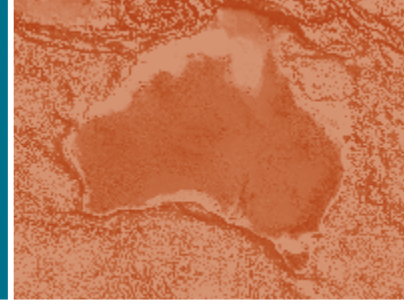




Australian Government  
Geoscience Australia



Record 2014/51 | GeoCat 82239

# Platinum-group elements in Australia

Geological setting, mineral systems, and potential

Editors: Hoatson, D.M. and Lewis, B.

Authors: Hoatson, D.M., Mieziitis, Y., Jaireth, S. and Huston, D.L.



# Platinum-group elements in Australia

Geological setting, mineral systems, and potential

GEOSCIENCE AUSTRALIA  
RECORD 2014/51

Editors: Hoatson, D.M. and Lewis, B.

Authors: Hoatson, D.M., Mieзитis, Y., Jaireth, S. and Huston, D.L.



**Australian Government**  

---

**Geoscience Australia**

## Department of Industry

Minister for Industry: The Hon Ian Macfarlane MP

Parliamentary Secretary: The Hon Bob Baldwin MP

Secretary: Ms Glenys Beauchamp PSM

## Geoscience Australia

Chief Executive Officer: Dr Chris Pigram

This paper is published with the permission of the CEO, Geoscience Australia



© Commonwealth of Australia (Geoscience Australia) 2014

With the exception of the Commonwealth Coat of Arms and where otherwise noted, all material in this publication is provided under a Creative Commons Attribution 3.0 Australia Licence.

(<http://www.creativecommons.org/licenses/by/3.0/au/deed.en>)

Geoscience Australia has tried to make the information in this product as accurate as possible. However, it does not guarantee that the information is totally accurate or complete. Therefore, you should not solely rely on this information when making a commercial decision.

Geoscience Australia is committed to providing web accessible content wherever possible. If you are having difficulties with accessing this document please email [clientservices@ga.gov.au](mailto:clientservices@ga.gov.au).

**ISSN 2201-702X (PDF)**

**ISBN 978-1-925124-45-3 (PDF)**

**GeoCat 82239**

**Bibliographic reference:** Hoatson, D.M. and Lewis, B. (eds.) 2014. *Platinum-group elements in Australia: geological setting, mineral systems, and potential*. Record 2014/51. Geoscience Australia, Canberra. <http://dx.doi.org/10.11636/Record.2014.051>

**Example chapter reference:** Jaireth, S. and Huston, D. 2014. Principal features of platinum-group-element mineral systems. In: Hoatson, D.M. and Lewis, B. (eds.) 2014. *Platinum-group elements in Australia: geological setting, mineral systems, and potential*. Record 2014/51. Geoscience Australia, Canberra. <http://dx.doi.org/10.11636/Record.2014.051>

**Front cover photographs:** Top right image: McIntosh Intrusion, Halls Creek Orogen, Western Australia. Image from Ian Oswald-Jacobs, IOJ Aerial Photography P/L, Adelaide. Left image: Stacked cyclic sequence of thin chromite (black) and olivine (replaced by white magnesite)-chromitite layers, Panton Intrusion. Image from senior author. Lower centre image: Panton Intrusion, Halls Creek Orogen, Western Australia. Image from Ian Oswald-Jacobs, IOJ Aerial Photography P/L, Adelaide. Lower right image: Massive sulphides in outcrop, Voisey's Bay nickel-copper deposit, Labrador, Canada. Image from Steve Tilley, CVRD-Inco, Canada.



*In memoriam:* This report is dedicated to the life and scientific contributions of our friend, colleague, and mentor, Dr David Henry Blake (22 August 1937–11 June 2014). A true gentleman, David was a distinguished field geologist who led several government field parties that mapped some of the most prominent Precambrian terranes in Australia. David joined the BMR in 1964, and commenced his eminent career by dissecting the geology and mineral systems of the Herberton Tin Field in northern Queensland. David subsequently led large traditional mapping programs in the Granites–Tanami, Mount Isa–Cloncurry, Davenport, and Kimberley regions of central and northern Australia. Many of the 1: 100 000 and 1:250 000 geological maps and reports derived from these programs remain today as the standard references for both explorers and the geological surveys of this country. This period of regional mapping was interrupted by volcanological investigations in the New Guinean islands of Bougainville and Buka, and David was regularly drawn to Iceland—a dynamic island characterised by diverging plate motions, repeated volcanism, and geothermal phenomena. David’s long list of scientific publications reveals an inquisitive mind that was prepared to challenge scientific principles and ‘established’ doctrines. His international scientific publications, BMR Bulletins, reports, map commentaries, and guidebooks on National Parks are considered models of geoscientific writing—composed in a clear and concise language, perfectly organised, and readily understood by all levels of audiences. David was a great mentor who readily passed his knowledge onto other geologists at BMR, State and Territory Geological Surveys, mining companies, and students. He always maintained ...“*that the best geologist is the geologist who has seen the most rocks in the field*”. David was certainly one of the best and most respected geologists who left an immeasurable and indelible legacy to Australian geoscience. A far-reaching record of significant scientific contributions will ensure that David Henry Blake will never be forgotten.

# Acknowledgements

In early 1983, the then Chief of the Petrology and Geochemistry Division at BMR, Dr John Ferguson, asked the senior author of this report to undertake a review of platinum in Australia. One of the major outputs from this request was BMR Record 1984/1—'*Potential for platinum group mineralisation in Australia. A review*'. With the publication of GA Record 2014/51, the senior author has after some thirty years returned full circle to those early investigations by discussing a similar theme in the same publication medium. During these three decades, the senior author (and co-authors) have drawn on the inspiration and advice on the geology and metallogeny of mafic-ultramafic igneous rocks provided by many colleagues at BMR–AGSO–GA, state and territory geological surveys, universities, and exploration companies. They include<sup>1</sup>. David Blake, David Champion, Jon Claoué-Long, Morrie Duggan, Andrew Glikson, Michael Huleatt, David Huston, Subhash Jaireth, Lynton Jaques, Lautaro Macias, Tony Meixner, Terrence Mernagh, Yanis Miezitis, Rodney Page, Russell Shaw, John Sheraton, Colin Simpson, Alastair Stewart, Shen Su Sun, David Wallace, Gladys Warren, Alan Whitaker, Lesley Wyborn (all of BMR–AGSO–GA); Tim Griffin, Franco Pirajno, Steve Sheppard, and Ian Tyler (Geological Survey of Western Australia: GSWA); Wayne Cowley, Sue Daly, and Marc Davies (Geological Survey of South Australia: GSSA); Christine Edgoose, Ian Scrimgeour, and Andrew Wygralak (Northern Territory Geological Survey: NTGS); Lawrence Glaser, Paul Hamlyn, Rebecca Sproule, and Alfonso Trudu (private consultants); Alan Boudreau (Duke University), Reid Keays (University of Melbourne), David Lambert (Monash University), Charter Mathison (University of Western Australia), Gerhard von Gruenewaldt (University of Pretoria); Steve Barnes, Martin Gole, Rob Hill, and Russell Hudson (CSIRO, Perth); and many others. In addition, Lynton Jaques and Reid Keays are acknowledged for their formal supervision of the senior author during his PhD study in the 1980s of PGE mineralisation in the Munni Munni Intrusion, Western Australia—a great foundation for a career devoted to PGEs.

This review has also compiled public information and data from several mineral commodity experts associated with the state and territory geological surveys. Don Flint and Abey Abeysinghe (GSWA), Tony Brown and Ralph Bottrill (Mineral Resources Tasmania–MRT), David Mason and Terry Denaro (Geological Survey of Queensland), Kathy Hill and Adele Seymon (Geological Survey of Victoria), Lindsay Gilligan and Peter Downes (Geological Survey of New South Wales), Ted Tyne, Mark McGeough, and Lachlan Rutherford (GSSA), Ian Scrimgeour and Mazhar Khan (NTGS) provided state and territory compilations of PGE occurrences that formed a basic framework for this report. Another important source of information was derived from many geologists associated with mining companies operating in Australia and elsewhere—unfortunately too many to acknowledge here.

Michelle Cooper, Lara Davis, Helen Dulfer, David Huston, Terrence Mernagh, Roger Skirrow, Alastair Stewart, and Jane Thorne (all GA) reviewed this report. The visual impact of the line figures and maps owes much to the cartographic skills of Neale Jeffery, Bianca Reese, and Veronika Galinec under the professional guidance of Silvio Mezzomo at GA. Alastair Stewart carried out a scientific edit of most of these figures. Chris Fitzgerald is acknowledged for his photographs skills evident in the mineral and rock textures portrayed in the pictorial atlas of Appendix L. Daniel Rawson prepared the report for online publication.

---

<sup>1</sup> Many of the geoscientists listed in the Acknowledgments have subsequently left GA or the organisation shown.

Bridgette Lewis is particularly thanked for her significant contributions in compiling, designing, and technical editing of this comprehensive and complex document.

Many people and organisations are acknowledged for providing photographs in Chapters 2, 4, 5, and 6. These include: Pat Workman at Johnson Matthey PLC (Figures 2-1, 2-2, 2-3, 2-4, 2-7, 2-10, 2-11, 4-2, 4-3, 4-4, 4-5, 4-6, 4-7, 4-8, 4-9, 4-10a,b; 4-11 a,b,d, 4-12, 4-15), Wikimedia Commons (Figures 2-5, 2-6, 2-8, 2-9, 4-1, 4-13c), and Theodore Gray (Figure 4-10c,d; 4-11c,e; 4-13a,b; 4-14) for photographs of the applications of PGEs; Carol Bacon and Michael Dix (MRT) for historical photographs of mining operations in Adamsfield (Figures 5-6, 5-7); Ralph Bottrill (MRT) for 'osmiridium' grains and miners in Tasmania (Figures 5-4 b,f; 5-5, 5-8); Jeffrey Gresham (Gresham Mineral Consulting Services) for historical images of Kambalda (Figures 5-9, 5-10, 5-11); Michael Organ for the picture of geological surveyor Stutchbury (Figure 5-1); Mitchell Library, State Library of New South Wales for Reverend Clarke (Figure 5-2); John Kaminsky (Rimfire Pacific Mining NL) for mining operations and Pt nuggets at Fifield (Figures 6-60, 6-61); Helix Resources NL for Pt nuggets at Fifield (Figure 6-62); and, in particular, Steve Barnes (CSIRO) is thanked for his quality photographs of komatiitic rocks in Appendix L (see below).

Most photographs in Appendix L belong to GA with additional photographs provided by:

- Figures L-1; L-2: Ian Oswald-Jacobs, IOJ Aerial Photography P/L, Adelaide.
- Figure L-5a: R.J. Perring, Pancontinental Mining, Perth.
- Figures L-5f; L-19f: Tim Ivanic, GSWA, Perth.
- Figure L-10: Reproduced with permission from Norilsk Nickel Australia Pty Ltd, Perth.
- Figure L-11a: Mike Donaldson, GSWA, Perth.
- Figures L-11b, d to f; L-21 to L-23; L-30 to L-32: Steve Barnes, CSIRO, Perth.
- Figure L-18a: Peter Hayden, Craton Geological Services, Perth.
- Figure L-18b: Western Mining Corporation Limited, Perth.
- Figures L-18e to f: Russell Hudson, CSIRO, Perth.
- Figure L-28: Steve Tilley, CVRD-Inco, Canada.

Most mineralised rock samples in Appendix L were collected by the senior author, with additional samples provided by: David Andrews (CRA Exploration Pty Ltd); Steve Barnes (CSIRO); Tim Callaghan (OZ Minerals Ltd); Jon Cloué-Long (GA); Julian Hanna (Western Areas NL); Jani Impola and Alistair Cowden (Vulcan Resources Ltd); Tony Green (Grenvyn Consulting Inc.); Peter Hayden and Colin Paterson (Craton Geological Services and Yilgarn Mining Ltd); David Singleton, Neil Hutchison, and Michael O'Mara (Poseidon Nickel Ltd); David Maidment (GA); Tim Kennedy and Somealy Sheppard (Lightning Nickel Pty Ltd and Independence Group NL); Aidan Trotter (BHP Billiton Ltd); and Alan Whitaker (GA).

# Executive summary

The platinum-group elements (PGEs) are a group of six rare metals comprising platinum (Pt), palladium (Pd), rhodium (Rh), iridium (Ir), osmium (Os), and ruthenium (Ru) that are classified as Transition Metals in the Periodic Table of Elements. They have unique physical and chemical properties and a high supply risk that make them 'global critical commodities' for many emerging and prominent technologies in today's society. For example, Os, Ir, and Pt are the densest metals known with densities up to  $22.59 \text{ g cm}^{-3}$ . Iridium is notable for being the most corrosion-resistant element, even at temperatures as high as  $2000^\circ\text{C}$ . The PGEs also have some of the highest melting points of all metallic elements, ranging from  $1555^\circ\text{C}$  for Pd to  $3033^\circ\text{C}$  for Os. Other important properties include strength, resistance to wear, a shiny lustre, ductility, malleability, electrical and thermal conductivity, and they are efficient catalysts. Commercial applications that have exploited these attributes are highlighted in the chemical, electrical, electronic, motor vehicle, aerospace, jewellery, dentistry, and agriculture industries, and in environmentally-based technologies (e.g., catalytic converters and fuel cells). Their scarcity in nature have made the PGEs strategically important in many industries, and highly valued as decorative and investment commodities.

As with other more common Transition Metals, such as iron, cobalt, and nickel, the PGEs tend to prefer either (1) metal-metal bonding over ionic bonding and consequently are often found in their native state, or (2) covalent bonding with sulphide ions in sulphide melt. These types of bondings reflect their strong dual siderophile (with iron) and chalcophile (with sulphur) behaviours in a variety of geological environments. Thus the presence of metallic and sulphide minerals generally determines the geochemical behaviour of the PGEs. The PGEs are truly rare metals with their relative abundances in the Earth's upper continental crust ranging from about 0.001 parts per million (ppm) for Ru, Pt, and Pd, to as low as 0.00001 ppm for the rarest PGE, Ir. The PGEs are useful for characterising petrogenetic and mineralising processes. They are strongly fractionated into a sulphide phase and can be used as a measure of the degree of partial melting in the mantle, and the sulphide saturation status of the magma—both important parameters for identifying fertile magmatic systems.

The world's current supply of PGEs is dominated by South Africa (Bushveld Igneous Complex) and Russia (Noril'sk–Talnakh). In 2013, 178.5 tonnes (t) of Pt were produced, with South Africa (71.8%) dominating followed by Russia (13.6%), Zimbabwe (6.9%) and North America (5.5%). Most of the 200 t of Pd were produced by Russia (42.0%) and South Africa (36.6%), with minor contributions from North America (14.5%) and Zimbabwe (4.8%). In the same year Australia produced 786 kg of Pd and Pt valued at ~\$20.4 million, which equates to ~0.2% of total global supply. This production was wholly derived as a by-product from Archean Ni-Cu-PGE sulphide deposits in Western Australia.

With the exception of a short period during the mid-1920s, when Tasmania was the largest producer of 'osmiridium' in the world, Australia has had an insignificant impact on the global PGE market. Australia's PGE production record comprises historical contributions from small-scale alluvial deposits in central New South Wales and from western Tasmania, and in more recent times from Western Australia. These three regions have accounted for more than 99% of Australia's total recorded production of 26 456.3 kg for Pt, Pd, 'osmiridium', and Ru between 1894 and 2013. Western Australia (24 843.9 kg Pt+Pd+Ru) has dominated PGE production followed by Tasmania (966.8 kg 'osmiridium'), New South Wales (633.5 kg Pt), and Victoria (12.1 kg Pt). Australia's PGE occurrences,

as elsewhere in the world are hosted by, or are derived from, ultramafic and/or mafic igneous rocks. The PGEs are found in a wide range of geological settings associated with orthomagmatic, hydrothermal, metamorphic, regolith-laterite, and placer environments. The ages of the host rocks in these geological settings encompass most of the geological time record from the Mesoarchean (~3.0 Ga) to the present.

The major aims of this report are to review the distribution, geological characteristics, resources, and potential of PGEs in Australia, and provide a mineral-systems-based framework for successful low-risk exploration.

A mineral-system approach has been used to classify ~500 PGE deposits and occurrences documented in this report. This approach focuses on mineral-forming processes critical to the formation of a particular deposit. It differs from descriptive classifications in that it can be used to predict new areas and types of PGE mineralisation. The classification used is hierarchical in structure, with the highest-level category of deposits called 'Mineral-System Class'. There are twelve major classes that fall within the broad-mineral systems: Orthomagmatic (classes 1 to 7), Hydrothermal-Metamorphic (class 8), Regolith-Laterite (class 9), Placer (class 10), Astrobleme-related (class 11), and a final class with minor or unknown economic importance (class 12).

The economic status of PGE deposits is dependent on a variety of petrogenetic processes that need to be efficient during the enrichment of background abundances to ore-grade abundances. Such concentration processes include: the generation of immiscible sulphide liquids; fractional crystallisation of high-temperature minerals (e.g., chromite, Ti-V spinel); remobilisation and transportation of metals during metamorphic and hydrothermal fluid activity; and mobility during regolith-related processes. The preservation-erosional status of the deposit is also critical to the viability of the deposit.

While PGEs have been explored in Australia for more than a century, a significant, economically viable PGE deposit remains elusive. This is in spite of Australia having favourable geological settings and an abundance of documented PGE occurrences that indicate fertile mineral systems have been active in many geological provinces. In this report, the potential for recognising a major PGE mineral system in Australia is examined at the continent-, province-, and local-intrusion-scale. Exploration strategies and guidelines for successful low-risk exploration are given for those mineral systems considered more prospective for forming large-tonnage PGE deposits. A complex set of parameters need to be considered for the discovery of such a deposit in Australia, namely: the early recognition of mineral potential; a thorough understanding of the mineral system(s); identification of various petrological and geochemical signatures indicating the sulphide-saturation status of magmas; a flexible multidisciplinary approach; exploration persistence; significant capital investment; and elements of serendipity are likely to be required.

This report concludes that, as seen globally, mineralised stratabound layers in Precambrian layered mafic-ultramafic intrusions in Australia are considered to have high potential for a major economic PGE resource. Such layers are attractive targets as they display: lateral continuity; have uniform grades (1 g/t to 6 g/t Pt+Pd+Au) and thicknesses; contain a significant component of the elements Pt, Pd, Rh, Au; and have potential for large-tonnage multi-element deposits (PGEs, Cr, Cu, Ni, Co, Au). Large Igneous Provinces may also provide opportunities for major economic PGE resource discoveries, despite the challenges of: defining favourable mineralised environments across large areas and under cover; lack of reliable geochronological and geochemical data for identifying different phases of the magmatic system; and a general perception that the global type example (Noril'sk–Talnakh in Russia) may be a 'unique' mineral system.

# Scope, rationale and objectives

The platinum-group elements are six precious metals (Pt, Pd, Rh, Ir, Ru, Os) that have unique physical and chemical properties that make them strategically important for today's society. The PGEs constitute essential components in the chemical, electrical, electronic, motor vehicle, aerospace, defence, jewellery, dentistry, and agriculture industries, and in environmentally-based technologies. Their sustained high prices reflect this expanding portfolio of applications and their narrow global supply base. Compared with other elements of commercial interest, the PGEs represent some of the most critical commodities of global economic importance. Consequently, the PGEs are attractive commodity targets for the minerals industry.–

This report produced by Geoscience Australia<sup>2</sup> reviews the distribution, geological characteristics, resources, and potential of PGEs in Australia. With the exception of historical accounts by Geary et al. (1956), Barrie (1965), Kalix et al. (1966), and Hoatson and Glaser (1989), no other publications have described the geological settings and resources of PGE occurrences at a national scale. This report provides a comprehensive and up-to-date summary of the diversity of PGE occurrences in Australia that draws upon data and information provided by all the state and territory geological surveys. In addition, despite Australia having favourable geological settings and an abundance of documented PGE occurrences (more than 500 described in this review) that indicate fertile mineral systems have been active in many geological provinces, this nation does not currently have a PGE deposit of economic status. Australia's insignificant global standing is also indicated by total PGE production (from by-products of Ni mining in Western Australia) equating to just ~0.2% of total global supply.

Geological information and locations for PGE deposits and occurrences in this report are derived from Geoscience Australia's National Mineral Location (MINLOC) database, which is based on the State and Northern Territory Geological Survey databases described in the introduction to Appendix K.

The major aims of this report are to: provide an up-to-date and comprehensive compilation of PGE occurrences in Australia; introduce a minerals-system framework that identifies those elements considered important for the formation of PGE deposits; assess the prospectivity and resource potential of PGEs in Australia; and provide prospectivity analyses and discovery strategies/guidelines that will minimise exploration risk. The information and main messages of a number of diverse themes presented in this review are intended to inform the public, student, and professional geoscientist.

---

<sup>2</sup> Geoscience Australia (GA: <http://www.ga.gov.au/>; formerly the Bureau of Mineral Resources, Geology and Geophysics–BMR; and the Australian Geological Survey Organisation–AGSO) is the Australian Government's geoscience agency which provides geoscientific information and knowledge to enable government and the community to make informed decisions about the exploitation of resources, the management of the environment, and the safety of critical infrastructure.

This report comprises eight chapters and twelve appendices that are structured as follows.

**Chapter 1** provides a general overview of the PGEs and a summary of the major geological settings of these rare metals. Supply, demand, and metal price dynamics are considered from both global and Australian perspectives, and the global critical importance of the PGEs are quantified against the many other elements of commercial significance.

**Chapter 2** discusses the historical applications of the PGEs from the earliest Egyptian civilisations dating back to ~1400 BC, to the skilled artisans of the Mayans, Incas, and Aztecs of Central and South America, to the influences of famous European scholars, alchemists, and jewellery craftsmen who had significant cultural impacts from the mid-16<sup>th</sup> century. The remarkable achievements of English chemists Wollaston and Tennant—the discoverers of Pd, Rh, Ir, and Os—are featured in the discovery record of the PGEs.

**Chapter 3** focuses on the different geochemical behaviours of the six PGEs. Metal abundances in mantle-crustal environments, various host igneous rock types and hydrothermal fluids, partitioning into magmas of different composition, and behaviours in hydrothermal fluids are compared within an evolutionary geochemical cycle framework.

**Chapter 4** describes the unique physical and chemical properties of the PGEs and examines how these attributes have been utilised in various commercial applications, such as catalytic converters, fuel cells, electronics, defence-aerospace, jewellery, watchmaking, laboratory apparatus, dentistry, medicine, photography, and investment.

**Chapter 5** presents a chronological history of Australia's PGE industry from the first discovery of Pt in central New South Wales in 1851, to Australia's first production of Pt at Fifield, to western Tasmania temporarily attaining the status of the largest producer of 'osmiridium' in the world, to the challenges of finding world-class Ni-Cu-PGE deposits in the Kambalda region of Western Australia.

**Chapter 6** summarises the geological settings of PGE deposits and occurrences in Australia. Major features, such as resources, current status and exploration history, stratigraphy, mineralisation environment, age and source of PGEs, and genesis are described for nineteen-type deposits and occurrences. This information is used to compile a mineral-system-based classification scheme that encompasses twelve major classes that are appropriate for Australia's many PGE occurrences.

**Chapter 7** incorporates the information provided by the type examples described in Chapter 6 and assesses those criteria considered critical for the formation of each particular deposit type. This mineral-system approach differs from descriptive-based classifications in that it can better predict potential new areas and types of PGE mineralisation.

**Chapter 8** draws on the main conclusions highlighted in the previous seven chapters. It explores the possible reasons for the apparent poor performance of the Australian PGE exploration industry in recent decades. The fertility status of tholeiitic and komatiitic magmatic mineral systems are assessed, and prospectivity analyses are undertaken at continent-, province-, and intrusion-scales. Exploration guidelines are provided for those mineral systems believed to have the highest potential for the discovery of a significant economic PGE resource in Australia.

**Appendices A to L** provide glossaries of resource and scientific terms, platinum-group minerals identified in Australia, national and global PGE resource data, useful websites, comprehensive inventory of Australia's PGE occurrences, and a pictorial atlas of diagnostic textures and mineralisation features associated with mafic and ultramafic igneous rocks from Australia and overseas.

# Contents

Acknowledgements .....	iv
Executive summary .....	vi
Scope, rationale and objectives .....	viii
1 What are platinum-group elements? .....	1
1.1 Overview of the platinum-group elements .....	1
1.2 General geological settings of platinum-group elements .....	4
1.3 Supply, demand, and metal prices .....	8
1.3.1 World supply .....	8
1.3.2 World demand .....	15
1.3.3 Australia's global profile—production, imports, and resources .....	15
1.3.4 Metal prices .....	18
1.4 Are the platinum-group elements of global critical importance? .....	21
1.5 Aims and sources of information .....	24
1.6 Other reviews of platinum-group elements in Australia .....	27
2 Historical aspects of the platinum-group elements .....	30
2.1 The earliest applications of platinum-group elements .....	30
2.2 The European influence .....	33
2.3 Scientific recognition and etymology .....	38
2.3.1 Platinum .....	40
2.3.2 Palladium .....	42
2.3.3 Rhodium .....	42
2.3.4 Ruthenium .....	44
2.3.5 Iridium and osmium .....	45
3 Geochemistry of platinum-group elements .....	46
3.1 General chemistry .....	46
3.2 Abundances of platinum-group elements on Earth .....	48
3.2.1 The mantle .....	49
3.2.2 The crust .....	49
3.2.3 Platinum-group-element concentrations in major rock types .....	50
3.3 Partition coefficients of platinum-group elements .....	57
3.4 Solubility of sulphur in mafic and ultramafic melts .....	58
3.4.1 Main factors controlling sulphur solubility .....	58
3.4.2 Equilibration of silicate and sulphide melts .....	61
3.5 Platinum-group elements in hydrothermal fluids .....	63
3.5.1 Fluid-melt partitioning .....	63
3.5.2 Platinum-group elements in fluids below 300°C .....	64
3.5.3 Platinum-group elements in fluids at 25°C .....	66
3.6 Conclusions .....	67
4 Properties and applications of the platinum-group elements .....	69
4.1 Introduction .....	69

4.2 Platinum .....	74
4.2.1 Catalytic converters .....	75
4.2.2 Jewellery.....	76
4.2.3 Fuel cells .....	78
4.2.4 Investment.....	78
4.2.5 Other uses .....	79
4.3 Palladium .....	82
4.3.1 Catalyst.....	83
4.3.2 Electrics and electronics.....	83
4.3.3 Other uses .....	84
4.4 Rhodium.....	85
4.5 Iridium .....	87
4.6 Osmium.....	89
4.7 Ruthenium.....	91
5 Evolution of Australia's platinum-group-element industry .....	94
5.1 Introduction .....	94
5.2 Evolution of Australia's platinum-group-element industry.....	95
5.2.1 1850 to 1890—Eastern Australian discoveries: an industry is born.....	95
5.2.2 1890 to present—Fifield: Australia's first platinum producer.....	99
5.2.3 1910 to 1960—Tasmania: largest producer of 'osmiridium' in the world .....	105
5.2.4 1960 to present—Kambalda: world-class Ni-Cu±PGE province .....	115
6 Platinum-group elements in Australia.....	121
6.1 Introduction .....	121
6.2 Spatial and temporal distribution of platinum-group-elements in Australia .....	129
6.3 Classification of platinum-group elements in Australia .....	131
6.4 Type examples of platinum-group-element deposits .....	136
6.4.1 Mineral-System Class 1: Layered tholeiitic mafic-ultramafic intrusions .....	138
6.4.2 Mineral-System Class 2: Massive to poorly layered tholeiitic mafic-dominant intrusions .....	180
6.4.3 Mineral-System Class 3: Komatiitic flows and related sill-like intrusions .....	199
6.4.4 Mineral-System Class 4: Alkaline mafic-ultramafic intrusions.....	227
6.4.5 Mineral-System Class 5: 'Alpine- and ophiolitic-type' ultramafic-mafic intrusions .....	233
6.4.6 Mineral-System Class 6: 'Alaskan- and Urals-type' mafic-ultramafic intrusions .....	248
6.4.7 Mineral-System Class 7: Continental flood basalts with associated sub-volcanic sills.....	265
6.4.8 Mineral-System Class 8: Hydrothermal-Metamorphic .....	265
6.4.9 Mineral-System Class 9: Regolith-Laterite.....	314
6.4.10 Mineral-System Class 10: Placer .....	322
6.4.11 Mineral-System Class 11: Astrobleme-related.....	330
7 Principal features of platinum-group-element mineral systems .....	331
7.1 Introduction—what is a mineral system? .....	331
7.2 Stages in the formation of platinum-group element and nickel- copper mineral systems .....	335
7.3 Mineral-system features of platinum-group element and nickel- copper mineral deposits .....	337
7.3.1 Mineral-system features of platinum-group-element deposits associated with layered tholeiitic mafic-ultramafic intrusions.....	338
7.3.2 Assessment criteria for layered tholeiitic mafic-ultramafic intrusions.....	340
7.3.3 Mineral-system features of platinum-group element deposits associated with massive to poorly layered tholeiitic mafic-dominated intrusions .....	342

7.3.4	Assessment criteria for massive to poorly layered tholeiitic mafic-dominated intrusions .....	344
7.3.5	Mineral-system features of platinum-group-element deposits associated with komatiitic flows and related sill-like intrusions .....	345
7.3.6	Assessment criteria for komatiitic flows and related sill-like intrusions .....	347
7.3.7	Mineral-system features of platinum-group-element deposits associated with 'Alpine- and ophiolitic-type' ultramafic-mafic intrusions.....	349
7.3.8	Assessment criteria for 'Alpine- and ophiolitic-type' ultramafic-mafic intrusions.....	351
7.3.9	Mineral-system features of platinum-group-element deposits associated with 'Alaskan- and Urals-type' mafic-ultramafic intrusions .....	352
7.3.10	Assessment criteria for 'Alaskan- and Urals-type' mafic-ultramafic intrusions .....	353
7.3.11	Mineral-system features of hydrothermal-metamorphic platinum-group-element deposits of primary and remobilised origin.....	354
7.3.12	Assessment criteria for hydrothermal-metamorphic PGE mineralisation .....	356
7.3.13	Mineral-system features of platinum-group-element deposits associated with continental flood basalts and sub-volcanic sills.....	357
7.3.14	Assessment criteria for continental flood basalts and sub-volcanic sills.....	358
8	Summary of exploration strategies, prospectivity, and guidelines .....	361
8.1	What is the status of Australia's exploration record?.....	361
8.2	Temporal distribution of platinum-group-element mineral systems .....	369
8.3	Fertility status of tholeiitic- and komatiitic-magmatic mineral systems .....	373
8.3.1	Tholeiitic magmatic systems: fertile versus barren .....	376
8.3.2	Komatiitic magmatic systems: fertile versus barren.....	382
8.4	Prospectivity analysis of platinum-group-element mineral systems in Australia .....	388
8.4.1	Prospectivity analysis—continent scale .....	391
8.4.2	Prospectivity analysis—province scale: large igneous provinces .....	397
8.4.3	Prospectivity analysis—intrusion scale .....	412
8.5	Prospectivity and exploration guidelines for platinum-group-element mineral systems in Australia .....	422
	References .....	447
	Appendix A Chemical elements .....	503
	Appendix B Glossary .....	505
	Appendix C Platinum-group minerals.....	511
	Appendix D World supply and demand for platinum-group elements.....	513
	Appendix E Platinum-group-element resources of world deposits .....	517
	Appendix F Production and value of platinum-group elements in Australia.....	521
	Appendix G Australia's national classification system for identified mineral resources.....	527
	Appendix H Useful links for information about platinum-group elements .....	532
	Appendix I Exploration reports by Sprent.....	535
	Appendix J Summary of Australian platinum-group-element deposits and occurrences.....	553
	Appendix K Australian platinum-group-element deposits and occurrences.....	581
	Appendix L Pictorial library of mafic-ultramafic rocks: a guide for exploration.....	950

# 1 What are platinum-group elements?

Dean M. Hoatson

## 1.1 Overview of the platinum-group elements

The platinum-group elements (PGEs<sup>3</sup>) comprise a group of six rare metals—platinum (shown as chemical symbol Pt), palladium (Pd), rhodium (Rh), iridium (Ir), osmium (Os), and ruthenium (Ru)—that are classified as Transition Metals on the Periodic Table of Elements<sup>4</sup> (Figure 1.1a; Appendix A). Transition Metals are typically ductile and malleable, conduct electricity and heat, and the valence electrons they use to combine with other elements, are present in more than one electronic shell. This is the reason why they exhibit several common oxidation states and different types of chemical bondings that determine their different geochemical behaviours (see Section 3.1). As with the other more common Transition Metals, such as iron (Fe), cobalt (Co), and nickel (Ni), the PGEs possess unfilled high-energy electronic d-orbitals containing unpaired electrons that may be engaged in metal-metal bonding or covalent bonding with sulphide ions in sulphide melt (Lorand et al., 2008). These types of bondings reflect the strong dual siderophile (with Fe) and chalcophile (with S) behaviours of the PGEs in a variety of geological environments that involve magmas, fluids, gases, and rocks.

The PGEs are often referred to as precious metals because of their rarity and desirability, and in some cases they are called noble metals based on their relative inactivity to combine or interact with most other elements or compounds. They are also regarded as strategic metals because of their growing use in advanced technologies related to the automotive, chemical, petroleum, electrical, electronic, medical, fuel cell, and aerospace industries. The United States Government also labels them strategic metals because they are considered a significant military resource. For many of these applications, it is not possible to substitute the PGEs economically and technically.

In the scientific literature the PGEs are sometimes divided into two subgroups (Rollinson, 1993): the Pd-subgroup (PPGEs) comprising Pt, Pd, and Rh; and the Ir-subgroup (IPGEs) of Ir, Os, and Ru.

Gold is sometimes associated with the former sub-group. The PPGEs and Au are often associated with the sulphides of Fe, Ni, and Cu and are found in norite, gabbro, and dunite, whereas, the IPGEs have a greater affinity for chromite as alloys or sulphides in dunite (Barnes et al., 1985). The two subgroups often display contrasting geochemical trends in different geological settings (e.g., layered mafic-ultramafic intrusions, ophiolites) and are therefore useful for characterising petrogenetic and mineralising processes. The PGEs are also very strongly fractionated into a sulphide phase and can be used as a measure of sulphide saturation in a melt, and they are also potentially useful as an indicator of the degree of partial melting in the mantle.

---

<sup>3</sup> The acronym PGEs is preferred to PGMs, which is often used in the literature, since the latter can be confused with the acronym for platinum-group minerals, i.e., PGMs. In this report, PGEs will be used for platinum-group elements, and PGMs will apply to platinum-group minerals (see Appendix B and Appendix C).

<sup>4</sup> The Periodic Table of Elements is a chart that summarises the physical, chemical, and other properties of 118 (as of March 2014) chemical elements and it provides a useful framework for classifying and comparing the different forms of chemical behaviour. The six PGEs occupy Groups (columns) 8 to 10 and Periods (rows) 5 to 6.

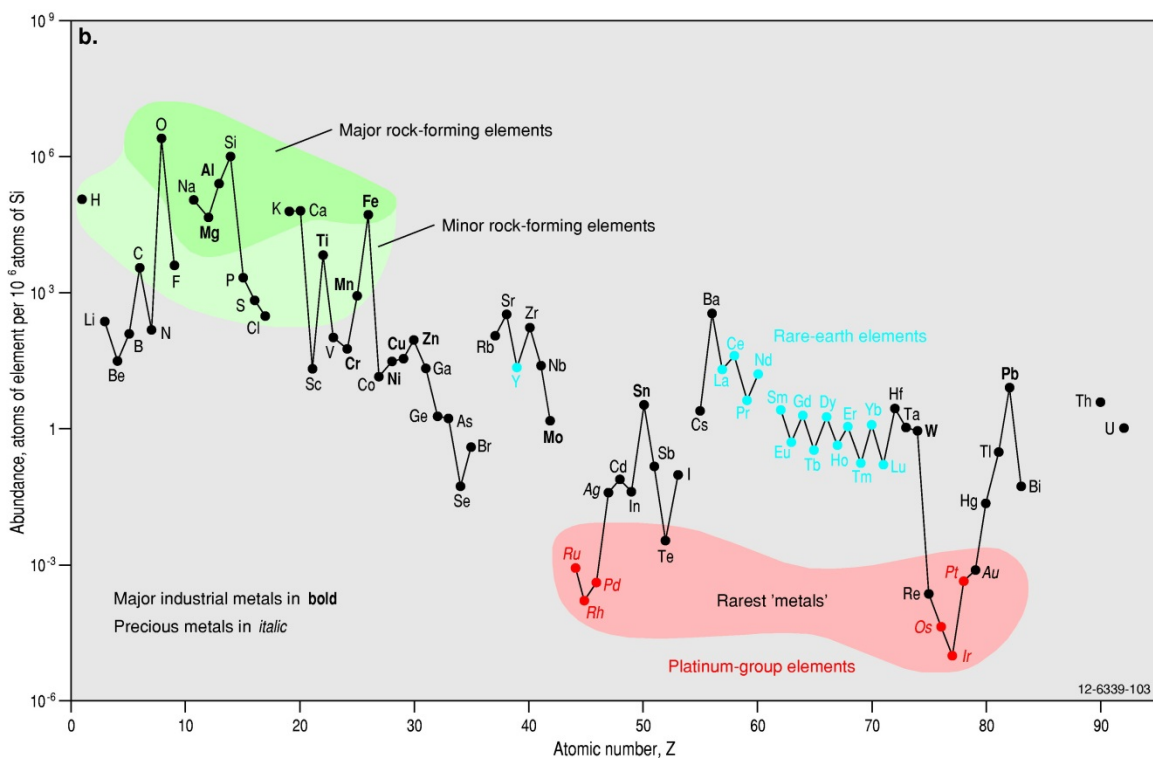
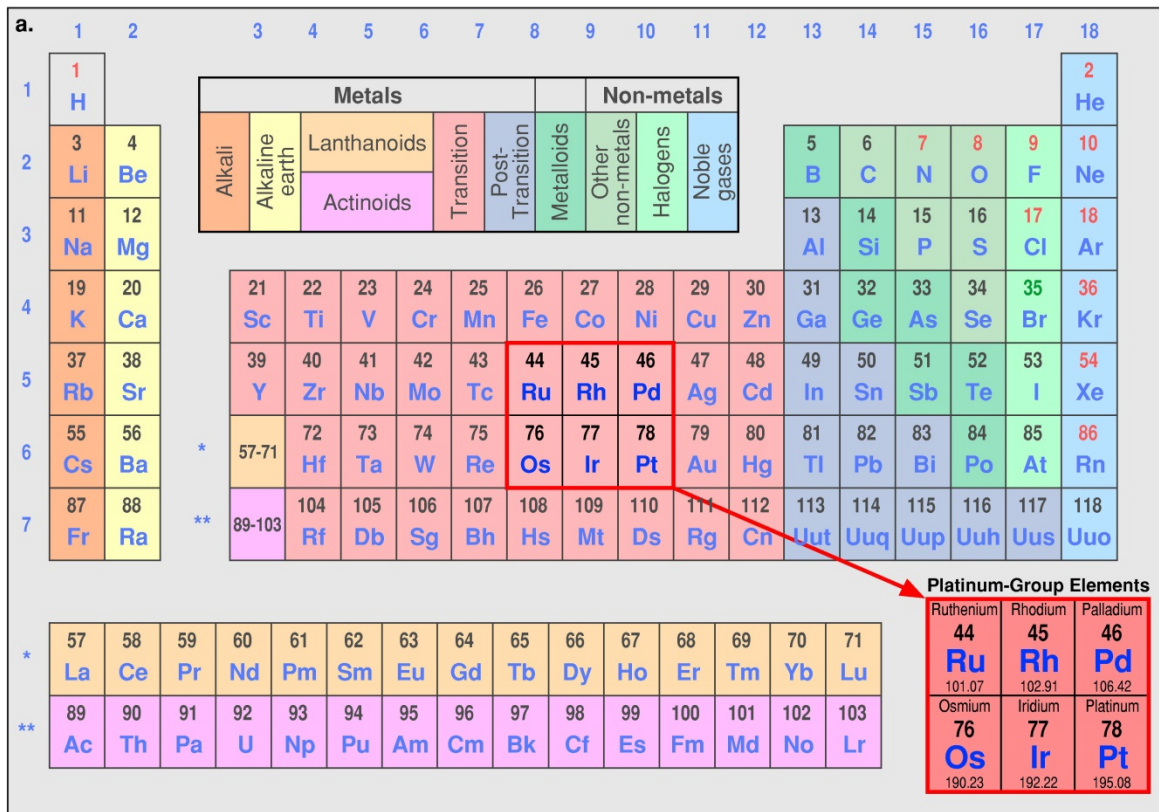


Figure 1.1 (a). Periodic Table of Elements. The six platinum-group elements are shown within the red box near the centre of the Periodic Table. Atomic weights are indicated in the enlarged inset. Modified from Dayah (1997). (b). Abundances (atom fractions) of the chemical elements in Earth's upper continental crust in reference to atomic number. Many of the elements are grouped into: (1) platinum-group elements (red font); (2) Rarest metals (pink field); and (3) Major and Minor rock-forming elements (dark and light green fields). Modified from Haxel et al. (2005).

The PGEs are most concentrated in the core of the Earth, becoming progressively less abundant in the successive outer shells of the mantle and crust<sup>5</sup> (Naldrett, 1989). The United States Geological Survey noted that their relative abundances in the Earth's upper continental crust range from about 0.001 parts per million (ppm) for the more common PGEs—Ru, Pt, and Pd, to 0.0001 ppm for Rh and Os, to as low as 0.00001 ppm for the rarest member of the group, Ir. Such low-crustal abundances represent less than 0.01% of the Earth's total PGE budget. In comparison, the more common rock-forming metallic elements like Cu, Ni, and Zn have crustal abundances of ~25 to ~100 ppm—about 5 orders of magnitude more than for Pt (Figure 1.1a; Haxel et al., 2005). Interestingly, the group of Rare-Earth Elements (REEs) shown in blue font of Figure 1.1b are actually not rare relative to the PGEs, which are at least three orders of magnitude less abundant than the more common REEs. The six members of the PGEs are truly rare metals. Actual abundance values of rare elements like the PGEs can be difficult to determine accurately, so published low-abundance values should be treated with caution. Examples cited on the internet often differ by up to several orders of magnitude from the generally accepted range of abundance values. Taylor and McLennan (2009) have estimated the PGE abundances of the combined mantle and crust of the Earth. In decreasing abundance they range from 6.6 parts per billion (ppb; 1000 ppb = 1 ppm) for Pt, 5 ppb for Ru, 3.6 ppb for Pd, 3.4 ppb for Os, 3.2 ppb for Ir, and 0.9 ppb for Rh. The PGEs are often associated with Cr, Ni, and Cu, and sometimes with Ti, Co, V, Au, and Ag, and their abundance ratios vary appreciably among the different types of mineral deposits. Although Au is a precious metal not belonging to the PGEs, it is commonly grouped with these metals when grades of deposits or products from smelters are discussed. The abundances of the PGEs throughout the Earth and from different rock types are discussed more in Chapter 3.

Possessing unique physical and chemical properties (see Chapter 4), the PGEs are increasingly becoming more important in today's society. Such properties as their high-melting points, resistance to corrosion and oxidation, electrical and thermal conductivity, and catalytic activity have been exploited in the chemical, electrical, electronic, motor vehicle, aerospace, agricultural, jewellery, and environmental industries. It has been estimated that approximately 20% of goods manufactured in the world today contain PGEs, or PGEs played a key role in their manufacturing process. Platinum and Pd are commercially the most significant PGEs followed by Rh. Osmium, Ir, and Pt are the densest metals known (Pt is 11% denser than Au and about twice the weight of the same volume of Pb and Ag), and Ir is the most corrosion-resistant element even at temperatures as high as 2000°C. They have some of the highest melting points (in excess of 3000°C) of all metallic elements, are hard-wearing, highly reflective, brittle, malleable, electrically and thermally conductive, and have unique catalytic characteristics.

The unique properties of the PGEs have also been highlighted in some international media announcements of technological advancements that created considerable controversy. One such example was on the 23<sup>rd</sup> of March, 1989, when Martin Fleischmann, then one of the world's leading electrochemists from the University of Southampton, and Stanley Pons of the University of Utah, declared that they had produced cold fusion—nuclear fusion of atoms at room temperature. The experiment involved electrolysis of heavy water on a Pd electrode, although subsequent experiments utilised electrodes made of Pt. The scientists documented anomalous heat production of a magnitude they asserted would defy explanation except in terms of nuclear processes. Their announcements raised hopes of a cheap and abundant new source of energy. Unfortunately, Fleischmann and Pons were subsequently unable to reproduce the heat-generating reactions to the satisfaction of the scientific community. If cold fusion became a reality, it would increase demand for PGEs.

---

<sup>5</sup> Upper part of the outermost layer or shell of the Earth which overlies the mantle and underlies the continents and the continental shelves; total continental crust ranges in thickness from about 35 km up to 60 km under mountain ranges.

## 1.2 General geological settings of platinum-group elements

Although the PGEs are commonly found together, deposits containing economic quantities of these precious metals are rare. Historically, alluvial placer deposits dominated the world production of PGEs, but this changed in the early 20<sup>th</sup> century when large hard-rock deposits in South Africa and Russia commenced mining. The most significant commercial quantities of PGEs today are associated with concentrations of Ni-Cu sulphides or chromite in igneous rocks of mafic to ultramafic composition. Enhancement of PGE abundances in these rocks may be attributed to multistage processes with concentration during high-temperature deposition of chromite, incorporation into immiscible sulphide-rich liquids, subsequent remobilisation during metasomatic and hydrothermal activity, and supergene enrichment in the weathering profile. Deposits that currently dominate global PGE production and resources can be broadly divided into three major groups.

1. Those deposits where the PGEs are produced as the primary products and have subordinate base-metal (e.g., Ni, Cu) sulphides and/or Cr-bearing spinels; are concentrated in laterally extensive stratabound layers, also often called 'reefs', at particular stratigraphic levels in large layered mafic-ultramafic intrusive complexes of Precambrian cratonic regions; and the host mineralised rocks are generally sulphide-poor (typically only containing a few % sulphides). The term 'reef' is derived from South African and Australian literature for a particular style of mineralisation that is represented by the rock layer that is mineralised and has a distinctive texture or mineralogy (Naldrett, 2004), or, the PGE-enriched sulphide mineralisation that occurs within the rock layer (Zientek, 2012). World-class mineralised stratabound layers are generally late Archean to Proterozoic in age and include: the Merensky Reef and UG-2 Chromitite layers in the Bushveld Complex of South Africa; the Main Sulphide Zone in the Great Dyke of Zimbabwe; and the J-M Reef in the Stillwater Complex, Montana, USA. Similar, but currently subeconomic Precambrian examples in Western Australia are the PGE-bearing sulphide and chromitite layers in the Munni Munni, Panton, Lamboo, Weld Range, and Windimurra layered mafic-ultramafic intrusions.
2. The second group includes those deposits that are mined primarily for their Ni, Cu, and Co credits, and the PGEs are produced as by-products; have formed from the interaction of mantle-derived magmas with crustal rocks that gave rise to early sulphide immiscibility; are mostly sulphide-rich (>5% sulphides); and may be associated with ultramafic- or mafic-dominated rocks. Such deposits are associated with primitive magmatic activity accompanying the early stages of formation of Precambrian greenstone belts. Significant examples include the Archean komatiitic-hosted deposits in Western Australia (e.g., Kambalda, Perseverance, Mount Keith, Cosmos) and similar Archean-Paleoproterozoic deposits in Canada (Raglan, Alexo, Thompson, Dumont, Bowden). Other important by-product contributions of PGEs are from sulphide concentrations located near the basal intrusive contacts (contact-type deposits of Zientek, 2012), or feeder conduits of massive or poorly layered mafic ± ultramafic intrusions. Important examples from overseas<sup>6</sup> include Voisey's Bay (Canada), Jinchuan (China), Kabanga (Tanzania), Pechanga (Russia), and prominent West Australian examples<sup>4</sup> include Nebo-Babel in the Musgrave Province, Savannah (formerly known as Sally Malay) in the Halls Creek Orogen, Radio Hill in the west Pilbara Craton, and the emerging Nova deposit in the Albany-Fraser Orogen.

---

<sup>6</sup> These deposits are Ni-Cu-Co dominant, but have minor concentrations of PGEs as reported in defined resources or in drill-hole intersections: see Table 6.2 and Appendix E and Appendix K.

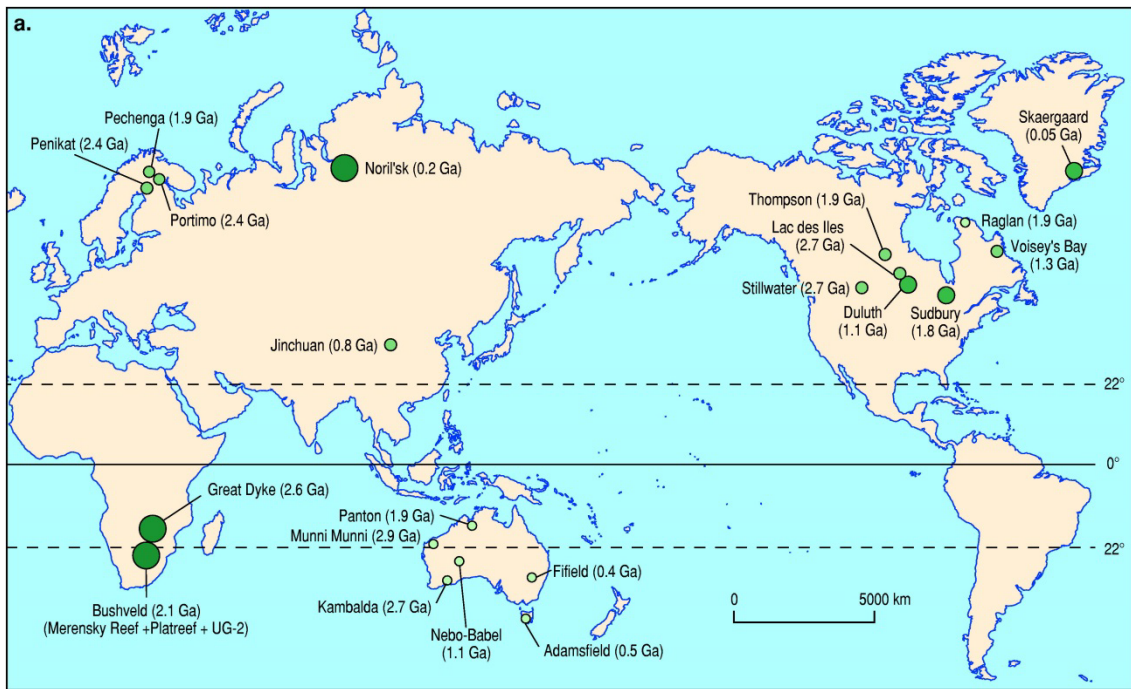
3. The final group includes two world-class deposits, or more correctly, two camps that contain many spatially close, 'comagmatic' mineral deposits. Having somewhat unconventional, possibly unique geological settings, these two camps have dominated the global production of Ni and Pd for many decades. They include the Ni-Cu-Co-PGE sulphide-rich deposits hosted by mafic-dominated rocks in the astrobleme-related Sudbury Intrusion in Ontario, Canada (Pye et al., 1984), and sub-volcanic picritic sills that are intrusive equivalents of comagmatic flood basalts associated with intracontinental rifting in the Noril'sk–Talnakh districts of Siberia, Russia (Naldrett, 2004). The Sudbury- and Noril'sk–Talnakh-types of deposits have created considerable exploration interest in Australia, however, such mineralisation styles have yet to be found.

In addition to these three major groups that dominate world production, relatively minor PGEs have also been mined in hard-rock and alluvial deposits associated with ophiolite-, alpine-, and Alaskan-Urals-type ultramafic-mafic complexes, in alkaline porphyry intrusions, skarns, and in hydrothermal, laterite, and sedimentary environments. However, a long history of exploration indicate that these geological settings offer little potential for large-tonnage deposits of world-class status, and their contributions to global production is insignificant relative to the three groups of globally significant deposits described above. Figure 1.2 shows the distribution of the major PGE deposits (a) and PGE-bearing Ni deposits (b) that make up these three important groups. The relative sizes of the colored symbols are an indication of the metal endowment (global resources<sup>7</sup>) in that deposit. In regard to the PGE deposits (Figure 1.2a), only three 'deposits' (Bushveld–South Africa; Great Dyke–Zimbabwe; and Noril'sk–Russia) have global resources of PGEs±Au exceeding 10 000 t. These large 'deposits' are followed by Sudbury (Canada), Duluth (USA), and Skaergaard (Greenland) with global resources ranging from 1000 t to 10 000 t. The six largest PGE deposits in Australia (Panton, Munni Munni, Kambalda group, Nebo–Babel, Fifield, and Adamsfield) have PGE±Au global resources of less than 100 t. The four world-class Ni sulphide deposits (Figure 1.2b) partly hidden behind the Kambalda (1.4 Mt global resource of Ni) symbol in Western Australia are Mount Keith (~3.4 Mt), Perseverance (~2.5 Mt), Yakabindie (~1.7 Mt), and Honeymoon Well (~1 Mt).

The following section summarises the distribution and genetic associations of platinum-group minerals (PGMs) in various geological settings. Further details of PGM associations can be found in the following geological settings: layered mafic-ultramafic intrusions—Kinloch (1982); Alaskan complexes—Johan (2002); hydrothermal—Tarkian and Stumpfl (1975); hypabyssal sills with associated flood basalts—Kozyrev et al. (2002); porphyry Cu deposits —Economou-Eliopoulos (2005); placer deposits—Weiser (2002); supergene environments—Oberthür and Melcher (2005); carbonaceous shale—Distler and Yudovskaya (2005); skarn—Yu, (1985); laterite—Lazarenkov et al. (2005); astrobleme-related—Cabri and Laflamme (1976); and general overviews—Cabri (1981; 2002) and Cabri et al. (1996).

---

<sup>7</sup> Global resource of metal (defined as total production plus remaining reserves and/or resources, i.e., total contained metal) will be used throughout this report unless otherwise stated. Resource data for the Australian deposits are from OZMIN—Geoscience Australia's national database of mineral deposits and resources.



Platinum-group-element deposit and platinum-group-element-bearing nickel deposit (Global resources of PGEs±Au)

- > 10 000 t
- 1000–10 000 t
- 100–1000 t
- < 100 t

Nickel sulphide deposit (Global resources of nickel metal)

- > 10 000 000 t
- 1 000 000–10 000 000 t
- < 1 000 000 t
- Associated platinum-group element deposits
- △ Nickel laterite deposit

12-6339-67

Figure 1.2 (a). World distribution of significant PGE and PGE-bearing deposits, and (b). nickel sulphide and nickel laterite deposits. The world-class nickel sulphide deposits partly hidden behind the Kambalda (1.4 Mt global resource of nickel) symbol in Western Australia are Mount Keith (~3.4 Mt), Perseverance (~2.5 Mt), Yakabindie (~1.7 Mt), and Honeymoon Well (~1 Mt). The distribution of laterite deposits is after Elias (2002) and the ages of deposits are from Hoatson et al. (2006).

Platinum production is dominated by large intrusive and hypabyssal bodies of mafic-ultramafic rocks, as described in groups 1 and 3 above. Platinum-group minerals typically comprise sulphides, sulpharsenides, tellurides, native metals, and Fe alloys, among many other species. These minerals occur with base-metal sulphides and Cr-bearing spinel in thin, laterally continuous stratabound layers often located near major compositional interfaces (ultramafic versus mafic) in the intrusions. The two most famous mineralised layers in the Bushveld Complex, the Merensky Reef and UG-2 Chromitite, have been mined for their PGEs since their discoveries in 1924 and 1906, respectively. Two other important economic settings in the Bushveld include a basal contact layer called the Platreef and hydrothermal dunite pipes (Onverwacht, Mooihoek, Driekop) that are discordant to the mafic-ultramafic stratigraphy of the complex. Platinum also occurs in a native state, often accompanied by small amounts of other PGEs, in alluvial and placer deposits in Colombia, Ontario, the Ural Mountains, and in the western American states. Placer alloys typically have either Pt-Fe or Ru-Ir-Os-Pt compositions; the latter display a compositional gap consistent with the limits of miscibility known from phase-equilibrium experiments (Cabri et al., 1996). Alluvial PGMs are also found in rivers draining major layered intrusions like the Great Dyke in Zimbabwe (Oberthür et al., 2013), but these deposits have lower economic significance relative to those alluvial deposits sourced by Urals- and Alaskan-type mafic-ultramafic intrusions. A significant amount of Pt and Pd is also produced commercially as a by-product of Ni-Cu sulphide ores from the Sudbury Complex in Ontario. Even though the quantity of Pt and Pd found in these ores is small (a few ppm), the large volume of Ni ores processed makes commercial recovery possible for these precious metals.

Palladium is often spatially associated with Pt in the sulphide- and chromite-bearing layers of the large intrusive bodies, such as the Bushveld Complex, and importantly, in the vast deposits hosted by the hypabyssal picritic intrusions of the Noril'sk–Talnakh region, Russia. It is also found as a free metal and alloyed with Pt and Au in placer deposits of the Ural Mountains of Eurasia, Ethiopia, and South and North America. As with Pt, it is commercially produced as a by-product of Ni-Cu sulphide ores at Sudbury. Remobilised Cu-rich vein-like ores at Sudbury also locally contain very high grades of associated Pd. Polymetallic hydrothermal deposits found on many continents are often enriched in Pd, Cu, Ag, and Au. Erratic precious-metal grades in these deposits are often a limitation on tonnage potential.

Rhodium occurs in ores that are mixed with other metals, such as Pd, Ag, Pt, Au, and consequently its industrial extraction processes are generally complex. It is principally found in Pt-rich ores of the Merensky Reef in the Bushveld Complex. Other important sources include the river sands of the Ural Mountains, in North and South America, and the Ni-Cu sulphide ores of Sudbury.

Iridium is found with Pt and other PGEs in alluvial deposits. Source rocks for these alluvial deposits range from ultramafic to mafic to alkaline in composition and they are usually found in Alaskan-type intrusions and tectonically-emplaced ophiolitic and alpine-type bodies. Naturally occurring Ir alloys include osmiridium and iridosmine, both of which are mixtures of Ir and Os.

Osmium-bearing minerals are found in Pt-bearing river sands in the Ural Mountains of Russia, and in North and South America. One of the most common PGMs is iridosmium, which is a naturally occurring alloy of Ir and Os. Trace amounts of Os also exist in Ni-bearing ores at Sudbury.

Ruthenium is generally found in ores with the other PGEs in the Ural Mountains and in North and South America. Small, but commercial quantities, are also found in the primary Ni sulphide mineral pentlandite that is extracted from the deposits at Sudbury.

Dill (2010) has provided the following brief compilation of the mineralogical-geological associations of some major PGMs and their PGE contents. For more comprehensive studies of the PGMs see Cabri (1981; 2002) and Kinloch (1982). Appendix C provides a summary of the major PGMs that have been documented with mafic-ultramafic rocks in Australia.

- Important host minerals of PGEs
  - Pt: pentlandite, chalcopyrite, pyrrhotite
  - Pd: maucherite, niccolite, gersdorffite
- PGE native minerals and alloys
  - Pt alloys with Pd, Ir, Os, Rh, Ru, and Fe (containing 10%–30% PGEs)
  - Pt is mainly related to Fe-rich magmas ('siderophile' character)
  - isoferroplatinum  $\text{Pt}_{2.25}\text{Pd}_{0.75}\text{Fe}^{0+}_{0.75}\text{Cu}_{0.25}$  (76% Pt, 13% Pd) Pt–Fe and Cu–Ni deposits in ultramafic rocks and placers
  - rustenburgite  $\text{Pt}_{2.25}\text{Pd}_{0.75}\text{Sn}$
  - atokite  $\text{Pd}_{2.25}\text{Pd}_{0.75}\text{Sn}$
  - chengdeite  $\text{Ir}_3\text{Fe}^{0+}$
- PGM sulphides ('chalcophile' character)
  - cooperite  $\text{Pt}_{0.6}\text{Pd}_{0.3}\text{Ni}_{0.1}\text{S}$  (62% Pt, 17% Pd) in norite
  - braggite  $\text{Pt}_{0.6}\text{Pd}_{0.3}\text{Ni}_{0.1}\text{S}$  (62% Pt, 17% Pd) in norite
  - laurite ( $\text{RuS}_2$ ) (61% Ru) in ultramafic rocks, and in placers
- PGM arsenides
  - sperrylite  $\text{PtAs}_2$  (56% Pt) in ultramafic rocks, and in placers
- PGM antimonides
  - geversite  $\text{PtSb}_{1.5}\text{Bi}_{0.5}$  (40% Pt) Pt–Fe–Cu–Ni deposits in ultramafic rocks
  - stibiopaladinite  $\text{Pd}_3\text{Sb}$

## 1.3 Supply, demand, and metal prices

### 1.3.1 World supply

Alluvial Pt deposits in South America and Russia were historically the major global sources of PGEs. Colombia (Chocó and Tumaco regions) and Ecuador (Esmeraldas region: see Chapter 2) in South America dominated the world's supply of Pt until the early 1820s when the alluvial Pt–Au deposits in the Ural Mountains of Russia were discovered. Platinum in the placer deposits of South America and Russia is generally associated with Ir and Os in the form of alloys, such as osmiridium and iridosmine. The PGE-bearing alloys are derived from the olivine-bearing ultramafic igneous rocks dunite and peridotite, or their altered equivalents serpentine.

The South American alluvial Pt deposits are described in Chapter 2 thus the following description will focus on the Russian and other similar placer deposits in the world. It is partly summarised from the report 'Part 1: Platinum placers and deposits' (Nevada Outback Gems, 2014).

The world's most productive Pt placers occurred on the eastern slopes of the Ural Mountains. Although hard-rock sources of Pt were discovered in ultramafic rocks on the Siberian side of the Urals in 1819, most production was from placers. The placers have been continuously mined for nearly two centuries and contributed to 90% of the world's Pt production until the eventual depletion of reserves. During periods of low demand the Russian Government supported the alluvial operations by incorporating almost half the production in the minting of Pt coins between 1828 and 1845 (see Section 2.2).

The major alluvial operations in the Ural Mountains were located in the Miass, Bogoslov, Nizhny Tagil, Biser, Goroblagdat, and Issovsk districts. The two principal centres of production were Nizhny Tagil and Blagodatk. Platinum nuggets occurred in the gravels of many streams, and all of the productive streams have serpentinite, peridotite, and/or pyroxenite bedrock in their headwaters. The platinum is associated with iridosmine, iridium, chromite, and some gold, but it is more abundant than the latter. It forms small rounded grains, and rarer larger nuggets that attain several kilograms in weight. The largest Pt nugget ever found (9.624 kg) was recovered from Tagil in 1843.

Many other placer deposits throughout the world have produced minor amounts of Pt and associated PGEs. Alluvium deposits derived from serpentine and gabbro in Borneo have yielded Pt. At the Congo Soco mines in Brazil, Pt occurs in the decomposed schistose rocks associated with Au. The placers of the River Tayaka in New Zealand, which are similar to those in the Urals, contain Os, Ir, and Pt grains derived from peridotite. At the Ruwe gold mine, in the Tanganyika district of Africa, alluvial deposits and certain sandstones carry Au, Pt, and Pd, but so far only the placers are worked. The Tulameen district of British Columbia in Canada has economic concentrations of Pt and chromite. In 1891, the British Columbia authorities supported the exploration of Pt placers with \$10 000, but that amount dwindled to \$3800 by 1895. Platinum associated with Au is also found in the Fraser, Tranquille, Yukon, Saskatchewan, and Chaudiere regions. In the United States of America, Pt derived from serpentinite or peridotite bedrock occurs in small quantities in the Au-bearing districts of northern and central California and in southwestern Oregon. Beach sands in northern California and southern Oregon host Pt and Au. Butte, Humboldt, Siskiyou, Trinity, Calaveras, Sacramento, and Del Norte have been the most productive California counties, with most production derived from bucket-line dredges. The Butte County alone accounted for 75% of the production from California. Platinum has also been mined in limited quantities in Arizona, Colorado, Georgia, and Idaho. Platinum metals were the primary metal mined by dredging for many years in the Goodnews Bay district of Alaska. Approximately 20 t of Pt were recovered from 1928 to 1975.

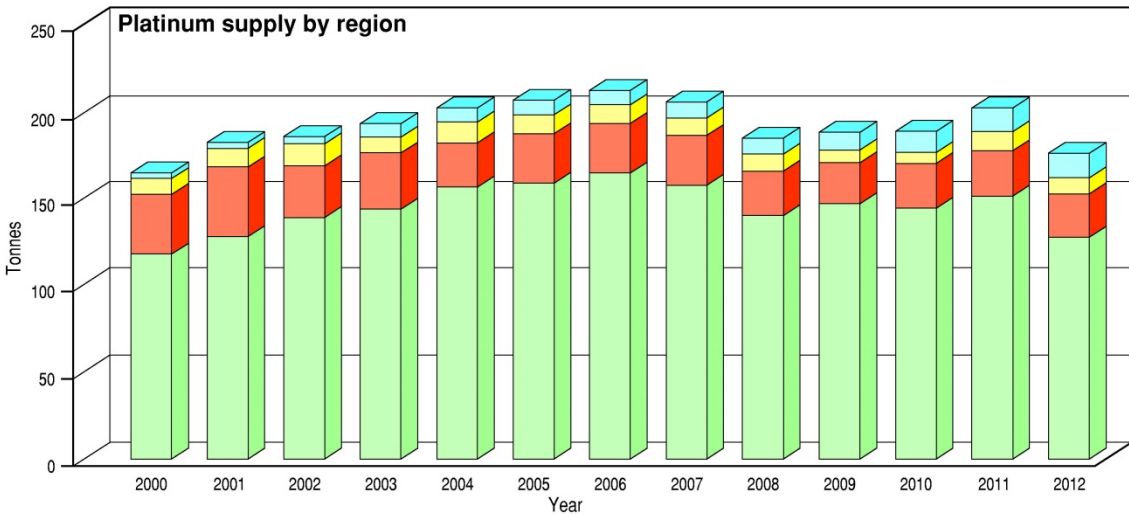
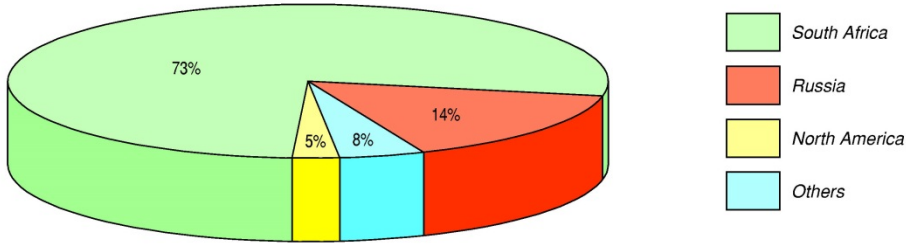
The period of global dominance of alluvial Pt deposits made way for hard-rock sources in Canada, South Africa, and Russia. The next new major source of PGE supplies was from the Sudbury region of Ontario, Canada. Nickel was discovered in mafic igneous rocks at Sudbury in 1856, and the first ores were produced in 1886 (Giblin, 1984). It was several decades later that the PGEs were recognised as an important by-product of the Ni-Cu sulphide ores. Canada was the world's leading producer of PGEs (majority of this from Sudbury) from 1934 to 1955 (Hulbert et al., 1988), and in some years Sudbury contributed 80% of the global Ni market. This global dominance changed with the subsequent discovery of the world's largest Pt deposits in the Bushveld Complex of South Africa, and the Ni- and Pd-rich deposits of Noril'sk in Siberia, Russia.

In 1924, alluvial Pt was found in the Transvaal Province of South Africa by a Lydenburg district farmer and amateur prospector Andries Lombaard. South African-born (German background) geologist Dr Hans Merensky (1871–1952) received an aspirin bottle from Lombaard containing heavy grey-white grains that were later identified as platinum. Following this discovery on what was later to become

known as the eastern limb of the Bushveld Igneous Complex, a mineralised group of rocks was traced with the assistance of Merensky over a distance of more than 160 km towards the north. This package of mineralised ultramafic rocks eventually became known as the Merensky Reef, which contains 75% of the world's known Pt resources. Mining quickly commenced at several locations on the Merensky Reef, and in several other mineralised environments in the Bushveld Igneous Complex. About the same time as the discovery of the Merensky Reef, production of PGEs switched from Pt-dominant alluvials in the Urals to hardrock Ni-Cu mining in the Noril'sk (discovered ~1926) and Talnakh (1960) districts of northern Siberia where Pd is an important by-product of Ni and Cu mining (Naldrett, 2004).

The world's current supply of PGEs is dominated by two countries, South Africa (from the Bushveld Igneous Complex) and Russia (Noril'sk–Talnakh). Significant, but lower amounts of PGEs are also produced by Canada (Sudbury Complex, Lac des Iles), Zimbabwe (Great Dyke of Zimbabwe), and the United States (Stillwater Complex). Other countries, such as Australia, China, Colombo, Finland, Japan, and Poland have in recent years provided very minor amounts of PGEs as by-products of hard-rock Ni-Cu and alluvial Au mining, or from ground stocks that accumulated over many years. Johnson Matthey (<http://www.platinum.matthey.com/publications/market-data-tables/>) has indicated that 178.5 t of Pt and 200 t of Pd were produced in 2013. South Africa (71.8%) dominated this supply of Pt followed by Russia (13.6%), North America (5.5%), and Zimbabwe (6.9%). Platinum in South Africa is largely derived from two famous mineralised layers in the Bushveld Igneous Complex, namely the Merensky Reef and the UG-2 Chromitite. Other important sources of PGEs in the Bushveld include the Platreef and various ultramafic pipes. Most Pd in 2013 was produced by Russia (42.0%) and South Africa (36.6%), with relative minor contributions from North America (14.5%) and Zimbabwe (4.8%). The Ni-Cu-PGE deposits of the Noril'sk-Talnakh region of Siberia are currently the major global producers of Pd. A number of other countries (including Australia) collectively produced relatively minor amounts of Pt (2.2%) and Pd (2.2%). Nearly 91.5% of the world's Rh production of 22.4 t in 2013 came from South Africa (79.9%) and Russia (11.6%). The balance of the Rh comes mainly from Zimbabwe and North America. Figure 1.3 to Figure 1.6 summarise the supply dynamics of Pt, Pd, Ru, Ir and Rh for various source regions for the period 2000 to 2012. World supply and demand statistics for the PGEs, up to and including 2013, are shown in Appendix D. The PGE resources of the major deposits in the world are summarised in Appendix E.

**Platinum supply by region 2012, Total: 175.5 tonnes**



**Platinum demand by application 2012, Total: 250.3 tonnes**

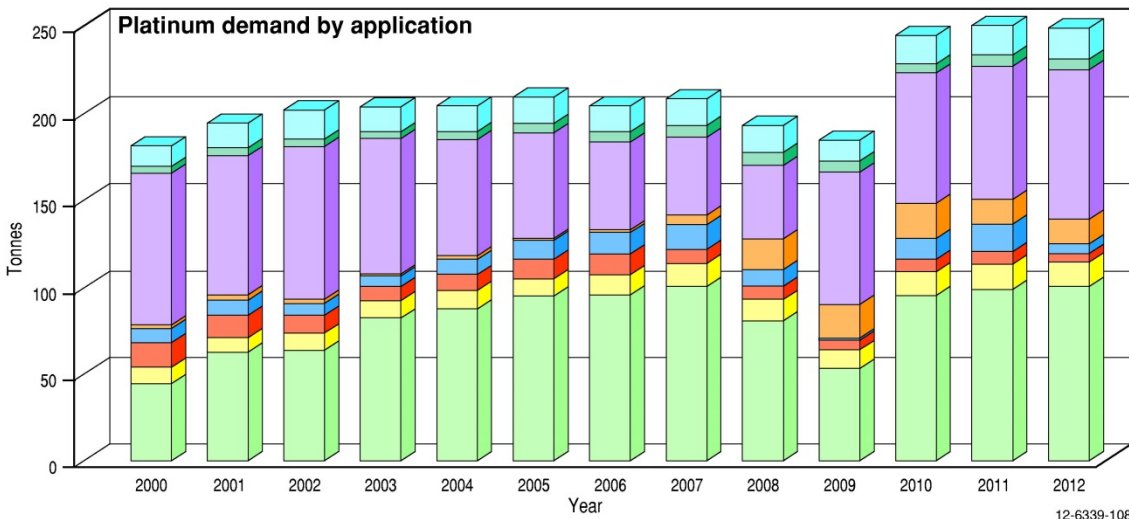
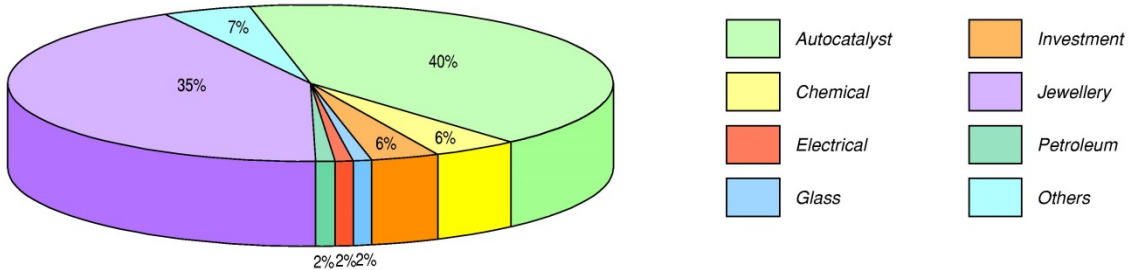
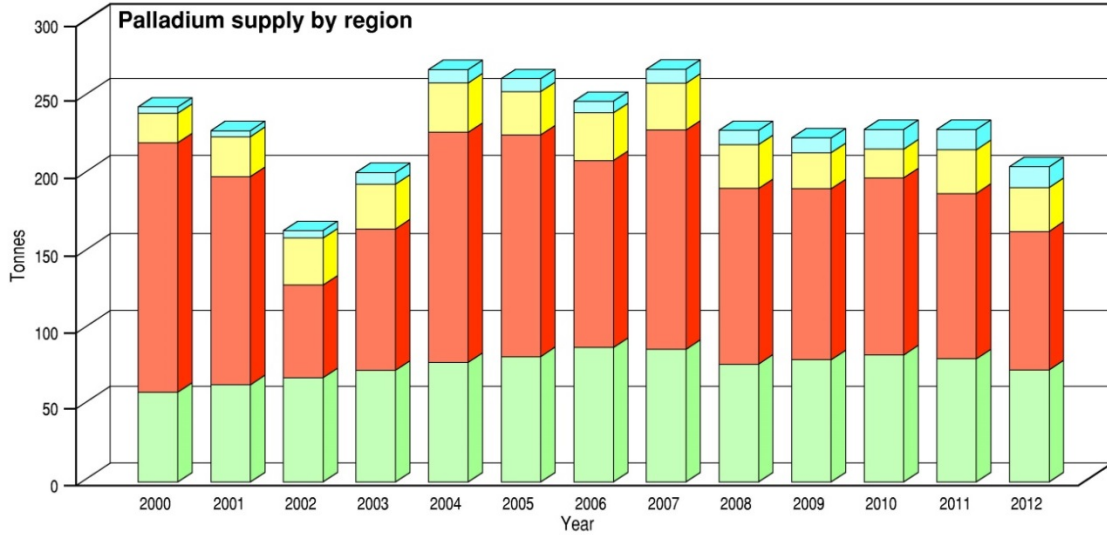
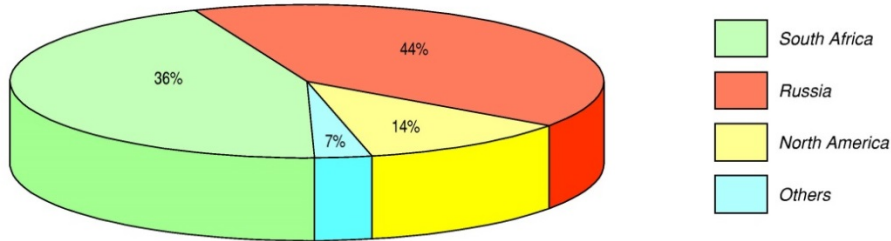


Figure 1.3 Supply and demand data (tonnes) for platinum from 2000 to 2012. Data from Johnson Matthey Market data tables at <http://www.platinum.matthey.com/publications/market-data-tables/>.

**Palladium supply by region 2012, Total: 203.5 tonnes**



**Palladium demand by application 2012, Total: 307.7 tonnes**

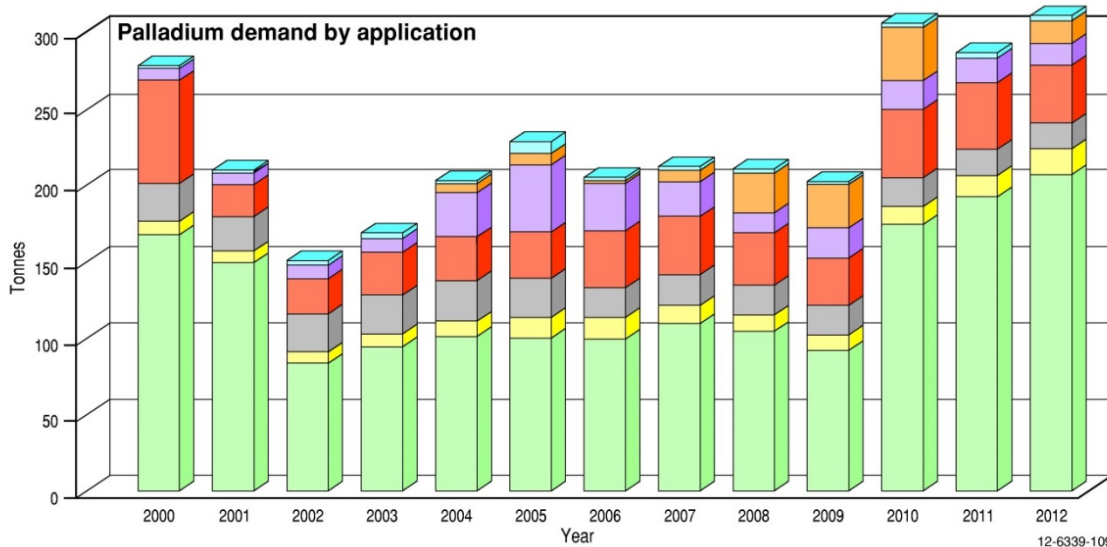
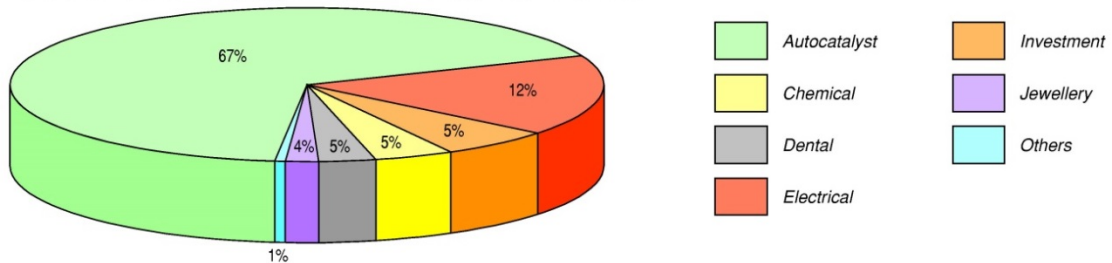
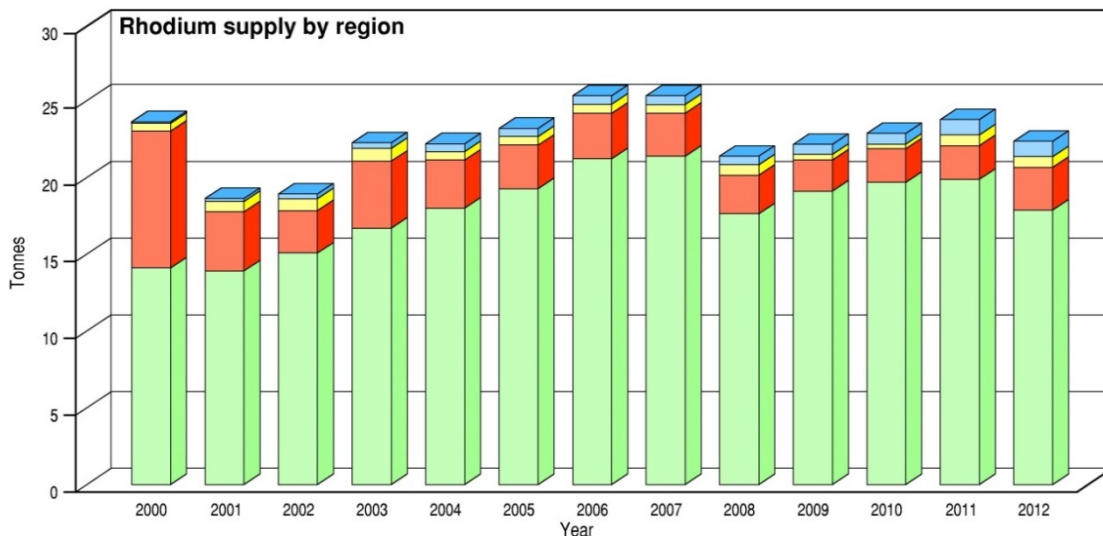
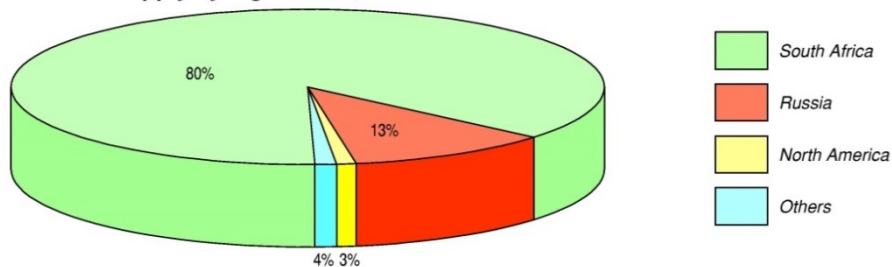


Figure 1.4 Supply and demand data (tonnes) for palladium from 2000 to 2012. Data from Johnson Matthey Market data tables at <http://www.platinum.matthey.com/publications/market-data-tables/>.

**Rhodium supply by region 2012, Total: 22.4 tonnes**



**Rhodium demand by application 2012, Total: 30.1 tonnes**

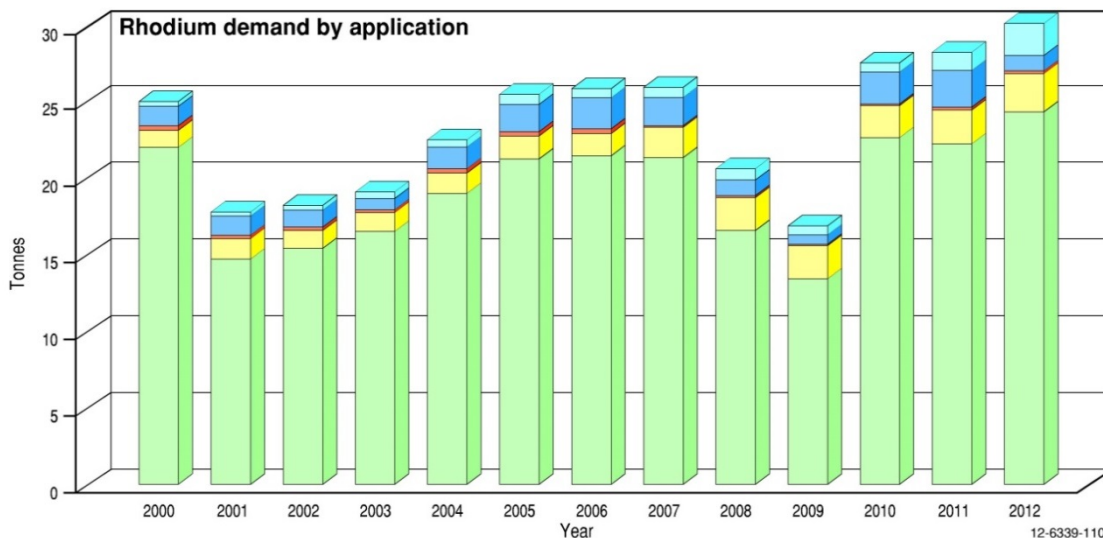
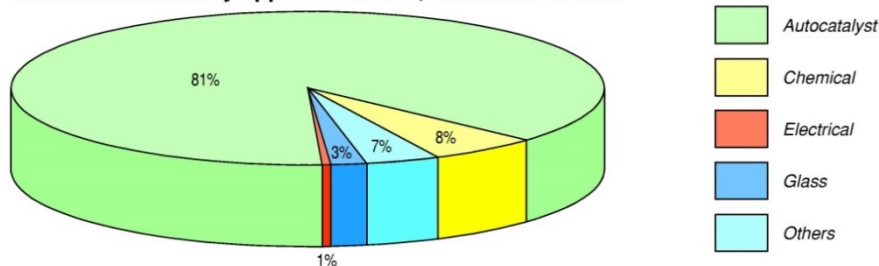
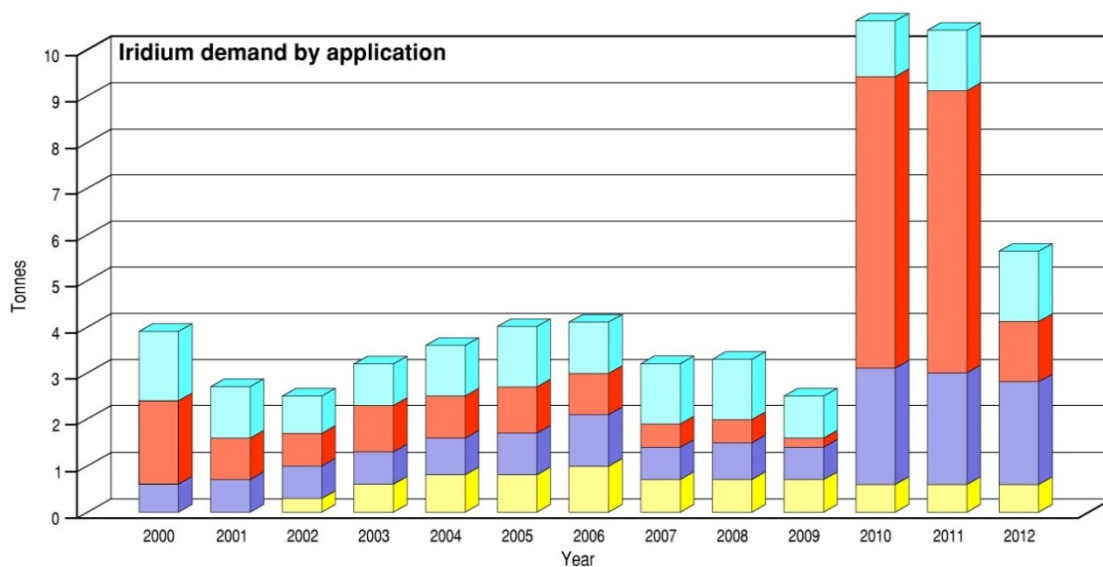
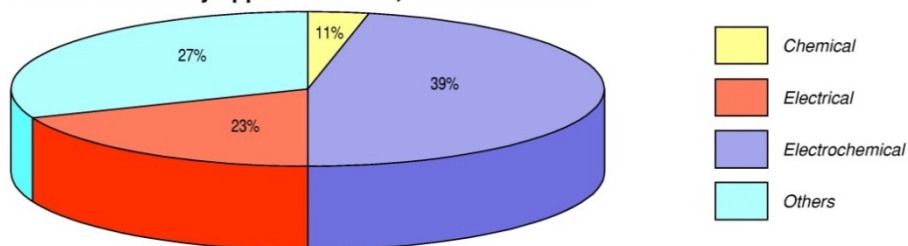
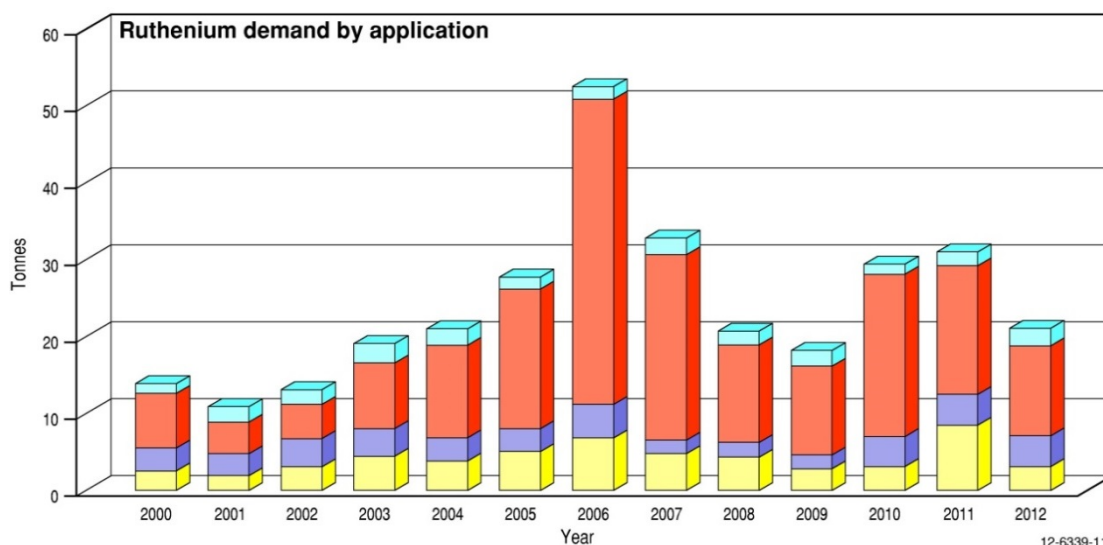
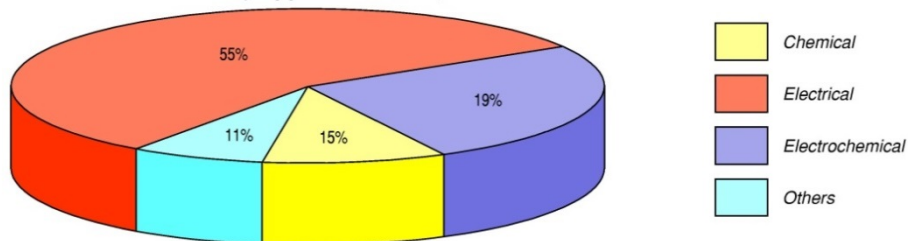


Figure 1.5 Supply and demand data (tonnes) for rhodium from 2000 to 2012. Data from Johnson Matthey Market data tables at <http://www.platinum.matthey.com/publications/market-data-tables/>.

**Iridium demand by application 2012, Total: 5.6 tonnes**



**Ruthenium demand by application 2012, Total: 21.1 tonnes**



12-6339-111

Figure 1.6 Demand data (tonnes) for iridium and ruthenium from 2000 to 2012. Data from Johnson Matthey market data tables at <http://www.platinum.matthey.com/publications/market-data-tables/>.

### 1.3.2 World demand

The diversity of applications and usage rates of the PGEs reflect their many unique chemical and physical properties (see Chapter 4) and the rapid growth needs of developing nations/regions (Europe, Japan, China, North America). Figure 1.3, Figure 1.4, Figure 1.5 and Figure 1.6 summarise the consumption patterns for Pt, Pd, Rh, Ir, and Ru during the period 2000 to 2012. The control of harmful emissions from vehicle exhaust using catalysts is the largest single application for PGEs, in 2013 (see Appendix D) accounting for 57% of gross world demand for Pd, Pt, and Rh combined. The largest industrial use for Pd and Pt has been automotive catalysts with Pd the preferred option for gasoline catalysts and Pt being the preferred metal for diesel-based catalytic systems. The demand for Pd in autocatalysts during 2013 accounted for 216.8 t (72.4%) of the total demand of 299.5 t, and for Pt, the demand was 97.2 t (37.1%) from a total of 261.9 t (Johnson Matthey, 2013a,b). Other minor applications for Pd included electrical (32.8 t: 11%), chemical (16.5 t: 6%), and dental (15.9 t: 5%), whereas jewellery (85.2 t: 33%) was the second most important application for Pt. The demand histograms of Figure 1.3 and Figure 1.4 also highlight the increasing attractiveness of Pt and Pd as investment options (e.g., coinage, bars, exchange traded funds and trusts) since 2007. More than 80% of Rh demand in 2013 was associated with autocatalysts (24.9 t of 31.6 t), whereas Ir demand (total 6.1 t) was dominated by electrochemical (1.8 t: 29.51%) and electrical (1.1 t: 18.0%) applications, and similarly Ru (total 25.8 t) was largely used for electrical (16.5 t: 64.0%) and electrochemical (3.9 t: 15.1%) needs.

Historical global market supply and demand statistics (Johnson Matthey, 2013a,b) for Pt (from 1975), Pd (from 1980), Rh (from 1985), Ir (demand only from 2005), and Ru (demand only from 2005) can be found at <http://www.platinum.matthey.com/publications/market-data-tables/>.

### 1.3.3 Australia's global profile—production, imports, and resources

The first official recorded annual production of PGEs in Australia was ~33 kg of Pt from NSW in 1894 (Appendix F). Mined credits of Pt, Pd, and 'osmiridium' have been recorded for nearly every year since the late 1800s. The production of PGEs has been dominated by Western Australia, followed by Tasmania, New South Wales, and a very minor contribution from Victoria. Despite this almost continuous record of PGE production, Australia has had an insignificant impact on the global supply of these rare metals.

The evolution of Australia's PGE industry is summarised in the production trends of Figure 1.7. Significant contributions of PGEs were provided by New South Wales (Pt), Tasmania (Os), and Western Australia (Pd, Pt) during the periods 1894 to 1913 (Pt), 1910 to 1932 (Os), and from 1970 to the present (Pd and Pt), respectively. Early historical production was dominated by alluvial deposits derived from ultramafic-mafic igneous rocks near Fifield in central New South Wales and from western Tasmania (see Chapter 5). Platinum and Pd production in more recent times has been derived from hard-rock Ni-Cu-sulphide deposits hosted by some of the oldest ultramafic rocks (Archean komatiites) in the Yilgarn Craton of Western Australia.

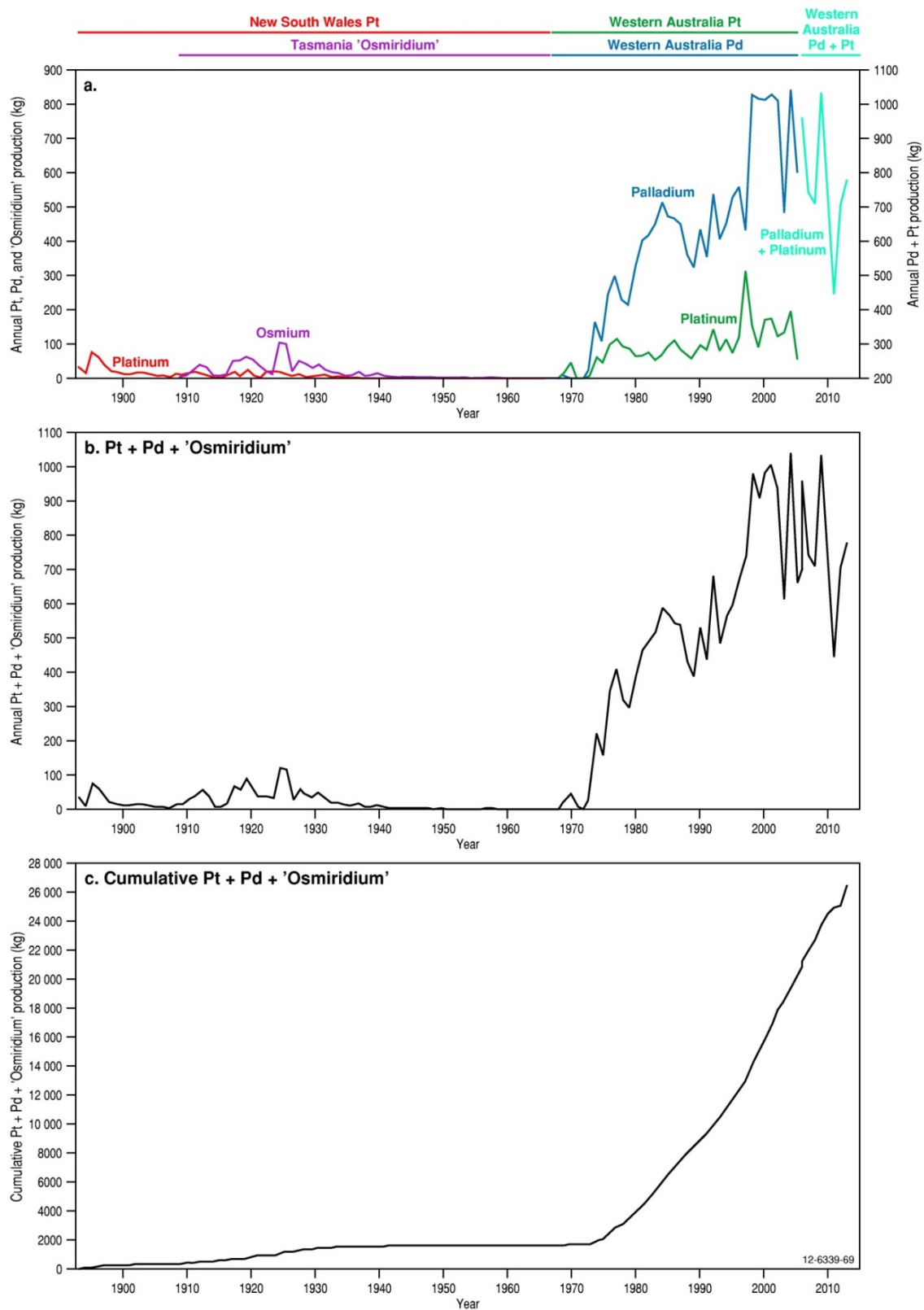


Figure 1.7 History of Australia's PGE production. (a). Platinum, palladium, and 'osmiridium' production (kg) from 1894 to 2013. (b). Total platinum plus palladium plus 'osmiridium' production (kg). (c). Cumulative platinum plus palladium plus 'osmiridium' production (kg). Data from: Geary et al. (1956); Kalix et al. (1966); Government of Western Australia Department of Mines and Petroleum Resource Data Files—Quantity and Value (<http://www.dmp.wa.gov.au/1521.aspx#1591>); Australian Mineral Industry Annual Reviews; pers. comm. D. Flint and P. Abeysinghe (GSWA, 2007, 2012).

Platinum in Australia was first mined in 1893 from the Fifield district of central New South Wales. Most of the ~635 kg of Pt was produced during the first ten years of mining, with intermittent minor production persisting up to the 1960s. Half of Tasmania's 'osmiridium' production of ~970 kg was from Adamsfield, and the balance was largely from the Heazlewood–Bald Hill area near Waratah. With the exception of minor 'osmiridium' produced in 1968 (0.4 kg), records of 'osmiridium' production ceased after 1959. Victoria's early modest production of ~9.6 kg of Pt was as a by-product from the Walhalla Cu mine in 1911 and 1913. Approximately 2.5 kg of Pt was also produced from Victoria in 1971. The hard-rock Ni-Cu-sulphide deposits hosted by Archean komatiitic rocks in the Eastern Goldfields Province of Western Australia have produced ~24 812 kg of Pd and Pt<sup>8</sup> as a by-product of Ni mining from 1969 (commencement of records) to including 2013. Many of the deposits in the Kambalda region are still being mined today after their discovery more than four decades ago to be Australia's major source of PGEs, with 300 kg to 850 kg of Pd and 50 kg to 320 kg of Pt produced annually. In the calendar year 2013, Australia produced 786 kg of Pd and Pt valued at ~\$20.4 million (WA Department of Mines and Petroleum: 2014). This national annual production equates to just ~0.2% of total global supply (379 t of Pt and Pd: Appendix D).

The Bureau of Resources and Energy Economics (BREE) does not include the PGEs in their statistical compilation of twenty-one exported mineral commodities, however, in regard to official national imports, there was 2099 kg of PGEs valued at A\$44 million imported in the 2012–13 financial year, which was down on the 2833 kg and A\$104 million recorded for imported PGEs in 2011–2012 (BREE, 2013). When comparing the national 2012–13 import statistics of PGEs (2099 kg; A\$44 million) with Australia's production statistics (all derived from Western Australia: WA Department of Mines and Petroleum) for the same financial year (658 kg; A\$15 million) it is clear that Australia is missing out on the inherent value of these precious metals in having to rely on significant volumes of imported PGEs to satisfy domestic needs. To emphasise this point, Australia imported 19 247 kg of PGEs valued at A\$717 million during the period 2006–2007 to 2012–2013.

The three mineralised regions of Fifield, western Tasmania, and Kambalda have accounted for more than 99% of Australia's total recorded production of 26 456.3 kg for Pt, Pd, 'osmiridium', and Ru<sup>8</sup> for the period 1894 to 2013, inclusive. Western Australia (24 843.9 kg Pt+Pd+Ru) has dominated PGE production followed by Tasmania (966.8 kg 'osmiridium'), New South Wales (633.5 kg Pt), and Victoria (12.1 kg Pt). The annual PGE production statistics for the state jurisdictions since 1894 are summarised in Appendix F and Figure 1.7 Geary et al. (1956) indicate that the actual production of Pt and 'osmiridium' during the early stages of the PGE industry would be significantly greater than the recorded figures as they mainly represent sales. Production statistics of Pt were not recorded before 1894, and not before 1910 in the case of 'osmiridium'. It is known that both these metals were sold to private buyers prior to these dates.

Australia's Economic Demonstrated Resources (EDR: see Appendix G for definitions) of PGEs remained unchanged at 4.7 t in 2012 (AIMR, 2013). Western Australia and the Northern Territory hold all of Australia's resources of EDR, but additional EDR in other states may be established if deposits currently being assessed become viable. Total Identified Resources of PGEs (EDR plus Subeconomic and Inferred Resources) total about 276 t. Of this amount, PGE-dominant deposits account for about 51%. The United States Geological Survey (USGS, 2014) state the global reserves of PGEs (Pt and Pd) were estimated at 66 000 t in 2013, with South Africa having by far the largest reserves with 63 000 t (~95%), followed by Russia with 1100 t (~1.7%), 900 t (~1.4%) for the USA, 310 t (0.5%) for Canada, and 800 t (1.2%) for the 'Other countries'. The USGS also assert in 2013, that the world

---

<sup>8</sup> The only documented production of Ru in Australia was 32 kg from the Kambalda region during the period 1886 to 1979.

resources of PGEs in mineral concentrations that can be mined economically are estimated to total more than 100 000 t. Australia's PGE endowment is insignificant when compared with the global PGE reserve base. Australia's status on the global stage is put into perspective when one considers that the three largest hard-rock PGE deposits of Nebo-Babel (70.6 t of global resources), Panton (65.6 t), and Munni Munni (63.7 t), that dominate Australia's PGE resources, but have not been mined, have a collective global metal resource of ~200 t of PGEs. With respect to the global PGE reserve base of 66 000 t as defined by the USGS above, the PGE endowment of Australia's three largest deposits represents only ~0.3% of the global reserve base.

Statistics on world PGEs supply from government and commercial online databases need to be interpreted with caution because of differences between national primary production, secondary production, and national sales. Countries such as Great Britain, Japan, and Switzerland refine and sell, but do not mine PGEs, while the sales of PGEs recovered from secondary scrap of previously imported PGEs also affects the figures. Additionally, there is little published information on production rates from the Soviet Union and South Africa, and much of the supply information must be gathered from traders and consuming industries (e.g., Johnson Matthey <http://www.platinum.matthey.com/publications/market-data-tables/>).

### 1.3.4 Metal prices

Platinum and Pd show flat price trends for the first half of the 20<sup>th</sup> century, with their prices generally within the range US\$20/troy ounce to US\$50/troy ounce and displaying insignificant annual fluctuations. During this period, these metals were largely used as catalysts for reactions involving acids, and Rh, Ru, Os, and Ir had limited applications in the chemical industry (see Chapter 4). However, from the 1970s onwards, the precious metal prices significantly increased and showed dramatic price fluctuations over short periods of time (Figure 1.8). The major driver for this rapid market growth was the increase in diversification of PGE applications for various emerging industries (e.g., autocatalysts, fuel cells, computer hard disks) and cultural developments (e.g., investment, jewellery).

Such application milestones and their impacts on PGE prices (US\$/troy ounce) since 1970 are summarised in Figure 1.9. This market growth was regularly stimulated by a number of different events, such as boom phases in the minerals and petroleum industries, technological developments, marketing opportunities, and changing environmental legislations. For example, one of the first major drivers for the market growth of Pt was the oil boom in the 1950s and the development of the petroleum refining industry. The PGEs became strategically important metals for catalytic processes in the expanding petroleum industry. In the 1960s, Pt growth was stimulated by a successful diamond jewellery promotion in Japan by De Beers. Another marketing opportunity for Pt jewellery was also created in Japan when the government restricted the private ownership of Au. The introduction of the United States Federal Clean Air Act in 1968 prolonged the growth surge of Pt, Rh, and Pd. This Act, which introduced legislation to restrict noxious gases emanating from vehicles, created a major new market for catalytic converters that today dominate the global demands for these precious metals. The general positive outlook for PGEs relative to most other metals, coupled with the perception that supplies from the dominant producing countries (South Africa, Russia) may be subject to disruption for political reasons also stimulated PGE markets and exploration in the 1970 and 1980s. In the early 1990s, Japan's booming economy provided sustained impetus to the Pt jewellery market to new record levels with at least 13 years of successive growth. Similarly, demand for Pt in jewellery during this period experienced a spectacular rise in China—today the world's biggest single market for Pt

jewellery. This phase of growth was joined by the rapidly expanding electronics and IT industries where Pd, Ru, and Pt are used in many high-technological components, e.g., computer hard-disk drive coatings, chip resistors, capacitors, integrated circuits, and fibre optic cables, etc. It is estimated that the IT industries alone increased the usage of PGEs by as much as 1000% during the 1990s. In more recent times, record prices of Ru (in 2007), Pt (2008), and Rh (2008) have been largely driven by the European diesel boom in the automotive sector and rapidly increasing consumer needs (e.g., jewellery, industrial, and investment) in emerging economies such as China and India.

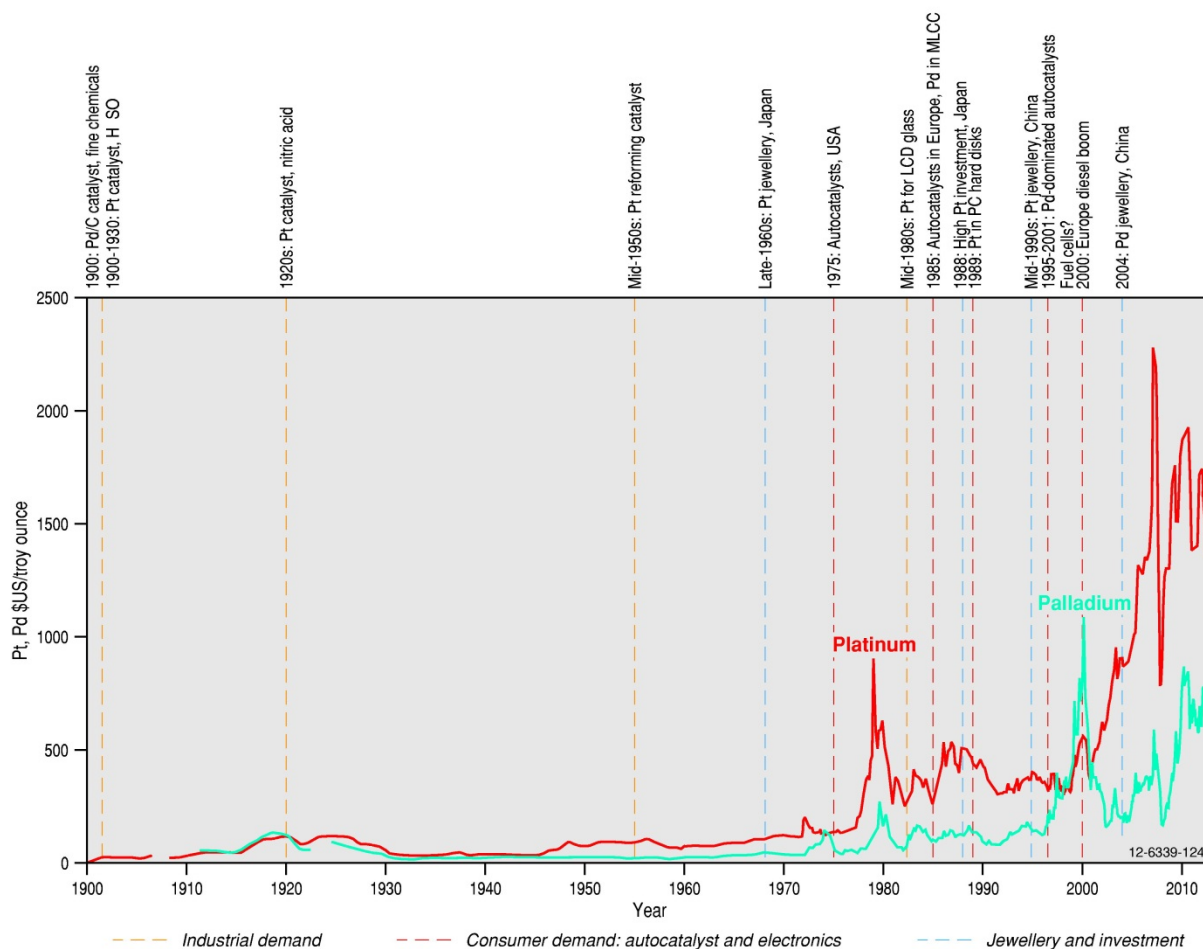


Figure 1.8 Impacts of application milestones with platinum and palladium prices from 1900 to 2013. The metal price trends for all PGEs from 1970 are shown in Figure 1.9. Modified from Butler (2012). Metal price data from Johnson Matthey at <http://www.platinum.matthey.com/prices/price-tables>; BASF(2014); and the USGS (2014).

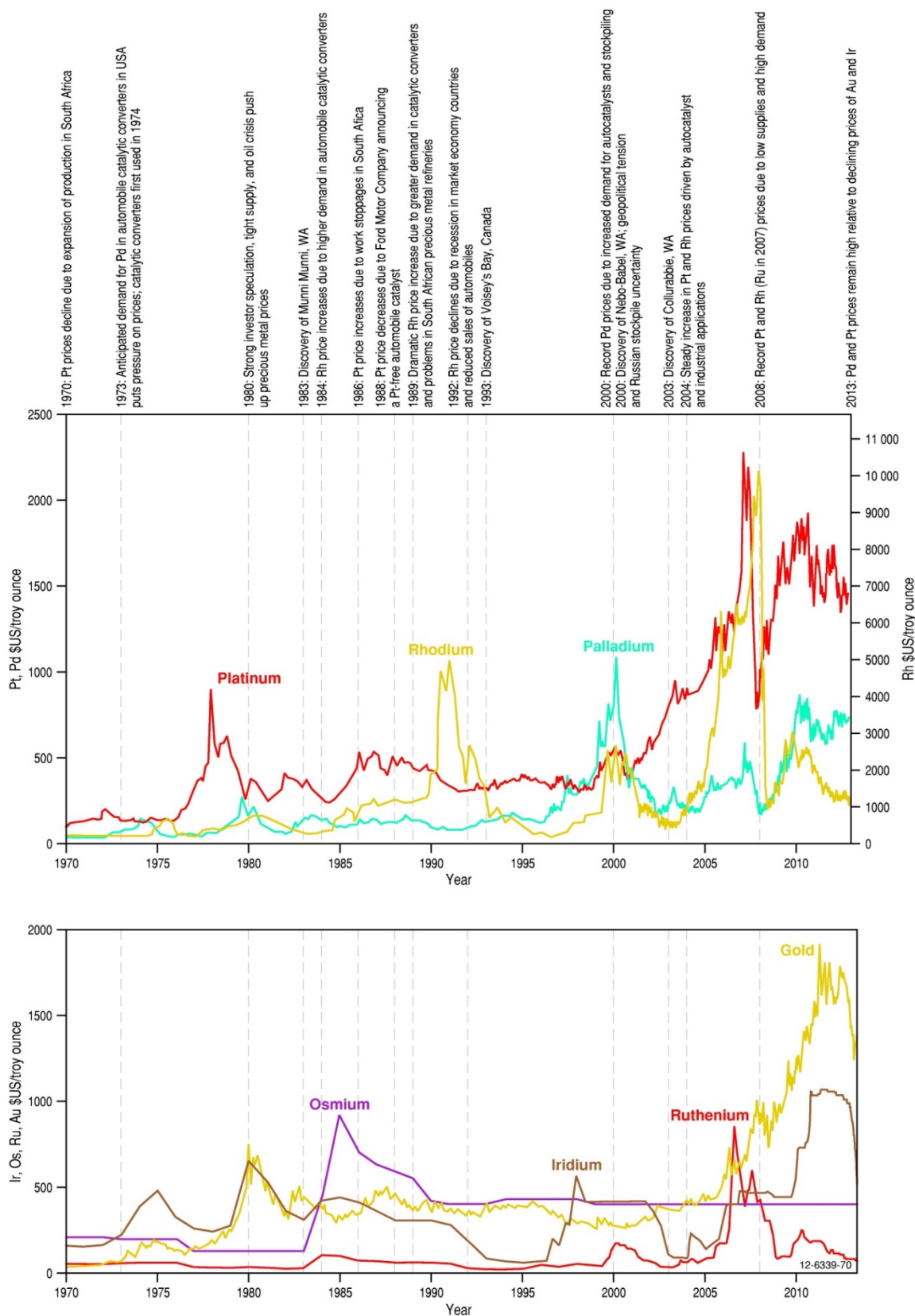


Figure 1.9 Impacts of application milestones and deposit discoveries with PGE prices from 1970 to 2013. Metal price data from Johnson Matthey at <http://www.platinum.matthey.com/prices/price-tables>; and BASF (2014).

Platinum and Pd prices (Figure 1.9) display protracted periods (years to several years) of generally upward price shifts that abruptly become terminated by dramatic price falls over short periods of time (e.g., Pt from ~1999 to ~2008). The final phase movement to the maximum metal price for each cycle is usually rapid, occurring over a few months duration. Peak metal prices tend to have a cyclic frequency of about ten years, with major price highs occurring at ~1980 (Ir), ~1985 (Os), ~1991 (Rh), ~2000 (Pd, Rh, and Ru), ~2007 (Ru), and ~2008 (Pt, Rh, and Pd). The cyclic growth and price volatility trends of Pt and Pd are attributed to sensitive imbalances between supply and demand, speculation, metal substitution, small size of market activities especially for the minor PGEs, and political instability of the major producing countries (South Africa, Russia). The market forces behind Ru, Rh, Os, and Ir are poorly constrained because of their minor production and consumption levels in comparison to Pt and Pd. The volatility of their prices may, in part, reflect the inelastic supply (dependent on the production of other metals) versus an elastic demand (periodic purchases for stockpiles and/or consumption in new applications).

Historically, Pt and Au prices have displayed a strong positive correlation with each other, although some short-term price reversals are evident during the past four decades. An example of this is a major divergence in the price of Pt relative to Au from around 1999. Prior to this year, both these metals were for most times close to, or at, price parity. However, after 1999 the price of Pt rapidly increased over the next nine years and outstripped the steadily increasing price of Au due to its escalating use in autocatalysts and jewellery. These diverging metal price trends have continued to present times, and the daily historical record price for Pt (US\$2278/troy ounce) reached on the 4<sup>th</sup> of May 2008 was more than twice than that for Au. The most expensive PGE, Rh, and its poorer relative Pd, show moderate correlations with the price trends of Pt and Au. Their trends feature two major price spikes near 1990 and 2000 that are largely attributed to the increased use of these precious metals in catalysts for the automobile industry. The price movements of the other less important PGEs, Os, Ir, and Ru display more independent and irregular trends. Their weak mutual correlations indicate they have vastly different supply, demand, and marketing systematics compared to each other and the other PGEs Pt, Pd, and Rh.

In regard to the Australian PGE industry, the impacts of historical phases of erratic PGE metal prices are exacerbated for aspiring Australian producers by the added volatility of the US\$/A\$ exchange rate. Ideal market conditions for the Australian PGE industry occur when the A\$ is low with respect to the \$US and when PGE prices are high (Moek et al., 2009).

## 1.4 Are the platinum-group elements of global critical importance?

Section 1.1 of this chapter describes the PGEs as a group of six precious metals that have unique physical and chemical characteristics (see Chapter 4) and the potential to contribute to the wellbeing of humans over a long time. Understanding the likelihood of disruptive fluctuations in the supply of such important metals as the PGEs for domestic applications, and making decisions about policies to reduce such disruptions, requires a thorough understanding of national and international mineral sources, mineral production technology, supply-demand dynamics, sustainability and recycling, market drivers, and potential impediments to the supply of PGEs<sup>9</sup>. It is therefore important to determine if the PGEs compared to the other elements of interest to mankind are critical commodities of global importance. The issue of criticality in the context of the PGEs will now be discussed.

---

<sup>9</sup> Most of these themes are outside the scope of this report, however, the reader can obtain details from Sehart and Grehl (2012) and McDonald and Hunt (1982).

What is a critical mineral or critical commodity? The United States National Academy of Sciences proposed in 2008 that *'a mineral can be regarded as critical only if it performs an essential function for which few or no satisfactory substitutes exist'*, and *'in addition, a mineral can be regarded as critical only if an assessment also indicates a high probability that its supply may become restricted, leading either to physical unavailability or to significantly higher prices for that mineral in key applications.'* The European Commission in 2010 stated: *'a raw material is labelled critical when the risks of supply shortage and their impacts on the economy are higher than for most of the other raw materials.'* Skirrow et al. (2013) stated that *'..... in essence a commodity is critical if it is both economically important and has high risk of supply disruption. These supply risks originate from four main causes: (1) scarcity of the commodity; (2) diversity and stability of supply; (3) production only as a by-product of other commodities; and (4) level of concentration of commodity production and processing within particular countries or by particular companies. The scarcity of a commodity may be determined by such factors as the geological abundance within the Earth; economics of extraction of the commodity; the extent of substitution of one material by another; and the extent of recycling. Criticality can also often change over time.'*

Three key studies with different methodologies have attempted to quantify the relative global importance of potential critical commodities, such as the PGEs. These are:

1. In 2010, the European Commission study 'Critical raw materials for the EU' (European Commission, 2010) recognised 14 raw mineral materials from 41 minerals and metals analysed, as critical to European industry (Figure 1.10a). The European Commission study used a methodology based on criticality, designed to account for the supply risk and the economic importance of each mineral and metal considered.
2. A two-year long study by the United States National Academy of Sciences ('Minerals, Critical Minerals, and the U.S. Economy', United States National Academy of Sciences, 2008) identified those minerals and metals considered critical, i.e., which ones were the bases of technologies that could not be actualised as practical devices without them, and also determined criteria for assessing the impacts of the interruption of their supply on United States industries and the general economy (Figure 1.10b).
3. A study by Geoscience Australia in 2013 ('Critical commodities for a high-tech world: Australia's potential to supply global demand', Skirrow et al., 2013) examined critical commodities from an Australian perspective and presented comprehensive geological information on Australia's resources and resource potential for these critical commodities (Figure 1.10c). Based upon a compilation of reports defining commodities considered critical by Australia's major trading partners (United Kingdom, Europe, USA, Japan, and Korea), a suite of commodities were identified that can be considered critical. Two major groups of commodities were identified: those with category one resource potential and those with category two resource potential. The different categories of resource potential were based on level of criticality; Australia's resources and potential for new discoveries; market size; and growth outlook.

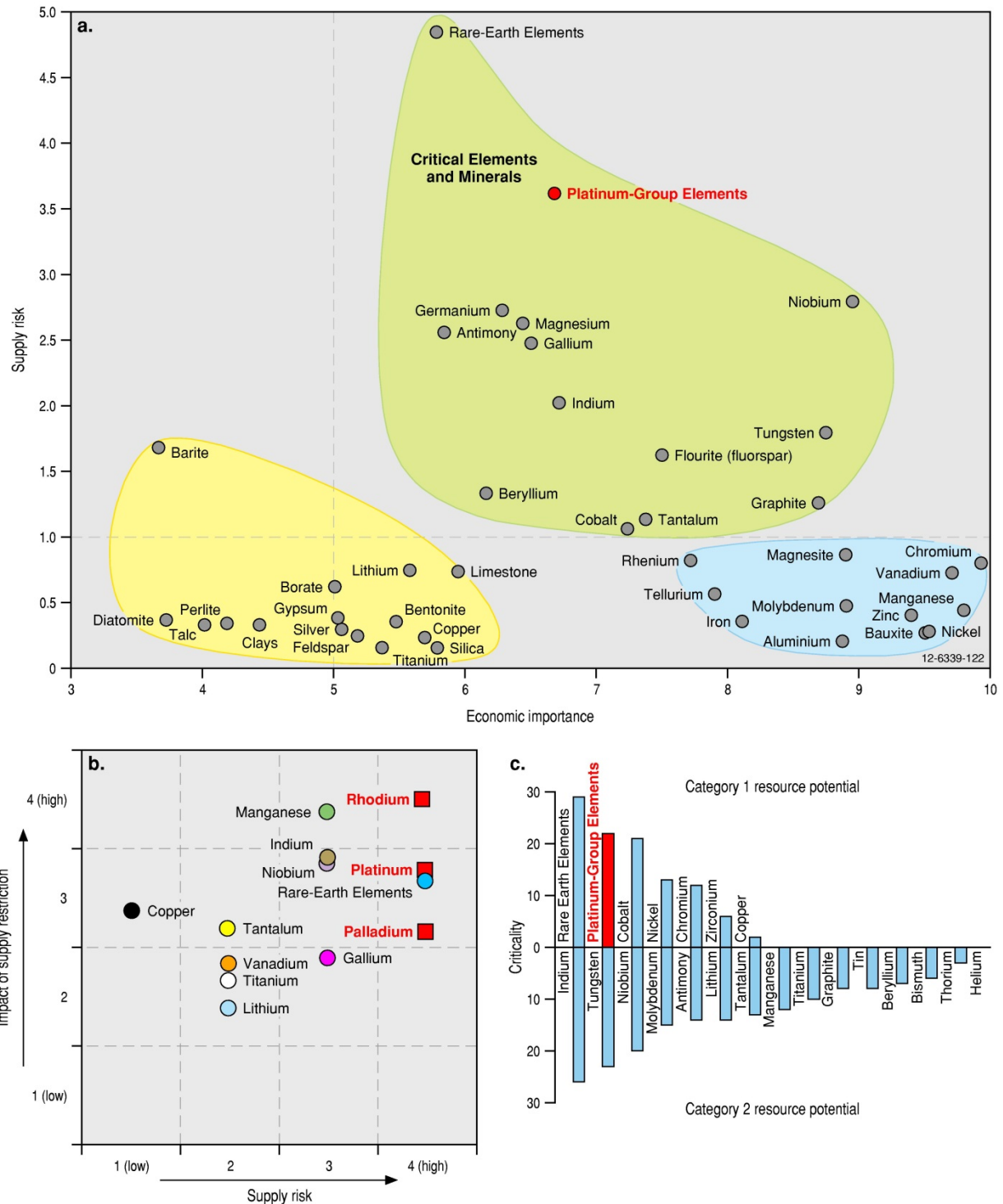


Figure 1.10 Three international organisations have used different methodologies in an attempt to quantify the relative global importance of potential critical commodities, such as the platinum-group elements (highlighted in red font). (a). European Commission (2010) 'Critical raw materials for the EU study' (European Commission, 2010). (b). United States National Academy of Sciences (2008) 'Minerals, Critical Minerals, and the U.S. Economy study' (United States National Academy of Sciences, 2008). (c). Geoscience Australia (Skirrow et al., 2013) 'Critical commodities for a high-tech world: Australia's potential to supply global demand study.'

The results of the three critical commodity studies are shown in Figure 1.10. The first two studies by the European Commission (Figure 1.10a) and the United States National Academy of Sciences (Figure 1.10b) developed concepts of criticality involving two-dimensional matrices which highlight the combinations of economic importance, impact of supply restriction, and availability or supply risk of the material in question. The key results from the Australian study are presented in a dual histogram (Figure 1.10c) summarising category one and category two resource potential assessments.

In regard to the European findings (Figure 1.10a), the PGEs are considered overall the second most critical elements that were investigated, having the second-highest supply risk ratings (to the REEs), and moderate ratings for economic importance. The United States criticality matrix (Figure 1.10b) shows that Rh has the highest impact of supply restriction rating (4) of all commodities studied and the equal highest supply risk rating (4). The other two PGEs assessed—Pt and Pd—have similar high ratings (4 and 3) for both axes variables. Consistent with these findings, the Australian-based study (Figure 1.10c) also nominated the PGEs with the second highest criticality rating (22) in the category one resource potential group. Only the REEs recorded a higher criticality rating (29) in this high-priority group.

In summary, all three independent criticality studies that used different methodologies identified the PGEs as having critical commodity status. In some assessments, Rh scored the highest ratings for impact of supply restriction and supply of all elements—metals studied, closely followed by Pt, Pd, and the REEs.

## 1.5 Aims and sources of information

The Australian continent contains a wide variety of igneous, sedimentary, and metamorphic rock types that record an almost continuous geological evolution of the Earth from the Hadean (~4600 Ma to 4000 Ma) times to the present. The antiquity of this continent is indicated by the ages of small zircon grains found in rocks from the granite-greenstone cratonic areas of Western Australia. The ages are from leucogabbro and meta-anorthosite inclusions and detrital zircons in quartzite from the Jack Hills region of the Manfred Complex in the Narryer Terrane, Yilgarn Craton, Western Australia. The rock inclusions have U-Pb zircon ages ranging up to 3730 million years—the oldest known rocks in Australia, and the detrital zircons record Hadean ages of up to 4404 million years—the oldest terrestrial material known on Earth (Froude et al., 1983; Kinny et al., 1988, 1990; Wilde et al., 2001; Wilde and Spaggiari, 2007). The Hadean age of the zircons has been confirmed by conventional radioactive decay of uranium to lead techniques, and also more recently by atom-probe tomography (Valley et al., 2014; Sydney Morning Herald, 2014).

Such ancient Precambrian and younger Phanerozoic rocks in Australia contain abundant and diverse mineral deposits that in some cases are of world-class importance. The largest deposits contain vast resources of Fe, coal, bauxite, Au, Cu, Pb, Zn, Ni, rutile, zircon, and the REEs that are of immense significance to the nation's economic and social development. The Bureau of Resources and Energy Economics have stated that income from all mineral and energy exports in 2012–13 was valued at A\$176 billion, which equates to 71% of the value of all Australia's merchandise exports (BREE, 2013). Iron ore, black coal, and Au are the leading export earners, and collectively they accounted for ~67% of Australia's mineral and energy export income. The PGEs are not included in the compilation of twenty-one exported mineral commodities.

Despite many phases of intensive exploration during the past four decades and the discovery of many PGE occurrences, no economic concentrations of PGEs (as the dominant commodities) have yet to be found in Australia. This is in contrast to the discovery rates during the early stages of the Australian PGE industry when many small-scale alluvial and hard-rock deposits of Pt and 'osmiridium' were readily found and mined in the eastern states of the continent. More than seventy years have elapsed since the last major PGE deposits (alluvial 'osmiridium' deposits in western Tasmania) were mined in Australia.

Many high-profile PGE and Ni-PGE prospects have been identified in the older crustal provinces of Western Australia. These prospects generally occur in Precambrian layered mafic-ultramafic intrusions (Eastman Bore, Jimberlana, Lamboo, Munni Munni, Narndee, Nebo-Babel–Giles Complex, Nova, Panton, Radio Hill, Savannah, Windimurra) and the PGEs are associated with Cr, Ni, Cu, and minor Au. Most of the prospects have experienced multiple phases of exploration during periods of favourable metal prices and 'indicated resources' have been defined in most cases. Although some of these prospects contain nationally-significant tonnages (~10 Mt to ~70 Mt) of PGE ores, their subeconomic status was largely determined by low grades, metallurgical complications, and/or various remoteness-logistical issues. Other different styles of PGE mineralisation that have also been investigated include hydrothermal (Broken Hill region, Coronation Hill), komatiite-associated (Kambalda district, The Horn, Waterloo), sedimentary-hosted (?Camel Bore), magnetite-hosted (Jameson Range: Haran–Canaan–Zen, Attutra: Casper–Coco), and laterite (Syerston, Owendale, Yarawindah Brook). The economic viability of these deposits is often hindered by erratic grades and low-tonnage status.

The two major aims of this report are to:

1. Provide an up-to-date and comprehensive compilation of all PGE occurrences in Australia. Many new occurrences and styles of PGE mineralisation have been documented since the last major national PGE compilation by Hoatson and Glaser (1989). Less than 70 occurrences of PGEs were described by those authors, whereas two decades later this inventory has increased to over 500 entries.
2. Introduce a minerals-system approach for assessing the prospectivity and resource potential of PGEs in Australia, and to minimise exploration risk in greenfields environments (particularly those under shallow cover).

Australia has favourable geological elements (e.g., all geological time periods represented, diverse geotectonic settings, rock types, and erosional regimes) for the formation and preservation of significant PGE deposit(s). The presence of many PGE occurrences in a variety of geological settings throughout the continent (see Chapter 6) indicates that fertile mineralising systems were active in many geological provinces over geological time. Australia boasts several world-class<sup>10</sup> deposits of Ni sulphides (Kambalda, Mount Keith, Yakabindie, Nebo-Babel) associated with mafic and ultramafic rocks—several of which contain significant by-product concentrations of PGEs—however, the continent is clearly under-represented with significant PGE and chromite deposits. The rarity of world-class PGE deposits is also seen at a global scale with only one such deposit (or groups of similar deposits) usually occurring in any particular nation or continent (e.g., South Africa–Bushveld; Russia–Noril'sk; Canada–Sudbury; Zimbabwe–Great Dyke; USA–Stillwater). The large number of PGE occurrences documented in Australia (see Appendix K), the vast volumes of mafic-ultramafic rocks in Precambrian provinces (Yilgarn, Pilbara, and Gawler cratons, Musgrave, Halls Creek, and Albany-Fraser orogens: Hoatson et al., 2006), and the recent recognition of Large Igneous Provinces

---

<sup>10</sup> Containing more than 1 million tonnes of Ni metal.

(LIPs, Warakurna, Kalkarindji, Hart, Gairdner: Pirajno and Hoatson, 2012) indicates Australia is prospective for a world class PGE deposit. Such a deposit could be under cover and its discovery may be dependent on smart science, cutting-edge geophysical, geochemical-isotopic, and deep-drilling techniques, and as often associated with the discovery of many mineral deposits, possibly an element of serendipity is involved. It is hoped that this review will reduce exploration risk in finding such a deposit.

Sources of information used in this review include (those entries indicated with an \* are inaccessible to the general public):

- MINLOC\* (Geoscience Australia's national database of mineral occurrences)
- OZMIN\* (Geoscience Australia's national database of mineral deposits and resources)
- Australian Mines Atlas (Geoscience Australia's national database of Australian minerals and energy deposits, mines, resources, and processing centres (<http://www.australianminesatlas.gov.au/>))
- Intierra's Resource Intelligence proprietary database for latest company reports (<http://www.intierra.com/Homepage.aspx>)
- Various geoscience websites at the Geoscience Portal (<http://www.geoscience.gov.au/>) which show the State, Territory, and Australian Government digital databases including:
  - Western Australia—MINEDEX (<http://www.dmp.wa.gov.au/3959.aspx>) mineral resources, and WAMEX (<http://www.dmp.wa.gov.au/3959.aspx>) company mineral exploration report databases
  - Tasmania—Mineral Resources Tasmania database; spatial and documentary (<http://www.mrt.tas.gov.au/portal/database-searches?inheritRedirect=true>)
  - New South Wales—DIGS (<http://digsopen.minerals.nsw.gov.au/>) documentary database
  - South Australia—SARIG database (<http://www.minerals.dmitre.sa.gov.au/sarighelp/home/>)
  - Victoria—GEOVIC database (<http://www.energyandresources.vic.gov.au/earth-resources/maps-reports-and-data/geovic>)
  - Queensland—interactive resource and tenure map site (<https://webgis.dme.qld.gov.au/webgis/webqmin/Run.htm>)
  - Northern Territory—STRIKE interactive map website ([http://geoscience.nt.gov.au/GeosambaU/strike\\_gs\\_webclient/default.aspx](http://geoscience.nt.gov.au/GeosambaU/strike_gs_webclient/default.aspx)) and various document search databases ([http://www.nt.gov.au/d/Minerals\\_Energy/Geoscience/](http://www.nt.gov.au/d/Minerals_Energy/Geoscience/))
- Company websites
- Australian Securities Exchange (ASX) company reports (<http://www.asx.com.au/>)
- 1:250 000 and 1:100 000 geological maps and associated explanatory notes available through State, Territory, and Australian Government geoscience agencies at the Geoscience Portal (see above)
- Annual historical and current PGE production data for Australia: Geary et al. (1956); Kalix et al. (1966); Government of Western Australia Department of Mines and Petroleum Resource Data Files—Quantity and Value (<http://www.dmp.wa.gov.au/1521.aspx#1591>); Australian Mineral Industry Annual Reviews

Relevant national and province reviews:

- Hoatson, D.M., 1984. Potential for platinum group mineralisation in Australia. A review. Bureau of Mineral Resources Australia, Record 1984/1, 84 pp.
- Marston, R.J., 1984. Nickel mineralization in Western Australia. Geological Survey of Western Australia, Mineral Resources Bulletin 14, 271 pp.
- Hoatson, D.M. and Glaser, L.M., 1989. Geology and economics of platinum-group metals in Australia. Bureau of Mineral Resources, Australia, Resource Report 5, 81 pp.
- Hoatson, D.M., 1990. Platinum group element mineralisation and potential in Australia. In: Hughes, F.E. (editor), *Geology of Mineral Deposits of Australia and Papua New Guinea*. Australasian Institute of Mining & Metallurgy, Melbourne, Monograph 14, 85–98.
- Hoatson, D.M., Wallace, D.A., Sun, S-S., Macias, L.F., Simpson, C.J. and Keays, R.R., 1992. Petrology and platinum-group-element geochemistry of Archaean layered mafic-ultramafic intrusions, west Pilbara Block, Western Australia. Australian Geological Survey Organisation Bulletin 242, 320 pp.
- Hoatson, D.M., 1998. Platinum-group element mineralisation in Australian Precambrian layered mafic-ultramafic intrusions. Special Jubilee Issue of Australian Geological Survey Organisation Journal of Australian Geology, Geophysics, 17(4), 139–151.
- Hoatson, D.M. and Blake, D.H. (editors), 2000. Geology and economic potential of the Palaeoproterozoic layered mafic-ultramafic intrusions in the East Kimberley, Western Australia. Australian Geological Survey Organisation Bulletin 246, 476 pp.
- Barnes, S.J. (editor), 2006. Nickel Deposits of the Yilgarn Craton: Geology, Geochemistry, and Geophysics Applied to Exploration. Economic Geology Special Publication Number 13, 210 pp.
- Hoatson, D.M., Jaireth, S. and Jaques, A.L., 2006. Nickel sulfide deposits in Australia: Characteristics, resources, and potential. *Ore Geology Reviews*, 29, 177–241.
- Koek, M., Kreuzer, O.P., Maier, W.D., Porwal, A.K., Thompson, M. and Guj, P., 2010. A review of the PGM industry, deposit models and exploration practices: Implications for Australia's PGM potential. *Resources Policy*, 35, 20–35.
- Pirajno, F. and Hoatson, D.M., 2012. A review of Australia's Large Igneous Provinces and associated mineral systems: Implications for mantle dynamics through geological time. *Ore Geology Reviews*, 48, 2–54.
- Thorne, J.P., Cooper, M., Claoué-Long, J.C., Hight, L., Hoatson, D.M., Jaireth, S., Huston, D.L. & Gallagher, R., 2014. Guide to Using the Australian Mafic-Ultramafic Magmatic Events GIS Dataset. Record 2014/039. Geoscience Australia, Canberra. [http://www.ga.gov.au/metadata-gateway/metadata/record/gcat\\_78742](http://www.ga.gov.au/metadata-gateway/metadata/record/gcat_78742).

Appendix H is a compilation of websites that provides information about the global aspects of the PGEs, namely historical and current production data, metal prices, supply and demand statistics, naming of PGMs, and government organisations involved with the research of PGEs, etc.

## 1.6 Other reviews of platinum-group elements in Australia

Many occurrences of PGEs have been documented throughout Australia since their first discovery in New South Wales in 1851 (see Chapter 5). Despite the protracted history of the Australian PGE industry, there have been very few comprehensive reviews that describe the distribution and geological settings of these precious metals. The earliest such reviews were state geological bulletins

and reports of significant and newsworthy discoveries, such as the 'osmiridium' deposits of western Tasmania. These historical documents written in the early 1900s provided invaluable information on the exploration exploits of the prospectors, geology of the alluvial and hard-rock deposits, mining methods, major markets for the industry, and production statistics. The major aims of these early reviews were to document mining activities and production statistics from the newly discovered areas and to promote exploration elsewhere in the state.

One of the earliest PGE reviews in Australia was published by the Tasmanian Department of Mines in 1914. Geological Survey Bulletin 17 that was written by Government Geologist Twelvetrees, describes the mining history of the Bald Hill Osmiridium Field in western Tasmania. It was the first of a series of Geological Survey Bulletins that summarised the emerging 'osmiridium' industry of Tasmania. Other bulletins that followed in this series included: Bulletin 32—Osmiridium in Tasmania by Reid (1921); Bulletin 39—The osmiridium deposits of the Adamsfield district by Nye (1929); and Bulletin 44—The geology and mineral deposits of Tasmania by Nye and Blake (1938). Brown (1919) also reviewed the 'osmiridium' mining industry of Tasmania. Nye (1930) wrote an historical report on the 'osmiridium' occurrences in the Main Creek area of Adamsfield. Elliston (1953), Ford (1981), Bottrill (1989, 2014), and Brown (1992, 1998) reviewed the mineralogy of the PGMs and their host rocks in Tasmania; Bacon (1992) described the mining-exploration history and production statistics of Adamsfield and Tasmania; and Bacon and Lynch (1993) compiled PGE data in the environmentally sensitive rainforest areas of western Tasmania.

Other PGE reviews at province or state scale (most published by State-Territory Geological Surveys: <http://www.geoscience.gov.au/>) include:

- **New South Wales**—Jaquet (1896), Morrison (1928), and Flack (1967) provided some of the earliest descriptions of PGE occurrences in the state; Suppel and Barron (1986a,b), Johan et al. (1990a,b), Elliott and Martin (1991), and Teluk (2001) described the field relationships and mineralogy of the mineralised Alaskan-type intrusions of the Fifield region, New South Wales.
- **Queensland**—Ball (1905), Dunstan (1917, 1921, 1926), and Connah (1961) provided historical accounts of Pt in heavy-mineral concentrates from mineral sands, and Dunstan (1920) gives one of the earliest accounts of PGEs in the state. A succinct summary of hard-rock and beach-sand PGE occurrences in the state is by Denaro et al. (2013).
- **Northern Territory**—Eupene Exploration Enterprises Pty Ltd (1989) described the PGE occurrences throughout the territory, and Hoatson et al. (2005a) investigated the PGE potential of mafic-ultramafic intrusions in the Arunta Region of central Australia.
- **Tasmania**—see above.
- **Victoria**—Seymon (2006) provides a state-wide appraisal of Ni mineralisation and potential in Victoria. The report identifies areas considered prospective for Ni based on the occurrence of analogue criteria and past exploration results, and it describes orthomagmatic, hydrothermal, and lateritic occurrences, including PGE-bearing Ni deposits (e.g., Thomson River).
- **South Australia**—The first published assessment of the Ni-Cu-PGE potential of the Late Archean Lake Harris Komatiite in the central Gawler Craton was provided by Hoatson et al. (2005b).
- **Western Australia**—Simpson (1914) recognised the potential association of 'platinoid metals' with 'basic and ultrabasic' type rocks throughout the state; Travis et al. (1976) and Ross and Keays (1979) investigated PGEs in gossans and ultramafic rocks from the Yilgarn Craton; Hudson and Donaldson (1984) and Hudson (1986) documented the compositions of PGMs from the Kambalda region; Harrison and Blockley (1990) and GSWA (1991) compiled Pt and Au data of mafic and ultramafic rocks for the state; Hoatson et al. (1992) and Hoatson and Blake (2000)

described PGE-bearing layered intrusions in the Pilbara Craton and the Halls Creek Orogen, respectively; and Morris and Pirajno (2005) highlighted the PGE potential of Proterozoic mafic sill complexes in the Bangemall Supergroup. Barnes (2006: and papers within) review Ni-Cu-PGE mineralisation associated with Archean komatiites in the Yilgarn Craton. Maier et al. (2014a,b) describe the mafic-ultramafic intrusions of the Giles Event in central Australia and considers the potential for magmatic Ni-Cu-PGE deposits.

No reviews of PGEs in Australia were published before 1955. The first significant national reviews of PGEs in Australia were brief government reports written by Geary et al. (1956) and Barrie (1965). These reports summarised the most significant PGE occurrences in each state-territory and production statistics of Pt and osmiridium for each jurisdiction. Kalix et al. (1966) compiled Australia's PGE production, import, and export data for the period 1894 to 1964. The Australian Mineral Industry Annual Reviews produced by the Bureau of Mineral Resources, Geology and Geophysics, summarised the salient PGE production statistics and exploration trends from 1975 to 1987. Reviews that highlight the potential of PGE deposits in different geological settings include Hoatson (1984) and Hoatson (1990). The summary of PGEs in Australia by Hoatson and Glaser (1989) describes the global marketing economics, historical mining, state occurrences, and the potential for new discoveries. Hoatson (1998) summarises orthomagmatic and hydrothermal mineral systems associated with Precambrian layered mafic-ultramafic intrusions in Australia. Hoatson et al. (2006) review the Ni sulphide deposits of Australia which encompasses descriptions of PGE deposits. Koek et al. (2009, 2010) assess the mining and marketing challenges, both domestically and globally, confronting the Australian PGE industry. Pirajno and Hoatson (2012) reviewed LIPs in Australia.

A review of PGEs in Australia by Geoscience Australia (GA) can be found at <http://www.ga.gov.au/minerals/mineral-resources/platinum.html>. Relevant maps, digital datasets, and publications relating to the PGEs and Ni are available for free download. Among the available maps and their associated GA Records that describe these maps are comprehensive summaries of Australian Mafic-Ultramafic Magmatic Events compiled in four resource packages, namely:

- Australian Mafic-Ultramafic Magmatic Events GIS Dataset  
[http://www.ga.gov.au/metadata-gateway/metadata/record/gcat\\_78742](http://www.ga.gov.au/metadata-gateway/metadata/record/gcat_78742)
- Map of Australian Archean Mafic-Ultramafic Magmatic Events  
[http://www.ga.gov.au/metadata-gateway/metadata/record/gcat\\_69347](http://www.ga.gov.au/metadata-gateway/metadata/record/gcat_69347)
- Map of Australian Proterozoic Mafic-Ultramafic Magmatic Events  
[http://www.ga.gov.au/metadata-gateway/metadata/record/gcat\\_70461](http://www.ga.gov.au/metadata-gateway/metadata/record/gcat_70461)
- Map of Australian Proterozoic Large Igneous Provinces  
[http://www.ga.gov.au/metadata-gateway/metadata/record/gcat\\_69213](http://www.ga.gov.au/metadata-gateway/metadata/record/gcat_69213).

These digital products show the geographic extent and age relationships of mafic and ultramafic rocks, and associated mineral deposits throughout the continent. To assist explorers, GA compiled a fact summary sheet of GA-produced products (up to 2008) including PowerPoint presentations related to those commodities (Ni, Cu, Co, Cr, PGEs, Ti, V) associated with Precambrian mafic-ultramafic rocks in Australia (Hoatson, 2008). Skirrow et al. (2013) briefly describe PGE-mineralising systems in Australia and examine the critical commodity status of PGEs.

Countries in proximity to Australia that have also produced national-wide reviews on PGEs include New Zealand (Douch, 1987; Challis, 1989; Christie and Challis, 1995) and Papua New Guinea (Power-Fardy, 1986; Bachmann et al., 1987; Power-Fardy et al., 1990; Weiser, 1998).

## 2 Historical aspects of the platinum-group elements

Dean M. Hoatson

### 2.1 The earliest applications of platinum-group elements

Naturally occurring Pt metal and Pt-bearing alloys can be traced throughout recorded history. It is most likely that Pt and the other precious metals of the group were not recognised as separate metals by early civilisations. Platinum has been identified in objects from various parts of the ancient world. Osmiridium inclusions (natural alloy of Os and Ir) have been identified in Egyptian Au pieces dating as far back as ~1400 BC (Scott and Bray, 1980), and adornments found in Egyptian tombs, decorated with Au and Pt, were imported from the ancient kingdom of Nubia in southern Egypt and from northern Sudan. Nubia had great natural wealth derived from Au mining, and trading of ivory, ebony, incense, and precious metals, all of which were highly coveted by neighbouring civilisations. The ~700 BC Casket of Thebes (Figure 2.1), a sarcophagus that contained the great high priestess Shepenupet, the daughter of the King of Thebes, is decorated with hieroglyphics of Au and Ag superimposed on a thin sheet of Pt. The Pt sheet had been hammered out in the same fashion that Thebian craftsmen treated Ag, suggesting it had been mistaken for Ag.



Figure 2.1 The daughter of the King of Thebes (~700 BC), the great high priestess Shepenupet, is buried in a sarcophagus decorated with gold, silver, and platinum. A small document casket made of platinum is also placed in her tomb, Johnson Matthey PLC Photograph Collection and Platinum Guild International–United Kingdom, Platinum History: <http://www.preciousplatinum.in/en/about-platinum/platinum-history>.

From Ancient Egyptians to South American native civilisations, to Spanish conquistadors, European scholars, and alchemists, the unique physical attributes, metallurgical properties, and applications of this rare metal were slowly revealed over time. A feature of the protracted evolutionary path of Pt is its sporadic appearance throughout history, mysteriously disappearing for centuries, to then rapidly re-emerge and become the priority precious metal of choice for skilled artisans and for the pleasure of kings and popes. Platinum's diverse uses during its early evolution ranged from decorations on ancient burial caskets, ceremonial jewellery pieces, chemical implements and apparatus, international standards of weight and measurement, and monetary items, to ornate pendants, crowns, and chalices of royalty and religious status.

During pre-Incan times (~100 BC), Pt was recovered by Colombian Indians during alluvial Au mining operations. The early South American civilisations of the Aztecs, Maya, Incas, Moche, Chibcha, and Canaras (Sutton, 2008) also used Pt and Au to create ceremonial jewellery (ear rings, nose pieces, pendants, face masks and studs), figurines, tweezers, needles, fish hooks, and various other artefacts (Figure 2.2). The most successful early exploitation of Pt was by the Esmeraldas people in northern Ecuador many centuries before the arrival of the Spanish. The Indians used sophisticated metallurgical processes for their intricate jewellery, such as the sintering of different precious metals at the La Tolita archaeological site. Danish metallurgist Paul Bergsøe (1872–1963) suggested that these jewellery items were made by heating Pt nuggets that were coated with Au dust, and then they were annealed and forged to produce a Au-Pt alloy surface. Radio carbon dating of many artefacts recovered from burial mounds and cemeteries in the mid-19<sup>th</sup> century obtained ages stretching back to the 1<sup>st</sup> and 4<sup>th</sup> centuries AD.

The Andean mountains were a rich source of Pt and Au for the South American civilisations. The Pt is associated with ultramafic rocks (dunite, peridotite, pyroxenite) along the seaward flanks of the western cordillera. Most Pt was obtained from the Chocó region of northwest Colombia, and the coastal regions of Tumaco and Esmeraldas near the border of Colombia and Ecuador. Platinum in the Chocó River and its tributaries occurs in gravels along the riverbeds and in Tertiary conglomerates. The Pt was in the form of water-borne grains and nuggets that contained approximately 50% to 80% Pt, with the balance comprising small amounts of Ru, Rh, Pd, Os, and Ir, in addition to Fe, Cu, and other base metals (McDonald and Hunt, 1982). Although some Pt nuggets are large (up to 700 g), most Pt grains are small and flattened due to fluvial transport (Scott and Bray, 1980). Placer concentrations were often contaminated by mercury and other heavy-black minerals, such as chromite and magnetite. Much of the Pt was also discarded because it could not be readily 'worked'. The local South American inhabitants often threw the silvery beads back into the river where they hoped with further 'ripening' they would return as little Au beads. Attempts to melt Pt failed, and the earliest efforts to fabricate the metal into objects were often restricted to the hammering out of single native iron-platinum grains. The desire for, and use, of Pt was 'lost' to civilisations for nearly two millennia, however, it reappeared in Europe around the mid-16<sup>th</sup> century.

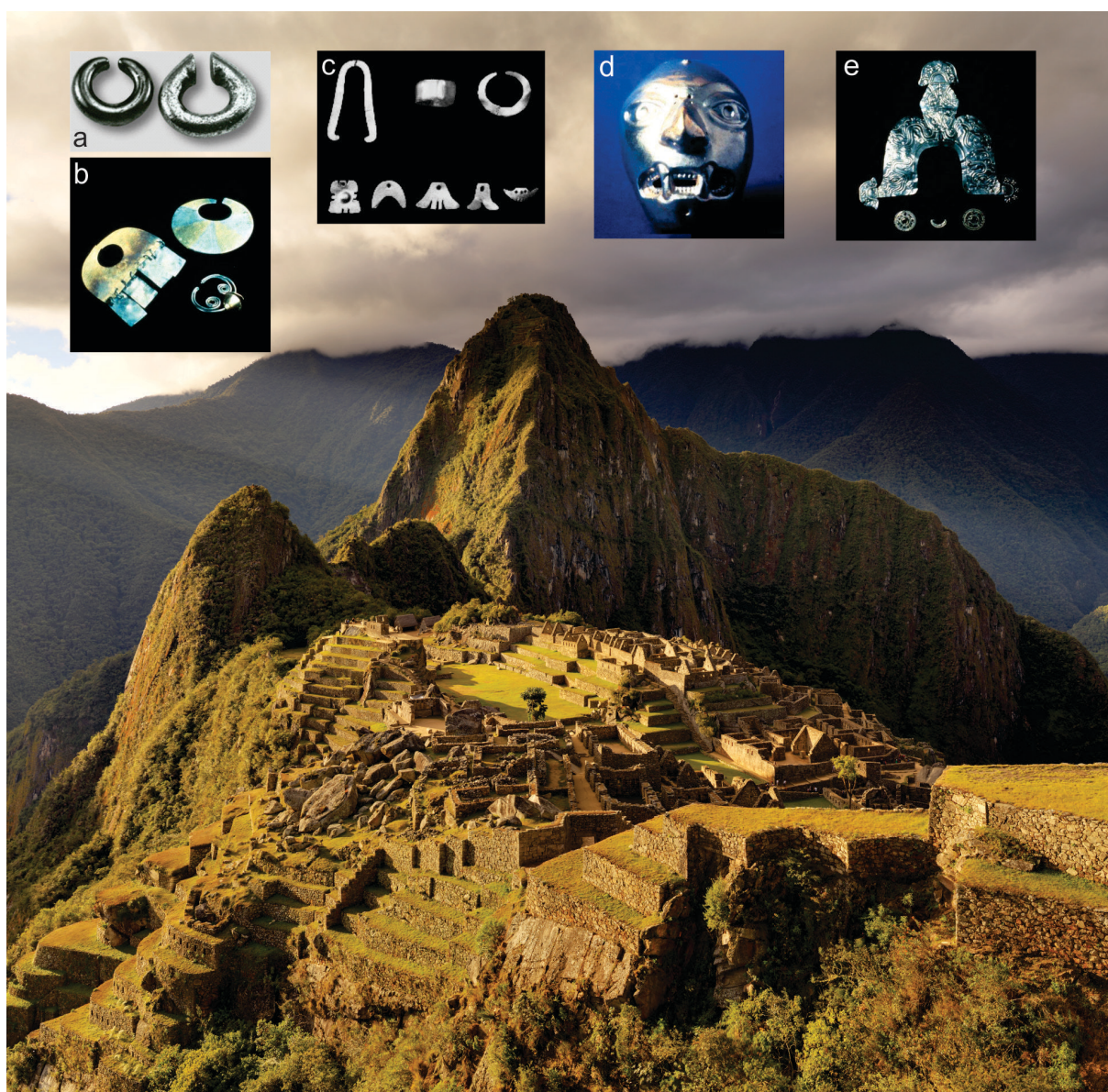


Figure 2.2 Platinum jewellery of the early South American civilisations. Background photograph is Machu Picchu —15<sup>th</sup>-century World Heritage-listed Inca site located ~2430 m above sea level in the Cusco Region of Peru. Photographer is Martin St-Amant. (a). Two platinum nose ornaments made by the Indians of Colombia. The piece on the left is a native iron-platinum alloy with small platinum inclusions visible on the surface; the piece on the right is made of a natural copper-platinum alloy with small inclusions of osmiridium. (b). Platinum ear rings made by the Incas. (c). Specimens of platinum-gold alloy jewellery from the Esmeraldas region of Ecuador. (d). Sheet metal face mask (7.1 cm-high) with human features and animal fangs from a gold alloy clad on both sides with a gold-platinum alloy made by the Incas. The platinum content varies from 2% to 30%. Mask was collected in the 1870s from the Rio Esmeraldas region of Ecuador (Scott and Bray, 1980). (e). Platinum head decoration made by the Incas. All images are from Johnson Matthey PLC Photograph Collection.

## 2.2 The European influence

The first reference to 'platinum' in Europe is believed to be in 1557, when Julius Caesar Scaliger (1484–1558), a well-known Italian scholar and poet who was familiar with South America, wrote *'Moreover, I know that in Honduras, a district between Mexico and Darien, there are mines containing a substance which it has not hitherto been possible to melt by fire or by any of the Spanish arts.'* The next important citation was published in Spain in 1590 by Jesuit priest José de Acosta (1539–1600), a Spanish missionary sent to the South American colonies in 1571. He states: *'Yea there is another kinde which the Indians call 'papas de plata' and sometimes they find pieces very fine and pure, like to small round rootes, the which is rare in silver but usual in gold'* (McDonald and Hunt, 1982).

From the late 16<sup>th</sup> century, the Spanish conquistadors plundered Au from the Incas in South America and dismissed the associated heavy metal as inferior and a nuisance since it interfered with their Au-mining activities. The Spanish consequently gave this metal the name 'platina', a derogatory diminutive of plata, meaning 'small silver'. It was also known as 'Platina del Pinto', after the Pinto River in New Granada, 'oro blanco', 'juan blanco' and a description that is still often used today, 'white gold'. The 17<sup>th</sup> century witnessed many published references to 'platina' by various European priests, alchemists, and scientists, however, the precious metal largely remained a mystery for many decades.

During the early 18<sup>th</sup> century, Pt metal arrived in Europe and was highly prized by alchemists who used it in an attempt to 'create gold from lead'. Virtually impossible to corrode with chemicals or gases, and heavier than Au, Pt was finally recognised in 1751 as a new metallic element possessing unique physical and chemical properties. In 1753, a small bag of Pt was sent to Spain with the note *'In the Bishopric of Popayan, Suffragan of Lima, there are several gold mines among which there is one called Choco. In a part of the mountains which contain it there is a large quantity of a sort of sand which the people of this country call platina and white gold.'*

Between 1730 and 1772, the extensive counterfeiting of Spanish doubloons by Au-coating Pt spurred the authorities to order the disposal of all Pt into the sea, but by 1788, the Spanish government was purchasing Pt at 8 shillings per pound. Platinum in 1780 was being used in France to make crucibles for glass production, and shortly later in 1784, it was used to make durable laboratory instruments in Berlin. European royalty and aristocrats, such as King Carlos III of Spain, King Louis XVI of France, and Pope Pius VI, appreciated the special physical qualities of Pt and commissioned a number of elite craftsmen of the day to make decorative chalices, bowls, watch-chains, expensive cutlery, coat buttons, and ceremonial crowns (Figure 2.3). Various items of Pt jewellery, such as brooches, pendants, rings, and necklaces, also became very fashionable throughout Europe (Figure 2.4).



Figure 2.3 Platinum ornaments and jewellery of European influence. (a). Ornate platinum chalice made by Francisco Alonso, 30 cm-high and weighing nearly two kilograms, presented by King Carlos III of Spain in 1788 to Pope Pius VI. (b). Fabergé platinum Easter egg created by Peter Carl Fabergé, famous jeweller to the Russian Tsars. (c). Fabergé platinum cigarette case. (d). Platinum crown holding the famous Koh-I-Noor diamond. (e). King Louis XVI of France asked his jeweller Marc Etienne Janety to make this ornate platinum sugar bowl. All Images from Johnson Matthey PLC Photograph Collection.



Figure 2.4. Intricate items of platinum jewellery that highlighted the skills of the elite craftsmen were very fashionable throughout Europe. (a). Art Nouveau pendant. (b). Floral-style red brooch. (c). Art Nouveau pearl-droplet brooch. (d). Matching necklace and ring. (e). Art deco pendant. (f). Three items of Art deco jewellery. All images are from the Johnson Matthey PLC Photograph Collection.

Industrial uses for PGEs early in the nineteenth century included Pd-Au alloys for navigating sextants and corrosion-resistant graduation plates for scientific instruments in 1812. In 1814, the Swedish chemist Jöns Jacob Berzelius (1779–1848; Figure 2.5), the Father of Swedish Chemistry, published a preliminary table of chemical elements based on atomic weights of all elements then known and also using O as 100. Berzelius's table showed data for Pt, Pd, and Rh, and he also proposed the use of the now familiar chemical symbols for the elements. The symbol Pt was suggested for platinum, while palladium was initially shown as Pl, and was later revised twice, ending with the presently accepted Pd.

The catalytic properties of PGEs were first noted in 1817 when British chemist and inventor Sir Humphry Davy (1778–1829) documented heterogeneous catalysis when a mixture of coal gas and air over Pt wire caused the wire to glow. Rhodium-Sn alloys in durable tips for pen nibs in the 1820s were later supplanted by the much harder osmiridium alloys (Griffith, 2003). Two Rh-Ir-Ag-steel razors were presented to the British scientist and philosopher Michael Faraday (1791–1867), and Os tetroxide was used for biological tissue preservation, an application that continues to this day. In 1862, Pt-Ir alloys were used in boiling vessels for the concentration of sulphuric acid, and towards the end of the century they were used in thermocouple and temperature measuring devices. Thomas Graham (1805–1869), Professor of Chemistry at University College, London, noted in 1866 that Pd can absorb up to six hundred times its own volume of H. The American inventor Thomas Alva Edison (1847–1931) in 1879 experimented with Pt and Ir filaments for incandescent light bulbs and Austrian chemist Carl Auer von Welsbach (1858–1929) used Os for metal-filament mantles in 1897 (Griffith, 2004). von Welsbach found working with Os was very difficult, but he developed a new method which mixed Os oxide powder with rubber or sugar into a paste, which he then squeezed through a nozzle and fired in a kiln. The paste burns away, leaving a fine wire of Os. Soon after the commercial introduction of the Oslamp in 1902, the Os filament in this lamp was replaced by the more stable metal tungsten (W: also called wolfram). Tungsten has the highest melting point of all metals and increases the luminous capacity and life of the incandescent lamps. The international light-bulb manufacturer OSRAM, which was formed by three German companies in 1906, derived its name from the components of OSmium and wolfram.

The wide-scale use of Pt in jewellery and coinage in the 19<sup>th</sup> century was hindered by its rarity, difficulty of crafting, and the need to alloy it with more expensive metals, such as Ir. However, this trend subsequently changed with the development of high-temperature torches that allowed jewellers to take advantage of the unique attributes of Pt (Sutton, 2008). In addition, the need for a regular global supply of Pt was later achieved by increased mining activities in Colombia and the discovery of the alluvial Pt-Au deposits in the Ural Mountains of Russia in 1823 (see Section 1.3.1). Many technical advances were associated with the discovery of the Ural deposits, including the processing of Pt to become malleable. In their attempt to support the alluvial mining activities in the Urals, the Russian Government were the first to mint Pt coins, namely the three-rouble (10.35 g Pt), six-rouble (20.70 g Pt), and twelve-rouble (41.41 g Pt) coins (Figure 2.6). About 75% of the 1 400 000 coins (equivalent to ~14.75 t of Pt) were subsequently returned to the Soviet treasury. With the advent of diamond mining in South Africa, Pt also became more fashionable as a setting for precious stones. From 1884, famous jeweller to the Russian Court, Peter Carl Fabergé (1846–1920) took advantage of these advances with the creation of decorated Fabergé Eggs (Figure 2.3b), such as the present for Tsar Alexander III and his wife Marie. In the early 1900s, the famous French jeweller and businessman Louis Cartier (1875–1942), known worldwide for elegant and extravagant watches and jewellery, used Pt to enhance the beauty of diamonds in his designs (Figure 2.7a). The Duchess of Windsor also raised the awareness of the applications of Pt in jewellery with her Pt-bearing engagement ring and wedding bands (Figure 2.7b). The popularity of Pt in jewellery has maintained its momentum to the present day.



Figure 2.5 The father of Swedish chemistry, Jöns Jacob Berzelius (1779–1848), published a table of elements in 1814 that included data and chemical symbols for platinum, palladium, and rhodium. Image from Wikimedia Commons.



Figure 2.6 Very rare, 1832 twelve roubles (41.4 g) Russian platinum coin minted in St. Petersburg: Tsar of Russia, Nikolai I Pavlovich (1796–1855). Image shows crowned double-headed imperial eagle facing with wings displayed, holding sceptre and orb, and central coat-of-arms of Moskva. Image from Wikimedia Commons.



Figure 2.7 (a). Bismarck Sapphire Necklace (1935) by renowned jewellery designer Louis Cartier. The necklace consists of a large blue sapphire (98.6 carat) and pairs of round brilliant cut diamonds on a single chain of platinum links. (b). The first 'testimonial' for platinum jewellery was the Duchess of Windsor. Her famous quotation "Even stupid people know that after 7 p.m. you can only wear platinum!" Here she wears her engagement ring—a huge emerald mounted in platinum—her wedding bands were also platinum. Image (a) is from Wikimedia Commons; image (b) is from the Johnson Matthey PLC Photograph Collection.

The British precious metal company Johnson Matthey in 1908 fashioned analytical crucibles of Ir, Rh, Ru, and Os. In particular, Ir was found to be harder than steel, resistant to attack by any chemical except caustic potash at red heat, and even in these conditions it had greater resistance than Pt. The use of Ir and Pt in crucibles still remains an important application today. German chemist Fritz Haber received the Nobel Prize for Chemistry in 1918 for his use of Os as a catalyst in the production of ammonia from N and H (Griffith, 2004).

## 2.3 Scientific recognition and etymology

The discovery, identification, and scientific characterisation of the six members of the PGEs is a testament to the exploits of eighteenth century Spanish and French explorers, in particular, Antonio de Ulloa y de la Torre-Girault (1716–1795: Figure 2.8a), and the years of laborious experimental trials undertaken by many European scientists. Two English chemists stand out for unravelling the mysteries of the PGEs at the beginning of the nineteenth century, namely William Hyde Wollaston (1766–1828: Figure 2.8b) and Smithson Tennant (1761–1815: Figure 2.9). Wollaston was the first to produce malleable Pt and he discovered Pd (1802) and Rh (1804), whereas Tennant found Ir (1803) and Os (1803). Some forty years later the remaining PGE, Ru (1844) was discovered in Russia. The following description of these scientific expeditions and experimental trials is in part from the excellent summary of the history of Pt and other related metals by McDonald and Hunt (1982) and from WebElements (<http://www.webelements.com/>).



Figure 2.8 Famous European scientists involved with the discovery of the platinum-group elements. Background photograph shows a group of European alchemists. (a). Antonio de Ulloa y de la Torre-Girault (1716–1795) was a Spanish general, explorer, astronomer, and is also credited with the 'discovery' of platinum in 1735. (b). Prominent English chemist William Hyde Wollaston (1766–1828) was an influential scientist who discovered palladium and rhodium, and produced the first malleable platinum. (c). Polish chemist Jędrzej Śniadecki (1768–1838) is alleged to have isolated ruthenium in 1807, but this claim was later discounted when his findings could not be ratified. (d). Russian chemist and botanist, Karl Karlovich Klaus (1796–1864), discovered ruthenium in 1844, and also investigated osmium, palladium, iridium, and rhodium. Images are from Wikimedia Commons.

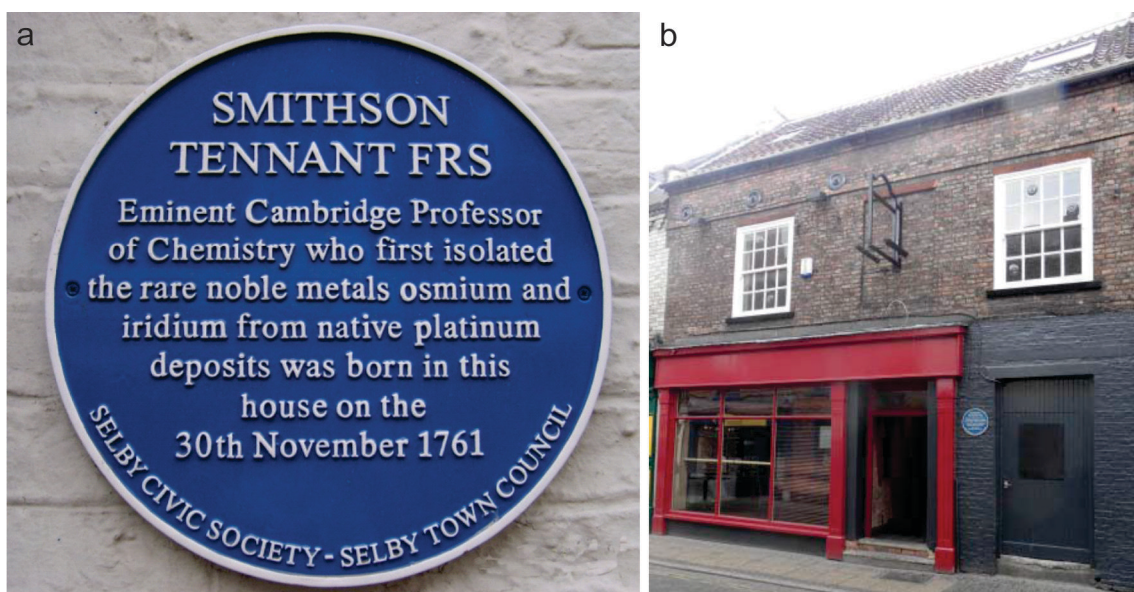


Figure 2.9 (a). A blue plaque commemorating the birthplace of Smithson Tennant FRS, discoverer of iridium and osmium. (b). 'Elizabethan' pub located in Finkle Street, Selby, United Kingdom showing plaque in (a). Image (a) from Wikimedia Commons; image (b) from Lewis (2011).

### 2.3.1 Platinum

Antonio de Ulloa y de la Torre-Girault was a Spanish general, explorer, author, astronomer, colonial administrator, the first Spanish Governor of Louisiana, and he was instrumental in raising the awareness of 'platina' in Europe (Figure 2.8). In this context, he is generally credited with the 'discovery' of Pt. In 1735, Ulloa, along with fellow Spaniard don Jorge Juan y Santacilia (1713–1773), was appointed by King Philip V to participate in the French Geodesic Mission. This was a scientific expedition organised by the French Académie des Sciences destined for Ecuador to measure the arc of a meridian at the equator in order to establish whether the Earth bulges at the equator as predicted by Newton. After arriving in Quito, Ecuador, in 1736, the two Spaniards made many observations of alluvial mining operations throughout Ecuador and Colombia, including the nuisance value of the resistant 'platina' grains. *"In the district of Chocó are many mines of lavadero or wash gold, like those we have just described.....Several of the mines have been abandoned on account of the platina, a substance of such resistance, that, when struck on an anvil of steel, it is not easy to be separated; nor is it calcinable; so that the metal enclosed within this obdurate body could only be extracted with infinite labour and charge."* Ulloa departed South America in 1745, and there is no evidence that the Spaniard took any samples of 'platina' to Europe. Three years later he wrote his accounts of the expedition in the publication 'Relación histórica del viage a la América Meridional'. A dozen copies of this report were sent to the Royal Society in London, and it was in this report that the above reference to 'platina' at Chocó was made. After publishing his report in 1748, Ulloa did not undertake any further investigations of the new metal. However, his report initiated wide-scale interest in Pt and consequently other chemists and metallurgists across Europe soon began studying Pt, including Torbern Bergman, Jöns Jakob Berzelius, William Brownrigg, William Lewis, Pierre Macquer, Sir William Watson, and Sir Charles Wood. The British metallurgist and assayer Charles Wood obtained some grains of 'platina' and forwarded them to chemist William Brownrigg for research and potential commercial applications. His findings were presented to the Royal Society on December 13<sup>th</sup>, 1750. He described Pt as being less pliable than Au, but with similar resistance to corrosion. Many researchers have proposed that the modern re-discovery of Pt should be credited to Wood and

Brownrigg since they were the first persons to undertake scientific investigations of this rare metal. In 1751, the Swedish scientist Henrik Theophil Scheffer (1710–1759) recognised the unique properties and rarity of Pt and declared it to be the seventh element known to exist up until that time.

The prominent English chemist William Hyde Wollaston was born in Norfolk and he lived most of his adult life in London. In 1793, he obtained a doctorate in medicine from Cambridge University. While practising medicine, he became interested in physiology, chemistry, physics, metallurgy, and crystallography. Wollaston discovered the first amino acid, cystine, and was the first to postulate that human hearing is limited to certain frequencies. He invented various optical instruments, and was the first to observe the dark lines in the solar spectrum which are a crucial tool used today in stellar astronomy. His many talents extended to demonstrating frictional and voltaic electricity and the design of voltaic batteries.

Early in the nineteenth century, Wollaston combined his immense skills and knowledge in chemistry, metallurgy, and crystal properties to fabricate malleable Pt. On the eve of Christmas 1800, Wollaston invested £795 for the purchase of 5959 ounces of alluvial Pt ore of South American origin. In February 1801, he set about purifying the mixed Pt in a laboratory behind his house near Fitzroy Square with his faithful servant John Dowse. He commenced his experiments by dissolving 16 or 20 ounce lots of Pt ore in aqua regia, followed by precipitation with sal-ammoniac (ammonium chloride flux), heating, and forging. During these early trials, the Pt ingots cracked or split on hammering, a problem that was partly corrected later by the removal of the previously unknown metals Pd and Rh. Further improvements were achieved by fine tuning the proportions of hydrochloric and nitric acids in the aqua regia, and using more dilute chemical mixtures. Wollaston then focussed his efforts on perfecting the powder metallurgy technique, and after three years of effort he eventually produced a saleable product of Pt. In later years, Wollaston purchased 47 000 ounces of crude Pt. From 1808 to 1819, he produced and marketed over 38 000 ounces of refined and malleable metal at an average price of 16 shillings per ounce. Such fabricated items included crucibles and their lids, balance and evaporation pans, blow-pipes, thermometers, touch-holes and pans for flintlock pistols, sulphuric acid boilers, knives, wire, bars, and ingots. Wollaston's supply of native platinum ended in 1820, when he ceased making products for industry. Sales of the Pt items amounted to about £30 000. His purification process remained a close secret for many years, and not until long after the experimental work had ceased did he consent to publish any account of his process shortly before his death from a fatal illness in 1828.

The scale and variety of Wollaston's research made him one of the most influential scientists of his time. The Wollaston Medal, in recognition of Wollaston's scientific achievements, is the highest award granted by the Geological Society of London. It was made of Pd when it was first awarded in 1832. In addition, the prestigious Royal Medal (also called The Queen's Medal), a Ag-gilt medal from the Royal Society of London was also awarded to Wollaston in 1828 for his communication, entitled, '*On a method of rendering Platina malleable, being the conclusion of a series of researches on the properties of the Metallic Bodies contained in the Ores of Platina.*' The legacy of Wollaston is also recognised by the calcium-bearing mineral wollastonite (CaSiO<sub>3</sub>) that commonly occurs in metamorphosed impure limestones.

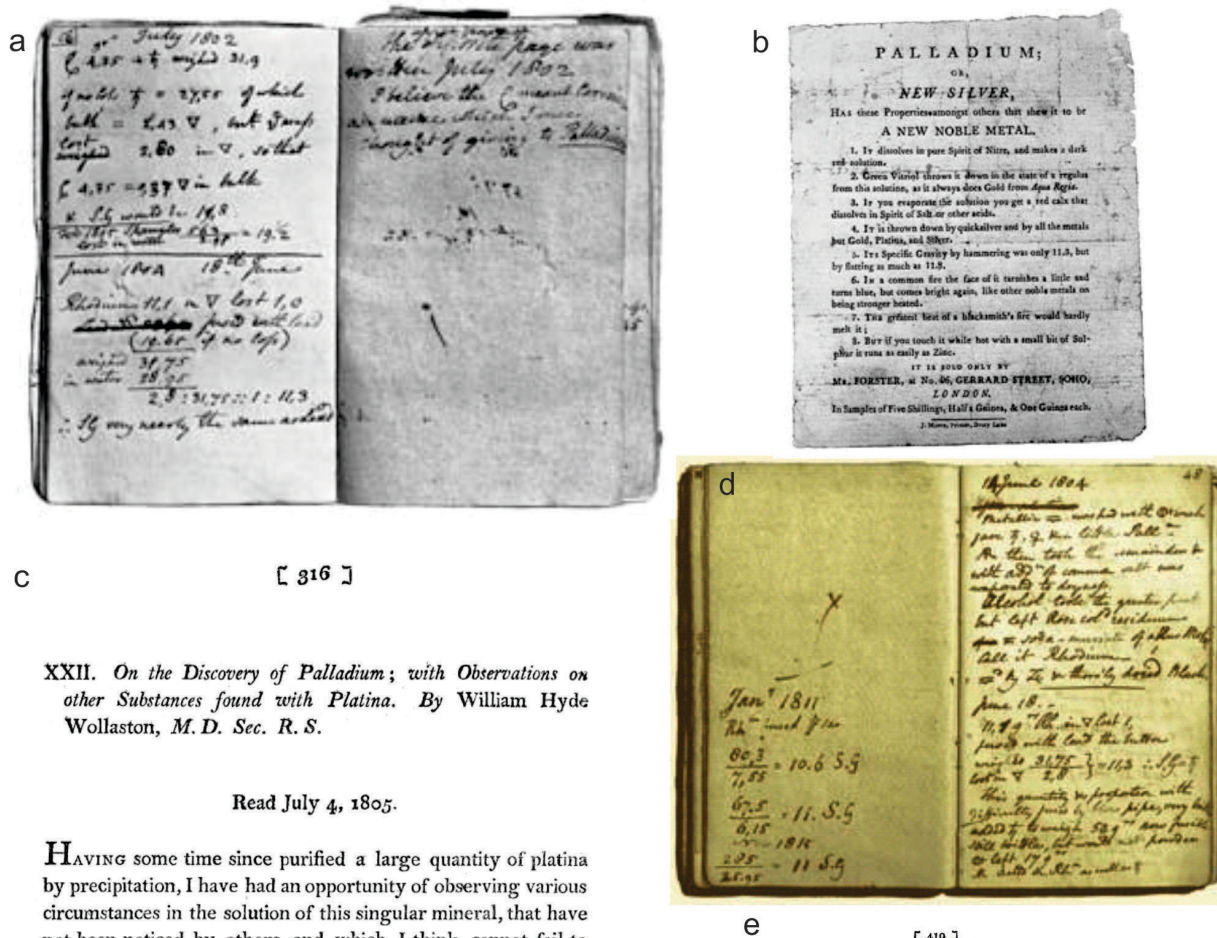
### 2.3.2 Palladium

English chemist Wollaston also identified Pd as a separate elemental metal in 1802. Early in his research on the solution of Pt in aqua regia, Wollaston suspected another metal was present in the precipitate that was neither Pt nor Tennant's Ir. The first reference to this is in one of his note-books dated July 1802 (Figure 2.10a), in which the properties of an alloy of lead with 'C' are described. On the facing page he later wrote: *'The upper part of the opposite page was written July 1802, I believe the 'C' means Ceresium, a name which I once thought of giving to Palladium.'* The successful recognition of Pd, and the other PGEs was due largely to the collaborative research between Wollaston and his fellow English chemist and close colleague Smithson Tennant. The two men entered into an informal partnership directed towards various chemically-based commercial endeavours, one of which was the production and marketing of malleable Pt. They knew that if such Pt could be produced, it could substitute for Au in many applications where an inert noble metal was required. Wollaston and Tennant had investigated South American ores for over 15 years. The Pt ore from South America (see above) was 'dissolved' in aqua regia with an insoluble black residue remaining. The two chemists decided that Wollaston would investigate the soluble component while Tennant would examine the insoluble residue. Wollaston neutralised the soluble acid component with sodium hydroxide (NaOH), and precipitated Pt out of solution by treatment with ammonium chloride (NH<sub>4</sub>Cl), as ammonium chloroplatinate. Palladium was then removed as Pd cyanide by treatment with mercuric cyanide. A new white metal (Pd) was produced from this cyanide by heating. Wollaston separated the Pd in 1802 and Rh in 1804. Tennant obtained Ir and Os from the insoluble residue in 1803 and announced his findings in 1804 (see Section 2.3.5).

Wollaston initially named the new metal 'ceresium' after the newly discovered asteroid Ceres. However, he changed this to palladium after another asteroid Pallas, one of the brightest asteroids discovered in 1802. In Greek mythology, Pallas is the Goddess of wisdom. Wollaston was reluctant to initially announce his discovery of Pd since he thought it would have commercial value. In April 1803, he anonymously sold some brief leaflets (Figure 2.10b) describing the properties of a new noble metal called Palladium or New Silver, and in January 1805 he formally announced the discovery of Pd to the scientific community (Figure 2.10c). His secrecy made him somewhat unpopular with his research colleagues who favoured open communication to facilitate scientific progress.

### 2.3.3 Rhodium

Wollaston's experiments that led to the discovery of Rh utilised the same South American Pt-bearing ores and initial procedures that were used for his Pt refining (see Platinum above). After the Pd was removed as Pd cyanide by treatment with mercuric cyanide, the remaining red precipitate containing sodium rhodium chloride (Na<sub>3</sub>RhC<sub>16</sub>·12H<sub>2</sub>O) salts from which Rh metal was obtained by reduction with H<sub>2</sub> gas and washed with water to remove the sodium chloride. An extract from Wollaston's laboratory notebook (Figure 2.10d) that describes the discovery and the naming of Rh is dated the 14<sup>th</sup> of June 1804. Shortly later on the 24<sup>th</sup> of June, only three days after the reading of Smithson Tennant's paper on Ir and Os (see below), Wollaston presented a paper (Figure 2.10e) to the Royal Society of London, titled 'On a new Metal, found in crude Platina'. In this paper he states: *'..... I design in the present Memoir to prove the existence, and to examine the properties of another metal, hitherto unknown, which may not improperly be distinguished by the name of Rhodium, from the rose-colour of a dilute solution of the salts containing it.'* Due to the colour of the chloride salts and of the respective aqueous solutions, Wollaston chose the name rhodium after the Greek *rhodon* for a rose.



XXII. On the Discovery of Palladium; with Observations on other Substances found with Platina. By William Hyde Wollaston, M.D. Sec. R. S.

Read July 4, 1805.

HAVING some time since purified a large quantity of platina by precipitation, I have had an opportunity of observing various circumstances in the solution of this singular mineral, that have not been noticed by others, and which, I think, cannot fail to be interesting to this Society.

As I have already given an account of one product obtained from that ore, which I considered as a new metallic substance, and denominated Rhodium, I shall on the present occasion confine myself principally to those processes by which I originally detected, and subsequently obtained another metal, to which I gave the name of *Palladium*, from the planet that had been discovered nearly at the same time by Dr. OLBERS.

In the course of my inquiries I have also examined the many impurities that are usually mixed with the grains of platina, but I shall not think it necessary to describe minutely substances which have already been fully examined by others.

§ I. Ore of Iridium.

I must however notice one ore, that I find accompanies the ore of platina, but has passed unobserved from its great resemblance to the grains of platina, and on that account is

XVII. On a new Metal, found in crude Platina. By William Hyde Wollaston, M.D. F. R. S.

Read June 24, 1804.

NOTWITHSTANDING I was aware that M. DESCOTILS had ascribed the red colour of certain precipitates and salts of platina, to the presence of a new metal; and although Mr. TENNANT had obligingly communicated to me his discovery of the same substance, as well as of a second new metal, in the shining powder that remains undissolved from the ore of platina; yet I was led to suppose that the more soluble parts of this mineral might be deserving of further examination, as the fluid which remains after the precipitation of platina by sal ammoniac, presents appearances which I could not ascribe to either of those bodies, or to any other known substance.

My inquiries having terminated more successfully than I had expected, I design in the present Memoir to prove the existence, and to examine the properties, of another metal, hitherto unknown, which may not improperly be distinguished by the name of *Rhodium*, from the rose-colour of a dilute solution of the salts containing it.

I shall also take the same opportunity of stating the result of various experiments, which have convinced me, that the metallic substance which was last year offered for sale by the name of *Palladium*, is contained (though in very small proportion) in the ore of platina.

Figure 2.10 Scientific documents by Wollaston that report the discoveries of palladium and rhodium. (a). Wollaston's notebook in which he records, probably for the first time, (left page) in July 1802, of palladium as 'C'. The right page states: 'The upper part of opposite page was written July 1802. I believe the 'C' meant Ceresium a name which I once thought of giving to Palladium.' (b). The handbill describing palladium which Wollaston published and distributed anonymously in April 1803. It offered for sale 'Palladium; or, New Silver... a New Noble Metal.' This handbill was later published in Nicholson's Journal. (c). Palladium discovery paper: William Hyde Wollaston (Wollaston, 1805). (d). Wollaston's notebooks showing the page for the 14<sup>th</sup> of June 1804, on which he describes the new metal rhodium. 'Using common salt he evaporated to dryness the remainder of a metallic precipitate after it was washed. Following treatment with alcohol, a rose coloured residue remained.' The metal he isolated from this he called Rhodium. (e). Rhodium discovery paper: William Hyde Wollaston: 'On a New Metal, Found in Crude Platina.' (Wollaston, 1804). Images (c) and (e) from Wikimedia Commons; images (a), (b), and (d) are from the Johnson Matthey PLC Photograph Collection.

### 2.3.4 Ruthenium

Several scientists laid early claims to the discovery of the sixth and last member of the PGEs Ru, including a Polish chemist, Jędrzej Sniadecki (1768–1838: Figure 2.8c). While at Vilnius University, Sniadecki in 1807 is alleged to have isolated 'ruthenium' (called vestium after the Roman goddess Vesta) from some Pt ores, but he withdrew his scientific claims when his findings could not be ratified. Similarly, Russian scientist Gottfried Wilhelm Osann (1797–1866), while studying the insoluble residues of Pt, also claimed, albeit incorrectly, he found Ru.

The credit of the authentic discovery of Ru is generally given to the Russian chemist, pharmacist, and botanist, Karl Karlovich Klaus (1796–1864: Figure 2.8d), who was also noted for his research on Os, Pd, Ir, and Rh. The identification of Ru had close connections with the alluvial native platinum operations in the Ural Mountains of Russia. In 1824, the mining of these extensive deposits, which sometimes contained very large Pt nuggets up to several kilograms in weight (Figure 2.11), made Russia the largest producer of Pt in the world. Klaus was appointed to a new chair of chemistry in the University of Kazan in 1838 where he worked mainly on industrial-scale analytical methods. Four years after starting his investigations of PGEs in 1840, Klaus successfully isolated the new metal Ru while investigating the waste residues of the platinum refinery in St. Petersburg. Klaus commenced his investigations on two pounds of residues and he was surprised to find they contained as much as 10% Pt in addition to four other PGEs. It was in the course of two years of arduous work that he discovered Ru by fusing insoluble osmiridium residue with potash and nitre in a Ag crucible. The bright red molten mass was poured into an Fe capsule to solidify in water and be dissolved in nitric acid to produce a black precipitate containing Ru and Os oxides. After several further stages of distillation and condensation, Klaus obtained six grams of a pure metallic sponge. Klaus named this metal ruthenium after the Latin word *Ruthenia*, which was Middle Latin for *Rus*, an early form of the Russian empire which extended across parts of Eastern Europe and modern-day Russia. The new name also acknowledged that Russia was now the major producer of the PGEs, and recognised the earlier scientific contributions of fellow Russian colleague Osann. Klaus published his findings as the experiments were being done in a series of short articles in the Bulletin of the Russian Academy of Sciences and in the 1845 book 'Chemical research of Ural platinum ore and ruthenium metal.'



Figure 2.11 Alluvial platinum deposits in the Ural Mountains of Russia are famous for large platinum nuggets up to several kilograms in weight. (a). Alluvial mining in the far east of Russia can produce large nuggets of ore which are extremely rich in PGEs. Photograph printed with permission from the Johnson Matthey PLC Photograph Collection. (b). Recovery of egg-sized nuggets of platinum is not uncommon at Kondyor. The largest nugget recovered from the operation weighed 3.52 kilograms.

### 2.3.5 Iridium and osmium

Credit for the discovery of Ir and Os in 1803 is generally given to the English chemist Smithson Tennant. Other English and French chemists, who also played important roles in their discoveries, included William Wollaston, Antoine de Fourcroy (1755–1809), Nicholas Vauquelin (1763–1829), and Hippolyte Collet-Descotils (1773–1815). In 1803–4, Tennant after studying the results of experiments carried out by these chemists, and using the large amount (~100 troy ounces) of by-product residues left from Wollaston's purification experiments of Pt, isolated two distinctive and unfamiliar elements in a dark residue which turned out to be Ir and Os. Tennant heated the black residue from Wollaston's Pt experiments, followed by hot fusion with caustic soda. The cooled solid was dissolved in water and the remaining black precipitate was treated with hydrochloric (marine) acid. The fusion process involving caustic soda and hydrochloric acid was repeated, until dark red crystals ( $?Na_2(IrCl_6) \cdot nH_2O$ ) appeared. After heating these crystals an unknown white powder formed of which Tennant wrote: '*.... appeared of a white colour, and was not capable of being melted, by any degree of heat I could supply..... As it is necessary to give some name to bodies which have not been known before, and most convenient to indicate by it some characteristic property, I should incline to call this metal Iridium, from the striking variety of colours which it gives, while dissolving in marine acid.*'

In parallel with his Ir research, Tennant melted the dark residue provided by Wollaston with alkalis and treated this with acid, distilled and then condensed, leading to a greasy liquid with a strong distinctive smell, and then to a semi-transparent solid. Tennant described this oxide: "*When the alkaline solution is first formed, by adding water to the dry alkaline mass in the crucible, a pungent and peculiar smell is immediately perceived. This smell, as I afterwards discovered, arises from the extrication of a very volatile metallic oxide; and, as this smell is one of its most distinguishing characters, I should on that account incline to call the metal Osmium.*"

The new results for Ir and Os were officially published in a paper Tennant read to the Royal Society of London on the 21<sup>st</sup> of June 1804 titled 'On two Metals, found in the black powder remaining after the solution of Platina'. Tennant published his results in haste since it was known that the French scientists de Fourcroy, Vauquelin, and Collet-Descotils were in hot pursuit.

Iridium is derived from iris, meaning in Greek mythology the personification of the rainbow and messenger of gods on account of the multiple colours of Ir salts, and Os for the Greek osme, 'a smell', after the distinctive odour of the compounded form of the element.

On the 22<sup>nd</sup> of February 1815, Tennant was riding his horse across a wooden bridge that subsequently collapsed when a securing bolt failed. He was thrown from his horse and he died an hour later from a fractured skull.

# 3 Geochemistry of platinum-group elements

Subhash Jaireth

## 3.1 General chemistry

The basic geochemistry of the PGEs is described in detail in several studies, such as Barnes et al. (1985), Barnes and Zhong-Li (1999), Cabri (1981, 2002), Mungall (2005a,b), Naldrett (1989, 1999, 2004, 2011), and Rollinson (1993). This brief overview uses material from these publications.

The PGEs are a group of six elements (Table 3.1) that belong to the Transition Metals (Groups 8, 9, and 10 of the periodic table: Figure 1.1a). Like Fe and Ni they tend to prefer metallic bonding over ionic bonding, as a result they are often found in their native state. They are classified as siderophile elements because of their affinity for Fe. Like Cu, Ag, and Au they also tend to form covalent bonds with S and hence behave like chalcophile elements. Thus in general, the presence of metallic and sulphide minerals determines their geochemical behaviour.

On the basis of their associations, the PGEs are divided into two sub-groups: the Iridium (Ir)-subgroup (IPGE— Ir, Ru, and Os), and the Palladium (Pd)-subgroup (PPGE—Pd, Pt, and Rh). The Ir-subgroup PGEs commonly have higher ionic charge (4) and higher ionic potential (6 to 6.5: Table 3.1) than the PGEs of the Pd-subgroup (2) with lower ionic potential (2 to 2.5: Table 3.1). On an ionic radius versus ionic charge diagram (Figure 3.1), the Pd-subgroup elements overlap with the transition elements, such as Ni and Cu, which may explain why they tend to be associated with the sulphides of Fe, Ni, and Cu. The PGEs of the Ir-subgroup on the other hand show closer association with Cr (chromite) as alloys (Barnes et al., 1985).

Table 3.1 Ionic radii (in Å) and ionic potential of PGEs (Shannon, 1976<sup>1</sup>).

Element	Group	Atomic number	Charge	Coordination	Ionic radius	Ionic potential	Melting point (°C)
Os	IPGE	76	4	VI	0.63	6.35	3033
Os	IPGE	76	5	VI	0.575		3033
Os	IPGE	76	6	V	0.49		3033
Os	IPGE	76	6	VI	0.545		3033
Os	IPGE	76	7	VI	0.525		3033
Os	IPGE	76	8	IV	0.39		3033
Ir	IPGE	77	3	VI	0.68		2466
Ir	IPGE	77	4	VI	0.625	6.40	2466
Ir	IPGE	77	5	VI	0.57		2466
Ru	IPGE	44	3	VI	0.68	4.41	2334
Ru	IPGE	44	4	VI	0.62	6.45	2334
Ru	IPGE	44	5	VI	0.565		2334

Element	Group	Atomic number	Charge	Coordination	Ionic radius	Ionic potential	Melting point (°C)
Ru	IPGE	44	7	IV	0.38		2334
Ru	IPGE	44	8	IV	0.36		2334
Rh	PPGE	46	2	unknown	0.86	2.33	1964
Rh	PPGE	45	3	VI	0.665		1964
Rh	PPGE	45	4	VI	0.6		1964
Rh	PPGE	45	5	VI	0.55		1964
Pt	PPGE	78	2	VI	0.8	2.50	1768
Pt	PPGE	78	4	VI	0.625		1768
Pt	PPGE	78	5	VI	0.57		1768
Pd	PPGE	46	1	II	0.59		1768
Pd	PPGE	46	2	VI	0.86	2.33	1555
Pd	PPGE	46	3	VI	0.76		1555
Pd	PPGE	46	4	VI	0.615		1555

IPGE: Iridium subgroup; PPGE: Palladium subgroup.

<sup>1</sup> Includes other references for melting point data shown in Table 4.1 and Table 4.2.

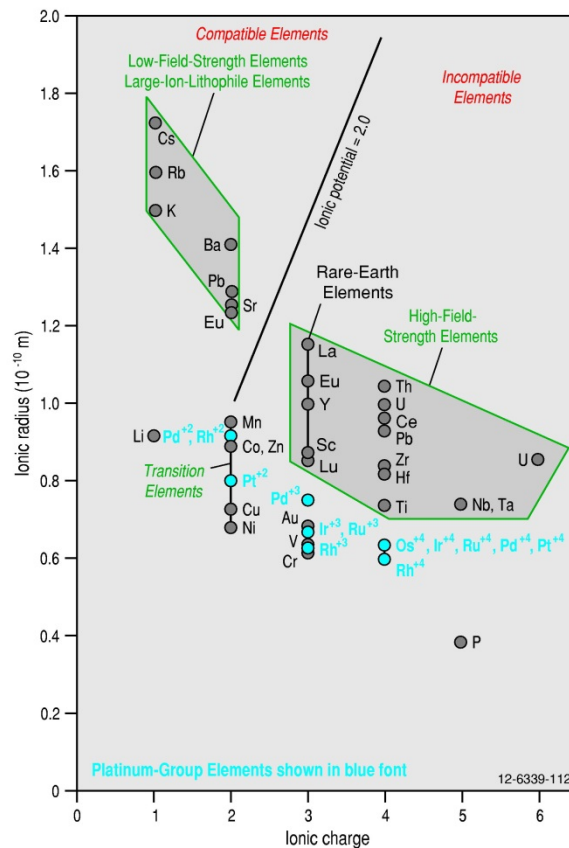


Figure 3.1 Ionic radii versus ionic charge diagram of trace elements showing that the PGEs are incompatible elements (modified from Rollinson, 1993).

## 3.2 Abundances of platinum-group elements on Earth

Natural abundances of PGEs have been discussed in detail by Crocket (1979, 2002), Mungall (2005a), and Barnes et al. (1985). Some of their data are summarised in Table 3.2 and Table 3.3. Naldrett et al. (1979) demonstrated that when PGE and Au concentrations are chondrite-normalised and plotted in order of decreasing melting point, they define curves similar to the curves of REEs (Figure 3.2). Brugmann et al. (1987) and Crockett (2002), however, show primitive mantle-normalised concentrations of PGEs.

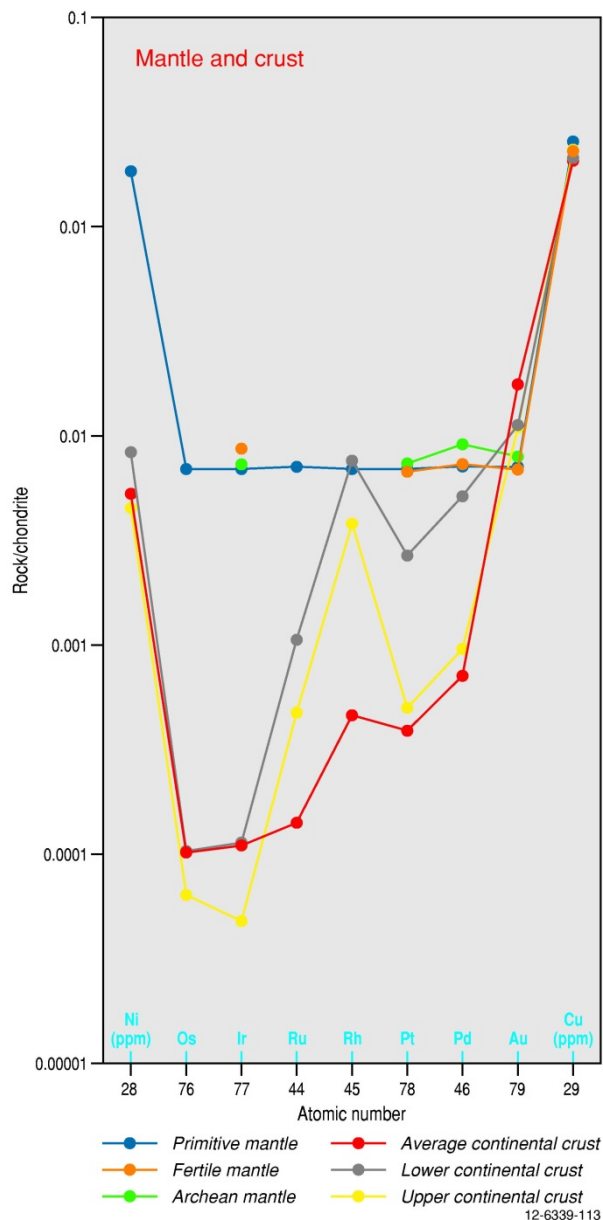


Figure 3.2 Average abundances of PGEs (ppb) in Earth's mantle and crust normalised to CI chondrite. Also shown are values for gold (ppb), nickel (ppm), and copper (ppm). Sources of data are shown in Table 3.2.

### 3.2.1 The mantle

The principal division of the Earth into core, mantle, and crust is the result of principally two processes: the formation of a metal core very early in the history of the Earth (~30 million years after the beginning of the solar system); and the formation of the crust by partial melting of the silicate mantle (Palme and O'Neill, 2007). The mantle is thought to be the Earth's largest chemical reservoir constituting ~82% of its total volume and ~65% of its mass. It comprises most of the silicate Earth, extending from the base of the crust (average thickness of ~40 km) to the top of the metallic core at ~2900 km-depth (Bennett, 2003).

The composition of the primitive mantle (the mantle before the onset of crust formation) has been estimated based on indirect approaches, such as: analogy with chondritic meteorites; critical evaluation of data derived from ultramafic mantle samples; and chemical and petrological models of peridotite-basalt melting relations (pyrolite model; see discussions in Frey, 1984; McDonough et al., 1992; and McDonough and Sun, 1995).

Compared to the CI chondrite, the primitive mantle (silicate Earth) is depleted in PGEs (Table 3.2); the depletion is of the same order for both Pd- and Ir-subgroups. It has been suggested that during segregation of metals from the silicate-part of the Earth to form the Fe-rich core, the primitive mantle was depleted in siderophile and chalcophile elements relative to lithophile elements (Newsom and Sims, 1991). The removal of Fe and Ni preferentially into the Fe core could have caused removal of PGEs as well.

The mantle is assumed to be the principle geochemical reservoir of PGEs. Melting of the mantle produces mafic and ultramafic melts relatively enriched in PGEs. However, the role of major rock-forming silicates in mafic and ultramafic rocks (as favourable hosts to PGEs) has been difficult to assess (Crocket, 2002). Several studies discussed in Crocket (2002) demonstrate a strong, positive and statistically significant correlation between a major element oxide (e.g., MgO) and a PGE (e.g., Ir). Brugmann et al. (1987) suggested that Ir might be present as a substitute in olivine. Chromite has also been proposed as a favourable host mineral for Os, Ir, and Ru (Agiorgitis and Wolf, 1978). However, available geochemical data on the concentrations of PGEs in silicate minerals show that major silicate minerals of mantle rocks including olivine, pyroxene, and garnet do not appear to be significant hosts for PGEs (Crocket, 2002). Chromite separates from both layered intrusions and ophiolites on the other hand, have much higher concentrations (up to 1060 ppb) of PGEs. In some chromites, PGEs are presents as mineral inclusions.

Minerals such as metallic alloys, tellurides, selenides, arsenides, sulpharsenides, and sulphides concentrate much higher levels of PGEs, but apart from sulphides, these minerals are rare in rocks that form from partial melting of mantle peridotites (Crocket, 2002).

### 3.2.2 The crust

The oceanic crust is thin (~7 km on average), is composed of dense rock types such as basalt, and is young ( $\leq 200$  Ma old). In contrast, the continental crust is thick (~40 km on average), composed of highly diverse rocks with an average intermediate or 'andesitic' bulk composition (Taylor and McLennan, 1985).

The continental crust comprises about 0.35% of the mass of the Earth. Although it contains substantial amounts (exceeding 30% of the bulk Earth budget) of the most incompatible elements, such as REEs (Taylor and McLennan, 1985), it is highly depleted in PGEs (Table 3.2).

The upper crust, which is more readily accessible to sampling, has been shown to have a granodioritic bulk composition. It is enriched in incompatible elements and contains an average of 1.9 ppb PGEs (Table 3.2). The lower crust, which has a bulk mafic composition, contains up to 7.4 ppb PGEs (Table 3.2).

### 3.2.3 Platinum-group-element concentrations in major rock types

The PGE concentrations of major mafic and ultramafic rock types are summarised in Table 3.3, Table 3.4, and Table 3.5. Felsic and alkaline rocks are not included in the table. The table also shows average concentration of magnesium in the rocks (arranged in decreasing order). The relative enrichment in PGEs in these rocks is also shown in Figure 3.3, which plots primitive, mantle-normalised concentrations of PGEs, Ni, Cu, and Au. Total concentrations of PGEs and the Pd- and Ir-subgroups of the PGEs are also shown in Figure 3.4.

The PGE concentrations in rocks show a general correlation with their magnesium concentrations (Table 3.3, Table 3.4, and Table 3.5), although it will be important to establish if the correlation is also valid for the magnesium concentrations of parent/primitive magma from which these rocks were formed from. Most data in the table are sourced from Crocket (2002), who also provides a comprehensive discussion of the variation of PGE concentrations in various rocks.

Orogenic and abyssal peridotites (Iherzolite and harzburgite) and ophiolites illustrate the behaviour of PGEs in the mantle (Crocket, 2002). The total concentration of PGEs in these rocks (~19 ppb to 32 ppb) is not very different from the concentration in primitive mantle (~24 ppb). The ratio of Pd- and Ir-subgroups is between 0.8 and 1.5, compared to 1 for the primitive mantle.

Komatiites commonly defined as ultramafic rocks with >18% MgO (Arndt and Nisbet, 1982), provide some idea on the effects of relatively high degrees of partial melting (30% to 60%) in the lower mantle. The Al-depleted komatiites (ADK- or Barberton-type with  $Al_2O_3/TiO_2 < 15$ ) are thought to result from ~30% partial melting of lower mantle at depths exceeding 300 km (Maier et al., 2009; Arndt et al., 2005). The Al-undepleted komatiites (AUDK- or Munro-type with  $Al_2O_3/TiO_2 = 15-25$ ), on the other hand, are formed from magma resulting from a higher degree (~50% to 60%) of partial melting of lower mantle at shallower depths (<300 km). Both types of magma are sulphide-undersaturated and become more undersaturated as they rise through the crust (Arndt et al., 2005). Both komatiites and spinifex-textured mafic rocks with komatiites (containing 9% to 18% MgO) have slightly higher total concentrations of PGEs (~30 ppb) compared to the primitive mantle (~24 ppb). In comparison with primitive mantle, these two rock-types are depleted in Ir-subgroup elements and Ni, and enriched in Pd-subgroup elements, Au, and Cu (Figure 3.3a). A more recent study on the concentrations of Pt and Pd (normalised to MgO concentration) in Archean komatiites shows systematic variation with age (Maier et al., 2009), increasing from ~2–5 ppb Pt (for ~3.5 Ga komatiites) to ~8–12 ppb Pt (for ~2.6 Ga komatiites).

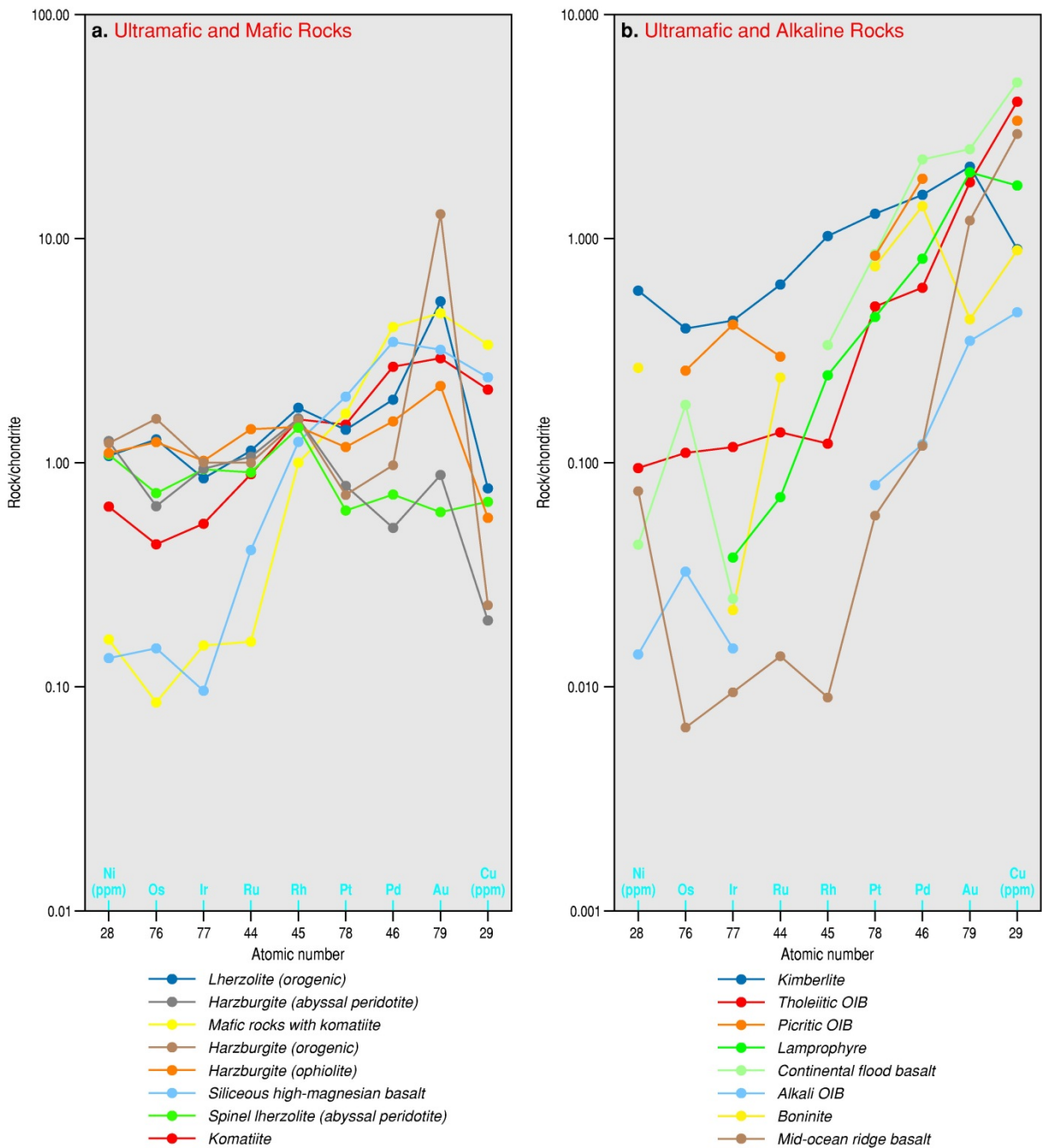


Figure 3.3 (a). Average abundances of PGEs (ppb) in major mafic and ultramafic igneous rock types normalised to CI chondrite. Also shown are values for gold (ppb), nickel (ppm), and copper (ppm). Sources of data are shown in Table 3.3 and Table 3.4. (b). Average abundances of PGEs (ppb) in major mafic, ultramafic, and alkaline igneous rock types normalised to CI chondrite. Also shown are values for gold (ppb), nickel (ppm), and copper (ppm). Sources of data are shown in Table 3.3, Table 3.4, and Table 3.5.

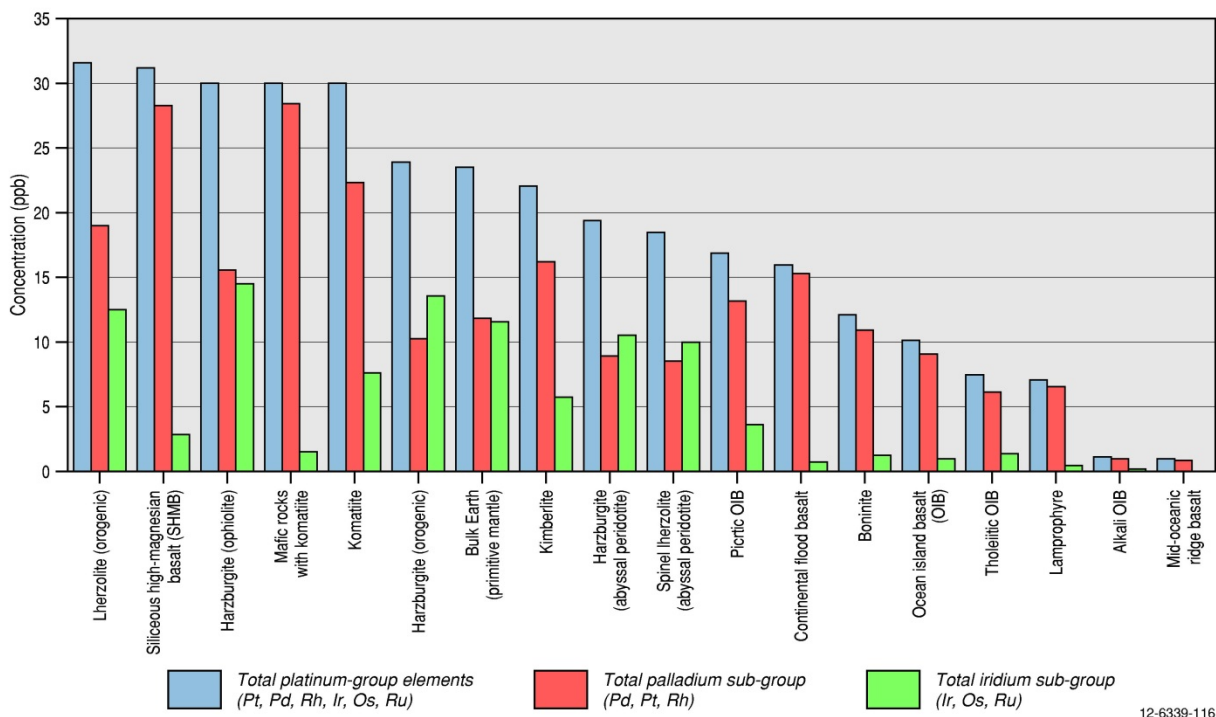


Figure 3.4 Total concentration of PGEs (in ppb) in important rock types. Sources of data are shown in Table 3.3-Table 3.5. Rocks or melts that are commonly associated with PGE deposits (shown on the x-axis) are located towards the left-hand side of the diagram. No PGE deposits are known to occur in association with melts that form tholeiitic Oceanic Island Basalt (OIB), lamprophyre, alkali OIB, and Mid-Ocean-Ridge Basalts.

Kimberlites and lamprophyres are generally thought to have been formed from a low degree of partial melting of mantle rocks. The kimberlites have a total PGE-concentration (~22 ppb) similar to that in the primitive mantle, but lamprophyres are much more depleted (~7 ppb). However, in comparison with primitive mantle, both rock-types are depleted in Ir-subgroup PGEs and Ni, but enriched in Pd-subgroup PGEs and Au (Figure 3.3b).

Ocean island basalts (OIBs) are formed from convective plumes in the mantle (Crocket, 2002). Both tholeiitic and alkali OIB have lower concentrations of PGEs than the primitive mantle (1 ppb to 8 ppb compared to 24 ppb). Picritic OIBs have higher PGE concentrations (~17 ppb). In comparison to the primitive mantle, the rocks are also depleted in Ir-subgroup PGEs and only picritic basalts show some enrichment in Pd (Figure 3.3b and Figure 3.4). Similarly, Mid-Ocean Ridge Basalts (MORBs), regarded to be derived from upper mantle are highly depleted in PGEs (Figure 3.3b).

Continental flood basalts are considered to have been formed from crustal contamination of melts generated by deep mantle plumes (Crocket, 2002). These rocks have an average total PGE concentration of 16 ppb (Table 3.4). The rocks are depleted in Ir-subgroup PGEs and slightly enriched in Pd-subgroup PGEs (Figure 3.3b and Figure 3.4).

An assimilation-fractional-crystallisation (ACF) model (Arndt and Jenner, 1986; Sun et al., 1991) is proposed to explain the genesis of Archean siliceous high-magnesian basalts (SHMB). The average concentration of total PGEs in SHMB is slightly higher than the concentration for the primitive mantle (Table 3.3). On the primitive-mantle normalised diagram, the SHMB curve is very similar to the curves for komatiites and mafic rocks associated with komatiites, showing enrichment in Pd-subgroup PGEs, Cu, and Au (Figure 3.3a).

Table 3.2 Abundances of platinum-group elements and other commonly associated elements in chondrite, primitive mantle, and continental crust.

Element	CI chondrite	Silicate Earth (primitive mantle)	Fertile mantle	Archean mantle	Lower continental crust	Upper continental crust	Average continental crust
Os	490	3.4			0.05	0.031	0.05
Ir	455	3.2	4	3.4	0.05	0.022	0.05
Ru	710	5			0.75	0.34	0.1
Rh	130	0.9			1	0.5	0.06
Pt	1010	7.1	7	7.5	2.7	0.5	0.4
Pd	550	3.9	4	5	2.8	0.52	0.4
Total	3345	23.5	15	15.9	7.35	1.913	1.06
Total Ir subgroup	1655	11.6	4	3.4	0.85	0.393	0.2
Total Pd subgroup	1690	11.9	11	12.5	6.5	1.52	0.86
Pd subgroup/Ir subgroup	1.02	1.03	2.75	3.68	7.65	3.87	4.30
Pd/Ir	1.21	1.22	1.00	1.47	56.00	23.64	8.00
Ni (ppm)	10 500	1960			88	47	56
Cu (ppm)	120	30	28		26	28	25
Au	140	1	1	0.75 to 1.5	1.6	1.5	2.5
Cr (ppm)	2650	2625			215	92	
Ni/Cu	87.5	65.33			3.38	1.68	2.24
Source	1	1	2	1	3	3	4

Source: 1–McDonough and Sun (1995); 2–Sun et al. (1991); 3–Rudnick and Gao (2003); 4–Wedepohl (1995). Concentrations of Rh in lower and upper continental crust from Taylor and McLennan (1995). Values in parts per billion (ppb) unless stated otherwise; ppm – parts per million.

Table 3.3 Average concentrations of platinum-group elements and other associated elements in major mafic and ultramafic igneous rocks.

Element	Bulk Earth (CI chondrite)	Bulk Earth (primitive mantle)	Lherzolite (orogenic)	SHMB <sup>1</sup>	Harzburgite (ophiolite)	Mafic rocks with komatiites	Komatiite
Os	490	3.4	4.3	0.5	4.2	0.29	1.5
Ir	455	3.2	2.7	0.306	3.3	0.49	1.7
Ru	710	5	5.6	2	7	0.8	4.4
Rh	130	0.9	1.6	1.1	1.3	0.9	1.4
Pt	1010	7.1	10	14	8.3	11.8	10.5
Pd	550	3.9	7.4	13.3	6	15.8	10.5
Total	3345	23.5	31.6	31.2	30.1	30.1	30
Total Ir subgroup	1655	11.6	12.6	2.8	14.5	1.58	7.6
Total Pd subgroup	1690	11.9	19	28.4	15.6	28.5	22.4
Pd subgroup/Ir subgroup	1.02	1.03	1.51	10.12	1.08	18.04	2.95
Pd/Ir	1.21	1.22	2.74	43.46	1.82	32.24	6.18
MgO (%)		37.8	39.6	11.8	38 to 44 <sup>2</sup>	12	35 to 52 <sup>3</sup>
Ni (ppm)	10500	1960	2068	257	2178	318	1246
Cu (ppm)	120	30	23	71.2	17	101	64
Au	140	1	5.3	3.2	2.2	4.7	2.9
Cr (ppm)	2650	2625					
Ni/Cu	88	65	90	4	128	3	19
Cu/Pd	0.2	7.7	3.1	5.4	2.8	6.4	6.1
Source	1	1	2	3 and 4	2	2	2

<sup>1</sup> SHMB = siliceous high-magnesian basalt; <sup>2</sup>Oshin and Crocket (1982); <sup>3</sup>Leshner (1989).

Source: 1–McDonough and Sun (1995); 2–Crocket (2002); 3–Barnes and Maier (2002); 4–Sun et al. (1991); Bennet (2003).

Values in parts per billion (ppb) unless stated otherwise; ppm – parts per million.

Table 3.4 Average concentrations of platinum-group elements and other associated elements in major mafic and ultramafic igneous rocks.

Element	Harzburgite (orogenic)	Kimberlite	Harzburgite (abyssal peridotite)	Spinel lherzolite (abyssal peridotite)	Picritic OIB	Continental flood basalt
Os	5.4	1.37	2.2	2.5	0.863	0.62
Ir	3.2	1.37	3	3	1.32	0.08
Ru	5	3.1	5.3	4.5	1.48	
Rh	1.4	0.92	1.4	1.3		0.3
Pt	5.1	9.3	5.6	4.4	5.94	6.2
Pd	3.8	6.1	2	2.8	7.32	8.8
Total	23.9	22.2	19.5	18.5	16.9	16
Total Ir subgroup	13.6	5.8	10.5	10	3.7	0.7
Total Pd subgroup	10.3	16.3	9	8.5	13.3	15.3
Pd subgroup/Ir subgroup	0.76	2.79	0.86	0.85	3.62	21.86
Pd/Ir	1.19	4.45	0.67	0.93	5.55	110
MgO (%)	44.3	9 to 35 <sup>c</sup>			24.4	6.09
Ni (ppm)	2368	1161	2438	2137		85
Cu (ppm)	7	58		20	103	152
Au	13	2.1	0.88	0.61		2.5
Cr (ppm)						
Ni/Cu	338	20		107	0	1
Cu/Pd	1.8	9.5		7.1	14.1	17.3
Source	1	1	1	1	2	1

Source: 1—Crocket (2002); 2—Bennet (2003).

Values in parts per billion (ppb) unless stated otherwise; ppm – parts per million.

Table 3.5 Average concentrations of platinum-group elements and other associated elements in major mafic, ultramafic, and alkaline igneous rocks.

Element	Boninite	OIB	Lamprophyre	Tholeiitic OIB	Alkali OIB	MORB
Os		0.25		0.38	0.11	0.022
Ir	0.07	0.28	0.12	0.38	0.047	0.03
Ru	1.2	0.44	0.35	0.69		0.067
Rh		0.24	0.22	0.11		0.008
Pt	5.4	4.3	3.2	3.6	0.56	0.41
Pd	5.5	4.6	3.2	2.4	0.47	0.46
Total	12.2	10.1	7.1	7.6	1.2	1
Total Ir subgroup	1.27	0.97	0.47	1.45	0.16	0.12
Total Pd subgroup	10.9	9.14	6.62	6.11	1.03	0.878
Pd subgroup/Ir subgroup	8.58	9.42	14.09	4.21	6.56	7.38
Pd/Ir	78.57	16.43	26.67	6.32	10	15.33
MgO (%)	17 <sup>1</sup>	6 to 11 <sup>2</sup>	6 to 14	8.27	4.7	7.4
Ni (ppm)	522	370	179	186	27	144
Cu (ppm)	27	119	52	125	14	88
Au	0.44	2.7	2	1.8	0.35	1.2
Cr (ppm)						
Ni/Cu	19	3	3	1	2	2
Cu/Pd	4.9	25.9	16.3	52.1	29.8	191.3
Source	2	1	1	1	1	2

<sup>1</sup> Brown and Jenner (1989); <sup>2</sup>Table 1A (Crocket, 2000).

Source: 1–Crocket (2002); 2–Peck and Keays (1990).

Values in parts per billion (ppb) unless stated otherwise; ppm – parts per million.

Boninites are considered to be derived from a peridotite source, which is more refractory than the residual material left after the generation of MORBs. This requires either higher temperatures than those required for the prior melting event, or the influx of hydrous fluids which can lower the solidus temperature (Crawford et al., 1989). The average concentration of total PGEs in boninites is much lower than in primitive mantle (~12 ppb compared to ~24 ppb: Table 3.5).

The PGE abundance data summarised in Table 3.3 Table 3.4 and Table 3.5, and in Figure 3.3 and Figure 3.4 indicate that rocks and/or melts, which are generally associated with known PGEs and PGE-enriched Ni-Cu deposits, are enriched in PGEs compared to the primitive mantle. The most potentially fertile rocks show a trend characterised by enrichment in Pd-subgroup PGEs (Figure 3.3a). Iridium-subgroup PGEs are either depleted or reach the concentration levels recorded in the primitive mantle. Abyssal peridotites (harzburgite, spinel lherzolite) show depletion in Pd-subgroup PGEs (Figure 3.3a).

### 3.3 Partition coefficients of platinum-group elements

An important guide of the behaviour of PGEs during partial melting, fractional crystallisation, and melt-melt immiscibility is provided by the Nernst partition coefficients of PGEs. The partition coefficients are derived from experimental studies and from direct measurements of concentrations in natural systems thought to represent an equilibrium between phases, such as sulphide globules on quenched MORB glasses or sulphide globules in a groundmass of basaltic rocks (Crocket, 2002). A detailed summary of partition coefficients can be found in Crocket (2002), Makovicky (2002), Naldrett (2004), and Mungall (2005a,b).

The partition coefficients clearly demonstrate the strong chalcophile behaviour of PGEs. For most PGEs, the partition coefficients between sulphide and coexisting silicate melt are at least an order of magnitude higher than those for Ni and Cu (Table 3.6). The partition coefficients of Ir- and Pd-subgroup PGEs are essentially similar. Copper is more chalcophilic than Ni. Thus, in the presence of a sulphide melt, all PGEs will preferentially dissolve in the sulphide melt, followed by Au, Cu, and Ni.

The partition coefficient between spinel and coexisting silicate melt shows that both Ir and Ru (Ir-subgroup) tend to prefer spinels, whereas both Pt and Pd (Pd-subgroup) prefer the melt. This may explain, to some extent, the commonly observed association between Ir-subgroup PGEs and chromite.

Table 3.6 Preferred values of partition coefficients ( $K_d$ )<sup>1</sup> of platinum-group elements and other related elements for magmas at ~1200°C and at fugacity of oxygen near the QFM buffer (Mungall, 2005a,b).

	Cu	Ni	Os	Ir	Ru	Rh	Pt	Pd	Au
Clinopyroxene/silicate liquid							1.5		
Olivine/silicate liquid				2	2.2	1.9	<0.01	0.01	
Spinel/silicate liquid				5–132	1000	75		0.14	0.08
Spinel/silicate liquid <sup>2</sup>				22–52	78–90		<0.02		
Sulphide/silicate liquid	1383	800	30 000	14 000, 26 000	6400	27 000 <sup>3</sup>	10 000	17 000, 23 000	1200, 15 000
Mss/sulphide liquid	0.2	0.6–1.5	4	5	10	4	0.05	0.1	0.005

<sup>1</sup> The Nernst partition coefficient (see Section 3.3) is defined by  $K_d = (\text{concentration in phase 1})/(\text{concentration in phase 2 melt})$ . A mineral-melt partition coefficient of 1.0 indicates that the element is equally distributed between the mineral and the melt. A value greater than 1.0 indicates that the element has a preference for the mineral phase (i.e., behaves compatibly) whereas a value less than 1.0 implies that the element prefers the melt (behaves incompatibly).

<sup>2</sup> Capobianco and Drake (1990).

<sup>3</sup> Bezmen et al. (1994).

MSS = monosulphide solid solution; QFM = quartz-fayalite-magnetite.

## 3.4 Solubility of sulphur in mafic and ultramafic melts

### 3.4.1 Main factors controlling sulphur solubility

As PGEs are highly chalcophilic, the capacity of mafic melts to transport PGEs depends on the solubility of S in the melts. Two types of S concentrations in melts are discussed in the literature (Mungall, 2005a): concentration of S in melts in response to the externally imposed S fugacity (concentration in the absence of sulphide phases in the melt); and the S concentration at sulphide saturation (SCSS: concentration of S in the melt in the presence of sulphide phases). This latter concentration determines if the melt is sulphide-saturated or sulphide-undersaturated.

Sulphide-saturated melts form a separate sulphide liquid phase as droplets suspended in the silicate melt into which PGEs can readily partition and concentrate.

Experimental studies on the solubility of S in mafic melts are discussed and summarised in many works such as those by Naldrett (1989, 2004, and 2011) and Mungall (2005a). These studies show that SCSS is determined by the composition of the melt, temperature, pressure, and fugacity of O.

The SCSS is found to increase with increasing temperature, but decreases with increasing pressure (Figure 3.5). At 1000°C the melt can dissolve up to 500 ppm S, whereas at 1600°C the concentration can vary from ~500 ppm (at 5 GPa pressure) to ~2500 ppm (at 0.5 GPa pressure: Mungall, 2005a). The temperature and pressure dependence of S solubility shows that melts can become sulphide-saturated during cooling.

However, melts during their ascent toward the surface of the Earth (i.e., decreasing pressure) will also become progressively sulphide-undersaturated. This means that a primary magma extracted from the mantle initially in a state of sulphide-saturation can become sulphide-undersaturated during its ascent. Rise of magma in the crust under adiabatic conditions is accompanied by simultaneous loss of pressure and lowering of temperature. The solubility of sulphide/S in such magmas progressively increases making them progressively undersaturated. According to Mungall (2005a) even magmas

which loose residual sulphides in the source region will remain sulphide-undersaturated as they reach the lithosphere and/or erupt at the surface.

Experimental studies also demonstrate that the solubility of S in mafic melts increases with an increase in the FeO content of the melt (Figure 3.6). At 1400°C and at a pressure of 30 kb, the solubility increases from ~500 ppm (for melts with 5.4% FeO) to ~1500 ppm (for melts with 17% FeO). The FeO content of the melt can change in response to several factors, one of which is felsification of melts due to mixing with felsic melts or due to assimilation of felsic rocks. Irvine (1975) investigated the effect of mixing felsic melt with a mafic melt with an adequately high Cr-content. He showed that such mixing, due to convective turn in a magmatic chamber, can result in the formation of chromitite layers and also generate immiscible sulphide melt.

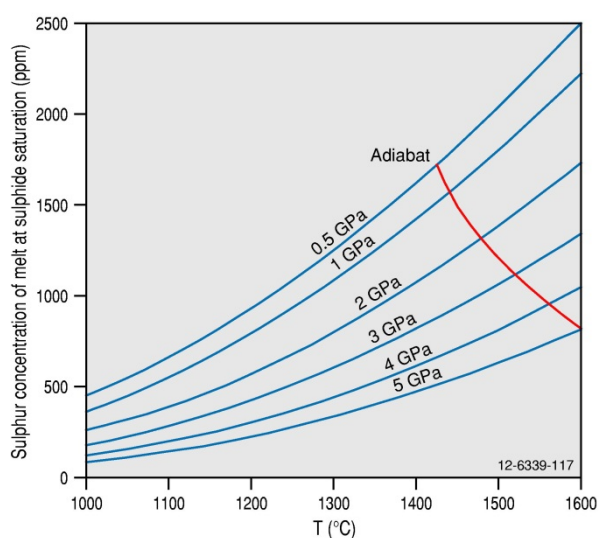


Figure 3.5 Solubility of sulphur (at sulphide saturation) in mafic melts as a function of temperature and pressure (modified from Mungall, 2005a).

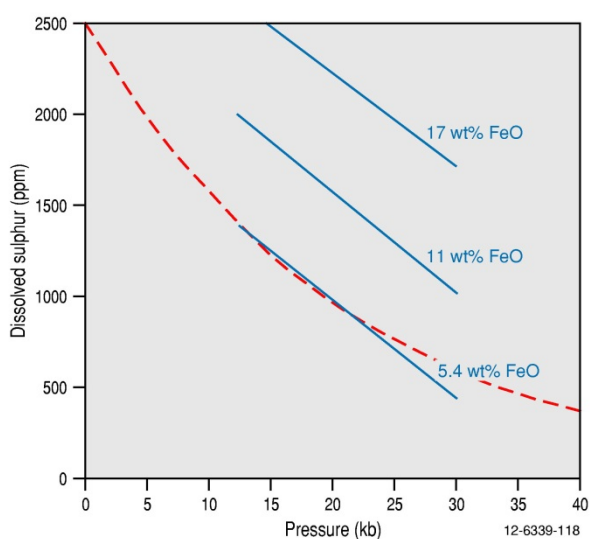


Figure 3.6 Solubility of sulphur in mafic melts as a function of pressure and FeO concentration of melts. Based on data from Wendlandt (1982). The data from Mavrogenes and O'Neill (1999) is shown by the red dashed line.

As the solubility of S in magma increases with increasing FeO concentration (Figure 3.6), Fe-rich melts will require more S to reach sulphide saturation, whereas Mg-rich melts (e.g., ultramafic melts) can reach sulphide saturation earlier and more easily. As a result, removal of PGEs by a sulphide melt formed from ultramafic melts can occur more easily in Mg-rich melts than in Fe-rich melts.

The role of fugacity of O in controlling the solubility of S is not clear (Naldrett, 2004). Shima and Naldrett (1975) studied the solubility of S in komatiitic melt and showed the concentration of S in the melt depended on the fugacity of S and O. It increased with an increase in the fugacity of S, but decreased with an increase in the fugacity of O. However, in their experiments the melt was sulphide-saturated only at  $fO_2 = 10^{-2.4}$  atm and  $fS_2 = 10^{-2}$  atm. At higher O fugacity, the melt remained sulphide-undersaturated. However, experiments performed by Buchanan and Nolan (1979) showed that the solubility of S decreased with an increase in the fugacity of O (Figure 3.7). Mavrogenes and O'Neil (1999), who experimentally determined solubility of S in sulphide-saturated conditions, noted that the S solubility (SCSS) was independent of  $fO_2$  and  $fS_2$ , except insofar as these two factors influence the nature of the sulphide liquid. More recent experimental studies (Jugo et al., 2005) indicate that at temperatures between 1300°C and 1355°C and at pressures between 1 GPa and 1.6 GPa (16 Kbar) basaltic melts can dissolve up to 1.5% S (under oxidised conditions where melt is saturated with sulphate liquid). This measured solubility of S is ten times lower (0.14%) if the basaltic melt is reduced (saturated with sulphide liquid). Thus a high-MgO basaltic magma similar to the Lower Zone (zone below the Critical Zone which hosts the Merensky Reef) of the Bushveld would be able to dissolve 1400 ppm S when saturated in Fe sulphides (Naldrett et al., 2008).

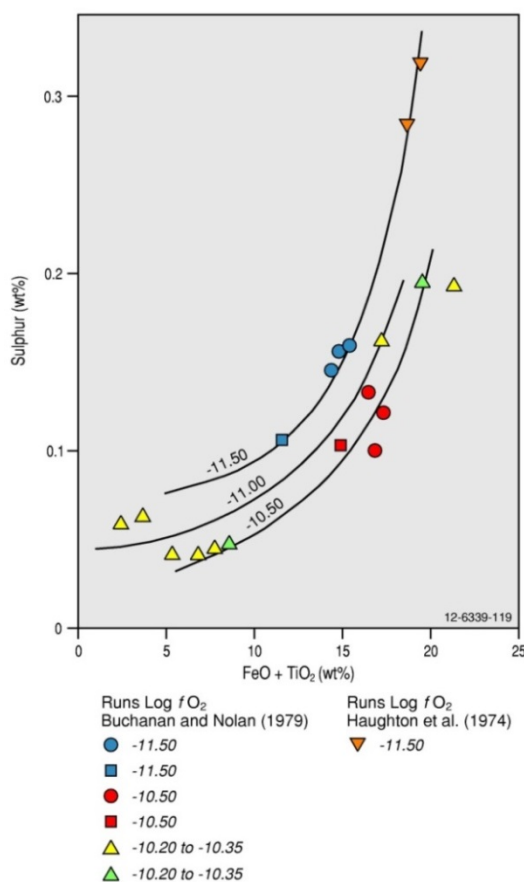


Figure 3.7 Sulphur content of silicate glass in equilibrium with sulphide melt. The solubility of sulphur increases with FeO content of the melts and with an increase in the fugacity of oxygen (modified from Naldrett, 2011).

In summary, sulphide saturation of a melt can be caused by a combination of factors such as:

- cooling;
- increase in pressure, which indicates that a mafic melt on its ascent will become progressively sulphide-undersaturated. Mavrogenes and O'Neil (1999) suggest that most basaltic magmas will never achieve saturation under near surface conditions unless they have undergone at least 60% fractional crystallisation or have acquired crustal S;
- felsification of mafic melt from assimilation of felsic rocks or due to mixing with more felsic melt; and
- assimilation of crustal S.

Sulphur solubility data (Jugo et al., 2005) suggests that sulphide saturation by assimilation of crustal S will depend on the nature of crustal S (sulphate versus sulphide). If crustal S is available as sulphate minerals (e.g., evaporite) a large amount of S (>~1.5%) would be required to achieve saturation. However, even in this case chalcophile elements such as PGEs, Cu, and Ni, which prefer sulphide phases may still remain incorporated into silicate melt (Jugo et al., 2005). A concomitant assimilation of reductant (e.g. carbonaceous sediments) can trigger conversion of sulphate S into sulphide S, and cause sulphide saturation because the solubility of S in basaltic magmas is in equilibrium with sulphide melt which is 10 times lower compared to when the magma is in equilibrium with sulphate melt (see above).

### 3.4.2 Equilibration of silicate and sulphide melts

Very high sulphide/silicate partition coefficients of PGEs indicate that their behaviour during evolution of parent mafic and ultramafic melts is predominantly controlled by processes that cause separation of sulphide liquid (i.e., attainment of sulphide saturation) and interaction between sulphide liquid and silicate melt (i.e., ratio of sulphide liquid and silicate melt). Naldrett (2004) summarises two approaches (R-factor and N-factor) for estimating the effect of silicate-melt to sulphide-liquid ratios.

The ratio achieved by bulk equilibration between silicate and sulphide melt is described by the R-factor. The final concentration of PGEs (and also for Cu and Ni) in the sulphide melt is represented by:

$$C_{sul} = C_o \times D^{sul/sil} [(R+1)/(R+ D^{sul/sil})]$$

In this equation,  $C_{sul}$  = final concentration of the element in the sulphide liquid;  $C_o$  = original concentration of the element in the silicate melt before sulphide saturation;  $D_{sul/sil}$  = partition coefficient of the element between sulphide and silicate melts. Modelling for a magma responsible for the Bushveld Complex shows (Naldrett, 2004) that at low values of R (between 100 and 2000), the Cu concentration of the sulphides reaches levels commonly observed for most Ni ores, whereas Pt concentrations are low. When the R-factor is raised to 10 000 or 100 000, concentrations of Cu and Pt in sulphides increases, but the increase for Pt is much higher and in the range typical of the Merensky Reef (Naldrett, 2004).

The N-factor represents a silicate-melt/sulphide-liquid ratio reached in a 'zone-refining' system. Droplets of sulphide melt separated from a silicate melt in the top part of the magma chamber settle through the magma and interact with successive portions of silicate magma, removing PGEs, Ni, and Cu. The same effect is generated in magma conduits along which fresh pulses of silicate melt can interact with sulphides. A comparison of R- and N-factor modelling of melts (see Figure 2.9 in Naldrett,

2004) shows that the effect of the two processes on the variation and the final concentrations of Cu and Pt in both types of systems are similar, but the increase in the concentration is more rapid for 'zone-refining' systems (N-factor).

In a recent study, Kerr and Leitch (2005) expanded the 'zone-refining' system by modelling a more complex open system in which the sulphide liquid is progressively redissolved by batches of mafic silicate magma interacting with it. It is suggested that this dynamic 'multistage dissolution upgrading' system may be intrinsically self-destructive, but may also be critical in the development of high-grade PGE ores. The extreme chalcophile behaviour of PGEs indicates that the fertility of mafic melts will be predominantly determined by four inter-related factors:

1. timing of sulphide saturation of melt;
2. rate of sulphide saturation of melt;
3. physical environment of sulphide saturation and formation of sulphide liquid; and
4. volume of silicate melt interacting with sulphide liquid (R- or N-factor).

The timing of sulphide saturation is also important during the partial melting of source rocks in the mantle. The PGEs are mainly trapped in sulphide minerals (mainly pyrrhotite), which constitute around 0.07% of the typical upper mantle (Lorand, 1990). Sulphur solubility in mantle-derived silicate melts of between 0.1% to 0.2% means that the silicate melt can attain saturation levels at around 30% of partial melting (Barnes and Maier, 2002). Lower levels of partial melting produces sulphide liquid which may remain undissolved in the silicate melt, and PGEs, which readily partition in to the sulphide liquid, may be sequestered from the silicate melt. A high degree of partial melting (at least ~30%) is considered important to produce melts (e.g., komatiitic and high-MgO basaltic) sufficiently enriched in PGEs to form PGE deposits (Li et al., 2001; see also Chapter 8).

The geochemically distinctive MORB are generated by low-pressure and low levels of melting. As a result, these lavas tend to have very low concentrations of PGEs (Table 3.5: Mungall, 2005a). Arc magmas are also characterised by low concentrations of PGEs (Table 3.5). They are produced by the melting of the mantle wedge above subduction zones and are contaminated by S. As a result, the melts become sulphide-saturated at the source region and thereby lose PGEs in the source region. Melting of S-enriched metasomatised mantle can also produce melts depleted in PGEs (Mungall, 2005a).

Both SHMB and boninites are generated by high degrees (>>30%) of partial melting of peridotite mantle. The high concentration of PGEs in such melts (Table 3.3) may be the result of the fact that they are not depleted in PGEs at the source of melting. The SHMB are also regarded as parental melts for fertile Stillwater and Bushveld complexes (Naldrett, 2004).

A PGE-enriched, sulphide-undersaturated melt can achieve saturation either gradually (fractional crystallisation and/or mixing with new pulses of melt introduced in the chamber), or more actively (assimilation of S-enriched rocks). Passive saturation initially produces small amounts of sulphide melt (hence high values of R-factor) with high concentrations of PGEs. In general, for a given size of magmatic system, high values of R achieved can lead to small tonnage of high-grade ores. Active assimilation can produce large quantities of sulphide melt (hence low values of R-factor) with low concentrations of PGEs. Magmatic systems under conditions of active assimilation can lead to high-tonnage of low-grade mineralisation (Mungall, 2005a).

Sulphide liquid and chromite are thought to be the two main collectors of PGEs. PGE-enriched melt can enter the chamber either saturated with collectors, or can form the collector at a suitable site in the

chamber. Magma conduits are considered to be ideal sites where collectors can accumulate. Such environments also ensure high cumulative values of R-factor. Conduits may take the form of dykes, sills, chonoliths, and other irregular-shaped cylindrical bodies. Local depressions, troughs, and embayments in the basal parts of magma chambers, entry points into and sites of widening of magma chambers, and abrupt changes in the orientation of the conduits can also provide favourable locations for the accumulation of collector phases (Mungall, 2005a).

## 3.5 Platinum-group elements in hydrothermal fluids

### 3.5.1 Fluid-melt partitioning

Many magmatic deposits of PGEs show remobilisation by aqueous fluids (e.g., Schiffries, 1982; Ballhaus and Stumpfl, 1986; Ballhaus et al., 1988; Boudreau and McCallum, 1992; Farrow, 1994). The PGEs also concentrate in many hydrothermal deposits, such as orogenic lode Au, porphyry Cu, unconformity-related U, and sediment-hosted Cu deposits (reviews by Wood, 2002; Hanley, 2005; Wilde, 2005). Transport of PGEs in low-temperature, surficial conditions is demonstrated by the presence of PGE-enriched zones in carbonaceous black shales and laterites (Kucha, 1982; Bowles, 1986).

Hanley and Mungall (2002) studied partitioning of PGEs in S-free, chloride-rich fluids at temperatures more than 600°C. Similar studies were reported by Ballhaus et al. (1994). In the two studies partitioning of Pt between melts and fluid was studied by trapping coexisting phases in synthetic fluid inclusions in quartz. Ballhaus et al. (1994) determined the partitioning of Pt between Ni-Cu-rich monosulphide solid solution (mss) and supercritical chloride fluid containing H<sub>2</sub>S. Hanley and Mungall (2002) investigated partitioning of Pt between S-free chloride-rich fluids and a coexisting melt. Ballhaus et al. (1994) reported highly variable and geologically unrealistic concentrations of Pt in fluids and explained this by suggesting that Pt could have formed multi-atom complexes.

Hanley and Mungall (2002) controlled both the HCl concentration and oxidation state of the fluid. They reported that Pt concentrations in the fluid were of the order of 1 ppm to 1000 ppm and between 35 ppb and 100 ppb in the coexisting melt, and suggested that the Nernst fluid-melt distribution coefficient for Pt was of the order of 100 to 1000. The experiments show that Pt can form chloride complexes. However, the presence of a strong negative correlation between salinity (concentration of chloride in the fluid) and the dissolved concentration of Pt indicates that, in high-salinity fluids, the role of other non-chloride complexes could have been reduced due to 'salting-out' effects.

Hanley (2005) reviewed solubility and speciation of PGEs in fluids at high-temperature magmatic-hydrothermal conditions and suggested that:

- fluids at high temperatures (800–900°C) may be able to dissolve very high (ppm-level) concentrations of Pt;
- the solubility of Pt may be controlled by complexing with HCl (e.g., PtCl<sub>3</sub>H), hydroxyl (e.g., PtOH<sub>2</sub>), or by the formation of heterogeneously distributed colloidal particles or clusters of hydrated Pt oxides or Pt hydroxides;
- in non-aqueous fluids vapour transport of PGEs is significant only at temperatures >1000°C and may be enhanced by the presence of Cl and S in the vapour phase; and
- theoretical predictions of PGE solubility significantly underestimates dissolved PGE solubility.

There is little information on the solubility and speciation of other PGEs in high-temperature hydrothermal fluids (Wood, 2002). Wood (2002) reports Os solubility ranging from between 3 ppb to 1700 ppb in experiments conducted between 400°C and 500°C in chloride fluid with its pH buffered by K-feldspar-muscovite-quartz, and its  $fO_2$  buffered by Ni-NiO buffers.

### 3.5.2 Platinum-group elements in fluids below 300°C

The bivalent PGEs are classified as soft acids and can complex preferentially with soft bases-ligands, such as  $I^-$ ,  $Br^-$ ,  $CN^-$ ;  $CO$ ,  $S^{2-}$ ,  $HS^-$ , and  $H_2S$  (Table 3.7). The PGEs are also known to form complexes with intermediate bases such as  $Cl^-$  (Wood, 2002). Those PGEs with high ionic charges (+4 and +5) are hard acids and will tend to form aqueous complexes with hard bases-ligands, such as  $F^-$ ,  $(OH)^-$ ,  $CO_3^{2-}$ , and  $SO_4^{2-}$ .

The solubility and speciation of Pt and Pd in aqueous fluids at temperatures up to 300°C have been studied by Gammons et al. (1992); Gammons and Bloom (1993); and Gammons (1995, 1996). A comprehensive review of experimental and geochemical modelling studies of PGEs in aqueous fluids at temperatures up to 300°C can be found in Wood (2002) and Hanley (2005).

The review of experimental and geochemical modelling data on the solubility and speciation of Pt and Pd in aqueous fluids at low temperatures reveals the following important conclusions (Wood, 2002):

- In their most common bivalent oxidation state, Pt and Pd form strong aqueous complexes with soft bases (e.g.,  $HS^-$ ) or borderline bases ( $Cl^-$ ). Hydroxide, thiosulphate, and organic complexes may be dominant in low-temperature surficial conditions. Ammonia, bromide, iodide, polysulphide, and sulphite complexes may become important under restricted conditions and are unlikely to cause transport of significant amounts of Pt and Pd.
- Geologically significant concentrations of Pt and Pd can be transported in either very oxidising and/or acidic (pH <4) conditions as chloride complexes, such as  $PtCl_3$  and  $PdCl_4^{2-}$  (Figure 3.8 and Figure 3.9). Thus fluids in equilibrium with hematite and/or clay minerals can transport more than 10 ppm of Pt or Pd. In contrast more reduced fluids (in equilibrium with pyrite, pyrrhotite, chlorite, and epidote) and/or fluids at neutral to alkaline conditions (pH >4) cannot transport enough Pt or Pd to form ore deposits.
- The role of bisulphide complexes in the transport of Pt and Pd is not clear. Bisulphide complexes such as  $Pt(HS)_2$  dominate in fluids with near-neutral pH and oxidising conditions, which are more reduced than the hematite-magnetite buffer. Under these conditions less than 0.5 ppb of Pt or Pd can be dissolved in aqueous fluids.
- Significant concentrations of Pt and Pd can be dissolved in either oxidising (oxidation state above magnetite-hematite buffer) and/or acidic conditions. Reactions causing an increase in pH, or a drop in  $fO_2$  (reduction), can trigger deposition of Pt and Pd. The solubility also increases with temperature. Hence, cooling can also cause deposition of Pt and Pd.
- The solubility of Pt and Pd as chloride and bisulphide complexes shows that Pt is slightly more soluble than Pd. However, the relative behaviour of Pt and Pd in hydrothermal systems will largely depend on the type of minerals Pt and Pd form in these systems.

Table 3.7 Classification of metals and ligands in terms of Pearson's (1963) hard and soft acids and bases principle.

Hard	Borderline	Soft
<b>Acids</b>	<b>Acids</b>	<b>Acids</b>
H <sup>+</sup>	Fe <sup>+2</sup> > Mn <sup>+2</sup> > Co <sup>+2</sup> > Ni <sup>+2</sup>	Au <sup>+</sup> > Ag <sup>+</sup> > Cu <sup>+2</sup> > Hg <sup>+2</sup> > Cd <sup>+2</sup>
Li <sup>+</sup> > Na <sup>+</sup> > K <sup>+</sup> > Rb <sup>+</sup> > Cs <sup>+</sup>	Cu <sup>+2</sup> , Zn <sup>+2</sup> > Pb <sup>+2</sup> , Sn <sup>+2</sup> , As <sup>+3</sup> , Sb <sup>+3</sup> , Bi <sup>+3</sup>	<b>Pt<sup>+2</sup> &gt; Pd<sup>+2</sup> &gt; other PGEs<sup>+2</sup></b> , Tl <sup>+3</sup> > Tl
Be <sup>+2</sup> > Mg <sup>+2</sup> > Ca <sup>+2</sup> > Sr <sup>+2</sup> > Ba <sup>+2</sup>		
Al <sup>+3</sup> > Ga <sup>+3</sup>		
Sc <sup>+3</sup> > Y <sup>+3</sup> ; REE <sup>+3</sup> (Lu <sup>+3</sup> > La <sup>+3</sup> )		
Ce <sup>+4</sup> > Sn <sup>+4</sup>		
Ti <sup>+4</sup> > Ti <sup>+3</sup> > Zr <sup>+4</sup> ~ Hf <sup>+4</sup>		
Cr <sup>+6</sup> > Cr <sup>+3</sup> ; Mo <sup>+6</sup> > Mo <sup>+5</sup> > Mo <sup>+4</sup> ;		
W <sup>+6</sup> > W <sup>+4</sup> ; Nb <sup>+5</sup> , Ta <sup>+5</sup> , Re <sup>+4</sup> > Re <sup>+6</sup> > Re <sup>+4</sup> ; V <sup>+6</sup> > V <sup>+5</sup> > V <sup>+4</sup>		
Mn <sup>+4</sup> ; Fe <sup>+3</sup> ; Co <sup>+3</sup> ; As <sup>+5</sup> Sb <sup>+5</sup>		
Th <sup>+4</sup> ; U <sup>+6</sup> ; U <sup>+</sup>		
<b>PGE<sup>+5</sup> &gt; PGE<sup>+4</sup></b>		
<b>Bases</b>	<b>Bases</b>	<b>Bases</b>
F <sup>-</sup> > H <sub>2</sub> O, OH <sup>-</sup> , O <sup>-2</sup> ; NH <sub>3</sub> > NO <sub>3</sub> ;	Cl <sup>-</sup>	I <sup>-</sup> > Br <sup>-</sup> , CN <sup>-</sup> ; CO
CO <sub>3</sub> <sup>-2</sup> > HCO <sub>3</sub> <sup>-2</sup> > SO <sub>4</sub> <sup>-2</sup> > HSO <sub>4</sub> <sup>-1</sup> ;		S <sup>-2</sup> > HS <sup>-1</sup> > H <sub>2</sub> S
PO <sub>4</sub> <sup>-3</sup> > HPO <sub>4</sub> <sup>-2</sup> > H <sub>2</sub> PO <sub>4</sub> <sup>-</sup>		Organic phosphines (R <sub>3</sub> P), organic thiols (RP); polysulphide, thiosulphate, sulphite
Carboxylates (acetate, oxalate, etc)		HSe <sup>-</sup> , Se <sup>-2</sup> , HTe <sup>-</sup> , Te <sup>-2</sup> ; AsS <sub>2</sub> <sup>-</sup> ; SbS <sub>2</sub> <sup>-</sup>
MoO <sub>4</sub> <sup>-2</sup> > WO <sub>4</sub> <sup>-2</sup>		

*Bold text indicates PGEs, where PGE = Platinum-group elements: platinum, palladium, rhodium, iridium, ruthenium, and osmium).*

*Note: In the case of hard species, the symbol > denotes 'harder than', and in the case of soft species it denotes 'softer than'. The symbol 'R' denotes an organic carbon chain.*

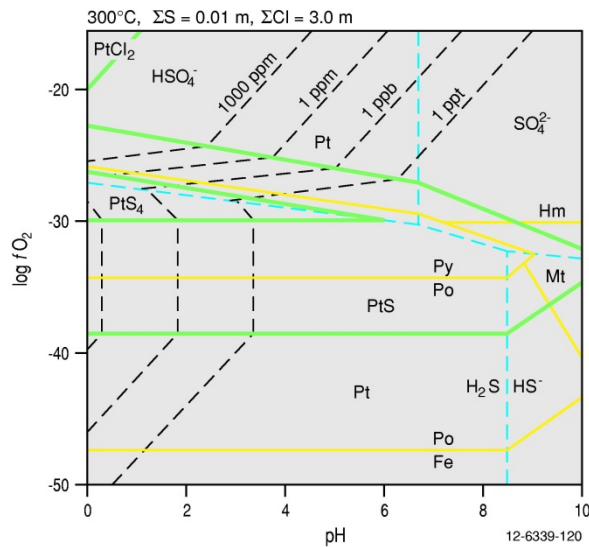


Figure 3.8  $\text{Log}f\text{O}_2$ -pH diagram for the Pt-S-Cl- $\text{H}_2\text{O}$  system at 300°C. The diagram is drawn for  $\Sigma\text{S} = 0.01 \text{ m}$  and  $\Sigma\text{Cl} = 3.0 \text{ m}$ . Heavy solid green lines separate fields of stability of platinum phases, and solid yellow lines define fields of solid phases in the system Fe-S-O. Dashed blue lines separate fields of aqueous sulphur species. The solubility of platinum as chloride complexes is shown as black dashed lines (modified from Wood, 2002).

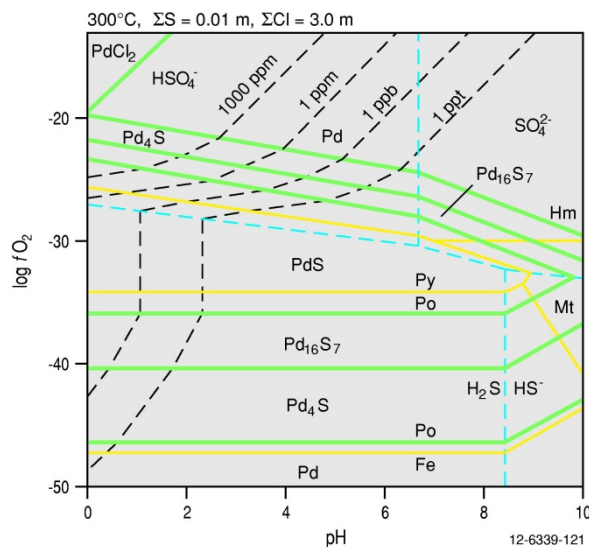


Figure 3.9  $\text{Log}f\text{O}_2$ -pH diagram for the Pd-S-Cl- $\text{H}_2\text{O}$  system at 300°C. The diagram is drawn for  $\Sigma\text{S} = 0.01 \text{ m}$  and  $\Sigma\text{Cl} = 3.0 \text{ m}$ . Heavy solid green lines separate fields of stability of Pd phases, and solid yellow lines define fields of solid phases in the system Fe-S-O. Dashed blue lines separate fields of aqueous sulphur species. The solubility of Pd as chloride complexes is shown as black dashed lines (modified from Wood, 2002).

### 3.5.3 Platinum-group elements in fluids at 25°C

There is mounting evidence of PGE mobility in surficial conditions. PGEs are known to be redistributed during weathering (e.g., Bowles, 1986; Bowles et al., 1993, 1994; Augé and Legendre, 1994; Olivo and Gammons, 1996; Eliopoulos and Economou-Eliopoulos, 2000; Kwitko et al., 2002; Traore et al., 2008). Enrichment of PGEs in black shales (e.g., Coveney et al., 1992; Pasava, 1993; Kucha and Przybyłowicz, 1999) may also be related to transport of PGEs in surface and/or shallow ground waters.

At low temperatures (25°C), speciation and solubility has been studied to some detail only for Pt and Pd (see reviews by Wood (2002) and Hanley (2005)). Bowles (1986) and Brookins (1988) have calculated an Eh-pH diagram showing the stability of aqueous species of Pt, Pd, Rh, Ru, Ir, and Os. However, the data of Brookins (1988) are only relevant for waters without dissolved chloride.

The PGEs at 25°C can form stable chloride, hydroxide, and carbonate complexes (Hanley, 2005). In certain specific conditions, the PGEs can also form complexes with ammonia or amino acids (Jaireth, 1992), humic substances (humic and fluvic acids: Wood, 1990) and carboxylic acids (Hanley, 2005). In saline fluids, the solubility of Pt and Pd is dominated by chloro-complexes, however, even under acidic (pH <4) and very oxidising conditions ( $\log fO_2 > -50$ ), the fluids can only dissolve between 0.01 ppb to 1 ppb Pt (Jaireth, 1992).

The Eh-pH diagram calculated by Bowles (1994) shows that under similar conditions Pd is more soluble than Pt although the solubility of both Pt and Pd is  $\sim 10^{-4}$  ppb. According to this diagram, Pd will tend to move to relatively deeper parts of the lateritic profile than Pt. Calculations by Brookins (1988) demonstrate some difference in the relative solubility of PGEs. Under oxidising conditions, Ru and Os are more soluble than the other PGEs because the aqueous species formed by them are more stable. Both Ir and Os are also soluble in oxidising and alkaline (pH >8) conditions, whereas other PGEs need more acidic conditions (pH <4).

### 3.6 Conclusions

The discussion on the igneous and hydrothermal geochemistry of PGEs, summarised in this chapter, shows why certain magmas produced under specific conditions are more favourable to form orthomagmatic ore deposits of PGEs. It also shows that, although PGEs can be dissolved and transported by hydrothermal fluids, they may be able to dissolve geologically significant concentrations of PGEs only at very high, near-magmatic, temperatures (>500°C). This review demonstrates the following important points relating to the fertility of PGE-forming mineral systems.

- The behaviour of PGEs in magmatic mineral systems is controlled by their highly pronounced chalcophilic character. All PGEs overwhelmingly favour sulphide phases (melts and solids) and thereby the S concentrations of melts and sulphide-saturation of melts affects the fertility of parental melts. The Ir-subgroup PGEs (Os, Ir, Ru) show more affinity to chromite and spinels than the Pd-subgroup PGEs (Rh, Pt, Pd). Sulphide and chromite/spinel phases are the two main collectors of PGEs.
- Amongst different types of parental magmas, MORB and normal arc magmas are considered to have low potential because they are significantly depleted in PGEs. In contrast, picritic and komatiitic parental melts form as a result of high degrees of partial melting of the mantle and because they are sulphide-undersaturated in the source region, they are sufficiently enriched in PGEs to form ore deposits. Any process (such as low-level partial melting, and presence of S-enriched material), which will cause sulphide-saturation at the site where the parental magma is generated, can make them potentially less favourable to form PGE deposits.
- Parental magmas produced from a high-degree of partial melting and remain sulphide-undersaturated in the source have the potential to be PGE fertile. Boninitic magmas, considered to have been formed from second-stage melting, can also be sulphide-undersaturated in the source region and thereby carry significant concentration of PGEs.

- Magmas containing PGEs undergo sulphide saturation after reaching the lithosphere, or after erupting. The sulphide-saturation can be caused by a combination of factors, such as cooling; assimilation of crustal S; and/or felsification of magma by either assimilation of felsic rocks or due to mixing with more felsic melt.
- The size of a PGE deposit generally depends on the amount of silicate magma equilibrating with the sulphide melt (the R- and N-factors). In layered mafic-ultramafic intrusions, a high R-factor is achieved by interaction of sulphide melt with silicate melt during crystal fractionation and during with fresh pulses of parental magma. Large magma chambers and associated extrusive magmatic settings that represent voluminous, open-magma systems (e.g., dynamic magma chambers with comagmatic flood basalts), and large-scale and efficient mixing processes will facilitate the formation of high R-factor PGE-enriched sulphide layers. High bulk silicate/sulphide ratio (N-factor) can also be achieved in magma conduits, local depressions, troughs and embayments in the basal parts of magma chambers, entry points into and sites of widening of magma chambers, and abrupt changes in the orientation of the conduits. It is envisaged that the R-factor of sulphide droplets perhaps buoyantly entrapped within a narrow conduit could be significantly enhanced by the flushing past of regular pulses of fertile silicate magma. All these sites are considered favourable locations for PGE-Ni-Cu and Ni-Cu-PGE deposits. Thus, economically important PGE deposits generally require a large volume of mafic-ultramafic magma.
- As sulphide-silicate partitioning coefficients for PGEs are significantly greater than those for Cu and Ni, saturation of magmas with sulphide causes abrupt changes in the concentration of these elements. The significance of the changes in Cu/Pd and Cu/Zr ratios in assessing sulphide-saturation of magmas and their application to exploration has been discussed in a number of studies (Hoatson and Keays, 1987a,b, 1989; Barnes et al., 1993; Hoatson, 1998; Maier et al., 1996, 2003; Maier, 2005) and is highlighted in Table 8.4.
- Limited data on the solubility of PGEs in hydrothermal fluids at high (near-magmatic) temperatures show that under certain conditions, hydrothermal fluids can significantly enrich and/or remobilise PGEs formed from magmatic melts. The solubility of PGEs in fluids at temperatures below 300°C is generally low and requires acidic and/or oxidising conditions to dissolve and transport geologically significant concentrations of PGEs.
- Effective exploration for PGE deposits depends on identifying various petrological and geochemical signatures, which can indicate that (1) a fertile (PGE-bearing) parental magma was sulphide-undersaturated in the source regions, and (2) reached sulphide-saturation in the magma chamber and/or after its eruption. The exploration applications of these petrological and geochemical signatures are summarised in Chapter 8 (e.g., Table 8.4).

# 4 Properties and applications of the platinum-group elements

Dean M. Hoatson

## 4.1 Introduction

The six PGEs—platinum, palladium, rhodium, iridium, osmium, and ruthenium—have unique physical and chemical properties (Table 4.1 and Table 4.2). These properties make them critical materials for many emerging technologies which are becoming increasingly commonplace in today's society. Their commercial applications are highlighted in the chemical, electrical, electronic, motor vehicle, aerospace, jewellery, dentistry, and agriculture industries, and in environmental-based technologies. Of the six metals, Pt and Pd are the most important commercially, with some of the other PGEs (e.g., Rh) expanding their commercial applications. Substitution by other cheaper metals is generally not a feature of these precious metals, although individual PGEs are sometimes replaced by another member of the group. Due to their scarcity and durable inert qualities, many industries have relied on recycling the PGEs for future needs. The recycling of Pt and other PGEs from nitric acid gauzes, glass fibre bushings, and reforming catalysts is becoming increasingly important for the marketing sustainability of these rare metals. Networks have been established for the recycling of automotive emission catalysts that have impacted on the global Pt, Pd, and Rh markets.

Table 4.1 Physical properties of the platinum-group elements.

	Platinum	Palladium	Rhodium	Iridium	Osmium	Ruthenium
Chemical symbol	Pt	Pd	Rh	Ir	Os	Ru
Element category	T M <sup>1</sup>	T M	T M	T M	T M	T M
Group, period, block	10, 6, d	10, 5, d	9, 5, d	9, 6, d	8, 6, d	8, 5, d
Atomic number	78	46	45	77	76	44
Atomic weight (g mol <sup>-1</sup> )	195.08	106.42	102.91	192.22	190.23	101.07
Atomic radius (pm)	139	137	134	136	135	134
Density (g cm <sup>-3</sup> )	21.45	12.02	12.41	22.56	22.59	12.45
Appearance	silvery white	silvery white	silvery white	silvery white	silvery white	silvery white
Characteristics <sup>2</sup>	l, s, m, d	l, s, m, d	l, d, h	h, b	l, h, b	h, b

<sup>1</sup> T M: Transition Metal.

<sup>2</sup> l—lustrous, s—soft, m—malleable, d—ductile, h—hard, b—brittle.

Sources: Johnson Matthey (1985); Info Comm (2009); Wikipedia (2009); Theodore Gray (2010) at [periodictable.com](http://periodictable.com); FindTheBest: Compare Chemical Elements (<http://chemical-elements.findthebest.com/>); WebElements (<http://www.webelements.com>).

Table 4.2 Abundance and other properties of platinum-group elements.

	Platinum	Palladium	Rhodium	Iridium	Osmium	Ruthenium
<b>Abundances</b>						
Earth's crust plus mantle (ppb) <sup>1</sup>	6.6	3.6	0.9	3.2	3.4	5
Meteorites (%)	0.000098	0.000066	0.000018	0.000054	0.000066	0.000081
Sun (10 <sup>-7</sup> %)	9	3	2	2	2	5
Universe (10 <sup>-7</sup> %)	5	2	0.6	2	3	4
<b>Other Properties</b>						
Crystal structure	FCC <sup>2</sup>	FCC	FCC	FCC	HCP <sup>3</sup>	HCP
Moh's hardness	4-4.5	4.75	6	6.5	7	6.5
Vickers hardness (MPa)	549	461	1246	1760	NA	NA
Brinell hardness (MPa)	392	37.3	1100	1670	3920	2160
Melting point (°C)	1768.3	1554.9	1964	2466	3033	2334
Boiling point (°C)	3825	2963	3695	4428	5012	4150
Heat of fusion (kJ mol <sup>-1</sup> )	22.17	16.74	26.59	41.12	57.85	38.59
Heat of vaporisation (kJ mol <sup>-1</sup> )	469	362	494	563	738	591.6
Specific heat capacity (J mol <sup>-1</sup> K <sup>-1</sup> ) <sup>4</sup>	25.86	25.98	24.98	25.10	24.7	24.06
Thermal conductivity (W m <sup>-1</sup> K <sup>-1</sup> ) <sup>5</sup>	71.6	71.8	150	147	87.6	117
Thermal expansion (µm m <sup>-1</sup> K <sup>-1</sup> ) <sup>6</sup>	8.8	11.8	8.2	6.4	5.1	6.4
Tensile strength (MPa)	125- 240	169.9	695	1096.5	NA	556
Poisson ratio	0.38	0.39	0.26	0.26	0.25	0.30
Electronegativity (Pauling scale)	2.28	2.2	2.28	2.2	2.2	2.3
Electrical resistivity (nΩ m) <sup>7</sup>	105	105.4	43.3	47.1	81.2	71
Electrical conductivity (10 <sup>6</sup> cm <sup>-1</sup> Ω <sup>-1</sup> )	0.0966	0.095	0.211	0.197	0.109	0.137
Istotopes <sup>8</sup>	6	6	1	2	7	7

<sup>1</sup> Abundance data of Earth's crust plus present mantle from Taylor and McLennan (2009).

<sup>2</sup> FCC: Face-Centred Cubic.

<sup>3</sup> HCP: Hexagonal Close-Packed.

<sup>4</sup> Specific heat capacity at 25°C.

<sup>5</sup> Thermal conductivity at 300°K.

<sup>6</sup> Thermal expansion at 25°C.

<sup>7</sup> Electrical resistivity at 20°C.

<sup>8</sup> Number of naturally occurring isotopes.

NA = Not Available.

Sources: Johnson Matthey (1985); Info Comm (2009); Theodore Gray (2010) at [periodictable.com](http://periodictable.com); FindTheBest: Compare Chemical Elements (<http://chemical-elements.findthebest.com/>); WebElements (<http://www.webelements.com>).

Osmium (density 22.59 g cm<sup>-3</sup>), Ir (22.56 g cm<sup>-3</sup>), and Pt (21.45 g cm<sup>-3</sup>) are the densest metals known. Platinum is twice as dense as Pb and 11% more dense than Au, whereas Ru (12.45 g cm<sup>-3</sup>), Rh (12.41 g cm<sup>-3</sup>), and Pd (12.02 g cm<sup>-3</sup>) are relatively lighter, with Pd having about the same density as Ag. Iridium is notable for being the most corrosion-resistant element even at temperatures as high as 2000°C. They have some of the highest melting points of all metallic elements. All six PGEs have melting points exceeding the melting point of Fe (1535°C), ranging from 1555°C for Pd to 3033°C for Os. The PGEs display a variety of attributes including strength, hard-wearing, lustrous, brittle, ductile, malleable, electrically and thermally conductive, and they are efficient catalysts. Their noble metal

characteristics reflect their inability to interact or combine with most other elements or compounds. The unusual physical and chemical characteristics described above, combined with their scarcity in nature (see Section 1.1), have made the PGEs strategically important in many industries, and highly valued as decorative and investment commodities. Currency crises, political turmoil, and inflation are some of the reasons why investors seek the investment opportunities of the PGEs.

The unique properties of the PGEs have in recent times made the PGEs increasingly important in a range of environmental-based technologies (e.g., catalytic converters, fuel cells, electronics). These favourable benefits for the environment have led them to be hailed as the 'environmental metals'. The catalytic properties of Pt, Pd, and Rh constitute one of their major values to the chemical, agriculture, and automotive industries. Catalysts are used to speed up or slow down chemical reactions without undergoing any change itself. Platinum, Pd, and Rh alloys are extensively used for the production of various acids and are an intermediate step in the production of Ni fertilisers, an important source of plant nutrients. The most significant industrial demand for PGEs is to catalyse key reactions involved in fuel production and engine emission control for the automotive industry. Brennan (2008) noted that the two key properties that allow the PGEs to be used in catalytic converters in modern cars are: (1) the stability of the PGEs in air at relatively high temperatures; and (2) the remarkable ability of the PGEs to chemisorb simple gaseous molecules, like O<sub>2</sub> and CO and, consequently, the rates of certain reactions are vastly accelerated by the presence of PGE-bearing metal surfaces. Catalytic converters were introduced into the USA car market in 1974, and they soon spread to Japan (1976), and later to South Korea (1987), Mexico (1989), the member states of the European Union (1993), Brazil (1994), and China (2000). Catalytic converters are now fitted to more than 85% of new cars in the world, and the automotive industry accounts for more than half the consumption of Pt, Pd, and Rh.

Research on fuel cells, which convert O and H to water and electricity through the catalytic activity of Pt, is increasing and there is potential for a major new market for Pt and Pt alloys. The high recyclability characteristics of the PGEs also minimises their load on the environment.

The high electrical and thermal conductivity, high resistance to corrosion and wear as alloys, selective resistance to acids, and extremely high-melting temperatures of the PGEs, make them particularly useful as electrical contacts in integrated circuits, in high-temperature electrical circuitry and thermocouples, in glass manufacture and laboratory apparatus. Alloys are used extensively in dentistry and medical hardware, and certain Pt compounds are used in anti-cancer chemotherapy.

The PGEs have been used in jewellery items over many centuries (see Section 2.1) and in more recent times, jewellery items made of the white metals Pt, Pd, 'white gold', and Ag have impacted on the traditional yellow gold market. The increasing growth of demand for Pd in jewellery over the last decade has largely been driven by Japan and China. Platinum is also highly valued in investment mediums such as 500 g and 1 kg bars and coins. Platinum was first used for coinage by the Imperial Russian Government in 1828. However, after the conversion of half a million ounces of Pt into coins, the minting of the Russian roubles in 1846 ceased. It was another ~150 years before Pt was once again used in a legal tender coin, namely the Isle of Man Noble in 1983, which was soon followed by coins from Australia, Canada, and the USA.

Platinum-group elements have also been traditionally used for standard unit measures. In 1874, Pt-Ir alloys were used as a standard metre length, but it was later revealed that some Fe and Ru impurities were also present. Some fifteen years later, a more pure alloy bar known as the 'International Prototype Meter' bar was cast with 90% Pt and 10% Ir and was accepted by the International Bureau of Weights and Measures in Paris as the standard length of one metre (Figure 4.1a). Twenty-nine

identical copies of the prototype were also made in 1889, and distributed to nations to serve as national standards. Small elliptical areas on the upper surface of the central rib at each end of the bars were highly polished, and three lines, nominally 0.5 mm apart, were ruled on these surfaces, the distance between the middle lines of each group defining the standard length of one metre measured at 0°C. This bar remained as the defining unit length until 1960 when more precise measurement methods involving a line in the atomic spectrum of krypton were implemented. The 'International Prototype Kilogram', that is defined by a cylinder of a Pt-Ir alloy made in 1879, still remains the international standard of mass (Figure 4.1b). It is stored in an airtight jar in the International Bureau of Weights and Measures in Sevres, Paris. The alloyed metals protect the cylinder from reacting with O and other chemicals in the air ensuring the standard's weight will always remain constant.

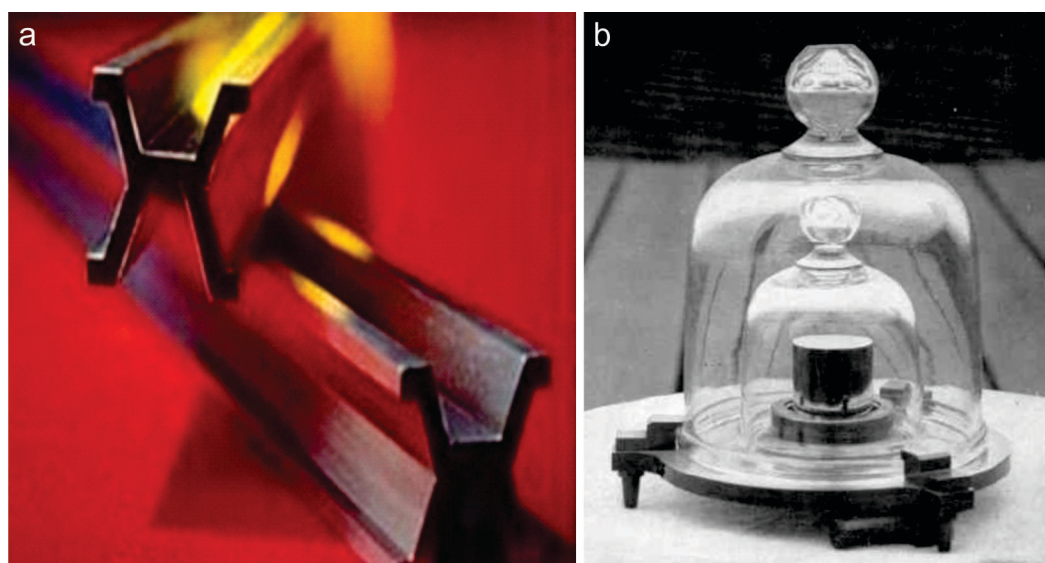


Figure 4.1 (a). International Prototype Metre standard bars made of 90% platinum and 10% iridium alloy. The bars have a distinctive 'X' cross-section to provide maximum rigidity. Image from Wikimedia Commons. (b). A standard kilogram weight of platinum-iridium alloy kept by the National Institute of Standards and Technology, USA, is an exact copy of the international prototype made in 1879 and now stored in the International Bureau of Weights and Measures in Sevres, Paris. It differs in mass from the prototype kilogram by about 75 micrograms. Image from Wikimedia Commons.

Table 4.3 and Table 4.4 summarise the major physical attributes and the applications of the six PGEs respectively. The 'uniqueness' of their attributes is reflected by the diversity of their applications in a wide range of industries, e.g., chemical, electrical, electronic, motor vehicle, aerospace, agricultural, jewellery, and environmental. In addition, the overlap in many of their attributes (e.g., all six PGEs have high-melting and boiling points and are electrically conductive) makes the PGEs ideal for combining as alloy metals for specialised applications.

The following section on the major properties and applications of the PGEs has been partly sourced from the annual Platinum reports and reviews by Johnson Matthey PLC (2000 to 2014), in particular, the Platinum Metals Review, Virtual Issue 5 'The Platinum Decathlon', August 2012 Johnson Matthey, (2012), Hoatson and Glaser (1989); and Info Comm (2009), provides a comprehensive summary of PGE applications and developments.

Table 4.3 Major physical attributes of the platinum-group elements.

	Platinum	Palladium	Rhodium	Iridium	Osmium	Ruthenium
High density	<input checked="" type="checkbox"/>			<input checked="" type="checkbox"/>	<input checked="" type="checkbox"/>	
Moderate density		<input checked="" type="checkbox"/>	<input checked="" type="checkbox"/>			<input checked="" type="checkbox"/>
Hard-wearing			<input checked="" type="checkbox"/>	<input checked="" type="checkbox"/>	<input checked="" type="checkbox"/>	<input checked="" type="checkbox"/>
Soft-wearing	<input checked="" type="checkbox"/>	<input checked="" type="checkbox"/>				
Malleable	<input checked="" type="checkbox"/>	<input checked="" type="checkbox"/>				
Ductile	<input checked="" type="checkbox"/>	<input checked="" type="checkbox"/>				
Brittle				<input checked="" type="checkbox"/>		
Lustre-reflectance	<input checked="" type="checkbox"/>	<input checked="" type="checkbox"/>	<input checked="" type="checkbox"/>		<input checked="" type="checkbox"/>	
Corrosion-oxidation resistant	<input checked="" type="checkbox"/>	<input checked="" type="checkbox"/>	<input checked="" type="checkbox"/>	<input checked="" type="checkbox"/>		<input checked="" type="checkbox"/>
Catalyst	<input checked="" type="checkbox"/>	<input checked="" type="checkbox"/>	<input checked="" type="checkbox"/>	<input checked="" type="checkbox"/>		
Chemical volatility		<input checked="" type="checkbox"/>			<input checked="" type="checkbox"/>	
High-melting point	<input checked="" type="checkbox"/>					
High-boiling point	<input checked="" type="checkbox"/>					
Conductive (electrical)	<input checked="" type="checkbox"/>					
Conductive (thermal)			<input checked="" type="checkbox"/>	<input checked="" type="checkbox"/>		<input checked="" type="checkbox"/>

Table 4.4 Applications of the platinum-group elements.

Applications	Platinum	Palladium	Rhodium	Iridium	Osmium	Ruthenium
Catalytic converters (vehicles)	M	M	M	m		
Catalytic converters (petroleum)	m	m	m	m		m
Jewellery	M	M	m			m
Electronic	m	M			m	M
Electrical	m	M	m	m	m	
Chemical	m	m	m	m	m	M
Defence-aerospace	m	m	m	m	m	m
Medical	m	m	m	m	m	m
Fuel cells	m	m			m	
Dental	m	m				
Laboratory	m		m	m	m	m
Financial investment	m	m				
Coinage	m	m	m			
Glass	m		m			
Decoration	m		m			
Magnets	m					
Photography		m				

*M = major application, m = minor application.*

## 4.2 Platinum

Platinum (pronounced PLAT–num) is represented by the chemical symbol Pt in Group 10 of the Periodic Table of Elements and it has an atomic number of 78 (Figure 1.1a; Table 4.1 and Table 4.2). Platinum is more precious than Au and Ag and it is considered the most important member of the PGEs. It is regarded today the most valuable precious metal because it has a small supply base and is used in many industrial applications (Figure 4.2–Figure 4.6). However, its expensive status does limit its use in every-day appliances. Platinum is also considered a strategically important metal by the United States Government due to its applications in the defence, medical, and telecommunications industries. This rare metal is stockpiled by the government for possible defence emergencies.

Platinum (with Ru) is the most abundant (0.001 ppm in lithosphere) of the PGEs, being about 300 times more abundant than Ir. However, Pt comprises only ~1–10 ng g<sup>-1</sup> of the Earth's crust making it a rare metal, with annual output less than a tenth of Au. Platinum is a soft, malleable, ductile, and lustrous precious metal. Platinum wire can be drawn down to 0.0006 mm diameter for commercial supply, which is much thinner than aluminium foil, and a gram of Pt can be stretched into a wire over 2 km-long. Platinum is one of the densest (21.45 g cm<sup>-3</sup>, i.e., a cubic centimetre of Pt weighs 21.45 times as much as a cubic centimetre of water) and heaviest of metals. For example, a fifteen centimetre-wide (~6 inch) cube of Pt weighs about as much as an average man (~72 kg). Platinum has a melting point of 1768°C and it is extremely resistant to oxidation and to corrosion with other chemical elements. It does not oxidise at any temperature and it is insoluble in hydrochloric and nitric

acids. However, it is corroded by halogens, cyanides, S, caustic alkalis, and dissolves in aqua regia (mixture of hydrochloric and nitric acids). Hydrogen and O gas mixtures explode in the presence of Pt wire. It is also a very good conductor of electricity and a powerful catalysing agent. It has been employed in catalysts since the early 1800s when Pt powder was used to catalyse the ignition of H. An unusual property of Pt is that it will absorb large quantities of H gas at high temperatures, similar to the way a sponge soaks up water. Its catalyst applications have expanded to the automobile industry, and in producing high-octane fuels and vegetable oils. The making of catalysts is the most important use for this precious metal. Platinum has generally maintained its monetary value over many centuries and it is often associated with Au as an investment item. All of these properties described above have been exploited for many industrial, chemical, electrical, and investment applications. Catalytic converters and jewellery dominate the global consumption of Pt, with both applications accounting for more than 74% of the world's supply of Pt.

#### 4.2.1 Catalytic converters

Platinum, Pd, and Rh are essential components of catalysts (Figure 4.2). In 1949, Universal Oil Products pioneered the use of Pt catalysts for the oil refining industry, as a means to upgrade low-octane petroleum naphtha to high-quality products. This technology subsequently became the principal method of producing high-octane fuels for automobiles and piston-engine aircraft. Autocatalysts that control noxious vehicle exhaust emissions have traditionally been one of the biggest applications of Pt. Autocatalysts were introduced in 1974 to assist with the more efficient burning of fuel in a car and the conversion of unburned hydrocarbons and carbon monoxide into less harmful carbon dioxide, N, and water vapour. Mixtures of Pt, Pd, and Rh were used, with Rh suitable for nitrogen oxide conversion and both Pd and Pt having excellent activity for oxidation reactions of carbon monoxide and hydrocarbon species. Demand for Pt in autocatalysts increased significantly in the 1970s when clean air legislation was introduced in USA and Japan. This demand has also grown in emerging countries which have introduced new environmental legislation. Platinum is also widely used in Europe because it is an essential element in diesel cars. In the 1990s, Pd was widely substituted for Pt in autocatalysts in the United States due to its relatively lower cost and superior performance. In recent years, various combinations of Pt, Pd, and Rh have been used for autocatalyst applications. These fluctuations in PGE demand were due to changing market conditions and advances in technology, such as fuel quality, especially S content; emissions legislation; vehicle technology including engine calibrations and fuelling systems; exhaust layout; and relative prices of the PGEs. The application of Pd and Rh in autocatalysts has recently gained favour relative to Pt. The demand for Pt in catalytic converters for emission control in the future may grow as stricter standards and regulations are approved. Being the largest consumer of the metal, Pt demand, and therefore price, is closely correlated to the various trends of the automotive industry.

Other catalytic applications involving Pt include in the production of formaldehyde, and sulphuric and nitric acids in the chemical industry, production of biodegradable elements for household detergents, production of fertilisers and synthetic fibres, and as a refining agent in the petroleum industry. In these catalytic processes, the catalyst material is not consumed and can be recycled for future use. Platinum gauze or mesh is used in cracking processes in crude oil refining. Crude oil must be treated before it is converted to high-octane fuel, fuel oil, and other petroleum products. The molecules are separated, rearranged, and compiled into new patterns.

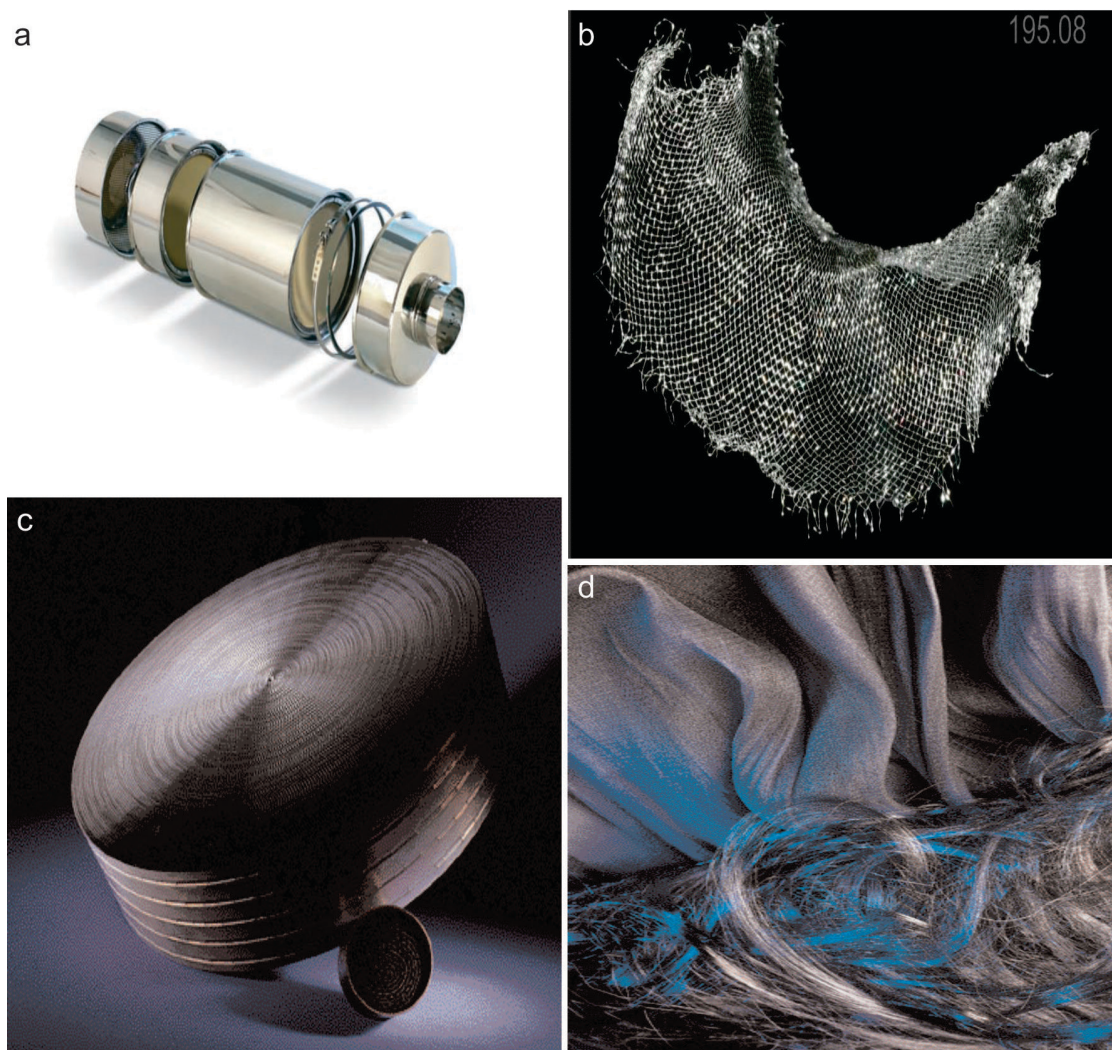


Figure 4.2 Modern applications of platinum. (a). Platinum-based catalyst that oxidises  $\text{NO}$  to  $\text{NO}_2$  which can then react with soot to produce carbon dioxide and nitrogen. A number of other filter systems use platinum, and sometimes palladium as well, for similar purposes. Catalytic systems being fitted to vehicles is one of the main factors behind the increase in platinum use in the automotive market. Johnson Matthey PLC (2007). (b). Fine ultrapure woven platinum cloth and mesh is used in catalytic cracking processes in crude oil refining. Reproduced with the permission of © 2010 Theodore Gray [periodictable.com](http://periodictable.com). (c). Autocatalysts for heavy-duty trucks have been growing markets for platinum. Reproduced with the permission of © 2010 Theodore Gray [periodictable.com](http://periodictable.com). (d). Platinum wire is knitted into catalyst gauze for nitric acid production. Johnson Matthey PLC (2001).

#### 4.2.2 Jewellery

The appealing silvery-white colour, high lustre, rarity, hardness, strength, hypo-allergenic, and resistance to tarnishing properties of Pt have led to it being widely used in such jewellery items as rings, bracelets, ear rings, watch bands, and pins (Figure 4.3). Platinum is alloyed with Pd, Ru, and Ir, and in some cases Cu and Co to optimise its strength and resistance to tarnish. It provides a secure framework setting for diamonds and other gemstones, and its flexibility is an important asset for jewellery designers. Gold is often used for large reflective sheet areas, but it is too soft (Vickers hardness 216 MPa) for some hard-wearing jewellery items. For these applications it can be alloyed with much harder Pt (Vickers hardness 549 MPa) or with other PGEs. In the 1960s, Japan became the world's principal Pt jewellery market, with such attributes as high purity, prestige, and white colour gaining status. A European revival began in Germany in the 1970s with the advent of stark modern

designs, followed by Italy in the 1980s, and Switzerland and the United Kingdom in the 1990s. During the last decade, the demand has steadily increased in North America with the appeal of Pt bridal jewellery, and in China its demand has surged where the white metal is regarded as the modern precious metal for the 'new millennium'. Platinum is used in the watch industry to produce cases and straps for high-quality watches that contain complex mechanical movements. Most of these watches are assembled in Switzerland. Patek Philippe, Vacheron Constantin, Rolex, and Breitling use Pt for producing their limited edition watch series. The market for Pt-bearing watches increased from 1200 watches in 1987 to 13 000 watches in 2004. Platinum watches are normally made from 95% Pt alloyed with Ru. It takes three times longer to produce a Pt case compared to one made in Au. Possessing different metallurgical properties to Au, the Pt is usually hand-polished by specialised polishers. Watchmakers highly appreciate the unique properties of Pt as it neither tarnishes nor wears out. The frame of the crown of Queen Elizabeth the Queen Mother, manufactured for her coronation as Consort of King George VI, is made of Pt. It was the first British crown to be made of Pt.



Figure 4.3 Modern applications of platinum. (a). A growing range of platinum chain designs is available to consumers. Johnson Matthey PLC (2002). (b). The silvery-white colour, high lustre, strength, and lack of tarnishing make platinum an ideal metal for rings. Johnson Matthey PLC (2006). (c). Stamped platinum washers are machined into wedding rings. Johnson Matthey PLC Photograph Collection. (d). Platinum watches from Patek Philippe. Johnson Matthey PLC Media Library.

### 4.2.3 Fuel cells

Fuel cells are devices for generating electric power by combining H (the fuel) and O (from air) through the catalytic activity of Pt. They have no moving parts, require no recharging, and run indefinitely when supplied with fuel. By generating power silently and only emitting pure water as a by-product, fuel cells have environmental advantages since they do not contribute to noise or air pollution. The superior energy efficiency of fuel cells will result in significant reductions of carbon dioxide and greenhouse gases. Fuel cells are used as an alternative to internal combustion engines in conventional vehicles and in more specialised mediums such as the Space Shuttle. In 1997, Daimler-Chrysler, Ford, and Ballard Power Systems formed a consortium to build fuel cell engines for motor vehicles. Thirty fuel cell buses went into service in Europe in 2004 to increase public awareness of fuel cells. Most fuel cells apply proton exchange membrane technology to produce energy for powering cars and buildings instead of batteries and generators. The major obstacle to fuel cell commercialisation is cost. Fuel-efficiency mandates by governments are accelerating research in fuel cells. In the United States and Japan this research is focussed at improving cell performance and developing low-cost materials to compete against batteries and conventional engines. Although fuel cells are currently subeconomic, advances in efficiency are predicted, and a major new market for Pt and Pt alloys may develop.

### 4.2.4 Investment

The relative scarcity, historical price performance, and unique fundamentals of Pt have made it an attractive commodity for investment opportunities (Figure 4.4). Investors have long used precious metals as a means of stabilising their investment portfolios and hedging assets against inflation. Precious metals also tend to appreciate in value during periods when other financial assets decline. Like Au and Ag, Pt provides an attractive means of exchange by virtue of its internationally standardised form and purity. Investment mediums include futures and options, Pt bars up to one kilogram (32.15 troy ounces) in weight, bullion coins and collectors' coins. The Arab Oil Embargo in 1975 initiated price increases in precious metals and investment Pt bars were introduced into Japan. Johnson Matthey & Co Ltd and Engelhard Corporation produced one and ten ounce Pt bars. During the early 1980s, interest in Pt bullion investment spread to Europe, the United States of America, Australia, and Canada. In 1983, The Isle Of Man issued a one ounce investment coin, the Noble Pt bullion coin, which became so popular that other mints issued their own Pt legal tender bullion coins. Such coins like the Australian Koala (1988), Canadian Maple Leaf (1988), and American Eagle Platinum (1997) were issued by the Perth Mint, Royal Canadian Mint, and United States Mint, respectively. For almost a decade, the Australian Koala and Canadian Maple Leaf were among the leading Pt coins in annual sales. The launch of the American Eagle Platinum proof coins in 1997 resulted in a near doubling of global investment demand and they became the most popular coins of their type in the world. The bullion Pt coins were produced in 1.0 ounce, 0.5 ounce, 0.25 ounce, and 0.1 ounce weights with a pure Pt rating of 0.9995. Investment demand for Pt reached its peak in the 1980s with the expansion of new investment products and the growing concerns about the impacts of apartheid in South Africa—this country being the major source of Pt in the world. In 1988, a total of 19 595 kg of Pt was sold in the form of bars and coins, representing 17% of world demand that year. Over subsequent years, dozens of limited edition Pt coins were released, such as the Panda coins by China and the Ballerina proof coins by Russia. In the mid 2000s, investment demand of Pt declined to less than 0.2%, but this steadily increased to 6% in 2011.



Figure 4.4 Modern applications of platinum. (a). Investment platinum bars and grain. Johnson Matthey PLC Media Library. (b). The 2007 American Platinum Eagle coin, proof reverse (top) and 1999 American Platinum Eagle coin, obverse side (bottom), (b) from Wikimedia Commons. (c). New platinum coins are regularly launched onto the international investment market, such as these pound and pence coins. (d). Large quantities of second-hand platinum jewellery is returned for resale or recycling. (c) and (d) from Johnson Matthey PLC (2008).

#### 4.2.5 Other uses

The high-melting point and chemical inertness of Pt make it a valuable element in a diverse number of medical, laboratory, and defence-aerospace applications. Platinum is widely used in anti-cancer drugs, neurosurgical apparatus, treatment of heart conditions, deafness, and Parkinson's disease, and in alloys for dental restorations (Figure 4.5). In certain chemical forms, Pt has the ability to inhibit the division of living cells. The discovery of this property in 1962, led to the development of Pt-based drugs to treat a wide range of cancers. PGE-based therapeutic applications include cisplatin  $[\text{Pt}(\text{NH}_3)_2\text{Cl}_2]$ , which is an effective drug for leukaemia, ovarian, testicular, head and neck cancers. Since its approval for treatment on humans in 1978, a number of cisplatin analogues (e.g., carboplatin) that show less toxicity and greater antitumour activity have been developed. It is claimed that the Pt-bearing drug satraplatin, being developed for the treatment of prostate cancer, has a higher survival rate than chemotherapy treatment regimes. Platinum is used as a catalyst in the manufacture of the silicone rubber and gel components of several types of medical devices (breast implants, joint

replacement prosthetics, bone pins, artificial knees, lumbar discs, artificial heart pacemakers, Pt-Cr and Pt-Ti coronary stents, vascular access ports). Owing to their biocompatibility, high electrical conductance, and resistance to corrosion from acids inside the body, Pt and Pt-Os-Ir alloys are important components of implant devices used for irregular heartbeat and in the replacement of defective heart valves. Heart pacemakers usually contain at least two Pt-Ir electrodes. Platinum is also widely used in X-ray-opaque guide wires and marker bands to help the surgeon navigate heart-assisting devices to the treatment site during angioplasty surgery. Platinum and Pd are the principal PGEs used in dental restorations. These metals are mixed with Au, Ag, Cu, and Zn in varying ratios to produce alloys for dental inlays, crowns, and bridges. Small amounts of Ir and Ru may be added. The metal alloys fall into two major groups, namely a high-Au type with only about 10% Pt, and a low Au-Pd-based alloy version containing 50% to 80% Pd. High-Au alloys have been used for several decades, but the use of Pd in dentistry has recently increased. Japan is the largest consumer of the Pd alloy types, followed by North America and Europe. The PGEs provide strength, stiffness, and durability, whereas the other alloyed metals contribute malleability. The most common use is in crowns, where the alloy forms the core onto which porcelain is bonded to build up an artificial tooth.



**Figure 4.5** Modern applications of platinum. (a). Platinum-based drugs are used to treat a number of cancers. Johnson Matthey PLC Photograph Collection. (b). Micro-machined platinum components have numerous surgical applications. Johnson Matthey PLC (2006). (c). Platinum wires are used in air-flow sensors in cars and in surgical procedures. Johnson Matthey PLC Media Library. (d). Platinum medical marker bands help the surgeon to navigate in angioplasty surgery. Johnson Matthey PLC Media Library.

Applications where long periods of operation at high-temperatures are required include crucibles, thermocouples, multi-layer ceramic capacitors, high-temperature electric furnaces, coatings for missile nose cones, and jet engine fuel nozzles. Platinum aluminide coatings protect rotating blades from oxidation in high temperature (>1500°C) turbofan jet engines, and Pt-tipped spark plugs are widely used in the automotive industry (Figure 4.6a). Other applications in cars include Pt wires in air-flow sensors that measure air flow in the cylinders of the engine, and in initiator sensors that facilitate the explosive release of air safety bags upon impact. Platinum's high conductivity is integral to its use in electrical contacts, particularly where alloys are used and resistance to both erosion and corrosion are required. The hardness and high-melting point attributes of Pt make it an ideal metal for the making of high-temperature glass products. Platinum and Pt-Rh alloys have applications in the fabrication of vessels that hold and channel molten glass since these metals do not react with glass or oxidise at high temperatures. The added Rh (5% to 30%) increases the strength of the Pt alloy and extends its life. Platinum's coefficient of expansion is similar to that of soda-lime-silica glass and thus it is used to make glass-sealed electrodes, textile glass fibre (also called reinforcement fibre), bushings and Liquid Crystal Displays (LCD), and cathode-ray tubes. Platinum-cobalt (75:25) alloys are used in some of the strongest magnets known. The alloy mixture has properties different from those of the individual metals. Platinum-based anodes are used in cathodic protection systems for large ships, pipelines, and steel piers. Platinum's ability to absorb large quantities of H is utilised in H gas purification processes. The increased production of computer hard-disk drive coatings, fibre optic cables, iPods, and infra-red detectors for military and commercial needs are contributing to the growth in demand for Pt (Figure 4.6b). The amount of data that can be stored on a hard drive of a computer depends on the strength of the magnetic field generated on surface layers of platters or disks. The addition of Pt to Co-based alloys in the hard disks enables data to be stored at higher densities and improve access times. All hard disks today contain Pt in their magnetic layers compared to around 50% in 1997. The ability of Pt-Rh alloys to resist corrosion from glass has become important for the production of liquid crystal flat screens in mobile phones, computers, and televisions. Platinum and Pd are both utilised for printmaking in photography since both metals are considered superior to conventional Ag in archival longevity and tonal quality. Their chemical stability facilitates long-lasting prints and they offer a greater range of tones compared to other black and white printing methods.

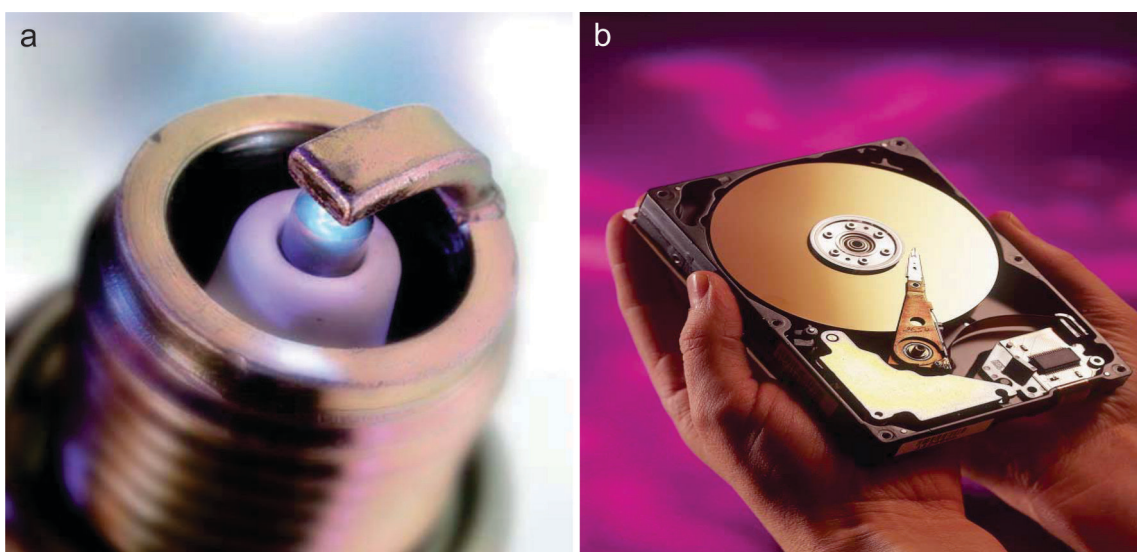


Figure 4.6 Modern applications of platinum. (a). Platinum-tipped spark plugs are increasingly fitted as they last several times longer than their base-metal predecessors. Johnson Matthey PLC (2006). (b). Platinum is used to increase the data storage capacity of computer hard disks. Johnson Matthey PLC (2002).

## 4.3 Palladium

Palladium (pronounced puh-LAH-dee-um) is represented with the chemical symbol Pd in Group 10 of the Periodic Table of Elements and it has an atomic number of 46 (Figure 1.1a; Table 4.1 and Table 4.2). It has the lowest density ( $12.02 \text{ g cm}^{-3}$ ) and melting point ( $1555^\circ\text{C}$ ) of all the PGEs, however, its remarkable qualities mean that it is no less crucial in a number of important applications (Figure 4.7–Figure 4.11). With Pt, Pd is considered the most important of the PGEs. It is a more affordable metal than Pt and Au, and it is one of the whitest metals available. Palladium's melting point is high relative to other popular metals (e.g., more than four and half times that of Pb) and it has high temperature stability and corrosion resistance. Palladium has similar unique physical and chemical properties to Pt that make it widely used in 'green' applications such as catalysts for the automotive industry. The market of Pd is very restricted, vulnerable to metal substitution, and its prices are consequently extremely volatile.

Palladium is silvery white in colour, does not tarnish in air, soft, malleable, and ductile, although cold working greatly increases its strength and hardness. Palladium is regarded the least noble of the PGEs because it is the most chemically reactive of the group. It combines poorly with O under normal conditions but will combust if ground into powder. The precious metal will combine with F and Cl when very hot. Palladium is a widely used catalyst for hydrogenation and dehydrogenation reactions. For example, it is known as the 'amazing soaking sponge' since at room temperature it has the unusual property of being able to absorb up to 900 times its own volume of H, which is released on heating, and therefore provides a means of purifying H gas. It resists high-temperature corrosion and oxidation, but it is attacked by nitric, sulphuric, and hydrochloric acids. Palladium has been used in modern jewellery since 1939 (Figure 4.7), as an alternative to Pt or 'white gold' (alloys of Au with Pd, Ni, or Ag). This is due to its natural white appearance that requires no Rh plating, and it is much lighter and about 12% harder than Pt. Important applications include medicine, dentistry, surgical instruments, and electrical contacts. Palladium is used in multi-layer ceramic capacitors and integrated circuits for domestic appliances, in the military and telecommunication industries, and in groundwater treatment. In many instances, Ag is being alloyed with Pd in electrical applications where previously Pd alone was used.

a



Figure 4.7 Modern applications of palladium. (a). Palladium is an attractive alternative to platinum for jewellery since it has a natural white colour, it is harder, and much lighter. Johnson Matthey PLC (2008). (b). The increased penetration of palladium jewellery throughout China, plus the introduction of Pd990 products, has led to strong rises in purchases of the metal by Chinese jewellery manufacturers. Johnson Matthey PLC (2006).

### 4.3.1 Catalyst

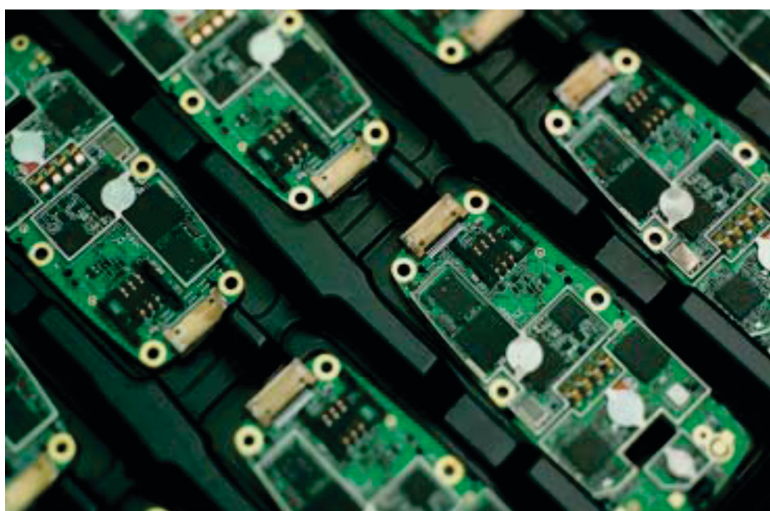
Palladium, Pt, and Rh are primary components in automotive catalysts (Figure 4.8) that convert up to 90% of harmful gases from auto exhaust (hydrocarbons, carbon monoxide, nitrogen oxide) into less harmful substances (carbon dioxide, nitrogen, and water vapour). The application of Pd in automotive catalysts is described in Section 4.2.1. Palladium's remarkable catalytic properties are instrumental for its widespread use in the chemical industry. The many chemical reactions in which Pd compounds serve as catalysts are collectively called Pd coupling reactions. The production of nitric acid for the manufacture of artificial fertilisers also requires significant amounts of this precious metal. It is also used in the production of sulphuric acid ( $\text{H}_2\text{SO}_4$ ), which is used in the manufacture of paper and fabric. Palladium is used in chemical processes that require H exchange between two reactants, such as that which produces butadiene and cyclohexane, the raw materials for synthetic rubber and nylon. Palladium catalysts have also had a remarkable impact in how exploratory drug compounds are synthesised in the pharmaceutical and biotechnology industries. Palladium metal is compatible with human tissue and is used in radioactive form, in the medical industry for the treatment of cancer. The radioactive isotope  $^{103}\text{Pd}$  has potential applications in the treatments of prostate and breast cancers. Palladium has other important catalytic applications such as the removal of toxic and carcinogenic substances from groundwater.



Figure 4.8 Modern applications of palladium. (a). Autocatalysts have historically been the dominant application for palladium. Johnson Matthey PLC (2005). (b). Scrapped palladium-bearing catalytic converters are an important recycled source of the precious metal. Johnson Matthey PLC (2007). (c). Smoptech palladium catalysts are based on a novel fibre support. Johnson Matthey PLC (2001).

### 4.3.2 Electrics and electronics

After autocatalysts, the largest demand sector for Pd is electrical and electronic applications. Its electrical conductivity and chemical stability make it a more effective and durable plating than Au in electronic components. Palladium-containing components are used in nearly all types of electronic device, from basic consumer products to complex military hardware. Although each component contains only a fraction of a gram of metal, the large volume of units produced results in significant consumption of this precious metal. Palladium is mainly used in the production of Multilayer Ceramic Capacitors (MLCC: Figure 4.9) and in conductive tracks in Hybrid Integrated Circuits (HIC). These capacitors, which help to control the flow of an electric current through a circuit by storing a charge of electricity until it is required, have diverse applications in mobile telephones, personal and notebook computers, fax machines, LCD televisions, and in auto and home electronics. Advances in technology are trying to reduce the use of Pd in MLCC. The industry in Japan and North America are using base metals, e.g. Ni, as an alternative for the conductive layers in MLCC. Other electronic applications for Pd include electronic circuits, as well as hybrid-integrated circuits.



*Figure 4.9 Modern applications of palladium. Palladium is an important component of the ongoing miniaturisation of electronic components in multilayer ceramic capacitors. Johnson Matthey PLC (2004).*

### **4.3.3 Other uses**

Two major types of Pd coins are available for the Pd investor. They are Pd bullion coins and collectible Pd coins. Palladium coins were issued by Tonga in 1967, and Canada, Soviet Union, France, Russia, China, Australia, and Slovakia subsequently followed with mainly special commemorative coins. Palladium ingots, bars, and wafers are also available and are sold at very little premium above the Pd value, but they may not be as easily available as Pd coins (Figure 4.10). Palladium-based alloys play a key role in the technology of fuel cells, which combine H and O to produce electricity, heat, and water. Palladium's adaptability, strength, resistance to tarnish in air, and its ability to be easily worked promote its use in dental alloy restorations (e.g., dental inlays, crowns, and bridges). The demand for Pd in dental applications, however, is susceptible to Au or base-metal alloy substitution. Palladium is extensively used in watchmaking and jewellery either on its own or as an element of 'white gold'. The addition of Pd causes the yellow colour of Au to fade and the alloy becomes whiter. Palladium-Au is a more expensive 'white gold' alloy than Au-Ni alloys, but rarely causes allergic reactions that may occur with the latter alloys. The addition of Pd to Au has the effect of increasing the strength, hardness, modulus of elasticity, and melting point of the alloy. Palladium is also alloyed with Au, Ag, and Cu in such products as ball bearings, springs, balance wheels of watches, and astronomical mirrors. Palladium is used in blood sugar test strips, aircraft spark plug electrodes, surgical instruments, as salts in photographic printing processes, and as a financial commodity, Pd bullion has international standard currency codes of XPD and 964. Ductile like Au, Pd can be beaten to a leaf thinness of 0.1  $\mu\text{m}$  (Figure 4.10d). Palladium leaf is used as a substitute for Ag and Al leaf in manuscript illumination.



Figure 4.10 Modern applications of palladium. (a). Russian palladium ingot. Johnson Matthey PLC Media Library. (b). Specification palladium bars. Johnson Matthey PLC (2002). (c). Palladium coins (technically a 'round' since such items are not legal tender) from Northwest Territorial Mint. (d). Palladium leaf is so thin that it conforms to the shape of the surface of the object it settles on, and will even show up the fine details of a fingerprint. Images (c) and (d) reproduced with the permission of © 2010 Theodore Gray [periodictable.com](http://periodictable.com).

## 4.4 Rhodium

Rhodium (pronounced ROH–dee–um) is represented by the chemical symbol Rh in Group 9 of the Periodic Table of Elements and it has an atomic number of 45 (Figure 1.1a; Table 4.1 and Table 4.2). It has a high melting point, high-temperature stability and reflectance, is extremely hard and durable, and its corrosion resistance make it a key component of many industrial applications, such as autocatalysts, metal alloy, acid, glass, glass fibre, in addition to medical apparatus and jewellery (Figure 4.11). Rhodium is the most costly PGE (often in the range 1000 to 10 000 \$US/troy ounce), and historically its price generally exceeds the next most expensive PGE, Pt, and Au by factors of about 5 to 10. It has the distinction of being the world's most expensive precious metal. Some of the most expensive consumer items in the world are made from Rh. Rhodium has a higher melting point (1964°C), lower density (12.41 g cm<sup>-3</sup>), and is harder than Pt. Oxygen is absorbed from the

atmosphere at the melting point of Rh, but the O is released upon solidification. Upon heating, it turns to the oxide producing a red colour, and at higher temperatures reverts back to the element. Rhodium is not affected by acids; it is completely insoluble in nitric acid and only slightly dissolves in aqua regia. It does not react with F, an element that reacts with most other elements. Like its sister elements, Pt and Pd, Rh has excellent catalytic properties.



Figure 4.11 Modern applications of rhodium. (a). Samples of rhodium nitrate are a key component of many gasoline autocatalysts. Johnson Matthey PLC (2003). (b). Rhodium foils are used in equipment for detecting cancer. Johnson Matthey PLC Media Library. (c). Rhodium-plated ring with tanzanite. Reproduced with the permission of © 2010 Theodore Gray [periodictable.com](http://periodictable.com). (d). Rhodium-platinum bushings are used to produce glass fibre by drawing molten glass through the holes. Johnson Matthey PLC Media Library. (e). Rhodium-plated cuff links. Reproduced with the permission of © 2010 Theodore Gray [periodictable.com](http://periodictable.com).

Increasing amounts of Rh are replacing Pd in new-generation catalytic converters with Pt (Figure 4.11a). Many complex Rh compounds form the basis of catalysts in a number of industrial-chemical processes. Such examples include the reduction of benzene to cyclohexane, synthesis of methanol for the production of acetic acid, and the manufacture of silicone rubbers. Due to its high mechanical and chemical resistance properties, Rh is employed in high-quality writing pen (Graf von Faber-Castell and Caran D'ache) surfaces. Rhodium has very low electrical resistance, high electrical and heat conductivity, and is resistant to corrosion, thus its application in electrical contacts. Rhodium plating is exceptionally hard and is used as a reflective surface in optical instruments, mirrors, and

search lights. It is also used as filters and foils in mammography medical scans because of the characteristic x-rays it produces, and Rh neutron detectors in Combustion Engineering Nuclear reactors measure neutron-flux levels (Figure 4.11b). Rhodium-Pt gauzes are used in the production of nitric acid. Rhodium is widely used in the jewellery and decoration industries (Figure 4.11c and e). The process of electroplating Rh onto 'white gold' and Pt jewellery to enhance a reflective white surface is called Rh flashing. Sterling Ag is also coated by Rh to inhibit tarnishing (silver sulphide). Solid (pure) Rh jewellery is rare because of the high melting point and poor malleability of the precious metal. Rhodium is silvery white to cool grey in colour, and has a high reflectance that is almost unique among all metals. Alloys of Rh with other PGEs have advantages over pure Pt and Pd in various industrial and research purposes. It is used extensively as an alloying agent to harden Pt and Pd for furnace windings, thermocouple elements, bushings for glass fibres, electrodes for aircraft spark plugs, and laboratory crucibles (Figure 4.11d).

## 4.5 Iridium

The rarest member of the PGE group of transitional metals, iridium (pronounced i-RID-ee-um), is identified with the chemical symbol Ir and the atomic number of 77 in Group 9 of the Periodic Table of Elements (Figure 1.1a; Table 4.1 and Table 4.2). Abundances in the Earth's crust are estimated to be as low as 0.00001 ppm (0.01 ppb). It has a melting point of 2466°C, is silvery white to slightly yellow, very hard (over four times that of Pt), brittle, and in its solid state is difficult to machine, form, or work. It is usually shaped at high temperatures. Iridium is the second densest (22.56 g cm<sup>-3</sup>) and most corrosion-resistant natural element known, even at temperatures as high as 2000°C, and it is the only metal to maintain good mechanical properties in air at temperatures above 1600°C. It is not attacked by acid, aqua regia, molten metals, or silicates. Iridium is unreactive at room temperatures. However, at higher temperatures it becomes more reactive with molten salts, such as sodium cyanide and potassium cyanide, as well as O and the halogens (particularly F) to form compounds like iridium dioxide (IrO<sub>2</sub>) and iridium trihalides. Fine Ir dust is reactive and can be flammable. The most important compounds in chemical applications are the salts and acids it forms with Cl and the organometallic compounds used in catalysis and in research. The name Ir is appropriate since the salts it forms are highly coloured.

Although it is one of the rarest elements in the Earth's crust, with annual production only about 3 t, Ir has many specialised industrial and scientific applications (Figure 4.12–Figure 4.13). High corrosion resistance and high melting point attributes are exploited in high-temperature laboratory crucibles, electrical contacts for spark plugs, electrodes for the production of Cl, electrical contacts, and industrial-engineering components such as dies (Figure 4.12). High-temperature Ir crucibles are also used to produce oxide single-crystals, such as sapphires, for use in computer memory devices and solid-state lasers. Iridium was used in radioisotope thermoelectric generators of unmanned spacecraft such as the Voyager, Viking, Galileo, and New Horizons. Iridium was chosen to encapsulate the <sup>238</sup>Pu fuel in these generators because it could withstand operating temperatures of up to 2000°C and it had great strength. Other sophisticated applications include high-precision optical components in X-ray telescopes. The mirrors of the Chandra X-ray Observatory (satellite launched by NASA on July 23<sup>rd</sup> 1999) are coated with a ~30 nm-thick layer of Ir. Iridium had superior qualities for deflecting X-rays compared to the other metals tested such as Ni, Au, and Pt. The Ir layer, which had to be smooth to within a few atoms, was applied by depositing Ir vapour under high vacuum on a base layer of Cr.

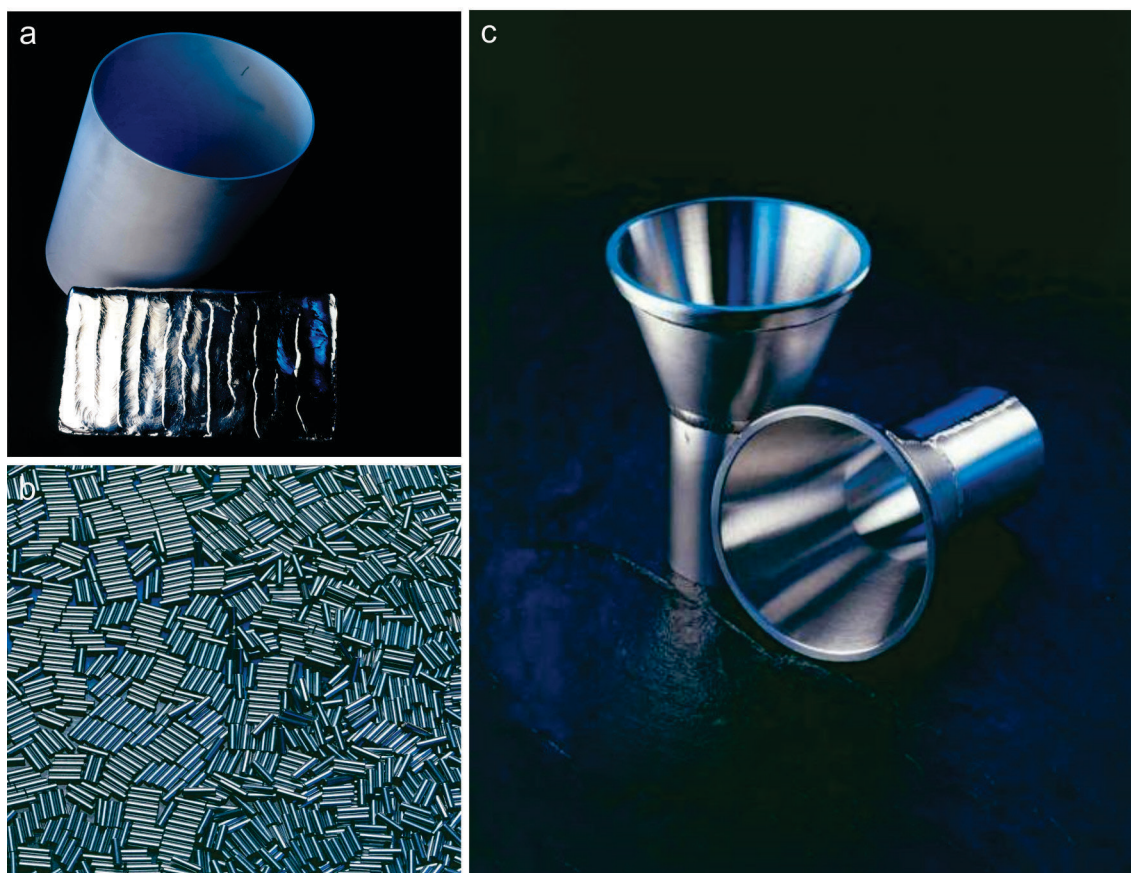


Figure 4.12 Modern applications of iridium. (a). Iridium crucibles for crystal growing are made from electron-beam melted ingots. Johnson Matthey PLC (2001). (b). Iridium spark plug tips. (c). Iridium dies. Images (c) and (d) from Johnson Matthey PLC Media Library.

Iridium is employed as a hardening agent for Pt, and when alloyed with Os, it is used in fountain pen points, phonograph needles, compass bearings, and balances (Figure 4.13a). The first use of these alloys on the tips of fountain pen nibs mounted in Au was in 1834. From 1944 onward, the 14 K Au nibs of famous Parker 51 fountain pens were tipped by an Ir (with 3.8% Ir) and Ru (96.2% Ru) alloy. These hardening alloys have subsequently been replaced by other metals like W.

Catalyst applications include the carbonylation of methanol to produce acetic acid, and in a car engine that was introduced in 1996 called the direct-ignition engine. Another kind of Ir catalyst is reported to capture sunlight and turn it into chemical energy similar to the photosynthesis process used by plants. Iridium also benefits the aerospace, defence, petroleum, and medical sectors. Long-life aircraft engine parts are made of Ir alloys, and Ir-Ti alloys are used for deep-water pipes because of their corrosion resistance. Medical and surgical advances, such as heart pacemakers, surgical pins, and hypodermic syringes have also relied upon iridium's unique qualities. The radioisotope  $^{192}\text{Ir}$  is an important source of energy used for industrial gamma-radiography in the treatment of cancer and also for the non-destructive testing of metals. The pigment *iridium black* is valued as a painting agent on porcelain because of its intense black colour.

Anomalous concentrations of Ir and other metals have been widely documented around the world in a 65 million year old clay layer located between the rocks of the Cretaceous and Tertiary geological time periods (Figure 4.13b). These precious metal concentrations, thousands of times greater than that

normally found in rocks that make up the Earth's crust, are interpreted by geoscientists to have been derived from an extra-terrestrial meteorite object that impacted on the earth. Such an impact has been proposed to be the cause of the extinction of the dinosaurs at the same point in geological time. The impact from a large meteorite object (~10 km diameter) threw enormous amounts of dust into the air which subsequently blocked out the sunlight and caused plants and animals to die. Such a large meteorite impact event occurred in the Yucatan Peninsula of Mexico at the same time the clay layer was deposited and the dinosaurs became extinct.

Meteorites often contain much higher abundances of Ir than the average abundances in the Earth's crust. An example is the Willamette Meteorite, the sixth-largest meteorite found in the world, which contains 4.7 ppm Ir (Figure 4.13c). The Fe-Ni-type of meteorite was discovered in the state of Oregon, USA. There was no impact crater at the discovery site; researchers believe the meteorite landed in what is now Canada or Montana, and it was transported as a glacial erratic to the Willamette Valley during the Missoula Floods at the end of the last Ice Age, some ~13 000 years ago.

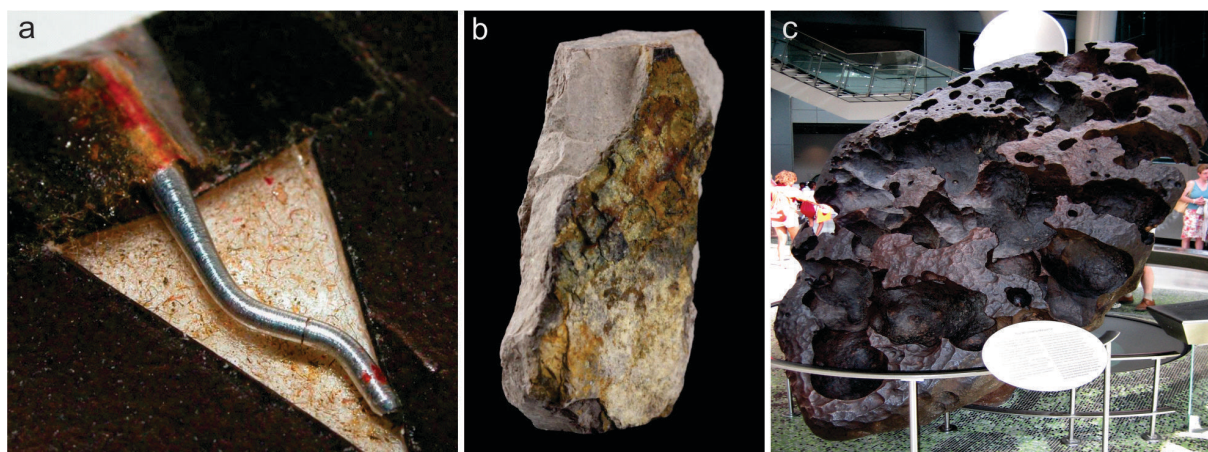


Figure 4.13 Applications and natural occurrences of iridium. (a) Iridium-tipped phonograph needle. (b) Dark, oxidised clay sample is from a thin iridium-rich layer at the boundary of the Cretaceous and Tertiary geological time periods, which can be traced around the world. (c) The iridium-bearing Willamette Meteorite is an iron-nickel meteorite discovered in the state of Oregon, USA. Images (a) and (b) reproduced with the permission of © 2010 Theodore Gray [periodictable.com](http://periodictable.com); image (c) from Wikimedia Commons.

## 4.6 Osmium

Osmium (pronounced OZ–mee–um) has the chemical symbol Os in Group 8 of the Periodic Table of Elements and it has an atomic number of 76 (Figure 1.1a; Table 4.1 and Table 4.2). It is a lustrous, silvery-bluish grey, extremely hard and brittle precious metal that is the densest ( $22.59 \text{ g cm}^{-3}$ ) natural element known, equating to twice the density of Pb. There has been controversy in the scientific literature to whether Os or its close relative Ir is the densest element. Since its discovery, Os has often held the title of densest metal, but for many decades in the twentieth century it was Ir that occupied that position. However, results from sophisticated density X-ray crystallographic techniques in the 1990s have indicated that Ir ( $22.562 \pm 0.009 \text{ g cm}^{-3}$ ) is about 0.1% less dense than Os ( $22.587 \pm 0.009 \text{ g cm}^{-3}$ ). Osmium is also the hardest (10 times harder than Pt), and has the highest melting point ( $3033^\circ\text{C}$ ) and lowest vapour pressure, of all the PGEs. Osmium's extraordinary hardening qualities are exhibited in applications where frictional wear, extreme durability, and high lustre attributes are required at elevated temperatures (Figure 4.14).



Figure 4.14 Modern applications of osmium. (a). Osmium tetroxide is very volatile and toxic. (b). Osmium phonograph needle package. (c). Osmium-tipped phonograph needle. (d). Osmiridium-tipped 'The Carter Pen'. Images (a)–(d) reproduced with the permission of © 2010 Theodore Gray [periodictable.com](http://periodictable.com).

Osmium's unusual physical and chemical properties determine why it has fewer commercial applications relative to the other PGEs. It is unworkable as a metal since it cannot be readily melted and shaped like most metals and it is rarely used in its pure state because of its volatility (reacts with O at room temperatures) and the extreme toxicity of its oxide. Osmium tends to be used mostly on alloys, often in small amounts to make metal stronger and more durable. The metal is very difficult to fabricate, but the powder can be sintered in a H atmosphere at temperatures of  $\sim 2000^{\circ}\text{C}$ . Osmium is dissolved by acids and by aqua regia after long exposure to these liquids, and when heated, the metal combines with O to form a powerful oxidising agent osmium tetroxide ( $\text{OsO}_4$ ). This oxide is used in chemical and biological research and is the only important commercial compound of Os (Figure 4.14a). It has a strong smell, is toxic, and is volatile. Concentrations as low as  $10^{-7}\text{ g m}^{-3}$  of osmium tetroxide in air can cause lung congestion, skin damage, and eye complications. Osmium is usually produced as a powder, or alloyed with other PGEs, principally Pt and Ir. Very hard alloys are used in instrument pivots, electrical contacts, and multi-pored spinnerets, through which a plastic polymer like rayon is extruded to form fibres. Medical applications include Pt-Os (90:10) alloys in surgical implants like pacemakers and pulmonary valve replacements.

Osmium is second to Ir as the rarest of stable elements (Figure 1.1b). Its average abundance in the Earth's crust is about 1 g per 200 t. Minor quantities of Os are obtained commercially as a by-product of refining Ni. Despite its rarity, Os is far less expensive than Au, partly because it has few commercial uses. Although its metallic form has few applications, osmium's chemical behaviour is impressive. It can exist in eleven different oxidation states, from -2 to +8; a versatility only matched by its chemical cousin Ru and a few other transition metals. Also the high +8 oxidation state reached by Os—along with Fe and Ru—is the highest observed for any chemical element under normal circumstances. In addition, Os metal strongly resists being compressed under pressure, so much that it rivals diamond as the least compressible of all known substances.

Stylus needles in early phonographs were made of Os, especially for 78-rpm long-playing records (Figure 4.14b–c). The Os was later to be substituted by sapphire and synthetic diamond in slower 45 rpm and 33 rpm records. Osmium and alloys of Os-Ir were valued for their durability and were also used in fountain-pen points or nibs (Figure 4.14d). The Os-Ir points of the fountain pens were subsequently replaced by other cheaper metals, and eventually the fountain pens lost fashion to 'ballpoint' ink pens.

Osmium's high reflectivity properties are exploited in specialised electromagnetic applications. Osmium has high reflectivity in the ultraviolet range of the electromagnetic spectrum, e.g., Os at 600 Å has a reflectivity twice that of Au. This high reflectivity is utilised in space-based ultraviolet spectrometers which have reduced mirror sizes due to the restrictions on available space. Osmium coated mirrors were used in several Space Shuttle missions. Its conductivity means Os is also used as an alternative to Au plating in electronic products.

As with the other PGEs, Os is an extremely efficient oxidation catalyst and contributes to the environment through its use in fuel cells. Osmium catalysts are used in the production of ammonia from the combination of H and N. Osmium tetroxide has been used as a catalyst in biomedical research purposes. Osmium has been applied to forensic science in the detection of fingerprints, as a stain for DNA samples, and in fixing and staining fatty tissue for optical and electron microscopy. As Os atoms are extremely electron dense, Os staining greatly enhances image contrast in transmission electron microscopy studies of biological materials.

## 4.7 Ruthenium

Ruthenium (pronounced roo–THEE–nee–um) is represented by the chemical symbol Ru in Group 8 of the Periodic Table of Elements and it has an atomic number of 44 (Figure 1.1a; Table 4.1 and Table 4.2). It is a cool silvery white metal, but it is rarely used by itself because it is extremely difficult to work. Ruthenium has fewer demand applications relative to the more dominant PGEs, Pt, Pd, and Rh (Figure 4.15). It has a melting point of 2334°C, is hard, has a lower density (12.45 g cm<sup>-3</sup>) relative to Os, Ir, and Pt, is white in colour, and only oxidises in air above 800°C. Ruthenium metal is chemically relatively unreactive. It is not attacked by acids or aqua regia, but dissolves in fused alkalis and reacts with halogens at high temperatures. Explosive oxidation reactions are obtained with potassium chlorate. The primary uses of Ru are in the electronics and chemical industries, where its important applications are dependent on its electrical and electrochemical attributes, catalytic activities, stability under varying operating conditions, and alloying and resistance to corrosion properties.

Principal applications in the electronics sector include resistors and in computer hard disks to increase the density of data storage (Figure 4.15a–b). Significant global consumption of Ru is accounted for by ruthenium dioxide, Pb and Bi ruthenates in thick film chip resistors. IBM scientists in 1990 discovered that a thin layer of Ru atoms created a strong anti-parallel coupling between adjacent ferromagnetic layers, stronger than any other nonmagnetic spacer-layer element. Such a Ru-layer was used in the first giant magnetoresistive read element for hard disk drives. In 2001, IBM announced a three-atom-thick Ru layer, informally referred to as 'pixie dust', which could quadruple the data density of current hard disk drive media.

Ruthenium adds two capabilities to a metal alloy; firstly it makes the alloy hard, and secondly, it makes the alloy resistant to attack by acid, O, and other chemicals. Ruthenium-Mo alloys are used in superconductors over a specific temperature range. Ruthenium is the most effective hardening alloy agent for Pt and Pd where electrical contacts require severe wear resistance, and also in Au jewellery alloys to impart hardness (Figure 4.15c–d). Because of its lower cost and similar properties compared to Rh, the use as plating material for electrical contacts is a major application. The coatings are either applied by electroplating or sputtering.

Advanced high-temperature Ru superalloys in turbine blades of jet engines reduce the CO<sub>2</sub> impact of air travel on the environment. The corrosion-resistance capabilities of Ti are improved 100 times by the addition of only 0.1% Ru. Ruthenium is used in electrolytic cells for chemical processes, such as generating Cl from saltwater, and in mixed-metal oxide (MMO) anodes used for cathodic protection of underground and submerged structures. It is also used in catalytic applications involving gas to liquids technology for the generation of S-free, high-quality fuels. Hydrogen sulphide can be isolated by light using an aqueous suspension of CdS particles containing ruthenium dioxide. This removal of H<sub>2</sub>S has applications in oil refineries and in other industrial processes. Although it is a versatile catalyst, Ru can be highly toxic in certain forms.

The biological stain, ruthenium red [(NH<sub>3</sub>)<sub>5</sub>Ru-O-Ru(NH<sub>3</sub>)<sub>4</sub>-O-Ru(NH<sub>3</sub>)<sub>5</sub>]Cl<sub>6</sub>·4H<sub>2</sub>O, stains polyanionic molecules such as pectin and nucleic acids for light microscopy and electron microscopy. The beta-decaying isotope <sup>106</sup>Ru is used in radiotherapy of eye tumours, mainly malignant melanomas of the uvea. Particular Ru chemicals that show resistance to hydrolysis and selective action on tumours are being researched for anticancer properties.

Ruthenium may be carcinogenic, and it is also bioaccumulates in the human body since the body has no way to process it, as it is not a dietary necessity. The pure element will also stain skin if handled directly, and certain Ru compounds and oxides are toxic.



Figure 4.15 Modern applications of ruthenium. (a). Ruthenium resistors. (b). Ruthenium sputtering targets are used in large numbers in the manufacture of hard disks. (c). Ruthenium-plated beaded necklace. (d). Ruthenium ring. Images (a) (c) and (d) reproduced with the permission of © 2010 Theodore Gray [periodictable.com](http://periodictable.com); image (b) from Johnson Matthey PLC (2007).

# 5 Evolution of Australia's platinum-group-element industry

Dean M. Hoatson

## 5.1 Introduction

The discovery in 1851 of a few grains of 'platina' in the Turon and Macquarie rivers, near Orange in central New South Wales, by geological surveyor Samuel Stutchbury represents a seminal event in the evolution of Australia's PGE industry. Stutchbury's announcement of Pt initiated a frenetic phase of exploration that resulted in the discovery of numerous PGE occurrences in eastern Australia. The PGEs were mainly found in alluvial deposits associated with ultramafic igneous rocks that outcrop from southern Tasmania to northern Queensland. Modest contributions of PGEs exploited during the early years of the industry were derived from the activities of individuals or small groups of prospectors throughout western Tasmania and New South Wales. It was not until the late-1960s that larger quantities of PGEs were obtained from hard-rock deposits in the Precambrian cratonic regions of Western Australia.

The Australian PGE industry has had a colourful history that highlights the hardships of exploring such harsh frontier environments as western Tasmania and remote Western Australia. The exploits of hardened explorers, prospecting identities, astute government geologists, distinguished men of the cloth, the discovery of world-class Ni deposits, and the dramatic 'boom and bust' cycles of Australia's rich mining history all feature along the evolutionary path of Australia's PGE industry.

With the exception of a short period during the mid-1920s when Tasmania was the largest producer of 'osmiridium' in the world (Reid, 1921; Geary et al., 1956), Australia has had an insignificant impact on the global markets of PGEs. Since the 1890s small quantities of Pt, Pd, Ru, and 'osmiridium' have been produced (generally less than ~1000 kg annually), and Australia has traditionally been a net importer of the PGEs accounting for less than 1% of world trade. Major world producers of PGEs, such as the Republic of South Africa, Russia, and Canada (see Section 1.3) have been relied on to satisfy Australia's domestic needs. In recent times, Australia's modest PGE production has been restricted to hard-rock deposits in Western Australia. Precious metals from the Eastern Goldfields Province in the Yilgarn Craton of Western Australia are important by-products from the mining of Ni-Cu sulphide deposits associated with Archean (majority of ~2705 million years in age) komatiitic rocks. Palladium (100 kg to 800 kg annually) is the dominant PGE produced followed by Pt (50 kg to 300 kg). The amounts of PGEs produced from Western Australia have gradually increased since the 1970s, however, these totals have in recent years fluctuated from between ~445 kg and 1035 kg. In 2013, Australia produced 786 kg of Pd and Pt, which equated to just ~0.2% of global supply (see Section 1.3.3). Nickel sulphide ore shoots on the Kambalda Dome have traditionally been the largest producers of by-product PGEs. These PGE-bearing shoots have close spatial and genetic associations with the other more conventional Ni sulphide deposits, which have had a long history of mining in the Eastern Goldfields Province. An important recent contribution to the national supply of PGEs has been the PGE-enriched types of Ni sulphide komatiite deposits discovered in other parts of the Yilgarn Craton (e.g., Cosmos, Prospero, and Waterloo).

The Ni-Cu sulphide deposits of the Eastern Goldfields Province have been the largest producers of Pd and Pt in Australia (Appendix F). The alluvial Pt deposits in the Fifield district of central New South Wales (described below) are often erroneously reported in the literature as being the largest producers of Pt in the country. The Western Australian Ni deposits have produced at least 7 times the inventory of Pt (not including Pd) compared to the deposits at Fifield.

The Australian PGE industry has witnessed protracted periods of relatively depressed metal prices, exploration inactivity, and low discovery rates, interspersed by short phases of frenetic exploration activities driven by buoyant global metal prices and high demand. Maximum PGE production has occurred at different relative stages during the three main mining periods at Fifield, New South Wales; western Tasmania; and Western Australia (Figure 1.7):

1. peak Pt production of 75.8 kg from the Fifield district was achieved in 1896, nine years after its discovery, and production rapidly decreased after this peak period;
2. 'osmiridium' production from western Tasmania reached its maximum of 104.7 kg in 1925 midway through its main 30-year producing period; and
3. Pd and Pt credits from the hard-rock Ni sulphide deposits in the Yilgarn Craton of Western Australia have generally continued to increase, albeit erratically, from 1970 onwards.

The Fifield production history conforms to a more typical discovery-production evolution pattern seen for most other mineral producing regions in Australia. These exploration histories are often characterised with the early discovery of the largest deposit(s) in the province and most of the metal obtained during the earliest phases of mining, and the discovery costs of further deposits increase as the exploration maturity of the province increases (Hronsky and Schodde, 2006). Australia's PGE exploration trends have generally behaved independently of other metals, such as Cu, and Zn.

## 5.2 Evolution of Australia's platinum-group-element industry

The following section introduces chronologically the first discoveries of PGEs in eastern Australia, and then it describes in more detail the three most important PGE-producing regions, namely Fifield (NSW), western Tasmania, and Kambalda (WA). A number of important reviews, many of historical context, that have been used for the following descriptions include: Earp (1852); Twelvetrees (1914); Brown (1919); Reid (1921); Nye (1929); Geary et al. (1956); Flack (1967); Mertie (1969); Marston (1984); Bottrill (1989; 2014); Hoatson and Glaser (1989); Elliott and Martin (1991); Gresham (1990; 1991); Bacon (1992); Teluk (2001); Hoatson et al. (2006); and Hronsky and Schodde (2006).

### 5.2.1 1850 to 1890—Eastern Australian discoveries: an industry is born

Samuel Stutchbury (1798–1859; Figure 5.1) was an English biologist, geologist, and naturalist who began his professional career at the Hunterian Museum of the Royal College of Surgeons in London. He departed for Australia, to become the geological surveyor for New South Wales from 1850 to 1855. Although his main work was devoted to marine biology he also engaged in geology and met most of the colonists interested in science. One of Stutchbury's early responsibilities was to document for the government the mining activities at Ophir in central New South Wales—the discovery site of the first payable Au in Australia. On the 19<sup>th</sup> May 1851 he wrote in his report to Governor FitzRoy '*... has been obtained in considerable quantity.... the number of persons engaged at work and about the diggings.... cannot be less than 400 of all classes.*'



Figure 5.1 Samuel Stutchbury (1798–1859) was an English biologist, geologist, naturalist, and the geological surveyor for New South Wales from 1850 to 1855. Stutchbury is credited with making the first reference to platinum in Australia in 1851. Image from Organ (1998).

Stutchbury's historic discovery of Pt in 1851 was made during his geological and mineralogical surveys that investigated the Au potential of the rivers in central New South Wales. He found in every place he tried, including the Macquarie and Turon Rivers, and Stony Creek near Orange. During his survey he made the remark "... *in no instance have I found in what I should consider its natural matrix. The bars and detritus of the rivers and creeks are the spots in which it is usually found, and in every case it presents the appearance of being waterworn.*" Stutchbury also found Pt and quicksilver (mercury) in more than one place (Earp, 1852). The first reference to Pt in Australia is found in Stutchbury's report dated the 9<sup>th</sup> of June 1851, in which, referring to the Macquarie and Turon Rivers, he says '*I have seen a few grains of platina, but it appears to be rare*' (Flack, 1967).

In the years that followed Stutchbury's discovery, there were several other reported occurrences of PGEs from the eastern states of Australia. Reverend William Branwhite Clarke (1798–1878), English geologist, Anglican clergyman, and headmaster at The King's School in Parramatta from 1839 to 1840, is considered by many to be the 'father of Australian geology' (Figure 5.2). Clarke's period of geological influence overlapped with that of Stutchbury, and his authority and writings in the 'Sydney Morning Herald' damaged the reputation of Stutchbury. Stutchbury also noted the bitter and disappointed feelings expressed by Clarke at his application for the appointment of colonial geological surveyor. Clarke predicted early the colony's mineral wealth, and he published important geological contributions relating to the Permo-Carboniferous coalfields and the fields of New South Wales, and he gave the first account of Silurian fossils in Australia. He described finding Au in both detrital deposits and in quartz reefs west of the Blue Mountains, in 1849 he made the first discovery of tin in Australia, he publicised the first occurrence of diamonds, and in his reports of 1860 he described Pt grains from the fields of New South Wales. Clarke published some eighty scientific papers, while his geological maps formed the basis of the first geological sketch maps of New South Wales, issued by the Department of Mines in 1880.

Alluvial Pt nuggets of up to 12 g were found in 1869 at Brickfield Gully on the Gympie Goldfield, Queensland (Dunstan, 1913).



Figure 5.2 Reverend William Branwhite Clarke (1798–1878), English geologist, Anglican clergyman, and school headmaster is considered by many to be the ‘father of Australian geology’. In 1860 he described platinum grains from the fields of New South Wales. Photograph (by J. Hubert Newman (Ref. PXA 1023/56) is from the Mitchell Library, State Library of New South Wales.

In 1882, Charles Percy Sprent (1849–1887, Figure 5.3) was appointed Deputy Surveyor-General and soon later tragically died from typhoid. Mount Sprent was later named after him. Sprent, who was educated at Hobart High School and became administrative head of the Tasmanian Lands and Surveys Department, is credited with the first discovery of ‘osmiridium’ in Tasmania (Reid, 1921). The informally named mineral ‘osmiridium’ is largely composed of a mixture of precious metal alloys dominated by Os, Ir, and Ru. Sprent carried out several expeditions that investigated the agricultural, pastoral, and mineral wealth potential of western Tasmania. His two expeditions of 1876 and 1876–1877 documented many occurrences of alluvial ‘osmiridium’ in the Pieman, Arthur, and Whyte Rivers near Mount Bischoff (Appendix I). Sprent’s important findings ultimately led to the discovery of many alluvial and rarer hard-rock ‘osmiridium’ deposits along the western side of Tasmania extending from Beaconsfield (Andersons Creek) in the north to Surprise Bay (New River, Osmiridium Beach) in the south. Alluvial deposits in the Nineteen Mile Creek–Bald Hill and Adamsfield (Florentine Valley, Boyes River, Fourteen Mile Creek, Styx River, Maydena) districts became the most significant producers in the state. Approximately 50% of Tasmania’s total ‘osmiridium’ produced (~964 kg) was obtained from the Adamsfield region (~477 kg) from 1925 to 1968. Other ‘osmiridium’-bearing regions included Mt Stewart, Badger Plains, Long Plains, Melba Flat, Macquarie Harbour (Spero Bay, Birches Inlet), Pieman River, Queenstown (Newall Creek), and from the Heazlewood, Castray, Wilson, and Huskisson rivers (Bottrill, 2014). Hard-rock sources of ‘osmiridium’ were found in foliated serpentinite at Caudry’s mine on Bald Hill, near Waratah, in 1913. This was considered by Reid (1921) to be the first discovery of ‘osmiridium’ *in situ* in the world. About 250 ounces of PGEs were produced from a zone containing magnesite, opal, and talc; the ‘osmiridium’ is intergrown with chromite and magnetite, which occurs in pods (Reid, 1921). In the same area, ‘osmiridium’ was shed from a decomposed serpentinite in Warners Creek and also from an opalised serpentinite at Purcell’s Prospect. A similar occurrence (Halls Open Cut) was later found in the headwaters of Main Creek, Adamsfield, adjacent to, and locally transecting, a barren, quartz-veined talcose zone near the eastern margin of the serpentinite (production from this zone was estimated at between 200 ounces to 400 ounces of PGEs: Nye, 1930). This deposit consists of a 300-m-long zone of dark coloured, foliated serpentinite with chromite pods and minor millerite and nickeloan carbonates, and ‘osmiridium’ nuggets to about

an ounce. 'Osmiridium' at Mt Stewart was found in schlieren transecting chromite and magnetite-rich serpentinite. Reid (1921) described 'osmiridium'-bearing limonitic, talcose joints in serpentinite at Wilson River as "schlieren". Some of the 'osmiridium' in these joints may be detrital, with the heavy 'osmiridium' grains being deposited in joints during erosion of the ultramafics. At Adamsfield there has also been considerable 'osmiridium' production from both serpentine-rich quartzose sandstone and a cemented fragmental serpentinite overlying the serpentinite, and the latter appears to constitute a shore-line placer of probable Ordovician age (Nye, 1929 and 1930; Carey, 1952; Elliston, 1953).



Figure 5.3 Charles Percy Sprent, Deputy Surveyor General 1882–1887. Image from DPIPW (2014).

Minor amounts of Pt associated with Au and Sn were found in beach sands in the Richmond River district of northern New South Wales in 1878. The beach-sand deposits of the Ballina District were mined for Au for many years (main producing period 1936–1938), but a small quantity of ~4 kg of Pt was recovered as a by-product (Flack, 1967; Hoatson and Glaser, 1989). In 1885, a German born chemist and mineralogist Fredrick Augustus Genth (1820–1893), reported osmiridium in association with cassiterite, native copper, and platinum in sand from the Aberfoil River, New South Wales. He described the Pt grains (iridosmine?) as forming tin-white flat scales, indistinct hexagonal plates, and mostly having irregular shapes. The Pt also contained as much as 30% of osmiridium (Reid, 1921). The alluvial Pt potential of the Fifield district in central New South Wales was first realised in 1887, but there was little production until 1896. Fifield has historically been the largest producer of alluvial Pt in Australia (see below for details). Platinum from the Broken Hill district was first detected in 1889 in samples of Ni-Cu ore submitted to the Department of Mines for assay (Mingaye, 1892). A field survey undertaken in 1892 showed that the PGE mineralisation was associated with ultramafic intrusions east of Broken Hill, notably at Little Darling Creek, Mulga Springs, and Red Hill (Jaquet, 1893).

One of the first examples of hard-rock Pt production from mainland Australia, albeit as a by-product of Cu-Ni-Au mining, was from the Thomson River copper mine (Vandenberg et al., 2006), at Coopers Creek near Walhalla, Victoria. Copper-Ni-Au mineralisation is hosted by mafic and ultramafic dykes of the Late Devonian Woods Point Dyke Swarm. Platinum-group elements are associated with several occurrences of Cu-Ni-Au mineralisation. Keays and Green (1974) reported that at least ten dykes in the Woods Point Dyke Swarm are mineralised and that for each 1% Cu, sulphides contain 1 ppm Pd and 1 ppm Pt. Platinum and Au were mined from three small open pits in the East Walhalla Copper and Platinum mine area. No production data are available, but samples taken in 1917 assayed up to 0.6% Cu, 2.93 ppm Pt, 1.02 ppm Au, and 5.23 ppm Ag (Cochrane, 1982; Vandenberg et al., 2006). The Thomson River Copper Mine was discovered in 1864, and mining commenced in September

1865 with an adit driven across a mineralised gabbro-monzonite-hornblendite dyke. Production between 1865 and 1881 was approximately 10 160 t of ore, with grades of up to 24.5% Cu, 3.75% Ni, and 186 ppm Ag (Cozens and Rangott, 1972). In 1874, the Walhalla Copper Mining Company erected roasting and smelting furnaces in the district. From 1906 to 1913, 2540 t of ore were mined, with estimated grades of 3.75% Cu, 0.34% Ni, 12.8 ppm Ag, 1.5 ppm Au, 2.3 ppm Pt, and 3.8 ppm Pd (Cozens and Rangott, 1972). Approximately 10 kg of Pt were produced in 1911 and 1913. The mine has had a chequered history of activities and interest since the early 1900s, but even in recent years, mining companies still actively explore the mineralised dyke systems in the Walhalla–Matlock region and assess the viability of the past mine workings.

Reid (1921) mentions several other minor alluvial occurrences of 'osmiridium' associated with sand and beach sand from New South Wales and Victoria, however, the years of their discoveries are not given. It should be noted that some of these occurrences and also the PGE species (e.g., osmiridium, platinum) reported may be of questionable authenticity. These occurrences include from New South Wales at Bingara, Mudgee, Bathurst, Ballina (see above), and also from the Dalmorton and Barnet River districts; and also in Victoria from Foster, Waratah Range, South Gippsland, Byron Bay, and within beach sands from several locations on the coastline. Table 5.1 summarises the major periods of historical and current PGE production in Australia.

Table 5.1 Platinum-group element mining centres in Australia.

Mining centre	Production (kg) <sup>1</sup>	Discovered	Main producing period(s)	Type of deposit	Reference(s)
Kambalda (WA)	24 812 (Pd, Pt) <sup>1</sup> 32 (Ru) <sup>1</sup>	1966	1974–	Hard-rock	Hudson (1986); Hudson and Donaldson (1984)
Fifield (NSW)	~635 (Pt)	1887	1893–1899	Alluvial	Flack (1967); Suppel and Barron (1986a)
Wilson River Mt Stewart Savage River (Tas)	~490 (Os, Ir)	1876	1913–1914 1918–1923	Alluvial	Reid (1921); Geary et al. (1956)
Adamsfield (Tas)	~480 (Os, Ir)	1925	1925–1934	Alluvial	Geary et al. (1956); Varne and Brown (1978)
Thomson River (Vic)	~10 (Pt)	1864	1911, 1913	Hard-rock	Cochrane (1982); Cozens and Rangott (1972)
Macquarie River (NSW)	~6 (Pt)	1851	1950–1954	Alluvial	Geary et al. (1956); Barrie (1965)
Ballina district (NSW)	~4 (Pt)	1878	1936–1938	Beach-sand	Flack (1967)

<sup>1</sup> Total mine production is for the period 1969 to 2013. The 32 kg of ruthenium produced in Western Australia occurred from the start of records at 1886 to 1979. Details of Australia's PGE production are shown in Appendix F.

Major sources of data: Geary et al. (1956); Kalix et al. (1966); Hoatson and Glaser (1989); Government of Western Australia Department of Mines and Petroleum Resource Data Files—Quantity and Value Tables (<http://www.dmp.wa.gov.au/1521.aspx>); Australian Mineral Industry Annual Reviews; pers. comm. D. Flint and P. Abeyasinghe (GSWA, 2007, 2012).

## 5.2.2 1890 to present—Fifield: Australia's first platinum producer

The Fifield district of central New South Wales was Australia's first significant producer of alluvial Pt in Australia, with Pt and Au occurring in Cenozoic gravels, buried leads, and in recent alluvium derived from both the gravels and leads (Bowman et al., 1982). Total production from the deep leads, which

occur in an area covering approximately 5 km by 10 km centred on Fifield, amounted to about 633 kg Pt and 178 kg of Au. Alluvial Pt was first found at Fifield in 1887, but there was little production until the discovery of the Platina Lead in 1893 (Geary et al., 1956). Production from the Fifield region peaked in 1896 when 75.8 kg Pt was recovered, but mining operations in subsequent years were often hampered by the lack of a regular water supply and thick clay that covered the flat-relief countryside. The miners reported that it required several tonnes of prospective soil material to ascertain if it contained economic quantities of Pt. Small dish samples or local shallow scrapings were generally inadequate to determine Pt-bearing from barren soils. The historical mining operations often consisted of horse-drawn scrapers that scooped up and carted large volumes of Pt-bearing soils and gravels to puddling plants that removed the Pt and Au nuggets from the alluvium.

The discovery of the nearby Gillenbine Tank Lead in 1917 provided a minor boost to the declining production rate from Fifield. The New South Wales Geological Survey in 1928 carried out the first systematic assessment of the mineral potential of the major deep leads. Extensive alluvial Pt was identified in a 79-hole program, however, details of these occurrences are not available. The Fifield region continued to produce minor amounts of Pt (0.1 kg to 25 kg) for over 70 years, with the final production (0.4 kg) recorded in 1966.

Most alluvial Pt grains from the Fifield region varied in size from tenths of millimetres to a few millimetres, with the majority around 1 mm. Large nuggets were also sometimes found, such as a rare example acquired in 1897 (and subsequently lost) by the Geological and Mining Museum in Sydney that measured 2.4 cm-across and weighed 42 g.

The three most important deep leads, the Platina Lead, Gillenbine Tank Lead, and the Fifield Lead, radiate out from the township of Fifield and are spatially near the Murga and Tout mafic-ultramafic intrusions. The deep leads are typically covered by thick sequences of alluvial clays and gravels. The regional radial pattern of the three major ancient watercourses indicate a potential source area south of Fifield, possibly related to a primary source in an undefined mafic-ultramafic intrusion(s) or a secondary Cenozoic gravel or laterite. The identification of the specific source(s) is hampered by the complex erosional and transportation histories of the precious metal grains apparent in the Fifield region. The most important paleo-drainage system, the Platina Lead, 5 km south of Fifield, produced approximately 478 kg of Pt at grades of 5 g/t–13 g/t and 124 kg of Au at grades of 1.5 g/t–4.6 g/t. The deep lead extended for approximately 3.5 km in a north-south direction, with the paleo-drainage direction towards the south. After its apparent confluence with the Un-Named Deep Lead from the west, the Platina Lead changed direction more towards the southeast. The Pt- and Au-bearing gravels were less than 1 m-thick and were concentrated in physical traps, such as cavities and gutters in the erosional surface of the basement Girilambone Group metasedimentary rocks. The gravels cropped out at the northern end of the lead, but towards the south they were covered by up to 22 m of Quaternary sands, clays, and gravels. A typical sequence consisted of thick units of reddish loam interspersed with patches of quartz rock and fragments of schistose and dolomitic rocks. The distribution of the old workings indicates the deep lead varied from 20 m to 45 m in width and was about 27 m-deep. The principal PGM in the gravels is isoferroplatinum, but the source of the Pt-alloys and Au is unknown. The PGE-bearing gravels have experienced a complex history of multiple cycles of transport and deposition.

The 2.5 km-long Gillenbine Tank Lead (6 kg Pt, 1 kg Au) and the 1 km-long Fifield Lead (145 kg Pt, 53 kg Au) produced minor quantities of Pt and Au. The Gillenbine Tank Lead a couple of kilometres east of Fifield was about 30 m-wide and 27 m-deep, whereas the north-trending Fifield Lead immediately north of Fifield was a much broader 200 m-wide channel not much more than 7 m-deep.

Waterworn Pt and Au grains were also found in the ferruginous cement of a quartz-bearing conglomerate of possible Cenozoic age at Jack's Lookout, 2 km east of Fifield (Flack, 1967). Total production from the paleoplacer conglomerate at Jack's Lookout was about 10 kg Pt and 1 kg Au.

In more recent times the Fifield region has continued to be a focus for Pt exploration, with several major and junior companies undertaking geophysical and drilling exploration programs. These phases of renewed exploration interest were generally stimulated by periods of buoyant global metal prices. Exploration activities have diversified from the alluvial Pt deposits worked at the turn of the century to also include hard-rock and supergene deposits associated with the intrusions.

The following summary of exploration activities and significant findings since the 1960s is largely from Teluk (2001), and from various chapter contributions by Elliot and Martin (Owendale Intrusion), Derrick (Tout Intrusion), and Jones (Kars and Gilgai intrusions) in Elliot and Martin (1991).

### **5.2.2.1 Alluvial deposits**

In 1969–70, Platina Developments and Mines Search carried out an extensive drilling program on the Platina and Gillenbine Tank deep leads and the Cenozoic conglomeratic paleoplacer at Jack's Lookout. A total of 211 holes were drilled into the Platina Lead, but results were equivocal due to sampling problems associated with clay. Conzinc Riotinto of Australia Exploration in the late 1970s undertook a geomorphological, auger and Rotary Air blast (RAB) drilling program that defined a large subeconomic platiniferous zone associated with the Platina Lead. Gold Shamrock Mines Limited in the mid-1980s commenced the most comprehensive phase on the Fifield alluvials. Sampling programs evaluated areas outside and within the known leads.

In the late 1980s, Helix Resources Limited through its extensive exploration programs for primary PGE mineralisation identified three subeconomic Pt-Au-bearing paleochannels within the Owendale intrusion 10 km north of Fifield:

1. Owendale Lead—northeasterly-trending paleo-valley up to 3 km-wide across the centre of the intrusion;
2. Milverton Lead—a 1.5 km-wide sub-parallel paleovalley up to 30 m-deep that traverses the southeastern corner of the intrusion; and
3. Cincinnati Lead—a smaller 100 m-wide northerly-trending channel along the eastern margin of the intrusion and flows into the main Owendale Lead.

The three mineralised paleochannel systems at Owendale have entrenched and partially stripped the early- to mid-Cenozoic regolith, thus indicating a post mid-Miocene age. The paleochannels appear to have their headwaters in the Tout Intrusion immediately to the south of the Owendale Intrusion, thus it is possible the source(s) of the alluvial Pt is associated with the Tout and/or Owendale intrusions. Sediments in the paleochannels comprise clay, sand, and poorly sorted gravel horizons that contain clasts of subrounded to angular vein quartz, goethite, and rare igneous rocks derived from the intrusions. Most clasts are 1 to 2 cm-across with rare examples attaining 10 cm.

Platinum grains in the deep leads are typically concentrated in gravel horizons overlying erosional unconformities at the base of the channels, or within the channels where a period of deposition has been followed by subsequent erosional and redepositional events. Maximum Pt grades of 0.14 g/loose cubic metres were obtained from bulk sampling of gravels at the Milverton Lead, and alluvial material from RAB holes at the Owendale Lead had grades of up to 0.4 g/t Pt. Typically the Pt grains have a bimodal size distribution, with most grains less than 1 mm, and a coarse fraction from 1 to 2 mm, with

some examples of centimetre-sized nuggets. Degree of rounding for the grains ranges from angular to subrounded. Over 90% of the grains are isoferroplatinum (Pt<sub>3</sub>Fe). Alloys of Os-Ir-Pt, cuprorhodsite, bowieite-kashinite (Rh, Ir, Pt, Cu, Fe, Os, S, As-bearing minerals), and Pd and Rh-Pd arsenides occurring as inclusions in isoferroplatinum were identified by Johan et al. (1990a,b). Irregular nuggets of Au up to 5 mm-long comprise less than 30% of the precious metals from the Milverton Lead. The Au is probably derived from quartz veins in schist country rocks (Girilambone Group).

High Pt prices in the 1990s initiated some further minor exploration activities on the thin and extensive colluvial and eluvial Pt placers north of the Platina Lead.

During the mid-2000s, Rimfire Pacific Mining NL undertook extensive soil sampling and subsoil auger drilling programs throughout the Platina and Gillenbine Tank lead region. They demonstrated the co-existence of coarse-grained Pt and Au in several locations. Soil and trenching programs at the 'Ebenezer' prospect located ~500 m southeast of the Platina and Gillenbine Tank deep lead area, indicated that the Pt is derived from residual or semi-residual soils, not alluvium. Trenching was a preferred technique to local spot drilling since it gave better geochemical coverage across the total width of the drainage systems. The rough exterior forms of the Pt grains indicated the sources were probably proximal and the grains had not travelled great distances. These findings questioned the previous mineral-system models of the Fifield region. Similar Pt anomalies were reported in residual soils at the 'Eastern Shear Zone' prospect near the Gillenbine Tank deep lead. The Pt anomaly at this prospect is continuous over 1 km and is parallel to the northeast-trending Gillenbine Tank Lead.

#### **5.2.2.2 Laterite deposits**

PGE-enriched Cenozoic laterites are spatially associated with a number of intrusions (e.g., Owendale, Tout-Syerston, Kars, Gilgai, Bulbodney Creek) in the Fifield–Nyngan region. These deposits are considered attractive, low-cost commercial targets (relative to the metallurgically complex sulphide and chromite associations seen in other types of PGE deposits) since:

- they contain the more valuable metal, Pt, relative to the other PGEs, and they usually have credits of Co and Ni;
- bulk-mining techniques involve low-stripping ratios of overburden and easy mechanical separation of the Pt and Au; and
- they can be quickly brought into production during periods of favourable metal prices.

The ferruginous laterite profile in the Owendale Intrusion is developed preferentially over olivine-rich ultramafic lithologies, such as dunite, wehrlite, and olivine pyroxenite. This style of mineralisation generally occurs above these lithologies throughout the intrusion, but is best developed in the Cincinnati and North Owendale areas. The laterite profile comprises an upper ferruginous zone overlying a mottled zone and a saprolite zone. It is enriched in Fe, Mn, Ni, Co, Cu, and Cr, and depleted in Mg and silica. The mineralisation generally consists of a high-grade elongate central zone some tens of metres wide and hundreds of metres long surrounded by a broad halo of low-grade mineralisation. Platinum is concentrated down the profile for thicknesses ranging from a few metres to 40 m, with maximum grades generally occurring at the base of, or immediately below, the upper ferruginous zone. Platinum grades are between 0.1 to 1.5 g/t with lesser Pd, and minor Os, Ir, and Rh. Maximum Pt grades attain 8 g/t over 1 m intervals in the Cincinnati prospect. Platinum to Pd ratios are usually 10:1 (similar to the primary mineralisation in the intrusion), and the Pt is enriched by a factor of ~27 compared to the underlying, unweathered ultramafic bedrock. The PGMs in the laterite are dominantly Pt-Fe alloys, and one such grain contained a small inclusion of osmiridium. The grains are

much smaller (<100 µm) than those in the alluvial placer deposits. There is no direct evidence to indicate large-scale supergene remobilisation of the PGEs in the lateritic environment.

The Syerston Pt-Ni-Co prospect, located in the Tout Intrusion, 8 km northwest of Fifield, is one of the most advanced lateritic prospects in the Fifield-Nyngan region. A resource of 1.0 million ounces @ 0.24 g/t Pt, with associated credits averaging 0.66% Ni and 0.11% Co, has been defined in the Syerston prospect. The Tout Intrusion is an elongate ultramafic-mafic-intermediate body, 16 km-long in a west-northwest direction, and up to 6.5 km-wide. Less than 1% of the intrusion is exposed, and drilling has defined six igneous rock sequences, namely hornblende quartz monzonite, hornblende melamonzonite-meladiorite, hornblende pyroxenite, clinopyroxene quartz monzonite-diorite, pyroxenite-gabbro, and dunite. These rock sequences are interpreted to represent individual magma pulses that were emplaced into an expanding magma chamber that progressively became more ultramafic with time. Parts of the intrusion are overlain by a thick, Cenozoic laterite profile comprising pisolitic laterite and massive to cavernous limonitic and siliceous laterite units. Nodular masses of magnesite locally invade goethitic clays in the laterite profile. The profile attains maximum development (>30 m) over the more weathered dunite rock types. Intensive drilling programs by Black Range Minerals in the late 1990s defined anomalous Pt grades (>2 g/t Pt) over an area of ~2000 m-long by 200 m- to 400 m-wide, indicating an underlying primary zone of mineralisation. Some of the higher Pt grades in the laterite profile include: 12 m @ 8.0 g/t, 4 m @ 8.0 g/t, 1 m @ 32 g/t, 14 m @ 3.3 g/t, 24 m @ 4.2 g/t, and 24 m @ 2.9 g/t. Metallurgical investigations indicate the Pt grain size varies from ultra-fine to coarse (nuggetty), and the dominant mineral is isoferroplatinum (alloy comprising ~80% Pt, 10% other PGEs, and 10% Fe). At least two geological periods of laterisation have resulted in residual enrichment of clays in different mobile metals (e.g., Cr, Ni, Co, and Pt). A moist period in the Early Cenozoic resulted in the development of various zones of hematite-rich pisolite, goethitic clay, and silicification at, or above, a high-level water table. A younger phase of laterisation in the Late Cenozoic witnessed more arid conditions and a falling water table level. As a result of these changing conditions, Cr, Ni, and Co were taken into solution and redeposited lower down in the profile, but Pt was not redistributed by these supergene processes.

The Kars Intrusion is a 700 m-wide, semi-elliptical ultramafic-mafic-intermediate body, located 22 km south of Fifield. The intrusion was defined by Platinum Search NL-Lachlan Resources NL using high-level Bureau of Mineral Resources, aeromagnetic data as a prominent high anomaly caused by the high magnetite content of the dunite-pyroxenite-monzonite lithologies of the intrusion relative to the non-magnetic metasedimentary country rocks of the Girilambone Group. The intrusion is poorly exposed, fault-bounded along the northwestern margin, and is locally unconformably overlain by Lower Devonian sandstone and conglomerate of the Derriwong Beds. Drilling has defined a sequence of very coarse-grained olivine pyroxenite, intermixed with zones of wehrlite and dunite, before passing into pyroxenite at greater depth. A 100 m-wide zone of hornblende monzonite mantles the southern extremity of the ultramafic lithologies. A region of lower magnetic intensity near the centre of the intrusion coincides with the major Pt-bearing lithologies. These include the more olivine-rich wehrlite, dunite, and olivine pyroxenite units which are cut by numerous dunite dykes and pods.

A near-surface Pt anomaly (averaging 0.42 g/t Pt) some 500 m-long by 50 m-wide was defined in soils and weathered bedrock above a small ultramafic-mafic dyke-like body in the Kars Intrusion. Costeans (shallow trench) over the anomaly confirmed the presence of widespread low-grade Pt (0.1 g/t to 2 g/t) mineralisation in weathered rocks. Drill intersections of the olivine-rich rock types included 42.28 m @ 0.43 g/t Pt from 20.7 m in DDH K1 and 59 m @ 0.33 g/t Pt from 79.0 m in DDH K4. Most of the disseminated Pt mineralisation is very fine-grained (<100 µm), comprises polyxene (Pt-PGE-Fe alloy) and isoferroplatinum (Pt<sub>3</sub>Fe), and is associated with magnetite in a chromite-depleted zone.

The poorly exposed Gilgai Intrusion, 25 km west of Nyngan, is interpreted to be a zoned body comprising an olivine-rich dunite core similar to the Owendale and Kars intrusions further south. A buried mineralised laterite cap, up to 45 m-thick, occurs above dunite and pyroxenite in the central part of the body. Shallow drilling and costeaming of the laterite have returned Pt grades of up to 2 g/t, with some enrichment of Ni and Cr, but Pd abundances are generally low. Diamond drilling tested a surface geochemical anomaly that covers an area of 250 m by 350 m. Dunite and olivine pyroxenite contain widespread low-grade Pt concentrations up to 0.4 g/t with local peaks of 1 g/t to 4 g/t over 1 m intervals. The mineralisation is characterised by extremely low S and Pd abundances.

### **5.2.2.3 Primary hard-rock deposits**

The hard-rock potential of the Fifield intrusions was initially highlighted in 1966–67 during a four-hole diamond-drill program of the Owendale Intrusion by Anaconda Australia Incorporated. High-grade Pt abundances (over 14 g/t Pt+Pd) in fresh pyroxenite from these drill-holes were confirmed some twenty years later by reanalysing of the core by New South Wales government geologists (Suppel and Barron, 1986a). Holes at the Kelvin Grove prospect on the southern margin of the Owendale Intrusion intersected a variety of alkaline ultramafic and mafic rocks including clinopyroxenite, biotite clinopyroxenite, meladiorite, hornblendite, hornblende-biotite clinopyroxenite, and serpentinite. High concentrations of Pt with subordinate amounts of Pd were recorded in medium- to coarse-grained clinopyroxenite. The most significant intersection was 1.4 m @ 13.2 g/t Pt, 0.93 g/t Pd (from DDH FKD 1: 302.36 to 303.76 m). The mineralisation is characterised by high Pt to Pd ratios (8 to 24) and uniformly low Au and Cr contents. There are no clear relationships between tenor of mineralisation and grain size or position of the mineralised pyroxenite unit. Suppel and Barron (1986a,b) described these transgressive monomineralic clinopyroxenites containing elevated Pt and Pd concentrations as 'P units' (see Section 6.4).

The Kelvin Grove hard-rock Pt discovery influenced a number of major companies (BHP 1974–5, CRA 1979–80, and Shell 1982–83) to undertake broad-spaced exploration over several intrusions in the Forbes–Fifield–Nyngan region. The brief exploration programs were generally not conceptually-based or sufficiently focussed towards detecting major primary mineralisation, although widespread enrichment of Pt was recorded in the laterite profiles. Drilling programs have recorded anomalous Pt concentrations in laterite above the Avondale (Rimfire Pacific Mining NL), Bulbodney Creek (Helix Resources Ltd), Gilgai (Platinum Search NL), Honeybugle (North Broken Hill Limited), Hylea (Lamadec Exploration Limited), Kars (Platinum Search NL), Murga (Austplat), Owendale (Helix Resources Ltd), and Tout (Anaconda Australia Incorporated) intrusions. The release of high-resolution airborne magnetics in 1997 by the New South Wales government Discovery 2000 program provided important new information on the intrusions under cover.

Rimfire Pacific Mining NL has been investigating in recent years the bedrock source(s) for the Pt and Au near the deep-lead systems southeast of Fifield. Excavated pavements of weathered bedrock revealed evidence of structurally-controlled alteration and mineralisation events. The structural corridors in the exposed bedrock coincide with the distribution of the historical (1920–30s) mining activities for Pt in the soil profile. The company concluded from examinations of the excavated bedrock pavements and heavy-mineral concentrates from overlying gravels that:

- coarse-grained Pt occurs in bedrock often associated with shear and breccia zones and non-magnetic mafic and possibly ultramafic dykes;
- the breccia zones contain significant alteration and re-brecciation features;

- open stockworks of gossanous veinlets, sulphide-carbonate veinlets, and small patches of near massive oxidised sulphides are locally associated with complex shear and breccia zones;
- the surface features of the Pt (isoferroplatinum) and Au grains from the overlying gravels and soils indicate two different travel distances of 0.1 to 0.5 km, and 1.5 to 4 km, respectively;
- the Pt and Au are derived from the same mineralising system;
- the grains are apparently primary as opposed to accreted in the weathering profile (i.e., they are not of supergene chemical origin) despite their coarse grain size (1 to 12 mm, and up to 7.4 g weight); and
- the Pt and Au grains are associated with magnetite, chromite, ilmenite, zircon, monazite, and cassiterite.

Rimfire Pacific Mining NL has documented a variety of mineralisation types (Pt, Au, Cu, Pb, Zn) that appear to be zoned within a narrow corridor of less than 10 km-wide immediately south of Fifield. They interpreted this corridor as being a complex volcanic rift setting potentially containing polymetallic deposits related to sub-volcanic intrusives with associated shearing, alteration, brecciation, and veining events at various scales. Gold occurs with minor Pt in the interpreted western margin of the rift, Pt is with some Au in the centre of the rift, and base metals are present on the eastern margin of the rift. Base-metal Cu soil anomalies and Cu-bearing barite gossans highlight the potential for Volcanic Massive Sulphide (VMS) deposits to be associated with the Pt mineralisation.

### 5.2.3 1910 to 1960—Tasmania: largest producer of 'osmiridium' in the world

The 'osmiridium' potential of Tasmania was first realised during Surveyor-General Charles Percy Sprent's expeditions of western Tasmania (Figure 5.3). 'Osmiridium' (often incorrectly recorded as platinum or palladium) occurrences were indicated in his reports (as platinum) that described his exploration of the Mount Bischoff region from February 1876 to April 1876 (Sprent, 1876: Appendix I), and they are also shown (as palladium) on his exploratory chart of the valley of the Wilson River. During his Mount Bischoff expedition, Sprent made the following observations regarding a heavy, tin-white metallic mineral that he and his colleagues found near Parson's Head Mountain in the Meredith Range, *'In this vicinity we obtained zircon sand and a little platinum. The platinum might be worth examination, but I am afraid that the place is too difficult of access to offer much encouragement to prospectors. On the west side of the Parson's Hood I am informed the formation is quite different, and consists of serpentine, diallage, hypersthene, with iron ores, asbestos, copper, and platinum, and in some places gold'* (Sprent, 1876, p. 2–3).

On December 21<sup>st</sup> 1876, Sprent commenced another expedition to the Pieman, Arthur, and Whyte Rivers, and revisited the Meredith Range in western Tasmania (Scott and Sprent, 1877: p. 10–11—Appendix I). Sprent described several occurrences of alluvial Au and Pt and he also makes the first description of 'osmiridium' in Australia. The most relevant references to these metals are *'Camped at the Whyte for a day whilst we examined the place where Long and Lord found ... The spot where we tried was on a small beach of the river. We obtained and platinum in every dish; quite enough to pay if there were any quantity of dirt, but unfortunately there is not.'* and near Parson's Hood *'As noticed in my last year's Report, Mr Harman discovered on the east side of Parson's Hood copper in small quantities in connection with serpentine rock, gold, and osmiridium... Gold occurs in small quantities almost everywhere. In two instances it occurs with osmiridium (a metal of the platinum class) in the vicinity of serpentine. Instances of serpentine being the mother rock of gold are by no means rare in Australia.'*

A few years after Surveyor-General Sprent's discovery of 'osmiridium' in 1876 prospectors working the Whyte and Savage Rivers of the Corinna field found 'osmiridium' in association with Au in the alluvial deposits. The 'osmiridium' was identified in gravels of the Savage River in 1881, with the earliest published reference in a report by Government Geologist A. Montgomery issued by the Tasmanian Department of Mines in 1894 (Reid, 1921). Later field reports of the 'osmiridium' deposits by Government Geologist W.H. Twelvetrees formed the basis of Geological Survey Bulletin 17 published by the Tasmanian Department of Mines in 1914. The 'osmiridium' in the Whyte and Savage Rivers formed small heavy, steel grey grains that were often associated with concentrations of alluvial Au grains. However, there was little demand for the 'osmiridium' and the prospectors considered it as an obnoxious impurity since because of its higher specific gravity than Au it was difficult to separate from it and a penalty of 7s. 6d. per ounce was imposed by the Mint for its removal. Most 'osmiridium' during this early phase of the industry was discarded and thrown away.

It was not until the turn of the century that small quantities of 'osmiridium' filtered through to foreign investors in London and New York, who appreciated the good quality and coarse grain size of the material. At about this time new applications were also being developed for the rare metal. Assistant Government Geologist Reid noted that although the price offered (25s. per ounce), was very small, it gave the diggers some incentive to continue their prospecting and mining activities (1921). Gold miners at Corinna were among the first individuals selling 'osmiridium' separately from Au resulting in a new industry being established. The mining techniques consisted of hand shovelling the prospective alluvium or 'wash' (gravel, sand, and clay) into riffled sluice boxes or cradles for treatment. Extracting 'osmiridium' from clay was more difficult as it involved 'puddling' or mixing the clay to a slurry before being treated in a sluice box. The miners referred to the 'osmiridium' as 'osie' or 'metal'. Some 'wash' was also obtained from the hosing down of trenches; this hosing of material *in situ* was called 'ground sluicing'. Larger operations had suction pumps called 'lifters', which extracted the prospective gravel and sand and pumped it directly into a sluice box. Local blasting of the creek bed enabled the upper ~30 cm of the creek bed to be broken up to obtain access to the 'osmiridium' that had settled into the crevices of the creek pavement. Production during these early days was mostly from small operations, often only one or two men with pans. This enabled the working of isolated deposits in remote areas.

From 1909, the price of 'osmiridium' started to increase with the collapse of the Russian PGE industry as a result of war and revolution. With the rising metal price, production also increased and the 'osmiridium' mining industry of Tasmania became established. In 1910 the Tasmanian Department of Mines commenced documenting the official amount and commercial value of 'osmiridium' produced in the state. Production statistics were maintained to 1968. Since 'osmiridium' was a precious metal requisite for munitions of war (osmic chloride was used in the making of poison gas), manufacturers who used the metal found some of their usual supplies cut off, and they turned their attention to Tasmania. Consequently production increased from 3.7 kg in 1910 to 62.3 kg in 1920. During this year, the price reached £38 per ounce and the Pieman fields produced 62 kg valued at £77 10s. 4d. Production increased erratically from 1910.

One of the most important 'osmiridium'-bearing areas during this early phase of the industry was Bald Hill situated on the Heazlewood River ultramafic-mafic intrusion in northwest Tasmania (Figure 5.4). The Nineteen Mile Creek, which defines the western margin of this intrusion, was the most productive source, with important alluvial contributions also from Linger and Die Creek, McGintys Creek, and Jones Creek. In 1914, ten nuggets weighing between 14 g and 50 g were purchased at Waratah by several museums from around the world. One of the largest 'osmiridium' nuggets in the world was discovered at Bald Hill. It was found by Tom Prouse in 1920 and weighed 4 ounces, 8 pennyweights, and 17 grains (~138 g). A nugget weighing over 2 ounces (~62 g) was also found in the same area in

1925. William Caudry attempted hard-rock 'osmiridium' mining at the head of McGintys Creek by crushing the serpentine host rock. Figure 5.5 shows alluvial 'osmiridium' and Au nuggets from the Bad Hill–Nineteen Mile Creek–Heazlewood region have quite variable and complex morphology and surface features.

Reid's comprehensive review 'Osmiridium in Tasmania' (1921) provides some useful early insights into the favourable host rocks and style of mineralisation. He states *'It has been definitely established as the direct result of the recent investigations of the Tasmanian fields that the occurrence of osmiridium is intimately related to the chemical and physical characters of serpentine rocks derived largely from bronzite rich in alumina, consequently the distribution of this mineral is determined by that of a particular variety of serpentine. For instance, in all the fields the osmiridium invariably accompanies serpentinised peridotite (olivine and bronzite), while the serpentines derived from pyroxenites and gabbros are barren. It is noteworthy that in these peridotites all metallic elements other than those that occur in combination with silica are found in alloy with one another or uncombined with other elements. It has been determined also that the deposits of osmiridium in the peridotite serpentine are almost exclusively confined to pockety accumulations distributed irregularly along structural planes in the rock..... It will be perceived from the foregoing that not only is it possible to distinguish the osmiridium-bearing serpentines from those that are barren and accurately delimit their boundaries, but the precise location of the deposits in these rocks can be fixed without difficulty.'*



Figure 5.4 Prospectors and alluvial-hardrock 'osmiridium' mining operations in western Tasmania. (a). Rare example of hard-rock mining of 'osmiridium' from serpentinite host rock, Caudry's mine, Nineteen Mile Creek, Bald Hill. (b). Alluvial operations for 'osmiridium', Bald Hill. (c). James McGinty, veteran pioneer 'osmiridium' miner. (d). Panning and sluicing for 'osmiridium', Mt Stewart. (e). Panning for 'osmiridium', Nineteen Mile Creek. (f). Miners camp, Bald Hill. (g). Typical miner's camp, Bald Hill. Images (a) and (c–e) from Brown (1919); (b and f) from R. Bottrill, *Mineral Resources Tasmania*.

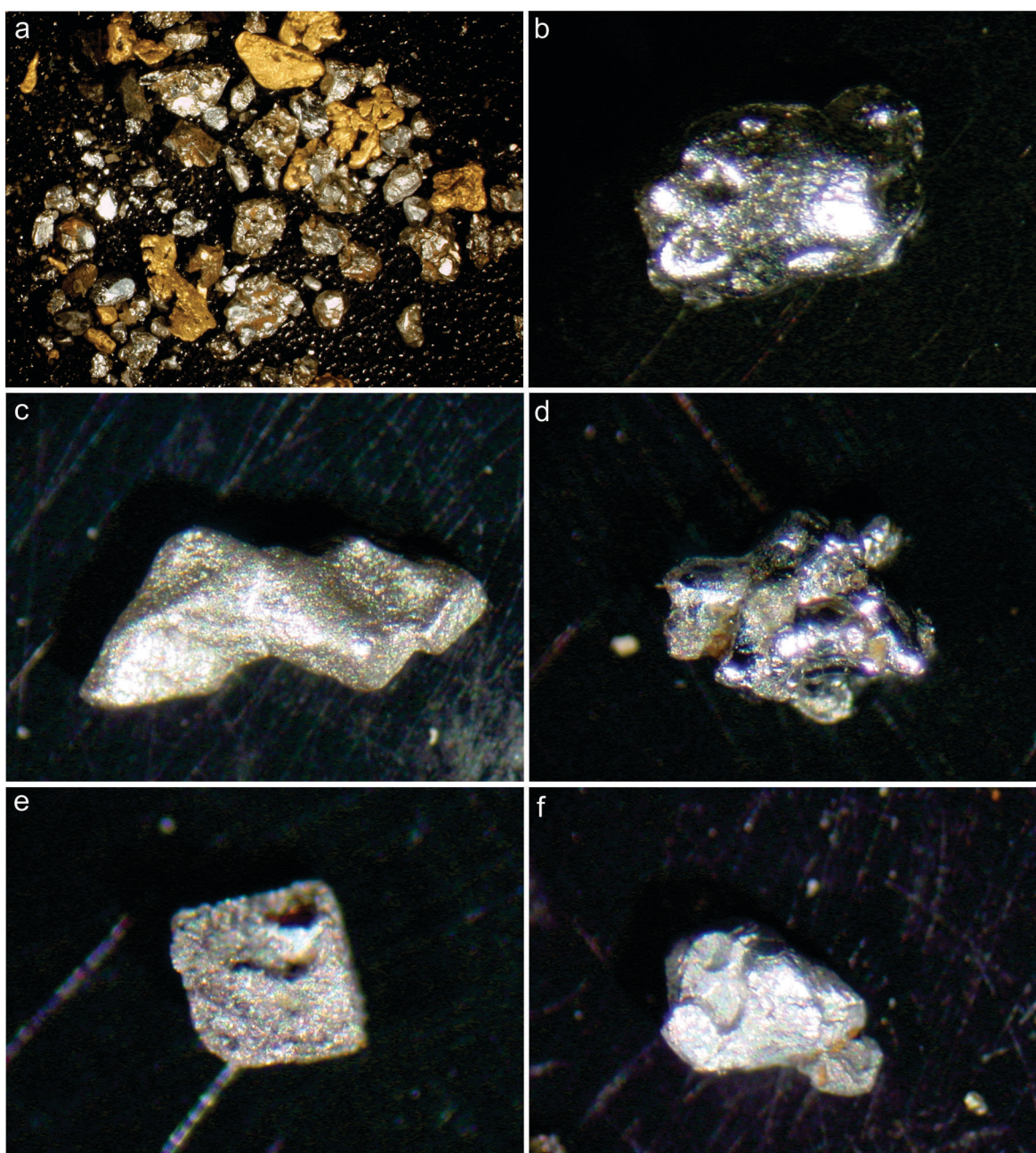


Figure 5.5 Alluvial 'osmiridium' nuggets from the Bald Hill–Nineteen Mile Creek–Heazlewood region, northwestern Tasmania. (a). Sub-rounded 'osmiridium' nuggets and more irregular, abraded, and flattened gold nuggets. (b). Sub-rounded 'osmiridium' nugget. (c). Sub-angular 'osmiridium' nugget. (d). Irregular 'osmiridium' nugget. (e). Sub-angular 'osmiridium' nugget. (f). Sub-rounded 'osmiridium' nugget. All images from R. Bottrill, *Mineral Resources Tasmania*.

The 'osmiridium' industry of Tasmania received considerable momentum in the 1920s with the discovery of shallow alluvial and hard-rock deposits in the Adam River valley (later to be known as Adamsfield) near Tyenna in the remote southwest corner of the state. The following summary of the discovery and life on the diggings at Adamsfield (Figure 5.6 and Figure 5.7) is in part from Bacon (1992). In 1909, Government Geologist W.H. Twelvetrees reported during his investigations of the mineral potential of the Tyenna and Gordon River region that the Clark brothers had found 'iridosmine' in Fourteen Mile Creek. Twelvetrees also documented small quantities of extremely fine-grained

'osmiridium' and Au in serpentinite rock about 1 mile beyond the Florentine River. However, further exploration activities indicated that the mineralisation was of limited extent and these early discoveries proved to be uneconomic. In December 1924, a group of prospectors comprising E. Boden, A. Wright, A.J. Stacey, and C.B. Stacey found 'osmiridium' in the Adam River Valley, above the falls (Adams Falls), and upstream near the Sawback Range. The news of the discoveries initiated a rush of many hopeful miners to the Adamsfield area—one of the last significant mining rushes to occur in Australia. The Department of Mines issued over 1000 Miners Right Claims in late 1925. The main 'osmiridium'-bearing area was along Main Creek from its source to below the junction with Smith Creek, and on the eastern, northern, and western slopes of Football Hill. The 'osmiridium' consisted of small (millimetre size) sub-angular to sub-rounded grains and rarer small nuggets (Figure 5.8). Production culminated in 1925 when 104 kg of 'osmiridium' was obtained from the alluvial deposits. In that year £105 570 was paid to the miners, and Tasmania was regarded the largest producer of free 'osmiridium' in the world (Reid, 1921; Geary et al., 1956). During these prosperous times, over 800 miners were working the Adamsfield alluvial deposits when the rare metal was nine times more valuable than Au. Adamsfield soon became the premier 'osmiridium' field of Tasmania producing about 477 kg, equating to 49% of the State's total production of ~970 kg.

In October 1929, Samuel McAteer found 'osmiridium' at Adamsfield in serpentinite rock adjacent to a talc-bearing ultramafic rock. He was granted a reward of ten acres for his discovery. The hard-rock workings consisted of trenching to expose mineralised veins, ground sluicing the surface of the lode, sinking shallow shafts and constructing drives (tunnels). During these early days no stamper or crusher was present to break down the rock, so treatment involved sluicing and re-sluicing piles of serpentinite, allowing the rock to weather and decompose, and sluicing again.

The prospectors generally endured a difficult lifestyle with the most pressing problems being the difficult access, the supply of fresh food provisions, bushfire hazards, and a suitable supply of water. Lack of water for sluicing at Adamsfield was a problem during the summer months, whereas for some low-lying areas too much water impacted on mining activities. The miners mainly lived on damper, tea with sugar, bacon, and 'tinned dog' (tinned meat). Food was expensive, with the cost of living in some mining centres 100% higher than more civilised settlements. Miners had to earn around £30 per month just to cover their food costs. Tents and paling huts were the common forms of accommodation for the miners.

During the peak of the mining boom in the mid-1920s, Adamsfield became a thriving town (Figure 5.6 and Figure 5.7). At one stage it boasted three general goods stores, a public bar, a community hall in which dances were regularly held, a church for monthly services, bush hospital, police station, school, Mines Department Office, and a butchery. Cattle for the butcher were taken into Adamsfield and killed for meat straight away since there was no grass suitable for grazing at Adamsfield. Towards the end of the 1920s the field traders were under financial pressure due to falling sales and the mining field started to decline. By 1932 low metal prices gradually caused the number of miners to dwindle and the minerals boom had finished with only £9075 paid to all miners in the state. In 1934, only sixty people were scattered throughout the Adamsfield mining field. Throughout the 1930s to 1940s a number of small 'osmiridium'-mining companies were floated on the Melbourne Stock Exchange to work the alluvial and hard-rock deposits. In June 1939, minor hard-rock lode material was crushed with the introduction of a 10-head stamper. In the late 1950s, small parcels of 'osmiridium' were sold at £100 per ounce compared to the world market price of around £30 per ounce. This anomalous price was due to the favourable coarse grain size of the Tasmanian 'osmiridium'.

Intermittent exploration activities that have involved 'modern' diamond drilling and geophysical techniques have occurred at Adamsfield in the last fifty years. In the 1960s, an increase in the use of 'osmiridium' in the electronics industry caused a small surge of exploration activities. Bulldozers were used to move 1000 t of material each day in exposing the lode. An aeromagnetic survey in 1965 identified a 1600  $\gamma$  anomaly over the host ultramafic rock sequence and this was followed up with ground geophysics. Exploration programs in the 1960s focussed on Ni and Cu, and in the 1980s the Au, PGE, and Cr potential were assessed. Today the historical mine sites at Adamsfield are largely reclaimed by dense natural bush.

For further details on the historical workings and life on the various mining fields, such as Bald Hill, Nineteen Mile Creek, Heazlewood, Mt Stewart, Long Plain, Wilson River, Huskisson Valley, Renison Bell, Dundas; the Gordon, Styx, Florentine, and Spero rivers; Birchs Inlet, Boyes and Hamilton Range areas, and Salisbury Goldfield, it is recommended that the reader refer to Twelvetrees (1914), Brown (1919), Reid (1921), and Nye (1929). Bacon (1992) provides a comprehensive summary of the historical and 'recent' mining activities on the Adamsfield mining field. The 'osmiridium' occurrences of Tasmania have been the subject of several petrological and mineralogical studies (Elliston, 1953; Cabri and Harris, 1975; Ford, 1981; Brown et al., 1988; Peck, 1990; Peck and Keays, 1990; Cabri et al., 1996). The following summary of the major findings from these studies is from Bottrill (2014).

The 'osmiridium' alloys from Tasmania generally occur as sparsely disseminated grains within chromitite pods, lenses, and layers hosted by serpentinised Cambrian ultramafic intrusive rocks (dunite, harzburgite) and in sedimentary rocks derived from these source rocks. Although PGE grades in the chromite-bearing host rocks locally attained 10 g/t, in most cases the grades of the primary deposits were too low to be economic. The host rocks of the primary deposits ranged from foliated serpentinite and talcose limonitic joints and schlieren (Halls Open Cut at Adamsfield, Caudry's Mine, Bald Hill, Wilson River), opalised serpentinite (Purcell's prospect), to schlieren transecting chromite and magnetite-rich serpentinite (Mt Stewart). The prospective zone at Caudry's Mine contained magnesite, opal, and talc, with the 'osmiridium' intergrown with chromite and magnetite. Source rocks at Adamsfield consisted of a 300 m-long zone of dark coloured foliated serpentinite containing chromite pods and minor millerite and nickeloan carbonates that was abutted on the eastern side by a barren, quartz-veined talcose shear zone. Considerable 'osmiridium' production at Adamsfield was also obtained from serpentine-rich quartzose sandstone and a cemented fragmental serpentinite overlying the host serpentinite, which may represent an ancient shore-line placer of probable Ordovician age.

A new style of PGE mineralisation associated with sulphide-bearing mafic rocks on the west coast of Tasmania was explored for during the late 1940s. The Cuni–Zeehan polymetallic deposits, located 2 km southwest of the Serpentine Hill Ultramafic Complex, consist of Cu-Ni-Pt-Pd pentlandite-rich ores hosted by a series of altered gabbroic dykes. The first reference to this mineralisation was by Reid (1921), who noted that Cu-Ni ore samples also contained 0.1 to 0.16 ounces per ton of Pt, ~1.4 ounces per ton Ag, and trace Au. The mineralised ?Neoproterozoic dykes occur in the Crimson Creek Formation and are unrelated to the Cambrian mafic-ultramafic 'osmiridium' source rocks that are widespread throughout western Tasmania. The ores at Cuni consist of magnetite-pyrite-pyrrhotite-pentlandite-chalcopyrite, with PGMs reported as native platinum and sperrylite (Hughes, 1965; Brown, 1998). Only a few thousand tonnes of ore have been mined from these small deposits which have generated renewed exploration interest for their Ni and precious metals in recent years (e.g., Melba Flats Ni-Cu-Co-Pt-Pd-Au prospect).

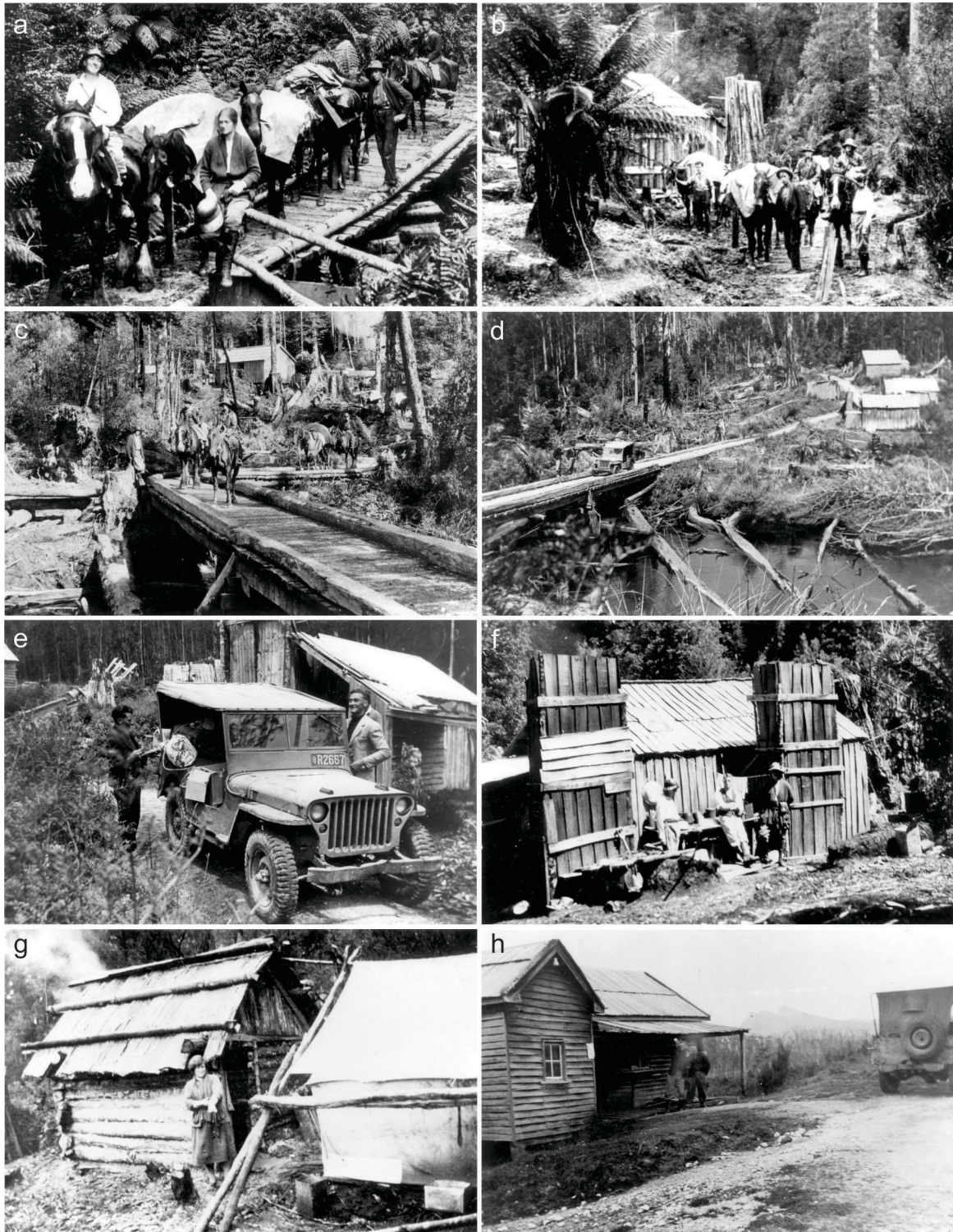


Figure 5.6 Infrastructure, accommodation, services, and mining activities being established, Adamsfield mining field, southwest Tasmania. (a). Pack horses en route to Adamsfield. (b). Pack horses near Florentine River, Adamsfield track. (c). Florentine River crossing. (d). Florentine River crossing, Adamsfield track, December 1948. (e). Arrival of first jeep to Adamsfield, Florentine River, December 1948. (f). Miner's slab hut ~1928. (g). Mrs Bidy Clark outside slab hut and canvas 'tent', ~1928. (h). General store at Adamsfield, with the first jeep to arrive in the town, December 1948. All images from Bacon (1992).



*Figure 5.7 Infrastructure, accommodation, services, and mining activities being established, Adamsfield mining field, southwest Tasmania. (a). Smith's general store at Adamsfield in ~1928. (b). Panorama of the early settlement of Adamsfield in ~1928. (c). Alluvial mining activities. (d). Processing 'wash' in a wooden sluice. (e). Alluvial mining activities. (f). Panning 'osmiridium', concentrates. (g). Processing 'wash' in a sluice. (h). Miners working the spoil heaps. All images from Bacon (1992).*

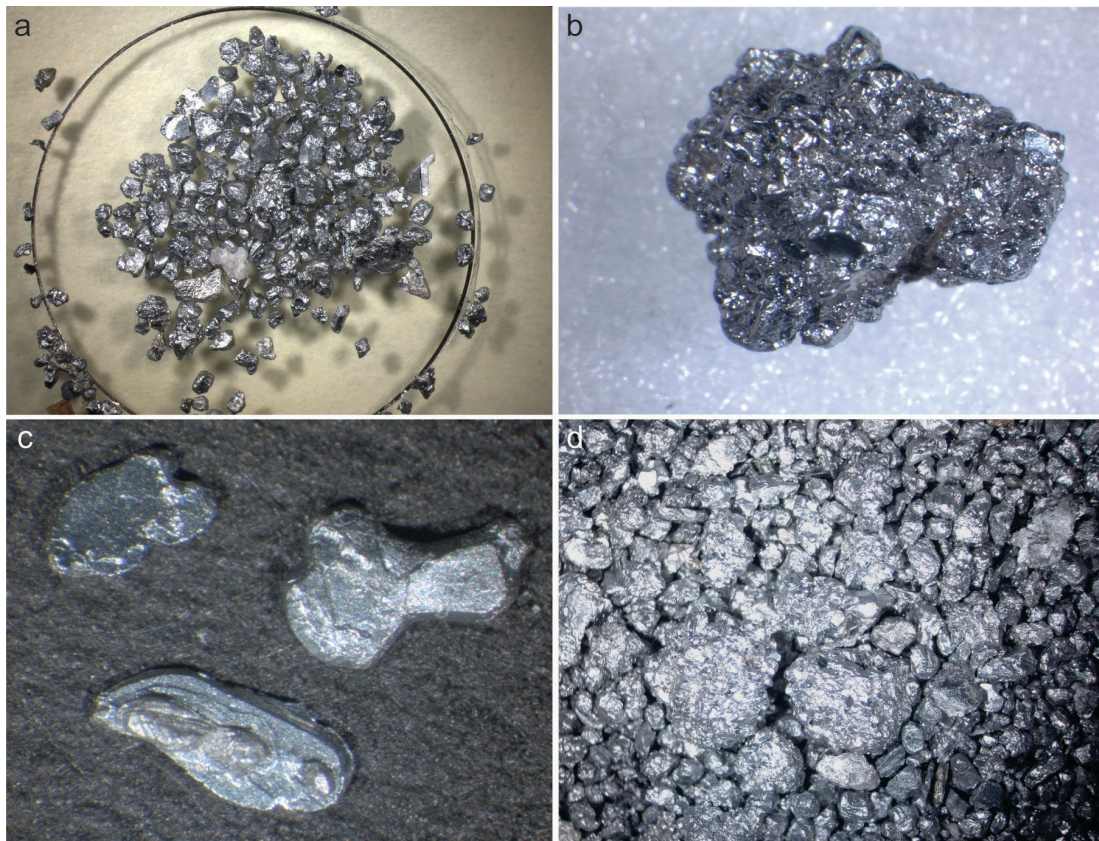


Figure 5.8 Alluvial 'osmiridium' grains and small nuggets from the Adamsfield mining field, southwest Tasmania. (a). Concentration of small sub-angular to sub-rounded 'osmiridium' grains and nuggets. (b). 'Osmiridium' nugget showing irregular pitted surface. (c). Three sub-angular 'osmiridium' nuggets. (d). Concentration of irregular 'osmiridium' grains and nuggets. All images from R. Bottrill, Mineral Resources Tasmania.

The majority of the Tasmanian 'osmiridium' production was derived from shallow Cenozoic alluvial and residual deposits spatially associated with the early Cambrian ultramafic-mafic source rocks. The small (<2 mm) tin-white to iron-grey irregular grains are harder than most metals and heavier than Au. Small nuggets can take the form of individual grains or weakly cemented aggregates of smaller grains up to 20 mm in diameter. Figure 5.5 and Figure 5.8 show some alluvial 'osmiridium' grains and small nuggets derived from the early-middle Cambrian ultramafic-mafic complexes of western Tasmania.

The informal name 'osmiridium' is entrenched in the early literature of the Tasmanian deposits to represent a poorly defined mixture of various PGE metals i.e. alloys. These alloys contain mainly Os, Ir, and Ru, with minor contributions from Pt, Pd, Rh, Au, Pt-Fe-Ni alloys, PGE arsenides, and sulphides. 'Osmiridium', and another equally incorrectly used mineral species 'iridosmine' that have been used for the Tasmanian examples have been abandoned in recent mineralogical classifications that are based on the major elements present. Harris and Cabri's (1991) classification of the natural Os-Ir-Ru alloys that is based on the elemental end-members (Ir, Os, and Ru) plus rutheniridosmine has shown there is complete solid solution between osmium, ruthenium, and rutheniridosmine, and a miscibility gap between these minerals and iridium (which may form a solid solution with Pt). Using this classification, most of the Tasmanian 'osmiridium' falls within the Osmium, Iridium, and Rutheniridosmine fields (see Figure 6.32). The tabular to hexagonal grains and scales are more likely to be osmium rather than iridium, which may show a crude cubic form. Other PGMs from Tasmania form microscopic inclusions in chromite and other minerals. The average composition of thirty

'osmiridium' concentrates from Adamsfield yielded 45.51% Os, 41.65% Ir, 6.40% Ru, 1.12% Pt, and 0.29% Rh, with traces of Pd, Au, Cu, and Fe (Nye, 1929). This average composition is considered by Bottrill (2014) to be typical of most of the Tasmanian deposits.

Bottrill (2014) has documented the PGM and Au minerals from the major mineralised provinces of western Tasmania (Adamsfield, Corinna, Fourteen Mile Creek, Heazlewood, Rosebery, Serpentine Hill, Wilson River, Zeehan). The minerals described include:

- Metals and Alloys:
  - auricupride ( $\text{Cu}_3\text{Au}$ ); ( $\text{Au,Ag}$ ); iridium ( $\text{Ir,Os,Ru,Pt}$ ); osmium ( $\text{Os,Ir,Ru}$ ); platinum ( $\text{Pt,Fe,Rh,Ni,Ir}$ ); ruthenidosmine ( $\text{Ir,Os,Ru}$ ); ruthenium ( $\text{Ru,Os,Ir}$ ); tetraferroplatinum ( $\text{PtFe}$ ); ferronickelplatinum ( $\text{Pt}_2\text{Fe}(\text{Ni,Cu})$ )
- Sulphides and Arsenides:
  - cherepanovite ( $\text{Rh,Pt,Ni,Fe}(\text{As,S})$ ); erlichmanite ( $\text{OsS}_2$ ); hollingworthite ( $(\text{Rh,Ir})\text{AsS}$ ); irarsite ( $(\text{Ir,Ru,Rh,Pt})\text{AsS}$ ); iridarsenite ( $\text{IrAs}_2$ ); kashinite ( $\text{Ir}_2\text{S}_3$ ); laurite ( $\text{RuS}_2$ ); ?safflorite ( $(\text{Co,Ru,Ni})\text{As}_2$ ); and sperrylite ( $\text{PtAs}_2$ )

## 5.2.4 1960 to present—Kambalda: world-class Ni-Cu±PGE province

The sampling of some curious green-stained Fe-rich rocks from a salt lake 60 km south of Kalgoorlie in the Eastern Goldfields of Western Australia represents an historic event in Australia's mining folklore. The identification of Ni-Cu-bearing gossans near the small township of Kambalda on the northern shoreline of Lake Lefroy was the catalyst for the discovery of some of the most significant Ni sulphide deposits in the world. In ensuing years, Western Australia would rival such countries as Canada, the Soviet Union, and New Caledonia as a major contributor to the global supply of Ni. The Ni sulphide deposits of the Eastern Goldfields produce mainly Ni, Cu, and Co, however, they have also produced significant amounts of Pd and Pt as a by-product of the other commodities. In fact, these deposits are historically and currently the largest producers of Pt and Pd in Australia. The Kambalda story is therefore an important chapter of the Australian PGE industry and for this reason it has been included in this report. The following description of the discovery and development of the Kambalda Ni deposit is largely derived from the excellent summary by Gresham (1991).

Interestingly, the discovery of the world-class Ni deposits in the Kambalda region involved a series of unrelated events that were linked to earlier Au and U mining booms. This part of the Australian continent has had a protracted history of Au exploration since its first discovery at Enuin (near the future site of the town Southern Cross) in 1887, but the importance of Ni was recognised much later. The township of Kambalda was gazetted in 1897, after the discovery of Au on the shores of Lake Lefroy in 1896. The town prospered for many years while Au was being mined at the area known as Red Hill. One of the most photographed Au specimens from Western Australia—the Golden Butterfly—came from the shallow workings at the Red Hill Au mine. Before the discovery of Au, the region was extensively investigated for its pastoral and grazing potential and Aboriginals frequented the area for centuries prior to the introduction of Europeans.

In 1939, Queensland prospector George Cowcill (Figure 5.9) brought his wife and two children to the Eastern Goldfields to chase the lure of Au that could be dollied and panned from outcropping rocks. It was during this time that Cowcill dug some shallow pits<sup>11</sup>, which later proved to contain the gossanous

<sup>11</sup> Marston (1984) provides a slightly different version of the initial gossan discovery. Marston states that the gossan was collected from the waste dumps of the abandoned Red Hill mine in 1947.

outcrops of the Lunnon Ni sulphide orebody. However, his main interest was Au, and he had to abandon these pits when water from a nearby well resulted in his family members falling ill. Several years later in 1954, spurred on by the first U exploration boom, Cowcill decided to continue his prospecting lifestyle. Cowcill's interest for U mineralisation was aroused by his observations of samples containing secondary green and yellow U minerals on display in the Mining Registrar office in Coolgardie (Marston, 1984). These colourful minerals reminded him of the gossanous rocks he had collected from the pits he dug in the Red Hill area in 1939 and he headed back to Kambalda. On the 4<sup>th</sup> of October 1954, he took the gossanous samples to Bill Cleverly, a senior lecturer in geology at the Kalgoorlie School of Mines, to assess the presence of radioactive minerals. Subsequent assays showed that the samples contained no U, but importantly they did record the presence of trace Ni. Cleverly reported *'in view of the very meagre Australian resources of nickel and the relatively high price, it might be worthwhile to explore the extent of the occurrence and to submit representative samples for nickel assay.'* Cowcill did collect more samples in January 1955, and Cleverly described these as *'ironstone of sulphide derivation with a few greenish stains which gave a positive test for nickel and a little pyrrhotite..... the percentage nickel would be almost insignificant and certainly not an economic proposition.'*



*Figure 5.9 Prospector George Cowcill inspects a piece of nickel gossan from the Lunnon deposit, Western Australia. Cowcill prospected in the Kambalda area for more than thirty years, before his persistence led to the discovery of the world-class Kambalda nickel deposit in the Eastern Goldfields (Gresham, 1991).*

In September 1964, further samples were submitted from Cowcill and his long-term colleague John Morgan to Roy Woodall (Figure 5.10a)—then Assistant Chief Geologist with Western Mining Corporation Limited (WMC: now merged into BHP Billiton)—whose company at the time was investigating the Au and base-metal potential of mafic-ultramafic rocks south of Kalgoorlie. Woodall had one of the samples submitted to the laboratory for a complete spectrographic chemical analysis. The sample contained about 0.7% Ni, 0.5% Cu, and anomalously high Mo, Te, and Ag. Woodall recognised the significance of this distinctive geochemistry, with the high tellurium in particular being typical of magmatic Ni-Cu sulphides. The sample was therefore interpreted to be a possible gossan derived from oxidised base-metal sulphides at depth. Woodall visited the prospective area with Morgan in September 1964. The discontinuous outcrop of gossans had a strike extent of over 450 m. The unusual geological setting (not previously recognised in Australia), combined with the distinctive geochemistry of the gossans and their extensive distribution, suggested that the gossans were leached from possibly a significant amount of magmatic Ni-bearing sulphides. Woodall wrote in a letter dated 23<sup>rd</sup> September 1964 to the General Superintendent of WMC (Laurence C. Brodie-Hall) *'I am not suggesting I have found an orebody but the occurrence is of great significance.'*

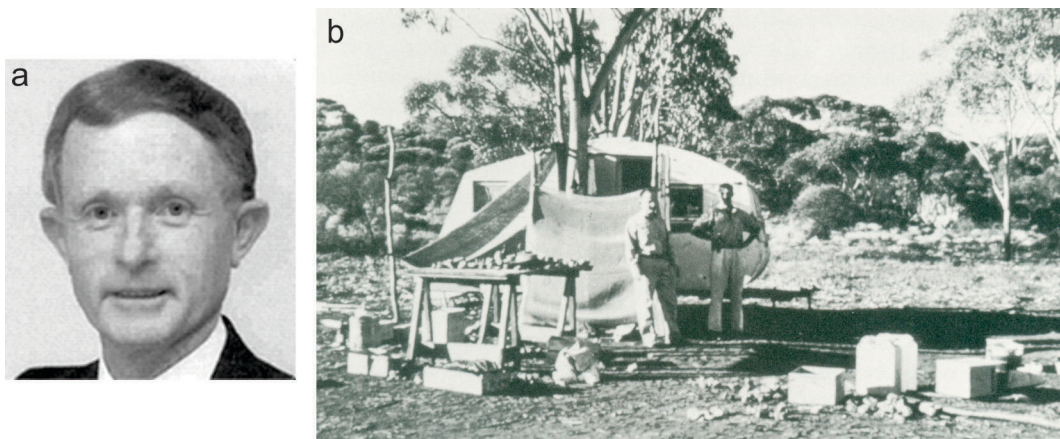


Figure 5.10 (a). Roy Woodall—Assistant Chief Geologist, Western Mining Corporation Limited—was instrumental in highlighting the base-metal potential of mafic-ultramafic rocks south of Kalgoorlie which led to the discovery of the Kambalda nickel deposit. (b). Roy Woodall with student John McKay at the Kambalda field camp 1964–65. McKay and fellow-student David Gamble carried out geological mapping of the Kambalda Dome region. They camped near a well that had served George Cowcill and other prospectors. The well was later preserved as an historical monument in Cowcill Street, Kambalda East (Gresham, 1991).

The prospective area of interest was geologically mapped in detail by university students John McKay and David Gamble in 1964–1965 under the supervision of WMC geologist Guy Travis (Figure 5.10b). The mapping defined a domal anticlinal structure plunging to the north and south (later to be known as the Kambalda Dome) and the gossans along a 21 km strike extent were situated near the base of thick sequences of ultramafic rocks overlain by pillowed metabasalt. Magnetic and induced polarisation (IP) geophysical surveys were employed to facilitate the location of diamond drill-holes. The IP surveys undertaken along 13.7 km of basalt-ultramafic contact indicated six anomalous zones around the domal structure. A strong IP anomaly defined the gossan in Cowcill's pits. Some of the other anomalies were found to be sourced by barren sulphide-rich sediments. A number of Ni and Cu anomalies were also delineated by geochemical soil sampling along the geophysical lines. WMC acquired extensive prospecting rights over the domal structure and further afield. The acquisition of new mining tenements was based on such criteria as the strike extensions of known ultramafic rocks and zones of magnetic anomalies as defined in regional airborne magnetic surveys. WMC had carried out detailed surface mapping in the area between Kalgoorlie towards Kambalda from 1962 to 1964. Ultramafic rocks had been recorded in this area, however, there were no documented mafic-ultramafic contacts similar to those at Kambalda, and consequently the Ni potential of the vast area north of Kambalda was downgraded. Hronsky and Schodde (2006) provide a comprehensive summary of the pioneering mapping criteria and methodologies used by WMC geologists. This expanding geological understanding was instrumental in the discovery of new Ni deposits in ensuing years. The early acquisition of extensive areas of prospective ground during the non-boom years also proved most advantageous for WMC during the pegging hysteria phase that followed in the late 1960s.

Woodall was given permission from WMC management to carry out a three diamond drill-hole program for a budget of about £22 500. The first drill-hole, KD1, drilled by Jack Lunnon was designed to test a combined geochemical-IP anomaly sourced below the original surface gossan found by Cowcill. The drill-hole initially penetrated a barren ultramafic-basalt contact at 130 m, then on the 28<sup>th</sup> of January 1966, it intersected 2.75 m of massive Ni-Cu sulphide ore that assayed 8.3% Ni and 0.5% Cu from 145.7 m to 148.4 m. Results of the next two holes were disappointing, with the second drill-hole barren, and the third failed to test the ultramafic-basalt contact due to drilling problems. Fourth drill-hole, KD4, on the western flank of the dome, intersected significant sulphides, and the ore

shoot was later named after the driller Derek Fisher. It was traditional practice by WMC to name the ore shoot after the driller responsible for drilling the first intersection. Further drilling near KD1 defined a significant Ni sulphide deposit (later to be called the Lunnon Shoot) hosted by komatiitic rocks. The company made a low-key announcement on 21<sup>st</sup> of February 1966: '*The Directors announce that in exploring the Kambalda area 30 miles south of Kalgoorlie for nickel, one drill hole has intersected significant nickel sulphide mineralisation. Additional drill holes are being put down in the area but it will be some time before any evaluation of the discovery can be made.*' On the 4<sup>th</sup> of April 1966 the managing Director W.M. (Bill) Morgan publicly announced the discovery of Kambalda: "*It is an important discovery. There have been small finds of a few hundred tons of nickel ore in Australia before, but none the size and quantity of the Kambalda body.*" Cowcill and Morgan were each granted \$25 000 for their roles in the discovery and bringing the prospect to WMC's attention.

The Kambalda project from 1966 to 1967 moved quickly from development to full-scale production. Official ore reserves of 735 580 t averaging 5.2% Ni for the Lunnon Shoot were announced in mid-1966. The rapid construction of the Lunnon Shaft (later to be called the 'Silver Lake Shaft') and headframe allowed production to commence less than 18 months after the drilling of the discovery hole (Figure 5.11). In March 1967, the first ore was intersected on the 380 level of the Lunnon shoot. The initial package of 2530 t of Ni concentrates was loaded onto the 'Botany Bay' boat at the port of Esperance, 330 km south of Kambalda, and exported to Vancouver on the 2<sup>nd</sup> of August 1967. After a development period of less than 20 months and a total cost of only ~\$6 million, WMC commenced to generate cash from its new mining adventure. Rapid development of the Lunnon Shoot was a key element in the successful development of the Ni field. Subsequent discoveries of the McMahon, Fisher, Durkin, and Jan shoots around the Kambalda Dome highlighted the wide distribution and potential of the field. In June 1967, known reserves for the Lunnon, Durkin, and Jan shoots were 4.7 Mt @ 3.7% Ni—a ~seven-fold increase on the figures announced 12 months earlier. In later years WMC discovered further deposits throughout the Eastern Goldfields and soon established itself as Australia's major Ni producer.



*Figure 5.11 The Silver Lake Headframe (previously called Lunnon Shaft) and ore bins, Kambalda nickel deposit, looking south over Lake Lefroy, Western Australia, 1966. The sinking of the shaft began in July 1966, less than six months after the drilling of the discovery drillhole KD1. The first nickel concentrate was produced in early June 1967, only 18 months after the discovery of the deposit. Image from Gresham (1991).*

The significant discovery at Kambalda heralded the initiation of Australia's Ni sulphide industry, an industry which has defined since 1966 a total Ni metal resource<sup>12</sup> of ~15.3 Mt and six deposits of world-class (>1 Mt of contained Ni metal) status.

The early exploration successes of WMC in delineating several deposits around the Kambalda Dome and by various junior companies exploring north of Kambalda, coupled with high demands for Ni, initiated a period from 1966 to 1971 of speculative exploration known as the 'nickel boom'. During the height of this boom (1969–70), most outcropping sequences of greenstone rocks in the Yilgarn Craton were being explored by prospectors, new Australian companies that were floated solely for Ni, and by various international mining groups. Large tracts of land that are now known to have little or no prospectivity for Ni were also being explored. In February 1970, the komatiite-hosted Mt Windarra deposit in the Eastern Goldfields featured in one of the most spectacular stock collapses in Australian share-market history—the 'Poseidon Crash'. Uncontrolled speculation drove the 80-cent stock rapidly upwards to a high of ~\$280, until its inevitable crash. Company and investors suffered significant losses and the negative media coverage tarnished the reputation of the mining industry. The 'Poseidon Crash' event initiated various government reviews and the emplacement of codes and regulations for the reporting of ore reserves, which provided the foundations for the present-day Joint Ore Reserves Committee (JORC; see Appendix G) code. The appetite for Ni in the early 1970s was substantially being driven by rising metal prices caused by a shortage of Ni in the world (due to industrial turmoil in the Canadian mines and the high demands of the Vietnam War) and excessively optimistic visions of major new exploration opportunities.

Australia's Ni industry grew rapidly in the first decade with many komatiite-hosted deposits commencing production within the first two years of their discovery. More than 75% of Australia's current total Ni metal resource derived from sulphide deposits (~15.3 Mt) was discovered during the relative short period of 1966 to 1973. The world-class Ni status (>1 Mt contained Ni metal) of the Eastern Goldfields Province was established when several large deposits were discovered between 1969 and 1973; namely Mount Keith (~3.4 Mt Ni), Perseverance (~2.5 Mt), Yakabindie (~1.7 Mt), and Honeymoon Well (~1 Mt). These deposits, in addition to those in the Kambalda camp (~1.4 Mt) still remain to this day, the largest Ni sulphide deposits in Australia.

The end of the 1970s witnessed the abrupt decline in the success rate of finding new komatiite-hosted Ni sulphide deposits. Reflecting market conditions of depressed metal prices due to a world oversupply of Ni, exploration during the early- to mid-1980s slowed, and Rocky's Reward (~65 km south of Mount Keith), was the only major komatiite-associated deposit discovered during this decade. This trend was broken in the 1990s when a significant new component to Australia's Ni inventory was the development of several large Ni laterite deposits (Murrin Murrin, Cawse, Bulong) during the 'nickel laterite boom' years of 1993 to 1999 (Brand et al., 1998; Elias, 2002, 2006; Flint et al., 2005; Hronsky and Schodde, 2006).

In addition to the more typical komatiite-hosted deposits of the Yilgarn Craton, several other more unusual deposits contain significant amounts of PGEs (~0.5–2 g/t Pd+Pt) that constitute an important by-product of the Ni mining. These deposits are mainly located in the northeastern part of the craton, with notable examples including Blair, Bodkin, Camel Bore, Carnilya Hill, Cosmos, Cruickshank, Fly Bore, Gunbarrel, Marshall Rock, Mount Windarra, Nepean, Polar Bear, Prospero, Ravensthorpe,

---

<sup>12</sup> Total resources of Ni metal (defined as total production plus remaining reserves and/or resources, i.e., total contained Ni resource) will be used throughout this paper unless otherwise stated. Many Ni sulphide deposits consist of several closely adjacent orebodies, therefore the definition of deposit is somewhat arbitrary. In the case of the mining camps of Sudbury and Noril'sk, the total resources indicated in this study are the collective resources of many individual deposits.

Redross, Scotia, Spargoville, The Bulge, The Horn, Waterloo, and several deposits clustered around the Kambalda Dome. The Collurabbie and Collurabbie South prospects in the northern part of the Duketon greenstone belt of the northeast Yilgarn Craton contain mineralised komatiitic sequences that have relatively low Ni/Cu ratios (<3) and are unusually enriched in the PGEs (up to 6 g/t) and Cu (2%). The high abundance of PGEs and low Ni/Cu ratios are features not normally associated with the typical komatiite-hosted deposits of the Yilgarn Craton. Such chemical characteristics are more typical of the Raglan Ni-PGE komatiite deposit (average grades of 2.7% Ni, 0.8% Cu, and 4 g/t PGEs: Seabrook et al., 2004) in northern Quebec and the Kuhmo Ni deposit in eastern Finland (Vulcan Resources Limited, 2005).

There appears to be a spectrum of PGE-bearing komatiitic-hosted deposits in Western Australia ranging from the PGE-rich variants (e.g., Collurabbie, Collurabbie South, Daltons), to those where the PGEs can form an important by-product component (Kambalda Dome, Waterloo, The Horn), to other more typical komatiitic deposits (Silver Swan, Mount Keith, Flying Fox) where the PGEs are of minor or background abundance. These deposits are described in more detail in Chapter 6.

During 2007, the Ni exploration industry was stimulated by record Ni prices (up to ~US\$54 400/t) that were largely driven by the increase in demand for Ni from China. This buoyant phase of the industry witnessed an increase in exploration activities at a number of komatiite-hosted deposits in the Eastern Goldfields and Southern Cross provinces. Some of these contained the highest Ni grades (5–8% Ni) in the world (e.g., Silver Swan, Cosmos, Prospero, Victor, Long, Flying Fox-T5, Spotted Quoll). In 2008 the price of Ni rapidly declined (to less than ~US\$10 000/t) due largely to the reduction in the demand for stainless steel and the global financial crisis. During these difficult times many Ni-based companies (sulphide and laterite) reassessed mining priorities and reduced annual production targets and exploration budgets.

The reader is referred to the following publications for a more comprehensive summary of the discovery, development, and geological setting of the komatiitic-hosted Ni deposits of Western Australia: Marston (1984); Hill et al. (1987); Leshner (1989); Naldrett (1989); Groves and Hudson (1990); Gresham (1990, 1991); Dowling and Hill (1998); Barnes et al. (1999); Leshner and Keays (2002); Arndt et al. (2005); Barnes (2006); Hoatson et al. (2006); Barnes and Fiorentini (2008); Fiorentini et al. (2010); Locmelis et al. (2011, 2013); Barnes and Liu (2012); Barnes et al. (2013); and Gole et al. (2013).

# 6 Platinum-group elements in Australia

Dean M. Hoatson

## 6.1 Introduction

Platinum-group elements have been documented from all Australian states and the Northern Territory, with Western Australia and Tasmania accounting for more than 80% of known occurrences. The number of PGE occurrences has rapidly increased from just a few examples described in the first national reviews of PGEs in Australia (Geary et al., 1956; Barrie, 1965; Kalix et al., 1966), to 68 in the late 1980s (Hoatson and Glaser, 1989), to the present inventory of over 500 entries described in this report (Appendix K). The rapid increase of documented PGE occurrences and their geological settings is attributed to several factors, including:

- diversification of exploration programs into more 'greenfields' geological environments (e.g., sedimentary, hydrothermal, marine) with less traditional exploration targets (carbonaceous sediments, porphyry Cu-Au deposits, volcanogenic-massive sulphides, Banded-Iron Formations (BIFs));
- introduction of cost-effective and now routine analytical techniques for PGEs that have sensitivity capabilities of parts per billion (e.g., inductively-coupled-plasma mass spectrometry, fire assay pre-concentration and neutron activation analysis);
- greater accessibility (and accountability) of company exploration activities and results via the World Wide Web (e.g., statutory reporting to State-Territory Geological Surveys, Australian Securities Exchange, Open-file reports); and
- improved prospectivity analysis through data-driven and knowledge-driven components, such as the application of mineral systems for PGEs and Ni.

Australia's extensive inventory of PGE occurrences range from those where the PGEs are the dominant commodity of a mineral deposit, to those where the PGEs constitute by-products of other mined mineral commodities (e.g., Ni, Cu, Co, Au), to prospects that have minor or no economic significance, to other occurrences that are merely of scientific or curiosity interest. The vast majority of Australia's PGE occurrences have the common feature that these rare elements are hosted by, or are derived from, ultramafic and/or mafic igneous rocks. Such intrusive and extrusive rock types in Australia cover the spectrum of ultramafic to mafic compositions, ranging from high-Mg primitive komatiite and dunite (with >30% MgO), to komatiitic basalt, high-Mg basalt, peridotite, and pyroxenite (30%–15% MgO), to more evolved gabbroic, basaltic, and in some rare cases those that have alkaline affinities (15%–2% MgO).

In Australia, PGEs are associated with igneous, metamorphic, and sedimentary rocks from a wide range of geological settings. Anomalous concentrations of PGEs have been documented in layered mafic-ultramafic intrusions, mafic-dominant intrusions, komatiitic flows and sills, alkaline igneous complexes, carbonatites, ultramafic-mafic complexes having alpine-, ophiolitic-, and 'Alaskan-type' affinities, structurally-controlled dyke and vein systems, hydrothermal breccias, unconformity U-Au deposits, porphyry Cu-Au deposits, volcanogenic-massive sulphide deposits, ?skarn deposits, BIFs, carbonaceous sedimentary rocks, laterite profiles, alluvial paleoplacers, and lherzolite nodules. The

ages of the host rocks in these geological settings encompasses most of the geological time record extending from the Mesoarchean (~3.0 Ga) to the present. The ~2.9 Ga layered mafic-ultramafic intrusions in the west Pilbara Craton of Western Australia (e.g., Munni Munni Intrusion) represent some of the oldest orthomagmatic mineralising systems in the world (Hoatson et al., 1992; Ruddock, 1999; Hoatson and Sun, 2002). The record of PGE-mineralising-systems continues into the Neoproterozoic with the formation of the ~2.8 Ga to ~2.7 Ga komatiitic-hosted deposits (Marston, 1984; Barnes, 2006; Grguric et al., 2006) and large layered mafic-ultramafic intrusions in the Yilgarn Craton (Ivanic, 2009; Ivanic et al., 2010). The Paleoproterozoic time period is represented by the mineralised ~1.85 Ga mafic-ultramafic intrusions of the Halls Creek Orogen (Sanders, 1999; Hoatson and Blake, 2000) and PGE-enriched unconformity U-Au deposits in the Pine Creek Orogen of the Northern Territory (Carville et al., 1990; Mernagh et al., 1994; McKay and Mieziotis, 2001). The Mesoproterozoic contains mineralised ~1.3 Ga and ~1.1 Ga mafic-dominant intrusions in the Albany-Fraser Orogen (Smithies et al., 2011) and Musgrave Province (Seat et al., 2007, 2009, 2011), respectively. Minor PGEs and Au are associated with Ni and Cu sulphides in ~1.1 Ga alkaline igneous complexes in central Australia (Nelson et al., 1989; Barnes et al., 2008). Fault-bounded early-Cambrian to Permian alpine- and ophiolitic-type ultramafic-mafic complexes along the eastern margin of Australia host podiform chromitites enriched in PGEs (Peck and Keays, 1990; Bottrill, 2014). Zoned 'Alaskan-type' alkaline mafic-ultramafic bodies were emplaced during the late Ordovician to late Devonian in central New South Wales (Johan et al., 1989; Elliott and Martin, 1991). Alkaline porphyry Cu-Au deposits with by-product PGEs (Scott, 1978, 1988; Morrison, 1998; Scott and Torrey, 2003) are coeval with, and spatially near, the 'Alaskan-type' intrusions. Cenozoic alluvial placers (Johan et al., 1990a,b; Slansky et al., 1991), residual laterites (Derrick, 1991; Shi, 1995; Platina Resources Ltd, 2012, 2013a, 2014a,b), and heavy-mineral beach deposits (Geary et al., 1956; Barrie, 1965; Flack, 1967; Hoatson and Glaser, 1989) throughout eastern Australia are the youngest PGE-mineralising systems recognised in Australia. Hydrothermal PGE occurrences (Purvis et al., 1972; Marston, 1984; Barnes, 1995; Marshall, 2000; Golden Cross Resources, 2011, 2013, 2014) are hosted by igneous, metamorphic, and/or sedimentary rocks in diverse geological settings. They feature throughout the total geological time record, i.e., they appear to have no spatial or temporal dependence.

Australia's current commercial production of PGEs is as a by-product of the Archean-hosted komatiite Ni-Cu sulphide deposits in Western Australia. Despite Australia only having very minor Economic Demonstrated Resources of PGEs (see Section 1.3.3), there are a number of deposits and prospects that highlight the potential for different styles of PGE mineralisation in Precambrian and Phanerozoic terranes. Details and additional references for these high-profile PGE occurrences that are listed below can be found in Section 6.4 and Appendix K.

- Munni Munni (Hoatson et al., 1992); Windimurra (Mathison and Ahmat, 1996); Weld Range (Parks, 1998), all WA—Archean layered mafic-ultramafic intrusion;
- Elizabeth Hill, WA (Barnes, 1995)—Archean structurally-controlled hydrothermal;
- Carr Boyd Rocks, WA (Purvis et al., 1972)—Archean hydrothermal bronzitite pipes;
- Mount Webber, WA (Haoma Mining NL., 2014)—Archean BIF;
- Collurabbie, WA (Bertuch, 2004)—Archean PGE-enriched komatiite;
- Panton (Perring and Vogt, 1991); Lamboo (Hoatson and Blake, 2000); Eastman Bore (Hoatson and Blake, 2000), Jemberlana (Keays and Campbell, 1981), all WA—Paleoproterozoic layered mafic-ultramafic intrusion;
- Nebo–Babel (Seat et al., 2007, 2009, 2011); Nova (Smithies et al., 2011); Savannah (Thornett, 1981), all WA—Proterozoic mafic-dominant intrusion;

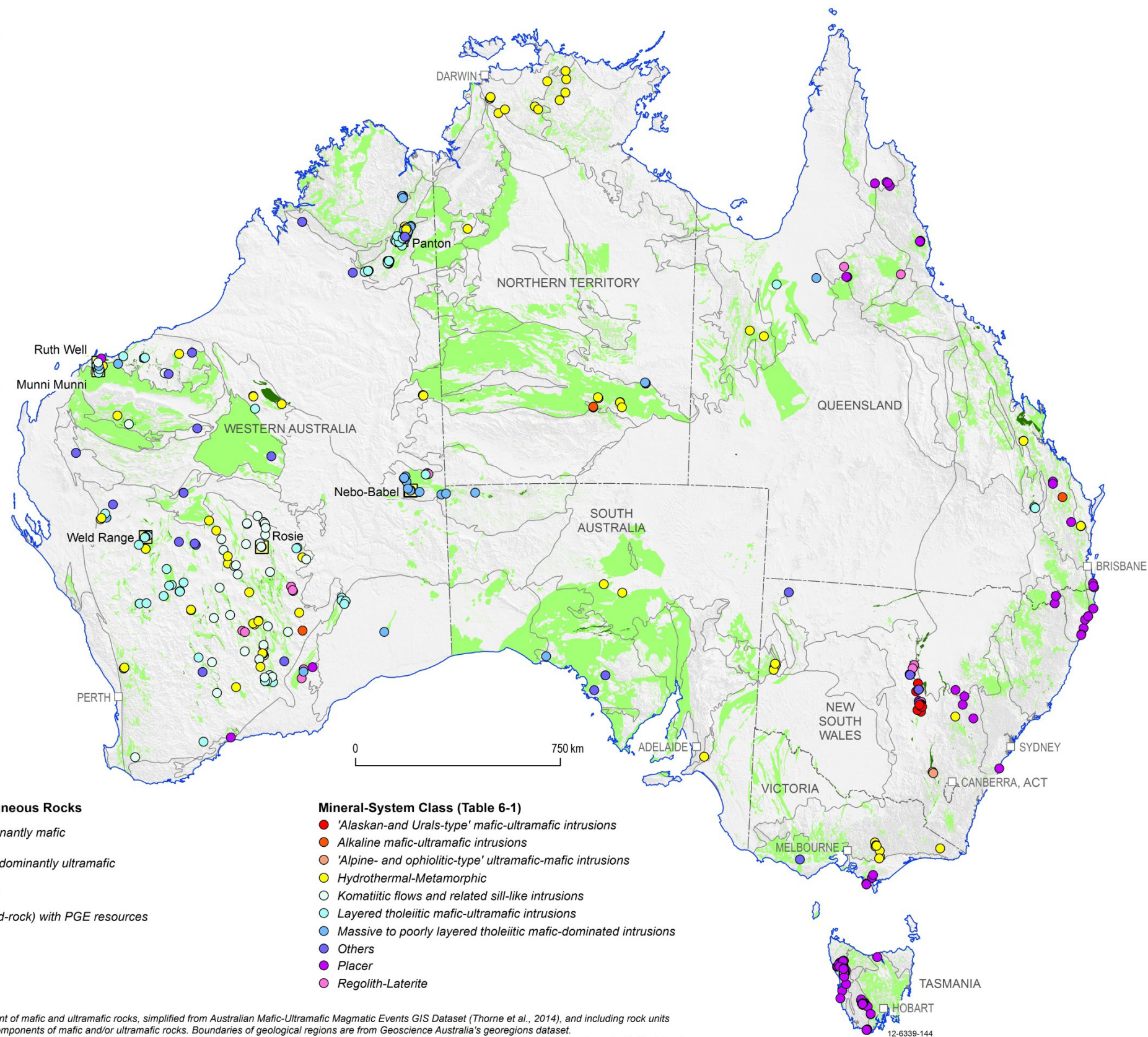
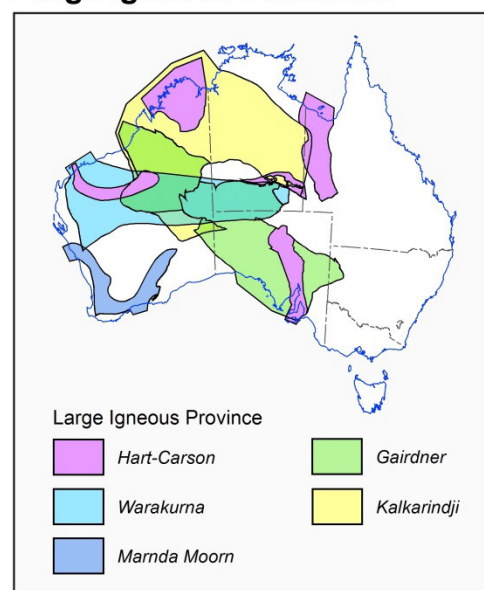
- Coronation Hill, NT (Mernagh et al., 1994)—Proterozoic hydrothermal–unconformity U-Au-PGEs;
- Jabiluka, NT (Hegge, 1977)—Proterozoic hydrothermal–graphite host;
- Haran, WA (Traka Resources Ltd, 2010a,b), Attutra, NT (Hoatson et al., 2005a)—Proterozoic oxide-bearing mafic-ultramafic intrusion;
- DeGrussa, WA (Sandfire Resources NL, 2009; 2011a,b)—Proterozoic volcanogenic-massive sulphide deposit;
- Kangaroo Dam, SA (Goldstream Mining NL, 2005a,b,c)—Proterozoic ?skarn;
- Mordor, NT (Barnes et al., 2008)—Mesoproterozoic alkaline mafic-ultramafic igneous intrusion;
- Mulga Springs, NSW (Golden Cross Resources, 2011; 2013)—Neoproterozoic structurally-controlled hydrothermal;
- Lake Acraman, SA (Williams and Gostin, 2005; 2010)—PGE enrichment in sedimentary rocks associated with Neoproterozoic impact structure;
- Adamsfield (Bottrill, 2014) and Heazlewood River (Peck and Keays, 1990), both Tas—Cambrian 'alpine-ophiolite-type' intrusion and Cenozoic alluvials;
- Owendale, NSW (Johan et al., 1989)—Paleozoic 'Alaskan-type' intrusion and Cenozoic alluvials;
- Copper Hill, NSW (Scott, 1978)—Ordovician porphyry Cu-Au deposit;
- Syerston (Derrick, 1991); Owendale (Elliott and Martin, 1991), both NSW—Cenozoic laterite.

The diversity of PGE occurrences in Australia in relation to geological settings and geological age is highlighted in the national maps of Figure 6.1 and Figure 6.2 and in Table 6.1.



# Australian Platinum-Group-Element (PGE) Deposits and Occurrences: Mineral-System Class

## Large Igneous Provinces



- Mafic and Ultramafic Igneous Rocks**
- Mafic and predominantly mafic
  - Ultramafic and predominantly ultramafic
  - Geological regions
  - Major deposit (hard-rock) with PGE resources

- Mineral-System Class (Table 6-1)**
- 'Alaskan-and Urals-type' mafic-ultramafic intrusions
  - Alkaline mafic-ultramafic intrusions
  - 'Alpine- and ophiolitic-type' ultramafic-mafic intrusions
  - Hydrothermal-Metamorphic
  - Komatiitic flows and related sill-like intrusions
  - Layered tholeiitic mafic-ultramafic intrusions
  - Massive to poorly layered tholeiitic mafic-dominated intrusions
  - Others
  - Placer
  - Regolith-Laterite

Outcrop and/or subsurface extent of mafic and ultramafic rocks, simplified from Australian Mafic-Ultramafic Magmatic Events GIS Dataset (Thorne et al., 2014), and including rock units with dominant or subordinate components of mafic and/or ultramafic rocks. Boundaries of geological regions are from Geoscience Australia's georegions dataset. The GEODATA 9 Second Digital Elevation Model (DEM-9S) Version 3 is a grid of ground level elevation points covering the whole of Australia derived from a Geoscience Australia dataset.

Figure 6.1 Distribution of Australian platinum-group-element deposits and occurrences: mineral-system class. Classification of deposits and occurrences is based on Table 6.1 and all occurrences are from Appendix K.

# Australian Platinum-Group-Element (PGE) Deposits and Occurrences: Major and Minor Commodities

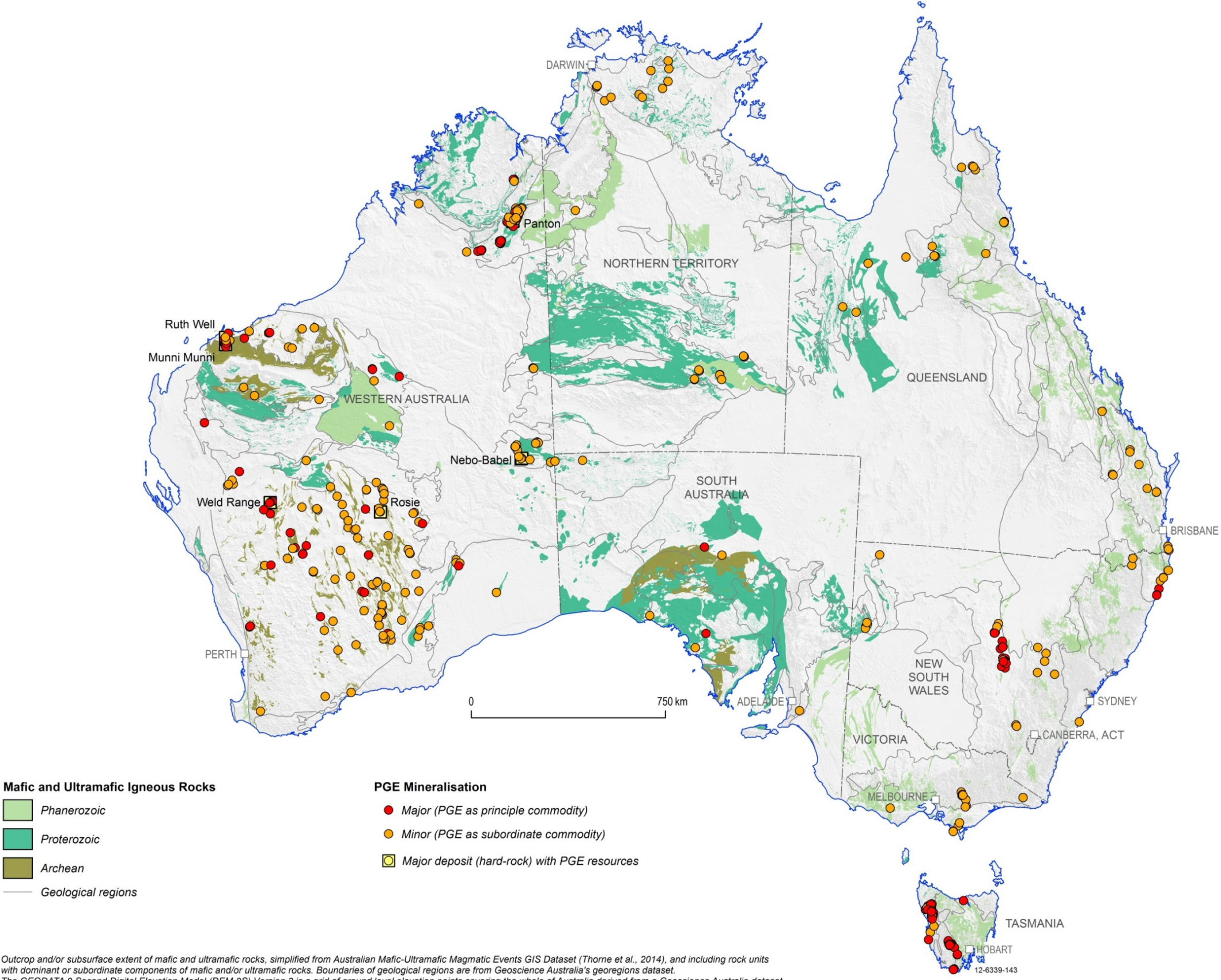


Figure 6.2 Distribution of Australian platinum-group-element deposits and occurrences: major and minor platinum-group-element commodities. Classification of deposits and occurrences is based on Table 6.1 and all occurrences are from Appendix K.

Table 6.1 Mineral-system classification of platinum-group-element deposits and occurrences in Australia.

Mineral-system class	Deposit type <sup>1</sup>	Australian examples <sup>2</sup>	International-type example	Metal association	Dominant PGEs	References <sup>3</sup>
1. Layered tholeiitic mafic-ultramafic intrusions	1.A. Stratabound PGE-bearing sulphide layers	<b>Munni Munni, WA</b> Windimurra, WA Windimurra, WA	Merensky Reef: Bushveld Complex (South Africa)	PGEs-Cu-Ni-Au	Pd, Pt, Rh	Donaldson (1974); Hoatson et al. (1992); Barnes and Hoatson (1994); Hoatson and Sun (2002)
	1.B. Stratabound PGE-bearing chromitite layers	<b>Panton, WA</b> Eastman Bore, WA Lambo, WA Plumridge, WA	UG-2 Chromitite: Bushveld Complex (South Africa)	Cr-PGEs-Ni-Cu-Au	Pd, Pt	Hamlyn (1975, 1977, 1980); Perring and Vogt (1991); Hoatson and Blake (2000); Platinum Australia Limited (2005)
2. Massive to poorly layered tholeiitic mafic-dominated intrusions	2.A. Segregations of Ni-Cu-Co-PGE sulphides in feeder conduits and basal contacts	<b>Nebo-Babel, WA</b> Nova, WA Radio Hill, WA Savannah, WA	Voisey's Bay (Canada) <sup>4</sup>	Ni-Cu-Co±PGEs	Pt, Pd	Hoatson and Blake (2000); Hoatson and Sun (2002); Dundas (2004); Seat et al. (2007, 2009, 2011)
	2.B. Stratabound PGE-bearing magnetitite layers	<b>Haran, WA</b> Canaan-Zen-Manchego, WA Casper-Coco-Attutra, NT	Stella (South Africa)	Ti-V-PGEs-Au-Cu	Pt, Pd, Rh	Glikson et al. (1996); WMC Ltd (2003); Traka Resources Ltd (2010a,b)
3. Komatiitic flows and related sill-like intrusions	3.A. Massive, matrix, and disseminated Ni-Cu-PGE sulphides in preferred lava pathways	<b>Kambalda, WA</b> Waterloo, WA Cosmos, WA Rosie, WA	Alexo (Canada)	Ni-Cu±Au±PGEs±Co	Pd, Pt, Ru	Marston (1984); Hill et al. (1987); Leshner and Keays (2002); Barnes (2006); Hoatson et al. (2006); Barnes et al. (2013)
	3.B. Disseminated Ni-Cu-PGE sulphides in central parts of thick dunite bodies	<b>Mount Keith, WA</b> Black Swan, WA Honeymoon Well, WA	Dumont (Canada)	Ni-Cu±PGEs±Co	Pd, Pt	Marston (1984); Hill et al. (1987); Grguric et al. (2006); Gole et al. (2013)
	3.C. PGE-enriched Ni-Cu sulphides associated with komatiitic and tholeiitic rocks	<b>Collurabbie, WA</b> ?Daltons, WA	Raglan (Canada)	Ni-Cu-PGEs	Pd, Pt	Bertuch (2004); Dundas (2004); Locmelis et al. (2011, 2013); Barnes and Fiorentini (2012)
4. Alkaline mafic-ultramafic intrusions	4.A. Stratabound and disseminated Cu-Au-PGE sulphides	<b>Orodruin-Mordor, NT</b> Ponton Creek, WA	Coldwell (Canada)	PGEs-Ni-Cu	Pt, Pd, Rh	Langworthy and Black (1978); Hoatson et al. (2005); Barnes et al. (2008)
5. 'Alpine- and ophiolitic-type' ultramafic-mafic intrusions	5.A. Podiform and stratabound chromitite	<b>Adamsfield, Tas</b> Heazlewood River, Tas Mount Mary Mines-Coolac, NSW	Semail Ophiolite (Oman)	Cr-PGEs-Ni-Cu-Au	Os, Ir, Ru, Pt, Pd	Varne and Brown (1978); Peck and Keays (1990); Bottrill (2014)
6. 'Alaskan- and Urals-type' mafic-ultramafic intrusions	6.A. PGE mineralisation in concentrically zoned mafic-ultramafic intrusions	<b>Owendale, NSW</b> Bulbodney Creek, NSW	Nizhni Tagil (Russia)	PGEs-Ni-Cu	Pt, Pd, Rh	Suppel and Barron (1986a,b); Johan et al. (1989, 1990a,b); Elliott and Martin (1991)
7. Continental flood basalts with associated sub-volcanic sills	7.A. Ni-Cu-PGE sulphides in sub-volcanic picritic-gabbroic sills with associated flood basalts	Unknown	Noril'sk-Talnakh (Russia) <sup>5</sup>	Ni-Cu-PGEs	Pd, Pt, Ir	Naldrett (1997, 2004, 2011); Cawthorn et al. (2005); Arndt (2011)
8. Hydrothermal-Metamorphic	8.A. Discordant-brecciated bronzitite pipes in mafic-ultramafic intrusions	<b>Carr Boyd Rocks, WA</b>	Dunite Pipes: Bushveld Complex (South Africa)	Ni-Cu-PGEs	Pt, Pd	Purvis et al. (1972); Marston (1984)
	8.B. Remobilised Ni-Cu-PGE±Au sulphides in komatiitic and metasedimentary rocks	<b>Juan Shoot-Kambalda, WA</b> Perseverance, WA Wannaway, WA	Thompson (Canada)	Ni-Cu-PGEs	Pd, Pt	Marston (1984); Barnes (2006)
	8.C. Magmatic breccias involving mafic, ultramafic, and felsic igneous rocks	<b>Elizabeth Hill, WA</b> ?Yarawindah Brook, WA	?Lac des Iles (Canada)	Ag-Pb-Ni-Cu-PGEs-Au-Ti-Mo	Pd, Pt	Barnes (1995); Marshall (2000); Hoatson and Sun (2002)
	8.D. Structurally-controlled remobilised Ni-Cu-PGE sulphides in mafic±ultramafic±felsic dykes/veins in shear zones	<b>Mulga Springs, NSW</b> Thomson River, Vic Westwood, Qld	New Rambler (USA)	Cu-Au-Ag-Ni-PGEs	Pd, Pt	Ostwald (1979); Cochrane (1982) Impact Minerals Ltd (2013); Golden Cross Resources (2014)

Mineral-system class	Deposit type <sup>1</sup>	Australian examples <sup>2</sup>	International-type example	Metal association	Dominant PGEs	References <sup>3</sup>
8. Hydrothermal-Metamorphic	8.E. Disseminated sulphides in alkaline to subalkaline porphyry Cu-Au deposit	<b>Copper Hill, NSW</b>	Ingerbelle (Canada)	Cu-Au-Mo-PGEs	Pd, Pt	Morrison (1998); Scott and Torrey (2003); Golden Cross Resources (2011, 2013)
	8.F. Unconformity-type U-Au-PGEs	<b>Coronation Hill, NT</b>	Beaverlodge (Canada)	U-Au-PGEs	Pd, Pt	Mernagh et al. (1994); McKay and Mieizitis (2001)
	8.G. U-Au-Pd-Pt mineralisation associated with graphitic schist and carbonaceous shale	<b>Jabiluka, NT</b> Camel Bore, WA	Kupferschiefer (Poland)	U-Au-PGEs	Pd, Pt	Hegge (1977); McKay and Mieizitis (2001)
	8.H. Mineralisation formed along mid-oceanic ridges	Unknown	Turtle Pits, Logachev (Mid-Atlantic Ridge) <sup>5</sup>	PGEs-Cu-Au-Co	Pd, Pt	Pašava et al. (2007); German et al. (2010)
9. Regolith-Laterite	9.A. PGE-bearing regolith developed on ultramafic-mafic igneous rocks	<b>Syerston, NSW</b> Weld Range, WA Owendale, NSW	Yubdo (Ethiopia)	Ni-Co-PGEs±Sc	Pt, Pd, Ir	Derrick (1991); Elliott and Martin (1991); Barron et al. (2004)
10. Placer	10.A. Alluvial placers derived from 'Alaskan- and Urals-type' mafic-ultramafic intrusions	<b>Fifield, NSW</b> Owendale, NSW	Goodnews Bay (Alaska)	PGEs-Au	Pt	Suppel and Barron (1986a,b); Johan et al. (1990a,b); Slansky et al. (1991); Elliott and Martin (1991)
	10.B. Alluvial placers derived from 'alpine- and ophiolitic-type' ultramafic-mafic intrusions	<b>Adamsfield, Tas</b> Bald Hill, Tas Nineteen Mile Creek, Tas	Zolotaya River (Russia)	PGEs-Cr-Au	Os, Ir, Ru, Pt, Pd	Rubenach (1973); Varne and Brown (1978); Bacon (1992)
	10.C. Alluvial placers	<b>Kennedy Creek, Qld</b> Nickol River East, WA	Chocó (Colombia)	PGEs-Au	Ir, Os, Ru, Pt	MINOCC (2011); Hudson and Horwitz (1985)
	10.D. Beach placers	<b>Ballina, NSW</b> Waratah Bay, Vic	South Island (New Zealand)	Au-PGEs	Pt, Os, Ir	Ferguson (1936); Flack (1967); Hoatson and Glaser (1989)
11. Astrobleme-related	11.A. Massive, vein, and disseminated Ni-Cu-PGE sulphides in mafic-ultramafic-felsic rocks and impact melts	Unknown	Sudbury (Canada) <sup>5</sup>	Ni-Cu-PGEs	Pd, Pt, Ir	Pye et al. (1984); Ames and Farrow (2007); Dare et al. (2012)
12. Others—minor or unknown economic importance	12.A. PGE enrichment in volcanogenic-massive sulphides	<b>DeGrussa, WA</b>	Outokumpu (Finland)	Cu-Au-Ag-Zn-PGEs	Pd, Rh	Sandfire Resources NL (2009; 2011a,b)
	12.B. Anomalous PGEs in sedimentary rocks associated with possible impact structure	<b>Lake Acraman, SA</b> McWhae Ridge, WA	Denmark, Italy, Spain, Mexico, Canada, USA, New Zealand	PGEs-V-Co-Ni-Cu-As-Sb-Pb-Th-REE	Ir, Pt	Playford et al. (1984); Gostin et al. (1989); Williams and Gostin (2005, 2010)
	12.C. Anomalous PGEs in banded-iron formations	<b>Mount Webber, WA</b>	Cauê, Minas Gerais (Brazil)	PGEs-Au-Ag	Pd, Pt, Ir	Haoma Mining NL (2012, 2014)
	12.D. PGE-bearing ultramafic nodules and xenoliths	<b>Mount Leura, Vic</b>	Noritic Ring Complex (Antarctica)	Ni-Cu-PGEs	Pt, Pd	Keays et al. (1981); Hoatson and Glaser (1989)
	12.E. Others—unknown geological setting	Kangaroo Dam, SA Bamboo Creek Tailings, WA		PGEs-Au	Pt, Pd	Goldstream Mining NL (2005a,b,c); Haoma Mining NL (2012, 2014)

<sup>1</sup> For convenience these are referred to as deposit in this table, however, some categories (e.g., 12.D) are obviously occurrences.

<sup>2</sup> Australian deposits shown in bold font are considered the 'Type Example' of that particular mineral-system class.

<sup>3</sup> Major references relate to the Australian-type example. If there is no such example in Australia, the references relate to a typical overseas example.

<sup>4</sup> Voisey's Bay deposit is associated with troctolite-anorthosite, and granite.

<sup>5</sup> Other economically important deposits from overseas (e.g., Noril'sk, Sudbury) have been included in this classification to highlight: (1) gaps in the record of Australian mineralising-system classes; and (2) potential exploration opportunities.

## 6.2 Spatial and temporal distribution of platinum-group-elements in Australia

Although PGEs in Australia have diverse geological settings, there still exist various characteristics relating to their formation (metal source, magma composition, metal associations with time, magma-fluid pathways; magmatic-hydrothermal-regolith processes, degree of preservation, etc) that can be used to formulate a particular genetic framework, or as promoted in this report—a mineral system—that could facilitate the discovery of further deposits (see Chapters 7 and 8).

Two major groups of PGE deposits associated with intrusive mafic±ultramafic igneous rocks have created considerable exploration interest over many decades in Australia. The first group is where the PGEs constitute the major economic commodities and are associated with sparsely dispersed Ni-Cu sulphides (up to ~3% sulphide) in stratabound layers, and/or with chromitite concentrations, in large- to medium-sized, differentiated mafic-ultramafic layered intrusions. In the second group, the PGEs form a subordinate component of Ni and Cu sulphide-rich ores (~5% to ~90% sulphide) in mafic-dominant sills and stocks. On a global scale, these two major groups of deposits (and in particular group 1) account for a significant amount of the world's supply of PGEs. Notable Australian examples<sup>13</sup> of the first group include: Munni Munni (Pilbara Craton); Windimurra, Weld Range, and Jimberlana (Yilgarn Craton); Panton, Lamboo, and Eastman Bore (Halls Creek Orogen); and Plumridge Lakes (Albany-Fraser Orogen). Group 2 is represented by: Radio Hill, Mt Sholl, and Andover (Pilbara Craton); Savannah (Halls Creek Orogen); Nebo–Babel (Musgrave Province); and Nova<sup>14</sup> (Albany-Fraser Orogen). Fractionated gabbroic bodies in the Musgrave Province (Jameson Range Intrusion: Haran–Canaan–Zen–Manchego prospects) and the Arunta Orogen (Attutra Metagabbro Intrusion: Casper–Coco prospects) contain PGE-enriched oxide layers at high stratigraphic levels in the tholeiitic intrusion.

Komatiitic-hosted Ni-Cu-PGE mineralisation is largely restricted to the eastern part of the Archean Yilgarn Craton (Eastern Goldfields, Northeastern Goldfields, and Southern Cross provinces), with several deposits in the Norseman–Wiluna (Kambalda Dome region, Cosmos, Prospero) and Gerry Well (Collurabbie, The Bulge, Rosie) greenstone belts having significant PGE concentrations (Barnes, 2006; Hoatson et al., 2006). Komatiitic-hosted deposits (Spotted Quoll, Flying Fox<sup>15</sup>) in the Forresteria greenstone belt to the west of the Norseman–Wiluna belt also have significant by-product PGEs. Recent exploration has highlighted a number of deposits and prospects that have unusual settings (e.g., atypical granite-hosted remobilised mineralisation at Flying Fox) and metal signatures. These include those komatiite deposits and prospects with exceptionally high Ni grades (e.g., Cosmos, Long, Spotted Quoll, Flying Fox–T0 to T7 ore shoots), with normal Ni/Cu ratios and high PGE grades (Waterloo), with low Ni/Cu ratios and high PGE grades (Collurabbie, Collurabbie South, Daltons).

Minor hard-rock occurrences of PGEs related to 'alpine-ophiolite-' and 'Alaskan-Urals-type' intrusions are Cambrian to Permian and Ordovician to Devonian age, respectively, and are confined to north-trending linear belts in the Delamerian, Lachlan, and New England orogens of eastern Australia (Hoatson and Glaser, 1989; Elliott and Martin, 1991; Bottrill, 2014). These types of mineralised intrusions have not been confirmed from Proterozoic or Archean terranes in Australia. Sub-parallel

<sup>13</sup> References for most of these specific Australian examples are cited in Sections 6.1 and 6.4, and Appendix K, and will not be repeated here.

<sup>14</sup> Sulphide intersections at Nova contain anomalous PGEs, e.g., DDH SFRC0026: 8 m @ 5.81% Ni, 2.26% Cu, 0.16% Co, 0.12 g/t Pd, 0.12 g/t Pt (Sirius Resources NL, 2012b,c,d; 2013a,b).

<sup>15</sup> Massive Ni ores from the Flying Fox Ni-Cu-PGE deposit in the Forresteria greenstone belt have PGE concentrations up to 2070 ppb Pt, 1060 ppb Pd, 208 ppb Rh, 142 ppb Ir, 296 ppb Os, and 1130 ppb Ru (Collins et al., 2012).

belts of tectonically emplaced, fault-bounded ultramafic–mafic bodies that were interpreted before the 1990s to have alpine and/or ophiolitic<sup>16</sup> affinities extend from western Tasmania, northwards through central Victoria, New South Wales, to northern Queensland. ‘Alaskan- and Urals-type’ mafic-ultramafic complexes have a more restricted distribution, with over 60 examples documented in the Fifield–Nyngan district of central New South Wales (Figure 6.35), and possibly a few representatives in the Wateranga area of southeastern Queensland. These intrusions overseas (e.g., Ural Mountains, Russia: Johan, 2002) commonly have clustered distributions comprising many comagmatic ovoid-shaped intrusions, thus further Fifield-like intrusions are likely to be found in eastern Australia. Placer deposits of Os-Ir-Ru and Pt alloys are derived from ultramafic rocks in intrusions from the western Tasmanian and central New South Wales regions, respectively. Historically, these occurrences were worked by the prospector and accounted for much of Australia’s early production of ‘osmiridium’ and Pt (see Chapter 8). Nickel-cobalt laterites containing elevated PGE and scandium concentrations are well developed near Fifield in central New South Wales and in the Greenvale region of northern Queensland. Most deposits occur in the deeply weathered profiles overlying olivine-rich ultramafic rocks in tropical or semi-tropical humid paleo-climates. Such PGE-bearing laterites are rarely associated with the ‘alpine-ophiolite’ ultramafic-mafic intrusions, which tend to be linear and narrow in shape and have more outcrop than the ovoid Alaskan- and Urals-type bodies.

Australian PGE occurrences related to hydrothermal-mineral systems cover a wide spectrum, ranging from deposits which are largely due to primary magmatic processes and having a minor hydrothermal overprint, through those involving late-stage hydrothermal remobilisation of PGEs derived from a nearby mafic-ultramafic rock source, to deposits which are strictly hydrothermal in origin. In the latter deposits, the PGEs show no association with, or obvious derivation from mafic-ultramafic rocks, and fluid movement has been the dominant mechanism for PGE transport (Hoatson and Glaser, 1989). The recognition of the importance of late- and post-magmatic processes in the transport and concentration of PGEs relative to those systems where the PGEs are exclusively associated with the early stages of mafic-ultramafic magma evolution has gained general acceptance in recent decades (Stumpfl, 1986, 1987; Stumpfl and Ballhaus, 1986; Ballhaus and Stumpfl, 1986; Distler et al., 2005; Wilde, 2005; Mungall and Naldrett, 2008; Dill, 2010).

Hydrothermal PGE mineralisation is diverse in its setting, and not bound by a specific time period, as known occurrences encompass the Archean, Proterozoic, and Phanerozoic time periods. The geological settings range from komatiitic volcanic-intrusive successions, layered mafic-ultramafic intrusions, ‘Alaskan-type’ intrusions, serpentinite sills, greenstone sedimentary and volcanic successions, to unconformity-related environments. Host rocks include peridotite and pyroxenite intrusives, ultramafic to felsic volcanics, porphyry, dioritic dykes, tuff, conglomerate, and various argillaceous and arenaceous sediments. In the Archean, hydrothermal PGE occurrences generally have a major magmatic component, with the remobilised mineralisation still preserving primary magmatic features and hosted by mafic to ultramafic rocks (Kambalda, Munni Munni and Radio Hill-basal contacts), but in the Proterozoic and Phanerozoic there may be no obvious spatial or genetic association with mafic to ultramafic rocks. Thus there appears to be a broad transition from occurrences in the Archean having a dominant magmatic-subordinate hydrothermal signature, to deposits in the Proterozoic and Phanerozoic which have experienced more wide-scale and intensive hydrothermal mineralising systems. Within these younger terranes disseminated mineralisation is prominent in the Proterozoic, whereas felsic-vein systems (often polymetallic with associated precious and base metals) are more typical of the Phanerozoic.

---

<sup>16</sup> Considerable controversy has persisted concerning the geotectonic significance of these bodies, i.e., whether they represent true complete fragments of oceanic crust—ophiolites (Crawford and Berry, 1992; Brown, 1998). In this report, the emphasis on alpine and ophiolite is reduced, and they will be referred to as ‘alpine- and ophiolitic-type’ ultramafic-mafic intrusions.

Minor concentrations of PGEs in other geological settings (Appendix K) include: alkaline mafic-ultramafic intrusions (Mordor, NT), porphyry Cu-Au deposits (Copper Hill, NSW), volcanogenic-massive sulphide deposits (DeGrussa, WA), skarn (?Kangaroo Dam, SA), BIFs (Mount Webber, WA), in sedimentary rocks associated with possible impact structures (Lake Acraman, SA), alluvial and beach placers (Waratah Bay, Vic), and lherzolite nodules and xenoliths (Mount Leura, Victoria). The economic status of a small proportion of these occurrences is as a potential by-product of other metals, most which have minor or unknown economic importance, or are of scientific interest only.

The majority of the more important PGE occurrences in Australia are associated with: (1) laterally continuous sulphide horizons at particular stratigraphic levels in large Archean and Proterozoic layered intrusions, or in komatiitic volcanic-intrusive sequences; (2) sulphide-bearing chromitite cycles in dismembered intrusions of Early Proterozoic orogenic zones; and (3) chromite in Paleozoic alpine peridotite or ophiolite and related placers in eastern Australia. This distribution reflects the secular variation of the PGEs associated with S and Cr from the Archean to the Proterozoic to the Phanerozoic. Platinum-group mineralisation associated with most Paleozoic concentrically zoned intrusions does not appear to show any clear affinity with sulphides or chromite. However, PGEs in hydrothermal settings are commonly associated with Cu and Ni in the Archean, Au and U in the Proterozoic, and with Au, Ag, Cu, Ni, Pb, and As in the Phanerozoic.

### 6.3 Classification of platinum-group elements in Australia

Platinum-group-elements are found in a wide range of orthomagmatic, metamorphic, hydrothermal, and residual-regolith environments. However, it is rare that PGEs occur in such concentrations in one location to enable exploitation. The economic status of PGE deposits is dependent on a variety of petrogenetic processes that need to be efficient during the enrichment of background abundances to ore-grade abundances. Such concentration processes that may involve several stages of evolution include: the generation of immiscible sulphide liquids; fractional crystallisation of high-temperature minerals (e.g., chromite and Ti-V-bearing spinels); remobilisation and transportation of metals during metamorphic and hydrothermal fluid activity; and mobility during regolith-related processes. The preservation-erosional status of the deposit is also critical to the viability of the deposit. The optimal approach for classifying PGE deposits requires the separation of radically different classes of mineralisation into a manageable number of categories, without permitting duplication of individual deposits into different categories (Macdonald, 1988). It also needs to allow the integration of significant deposits from overseas and new types of deposits.

Previously proposed classification schemes of PGE and Ni deposits have often used equivocal and cumbersome criteria, such as: 'petro-tectonic' and 'geotectonic' settings (Naldrett, 1981, 1989, 2004, 2011; Barnes and Lightfoot, 2005); ambiguous lithological terms (dunite versus peridotite: Marston, 1984; Leshner, 1989); detailed petrographic terms for different ore types that can be difficult to apply and can occur together in a single deposit (e.g., blebby, cloudy, interstitial, off-set: Leshner and Keays, 2002); and uncertain genetic qualifiers (intrusive versus extrusive, stratiform versus stratabound: Marston, 1984; Leshner, 1989; Leshner and Keays, 2002; Arndt et al., 2005). Macdonald's (1988) classification of PGE deposits was based on the inferred process by which the PGEs were concentrated, and whether the PGEs are the primary product, a co-product, or a by-product. His proposed scheme was simply divided into the three deposit classes of orthomagmatic, alluvial, and hydrothermal. Similarly, Eckstrand (2005) and Dill (2010) based their classifications on four group criteria, namely: Magmatic, Sedimentary, Hydrothermal, and Laterite; and Magmatic, Sedimentary, Structure-related, and Metamorphic, respectively.

This report uses a mineral-system approach to classify PGE deposits and occurrences in Australia (Table 6.1; Figure 6.1 and Figure 6.2). This approach focuses on mineral-forming processes (see Section 7.1 for a definition of a mineral system) and has the advantage over more traditional descriptive classifications in that it attempts to identify those geological processes considered critical to the formation of a 'group or clan' of deposit types that share common parameters. This information can then be applied in a predictive sense to assist mineral exploration in the identification of potential new areas and types of PGE mineralisation. The mineral-system-based scheme proposed here is also flexible to permit modification in response to an increased understanding of the mineralisation process in question, and can easily accommodate new types of mineralisation identified in the future. An example of the latter challenge is the discovery of atypical styles of sulphide-poor, PGE-enriched mineralisation in thick komatiitic sequences at Mount Clifford (Locmelis et al., 2009) and Wiluna (Fiorentini et al., 2007a) in the Agnew–Wiluna greenstone belt. The PGE mineralisation at these two locations has been described by the authors as having similarities to two different styles of stratiform PGE mineralisation, namely disseminated sulphides in fractionated komatiitic cumulates (i.e., type III of Leshar and Keays (2002) mineralised komatiite classification), and 'off-set reefs' that occur in tholeiitic layered intrusions, such as the Munni Munni Intrusion (Barnes et al., 1992) and the Great Dyke of Zimbabwe (Prendergast and Keays, 1989; Wilson and Tredoux, 1990). Obviously the new style of PGE mineralisation at Mount Clifford and Wiluna should not have both komatiitic and tholeiitic mineral-system-based characteristics. Further geochemical-isotopic studies and a review of classification schemes of mineralised komatiitic and tholeiitic rocks may resolve this dilemma.

The mineral-system classification shown in Table 6.1 is hierarchical in structure, with the highest-level category of deposits called 'Mineral-System Class'. This category is divided into twelve major classes of varying economic importance that encompass the broad mineral systems of Orthomagmatic (Classes 1 to 7), Hydrothermal/Metamorphic (Class 8), Regolith/Laterite (Class 9), Alluvial/Placer (Class 10), Astrobleme-related (Class 11), and a final class of deposits that has minor or unknown economic significance (Class 12). Table 6.2 summarises Australia's resources of PGEs associated with the different Mineral-System Classes. The subdivision of the large Orthomagmatic class is based on the dominant chemical affinities of the host magma (e.g., tholeiitic, komatiitic, and alkaline) and the broad geological settings of the mafic-ultramafic rocks (Alpine, Alaskan, continental flood basalt). 'Deposit types' are largely defined according to the spatial distribution of the PGE mineralisation (e.g., stratabound layers, basal contact, feeder contact, discordant pipes, remobilised, brecciated, unconformity, etc). The type example of each Mineral-System Class is shown for both Australia and overseas in Table 6.1. Some economically important deposits from overseas (e.g., Sudbury, Canada, and Noril'sk–Talnakh, Russia) do not currently have confirmed analogues in Australia. They have been included in this classification scheme because: (1) of their global economic importance; (2) they highlight significant gaps in the Australian 'bar-code record' of mineralising-system classes; and (3) they indicate potential new exploration opportunities in Australia, particularly in greenfields-type environments. For example, in regard to astrobleme-related deposits, very low concentrations of PGEs have been documented in sedimentary rocks associated with the Lake Acraman impact structure in South Australia (Williams and Gostin, 2005, 2010; Appendix K), and exploration at the Yarrabubba impact structure near Meekatharra in Western Australia (Bunting and MacDonald, 2004; Impact Minerals, 2014a?) has been targeted for magmatic and hydrothermal deposits similar to the Sudbury Ni-Cu-PGE deposits in Canada.

Table 6.2 Platinum-group-element resources in Australia.

Mineral-system class	Deposit	Province	Deposit type <sup>1</sup>	Resource	References
Layered tholeiitic mafic-ultramafic intrusions	Munni Munni, WA (central and western parts of mineralised Porphyritic Websterite Layer: PWL)	Pilbara Craton	1.A	12.4 Mt @ 1.1 g/t Pt, 1.4 g/t Pd, 0.1 g/t Rh, 0.09% Cu, 0.07% Ni, 0.2 g/t Au (Meas R); 9.8 Mt @ 1.1 g/t Pt, 1.6 g/t Pd, 0.1 g/t Rh, 0.22% Cu, 0.11% Ni, 0.3 g/t Au (Ind R); 1.4 Mt @ 1.1 g/t Pt, 1.6 g/t Pd, 0.1 g/t Rh, 0.15% Cu, 0.09% Ni, 0.3 g/t Au (Inf R); 23.6 Mt @ 1.1 g/t Pt, 1.5 g/t Pd, 0.1 g/t Rh, 0.15% Cu, 0.09% Ni, 0.2 g/t Au (Total Min R)	Helix Resources Ltd (2004a); Platina Resources Ltd (2014a)
	Panton, WA (Main Chomitite Layer: MCL)	Halls Creek Orogen	1.B	14.32 Mt @ 2.19 g/t Pt, 2.39 g/t Pd, 0.27% Ni, 0.07% Cu, 0.31 g/t Au (Meas R+Ind R+Inf R)	Platinum Australia Ltd (2005)
Massive to poorly layered tholeiitic mafic-dominated intrusions	Mount Sholl, WA	Pilbara Craton	2.A	0.633 Mt @ 0.59% Ni, 0.64% Cu, 0.5 g/t PGEs <sup>2</sup> (Ind R); 5.324 Mt @ 0.53% Ni, 0.62% Cu, 0.5 g/t Pd <sup>2</sup> (Inf R)	Fox Resources Ltd (2007)
	Nebo-Babel, WA	Musgrave Province	2.A	392 Mt @ 0.3% Ni, 0.33% Cu, 0.18 g/t PGEs (Prelim R)	Phaceas (2007)
	Radio Hill, WA	Pilbara Craton	2.A	1.181 Mt @ 0.79% Ni, 1.09% Cu, 0.04% Co, 0.5 g/t Pd (Ind R); 0.94 Mt @ 0.7% Ni, 0.9% Cu, 0.03% Co, and 0.4 g/t Pd (Inf R)	Fox Resources Ltd (2007)
	Savannah, WA (previously called Sallay Malay)	Halls Creek Orogen	2.A	4.74 Mt @ 1.48% Ni, 0.72% Cu, 0.08% Co, ~0.2 g/t PGEs <sup>2</sup> (Meas R+Ind R+Inf R)	Panoramic Resources Ltd (2008)
Komatiitic flows and related sill-like intrusions	Mount Windarra (F Shoot), WA	Yilgarn Craon	3.A	900 000 t @ 0.6% Ni, 0.77 g/t Pt, 0.15 g/t Pd (Ind R)	Western Mining Corporation Ltd (1993)
	Rosie, WA	Yilgarn Craton	3.A	1.744 Mt @ 1.7% Ni, 0.4% Cu, 0.8 g/t Pt, 1.1 g/t Pd	Arrowhead (2012)
	Ruth Well, WA	Pilbara Craton	3.A	60 000 t @ 0.99% Ni, 0.87% Cu, 0.04% Co, 0.27 g/t Pd (Ind R); 9000 t @ 1.05% Ni, 0.87% Cu, 0.04% Co, 0.24 g/t Pd (Inf R)	Fox Resources Ltd (2007)
	The Horn, WA	Yilgarn Craton	3.A	0.6 Mt @ 1.39% Ni, 0.3% Cu, 0.5 g/t Pt+Pd (Inf R)	Breakaway Resources Ltd, ASX Release 14 April 2008
	Waterloo, WA	Yilgarn Craton	3.A	299 000 t @ 3.5% Ni, 0.26% Cu, 1.13 g/t PGEs (Ind R); 354 000 @ 2.2% Ni, 0.14% Cu, 0.63 g/t PGEs (Inf R)	LionOre International Mining Ltd (2004)

Mineral-system class	Deposit	Province	Deposit type <sup>1</sup>	Resource	References
'Alpine- and ophiolitic-type' ultramafic-mafic intrusions	Adamsfield (Halls Open Cut), Tas	Delamerian Orogen	5.A	14 500 t @ 6.5 g/t Ir, 7.3 g/t Os, 0.13 g/t Pt (Inf R)	Shree Minerals Ltd (2009)
Hydrothermal–metamorphic	Copper Hill, NSW (Gold-rich zone)	Lachlan Orogen	8.E	18.5 Mt @ 0.55% Cu, 0.55 g/t Au, 0.02 g/t Pd	Scott and Torrey (2003)
	Coronation Hill, NT	Pine Creek Orogen	8.F	4.85 Mt @ 4.31 g/t Au, 0.19 g/t Pt, 0.65 g/t Pd (Ind R); 3.49 Mt @ 5.12 g/t Au, 0.21 g/t Pt, 0.56 g/t Pd (Ind R); 2.87 Mt @ 7.25 g/t Au, 0.35 g/t Pt, 1.31 g/t Pd (Inf R)	Carville et al. (1990); Mernagh et al. (1994)
	Gold Ridge, NT	Pine Creek Orogen	8.F	32 000 t @ 4.5 g/t Au, 0.3 g/t Pt, 0.5 g/t Pd (Inf R)	Ahmad et al. (2009)
	Red Hill Mine, NSW	Curnamona Craton	8.D	500 t @ 5 to 41 g/t PGEs, 2 to 4% Cu, 2 to 3% Ni, 22 to 70 g/t Ag	Impact Minerals Ltd (2013)
	Yarawindah Brook, WA	Yilgarn Craton	?8.C	0.31 Mt @ 0.5 g/t Pt+Pd	Butt et al. (2006)
	Thomson River, Vic	Lachlan Orogen	8.D	40 000 t @ 3.2 ppm Pt, 3.6 ppm Pd, 2.7% Cu, 9.5 ppm Ag, 2.5 ppm Au	Hoatson and Glaser (1989)
Regolith–laterite	Cincinnati, Fifield (Owendale Intrusion), NSW	Lachlan Orogen	9.A	9 Mt @ 0.5 g/t Pt (Inf R); 2.6 Mt @ 0.7 g/t Pt (Ind R); 2.2 Mt @ 0.7 g/t Pt (Inf R)	Helix Resources Ltd (2004b); Platina Resources Ltd (2012, 2013a)
	Milverton, Fifield (Owendale Intrusion), NSW	Lachlan Orogen	9.A	1.3 Mt @ 0.6 g/t Pt (Inf R)	Platina Resources Ltd (2013a)
	Owendale North, Fifield (Owendale Intrusion), NSW	Lachlan Orogen	9.A	10 Mt @ 0.58 g/t Pt, 0.20% Ni, 0.05% Co (Ind R); 21 Mt @ 0.49 g/t Pt, 0.12% Ni, 0.05% Co (Inf R); 31 Mt @ 0.52 g/t Pt, 0.15% Ni, 0.05% Co (Total Min R)	Platina Resources Ltd (2014a)
	Owendale Project, NSW	Lachlan Orogen	9.A	31.1 Mt @ 0.52 g/t Pt, 48 ppb Pd, 0.15% Ni, 0.05% Co, 248 ppm Sc, 2.6% MgO, 47.4% Fe <sub>2</sub> O <sub>3</sub> (Ind R + Inf R)	Platina Resources Ltd (2014b)
	Mount Carnage (Ora Banda Intrusion), WA	Yilgarn Craton	9.A	10 Mt @ 1 g/t PGEs	Pre-1993 exploration
	Syerston, Fifield, (Tout Intrusion), NSW	Lachlan Orogen	9.A	137 Mt @ 0.24 g/t Pt and 96 Mt @ 0.69% Ni, 0.12% Co (Meas R+Ind R+Inf R)	Black Range Minerals NL (2000)
	Weld Range (Weld Range Intrusion), WA	Yilgarn Craton	9.A	14.76 Mt @ 0.6 g/t Pt, 0.5 g/t Pd; 6.3 Mt @ 1.6 g/t Pt+Pd+Au (Inf R)	Parks (1998); Minara Resources Ltd (2005)

Mineral-system class	Deposit	Province	Deposit type <sup>1</sup>	Resource	References
	Yarawindah Brook, WA	Yilgarn Craton	9.A	2.9 Mt @ 0.79 g/t Pt+Pd (R); 2.7 Mt @ 0.9 g/t Pt+Pd (Inf R)	Cornelius (2005); Washington Resources Ltd (2005); Butt et al. (2006)

*R = Resource; Prelim R = Preliminary Resource; Meas R = Measured Resource; Ind R = Indicated Resource; Inf R = Inferred Resource; Total Min R = Total Mineral Resource.*

<sup>1</sup> Deposit Type is from the classification scheme in Table 6.1, namely 1.A = Stratabound PGE-bearing sulphide layers; 1.B = Stratabound PGE-bearing chromitite layers; 2.A = Segregations of Ni-Cu-Co-PGE sulphides in feeder conduits and basal contacts; 3.A = Massive, matrix, and disseminated Ni-Cu-PGE sulphides in preferred lava pathways; 5.A = Podiform and stratabound chromitites; 8.C = Magmatic breccias involving mafic, ultramafic, and felsic igneous rocks; 8.D = Structurally-controlled remobilised Ni-Cu-PGE sulphides in mafic±ultramafic±felsic dykes/veins in shear zones; 8.F = Unconformity-type U-Au-PGEs; 9.A = PGE-bearing regolith developed on ultramafic-mafic igneous rocks.

<sup>2</sup> Approximate estimate of PGE grades by Hoatson and Blake (2000) from limited analyses of massive and matrix sulphides in drill core.

Source: Company Announcements to the Australian Securities Exchange; Minmet Australia, March 2006; Register of Australian Mining (various years).

## 6.4 Type examples of platinum-group-element deposits

This section summarises the major geological and resource characteristics of those occurrences of PGEs considered the type example of a particular mineral system in Australia. Platinum-group-element occurrences are widespread throughout the Precambrian and Phanerozoic terranes of Australia, however, no economic resources of PGEs as the major commodity are mined (as of late 2014). Geological data and resource statistics for over 500 PGE occurrences have been sourced from Geoscience Australia's national databases MINLOC (mineral occurrences) and OZMIN (mineral deposits and resources)<sup>17</sup>. These national databases have been complemented by the seven mineral occurrence databases available from the State and Northern Territory geological surveys as summarised in the introduction to Appendix K. The PGE occurrences have been divided into the following 12 mineral-system classes and deposit types that form the basis of Australia's PGE classification scheme (Table 6.1). The PGE occurrence considered the type example of that particular deposit category is shown in parentheses.

- **Mineral-System Class 1:** Layered tholeiitic mafic-ultramafic intrusions.
  - 1.A. Stratabound PGE-bearing sulphide layers (Munni Munni, WA).
  - 1.B. Stratabound PGE-bearing chromitite layers (Panton, WA).
- **Mineral-System Class 2:** Massive to poorly layered tholeiitic mafic-dominant intrusions.
  - 2.A. Segregations of Ni-Cu-Co-PGE sulphides in feeder conduits and basal contacts (Nebo-Babel, WA).
  - 2.B. Stratabound PGE-bearing magnetitite layers (Haran, WA).
- **Mineral-System Class 3:** Komatiitic flows and related sill-like intrusions.
  - 3.A. Massive, matrix, and disseminated Ni-Cu-PGE sulphides in preferred lava pathways (Kambalda, WA).
  - 3.B. Disseminated Ni-Cu-PGE sulphides in central parts of thick dunite bodies (Mount Keith, WA).
  - 3.C. PGE-enriched Ni-Cu sulphides associated with komatiitic and tholeiitic rocks (Collurabie, WA).
- **Mineral-System Class 4:** Alkaline mafic-ultramafic intrusions.
  - 4.A. Stratabound and disseminated Cu-Au-PGE sulphides (Orodruin-Mordor, NT).
- **Mineral-System Class 5:** 'Alpine- and ophiolitic-type' ultramafic-mafic intrusions.
  - 5.A. Podiform and stratabound chromitite (Adamsfield, Tas).
- **Mineral-System Class 6:** 'Alaskan- and Urals-type' mafic-ultramafic intrusions.
  - 6.A. PGE mineralisation in concentrically zoned ultramafic-mafic intrusions (Owendale, NSW).
- **Mineral-System Class 7:** Continental flood basalts with associated sub-volcanic sills.
  - 7.A. Ni-Cu-PGE sulphides in sub-volcanic picritic-gabbroic sills with associated flood basalts (no confirmed example in Australia).

---

<sup>17</sup> See Section 1.5 for further details of these databases.

- **Mineral-System Class 8:** Hydrothermal-Metamorphic.
  - 8.A. Discordant-brecciated bronzitite pipes in mafic-ultramafic intrusions (Carr Boyd Rocks, WA).
  - 8.B. Remobilised Ni-Cu-PGE±Au sulphides in komatiitic and metasedimentary rocks (Juan Shoot–Kambalda, WA).
  - 8.C. Magmatic breccias involving mafic, ultramafic, and felsic igneous rocks (Elizabeth Hill, WA).
  - 8.D. Structurally-controlled remobilised Ni-Cu-PGE sulphides in mafic±ultramafic±felsic dykes/veins in shear zones (Mulga Springs, NSW).
  - 8.E. Disseminated sulphides in alkaline to subalkaline porphyry Cu-Au deposit (Copper Hill, NSW).
  - 8.F. Unconformity-type U-Au-PGEs (Coronation Hill, NT).
  - 8.G. U-Au-Pd-Pt mineralisation associated with graphitic schist and carbonaceous shale (Jabiluka, NT).
  - 8.H. Mineralisation formed along mid-oceanic ridges (no confirmed example in Australia).
- **Mineral-System Class 9:** Regolith-Laterite.
  - 9.A. PGE-bearing regolith developed on ultramafic-mafic igneous rocks (Syerston, NSW).
- **Mineral-System Class 10:** Placer.
  - 10.A. Alluvial placers derived from 'Alaskan- and Urals-type' mafic-ultramafic intrusions (Fifield, NSW).
  - 10.B. Alluvial placers derived from 'alpine- and ophiolitic-type' ultramafic-mafic intrusions (Adamsfield, Tas).
  - 10.C. Alluvial placers (Kennedy Creek, Qld).
  - 10.D. Beach placers (Ballina, NSW).
- **Mineral-System Class 11: Astrobleme-related.**
  - 11.A. Massive, vein, and disseminated Ni-Cu-PGE sulphides in mafic-ultramafic-felsic rocks and impact melts (no confirmed example in Australia).
- **Mineral-System Class 12:** Other occurrences—minor or unknown economic importance.
  - 12.A. PGE-enrichment in volcanogenic-massive sulphides (DeGrussa, WA).
  - 12.B. Anomalous PGEs in sedimentary rocks associated with possible impact structure (Lake Acraman, SA).
  - 12.C. Anomalous PGEs in banded-iron formations (Mount Webber, WA).
  - 12.D. Platinum-group minerals in ultramafic nodules and xenoliths (Mount Leura, Vic).
  - 12.E. Others—unknown geological setting (Kangaroo Dam, SA).

The following section describes the type example of 19<sup>18</sup> major styles of PGE occurrences in Australia using the classification scheme of Table 6.1 and a pro-forma template that contains the following attributes:

Overview	Australian deposits/prospects/hosts
Significant global example(s)	Type example in Australia
Location	Geological province
Resources	Current status and exploration history
Economic significance	Geological setting
Mineralisation environment	PGE mineralisation
Age of mineralisation	Genesis
Key references	

## 6.4.1 Mineral-System Class 1: Layered tholeiitic mafic-ultramafic intrusions

### 6.4.1.1 Deposit Type 1.A: Stratabound PGE-bearing sulphide layers

#### Overview

Precambrian layered mafic-ultramafic intrusions of tholeiitic affinity have generated considerable exploration interest in the stable Precambrian cratons for their PGE potential. Stratabound sulphide-bearing layers in these intrusions are an attractive target since they generally have: great lateral continuity (at least 60 km in the Munni Munni Intrusion, west Pilbara Craton); uniform grades (1 to 6 g/t Pt+Pd+Au) and thicknesses (0.5 to 3 m); a significant component of the more valuable precious metals (Pt, Rh, Au); and potential for large tonnage (up to 30 Mt) multi-element deposits (PGEs, Cr, Cu, Ni, Co, Au). Disseminated PGE-enriched Cu-Ni sulphides (<2%) usually occur in 1- to 3-m-thick laterally extensive layers at particular stratigraphic levels in the mafic-ultramafic stratigraphy, as shown by the economically important global examples of the Merensky Reef (Bushveld Complex, Republic of South Africa: Viljoen, 1999) and J-M Reef (Stillwater Complex, Montana, USA: Czamanske and Zientek, 1985). The mineralised layers, which are usually pyroxenitic, often form porphyritic or pegmatoidal 'reefs' from 20 m below (Munni Munni, Great Dyke of Zimbabwe) to 500 m above (Merensky Reef, J-M Reef), the stratigraphic level where plagioclase first becomes a cumulus mineral, i.e., the stratigraphic level first dominated by gabbroic rather than ultramafic cumulates (Hoatson, 1998). Stratabound PGE-enriched sulphide layers can be difficult targets to explore, particularly in poorly exposed terranes. This is because they typically form narrow targets (e.g., Merensky Reef is a 0.8-m-thick layer within a ~9000-m-thick stratigraphic succession Bushveld Complex) and they have weak geophysical and geochemical signatures due to their low disseminated sulphide content of a few percent.

Exploration in Australia has largely focussed on large differentiated Archean layered mafic-ultramafic intrusions in the Yilgarn, Pilbara, and Gawler cratons, and to a lesser extent, tectonically dismembered bodies in the Proterozoic Halls Creek, Albany-Fraser, and Musgrave orogens. The most intensively explored intrusions (Hoatson, 1984) include Munni Munni, Mount Sholl, and Andover (Pilbara Craton), Windimurra, Narndee, Weld Range, Jemberlana (Yilgarn Craton), which in some cases contain sub-economic concentrations of PGEs, Cr, Au, and associated minor base-metal sulphides. Intensive

<sup>18</sup> Those minor deposit types not discussed in the following section (e.g., placer occurrences 10.B, 10.C, and 10.D, and 'Other occurrences of minor or unknown economic importance' 12.A to 12.E) are described in Appendix K.

geophysical-geochemical investigations of large layered mafic-ultramafic intrusions in the Proterozoic Musgrave Province of central Australia have largely been unsuccessful for Type 1.A mineralisation. Stratabound PGE-enriched sulphide deposits in Australia are typically late Archean to Early Proterozoic (~2.9 Ga to ~2.4 Ga) in age, with no significant mineralised layers recorded in Phanerozoic intrusions. The type example of Deposit Type 1.A in Australia is the PGE-enriched Porphyritic Websterite Layer (PWL) directly below the ultramafic-gabbroic zone contact in the ~2.9 Ga Munni Munni Intrusion, similar to the Main Sulphide Zone in the Great Dyke of Zimbabwe (Wilson et al., 1989; Wilson and Tredoux, 1990).

#### *Australian deposits/prospects/hosts*

Munni Munni Intrusion (Pilbara Craton, WA); Weld Range Intrusion, Jimberlana Intrusion, and Windimurra Igneous Complex (all Yilgarn Craton, WA).

#### *Significant global example(s)*

Merensky Reef, Bushveld Complex (Republic of South Africa); J-M Reef, Stillwater Complex (USA); Main Sulphide Zone, Great Dyke of Zimbabwe (Zimbabwe); SK and RK Reefs, Portimo Complex, and S J Reef, Penikat Complex (both Finland).

#### *Type example in Australia*

Munni Munni Intrusion, Western Australia

#### *Location*

Longitude 116.829597°E, Latitude: -21.116989°S; 1:250 000 map sheet: Yarraloola (SF 50–06), 1:100 000 map sheet: Pinderi Hills (2255); ~45 km south of Karratha, Western Australia.

#### *Geological province*

West Pilbara Granite-Greenstone Terrane, Pilbara Craton, Western Australia.

#### *Resources*

Porphyritic Websterite Layer—Measured Resource of 12.4 Mt @ 1.1 g/t Pt, 1.4 g/t Pd, 0.1 g/t Rh, 0.09% Cu, 0.07% Ni, 0.2 g/t Au; Indicated Resource of 9.8 Mt @ 1.1 g/t Pt, 1.6 g/t Pd, 0.1 g/t Rh, 0.22% Cu, 0.11% Ni, 0.3 g/t Au; Inferred Resource of 1.4 Mt @ 1.1 g/t Pt, 1.6 g/t Pd, 0.1 g/t Rh, 0.15% Cu, 0.09% Ni, 0.3 g/t Au; Total Mineral Resource of 23.6 Mt @ 1.1 g/t Pt, 1.5 g/t Pd, 0.1 g/t Rh, 0.15% Cu, 0.09% Ni, 0.2 g/t Au (from Platina Resources Ltd, 2014; Table 6.2):

#### *Current status and exploration history*

Undeveloped PGE-Ni-Cu-Au sulphide deposit with JORC-compliant resources. One of the most extensively explored layered intrusions in the west Pilbara Craton, and indeed in Australia. The potential for PGE mineralisation in the west Pilbara layered mafic-ultramafic intrusions was not fully realised during the early phases of Ni-Cu exploration. Limited PGE analyses were carried out on Ni-rich intervals from near the basal contacts, and little consideration was given to possible PGE enrichment at higher stratigraphic levels, or in different settings, such as structurally-controlled hydrothermal types of mineralisation. The Bureau of Mineral Resources, Geology and Geophysics (now Geoscience Australia) began a study of the Munni Munni Intrusion in 1983, as part of a regional evaluation of the PGE potential of layered intrusions in Western Australia. Of particular interest was the Archean age and large size of the intrusion and the presence of a porphyritic pyroxenite unit reported by Donaldson (1974) at the interface between the ultramafic and gabbroic zones. By analogy

with large overseas intrusions where PGE mineralisation is commonly hosted by coarse-grained sulphide-bearing layers close to where plagioclase becomes an early-crystallising phase, it was believed by Hoatson (1984, p. 45) that the Munni Munni Intrusion was prospective for PGE mineralisation at the base of cyclic units in the ultramafic zone, or more likely, in the porphyritic pyroxenite layer at the interface between the ultramafic and gabbroic zones, i.e. in the vicinity of the first appearance of cumulus plagioclase at the expense of cumulus olivine. Follow-up field sampling by BMR in mid-1983, as part of the regional geochemical program that assessed the PGE prospectivity of intrusions in the Pilbara Craton and Halls Creek Orogen (Hoatson, 1984; Wallace and Hoatson, 1990), located and sampled a sulphide-bearing porphyritic plagioclase websterite unit containing anomalous PGE concentrations near the ultramafic/gabbroic interface. The mineralised websterite samples showed very similar mineralogical and textural features to the pegmatoidal phase of the Merensky Reef and contained at least ~30 times background concentrations of Pt and Pd.

In 1984, Hunter Resources Ltd carried out a 400-m line-spaced soil geochemical survey and confirmed that the ultramafic/gabbroic contact zone region had potential for stratabound-type PGE mineralisation. Subtle geochemical signatures occurred on eight of the 11 soil traverses at the same stratigraphic position. Maximum soil geochemical results were 93 ppb Pt and 430 ppb Pd. Trenching intersected significant PGE anomalies in nine of the 15 trenches, and included a best intersection of 2 m @ 2.3 ppm Pt and 1.7 ppm Pd in the Porphyritic Websterite Layer (PWL). To 1992, 66 diamond drill-holes were completed along a 7.5 km strike-length section of the mineralised layer, 63 of which intersected the mineralised zone at the same stratigraphic level. The best intersection was in DDH MM34, which was drilled in the central part of the complex and obtained 5.5 m (543.0 m–548.5 m) @ 1.4 ppm Pt, 2.8 ppm Pd, 0.5 ppm Au, 0.7% Cu, and 0.3% Ni. A preliminary potential resource of 20 to 30 Mt of ~2.9 ppm Pt+Pd+Au, 0.3% Cu, and 0.2% Ni was delineated to a depth of 500 m. Rhodium and Au average 42 ppb and 300 ppb, respectively, while Ru, Os, and Ir are present in minor amounts. The prospect was being re-appraised by companies in 2001–2002, with in-fill drilling along a 1.3-km-long section of the PWL defining a 13.5 Mt resource of 1.1 ppm Pt, 1.6 ppm Pd, 0.1 ppm Rh, and 0.2 ppm Au (Australia's Paydirt, May 2001). Anomalous PGE grades of around 1 ppm were defined by Hunter Resources Ltd in altered pyroxenite and gabbroic rocks along the southeastern contact of the Munni Munni Complex, near the Zebra Hill Dyke. These rocks are the southern extension of the mineralised porphyritic websterite layer. The Munni Munni Intrusion was explored by Helix Resources Limited up to 2006 when the company redirected its PGE interests into a new company—Platina Resources Limited. Reviews of earlier drilling programs indicated that holes that were designed to test for extensions of the PWL under cover were not accurately located. Seismic reflection surveys and new drilling were successful in targeting the mineralised PWL along its projected 40 km strike extent under the Fortescue Group platform cover to the southwest. In 2008, a JORC-compliant total resource (inferred, indicated, measured) of 23.6 Mt of ore for 2000 000 ounces of Pt+Pd+Au was announced by Platina Resources Limited. However, a scoping study concluded that Munni Munni was economically marginal given the large capital expenditure requirement relative to the small size of the known resource and unfavourable US\$/A\$ exchange rates (Koek et al., 2010).

### *Economic significance*

One of the most significant PGE deposits in Australia that has experienced several phases of intensive exploration since its discovery in the early 1980s. The deposit contains one of the largest resources of PGEs (global resource of 63.7 t: Table 6.2) associated with a layered mafic-ultramafic intrusion in Australia. The Munni Munni and Panton (see Deposit Type 1.B) PGE deposits are generally regarded as two of the most important PGE deposits associated with layered mafic-ultramafic intrusions in Australia.

## *Geological setting*

The Pilbara Craton (Hickman, 1983, 1997; Smithies et al., 1999; Huston et al., 2002; Van Kranendonk et al. 2002; Hickman and Van Kranendonk, 2008) is the best exposed Archean-Proterozoic granite-greenstone-platform terrane in Australia. It consists of two contrasting tectonic components:

1. the North Pilbara Terrain—an elongate east-west-trending Archean (~3.51–2.85 Ga) granite-greenstone terrane comprising ovoid granitic batholiths separated by synclinal belts of greenschist- to amphibolite-facies metasediments and metavolcanics; and
2. a Late Archean to Paleoproterozoic (~2.77–2.45 Ga) volcano-sedimentary platform cover sequence (Mount Bruce Supergroup of the Hamersley Basin) that unconformably overlies the North Pilbara Terrain to the south and east.

The layered mafic-ultramafic intrusions of the west Pilbara Craton form two geographical groups with contrasting outcrop patterns (Figure 6.3, Table 6.3). The western group (Andover, Bullock Hide, Dingo, Maitland, Mount Sholl, Munni Munni, North Whundo, and Radio Hill) form large differentiated mafic-ultramafic bodies, shallow-dipping mafic sheets, and small ultramafic plugs. All intrusions occur in a north- to northeasterly-trending corridor (80 km long by 25 km wide), which is coincident with a prominent regional aeromagnetic low lineament that probably represents a deep-seated crustal structure. The western group of intrusions host the most significant mineral deposits in the west Pilbara. The eastern group of layered intrusions (Sherlock, Opaline Well) form arcuate mafic sills and dykes near the margins of the ovoid ~3095–2925 Ma Caines Well Granitoid Complex in the Mallina Basin. They are fairly evolved thin bodies that contain deposits of titaniferous magnetite and remobilised base-metal sulphides. Published resources of the west Pilbara intrusions are summarised by Hoatson and Sun (2002) and in Table 6.3.

The ~2.9 Ga Munni Munni, Andover, Radio Hill, Mount Sholl, and Sherlock layered intrusions (Figure 6.3) are a cogenetic suite of high-level (<5 kb) bodies that represent some of the oldest mineralising systems of their type in the world. Although they display similar field relationships and mineralogical, geochemical, and isotopic features, their contrasting chalcophile metal distribution patterns show that the timing and mechanism of the sulphide-saturation event were critical for the development of PGE-enriched sulphide-bearing layers and basal segregations of base-metal sulphides. The intrusions form thick (>5.5 km) 'dyke'-like bodies or relatively thin (0.5 km–2 km) sheets and sills emplaced at different levels along major lithological discontinuities in the upper crust. Rhythmically layered ultramafic components are generally thinner than, and occur along the northern sides of, more massive overlying mafic components. The ultramafic zones consist of dunite, lherzolite, wehrlite, olivine websterite, clinopyroxenite, and websterite. Inverted pigeonite gabbro, magnetite gabbro, olivine gabbro, anorthositic gabbro, and anorthosite comprise the mafic sequences. Olivine and clinopyroxene were generally the first minerals to crystallise, except in the Andover Intrusion, where orthopyroxene preceded clinopyroxene and possibly reflects greater contamination of the parent magma by felsic crustal material. The crystallisation of chromite was inhibited in the ultramafic zones by the partitioning of Cr into early-crystallising clinopyroxene, thus downgrading the potential for PGE-chromite associations.

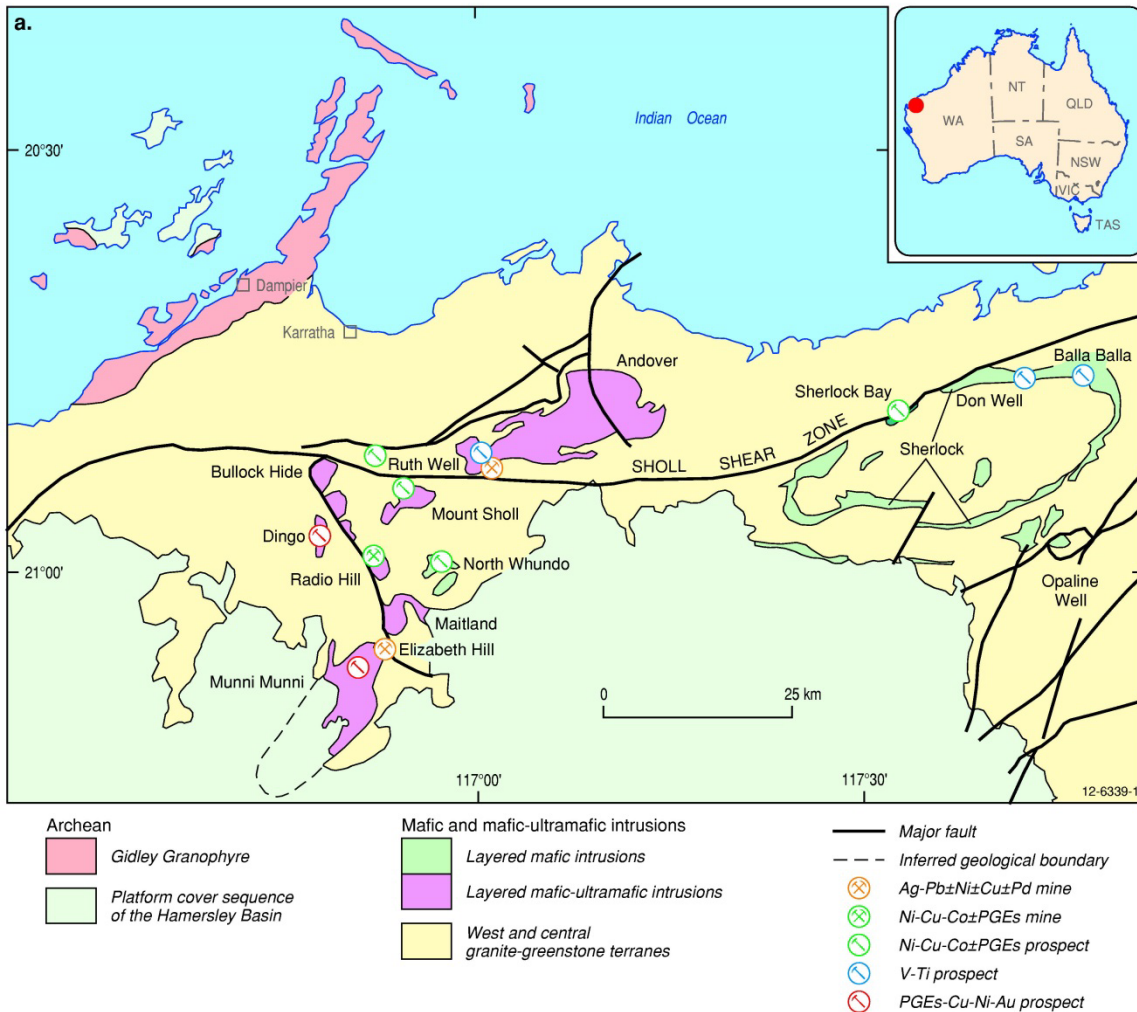
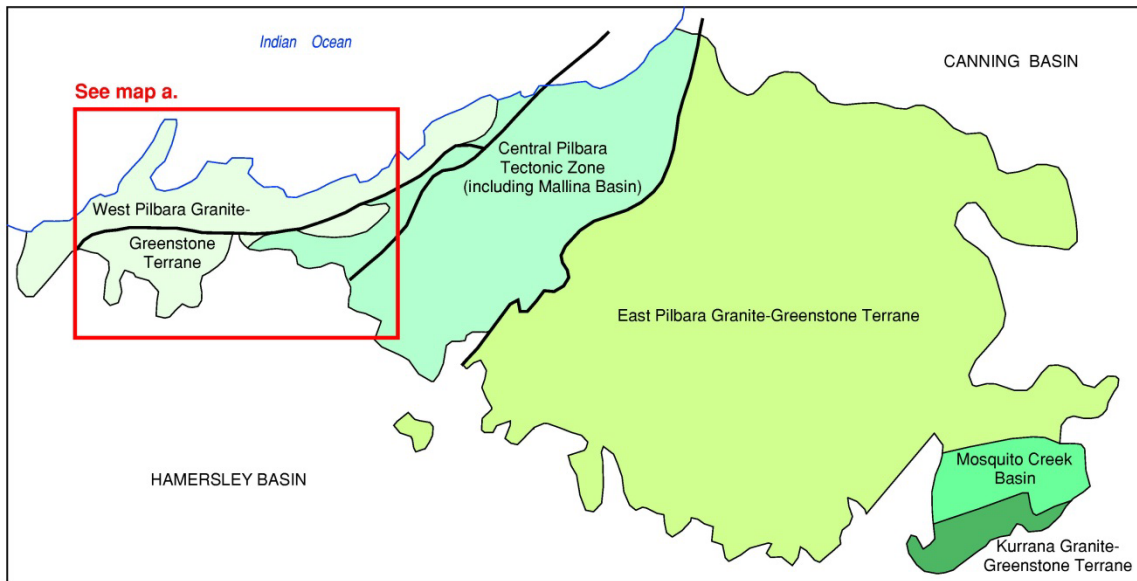


Figure 6.3 Distribution of Archean layered mafic-ultramafic intrusions and associated mineral deposits in the West Pilbara Granite-Greenstone Terrane, Pilbara Craton, Western Australia (intrusions are modified from Ruddock, 1999). The southwestern extension of the Munni Munni Intrusion beneath the Hamersley Basin is indicated by dashed line. The boundaries for the lithotectonic elements shown in the regional map (top figure) are from Van Kranendonk et al. (2002). Modified from Hoatson and Sun (2002).

Table 6.3 Major mafic-ultramafic intrusions in the west Pilbara Craton.

Intrusion	Extent (km)	Thickness (km)	Major rock types	Mineralisation	Resource(s) (Mt or t)	References
<b>Western Group</b>						
Andover	7 x 20	2	Per, Gab, Px,	V, Ti	3 Mt @ 0.92% V <sub>2</sub> O <sub>5</sub>	Connolly (1959) Hickman (1983) Wallace (1992, ab)
Bullock Hide	2 x 3	<0.5?	Per, Gab, Px			Ruddock (1999)
Dingo	1.5 x 1.5	<0.5?	Per, Gab, Px	PGEs, Ni, Cu		Mathison and Marshall (1981) Hoatson et al. (1992)
Elizabeth Hill <sup>1</sup>				Ag-Cu-Pd	24 100 t @ 0.42% Ag <sup>3,4</sup> (upper pod) 22 700 t @ 0.12% Ag <sup>3</sup> (lower pod)	Barnes (1995) Murphy (2000)
Gidley Granophyre	10 x 50	3	Gran, Gab, Dior			de Laeter and Trendall (1971) Hickman (1983)
Maitland	3.5 x 4	2	Gab, An, Per			Hoatson et al. (1992)
Mount Sholl	3 x 6	1–2	Gab, Per, Px	Ni, Cu, PGEs	0.633 Mt @ 0.59% Ni, 0.64% Cu, 0.5 g/t PGEs <sup>4,6</sup> 5.324 Mt @ 0.53% Ni, 0.62% Cu, 0.5 g/t Pd <sup>3,6</sup>	Mathison and Marshall (1981) Hoatson et al. (1992) Murphy (2000) Fox Resources Ltd (2007)
Munni Munni	9 x 25 <sup>2</sup>	>5.5	Gab, Px, Per	PGEs, Cu, Ni	23.6 Mt @ 1.1 g/t Pt, 1.5 g/t Pd, 0.1 g/t Rh, 0.15% Cu, 0.09% Ni, 0.2 g/t Au <sup>5</sup>	Hoatson and Keays (1989) Williams et al. (1990) Hoatson et al. (1992) Barnes and Hoatson (1994) Platina Resources Ltd (2014)
North Whundo	0.5 x 4		Gab, Nor, An			Hickman (1997)
Radio Hill	1.8 x 2	>1.2	Gab, Per, Px	Ni, Cu, Co	1.181 Mt @ 0.79% Ni, 1.09% Cu, 0.04% Co, 0.5 g/t Pd <sup>4</sup> ; 0.94 Mt @ 0.7% Ni, 0.9% Cu, 0.03% Co, 0.4 g/t Pd <sup>3</sup>	de Angelis et al. (1987, 1988) Hoatson et al. (1992) Murphy (2000) Fox Resources Ltd (2007)
<b>Eastern Group</b>						
Opaline Well	5 x 1	0.5?	Gab, Gran, Per			Smithies (1998)

Intrusion	Extent (km)	Thickness (km)	Major rock types	Mineralisation	Resource(s) (Mt or t)	References
Sherlock	15 x 1.2	1?	Gab, An, Nor, Gran, Per	V, Ti, Ni, Cu	Balla Balla—117 Mt @ 0.7% V <sub>2</sub> O <sub>5</sub> <sup>3</sup> Don Well—40.8 Mt @ 0.57% V <sub>2</sub> O <sub>5</sub> , 12.3% TiO <sub>2</sub> <sup>3</sup> Sherlock Bay—16 Mt @ 0.75 Ni, 0.09% Cu <sup>3</sup>	Baxter (1978) Smithies (1998) Ruddock (1999) Miller and Smith (1975) Marston (1984)

*Per*—Peridotite; *Px*—pyroxenite; *Nor*—norite; *Gab*—gabbro; *An*—anorthosite; *Gran*—granophyre.

*Rock types are arranged in order of decreasing abundance.*

<sup>1</sup> Hydrothermal polymetallic deposit on northern margin of the Munni Munni Intrusion (see Deposit Type 8.C in Section 6.4.8.3).

<sup>2</sup> Includes unexposed part beneath platform cover rocks of the Fortescue Group.

<sup>3</sup> Inferred Resource.

<sup>4</sup> Indicated Resource.

<sup>5</sup> Total Mineral Resource.

<sup>6</sup> Approximate estimate of PGE grades by Hoatson (GA) from limited analyses of massive and matrix sulphides in drill core.

### *Mineralisation environment*

The 2927 Ma Munni Munni Intrusion (Figure 6.4) is an elongated mafic-ultramafic body that crops out over an area of ~4 km by ~9 km (Hoatson and Keays, 1989; Hoatson et al., 1992; Barnes and Hoatson, 1994). The southwestern extension of the intrusion is unconformably overlain by 2.77 Ga sedimentary and volcanic rocks of the Fortescue Group, but near coincident aeromagnetic and gravity highs suggest the overall dimensions of the intrusion are ~9 km by ~25 km. Hoatson (1991a,b) subdivided the intrusion into a lower 1850-m-thick ultramafic zone and an overlying gabbroic zone which has a minimum thickness of 3600 m. The ultramafic zone consists of nine subzones containing macrorhythmic cycles of olivine-rich and clinopyroxene-rich mesocumulates and adcumulates. Preferential erosion of the ultramafic stratigraphy has resulted in a distinctive undulating landform comprising alternating valleys equating to the olivine-rich units and ridge-forming pyroxenite cycles. Dominant rock types are dunite, lherzolite, wehrlite, olivine websterite, clinopyroxenite, and websterite, with orthopyroxenite, norite, and spinel-bearing xenolithic units prominent in the upper parts of the lower zone.

The upper part of the ultramafic zone contains a distinctive 30-m- to 80-m-thick, mineralised porphyritic websterite layer (PWL). The main host rock in the PWL is a porphyritic plagioclase websterite unit that is a texturally distinctive orthocumulate containing 40% to 80% augite and 10% to 40% hypersthene as cumulus phases, and up to 20% intercumulus plagioclase. Accessory minerals include biotite, ilmenite, magnetite, alkali feldspar, apatite, sulphides, and secondary clin amphibole and carbonate minerals. Hypersthene forms large (up to 3 cm) euhedral cumulus grains that are mantled by intercumulus plagioclase, whereas clinopyroxene occurs as smaller subhedral granular grains. Chemical and mineralogical data indicate that the PWL is transitional in character between the ultramafic and gabbroic zones. Cumulus olivine disappears, orthopyroxene becomes cumulus with clinopyroxene, and plagioclase appears as an intercumulus mineral. In the overlying gabbro zone, plagioclase, clinopyroxene, and orthopyroxene as inverted pigeonite are cumulus. Persistent PGE mineralisation associated with disseminated chalcopyrite, pentlandite, and pyrrhotite (up to 2%) blebs occurs along the exposed 22-km-strike extent of the PGE-enriched layer. The PWL parallels the basal contact of the gabbroic zone, but its base is discordant to arcuate layering trends in the upper part of the ultramafic zone indicative of magmatic erosion during magma mixing. A number of minor rock types, namely olivine orthopyroxenite, orthopyroxenite, chromitite, norite, and mixed orthopyroxenite-norite rocks form a package of interfingering lenses of up to 200-m-strike length in the PWL (Hoatson and Keays, 1989).

The base of the gabbroic zone marks the departure of cumulus olivine and the first major appearance of cumulus plagioclase and inverted pigeonite in the intrusion. The dominant mafic rocks in the gabbroic zone are laminated and massive intergranular gabbro-norite, leucogabbro, and magnetite gabbro. Carbonate-altered granophyric gabbro, quartz monzonite, and quartz syenite abutting the Fortescue Group rocks to the south represent the most evolved rocks exposed in the intrusion.

The intrusion is interpreted as a slightly asymmetric boat-like structure, plunging moderately to the south-southwest, with the cyclic units thickening along the axis of the intrusion (Figure 6.5). The PWL in the central part of the intrusion generally maintains its thickness and moderate southerly dips to depths of 600 m. An isolated north-trending body of pyroxenite on the northwestern side of the intrusion, referred to as the Cadgerina Dyke, was interpreted by Barnes and Hoatson (1994) to be a feeder conduit to the gabbroic zone and upper parts of the ultramafic zone. The intersection of the projected southerly extension of this dyke with the central axis of the ultramafic zone coincides with a regional gravity high over the intrusion.

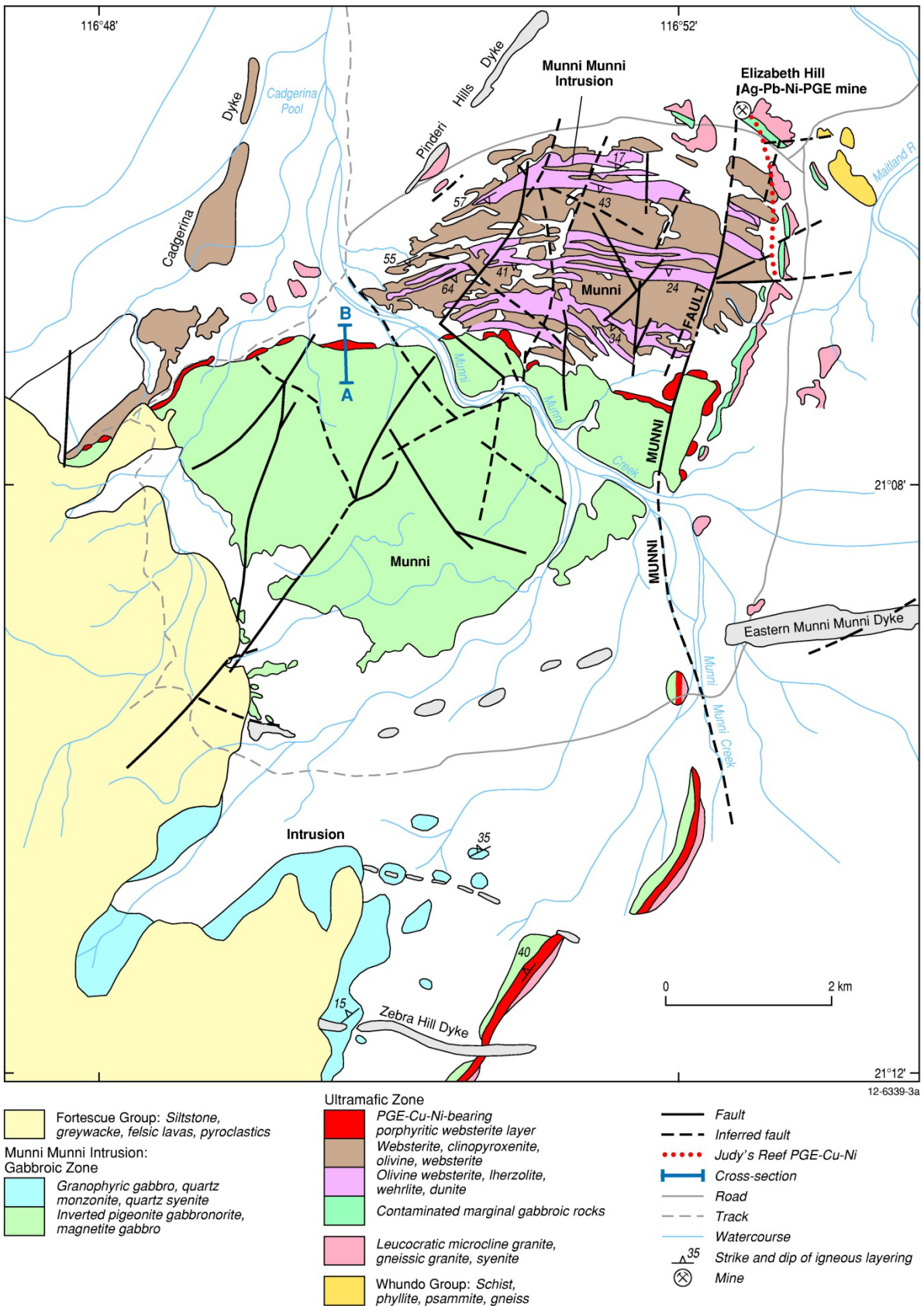


Figure 6.4 Geology of the 2927 Ma Munni Munni Intrusion, west Pilbara Craton, Western Australia (after Hoatson, 1986, 1992; Williams et al., 1990). The unornamented areas within and surrounding the intrusion largely represent alluvium. Modified from Hoatson and Sun (2002).

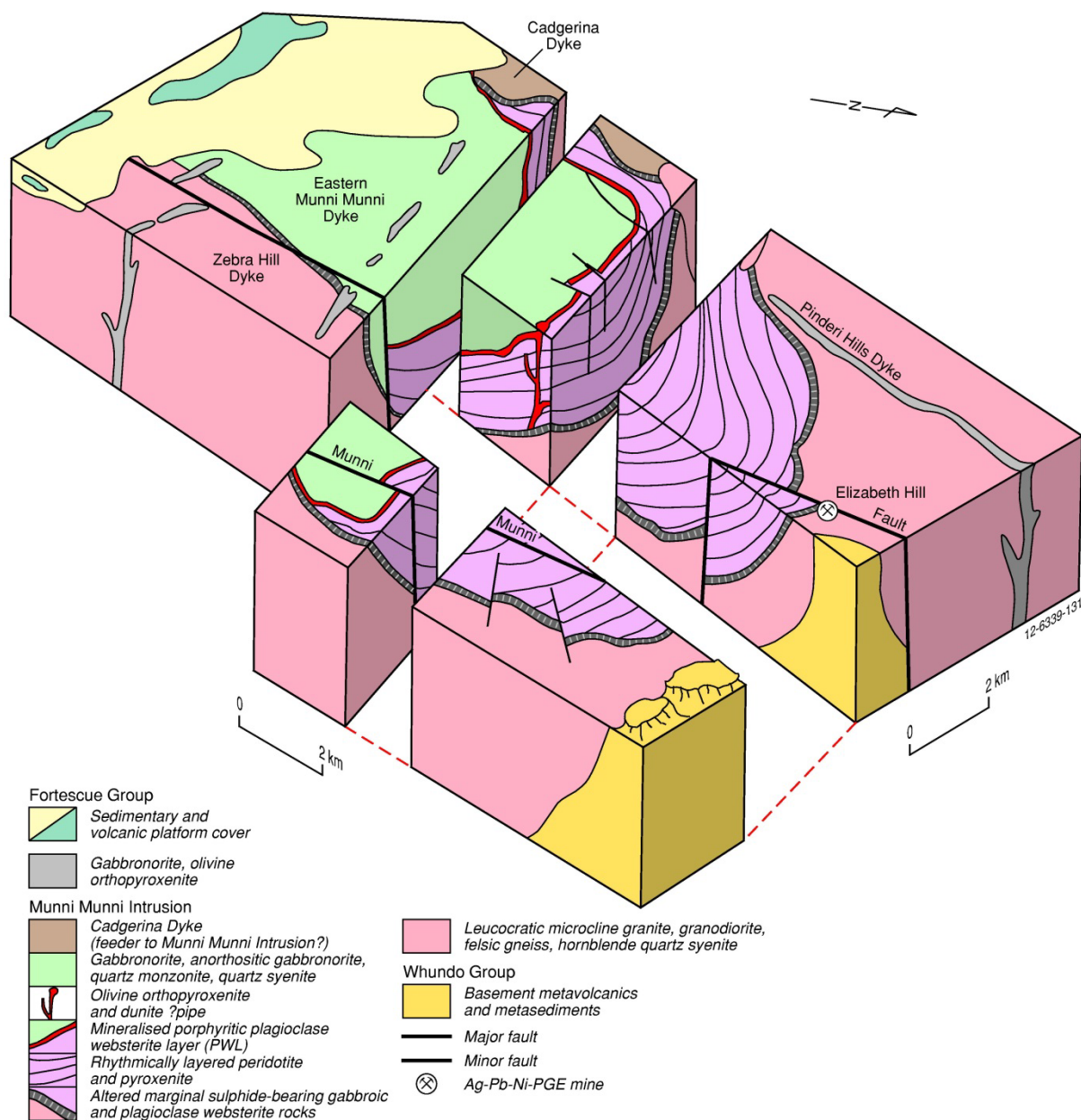


Figure 6.5 Interpretive block diagram of the Munni Munni Intrusion. The lateral continuity of the mineralised porphyritic websterite layer (PWL) is highlighted near the contact between the ultramafic and gabbroic zones. Modified from Hoatson (1992).

### PGE mineralisation

Four different styles of PGE mineralisation have been documented in the Munni Munni Intrusion.

1. A thin veneer of gabbronorite, gabbro, and plagioclase websterite along the northern basal contact of the ultramafic zone hosts disseminated pyrrhotite, chalcopyrite, and minor pentlandite (up to 6.0% total sulphides). The basal sulphides generally have low Ni/Cu ratios of 0.4 and Pt and Pd abundances of less than 40 ppb and 60 ppb, respectively. The mafic-hosted sulphides probably formed during localised supercooling and/or contamination processes that involved the first ultramafic magma pulses in the basal parts of the magma chamber and the country rocks.

2. Judy's Reef is a 1-m- to 2-m-thick Pd-enriched layer along the northeastern basal contact of the ultramafic zone (Barnes, 1995). Polymetallic mineralisation occurs 20 m to 30 m above the basal contact for a distance of 2 km south of the Elizabeth Hill Ag deposit (see Deposit Type 8.C). The reef is enriched in Pd, Ni, Cu, Co, and Ag, with Pd constituting about 80% of the total metal content. Typical drill-hole intersections include 1 m to 2 m @ 0.2 ppm to 1.9 ppm Pd+Pt+Au, 0.3% to 2.9% Ni+Cu, and 28 ppm to 260 ppm Ag. Erratic metal grades and ratios and the non-coincident character of Pd and Ag anomalies over several metres suggest a possible hydrothermal origin similar to the nearby Elizabeth Hill Ag deposit.
3. Thin (1 m to 3 m) pegmatoidal websterite layers and lenses containing 0.3 to 1 ppm Pd occur about one-third of the way up the ultramafic zone of the intrusion (Barnes, 1995).
4. The PWL contains the most significant PGE mineralisation in the intrusion.

The PGE enrichment in the PWL occurs at the base of a 5-m- to 15-m-thick interval of disseminated Cu-Ni sulphides generally within 20 m of the overlying ultramafic-gabbroic zone contact (Figure 6.6). The PWL is exposed along a 22 km strike extent and it is interpreted to extend for another 40 km along strike beneath the Fortescue Group platform cover to the southwest. One of the best drill-hole intersections of the PWL is DDH MMD 34: 5.5 m @ 4.3 ppm PGEs+Au from near the central part of the intrusion. This drill-hole indicates an apparent increase in grade and width of the mineralised horizon with depth. Figure 6.7 illustrates that there was minor Pt, Pd, and Au enrichment near the base of the ultramafic zone (see above). However, for most of the ultramafic zone, the incompatible chalcophile elements Pt, Pd, Ir, and Au had low abundances (<2 ppb Pt, <3 ppb Pd, <1.5 ppb Ir, <0.6 ppb Au) in sulphide-undersaturated conditions. This trend changed in the upper parts of the ultramafic zone, where the PGEs behaved incompatibly as they were concentrated in the melt during fractionation. This mineralising process pre-empted the sulphide-saturated conditions induced by the emplacement of, and mixing with, the sulphide-saturated tholeiitic mafic magmas(s) that formed the gabbroic zone. The PGEs were enriched in disseminated sulphides (to ppm concentrations) in the hybrid PWL, and above this layer, they were rapidly depleted in the lower parts of the gabbroic zone due to their exceptionally high partition coefficients for S in the PWL. The geochemical trends of Pt, Pd, Cu, and Ni for the mineralised environment are shown in DDHs MMD1 and MMD5 of Figure 6.7. Barnes et al. (1990) noted that for about 40% of the mineralised intersections in the intrusion, peak Pd, Pt, Au, Cu, and Ni grades are coincident, whereas for the remainder the peak PGE grades are offset about 1 m to 4 m below the peak Cu and Ni peaks. The decoupling of the precious metals from the base metals and the increasing Pt/Pd ratio with increasing fractionation are features also seen in the PGE-rich horizons in the Wedza (Prendergast and Keays, 1989) and Darwendale (Wilson and Tredoux, 1990) subchambers of the Great Dyke of Zimbabwe. The PGMs (Hoatson and England, 1986; Hoatson and Keays, 1989) in the PGE-enriched PWL comprise arsenides, sulpharsenides, tellurides, native metals, and mercury-bearing phases that form small (2 µm to 10 µm; rarely up to 20 µm) grains enclosed within silicate minerals or along silicate grain boundaries (78% of occurrences), or are associated with chalcopyrite-pyrrhotite-pentlandite blebs (22%). Major mineral species identified by SEM analysis include cooperite, braggite, vysotskite, moncheite, potarite, atheneite, temagamite, michenerite, sperrylite, platarsite, native Pt, and native Pd (Hoatson and England, 1986). Significant diamond drill-hole intersections of the PGEs are shown in Table 6.4.

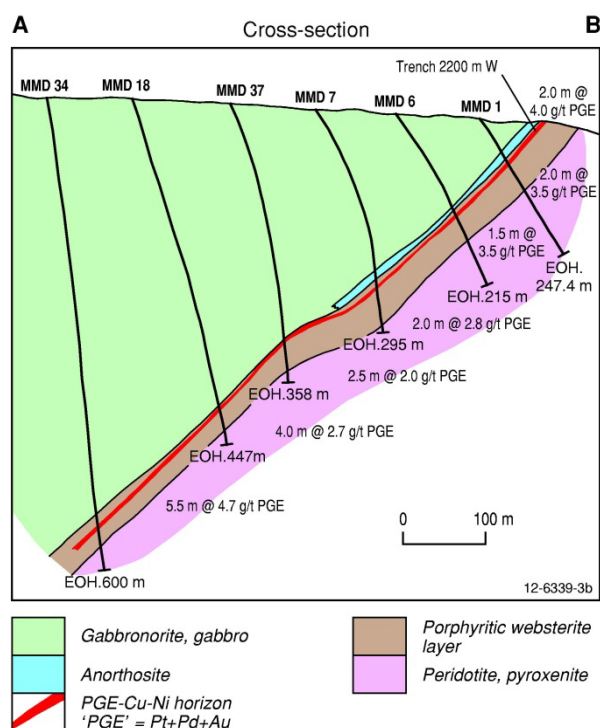


Figure 6.6 Schematic north-south cross-section of the PGE-enriched porphyritic websterite layer and associated rocks in the central part of the Munn Munn Intrusion. The location of cross-section A–B is shown in Figure 6.4. Modified from Williams et al. (1990).

Table 6.4 Significant PGE intersections from the Munn Munn Intrusion.

Drill-hole	interval (m)	Pt (ppm)	Pd (ppm)	Au (ppm)	Pt+Pd+Au (ppm)
MMD 1	64.0–66.5	1.28	2.03	0.15	3.46
MMD 3	76.0–79.0	0.98	1.74	0.13	2.85
MMD 5	42.0–45.0	0.69	1.20	0.09	1.98
MMD 7	236.0–241.0	0.62	1.11	0.15	1.88
MMD 11	109.0–118.5	0.63	1.06	0.20	1.89
MMD 15	87.0–92.0	0.81	1.47	0.54	2.82
MMD 28	231.0–232.5	2.25	3.77	0.71	6.73
MMD 34	543.0–548.5	1.2	2.6	0.5	4.3
MMD 38	224.0–229.0	0.6	1.1	0.1	1.8
MMD 42	384.5–387.5	0.7	1.3	0.1	2.1
MMD 47A	202.5–205.5	0.4	1.6	0.2	2.2
MMD 52	30.5–32.0	0.8	1.7	0.3	2.8

Source: Several Hunter Resources Ltd exploration reports to the Australian Securities Exchange cited in Hoatson and Glaser (1989).

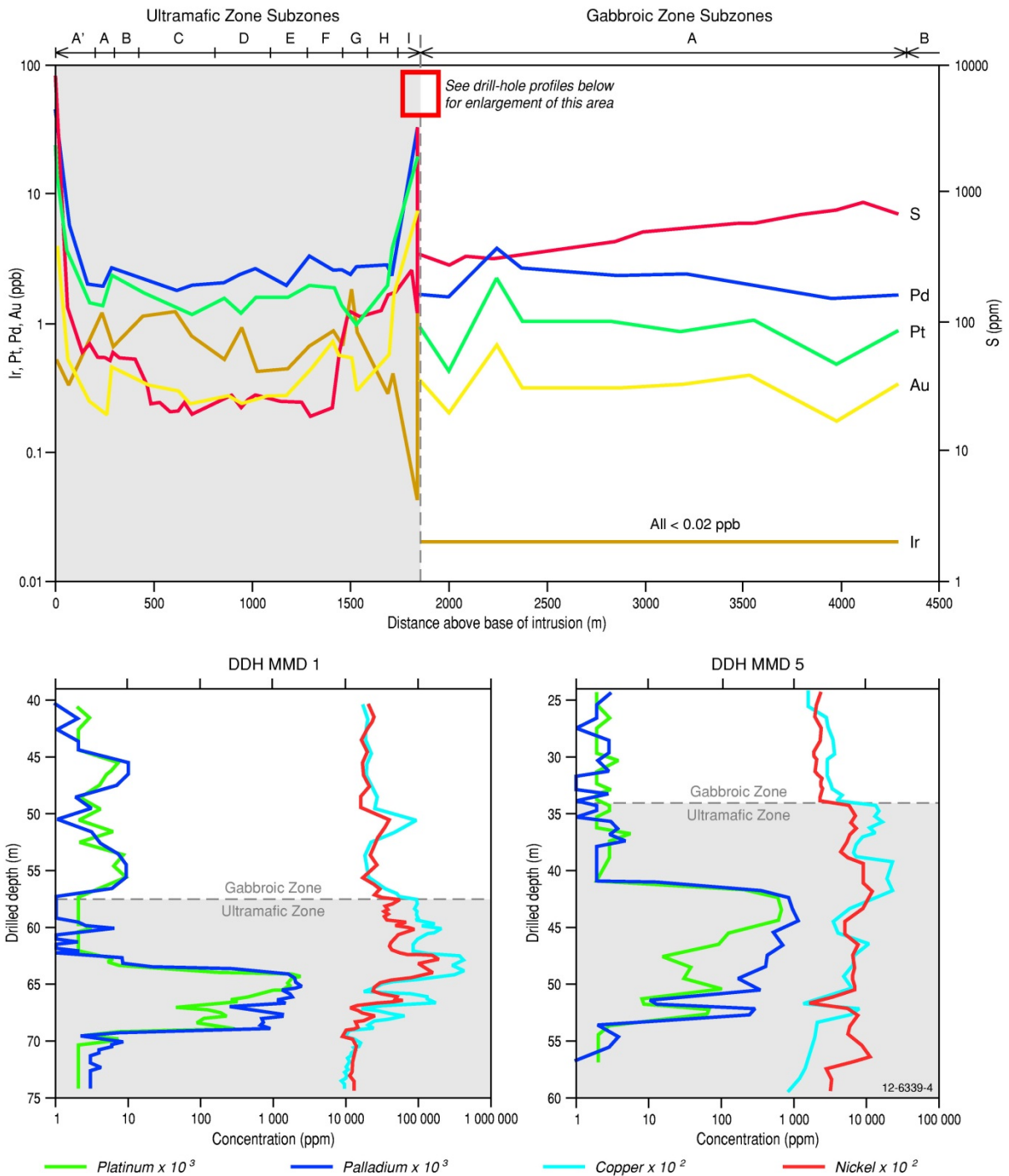


Figure 6.7 Geochemical profiles (top figure) of whole-rock platinum, palladium, iridium, gold, and sulphur concentrations in the ultramafic and gabbroic zones of the Munni Munni Intrusion. Geochemical profiles (bottom figures) of platinum, palladium, copper, and nickel concentrations across the porphyritic websterite layer in the upper part of the ultramafic zone in the Munni Munni Intrusion. The location of diamond drill-hole MMI is shown on Figure 6.6. DDH MM5 was collared 1.5 km along a southerly strike from DDH MM1 in laminated gabbronorite. Modified from Hoatson and Keays (1989).

The PGE mineral systems in the Munni Munni Intrusion have been described by Hoatson (1984, 1991a,b, 1998); Hoatson and England (1986); Hoatson and Keays (1987a,b, 1989); Williams et al. (1990); Barnes et al. (1990, 1991b, 1992); Sun et al. (1991); and Hoatson and Sun (2002).

### *Age of mineralisation*

A minimum age for the Munni Munni Intrusion is indicated by the age of the Fortescue Group, which unconformably overlies the southern two-thirds of the intrusion. The age of the basal Fortescue Group is constrained by:

- the average age of 2765 Ma from six U-Pb zircon ages of various basal Fortescue Group volcanic and sedimentary units (Arndt et al., 1991);
- U-Pb zircon age of  $2768 \pm 16$  Ma from the Spinaway Porphyry which intrudes the Hardey Sandstone (Pidgeon, 1984); and
- Pb model age of  $2760 \pm 30$  Ma for the Kylene Basalt (Richards and Blockley, 1984).

Therefore the best estimate for the age of the base of the Fortescue Group is about 2765 Ma, which provides a minimum age for the Munni Munni Intrusion.

Mineral separates of clinopyroxene, plagioclase, and orthopyroxene from three samples in the Munni Munni Intrusion were analysed to obtain Sm-Nd mineral isochrons. Pooled data for rock samples from the PGE-enriched porphyritic websterite layer and the gabbroic zone gave a weighted mean age of  $2927 \pm 13$  Ma ( $2\sigma$ : Hoatson and Sun, 2002), which agrees well with the SHRIMP zircon U-Pb age of  $2925 \pm 16$  Ma by Arndt et al. (1991) for a ferrogabbro pegmatite near the top of the ultramafic zone. The pegmatite is believed to have been derived from late-crystallising intercumulus liquid, and therefore the age is interpreted as a reliable estimate for the crystallisation of the intrusion, and is not an inherited age from xenocrystic zircon. The  $2927 \pm 13$  Ma age is further constrained by a SHRIMP U-Pb zircon age of  $2924 \pm 5$  Ma for a granitic dyke that cuts pyroxenite and gabbro of the intrusion (Nelson, 1998). The crystallisation ages of  $2927 \pm 13$  Ma and  $2925 \pm 16$  Ma for the Munni Munni Intrusion are also reliable ages for the orthomagmatic PGE mineralisation in the PWL immediately below the contact of the gabbroic-ultramafic zones.

The ~2.89 to 2.93 Ga Munni Munni, Radio Hill, Andover, and Sherlock intrusions (all within error) of the west Pilbara Craton represent some of the oldest mineralised layered intrusions in the world. The Andover Intrusion has been tentatively assigned to the ~2925 Ma intrusions of the west Pilbara Craton. However, a U-Pb age of  $3016 \pm 4$  Ma (Nelson, 2001) for a discordant monzodiorite body within this intrusion may indicate that it is older than the other west Pilbara intrusions. The large ~2800 Ma mafic-ultramafic intrusions of the Murchison Domain in the Yilgarn Craton (Ahmat and Ruddock, 1990; Ivanic et al., 2010) and the 1860–1840 Ma intrusions in the Halls Creek Orogen, East Kimberleys (Hoatson and Blake, 2000) are some of the oldest intrusions in Australia that have been accurately dated. Important mineralised intrusions from overseas that are of Archean or Proterozoic age include the Stillwater Complex ( $2701 \pm 8$  Ma: De Paolo and Wasserburg, 1979); Great Dyke ( $2587 \pm 8$  Ma: Mukasa et al., 1998); Bushveld Complex ( $2060 \pm 3$  Ma: Kruger et al., 1986); Sudbury ( $1850 \pm 1$  Ma: Krogh et al. (1984); and Voisey's Bay ( $1333 \pm 1$  Ma: Amelin et al., 1999).

### *Genesis*

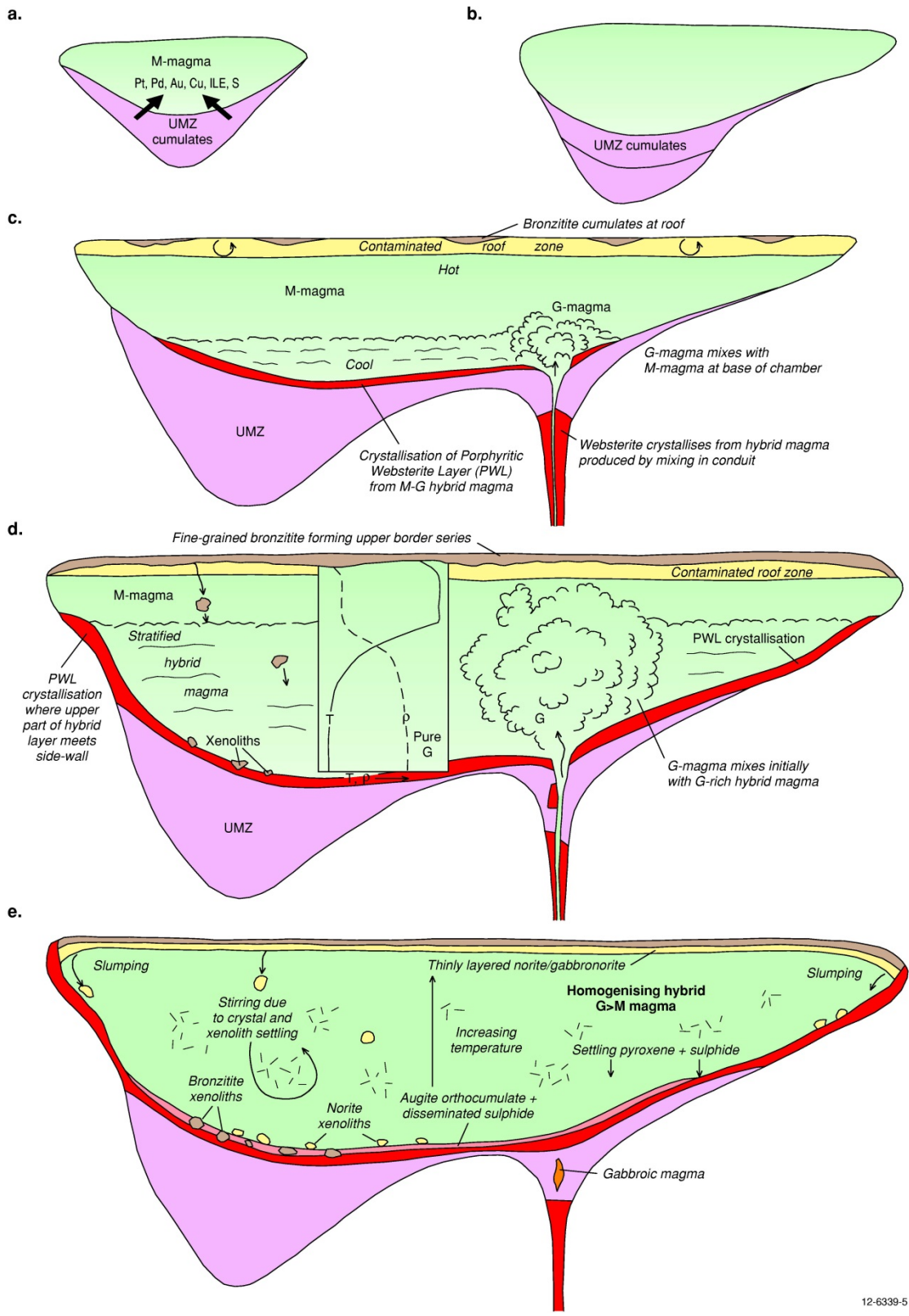
The Munni Munni Intrusion was emplaced near the contact between the Cherratta Granitoid Complex and metavolcanic-metasedimentary rocks of the Whundo Group. It crystallised at upper crustal pressures of 3.5 kb to 5 kb, temperatures of 1050°C to 1100°C, and under low  $P_{\text{H}_2\text{O}}$  conditions.

Oxygen fugacities were equivalent to the fayalite-magnetite-quartz buffer (Hoatson et al., 1992). Periodic reversals towards more primitive olivine and pyroxene compositions within a restricted compositional range in the ultramafic zone imply open-system crystallisation involving periodic replenishment by new primitive magma pulses that mix with residual differentiated magma. In contrast, a steady decrease in the magnesium content of clinopyroxene and inverted pigeonite and the anorthite content of plagioclase in the gabbroic zone indicates closed-system fractionation with little if any magma replenishment.

Hoatson and Keays (1989) proposed that the PGE mineralisation in the PWL resulted from the combined processes of crystal fractionation and mixing of chemically distinct magma types (Figure 6.8). Chalcophile element trends through the intrusion showed that the PWL marks the onset of sulphide saturation and sulphide accumulation in the chamber. The early development of the intrusion involved repeated influxes of a sulphide-undersaturated, PGE-bearing magnesian magma (M magma), followed by a dramatic expansion of the chamber that culminated in a large influx of fractionated sulphide-saturated tholeiitic gabbroic magma (G magma) (Barnes et al., 1990). Mixing of the magmas during this influx gave rise to the PGE-bearing PWL.

Barnes and Hoatson (1994) provided further details of the crystallisation and magma-mixing model of the intrusion. The cyclicity of the ultramafic zone cumulus stratigraphy, the geometry of the layering, and the overall shape and structure of the intrusion are all consistent with a model for progressive expansion of the magma chamber during emplacement of successive pulses of magma. Injection of fractionated tholeiitic magma into more primitive high-Mg basalt resident magma formed a turbulent fountain, which entrained the resident magma and formed a cool, dense basal hybrid layer. Crystallisation of the PWL occurred where the top of this hybrid layer impinged on the sloping floor. Continuing injection of tholeiitic magma expanded the thickness of the hybrid layer, causing the PWL to accrete progressively up the sloping floor and the walls. After the conclusion of the influx phase, the hybrid layer became homogenised to a final tholeiite-rich composition, which eventually crystallised to form the thick Gabbroic Zone.

The siliceous high-magnesian basaltic parent magmas proposed by Hoatson and Keays (1989) and Hoatson and Sun (2002) for the Munni Munni and other nearby west Pilbara layered mafic-ultramafic intrusions (e.g., Andover, Radio Hill, Mount Sholl) show distinctive crustal characteristics, such as enrichment of Th and light rare-earth elements (REE), but low Nb/Th and Nb/La (~0.2–0.3). Such features could be a result of crustal contamination and/or recycling of crustal material through lithospheric subduction and modification of the magma source region. Sun et al. (1991) showed that high FeO (11.5%) and low Al<sub>2</sub>O<sub>3</sub> (8.5% to 10%) and Al<sub>2</sub>O<sub>3</sub>/TiO<sub>2</sub> ratios of ~11 for these siliceous high-magnesian basalts exclude an origin mainly by melting of a metasomatised refractory lithospheric mantle (poor in Fe and Ti). Hoatson and Sun (2002) indicated that the siliceous high-magnesian basalts that formed the Munni Munni Intrusion and other west Pilbara intrusions were of Al-depleted komatiitic affinity (Barberton-type) with 9–12% MgO, 15–25 ppm Sc, 12–18 ppm Y, and light-REE enrichment (chondrite-normalised La/Sm = 2.7, La/Lu = 9.0). They were generated with garnet in the residual asthenospheric mantle with probable involvement of a pre-3.0 Ga subduction-modified lithospheric mantle. Isotopic and geochemical modelling suggests that the magmas were contaminated by ~3.0–3.3 Ga Archean tonalitic to granodioritic crust before being emplaced into high-level magma chambers. The fertile parent magma responsible for the formation of the ultramafic zone is estimated to have contained 10% to 15% MgO, 10 ppb to 15 ppb Pt, 15 ppb to 20 ppb Pd, 2 ppb to 4 ppb Au, 85 ppm Cu, 62 ppm Zr, 220 ppm Sr, and 530 ppm S (Hoatson and Keays, 1989). These values are similar to those reported by Davies and Tredoux (1985) for the magnesian parent magma suite (MgO ~12%) of the Bushveld Complex.



12-6339-5

Figure 6.8 Conceptual representation of the evolution of the Munni Munni Intrusion. The various stages show the enrichment of PGEs, Au, Cu, S, and the ILE by crystal fractionation processes in the S-undersaturated resident magma (M-magma) in the chamber (stage a), the rapid enlargement of the magma chamber (stage b), and the formation of the mineralised PWL from the mixing of a fractionated S-saturated gabbroic magma (G-magma) with the PGE-enriched M-magma in a prolonged fountain-type injection (stages c to e). Predictive qualitative profiles of temperature and density gradients are also shown in stage d. Modified from Barnes and Hoatson (1994).

Hoatson et al. (1992) and Hoatson and Sun (2002) showed that the ~2.9 Ga Munnii Munnii, Andover, Radio Hill, Mount Sholl, Maitland, and Sherlock layered mafic-ultramafic intrusions are a cogenetic suite of high-level (<5 kb) bodies that represent some of the oldest mineralising systems of their type in the world. Although they display similar field relationships and mineralogical, geochemical, and isotopic features, their contrasting chalcophile metal distribution patterns show that the timing and mechanism of the sulphide-saturation event were critical for the development of PGE-enriched sulphide-bearing layers and basal segregations of base-metal sulphides. For example, mineral compositional trends and Nd isotopic data for Munnii Munnii indicate that the PGE-bearing siliceous high-magnesian basaltic parent magma was frequently injected into the magma chamber and the PGEs increased in concentration by crystal fractionation processes within a sulphide-undersaturated environment. A major influx of more fractionated, sulphide-saturated tholeiitic gabbroic magma related to the resident magnesian basaltic magma, rapidly inflated the chamber and induced turbulent magma mixing that resulted in the formation of the PGE-bearing PWL at a relatively high stratigraphic level in the intrusion (i.e., at a major compositional interface in the complex, such as the ultramafic zone and gabbroic zone contact). In contrast, the parent magmas that formed the Radio Hill, Mount Sholl, Andover, and Maitland intrusions were saturated in S before they were emplaced into the magma chambers. In these intrusions (which host Type 2.A deposits as described in this report), gravitational and structural controls, and the dynamics of magma flow (i.e., turbulent versus slow) were important for the formation of PGE-poor (5 ppb to 400 ppb Pt+Pd+Au) massive sulphides. These sulphides concentrated in depressions and structural embayments along the basal contacts beneath the thickest sequences of mafic-ultramafic cumulates (e.g., Radio Hill, Mount Sholl, Andover, ?Maitland) and/or in feeder conduits (Radio Hill).

The evolution of the Munnii Munnii Intrusion is described by Hoatson and Keays (1989); Hoatson (1991a); Barnes and Hoatson (1994); and Hoatson and Sun (2002). Company, academic, and government investigations of the west Pilbara Intrusions are summarised in Table 6.5.

*Table 6.5 Investigations of mafic-ultramafic intrusions in the west Pilbara Craton, Western Australia. Source: Hoatson and Sun (2002).*

Reference	Intrusion(s)	Investigation(s)
de Laeter and Trendall (1971)	Gidley Granophyre	Geochronology
Donaldson (1974)	Munnii Munnii	Petrology, mineralogy, whole-rock geochemistry
Fitton et al. (1975)	Various intrusions	Stratigraphy, geochronology
Baxter (1978)	Andover, Balla Balla	Geology, mineralisation
Mathison and Marshall (1981)	Mount Sholl	Petrology, mineral and whole-rock geochemistry
Nisbet and Chinner (1981)	Ruth Well	Geology, stratigraphy, mineralisation
Hickman (1983)	Various intrusions	Regional setting, geology, mineralisation
Hoatson (1984)	Munnii Munnii	Geology, mineralisation
Marston (1984)	Various intrusions	Regional setting, geology, mineralisation
Hudson and Horwitz (1985)	Andover region	Mineralogy of platinum-group minerals
Hoatson and England (1986)	Munnii Munnii	Mineralogy of platinum-group minerals
Korsch and Gulson (1986)	Millindinna	Geochronology, Sm-Nd and Pb-Pb isotopes
de Angelis et al. (1987)	Radio Hill	Geology, geophysics, mineralisation

Reference	Intrusion(s)	Investigation(s)
Hoatson and Keays (1987a,b)	Munni Munni	Stratigraphy, mineralogy, geochemistry, mineralisation
Peters and de Angelis (1987)	Radio Hill	Exploration, geology, geophysics
de Angelis et al. (1988)	Radio Hill	Exploration, geology, geophysics
Horwitz (1988a)	Radio Hill	Geology, stratigraphy
Simpson et al. (1988)	Munni Munni, Andover	Remote sensing
Hoatson and Glaser (1989)	Munni Munni	Geology, mineralisation
Hoatson and Keays (1989)	Munni Munni	Stratigraphy, mineralogy, geochemistry, mineralisation
Barnes et al. (1990)	Munni Munni	Geology, mineralisation
Macias and Simpson (1990)	Munni Munni, Andover	Remote sensing
Wallace and Hoatson (1990)	Various intrusions	Geology, petrology, whole-rock geochemistry
Williams et al. (1990)	Munni Munni	Exploration, geology, mineralisation
Arndt et al. (1991)	Munni Munni	Geochronology
Barnes et al. (1991b)	Munni Munni	Geology, stratigraphy, mineralisation
Hoatson and Barnes (1991)	Several intrusions	Geology, stratigraphy, mineralisation
Sun et al. (1991)	Munni Munni, Andover	Whole-rock geochemistry, Sm-Nd isotopes
Barnes et al. (1992)	Munni Munni	Geology, pyroxene compositions, mineralisation, genesis
Hoatson et al. (1992)	Various intrusions	Geology, geochemistry, mineralisation, genesis
Wallace (1992)	Andover	Geology, geochemistry, mineralisation, genesis
Boudreau et al. (1993)	Munni Munni, Radio Hill	Geochemistry of apatite, stratigraphy, genesis
Barnes and Hoatson (1994)	Munni Munni	Geology, structure, mineralisation, genesis
Starkey (1994)	Sherlock, Balla Balla	Geology, geophysics
Barnes (1995)	Elizabeth Hill	Exploration, geology, mineralisation, resources
Mernagh and Hoatson (1995)	Munni Munni	Laser Raman study of platinum-group minerals
Mernagh and Hoatson (1997)	Munni Munni	Laser Raman study of pyroxene
Lambert et al. (1998)	Munni Munni, Ruth Well	Geochemistry, Re-Os isotopes
Smithies (1998)	Sherlock, Opaline Well	Geology, mineralisation
Ruddock (1999)	Several intrusions	Exploration, geology, mineralisation
Mernagh et al. (2000)	Munni Munni	Laser Raman study of chromite
Frick et al. (2001)	Radio Hill	Geology, geochronology, Re-Os isotopes
Miele et al. (2001)	Ruth Well	Geochronology, Re-Os isotopes
Hoatson and Sun (2002)	Various intrusions	Geology, geochronology, mineralisation, genesis
Hoatson et al. (2006)	Various intrusions	Geology, geochronology, mineralisation, genesis
Hoatson et al. (2009a,b)	Various intrusions	Geology, geochronology, correlations, mineralisation
Pirajno and Hoatson (2012)	Large Igneous Provinces	Geology, geochronology, mineralisation, genesis

## *Key references*

- Donaldson (1974): geological maps at various scales; geological setting; stratigraphy; petrology; layering structure; whole-rock geochemistry.
- Hoatson (1984): geological setting; highlighted PGE potential of Munni Muni Intrusion; comparisons with Bushveld and Stillwater intrusions, exploration strategies.
- Hoatson and England (1986): scanning-electron-microprobe study; PGMs; sulphide mineralogy; mineralisation models.
- de Angelis et al. (1988): geophysical techniques; geology; exploration.
- Hoatson and Keays (1989): regional geological setting; stratigraphy; PGE mineralisation; geochemistry; petrogenesis.
- Wallace and Hoatson (1990): petrology; whole-rock geochemistry; mineralisation.
- Williams et al. (1990): geology; stratigraphy; mineralisation; mineral resource.
- Barnes et al. (1991b): geology; stratigraphy; structure; mineralisation.
- Hoatson (1991a): Pilbara layered intrusions; geological maps; field relationships; layering; petrology; PGE geochemistry; whole-rock and mineral chemistry; isotopes; parent magmas; exploration.
- Hoatson (1991b): 1:20 000 scale geological maps of the Munni Munni, Mount Sholl, Maitland, and Radio Hill layered intrusions.
- Barnes et al. (1992): mineralogy of porphyritic websterite layer; sulphide assemblage; mineral geochemistry; mineralisation; petrogenesis.
- Hoatson et al. (1992): Pilbara layered mafic-ultramafic intrusions; geological maps; field relationships; layering; geochronology; petrology; PGE geochemistry; whole-rock and mineral chemistry; isotopes; parent magmas; remote sensing; exploration.
- Barnes and Hoatson (1994): stratigraphy; structure; petrogenesis.
- Boudreau et al. (1993): Pilbara intrusions; mineral chemistry; stratigraphy; mafic rocks; apatite geochemistry; fluid activities; mineralisation; exploration potential.
- Mernagh and Hoatson (1995): Laser Raman microprobe study of PGMs; mineralogy; petrogenesis of PGMs.
- Mernagh and Hoatson (1997): Laser Raman microprobe study of pyroxene; mineralogy; evolution trends of pyroxenes.
- Hoatson (1998): Pilbara layered intrusions; Munni Munni Intrusion; regional geological setting; stratigraphy; mineralisation.
- Hoatson and Sun (2002): oldest mineralising systems in world; Pilbara layered intrusions; Munni Munni Intrusion; regional geological setting.
- Hoatson et al. (2006): geological setting, Ni-mineral systems, resources, genesis, potential.
- Hoatson et al. (2009a,b): spatial and temporal correlations of Archean mafic-ultramafic intrusions, geology, geochronology, mineralisation.

### **6.4.1.2 Deposit Type 1.B: Stratabound PGE-bearing chromitite layers**

#### *Overview*

Chromitite layers are relatively common in large layered Precambrian mafic-ultramafic intrusions. They have been widely documented throughout the world and they are an important source of Cr, PGEs, and minor base-precious metals. The single most PGE-enriched rock formation in the world is the UG-2 Chromitite layer in the Bushveld Complex, Republic of South Africa. This layer can be traced for many tens of kilometres without any physical breaks, and for distances of at least 300 km (Cawthorn, 1999). The estimated global resource of 32 730 t of PGEs for the UG-2 Chromitite layer (Naldrett, 1989, 2004, 2011) exceeds those resources estimated for the Merensky Reef (26 160 t) and the Great Dyke of Zimbabwe (13 945 t).

The most important stratabound PGE-bearing chromitite layers in Australia are hosted in ultramafic-dominant intrusions in Proterozoic orogenic zones, with other minor examples including Archean mafic-ultramafic intrusions of Archean granite-greenstone cratons. Relative to the stratabound PGE-bearing sulphide deposits of Type 1.A, PGE-enriched chromitites are more widespread throughout Australia's Proterozoic and Archean terranes. Stratabound chromitite layers that range in thickness from a few cm to 2.4 m occur within dunite (Panton Intrusion: Perring and Vogt, 1991), troctolite (Wilagee Intrusion: Hoatson and Blake, 2000), and/or near the base of cyclic dunite-bronzite units (Windimurra Intrusion: Mathison and Ahmat, 1996) similar to the UG-2 Chromitite of the Bushveld Complex, Republic of South Africa (Naldrett, 1989, 2004, 2011; Cawthorn, 1999, 2010). Concentrations of PGEs in these deposits are generally <3 g/t total PGEs+Au, however, some localised values up to 10 g/t over a few metres width have been documented. Generally most sulphide-enriched chromitites close to, or above the level where plagioclase first enters as a cumulus mineral, are particularly enriched in PGEs. The lateral continuity of both grades and widths of mineralised units often determines the economic viability of these deposits in the orogenic belts of Australia.

The Paleoproterozoic Panton Intrusion in the Halls Creek Orogen (HCO), contains the largest resource of PGEs (global resource of 65.6 t: Table 6.2) associated with chromite in Australia. The intrusion has had a protracted history of exploration since the discovery of chromitites in 1962, and it is considered the most advanced prospect with potential to become Australia's first mineable resource of PGEs. Other notable examples include Lamboo and Eastman Bore (both HCO) and Salt Creek–Plumridge Lakes (Albany-Fraser Orogen, WA: Hoatson and Glaser, 1989).

The HCO contains the largest number of PGE-bearing chromitite deposits of any province in Australia. The other major Proterozoic mafic-ultramafic igneous province in Australia—Musgrave Province of central Australia (Glikson et al., 1995, 1996; Howard et al., 2009; Evins et al., 2010)—contains very few mineralised chromitites in the large Mesoproterozoic intrusions of the Giles Complex. Minor chromitites have been documented in the Mount Davies and Hinckley Range intrusions (Daniels, 1974; Glikson et al., 1995, 1996; Howard et al., 2009; Evins et al., 2010). The paucity of chromitites in the Giles Complex may be attributed to the clinopyroxene-dominance of the ultramafic cumulates. Chromitite layers enriched in PGEs are generally associated with olivine and/or orthopyroxene (not clinopyroxene) cumulates in the upper parts of the ultramafic zone, similar to the Panton Intrusion and the UG-2 Chromitite in the Bushveld Complex (Mondal and Mathez, 2007). PGE-enriched chromitites in large differentiated Archean mafic-ultramafic intrusions, such as Windimurra (Mathison et al., 1991; Mathison and Ahmat, 1996) and Weld Range (Parks, 1998) in the Yilgarn Craton have also been a focus for exploration. The Coobina Intrusion (Tyler, 1991; Barnes and Jones, 2013) in the Pilbara region of Western Australia hosts the only Precambrian chromitite deposit that has been mined in

Australia. This Archean intrusion in the Sylvania Dome contains a number of tectonically dislocated and folded chromitite seams within a strongly deformed ultramafic-mafic layered intrusion. Despite the chromitites having anomalously high Cr contents relative to layered intrusions worldwide, low abundances of Pt and Pd in the chromitites are attributed to their crystallisation from uniformly sulphide-undersaturated magmas.

#### *Australian deposits/prospects/hosts*

Panton Intrusion, Lamboo Intrusion, Eastman Bore Intrusion (Halls Creek Orogen, WA); Salt Creek–Plumridge Lakes (Albany-Fraser Orogen, WA); Coobina Intrusion (Sylvania Dome, WA); Windimurra Igneous Complex, Bulong Intrusion, Imagi Well, Taccabba Well, West Bending (Yilgarn Craton); Pear Creek, Nobs Well (Pilbara Craton).

#### *Significant global example(s)*

UG-2 Chromitite, Bushveld Complex (South Africa); Chromitites in Ultramafic Sequence, Great Dyke of Zimbabwe (Zimbabwe); Lower Chromitites in Ultramafic Series, Stillwater Complex (USA); Kemi Intrusion (Finland).

#### *Type example in Australia*

Panton Intrusion, Western Australia.

#### *Location*

Longitude 127.831596°E, Latitude -17.751530°S; 1:250 000 map sheet: Dixon Range (SE 52–06), 1:100 000 map sheet: McIntosh (4462); ~55 km north-northeast of Halls Creek, Western Australia.

#### *Geological province*

Central Zone, Lamboo Province, Halls Creek Orogen (HCO), Western Australia.

#### *Resources*

Top Chromitite Reef and Middle Chromitite Reef—Combined Measured, Indicated, and Inferred Resources of 14.32 Mt @ 2.19 g/t Pt, 2.39 g/t Pd, 0.27% Ni, 0.07% Cu, 0.31 g/t Au (Panoramic Resources Limited, 2014).

#### *Current status and exploration history*

Undeveloped, but advanced PGE-Ni-Cu deposit with JORC-compliant resources. The layered mafic-ultramafic intrusions in the HCO have been explored for PGEs, Cr, Ni, Cu, Co, Ti, V, and Au since the early 1960s. Although significant amounts of these commodities have been found in many of the intrusions, no economic deposits (except the Savannah Ni-Cu-Co sulphide deposit in the Savannah Intrusion<sup>19</sup>) have been located to date. The Panton and Savannah intrusions are among the most intensively explored Proterozoic layered intrusions in Australia.

---

<sup>19</sup> Previously known as the Sally Malay Intrusion and Sally Malay deposit; renamed by Panoramic Resources Limited.

There have been four major phases of exploration relating to the HCO intrusions since the 1960s. Interest was stimulated during:

1. the 1960s—first systematic geological mapping of the East Kimberleys by the BMR and GSWA (impacts mainly for Cr-PGEs, Fe-Ti-V, and Ni-Cu-Co);
2. the early 1970s (the 'nickel boom years')—discovery in 1966 of komatiite-hosted Ni-Cu deposits in the Kambalda region of Western Australia (Ni-Cu);
3. the mid- to late-1980s—buoyant world PGE metal prices (Cr-PGEs); and
4. the early-1990s to 2000s—second-generation mapping of the HCO by GA and GSWA, and the discovery in 1993 of the world-class Voisey's Bay Ni-Cu-Co deposit in Canada (Ni-Cu-Co).

Pickands Mather and Company International and Australian Anglo American Limited carried out some of the earliest regional exploration programs in the Kimberleys from the early 1960s to the mid-1970s. The potential of the Panton Intrusion was highlighted in a large (80 000 km<sup>2</sup>) stream-sediment geochemical exploration program throughout the east Kimberleys. The other major discovery during these regional programs was the surface gossans of the Savannah Ni-Cu-Co-PGE deposit in 1974. Interest in the PGE-Cr potential of the Panton Intrusion was initiated when PGE-bearing chromitites were discovered in 1962 during the first generation geological mapping of the Dixon Range 1:250 000 geological sheet (Dow and Gemuts, 1967) by the Bureau of Mineral Resources, Geology and Geophysics and the Geological Survey of Western Australia. Anomalous amounts of Pt and Ni were recorded in primary chromitite bands and secondary chromite veins in the ultramafic sequences. The primary bands, which consist of alternating chromitite layers (2.5-cm-thick) and altered ultramafic rocks, were reported by Dow and Gemuts (1969) to be up to 10-m-thick and assaying 0.4 dwt/long ton (0.6 ppm) Pt and 0.15% Ni. The secondary chromite-rich veins in magnesite were up to 100-m-long and 0.7-m-wide, and contained a maximum of 2.0 dwt/long ton (~3.1 ppm) Pt and 0.2% Ni.

Many companies have evaluated the PGE-Cr-Ni-Au resources of the Panton Intrusion. Systematic exploration programs commenced some eight years after the discovery of the PGE-bearing chromitites. From the 1970s to the early 1980s, Minsaco Resources Pty Ltd mapped the intrusion in detail, and identified and drilled the main PGE-bearing chromitite layer. A feasibility study by Helix Resources Limited in 1989 assessed the Panton Intrusion to be uneconomic. Pancontinental Mining Ltd and Degussa Explorations GmbH carried out further investigations of the chromitites from 1989 to 1991. Closely spaced drilling of stratabound chromitite layers on the northwestern side of the intrusion defined a small high-grade resource of 2 Mt @ 6.02 ppm Pt+Pd+Au, 0.28% Ni, 0.06% Cu, and 8.49% Cr (using 3 ppm PGEs+Au cut-off: Perring and Vogt, 1991; Helix Resources, 1993a). In the mid-1990s, Helix Resources Limited focussed their exploration efforts on styles of magmatic and hydrothermal PGE mineralisation not considered by previous explorers. A stream-sediment geochemical orientation survey over the intrusion in 1994 identified anomalous Pt, Pd, Au, Ni, Cu, and Cr. A review of the open-cut potential of the PGE resource was carried out in 1997, but results were discouraging. During the 2000s, companies continued to define the PGE resources of the intrusion and submitted bulk samples of the different chromitite layers for metallurgical testing. Thundelarra Exploration Limited in 2001 defined a coincident Pt, Pd, Au, Cu, and Ni soil anomaly at the northern end of the Panton Intrusion. The anomaly ('Northern Anomaly') with maximum values of 715 ppb Pt+Pd, 856 ppb Au, 0.37% Ni, and 0.24% Cu has a strike extent of over 2 km and appears to be related to sulphides rather than chromitites. Drill intercepts of the anomaly included 128 m @ 0.55 g/t Pt+Pd+Au and 136 m @ 0.49 g/t Pt+Pd+Au (Thundelarra Exploration Limited, 2001). In the early 2000s, Platinum Australia Limited considered the potential for extensions of known mineralisation and new discoveries. Drilling programs confirmed substantial mineralisation above the known resource. In

2003, the Panton Intrusion was assessed to contain one of Australia's highest grade and largest tonnage PGE resources with a potential in-ground value of at least A\$2 billion. Platinum Australia Limited proposed a stand-alone operation, initially as an open pit, but with the option of continuing as a long-life underground mine. However, decreasing Pd prices and a strong Australian dollar were detrimental to the feasibility status of the proposed mining operation. More recently with the improvement of PGE prices, the focus of drilling turned to the high-grade mineralised zones. In 2012, Platinum Australia Limited reviewed potential development concepts that proposed combined open pit and underground mining operations that involved the processing of 600 000 t of ore for an annual production of 83 000 ounces of Pt+Pd+Au. This operation assumed a head grade of 5.47 g/t Pt+Pd+Au and a metal recovery of 79% for these three metals. Platinum Australia Limited (2014) developed a new metallurgical process for the recovery of PGEs and Au. The 'Panton Process' consists of two parts: (1) a calcine leach process in which a low-grade flotation concentrate is subjected to low-temperature calcination followed by cyanide leaching at elevated temperatures to dissolve the PGMs, Au, and base metals; and (2) a metals recovery process which recovers the dissolved metals from the leach solution by precipitation, and these metals are further upgraded to a separate high-grade PGE concentrate and base-metal concentrate. Platinum Australia Limited considers the 'Panton Process' to be superior to the traditional smelter route.

After more than half a century of exploration, detailed drilling programs, and feasibility studies, the Panton Intrusion is still regarded as uneconomic (as of October 2014), and mining is unlikely to proceed in the near future. The 'Panton story' is a well-documented case study where such a high-profile PGE project in Australia, despite being thoroughly assessed by many companies and agencies to be technically sound, is still very much dependent on favourable global metal prices, US\$/A\$ exchange rates, and metallurgical characteristics.

Further details describing the exploration of layered mafic-ultramafic intrusions in the HCO can be found in Marston (1979), Hoatson (1993a), Sanders (1999), Hoatson and Blake (2000), and in unpublished open-file reports in the Western Australian Department of Minerals and Energy.

### *Economic significance*

Significant PGE deposit in Australia which contains the largest resource of PGEs (~65.6 t of contained PGE metal) associated with chromitites in Australia. The Panton and Munni Munni (see Deposit Type 1.A) PGE deposits are generally regarded as two of the most important PGE occurrences associated with layered mafic-ultramafic intrusions in Australia.

The discovery of PGE-enriched chromitite layers in the Panton Intrusion had a profound influence on the direction of exploration in the East Kimberley. Mineral exploration companies decided to focus their exploration strategies on finding stratabound chromitite layers in the ultramafic zones of other ultramafic-dominant intrusions. PGE-bearing chromitite layers were subsequently found in the Big Ben, Eastman Bore, Highway, Lamboo, Mini, South Melon Patch, Melon Patch, Mini, West McIntosh, West Panton, and Wilagee intrusions, but all were subeconomic. For many years, exploration companies new to the East Kimberley often duplicated previous exploration programs, and other styles of magmatic or hydrothermal mineralisation at higher stratigraphic levels in the intrusions, or in the country rocks, were rarely evaluated or even considered. Open-file company reports at the Western Australian Department of Minerals and Energy indicate that most mineral exploration companies were searching for large-tonnage stratabound mineralised layers similar to those in the Bushveld Complex of South Africa, such as the Merensky Reef and the UG-2 chromitite layer (Naldrett, 2004, 2011; Cawthorn, 2010).

## Geological setting

The Paleoproterozoic layered mafic-ultramafic intrusions in the HCO of the East Kimberley (Hoatson and Blake, 2000) represent one of the most extensively mineralised igneous associations of their type in Australia (Figure 6.9, Figure 8.21, and Table 6.6). They contain a range of magmatic and hydrothermal deposits of PGEs, Cr, Ni, Cu, Co, Ti, V, Fe, and Au. The intrusions are restricted to the central and western zones of the HCO (Tyler et al., 1995)—a well-exposed north-northeasterly trending orogenic belt of variably deformed and metamorphosed sedimentary, volcanic, and intrusive Paleoproterozoic rocks. The orogen formed initially during the Paleoproterozoic between a postulated Kimberley Craton, underlying the Kimberley Basin to the northwest, and a composite craton involving Archean rocks in the Pine Creek and The Granites-Tanami provinces to the east. Sedimentary and volcanic sequences in Mesoproterozoic, Neoproterozoic, and Paleozoic basins cover much of the composite craton (Tyler et al., 1995). Marked gravity highs along the HCO can be attributed to large mafic intrusions and high-grade (granulite facies) metamorphic rocks, and most intrusions are moderately to highly magnetic.

Hoatson (1993b, 1995, 2000) and Hoatson and Tyler (1993) assigned the layered intrusions of the HCO to seven major groups (designated I–VII) on the basis of rock types, U–Pb geochronology, contact relations with country rocks, metamorphic-structural history, types of mineralisation, trace-element chemistry, and Sm–Nd isotopic composition. The Panton Intrusion is the type example of the ~1855 Ma group I intrusions, and it is coeval with the group II and III intrusions. Intrusions that show no compositional layering and generally form small irregular mafic bodies are also common throughout the HCO. The layered intrusions form folded sheets, shallowly dipping basal bodies, composite multi-chambered bodies, funnel-shaped bodies, steeply plunging plugs, fault-bounded blocks, narrow dyke-like bodies, and screens between granite plutons. Chilled and contaminated margins, contact aureoles, ribbon-like comagmatic satellite intrusions, net-vein complexes (resulting from mingling of mafic and felsic magmas), and feeder conduits indicate that the intrusions crystallised *in situ*, rather than being tectonically emplaced blocks that crystallised elsewhere.

The economically important 1855 Ma group I mafic-ultramafic intrusions have the greatest ratio of ultramafic to mafic rock types in the HCO and they commonly host stratabound PGE-enriched chromitite layers. They are strongly differentiated and deformed folded bodies containing a variety of rock types ranging from primitive olivine-rich cumulates to evolved gabbroic and anorthositic types near the top of the bodies. Most group I intrusions are confined to a northeast-trending narrow corridor (see Figure 8.21) that borders the western flank of the prominent landscape feature of the McIntosh Intrusion (Figure 6.13). The group I intrusions in this corridor include the Panton, West Panton, Highway, Mini, West McIntosh, and South Melon Patch group, which all contain PGE-bearing chromitite layers in the upper parts of the ultramafic zones. The chromitites have been a focus of exploration for several decades. The 2-km-thick Big Ben mafic-ultramafic Intrusion is located on the west side of the Panton Fault, some 15 km south of the Panton Intrusion. Hoatson (1993b) proposed that the Big Ben body is a transposed fault-bounded block that once represented the southern part of the Panton Intrusion.

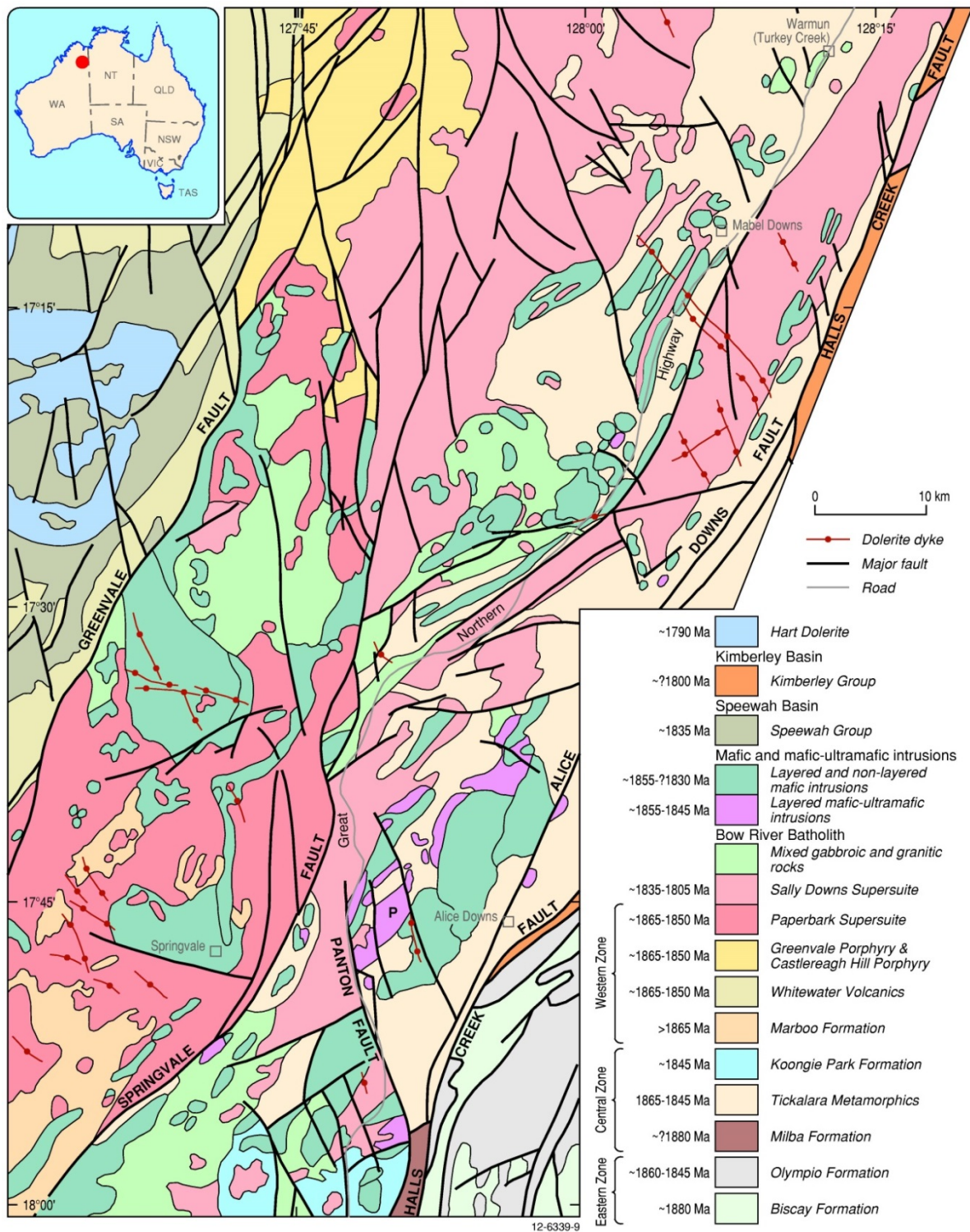


Figure 6.9 Regional geological setting of the Paleoproterozoic mafic and mafic-ultramafic intrusions in the Halls Creek Orogen of the East Kimberley. Names of individual intrusions are shown on Figure 8.19. The Panton mafic-ultramafic Intrusion is indicated by the letter 'P', west of Alice Downs Homestead in the lower central part of the figure. Modified from Hoatson and Blake (2000).

Table 6.6 Major mafic and mafic–ultramafic intrusions in the Halls Creek Orogen, East Kimberleys, Western Australia.

	Intrusion (group <sup>1</sup> )	Extent (km)	Thickness (km)	Form	Country rocks	Major rock types <sup>2</sup>	Mineralisation
1	Faulted (C g)	2 x 4	1.4	Steeply dipping basin	Metasediments, migmatite	BiotGabn, BiotGab, MtGab, HbGab	
2	Turkey Creek (?T M)			?Small lens	Amphibolite, gneiss, migmatite	MGran	Ni, Cu, Co
3	Mabel Downs West (C g)	1.5 x 2.2	?1	?Steeply plunging plug	Granite, gabbro, migmatite	BiotGabn, BiotGab, MtGab, Ton	
4	Mabel Downs Homestead (V)	0.5 x 1	0.5	Steeply dipping sheet	Gabbro (C g), granite, migmatite	OGab, Gab, LGab, An	
5	Mabel Downs Southwest (V)	0.8 x 1.2	1	Steeply dipping sheet	Gabbro (C g), granite, migmatite	MtGab, BiotGab, OGab	Ti, V
6	Nine Mile (C g)	2.5 x 8	?2	Elongate body	Granite, metasediments, migmatite	MtGab, BiotGab, OGab	
7	Norton (T M)	1.5 x 9	1	Steeply dipping elongate body	Metasediments, migmatite, granulite	MGran, HbMGab, HbMtMGab	Ni, Cu, Co, PGEs
8	Frog Hollow (V)	1 x 8	?0.8	Steeply dipping elongate body	Metasediments, migmatite, granite	MtGab, Gab, OGab, LGab, An	Ti, V
9	Foal Creek (II)	1 x 2.2	?1	Dipping sheet	Gabbro (C g), granite	OGab, Gab, Troc, LGab, An	
10	Keller Creek (V)	0.3 x 1.5	0.3	Folded lens	Pelite, migmatite, granulite, granite	OGab, LGab	Ni, Cu, Co
11	Corkwood (V)	0.2 x 2.2	0.2	Steeply dipping sheet	Pelite, marble, migmatite, granulite	MGab, OMGab, OGab, Amph	Ni, Cu, Co
12	Greenvale Fault (C g)	3 x 28	?	Irregular ?sheet	Felsic volcanics, granite	BiotGabn, BiotGab, MtGab, Ton	
13	Savannah (V)	1.5 x 3	1.7	Elliptical sub-chambers/feeders	Metasediments, migmatite, granulite	Du, Troc, OGab, LGab, N, An	Ni, Cu, Co
14	Three Nuns (V)	0.3 x 0.3	?0.2	?Lens	Granulite, metasediments, migmatite	MGab, OMGab, Amph	Ni, Cu, Co

	Intrusion (group <sup>1</sup> )	Extent (km)	Thickness (km)	Form	Country rocks	Major rock types <sup>2</sup>	Mineralisation
15	Oxide (V)	0.3 x 0.3	?0.2	?Lens	Metasediments, migmatite, granulite	MtGab, Gab	Ti, V
16	Fletcher Creek (V)	0.5 x 9	?0.3	Composite lenticular sill	Metasediments, migmatite, marble, granite	OGab, Troc, LGab,	Cu
17	Dave Hill (V)	1 x 3.5	0.8	Steeply dipping folded sheet	Migmatite, granulite, gabbro (T Ck)	OGab, OGabn, Troc, LGab, An, Du	Ni, Cu, Co
18	Amphitheatre (VII)	0.2 x 0.8	0.2	Steeply plunging plug	Gabbro (C g), granite	OGabn, OGab, Troc	
19	Wilson Creek (V)	3 x 6	?2	Steeply plunging plug and irregular lobate body	Gabbro (T Ck), granite, migmatite	OGab, An, Du, OGabn, Troc, LGab	Ni, Cu
30	Spring Creek (V)	4 x 4	2.5	Moderately dipping ovoid body	Gabbro, granite	OGab, OGabn, Troc, LGab, An	Ni, Cu
21	Bulldust Flat (?T M)			Conformable dipping pod	Granulite, metasediments, calc-silicates	MGran, N, MGab	Cu, Ni, Co
22	Cattle Creek (?T M)			Steeply dipping ?pod	Granulite, metasediments, calc-silicates	MGran, N, MGab	Cu, Ni, Co
23	Wills Creek (?T M)			Dipping sills, dykes	Metasediments, paragneiss, amphibolite	Pyrox, Gab, BiotGab, MPyrox, Amph MPer, Amphibole-talc-chlorite dyke	Cu, Ni, Co, PGEs
24	McKenzie Spring (V)	1.2 x 15	?1	Lenticular sill	Metasediments, granite, amphibolite	OGab, MtGab, Troc, An, LGab, Pyrox	Ni, Cu, Co
25	Egg (VII)	0.7 x 1	?0.5	Steeply plunging plug	Granite, gabbro (C g)	Troc, OGab, OGabn, Gab	
26	Toby (III)	12 x 20	?2	Shallow-dipping basin	Granite, gabbro (group II)	BiotGab, OGab, Du, non-cumulates	
27	Sandy Creek (C g)	2 x 14	?1	Irregular dyke	Granite	OGab, BiotGab, MtGab, LGab, An	Cu, Ni, PGEs
28	Wilagee (II)	2 x 10	1.3	Fault-bounded block and sheet	Granite, gabbro (group III)	OGab, Troc, LGab, An, N, Du, Cr	Cr, PGEs, Ni
29	Togo (VI)	1.5 x 3.5	?0.5	Fault-bounded block	Granite, amphibolite, metasediments	Gab, OGab, LGab, An	

	Intrusion (group <sup>1</sup> )	Extent (km)	Thickness (km)	Form	Country rocks	Major rock types <sup>2</sup>	Mineralisation
30	Melon Patch (I)	0.6 x 3	?0.5	Steeply dipping lenses	Metavolcanics, calc-silicate, amphibolite, granite	Du, Amph, Tr-An, Gab, An, N, Cr	Cr, PGEs, Ni
31	White Rock Well West			Small pods, ?sill	Granite	N, Gabn	Cu, Ni, Co
32	Billymac Yard (C g)	1 x 6	?0.5	Moderately dipping dyke	Granite	Gab, MtGab, BiotGab, An, N, Pyrox, Per	Cu, Ni, PGEs
33	Juries (C g)	3 x 4	?1	Folded and faulted sheets	Granite, metasediments	Gab, OGab, BiotGab	Cu
34	Black Hills Yard (VII)	0.4 x 1	?0.3	Plugs and sheets	Gabbro (C g), granite	Troc, OGab, LGab, BiotGab, Lherz	
35	South Melon Patch (I)	2.5 x 5.5	1	Plunging anticline	Granite, amphibolite, metasediments, gabbro (groups IV & VI)	Du, Cr, Ha, Amph, Tr-An, Gab, Gabn, N, LGab, An	Cr, PGEs, Ni
36	Copernicus-Alice Downs (U g)			Layered sill-plunging lens	Metasediments, paragneiss, granodiorite, mafic granulite, calc-silicates, amphibolite	Pyrox, Gab	Ni, Cu, Co, PGEs
37	Paperbark (C g)	1 x 11	?0.5	Irregular dyke	Granite	MtGab, Gab, BiotGab	
38	West McIntosh (I)	0.5 x 8	0.5	Steeply dipping sheet	Metasediments, gabbro (group VI)	Du, Cr, Amph, Tr-An, Gab, Gabn, N, An	Cr, PGEs, Ni, Cu
39	Mini (I)	0.3 x 2.5	0.2	Folded sill	Metasediments, granite	Du, Cr, Amph, Tr-An, Gab, N	Cr, PGEs
40	McIntosh (VI)	6 x 14	7.8	Shallow- to steeply dipping funnel	Gabbro (groups I & IV), calc-silicate, metavolcanic, granite	OGab, OGabn, Troc, MtGab, LGab, Lherz	Ti, V
41	Eileen Bore (U g)			Semi-concordant sills	Metasediments, amphibolite, gneiss	Amph, Pyrox, Per, Hb	Cu, Ni, Co, PGEs, Au
42	Highway (I)	0.3 x 2.2	0.2	Steeply dipping sheet	Metasediments, granite, gabbro (group IV)	Du, Cr, Amph, Tr-An, An, Gab	Cr, PGEs
43	West Panton (I)	0.5 x 1.2	0.5	Steeply dipping sheet	Metasediments, gabbro (group IV)	Du, Cr, Amph, Tr-An, Gab, An	Cr, PGEs

	Intrusion (group <sup>1</sup> )	Extent (km)	Thickness (km)	Form	Country rocks	Major rock types <sup>2</sup>	Mineralisation
44	Springvale (II)	6 x 13	2	Moderately dipping lobes	Granite, metasediments, gabbro (C g)	Gab, OGab, Troc, LGab, An	Cr, PGEs, Cu, Ni
45	Springvale Track (I)	0.2 x 0.6	?0.2	Discontinuous lenses	Amphibolite, metasediments	Du, Tr-An	
46	Panton (I)	2.5 x 10.5	1.6	Plunging syncline	Metasediments, amphibolite, granite	Du, Ha, Cr, Tr-An, Gab, Gabn, N, LGab, An, FGab	Cr, PGEs, Cu, Ni, Au
47	Wild Dog Creek (IV)	6 x 10	?2	Shallow-dipping sheets	Metavolcanics, calc-silicate, granite, gabbro (groups I & VI)	MtGab, BiotGab, OGab, Ton, Amph	
48	West Robin Soak (I)	0.2 x 0.8	?0.1	Discontinuous lenses	Amphibolite, metasediments, granite	Du, Tr-An, Gab	Cr, PGEs, Ni, Cu
49	Panton River (U g)	5 x 8	?2	Fault-bounded ?sheet	Granite, gabbro, metavolcanics	OGab, Gab, LGab	
50	Big Ben (I)	2.5 x 2.5	2	Fault-bounded block	Metavolcanics, gabbro (group IV), granite	Du, Tr-An, An, Gab, LGab, Pyrox	Cr, PGEs, Cu, Ni, Au
51	Margaret River (C g)	1 x 4	?	Irregular dyke	Metasediments, granite	Gab, LGab	
52	Three Sisters (U g)	2 x 10	?1.5	Moderately dipping sheet	Granite, metavolcanics, gabbro	Gab, OGab, LGab, An	
53	Armanda (VI)	1.5 x 2.5	0.7	Moderately dipping sheet	Metavolcanics, metasediments	OGab, OGabn, Gab, LGab, An	

<sup>1</sup> Intrusion group: Groups I to VII as defined by Hoatson (2000); (C g) = Corridor gabbro; (T Ck) = Turkey Creek microgabbro-norite; (T M) = Tickalara Metamorphics; (U g) = Undivided gabbro.

<sup>2</sup> Major rock types are arranged in approximate order of decreasing abundance. Amph = amphibolite; An = anorthosite; BiotGab = biotite gabbro; BiotGabn = biotite gabbro-norite; Cr = chromitite; Du = dunite; FGab = ferrogabbro; Gab = gabbro; Gabn = gabbro-norite; Ha = harzburgite; Hb = hornblende; HbGab = hornblende gabbro; HbMGab = hornblende metagabbro; HbMtMGab = hornblende-magnetite metagabbro; LGab = leucogabbro; Lherz = lherzolite; MGab = metagabbro; MGran = mafic granulite; MPer = metaperidotite; MPyrox = metapyroxenite; MtGab = magnetite-ilmenite gabbro; N = norite; OGab = olivine gabbro; OGabn = olivine gabbro-norite; OMGab = olivine metagabbro; Per = peridotite; Pyrox = pyroxenite; Ton = tonalite; Tr-An = tremolite-anthophyllite peridotite; Troc = troctolite.

### *Mineralisation environment*

The Panton Intrusion (Hamlyn, 1977, 1980; Perring and Vogt, 1991; Hoatson, 2000) is a steep-sided, 1550-m-thick asymmetric syncline, 10.5 km long by 2.5 km wide, that plunges moderately towards the southwest (Figure 6.10 and Figure 6.11). The elongate shape of the body is attributed to tight, upright, northeasterly-trending folding of an original mafic-ultramafic lopolith. Layering on the southeastern limb dips towards the centre of the intrusion at 60–68°. The northwestern limb has steeper to locally overturned dips, and the axial region has inward dips of 30–45°. Ultramafic cumulates have a steeply dipping axial plane cleavage. Parallel north-northwest-trending faults with sinistral strike-slip and vertical displacements cut the intrusion, and the body is truncated in the south by the Panton Fault. A ~50-m-wide contact aureole on the northwestern margin of the intrusion comprises late-crystallising sillimanite overprinting andalusite porphyroblasts of regional metamorphic origin in hornfelsed pelitic migmatite and schist of the Tickalara Metamorphics. The metamorphic grade of the intrusion is middle amphibolite facies.

The well layered differentiated mafic-ultramafic body comprises a lower 650-m-thick Ultramafic Series of contaminated basal contact rocks and ultramafic cumulates, and a stratigraphically overlying 900-m-thick Gabbroic Series of mafic and minor ultramafic cumulates (Hoatson, 2000). The Ultramafic and Gabbroic Series is divided on the basis of the distribution of cumulus olivine and cumulus plagioclase, with the Gabbroic Series further subdivided into Lower, Middle, and Upper Mafic Zones according to different rock types and field relationships. A complete differentiated ultramafic to mafic cumulate sequence, and both the floor and roof rocks of the intrusion are well exposed.

The Ultramafic Series consists of a basal sequence of shallowly dipping dunite and porphyritic harzburgite. The harzburgite is a distinctive unit containing large oikocrysts of orthopyroxene, which is most abundant along the northern margin of the intrusion. Its close spatial association with the margins of the intrusion and its irregular distribution indicate that silica contamination of the primitive magma by felsic country rocks initiated orthopyroxene crystallisation at the expense of olivine. The introduction of hotter, uncontaminated primitive magma into the chamber arrested the crystallisation of orthopyroxene. Most of the Ultramafic Series consists of cyclic units of massive and well-layered medium-grained dunite with minor lherzolite and chromitite more prominent in the upper parts of the series (Perring and Vogt, 1991).

The overlying Gabbroic Series contains a cyclic distribution of rock types that indicate an open-magmatic system where the upper levels of the magma chamber were periodically replenished by new influxes of mafic magma of different composition, and more rarely, by ultramafic magma. Rhythmically layered and laminated gabbro, gabbro-norite, and norite feature in the Lower Mafic Zone, whereas the Middle Mafic Zone consists of melagabbro, gabbro-norite, and chromite-bearing dunite lenses. The Upper Mafic Zone is a composite sequence of foliated ferrogabbro and mottled anorthosite—these are the most fractionated cumulates in the intrusion. Homogeneous schistose biotite granite and schist along the synclinal axis of the southern part of the intrusion are remnants of deformed country rocks that formed the roof of the intrusion. The biotite granite resembles migmatized Rose Bore Granite (Page and Hoatson, 2000: see Age of mineralisation below).

Fine-grained marginal rocks of the Ultramafic Series contain hornblende after clinopyroxene, plagioclase, graphic intergrowths of quartz and feldspar, interstitial quartz, minor apatite, magnetite, chlorite, and trace sulphides. The high quartz content and fractionated Fe-rich compositions of the marginal rocks are considered to be due to alteration by fluid activity and/or SiO<sub>2</sub> contamination from the country rocks. Dominant rocks of the Ultramafic Series are intensely serpentinised ultramafic

cumulates containing only two cumulus minerals—olivine and/or chromite. There is a complete gradation from dunite containing no chromite, to chromite-bearing dunite, to chromitites with no silicate minerals. Adcumulus granular textures are preserved for the dunites as a tight interlocking array of subhedral olivine grains (1 mm–3 mm) surrounded by discontinuous trains of euhedral chromite grains. Chromite also occurs as rare subhedral inclusions in olivine. Olivine locally has well-developed coronas of amphibole, Al spinel, and chlorite. Hamlyn (1975) and Hamlyn and Keays (1979) reported narrow Al-Mg-enrichment and Fe-Cr-Ti-depletion alteration zones along the margins and fractures of chromite grains, and olivine is altered to serpentine minerals, magnetite, hematite, chlorite, iddingsite, calcite, and magnesite. Hamlyn (1980) maintains that olivine ( $\text{Fo}_{81-91}$ ) was stable during middle amphibolites-facies regional metamorphism, and chromite suffered only minor ferritchromite alteration, but the postcumulus minerals were extensively replaced by chlorite, tremolite, and clinozoisite. Cumulus plagioclase is restricted to rare chromite-bearing ultramafics above the 375 m stratigraphic interval. Orthopyroxene forms large (up to 3 cm) oikocrysts in harzburgite near the base of the intrusion and, with clinopyroxene, forms a minor cumulus component in rare lherzolite mesocumulates near the top of the Ultramafic Series (Perring and Vogt 1991). Sulphide-saturated conditions for most ultramafic cumulates are indicated by trace amounts of pentlandite, chalcopyrite, pyrite, and pyrrhotite in veinlets and as small anhedral at grain boundaries of silicates.

The base of the Gabbroic Series marks the introduction of cumulus plagioclase at the expense of cumulus olivine in the intrusion. Medium-grained gabbro, melagabbro, gabbronorite, and minor norite adcumulates in the Lower Mafic Zone and Middle Mafic Zone contain similar cumulus assemblages, but are subdivided on the basis of contrasting layering and outcrop features. Gabbros of these two zones contain subhedral to anhedral tabular plagioclase laths, uralitised clinopyroxene and orthopyroxene, accessory apatite, zircon, granular green spinel, sphene, chromite, and sulphides, and very rare Fe-Ti oxides and primary biotite. Widespread uralitisation and sericitisation, and local tourmalinisation alteration have largely destroyed cumulus textures and primary mineralogy. Hamlyn (1980) described deformational features, such as undulose extinction, bent lamellae twins, local subgrain recrystallisation, and metamorphic schistosity of prismatic amphibole overprinting igneous lamination of aligned plagioclase laths. Mottled textures in anorthosite mesocumulate from the Upper Mafic Zone are defined by large (up to 5 mm) broad plagioclase laths with postcumulus overgrowths enclosed by centimetre-sized intercumulus clinopyroxene grains that are replaced by hornblende, magnetite, tremolite, chlorite, clinozoisite, and epidote. Primary accessory apatite, zircon, and brown biotite are prominent in the middle part of the zone. Foliated ferrogabbro cyclic units from the top of the Upper Mafic Zone contain decussate aggregates of poikilitic hornblende with associated Fe-Ti oxide and sphene anhedral, and fine-grained interstitial plagioclase. Hamlyn (1977, 1980) attributed the calcic compositions of plagioclase ( $\text{An}_{83-100}$ ) in the Gabbroic Series to the metamorphic re-equilibration of this mineral with adjacent hornblende.

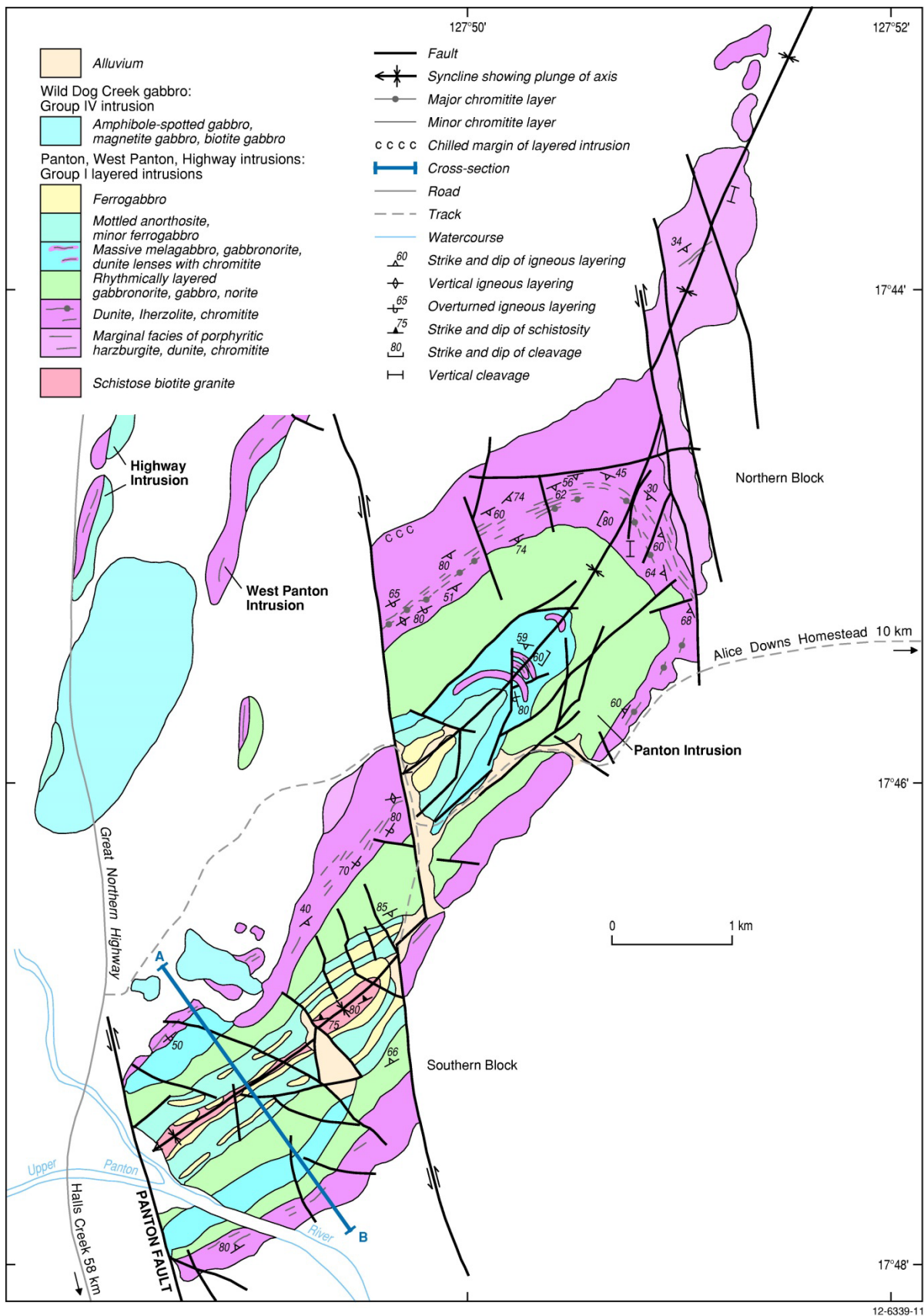


Figure 6.10 Geology of the 1856 Ma (group I) Panton mafic-ultramafic intrusion. Modified from Hoatson (2000).

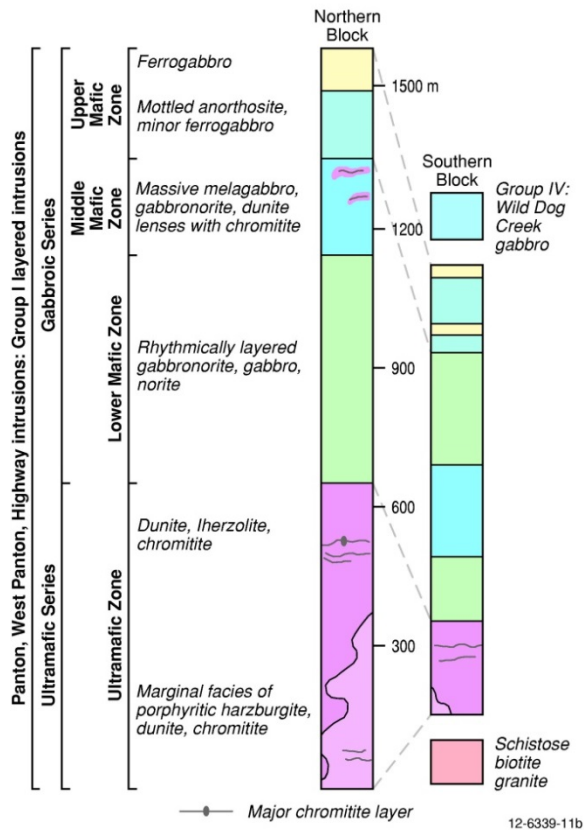
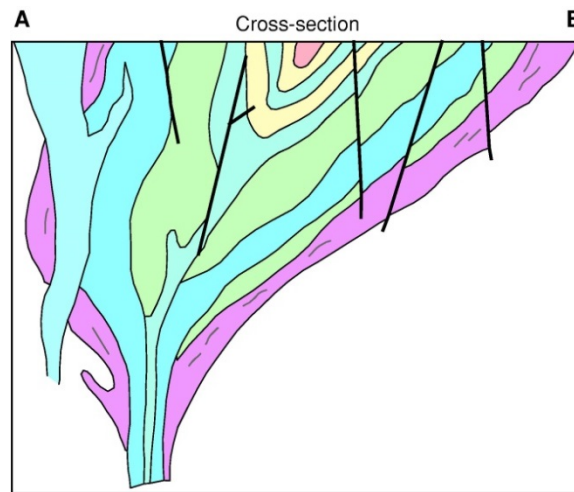


Figure 6.11 Schematic northwest-southeast cross-section A–B of the Southern Block of the Panton mafic-ultramafic intrusion (see Figure 6.10). Stratigraphic columns for the Northern and Southern blocks are also shown. Modified from Hoatson (2000).

## *PGE mineralisation*

Stratabound PGE-bearing chromitite layers (Table 6.7) occur in three major stratigraphic levels in the intrusion (Perring and Vogt, 1991; Helix Resources Limited, 1993a; Hoatson, 2000).

1. **Lower Chromitite Group** ('D- and E-seam chromitites' of Perring and Vogt, 1991). Thin chromitite layers are hosted by harzburgite and dunite in the basal parts of the Ultramafic Series. Chromitite layers in this group rarely attain more than 10 cm in thickness and they occur as discontinuous layers and lenses 600 m to 650 m below the Gabbroic Series–Ultramafic Series contact. Relative to chromitites in the upper part of the Ultramafic Series, these chromitites have a lower average precious metal concentrations ranging from 1215–1500 ppb Pt, 1350–1975 ppb Pd, 80–125 ppb Rh, 250–310 ppb Ru, 76–100 ppb Os, 75–80 ppb Ir, and 50–55 ppb Au.
2. **Middle Chromitite Group** ('A-, B-, and C-seam chromitites' of Perring and Vogt, 1991). This economically important package of PGE-enriched layers, which includes the Main Chromitite Layer (MCL), is hosted by dunite about 120 m to 150 m below the Gabbroic Series–Ultramafic Series contact (Figure 6.12). The MCL can be traced along strike for at least 12 km at a stratigraphic level of ~120 m below the Gabbroic Series–Ultramafic Series contact. The MCL represents the thickest and most PGE-enriched chromitite layer in the intrusion. Average thickness is 80 cm, and average metal endowment is 3175 ppb Pt, 3730 ppb Pd, 70 ppb Rh, 140 ppb Ru, 93 ppb Os, 62 ppb Ir, and 530 ppb Au. The MCL is the most variable layer in terms of morphology, with its thickness ranging from 0.1 m to 2.4 m over short distances. The rapid variations in thickness are attributed to both the magmatic depositional environment and post-magmatic slumping of the layer. Chromitite layers generally do not bifurcate along strike. Changes in the number of chromitite layers that make up the MCL is achieved by one or more layers lensing out, while at the same general stratigraphic position new layers lens in only a few centimetres above or below. Other chromitite layers in the Middle Group display intense magnesite alteration that imparts a distinctive bleached white colour to outcrops. Despite the olivine being totally replaced by magnesite and other carbonates, the cumulus textures of olivine and chromite are still preserved.
3. **Upper Chromitite Group** in the Middle Mafic Zone of the Gabbroic Series. Intensely fractured, locally thickened (up to 30 cm) chromitite layers and lenses occur in a stacked sequence of arcuate dunite lenses in the upper parts of the Middle Mafic Zone approximately 200 m below the roof of the intrusion. The mafic-hosted ultramafic lenses in the Northern Block are truncated by faults and are gently folded around the synclinal axis of the intrusion. The limited strike extent of these chromitites (metres to tens of metres) is attributed to the thin dimensions of the ultramafic-host rocks and faulting. Relative to the other two major groups of chromitites in the Ultramafic Series, these chromitites have lower economic potential because of their restricted strike extent and lower metal concentrations, namely 200 ppb Pt, 68 ppb Pd, 4 ppb Au, 1 ppm Cu, and 925 ppm Ni.

In addition to the three major settings of chromitites described above, many other thin (millimetre to centimetre) chromitite layers, stringers, and lenses occur throughout the intrusion, particularly in the upper stratigraphic levels of the Ultramafic Series.

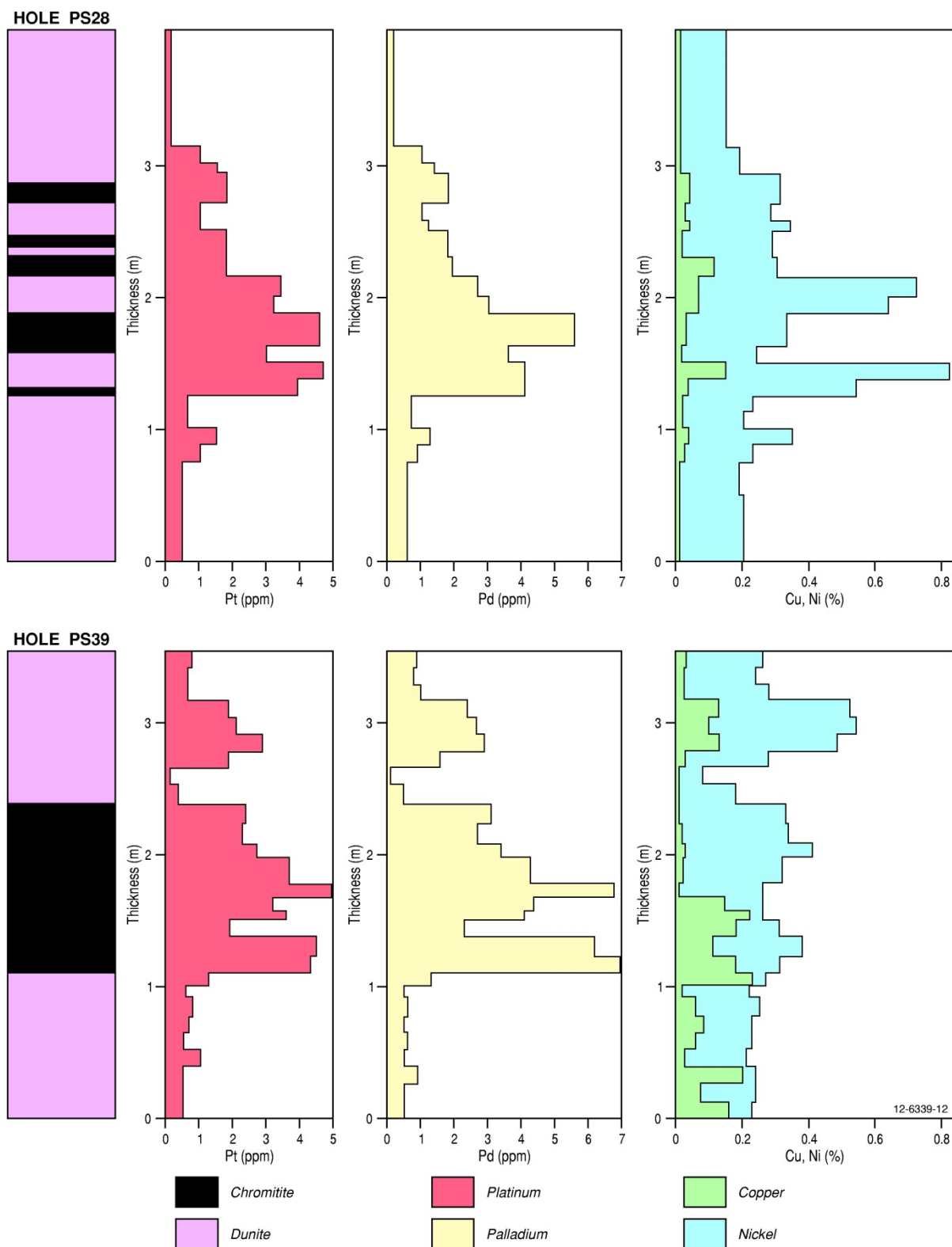


Figure 6.12 Variations in the whole-rock Pt (ppm), Pd (ppm), Cu (%), and Ni (%) concentrations across the Main Chromitite Layer in diamond holes PS28 and PS39, Panton mafic-ultramafic intrusion. Modified from Perring and Vogt (1991).

Table 6.7 Platinum-group-element and gold geochemistry of chromitite layers in the Ultramafic Series of the Panton Intrusion in ppb.

Chromitite layer <sup>1</sup>	Stratigraphic height (m) <sup>2</sup>	Thickness (cm)	Pt	Pd	Rh	Ru	Ir	Os	Au	Pt/Pd	Pd/Ir	(Pt+Pd)/(Ru+Ir+Os)
A	530	80	3175	3730	70	140	62	92	53	0.85	60.2	23.5
B	515	10	2070	1785	82	132	56	66	108	1.16	31.9	15.2
C	500	15	295	440	42	85	30	32	30	0.67	14.7	5
D	40	10	1215	1350	80	250	80	76	50	0.90	16.9	6.3
E	15	10	1500	1975	125	310	75	100	55	0.76	26.3	7.2

<sup>1</sup> Source of data and classification of chromitite layers: Perring and Vogt (1991). Chromitite layers A, B, and C (terminology used by Perring and Vogt, 1991) are equivalent to the Middle Chromitite Group (terminology used in this report), and Chromitite A is equivalent to the Main Chromitite Layer (MCL); and also Chromitite layers D and E are equivalent to the Lower Chromitite Group.

<sup>2</sup> The contact between the Gabbroic Series and the underlying Ultramafic Series is at the 650-m stratigraphic level above the base of the intrusion.

The MCL is a fine- to medium-grained (0.1 mm–2 mm) massive adcumulate, comprising tightly packed fragmented and fractured chromite anhedral in a groundmass of serpentine, carbonate, tremolite, chlorite, and iddingsite. Some chromite grains are embayed and doughnut-shaped. Pyrite, pentlandite, pyrrhotite, chalcopyrite, bornite, and covellite form trace anhedral interstitial grains. Dominant PGMs with the chromite are Pt arsenides (sperrylite), Pd sulphides, tellurides, and bismuthinides. The Cr<sub>2</sub>O<sub>3</sub> concentration is fairly constant across the MCL, which contains 24% Cr<sub>2</sub>O<sub>3</sub>, 0.31% Ni, and 0.06% Cu. Chromitites with a greater abundance of olivine, about 20 m below the MCL, have net textures, comprising disseminated chromite subhedra mantling olivine grains that are replaced by magnesite and lesser serpentine. Chromitites of the Lower Chromitite Group contain fine-grained (0.1 mm–0.3 mm) euhedral chromite grains, with brittle fracturing of grains characterising thin (<0.5 mm) shear zones, and carbonate alteration of olivine is subordinate to serpentinisation. The very low sulphide contents of most chromitites in the Ultramafic Series relative to adjacent sulphide-saturated silicate cumulates may be due to remobilisation of sulphides during intense serpentinisation of Cr-Fe-Mg-rich assemblages. Hamlyn and Keays (1979) attributed olivine's more primitive compositions in chromite-rich peridotite (Fo<sub>84–91</sub>)<sup>20</sup> compared to chromite-poor peridotite (Fo<sub>81–85</sub>) to the postcumulus re-equilibration of olivine with the surrounding magma.

### *Age of mineralisation*

Prior to the mid-1990s, no reliable crystallisation ages of the layered mafic-ultramafic intrusions in the East Kimberley existed, and most of the intrusions were often simply assigned as Paleoproterozoic or Early Proterozoic. Relative ages of the Panton Intrusion can be determined from the contact relationships of the body with its surrounding rocks. For example, the intrusion crosscuts, and hence post-dates, the main structural fabrics in andalusite-muscovite-feldspar-quartz schist country rocks of the ~1880 Ma–1850 Ma Tickalara Metamorphics. In addition, a narrow contact aureole (see Mineralisation environment above), localised *in situ* melting of migmatites, and chilled marginal rocks along the northwestern contact of the Ultramafic Series are indicators of an intrusive contact with rocks of the Tickalara Metamorphics. Hybrid biotite granite and tonalite belonging to the 1835 Ma–1805 Ma Sally Downs supersuite of the Bow River Batholith (Sheppard et al., 1995, 1997), and mafic rocks of the undated Wild Dog Creek gabbro (Hoatson, 2000), intrude dunite units on the northwestern margin of the southern block of the Panton body.

Geochronological studies of the layered mafic-ultramafic intrusions in the HCO (Page et al., 1995; Page and Hoatson, 1997, 2000) endeavoured to determine the crystallisation ages for the more important intrusions, the relative timing of these intrusions and granite plutonism, and possible links between mafic-ultramafic and felsic magmatism and high-grade metamorphism. The SHRIMP U-Pb dating of zircon and baddeleyite was integrated with field relationships, petrology, and geochemistry of the mafic-ultramafic intrusions. Page and Hoatson (2000) determined ages for five major layered mafic-ultramafic intrusions in the HCO, including the Panton, Springvale, Toby, Savannah, and McIntosh bodies.

A direct U-Pb zircon age for the Panton Intrusion was obtained from a fractionated mottled anorthosite in the upper part of the Gabbroic Series near the centre of the Panton intrusion (Figure 6.10). Mottled anorthosites are common fractionated cumulates of groups I and V intrusions (Page et al., 1995; Page and Hoatson, 1997). The mottled texture is defined by centimetre-scale irregular clots of uralitised

---

<sup>20</sup> The Forsterite (Fo) number is a chemical ratio of magnesium (Mg) and ferrous iron (Fe<sup>2+</sup>) that provides an indication of the primitive (or evolved) status of olivine, i.e., a semi-quantitative fractionation index. The higher the Fo content the more primitive is the olivine. The mg number (mg) is a similar chemical ratio (involving Mg, Fe<sup>2+</sup>, Fe<sup>3+</sup>) used in whole-rock geochemical studies.

intercumulus clinopyroxene within partly sericitised cumulus plagioclase. The distinctive suite of zircons from the mottled anorthosite form partly altered, squat, euhedral to subhedral grains. Some zircon grains are moderately zoned; others appear unzoned. All analyses have very high U (2360 ppm–5930 ppm), high Th/U (1.0–3.1) and are highly radiogenic with very large measured  $^{206}\text{Pb}/^{204}\text{Pb}$  (Page and Hoatson, 2000). A weighted mean of  $1856 \pm 2$  Ma for the crystallisation age of the Panton Intrusion is in accord with the age constraints (see below) provided by the older Rose Bore Granite ( $1863 \pm 3$  Ma) and a younger pegmatite dyke ( $\sim 1823$  Ma). The internal coherence and concordance of the data indicate that the measured age is the igneous crystallisation age of the Panton intrusion. An alternative explanation, that all these grains are xenocrysts derived from 1856 Ma felsic rocks underlying the intrusion, cannot be seriously considered, given the morphology and unusual Th/U chemistry (up to 3.1) of the zircons. High Th/U zircons are also characteristic of other mafic-ultramafic intrusions in the East Kimberley (Page and Hoatson, 2000).

Relative ages for the Panton Intrusion are also determined from the dating of the Rose Bore Granite and a muscovite pegmatite dyke (Page et al., 1995; Page and Hoatson, 1997, 2000). The Rose Bore Granite is a strongly gneissic migmatitic granite that crops out in the Upper Panton River near the southern end of the Panton body. The migmatitic granite consists of knots of biotite and muscovite in a matrix of quartz, plagioclase, sillimanite (mostly fibrolite), garnet, with complex small-scale folding and local partial melting adjacent to ultramafic rocks of the Panton Intrusion. Migmatised metasediments of the Tickalara Metamorphics are also associated with the granite in the contact aureole. A U-Pb zircon age of  $1863 \pm 3$  Ma was interpreted for the crystallisation of the Rose Bore Granite, which is a maximum age for the Panton Intrusion and a minimum age for the host paragneisses and schists of the Tickalara Metamorphics (Page and Hoatson, 2000). A muscovite–tourmaline pegmatite dyke, about 50-m-long and 3-m-wide, cuts serpentinitised ultramafic rocks in the southeast of the Panton Intrusion. A U-Pb zircon age of  $1823 \pm 4$  Ma was obtained for the muscovite pegmatite. Although this age cannot be regarded as a particularly accurate crystallisation age for the pegmatite (due to altered zircon having very high U and significant common Pb), it is consistent with the geological relationships of the Panton Intrusion. This pegmatite could well be an apophysis from a nearby granite belonging to the 1835–1805 Ma Sally Downs supersuite of the Bow River Batholith (Sheppard et al., 1995, 1997).

The age of the orthomagmatic PGE-chromite mineralisation in the Panton Intrusion is therefore  $1856 \pm 2$  Ma. Crystallisation U-Pb ages for other near-by intrusions (Page and Hoatson, 1997; 2000), and their contained comagmatic mineralisation, if present, are: Springvale ( $1857 \pm 2$  Ma–zircon); Toby ( $1855 \pm 2$  Ma–zircon); Savannah ( $1844 \pm 3$  Ma–zircon;  $1846 \pm 5$  Ma–baddeleyite); and McIntosh ( $1830 \pm 3$  Ma–zircon).

### *Genesis*

The layered mafic-ultramafic intrusions of the HCO were emplaced into the crust at depths ranging from  $\sim 8$  km to 23 km (2.4 kb–6.7 kb) and there were at least three major periods of emplacement—1855 Ma, 1845 Ma, and 1830 Ma (Hoatson and Blake, 2000). Emplacement of the 1855 Ma intrusions (groups I–III), including the Panton Intrusion, was contemporaneous with granite plutonism (part of the Bow River Batholith) and felsic volcanism (Whitewater Volcanics) during a major magmatic event that represented a large flux of heat into the crust. Most of the layered intrusions can be classified as late orogenic to postorogenic bodies that were emplaced during quieter phases between periods of active tectonism in a complex orogenic belt.

The mafic-ultramafic intrusions were derived from olivine tholeiite and quartz tholeiite parent magmas of basaltic affinity (i.e., relatively fractionated magmas with  $mg = 67$  or less).

Incompatible-trace-element abundances are consistent with compositions ranging from MORB to continental tholeiite. High average S content (520–1570 ppm) in cumulate rocks from most groups of intrusions indicates early sulphide saturation of the parent magmas.

Hoatson (2000) showed that the regional distribution of the major mineralised intrusions (groups I, II, and V) defines two parallel northeast-trending corridors, which can help focus exploration for Cr-PGEs-Ni-Cu±Au (chromite association) and Ni-Cu-Co±PGEs (sulphide association) mineralisation (see Figure 8.21). PGE-bearing chromitite layers similar to that in the Panton Intrusion occur in the Mini, South Melon Patch, Melon Patch, West McIntosh, West Panton, Big Ben, and Highway intrusions (Figure 6.13). Magma mixing, crustal contamination, and the dynamics of magma flow (e.g., fast, slow, turbulent, passive) were significant mineralising processes in the petrogenesis of these intrusions.

Geochemical studies of the Panton Intrusion by Hamlyn et al. (1988), Perring and Vogt (1991), Hoatson (2000), and Sproule et al. (2002a) have provided useful insights into the genesis of the intrusion. Variations in the major oxide profiles throughout the whole intrusion (Hamlyn et al., 1988; Hoatson, 2000) largely reflect gross compositional changes, as defined by the variable proportions of olivine, chromite, and, to a lesser extent, plagioclase in the Ultramafic Series, and plagioclase, clinopyroxene, orthopyroxene, and Fe–Ti oxides in the Gabbroic Series. Fractionated compositions of the basal ultramafic chill rocks (high FeO, MnO, TiO<sub>2</sub>, Al<sub>2</sub>O<sub>3</sub>, Na<sub>2</sub>O, and K<sub>2</sub>O and low mg<sub>32.6–36.5</sub>) relative to the overlying dunites are attributed to rapid cooling and contamination along the basal contact. Mixing between a silica contaminated resident magma, and new pulses of hot primitive magma resulted in chromite saturation and deposition in thin massive layers on the floor of the chamber. Hamlyn et al. (1988) recognised two megacyclic units for the main part of the Ultramafic Series—lowermost unit is delineated by increasing Al<sub>2</sub>O<sub>3</sub> and decreasing Cr, Ir, and Ni abundances to approximately the 400-m level, where rare cumulus plagioclase is present. An abrupt discontinuity at this level defines the base of the second megacyclic unit, above which the highly compatible behaviour of decreasing Cr, Ir, and Ni indicate closed-system fractionation to 950 m. Pronounced fluctuations in Cr, Ir, Pt, and Pd concentrations from 950 m to about 1350 m coincide with more open-system fractionation, involving the reappearance of thin dunite lenses in gabbro-hosted chromitite layers. Marked changes in K<sub>2</sub>O, Na<sub>2</sub>O, Al<sub>2</sub>O<sub>3</sub>, TiO<sub>2</sub>, mg, and increases in most trace-element abundances above 1350 m correlate with fractionated anorthosite and ferrogabbro cyclic units of the Upper Mafic Zone.

Platinum, Pd, Ir, and Au concentrations generally show sympathetic decreasing trends with S throughout the intrusion, and no marked discontinuity at the contact of the Ultramafic Series and Gabbroic Series. High S contents of most ultramafic (300 ppm–1750 ppm) and gabbroic (340 ppm–920 ppm) cumulates testify to sulphide-saturated conditions, which were probably induced by repeated mixing events between the slightly evolved resident magma and influxes of hotter more primitive magma. The small size of the intrusion may have assisted in a relatively steep thermal gradient in the body, and this facilitated in localised magma mixing and oscillating chromite and olivine saturation. In some parts, olivine or just chromite crystallised alone, whilst in others olivine and chromite crystallised alternately or together. Chromitite layers in the Ultramafic Series have markedly different concentrations and ratios of the PGEs and Au. Platinum and Pd show similar enrichment trends in the lower parts of the MCL, whereas Cu and Ni show weak and no correlations, respectively.

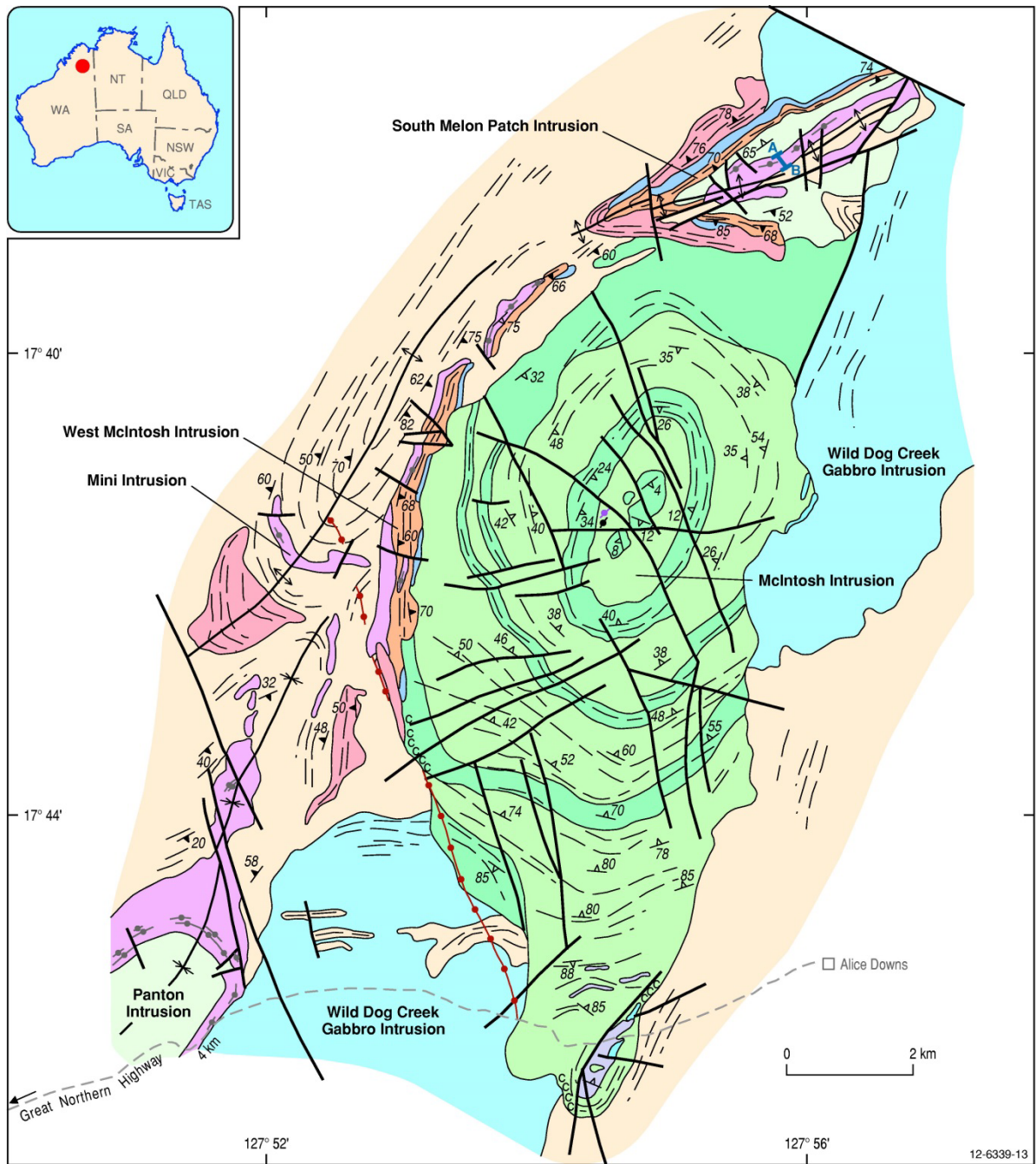


Figure 6.13 Geological setting of the Paleoproterozoic Panton (part of), Mini, West McIntosh, and South Melon Patch mafic-ultramafic intrusions (all group I), Wild Dog Creek (group IV) mafic intrusion, and the large McIntosh mafic intrusion (group VI), Halls Creek Orogen, Western Australia. Modified from Hoatson (2000).

Soil geochemical programs in the intrusion indicate that the most sensitive indicators of PGE-enriched chromitites are Pt and Cr, with elevated Ni/Cu ratios directly above the MCL due to preferential partitioning of Cu into sulphide minerals in the chromitites. Nickel is not a useful indicator, since its broad distribution reflects its association with both sulphides and olivine.

The 2-km-thick Big Ben mafic-ultramafic intrusion (Figure 6.14) is located on the west side of the Panton Fault, some 15 km south of the Panton Intrusion (Hoatson, 1993b). Thunderalla Exploration Limited (2001) defined chromitites up to 2-m-thick in the Big Ben Intrusion with maximum Pt+Pd values of 1.61 g/t. It is the only group I body outside the Cr–PGEs–Ni–Cu±Au metallogenic corridor as defined by Hoatson (1993b; Figure 8.21). Restoration of common rock units (gabbro of the Wild Dog Creek intrusion and granite of the Sally Downs supersuite) across the Panton Fault, and similar mineralogical and chemical features (see below) indicate that the Big Ben Intrusion is probably a transposed fault-bounded block that was originally part of the mineralised Panton Intrusion (Hoatson, 1993b). Sinistral displacement of about 15 km along the Panton Fault accounts for it being outside the metallogenic corridor. ‘Tectonic fragmentation’ of the southwestern end of the Panton Intrusion is also indicated by another smaller transposed mafic–ultramafic block just east of the Panton Fault, about 2.5 km south-southeast of the Panton Intrusion. The high ratio of ultramafic to mafic cumulates in the Big Ben Intrusion (5.5:1) relative to the Panton Intrusion (0.7:1) is attributed to the deeper erosion of the former intrusion caused by upward dip-slip movement along the Panton Fault. The Big Ben and Panton intrusions have similar:

- cumulus assemblages in the ultramafic (cumulus olivine, chromite, and, locally, plagioclase, intercumulus orthopyroxene) and gabbroic (cumulus plagioclase, clinopyroxene, and orthopyroxene) zones;
- coronas of amphibole and Al spinel around embayed olivine;
- unusual calcic compositions (Big Ben—An<sub>89–100</sub>, Panton—An<sub>83–100</sub>) for plagioclase, owing to its re-equilibration with metamorphic hornblende;
- Pt/Pd ratios for chromitites in the ultramafic zones (Big Ben—0.54–0.90, Panton—0.67–1.16); and
- the same estimated depths of emplacement of ~11 km (Trudu and Hoatson, 1996, 2000).

If the Big Ben and Panton intrusions were originally part of the same body, this enhances the prospectivity of the former intrusion, and other mineralised group I intrusions near the Panton Fault.

The Coobina Intrusion (Tyler, 1991; Barnes and Jones, 2013) in the Pilbara region of Western Australia is significant in that it is the only Archean chromitite deposit that has been mined in Australia, and it is a rare example of a Cr-bearing intrusion emplaced into an Archean greenstone belt. Over 200 chromitite pods and lenses have been tectonically disrupted in an Archean dyke-like body that has been intensively serpentinised. Consolidated Minerals Limited has defined a JORC compliant resource (for the Newlands and Wrights deposits) of 1.5 Mt @ 29.4% Cr (as at 30 June, 2011). The chromitites have compositions at the more Cr-rich end of the range observed in layered intrusions worldwide, and Cr contents and Cr/Al ratios are indicative of a parent magma of komatiitic affinity (Barnes and Jones, 2013). The chromitites are consistently Pt and Pd poor, have typical 100-ppb levels of Ru and Ir, and show no systematic relationship to stratigraphy or major element chromite chemistry. The absence of Pt and Pd enrichment implies crystallisation from uniformly sulphide-undersaturated magmas, consistent with evidence for high temperatures of formation. Barnes and Jones (2013) propose that positive Ru anomalies are attributed to incorporation of Ru in the chromite lattice.

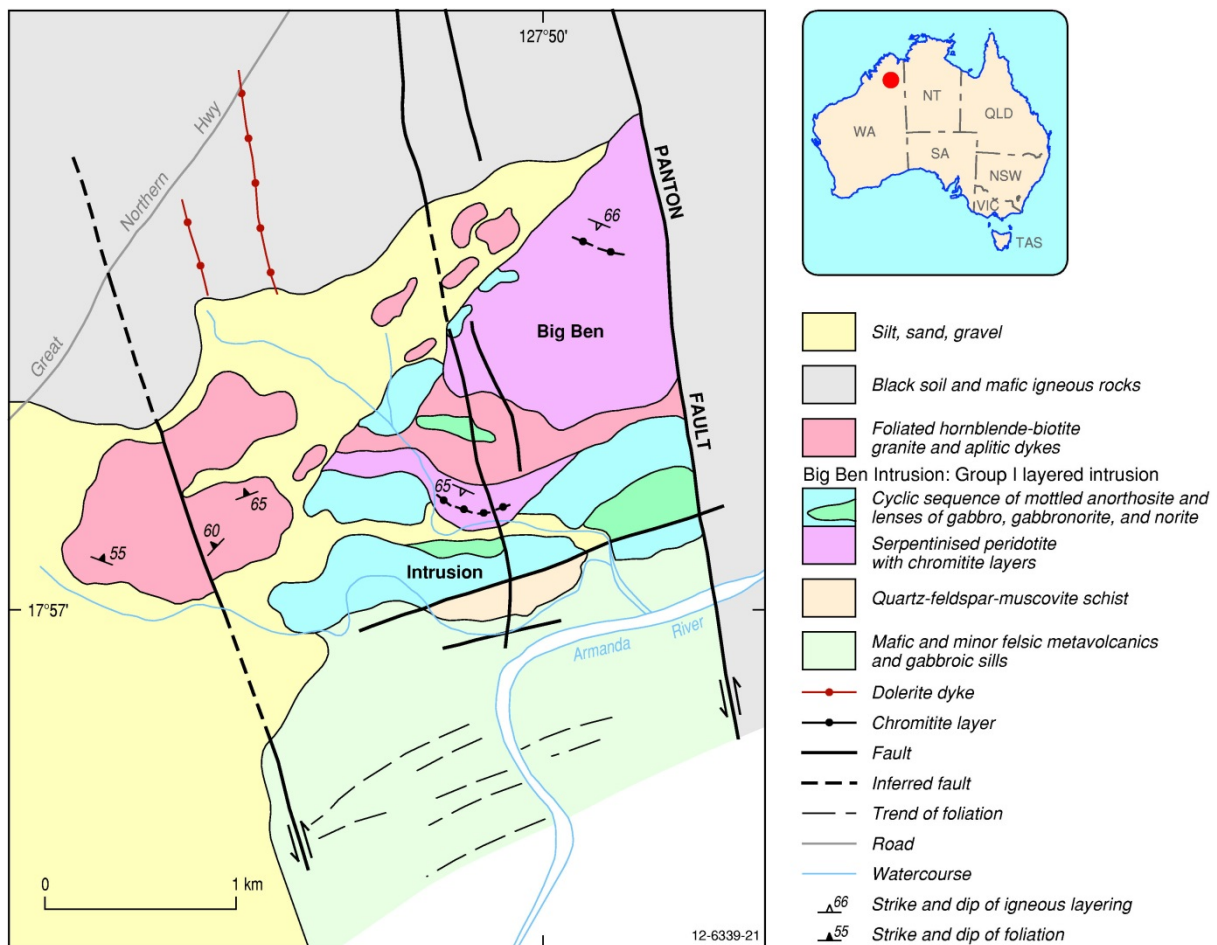


Figure 6.14 Geology of the Paleoproterozoic (group I) Big Ben mafic-ultramafic intrusion, Halls Creek Orogen, Western Australia. Modified from Hoatson (2000).

### Key references

- Hamlyn (1975): geology of Panton sill; stratigraphy; chromite alteration; mineral chemistry; fluid activity; mineralisation.
- Hamlyn (1977): regional mapping; geological setting of Panton and McIntosh intrusions; stratigraphy; layering; structure; petrogenesis.
- Hamlyn and Keays (1979): stratigraphy; spatial distribution of chromitites; mineral chemistry; compositional variation of chromitites; mineralisation; Panton sill.
- Hamlyn (1980): stratigraphy; structure; chromitites; petrogenesis; phase chemistry; modelling.
- Wallace and Hoatson (1990): petrology; whole-rock geochemistry; mineralisation.
- Perring and Vogt (1991): rock types; stratigraphy; chromitites; mineralisation; PGE resource.
- Hoatson (1998): East Kimberley layered mafic-ultramafic intrusions; Panton Intrusion; regional geological setting; stratigraphy; mineralisation; petrogenesis.
- Sproule (1999): regional geology; Panton Intrusion; stratigraphy; whole-rock and mineral chemistry; Re-Os isotopes; geochronology; parent magma; petrogenesis of chromitites.
- Hoatson (2000): East Kimberley layered mafic-ultramafic intrusions; Panton Intrusion; geological maps; field relationships; layering; geochronology; petrology; PGE geochemistry;

whole-rock and mineral chemistry; pressure-temperature evolution of intrusions; Laser Raman study of chromite; isotopes; parent magmas; remote sensing; geophysics; geochronology; petrogenesis; exploration potential.

- Sproule et al. (2002a): geology of Panton Intrusion; stratigraphy; decoupling of Sm-Nd and Re-Os isotopic systems; sulphide-saturated magmas; mineral potential.
- Boudreau and Hoatson (2004): Panton Intrusion; Group I mafic-ultramafic intrusions; mineral chemistry; stratigraphy; mafic rocks; apatite geochemistry; fluid activities; mineralisation; exploration and PGE potential.
- Hoatson et al. (2008a,b): spatial and temporal correlations of Proterozoic mafic-ultramafic intrusions, geology, geochronology, mineralisation.

## **6.4.2 Mineral-System Class 2: Massive to poorly layered tholeiitic mafic-dominant intrusions**

### **6.4.2.1 Deposit Type 2.A: Segregations of Ni-Cu-Co-PGE sulphides in feeder conduits and basal contacts**

#### *Overview*

The discovery of the Voisey's Bay Ni-Cu-Co deposit, Canada (Ryan et al., 1995; Naldrett et al., 1996), in 1993 had a significant impact on exploration philosophies in Australia. Companies changed their exploration focus from komatiitic- and ultramafic-hosted deposits to small- and medium-sized mafic-dominant intrusive bodies in Proterozoic orogenic zones (Halls Creek, Musgrave, Paterson, Albany-Fraser, Litchfield) and Archean cratons (Yilgarn, Pilbara, Gawler). In addition, the Voisey's Bay deposit showed that magmatic Ni-Cu sulphides can occur in anorthosite-troctolite complexes previously regarded as unprospective, and a relatively small intrusion can host a world-class magmatic Ni-Cu-Co sulphide deposit.

Western Australia is relatively well endowed with Type 2.A deposits. Several Precambrian provinces have at least one major deposit that has been mined, or contains significant Ni-Cu-Co-PGE resources. Such examples include Savannah (HCO: Thornett, 1981), Radio Hill, Mount Sholl, Andover (Pilbara Craton: Hoatson et al., 1992), Nebo-Babel (Musgrave Province: Seat et al., 2007, 2009, 2011), Nova-Bollinger (Albany-Fraser Orogen: Smithies et al., 2011), and ?Sandy Creek (Litchfield Province, NT: Eupene Exploration Enterprises, 1989). The host intrusions are typically small- to medium-sized (1-km- to 5-km-thick) mafic-dominant bodies that have had early S saturation (i.e., in the conduit or prior to their emplacement into the chamber). They are generally composed of a thicker mafic sequence of primitive and fractionated gabbroic and anorthositic rocks that overly a thinner ultramafic sequence usually dominated by olivine-rich cumulates. The host rocks to the sulphide mineralisation often form a thin (<50-m thick) marginal 'vener' of gabbroic rocks located along the basal contact region between the country rocks and overlying ultramafic cumulates. Massive and disseminated pyrrhotite-pentlandite-chalcopyrite±pyrite±magnetite assemblages contain low (tens to hundreds of ppb PGEs) to moderate (<0.6 g/t) concentrations of Pt, Pd, and lesser Rh. Very rich Pd-Cu-Au remobilised vein-type ores (e.g., Radio Hill: Hoatson et al., 1992) may traverse the basal contact and country rocks. The massive sulphides are often localised in, or over, structural embayments or depressions in the footwall contact beneath the thickest sequence of cumulates (Radio Hill, Mount Sholl), or in feeder conduits (Babel, Savannah, ?Nova-Bollinger). To attain economic grades, massive sulphides need to be concentrated in depressions or structural embayments of the footwall contact or in feeder conduits. The dynamics of magma flow, e.g., decrease in the velocity of magma flow from

narrow vertical conduits to broad open magma chambers, are also important for the deposition and concentration of the heavy massive sulphides into structural traps.

#### *Australian deposits/prospects/hosts*

Nebo–Babel Intrusion (Musgrave Province, WA); Halleys–Saturn Intrusion (Musgrave Province, WA); Nova deposit (Albany–Fraser Orogen, WA); Radio Hill Intrusion (Pilbara Craton, WA); Savannah Intrusion (HCO, WA); ?Sandy Creek Intrusion (Litchfield Province, NT).

#### *Significant global example(s)*

Voisey's Bay (Canada); Jinchuan (China); Pechenga (Russia); Kabanga (Tanzania); Kotalahti (Finland).

#### *Type example in Australia*

Nebo–Babel Intrusion, Western Australia.

#### *Location*

Longitude 127.7274°E, Latitude -26.09538°S; 1:250 000 map sheet: Cooper (SG 52–10), 1:100 000 map sheet: Cooper (4445); ~25 km south of Jameson and ~125 km west of the South Australia–Northern Territory–Western Australia border junction.

#### *Geological province*

Musgrave Province, Western Australia.

#### *Resources*

Preliminary Resource estimate based on 90 drill-holes is 392 Mt @ 0.3% Ni, 0.33% Cu, 0.18 g/t PGEs (Phaceas, 2007). Approximately 70% of this resource is in the Babel deposit.

#### *Current status and exploration history*

Large undeveloped Ni-Cu-Co-PGE sulphide deposit. The discovery of the Nebo–Babel deposit in 2000 initiated much exploration interest in the Musgrave Province of central Australia. To date it represents the largest Ni sulphide deposit discovered since Voisey's Bay, Canada, in 1993 (Hoatson et al., 2006), and the most significant mafic-hosted Ni sulphide deposit in Australia that also contains PGEs. Nebo–Babel has the largest global resource of PGEs (70.6 t) in Australia, marginally larger than the Panton (65.6 t) and Munni Munni (63.7 t) intrusions. Its PGE inventory also probably exceeds the currently undefined PGE credits in the Nova–Bollinger Ni sulphide deposit that was discovered in 2012, and which has highlighted the prospectivity of the Albany–Fraser Orogen.

Nebo–Babel was a geophysical-geochemical discovery that also utilised mineral-system comparisons with major mafic-intrusive-hosted deposits overseas. Western Mining Corporation Limited (WMC Ltd was purchased by BHP Billiton in 2005) targeted the Musgrave Province in Western Australia in 1995 with the objective of discovering a major greenfields Ni–Cu–PGE sulphide deposit similar to that at Voisey's Bay, Canada (e.g., Naldrett, 1997; Amelin et al., 1999; McKenzie, 2000; Scoates and Mitchell, 2000; Lightfoot et al., 2012; Hiebert et al., 2013). Hoatson et al. (1997) also highlighted the potential of several large 1.08-Ga troctolitic-gabbroic intrusions in the Musgrave Province (Jameson Range, Blackstone Range, Bell Rock Range: Glikson et al., 1996) to host Voisey's Bay-type Ni

sulphide mineralisation<sup>21</sup>. Exploration tenements in the west Musgrave province were acquired in 1996, and in mid-1999, reconnaissance exploration led to the recognition of a coincident geochemical, magnetic, and gravity anomaly. Follow-up geophysical-geochemical programs outlined a significant east–west trending electromagnetic conductor that extended intermittently for more than 5 km: the Nebo–Babel Ni-Cu-Co-PGE sulphide deposit. Lag (siliceous and/or ferruginous stony material forming veneer or pavement on desert land surface) sampling was pivotal to the discovery of the deposit. An area of 1100 km<sup>2</sup> was covered with 1747 deflation lag samples collected on a 1000-m by a 500-m grid. A multi-element geochemical program involving 35 elements (including Pt, Pd, and Au) led to the identification of the Babel deposit. Two lag samples (545 ppm and 566 ppm Ni; 660 ppm and 950 ppm Cu; 11 ppb and 27 ppb Pt) on a median background of 47 ppm Ni and 53 ppm Cu were indicative of weathered Ni-Cu sulphides from among many stronger Ni or Cu and Pt anomalies (Baker and Waugh, 2005; Butt et al., 2006). The Babel deposit is a large low-grade disseminated deposit that locally has sub-crop through thin sand cover. The Nebo deposit lies 2 km to the northeast under a few metres of aeolian dune sand and is smaller, but contains a number of high-grade massive sulphide pods. The lag sampling program was effective where the aeolian cover was shallow (<2 m), however, it was unable to detect the sulphides at Nebo, where the cover is up to 5 m-thick. Two drill-holes targeting geophysical-geochemical anomalies in 2000 intersected 148.9 m of predominantly disseminated mineralisation grading 0.30% Ni, 0.42% Cu, and 0.29 g/t Pt+Pd+Au at Babel, and 26.55 m of massive sulphides grading 2.45% Ni, 1.78% Cu, 0.09% Co, and 0.74 g/t Pt+Pd+Au at Nebo. These drill intersections also highlight the significant by-product potential of the PGEs. Following these results, a major exploration and resource definition-drilling program, including a 200-m spaced grid of 90 diamond-drill-holes, was completed in 2002. More than 11 000 drill-core samples were collected and assayed for the purposes of geological and resource model definition. A preliminary resource of 392 Mt @ 0.30% Ni, 0.33% Cu, and 0.18 g/t PGEs, that comprised ~1.2 Mt contained Ni, ~1.3 Mt contained Cu and Co, and ~70.6 t of PGEs, had an in-ground Ni-Cu-Co value of about A\$25 billion (Phaceas, 2007). A more detailed account of the exploration philosophy, discovery, and exploration program of Nebo–Babel is provided by Baker and Waugh (2005).

### *Economic significance*

Nebo–Babel is the largest Ni sulphide discovery since Voisey's Bay, Canada, and provides an excellent example of greenfields success through conceptual targeting. It contains a world-class resource (>1 Mt of contained Ni metal) of Ni with relatively minor credits of Cu, Co, Pt, and Pd, and lesser Rh and Ru. The relatively low Ni (0.3%), Cu (0.33%), and PGE (0.18 g/t) grades, remote location, lack of basic infrastructure, and impending uncertain times for WMC Ltd (e.g., takeover attempts by Xstrata PLC in 2004 and BHP Billiton in 2005), were factors that led to the uneconomic status of the deposit. However, Nebo–Babel highlighted the economic potential of the Musgrave Province and it is one of the most important examples in Australia of an orthomagmatic Ni-Cu-Co-PGE mineral system in a mafic-dominant intrusion. Several phases of frenetic tenement uptake occurred throughout the Musgrave Province soon after the announcement of promising drill-hole results and its discovery was also responsible for stimulating exploration in other Proterozoic provinces in Australia. Most mining companies exploring mafic intrusions in Australia and elsewhere now often use Voisey's Bay- and Nebo–Babel-type mineralising systems in their exploration strategies (see Chapter 7).

---

<sup>21</sup> The Nebo–Babel deposit is located in a poorly outcropping area near the interpreted southern extension of the Jameson Range Intrusion and northwest of the Cavenagh Range Intrusion (Figure 6.16).

## *Geological setting*

The Musgrave Province (Glikson et al., 1996; Edgoose et al., 2004a,b; Howard et al., 2009; Evins et al., 2010) is an east-west trending, Mesoproterozoic orogenic belt in central Australia (Figure 6.15). Amphibolite and granulite-facies basement gneiss with predominantly igneous protoliths cover vast areas of South Australia, Western Australia, and the Northern Territory. These basement lithologies have been intruded by several generations of mafic-ultramafic and felsic bodies; multiply deformed, and metamorphosed between 1600 million years and 500 million years. The ~1070 Ma Giles Complex (Ballhaus and Glikson, 1995; Glikson et al., 1996) occurs in all three jurisdictions and is part of a more extensive magmatic system called the Warakurna LIP: Wingate et al., 2004; Hoatson et al., 2008a,b; Claoué-Long and Hoatson, 2009a,b), that has more recently been referred to as the Warakurna Supersuite (Evins et al., 2010). The ~1070 Ma Warakurna LIP includes time-equivalent mafic-ultramafic magmatism in a ~2000-km-long east-trending belt across the West Australian Crustal Element and the southern margin of the North Australian Crustal Element. In addition to large mafic-ultramafic bodies that characterise the Giles Complex, various swarms of dolerite dykes traverse the Musgrave Province, Edmund Basin, Collier Basin, Hamersley Basin, and Earraheedy Basin (Hoatson et al., 2008a,b; Claoué-Long and Hoatson, 2009a,b). The relatively short duration of magmatism in the Warakurna LIP between 1078 and 1070 million years and the large areal extent of the magmatism across central and western Australia have been used as evidence for mantle plume activity (Wingate et al., 2004; Morris and Pirajno, 2005). The Giles Complex consists of a suite of layered mafic-ultramafic intrusions, mafic and felsic dykes, and temporally associated with volcanic rocks and granites. In the Musgrave Province it forms an easterly-trending belt about 85 km-wide, stretching from the Bedford Range in Western Australia to the eastern end of the Musgrave Province in South Australia. Minor exposure of the Giles Complex is known in the southwestern corner of the Northern Territory (Edgoose et al., 2004a,b). The Giles Event, encompassing the Giles Complex, has been divided into at least eight mafic and felsic magmatic events by Evins et al. (2010). They suggested that all this magmatism occurred at relatively shallow crustal levels within a long-lived, failed intracontinental rift called the Ngaanyatjarra Rift. The extended time period (at least ~50 million years) of magmatism and deformation during the Giles Event precludes a single mantle plume as its sole cause. Evins et al. (2010) proposed that the Giles Event may be the result of a long-lived thermal anomaly underlying the Musgrave Province since the beginning of the 1220 Ma–1120 Ma Musgrave Orogeny. Several crustal-scale fault zones (Cavenagh Fault, Mt West Fault, Lasseter Shear Zone, etc) may have played an important role for the emplacement of the magmas during the Giles Event (i.e., a dynamic crustal-scale magma pathways). Many of these faults show changing kinematics during the Giles Event.

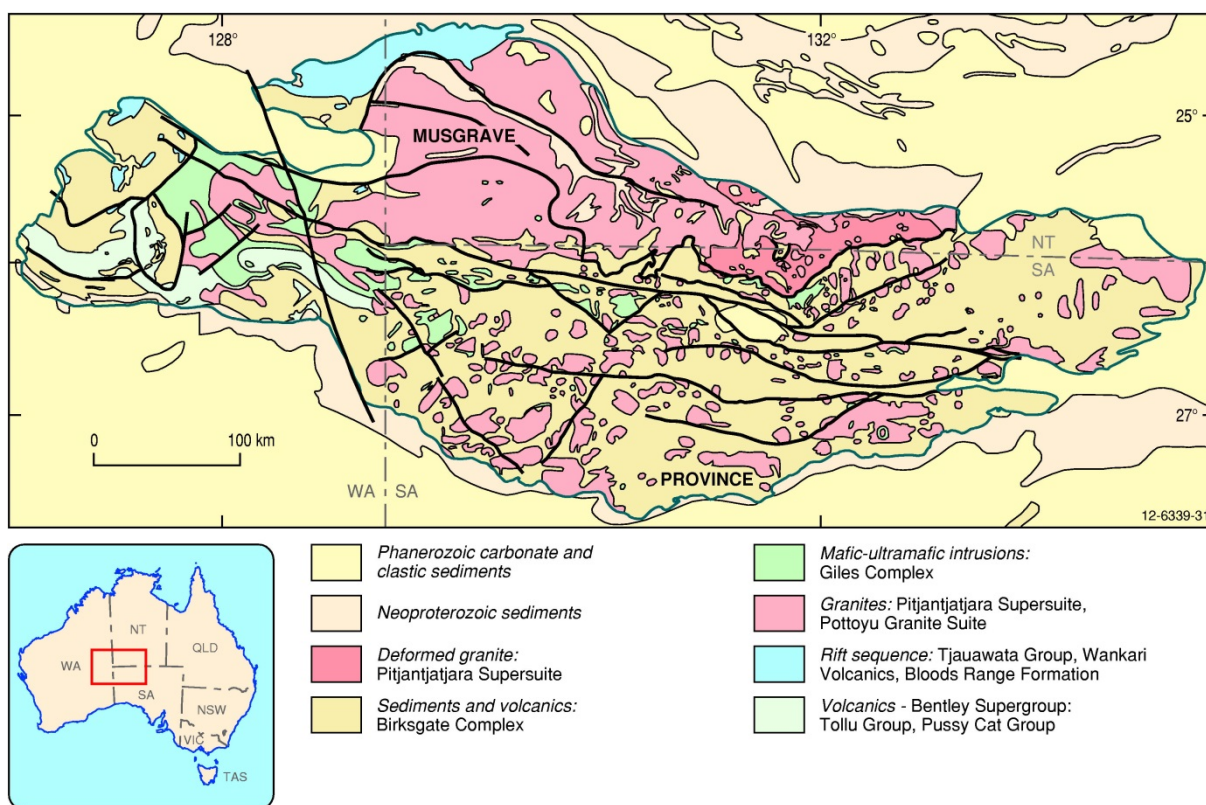


Figure 6.15 Generalised geology of the Musgrave Province, central Australia. The Mesoproterozoic mafic-ultramafic intrusions of the Giles Complex are shown in green. Modified from Glikson et al. (1995, 1996).

Over twenty major intrusions and numerous smaller bodies of layered cumulates have been defined in the Musgrave Province (Ballhaus and Glikson, 1995; Glikson et al., 1996). Ultramafic bodies dominate in the northeast, whereas tholeiitic gabbroic bodies dominate in the centre, and troctolitic variants are common in the western most part of the province (Figure 6.16). Igneous layering ranges from large-scale cyclic units, through rhythmic layering, intercumulus layering and cryptic layering. The intrusions are interpreted to have crystallised at crustal depths between 15 km and 30 km and are generally undeformed and unmetamorphosed. The bodies display a trend to increasing fractionated composition from east to west, inferring progressive shallower crustal levels of emplacement. In addition to Nebo–Babel, several other mineral systems have been identified with the Giles layered mafic-ultramafic intrusions (DMITRE, 2014). These include disseminated and massive primary sulphides in the Tomkinson and Mann Ranges believed to be associated with late-stage dolerite dykes of the Giles Complex intrusions. Rare chromitite seams up to 1.5 cm-thick are found within alternating layers of pyroxenite and olivine gabbro in the Tomkinson Ranges and in the Wingellina Hills. Substantial deposits of V-bearing titaniferous magnetite sometimes enriched with PGEs (see next Deposit Type 2.B) are found in the upper parts of the Jameson Range Intrusion in Western Australia. The mineralisation occurs as magmatic segregations in layers up to 5 m-thick over strike lengths of tens of kilometres. In South Australia, Fe-Ti-V oxide mineralisation is hosted by anorthosite in the Kalka Intrusion. Grades of up to 1.28%  $V_2O_5$  and 10%  $TiO_2$  are recorded. Similarly, anorthosite in the Caroline Intrusion has grades of 0.54%  $V_2O_5$  rising to 0.7%  $V_2O_5$  in lateritised equivalents. Secondary enrichment during Cenozoic weathering processes has resulted in the formation of large Ni laterite deposits over deeply weathered olivine-rich ultramafic rocks in the Claude Hills and Tomkinson Ranges. In the 1960s Southwestern Mining Limited outlined a resource at Wingellina Hills in the

Tomkinson Ranges, Western Australia of 61 Mt @ 1.32% Ni. Government investigations in the late 1960s delineated a Ni laterite deposit in the Claude Hills area containing 4.57 Mt @ 1.5% Ni. The Halleys Ni-Cu-PGE prospect on the southwestern margin of the Saturn body in the Blackstone region of Western Australia has geological similarities to Nebo–Babel. Disseminated sulphides with significant Cu-PGE grades (>0.1% Cu and 200 ppb PGE) are hosted by a zoned, ovoid-shaped pipe.

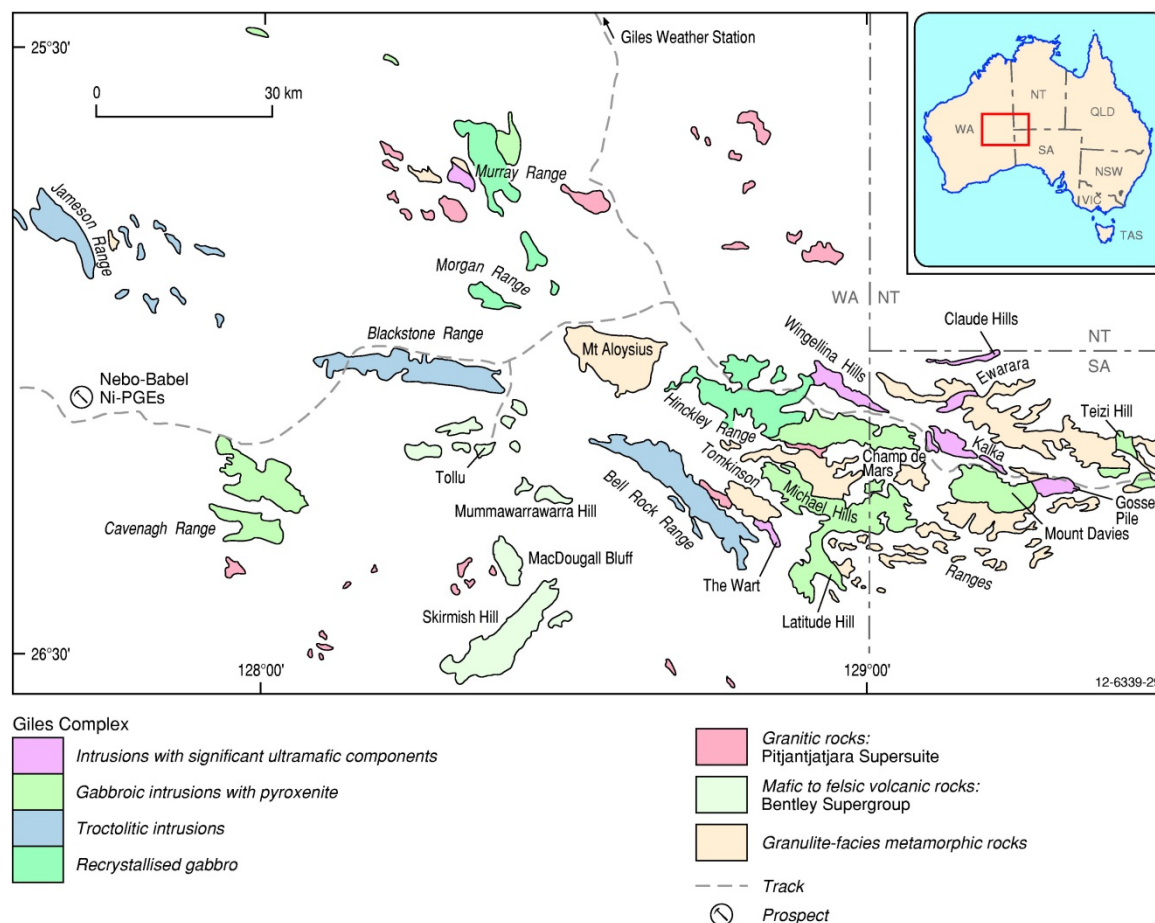


Figure 6.16 Geological setting of the major mafic-ultramafic intrusions of the Giles Complex in the Tomkinson Ranges–Blackstone Range–Jameson Range region, western Musgrave Province, central Australia. The Nebo–Babel Ni-Cu-PGE deposit is located south of the Jameson Range in the western part of the figure. Modified from Glikson et al. (1995, 1996).

The Geological Survey of South Australia has documented the following features that highlight the potential for magmatic Ni-Cu-PGE deposits in the Giles Complex (DMITRE, 2014).

- The Giles Complex (~1070 Ma) is an extensive voluminous mafic-ultramafic intrusive sequence that is scattered over an area of some 2500 km<sup>2</sup>.
- The layered mafic-ultramafic bodies experienced a multiple metamorphic-deformational history.
- The E-W-trending Mann–Hinckley Fault and pre-existing N- to NNE-trending deep basement structures are crustal scale-fractures that were active around the time of the emplacement of the Giles Complex and could potentially have been the corridor that allowed for the emplacement of Ni-Cu-bearing upper-mantle magmas.

- The interaction of later stage olivine-dolerite dykes/sills with earlier peridotite, gabbro, and troctolite has the potential to form Voisey's Bay style Ni-Cu mineralisation.
- The Giles Complex exhibits a series of vertically stacked magma chambers and associated feeder dykes that could potentially act as traps for immiscible Ni-Cu sulphides.
- The emplacement of the melts coincided with an extensional period during granulite facies metamorphism.

Maier et al. (2013) and the Geological Survey of Western Australia have provided the following thoughts on the prospectivity of the Giles Complex and the larger region encompassing the Musgrave Province. Large magmatic events dominated by mafic-ultramafic magmas, like the ~1070 Ma Giles Complex, result in enhanced heat flux into the crust, triggering crustal melting, devolatilisation, and large-scale fluid flow. Deposit types favoured by such regimes include magmatic PGE-Cr-Fe deposits in large layered intrusions, Ni-Cu sulphide ores formed through assimilation of S-rich strata in magma feeder conduits or at the base of layered intrusions, and hydrothermal deposits of variable style, notably in the roof and side walls of the largest intrusions. Pirajno et al. (2006) made comparisons between the Giles Event and the Bushveld Complex of South Africa. Both are associated in space and time with bimodal volcanic rocks which, in the case of the Bushveld Complex, are well endowed with a wide range of hydrothermal ore deposits, ranging from greisen-style deposits, breccia pipes with Sn-W, to epithermal and mesothermal lode-Au and Fe oxide-Cu-Au (IOCG) deposits. The Musgrave region also has a high potential for such deposits, as highlighted by the discovery of Cu-Au vein-style mineralisation in the felsic volcanic rocks of the Tollu Group, to the north of the Cavenagh Range.

### *Mineralisation environment*

The following descriptions of the Nebo–Babel Intrusion are largely from Seat (2008), Seat et al. (2007, 2009, 2011), and Godel et al. (2011). The Nebo and Babel prospects, which are part of the same mineralising system, are off-set ~1.5 km from each other by the north-south trending Jameson Fault (Figure 6.17). The two mafic-hosted deposits have almost identical morphology and marginal intrusive units, but differ significantly in their mineralisation styles. Mineralised zones are confined to the top of a conduit and comprise net-textured magmatic sulphides at Babel and massive sulphide lenses that host most of the mineralisation at Nebo. Massive sulphides (Nebo) and disseminated sulphides (Babel) occur in a concentrically zoned, olivine-free gabbro-norite tube-like (chonolithic) feeder conduit that intruded sulphide-free granulite facies granitic gneiss and mafic country rocks (Figure 6.18). The dominant country rock is the granitic gneiss which comprises K-feldspar, plagioclase, and quartz forming ~80% of the rock; the remainder is amphibole, biotite, oxides, apatite, and trace orthopyroxene. The conduit extends for 5 km and has a cross-section size of 0.5 km by 1 km. It has a gentle west-southwest plunge of less than 10° and dips to the south at ~15°. The tube-like intrusion was emplaced in felsic orthogneiss that has ages ranging from 1260 Ma to 1140 Ma. Seat and co-authors noted that this basement has whole-rock S abundances of less than 100 ppm which, in their view, precludes basement rocks as a possible S contaminant for the precipitation of Ni-Cu sulphides.

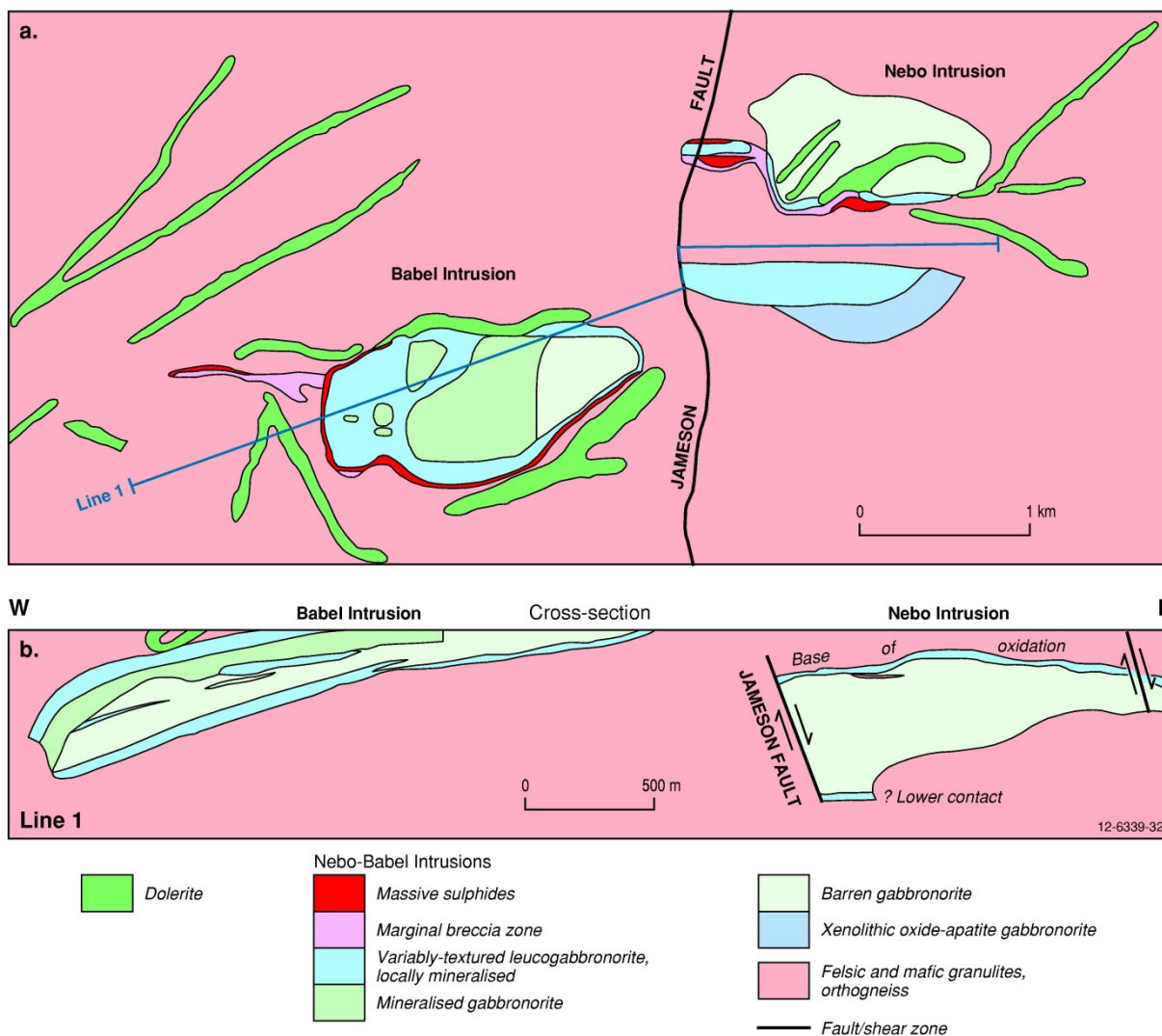


Figure 6.17 Geology of the 1068 Ma Nebo–Babel Intrusion, Musgrave Province, central Australia. (a). Surface projection of the gabbronorite units, mineralised domains, and major structural elements. Modified from Seat et al. (2007). (b). Longitudinal east–west cross-section (Line 1) through the Nebo and Babel components of the intrusion. Modified from Seat et al. (2007).

Geological and geochemical studies have shown that the Nebo–Babel is a composite body consisting of chemically related, but temporally distinct magma pulses. The initial magma pulses, which were the most primitive and the most contaminated, formed the marginal units of the conduit. The later pulses were emplaced into the core of the conduit. The chilled margin rocks (7%–9% MgO) contain sulphide globules. Igneous mineralogy, fabrics and textures of the intrusive have been well preserved and allow the recognition of the lithostratigraphy which includes Variably-textured LeucoGabbroNorite (VLGN) that forms an outer shell around Mineralised GabbroNorite (MGN), with Barren GabbroNorite (BGN) and Oxide-Apatite GabbroNorite (OAGN) in the middle and lower parts of the conolith. The mineralised gabbronorite rocks have a uniform grain size (5 mm–20 mm), with major minerals being plagioclase (55%–65%), orthopyroxene (15%–25%), and clinopyroxene (5%–10%). Minor minerals include ilmenite, magnetite, biotite, and apatite. Dominant sulphides include monoclinic pyrrhotite, pentlandite, chalcopyrite, and pyrite, with trace sulphides represented by bravoite, sphalerite, galena, tellurides, and altaite (lead telluride). Oxide-apatite-bearing gabbronorite features at the eastern end of

the Nebo body. Breccias contain abundant country-rock xenoliths, chilled margin fragments, and VLGN and sulphide xenoliths in a massive sulphide or chill matrix. The chilled margin rocks consist of fine-grained ferro-gabbronorite. Mineral and whole-rock geochemistry indicate that the mafic units become progressively more evolved in the order: VLGN, MGN, BGN, and OAGN, and that incompatible trace-element concentrations increase downwards within the MGN and BGN. Major- and trace-element compositional trends throughout the mafic stratigraphy are controlled by the relative proportions of cumulus plagioclase, pyroxene, and trapped silicate liquid.

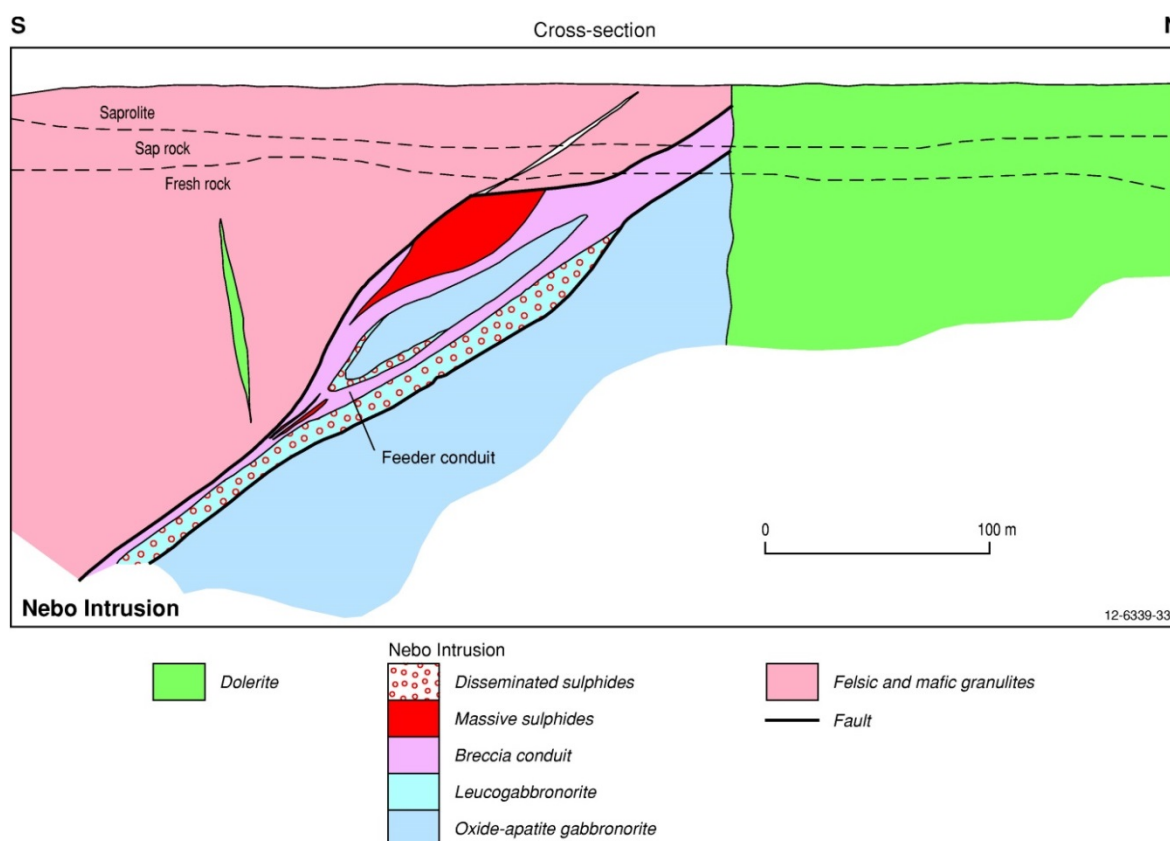


Figure 6.18 Schematic north-south cross-section of the Nebo component of the Nebo-Babel Intrusion highlighting the rock types and mineralisation features of the moderately plunging feeder conduit. The relative positions of the sulphide ores, e.g., massive sulphide body adjacent to the hanging wall contact, indicate the conduit is probably overturned. Modified from Seat et al. (2007).

The Ni-Cu-PGE mineralisation, which is confined to the early, more primitive units (VLGN and MGN), occurs as massive sulphide breccias and stringers and as disseminated gabbronorite-hosted sulphides mainly in the upper parts of the intrusion. The metal tenors of the sulphides are mostly 5% to 6% and 2% to 8% Cu (Cu/Ni ratio around unity) and up to several ppm Pt and Pd each (Seat et al., 2009). Sulphur isotopic data reveal a remarkably narrow range of  $\delta^{34}\text{S}$  values from 0.0‰ to +0.8‰.

### PGE mineralisation

Seat (2008) and Seat et al. (2009) compared the PGE geochemistry of disseminated and massive sulphides (Table 6.8). Combined PGE contents of disseminated sulphides range from 103 ppb and 448 ppb with Pt and Pd predominating. Two massive sulphide samples from Babel were significantly different geochemically to the disseminated sulphide sample. Total PGE contents (excluding Os) for

the massive sulphides are 798 ppb and 628 ppb, and Ni/PGE ratios are very high (60 000 to 116 000) relative to the disseminated sulphides (7300 to 24 000). These differences, and the fact that the massive sulphides have significantly higher relative Ru, Os, and Ir abundances indicate either a different source for the massive sulphides or, that the massive sulphide component underwent sulphide-melt fractionation (Barnes and Maier, 1999). Seat (2008) suggests many of the PGMs are tellurides hosted by silicate minerals rather than sulphides. Preliminary scanning electron microscope studies identified moncheite (PtTe<sub>2</sub>), merenskyite (PdTe<sub>2</sub>), michenerite (PdBiTi), and melonite (NiTe<sub>2</sub>) where significant Pd substitutes for Ni. The PGMs typically form small anhedral grains (1 µm to 4 µm; rarely up to 10 µm across) in pyroxene, plagioclase, pyrrhotite, K-feldspar, and quartz. All of the Nebo–Babel rock units are slightly PGE depleted with Cu/Pd ratios higher than primitive mantle, indicating early saturation and segregation of a sulphide and/or PGE removal. Rocks with trace cumulus sulphides have the lowest Cu/Zr and highest Cu/Pd ratios and the most fractionated metal patterns, indicating that these units have undergone the highest degrees of Ni, Cu, and PGE depletion. The chalcophile metal depletion in these units has occurred prior to the final emplacement of the Nebo–Babel Intrusion. The massive sulphides were emplaced late into the intrusive sequence, have different PGE chemistry and Cu tenor to the disseminated sulphides, and have undergone sulphide fractionation. The fractional crystallisation of the sulphide liquid produced a cumulate of monosulphide solution relatively enriched in Os, Ir, and Ru, and depleted in Pt, Pd, and Au.

Table 6.8 Precious metal geochemistry of mineralised samples from Nebo–Babel.

Sample	Style	Unit	Ni%	Cu%	S%	Pt ppb	Pd ppb	Rh ppb	Ir ppb	Ru ppb	Au ppb
1018–113	Chilled	Margin	0.02	0.03	0.14	16	17	0.90	0.62	0.80	7.70
1031–062	Chilled	Margin	0.04	0.03	0.22	19	20	1.45	0.72	1.18	7.06
1031–026	Mass	Mass S	7.26	0.25	32.10	23	150	122	96	238	10
1092–010	Dissem	MGN	0.64	0.20	4.14	97	147	8	4	8	43
1018–061	Dissem	VLGN	0.36	0.33	2.31	242	197	16	11	22	91
31–004	Dissem	VLGN	0.33	0.40	2.22	88	112	4	3	6	95
70–004	Dissem	Troctolite	0.17	0.19	1.13	45	48	3	2	5	41
1031–006	Blebby	FGMGN	0.63	0.94	5.70	63	60	2	2	3	33
1031–016	Blebby	FGMGN	0.60	0.69	4.13	163	350	4	2	3	141
31–012	OAGN	OAGN	0.10	0.12	1.30	35	20	0.72	0.53	0.99	10.23

Mass—Massive; Dissem—Disseminated; FGMGN—Fine-Grained Mineralised Gabbro-norite; MGN—Mineralised Gabbro-norite; VLGN—Variably-Textured Leucogabbro-norite; OAGN—Oxide-Apatite Gabbro-norite.  
Source: Seat (2008) and Seat et al. (2009).

### Age of mineralisation

More than 400 euhedral zircon crystals from two barren gabbro-norite samples from Babel (sample 1018–097) and Nebo (70–019) were used by Seat (2008) and Seat et al. (2011) to determine the crystallisation age the Nebo–Babel Intrusion. A U–Pb zircon crystallisation age of  $1068.0 \pm 4.3$  Ma was obtained by combining the individual <sup>207</sup>Pb/<sup>206</sup>Pb ages of the Babel ( $1071.7 \pm 4.7$  Ma) and Nebo ( $1063.7 \pm 8.7$  Ma) bodies. The emplacement of Nebo–Babel at  $1068.0 \pm 4.3$  Ma indicates it was part of the ~1070 Ma Giles Complex, an important component of the Warakurna LIP—a major Mesoproterozoic magmatic event that impacted on central and western Australia (Wingate et al., 2004).

## Genesis

The distribution of disseminated sulphides, which are primary magmatic in origin, is related to chonolith geometry and magma flow regimes, rather than to gravitational settling. Sulphur-bearing country rocks are absent in the Nebo–Babel deposit area, and thus, local crustal S addition was unlikely to have been the major mechanism in achieving sulphide immiscibility. The Nebo–Babel intrusion is part of an originally continuous magma chonolith that formed from multiple and related magma pulses. The parental magma was a medium- to low-K tholeiite containing 8% to 9% MgO. The enormous amount of magmatism in the Musgrave Province coupled with static geodynamics requires an enormous amount of upper-mantle melting. Godel et al. (2011) suggest that the Nebo–Babel parent magma represents 5%–10% partial melting. Seat et al. (2007) showed the initial magma pulse (VLGN: see description of mineralisation environment above), the most primitive and sulphide saturated, was emplaced along a linear weakness in the country rock, i.e., a shear zone or a fault, more or less parallel to the regional foliation. After crystallisation of VLGN, marginally more fractionated, sulphide-saturated magma was injected through the thermally insulated core of the conduit, forming the MGN. Massive sulphides in the MGN underwent fractional crystallisation of the sulphide liquid. This process can produce an Fe-rich olivine cumulate with Os, Ir, Ru and a Cu-rich liquid, enriched in Au, Ag, Pt, and Pd. Sulphide globules in chilled margins indicate that sulphide segregation was an early process in the parental magma and, as such, it may have occurred prior to its intrusion. Furthermore, widespread distribution of trace amounts of sulphide blebs indicates that the entire magmatic system must have been sulphide-saturated. Successive pulse(s) of more fractionated magma (BGN) were emplaced in the core of the intrusion. After magma flow ceased, closed-system crystal fractionation produced consistent mineral and chemical fractionation trends within BGN and OAGN. After crystallisation, the Nebo–Babel body was intruded by dyke suites, overturned, and then off-set by the Jameson Fault resulting in the apparent 'reverse' chemical and mineral trends observed.

Geochemical modelling by Godel et al. (2011) showed that the Nebo–Babel Intrusion and its associated Ni-Cu-PGE sulphide mineralisation formed in the crust between the low- and high-Ti basalts and may have originated from mixing between these two magma types. This observation is strengthened by the modelling of the S concentrations at sulphide saturation—the assimilation of country-rock orthogneiss by the mixed magma caused a drop in S solubility, which led to sulphide saturation in the early stages of the mixing and/or assimilation, and potentially to the formation of the Nebo–Babel deposit. Seat (2008) and Seat et al. (2009) indicated that  $\delta^{34}\text{S}$  values for the massive and disseminated sulphides range from 0.0‰ to 0.8‰ (average of  $0.4\text{‰} \pm 0.2\text{‰}$ ) and are consistent with the S being of mantle origin and similar to other magmatic mineralising systems, e.g., Voisey's Bay and Jinchuan (Pirajno and Hoatson, 2012). Noticeable is the remarkable difference in  $\delta^{34}\text{S}$  values compared to sulphides from the Noril'sk deposits in Russia, where the S was probably derived from country rocks (evaporites). Sulphide saturation at Nebo–Babel did not occur *in situ* and is inferred to have been triggered by assimilation of felsic orthogneiss, perhaps in the parental magma chamber. The initial magma pulse with entrained sulphides into the chamber formed the marginal units of the Nebo–Babel Intrusion. Some of the entrained sulphides accumulated within physical traps on the way into the conduit and/or at exit from the chamber. These sulphides were later emplaced along the footwall contact as massive and/or marginal fragment-laden sulphide liquid. Distribution of the disseminated sulphides was influenced by the conduit geometry and magma flow dynamics. The final and volumetrically dominant barrel-magma pulse underwent crystal fractionation and oxide precipitation in the core of the Nebo–Babel Intrusion, which in turn caused sulphide saturation and formed trace PGE-depleted sulphides in these units. Calculated metal concentrations of the parental magma by Godel et al. (2011) from which the Ni-Cu-PGE mineralisation formed are: 165 ppm Ni,

150 ppm Cu, 3.40 ppb Pt, 3.30 ppb Pd, 0.15 ppb Ir, 0.30 ppb Ru, and 0.22 ppb Rh. These metal concentrations are similar to those for low-Ti basalt compositions after they experienced a small amount (<0.001%) of sulphide segregation prior to their final emplacement.

Seat et al. (2011) showed that emplacement of Nebo–Babel occurred at about 10 km to 12 km-depth. All of the Nebo–Babel units can be related by crystal fractionation of the parental tholeiitic magma. Mineral  $\delta^{18}\text{O}$  values are of typical mantle values and preclude large-scale crustal contamination of the parental magma with anything other than material with similar values. Although even the least contaminated intrusive units have negative Nb anomalies and enriched  $^{87}\text{Sr}/^{86}\text{Sr}$  initial ratios compared to bulk earth at the time, the crustal assimilation must have been significantly less than 10% based on mantle-like  $\delta^{18}\text{O}$  values and  $^{143}\text{Nd}/^{144}\text{Nd}$  ratios. Trace-element geochemical studies by Seat et al. (2011) indicate that primitive Nebo–Babel melts equilibrated with spinel-facies mantle implying shallow melting beneath a lithosphere less than 80 km-thick.

Seat (2008) notes that the Nebo–Babel Intrusion has several features in common with other Ni-Cu-PGE deposits hosted in dynamic magma conduits (e.g., Voisey's Bay), such as multiple magma pulses and sulphide entrainment from depth rather than *in situ* sulphide segregation. The major difference between Nebo–Babel and other non-komatiitic magmatic Ni-Cu-PGE deposits is there is no evidence to support external S addition in Nebo–Babel, rather sulphide saturation was primarily triggered by silica addition through crustal assimilation.

In contrast to the findings of Seat (2008), Maier et al. (2014) propose that there is compositional and lithological evidence for country rock contamination at Nebo–Babel, and the fact that the basement contains lithologies that may have provided juvenile S to the magma, indicates that addition of external S to the magma remains a possibility. External addition of juvenile volcanic rocks would be consistent with the relatively high Cu/Pd and Cu/Ni ratios (due to addition of crustal Cu) and high Au/Pd ratios (due to addition of crustal Au) at Nebo–Babel. Maier et al. (2014) also point out that some samples of chilled margin (Godel et al., 2011) have ~1000 ppm S, 10 ppb to 20 ppb Pt and Pd each (i.e., levels similar to fertile basaltic magmas) suggesting some of the initial magmas intruded in a sulphide-undersaturated state.

The genetic implications and the economic potential of swarms of tholeiitic dolerite dykes and sills (Figure 6.19) that traverse the Musgrave Province, Edmund Basin, Collier Basin, Hamersley Basin, and Earraheedy Basin (Hoatson et al., 2008a,b; Claoué-Long and Hoatson, 2009a,b) and any possible comagmatic extrusive components (e.g., flood basalts) should also be investigated for PGE-Ni-Cu mineralisation.

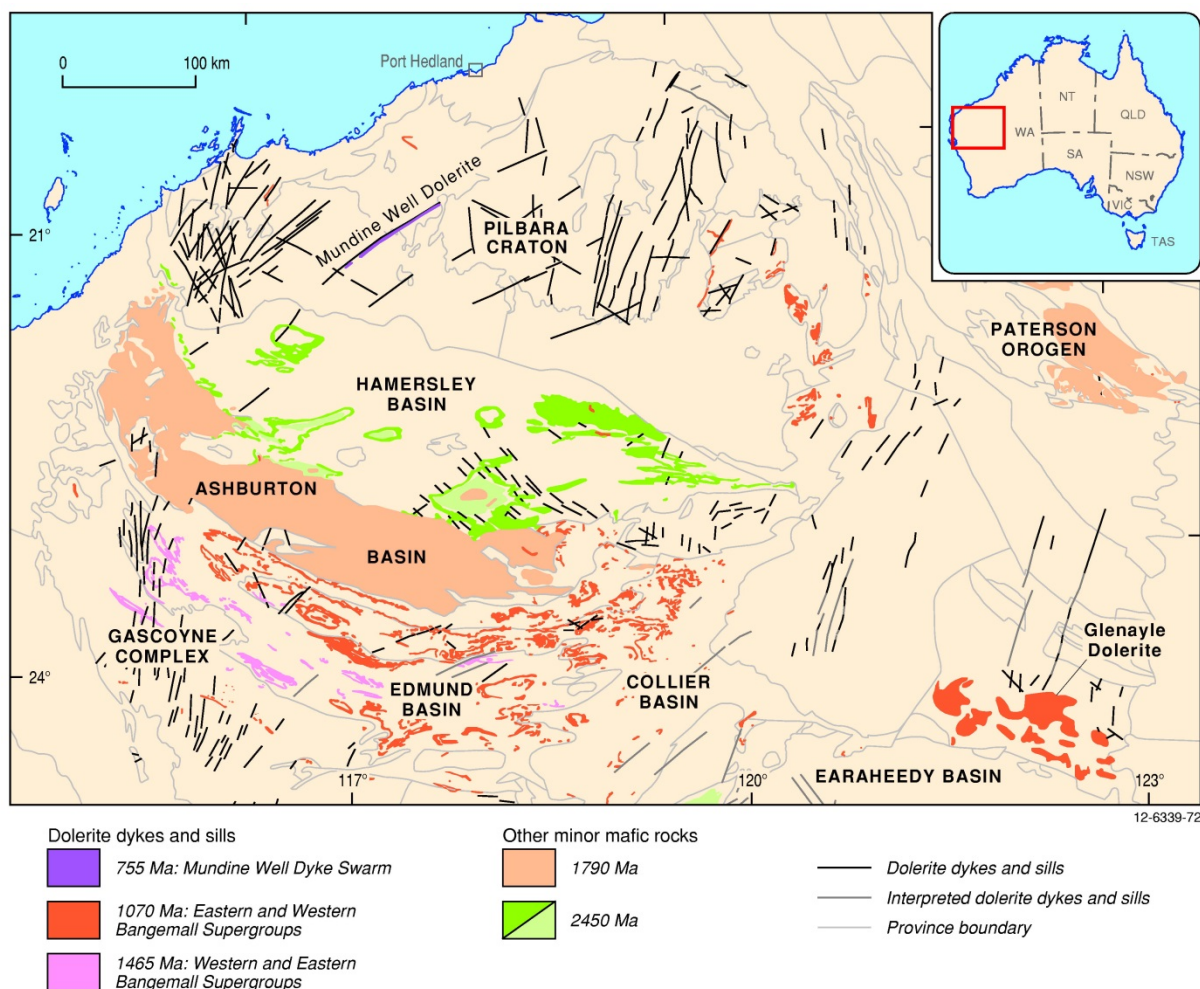


Figure 6.19 Proterozoic mafic dyke swarms, sills, and intrusions in various sedimentary basins of central Western Australia. The ~1070 Ma Warakurna LIP encompasses the ~1070 Ma Eastern and Western Bangemall Supergroup of dolerite dykes and sills prominent in the Edmund and Collier basins and the ~1070 Ma Glenayle Dolerite located further east. The distribution and age relationships of mafic rocks are derived from Hoatson et al. (2008a,b) and references within.

### Key references

- Glikson (1995): regional geology; geochronology; petrology and geochemistry; stratigraphy; Giles mafic-ultramafic complex.
- Glikson et al. (1996): geochronology, stratigraphy, petrology, and geochemistry of Giles mafic-ultramafic intrusions, genesis, economic potential.
- Hoatson et al. (1997): comparisons of the Sally Malay Intrusion to Voisey's Bay and Nebo–Babel-type deposits; geological setting; feeder zone; genesis.
- Close et al. (2003a): compilation of geochronological data for northwestern Musgrave Block.
- Baker and Waugh (2005): exploration history; targeted Musgrave Province; geochemical-geophysical program; electromagnetic anomalies, geochemical lag discovery; drill intersections of disseminated and massive sulphides.
- Hoatson et al. (2006): classification of intrusion; Nebo–Babel geological setting; resources.

- Seat et al. (2007): geology; structure; stratigraphy; petrology; sulphides; geochemistry; architecture and emplacement of intrusion.
- Seat (2008): geology; petrology; mineral and whole-rock chemistry; stable and radiogenic isotope systematics; Ni-Cu-PGE mineralisation of the Nebo–Babel intrusion.
- Howard et al. (2009): geochronology and geochemistry; Alcurra Suite in west Musgraves; potential for orthomagmatic Ni-Cu-PGE mineralisation; Giles Event.
- Seat et al. (2009): S assimilation; PGE distribution and geochemical trends; S saturation of magmas; mineralisation; genesis.
- Evins et al. (2010): new geochronology and geological mapping; definition of eight mafic and felsic magmatic pulses; redefining Giles Event; Ngaanyatjarra Rift; genesis of west Musgrave Province.
- Seat et al. (2011): U/Pb zircon geochronology; whole-rock and mineral chemistry; and O-Sr-Nd isotope compositions.
- Godel et al. (2011): parental magma composition; magma mixing; geochronology and geochemistry of dykes; geochemical modelling; genesis; exploration potential.
- Joly et al. (2013): analysed the mineral potential of the west Musgrave Province; several commodities investigated including PGEs, Ni, and Cu; used a knowledge driven mineral-systems approach; exploration potential.
- Maier et al. (2014a,b): tectonomagmatic events of the Musgrave Province; Giles Complex, geochronology and geochemistry of intrusions; mineral prospectivity.

#### **6.4.2.2 Deposit Type 2.B: Stratabound PGE-bearing magnetite layers**

##### *Overview*

Concentrations of V-bearing titanomagnetite and ilmenite occur widely and almost exclusively throughout the Archean and Proterozoic of western and central Australia, notably in the Archean Yilgarn, Pilbara, and Gawler cratons and in the Proterozoic Musgrave Province and HCO. The oxide-rich layers have been explored for Ti and V, however, from analogies with overseas deposits (Stella Intrusion and Bushveld Complex in South Africa: Maier et al., 2003), such layers can be enriched in PGEs. Typical grades for magnetite layers in Australian deposits are 0.4% to 1.3% V<sub>2</sub>O<sub>5</sub>, 2% to 20% TiO<sub>2</sub>, 100 ppb to 600 ppb Pt+Pd+Au, and 0.2% Cu (Hoatson, 1984). The magnetite takes the form of disseminated grains and as magnetite layers commonly at the base of magmatic cycles in the upper parts of large differentiated gabbroic-anorthositic intrusions. The most mineralised magnetite layers are often not the lowest member in the mafic stratigraphy. Principal ore minerals include titanomagnetite and V-bearing magnetite, with associated minerals being ilmenite, hematite, spinel, and sulphide minerals (pyrite, pyrrhotite, chalcopyrite). The Fe- and Ti-oxide phases form by crystal settling or filter pressing during crystallisation of the gabbroic magmas, resulting in laterally persistent layers and segregations. Daniels (1974), Baxter (1978), Hoatson (1984), Glikson et al. (1996), Hoatson (2000), and Hoatson and Stewart (2001) have described Ti-V occurrences at Barrambie, Bremer Range, Buddadoo, Coates, Gabanintha, Tallanalla Gabbro, Windimurra, Yarrabubba (Yilgarn Craton, WA); Andover, Balla Balla (Pilbara Craton, WA); Frog Hollow, Mabel Downs Southwest, McIntosh, Oxide (HCO, WA); Speewah Central (Kimberley Basin, WA); Bell Rock, Blackstone Range, Caroline, Jameson Range—Haran—Canaan—Zen, Kalka (Musgrave Province, WA); and Attutra Metagabbro—Casper—Coco (Arunta Orogen, NT). Cyclic magnetite layers hosted by gabbro and anorthosite in the large Windimurra Igneous Complex have had an intermittent history of mining. With the exception of the Haran group of prospects in the Jameson Intrusion, Casper

Prospect–Attutra, and the Speewah Central deposits that are associated with the Hart Dolerite near the margins of the Kimberley Basin, very few of the magnetite deposits listed above have published data of associated PGE concentrations.

#### *Australian deposits/prospects/hosts*

Haran, Canaan, Zen, Manchego (prospects in Jameson Intrusion, Musgrave Province, WA); Casper–Coco (prospects in Attutra Metagabbro Intrusion, Aileron Province, NT); Speewah Central (Kimberley Basin, WA).

#### *Significant global example(s)*

Stella Intrusion, Bushveld Intrusion (both South Africa); Rio Jacaré Intrusion, (Brazil); Rincon del Tigre Complex (Bolivia); Duluth Intrusion (USA); Coldwell Complex (Canada); Skaergaard Intrusion (Greenland); Panzihua (China).

#### *Type example in Australia*

Haran, Western Australia.

#### *Location*

Longitude 127.5287°E, Latitude -25.7173°S; 1:250 000 map sheet: Scott (SG 52–06), 1:100 000 map sheet: Finlayson (4446); ~110 km east-northeast of Warburton.

#### *Geological province*

Musgrave Province, Western Australia.

#### *Resources*

Unknown.

#### *Current status and exploration history*

Prospect.

#### *Economic significance*

Unusual deposit in the Musgrave Province that highlighted the potential of PGE-enriched Fe-Ti-V oxides in the upper parts of fractionated mafic-dominant layered intrusions. Another similar PGE-oxide deposit called the Jamieson Prospect (see Appendix K) is located ~10 km southeast of Haran (Longitude 127.57361 E, Latitude -25.79778 S). The uneconomic Stella Intrusion in South Africa (Maier et al., 2003) is generally considered the global type example of this mineralising system.

#### *Geological setting*

The Musgrave Province (Glikson et al., 1996; Edgoose et al., 2004a,b; Howard et al., 2009; Evins et al., 2010) is an east-west trending, Mesoproterozoic orogenic belt in central Australia (Figure 6.15). Amphibolite and granulite-facies basement gneiss with predominantly igneous protoliths cover vast areas of South Australia, Western Australia, and the Northern Territory. These basement lithologies have been intruded by several generations of mafic-ultramafic and felsic bodies; multiply deformed, and metamorphosed between 1600 million years and 500 million years. The ~1070 Ma Giles Complex (Ballhaus and Glikson, 1995; Glikson et al., 1996) occurs in all three jurisdictions and is part of a more extensive magmatic system called the Warakurna LIP (Wingate et al., 2004; Hoatson et al., 2008a,b;

Claoué-Long and Hoatson, 2009a,b), that has more recently been referred to as the Warakurna Supersuite (Evins et al., 2010). The ~1070 Ma Warakurna LIP includes time-equivalent mafic-ultramafic magmatism in a ~1500-km-long east-trending belt across the West Australian Crustal Element and the southern margin of the North Australian Crustal Element. In addition to large mafic-ultramafic bodies that characterise the Giles Complex, various swarms of tholeiitic dolerite dykes and sills (Figure 6.19) traverse the Musgrave Province, Edmund Basin, Collier Basin, Hamersley Basin, and Earraheedy Basin (Hoatson et al., 2008a,b; Claoué-Long and Hoatson, 2009a,b). The geochemistry and Ni-Cu-PGE potential of the mafic dykes and sills in these basins have been preliminary assessed by Morris and Pirajno (2005). The relatively short duration of magmatism in the Warakurna LIP between 1078 and 1070 million years and the large areal extent of the magmatism across central and western Australia have been used as evidence for mantle plume activity (Wingate et al., 2004; Morris and Pirajno, 2005).

The Giles Complex consists of a suite of layered mafic-ultramafic intrusions, mafic and felsic dykes, and temporally associated with volcanic rocks and granites. In the Musgrave Province it forms an easterly-trending belt about 85 km-wide, stretching from the Bedford Range in Western Australia to the eastern end of the Musgrave Province in South Australia. Minor exposure of the Giles Complex is known in the southwestern corner of the Northern Territory (Edgoose et al., 2004a,b). The Giles Event, encompassing the Giles Complex, has been divided into at least eight mafic and felsic magmatic events by Evins et al. (2010). They suggested that all this magmatism occurred at relatively shallow crustal levels within a long-lived, failed intracontinental rift called the Ngaanyatjarra Rift. The extended time period (at least ~50 million years) of magmatism and deformation during the Giles Event precludes a single mantle plume as its sole cause. Evins et al. (2010) proposed that the Giles Event may be the result of a long-lived thermal anomaly underlying the Musgrave Province since the beginning of the 1220 Ma–1120 Ma Musgrave Orogeny.

Over twenty major intrusions and numerous smaller bodies of layered cumulates have been defined in the Musgrave Province (Ballhaus and Glikson, 1995; Glikson et al., 1996). Ultramafic bodies dominate in the northeast, whereas tholeiitic gabbroic bodies dominate in the centre, and troctolitic variants are common in the western most part of the province (Figure 6.16). Igneous layering ranges from large-scale cyclic units, through rhythmic layering, intercumulus layering and cryptic layering. The intrusions are interpreted to have crystallised at crustal depths between 15 km and 30 km and are generally undeformed and unmetamorphosed. The bodies display a trend to increasing fractionated composition from east to west, inferring a progressively shallower crustal level of emplacement. In addition to Nebo–Babel, several other mineral systems have been identified in close association with the Giles layered mafic-ultramafic intrusions (DMITRE, 2014). These include disseminated and massive primary sulphides in the Tomkinson and Mann Ranges believed to be associated with late-stage dolerite dykes of the Giles Complex intrusions. Rare chromitite seams up to 1.5 cm-thick are found within alternating layers of pyroxenite and olivine gabbro in the Tomkinson Ranges and in the Wingellina Hills. Substantial deposits of V-bearing titaniferous magnetite sometimes enriched with PGEs (see next Deposit Type 2.B) are found in the upper parts of the Jameson Range Intrusion in Western Australia. The mineralisation occurs as magmatic segregations in layers up to 5 m-thick over strike lengths of tens of kilometres. In South Australia, Fe-Ti-V oxide mineralisation is hosted by anorthosite in the Kalka Intrusion. Grades of up to 1.28%  $V_2O_5$  and 10%  $TiO_2$  are recorded. Similarly, anorthosite in the Caroline Intrusion has grades of 0.54%  $V_2O_5$  rising to 0.7%  $V_2O_5$  in lateritised equivalents. Secondary enrichment during Cenozoic weathering processes has resulted in the formation of large Ni laterite deposits over deeply weathered olivine-rich ultramafic rocks in the Claude Hills and Tomkinson Ranges. In the 1960s Southwestern Mining Limited outlined a resource at

Wingellina Hills in the Tomkinson Ranges, Western Australia of 61 Mt @ 1.32% Ni. Government investigations in the late 1960s delineated a Ni laterite deposit in the Claude Hills area containing 4.57 Mt @ 1.5% Ni. The Halleys Ni-Cu-PGE prospect on the southwestern margin of the Saturn body in the Blackstone region of Western Australia has geological similarities to Nebo–Babel. Disseminated sulphides with significant Cu-PGE grades (>0.1% Cu and 200 ppb PGE) are hosted by a zoned, ovoid-shaped pipe.

### *Mineralisation environment*

Anomalous concentrations of PGEs are associated with magnetite bands interlayered with gabbro and anorthositic gabbro in the Jameson Range intrusion. The Jameson Range Intrusion is composed of approximately 2500 m of layered Fe-rich troctolite, gabbroic troctolite, and anorthosite adcumulates, with the more fractionated mafic rocks containing concentrations of disseminated and massive magnetite (Gliksun et al., 1996). Daniels (1974) estimated the intrusion to be up to 4500 m-thick, and he divided the stratigraphy into four zones. Zone 1 at the base, about 460 m-thick and characterised by glomeroporphyritic gabbro; Zone 2, up to 320 m-thick, consists of kaersutite<sup>22</sup> lherzolite and gabbroic rocks with titaniferous magnetite bands, the gabbro rocks contain anorthite, kaersutite, olivine, orthopyroxene, and clinopyroxene with various amounts of titaniferous magnetite; Zone 3, about 760 m-thick and characterised by rhythmically layered troctolite units; Zone 4, up to 3000 m-thick, is a layered sequence of hypersthene troctolite, troctolite, olivine gabbro, and hypersthene gabbro, with titaniferous magnetite bands. Zone 2 in the northeast of the Range contains 20% to 50% of opaques (probably all titanomagnetite) in the ultramafic-mafic layers, with the V<sub>2</sub>O<sub>5</sub> tenor estimated at about 1.4%. Zone 4, located in the southwest, has at its base a band of titaniferous magnetite, which has been traced along strike for about 19 km. At one locality this band reaches a thickness of 15 m. Analyses of samples from this band yield an average of 0.9% V<sub>2</sub>O<sub>5</sub> and 23.4% TiO<sub>2</sub> (table 35, in Daniels, 1974). Zone 4 has more titaniferous magnetite layers towards the upper parts of the sequence, where one of these bands can be traced intermittently for 37 km, with thicknesses of up to 60 m at an average of 0.79% V<sub>2</sub>O<sub>5</sub>. Daniels (1974) also noted compositional variations of V, Ti, Fe, Cr, and P with stratigraphic height. The higher magnetite bands have lower V, Ti, and higher Fe, Cr and P, which he attributed to the more advanced fractionation of the evolving magmatic liquids.

### *PGE mineralisation*

The Haran Ti-V-PGE prospect is a PGE-bearing massive Fe-Ti oxide layer associated with anorthosite, anorthositic gabbro, gabbro, and troctolite in the Jameson Range Intrusion (Figure 6.20). The polymetallic character of the mineralisation is indicated by an average drill-hole intersection of 2.8 m @ 20% TiO<sub>2</sub>, 0.8% V<sub>2</sub>O<sub>5</sub>, 50% Fe<sub>2</sub>O<sub>3</sub>, 0.6 g/t Pt+Pd+Au, and 0.2% Cu. The Jameson Range Intrusion contains a stacked sequence of magnetite layers with the main PGE-enriched layer—the Haran Band—trending northwest-southeast over tens of kilometres. Other magnetite layers that have moderate dips toward the southwest occur stratigraphically above and below the Haran Band. The Jamieson Prospect, located about 10 km southeast of the Haran prospect, has a similar geological setting to the Haran deposit. A titaniferous magnetite rock layer that extends over 10 km in strike length has returned rock-chip sample analyses of 0.1 g/t to 2.1 g/t Pt+Pd+Au. The average combined grade is 1.3 g/t with the Pt component comprising 0.96 g/t. The average V and Ti composition was reported to be 1.18% V<sub>2</sub>O<sub>5</sub> and 23.2% TiO<sub>2</sub> and the Fe content of the rock averages 44% Fe with 442 ppm Cu and 280 ppm Ni.

<sup>22</sup> A dark brown to black Ca-Ti-bearing amphibole NaCa<sub>2</sub>[(Mg,Fe<sup>2+</sup>)<sub>4</sub>Ti](Si<sub>6</sub>Al<sub>2</sub>)O<sub>22</sub>(OH)<sub>2</sub>

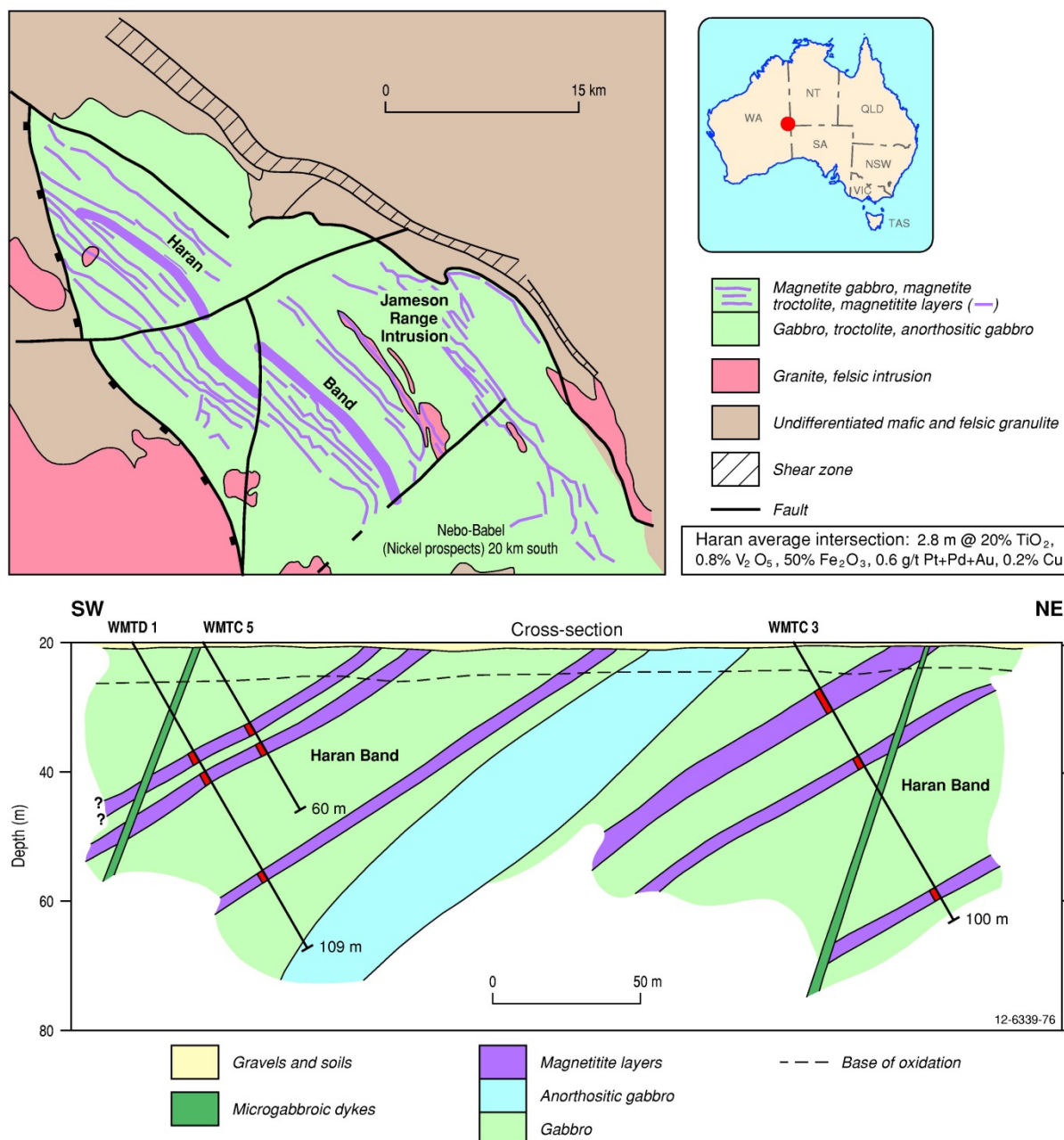


Figure 6.20 Geology and schematic northeast-southwest section of the Haran magnetitite deposit in the Jameson Range Intrusion, Musgrave Province, Western Australia. The PGE-enriched magnetitite layers occur in fractionated gabbro, anorthosite, and troctolite in the evolved mafic stratigraphy. Modified from Western Mining Corporation Limited (2003).

### Age of mineralisation

The Jameson Range Intrusion (Gliksen et al., 1996) is part of the ~1070 Ma Giles Complex, which is an important mafic-ultramafic igneous component of the regional extensive Warakurna LIP (Wingate et al., 2004). The PGE-enriched Haran and associated oxide layers have formed from primary orthomagmatic processes, or they formed late in the magmatic mineralising system, hence their age of formation is inferred to be ~1070 Ma.

## *Genesis*

No published studies on the genesis of the Haran deposit are known. However, Pirajno and Hoatson (2012) provide the following salient points for these mineralising systems. Magmatic deposits of V-Ti-Fe±PGE oxides consist of layers and lenses of massive, disseminated titanomagnetite or V-magnetite, with minor amount of ilmenite and chromite, in differentiated gabbroic intrusions. The host rocks are typically norite, gabbronorite, and troctolite. The mineralised layers usually occur near, or at the tops of the fractionated mafic stratigraphy. Mafic-ultramafic pipes may be associated with the intrusions. The principal ore minerals are titanomagnetite and V-bearing magnetite, with associated minerals being ilmenite, hematite, spinel, and sulphide minerals (pyrite, pyrrhotite, chalcopyrite). The Fe- and Ti-oxide phases form by crystal settling or filter pressing during crystallisation of the gabbroic magmas, resulting in laterally persistent layers and segregations. Closed-fractionation systems involving little magma input into the upper parts of the chamber and favourable oxygen fugacity conditions promote the formation of these deposits in large mafic-dominant intrusions.

Important global examples of this type of mineralisation are the vanadiferous magnetite layers in the Upper Zone (gabbro) of the ~2.06 Ga Bushveld Complex in South Africa (Eales and Cawthorn, 1996) and in Western Australia, where the ~2.8 Ga Windimurra Igneous Complex in the western Yilgarn Craton hosts layers of Fe-Ti-V oxides (Mathison and Ahmat, 1996; Ivanic et al., 2010). Importantly, it has been shown that PGE minerals can be hosted in magnetite-rich layers of gabbro intrusions (Maier et al., 2003), thereby extending the PGE prospectivity to the upper gabbroic parts of layered mafic-ultramafic intrusions.

## *Key references*

- Daniels (1974): regional geology; structure; stratigraphy of the Blackstone region; Giles intrusions; Jameson Intrusion; magnetite layers; mineralisation.
- Glikson et al. (1996): geological setting of Giles mafic-ultramafic intrusions; Jameson Intrusion; structure; stratigraphy; whole-rock and mineral chemistry; magnetite layers.
- Hoatson et al. (2008a,b): Australian Proterozoic Mafic-Ultramafic Magmatic Events: Time-Space-Event Chart.
- Howard et al. (2009): geochronology and geochemistry; Alcurra Suite in west Musgraves; potential for orthomagmatic Ni-Cu-PGE mineralisation; Giles Event.
- Evins et al. (2010): new geochronology and geological mapping; definition of eight mafic and felsic magmatic pulses; redefining Giles Event; Ngaanyatjarra Rift; genesis of west Musgrave Province.
- Pirajno and Hoatson (2012): Jameson Range stratiform vanadiferous magnetite deposits; PGE-bearing magnetite layers; evolved gabbro; Proterozoic Giles Complex; drill intersections mineral resource.
- Joly et al. (2013): analysed the mineral potential of the west Musgrave Province; several commodities investigated including PGEs, Ni, and Cu; used a knowledge driven mineral-systems approach; exploration potential.
- Maier et al. (2014a,b): tectonomagmatic events of the Musgrave Province; Giles Complex, geochronology and geochemistry of intrusions; mineral prospectivity.

### 6.4.3 Mineral-System Class 3: Komatiitic flows and related sill-like intrusions

#### 6.4.3.1 Deposit Type 3.A: Massive, matrix, and disseminated Ni-Cu-PGE sulphides in preferred lava pathways

##### Overview

Australia's Ni sulphide production is dominated by the ~2705 Ma komatiite-hosted deposits in the Eastern Goldfields Province of the Yilgarn Craton (Barnes, 2006; Hoatson et al., 2006). Archean komatiitic magmatism is a global feature of evolving Archean greenstone-granitoid terranes and intracratonic rift zones or extensional zones. These distinctive high-temperature, mantle-derived lavas and their associated Ni-sulphide deposits provide valuable insights into their geodynamic settings and the evolution of the Archean lithosphere. For example, the spatial distribution of komatiitic lavas indicate they were emplaced without significant differentiation or heat loss along major lithospheric discontinuities, such as craton margins and extensional zones within cratons. Since the komatiite-associated Ni-Cu-PGE deposits in the Yilgarn Craton occur in broadly parallel, north-northwest-trending greenstone belts that traverse the craton and occur at high angles to the margins of the craton, a geodynamic setting of intracratonic extensional zones may be relevant to their evolution.

The Yilgarn Craton contains the largest concentration of Archean komatiite-hosted Ni deposits in the world, and includes such world-class examples as Kambalda (Deposit Type 3.A), Perseverance, Yakabindie, Honeymoon Well, and Mount Keith (the latter four deposits belong to Deposit Type 3.B, of which Mount Keith is the type example). Type 3.A Ni-Cu-PGE deposits (Kambalda Dome deposits, Cosmos, Wedgetail, Waterloo, Maggie Hays, Prospero) are prominent throughout the Eastern Goldfields province. Other similar deposits occur in the Southern Cross (~3030 Ma to ~2720 Ma) and Northeastern Goldfields (>2900 Ma to ~2710 Ma) provinces, however, in comparison the Murchison (~3000 Ma to ~2750 Ma) and South West (~2670 Ma) provinces are poorly mineralised (Hoatson et al. 2006). The Narryer Province in the northwest of the Yilgarn Craton has no recorded komatiites. Kambalda-type deposits are spatially associated with the Kambalda Komatiite Formation—a complex ~2705 Ma volcanic-minor sedimentary sequence—that overlies pillowed tholeiitic basalts of the Lunnon Basalt (Marston, 1984; Cowden and Roberts, 1990; Barnes, 2006). The stratigraphy has been multiply deformed, metamorphosed to lower amphibolite facies, and intruded by felsic dykes. The deposits typically comprise accumulations of massive sulphide ores (>35% sulphides) localised in lava pathways at the base of thin (metres to tens of metres thick) komatiite flows. They are small-tonnage orebodies (0.5 to 5 Mt) with moderately high-Ni grades (2 to 4% Ni); although some deposits (Cosmos, Silver Swan) have the highest primary magmatic Ni grades (up to 9% Ni) in the world (Hoatson et al., 2006). Kambalda Type 3.A deposits are Australia's major source of PGEs, with ~24 812 kg of Pd and Pt produced as a by-product of Ni, which equates to almost 94% of Australia's total historical PGE production (see Section 1.3.3). However, this PGE by-product is largely unpublished for individual deposits.

The komatiite-hosted deposits of the Yilgarn Craton have distinctive Ni to Cu ratios that provide a useful criterion for their classification. Type 3.A (Kambalda: Barnes, 2006) deposits have Ni to Cu ratios of 7 to 20, Type 3.B (Mount Keith: Grguric et al., 2006) are more Ni-rich with ratios generally greater than 20, whereas Type 3.C (Collurabbee: Bertuch, 2004) deposits have distinctly lower Ni to Cu ratios of 0.5 to 1.5 (Hoatson et al., 2006). The Pilbara Craton has several phases of komatiitic magmatism that range in age from ~2880 Ma to ~3460 Ma (Hoatson et al. 2009a,b), and the ~2520 Ma Lake Harris Komatiite in the central Gawler Craton, South Australia, is the youngest, and most eastern known occurrence of these primitive rocks in Australia (Hoatson et al., 2005b). Komatiitic flows coeval with the Lake Harris Komatiite also occur near Mount Hope on the western Eyre

Peninsula of the southern Gawler Craton. On existing evidence, komatiitic rocks in the Pilbara and Gawler cratons have significantly lower metal endowment and potential relative to those in the Yilgarn Craton. Hoatson et al. (2006) indicate fertile komatiitic sequences in the Yilgarn Craton generally have Al-undepleted ( $\text{Al}_2\text{O}_3/\text{TiO}_2 = 15\text{--}25$ ) chemical affinities, and often occur with S-bearing country rocks in dynamic high magma-flux environments, such as compound sheet flows with internal pathways facies (Kambalda-type), or dunitic compound sheet flow facies (Mount Keith-type). Barnes (2006) states that mineralisation is associated with favourable stratigraphic and volcanological facies. Favourable host komatiite sequences are voluminous compound flows with well-developed pathways, and the most favourable circumstances occur when these pathways are emplaced above potentially sulphide-bearing substrates that can be readily eroded.

### *Australian deposits/prospects/hosts*

Several Kambalda–Widgiemooltha deposits; Cosmos; Prospero; Flying Fox; Waterloo; Rosie (all Yilgarn Craton, WA).

### *Significant global example(s)*

Alexo, Katinniq (Canada).

### *Type example in Australia*

Kambalda, Western Australia.

### *Location*

Longitude 121.749747°E, Latitude -31.340037°S; 1:250 000 map sheet: Widgiemooltha (SH 51–14), 1:100 000 map sheet: Cowan (3234); ~52 km south-southeast of Kalgoorlie, Western Australia.

### *Geological province*

Eastern Goldfields Province, Yilgarn Craton, Western Australia.

### *Resources*

Collective resources of deposits in the Kambalda Dome and St Ives–Tramways regions (Otter, Long–Victor, Lunnon, Durkin, Foster, etc) are 42 Mt @ 3.3% Ni—a global resource of ~1.4 Mt of contained Ni, with variable credits of Cu, Au, Co, Pt, and Pd (Hoatson et al., 2006).

### *Current status and exploration history*

Developed world-class Ni-Cu±PGE deposits with JORC-compliant resources; operating mines. The exploration history of the Kambalda Ni deposits is described by Marston (1984), Gresham (1990, 1991), and Barnes (2004a), and is summarised in Section 5.2.4.

### *Economic significance*

The Yilgarn Craton in Western Australia contains most of Australia's Ni resources, both sulphide and laterite, and is one of the world's great Ni provinces (Figure 6.21). Hronsky and Schodde (2006) state that the Yilgarn Craton contains about 31.5 Mt of Ni metal with an *in situ* value of about \$350 billion on a pre-mining basis, amounting to 13.5% of the world's known Ni resources. More than 90% of the nation's known global resources<sup>23</sup> of Ni metal from sulphide sources were discovered during the

<sup>23</sup> Global resources of Ni metal are defined as total production plus remaining reserves and/or resources, i.e., total contained Ni metal.

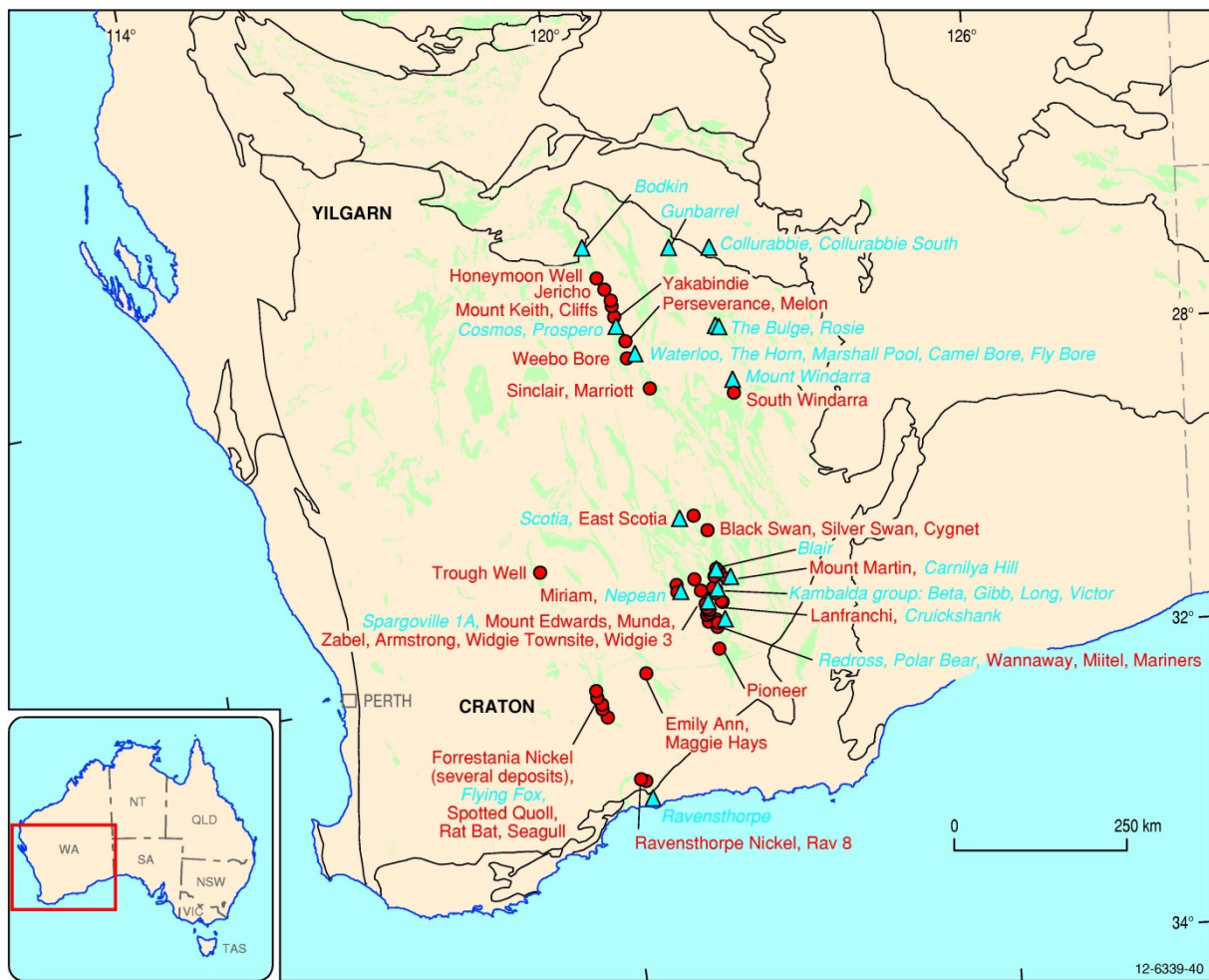
narrow time period of 1966 to 1973 (Hoatson et al. 2006). Nickel sulphide deposits in this craton are almost exclusively associated with komatiitic rocks, the one exception being the Carr Boyd Rocks deposit (see Deposit Type 8.A), 125 km north of Kambalda. Nickel laterites in the Yilgarn Craton are exclusively developed over komatiitic rocks (Barnes, 2006). The world-class Ni sulphide deposits of the Yilgarn Craton include Mount Keith (~3.4 Mt of contained Ni metal), Perseverance (~2.5 Mt), Yakabindie (~1.7 Mt), Honeymoon Well (~1 Mt), and deposits from the Kambalda Dome region have a collective global resource of ~1.4 Mt of Ni. The combined total resource of these world-class deposits is ~10 Mt of Ni metal, equivalent to almost 78% of Australia's global Ni sulphide resources (Hoatson et al., 2006). Most PGEs produced from the komatiitic-hosted Ni sulphide deposits in the Yilgarn Craton are from Kambalda-type (see Deposit Type 3.A). Many of the major Ni-Cu±PGE deposits associated with komatiitic rocks at the Kambalda Dome (e.g., Long–Victor, Lunnon, Foster, Fisher, Hunt-Beta, Carnilya Hill) and in the nearby St. Ives, and Tramways areas have been in production from 1966 to at least 2000. Other developed deposits (Silver Swan, Cosmos, Prospero, Cosmic Boy, Digger Rocks, Flying Fox, Miitel, Nepean, Redross, Spargoville, Maggie Hays, Widgiemooltha North<sup>24</sup>) similar to Kambalda occur in the Forrestania, Honeymoon Well, Lake Johnston, Ravensthorpe, and Widgiemooltha regions of the Yilgarn Craton. The PGE by-product contributions, if present, are unpublished for most of these individual Ni-Cu deposits. Type 3.A komatiitic Ni sulphide deposits are currently Australia's only major source of PGEs, with approximately 300 kg to 850 kg of Pd and 50 kg to 320 kg of Pt produced annually. For the period 1966 to 2013, these deposits have collectively produced ~24 812 kg of Pd and Pt as a by-product of Ni, which equates to almost 94% of Australia's total historical PGE production. The vast majority of this PGE production has been generated by the Kambalda group of deposits in contrast to the Mount Keith-type of deposits (see Deposit Type 3.B). Therefore, Kambalda Type 3.A deposits of the Yilgarn Craton are of global economic significance in relation to sulphide and lateritic Ni, with the former also an important source of by-product Pd and Pt.

### *Geological setting*

The Kambalda deposits are located within a 30-km-long by 10-km-wide corridor between the Kambalda Dome (Figure 6.22) and the Tramways Dome near the southern part of the Norseman–Wiluna greenstone belt of the Yilgarn Craton. Nickel sulphide deposits are spatially associated with Archean komatiitic rocks in this economically important belt that has a north-northwest to south-southeast trend and is bounded by large terrane-scale faults and granitoid bodies. The Kambalda Dome is a doubly plunging D<sub>3</sub> anticline superimposed on a regional D<sub>2</sub> anticline that is characterised by extensive parasitic folding and thrusting. Most of the thrusting was localised along the zone of competency contrast at the contact between the mineralised komatiite and underlying basalt (Barnes, 2006).

---

<sup>24</sup> Many of the Ni deposits in the Yilgarn Craton and elsewhere can contain more than one style of mineralisation relating to orthomagmatic (3.A and 3.B), hydrothermal-metamorphic (8.B), and regolith-laterite (9.A) mineral systems associated with ultramafic rocks.



Deposits and prospects shown in italics have associated PGEs

Figure 6.21 Distribution of Archean komatiite-associated Ni-Cu (red dot) and Ni-Cu-PGE (blue triangle) sulphide deposits in the Yilgarn Craton, Western Australia. The Kambalda group of nickel deposits occur just below the centre of the figure. Background map of Precambrian mafic and ultramafic rocks in Western Australia is from Hoatson et al. (2009a,b).

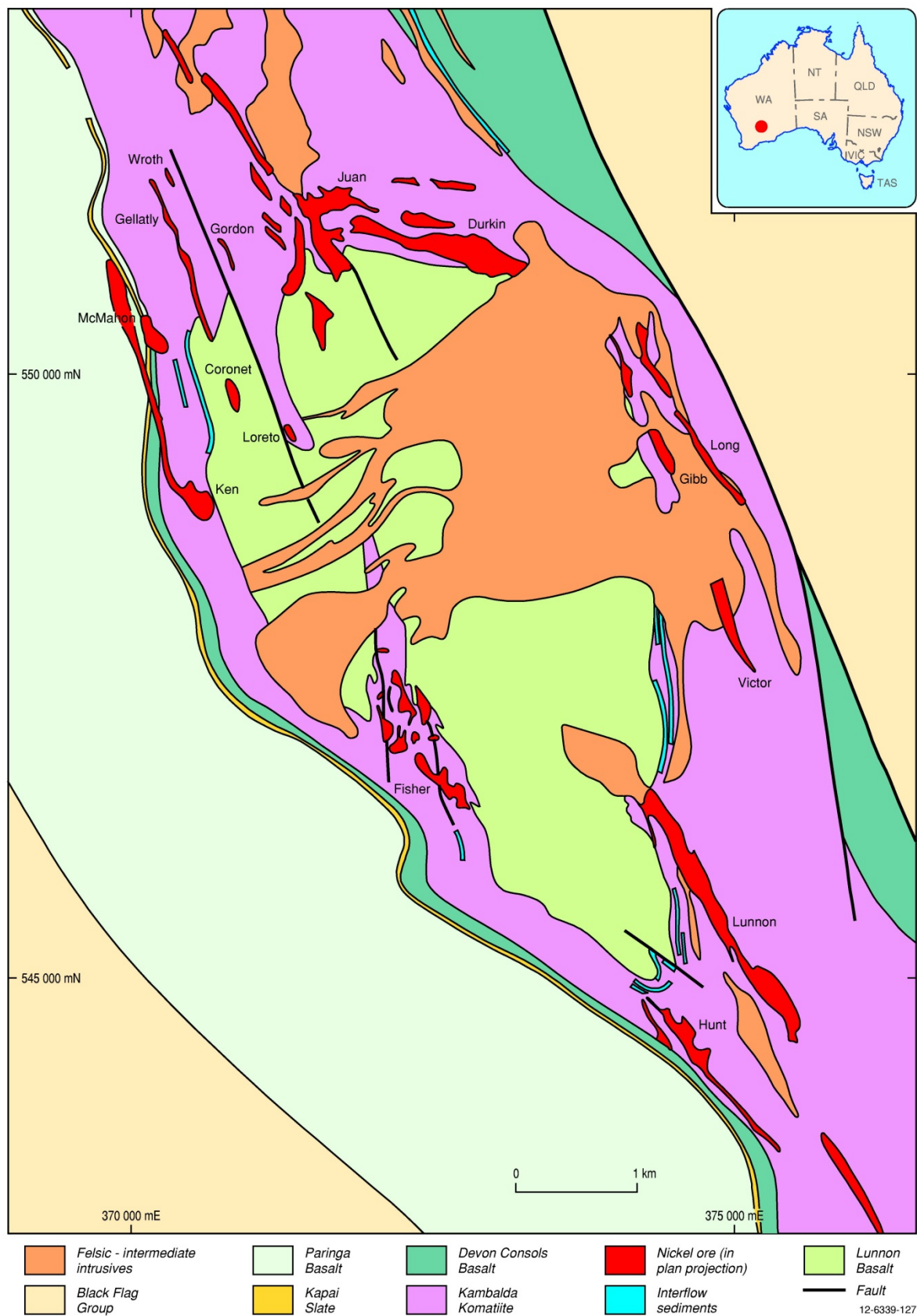


Figure 6.22 Geology of the Kambalda Dome showing the horizontal projection of the main sulphide ore shoots. The shoots generally form irregular lensoidal bodies associated with the Kambalda Komatiite. Modified from Stone and Masterman (1998).

### *Mineralisation environment*

The following summary of the host komatiitic rocks in the Kambalda district is from Dowling and Hill (1998); Barnes et al. (1999); Leshner and Keays (2002); Barnes (2004b, 2006); Beresford and Stone (2004); Stone et al. (2005); and Hoatson et al. (2006). Nickel sulphide deposits in the Kambalda Dome are spatially associated with the Kambalda Komatiite Formation—a complex ~2705 Ma volcanic, minor sedimentary sequence—that overlies pillowed tholeiitic basalts of the Lunnon Basalt. The economically important Silver Lake Member of this formation contains spinifex-textured differentiated flow units and thicker olivine cumulate units. The ultramafic stratigraphy has been multiply deformed, metamorphosed to lower amphibolite facies, and intruded by different generations of felsic dykes. The Kambalda Komatiite Formation displays considerable lateral continuity and systematic variation in rock types and facies up the sequence. Beresford and Stone (2004) describe three to six high-Mg (up to 45% MgO) komatiite flows (25 m- to 100 m-thick) at the base (Silver Lake Member), which transgress upwards to multiple thin (<10 m thick), less magnesian (15% to 35% MgO) spinifex-textured flows at the top of the sequence (Tripod Hill Member). Stone et al. (2005) and Barnes (2006) describe the Silver Lake Member as a komatiitic unit consisting primarily of thick, cumulate-rich flows 40 m- to 100 m-thick, and containing up to 20 distinct cooling units in the vertical section. Sulphide mineralisation is generally restricted to the basal flow, which is commonly the thickest flow, and contains the highest proportion of forsteritic olivine mesocumulates to orthocumulates with MgO contents greater than 45% (anhydrous). Intercalated thinly laminated sulphidic sediments are restricted to the basal member. Lateral variations of stratigraphic units, flow compositions, and distribution of interflow sediments within the Silver Lake Member define lava channel (ore environment) and sheet flow (non-ore environment) facies (Cowden and Roberts, 1990). The mineralised channel facies (pathway facies is also used in the literature to avoid any prejudgment of intrusive or extrusive origin: Barnes, 2006), which is interpreted to represent the main locus of flow within an active lava flow, consists of a stacked sequence of thick primitive flows and an absence of interflow sedimentary units. The channel facies is also defined by the thickening of the flow unit associated with linear troughs in the underlying Lunnon Basalt, and can be traced over up to 15 km in length and 500 m in width. The more distal sheet flow facies is characterised by thinner (10 m to 20 m) and more evolved flows and thin interflow sedimentary unit are common.

The Ni sulphide orebodies are hosted by specific volcanic facies within the long linear and anastomising lava pathways or channels. Lenticular shoots of massive (>35% sulphides), matrix, and disseminated (a few % interstitial sulphides) sulphide ores occur at the base of the flows, commonly confined by shallow embayments or depressions in the basal ultramafic-basalt contact of the channel facies (called contact ore), and, more rarely in the overlying flows (hanging wall ore) and in crosscutting structures (off-set ore). Figure 6.23a–e shows reconstructed stratigraphic sections through various types of Kambalda-type Ni-Cu-PGE deposits associated with komatiitic rocks in Australia and Canada. The contact massive ores form continuous linear, ribbon-like ore shoots, up to 3 km-long and 300 m-wide, usually less than 5 m-thick, or more rarely as equidimensional pods at the basal contact of the Silver Lake Member. Resources in these deposits typically range from less than 0.5 Mt up to 10 Mt. The contact ores are by far the most economically important ore type constituting more than 80% of the total Ni resources in these deposits. Approximately half the ore shoots consist of massive ore overlain by matrix ore; some shoots have massive and disseminated ore only; others have matrix without massive ore; and most have a halo of low-grade disseminated ore. Major minerals in the massive and disseminated ores are pyrrhotite, pentlandite, pyrite, chalcopyrite, magnetite, and chromite, with rare millerite and heazlewoodite generally confined to disseminated ores. The host komatiitic rocks are generally extensively reconstituted to talc-carbonate assemblages with no

preservation of original texture in cumulates and local preservation in spinifex zones. Lesher (1983) and Beresford et al. (2002) describe the preservation of serpentinites in rare pockets in the Durkin and Victor shoots. Postmagmatic processes (tectonic, metamorphic, intrusive, and weathering events) have also resulted in a spectrum of mineralisation types, ranging from dislocation (faulted ores), and more localised mobilisation (stringer sulphides), through metamorphic replacement (interpillow-interbreccia sulphides), hydrothermal dissolution and redeposition (vein-type sulphides), to lateritisation-oxidation enrichment (supergene sulphides-oxides).

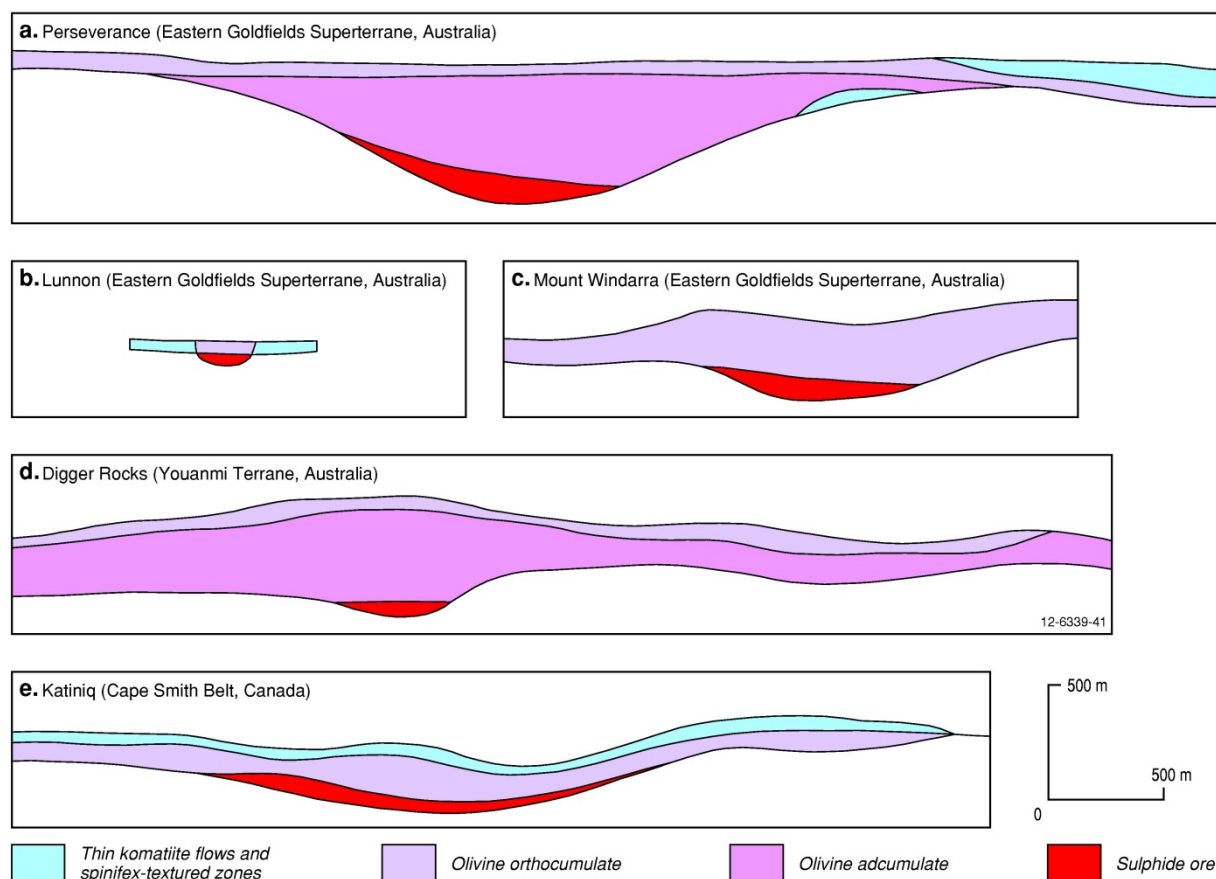


Figure 6.23 Reconstructed stratigraphic sections through various types of Kambalda-type (Deposit Type 3.A) Ni-Cu-PGE deposits associated with komatiitic rocks in the Yilgarn Craton and Cape Smith Belt, Canada. The Lunnon ore shoot from the Kambalda Dome is shown in (c) and also on Figure 6.22. All sections are to the same approximate scale. Represents early version of Figure 3 in Chapter 3 of Barnes (2006).

### PGE mineralisation

In their studies of the PGE concentrations in the ores and host rocks of the Kambalda deposits, Ross and Keays (1979) and Keays et al. (1981a) found Pd to be enriched in pentlandite relative to other sulphide phases, whereas Ir occurred in pentlandite, pyrrhotite, pyrite, and chalcopyrite, and Au was enriched in pyrite and chalcopyrite. These workers concluded that discrete PGMs were rare in the massive and matrix ores, and the chalcopyrite-rich footwall stringers were enriched in Pd and Au, owing to the remobilisation of these elements from the massive ores. Hudson and Donaldson (1984) noted that the Kambalda Ni ores contain (concentrations recalculated to 100% sulphides are shown in brackets) 2.96% Ni (14.45%), 0.22% Cu (1.10%), 8.09% S (39.95%), 326 ppb Pt (1630 ppb), 425 ppb Pd (2104 ppb), 110 ppb Os (537 ppb), 60 ppb Ir (293 ppb), 50 ppb Rh (240 ppb), 220 ppb Ru

(1074 ppb), and 339 ppb Au (1721 ppb). Cowden et al. (1986) confirmed previous observations that PGE values were highest in high tenor Ni ores, and Pd, Os, Ir, Rh, and Ru correlate strongly with Ni, but Pt has only a weak to moderate correlation with Ni. Geochemical profiles of the Lunnon Shoot, Juan Complex, and Long Shoot by Cowden et al. (1986) showed that Pt, Pd, and Au were much lower in massive ores compared with overlying matrix and disseminated ores. In contrast, Os, Ir, Rh, and Ru contents, although variable, were similar in both ore types. The lower PGE concentrations in massive ores were explained as redistribution and remobilisation of Pt, Pd, and Au into stringers and fracture fillings. Keays and Davison (1976) and Cowden et al. (1986) provide useful early compilations of PGE data for different ores types and deposits throughout the Yilgarn Craton, whereas more recent PGE data can be found in the many references cited in Barnes (2006).

Hudson and Donaldson (1984) and Hudson et al. (1991) reported that significant Pt, Pd, and Au occur as discrete mineral phases in typical Kambalda Ni ores. Major PGMs documented included: sperrylite ( $\text{PtAs}_2$ ); moncheite ( $\text{Pt,Pd,Ni}(\text{Te,Bi})_2$ ); sudburyite ( $(\text{Pd,Pt,Ni})(\text{Sb,Te,Bi})$ ); and stibiopalladinite ( $\text{Pd}_5\text{Sb}_2$ ); together with palladian arsenides, palladian melonites, and native gold. Michenerite, merenskyite, and testibiopalladinite also occurred within Kambalda ores (Hudson et al., 1991). Apart from a single grain of irarsite ( $\text{IrAsS}$ ), no discrete PGMs containing Os, Ir, Rh, and Ru were identified (Cowden et al., 1986; Hudson, 1986). Sperrylite occurred within massive pyrrhotite-pentlandite ores and was particularly abundant in chalcopyrite-rich ores. The correlation of Os, Ir, Ru, and Rh with both Ni and pentlandite, and the fact that discrete phases containing these elements are extremely rare, suggest that these elements either occur largely in solid solution or as minute inclusions within pentlandite.

Discrete Pd-bearing minerals were most abundant in sulphide stringers in the footwall to the ore, in cross-cutting sulphide veins, or in reaction zones associated with hydrothermal veins and porphyries. Coarse discrete Pd minerals were rare in massive and matrix sulphides. The occurrence within the ore zones of Pt as sperrylite and Pd possibly dispersed in pentlandite is thought to reflect a primary magmatic distribution. However, the presence of sudburyite, moncheite, merenskyite, michenerite, testibiopalladinite, and palladian melonite in stringers and reaction zones indicated that their formation may be related to postmagmatic processes, in particular metamorphic segregation of sulphides and the interaction of ore sulphides with younger hydrothermal fluids (Hudson et al., 1991).

The Ni-Cu matte (73% Ni, 5.5% Cu) produced in treating the ore contains about 4.2 ppm Pt, 10.9 ppm Pd, 1.2 ppm Rh and 4.1 ppm Ru (Hudson and Donaldson, 1984).

The Ni and PGE tenors of the sulphide ores on the Kambalda Dome vary considerably both between, and within, ore shoots. Neighbouring ore shoots such as the Victor and Long shoots have markedly contrasting tenor. Barnes (2006) attributes the different metal grades to variable fluid dynamic conditions determining the extent of equilibration between the komatiite lava and the sulphide-bearing ore magma. The wide variability within shoots on a hand-size scale is attributable to metamorphic effects (Keays et al., 1981a; Stone et al., 2004). Several other Ni-Cu deposits in the Norseman–Wiluna greenstone belt contain moderate to high PGE concentrations associated with massive and disseminated ores. These deposits have similar settings and age (~2705 Ma) to Kambalda, with the Ni-Cu mineralisation being associated with komatiitic and tholeiitic mafic-ultramafic flows. Maximum PGE contents for these deposits as reported by Keays and Davison (1976) and Travis et al. (1976) are: Nepean—31.30 ppm Pd (with 19.8% Ni, 0.16% Cu); Scotia–Broad Arrow—2.35 ppm Pd, 1.09 ppm Ir (19.0% Ni, 0.81% Cu); Carnilya Hill—1.50 ppm Pd (10.4% Ni, 1.22% Cu); and Redross—1.99 ppm Pd (17.6% Ni, 0.08% Cu). Nickel gossans in the region have anomalous PGE levels, and these include: Carnilya Hill—1.50 ppm Pd (0.35% Ni, 0.27% Cu); Mount Clifford—1.70 ppm Pd (2.52% Ni, 1.40% Cu); Kurnalpi—3.63 ppm Pd (2.70% Ni, 5.05% Cu); and Bronzite Ridge–Jimberlana Dyke—2.49 ppm Pd (1.25% Ni, 0.35% Cu).

### *Age of mineralisation*

The age of the komatiitic stratigraphy is Archean (~2705 Ma) from the dating of komatiitic and associated felsic rocks in the Kambalda region, and also from analogy with similar mineralised greenstone belts and other Ni sulphide deposits in the Eastern Goldfields Superterrane that have been dated (Nelson, 1997). Such important U-Pb zircon ages that constrain the mineralised komatiites include a direct age of  $2705 \pm 4$  Ma for a fragmental felsic tuff (GSWA no. 100726) intercalated in the Kambalda Komatiite, Bulong;  $2708 \pm 7$  Ma age for coeval dacite in komatiite, Ballarat–Last Chance mine;  $2704 \pm 4$  Ma and  $2706 \pm 5$  Ma rhyolite in komatiite; and  $2708 \pm 5$  Ma volcanogenic sandstone in komatiite (Nelson, 1997; Kositcin et al., 2008). Hoatson et al. (2009a,b) provide additional age data and national magmatic event maps that highlight the important mineralising event at ~2705 Ma. Hoatson et al. (2006, 2009a,b) have compiled U-Pb zircon and baddeleyite ages of komatiite and associated rocks in Australia. The ages of these rocks are constrained by felsic units intercalated with komatiitic sequences (i.e., direct age of komatiites), felsic footwall units (maximum age), felsic hanging wall units (minimum age), and felsic dikes cutting the komatiitic sequences (minimum age). Most Ni sulphide deposits in the Norseman–Wiluna greenstone belt fall within a very narrow age span of 2705 million years, part of a global komatiite event within 10 to 15 million years. Campbell et al. (1989) indicated that extensive outpourings of primitive lava within a very short time span is a hallmark of magmatism related to the first arrival of mantle plumes at crustal levels.

### *Genesis*

During the early years of Au and Ni exploration in the 1960s, unusual ultramafic rocks in the southeastern Yilgarn Craton were recognised to have komatiitic affinities based on their similarities in composition (>18% MgO) and textures (spinifex-textured flows) to komatiitic lava flows in the Komati River Valley of the Barberton greenstone belt in the Kaapvaal Craton of southeastern Africa (Viljoen and Viljoen, 1969). Several important papers (McCall and Leishman, 1971; Williams, 1971; Hallberg and Williams, 1972) describing the Western Australian occurrences were published shortly after the original Viljoen paper.

The genesis of the Kambalda Ni sulphide ores has been the subject of many investigations since their discovery in the mid 1960s. Barnes (2006) has summarised the changing evolution of these concepts which in some cases still remain controversial today. During the early phases of mining at Kambalda (see Section 5.2.4), the ores were first thought to be the result of gravitational settling and accumulation of mantle-derived sulphide melt transported from great depths to the surface by komatiitic magma (Naldrett and Cabri, 1976; Naldrett and Turner, 1977). Detailed studies in the mine environments on the Kambalda Dome in the early 1980s led to the idea that the Ni-Cu sulphides were derived by thermal erosion or 'ground melting' of sulphidic sedimentary rocks in the immediate substrate to the lava, and the sulphides were deposited in linear thermal erosion troughs (Huppert et al., 1984; Leshner et al., 1984; Huppert and Sparks, 1985). Although this model has received considerable acceptance in the exploration industry, aspects of the thermal erosion model have been challenged on the basis of Re-Os isotopic data and volcanological-structural evidence (Foster et al., 1996; Cas et al., 1999; Stone and Archibald, 2004). Barnes (2006) also notes that the origin of the mineralised trough structures at Kambalda remains one of the most contentious issues and centres on whether they are primary or tectonic in origin. Researchers who have undertaken detailed investigations of the komatiite-basalt contact have proposed a number of origins for the troughs that include: synvolcanic grabens (Ross and Hopkins, 1975; Brown et al., 1989); eruptive fissures (Gresham and Loftus-Hills, 1981); topographic sea-floor depressions between linear parallel basalt flows modified by deformation (Leshner et al., 1984; Leshner, 1989); thermal erosion of underlying basalt

(Huppert and Sparks, 1985); combinations of various primary topographic features unrelated to thermal erosion enhanced by deformation (Squire et al., 1998); entirely structural features (Stone and Archibald, 2004); and drained lava tubes or channels within the uppermost flows of the Lunnon Basalt (Barnes, 2006). Further information on the genesis and structural controls (e.g., tectonic versus volcanic, assimilation, ground melting) of the Kambalda deposits can be found in Stone and Archibald (2004), Barnes et al. (2004a), Barnes (2006), Fiorentini et al. (2010), and Barnes et al. (2013).

A study of the major komatiitic provinces in the world by Hoatson et al. (2006) indicated that fertile komatiitic sequences for Ni sulphides are generally of late Archean (~2700 Ma) or Paleoproterozoic (~1900 Ma) age, have dominantly Al-undepleted ( $Al_2O_3/TiO_2 = 15-25$ ) chemical affinities, and often occur with S-bearing country rocks in dynamic high magma-flux environments (Figure 6.24), such as compound sheet flows with internal pathways facies (Kambalda-type), or dunitic compound sheet flow facies (Mount Keith-type).

Detailed geochemical and structural investigations of the Flying Fox Ni-Cu-PGE deposit in the Forrestania greenstone belt of the Yilgarn Craton (Collins et al., 2012) have shown that the deposit is characterised by intense brittle-ductile deformation, a strong variability in Ni tenor unrelated to mineralisation style, and significant pyrite content formed from mechanical processes and circulating Fe-, S-, Cu-, and As-enriched hydrothermal fluids generated during deformation. Massive ores contain the highest PGE concentrations (2070 ppb Pt, 1060 ppb Pd, 208 ppb Rh, 142 ppb Ir, 296 ppb Os, 1130 ppb Ru) relative to breccia, stringer, and stringer/vein ores. The PGEs show strong linear correlations between Ir, Os, Ru, and Rh, but poor correlation between Pt, Pd, and Cu. The authors contend that the mobilisation of Ni within mineralised ultramafic belts cannot be directly linked to metamorphic and tectonic events, thus further investigations are required to identify that conditions that control Ni solubility.

### *Key references*

- Travis et al. (1976): gossan mineralogy; Pd and Ir concentrations in Ni gossans from Western Australia; potential.
- Keays and Davison (1976): Pd, Ir, and Au concentrations of ores and host rocks; Ni-sulphide deposits in Western Australia; exploration potential.
- Keays et al. (1981a): PGE concentrations of Kambalda ores; distribution within ores and host rocks; magmatic and hydrothermal processes; mineralisation models.
- Marston (1984): Ni sulphide deposits of Western Australia; Kambalda Dome deposits; stratigraphy; structure; mineralisation; exploration results; mining companies.
- Hudson and Donaldson (1984): PGMs from Kambalda; mineralogy.
- Leshner and Keays (1984, 2002): metamorphic and hydrothermal mobilisation of Ni-Cu sulphides and PGEs; genesis.
- Hudson (1986): PGMs from Kambalda; mineralogy.
- Gresham and Loftus-Hills (1981): geology of Kambalda; exploration methods, mining.
- Arndt and Jenner (1986): crustal contamination of komatiites and basalts from Kambalda; genesis.
- Leshner (1989): komatiite-associated Ni sulphide deposits; stratigraphy; mineralisation; Kambalda-type deposits; volcanology; genesis.
- Cowden and Roberts (1990): overview of komatiite-hosted Ni-sulphide deposits; stratigraphy; exploration history; resources.

- Gresham (1990, 1991): discovery of Kambalda deposits; exploration philosophy and techniques; mining practices; drill intersections and resources.
- Foster et al. (1996): Re-Os isotopic system; comparing isotopic data for Kambalda, Mount Keith, and Perseverance deposits; crustal contamination; ore genesis; model precludes significant bulk assimilation of sulphidic sediments; ore-forming komatiites from a depleted upper-mantle source.
- Barnes et al. (1999, 2004a): komatiite flow fields and associated Ni-sulphide mineralisation; volcanology; Kambalda Ni mineralisation; lithochemistry, potential.
- Beresford and Stone (2004): overview of komatiite-hosted Ni-Cu-PGE deposits of the Kambalda Ni camp; volcanic and structural controls of ore shoots; stratigraphy and deformation of Kambalda Dome; mineralised volcanic channels and troughs.
- Beresford et al. (2005): volcanological study of the Ni-Cu-(PGE) Coronet deposit; structural evolution of Coronet trough and Kambalda Dome; Kambalda Komatiite; volcanic facies.
- Barnes (2006): komatiite-hosted deposits of the Yilgarn Craton; Kambalda-type deposits; stratigraphy; lava channels; mineralisation; genesis.
- Hoatson et al. (2006): classification of Australia's Ni deposits; stratigraphy; mineralisation; genesis; and potential for new discoveries.
- Barnes and Fiorentini (2008): Ir, Ru, and Rh abundances in komatiites; Kambalda-type deposits; alloy saturation; partition coefficients; thermodynamic modelling.
- Thebaud et al. (2009): tectonostratigraphic controls; localisation of Archean komatiite-hosted Ni-sulphide deposits in the Yilgarn Craton; Kambalda-type Ni deposits; structural framework of the Yilgarn Craton and emplacement of Ni deposits.
- Fiorentini et al. (2010): Kambalda-type deposits; PGE geochemistry of mineralised and non-mineralised komatiites; depletion and enrichment of PGEs; physical volcanology; ore-forming processes; exploration potential.
- Collins et al. (2012): Flying Fly Ni-Cu-PGE deposit, Forresteria greenstone belt; geochemical-structural investigations; brittle and ductile deformation; geochemical behaviour of PGEs; introduction of pyrite by hydrothermal fluids; mobilisation of Ni associated with metamorphic and tectonic events; mobility of Ni during deformation and implications for exploration.
- Barnes et al. (2013): abundance profiles of PGEs in komatiites; Long-Victor deposit; PGE-enrichment halo; geochemical footprints; channel and flank facies; prospect-scale prospecting.

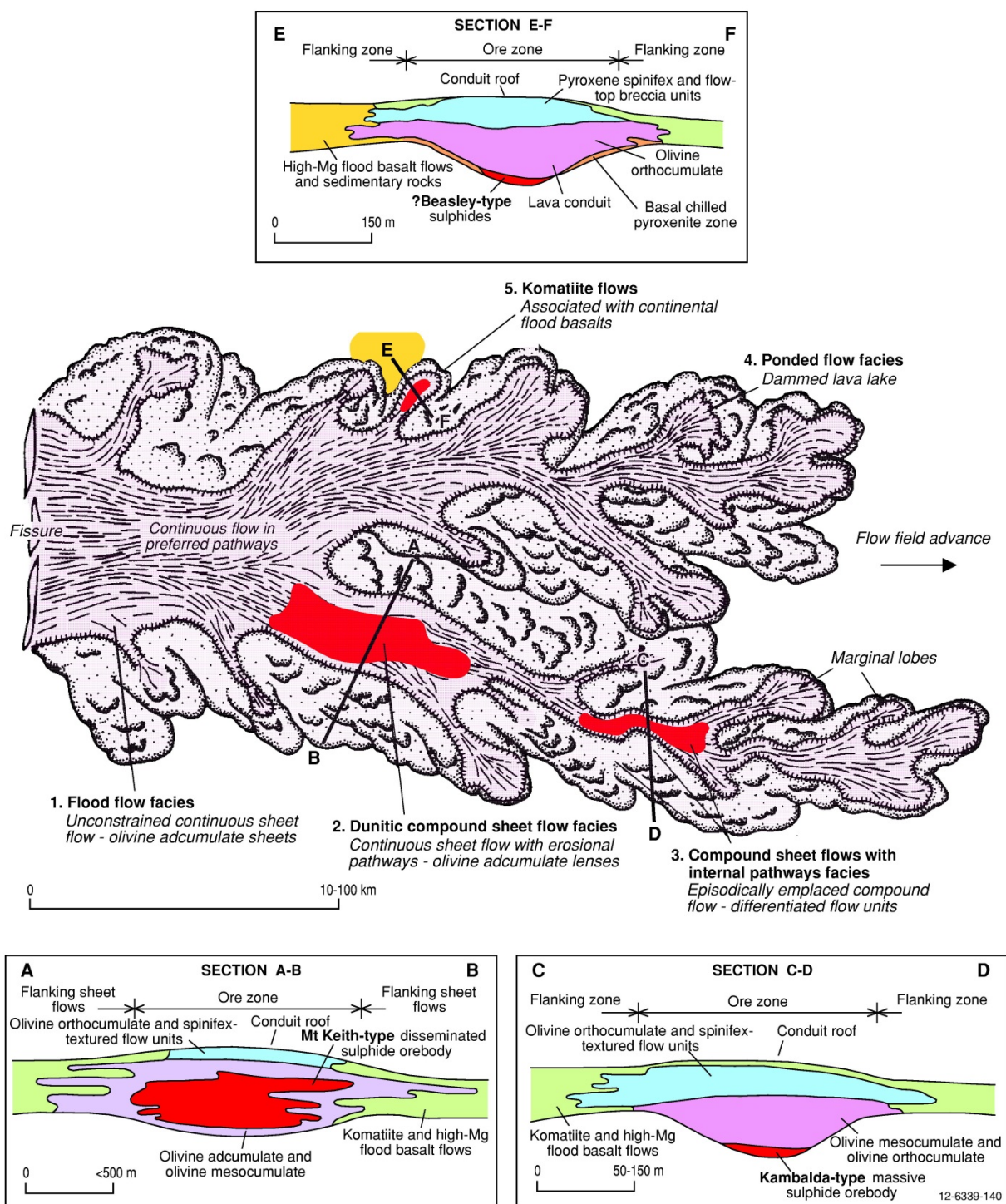


Figure 6.24 Schematic section through an inflationary komatiite flow field that developed through sustained eruption of komatiite. The spatial relationships between various komatiite facies and types of nickel mineralisation are shown for the Kambalda—Type 3.A (section C–D), Mount Keith—Type 3.B (section A–B), and Beasley—Type 3.C (section E–F) deposits. Modified from Dowling and Hill (1998).

### **6.4.3.2 Deposit Type 3.B: Disseminated Ni-Cu-PGE sulphides in central parts of thick dunitic bodies**

#### *Overview*

Australia's Ni resources, both sulphide and laterite, are largely associated with Archean komatiitic rocks in the Yilgarn Craton of Western Australia. Archean komatiitic magmatism is a global feature of evolving Archean greenstone-granitoid terranes and intracratonic rift zones or extensional zones. The most important Type 3.B Ni sulphide deposits (Mount Keith, Perseverance, Yakabindie, and Honeymoon Well) occur in the northern part of the Norseman–Wiluna greenstone belt of the Eastern Goldfields Province, where they are often spatially associated with Type 3.A deposits. The deposits are characterised by small- to large-tonnage ores (up to hundreds of millions of tonnes) with relatively low Ni grades (0.5% to 1.5% Ni).

The Mount Keith Ni deposit contains one of the largest resources of Ni (global resource of Ni metal of ~3.4 Mt) that are associated with komatiitic rocks in the world (Hoatson et al., 2006). It is the type example of a low-grade, large-tonnage disseminated Ni sulphide deposit located in the central zones of thick dunitic bodies. The 650-m-thick serpentinised host body consists of a basal zone of olivine orthocumulate overlain by a thick zone of barren olivine adcumulate and a thick zone of layered mineralised olivine adcumulate and olivine mesocumulate (MKD5 orebody: Grguric et al., 2006). Most of the primary magmatic Ni-Cu±PGE sulphides are confined to the central olivine adcumulate zone. Disseminated sulphides typically have Ni grades ranging from 0.1% to 1.0% (averaging 0.6%) and low to moderate concentrations of PGEs (combined 100 ppb to 700 ppb). Dominant PGMs in areas of high As include sperrylite (PtAs<sub>2</sub>) and irarsite (Ir,Ru,Rh,Pt)AsS (Grguric, 2003; Grguric et al., 2006). Barnes et al. (1999) proposed that the Mount Keith body was a large lava pathway or lava tube that experienced a prolonged period of continuous eruption and flow of komatiitic lava. Fertile komatiitic sequences in the Yilgarn Craton generally have Al-undepleted (Al<sub>2</sub>O<sub>3</sub>/TiO<sub>2</sub> = 15–25) chemical affinities, and often occur with S-bearing country rocks in dynamic high magma-flux environments, such as lava pathways associated with dunitic compound sheet flow facies (Mount Keith-type), or compound sheet flows with internal pathways facies (Kambalda-type).

#### *Australian deposits/prospects/hosts*

Mount Keith (MKD5 orebody); Betheno; Cliffs-Charterhall; Perseverance (previously called Agnew); Yakabindie; Black Swan; Honeymoon Well; Marriott; Durkin shoot at Kambalda; Six Mile Well; Goliath North (all Yilgarn Craton, WA).

#### *Significant global example(s)*

Dumont (Canada).

#### *Type example in Australia*

Mount Keith MKD5, Western Australia.

#### *Location*

Longitude 120.543341°E, Latitude -27.230066°S; 1:250 000 map sheet: Sir Samuel (SG 51–13), 1:100 000 map sheet: Mount Keith (3043); ~80 km south-southeast of Wiluna, Western Australia.

#### *Geological province*

Eastern Goldfields Province, Yilgarn Craton, Western Australia.

## *Resources*

Large low-grade pre-mining resource of 600 Mt @ 0.57% Ni and a global resource of ~3.4 Mt of contained Ni; minor Cu, and relatively low abundances of Pt and Pd (Hoatson et al., 2006).

## *Current status and exploration history*

World-class Ni-Cu±PGE deposit with JORC-compliant resources; operating mine. The following description of the discovery of Mount Keith is from Grguric et al. (2006). Mount Keith, a small hill located 100 km north of Leinster, is believed to have been named after Lord Kintore in the 1890s, the Governor of South Australia, whose additional title was Lord Keith of Aberdeenshire. The discovery of Au at Wiluna in 1896 attracted prospecting parties to the Mount Keith region. During the period 1911 to 1923, 7946 ounces of Au from 9875 t of ore were produced from an outcropping quartz reef west of Mount Keith. Jim Jones was the manager of Mount Keith Station in the 1960s and he was also a keen amateur prospector. His interest in Ni was initiated by the discovery of the Kambalda deposit by Western Mining Corporation in 1966 (see Section 5.2.4). Jones drilled a RC drill-hole to test a gossanous ultramafic rock, and disseminated Ni sulphides were obtained in talc-carbonate ultramafic cumulate rock at 70 m—a discovery that was later called the Golgotha prospect. Metals Exploration commenced a detailed exploration program of the region in January 1969. The very poor outcrop and deep weathering profile necessitated reliance on magnetic data to define ultramafic bodies. In November 1969, diamond drill-hole MKD5 intersected 176 m @ 0.60% Ni highlighting the economic potential of the Mount Keith deposit. Mining was delayed for two decades by low-metal prices and metallurgical problems. Western Mining Corporation Resources Limited acquired ownership of the project in 1993 and begun production of the world-class resource in October 1994.

## *Economic significance*

The Agnew–Wiluna greenstone belt in the Yilgarn Craton Western Australia is the most highly Ni endowed komatiite belt in the world, containing two world-class nickel deposits, Mount Keith and Perseverance, and several smaller economic deposits (Fiorentini et al., 2012). The Agnew–Wiluna greenstone belt is better endowed than the next best nickel-bearing komatiite belt by a factor of 5 (Hoatson et al., 2006; Mamuse et al., 2010). Over thirty Ni-Cu±PGE deposits (Ni accounts for well over 90% of the value of the ore in all cases) occur along the length of the Agnew–Wiluna greenstone belt, extending from Honeymoon Well in the northwest to Sinclair in the southeast (Figure 6.21). All the Ni deposits are hosted by komatiitic olivine-rich cumulate rocks, and they occur in groups associated with specific komatiite facies (Leshner and Keays, 2002). In addition to the Mount Keith (Cliffs) and Perseverance areas, the major deposits are predominantly Type 3.B, low-grade disseminated orebodies in the Honeymoon Well (Harrier, Hannibals, Corella, Wedgetail, Harakka) and Yakabindie (Betheno, Six Mile Well, Goliath, David, Kathleen East) areas. High-grade Type 3.A ores are found in the Cosmos (Cosmos, Tapinos, Prospero) and Waterloo areas (Waterloo, Amorac), and also at Sinclair (Fiorentini et al., 2012).

The disseminated Ni sulphide Type 3.B ores also have relatively lower grades of PGEs (<0.5 g/t) and Ni (<1%) compared to the high-grade 3.A ores represented in the Kambalda-type deposits. Barnes (2006) and Barnes et al. (2011a,b; 2012) have reviewed the main Ni-Cu±PGE sulphide deposits of the Agnew–Wiluna greenstone belt.

## *Geological setting*

The Mount Keith Ultramafic Complex hosts the Mount Keith Ni sulphide deposit in a narrow section of the Agnew–Wiluna greenstone belt in the northern part of the Eastern Goldfields Province of the

Yilgarn Craton (Figure 6.21). This belt is one of the most highly Ni-endowed domains in the world (Hronsky and Schodde, 2006), and contains several world-class Ni-Cu-(PGE) deposits, including two of the largest known komatiite-hosted ore deposits at Mount Keith and Perseverance. The Agnew–Wiluna greenstone belt has a north-northwest to south-southeast trend and is bounded by large terrane-scale faults and granitoid bodies. The belt is at its most attenuated in the Mount Keith area with a maximum thickness of 6 km and it also changes strike here, possibly indicating the influence of some underlying primary structural control (Grguric et al., 2006). The Agnew–Wiluna greenstone belt comprises a ~2.7 Ga sequence of felsic-to-intermediate volcanic and volcanoclastic rocks, sulphidic chert, carbonaceous shale, and laterally variable komatiite including cumulates, thin spinifex-textured units, and komatiitic basalts (Barnes et al., 2011). The komatiite stratigraphy of the Mount Keith deposit can be correlated for over 100 km along strike from the Perseverance deposit in the south to the Honeymoon Well deposit in the north of the greenstone belt (Figure 6.21). The relationships of disseminated mineralisation with rock types and volcanic facies for Mount Keith are summarised in the schematic komatiite flow field and section A–B of Figure 6.24. Regional metamorphism in the Mount Keith region attained mid-greenschist facies (Barrett et al., 1977).

### *Mineralisation environment*

The volcanological architecture of the Mount Keith Ultramafic Complex has been interpreted by Fiorentini et al. (2007b) and Rosengren et al. (2005; 2007) to be a subhorizontal, subvolcanic sill comprising a central conduit acting as a feeder to overlying komatiite flows. This ~650 m-thick serpentinised ultramafic sill, which consists of adcumulus-textured pods and lenses, grades laterally and vertically into an upper zone of olivine orthocumulate, spinifex-textured flows, and other minor ultramafic and gabbroic lithologies. Footwall rocks to the sill are dominantly fragmented dacitic to andesitic volcanics interpreted as submarine lavas and breccias as associated autoclastic facies (hyaloclastite, autobreccia). Hanging wall units include dacitic to andesitic volcanics similar to the felsic footwall lavas, minor thin pyritic chert and mafic units, and rare sulphidic graphitic pelite.

Grguric et al. (2006) divided the MKD5 orebody into seven primary lithological units, the boundaries of which are generally parallel to the regional trend of the Mount Keith Ultramafic Complex (Figure 6.25). The units dip steeply towards the west and they generally become more magnesian and closer packed olivine cumulates from west to east, indicating a westward-facing direction for the complex. The main ore domain in the MKD5 orebody is unit 104 where sulphides are crudely layered throughout on a scale of tens of centimetres. Disseminated Fe-Ni-(Cu) sulphide blebs occur interstitial to former olivine crystals, and are concentrated in lensoidal ultramafic bodies. Barnes (2006) described the sulphides as interstitial blebs ranging in size from 40 µm to 1.5 mm. These blebs consist of aggregates of Ni-Fe sulphide grains in some cases surrounded by a corona of magnetite. The sulphide mineralogy through the orebody consists almost entirely of pentlandite, pyrrhotite, and minor chalcopyrite, with trace pyrite and minor magnetite developed as rims and fracture fills. Pentlandite forms coarse, blocky grains, which in places appear to be fragmented and infilled with pyrrhotite. This texture is possibly attributable to volume expansion of the host rock during serpentinisation.

The dominant ultramafic protolith rocks of the Mount Keith Ultramafic Complex are olivine cumulates (dunite, peridotite) that have been pervasively altered to serpentine, with less abundant talc carbonate assemblages (Barnes, 2006; Grguric et al., 2006). The rocks are lizardite-brucite-hydroxycarbonate serpentinites with minor chlorite and carbonate, and accessory relic igneous chromite with secondary magnetite overgrowths. Minor associated rocks include pyroxene±olivine cumulates (pyroxenite) and plagioclase-pyroxene±olivine±quartz cumulates (gabbro). The ultramafic rocks in the complex are Al-undepleted with near chondritic  $Al_2O_3/TiO_2$  ratios of ~20 and olivine compositions from  $Fo_{87}$  to  $Fo_{90.7}$ .

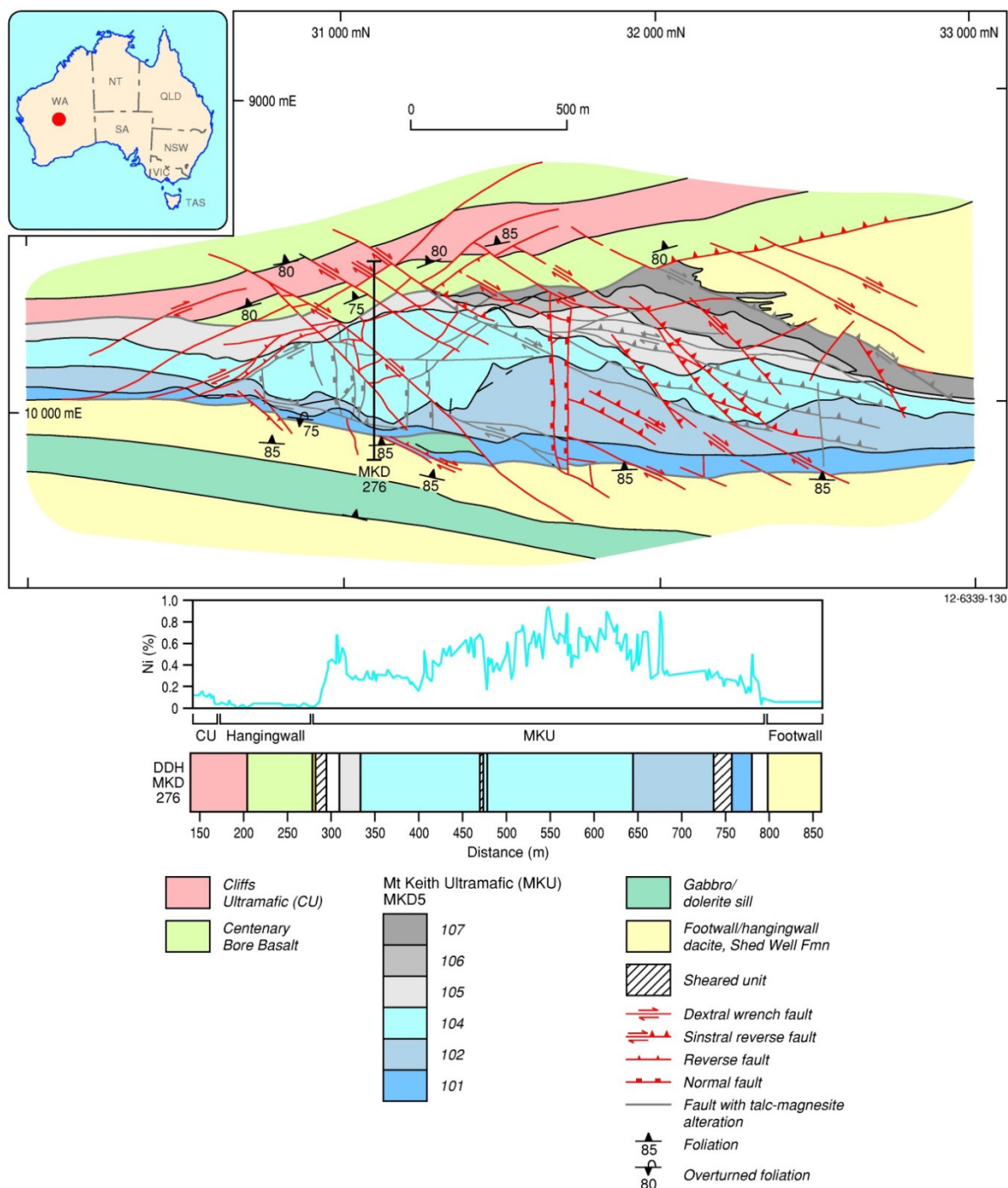


Figure 6.25 Schematic plan view showing primary lithologic units of the Mount Keith Ultramafic (MKU) Complex, Agnew–Wiluna greenstone belt, Yilgarn Craton, Western Australia. Plan is constructed at 400RL (ground surface is at 544RL), and north is orientated to the right. Figure below shows the lithologic units of MKU projected to 300RL and the variation of nickel concentrations for DDH MKD 276. Modified from Hayward (2004), Rosengren (2004), and Barnes (2006).

### PGE mineralisation

The diverse mineralogy of the Mount Keith deposit is the result of primary magmatic, secondary hydrothermal, and weathering processes (Grguric, 2003; Grguric et al., 2006). Most of the primary magmatic Ni-Cu±PGE sulphides are confined to the central olivine adcumulate zone. The sulphides

are typically disseminated and layered, with Ni grades ranging from 0.1% to 1.0% and averaging 0.6%. Pyrrhotite, pentlandite, magnetite, pyrite, chalcopyrite, and chromite are the major phases in ores grading more than 1% Ni, whereas millerite, heazlewoodite, godlevskite, and polydymite occur in ores less than 1% Ni. Supergene minerals often include violarite, pyrite, and marcasite. Magmatic sulphide mineralisation in unit 102 of the MKD5 orebody occurs as discrete pods that appear to plunge steeply and are associated with elevated PGE (combined 100 ppb to 700 ppb) and Cu (100 ppm to 900 ppm) concentrations. Arsenic-bearing minerals, such as gersdorffite (NiAsS), nickeline (NiAs), cobaltite (CoAsS), and maucherite (Ni<sub>11</sub>As<sub>8</sub>), often replace pyrrhotite and pentlandite and are paragenetically late. In areas of high arsenic, the PGEs occur in minute amounts as discrete PGMs, namely sperrylite (PtAs<sub>2</sub>) and irarsite (Ir,Ru,Rh,Pt)AsS (Grguric, 2003; Grguric et al., 2006). In other parts of the Mount Keith deposit, the PGEs typically constitute a trace component (100 ppb to 200 ppb combined) with the highest concentrations associated with the common sulphide phases. Low levels of Co (100 ppm to 200 ppm) characterise the Mount Keith deposit, where it is hosted predominantly in pentlandite, pyrite, and hypogene violarite. Copper is also a minor component (100 ppm to 600 ppm), and it is represented by chalcopyrite, bornite, native copper, and tochilinite-valleriite series minerals. Nickel enrichment of the sulphides occurred during the re-equilibration of olivine with a residual sulphide-rich melt prior to complete crystallisation, and also during the serpentinisation of olivine that accompanied greenschist-facies metamorphism. Rödsjö (1999) and Grguric et al. (2006) have summarised the mineralogy and geochemistry of the primary mineralisation and Butt and Nickel (1981) and Butt et al. (2006) have reviewed the supergene zone.

Dowling and Hill (1992) documented the distribution of PGEs in their designated Western and Central ultramafic units at Mount Keith. The units include thin flows up to 25 m-thick, with spinifex-textured varieties common. Olivine-bearing spinifex-textured flows from the Western ultramafic unit are consistently more magnesian ( $\geq 32\%$  MgO vs 26%–30% MgO) than their counterparts from the Central Unit and contain significantly lower amounts of all PGEs. The olivine-bearing flows exhibit irregular and complex PGE distribution patterns. Platinum, Pd, and Rh exhibit incompatibility with respect to olivine, and Ir and Ru behave in both a compatible and incompatible manner. Higher incompatible PGE concentrations in pyroxene spinifex-textured flows, over their olivine-rich counterparts are consistent with a genetic link by olivine fractionation. Negative Pt anomalies (relative to abundances of Rh and Pd) characterise all olivine-bearing flows. The pyroxene-bearing flows do not exhibit this anomaly, suggesting the possible involvement of a Pt metal phase.

A detailed study of PGE and trace-element concentrations through the Mount Keith Ni orebody by Barnes et al. (2012) revealed a complex trend of covariance between the original cumulus components of a thick sequence of almost pure olivine-sulphide liquid accumulates. The geochemical profile divided the ultramafic stratigraphy into several chemostratigraphic zones based on original olivine compositions (Mg#) and PGE/sulphide ratios (Pt/S). Inferred olivine compositions range from about Fo<sub>92</sub> to Fo<sub>94.6</sub>, and show a broad decrease up the sequence complicated by numerous reversals, revealing crystallisation in an open-conduit system. PGE and Ni tenors of Mount Keith sulphide ores have typical values similar to Type 3.A ores from the Kambalda Dome. Tenors (recalculated to 100 weight % sulphides, and all units in ppb, except for Ni) for the various chemostratigraphic zones range from: 370–1540 Pt; 970–3670 Pd; 100–460 Ir; 170–460 Rh; 710–1260 Ru; and 12–22% Ni. Platinum, Pd, and Rh tenors are very strongly correlated, but the IPGEs (Ir and Ru) less so. Tenor variations are predominantly controlled by variations in the magma:sulphide ratio R (100–350) and minor variance from equilibrium crystallisation trends in the parent magma. Ratios of the PGEs to one another are similar to those in the host komatiite magma, with the exception of Pt, which is systematically depleted in ores, relative to Rh and Pd and relative to the host magma, by a consistent

factor of about 2 to 2.5. The consistent nature of this depletion, and particularly the very strong correlation between Pt, Pd, and Rh in the Mount Keith deposit, argue that this depletion is a primary magmatic signal, and is not due to alteration.

Barnes et al. (1988a,b; 1995) have documented the PGE geochemistry of the major ore types for the Perseverance and Rocky's Reward Ni deposits (~65 km south of Mount Keith), which have similar geological settings to the Mount Keith deposit. The Perseverance deposit consists of a central dunite lens, 700 m-thick by 3 km-wide, flanked by olivine orthocumulate and spinifex-textured komatiite. For massive, matrix, and vein-filling sulphide ores, maximum concentrations (recalculated to 100 weight percent sulphides, and all units in ppb) are: 410, 210, 360 Pt; 830, 300, 1 200 Pd; 260, 50, 32 Os; 210, 36, 28 Ir; 150, 20, 49 Rh; 590, 92, 110 Ru; and 110, 27, 23 Au, respectively. The chalcophile element (Ni, Ir, Ru, Pt, Pd, Au, and Cu) concentrations in spinifex-textured flows flanking the central dunite (A-zone samples) are typical of komatiites (Barnes et al., 1988a,b; 1995). Komatiites from the Perseverance mineralised units and from Rocky's Reward show evidence of depletion of the more strongly chalcophile PGEs relative to Ni and Cu. This feature is also evident in massive and matrix sulphide ore samples, although less evident in the main Perseverance cloud sulphides. The major element, PGE, and REE chemical data is consistent with derivation by combined assimilation of felsic material and crystallisation of olivine from a primitive komatiitic magma. The geochemical features of mineralised and unmineralised basal komatiite units indicate the effects of crustal assimilation. This is consistent with genetic models for Ni sulphide deposits, based largely on Kambalda, which emphasise the role of thermal erosion of sulphidic footwall sediments.

### *Age of mineralisation*

The age of the mineralised komatiitic stratigraphy at Mount Keith is Archean, and has previously been considered of similar age (~2705 Ma) by analogy with and the proposed episode of komatiite volcanism recorded elsewhere in the Eastern Goldfields Province at ~2705 Ma (Nelson, 1997). Hoatson et al. (2006, 2009a,b) have compiled U-Pb zircon and baddeleyite ages of komatiite and associated rocks throughout the Yilgarn Craton and other parts of Australia. Most Ni sulphide deposits in the Norseman–Wiluna greenstone belt fall within a very narrow age span centred at 2705 million years, part of a global komatiite event within 10 to 15 million years. Fiorentini et al. (2012) describe SHRIMP U-Pb ages on magmatic zircon and titanite grains from the Mount Keith Dacite (which has primary contact relationships with the mineralised Mount Keith ultramafic unit) in the footwall and hanging wall of the unit as, respectively,  $2713 \pm 6$  Ma and  $2706 \pm 6$  Ma (Fiorentini et al., 2005). In all samples, numerous detrital and xenocrystic zircon grains also yield a wide range of ages from ~2740 Ma to ~2730 Ma (Fiorentini et al., 2005). At Albion Downs, ~25 km north of Mount Keith, where the dacitic volcanic sequence in the footwall and hanging wall of the unit is texturally best preserved, SHRIMP U-Pb ages on magmatic zircons are  $2711 \pm 6$  Ma (Fiorentini et al., 2005). These ages are within error of the Re/Os isotopic age of  $2706 \pm 36$  Ma obtained for the Mount Keith ultramafic unit by Foster et al. (1996).

### *Genesis*

Mount-Keith-type deposits were formerly classified as 'intrusive-dunite associated' (Marston, 1984), 'dunite-hosted deposits' (Donaldson et al., 1986), and 'type 2 deposits' (Dowling and Hill, 1998). Much controversy has related to their origin with interpretations ranging from extrusive (i.e., slowly-cooled bodies that are integral parts of the extrusive komatiite stratigraphy: Hill et al., 1996; Barnes et al., 1999) to more intrusive origins involving subvolcanic lava feeder zones or sill-like emplacement into a volcanic pile (Rosengren et al., 2005). On the basis of type and distribution of lithologies, igneous

textures, and whole-rock geochemistry, Barnes et al. (1999) suggested that the Mount Keith body represents a large lava pathway or lava tube that experienced a prolonged period of continuous eruption and flow of komatiite lava. The relationships of disseminated mineralisation with rock types and volcanic facies are summarised in the schematic komatiite flow field of Figure 6.24.

The petrographic-geochemical studies of Barnes (2007) and Barnes et al. (2011a,b; 2012) indicated that the Mount Keith Ultramafic Complex formed in a dynamic open magmatic system where successive (or continuous) pulses of magma fluctuated in composition during accretion or accumulation of the cumulus pile. Fluctuations in olivine and sulphide compositions reflect the processes of crystallisation in a high-flux magma conduit. Based on microtextural features of olivine and sulphide droplets, accumulation of the ore zone involved a combination of *in situ* nucleation and growth of olivine at the floor of the flow coupled with mechanical sedimentation and deposition of transported sulphide droplets and olivine. Sulphur isotopic data indicate the S component of the komatiite-hosted ores was derived from crustal sources. Non-mantle signatures are evident both in  $^{34}\text{S}/^{32}\text{S}$  and in  $^{33}\text{S}/^{32}\text{S}$ , which shows evidence of mass-independent atmospheric fractionation (Fiorentini et al. 2011). Externally derived S also accounts for the very high S/Se ratios in the ores, and lithophile trace element data also support extensive assimilation of felsic country rocks (Fiorentini et al., 2007b).

Fiorentini et al. (2012) interpreted the Mount Keith Ultramafic Complex (Figure 6.25) to represent a continuous sill extending along the Agnew–Wiluna greenstone belt from north of Albion Downs to Perseverance. The sheet or tabular sill in the Wiluna area (Fiorentini et al., 2007a) is probably the lateral equivalent of the Mount Keith body. The lens geometry of the dunites is interpreted to reflect proximal channelisation within a laterally extensive sill, whereas sheet or tabular sills represent more distal facies. Channelisation of sills was a near-vent process that involved high-magma flux and turbulent flow. In the Mount Keith open-cut mine, there are abundant apophyses exposed along the top and bottom contacts of the Mount Keith dunite that confirm an intrusive origin (Rosengren et al., 2005). Fiorentini et al. (2012) exclude an invasive flow origin because of the coherent nature of the felsic volcanic rocks. These authors also note that pyritic exhalative sulphides of inferred VMS origin are spatially associated with the axis of the Agnew–Wiluna greenstone belt and felsic volcanic rocks and are absent from the northern, southern, and lateral portions of the Agnew–Wiluna greenstone belt. Fiorentini et al. (2012) contend that these pyritic massive sulphide lenses are the main source of S in komatiite-hosted Ni-Cu-(PGE) deposits of the Agnew–Wiluna greenstone belt. Similarly, Bekker et al. (2009) used multiple S isotopes to indicate that pyritic exhalative sulphides, and not sedimentary sulphides, were probably the source of S for komatiitic Ni-Cu-(PGE) deposits.

Barnes et al. (1995) have also modelled compositions of komatiitic liquids, sulphides, and cumulus olivine at the nearby Perseverance deposit to indicate varying degrees of batch equilibration between komatiite magma, olivine, and assimilated sulphidic sedimentary rocks. Models involving combined assimilation and fractional crystallisation, in which olivine and sulphide are fractionally segregated as they form, are much less successful at matching the data. This suggests that the mineralisation is due to wholesale assimilation of floor rocks close to the site of sulphide accumulation.

A study of the major komatiitic provinces in the world by Hoatson et al. (2006) indicated that fertile komatiitic sequences for Ni sulphides are generally of late Archean (~2700 Ma) or Paleoproterozoic (~1900 Ma) age, have dominantly Al-undepleted ( $\text{Al}_2\text{O}_3/\text{TiO}_2 = 15\text{--}25$ ) chemical affinities, and often occur with S-bearing country rocks in dynamic high magma-flux environments, such as dunitic compound sheet flow facies (Mount Keith-type), or compound sheet flows with internal pathways facies (Kambalda-type).

## *Key references*

- Marston (1984): Ni sulphide deposits of Western Australia; Mount Keith-type deposits; stratigraphy; structure; mineralisation; exploration results; mining companies.
- Gresham and Loftus-Hills (1981): geology of Ni-Cu sulphide deposits in Yilgarn Craton; exploration methods and mining.
- Barnes et al. (1988a,b): structure and stratigraphy of Agnew komatiite Ni sulphide deposit; sulphide geochemistry; distribution and mineralogy of PGMs; PGE contents of massive, matrix, disseminated, and remobilised ores.
- Lesher (1989): komatiite-associated Ni sulphide deposits; stratigraphy; mineralisation; Mount Keith-type deposits; volcanology; petrogenesis.
- Cowden and Roberts (1990): overview of komatiite hosted Ni sulphide deposits; stratigraphy; exploration; resources.
- Gresham (1990, 1991): discovery of Mount Keith-type deposits; exploration philosophy and techniques; mining practices.
- Dowling and Hill (1992): distribution of PGEs in fractionated Archean komatiites; Western and Central ultramafic units in Mount Keith region; olivine-bearing flows exhibit irregular and complex PGE distribution patterns; Pt, Pd, and Rh show incompatibility with respect to olivine, and Ir and Ru behave in both a compatible and incompatible manner.
- Barnes et al. (1995): whole-rock major and PGE geochemistry; geology of Perseverance and Rocky's Reward deposits; discriminating barren from mineralised komatiite; fractionation and contamination models.
- Foster et al. (1996): Re-Os isotopic system; comparing isotopic data for Mount Keith, Perseverance, and Kambalda deposits; crustal contamination; ore genesis; model precludes significant bulk assimilation of sulphidic sediments; ore-forming komatiites from a depleted upper-mantle source.
- Hopf and Head (1998): geology of Mount Keith Ni deposit; stratigraphy; structure; mineralisation.
- Rosengren et al. (2005, 2007): emplacement origins for the komatiitic-dunite hosted Mount Keith deposit; internal stratigraphic architecture of the MKD5 orebody; volcanology; structure; stratigraphy; mineralisation; Mount Keith komatiitic dunite bodies are subvolcanic sills emplaced within and below an extrusive komatiite pile.
- Barnes (2006): komatiite-hosted deposits of the Yilgarn Craton; Mount Keith-Black Swan-Perseverance-type deposits; stratigraphy; lava channels; mineralisation; petrogenesis.
- Butt et al. (2006): weathering history; supergene and lateritic enrichment processes; gossan formation; mineralogy and geochemistry of supergene zone; Mount Keith deposit; Ni sulphide deposits of Western Australia.
- Grguric et al. (2006): history and discovery, geology, mineralogy, and processing of the Mount Keith and Yakabindie orebodies.
- Hoatson et al. (2006): classification of Mount Keith-type deposits; stratigraphy; geochronology; mineralisation; Ni resources, genesis; potential for new discoveries.
- Barnes (2007): cotectic precipitation of olivine and sulphide liquid; komatiite magmas; genesis of komatiite-hosted disseminated Ni sulphide mineralisation at Mount Keith and Yakabindie; Western Australian Ni deposits; geochemical modelling.

- Fiorentini et al. (2007b): emplacement and genesis of Mount Keith and Sarah's Find Ni–Cu–PGE deposits; PGEs; chilled margin composition; disseminated and massive sulphides; alteration and metasomatism; petrogenesis.
- Barnes and Fiorentini (2008): Ir, Ru, and Rh abundances in komatiites; Mount Keith–Perseverance-type deposits; alloy saturation; partition coefficients; thermodynamic modelling.
- Locmelis et al. (2009): unusual S-poor PGE mineralisation at Mount Clifford; PGEs in lower part of 1000-m-thick komatiitic dunite body; PGEs associated with base-metal sulphides and show off-set distribution patterns; PGMs include Pd antimonides, Pt-dominant PGMs, and Pt-bearing Ni antimonides.
- Thebaud et al. (2009): tectonostratigraphic controls; localisation of Archean komatiite-hosted Ni-sulphide deposits in the Yilgarn Craton; Mount Keith-type Ni deposits; structural framework of the Yilgarn Craton and emplacement of Ni deposits.
- Fiorentini et al. (2010): Mount Keith-type deposits; PGE geochemistry of mineralised and non-mineralised komatiites; depletion and enrichment of PGEs; physical volcanology; ore-forming processes; exploration potential.
- Barnes et al. (2011a,b): Betheno–Mount Keith deposits; Ni-rich Fe-Ni sulphides in komatiitic dunite; PGEs; Fe-Ni-S phase equilibria; distribution coefficients; primary magmatic origins.
- Barnes and Liu (2012): mobility of PGEs in komatiitic rocks; Mount Keith–Black Swan–Perseverance-type disseminated and massive sulphides in dunite; petrogenetic tracers; exploration potential.
- Barnes et al. (2012): PGE and Ni concentrations of Mount Keith deposit; magmatic sulphides; chemostratigraphic zones; olivine compositions; R factor; magmatic versus alteration processes.
- Fiorentini et al. (2012): regional sulphur isotope study; genesis of komatiite-hosted nickel deposits; Agnew–Wiluna greenstone belt; district-scale controls on Ni sulphide mineralisation.
- Gole et al. (2013): emplacement origin for Mount Keith ultramafic body; structural modifications; thick olivine cumulate pile; spinifex textures and ponded fractionated cumulates at top of Mount Keith ultramafic unit; extrusive lava mineral system rather than a sill origin.

#### **6.4.3.3 Deposit Type 3.C: PGE-enriched Ni-Cu sulphides associated with komatiitic and tholeiitic rocks**

##### *Overview*

In November 2004, Western Mining Corporation Limited (now BHPB) announced a high-grade massive sulphide intersection (5.8 m @ 3% Ni, 2% Cu, 5.3 g/t PGEs) at the Olympia Prospect, Collurabbie, near the northern margin of the Yilgarn Craton. This high-value-type of mineralisation has not been previously documented in the Yilgarn Craton and it defined a new metallogenic province in the Gerry Well (also called Duketon) greenstone belt. The Olympia Prospect consists of a steeply dipping sequence of komatiitic and ultramafic rocks within a dominantly basaltic sequence. The igneous rocks have chemical affinities with both komatiitic and tholeiitic mineral systems. Structurally remobilised massive sulphides have the highest grades of Ni, Cu, Co, Au, and PGEs and are spatially associated with matrix and disseminated sulphides near contacts of the ultramafic rocks. The high concentrations of PGEs and low Ni/Cu ratios (<3) that characterise the Collurabbie sulphides are not typical of other komatiite-hosted deposits in the Yilgarn Craton. However, they are features seen in the Raglan Ni-PGE komatiite deposit of northern Quebec (average grades 2.7% Ni, 0.8% Cu, and 4 g/t PGEs: Seabrook et al., 2004) and in the Kuhmo Ni prospect in eastern Finland (Vulcan Resources

Limited, 2005). Two other Ni prospects in northern Western Australia—Beasley and Daltons—have similar geological settings to Collurabbie. The Beasley Ni-Cu-PGE prospect (AusQuest Limited, 2003, 2004, 2006) in the Hamersley Basin contains mineralised komatiite rocks interpreted to be comagmatic with basaltic rocks of the Late Archean (~2770 Ma) Fortescue Group—an extensive platform sequence on the southern margin of the Pilbara Craton. The mineralised basaltic komatiite sequence is associated with andesitic basalt and gabbroic sills. A typical 150-m-thick flow is shown in section E–F of Figure 6.24. Magmatic sulphides are concentrated in serpentinised olivine cumulates within the lowermost komatiite unit. Gossans near the base of an interpreted channel flow facies have unusually low Ni/Cu ratios and elevated PGE concentrations (1.8% Ni, 0.6% Cu, 3.4 g/t Pd, 1 g/t Pt, and 1.1 g/t Au) for komatiitic systems. High-Mg ultramafic sequences with very high metal grades (up to 13.5% Ni, 17.5% Cu, 52 g/t PGEs+Au) occur at the Daltons Ni-Cu-PGE prospect in the southeast Pilbara Craton (Giralia Resources NL, 2004). Basal massive and disseminated sulphides in peridotite and remobilised sulphides in a footwall chert unit have elevated PGEs and low Ni/Cu ratios (<4) similar to the Beasley and Collurabbie-Olympia prospects.

#### *Australian deposits/prospects/hosts*

Collurabbie (Yilgarn Craton, WA); Dalton (Pilbara Craton, WA); ?Beasley (Hamersley Basin, WA).

#### *Significant global example(s)*

Raglan (Canada), Kuhmo and Keivitsansarvi (Finland).

#### *Type example in Australia*

Collurabbie, Western Australia.

#### *Location*

Longitude 122.216003°E, Latitude -26.886450°S; 1:250 000 map sheet: Kingston (SG 51–10), 1:100 000 map sheet: Collurabbie (3344); ~200 km north of Laverton, Western Australia.

#### *Geological province*

Burtville Terrane, Eastern Goldfields Superterrane, Yilgarn Craton, Western Australia.

#### *Resources*

Unknown.

#### *Current status and exploration history*

Prospect with advanced exploration. In July 2003, disseminated Ni-Cu-PGE sulphide mineralisation was discovered in the first aircore drilling program at Collurabbie. The announcement by WMC Limited in November 2004 of a high-grade massive sulphide intersection (5.8 m @ 3% Ni, 2% Cu, 5.3 g/t PGEs) at the Olympia prospect highlighted the PGE potential of Archean greenstone sequences near the northeastern margins of the Yilgarn Craton. Follow-up drilling at this greenfields discovery indicated the mineralisation extended over a strike length of at least 7 km. Aircore drilling in 2004 intersected geochemical dispersion halos interpreted to be derived from Ni sulphides. Subsequent deep drilling confirmed the presence of significant Ni-PGE sulphides at depth. Regional exploration in the previously poorly explored Gerry Well greenstone belt defined a 40-km-long prospective ultramafic belt that contained a number of other spatially close and similar Ni-Cu-PGE prospects (e.g., Agora, Argus, Leros, Naxos, Paros, Rhodes East, Spartacus, Troy, and Zeus: Figure 6.26). The next

ultramafic unit to the east of Olympia contains the Paros and Naxos prospects, and is interpreted by Falcon Minerals to have potential for medium- to high-grade Ni, Cu, and PGEs. The strike length of the prospective ultramafic stratigraphy is around 2.5 km and it is open to the south. Another major ultramafic belt further east hosts the Zeus prospect. Follow-up drilling at Olympia and other nearby prospects in 2005 and 2006 returned lesser intersections of sulphides and this, coupled with a change of management (from WMC to BHPB) led to the suspension of mineral exploration. Regis Resources Limited (2007a,b) highlighted the regional extent of sulphides at Collurabbie when they announced a drill intersection of 153 m of sulphides at their Mocha Prospect (Figure 6.26), some 35 km south of the Olympia prospect. The intersection comprised four zones of massive sulphides (mainly pyrrhotite and pyrite) totalling 17.6 m with matrix and disseminated sulphides in a pyroxenite-diorite host. In 2009, Falcon Minerals Limited negotiated a new agreement with BHPB and recommenced diamond drilling in June 2010. Falcon completed three drilling campaigns (25 holes for 7472 m) to test the continuity and better define the geometry of massive and matrix sulphide mineralisation at Olympia and to test electromagnetic conductors and embayment positions within ultramafic lithologies at the Spartacus prospect, 6 km north-northwest of Olympia. At Olympia, massive and matrix Ni-Cu-PGE sulphide mineralisation up to 9-m-thick was detected over a 300 m-strike length. The Olympia deposit is small and is regarded as sub-economic. At Spartacus, low-grade disseminated Ni-Cu-PGE sulphides are widespread throughout an ultramafic host. Broad zones up to 20-m-thick consistently return grades around 0.4% Ni. This mineralisation appears continuous over several strike kilometres, but at these grades it is regarded in 2014 as sub-economic. Higher-grade disseminated Ni mineralisation occurs further north in the same host rock at the Troy prospect (CLD040: 20 m @ 0.68% Ni, 0.28% Cu, and 0.62 g/t PGEs). Future exploration will shift away from the Olympia prospect and focus on the regional Olympia trend which has only received limited attention in the past. In particular, areas will be targeted where the Olympia trend intersects northeast-trending faults as these structures are considered important in the Olympia mineralising event. Falcon Mineral Limited considers there is significant potential in the district to discover further massive Ni-Cu-PGE sulphides. Major exploration methods used by various companies in the Gerry Well greenstone belt include aeromagnetics, ground magnetics, electromagnetics, down-hole electromagnetics, diamond and aircore drilling, regolith mapping, soil geochemistry, and 3-D modelling of mineralised zones.

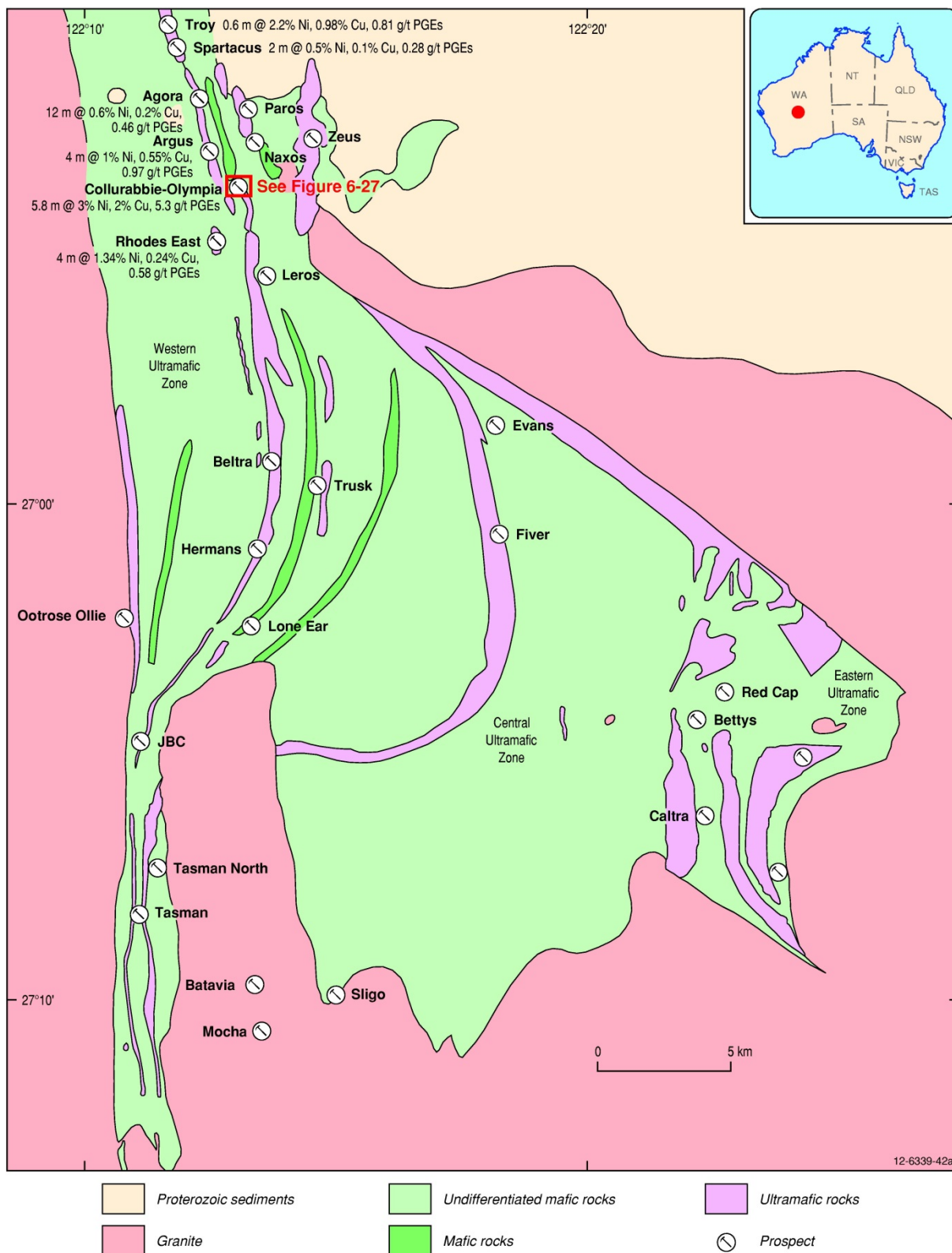


Figure 6.26 Regional geological setting of Ni-Cu-PGE sulphide prospects in the northern part of the Gerry Well greenstone belt of the Burtville Terrane, Yilgarn Craton, Western Australia. The PGE-enriched Collurabbie-Olympia prospects are highlighted in the northern part of the greenstone belt. The drill-hole section for the Olympia prospect is shown in Figure 6.27. Modified from Regis Resources NL (2007b).

### *Economic significance*

The delineation of massive sulphides at Collurabbie has highlighted the potential of poorly exposed Archean greenstone sequences (Figure 6.21 and Figure 6.26). A thin layer of transported sand and younger Proterozoic sedimentary rocks overlying the basement rocks has impeded exploration for Ni sulphides in this area. The group of prospects at Collurabbie are hosted by Archean high-Mg ultramafic sequences that contain multiple zones of sulphides with unusually high abundances of PGEs (2 to 5 g/t Pt+Pd) and Cu (up to 2%) relative to other typical komatiite deposits (e.g., Kambalda, Mount Keith). In addition, their distinctly low Ni to Cu ratios of less than 3 are more typical of tholeiitic mafic magmatic systems rather than those associated with komatiitic rocks. The discovery of Collurabbie is therefore significant in that it represents a style of PGE mineralisation not previously encountered in Australia, and it has highlighted a potentially new Ni-Cu-PGE province. Globally there are very few komatiitic-associated deposits enriched in PGEs, with perhaps the Raglan Ni sulphide deposit in Canada (see Genesis below) being a Proterozoic analogue of Collurabbie.

### *Geological setting*

The Collurabbie Ni-Cu-PGE prospect is located in the Gerry Well greenstone belt in the Burtville Terrane (northeastern part of the Eastern Goldfields Superterrane). The geological setting of this unusual deposit is not well documented, with information limited to industry reports, a regional aeromagnetic interpretation (Whitaker and Bastrakova, 2002), and two petrological studies that investigated Ru signatures in chromite from komatiitic rocks (Locmelis et al., 2011, 2013; Bertuch, 2004). Two parallel zones of high-amplitude linear aeromagnetic anomalies trending north-northwest define the distribution of the prospective ultramafic-mafic stratigraphy. These regional anomaly trends indicate strike extensions of the stratigraphy persist northwards unconformably beneath Proterozoic sedimentary rocks of the Yerida and Earraheedy basins (Hoatson et al. 2006). In the vicinity of Olympia prospect, the anomalies are narrow (<1 km wide), but these broaden (2 km to 5 km) significantly toward the north. The Olympia Prospect at Collurabbie consists of a parallel series of narrow ribbon-like bands of komatiitic and ultramafic rocks that steeply dip towards the west within a dominantly basaltic sequence (Figure 6.27). The mafic-ultramafic stratigraphy consists of clastic rocks, basaltic hyaloclastic breccia associated with pillowed basalt and basalt, fractionated gabbro, olivine gabbro, pyroxenite, and various olivine-bearing ultramafic rocks. Minor associated lithologies include carbonaceous shale, mafic and ultramafic schist, and sulphidic quartz veining. The mafic-ultramafic igneous rocks appear to have both komatiitic and tholeiitic affinities. Narrow zones of massive sulphides, often structurally remobilised and containing the highest grades of Ni, Cu, Co, Au, and PGEs, are spatially associated with matrix and disseminated sulphides near the contacts of the ultramafic and basaltic lithologies. The komatiitic basalts dominate and they occur as random spinifex-textured lava flows with MgO liquid compositions of ~16 wt % MgO (anhydrous). Oikocrystic peridotite, pyroxenite, and gabbro were emplaced as a layered subvolcanic sill (Bertuch, 2004). Locmelis et al. (2013) described two different horizons in the complex, one mineralised, the other apparently barren:

1. The Beta horizon hosts two different styles of mineralisation: (a) localised poddy stratabound basal matrix Ni-Cu-PGE mineralisation; and (b) laterally extensive disseminated hanging-wall Ni-Cu-(PGE) mineralisation (Bertuch, 2004). The Beta horizon is a narrow (<250 m) tabular sheet-like mafic and/or ultramafic horizon interpreted to represent a sill, which extends over a length of more than 5 km with a variable thickness between 10 m and 250 m.
2. The Gamma horizon is a sequence of differentiated spinifex-bearing layered and porphyritic komatiitic basalt flows that contain no known mineralisation. Ultramafic cumulates have high-MgO contents ranging from ~35 to 43 wt % MgO.

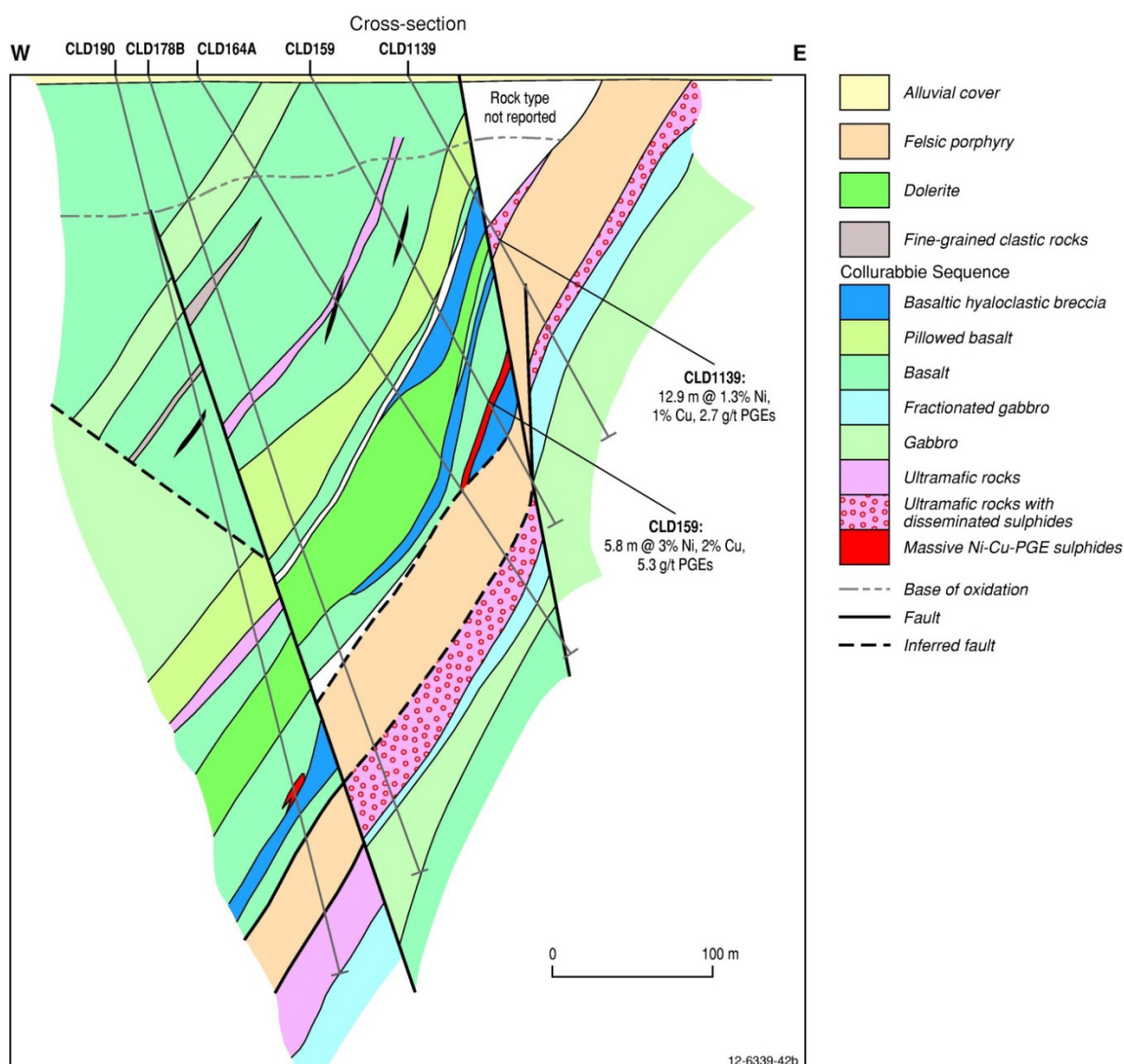


Figure 6.27 Schematic east-west cross-section of the Olympia Ni-Cu-PGE prospect at Collurabbie. Modified from Falcon Minerals Limited (2006).

### Mineralisation environment

Olivine-rich ultramafic komatiites, komatiitic basalts, high-MgO basalts, and basaltic lithologies. The Olympia Prospect consists of a parallel series of narrow ribbon-like bands of komatiitic and ultramafic rocks that steeply dip within a dominantly basaltic sequence. Narrow zones of massive sulphides, often structurally remobilised and containing the highest grades of Ni, Cu, Co, Au, and PGEs, are spatially associated with matrix and disseminated sulphides near the contacts of the ultramafic rocks.

### PGE mineralisation

Unusual PGE occurrences that are characterised by anomalously high concentrations of PGEs (up to 8 g/t Pt+Pd) associated with komatiitic and tholeiitic mafic-ultramafic igneous rocks (Table 6.9). This high-value-type of mineralisation has not been previously documented in the Yilgarn Craton. The PGEs are approximately an order of magnitude higher in concentration and the deposits have lower Ni/Cu ratios (<3) than those associated with more typical komatiitic sequences (e.g., Kambalda-type).

Table 6.9 Drill-hole intersections from the Olympia and Spartacus nickel-copper-PGE prospects.

Drill-hole	Ni%	Cu%	Ni/Cu	Pt+Pd (g/t)	Thickness (m)	From (m)
CLD122	2.93	2.60	1.13	2.24	0.08	200.18
CLD125	1.23	1.62	0.76	3.82	8.00	64.00
CLD127	1.00	0.55	1.82	0.97	4.00	82.00
CLD136	3.64	2.77	1.31	6.95	1.90	176.00
CLD136	3.67	3.12	1.18	7.78	1.10	184.90
CLD137	2.85	1.77	1.61	2.52	2.00	136.00
CLD139	1.33	0.95	1.40	2.69	12.86	131.64
CLD159	3.00	1.96	1.53	5.29	5.77	279.43
CLD195	1.44	0.44	3.27	2.37	0.56	231.55
CLD196	2.03	1.06	1.92	2.00	2.74	218.16
CLD197	1.13	0.73	1.55	1.34	1.42	268.27
CLD198	2.73	2.16	1.26	6.51	1.17	277.30
CLD199	1.05	0.89	1.18	1.74	5.32	226.27
CLD201	1.47	1.59	0.92	4.43	3.74	163.75
CLD201	1.29	0.79	1.63	2.98	0.44	170.01
CLD202	3.01	2.57	1.17	0.001	0.30	130.95
CLD202	1.74	1.05	1.66	2.37	3.82	153.88
CLD203	0.82	0.30	2.73	0.76	4.38	376.10
CLD208	0.96	1.25	0.77	3.49	2.0	143.0
CLD208	0.34	0.24	1.42	0.51	6.8	163.9
CLD211	2.21	1.82	1.21	3.53	3.8	189.8
CLD211	0.51	0.37	1.38	0.54	5.1	233.0
CLD213	0.94	0.66	1.42	1.89	0.5	320.0
CLD213	0.55	0.15	3.67	0.24	0.6	383.1
CLD215	0.36	0.14	2.57	0.25	8.4	215.6
CLD217	0.43	0.13	3.31	0.23	12.3	233.4
CLD218	0.43	0.20	2.15	0.33	5.2	190.8
CLD219	0.38	0.10	3.80	0.13	20.3	188.8

Source: Falcon Minerals Limited (2014).

### Age of mineralisation

The age of the komatiitic stratigraphy is probably Archean (~2705 Ma) by analogy with similar mineralised greenstone belts and Ni sulphide deposits in the Eastern Goldfields Superterrane that have been dated (Nelson, 1997; Hoatson et al., 2006; Hoatson et al., 2009a,b; Locmelis et al., 2013).

## *Genesis*

Very few detailed studies have been undertaken on the genesis of the Collurabbie prospects. Bertuch's (2004) geological mapping and petrological studies have shown the PGE-rich Ni-Cu sulphide mineralisation is hosted in an Archean layered subvolcanic ultramafic sill emplaced in a basaltic-dominant environment. Details of the emplacement of this ultramafic-mafic body into the volcanic stratigraphy may take considerable time if the Mount Keith deposit is a guide. The nature of the emplacement of the economically important ultramafic host body at Mount Keith (i.e., extrusive versus intrusive: Barnes, 2006) has been the subject of many detailed studies since its discovery in 1968, and remains controversial even today. The presence of hyaloclastic breccias and pillowed basalts in the Olympia stratigraphy suggest paleo-environments characterised by mafic volcanism under water, under ice, or the interaction of subaerial flows with the sea or other bodies of water. Fiorentini et al. (2011) indicated that the komatiitic basalts from Collurabbie have similar primitive mantle normalised PGE patterns to komatiites from elsewhere in the greenstone belt, but have a slightly higher Pd/Ir ratio attributable to the generally more fractionated, less magnesian nature of the suite. Very few komatiitic-hosted Ni sulphide deposits in Western Australia contain such high PGE contents as Collurabbie. A possible exception may be the Daltons Ni-Cu-PGE prospect in the southeast Pilbara Craton (Giralia Resources NL, 2004). High-Mg ultramafic lithologies have metal grades of up to 13.5% Ni, 17.5% Cu, and 52 g/t PGEs+Au. A narrow basal layer of massive and disseminated sulphides in peridotite and remobilised sulphides in a footwall chert unit have elevated PGEs and low Ni/Cu ratios (<4) similar to the Collurabbie-Olympia prospects. The high abundance of PGEs and low Ni/Cu ratios (<3) at Collurabbie are features characteristic of the ~1.9 Ga Raglan Ni-Cu-Co-PGE komatiite deposit in northern Quebec (average grades of 2.7% Ni, 0.8% Cu, and 4 g/t PGEs: Seabrook et al., 2004) and the ~2.8 Ga Kuhmo Ni deposits in eastern Finland (Vulcan Resources Limited, 2005). The distinctive chemical signatures of these Australian and overseas deposits could be a legacy of unusual parent-magma composition(s); mineralising systems that involved both komatiitic and tholeiitic components; and/or certain magmatic-crustal processes that operated during the ascent of the primitive magma(s) will only become apparent with further detailed investigations of these important deposits. In addition to the more typical komatiite-associated Ni deposits of the Yilgarn Craton (e.g., Kambalda- and Mount Keith-types), recent exploration at greater depths and in less traditional environments has defined an increasing number of deposits and prospects that have unusual settings and metal signatures (Hoatson et al., 2006). These include those komatiite deposits and prospects with exceptionally high Ni grades (e.g., Cosmos, Long, Flying Fox–T5, Spotted Quoll); with normal Ni/Cu ratios and high PGE grades (Waterloo); with low Ni/Cu ratios and high PGE grades (Collurabbie, Collurabbie South, Daltons). This diversity of mineralisation styles, which enhances the prospectivity of this magmatic association, is likely to expand in the future with the increasing emphasis of exploration away from the more traditionally explored parts of the greenstone belts.

## *Key references*

- Bertuch (2004): geological mapping, stratigraphy, mineralisation, genesis.
- Hoatson et al. (2006): regional geology; stratigraphy; structure; drilling; mineralisation.
- Fiorentini et al. (2010): Collurabbie-type deposits; PGE geochemistry of mineralised and non-mineralised komatiites; depletion and enrichment trends of PGEs; physical volcanology; ore-forming processes; exploration potential.
- Fiorentini et al. (2011): komatiitic basalt; Gerry Well greenstone belt, Kurnalpie Terrane; high Pd/Ir ratios indicate fractionated and less magnesian nature of suite.

- Locmelis et al. (2011, 2013): variations of Ru contents in chromite from komatiites and komatiitic basalts at Collurabie; Ru signatures in chromite; discriminate mineralised from barren komatiite and komatiitic basalt units; prospectivity indicator.
- Barnes and Fiorentini (2012): komatiite basalt-associated subvolcanic intrusions; Collurabie in the Gerry Well greenstone belt; PGEs; Ni sulphide deposits; komatiites emplaced under sulphide undersaturation; derived from sources with remarkably similar PGE contents.

## 6.4.4 Mineral-System Class 4: Alkaline mafic-ultramafic intrusions

### 6.4.4.1 Deposit Type 4.A: Stratabound and disseminated Cu-Au-PGE sulphides

#### Overview

The Mesoproterozoic Mordor Igneous Complex is a rare example in Australia of PGE mineralisation associated with an alkaline mafic-ultramafic intrusion. Such intrusions are most abundant in the Proterozoic and Phanerozoic (especially Mesozoic and Cenozoic) terranes of Australia. Their geological setting is mainly continental (anorogenic) rift zones, with some alkaline bodies (e.g., carbonatites) near plate margins (collisional and divergent) and margins of cratons. They invariably occur in association with alkalic rocks and they are spatially related to deep crustal (lithospheric?) structures that control multiple intrusion events. Very few examples are enriched in PGEs and the main focus of exploration is generally for REEs (Hoatson et al., 2011; Jaireth et al., 2014). Mineralisation is in lava, flows, and composite plugs, cone sheets, dykes, and rare sills, but never in large homogeneous plutons. The emplacement of this steeply plunging, plug-like  $1133 \pm 5$  Ma Mordor Igneous Complex (Claoué-Long and Hoatson, 2005) may have been facilitated during the Mesoproterozoic by the nearby deep crustal structures of the Redbank Thrust and/or the Woolanga Lineament. This composite alkaline ultramafic-mafic body can be broadly subdivided into a western zone of homogeneous syenite and an eastern zone comprising a highly fractionated comagmatic suite of alkaline felsic and mafic rocks (syenite, monzonite, melamonzonite, shonkinite) spatially associated with phlogopite-bearing ultramafic cumulate rocks (wehrlite, olivine clinopyroxenite, lherzolite, dunite, pyroxenite) that make up less than 5% of the complex.

The Mordor Igneous Complex consists of a differentiated ultrapotassic suite of rocks with silica contents ranging from 43% to 53%, and which is enriched in K, Al, Rb, Ba, Sr, and La. The alkaline felsic rocks and discordant carbonate-bearing dykes have been drilled for REEs, U, and Th, whereas the alkaline ultramafic rocks have been assessed for PGEs, Cu, Ni, Cr, Au, phlogopite, and vermiculite. The Orodruin Prospect (type example of Deposit Type 4.A) near the centre of the complex consists of stratabound PGE mineralisation (8 m @ 0.67 ppm Pt+Pd+Au) hosted by cyclic sequences of ultramafic rocks (Barnes et al., 2008). Another mineralised body similar to Mordor is the ~2025 Ma Ponton Creek carbonatite (previously called Cundeelee), located at the southeastern margin of the Archean Yilgarn Craton near the intersection of a shear system associated with the Fraser Complex to the southeast and the southern extensions of the Laverton Tectonic Zone. The emplacement of the Ponton Creek complex may have been facilitated by the intersection of these two regional structural corridors. The main basement lithologies comprise granitic gneiss, migmatite, and intrusives overprinted by the northeast-trending tectonic fabrics of the Proterozoic Albany-Fraser Orogen. Anomalous concentrations of PGEs are associated with REEs.

### *Australian deposits/prospects/hosts*

Orodruin Prospect–Mordor Igneous Complex (Aileron Province, Arunta Orogen, NT); Ponton Creek (Yilgarn Craton, WA).

### *Significant global example(s)*

Coldwell, Coryell, Marathon, Sappho, Entwine Lake, Roaring River complexes (Canada); Volkovsky Deposit, Baron Prospect, Guli Intrusion (Russia); Palabora (South Africa); Catalão, Ipanema (Brazil); Loch Borrallan and Loch Ailsh intrusions (Scotland); Longwoods Intrusive Complex (New Zealand).

### *Type example in Australia*

Orodruin Prospect–Mordor Igneous Complex, Northern Territory.

### *Location*

Longitude 134.479966°E, Latitude -23.439744°S; 1:250 000 map sheet: Alice Springs (SF 53–14), 1:100 000 map sheet: Laughlen (5751); ~70 km northeast of Alice Springs, Northern Territory.

### *Geological province*

Aileron Province, Arunta Orogen, Northern Territory.

### *Resources*

Unknown.

### *Current status and exploration history*

Prospect. The Mordor alkaline mafic-ultramafic complex and associated carbonate veins have been extensively explored by many companies (including a 20-year program by CRA Exploration-Rio Tinto) for Ni, Cu, Cr, PGEs, diamonds, vermiculite, phlogopite, U, Th, and REE. Despite the protracted history of exploration for these different commodities, no deposits of significant size have been found. The most significant PGE occurrence was found by Tanami Gold NL in 2001, when a rock chip and drill program tested a strong Pt, Pd, Ni, and Cu soil anomaly at the Orodruin Prospect (previously called Mithril Prospect: Figure 6.28) near the centre of the complex. Follow-up rock chip sampling was undertaken over one of the strongest soil anomalies and returned highly anomalous values for Cu, Ni, and PGEs. The drilling defined stratabound PGE mineralisation with grades of up to 1.5 g/t PGEs+Au in a cyclic sequence of pyroxenite and wehrlite. Polymetallic mineralisation with anomalous PGE concentrations (30.4 m @ 0.25% Cu which included 1 m @ 1.4% Cu, 0.3% Ni, 0.4 g/t Pt+Pd, and 0.1 g/t Au) has also been defined at the Braveheart Ironstone Prospect (Figure 6.28)—an ironstone gossan on the southeast margin of the complex. The mineralisation is hosted in porphyritic shonkinite and is associated with a zone of sulphide enrichment (pyrrhotite, chalcopyrite, pyrite) which dips at 55° towards the northwest. Induced polarisation and magnetic surveys defined the mineralised zone which had a strong electromagnetic conductivity, elevated chargeability, and enhanced magnetic susceptibility response.

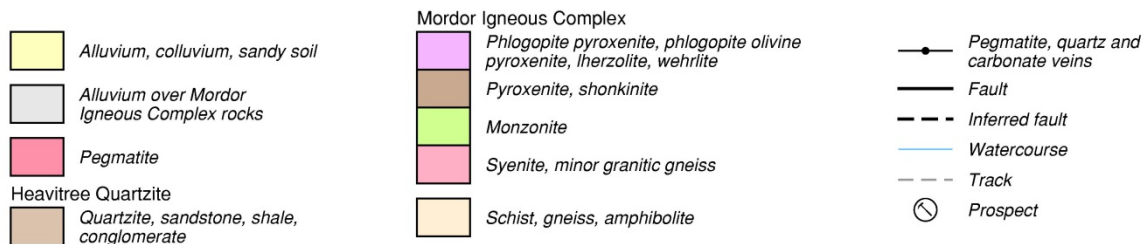
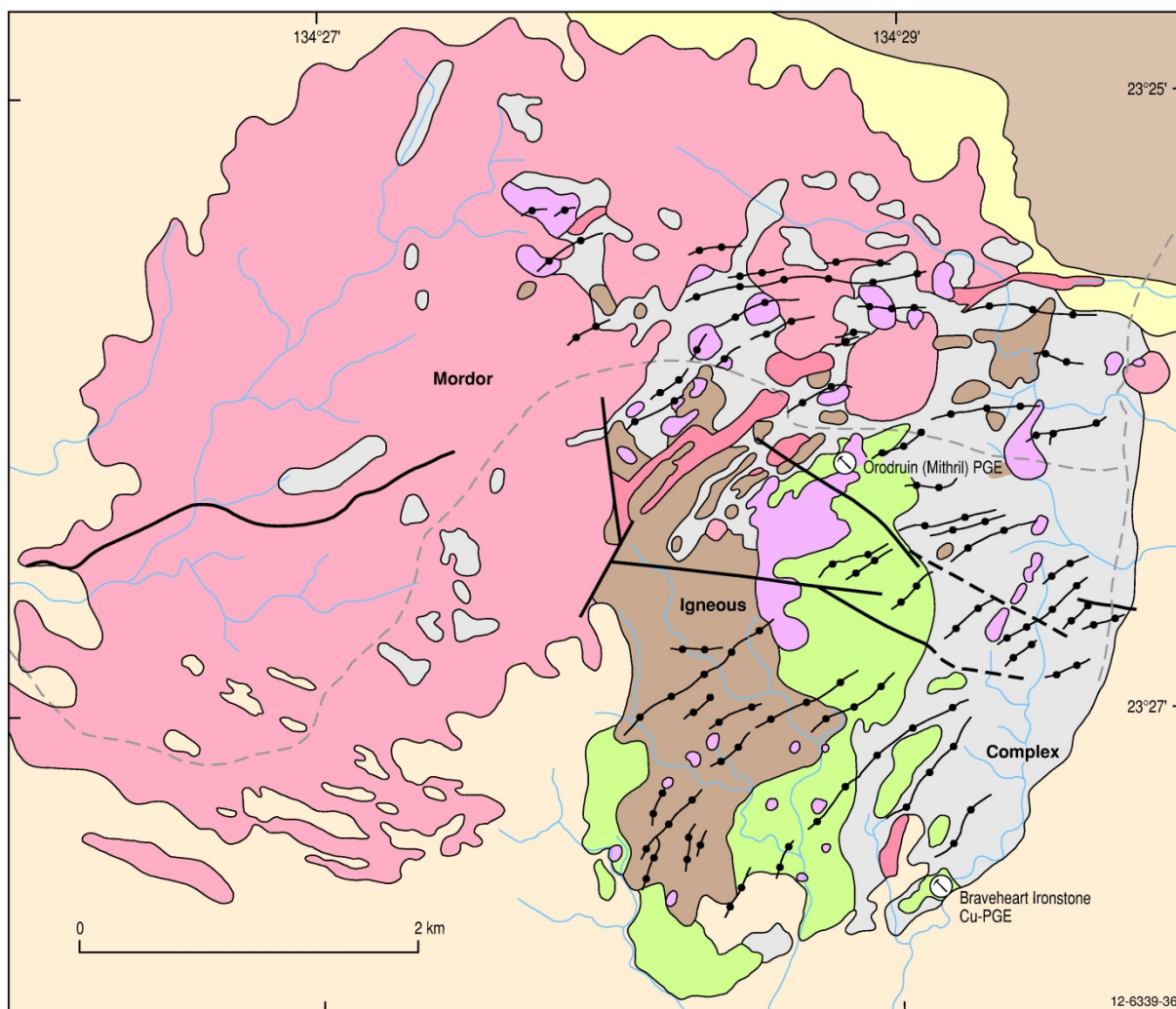


Figure 6.28 Geology of the Mordor Igneous Complex, Arunta Orogen, Northern Territory. The Orodruin PGE-Cu-Ni-Au prospect is located near the right central part of this unusual alkaline complex, and the Braveheart Ironstone Cu-PGE prospect occurs on the southeastern margin of the complex. Modified from Langworthy and Black (1978) and Hoatson et al. (2005a).

### Economic significance

The Orodruin Prospect in the Mordor Igneous Complex is a rare example in Australia of PGE mineralisation being associated with an alkaline mafic-ultramafic intrusion of lamprophyric or potassic parentage. Reef-style PGE mineralisation in the Orodruin Prospect is the only known example of stratabound PGE-sulphide mineralisation in the Northern Territory.

## *Geological setting*

The plug-like alkaline-ultramafic Mordor Igneous Complex (Figure 6.28) in the Aileron Province of the Arunta Orogen intrudes high-grade Paleoproterozoic granitic gneisses and amphibolites near the intersection of the easterly extension of the Redbank Thrust, a complex east-trending mylonite zone up to 10 km wide (Shaw and Black, 1991), and the Woolanga Lineament, a deep-seated northwest-trending crustal dislocation (see Figure 8.13). Claoué-Long and Hoatson (2005) suggest the Mordor Igneous Complex, was part of the ~1130 Ma Teapot Event, a period of elevated crustal temperatures (amphibolites facies) in the southern part of the Arunta Orogen. The complex crops out over 6 by 6 km inside the Mordor Pound, a three-sided box-shaped low-relief feature bounded by sheer cliffs of unconformably overlying sandstone and conglomerate (~820 Ma Heavitree Quartzite of the Amadeus Basin). Modelling of aeromagnetic data by Meixner and Hoatson (2003) showed that the steep-sided complex corresponds to a circular region of moderate magnetic intensity comprising four separate very intense anomalies. The undeformed composite intrusion can be broadly subdivided into a northwestern zone of homogeneous coarse-grained syenite and a southeastern zone comprising a highly fractionated comagmatic suite of alkaline felsic and mafic rocks (monzonite, melamonzonite, syenite, clinopyroxene syenite—previously called mafic shonkinite) spatially associated with phlogopite-bearing ultramafic rocks (wehrlite, olivine clinopyroxenite, lherzolite, dunite, pyroxenite: Figure 6.28). Isolated pods and cross-cutting apophyses of the ultramafic-mafic phase in the northwestern syenitic phase, suggest that the more primitive ultramafic-mafic phase has intruded the essentially coeval syenitic phases (Hoatson and Stewart, 2001; Barnes et al. 2008). Numerous late stage pegmatite dykes and lesser quartz- and quartz-carbonate veins with prominent northeast to east-northeast trends crosscut the ultramafic cumulates. Some of the dykes are up to 6 m-wide and are radioactive with rock chips returning 0.33% U, 0.1% Th, and 0.37% Nb (Core Exploration Limited, 2013). Swarms of syenitic dykes formed from the late migration of interstitial magma expelled during the compaction of the cumulate pile. Gamma-ray spectrometrics (potassium band) indicate that the ultramafic rocks make up less than 5% of the intrusion. The largest ultramafic body (0.5 km by 1.2 km) near the right centre of the intrusion is flanked to the north and east by a curvilinear cluster of outcrops that may have intruded along a ring fracture. The ultramafic rocks are generally massive, show no obvious gross compositional layering or metamorphic recrystallisation, and have well-preserved primary mineral assemblages of abundant phlogopite, and cumulus clinopyroxene, orthopyroxene, olivine, and chromite. The more fractionated alkaline mafic-felsic rocks contain cumulus magnetite/ilmenite, apatite, and K-feldspar. Barnes et al. (2004b) documented an incipient lamination in wehrlite that was conformable with a lamination defined by the alignment of large tabular alkali feldspar phenocrysts in the shonkinite. They therefore suggested that the olivine-bearing ultramafic rocks are part of an inward-dipping cyclic cumulate sequence forming a funnel-shaped intrusion, rather than being a separate body in a composite intrusion. These phlogopite-bearing ultramafic rocks have unusual alkaline-ultramafic affinities (Langworthy and Black, 1978; Barnes et al., 2004b) with elevated MgO (16.5%–25.3%), K<sub>2</sub>O (0.5%–2%), P<sub>2</sub>O<sub>5</sub> (0.3%–0.9%), and low Al<sub>2</sub>O<sub>3</sub> (2.5%–4.8%) and Na<sub>2</sub>O (0.2%–0.5%) abundances. The rocks are also enriched in many trace elements (Rb, Ba, Sr, Zr, La, Ni, Cr, Cu) relative to other intrusions.

## *Mineralisation environment*

Mordor is an unusual differentiated alkaline mafic-ultramafic body of lamprophyric or potassic parentage that contains primary magmatic PGE-enriched sulphides. The Orodruin PGE Prospect near the centre of the intrusion is a stratabound PGE-sulphide deposit in a cyclic sequence of alkaline ultramafic cumulates. The host rock sequences are phlogopite-rich pyroxenitic cumulates, with an inward dipping conformable layer of olivine-bearing cumulates that can be divided into a number of

cyclic units. Barnes et al. (2008) provide detailed descriptions of the mineralogy and trace-element geochemistry across the mineralised horizons in the Orodruin Prospect (Figure 6.28).

### *PGE mineralisation*

The PGEs are associated with disseminated primary magmatic sulphides (up to 1% chalcopyrite, pyrrhotite, and pentlandite) at the contact of pyroxenite and overlying peridotite cyclic units. Table 6.10 summarises the PGE contents of samples from the Orodruin Prospect. Barnes et al. (2008) describe two types of stratiform-disseminated sulphide accumulations:

1. disseminated layers at the base of cyclic units, with relatively high PGE tenors; and
2. patchy PGE-poor disseminations within magnetite-bearing upper parts of cyclic units.

Sulphide-enriched layers at cycle bases contain anomalous PGE contents with grades up to 1.5 g/t Pt+Pd+Au over 1-m intervals. A 2-m-wide mineralised zone containing 1.1 ppm Pt+Pd+Au occurs within an 8-m-wide zone that assayed 0.67 g/t Pt+Pd+Au.

*Table 6.10 Platinum-group-element chemistry of selected sulphide-bearing samples from the Orodruin Prospect area, Mordor Igneous Complex (Barnes et al., 2008).*

Sample	Zone	Ni ppm	Cu ppm	Pt ppb	Pd ppb	Rh ppb	Ir ppb	Ru ppb	Au ppb	Pd/Ir	Pt/Pd
MOD1–202	MOD SL1	687	10	98	89	8	9	4	5	9.9	1.10
MOD1–206	MOD SL1	737	1486	440	710	29	33	19	224	21.5	0.62
MOD1–216	MOD SL1	592	1658	78	115	4	5	4	62	23.0	0.68
MOD2–28	MOD2 upper	492	869	49	90	3	2	1	38	45.0	0.54
MOD2–63	MOD2 upper	543	1160	38	45	2	1	2	41	45.0	0.84
24109MC <sup>1</sup>	MOD1 SLI	718	666	183	287	14	17	8	72	16.6	0.64

<sup>1</sup> Outcrop sample, all other samples from drill-holes.

### *Age of mineralisation*

Plagioclase pyroxenite (containing 112 ppm Zr) from the northeastern corner of the intrusion has an interpreted U-Pb zircon age of  $1133 \pm 5$  Ma (Claoué-Long and Hoatson, 2005). This age is considered the most reliable age for the crystallisation of the Mordor Igneous Complex and its orthomagmatic Cu-Ni-PGE sulphide mineralisation at the Orodruin Prospect. It is consistent with the mineral Rb-Sr isochron ages of  $1128 \pm 20$  Ma and  $1118 \pm 17$  Ma and whole-rock Rb-Sr isochron age of  $1180 \pm 90$  Ma (Langworthy and Black, 1978; recalculated by Nelson et al., 1989), and the Sm-Nd isochron age of  $1100 \pm 280$  Ma (Nelson et al., 1989).

### *Genesis*

Barnes et al. (2008) interpreted the PGE-enriched sulphide layers at the base of magmatic cycle bases that are truncated by narrow barren intervals and reversals in normal fractionation trends to be caused by new magma influxes into a continuously replenished magma chamber. The PGE-enriched layers at the base of cyclic units have decoupled Cu and PGE peaks reflecting increasing PGE tenors up-section, due to increasing R factors during the replenishment episode, or progressive mixing of between resident PGE-poor magma and more PGE-enriched replenishing magma. The details of the

cyclicality within the Mordor Igneous Complex imply that the chamber was a more or less continuously open system, with new magma influx varying between a steady trickle and occasional larger pulses followed by periods of quiescence and *in situ* fractionation. Successive influxes formed hybrid layers at the bottom of the chamber; these may have been discontinuous if the topography of the chamber floor was rugged, possibly accounting for poor continuity within and between units.

Claoué-Long and Hoatson (2005) proposed the Mordor Igneous Complex was part of the ~1150–1130-Ma Teapot Event that involved local intrusions and thermal effects across the southern part of the Arunta Orogen. This event may represent a transition to within-plate magmatism, since the subsequent ~500–460 Ma Larapinta Event in the eastern Arunta Orogen appears to be part of a major within-plate extension that was accompanied by large volumes of mafic magmatism. The emplacement of the Mordor Igneous Complex, and that of the much later Mud Tank Carbonatite plug-like body at ~730 Ma (Black and Gulson, 1978; Knutson and Currie, 1990), located ~50 km to the north-northwest, may have been facilitated by the nearby Woolanga Lineament. The early investigations of Langworthy and Black (1978) showed the rocks of the complex were produced by fractional crystallisation from an ultrapotassic mafic magma in an intermediate-level magma chamber. Magma genesis possibly involved modification during the ascent of potassic partial melt derived from a phlogopite-bearing atypical upper mantle source rock. Nelson et al. (1989) suggested that the parent magma to the 1133 Ma Mordor Igneous Complex was derived from an enriched lithospheric mantle that was metasomatised by subduction of sediment during the early history of the Arunta Orogen. The presence of PGE-enriched sulphides in cumulates from a lamprophyric magma implies that low-degree partial melts do not necessarily leave sulphides and PGEs in the mantle restite during partial melting (Barnes et al. 2008).

The Mordor Igneous Complex is unusual in that its alkaline-ultramafic rock types and steep-sided plug-like form are similar features to those in 'Alaskan-type' ultramafic-mafic complexes (Johan, 2002), whereas the stratabound PGE mineralisation (e.g., Orodruin Prospect) is more typical of tholeiitic layered mafic-ultramafic intrusions (Naldrett, 1989). More detailed geochemical and isotopic studies similar to that done by Barnes et al. (2008) are required before this unusual intrusion can be assigned to a particular mineralising system. The presence of PGE-enriched magmatic sulphides in a lamprophyric setting has important exploration implications. A wider range of magmas than is conventionally accepted may have potential for magmatic sulphide mineralisation of a range of types (Barnes et al. 2008).

### *Key references*

- Langworthy and Black (1978): differentiated potassic character of Mordor Igneous Complex; whole-rock geochemistry; stratigraphy; structure.
- Nelson et al. (1989): geology; stratigraphy; geochronology; Sm-Nd and U-Pb whole-rock isochrons; enriched mantle sources.
- Hoatson and Stewart (2001): regional geological setting of Mordor and other Arunta intrusions; stratigraphy; field relationships; mapping; mineralisation.
- Barnes et al. (2004b): PGE mineralisation; cyclic layering; PGE-enriched magmatic sulphides; ultrapotassic hydrous magma.
- Hoatson et al. (2005a): geological setting of Mordor and other Proterozoic mafic-ultramafic intrusions; Arunta Orogen; stratigraphy, mineralisation.
- Claoué-Long and Hoatson (2005): event chronology and regional correlations of Mordor and Arunta Intrusions; geochronology; whole-rock geochemistry; regional temporal correlations.

- Rowan et al. (2004, 2005): lithological mapping of the Mordor Igneous Complex; remote sensing of environment; hyperspectral analysis; Advanced Spaceborne Thermal Emission and Reflection Radiometer (ASTER).
- Barnes et al. (2008): stratigraphy, drilling; whole-rock geochemistry; PGE mineralisation; PGE-enriched disseminated sulfide layers; cumulates; alkaline character of the Mordor Alkaline Igneous Complex.

## 6.4.5 Mineral-System Class 5: 'Alpine- and ophiolitic-type' ultramafic-mafic intrusions

### 6.4.5.1 Deposit Type 5.A: Podiform and stratabound chromitite

#### Overview

Ophiolites represent fragments of upper mantle and oceanic crust that were emplaced during plate collision or rifting of continental lithosphere (i.e., the early, solid-state intrusive stage in tectonically unstable terranes) in convergent plate boundaries. They have similar tectonic settings and geochemical features to the alpine serpentinite complexes, but the associated volcanics and chemical sediments are generally absent from the alpine intrusions. Most major podiform chromitite deposits associated with ophiolites in the world are Phanerozoic in age ranging from 500 Ma (Thetford, Canada) to 10 Ma (New Caledonia) (Stowe, 1994; Mosier et al., 2012). Complete ophiolitic suites (Stowe, 1987) comprise a basal mantle peridotite zone of dominantly harzburgite with interlayered lenses of dunite, a transitional tectonised peridotite zone, and an overlying crustal cumulate sequence of layered peridotite to massive gabbro rock types, with pillow lavas, sheeted dykes and cherts forming the upper levels. Disseminated chromite and more rarely podiform PGE-bearing chromitites can occur in either dunite of the mantle sequence, the mantle-harzburgite and crustal-cumulate transition zone, or above this transition in the lowest crustal cumulate dunite. The deposits are often associated with shear zones, formed in or around zones of weakness in pre-existing chromitite bodies, and may themselves be displaced by faulting and intensely deformed by tectonic processes. There appears, however, to be no relation of the size of the deposits to the size of the ultramafic host rock (Mosier et al., 2012). Massive chromite lenses may be continuous for tens of metres, or they may pinch and swell abruptly, and individual lenses may be widely separated. Discordant chromite bodies may have their primary origins in vertical conduits, feeding magma across enclosing mantle harzburgite, and some orebodies have been sheared into concordance. Massive pods may have associated lateral zones of disseminated chromite which can be traced for hundreds of metres. Massive chromite ores typically contain 40% to 60% Cr<sub>2</sub>O<sub>3</sub>, whereas schlieren, stringer, and disseminated chromite zones contain 10% to 30% Cr<sub>2</sub>O<sub>3</sub>. The chromite-bearing zones are usually enriched in Os, Ir, and Ru, and in some cases by Pt, Pd, and Rh. Common PGMs include Os, Ir, and Ru alloys, laurite, erlichmanite, irarsite, hollingworthite, and various Pt-, Pd-, and Rh-bearing minerals (see references within Mosier et al., 2012).

Podiform and rare stratabound chromitite layers are associated with tectonically emplaced ultramafic-mafic bodies throughout the Lachlan and New England orogens of eastern Australia. The intrusions form north-trending linear belts that extend from southern Tasmania, across central-eastern Victoria and New South Wales, to northern Queensland. They range in age from Cambrian (~510 Ma) in Tasmania and central New South Wales (~530 Ma), to Permian in northern New South Wales and Queensland. The intrusions have previously been referred to in the literature as 'ophiolite', 'dismembered ophiolite', fault-bounded alpine serpentinites, and serpentinite mélanges. However,

Crawford and Berry (1992) recommended that since complete ophiolite sequences have not been observed in Australia, such labels as ophiolite with its genetic connotation of mid-ocean ridge-generated oceanic crust and upper mantle, be abandoned for the Tasmanian ultramafic-mafic complexes. Notable intrusions occur along the western margin of Tasmania (e.g., Adamsfield, Heazlewood River, Serpentine Hill, Wilson River, Andersons Creek, and Beaconsfield: Bacon, 1992; Bottrill, 2014; Corbett et al., 2014), in the Coolac Serpentinite (Tumut–Coolac–Gundagai–Wallendbeen), Great Serpentinite (Nundle–Bingara), Gordonbrook Serpentinite (Copmanhurst–Gordonbrook) belts of New South Wales (MacNevin, 1975a,b; Leitch, 1980; Aitchison and Ireland, 1995; Och et al., 2007; NSW DPI, post-2007), and in the Rockhampton district of southern Queensland (INAL Staff, 1975). The regional distribution of the ultramafic-mafic complexes in eastern Australia is strongly controlled by steeply dipping northwest- to northeast-trending fault systems, hence they represent fault-bounded intrusive blocks within well-defined linear belts. Dunite, orthopyroxenite, and harzburgite are the dominant rock types, with syn-emplacement deformation fabrics and serpentine alteration overprinting primary igneous textures and mineralogy. Massive podiform chromitite horizons appear to be more prominent in the younger complexes, whereas disseminated chromite is more typical of the Cambrian examples in Tasmania. Contact metamorphism is weak to absent since emplacement is generally via faults. The heterogeneous distribution of the Os-Ir-Ru alloys in the Tasmanian complexes largely reflects the erratic nature of the chromite mineralisation in the ultramafic rocks. The best documented intrusions are those from western Tasmania, which are interpreted to represent allochthonous sheets tectonically emplaced from the east and northeast. Their orthopyroxene-rich cumulate sequences, highly magnesian cumulate olivine compositions (Mg# up to 94), and exceptionally Cr-rich chromites indicate they crystallised from boninitic to low-Ti magnesian quartz tholeiite basaltic magmas (Bottrill, 2014; Corbett et al., 2014).

The structurally controlled ultramafic-mafic intrusions of eastern Australia are believed to hold little potential for a large-tonnage hard-rock resource of PGEs, since they often have predictable distributions in north-trending linear belts, they form hills, are often associated with earlier discovered placer deposits, have been extensively explored by prospectors, and the primary podiform PGE-Cr mineralisation generally has an erratic distribution (Hoatson, 1984).

#### *Australian deposits/prospects/hosts*

Adamsfield Intrusion (Thylacine Province, Delamerian Orogen, Tas); Heazlewood River Intrusion (Thylacine Province, Delamerian Orogen, Tas); Mount Mary Mines–Coolac Serpentinite Belt (Lachlan Orogen, NSW); Rockhampton (New England Orogen, Qld).

#### *Significant global example(s)*

Semail Ophiolite (Oman); Unst Ophiolite–Cliffs Deposit, (United Kingdom); Zambales (Philippines); Kempirsai (Russia); Al Ays (Saudi Arabia); and many podiform chromitite deposits in Turkey, Cyprus, Greece, Iran, Oman, New Caledonia.

#### *Type example in Australia*

Adamsfield Intrusion, Tasmania.

#### *Location*

Longitude 146.330000°E, Latitude -42.730000°S; 1:250 000 map sheet: Queenstown (SK 55–10), 1:100 000 map sheet: Wedge (8112); ~80 km west-northwest of Hobart, near Lake Gordon, Tasmania.

## *Geological province*

Thylacine Province, Delamerian Orogen, Tasmania.

## *Resources*

Inferred Resource at the Halls Open-Cut of 14 500 t @ 6.5 g/t Ir, 7.3 g/t Os, 0.13 g/t Pt (Shree Minerals Ltd, 2009).

## *Current status and exploration history*

Undeveloped deposit. Many prospectors and mining companies have investigated the alluvial and hard-rock PGE potential of the Adamsfield Intrusion since its discovery in 1924 (see Section 5.2.3). The earliest phase of exploration from the mid-1920s to the 1950s was dominated by individual or small groups of prospectors working small alluvial deposits with pans and sluices on the plains draining the ultramafic rocks. Exploration from the 1950s to the 1970s concentrated on Ni, with very few assays undertaken for the PGEs. Activities involved airborne magnetics, with localised ground geophysical-geochemical surveys, and drilling. Other historical activities included auger sampling of alluvial material to depths of 3 m west of the main hard-rock PGE occurrences, but results were discouraging. After the 1980s, the focus of small-scale exploration programs turned to both hard-rock targets in the Adamsfield Intrusion and nearby alluvial deposits.

Exploration activities for 'osmiridium' at the Halls Open-Cut prospect on the northeastern margin of the intrusion commenced more than 70 years ago. Grades of 42 g/t Os+Ir were reported within a narrow (1–2-m-wide), sheared serpentinitised ultramafic unit. Activities at the Halls Open-Cut prospect by Metals Exploration Limited in the mid-1980s consisted of geochemical sampling, percussion drilling, and diamond drilling (3 holes for 190.7 m). Diamond drilling down-dip of the excavated lode obtained low-grade visible Au, base-metal sulphides, and weakly anomalous PGE concentrations. Subsequent percussion drilling (12 holes for 461 m) reported significant narrow mineralised intercepts, e.g., AHP1: 1 m @ 14 g/t Ir, 18 g/t Os and 0.25 g/t Pt. Shree Minerals Limited (2009) undertook further drilling to define an Inferred Resource at Halls Open-Cut (see above), and combined new geological concepts and datasets to generate exploration targets. They considered three major targets in the Adamsfield region:

1. stratiform PGE, Cr, and Ni sulphide mineralisation in layered serpentinite and dunite;
2. paleoplacers within the overlying Cambro-Ordovician clastic sequences; and
3. placer accumulations in the Quaternary sedimentary sequences.

An important aspect of their exploration strategy was to map out and sample the layered ultramafic stratigraphy and establish favourable positions for PGE and Ni mineralisation. Shallow-hole angled drilling and ground-based magnetic and induced polarisation surveys were considered the most appropriate methods. Bacon (1992) provides a comprehensive summary of the mining activities and production statistics of the Adamsfield mining field.

## *Economic significance*

The Adamsfield ultramafic-mafic intrusion in southwestern Tasmania has attracted considerable interest since its PGE potential was first realised in 1924 (see Section 5.2.3). Hardrock and alluvial deposits of 'osmiridium' (~477 kg) associated with the Adamsfield ultramafic-mafic intrusion have accounted for approximately 50% of Tasmania's total production of 'osmiridium' (~964 kg) from 1925 to 1968. Adamsfield, Savage River, Mount Stewart, and Wilson River have collectively produced about

970 kg. Production at Adamsfield culminated in 1925 when 104 kg of 'osmiridium' was obtained from the alluvial deposits. In that year £105 570 was paid to the miners, and Tasmania was regarded the largest producer of free 'osmiridium' in the world (Reid, 1921; Geary et al., 1956). During these prosperous times, over 800 miners were working the Adamsfield alluvial deposits. Exploration programs from the 1960s to recent times have regularly reviewed and evaluated the hardrock, and, in particular, the alluvial mineralisation potential of the Adamsfield region.

### *Geological setting*

Structurally-emplaced early- to middle-Cambrian ultramafic-mafic intrusions occur in Cambrian sedimentary troughs between regions of Precambrian basement in the Delamerian Orogen of western Tasmania (Figure 6.29). Corbett et al. (2014) describe their distribution as dispersed along the western margin of the Dundas Trough in western Tasmania, and deformed relics of the same bodies at other locations. Amphibolite mylonites along the bases of several complexes indicate their emplacement took the form of one or more allochthonous sheets from the east and northeast. Most intrusions occur along a north-south-trending arcuate 'corridor', extending from near Beaconsfield in the north, across to the northwestern and western coasts, and southwards through central Tasmania, to Rocky Boat Inlet on the southern coast (Figure 6.29). Based on the interpretation of geophysical data, additional Cambrian ultramafic-mafic complexes are likely to occur at depth throughout southeastern Tasmania, and are now covered by Late Carboniferous-Jurassic sedimentary rocks and dolerite dykes and sills (Figure 6.30). The common features of the Tasmanian ultramafic-mafic intrusions are that they are high-magnesian, well layered, and dominated by olivine and orthopyroxene. Clinopyroxene and plagioclase are minor phases and generally only occur as post-cumulus minerals (Brown, 1992). The intrusions have distinctive orthopyroxene-rich cumulate sequences and very low-Ti lavas (Crawford and Berry, 1992). Brown (1986) identified three major ultramafic cumulate associations, namely:

1. layered dunite-harzburgite cumulate sequences (LDH) that contain highly magnesian cumulus olivine and orthopyroxene ( $Mg\# = 100Mg/(Mg+Fe^{2+}) = 92-94$ ), refractory Cr-spinel ( $Cr\# = 100Cr/(Cr+Al) = 87-94$ ), and CaO and  $Al_2O_3$  contents of orthopyroxene less than 0.5%;
2. layered pyroxenite-dunite succession (LPD); and
3. layered peridotite-pyroxenite-gabbro succession (LPG).

Petrographically the LPG cumulates differ from the LPD cumulates by the presence of post-cumulus plagioclase. Both the LPD and LPG cumulates are chemically similar with olivine and orthopyroxene having  $Mg\# = 85-90$ , and chromite  $Cr\# = 52-80$ . Both CaO (0.6%–2%) and  $Al_2O_3$  (0.75%–2%) contents of orthopyroxene are higher than those in the LDH cumulates. The orthopyroxene-rich cumulate sequences, highly magnesian cumulate olivine compositions ( $Mg\#$  up to 94), and exceptionally Cr-rich chromites indicate that the cumulate sections of these complexes crystallised from boninitic to low-Ti magnesian quartz tholeiite basaltic magmas. Lava sections of both boninitic and low-Ti tholeiite compositions form the volcanic components of the best preserved complexes (Corbett et al., 2014).

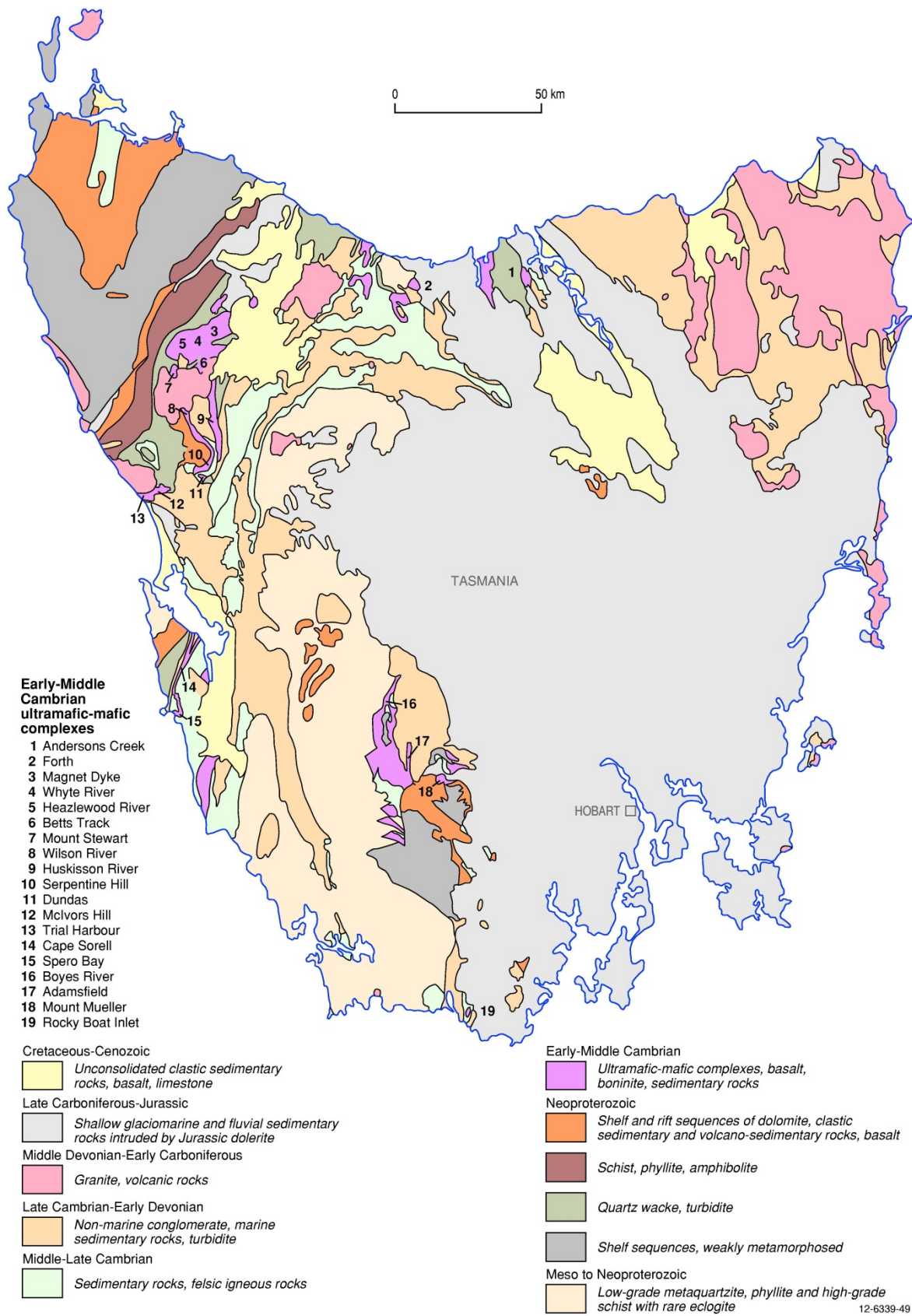


Figure 6.29 Generalised geology of Tasmania. The early to middle Cambrian ultramafic-mafic complexes extend along the western half of the state from Andersons Creek to Rocky Boat Inlet. Most of these complexes have associated hard-rock and/or alluvial 'osmiridium' deposits. Modified from Seymour et al. (2007).

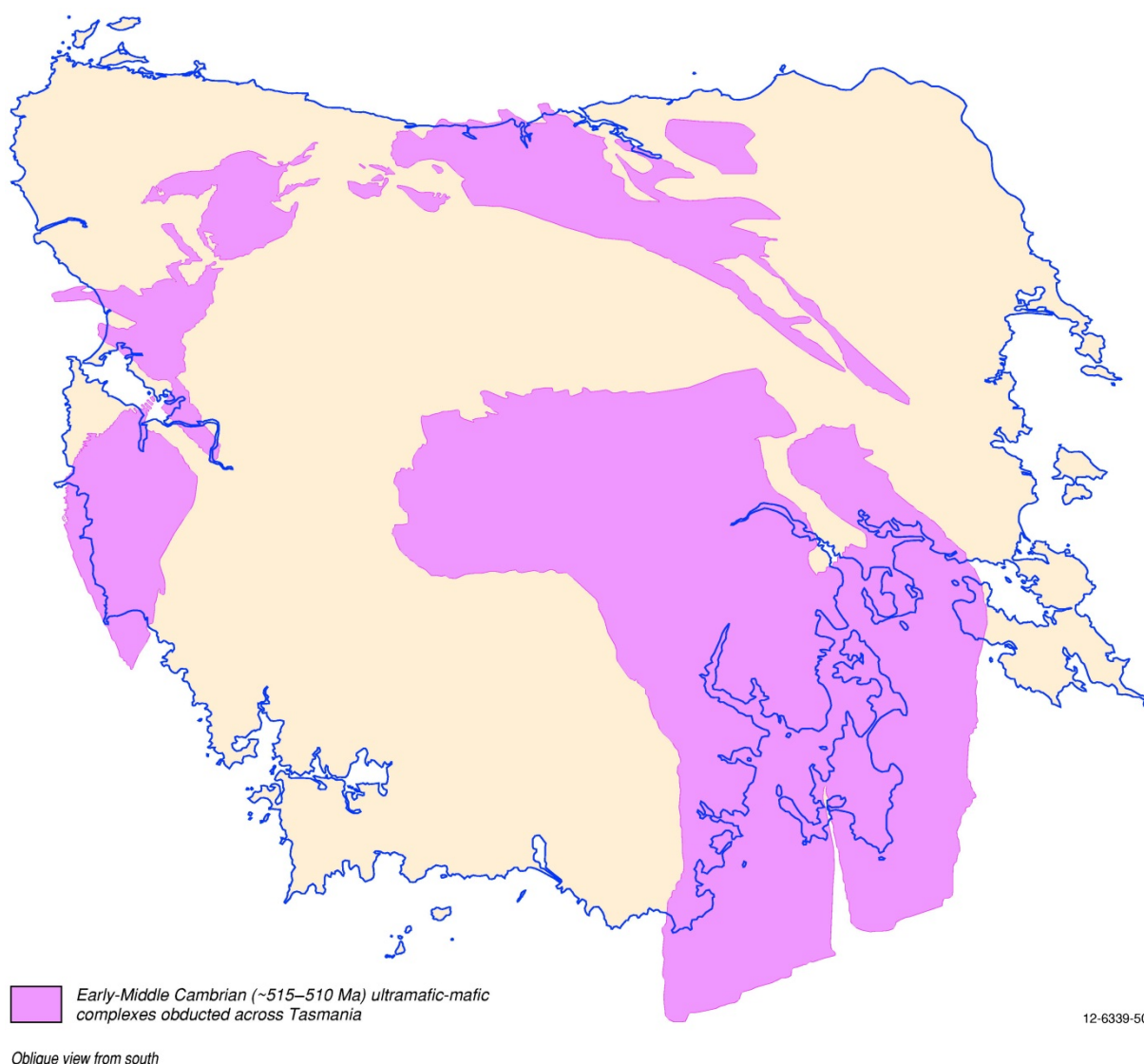


Figure 6.30 Interpreted 3-D geological model showing extent of outcropping and concealed early to middle Cambrian ultramafic-mafic intrusions on mainland Tasmania. Oblique view from the south. Modified from Seymour et al. (2007).

Primary and alluvial 'osmiridium' deposits are spatially associated with the intrusions. The compositional Os-Ir-Ru dominance of the Tasmanian 'osmiridium' was highlighted in the early twentieth century when an average of thirty analyses of Os-Ir concentrates yielded 45.51% Os, 41.65% Ir, 6.40% Ru, 1.12% Pt, and 0.29% Rh (Nye, 1929). Cabri and Harris (1975) analysed 15 grains from Tasmania, comprising 6 grains from the Adamsfield Intrusion and 9 grains from 19 Mile Creek near the Heazlewood River Intrusion. They identified iridosmine, rutheniridosmine, osmiridium, ruthenosmiridium, and irarsite, and documented unusual compositional zoning trends in the Heazlewood River Os-Ir alloys. From the centre of some grains to the margins, the Ru content remained constant and Ir increased with the antipathetic decrease in Os, while in other grains there were complex enrichment-depletion features of Ir and Os towards the margins, Ru again remaining uniform. Heavy minerals associated with the rutheniridosmine include Au, Au-Pt alloys, chromite, picotite, magnetite, pyrrhotite, and pyrite (Mertie, 1969). More recent investigations of these same samples by Cabri et al. (1996), and using a revised classification of osmium, iridium, and ruthenium

alloys based on the major elements present by Harris and Cabri (1991), showed the grains were mainly osmium and iridium, with one grain classified rutheniridosmine. Irarsite occurred as either inclusions, or in veins traversing the grains. A previously unanalysed grain from Tasmania was described as a 4.5 mm composite aggregate of Pt-Fe alloy and fractured subgrains of osmium and iridium. Associated heavy minerals included gold, gold alloyed with platinum, chromite, Cr-spinel, magnetite, pyrrhotite, and pyrite. Ford's (1981) investigations of 300 grains from Adamsfield, Heazlewood River, and Fourteen Mile Creek confirmed the Tasmanian PGMs were dominated by osmium. He described the alluvial 'osmiridium' grains as rounded, with some having hexagonal cross-sections and others having abraded features. Ford (1981) showed that Pt and Rh were concentrated in the Ir-rich phase, which being of cubic system, acted as a collector for these metals that otherwise would tend to be rejected by the dominant (Os-Ru) hexagonal phase. Samples from Fourteen Mile Creek had maximum amounts of Rh at 17.28%. Only five grains had Pt as a major component, and Fe was more abundant in the Pt-rich grains since it preferred the cubic structure. Ford (1981) noted that there was a maximum variation of about 1% for compositionally zoned grains. 'Osmiridium' grains from different intrusions display subtle changes in composition, and in particular they differ in their average Ru contents. For example, based on the Os-Ru-Ir fields of Harris and Cabri (1973), grains from Adamsfield all fall in the iridosmine field, grains from Heazlewood River are dominantly rutheniridosmine with some very-high Ru values, while the Fourteen Mile Creek grains straddle the iridosmine-rutheniridosmine boundary. Table 6.11 summarises the average PGE contents of the major ultramafic-mafic complexes in Western Tasmania.

Table 6.11 Average platinum-group-element concentrations for ultramafic-mafic complexes in Western Tasmania.

Intrusion	Pt (ppb)	Pd (ppb)	Rh (ppb)	Ru (ppb)	Ir (ppb)
Anderson Creek	29.0 (4)	<1	<1	<100	<20
Heazlewood River–North	16.0 (4)	1 (1)	<1	<100	<20
Heazlewood River–South	18.3 (6)	<1	<1	<100	<20
Huskisson River–Lynch Hill	16.3 (3)	1 (3)	1 (2)	<100	<20
Huskisson River–14 km quarry	22.5 (2)	1 (2)	2 (1)	<100	<20
Melba Flat	1240 (1)	4.5 (2)	54 (1)	180 (1)	70 (1)
Serpentine Hill–opx-rich sequence	36 (4)	1.7 (3)	2.0 (3)	<100	<20
Serpentine Hill–ol-rich sequence	33.4 (12)	2.3 (9)	5.0 (6)	<100	<20
Serpentine Hill–gabbroic sequence	36.0 (4)	10.3 (4)	1 (1)	<100	<20
Serpentine Hill–chromitite	44.5 (6)	3.4 (5)	6.2 (6)	270 (6)	68.3 (6)
Serpentine Hill–dunite	22.3 (6)	1.8 (5)	<1	<100	<20
Wilson River–Serpentine Ridge	16.2 (5)	1.3 (3)	6.5 (2)	150 (1)	40 (1)
Wilson River–Riley Knob	41.5 (2)	1.5 (2)	<1	<100	<20

Number of samples is indicated in parentheses.

opx = orthopyroxene; ol = olivine.

Source: Brown et al. (1988).

In addition to PGE mineralisation associated with 'Alpine- and ophiolitic-type' ultramafic-mafic intrusions, Bottrill (2014) described another style of Cu-Ni-PGE mineralisation he classified as 'high-sulphidation Cuni-style'. Massive Cu-Ni-Fe-Pd-Pt-Au sulphide ores were mined from several small, but locally very rich, deposits in mafic intrusions of late Neoproterozoic age, east of Zeehan.

Five main orebodies (North Cuni, South Cuni, and Vandeau mines, and the Nickel Reward and Devereaux prospects) were worked or prospected along a 2500 m-long north-trending belt. The deposits occur in small sulphide zones in altered dolerite or gabbro dykes or sills that intrude volcanoclastic rocks correlated with the Crimson Creek Formation. Massive ores contain 4% to 14% Cu and 8% to 17% Ni, with up to 5 g/t Pt+Pd+Au. Platinum and sperrylite occur in the sulphide ores. The deposits have been variously described as orthomagmatic with associated phases of magmatic segregation, wall-rock contamination, and minor remobilisation, to other mineral systems that involved hydrothermal fluids and replacement vein-type processes.

### *Mineralisation environment*

The Adamsfield ultramafic-mafic intrusion is a north-south-trending arcuate body, 15 km-long and up to 1.4 km-wide, on the western flank of the Sawback Range (Figure 6.31). The ultramafic complex was tectonically emplaced and exposed to erosion, prior to being subsequently re-emplaced into the core of a large anticline of upper Cambrian and Ordovician flysch and molasse-type sedimentary rocks during the Middle Devonian Tabberabberan Orogeny (Corbett et al., 2014). Brown (1986) showed that the complex consists of fault-juxtaposed blocks. The intrusion is almost wholly made up of three major rock types: serpentinitised dunite; olivine orthopyroxenite; and orthopyroxenite. These ultramafic rocks form an anticlinal structure, with well-developed layering of all lithologies in the northern part of the complex, whereas the southern part consists of massive dunite and orthopyroxenite. The transition from massive to layered rocks is defined by a zone of intense, high-temperature deformation where layers are folded and boudinaged. The northern part of the intrusion consists of elliptical masses of partly serpentinitised ultramafic rocks, sheathed in sheared serpentinite, with their long axes aligned sub-parallel to the north-south anticlinal axis and the steeply-dipping bounding faults of the complex. Layering in the ultramafic rocks also strikes near north-south, which is parallel to schistosity in the serpentinite. Alternating isomodal layers (2 cm- to 2 m-thick) of dunite (olivine Fo<sub>87</sub>) and orthopyroxenite have sharp contacts and are persistent along strike. Euhedral Cr-spinels (Cr# 58–68) are also present. The central part of the complex is less well layered and consists of massive dunite, interdigitating with massive orthopyroxenite containing rare layers of dunite and chromitite. Olivine and spinel grains are commonly elongated parallel or near parallel to grain size banding in the dunite. Olivine (Fo<sub>92-93</sub>), enstatite (En<sub>92-95</sub>), and spinel (Cr# 89–96) have more refractory compositions than in the layered ultramafic cumulates to the north (Varne and Brown, 1978; Corbett et al., 2014). Layered orthopyroxenites have lower Mg/(Mg+Fe) than massive orthopyroxenite, the orthopyroxene extends into bronzite compositions, and the associated spinel is Cr-rich. Varne and Brown (1978) noted that the spinel, which forms a minor, but widely disseminated phase in the complex, as having Mg/(Mg+Fe<sup>+2</sup>) = 0.57 to 0.24, and Cr/(Al+Cr+Fe<sup>+3</sup>) = 0.95 to 0.56. To the south, the intrusion passes into a mélange of interspersed lenses of serpentinite, amphibolite, boninite, low-Ti basalt, and mudstone.

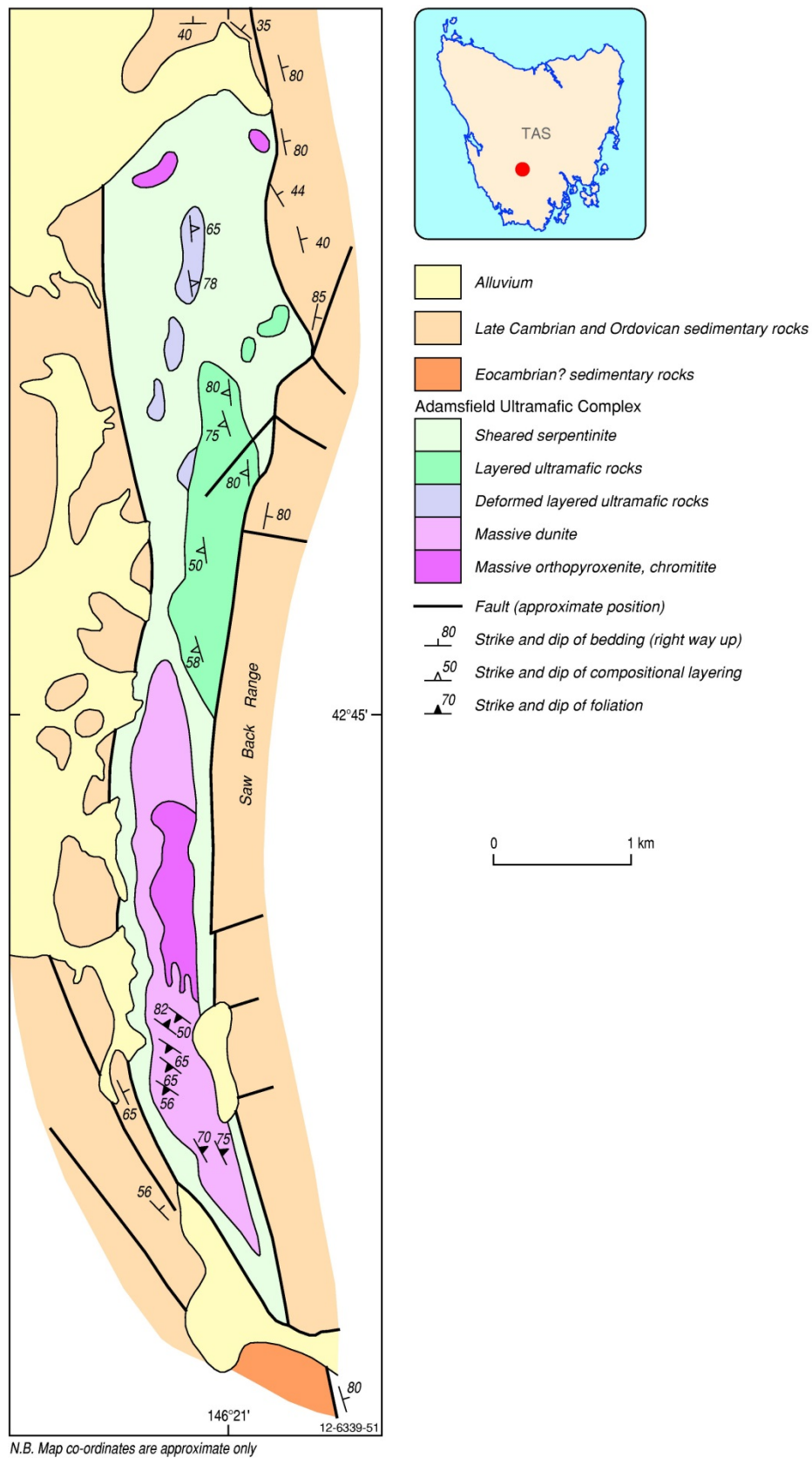


Figure 6.31 Geology of the Adamsfield ultramafic-mafic intrusion, Delamerian Orogen, Tasmania. Modified from Varne and Brown (1978).

## *PGE mineralisation*

'Osmiridium' in the Adamsfield district occurs in three major settings (Reid, 1921; Nye, 1929, 1930; Cabri and Harris, 1975; Bacon, 1992; Bottrill, 2014):

1. Primary occurrences in the ultramafic rocks of the complex. The PGMs occur as sparsely disseminated grains spatially associated with chromite in the ultramafic rocks. These primary deposits were, however, rarely of sufficient grade to be worked economically, in contrast to the associated alluvial and residual deposits. 'Osmiridium' has been reported in serpentinite, but no occurrence has been documented in unaltered peridotite. One such occurrence of *in situ* 'osmiridium' occurs at Halls Open Cut in the headwaters of Main Creek. This occurrence is adjacent to, and locally transects, a barren, quartz-veined talcose shear zone near the eastern margin of serpentinite. Production from this zone was estimated at between 200 ounces to 400 ounces of PGEs (Nye, 1930). The deposit consists of a 300-m-long zone of dark coloured, foliated serpentinite with chromitite pods and minor millerite and nickeloan carbonates, and 'osmiridium' nuggets to about an ounce. More recent analyses of percussion drill samples with more reliable assay techniques are reported to have returned 1 m @ 14 g/t Ir, 18 g/t Os, and 0.25 g/t Pt from a drill-hole depth of 21 m. An inferred resource statement for the Halls Open Cut reported 14 500 t @ 6.5 g/t Ir, 7.3 g/t Os, and 0.13 g/t Pt (Shree Minerals Limited, 2009). Past attempts at hard-rock mining at Adamsfield do not appear to have been highly productive. The PGE potential of the Adamsfield region lies in the discovery of small- to moderate-sized alluvial deposits, and possibly the location of the hard-rock source of PGEs.
2. Alluvial concentrations in Holocene sand and gravel. Most of the 'osmiridium' occurs in chromite-rich alluvial drifts derived from the ultramafic rock types. Alluvial 'osmiridium' and chromite was largely mined from the Main Creek, Adam River, and Football Hill areas. The 'osmiridium' generally forms irregular grains 0.5 mm to 1.5 mm across, but nuggets up to 50 g have been found.
3. Late Cambrian sedimentary rocks that were derived from, and unconformably overly, the ultramafic rocks of the complex. Minor 'osmiridium' production occurred from serpentine-rich quartzose sandstone and a cemented fragmental serpentinite overlying the serpentinite, and the latter appears to constitute a shore-line placer of probable Ordovician age (Nye, 1929, 1930; Carey, 1952; Elliston, 1953).

The PGMs from Tasmania have previously been described as osmiridium and/or iridosmine (Twelvetrees, 1914; Brown, 1919; Reid, 1921; Nye, 1929; Cabri and Harris, 1975; Ford, 1981), but Harris and Cabri (1991) have redefined most of the natural osmium, iridium, and ruthenium alloys to the elemental end-members of Os, Ir, and Ru (and rutheniridosmine: Figure 6.32). There is complete solid solution between Osmium, Ruthenium, and Rutheniridosmine, and a miscibility gap between these minerals and iridium (which may form a solid solution with Pt). The reclassification scheme of Harris and Cabri (1991) indicates that the 'osmiridium' from Tasmania falls within the fields of osmium, iridium, and rutheniridosmine (Figure 6.32).

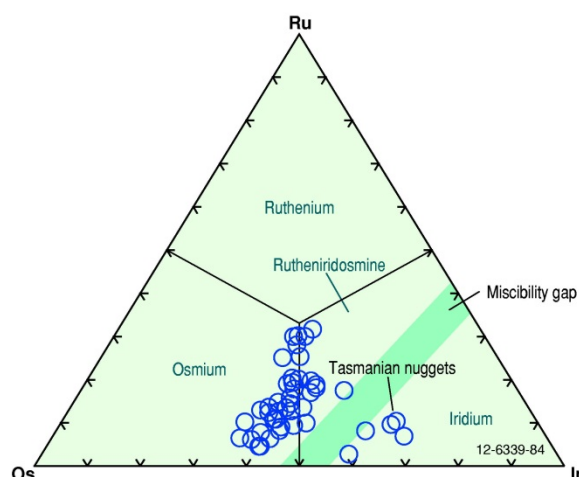


Figure 6.32 Ternary diagram showing compositional fields for Os-Ir-Ru minerals associated with the Tasmanian ultramafic-mafic intrusions based on the classification by Harris and Cabri (1991). The diagram highlights the two tight compositional groups (encompassing Osmium, Iridium, and minor Rutheniridosmine) on both sides of the miscibility gap for the 'osmiridium' grains.

### Age of mineralisation

Very few of the ultramafic-mafic complexes that extend along the western half of Tasmania have direct age determinations. One exception is the Heazlewood River Complex near the northwestern corner of the state (Figure 6.33) which has a similar geological setting and style of PGE-chromite mineralisation to the Adamsfield ultramafic-mafic intrusion. A U-Pb zircon age of fractionated tonalitic rocks from the upper part of the stratigraphy indicates a middle Cambrian crystallisation age of  $513.6 \pm 5$  Ma (Turner and Bottrill, 2001) for the complex. This age is more refined than the previously published ages for the same rock of  $510 \pm 6$  Ma (62 analyses of zircon: Turner et al., 1998), and 520 Ma ( $519 \pm 7$  Ma and  $522 \pm 6$  Ma for two size fractions by conventional U-Pb multigrain zircon dating: Kimbrough and Brown, 1992). This middle Cambrian age may be applicable to the Adamsfield Intrusion and its primary PGE-chromite mineralisation. Most alluvial 'osmiridium' deposits derived from the Tasmanian ultramafic-mafic intrusions are of Cenozoic age (Reid, 1921; Nye, 1929, 1930; Bottrill, 2014), but some examples may extend as far back as the mid-Cambrian. Eluvial and placer deposits of PGEs derived from the Heazlewood River Complex are buried by Cenozoic lavas.

### Genesis

The ultramafic-mafic complexes of western Tasmania are important to the interpretation of the Cambrian evolution of Tasmania. However, despite several decades of detailed research, the origin of these complexes still remains controversial today. The complexes have often been referred to in the literature as 'ophiolite', dismembered 'ophiolite', and fault-bounded alpine intrusions (Rubenach, 1973, 1974; Williams, 1978; Brown et al., 1979). Complete ophiolite sequences typically comprise a basal zone of tectonised peridotite overlain by a sequence of mafic and ultramafic cumulates (ranging from peridotite to gabbro in composition), pillow lavas, feeder dykes, and cherts. Alpine serpentinite complexes have similar tectonic settings and geochemical features to ophiolites, but they generally lack the volcanics and chemical sediments that are associated with ophiolites. Tasmanian complexes that have been often compared to 'ophiolites' include the Heazlewood River (Figure 6.33), Serpentine Hill (Figure 6.34), Wilson River, Anderson's Creek, Forth, and Cape Sorell complexes in northwest Tasmania.

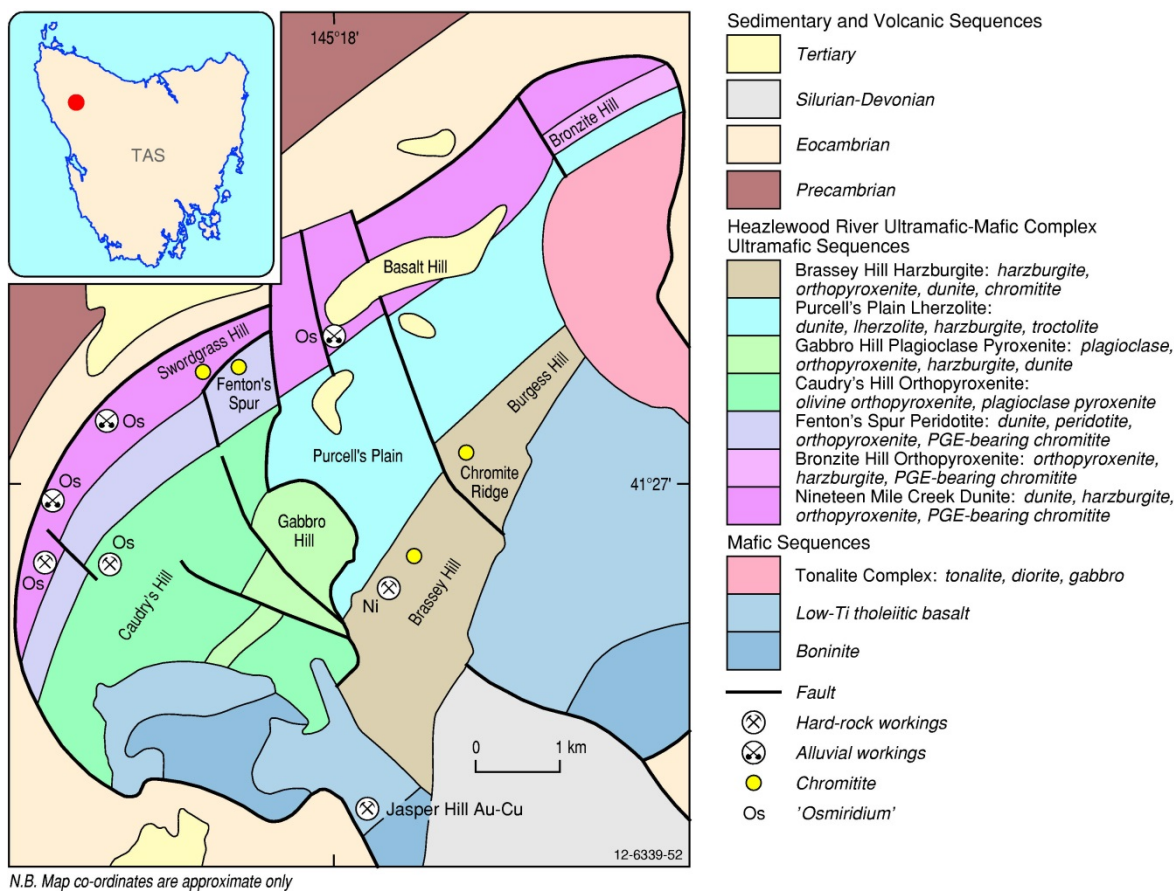


Figure 6.33 Generalised geology of the 513 Ma Heazlewood River ultramafic-mafic intrusion, Delamerian Orogen, Tasmania. Modified from Peck and Keays (1990b).

Williams (1978) interpreted the complexes as representing fragments of oceanic crusts which were thrust up into Crimson Creek Formation sedimentary sequences shortly before the middle Cambrian. The Serpentine Hill Complex according to Rubenach (1974) was tectonically emplaced as an east-dipping thrust sheet over Crimson Creek Formation sediments before the middle Cambrian. Berry and Crawford (1988) considered the Tasmanian complexes were emplaced as an extensive sheet along a sub-horizontal thrust in the early-middle Cambrian, and that this sheet and thrust surface were folded during a Middle Devonian orogenic event. Brown et al. (1979) interpreted the complexes to be slices of oceanic crust that were formed during the waning stage of igneous activity associated with abortive Cambrian rifting of continental lithosphere, and the formation of sedimentary troughs, i.e., a continental rift setting. Other theories invoke an active continental-margin origin (Berry and Crawford, 1988), with emplacement of the oceanic slices during plate collision.

Varne and Brown (1978) showed that the Adamsfield Intrusion probably originally crystallised at low pressures from highly magnesian, titania-poor tholeiitic or andesitic magmas. Equilibration temperatures for coexisting mineral assemblages range from magmatic values ( $1200 \pm 100^\circ\text{C}$ ) for undeformed rocks down to subsolidus values ( $\sim 950^\circ\text{C}$ ) for deformed and altered assemblages. Varne and Brown (1978) also noted that a chemically distinctive group of fine-grained volcanic rocks, including high-magnesia andesites, are associated with some of the Tasmanian ultramafic-mafic intrusions. They proposed that this group be called a Low-titania Ophiolite Association, that was poor in  $\text{TiO}_2$  ( $<0.5\%$ ),  $\text{P}_2\text{O}_5$  ( $<0.1\%$ ), and Zr, and rich in MgO, Ni, and Cr. Crawford and Berry (1992)

characterised mafic volcanics associated with the intrusions as high-Mg basalts of boninitic affinity, low-Ti basalts, and highly depleted magnesian quartz tholeiites. Such distinctive lithologies are only known from forearc regions of oceanic island arcs, and they are difficult to reconcile with an intra-cratonic rift setting. This prompted suggestions that the ultramafic-mafic complexes were derived from an exotic terrane and tectonically introduced to western Tasmania.

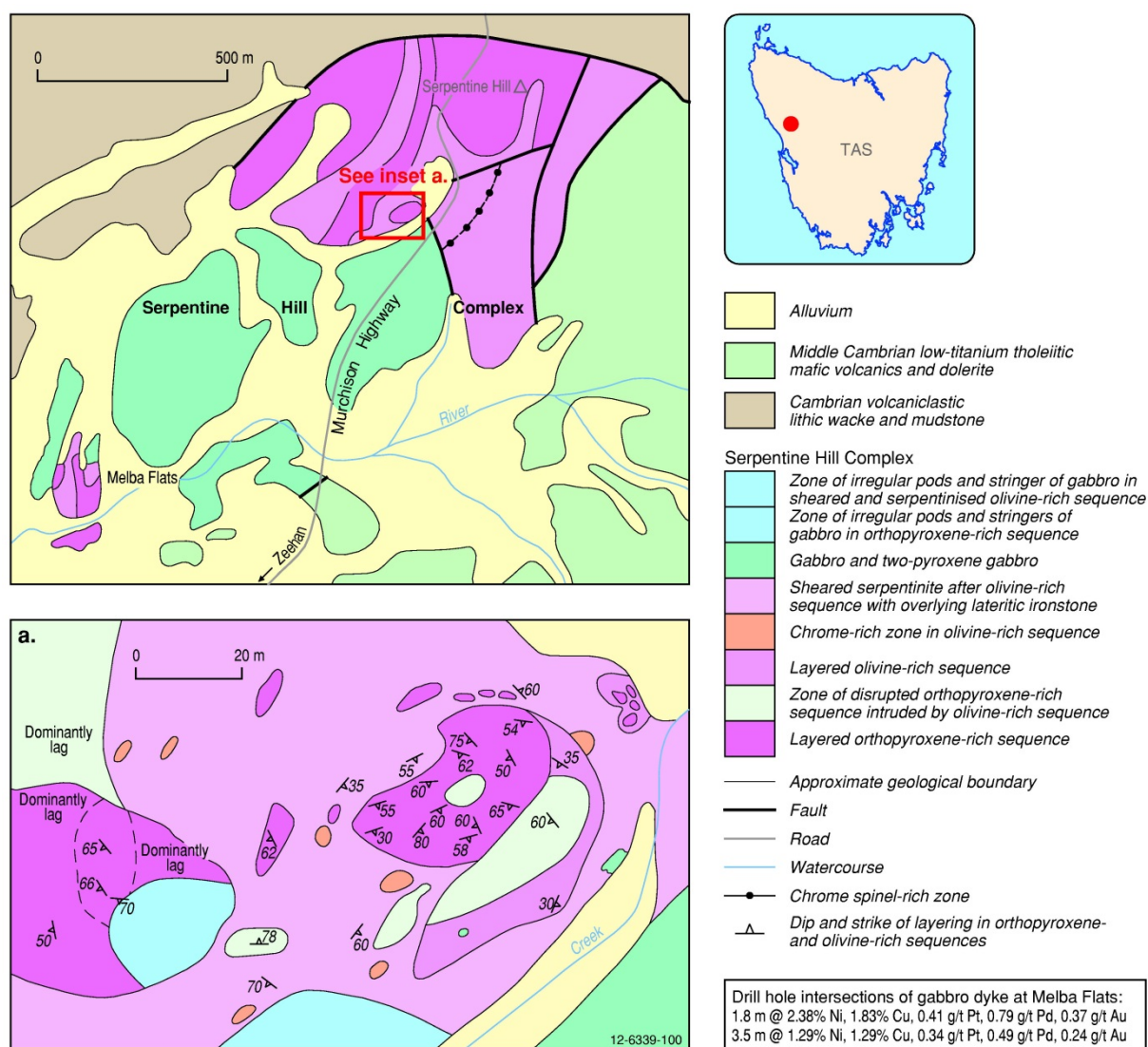


Figure 6.34 Geology of the Serpentine Hill ultramafic-mafic intrusion, Delamerian Orogen, Tasmania. Inset (a) shows detailed geology of central part of Serpentine Hill intrusion. Modified from Brown et al. (1988).

Varne and Brown (1978), Brown (1986), and Crawford and Berry (1992) emphasised that complete ophiolite sequences are rarely preserved in Australia and have never been recorded in Tasmania. On this basis, Crawford and Berry (1992) recommended that the term 'ophiolite', with its genetic connotations of mid-ocean ridge-generated oceanic crust and upper mantle, be abandoned for the Tasmanian ultramafic-mafic complexes. Brown (1986) proposed that the complexes represent tectonically dismembered and multiply re-replaced crystal cumulate bodies generated within a failed continental rift, rather than a supra-subduction zone setting. He concluded they were remnants of

high-temperature-low pressure cumulate magma chambers formed within stretched and rifted continental crust above a rising mantle diapir.

Brown (1992) considered the PGE-bearing ultramafic rocks of western Tasmania formed from parent liquids which produced boninitic and low-Ti basaltic lavas and associated gabbroic rocks. Similar lavas and associated rocks are found within the Cenozoic to Recent Western Pacific Island-arc system between New Guinea and Japan. The present juxtaposition of rock successions in western Tasmania is considered by Brown (1992) to be the result of obduction of parts of a Cambrian island-arc system onto a continental terrane at the end of the middle Cambrian, followed by further deformation during a Mid-Devonian orogeny.

Some historical reports (Reid, 1921; Nye, 1929, 1930) briefly describe the genesis of the 'osmiridium' mineralisation in the Adamsfield ultramafic-mafic intrusion, however, no detailed findings related to this intrusion have been published in recent years. Ford's (1981) investigations of 'osmiridium' grains from Tasmania (including Adamsfield) described three types of silicate inclusions in the PGMs, that range from 0.025 mm to 0.05 mm in size. The inclusions included: olivine ( $\text{Fo}_{89-94}$ ); Mg-Fe pyroxene containing up to 3%  $\text{Al}_2\text{O}_3$ ; and highly aluminous, calcic pyroxenes that were non-stoichiometric. The inclusions suggest formation temperatures as high as 1700°C (unrealistically high since more primitive high-Mg komatiitic magmas have typical liquidus temperatures of ~1600°C: Arndt et al., 2005), and tend to show a trend toward lower magnesium values that may reflect the changes of an evolving magmatic system. From a petrogenetic point of view, Ford (1981) favoured the production of the PGMs by an exsolution process as the parent magma began to crystallise, rather than from crystallisation of a separate melt.

The following summary of the genesis of the Tasmanian Os-Ir-Ru deposits is from Bottrill (2014). The origin of the primary 'osmiridium' mineralisation at Adamsfield is not well understood, but in similar deposits worldwide the Os-Ir-Ru alloys are found to originate in chromitite, dunite, and related ultramafic rocks derived from high-Mg magmas (Boudreau 1995; Brown et al., 1988; Brenker et al., 2003; Peck and Keays, 1990). The high-melting points and low solubility of Ir, Os, and Ru in these magmas results in these metals precipitating with chromite at high temperature, early in the cooling of the magma, usually as a variable mixture of alloys, arsenides, and sulphides, depending on the S and As contents of the magma (Stockman and Hlava 1984; Barnes et al., 1985; Torres-Ruiz et al., 1996; Krstic and Tarkian, 1997). The PGE contents of the ultramafic rocks are related to the degree of mantle melting, and Hattori and Cabri (1992) confirmed a mantle origin for the PGE alloys using  $^{187}\text{Os}/^{186}\text{Os}$  isotopes. A low  $(\text{Pt}+\text{Pd})/(\text{Os}+\text{Ir})$  ratio in ultramafic rocks is probably indicative of a low S fugacity in relatively unfractionated magmas, as Pt and Pd are scavenged by sulphides in the melts and precipitate in chromite (Barnes et al., 1985). Bai et al. (2000) suggested that the PGMs form deep in the mantle and are captured by rising mantle plumes, but Boudreau (1995) and Brenker et al. (2003) considered them to have a hydrous magmatic origin, with elevated concentrations in saline hydrous fluids in the shallow upper mantle. Peck and Keays (1990) thought that laurite ( $\text{RuS}_2$ ) was an important early cumulus phase, which was largely entrained in chromite grains, cumulating in chromitites with interstitial, altered, Os-Ir-Ru alloys and later-formed Pd-group arsenides and sulpharsenides. Torres-Ruiz et al. (1996) considered the PGEs to be precipitated firstly mostly as arsenides and sulphides, with the alloys forming much later by reduction of these minerals, perhaps by hydrogen generated during serpentinisation (as for Ni-Fe alloys: Andersen et al., 2002). Elhaddad (1996) considered the magmatic PGEs were modified by low-temperature processes. The Tasmanian PGE deposits have a low  $(\text{Pt}+\text{Pd})/(\text{Os}+\text{Ir})$  ratio, which Cabri and Harris (1975) noted to be typical of relatively 'old' Alpine-type intrusions, with large obducted sheets, whilst generally the 'Alaskan-type' with multiple intrusions usually have a high value. Cabri and Harris (1975) and Barnes et al. (1985)

tentatively suggested that the (Pt+Au)/(Os+Ir) ratio is indicative of the degree of fractionation of the parent magma. Peck and Keays (1990) noted the ratio depends on the S content of the magma: with increasing S content the Ir group (Ir-Os-Ru) minerals are precipitated first, and with S saturation the Pd-group (Pt-Pd-Rh) minerals are precipitated. Peck et al. (1992) concluded that the Tasmanian Os-Ir-Ru-Pt alloys crystallised before the emplacement of boninitic parent magmas into crustal magma chambers. Some of the richest primary occurrences of 'osmiridium' in Tasmania are, however, in highly altered schlieren and foliated serpentine zones possibly representing late-stage shear zones. This may indicate post-magmatic alteration and mobilisation (or perhaps just physical entrapment during erosion). The 'osmiridium' nuggets cemented by Au or Pt-Fe alloys and the Os-Ir grains cemented, veined, and rimmed by irarsite (IrAsS) also indicate post-magmatic alteration, at moderate temperature. These occurrences require further research, but there is good evidence for a high-temperature origin, but with some modification by poorly understood low-temperature processes.

### *Key references*

- Reid (1921): early account of 'osmiridium' in Tasmania (including Adamsfield); rock types; geology; prospects; alluvial deposits.
- Nye (1929, 1930): historical accounts of mining operations at Adamsfield; geology of alluvial and hard-rock deposits; production statistics; prospectors.
- Cabri and Harris (1975): Os-Ir-Ru alloys from Tasmania (including Adamsfield); morphology and mineralogy of alluvial 'osmiridium' grains and nuggets; compositional variations in grains; chemical zonation; comparisons with other deposits; origin of Os-Ir-Ru alloys.
- Varne and Brown (1978): geological map; stratigraphy; petrology; mineralogy; geochemistry; PGEs; distribution of chromite; economic potential of Adamsfield Intrusion.
- Ford (1981): geology; mineralogy of PGMs; alluvial grains and nuggets from Adamsfield; comparisons with other PGE deposits.
- Bacon (1992): history of mining at Adamsfield; mining culture; prospectors; photographs of historical mining activities; statistics of 'osmiridium' production in Tasmania; exploration.
- Crawford and Berry (1992): tectonic setting of Late Proterozoic–Early Paleozoic igneous rock associations in western Tasmania; geochemically classified mafic volcanic rocks as high-Mg basalts of boninitic affinity, low-Ti basalts, and highly depleted magnesian quartz tholeiites; questioned status of ophiolite definition for Tasmanian ultramafic-mafic complexes; genesis.
- Franklin et al. (1992): remobilisation of PGEs in podiform chromitites; alpine-type ultramafic body; Coolac Serpentinite Belt; mineralogical study; genesis.
- Bottrill (2014): PGEs and Ni mineralisation of mafic-ultramafic complexes in Tasmania; rock types; mineralogy; PGMs; exploration history; mineral prospects and deposits associated with complexes; mining; production statistics.
- Corbett et al. (2014): mafic-ultramafic complexes of Tasmania; geological setting of Adamsfield Intrusion; Cambrian geology of Tasmania; Cambrian tectonics.

## 6.4.6 Mineral-System Class 6: 'Alaskan- and Urals-type' mafic-ultramafic intrusions

### 6.4.6.1 Deposit Type 6.A: PGE mineralisation in concentrically zoned mafic-ultramafic intrusions

#### Overview

'Alaskan- and Urals-type' or concentrically zoned complexes (Johan, 2002; Tolstykh et al., 2005) intrude orogenic zones during, or after, the late stages of the main deformation event, but generally before the emplacement of granite batholiths. Some of the most important overseas PGE placer deposits are associated with zoned ultramafic intrusions. These include the Goodnews Bay in Alaska, Ural Mountains in Russia, the Tulameen area in British Columbia, Venezuela, and northern California, USA (Mertie, 1969; Irvine, 1974; Gray et al., 1986; Nixon and Hammack, 1991; Johan, 1992; Tolstykh et al., 2005).

With the exception of the Fifield region of central New South Wales, 'Alaskan- and Urals-type' mafic-ultramafic intrusions appear to be rare in Australia. This may be due in part to post-emplacement deformation that has destroyed the concentric form and primary mineralogy of these small intrusions making recognition difficult, and/or their poor surface preservation during protracted erosional-lateritisation events during the Cenozoic. In the Girilambone Anticlinorial Zone of central New South Wales, more than 60 late Ordovician to late Silurian (e.g., 450 to 420 million years) 'Alaskan-type' intrusions form a ~250-km-long north-northwest trending belt that coincides with the Parkes Terrace—a composite structural zone bounded by major faults and containing regionally elevated twin-ridge gravity anomalies. Trace-element geochemical studies by Wyborn (1988, 1990) indicate the intrusions near Fifield have shoshonitic affinities, and possibly represent deep cumulate feeder zones to Ordovician volcanics and high-level sills that occur to the east and south of Fifield. Linear alpine-type serpentinites are commonly associated with the zoned intrusions. Mafic rocks are dominated by diorite, monzonite, syenite, and hornblendite, and ultramafic rocks comprise dunite, wehrlite, peridotite, clinopyroxenite, olivine clinopyroxenite, biotite clinopyroxenite, and magnetite clinopyroxenite. The lithologies often display a crude concentric zonation with ultramafic rock types in the core surrounded by mafic and alkaline rocks. Primary and secondary concentrations of PGEs are associated with the intrusions in orthomagmatic and hydrothermal vein-type mineral systems in ultramafic rocks (Deposit Type 6.A), deep laterite profiles above ultramafic lithologies (Deposit Type 9.A), and in alluvial paleoplacer deposits (Deposit Type 10.A). The intrusions generally display broad petrological and geochemical similarities to PGE-bearing Phanerozoic mafic-ultramafic intrusions that represent type examples in Alaska (USA) and the Urals (Russia: Johan, 2002).

Alaskan and placer-type PGE mineralisation has also been investigated in a group of small composite Paleozoic-Mesozoic complexes (Wateranga, Goondicum, Hawkwood, and Boyne) along major lineaments in the New England Orogen of southeast Queensland. The Wateranga Intrusion (28 km<sup>2</sup> in area, >500-m thick) is an undeformed, unmetamorphosed, Permo-Triassic layered gabbroic pluton intruded into late Carboniferous sedimentary rocks (Talusani et al., 2005). Dominant rocks include gabbro and norite, with subordinate troctolite, anorthosite, orthopyroxenite, and rare picrite. The ovoid-shaped body shows evidence of extreme fractionation of incompatible trace elements (e.g., Ti, Zr, P) as evidenced by the development of titaniferous magnetite horizons. Minor PGMs have been reported in the intrusion (Talusani et al., 2005).

### *Australian deposits/prospects/hosts*

Owendale Intrusion, Tout Intrusion, Kars Intrusion, Honeybugle Intrusion, Hylea Intrusion, Bulbodney Creek Intrusion (all Central NSW–Omeo Province, Lachlan Orogen, NSW); Wateranga (New England Orogen, Qld).

### *Significant global example(s)*

Nizhny Tagil Complex, Katchkanar Complex, Svetli Bor Complex, Konder Complex, Inagli Complex (all Russia); Goodnews Bay (Alaska); Tulameen Complex (Canada); Alto Condoto Complex (Colombia); Yubdo Complex (Ethiopia).

### *Type example in Australia*

Owendale Intrusion, New South Wales.

### *Location*

Longitude 147.469850°E, Latitude -32.69219°S; 1:250 000 map sheet: Narromine (SI 55–03), 1:100 000 map sheet: Boona Mount (8332); ~15 km north of Fifield, New South Wales.

### *Geological province*

Central NSW–Omeo Province, Lachlan Orogen, New South Wales.

### *Resources*

No resources have been published for primary PGE mineralisation associated with 'Alaskan- and Urals-type' mafic-ultramafic intrusions in Australia. However, several exploration companies have defined Pt resources (Table 6.2) in laterite deposits associated with these intrusions, namely:

- Owendale North Prospect—31 Mt @ 0.52 g/t Pt, 0.15% Ni, 0.05% Co (Total Mineral Resource: Platina Resources Ltd, 2014b);
- Cincinnati Prospect—9 Mt @ 0.5 g/t Pt (Inferred Resource: Helix Resources Ltd., 2004b), 2.6 Mt @ 0.7 g/t Pt (Indicated Resource: Platina Resources Ltd., 2012); 2.2 Mt @ 0.7 g/t Pt (Inferred Resource: Platina Resources Ltd., 2013a); and
- Milverton Prospect—1.3 Mt @ 0.6 g/t Pt (Inferred Resource: Platina Resources Ltd., 2013a).

### *Current status and exploration history*

Prospects with advanced exploration. The 'Alaskan-type' mafic-ultramafic intrusions of central New South Wales are generally poorly exposed and most have been explored by modern geophysical and geochemical techniques. The identification of the intrusions was facilitated by the release in 1961 of the first regional airborne magnetic survey by the BMR. The survey delineated many mafic and ultramafic intrusions concealed under shallow alluvium and laterite cover. The hard-rock potential of the Fifield intrusions was initially highlighted in 1966 during a four-hole diamond-drill program of the Owendale Intrusion by Anaconda Australia Incorporated. Original high-grade Pt abundances (1.4 m from 302.36 m @ 13.2 g/t Pt, 0.93 g/t Pd: Teluk, 2001) reported in fresh pyroxenite from the Kelvin Grove prospect were confirmed some twenty years later by reanalysing of the drill core by New South Wales government geologists (Suppel and Barron, 1986a). The Owendale Intrusion was extensively explored for PGEs after the mid-1980s. For the period 1985 to 1991, Helix Resources NL undertook 6000 m of trenching, and 31 000 m of rotary air blast (RAB), reverse circulation, and diamond drilling. Several junior exploration companies followed up these new findings with regional

geophysical-geochemical surveys that relied on shallow-drilling programs to penetrate the Quaternary clays and sands that cover the flat-relief countryside. Exploration programs in the Owendale Intrusion have focussed on primary concentrations of Pt in ultramafic lithologies (e.g., clinopyroxenite), alluvial deep leads of Pt, and Pt-Sc-bearing laterites. Further details of the exploration history of the 'Alaskan-type' intrusions in the Fifield region can be found in Chapter 5.

Many of the intrusions near Fifield have been described in detail, largely in the form of many unpublished company reports. From the late 1980s to 2000 there was a significant increase in available published information relating to the intrusions, including government geological survey (Suppel and Barron, 1986a,b; Barron et al., 1987; Suppel et al., 1987; Wyborn, 1988, 1990; Wyborn and Cameron, 1990; Barron et al., 2004) and university investigations (Agnew, 1987; Agnew et al., 1987; Brill and Keays, 1989a,b, 1990; Shi, 1995; Stojanovic, 1995). During this period, there were also a number of important reviews (Elliott and Martin, 1991; Teluk, 2001) and several international studies (Bowles, 1989; Johan et al., 1989, 1990a,b; Slansky et al., 1991) that documented the mineralogy and genesis of PGEs from the Fifield region.

### *Economic significance*

The Fifield district in central New South Wales was Australia's first significant producer of alluvial Pt. Platinum was found in 1887, but there was little production until the discovery of the Platina Lead in 1893. The three most important deep leads, the Platina Lead, Gillenbine Tank Lead, and the Fifield Lead, are located south of the Owendale Intrusion, near the Tout and Murga mafic-ultramafic intrusions. Total production from the deep leads amounted to about 633 kg Pt and 178 kg of Au, with the most productive year being 1896 (75.8 kg Pt). The different styles of primary and secondary PGE mineralisation that have been defined in the 'Alaskan-type' intrusions indicate the Fifield region has significant economic potential. A diverse group of other commodities (e.g., Ni, Co, Cu, Au, Cr, Sc, and vermiculite) associated with the intrusions has protracted the exploration interest of these intrusions. Despite intensive phases of exploration by many junior companies and investigations by New South Wales government geologists, no primary or secondary PGE deposits associated with the intrusions are economic (as of late 2014).

The best documented Alaskan-type intrusion in Australia is probably the Owendale Intrusion. The Owendale intrusion, which was first regarded as having Alaskan-type affinities by Bowman et al. (1982), has subsequently been used as a standard for the classification of other similar bodies in central New South Wales.

### *Geological setting*

More than sixty 'Alaskan-type' mafic-ultramafic intrusions are interpreted to form a north-northwest-trending belt in the Girilambone Anticlinorial Zone—a major tectonostratigraphic province of the Lachlan Orogen in central New South Wales (Table 6.12, Figure 6.35). Many of the poorly exposed intrusions in the belt have been detected by aeromagnetic data and their 'Alaskan-type' classification has still to be confirmed since they are poorly described or have very small or non-existent ultramafic components (Elliott and Martin, 1991). The intrusions extend for over ~250 km northwards from just south of Condobolin through Fifield to at least 50 km north of Nyngan, and possibly further north to Doradilla near Bourke. This regional province coincides with a 80 km-wide north-trending belt of gravity highs known as the Parkes Terrace—a regional zone of crustal thinning, possibly containing deep penetrative crustal structures (sutures, detachments, etc) that focussed the emplacement of the 'Alaskan-type' intrusions into mid-crustal levels from source areas in upwelling lithospheric mantle (Suppel and Barron, 1986a; Derrick, 1991). The oldest outcropping unit of this province is the

Girilambone Group, a northerly-trending belt of sediments deposited during the late Cambrian to Early Devonian age. Bounding the Girilambone Group to the east are late Silurian to early Devonian felsic volcanic and sedimentary rocks and to the west, middle Devonian sedimentary rocks of the Tullamore and Murga synclines. The Girilambone Group is believed to have accumulated as a flysch sedimentary sequence on the continental slope and within the adjacent trench. The rocks of the Girilambone Group are strongly deformed and are usually steeply dipping.

The 'Alaskan-type' intrusions typically form composite plug-like bodies with steeply dipping internal contacts and comprising a variety of alkaline mafic and ultramafic rocks. Outcrop is rare, and most bodies are generally covered by shallow thicknesses of soil, eluvium, sheet wash, and buried drainage channels containing gravel, sand, and clay. Their near circular, ovoid, elliptical, and curvilinear outlines are well preserved in aeromagnetic data. Mafic rocks are dominated by diorite, monzonite, syenite, and hornblendite, and ultramafic rocks comprise dunite, wehrlite, peridotite, clinopyroxenite, olivine clinopyroxenite, biotite clinopyroxenite, and magnetite clinopyroxenite. The intrusions generally display broad petrological and geochemical similarities to PGE-bearing Phanerozoic mafic-ultramafic intrusions that occur in Alaska (USA) and the Urals (Russia: Johan, 2002). Their multiple and clustered distributions suggest further intrusions may occur along extensions of the presently defined province. Figure 6.36 shows that several intrusions between Nyngan and Fifield have recorded significant intersections of anomalous PGEs. In general, the Fifield intrusions have high average background PGE contents compared with other types of ultramafic intrusions. Background contents of PGEs commonly exceed 30 ppb Pt+Pd in ultramafic lithologies (Elliott and Martin, 1991). Linear alpine serpentinite bodies thought to represent the remains of a subduction zone active during the Ordovician are spatially associated with some of the larger zoned intrusions (e.g., Honeybugle). The emplacement of the 'Alaskan-type' intrusions is thought to have occurred during the Devonian, proximal to the Gilmore Suture in the western half of the Parkes Terrace. Ordovician-Silurian volcanic and related intrusives found to the east, are spatially related, and possibly genetically related, to the 'Alaskan-type' intrusions. During the late Paleozoic, deep erosion exposed the intrusive complexes whilst continued weathering during the Cenozoic saw the development of up to 50 m-thick laterite profiles, and the scouring of paleo-alluvial channels in the underlying intrusions. Anomalous concentrations of Pt in the most explored intrusions (e.g., Owendale, Tout, Kars, Honeybugle, Bulbodney Creek, Hylea, and Murga) occur in three major settings:

1. primary orthomagmatic and hydrothermal hard-rock deposits hosted by ultramafic lithologies;
2. laterite profiles overlying ultramafic lithologies (see Deposit Type 9.A); and
3. Cenozoic gravels, buried leads, and in recent alluvium derived from the intrusions and associated rocks (see Deposit Type 10.A).

The intrusions shown in Table 6.12 are compiled from exploration reports of the Geological Survey of New South Wales.

Table 6.12 'Alaskan-type' mafic-ultramafic intrusions in the Fifield–Nyngan region, New South Wales.

	Intrusion	Extent (km <sup>2</sup> )	Form	Major rock types <sup>1</sup>	Reference(s) <sup>2</sup>
1	Carlton	6			1989/221
2	Horton Park	23			1989/221
3	Gerar	23	Annular	Dior	1984/104

	Intrusion	Extent (km <sup>2</sup> )	Form	Major rock types <sup>1</sup>	Reference(s) <sup>2</sup>
4	Fairfield	2.5			
5	Kidbull	<1			1991/209
6	Kidgery	1	Dyke		1991/209
7	Gundaur	4			1991/209
8	Gilgoenbon	3			1991/209
9	Bonna	1			
10	West Lynne North	2		Du, Per	1991/209
11	West Lynne	2			1991/209
12	Lynch	3	Dyke		1988/210
13	Redlands	3		Du	1991/209
14	Rosedale	4			1991/209
15	Nyngan	2		Pyrox, Per	1984/104
16	Cooreen	1	Dyke, annular		1988/210
17	Nyngan South	3			2001/253
18	Whitbarrow Creek–Gilgai	20	Faulted dyke	Pyrox, Du, Serp, Hb, Dior, OP-unit, Lamp	2001/216
19	Koonora	4			1988/210
20	Whitbarrow	2.5	Dyke		1988/210
21	Rutherglen	5			1988/210
22	Darouble	1.5			1988/210
23	Neerock	4			1988/210
24	Keenan	3			1988/210
25	Pangee	3			1988/210
26	Summerlea	4.5			1988/210
27	River	5			1988/210
28	Honeybugle	148	Annular, composite, oval, linear	Monzodi, Pyrox, Hb, Dior	1986/198
29	Hermitage Plains (New Haven)	1		Pyrox, Dior, P-unit	EXP NSW
30	Trangie	<1		Pyrox, Gab	1992/217
31	Widgelands–Homeville–Collerina	15	Linear, dyke	Du, Serp	
32	Sampsons Tank	<1			1989/269
33	Laceys	<1		Mafic and ultramafic rocks	1989/269
34	Minemoorong	38			1999/404
35	Hillview	1		Pyrox	1995/281
36	Bulbodney Creek	37	Annular		1995/281

	Intrusion	Extent (km <sup>2</sup> )	Form	Major rock types <sup>1</sup>	Reference(s) <sup>2</sup>
37	East Albert, Rosehill	1		Pyrox	1992/334, 1995/079
38	Tanthitha	3.5	Composite, faulted, oval	Du, Hb, Gab, Pyrox, Dior, Serp	
39	Hylea	22	Annular, faulted, oval	Monz. Hb, Dior, Du, Pyrox	1989/133, 1991/262, 1994/055
40	Glenoma	2		Cpyrox, Monz	1988/315
41	Middletons	2.5			
42	Jumble Plains West	1			2003/057
43	Jumble Plains East	<1			2001/492
44	Tresylva	4.5		Pyrox, Gab, Hb	1988/276
45	Glen Lyon	<1	Plug	Hb	1988/276
46	Owendale	55	Annular, oval	Du, Per, Pyrox, Hb, Monzodi, Monz, P-unit	1991/059
47	South Cleveland	<1		Hb	1988/315
48	Looney	28	Oval, dyke	Gab, Dior	
49	Tout–Flemington–Syerston	55	Annular, composite, oval	Du, Per, Pyrox, Hb, Gab, Monzodi, Monz	1991/023
50	Rosedale?	2		Gab, Dior	
51	Glen Iris	<1		Gab, Dior	1988/276
52	Murga–Wandabye	6	Annular, linear	Gab, Hb, Dior, Monzodi, Pyrox	EL4450
53	Yoes	3		Dior	1988/276
54	Karra Karra	<1	Plug	PyroxHb, Monzodi	1989/225, 1988/160
55	Carlisle	<1	Linear		1988/276
56	Ellon Lea				
57	Grassdale				
58	Forest View	<1		Pyrox, Gab, HbPyrox	1989/225
59	Ionumba	<1			
60	Avondale	3	Dyke, annular, faulted	Pyrox, Du, Serp, Hb, Dior, OP-unit, Lamp	1989/225
61	Mt Derriwong–Murrumbogie	1.5	Annular, oval	Dior, Pyrox, Du, Hb, Lamp	1989/335
62	Kars	<1	Composite, dyke, faulted	Pyrox, Per, OP-unit, Monz, Lamp	1989/335
63	Kookaburragong	<1		Pyrox	1995/208
64	Morrison	<1		Dior, Hb, Pyrox	1983/355

<sup>1</sup> Amph = amphibolite; CPyrox = clinopyroxenite; Dior = diorite; Du = dunite; Gab = gabbro; Hb = hornblende; HbPyrox = hornblende pyroxenite; Lamp = lamprophyre; Monz = monzonite; Monzodi = monzodiorite; Per = peridotite; Pyrox = pyroxenite; PyroxHb = pyroxene hornblende; Serp = serpentinite.

<sup>2</sup> References refer to exploration reports from the Geological Survey of New South Wales.

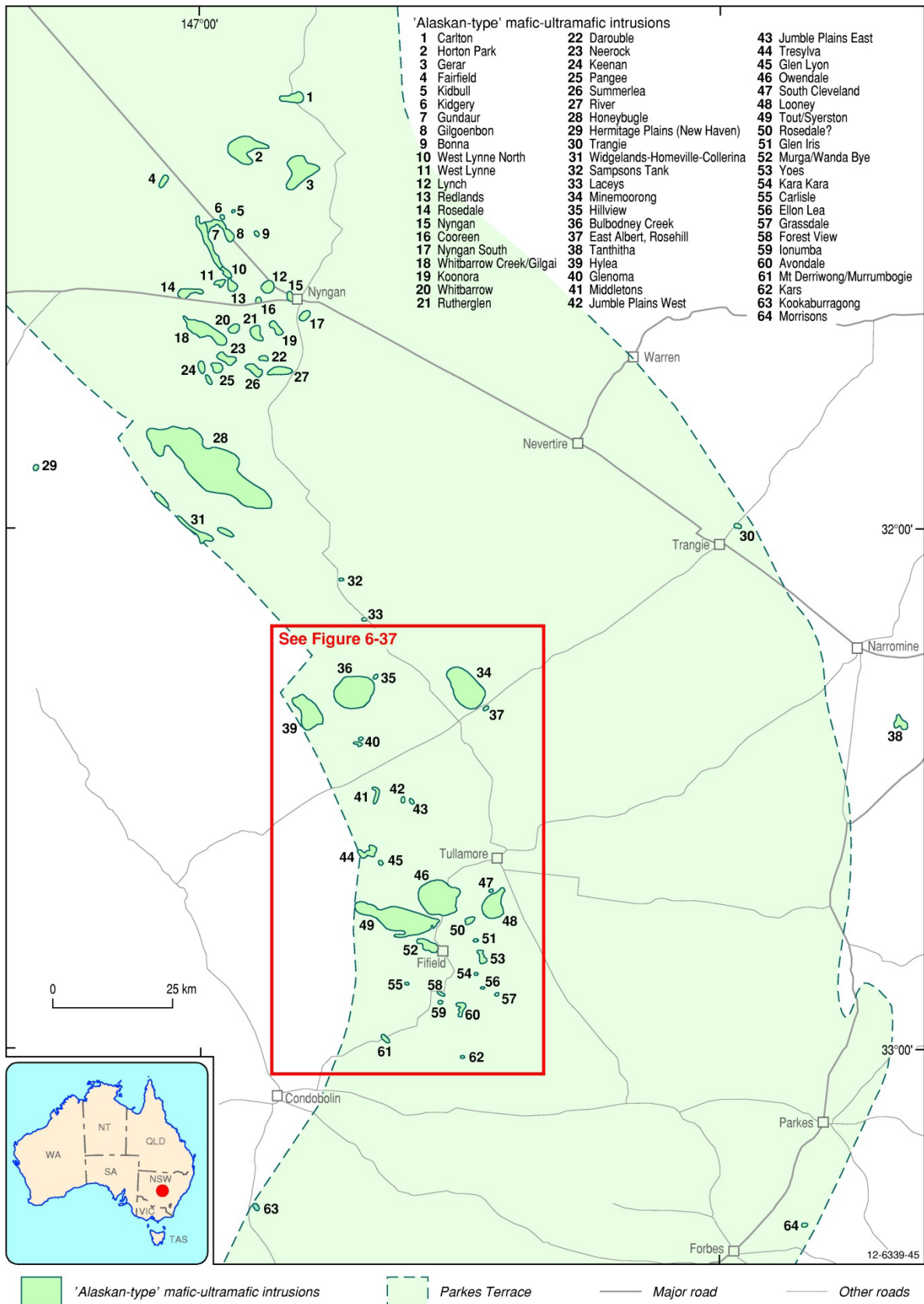


Figure 6.35 Distribution of 'Alaskan-type' mafic-ultramafic intrusions in the Parkes Terrace of the Lachlan Orogen, central New South Wales. The intrusions numbered from 1 to 64 are described in Table 6.12; the geological settings of the intrusions in the inset box are shown in Figure 6.37.

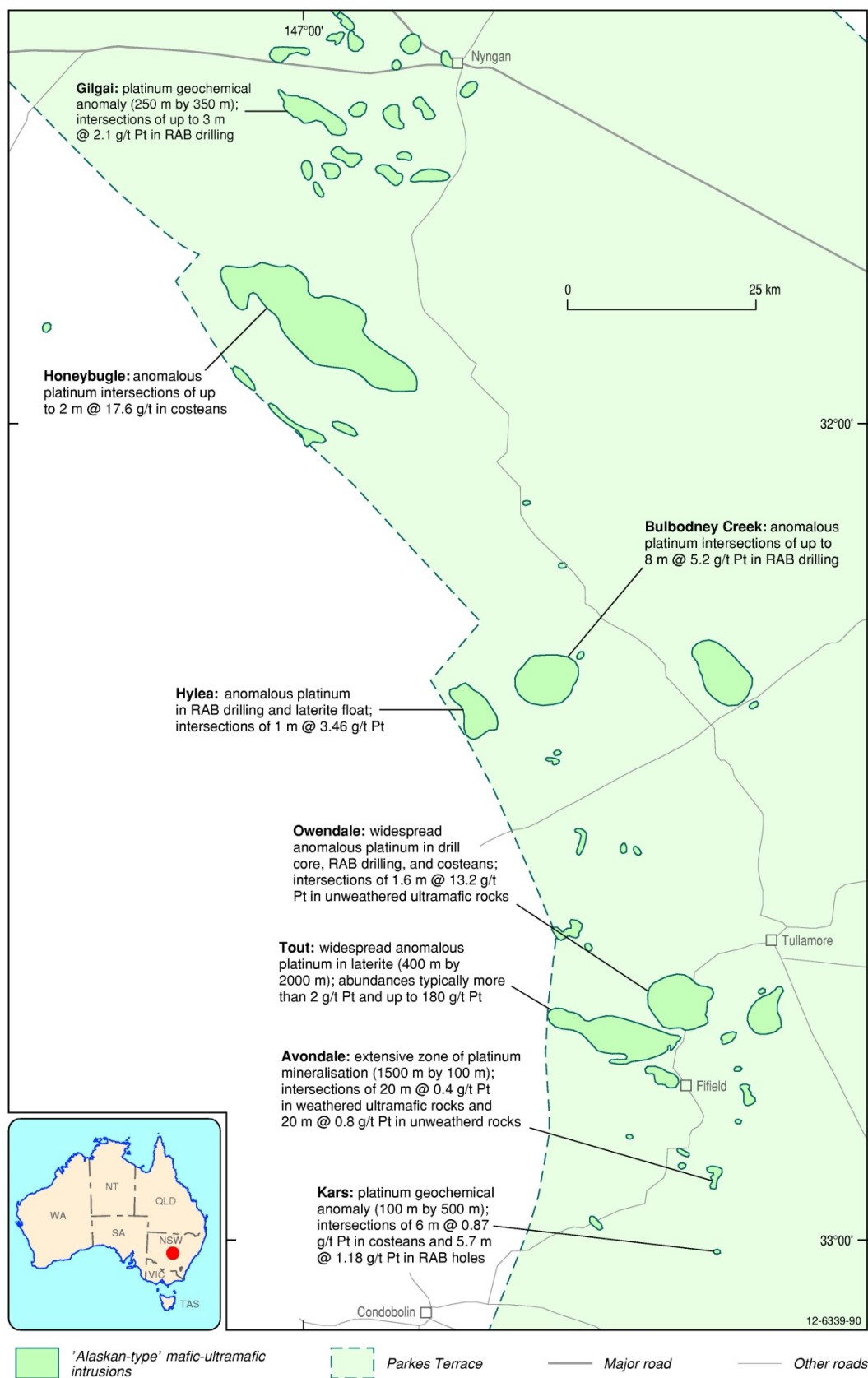


Figure 6.36 Significant geochemical intersections for hard-rock and laterite platinum deposits associated with the 'Alaskan-type' mafic-ultramafic intrusions between Nyngan and Fifield. Geochemical data compiled by senior author from many company announcements to the Australian Securities Exchange.

### *Mineralisation environment*

The Owendale Intrusion (Figure 6.37 and Figure 6.38) is a steeply plunging, pipe-like body, with a near circular plan view measuring ~8 km by ~7 km. The complex comprises three distinct lithological groups based on mineralogy and stratigraphic position. An Ultramafic Series comprise approximately one-third of the surface area of the complex and, apart from an isolated body near the centre of the complex, forms a continuous zone along the eastern part of the intrusion. This zone has been further sub-divided into the North Owendale (northeast), Cincinnati (east), and Kelvin Grove (south) areas. Mafic-Felsic Series lithologies comprise most of the western two-thirds of the complex. The Marginal Series occurs, for the most part, adjacent to the external contacts of the complex. Crude layering in drill core from the Kelvin Grove area indicates the presence of steeply dipping units which appear to parallel the external contacts of the complex. Poorly developed cyclical layering on a scale of several metres to tens of tens of metres show a general increase in olivine from clinopyroxenite to wehrlite towards the centre of the complex. Peripheral to the intrusion are contact metamorphosed sedimentary rocks—metawacke, quartz mica schist, and slate—of the Cambro-Ordovician Girilambone Group. All rocks of the intrusion are weathered to depths from a few metres to 80 m and are covered by a thin veneer of soil and clay/sand/gravel alluvium up to 40 m deep.

Lithologies in the Ultramafic Series include biotite-, magnetite-, and olivine-bearing clinopyroxenite, dunite, and wehrlite. Dunite and surrounding envelopes of wehrlite are the products of late-stage magmatic alteration. Hornblende clinopyroxenites are interlayered with the Ultramafic Series lithologies, but are generally restricted to the margins of the intrusion and are therefore included in the Marginal Series. Clinopyroxene-rich ultramafic lithologies contain diopsidic augite with varying amounts of minor biotite, magnetite, and olivine, and accessory hornblende, plagioclase and rare K-feldspar. Wehrlite comprises 40% to 85% olivine and dunite greater than 85% olivine. The PGE-enriched monomineralic clinopyroxenite units ('P units') are locally pegmatitic and are devoid of accessory minerals. No orthopyroxene is present in the Ultramafic Series lithologies.

Lithologies in the Mafic-Felsic Series can be broadly subdivided into a central core of monzonite and an outer zone of diorite which is in contact with rocks of the Ultramafic Series and Marginal Series. Further subdivisions of this series based on the proportions of primary and accessory minerals reveals a crude concentric zoned pattern to the units. Plagioclase, augite, and orthoclase are the principal minerals in this series, with minor magnetite and biotite. Some mafic rocks also contain hypersthene or hornblende, and quartz is restricted to the margins of the intrusion.

Marginal Series lithologies are confined to the margins of the intrusion, and locally between Mafic-Felsic Series and Ultramafic Series rocks west of Cincinnati. Marginal Series rocks are interlayered with, and to some extent gradational to, rocks of the other two Series. They are characterised by an abundance of hornblende with the hornblende content being a good mineralogical discriminator for rocks of this Series from those of the Ultramafic and Mafic-Felsic Series. Major lithologies include hornblendite, pyroxene hornblendite, hornblende clinopyroxenite, and hornblende gabbro. Hornfels are also interlayered with rocks of the Marginal Series.

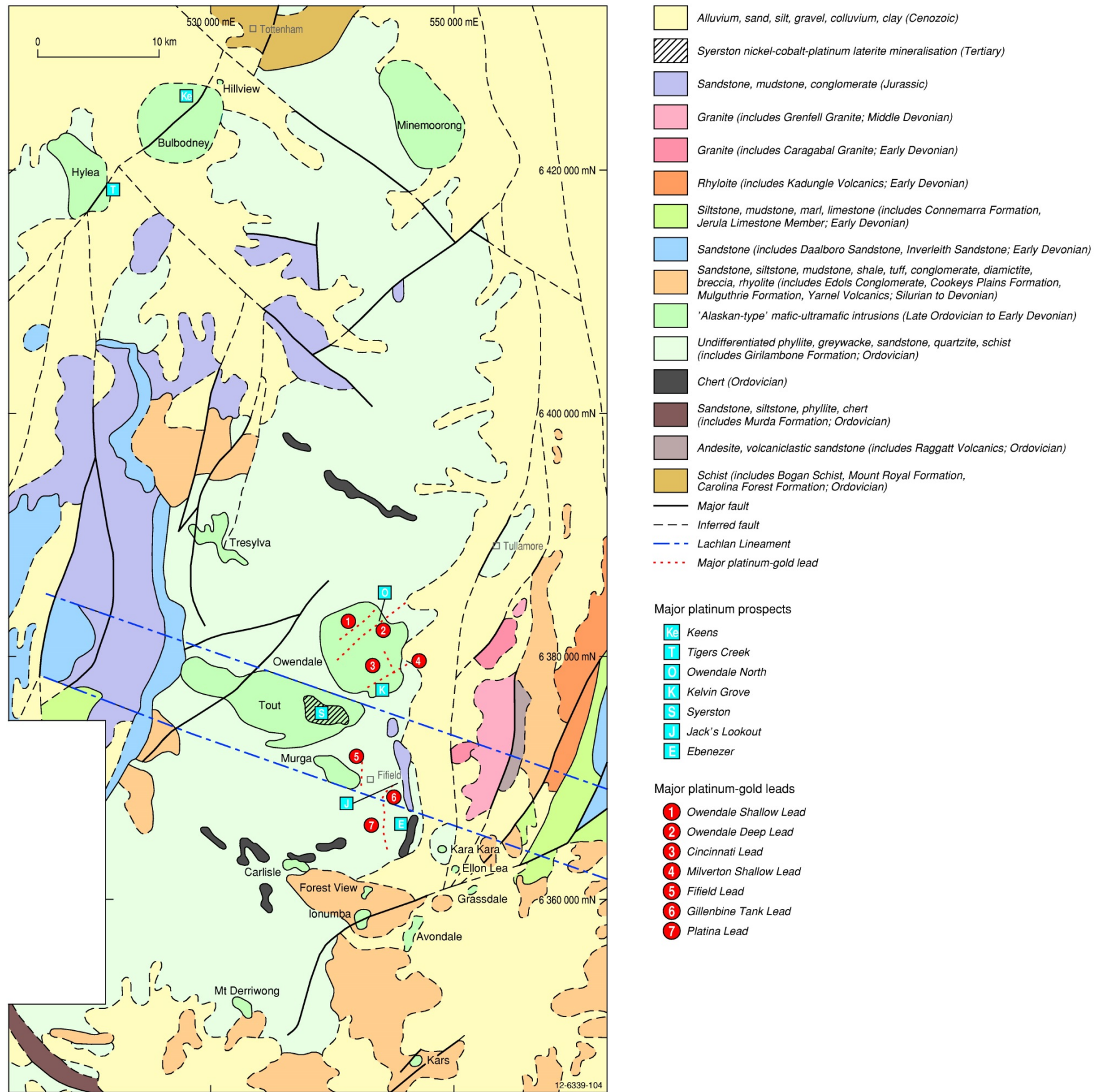
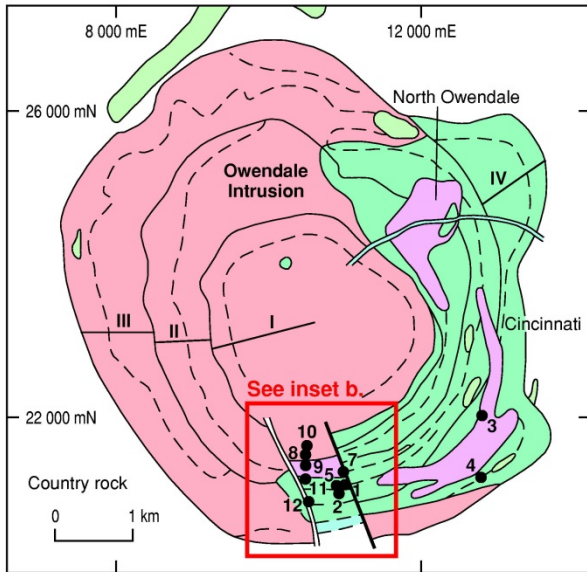


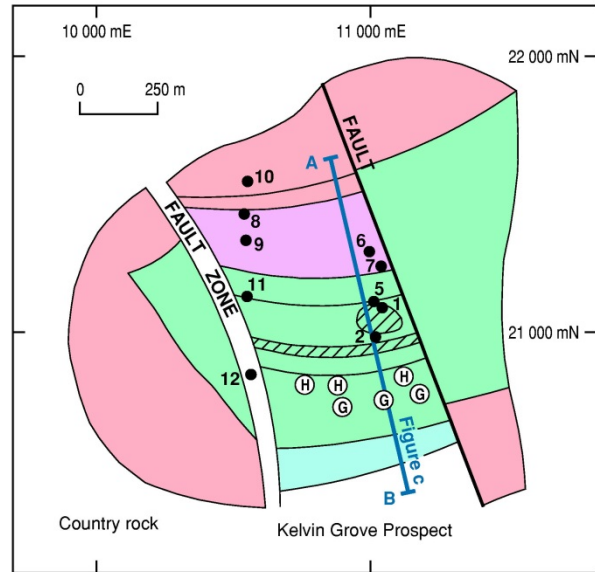
Figure 6.37 Geology of 'Alaskan-type' mafic-ultramafic intrusions, platinum prospects, and platinum-gold leads in the Fifield-Tottenham region. Modified from Rimfire Pacific Mining (2009).



**a. Owendale Intrusion**



**b. Kelvin Grove Prospect**



**c. Kelvin Grove Prospect**

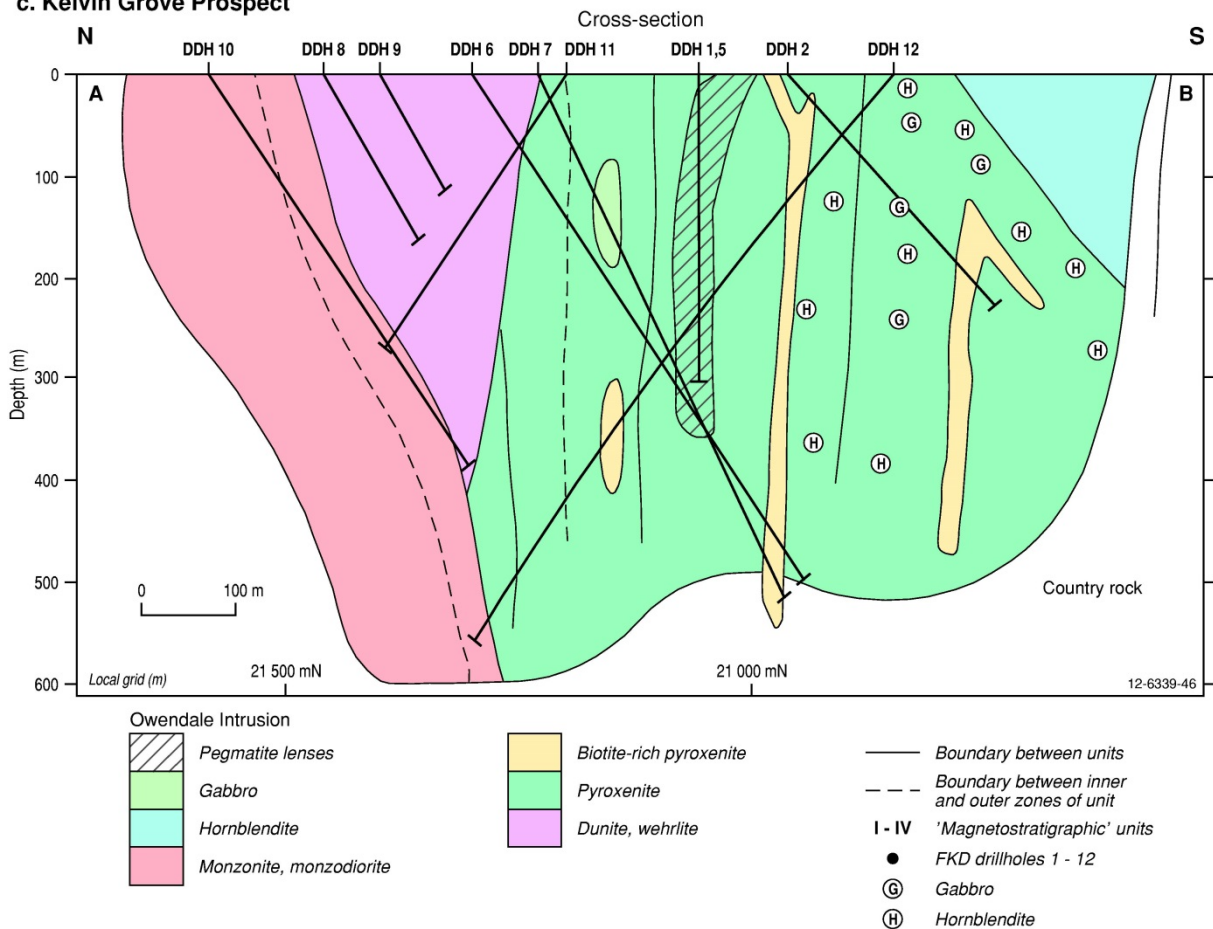


Figure 6.38 Geology of the Owendale mafic-ultramafic intrusion. Modified from Johan et al. (1989). (a) The Owendale Intrusion displays a ovoid-shape and crude concentric form typical of 'Alaskan-type' mafic-ultramafic intrusions. The Kelvin Grove PGE prospect is located on the southern side of the intrusion. (b) Geology of the Kelvin Grove prospect. (c) Schematic north-south cross-section of the Kelvin Grove prospect.

### *PGE mineralisation*

Four major types of PGE mineralisation have been defined in the Owendale Intrusion, the first two of being of primary hard-rock origin, and are discussed here. The laterite (3) and alluvial (4) Pt deposits are described in Deposit Types 9.A and 10.A, respectively:

1. Pt-Pd-Rh in 'P units' in clinopyroxenite (Figure 6.39);
2. structurally-controlled Pt-Pd-Cu veins in dunite and wehrlite;
3. residual Pt in laterite; and
4. alluvial Pt associated with paleochannels.

The following two descriptions of the hard-rock mineralised settings in the Owendale Intrusion are partly from Elliott and Martin (1991).

1. 'P units' in biotite clinopyroxenite (Figure 6.39)
  - Anomalous Pt and Pd concentrations are associated with transgressive monomineralic clinopyroxenite (the 'P units' of Suppel and Barron, 1986b) in biotite-hornblende clinopyroxenite. This unusual type of PGE mineralisation has been defined by drilling at the Kelvin Grove prospect near the southern margin of the intrusion. The 'P units' often have pegmatoidal textures and form irregular thin lenses, individual veins, and swarms of closely-spaced veins that have widths from a few millimetres to 2 m and their lengths rarely exceed a few tens of metres. They often appear to be discontinuous and they are invariably enclosed within biotite-magnetite clinopyroxenite with which they have contacts varying from apparently conformable to cross-cutting and sharp to gradational. Increased modal concentrations of biotite in the clinopyroxenite host often define the contacts. Platinum comprises 90% of the total PGE content with lesser Pd, and minor Os, Ir, and Rh. Significant intersections include, DDH FKD 1: 1.57 m @ 13.19 g/t Pt, 0.90 g/t Pd, and 0.5 g/t Rh, and DDH FKD 6: 0.41 m @ 10.35 g/t Pt, 0.5 g/t Pd. Suppel and Barron (1986b) found that the mineralised clinopyroxenites are characterised by low concentrations of S (S < 0.04%), Se, Te, Sb, Bi, As, and Sn, but high Pt/Pd ratios  $\geq 10$ . There is no definitive relationship between PGE content and grain size, or position of the 'P units'. Many 'P units' contain only background concentrations of PGEs. The PGMs in the 'P units' occur as discrete phases, or as inclusions in clinopyroxene, on grain boundaries, and within fractures in chrome-bearing magnetite. Barron et al. (1987) found that the PGMs occur as 15  $\mu\text{m}$  to 30  $\mu\text{m}$  euhedral grains of Fe-Pt co-existing with Rh-bearing erlichmanite, Al-F-sphene, and fluorite that were trapped in fractures in magnetite. An early high-temperature assemblage of cooperite (PtS), tetraferroplatinum (Pt<sub>3</sub>Fe), and erlichmanite (Os<sub>2</sub>S<sub>2</sub>) is overprinted by a lower-temperature assemblage of isoferroplatinum (Pt<sub>3</sub>Fe), sperrylite (PtAs<sub>2</sub>), and geversite (PtSb<sub>2</sub>), in addition to several other minor PGMs (platarsite, stibiopalladinite). Associated base-metal sulphides constitute only trace amounts and are not enriched relative to the surrounding unmineralised biotite-magnetite clinopyroxenite. Most rocks have variable amounts of Ti-poor magnetite ranging from 5% to 25%, and chromite forms a rare component in the intrusion. A later petrological study of the 'P units' by Johan et al. (1989) identified a similar PGM inventory to Barron et al. (1987) of erlichmanite, isoferroplatinum, tetraferroplatinum, cooperite, cuprorhodsite, malanite, geversite, sperrylite, stumpflite, and several unidentified Pd-antimonides. The early PGMs (erlichmanite, (Pt-Fe) alloys, cooperite) were deposited from fluid-rich systems slightly before the end of clinopyroxene crystallisation. Late PGMs are dominated by sperrylite-geversite solid solution resulting from the reaction of early PGMs

with a fluid phase. These mineral extensively replace cooperite and locally remobilise the PGE stock. Isoferroplatinum appears as a reaction product during the metasomatic replacement indicating a high-Fe activity in the fluid phase. Johan et al. (1989) estimate that the temperature range of formation of PGMs and base metals at Kelvin Grove in the Owendale Intrusion is 850°C to 650°C.

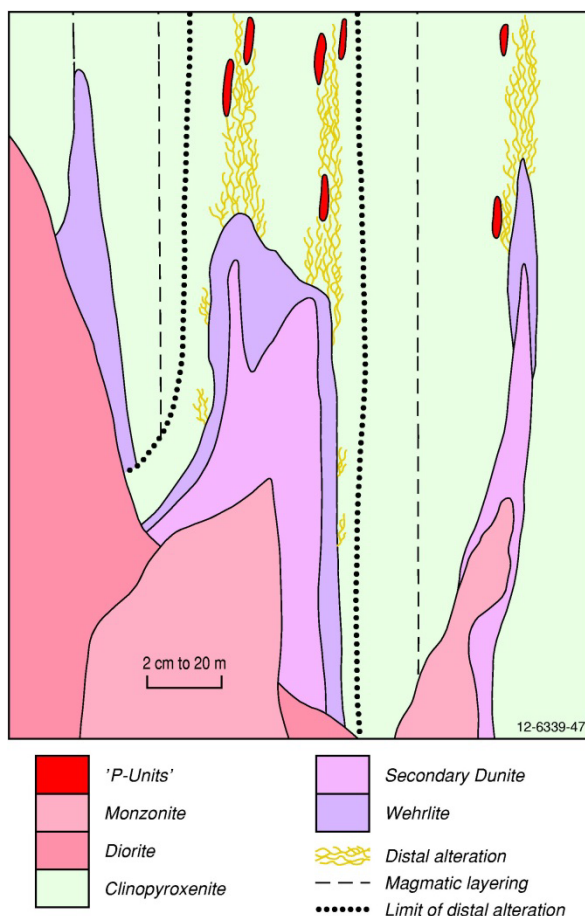


Figure 6.39 Conceptual section showing primary platinum mineralisation styles in the Owendale Intrusion. Modified from Turvey (1990) and Elliott and Martin (1991).

## 2. Structurally-controlled platinum-palladium-copper veins in dunite and wehrlite

- Veins enriched in Pt-Pd-Cu have been defined by drilling at the North Owendale prospect in the northeast corner of the intrusion. The veins are interpreted to occur along a northeast-trending structure that is discordant to a dunite-wehrlite-olivine pyroxenite body. Anomalous PGE contents occur in both dunite and wehrlite, but the highest grades are more typical of serpentinised dunite. Two subtypes of mineralisation have been identified: (a) fine disseminations and microveins of native copper in Pd-enriched pegmatite, clinopyroxenite, and dunite; and (b) Cu sulphides and PGMs within, and near, chrome-bearing magnetite veins. The high-temperature hydrothermal mineralisation is represented by a variety of oxides (chrome-bearing spinel, magnetite, baddeleyite), native metals, base-metal sulphides, and several complex Pd-bearing PGMs. Significant drill intersections include DDH FKD13 from 88.0 m: 2.0 m @ 1.71 g/t Pt; DDH FKD 15 from 98.0 m: 7.0 m @ 1.9 g/t Pt, 0.6% Cu; and DDH FKD16 from 312.0 m: 4.0 m @ 1.5 g/t Pt, 0.3% Cu.

- The compositional ternary diagram of Figure 6.40 shows the diverse nature of different primary sources generating these PGE-mineral systems, reflecting not only their geochemical features, but also differences in the temperature of ore deposition from the nuggets, to the weathered outcrop, to the 'P units' (Slansky et al., 1991).

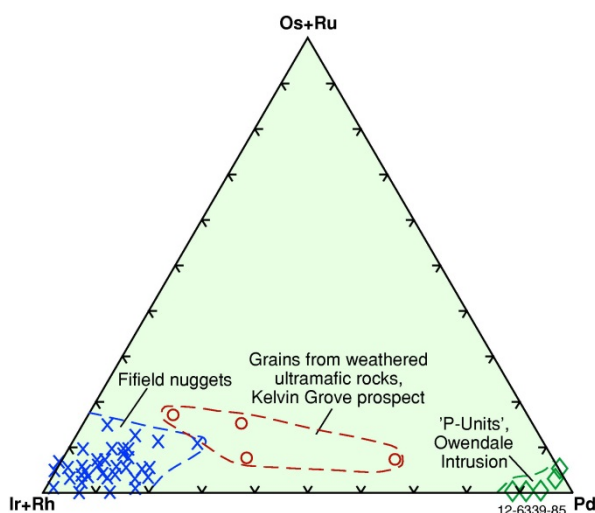


Figure 6.40 Ternary diagram showing distribution of minor elements (at. %) in isoferroplatinum from: nuggets at Fifield; grains from weathered ultramafic rocks from the northwestern part of the Kelvin Grove prospect; and from 'P-units' of the Owendale Intrusion. Modified from Slansky et al. (1991).

### Age of mineralisation

The crystallisation ages of the Owendale and other intrusions in the Fifield region are generally poorly defined. The ages, which appear to be dependent on the dating method used, extend from the late Ordovician to late Devonian. The most recent and robust geochronological methods involving the dating of zircon indicate a late Ordovician to late Silurian age (e.g., ~450 Ma to ~420 Ma) for the Fifield intrusions. Early whole-rock K-Ar geochronology studies by Thomson (1974) indicated that the Tout and Hylea intrusions were coeval at  $397 \pm 16$  Ma and  $397 \pm 12$  Ma, respectively. Pogson and Hilyard (1981) recorded a within error K-Ar age of 405 Ma for the same two intrusions. Barron et al. (2004) compiled whole-rock Rb-Sr ages of  $446.1 \pm 10.8$  Ma and  $365 \pm 10$  Ma for the Owendale Intrusion (both ages pers. comm., Whitford, 1991), and  $428 \pm 4$  Ma for the Tout Intrusion (Stojanovic, 1995). SHRIMP U-Pb zircon ages of  $445 \pm 6$  Ma and  $448 \pm 4$  Ma were obtained for the Honeybugle and Bulbodney Creek intrusions, respectively (pers. comm., R.I. Hill, Australian National University, Canberra, in Elliott and Martin, 1991). More recent ICPMS zircon ages of  $424 \pm 11$  Ma (pers. comm., A.J., Crawford, 2001),  $436 \pm 12$  Ma and  $444 \pm 3$  Ma (both ages pers. comm., S. Meffre, 2003, as reported in Barron et al., 2004) indicate a late Ordovician to early Silurian age for the Owendale Intrusion.

The 'P unit' mineralisation interpreted by Raedeke (1988) and Turvey (1990) to be late-stage magmatic alteration related to the formation of secondary dunite-wehrlite bodies. Similarly, the structurally-controlled hydrothermal PGE vein systems also formed late in the magmatic evolution of the intrusion. Therefore the best estimate for the maximum age of these styles of hard-rock PGE mineralisation in the Owendale Intrusion is late Ordovician to late Silurian (e.g., 450 to 420 million years). The laterite profile in the Owendale Intrusion is very similar to the mineralised laterites at

Syerston in the nearby Tout Intrusion (see Deposit Type 9.A; see Figure 6.37). The laterites at Syerston formed during the ?Early and Late Cenozoic time era (Derrick, 1991), thus a similar age range is likely for the formation of laterites at Owendale. The three mineralised paleochannel systems in the Owendale Intrusion (see Deposit Type 10.A; see Figure 6.37) have eroded the early- to mid-Cenozoic regolith, thus indicating a post mid-Miocene age for this mineral system.

### *Genesis*

The small size, equidimensional and pipe-like forms; zoned nature (particularly evident from aeromagnetic trends); clustered distribution of many intrusions; alkaline compositions, principal rock types of clinopyroxenite, olivine clinopyroxenite, wehrlite, biotite clinopyroxenite, dunite, monzonite, syenite, diorite, and hornblendite; paucity of orthopyroxene in the ultramafic rocks; forsteritic composition of olivine; magnetite forming a major mineral (up to 20% modal) in clinopyroxenite; Pt-dominance and localised irregular distribution of the primary mineralisation; and the spatial association with Pt-bearing placers collectively indicate the intrusions near Fifield have affinities with Alaskan-type intrusions (Hoatson and Glaser, 1989; Johan, 2002). However, K-feldspar and biotite are far more abundant than in typical Alaskan and Ural intrusions indicating more K-rich parent magmas, and dunite in these intrusions generally contain chrome-rich accessory minerals, which is not apparent for the Fifield intrusions. In addition, some of the latter intrusions display a reverse zoning of ultramafic rocks mantling an inner core of more fractionated rocks.

The 'Alaskan-type' intrusions in central New South Wales have been regarded in a number of studies (Agnew, 1987; Agnew et al., 1987; Wyborn, 1988, 1990; Wyborn and Cameron, 1990; Derrick, 1991) as part of an extensive regional igneous province that contains Ordovician shoshonitic volcanic and associated intrusive rocks. The Fifield intrusions have similar trace-element geochemical signatures to Ordovician volcanic rocks from Kiandra, Orange, and Wellington, and with modern shoshonites from other parts of the world (e.g., Lihir Island, Fiji, western USA, Mount Hagen–Papua New Guinea). Derrick (1991) states that the shoshonitic association is characterised by high K, Sr, Ba, and P, and low Ti, Zr, Y, and Nb, and appears to be derived from metasomatically-altered subcontinental lithosphere rather than from subducted oceanic crust. The presence of many Au deposits and Pt-bearing Alaskan-type' intrusive in the Ordovician igneous suite in central New South Wales suggests that the shoshonitic magmas were derived from sulphide-undersaturated and Au- and PGE-enriched lithosphere. Derrick (1991) also mentions these enriched shoshonitic magmas underwent further fractional crystallisation in the crust. The Goonumbla porphyry Au system and the Pt-bearing Owendale Intrusion are typically S-poor (Wyborn and Cameron, 1990).

A group of small composite Paleozoic-Mesozoic complexes (Wateranga, Goondicum, Hawkwood, and Boyne) similar to the intrusions near Fifield have been identified in the New England Orogen of southeast Queensland. The Wateranga Intrusion is an undeformed, Permo-Triassic layered gabbroic pluton intruded into late Carboniferous sedimentary rocks (Talusani et al., 2005). The >500-m thick, ovoid-shaped intrusion consists mainly of gabbro and norite, with minor troctolite, anorthosite, and orthopyroxenite, and rare picrite. Extreme fractionation of incompatible trace elements (e.g., Ti, Zr, P) is indicated by the development of titaniferous magnetite horizons in the more evolved rocks. Fine-grained Fe-Ni-Cu sulphides occur throughout the intrusion. Talusani et al. (2005) identified rare Rh-Ru inclusions in orthopyroxene grains from norite, and the Queensland Department of Mines reported PGE values of 9 ppm and 14 ppm in a magnetite-apatite-bearing pyroxenite from the Wateranga Gabbro (Hoatson and Glaser, 1989). Talusani et al. (2005) determined crystallisation temperatures of 1057°C to 927°C and pressures of 2 kbar to 4 kbar for the intrusion. The authors state the variation trend of anorthite content of plagioclase versus the forsterite content of olivine precludes an

arc-related magma source. The composition and geological setting of the intrusion are consistent with emplacement in a post-subduction extensional tectonic environment.

A number of investigators have proposed hydrothermal solutions that were derived from, or driven by, late dunite intrusive bodies, remobilised the PGEs into the monomineralic clinopyroxenite 'P unit' zones in the Owendale Intrusion. Raedeke (1988) and Turvey (1990) interpreted the PGE mineralisation in the intrusion to be being directly related to late-stage magmatic alteration mineral systems that were responsible for the formation of the secondary dunite-wehrlite bodies. These olivine-rich bodies were possibly formed by the addition of water to the melt, and with the increase in water fugacity, clinopyroxene was resorbed to form olivine. Various styles of alteration, some of which were mineralised, are associated with the ultramafic lithologies. The end members of this alteration series are the secondary dunite bodies and the pegmatitic clinopyroxenite, with the other intervening alteration styles being characterised by pseudomorph and incipient replacement of clinopyroxene by olivine, biotite, and, to a lesser extent, hornblende. The PGEs associated with these alteration styles were transported to their present position by uncharacterised fluids which were responsible for the alteration and subsequent deposition of the metals. Turvey (1990) described the alteration and associated mineralisation to be vertically zoned and to favour lithologies with the highest contents of magmatic olivine. The alteration and mineralisation therefore approximately parallels the sub-vertical magmatic stratigraphy, although the host dunite-wehrlite bodies may be markedly discordant. Elliott and Martin (1991) provide further details on these genetic models.

Investigations of laterite mineralisation in the North Owendale area by Brill and Keays (1989a,b) indicated that Pt is enriched by a factor of 27 compared to the underlying, unweathered bedrock. This high enrichment factor implies that the Pt was originally very erratically distributed in the primary ultramafic rocks prior to weathering and that the high grades now observed in the laterite profile reflect a primary protore which has subsequently been entirely weathered.

Ultramafic lithologies in the 'Alaskan-type' intrusions are critical to the formation of the mineralised laterite profiles. The types of lateritic mineralisation show strong correlations with particular basement lithologies, including: Pt-Cu mineralisation overlying dunite-wehrlite rocks with variable Co, Ni, and Au contents; Co-Ni mineralisation with Pt credits associated with underlying olivine pyroxenite; and elevated Cr and Sc where dunite-wehrlite lithologies dominate.

The PGE mineralisation in the primary rocks and laterite in the Fifield region has demonstrated a good example of multi-stage process mineralisation including primary high-temperature magmatic formation, low temperature postmagmatic hydrothermal alteration, and residual lateritic enrichment.

### *Key references*

- Suppel and Barron (1986a,b): Pt-bearing intrusions in Fifield province; regional setting; general geology; mineralisation, PGEs.
- Agnew et al. (1987): Owendale and Tout intrusions; petrology and geochemistry; mineralisation potential.
- Barron et al. (1987): petrology; geochemistry; mineralogy; PGE mineralisation of Owendale Intrusion.
- Suppel et al. (1987): alluvial and hard-rock deposits; PGEs in mafic-ultramafic complexes; rock types; stratigraphy; host rocks of PGEs.
- Wyborn (1988, 1990): petrology and geochemistry; shoshonitic magmatism; Au mineralisation, tectonic model for the Ordovician and Silurian; Au and Pt potential of the Lachlan Orogen.

- Johan et al. (1989, 1990a,b): Pt mineralisation in Kelvin Grove Prospect; Alaskan intrusions in Fifield region; mineralogy; clinopyroxenite host rocks; PGEs; placer deposits; PGM nuggets.
- Turvey (1990): review of PGE mineralisation in Fifield region; geology and mineralisation of Owendale Intrusion; rock types; stratigraphy; drilling results; exploration potential.
- Elliott and Martin (1991): regional geological setting of Fifield platinum province; mining history; comprehensive summaries of residual, alluvial, and hard-rock PGE mineralisation; Owendale Intrusion; stratigraphy; PGE resources.
- Slansky et al. (1991): geology of Alaskan-type intrusions near Fifield; placer deposits; formation and distribution of PGMs; genesis of alluvial Pt deposits.
- Shi (1995): Owendale Intrusion; geochemistry and mineralisation; mineralogy; primary and secondary PGMs.
- Stojanovic (1995): petrology; geochemistry and isotope geochemistry of host rocks; PGE mineralisation; genesis.
- Teluk (2001): regional geophysics; aeromagnetic expression of intrusions; Pt metallogenesis; Fifield intrusions; Owendale Intrusion; Ural-Alaskan type complexes.
- Barron et al. (2004): geological setting of Fifield Alaskan-type mafic-ultramafic intrusions; geochronology; PGE mineralisation.

#### **6.4.7 Mineral-System Class 7: Continental flood basalts with associated sub-volcanic sills**

##### ***6.4.7.1 Deposit Type 7.A: Ni-Cu-PGE sulphides in sub-volcanic picritic-gabbroic sills with associated flood basalts***

(e.g., Noril'sk-Talnakh)—no confirmed examples documented in Australia.

#### **6.4.8 Mineral-System Class 8: Hydrothermal-Metamorphic**

##### ***6.4.8.1 Deposit Type 8.A: Discordant-brecciated bronzitite pipes in mafic-ultramafic intrusions***

###### *Overview*

The Carr Boyd Rocks Intrusion, located ~72 km north-northeast of Kalgoorlie, is the most significant example of hydrothermal PGE mineralisation associated with discordant bronzitite pipes in Australia. Carr Boyd Rocks also has the distinction of being the only non-komatiitic-hosted Ni-Cu-PGE sulphide deposit that has been mined (for Ni, Cu) in the Yilgarn Craton. Carr Boyd Rocks shows mineralogical and chemical similarities to the olivine-bronzite-plagioclase pegmatoids that encase the high-grade (up to 2050 g/t PGEs) PGE dunite pipes of the Bushveld Complex (Peyerl, 1982; Schiffries, 1982; Scoon and Mitchell, 2004).

Carr Boyd Rocks is a poorly exposed mafic-ultramafic intrusion derived from a tholeiitic magma which progressively became richer in normative plagioclase and poorer in normative orthopyroxene (Purvis et al., 1972). The Ni-Cu-PGE mineralisation occurs in cross-cutting, steeply plunging, pipe-like pegmatoidal bodies and vein stockworks of coarse-grained altered bronzite. The pegmatoidal phases include bronzite (Fs<sub>24</sub>), olivine (Fa<sub>16</sub>), clinopyroxene, hornblende, biotite, plagioclase (An<sub>62</sub>), chrome titanomagnetite (6–18% Cr<sub>2</sub>O<sub>3</sub>, 0.3–1.5% V<sub>2</sub>O<sub>5</sub>). The pegmatoidal pipes attain 60 m in width and have

both structural and stratigraphic controls. Massive sulphides average about 6% Ni and 2% Cu, and matrix sulphides contain up to 4% Ni. The Ni/Cu and Ni/Co ratios of the deposit are 3.09 and ~30, respectively (Marston, 1984). The three major ore shoots in the deposit average 1.5% Ni and 0.5% Cu, with Pt concentrations ranging from ~6 ppb to ~300 ppb for the highest Ni grades of ~5%.

Massive Ni-Cu sulphide-bearing breccia pipes within off-set dykes (or satellite dykes) adjacent to the 2411 Ma Jimberlana Dyke in the Yilgarn Craton contain significant mineralisation (e.g., 13.7 m @ 2.6% Ni, 0.8% Cu). The breccia pipes are located below the PGE-enriched stratabound sulphide layers (14 m @ 0.5 g/t Pt+Pd) in the upper part of the Ultramafic Series and are sub-parallel to the basal intrusive contact of the intrusion. Orthopyroxenite and olivine orthopyroxenite pipes truncate the PGE-enriched porphyritic websterite layer in the upper part of the Ultramafic Zone in the Munni Munni Intrusion (see Deposit Type 1.A). However, these particular pipes carry abundant Cr-poor, Al-rich spinels and no PGE mineralisation (Hoatson et al., 1992). Mineralised breccia pipes are also commonly observed in the world's largest Ni deposits, e.g., Sudbury, Noril'sk, Voisey's Bay, and Jinchuan.

#### *Australian deposits/prospects/hosts*

Carr Boyd Rocks<sup>25</sup> (Yilgarn Craton, WA); Jimberlana Dyke (Yilgarn Craton, WA).

#### *Significant global example(s)*

Onverwacht–Mooihoek–Driekop–Maandagshoek dunite pipes, Bushveld Complex (South Africa); Sudbury and Voisey's Bay (Canada); Jinchuan (China); and Noril'sk (Russia).

#### *Type example in Australia*

Carr Boyd Rocks, Western Australia.

#### *Location*

Longitude 121.626099°E, Latitude -30.065901°S; 1:250 000 map sheet: Kurnalpi (SH 51–10), 1:100 000 map sheet: Gindalbie (3237); ~72 km north-northeast of Kalgoorlie and ~125 km north of Kambalda, Western Australia.

#### *Geological province*

Eastern Goldfields Province, Yilgarn Craton, Western Australia.

#### *Resources*

Global resources of 1 018 000 t @ 1.17% Ni (contained Ni metal of 11 950 t: Hoatson et al., 2006); unknown PGE resources.

#### *Current status and exploration history*

Historical Ni-Cu mine. An airborne magnetometer survey of the Kurnalpi 1:250 000 map sheet by the Bureau of Mineral Resources in 1958 (published in 1961) revealed a group of aeromagnetic anomalies near Carr Boyd Rocks. In 1968, Great Boulder and Northern Kalgurli followed up these anomalies with a geological mapping and soil geochemical program. The first ore shoot was found through its gossan, which has a weak Ni and Cu soil anomaly. There was no obvious magnetic anomaly with the gossan. Mafic rocks stained with Ni and Cu carbonates assayed 0.57% Ni and

---

<sup>25</sup> Also has been incorrectly called in the literature as Carr Boyd, which is a Au deposit in the Yilgarn Craton, Western Australia.

0.55% Cu, and follow-up costeans with gossanous ultramafic rocks contained 1.75% Ni and 0.50% Cu. A 107 diamond drill-hole program in 1969 defined a resource of 1.361 Mt @ 1.65% Ni and 0.57% Cu in three shoots numbered 1, 2, and 3 (Marston, 1984). Additional lower grade ore is not included in this resource. Development of the number 1 shoot commenced in ~1971 and after some brief early periods of production during the mid-1970s, the mine was closed in 1977 due to increased costs, low productivity, and a lack of underground development. The deposit has subsequently experienced a long intermittent history of evaluation, development, and production by WMC Ltd and a number of junior companies.

### *Economic significance*

The only non-komatiitic-hosted Ni-Cu-PGE sulphide deposit that has been mined in the Yilgarn Craton. Elevated concentrations of PGEs are associated with Ni-Cu sulphides in breccia pipes, but mining-refining operations have focussed on Ni and Cu, and details of PGE resources are unknown. The Carr Boyd Rocks deposit is significant as it is one of the best Australian examples of hydrothermal mineral systems involving the PGEs. The economic significance of the PGE credits may become more apparent in this poorly understood intrusion during periods of advantageous PGE metal prices.

### *Geological setting*

The Carr Boyd Rocks Complex intrudes mafic volcanic and sedimentary rocks of the Archean Morelands Group and is itself intruded by Archean granites on the northern side in the Eastern Goldfields Province of the Yilgarn Craton (Figure 6.41). The immediate country rocks appear to be folded, possibly into small local basinal structures. The geological setting of the mafic-ultramafic complex is poorly understood due to limited exposure. This ?2700 Ma body is lobate in outline and the mafic and ultramafic rock types with an aggregate thickness of ~3000 m cover an area of 75 km<sup>2</sup>. The western, southern, and eastern lobes contain ultramafic rocks, while the centre and north are characterised by overlying mafic and minor ultramafic units. Purvis et al. (1972) subdivided the stratigraphy into five units (I to V) of which three are ultramafic and two are mafic. Rock types in most units (except unit IV) display cyclic layering and are partly to completely altered to metamorphic assemblages of serpentine, magnetite, chlorite, talc, tremolite-actinolite, anthophyllite, and cummingtonite. Rock types in the five units are:

- Unit V—troctolite, olivine anorthosite, norite, and minor dunite, bronzitite, augite norite (approximate thickness 1000 m<sup>+</sup>);
- Unit IV—dunite (250 m);
- Unit III—dunite-harzburgite-bronzitite cycles (200 m), dunite (50 m), and bronzitite (?200 m);
- Unit II—norite, augite norite, olivine norite, harzburgite, and dunite (200 m to 800 m); and
- Unit I—dunite harzburgite-bronzitite cycles (50 m), bronzitite (150 m), dunite-harzburgite-bronzitite cycles (50 m), and bronzitite (150 m).

Intrusive rocks of various lithologies are discordant to the above layered series. Bronzite pegmatoids and sulphide-bearing noritic pegmatoids are associated with the economically important sulphide-bearing bronzite pegmatoidal bodies (see Mineralisation Environment) with most of the latter types confined to the base of Unit V. Other intrusions of micronorite, olivine-augite micronorite, andesite, and microgranodiorite are common. The gabbroic rocks dip inwards towards the centre of the complex, whereas igneous layering in the vicinity of the deposit generally dips towards the southeast.

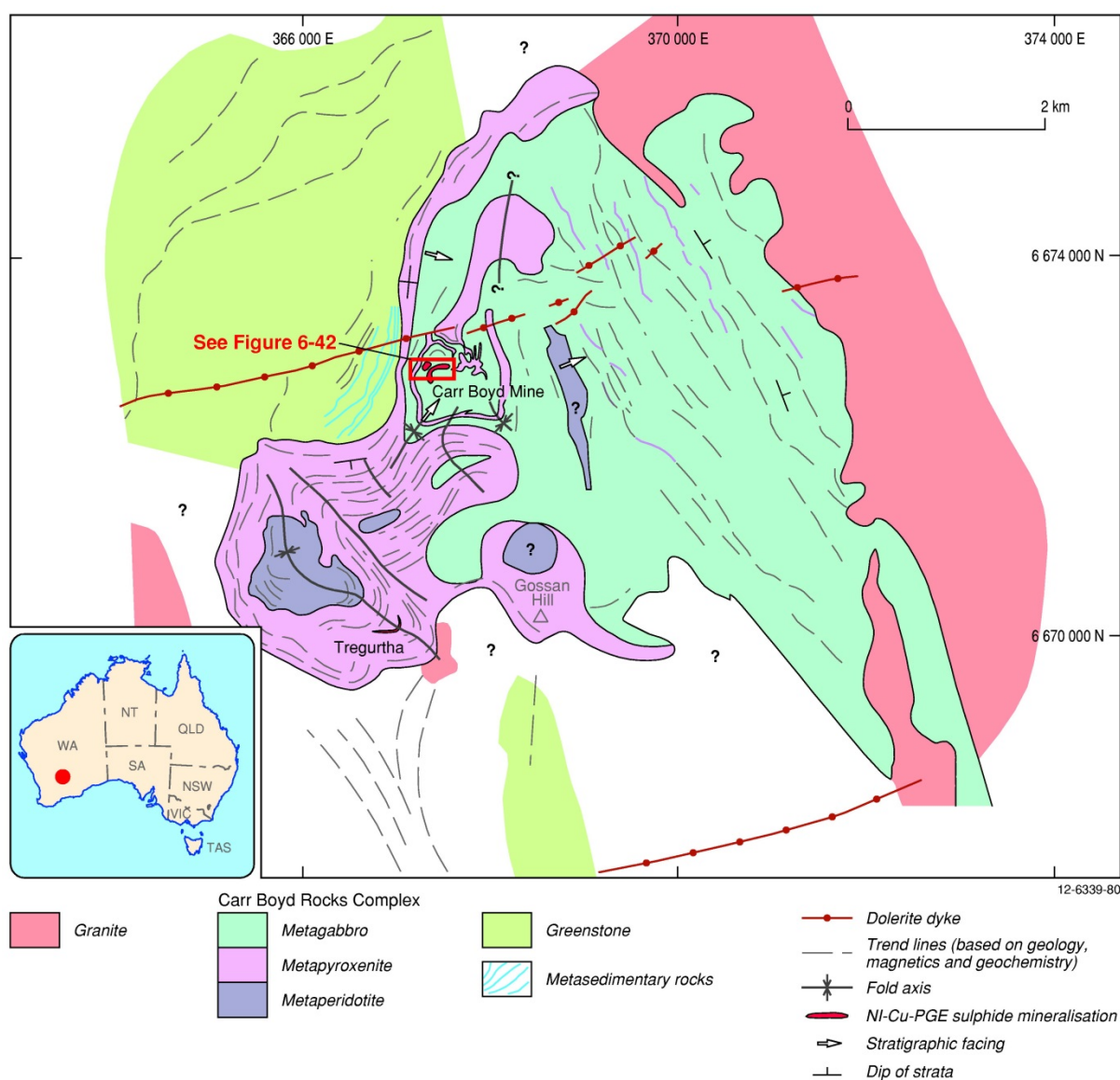


Figure 6.41 Geological setting of the Carr Boyd Rocks Intrusion, Yilgarn Craton, Western Australia. Figure provided from Yilgarn Mining Limited (Brockman Resources Limited) in 2007.

### Mineralisation environment

The following descriptions are largely from Schultz (1975) and Marston (1984). The Ni-Cu-PGE mineralisation occurs in a small cluster of ore shoots that take the form of cross-cutting, steeply inclined pegmatoidal pipe-like bodies that spiral down plunge, possibly due to folding (Figure 6.42). The pegmatoidal pipes are generally amphibole-sulphide-breccia bodies that attain 60 m in width and occur in an east-northeast-trending zone about 800 m-wide, bisecting the intersection of two major faults and are confined to Unit V, indicating both a structural and stratigraphic control. The pegmatoidal phases include bronzite ( $Fs_{24}$ ), olivine ( $Fa_{16}$ ), clinopyroxene, hornblende, biotite, plagioclase ( $An_{62}$ ), chrome titanomagnetite (6–18%  $Cr_2O_3$ , 0.3–1.5%  $V_2O_5$ ). Disseminated and massive sulphides consist of monoclinic pyrrhotite, pentlandite, pyrite, chalcopyrite, and cubanite. Associated with the pipes are vein stockworks of medium- to very coarse-grained bronzite altered to anthophyllite, tremolite-actinolite, talc, chlorite, and plagioclase, with some relict igneous pyroxene.

The three mineralised ore shoots (Number 4 ore shoot was defined post-1984) are relatively small and consist of a central zone of breccia and massive sulphides and high-grade disseminated sulphides of at least 1% Ni, and an enveloping mineralised zone comprising veins of bronzitite in gabbronorite with patchy disseminated sulphides and veinlets developed in bronzitite (Figure 6.43). The three ore shoots plunge steeply west and are displaced by west-dipping faults. The Number 3 ore shoot averages 1.72% Ni and 0.45% Cu, and the Number 1 and 2 ore shoots average 1.41% Ni and 0.50% Cu. The average composition of the shoots by volume is: silicate inclusions—bronzitite and gabbronorite (70%); nickeliferous (0.5%) monoclinic pyrrhotite (20%); pentlandite (4%); chalcopyrite (2%); pyrite (2%), chrome-titanomagnetite (2%), and minor cubanite. The silicate inclusions range in size from individual crystals to irregular blocks up to 10 m wide. The sulphide/silicate ratio decreases outwards.

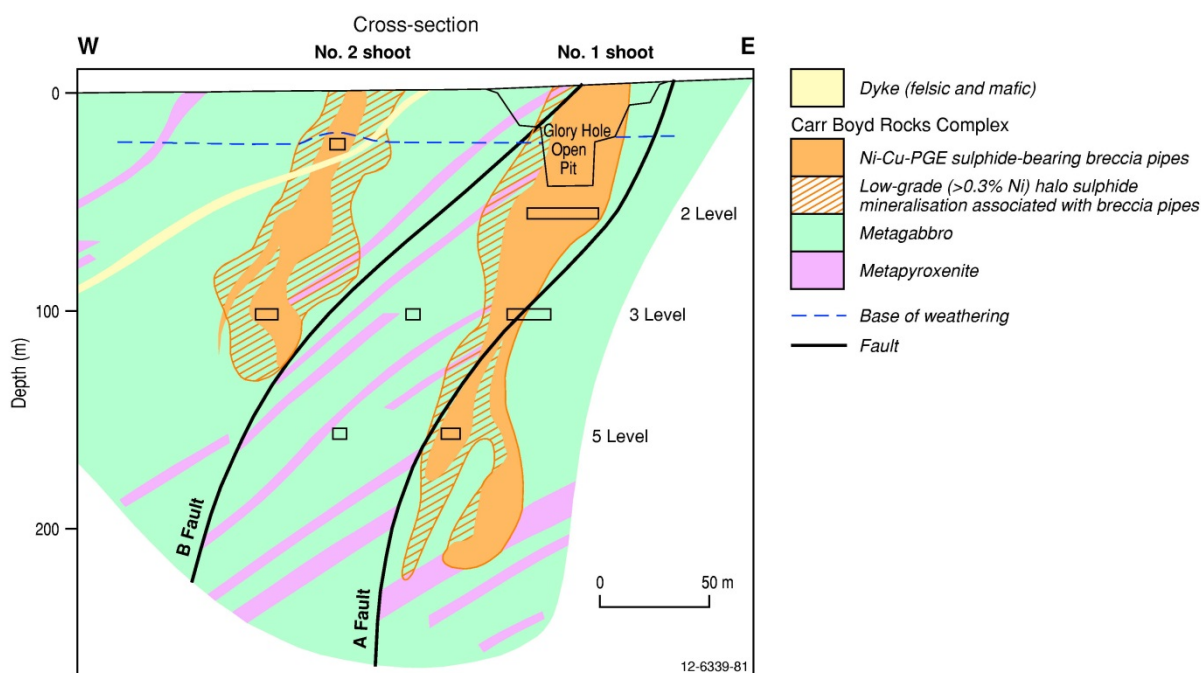


Figure 6.42 Schematic east-west cross-section of the steeply plunging Number 1 and 2 ore shoots, Carr Boyd Rocks Ni-Cu-PGE deposit. Figure provided from Yilgarn Mining Limited (Brockman Resources Limited) in 2007.

### PGE mineralisation

Very little PGE data and information on the PGMs for the complex have been published. Figure 6.44 shows that most samples in the four ore shoots generally have a similar range of Pt concentrations from 6 ppb to ~300 ppb for Ni grades up to ~5%. Ore shoots 1 and 4 have marginally higher Pt concentrations relative to the other two shoots. Greater variations are observed for the Ni grades, which range from ~5% for ore shoots 2 and 4, down to maximum grades of ~3.5% for shoots 1 and 3. Average metal concentrations for ~370 mineralised samples from the ore shoots are 1.68% Ni, 68 ppb Pt, 195 ppb Pd, and 49 ppb Au. Anomalous Pt and Pd concentrations have also been detected from a pyroxenite unit near the base of the mafic-ultramafic stratigraphy and also in stream sediments distant from the mine.

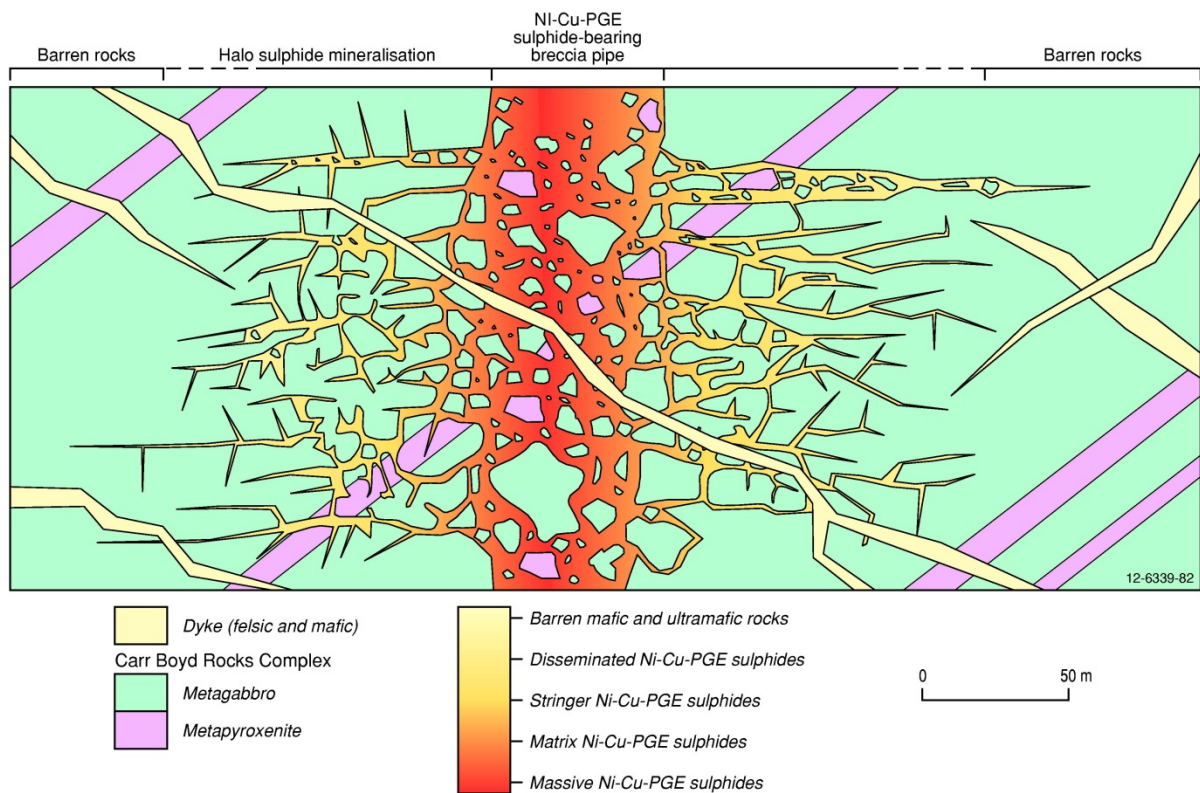


Figure 6.43 Conceptual section of Ni-Cu-PGE sulphide-bearing breccia pipe and associated styles of mineralisation, Carr Boyd Rocks Ni-Cu deposit. Figure provided from Yilgarn Mining Limited (Brockman Resources Limited) in 2007.

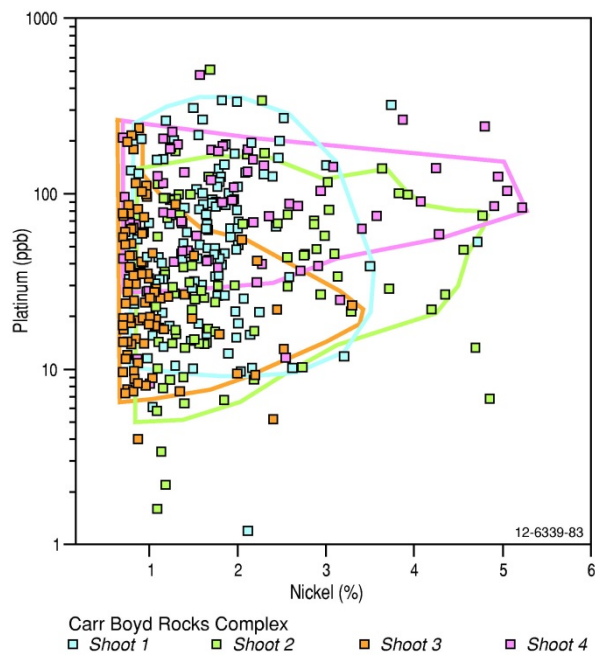


Figure 6.44 Relationships of platinum (ppb) versus nickel (%) concentrations in ore shoots 1, 2, 3, and 4, Carr Boyd Rocks Ni-Cu deposit. Figure provided from Yilgarn Mining Limited (Brockman Resources Limited) in 2007.

### *Age of mineralisation*

The age of the undated complex is tentatively assigned to ~2700 million years equating to a major mafic-ultramafic magmatic and mineralising event in the Eastern Goldfields Province, which provides a maximum age constraint for the discordant sulphide-bearing pipe-like bodies.

### *Genesis*

The Carr Boyd Rocks intrusion is characterised by its complex structural setting, intricate cyclic layering, absence of cryptic layering, and the presence of high-pressure crystallisation features (crystallisation depth estimated at 23 km to 26 km). The layered sequence is believed by Purvis et al. (1972) to be derived from a tholeiitic magma which progressively became richer in normative plagioclase and poorer in normative orthopyroxene. Three compositionally different, but related magmas, gave rise to three crystallisation sequences, involving progressively earlier crystallisation of plagioclase, and later crystallisation of orthopyroxene.

Purvis et al. (1972) interpreted the mineralised pegmatoidal bodies at Carr Boyd Rocks to have formed from residual liquids derived from the crystallisation of mafic sequences and subsequently forcefully emplaced during a period of deformation. They show mineralogical and chemical similarities to the envelopes of olivine-bronzite-plagioclase pegmatoids that encase the high-grade (up to 2050 g/t PGEs) PGE dunite pipes of the Bushveld Complex (Peyerl, 1982; Schiffries, 1982; Scoon and Mitchell, 2004). In the Onverwacht region of the East Bushveld, the pipes consist of a central 20 m-wide zone of hortonolite dunite (Fo<sub>22</sub>) which taper downward and is encased within a 100 m-wide zone of dunite (Fo<sub>80-92</sub>). The scale, geometry, pegmatoidal character, mineralogy, and envelope olivine compositions appear to be similar in both complexes. However, genetic interpretations appear to differ with the Bushveld pipes resulting from replacement of bronzite by hot aqueous solutions which leached SiO<sub>2</sub>, Al<sub>2</sub>O<sub>3</sub>, and Na<sub>2</sub>O, and introduced FeO, TiO<sub>2</sub>, V, and PGEs. In contrast, the mineralised and barren pegmatoidal bodies at Carr Boyd Rocks appear to have formed from residual liquids from crystallisation, derived from Unit V troctolite-olivine anorthosite sequence and subsequently been forcefully emplaced during a period of incipient deformation. It is likely that the stresses that caused the deformation also caused the observed shear trends, and that the intersection of these trends provided loci for ore intrusion. Another possible connection with the Bushveld Complex is that the pegmatoids from the Vlaktefontein district are structurally similar, with the orebodies also being associated with norite-pyroxenite pegmatoids. Similarly, the Cu/(Cu+Ni) ratios are comparable for both regions—0.2 for Carr Boyd Rocks and 0.217 for Vlaktefontein for Ni grades less than 3%.

### *Key references*

- Purvis et al. (1972): regional geological setting; Yilgarn Craton; geology of Carr Boyd Rocks Intrusion; stratigraphy; petrography; mineralogy; Ni-Cu sulphides; bronzite pegmatoids; intrusive breccia pipes; contemporaneous fault off-sets; S-oxygen fugacities; exploration.
- Schultz (1975): history of discovery; geological setting; mineral reserves; ore deposits; breccia pipes; structure; genesis.
- Marston (1984): regional setting of mafic-intrusive hosted Ni sulphides in Western Australia; geological setting of Carr Boyd Rocks Intrusion; stratigraphy; exploration and discovery histories; drill results; exploration.
- Barnes et al. (1991a): regional geological setting of layered mafic-ultramafic complexes in Western Australia; magma composition of Carr Boyd Rocks Intrusion; cyclic layering.
- Ahmat (1993): crustal evolution; geochronology; geological setting; mineralisation.

#### **6.4.8.2 Deposit Type 8.B: Remobilised Ni-Cu-PGE±Au sulphides in komatiitic and metasedimentary rocks**

##### *Overview*

Various postmagmatic processes have modified the distribution, structure, texture, mineralogy, and chemistry of the Ni-Cu-PGE sulphide ores associated with Archean komatiitic volcanism in the Yilgarn Craton of Western Australia. These processes have resulted in a spectrum of sulphide mineralisation types, ranging from complete dislocation (faulted ores), and more localised mobilisation (stringer sulphides), through metamorphic replacement (interpillow-interbreccia sulphides), to hydrothermal dissolution and redeposition (vein-type sulphides). These different mineralisation types are observed for most deposits throughout the Yilgarn Craton, and they are particularly well developed in the ore shoots that characterise the flanks of the Kambalda Dome (e.g., Otter–Juan, Long–Victor, Lunnon, Durkin, Foster, Hunt, etc).

Hudson (1986) showed that the Pd-bearing minerals sudburyite, moncheite, merenskyite, michenerite, testibiopalladite, and palladian melonite occur within veins in the massive and matrix ores, within stringers of sulphide in the footwall rocks, or in association with post-ore hydrothermal veins and porphyries. These PGMs appear to have formed as the result of post-magmatic processes, in particular, metamorphic segregation of sulphides and the interaction of Pd-bearing ore sulphides (pentlandite) with younger hydrothermal veins. Barnes (2006) proposed deformation demonstrably played an important role in localising economically significant bodies of massive ore, particularly in areas of intense deformation at medium- and high-metamorphic grade. However, what is less clear is whether deformation has played any role in concentrating or upgrading sulphides, or in localising medium-grade matrix ores, which often form the bulk of the economic resource. Barnes (2006) states that there is no compelling evidence that it does, and the PGE chemistry of massive, matrix, and disseminated ores argues strongly that tectonic upgrading is not an important process, even in areas of severe deformation, such as Perseverance where it might be most likely.

##### *Australian deposits/prospects/hosts*

Juan Shoot–Kambalda, Wannaway, Perseverance, Emily Ann, Harmony, Rocky's Reward, Nepean (all Yilgarn Craton, WA).

##### *Significant global example(s)*

Thompson (Canada).

##### *Type example in Australia*

Otter–Juan deposits Kambalda, Western Australia.

##### *Location*

Longitude 121.641666°E, Latitude -31.159722°S; 1:250 000 map sheet: Widgiemooltha (SH 51–14), 1:100 000 map sheet: Cowan (3234); northern end of Kambalda Dome, ~52 km south-southeast of Kalgoorlie, Western Australia.

##### *Geological province*

Eastern Goldfields Province, Yilgarn Craton, Western Australia.

## *Resources*

Unknown for Juan Shoot. An important member of the Kambalda Ni-Cu±PGE deposits (e.g., Otter–Juan, Long–Victor, Lunnon, Durkin, Foster, Hunt, etc)—42 Mt @ 3.3% Ni, a global resource of ~1.4 Mt of contained Ni, with variable credits of Cu, Au, Co, Pt, and Pd (Hoatson et al., 2006). The vast majority of this resource is attributed to 'primary' massive, matrix, and disseminated sulphide ores, however, the contribution from remobilised ores, which is unknown, would be relatively minor. Such metals as Pd, Cu, and Au are enriched in remobilised stringer and vein-type ores relative to the other metals mined in the Kambalda Dome region. Ore shoots in the Juan and Hunt deposits that contain these styles of mineralisation may have larger mined credits of Pd, Cu, and Au relative to other shoots.

## *Current status and exploration history*

Developed deposits. Mineralisation associated with the Juan deposit is blind at surface, however, the nearby Otter deposit is defined by small gossans after massive and disseminated sulphides. These gossans were discovered by soil geochemical programs in 1965–1966 during the earliest phases of regional exploration. A gossan sample after massive sulphides contained 10.4% Ni, 1.05% Cu, 3580 ppb Pd, and 1930 ppb Ir. The gossans are also characterised by irregular pale to apple green veinlets of gaspeite (rare Ni carbonate mineral) in veinlets up to 8 cm-thick (Marston, 1984). The shoots were operated by Western Mining Corporation from 1967 to 1999. Between 1998 and 2001, Western Mining progressively sold their Ni interests in the Kambalda region. The Otter mine was purchased by GBF Mining Pty Ltd in 2001, and later that year, the mine was re-opened. In 2007, Mincor Resources Ltd purchased the mine, and this company operates several Ni mines on the Kambalda Dome. More recent mining-exploration activities have focussed on potential new ore resources in the spatially close Otter and Juan shoots.

## *Economic significance*

The Yilgarn Craton in Western Australia contains most of Australia's Ni resources, both sulphide and laterite, and is one of the world's great Ni provinces (Figure 6.21). Hronsky and Schodde (2006) state that the Yilgarn Craton contains about 31.5 Mt of Ni metal with an *in situ* value of about \$350 billion on a pre-mining basis, amounting to 13.5% of the world's known Ni resources. More than 90% of the nation's known global resources of Ni metal from sulphide sources were discovered during the narrow time period of 1966 to 1973 (Hoatson et al. 2006). Nickel sulphide deposits in this craton are almost exclusively associated with komatiitic rocks, the one exception being the Carr Boyd Rocks deposit (see Deposit Type 8.A). Nickel laterites in the Yilgarn Craton are exclusively developed over komatiitic rocks (Barnes, 2006). Many of the major Ni-Cu±PGE deposits associated with komatiitic rocks at the Kambalda Dome (e.g., Otter, Long–Victor, Lunnon, Durkin, Foster, Fisher, Hunt-Beta, Carnilya Hill) and in the nearby St. Ives, and Tramways areas have been in production from 1966 to at least 2000. The Otter–Juan Ni sulphide deposits are some of the largest and richest in the Kambalda Dome. They contain about 25% of the geological ore reserves of the Kambalda group and the Otter–Juan mine accounted for about 30% of the early annual Ni production (Marston, 1984).

## *Geological setting*

The Kambalda group of Ni-Cu±PGE sulphide deposits are located within a 30 km-long by 10 km-wide corridor between the Kambalda Dome (see Figure 6.22) and the Tramways Dome near the southern part of the Norseman–Wiluna greenstone belt of the Yilgarn Craton (see Deposit Type 3.A).

The Otter–Juan Ni-Cu±PGE deposits on the northern boundary of the Kambalda Dome (Figure 6.22) contain over 60 individual ore shoots that generally trend northwest-southeast for about 4 km. Major productive ore shoots include the Juan Complex (containing several ore subshoots), Juan West, Durkin, and Otter (Marston, 1984). These shoots form part of a northeastern belt of mineral systems, with the Durkin, Gibb, Long, and Victor shoots, and they straddle the north-northwest plunging anticlinal axis of the Kambalda Dome. The Juan Fault in this axial zone separates the mineralisation into north-dipping ore surfaces to the east and generally west-dipping ore surfaces in the west. The formerly more continuous ore shoots have been broken up by large-scale folding, followed by high-angle reverse faulting, and finally strike- to oblique-slip movement along the Juan Fault with associated small-scale folding and low-angle reverse faulting (Marston, 1984). A reconstruction of the original configuration of the shoots and subshoots shows two arcuate belts of ore with contrasting Ni tenors separated by a horst-like structure, which is interpreted as representing an original topographic high. Felsic dykes and sills strike west to west-northwest and dip steeply south. Minor movements post-dating the felsic intrusions are evident on the Juan Fault and parallel to some subshoots.

### *Mineralisation environment*

As is typical of most deposits on the Kambalda Dome (Beresford and Stone, 2004; Barnes, 2006), the ore shoots of the Otter–Juan deposits are hosted by basal komatiitic rocks—generally high-MgO (~25% to ~45% MgO) metaperidotites and metadunites replaced by talc-magnesite-chlorite-carbonate±serpentine±magnetite±dolomite assemblages—of the Kambalda Komatiite Formation, and they directly lie on basaltic rocks of the Lunnon Basalt (Figure 6.45). The footwall metabasalts are fine-grained dark grey-green massive rocks, locally traversed by quartz veinlets, and replaced by epidotic alteration or silicification. Concentrations of sulphides locally occur between pillows in the metabasalts. Metasomatic reaction zones containing abundant chlorite, biotite, phlogopite, and tremolite occur between the metabasalt and ultramafic rocks, or felsic porphyry intrusions and ultramafic rocks (Figure 6.45). Such reaction zones are only developed where massive ore is very thin or locally missing, or where breccia ore is present (Marston, 1984). Massive ores that range in thickness from 0.2 m to 4 m generally contain 80% to 100% sulphides at 10% to 17% Ni to 0.8 m above the footwall basalt. Above this are metre-thick layers of matrix ore containing 40% to 80% sulphides and 2.5% to 7% Ni. Disseminated-type ores with 10% to 40% sulphides and 0.5% to 2.5% Ni are located above the massive and matrix ores. Marston (1984) showed the subshoots have irregular ore distribution and structure. Massive and matrix-disseminated ores are very variable in thickness and commonly have irregular contacts with the footwall metabasalt. Disseminated to matrix ore is commonly two to seven times thicker than the massive ore which it overlies. Veins of massive ore, inclined at various angles penetrate up to a few metres into the footwall metabasalt, disseminated-matrix ore, or barren ultramafic rock (Figure 6.45). The primary sulphides consist of pentlandite-pyrrhotite-pyrite and pentlandite-millerite-pyrite assemblages, altered in the supergene zone to violarite and pyrite. This decomposes further by oxidation to a goethitic residue in which most of the secondary Ni species are deposited. The material is found around 20 m below the surface, at the base of the oxidised zone, in a supergene weathering area. The Otter–Juan mine is recognised for its variety of unusual secondary minerals in the supergene zone (Nickel and Wildman, 1981; Nickel and Robinson, 1985). Kambaldaite, gaspeite, reevesite, and some aragonite are found on fracture surfaces in goethite. Some of these rare species developed in this zone are from the dissolution of violarite, high sodium content from saline seepage from nearby salt lakes, and the dissolution of carbonates from the wall rock and ore (Mindat, 2014).

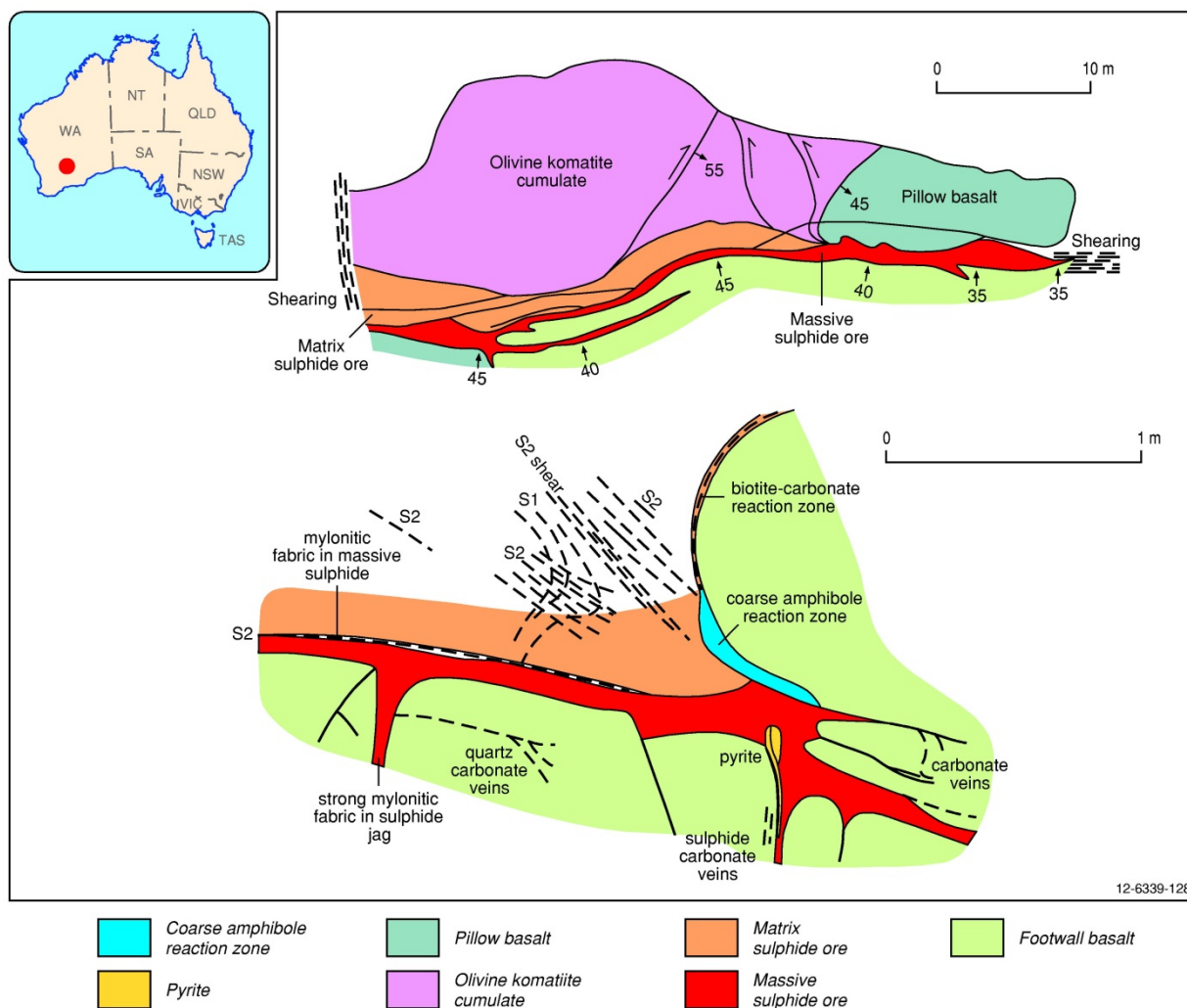


Figure 6.45 Detailed maps of basalt-ore-basalt pinchouts, and distribution of massive, matrix, remobilised, and vein-type sulphide ores, Juan Mine, Kambalda Dome, Western Australia. Modified from Lesher (1989), Stone and Archibald (2004), and Barnes (2006).

### PGE mineralisation

Ross and Keays (1979) and Keays et al. (1981a) studied the distribution of PGEs and other metals in the different types of sulphide ores and host rocks from the Juan and other ore shoots in the Kambalda district. They found that Pd was enriched in pentlandite relative to other sulphide phases, whereas Ir occurred in pentlandite, pyrrhotite, pyrite, and chalcopyrite, and Au was enriched in pyrite and chalcopyrite. These workers concluded that discrete PGMs were rare in the massive and matrix ores, and the remobilised chalcopyrite-rich footwall stringers were enriched in Pd and Au, owing to the remobilisation of these elements from the massive ores.

Hudson and Donaldson (1984) and Hudson et al. (1991) reported that significant amounts of Pt, Pd, and Au occur as discrete mineral phases in the Kambalda Ni ores. Major PGMs documented included: sperrylite ( $\text{PtAs}_2$ ); moncheite ( $\text{Pt,Pd,Ni}(\text{Te,Bi})_2$ ); sudburyite ( $(\text{Pd,Pt,Ni})(\text{Sb,Te,Bi})$ ); and stibiopalladinite ( $\text{Pd}_5\text{Sb}_2$ ); together with palladian arsenides, palladian melonites, and native gold. Michenerite, merenskyite, and testibiopalladinite also occurred within Kambalda ores (Hudson et al., 1991). Apart from a single grain of irarsite ( $\text{IrAsS}$ ), no discrete PGMs containing Os, Ir, Rh, and Ru were identified

(Cowden et al., 1986; Hudson, 1986). The correlation of Os, Ir, Ru, and Rh with both Ni and pentlandite, and the fact that discrete phases containing these elements are extremely rare, suggest that these elements either occur largely in solid solution or as minute inclusions within pentlandite.

Hudson's (1986) detailed study that focussed on the distribution of PGMs from the Juan, Lunnon, and Ken ore shoots in the Kambalda Dome showed that sperrylite was the most abundant PGM in the massive ores, whereas sudburyite, moncheite, merenskyite, michenerite, testibiopalladite, and palladian melonite occur predominantly within veins in the massive and matrix ores, within stringers of sulphide in the footwall rocks, or in association with post-ore hydrothermal veins and porphyries. These discrete Pd-bearing phases appear to have formed as the result of post-magmatic processes, in particular, metamorphic segregation of sulphides and the interaction of Pd-bearing ore sulphides (pentlandite) with younger hydrothermal veins.

### *Age of mineralisation*

The age of the komatiitic stratigraphy in the Otter–Juan shoots is well established as Neoproterozoic from the dating of komatiitic and associated felsic rocks in the Kambalda Dome region, and also from analogy with similar mineralised greenstone belts and other Ni sulphide deposits in the Eastern Goldfields Superterrane that have been dated (Nelson, 1997). Most komatiitic-hosted Ni sulphide deposits in the Norseman–Wiluna greenstone belt fall within a very narrow age span between 2710 Ma and 2700 Ma (Hoatson et al., 2006). Therefore the maximum age constraint for the event(s) forming the remobilised Ni-Cu-PGE±Au-bearing sulphides at Otter–Juan is approximately 2705 Ma. Since remobilised ores can form through many different processes, e.g., late magmatic-metasomatic-metamorphic-deformational-hydrothermal-regolith (see next section Genesis), and knowing that the Kambalda ores have undergone a complex history of polyphase deformation and metamorphism (Cowden et al., 1986), it is unlikely that any determined ages could be confidently assigned to a particular post-emplacement event.

### *Genesis*

Leshner and Keays (1984) found that the komatiitic peridotite-hosted mineralisation at Kambalda is largely magmatic, but various postmagmatic processes have modified the distribution, structure, texture, mineralogy, and chemistry of the sulphide ores. These processes have resulted in a spectrum of sulphide mineralisation types, ranging from complete dislocation (faulted ores), and more localised mobilisation (stringer sulphides), through metamorphic replacement (inter-pillow-interbreccia sulphides), to hydrothermal dissolution and redeposition (vein-type sulphides).

Geochemical profiles of PGEs through typical ore zones at the Juan, Lunnon, and Long shoots by Cowden et al. (1986) showed that Pt, Pd, and Au concentrations are lower in massive ore relative to overlying matrix and disseminated ores, whereas the other PGEs have a more uniform distribution through these ore types. Platinum, Pd, and Au are strongly concentrated at the footwall metabasalt-massive ore contact and in small sulphide-filled fractures within the footwall metabasalt. The other PGEs are concentrated to a lesser extent at this position. Some magnetite selvages immediately above massive ores are depleted in Os, Ir, and Ru. The concentration of PGEs in the late fractures is attributed to metamorphic remobilisation.

Sulphur isotope data of coexisting sulphides from a wide range of ore types from the Juan and Lunnon shoots by Secombe et al. (1981) show a very restricted range of  $\delta^{34}\text{S}$  of 4.3‰. The mean value was 2.4‰ and standard deviation of +0.8‰. These data support a magmatic source for the Fe-Ni-Cu sulphide ores, and the slightly positive mean  $\delta^{34}\text{S}$  value was attributed to  $\text{S}^{2-}$ - $\text{HS}^-$  fractionation during

segregation of sulphide-oxide liquid from the silicate melt. The authors also proposed that massive and matrix ores may have crystallised independently, and there was late-stage S addition to the massive sulphides with generation of fine-grained pyrite layers.

Remobilised sulphide ores have also been documented in other komatiite-hosted deposits distant from the Kambalda Dome. These include Waterloo–Amorac, Emily Ann, Wannaway, and potentially other small pods of remobilised and structurally complicated sulphides (e.g., Wedgetail prospect at Honeymoon Well). In most cases, the sulphides have moved less than 100 m, although in the case of Emily Ann, over 600 m of displacement has been documented. Ross and Keays (1979) suggested that some Pd and Au was lost from Ni ores during metamorphism, and Keays (pers. comm. in Cowden et al., 1986) proposed that up to 80% of the original Au content was lost to metamorphic fluids, thus providing a possible source for Archean lode Au deposits.

### *Key references*

- Marston and Kay (1980): geological setting; petrology; different types of Ni ores; genesis of the Juan Complex.
- Keays et al. (1981a): PGEs contents of Kambalda ores; distribution within ores and host rocks; magmatic and hydrothermal processes; mineralisation models.
- Seccombe et al. (1981): S isotopes; textures of sulphides; generation of pyrite; S paragenesis and mobility; ore modification of the Juan and Lunnon main shoots.
- Marston (1984): Ni sulphide deposits of Western Australia; Kambalda Dome deposits; stratigraphy; structure; mineralisation; exploration results; mining companies.
- Leshner and Keays (1984, 2002): metamorphic and hydrothermal mobilisation of Ni-Cu sulphides and PGEs; petrogenesis.
- Cowden et al. (1986): PGE and Au contents of Kambalda komatiites; Pt, Pd, and Au are strongly concentrated at the footwall metabasalt-massive ore contact and in small sulphide-filled fractures within footwall metabasalt; remobilisation of PGEs due to metamorphic processes.
- Hudson (1986): distribution of PGMs in massive sulphides, veins, stringers and reaction zones; hydrothermal remobilisation; metamorphic processes.
- Leshner (1989): komatiite-associated Ni sulphide deposits; stratigraphy; mineralisation; Kambalda-type deposits; volcanology; petrogenesis.
- Barnes et al. (1999): komatiite flow fields and associated Ni-sulphide mineralisation; volcanology; Kambalda Ni mineralisation.
- Beresford and Stone (2004): overview of komatiite-hosted Ni-Cu-PGE deposits of the Kambalda Ni camp; volcanic and structural controls of ore shoots; stratigraphy and deformation of Kambalda Dome.
- Stone et al. (2005): three-dimensional structural study of Ni shoots at the Kambalda Dome; deformation and remobilisation of Otter–Juan shoots; structural deformation and alteration of Juan ore shoot; displacement, transport, and off-set of ore shoots have implications for new exploration targets.
- Barnes (2006): komatiite-hosted deposits of the Yilgarn Craton; Kambalda-type deposits; stratigraphy; lava channels; mineralisation; petrogenesis; hydrothermal and magmatic origins.
- Hoatson et al. (2006): classification of Kambalda deposits; stratigraphy; mineralisation.
- Barnes and Fiorentini (2008): Ir, Ru, and Rh abundances in komatiites; Kambalda-type deposits; alloy saturation; partition coefficients; thermodynamic modelling.

- Fiorentini et al. (2010): Kambalda-type deposits; PGE geochemistry of mineralised and non-mineralised komatiites; depletion and enrichment of PGEs; physical volcanology; ore-forming processes; exploration potential.
- Barnes et al. (2013): abundance profiles of PGEs in komatiites; Long–Victor deposit; PGE-enrichment halo; geochemical footprints; channel and flank facies; prospect-scale prospecting.

#### **6.4.8.3 Deposit Type 8.C: Magmatic breccias involving mafic, ultramafic, and felsic igneous rocks**

##### *Overview*

Polymetallic hydrothermal PGE deposits in Australia range from localised *in situ* remobilisation of sulphides along the basal contacts of layered mafic-ultramafic intrusions (Abrahams Find–Joshua, Edison, Jimberlana, Munni Munni, Nova, Radio Hill, Savannah, Tom Tit, Jason) and komatiitic lavas (Kambalda ore shoots, Perseverance), to shear-related mineralisation in mafic-ultramafic dykes and sills (Jacks Hill, Koppany, Melba Flat, Mulga Springs, Thomson River), to more distal deposits associated with shear zones in mafic volcanic and siliciclastic rocks (Alma, Cunig, Great New Zealand, Halleys, Lady Mary North, Lucknow) and felsic rocks (Andover, Copper Hill, Copper King, Copper Queen, Doolena Gap, Elizabeth Hill, Pokali). Sub-economic concentrations of Pd, Rh, and/or Pt are associated with precious and base metals that were transported by various types of hydrothermal fluids along major structural elements, such as faults, fracture, and dilational zones. For all these deposits shown above (see Appendix K for descriptions), the PGEs are spatially associated with mafic-ultramafic, and to a lesser degree, felsic igneous rocks, but are all derived from the former rocks.

Regional lineament studies in the west Pilbara Craton in the late 1980s identified structurally controlled precious metal mineralisation near the northern margin of the Munni Munni Intrusion (see Deposit Type 1.A). Strong hydrothermal Ag mineralisation was defined on the Munni Munni Fault where it cuts basement Archean granitic and meta-sedimentary rocks. Elizabeth Hill is an unusual example in Australia of an Archean hydrothermal breccia deposit that has anomalous concentrations of PGEs hosted by felsic rocks in the primary and supergene zones. High-grade ore pods are hosted by a variety of felsic and mafic-ultramafic igneous rocks, including granite, monzogranite, gabbro, and pyroxenite. The mineralised veins consist of calcite-quartz breccias that contain spectacular Ag grades (up to 16% Ag) and anomalous Pd, Cu, Au, Pb, Ni, Ti, Ba, and Mo (de Angelis et al., 1988). Over 60 different ore minerals characterise this unusual deposit formed from the interplay of different metal sources. The juxtaposition of magmatic and hydrothermal sulphides and an exotic suite of Ag and base-metal sulphides are consistent with magmatic sulphide assemblages being overprinted by hydrothermal fluids in a possible low-pressure and low- to moderate-temperature environment. Marshall (2000) cites the geometry, textures, and mineralogy of the mineralised veins as evidence for an epithermal origin for the Elizabeth Hill deposit.

Barnes (1995) notes that there are similarities between Elizabeth Hill and overseas deposits where quartz veins intersect mafic units that contain Ni, Co, Pd, and Ag mineralisation. Such ‘exotic Ag vein’ deposits include: Cobalt, Ontario; Bou Azzer, Morocco; Jachymov, Czech Republic; and Saxony, Germany. Hydrothermal Pb-Ag veins also occur at the contact between gabbro and granite on the southern margin of the Andover Intrusion (Andover Ag-Pb mine: Wallace, 1992b), near Roebourne (Figure 6.3).

### *Australian deposits/prospects/hosts*

Elizabeth Hill (Pilbara Craton, WA); ?Yarawindah Brook–New Norcia (Yilgarn Craton, WA).

### *Significant global example(s)*

Platreef and Waterberg, Bushveld Complex (Republic of South Africa); ?Lac des Iles (Canada).

### *Type example in Australia*

Elizabeth Hill, Western Australia.

### *Location*

Longitude 116.871385°E, Latitude -21.086066°S; 1:250 000 map sheet: Yarraloola (SF 50–06), 1:100 000 map sheet: Pinderi Hills (2255); small underground mine ~42 km south of Karratha, west of the Karratha–Tom Price Road, Western Australia.

### *Geological province*

West Pilbara Granite-Greenstone Terrane, Pilbara Craton, Western Australia.

### *Resources*

Approximately 16 800 t of ore grading 2100 g/t Ag (70 ounces/t) were mined to produce 1 170 000 ounces of Ag, valued in 2009 at AUD\$21 million. The bulk of production, in the form of sulphide concentrates, was shipped to South Africa for treatment and the high-grade coarse Ag was shipped to the Perth Mint for direct smelting. A shallow resource of 7000 t grading 700 g/t Ag (22 ounces/t) for 157 000 ounces remains. Inferred and Indicated Resources for the upper Ag pod are 24 100 t @ 0.42% Ag; Inferred Resource for the lower Ag pod is 22 700 t @ 0.12% Ag (Barnes, 1995; Murphy, 2000). An Inferred Resource of 2.7 Mt of ore grading 0.9 g/t Pt and Pd was announced by Washington Resources Limited (2005).

### *Current status and exploration history*

Developed mine; not operating in 2014. The outcrop of this high-grade vein deposit was discovered by AGIP Australia in 1987 during company investigations of regional lineaments for hydrothermal mineralisation (de Angelis et al., 1988). Spectacular secondarily-enriched Ag intersections were defined on the Munni Munni Fault, near the basal contact of the ultramafic zone of the Munni Munni Intrusion with the granite country rock. Percussion hole PH MM9 contained 6 m @ 3478 ppm Ag, including a peak of 2 m @ 6800 ppm Ag. Maximum values of 6450 ppm Cu, 3130 ppm Ti, 2180 ppm Ni, 1550 ppm Pb, and 494 ppm Mo were also present in the drill-hole. Drill-hole PH MM12 contained 9 m @ 0.21 ppm Au and 0.59 ppm Pd. The underground mining of a series of small, but rich ore pods was undertaken by Global Strategic Metals and Legend Mining between 1998 and 2000. Electromagnetic geophysical surveys have also identified anomalies within 400 m of the mine and Sub-Audio Magnetic (SAM: also called Total Field Magnetometric Resistivity: TFMRR) surveys have defined lower grade, remnant Ag resources in the mine workings. The SAM surveys can identify structural and alteration features, which show up as lower relative electrical resistance than surrounding basement/host rocks.

### *Economic significance*

The Elizabeth Hill deposit is a rare example in Australia of an Archean hydrothermal polymetallic deposit that has anomalous concentrations of PGEs in the primary and supergene zones. In addition,

such deposits have been rarely mined (albeit not for PGEs) in recent times. A giant Ag nugget weighing 165 kg—believed to be the largest example of primary Ag mineralisation in Australia—was found in 2000 (Australia's Paydirt, May 2000).

### *Geological setting*

The structurally-controlled Elizabeth Hill Ag deposit (Barnes, 1995; Marshall, 2000) has a spatial and possible genetic association with the 2927 Ma Munni Munni Intrusion (Figure 6.3 and Figure 6.4). The Elizabeth Hill deposit is located on the northern basal contact of the Munni Munni Intrusion where the Munni Munni Fault—a major north-trending vertical sinistral structure—cuts ultramafic rocks of the intrusion and granitic rocks of the Cherratta Granitoid Complex (Figure 6.5 and Figure 6.46). The Munni Munni Fault and the basal contact of the Munni Munni Intrusion, which dips 15° to 45° towards the south, are the major controls on the geometry of the vein system. Four high-grade ore pods, 20 m- to 80 m-long, and 5 m- to 15 m-wide, plunge shallowly to the south to depths of 120 m, formed in a shear structure linked to the Munni Munni Fault immediately to the west. They are enclosed within a discordant en échelon body containing a lower-grade envelope (Ferguson, 1999; Marshall, 2000). Hydrothermal Pb-Ag veins also occur at the contact between gabbro and granite on the southern margin of the Andover Intrusion, near Roebourne (Figure 6.3). Silver anomalies have been recorded in layered mafic-ultramafic intrusions from overseas, including Dunka Road (USA), Fiskenaeset (Greenland), and from the Ukraine.

### *Mineralisation environment*

The deposit is hosted by a variety of felsic and mafic-ultramafic igneous rocks, including granite, monzogranite, gabbro, and pyroxenite. The last two rock types form rafts, 2 m to 50 m in size within the granite, dipping west. The mineralised veins consist of calcite-quartz breccias that contain fragments of pyroxenite, gabbro, and granite. The 82 m-level of the mine exposes the vein system as a 1.5-m-wide body of carbonate-quartz breccia with about 25% clasts predominantly of pyroxenite with lesser granite (Marshall, 2000). The selvedges of the shoot show anastomosing quartz-carbonate and sulphide veins and stringers in silicified, carbonatised, and chloritised country rock.

### *PGE mineralisation*

The mineralised veins contain spectacular Ag grades (up to 16% Ag) and anomalous concentrations of Pd, Cu, Pb, Zn, Ni, Ti, Ba, and Mo (de Angelis et al., 1988). Marshall (2000) notes that although there are local erratic high levels of Au, it would appear that the mineral system does not contain significant Au. Notable drill-hole intersections that highlight the polymetallic character of the deposit include 7.5 m @ 2.3% Ag, 5 m @ 2% Pb, and 9 m @ 0.6 ppm Pd and 0.2 ppm Au. Over 60 ore minerals, including native metals, alloys, and sulphides occur in the mineralised veins and country rock. These include suites of sulphides and native metals typical of magmatic deposits in layered intrusions (pyrrhotite, chalcopyrite, pentlandite, native PGMs), hydrothermal Cu-Zn-Pb deposits (pyrite, chalcopyrite, sphalerite, galena), and an exotic suite of Ag sulphide minerals containing Ni, Co, Cu, Pb, Zn, As, and Sb. Dominant Ag-bearing minerals are native silver, argentopentlandite, acanthite, and argentite. Many of these minerals are late in the paragenesis of the ores, with acanthite widespread in siderite silicates and quartz assemblages (Marshall, 2000). Native silver occurs as veins, sheets, crystalline wire, globules, dendrites, and in large carbonate-hosted nuggets weighing up to 165 kg. A 100 t bulk sample from the 82 m level averaged about 1% Ag, 20% of which occurred as native silver and the remainder comprised a complex group of Ag sulphides and sulphosalts and base-metal sulphides. Calcite, quartz, calcian siderite, and chlorite are the major gangue minerals. The Ag mineralisation is dominantly primary, although supergene sulphides locally extend to depths of

100 m in the mine. Vanadanite, chalcantite, galena, and unidentified Ag halides occur in the ore stockpiles. The very high Ag content of the deposit is attributed to both primary and supergene enrichment processes. The complexity of the ore assemblages may reflect primary magmatic sulphides overprinted by Ag-base metal rich, hydrothermal fluids with subsequent supergene sulphide deposition and partial oxidation of the entire assemblage (Marshall, 2000). Gossans that can be traced over 600 m on the surface contain Ag (up to 300 ppm), Pd (up to 10 ppm), Rh (up to 1 ppm), and minor Cu, Ni, Pb, Zn, but no Pt or Au (Barnes, 1995).

### *Age of mineralisation*

Miller (2000) states that the structurally controlled mineralised vein system at Elizabeth Hill is clearly younger than the 2927 Ma Munni Munni Intrusion. The deposit is located immediately adjacent to the Munni Munni Fault—the most prominent sinistral fault along the eastern side of the Munni Munni Intrusion (Figure 6.4). Lead/lead isotope studies (Huston et al., 2002) of galena from veins in the Elizabeth Hill deposit indicate a maximum age of 2867 Ma for the precipitation of metals, i.e., at least ~50 million years younger than the nearby 2927 Ma Munni Munni Intrusion. They suggest that the deposit may be related to an early Fortescue mineralising event at 2750 to 2700 Ma.

### *Genesis*

Elizabeth Hill is an unusual, very high-grade polymetallic deposit. A number of different origins for the mineralisation have been proposed. On the basis of petrological data, Barnes (1995) considered three possible origins:

1. supergene enrichment;
2. hydrothermal veins associated with felsic rocks along the Munni Munni Fault; and
3. a late-stage Ag-rich phase differentiated from the Munni Munni Intrusion following assimilation of country rock.

Barnes (1995) also infers a close connection with stratabound PGE-Cu-Ni layers in the Munni Munni Intrusion that contain anomalous Ag (e.g., Judy's Reef). de Angelis et al. (1988) were the first investigators to suggest the very high Ag contents of the Elizabeth Hill deposit were the result of supergene enrichment. However, Marshall (2000) notes that Ag mineralisation at the 82 m-level of the mine is dominantly a primary assemblage, although supergene sulphides (e.g., marcasite, violerite, millerite, and mckinstryite-(Ag,Cu)<sub>2</sub>S) and oxidised products (goethite) extend to 100 m-depth.

Company geologists have more recently proposed that the Elizabeth Hill deposit may have formed from the Munni Munni Intrusion assimilating a VMS deposit as it was emplaced in an area of structural weakness (Proactive Investors, 2014). A number of small VMS deposits occur immediately north of the Munni Munni intrusion and elsewhere throughout the west Pilbara Craton. The Elizabeth Hill deposit shows many characteristics of a complex hydrothermal carbonate-quartz vein system that involved multiple sources of metals. The Munni Munni Fault and associated shear-link structure localised the movement of metal-bearing hydrothermal fluids through the Munni Munni Intrusion and country rocks. The variety of metals in the deposit implies they were derived from the layered mafic-ultramafic intrusion and the felsic igneous country rocks. Precipitation of the metals from the fluids was probably initiated by the chemical interaction of the fluids with reactive rocks near the basal contact of the intrusion or with ascending basement-derived fluids. The presence of such minerals as nickeliferous pyrrhotite and argentopentlandite; Pd, Rh, Ni, and Cu in gossans; and the similar chemistry of the nearby Judy's Reef suggest that the sulphide-bearing rocks in the lower part of the ultramafic zone of the Munni Munni Intrusion were a source of metals for the Elizabeth Hill deposit.

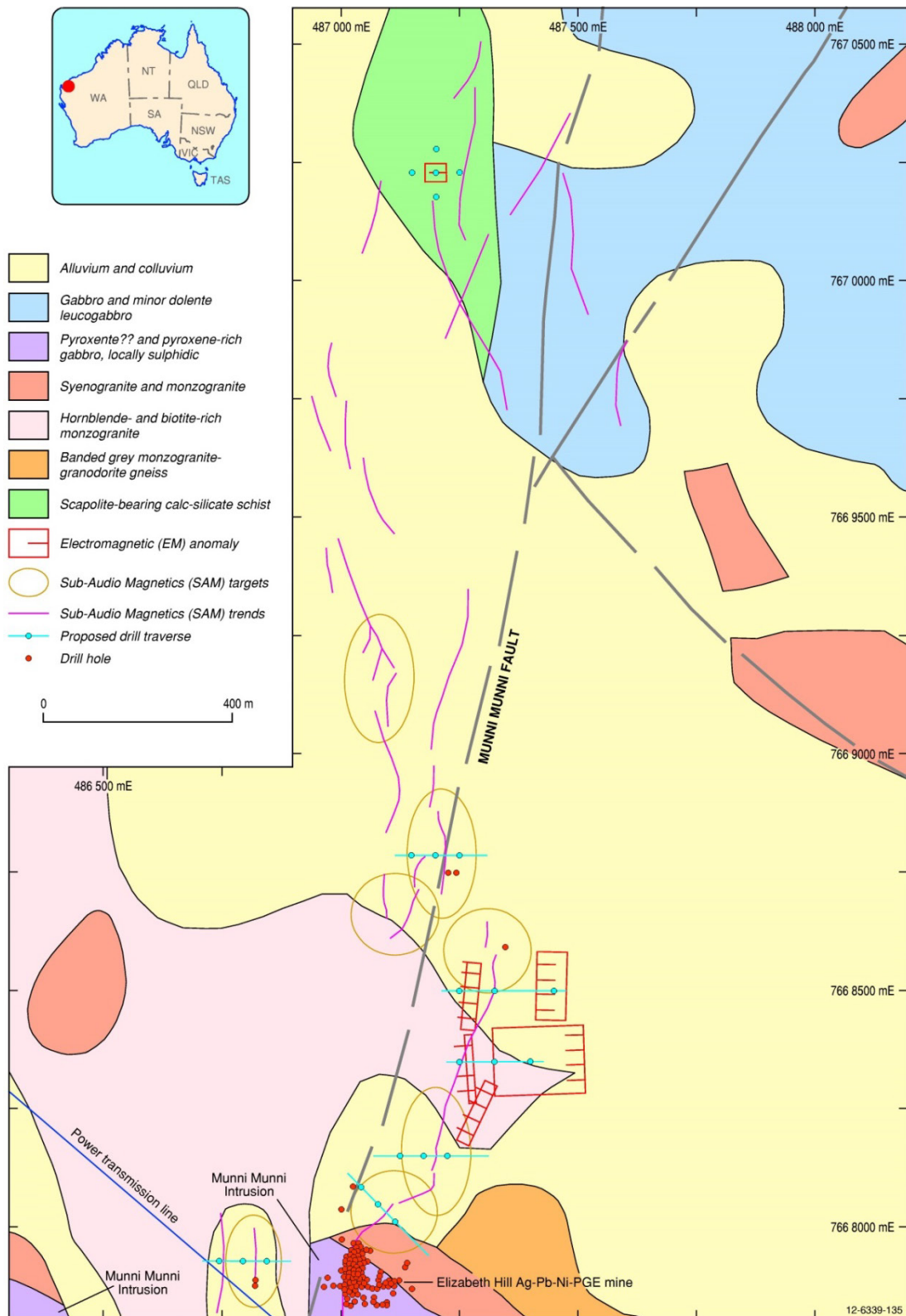


Figure 6.46 Generalised geological setting of the hydrothermal Elizabeth Hill Ag-Pb-Ni-PGE deposit located on the Munni Munni Fault, immediately north of the Munni Munni Intrusion, west Pilbara Craton, Western Australia. Electromagnetic anomalies and trends are shown subparallel to the Munni Munni Fault. Modified from East Coast Minerals NL (2009).

Marshall (2000) cites the geometry, textures, and mineralogy of the mineralised veins as evidence for an epithermal origin for the Elizabeth Hill deposit. The juxtaposition of magmatic and hydrothermal sulphides and the exotic suite of Ag and base-metal sulphides are consistent with magmatic sulphide assemblages being overprinted by hydrothermal fluids in a possible low-pressure and low- to moderate-temperature environment. Barnes (1995) notes that there are some obvious broad similarities between Elizabeth Hill and overseas deposits where quartz veins intersect mafic units that contain Ni, Co, Pd, and Ag mineralisation. Such 'exotic Ag vein' deposits are referred by Ruzicka and Thorpe (1996) as arsenide vein Ag-Co, and arsenide vein Ag-U deposits, and include Cobalt, Ontario; Bou Azzer, Morocco; Jachymov, Czech Republic; and Saxony, Germany. However, as Marshall (2000) points out Elizabeth Hill arsenides are uncommon, and U or Ra minerals are yet to be identified.

### *Key references*

- de Angelis et al. (1988): geological setting of the Elizabeth Hill Ag deposit; secondary Ag mineralisation, exploration history; Radio Hill and Munni Munni intrusions; integrated exploration techniques.
- Barnes (1995): exploration, mining practices; geological setting; carbonate-hosted mineralisation; polymetallic deposit; PGEs, fluid activity.
- Ruddock (1999): regional geology of west Pilbara Craton; Elizabeth Hill polymetallic deposit; mineralisation; drilling; exploration activities and potential.
- Marshall (2000): mineralogy of ores; paragenesis of polymetallic ores; sulphides and native metals typical of magmatic and hydrothermal deposits; low temperature-low pressure epithermal origin.
- Hoatson and Sun (2002): discovered during regional lineament study; structurally-controlled polymetallic deposit; located in fault linked to Munni Munni Fault; high-grade veins and ore pods; calcite-quartz breccia; high Ag grades up to 16% Ag; primary and supergene sulphides; multiple sources of basement-derived fluids.
- Huston et al. (2002): lead/lead isotopes; maximum age of 2867 Ma for precipitation of metals in veins; deposit is ~50 million years younger than abutting 2927 Ma Munni Munni Intrusion; possibly related to Fortescue-aged (~2750 Ma) mineralising event.
- Hickman and Van Kranendonk (2008): regional geology and metallogenesis of northern Pilbara Craton; geology of Elizabeth Hill deposit; crustal evolution.
- East Coast Minerals (2009): electromagnetic anomalies; drill results; new geological model; assimilation of volcanogenic massive sulphide deposit by the Munni Munni Intrusion.

#### **6.4.8.4 Deposit Type 8.D: Structurally-controlled remobilised Ni-Cu-PGE sulphides in mafic±ultramafic±felsic dykes/veins in shear zones**

##### *Overview*

Some 30 years ago there was considerable debate about the relative importance of magmatic processes versus fluid-volatile processes in the formation of PGE deposits (Boudreau et al., 1986; Stumpfl, 1986, 1987; Stumpfl and Ballhaus, 1986; Naldrett, 1989, 2004). Remobilised PGE occurrences encompass a wide range of temperatures and fluid compositions. These include C-O-H-S-Cl volatile-fluid systems at temperatures greater than 600°C in pegmatoidal pyroxenite horizons in layered intrusions, to chlorine brines around 300°C, down to temperatures of 4°C in seawater (Stumpfl, 1986). There is now general consensus that hydrothermal mineral systems play a critical role

in the formation and economic status of particular PGE deposits. Australian PGE occurrences related to remobilised-hydrothermal systems can be classified into deposits which are mainly due to primary magmatic processes and having a minor hydrothermal overprinting (Deposit Type 8.D), through those involving late-stage hydrothermal remobilisation of PGEs derived from a nearby mafic-ultramafic rock source, to deposits which are strictly hydrothermal in origin (i.e., the PGEs show no obvious derivation from mafic-ultramafic rocks, are commonly associated with Au, U, and/or base metal sulphides, and fluid movement was the dominant mechanism for PGE transport in a region which had a favourable structural framework: Deposit Type 8.F).

Structurally-controlled, remobilised Ni-Cu-PGE mineral systems associated with dyke and sill-like bodies of mafic±ultramafic igneous rocks are most prominent in Proterozoic and Phanerozoic terranes of Australia. Examples described in Appendix K and by Hoatson and Glaser (1989) include Baldrick, Blackadder, Kongo (NT), Koppany, Westwood (Qld) Mulga Springs (NSW), Thomson River (Vic), and Melba Flat (Tas). Mulga Springs is the type example of a Ni-Cu-PGE orthomagmatic mineral system overprinted by hydrothermal processes in close proximity of mafic-ultramafic rocks. Mulga Springs is one of several serpentinised dykes, sills, and thin lensoidal bodies that have intruded along late shear and fault zones, possibly related to the Rodinia continental breakup event that affected Australia from around ~850 Ma (Blewett, 2012). The Back Ridge, Little Broken Hill Gabbro, Little Darling Creek, Mulga Springs, Round Hill, Moorkaie, Mulga Springs, and Razorback Ni-Cu±PGE prospects are associated with the intrusions that form a thin arcuate belt in the southeastern corner of the Curnamona Craton. Platinum-group-element mineralisation at Mulga Springs has been delineated in three major settings. Platinum, Pd, and Au concentrations are associated with chalcopyrite-pentlandite-pyrrhotite mineralisation near the basal contacts of the intrusions, in remobilised sulphides in the footwall gneissic rocks, and in surface gossans spatially above the sulphides. Gossans at Mulga Springs and Back Ridge are unusually enriched in all PGEs and base metals, namely 19.6 g/t Pt, 50 g/t Pd, 3 g/t Rh, 4.4 g/t Ir, 3 g/t Os, 2 g/t Ru, 0.57 g/t Au, 0.34% Ni, and 0.71% Cu. The extremely high PGE abundances, erratic Pt to Pd ratios, and the irregular distribution of remobilised sulphides along the basal contacts of the intrusions are features indicative of hydrothermal-mineralising systems. The heterogeneous nature of the PGE mineralisation (i.e., lack of lateral continuity of grades and widths of mineralisation) makes delineation of ore resources difficult and these types of deposits generally have low potential for large-tonnage deposits. An example of structurally controlled, remobilised PGE mineralisation that operated in the Phanerozoic is the Thomson River Cu-Au mine (also called Coopers Creek) at the southern end of the Walhalla–Woods Point auriferous belt, central Victoria (see Appendix K). Thomson River is also significant since it is probably the first notable example of hard-rock PGE mining in Australia, albeit as a by-product of Cu-Ni mining. After being discovered in 1864, the Thomson River Copper mine had several phases of mining activity, with production up to 1881 amounting to 10 000 t of Cu-rich ores (>10% Cu). The mineralisation is an example of hydrothermal remobilisation of Au, and to a lesser degree Pt and Pd. The host rock for the mineralisation is a Devonian hornblendite dyke, faulted, sheared, and hydrothermally altered by carbonate-bearing solutions (Keays and Kirkland, 1972).

#### *Australian deposits/prospects/hosts*

Mulga Springs Intrusion (Curnamona Craton, NSW); Thomson River Copper mine (Lachlan Orogen, Vic); Westwood (New England Orogen, Qld); Kongo–Copper King–Copper Queen (Arunta Orogen, NT); Melba Flat (Delamerian Orogen, Tas).

### *Significant global example(s)*

Messina, Waterberg (both South Africa); New Rambler (USA); Rathbun Lake (Canada); Hitura (Finland).

### *Type example in Australia*

Mulga Springs Intrusion, New South Wales.

### *Location*

Longitude 141.665109°E, Latitude -31.885816°S; ~25 km northeast of Broken Hill, New South Wales; 1:250 000 map sheet: Broken Hill (SH 54–15), 1:100 000 map sheet: Taltingan (7234).

### *Geological province*

Curnamona Craton, New South Wales.

### *Resources*

Unknown. Around 500 t of ore was mined from the historic Red Hill mine between 1906 and 1937, with face rock samples having grades ranging from 5 g/t to 41 g/t PGEs, 2% to 4% Cu, 2% to 3% Ni, and 22 g/t to 70 g/t Ag (Impact Minerals Limited, 2013, 2014).

### *Current status and exploration history*

Prospect with advanced exploration. Early exploration in the southern Curnamona Craton focused on Broken Hill-style Pb-Zn-Ag mineralisation, however, a number of exploration programs from the 1960s recognised the association of small PGE-Ni-Cu gossans associated with mafic-ultramafic intrusive complexes which are much younger than the Broken Hill deposit-host rocks. Geological mapping by the NSW Geological Survey outlined a discontinuous, locally highly sheared zone of ultramafic and mafic rocks extending from Mulga Springs, almost 9 km to the northwest to the Moorakaie prospect. In the 1960s, the Zinc Corporation, among many other companies, assessed the Ni potential of ultramafic rocks in the Willyama Complex. Mapping at Mulga Springs and Mount Gipps showed that the ultramafic rocks formed steeply dipping, narrow serpentinised bodies, up to 10 m-thick, and 40 m-thick lensoidal bodies, with outcrop generally limited by regolith and alluvial cover. Shallow auger drill lines at Mulga Springs revealed the ultramafic rocks were more extensive than inferred from outcrop. The ultramafic bodies were considered to have similarities with 'alpine-type' intrusions related to major fault/shear zones (pers. comm., A. McKay, GA, July 2013). Sampling of gossans returned spectacular grades of PGEs and Au, e.g., 40 g/t Pt+Pd at the Back Ridge gossan. In the 1970s, CRA drilled the Mulga Springs prospect and recorded a 2- to 3-m-thick intersection of banded pyrrhotite-pentlandite-chalcopyrite associated with cumulate textured olivine rich mafic rocks (Golden Cross Resources, 2014). Whilst the tenor of this drill-hole was assessed, no systematic analyses for PGEs were undertaken. Golden Cross Resources drilled close by in 2001 and returned an intersection of 2 m @ 10.9 g/t Pt, 23.6 g/t Pd, 0.94 g/t Au, 6.12% Cu, and 4.45% Ni in massive sulphides. Several companies carried out ground magnetics, soil geochemistry, and RAB/aircore drilling programs in areas of residual soil and cover marginal to the intrusions. Drilling of the Little Broken Hill Gabbro by Vale (previously CVRD-Inco) in 2006 recorded anomalous Cu and Ni values in several holes. In addition, the drilling confirmed the extension of the mafic-ultramafic sequences under cover opening up the potential for hidden mineralisation. Moving loop Electro Magnetic surveying failed to identify massive sulphide accumulations in potential feeder zones at the Little Broken Hill Gabbro and Mt Darling Creek complexes. Exploration by Endeavour Minerals Pty Ltd since 2012 involved surface soil

and rock geochemical programs at the Little Broken Hill Gabbro, Round Hill, Little Darling Creek, and at Back Ridge and Southern Slope, north of Mulga Springs.

The Red Hill mine is located ~15 km southeast of Broken Hill in ultramafic rocks that cross cut deformed and metamorphosed rocks of the Broken Hill Group (Impact Minerals Limited, 2013, 2014). The ultramafic rocks outcrop over an area of 500 m by 250 m and mineralisation occurs close to the western contact. Red Hill was mined for Cu between 1906 and 1937 both at surface and underground, from a vertical shaft to a depth of 36 m. Old mine records indicate that about 500 t of ore was mined from four parallel 'lodes', each 1 m to 2.5 m wide. Recent sampling from the underground mine returned anomalous PGE and Cu-Ni-Ag concentrations shown in 'Resources' above. The lodes are open along strike and at depth. About 70 rock chip samples taken over a 130 m by 30 m area trending northeast from the Red Hill mine returned assays with a grade range of 1 g/t to 36 g/t PGE and 0.2% to 6.1% Cu near the western contact of the ultramafic rocks. Rock and soil geochemical studies by Impact Minerals Limited (2014) suggest the host ultramafic body at Red Hill has a Ni-enriched core surrounded by a precious metal-Cu-enriched margin. Outcrop samples from the Red Hill mine shaft returned up to 16 g/t Pt, 12.1 g/t Pd, 4.2% Ni, 7.7% Cu, 1.3 g/t Au, and 221 g/t Ag. Rock-chip samples from Simons Find, 150 m north of the Red Hill mine shaft, returned up to 0.7 g/t Pt, 1.7 g/t Pd, 0.4% Ni, 0.1% Cu, 1.9 g/t Au, and 6.6 g/t Ag, and slightly higher assays of 1.0 g/t Pt, 2.6 g/t Pd, 0.9% Ni, 0.8% Cu, 1.8 g/t Au, and 3.3 g/t Ag were obtained from Red Hill South, 100 m south of the shaft (Impact Minerals Limited, 2014).

Hoatson and Glaser (1989: p. 51) provide a summary of exploration activities and results prior to 1989 for the ultramafic intrusions of the Broken Hill district.

### *Economic significance*

The PGEs reported in drill-hole intersections and surface gossans at Mulga Springs, Back Ridge gossan, and Forners Prospect are some of the highest concentrations reported in Australia. Gossan outcrops in the Mulga Springs Intrusion are noted for the complete suite of the six PGEs, including the rarer members Ir, Os, and Ru (see PGE mineralisation below).

### *Geological setting*

The Little Broken Hill Gabbro, Little Darling Creek, Mulga Springs, Round Hill, Back Ridge, Moorkaie, and Razorback PGE-Ni-Cu prospects occur in serpentinised ultramafic intrusions that form a thin arcuate belt near the southeastern corner of the Curnamona Craton (Figure 6.47). This region contains high-grade Proterozoic metasedimentary and intrusive rocks of the Willyama Supergroup—a predominantly terrigenous, clastic depositional sequence, with minor metavolcanics, syn-depositional dolerite and gabbro (now mafic gneiss) dykes and sills, and granite (now granite gneiss) sills, laid down in an intracratonic rift during the period ~1730 Ma to ~1650 Ma (Golden Cross Resources, 2014). The exposed Proterozoic sequences in the southeast Curnamona Craton include the Thorndale Composite Gneiss, Cues Formation, Himalaya Formation, and the Purnamoota Subgroup. The first three components belong to the Thackaringa Group, which occurs in the lower stratigraphy of the Willyama Supergroup, whereas the Purnamoota Subgroup, is interpreted to be a lateral facies equivalent of the Broken Hill Group that hosts the Broken Hill Pb-Zn-Ag lode.

The most intensively explored ultramafic intrusions are Little Darling Creek, Mulga Springs, Red Hill, and Little Broken Hill Gabbro, with the latter being the largest intrusion, but with no known significant mineralisation. They extend along a ~35-km-long thin belt extending from Little Broken Hill Gabbro in the south to Moorkaie in the north (Impact Minerals Limited, 2013; Golden Cross Resources, 2014).

The larger ultramafic bodies are now mostly serpentinites or chlorite-amphibole rocks after peridotite and pyroxenite, respectively. Smaller and thinner dykes tend to be doleritic in texture, particularly those forming NW–SE and SSW–NNE dyke swarms. Numerous, variably orientated shear zones cut the metamorphics. These also post-date the mafic-ultramafic dykes, at least in terms of their latest movement. They are characterised by intense schistose deformation and retrograde mineral assemblages. Golden Cross Resources (2014) consider the shears to be the result of the superimposed Cambro-Ordovician Delamerian Orogeny (~520–480 Ma). This orogeny is believed to be related to accretion of various Phanerozoic sequences onto the eastern margin of the Curnamona Craton. Some of the ultramafic bodies are strongly magnetic and contain coarse magnetite. In others, the opaque mineral is magnetite-coated chromite. While there is excellent preservation of cumulus textures in some areas (particularly within central parts of pod-like masses), most are strongly schistose, or even composed of crenulated phyllite near contacts. Foliations are generally parallel to dyke margins. Talc and talc dolomite alteration occurs locally. Shallow pits are commonly developed on some coarse-grained magnesite pods and rare fibrous white asbestos veins.

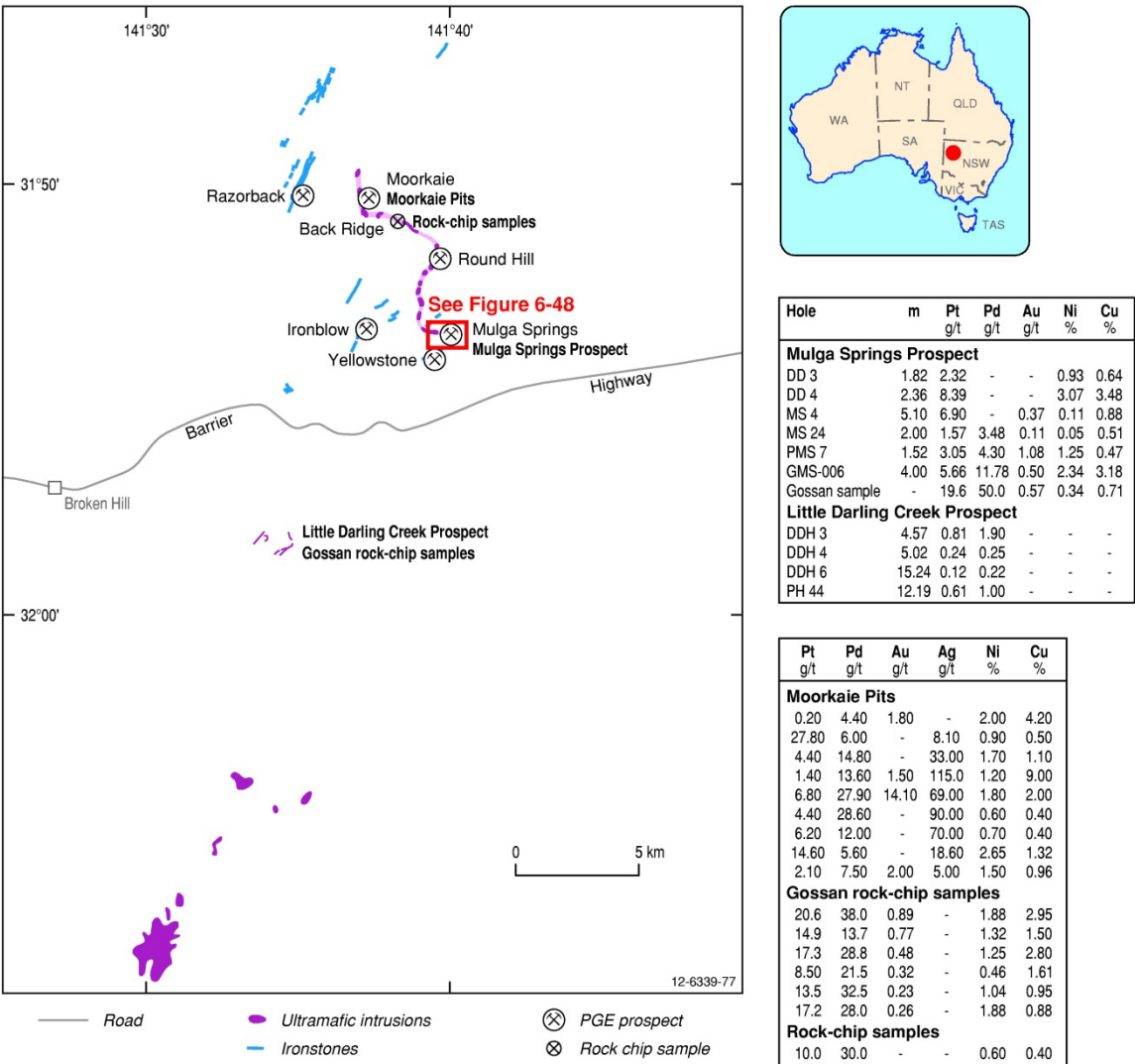


Figure 6.47 Regional distribution of Neoproterozoic ultramafic intrusions east of Broken Hill, Curnamona Craton, New South Wales. Mineralised gossan and ultramafic samples from the linear serpentinitised lensoidal bodies generally have high PGE abundances, erratic PGE ratios, and heterogeneous mineralisation trends along strike that are indicative of hydrothermal mineral systems. Modified from Golden Cross Resources (2014).

### Mineralisation environment

The host ultramafic bodies are altered and serpentinised harzburgite dykes and sills up to several hundred metres long and several tens of metres wide. The Mulga Springs line of intrusions (informally called by companies as the 'Mulga Springs Gabbro') consists of a series of shallow northeast-dipping ultramafic-mafic sills extensively developed over a 10 km strike extent from Mulga Springs in the south to Moorkaie in the north (Impact Minerals Limited, 2013). The type intrusion is the Mulga Springs Intrusion, which is an irregular shaped elongate body that extends over ~400 m east-east and ~100 m north-south. Displacements along inferred faults under cover partly account for the irregular shape of the body. The ultramafic unit extends along strike in a southeasterly direction under cover. Mineralisation at Mulga Springs is situated along the basal contact of an olivine-rich cumulate unit. Drilling has focused along an inferred north-trending fault that traverses the widest part of the serpentinised ultramafic sill (Figure 6.48). Erratic high-grade PGE intersections are associated with thin massive sulphides on the northern side of the sill (Figure 6.49).

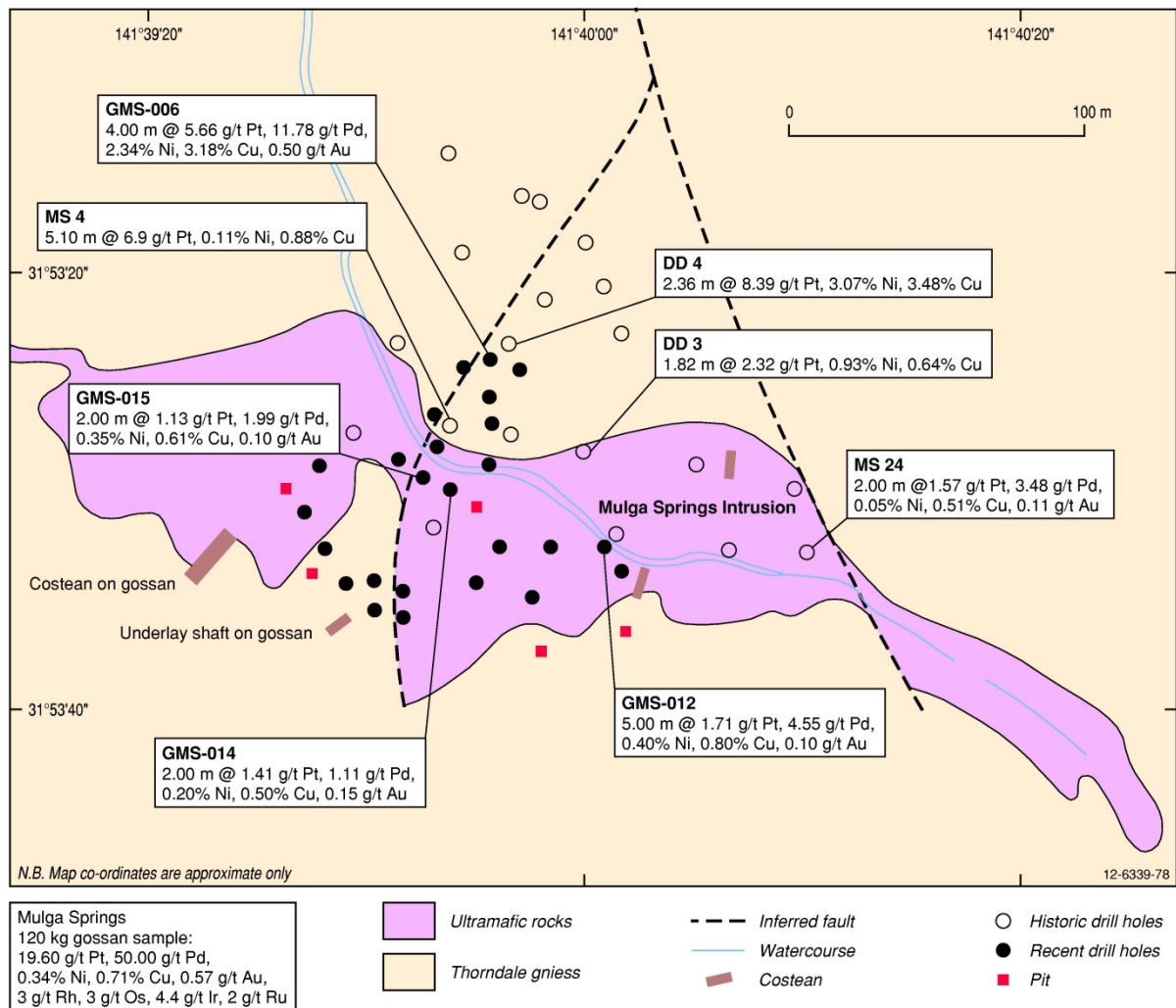


Figure 6.48 The Mulga Springs Intrusion has attracted considerable exploration interest with local high-grade PGE intersections. Modified from Golden Cross Resources (2014).

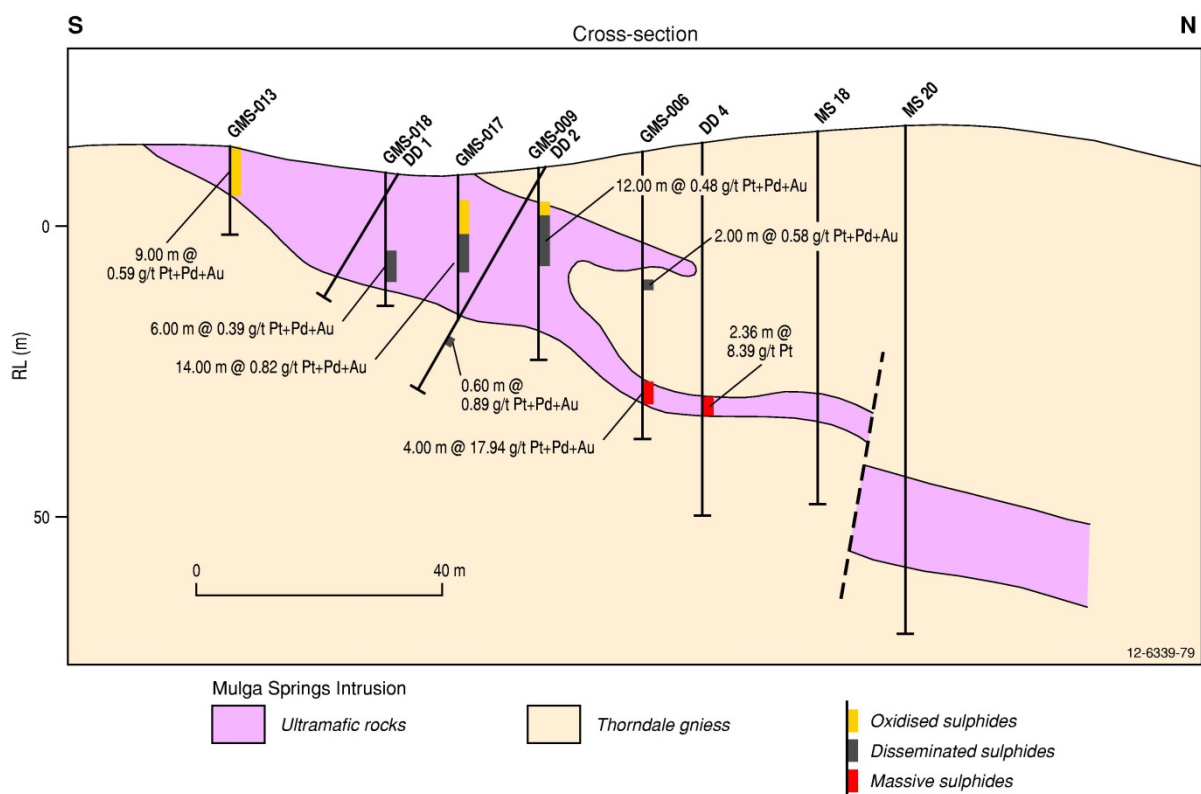


Figure 6.49 Schematic north-south cross-section of the Mulga Springs Intrusion. Section line 5692975E. Modified from Golden Cross Resources (2014).

### PGE mineralisation

Platinum-group-element mineralisation has been delineated in three major settings. Platinum, Pd, and Au concentrations are associated with chalcopyrite-pentlandite-pyrrhotite mineralisation near the basal contacts of the intrusions, in remobilised sulphides in the footwall gneissic rocks, and in surface gossans spatially above the sulphides. The PGEs reported (Impact Minerals Limited, 2013; Golden Cross Resources, 2014) in drill-hole intersections and surface gossans in the Mulga Springs region include: (DDHMS4: 2 m @ 18.0 g/t Pt, 24.6 g/t Pd); Red Hill mine (5 to 41 g/t PGEs, 2 to 4% Cu, 2 to 3% Ni, 22 to 70 g/t Ag); Back Ridge gossan (40 g/t PGEs); and Forners Prospect (9.4 g/t Pd, 1.2 g/t Pt, 37.5 g/t Ag, 0.3 g/t Au, 1.52% Cu, 0.66% Ni). The gossans are enriched in all PGEs and base metals, namely 19.6 g/t Pt, 50 g/t Pd, 3 g/t Rh, 4.4 g/t Ir, 3 g/t Os, 2 g/t Ru, 0.57 g/t Au, 0.34% Ni, and 0.71% Cu. Hoatson and Glaser (1989: p. 51) summarise the recorded PGE intersections prior to 1989 for the ultramafic intrusions of the Broken Hill district.

### Age of mineralisation

Neoproterozoic or younger? The ultramafic intrusions have previously been regarded as Cambrian in age, however, the ?coeval Little Broken Hill Gabbro Intrusion has a U-Pb zircon-baddeleyite crystallisation age of  $827 \pm 9$  Ma (Wingate et al., 1998).

### Genesis

The PGE-bearing ultramafic intrusions in the Mulga Springs region consist of serpentised plugs, dykes, and thin lensoidal bodies that appear to have intruded structural weaknesses, possibly initiated by the ~850 Ma Rodinia continental breakup of Australia (Blewett, 2012). One of the earliest

manifestations of the rifting events associated with this breakup was the northwest-trending ~825 Ma Gairdner LIP, which comprises extensive mafic dyke swarms, basaltic lavas, and mafic-ultramafic intrusives across much of South Australia and Western Australia (Zhao et al., 1994; Hoatson et al., 2008a,b; Claoué-Long and Hoatson, 2009a,b). The 827 ± 9 Ma Little Broken Hill Gabbro (Wingate et al., 1998), a small mafic body ~20 km south-southeast of Broken Hill, represents a coeval component of the ~825 Ma Gairdner LIP. The Little Broken Hill Gabbro is associated with faulting and is located in the same arcuate structural trend as the mineralised ultramafic intrusions, indicating a possible common genesis.

Anomalous concentrations of PGEs are also associated with Cu-Ni mineralisation in ultramafic intrusives at three occurrences near Magnetic Hill, southwest of Broken Hill (Hoatson and Glaser, 1989). The Magnetic Hill and Round Hill, Mulga Springs, Little Darling PGE prospects further east occur along a broad northeast-southwest trend coinciding with the Broken Hill base-metal sulphide lode direction, and possibly reflecting a structural control in the emplacement of the mineralised ultramafic intrusions.

The extremely high PGE abundances, erratic Pt to Pd ratios, and the heterogeneous distribution of remobilised sulphides along the basal contacts of the serpentinised intrusions in the Broken Hill district are features indicative of hydrothermal-mineralising systems. The lack of lateral continuity of PGE grades and widths of mineralisation makes delineation of ore resources difficult, and these types of deposits generally have low potential for large-tonnage deposits.

#### *Key references*

- Andrews (1922): regional setting, geological setting of prospects, vein deposits near margins of ultramafic hosts rocks; fluid activity.
- Stevens et al. (1975): regional geology; several ultramafic intrusions with elevated PGEs; basal setting of mineralisation; sulphides as disseminations and thin veins; associated Cu, Ni, Co, Au, Fe, and quartz; shallow pits and shafts.
- Hoatson and Glaser (1989): serpentinite body; PGE-enriched sulphides near basal contact and in footwall gneissic rocks; structural control; hydrothermal-remobilised mineralisation; heterogeneous PGE grades.
- Impact Minerals Ltd (2013): extensive mafic-ultramafic sills, dykes and stocks; gossans and fresh outcrops with very high-grade PGE's, Ni, Cu, Au and Ag mineralisation; highest-grade PGE-Ni-Cu-Au-Ag gossans in Australia; anomalous Pt, Pd, Os, Ir, and Ru; potential for bulk-tonnage PGEs; electromagnetic surveys anomalies at Red Hill mine.
- Golden Cross Resources (2014): historical exploration of Broken Hill region; exploration activities at Mulga Springs prospect; drill-hole profiles; PGE-Ni-Cu gossans; remobilised PGE mineralisation.

#### **6.4.8.5 Deposit Type 8.E: Disseminated sulphides in alkaline to subalkaline porphyry Cu-Au deposit**

##### *Overview*

Porphyry Cu±Au±Mo±PGE deposits are spatially and genetically associated with porphyritic intrusions of alkaline and calc-alkaline igneous rocks, emplaced at relatively high levels (<2 km) in the crust (Economou-Eliopoulos, 2005). The majority of the largest deposits (Grasberg, Mamut, Ok Tedi, Panguna) are located in the circum-Pacific region—a linear zone of volcanism at the boundary between the Pacific and adjacent Australia-India, Philippines, and Eurasia plates that define the 'ring

of fire'. Many giant Au-rich mineral systems are generated at convergent margins during or immediately following the subduction of lithosphere (Economou-Eliopoulos, 2005). Elevated concentrations of PGEs, particularly Pd and Pt, have been reported from several alkaline porphyry deposits in the Cordillera of British Columbia (Copper Mountain, Galore Creek), USA (Allard Stock, La Plana Mountains, Copper King Mine), Greece (Skouries), Bulgaria (Elatsite), and the Philippines (Santo Tomas II). Tarkian and Stribrny (1999) and Economou-Eliopoulos (2005) review the global distribution and evolution of the PGE-bearing porphyry mineral systems, critical factors for their formation, and key exploration criteria.

The most important and advanced deposits in Australia are associated with Late Ordovician mineral systems in the Lachlan Orogen of eastern Australia. The Copper Hill Igneous Complex in central New South Wales is an important member of a group of economically significant multi-phase dacite-tonalite intrusions that occur within a north-south trending sequence of Ordovician basaltic andesitic lavas. The Copper Hill and nearby Cadia and Goonumbra deposits represent some of the most important examples of porphyry-style polymetallic mineralisation in Australia. The ~450–445 Ma Copper Hill Igneous Complex is a composite porphyry body comprising an early quartz diorite in its southeastern third and several later phases of porphyritic dacite in the remainder. Copper-Au±PGE mineralisation is hosted in zones of quartz stockwork within porphyritic dacite. The stockworks occur in structural corridors in two structural orientations that trend east-southeast and north-northwest. A resource of 18.5 Mt @ 0.55% Cu, 0.55 g/t Au, and 0.02 g/t Pd was identified in a 200 m-long by 50 m-wide area of potassic alteration (K-feldspar and biotite) associated with early quartz-magnetite stockwork and sheeted veins. Palladium correlates with the best Au grades and is represented by the telluride-bearing mineral merenskyite. Quartz-magnetite-chlorite stockworks at the Open Cut prospect also contain high Au and Pd zones (e.g., 1 m @ 8.17 g/t Au and 0.91 g/t Pd). Copper generally has a broader occurrence throughout both quartz-sericite and chloritic-altered zones as chalcopyrite associated with disseminated pyrite. A good correlation between Au, Cu, and Pd occurs in stockwork zones (Torrey, 1990; Erceg, 1992).

The economic significance of PGEs, as by-products or potential by-products, in porphyry deposits throughout Australia has yet to be fully realised. Phanerozoic terranes in eastern Australia (in particular, New South Wales and Queensland) contain large, well-developed granitoid-associated porphyry deposits that have significant metal endowments and are well preserved. The main porphyry-epithermal province in Australia is the Siluro-Ordovician Macquarie Arc in New South Wales, which contains the porphyry Cu-Au deposits at Cadia (global resource of 1.31 Gt at 0.31% Cu and 0.74 g/t Au) and Northparkes (global resource of 153 Mt at 1.03% Cu and 0.46 g/t Au; Cooke et al., 2007). In contrast, Archean porphyry Cu-Mo-Au, Cu-Mo, and Cu-Au systems in the Yilgarn Craton of Western Australia are spatially and temporally associated with volumetrically small, pervasively altered, felsic plutons and dykes surrounded by altered and mineralised supracrustal country rock (Duuring et al., 2007). Relative to the eastern Australian examples, these deposits (except the Boddington 'porphyry' deposit in the Archean Saddleback greenstone belt) generally contain much smaller metal inventories and are poorly preserved because of protracted erosion. Various studies of porphyry Cu deposits from different geodynamic settings in the world (Tarkian and Stribrny, 1999; Sinclair, 2007) indicate these deposit types contain anomalous amounts of Pd and Pt, and therefore they potentially represent an important source of these precious metals. Some porphyry Cu-Au deposits contain significant amounts of PGEs; the Afton deposit in Canada, for example, has a measured and indicated resource of 68.7 Mt grading 1.1% Cu, 0.9 g/t Au, 2.6 g/t Ag, and 0.1 g/t Pd (Bradbrook, 2006). Tarkian and Stribrny's (1999) reconnaissance global study of the PGE contents of 33 porphyry Cu deposits from 17 countries showed that 7 deposits (six of island arc and one of

continental margin setting) have relatively high Pd contents (130 ppb–1999 ppb), which are associated with high Au contents (1 ppm–28 ppm). Palladium and Pt concentrations were above the analytical detection limit (>8 ppb) in 70% and 30%, respectively, of the deposits studied. The concentrations of Os, Ir, Ru, and Rh were below the detection limit for all samples. Discrete PGMs (merenskyite, sperrylite, unidentified Pd-Sb telluride) were identified in five of the deposits in accordance with their elevated Pd contents. Tarkian and Stribny (1999) concluded that Au-rich island arc porphyry Cu deposits appear to host more Pd and Pt than those deposits from continental margin settings. Other parameters, such as geological age, chemical composition, and magma type do not seem to influence PGE endowment. These criteria should be considered when exploring for porphyry Cu-Au±PGE mineral systems. One of the most fundamental problems in exploring porphyry deposits is to identify factors that can distinguish the relatively few fertile igneous complexes from the many that are not. Despite the close association of porphyry deposits with intermediate to felsic intrusive rocks and their formation involves the separation of metalliferous fluids from ore-related magmas, the processes that form porphyry deposits are diverse and significant knowledge gaps still remain (Sinclair, 2007).

#### *Australian deposits/prospects/host*

Copper Hill (Lachlan Orogen, NSW).

#### *Significant global example(s)*

Ingerbelle (Canada); Robinson, Allard Stock (USA); Aksug (Russia); Santo Tomas II (Philippines); Skouries (Greece); Elatsite (Bulgaria).

#### *Type example in Australia*

Copper Hill mine, New South Wales.

#### *Location*

Longitude 148.86793°E, Latitude -33.05219°S; 1:250 000 map sheet: Bathurst (SH 55–08), 1:100 000 map sheet: Molong (8631); ~5 km north of Molong, New South Wales.

#### *Geological province*

Lachlan Orogen, New South Wales.

#### *Resources*

Total Geological Resource of 215 Mt @ 0.3% Cu, 0.24 g/t Au; Constrained Resource of 155 Mt @ 0.33% Cu, 0.27 g/t Au, containing 493 000 t of Cu and 1.33 million ounces of Au (Golden Cross Resources, 2013). Minor concentrations of Pd are associated with Cu and Au. There are no Pd values in the resource figures.

#### *Current status and exploration history*

Undeveloped porphyry Cu-Au deposit with JORC-compliant resources. The earliest record of the Copper Hill mine is in a report by James Ranken of Bathurst that stated that mining operations commenced in 1845. Mining continued for the next six years, when 3300 t of supergene Cu ore averaging 1.4% was mined, with only sporadic production thereafter (Scott and Torrey, 2003). Gold was discovered in 1851 with 14 t produced from ore averaging 6.12 g/t. Geological Surveyor Stutchbury said Copper Hill was deserted in 1852 and the mine region consisted of decomposed clayslates followed by porphyries, with occasional altered slates (Goldencross, 2014b). In 1885,

Government Geologist C.S Wilkinson described it as a huge mass of felsites, with hornblende porphyry in places, traversed by numerous lodes or dykes of porous ferruginous quartz. The porphyry Cu potential of the deposit was first recognised in the late 1960s when Anaconda Australia Incorporated and Amax Exploration (Australia) Incorporated used soil geochemistry, induced polarisation, and diamond drilling to define a resource of 130 Mt @ 0.15% Cu. With the improvement of the Au price in the 1980s, the emphasis of exploration turned to Au. Homestake Gold of Australia Limited encountered one of the best intersections of 217 m @ 1.67 g/t Au and 0.72% Cu in Hole 58 (Scott and Torrey, 2003).

### *Economic significance*

The Copper Hill mine is the oldest mined Cu deposit in NSW (Scott and Torrey, 2003). The Copper Hill and the nearby Cadia and Goonumbla deposits represent the most important examples of Ordovician porphyry-type polymetallic mineralisation in the Lachlan Orogen, and indeed within Australia. The economic significance of potential PGE credits in similar deposits throughout eastern Australia is yet to be fully realised. Porphyry intrusions in Australia have considerable potential to host large-tonnage, low-grade Cu-Au deposits that have enhanced concentrations of PGEs.

### *Geological setting*

The Copper Hill mine is located near the northern end of the Molong Rise, which forms part of the Molong–South Coast Anticlinorium (Figure 6.50). Geological mapping identified several centres of intense sericite-chlorite-carbonate alteration within a major structural corridor hosting Cu-Au±PGE mineralisation. The Copper Hill Igneous Complex (CHIC) is an important member of a group of economically significant Late Ordovician multi-phase dacite-tonalite intrusions that occur within a north-south trending sequence of Ordovician basaltic andesitic lavas. Glen et al. (2003) classified the porphyries of the CHIC as Group 3, being emplaced at the beginning of the 3rd phase of regional arc volcanism at ~450–445 Ma. Intrusives of this age form common, but relatively small-volume mainly felsic intrusives in various volcanic belts. Mainly of dacitic composition, although sometimes extending to diorite to gabbroic compositions, this suite is expressed mineralogically by quartz and hornblende phenocrysts in rocks with >60% SiO<sub>2</sub>, and K-calc-alkaline chemical affinities. The porphyries contain significant amounts of mineralisation in the Molong Volcanic Belt (Copper Hill and Cargo deposits) and in the Narromine Igneous Complex in the Junee-Narromine Volcanic Belt.

A number of investigators (Chivas and Nutter, 1975; Scott, 1978; Poltock, 2001; Blevin, 2002; Scott and Terry, 2003) have long recognised that different types of alteration facies and styles of mineralisation are associated with the hydrothermal mineral system at Copper Hill. The initial investigators (Chivas and Nutter, 1975; Scott, 1978) delineated two major dacite phases in the complex with the earlier phase extensively hydrothermally altered and the later phase less altered. However, Poltock (2001) proposed multiple phases of intrusive dacite stopping out earlier phases to explain the distribution of mineralisation. Scott and Torrey (2003) describe the CHIC as a composite porphyry body comprising an early quartz diorite in its southeastern third and several later phases of porphyritic dacite in the remainder. The most widespread alteration type characterising the earlier dacite phase of Chivas and Nutter (1975) and Scott (1978) is pervasive quartz-sericite-chlorite, with variable amounts of pyrite and chalcopyrite as disseminations in the groundmass or in fractures. This variability in sulphide content and the irregular intensity of fracturing gives rise to variable Cu grades. Peripheral propylitic alteration comprising veinlets of epidote-pyrite and rare chalcopyrite pervades the margins of the host dacite and extends for at least 100 m into the surrounding andesitic volcanics. The less altered dacite phase displays epidote-magnetite-chlorite alteration with minor groundmass

silicification and poorly developed fracturing. Mineralisation styles include quartz-magnetite-chalcopyrite-stilbite and quartz carbonate±sphalerite±tetrahedrite±molybdenite in fracture zones, and rare quartz-molybdenite in veinlets. The final hydrothermal events are represented by calcite-sphalerite and calcite-galena-barite veins, which extend for several hundred metres peripheral to the Cu-bearing zone. Exposure of the CHIC during the Cenozoic has resulted in a supergene-enriched profile comprising a leached capping and a thin blanket of secondary Cu enrichment. Leached cappings over pyrite-rich areas contain clay minerals, gypsum, hematite, and several varieties of limonite. Supergene Cu-Au-rich layers, up to 5 m-thick above the primary mineralisation, are composed of chalcocite, digenite, native copper, malachite, and azurite. The ferruginous capping zones of the CHIC define the topographic highs of the Copper Hill and Wattle Hill deposits.

### *Mineralisation environment*

Mineralisation at the Copper Hill deposit covers an approximate area of 1 by 2 km within the central part of the intrusive complex (Scott and Torrey, 2003). Quartz-pyrite-chalcopyrite and quartz-magnetite-chalcopyrite stockworks and veins are associated with hydrothermally altered variants of intermediate to felsic igneous rocks that include diorite, quartz diorite, dacite, tonalite, and andesite. These rocks are commonly referred to in the literature as a 'dacite porphyry'. The pre-alteration mineralogy of mineralised dacite porphyries was dominated by plagioclase-quartz-hornblende assemblages that were replaced during multiple mineralisation-alteration events. Scott (1978) and Blevin (2002) provide detailed petrographic descriptions for the mineralised igneous rocks of the CHIC and surrounding Fairbridge Volcanics.

### *PGE mineralisation*

Copper-Au±PGE mineralisation is hosted in zones of quartz stockwork within the porphyritic dacite intrusives of the CHIC. Stockworks occur in structural corridors in two structural orientations and trend east-southeast and north-northwest. These form a conjugate fault set and are approximately bisected by the elongate axis of dacite intrusions. In the late 1980s, MIM Exploration Pty Ltd and Newcrest Mining Limited delineated Cu-Au-Pd mineralisation over an area 200 m-long, 50 m-wide, and up to 200 m-deep. Within this zone, 18.5 Mt @ 0.55% Cu, 0.55 g/t Au, and 0.02 g/t Pd was identified (Scott and Torrey, 2003). Potassic alteration (K-feldspar and biotite) occurs in the central part of the deposit, where it is associated with early quartz-magnetite stockwork and sheeted veins and Cu-Au-Pd mineralisation (Girvan, 1992; Trudu, 1994). The highest Au grades (Hole 58: 217 m @ 1.67 g/t Au, 0.72% Cu) define an area of about 300 m by 50 m. Palladium correlates with the best Au grades and is represented by the telluride-bearing mineral merenskyite. Similarly, geochemical sampling by Cyprus in 1989 intersected significant Au-Cu-Pd mineralisation in quartz-magnetite-chlorite stockworks at the Open Cut prospect. Oxidised surface rock chips returned maximum concentrations of ~5 g/t Au and 1 g/t Pd, whereas maximum values in unoxidised core samples over 1 m intervals were 8.17 g/t Au and 0.91 g/t Pd. These high Au and Pd zones have elevated Cu concentrations of up to 1.8%. Copper generally has a broader occurrence throughout both quartz-sericite and chloritic-altered zones as chalcopyrite associated with disseminated pyrite. A good correlation between Au, Cu, and Pd occurs in stockwork zones (Torrey, 1990; Erceg, 1992).

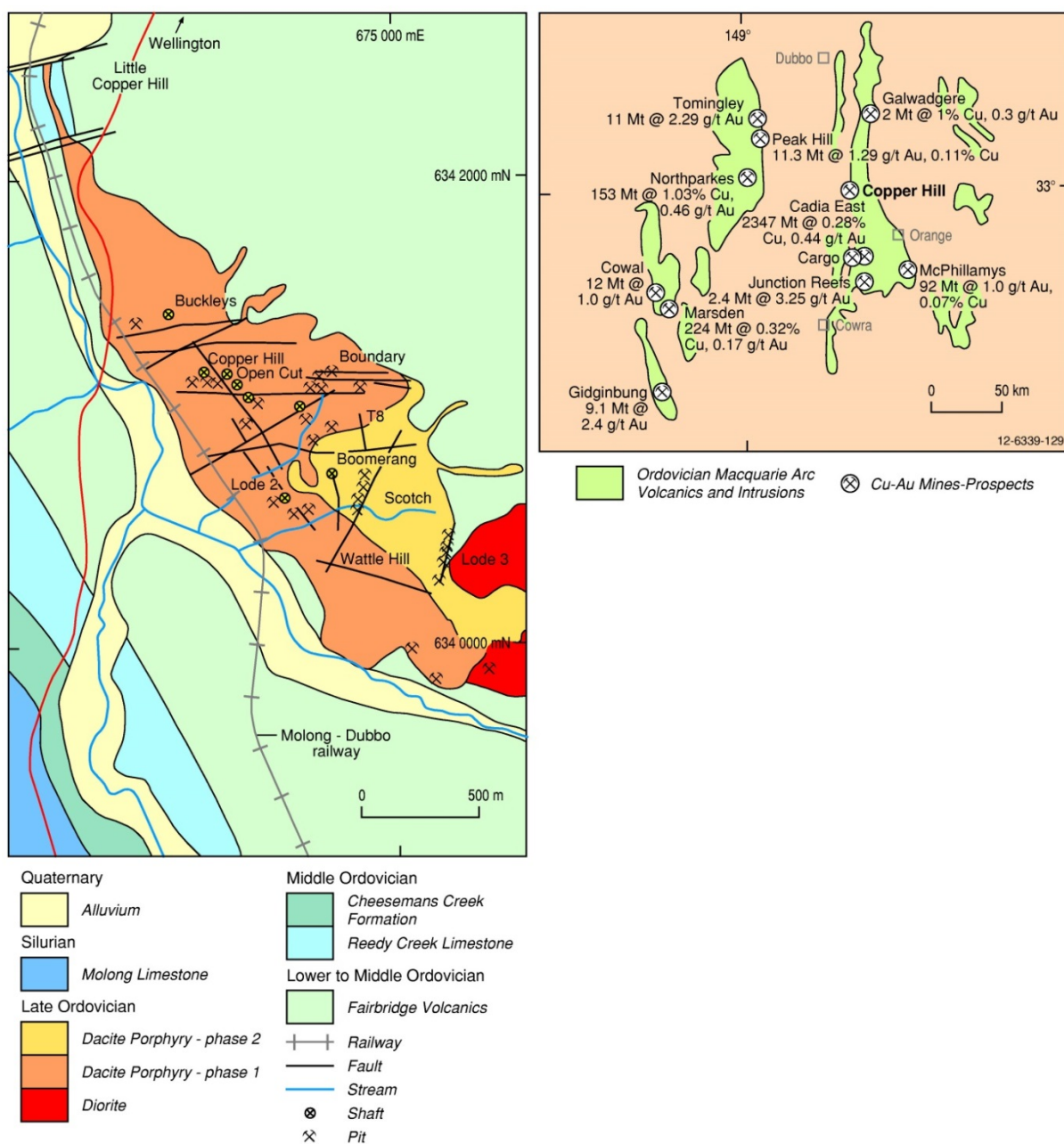


Figure 6.50 Geological setting of the Copper Hill porphyry Cu-Au deposit and surrounding deposits and prospects, Lachlan Orogen, central New South Wales. Small map (at right) shows copper and gold resources for porphyry-type deposits associated with the Ordovician Macquarie Arc volcanics and intrusions in the Dubbo-Cowra region. Modified from Scott and Torrey (2003).

### Age of mineralisation

The porphyry Cu-Au mineralising system associated with altered dacite porphyry and quartz dacite intrusions at Copper Hill is probably similar in age to the host intrusive rocks (Carr et al., 1995). Girvan (1992) indicates the CHIC was emplaced during the Late Ordovician at  $447 \pm 5$  Ma, which is consistent with the regional classification scheme ( $\sim 450$ – $445$  Ma for Group 3) of Glen et al. (2003). Blevin (2002) has summarised mineral ages from diorite and dacite units in the CHIC and contiguous Fairbridge Volcanics. Dating of magmatic hornblende from quartz diorite phases of the CHIC units and

the Fairbridge Volcanics yielded  $^{40}\text{Ar}$ – $^{39}\text{Ar}$  ages of  $449.1 \pm 1.5$  Ma and  $455.4 \pm 1.0$ , respectively (Perkins et al., 1995). K-Ar dating of amphibole by Chivas (1976) yielded  $447 \pm 5$  Ma for a quartz diorite unit and  $446 \pm 6$  Ma for a dacite porphyry (using new constants). Perkins et al. (1995) obtained a U-Pb age of  $450 \pm 6$  Ma on zircon from a dacite porphyry. These ages indicate that the CHIC and the Fairbridge Volcanics are broadly contemporaneous. However, Scott and Torrey (2003) state the CHIC intrudes intermediate to mafic volcanic and volcanoclastic rocks of the lower Ordovician Fairbridge Volcanics and, at Little Copper Hill, the middle Ordovician Reedy Creek Limestone.

### *Genesis*

Moderate to strong hydrothermal alteration accompanied the Late Ordovician dacites of the CHIC, giving rise to potassic, chloritic, sericitic, and propylitic alteration in both the intrusive and adjacent volcanic rocks (Scott and Torrey, 2003). Stratigraphic considerations and the present erosional level of the host porphyry imply a shallow emplacement for the CHIC between 1 km and 2 km from the Late Ordovician ground surface (Chivas and Nutter, 1975). Contact metamorphism up to 200 m into the intruded limestone and volcanic rocks and prehnite-pumpellyite regional metamorphism is evident in the volcanic rocks further from the intrusive contacts. Mineralisation takes the form of quartz-pyrite-chalcopyrite and quartz-magnetite-chalcopyrite stockworks and veins, and as sulphides in carbonate veins. There are apparently no consistent paragenetic relationships between different types of veins. Morrison (1998) proposed the highest mineralisation grades are located where late-stage structurally-controlled basement Au systems overprint an earlier strongly developed vein network. Morrison's structural studies showed that Au and Cu occur in structurally-controlled fractures and quartz veins with two to three dominant sets of fracture directions. Down-hole geochemistry indicates four different structural regimes, differing markedly between holes only 200 m apart. Poltock (2001) postulated multiple phases of intrusive dacite stoping out earlier phases could explain the spatial distribution of the Cu and Au mineralisation. Supergene mineralisation comprising leached limonite cappings and secondary Cu-enriched layers superimpose the primary mineralisation at the topographic high of Copper Hill.

Blevin's (2002) geochemical studies show that the variably K-enriched magmatic suites associated with the mineralised Ordovician porphyry intrusions (e.g., Copper Hill, Cadia, Goonumbla: Figure 6.50) in the Lachlan Orogen have trace-element geochemical patterns of enrichment and depletion typical of magmas from subduction-related tectonic settings. In particular, there are negative anomalies for Ti, Nb, and Ta, and strong enrichments in mantle incompatible elements such as Ba, Rb, Th, and K. Relative to the other Ordovician porphyry deposits in the Lachlan Orogen, the magmas that formed the CHIC were primitive, incompatible-element poor, medium K-enriched, and had high  $\epsilon_{\text{Nd}}$  and unradiogenic Pb isotope signatures. In contrast, the magmas that formed the other nearby, but larger Cadia and Goonumbla-Endeavour deposits, had high-K to shoshonitic character, were incompatible-element enriched, and had lower  $\epsilon_{\text{Nd}}$ , but more evolved Pb signatures (Blevin, 2002). The Ordovician magmas could have been sourced from a heterogeneous, variably-enriched lithospheric mantle, or they could represent mixing between enriched lithospheric mantle and more primitive asthenospheric mantle sources (see Carr et al., 1995). Alternatively, the source region of the magmas was progressively enriched over time. The mineralised Ordovician magmas of the Lachlan Orogen contrast markedly from those of the Silurian, Devonian, and Carboniferous, in that the former are typically more strongly oxidised, and are significantly less compositionally evolved (Blevin, 2002).

## Key references

- Scott (1978): regional geology; CHIC stratigraphy; mineralogy; country rocks; whole-rock chemistry; alteration-mineralisation zonation.
- Scott (1988): mineralogy of weathered profile; mineralogy, geochemistry, genesis.
- Girvan (1992): Copper Hill porphyry deposit; geology and mineralisation; stratigraphy; petrography; mineralisation; petrogenesis.
- Trudu (1994): Copper Hill porphyry deposit; geology and mineralisation; mineralogy, Cu, Au, and PGEs.
- Carr et al. (1995): regional setting of porphyry Cu-Au deposits; Lachlan Fold Belt; Pb/Pb isotope geochronology of Copper Hill deposit; fingerprinting hydrothermal and metallogenic events; mantle-crust mixing processes; petrogenesis; exploration implications.
- Perkins et al. (1995): Ar-Ar, K-Ar, and U-Pb geochronology of Copper Hill deposit; metallogenic episodes; Tasman Fold Belt; geochemistry and tectonic setting.
- White et al. (2001): geophysical-geochemical surveys, induced polarization study; structural trends; 3D mineralisation inversion model.
- Blevin (2002): regional geology of Ordovician porphyry Cu-Au deposits; Copper Hill deposit; Lachlan Fold Belt; alteration-mineralisation zonation; petrography and major-trace-element geochemistry; classification of intrusions; shoshonite magmatism; tectonic settings; petrogenesis.
- Glen et al. (2003): regional setting of Ordovician porphyry Cu-Au deposits; Copper Hill Suite; Lachlan Fold Belt; petrography, geochemistry; geochronology; late-Ordovician calc-alkaline, multi-phase dacite-tonalite intrusions.
- Scott and Torrey (2003): discovery history; geological setting; regolith expression; porphyry mineralisation; supergene mineralisation.
- Smith (2007): porphyry Cu-Au-PGE deposits overseas; hydrothermal Au-PGE deposits; carbonaceous shale-hosted PGE mineralisation; unconformity-related PGE-Au deposits.
- Golden Cross Resources (2011): exploration results; porphyry-style Cu-Au deposit; Ordovician Macquarie Arc; resources.

### 6.4.8.6 Deposit Type 8.F: Unconformity-type U-Au-PGEs

#### Overview

Unconformity-type U-Au-PGE deposits in the Proterozoic Pine Creek Orogen of the Northern Territory occur at, or just below, the unconformity between the gently folded Coronation Sandstone and the underlying highly folded Proterozoic succession that includes the Koolpin Formation (carbonaceous shale and ferruginous siltstone) and Zamu Dolerite. The underlying succession hosts the deposits and prospects in the South Alligator Valley Uranium Field. The deposits in Australia typically exhibit a wide range of ore tonnages and grades (generally between 0.1% and 1.8%  $U_3O_8$ ; Lambert et al., 2005).

Unconformity-related U deposits are also prominent in the Athabasca Basin in Saskatchewan, Canada (e.g., some of these having the highest grades of U—up to 26%  $U_3O_8$ —in the world, namely Cigar Lake, Rabbit Lake, McArthur River: Lambert et al., 2005; Jefferson et al., 2007; Richard et al., 2012; Reid et al., 2014) and in Zaire, however, very few of these deposits are known to contain PGEs.

The Coronation Hill U-Au-PGE deposit in the South Alligator Valley Uranium Field of the Pine Creek Orogen is often regarded as the type global example of this unusual PGE mineral system. Coronation

Hill is unusual in that the PGE mineralisation shows no obvious spatial association with, or derivation from, mafic-ultramafic rocks. Mineralisation occurs in microfractures and veinlets in felsic porphyry, volcanoclastic siltstone, debris flow conglomerate, and diorite. The dominant styles of alteration associated with the fine-grained disseminated Au-PGE mineralisation (invisible to the naked eye) are sericitisation and silicification, with minor hematite, chlorite, and pyrite. There is a positive correlation between Au and the dominant PGEs, Pt, and Pd, with the latter metals contributing up to 20% of the precious-metal gross value of the deposit.

Recent exploration in the Pine Creek Orogen has defined a number of PGE-bearing U-Au prospects that have similar mineral-system features to Coronation Hill. These include Airstrip, Devils Elbow, Flying Ghost, Gold Ridge, Goldeneye, Hardtop, Sargent, Sargent North, and Stevens, in addition to the established deposits at El Sherana, El Sherana West, Palette, Ranger 3, and Rockhole (see Appendix K). Mineralisation at Gold Ridge occurs within a shear zone traversing granite, and the main host at Sargent North is a hematite-quartz breccia. The Kintyre U deposit (Jackson and Andrew, 1988, 1990; Cameco Australia, 2014) in the Proterozoic Paterson Province of Western Australia also has similar stratigraphic and mineralisation features to the unconformity-related U deposits in the Pine Creek Orogen.

#### *Australian deposits/prospects/hosts*

Airstrip, Coronation Hill, Devils Elbow, El Sherana, Flying Ghost, Gold Ridge, Goldeneye, Hardtop, Palette, Ranger 3, Rockhole, Sargent, Sargent North, Stevens (all Pine Creek Orogen, NT); ?Kintyre U prospect (Paterson Province, WA).

#### *Significant global example(s)*

Beaverlodge–Nicholson Bay, Rabbit Lake, Maurice Bay, Cigar Lake (Canada); Musonoi, Shinkolobwe (Zaire); Serra Pelada (Brazil).

#### *Type example in Australia*

Coronation Hill, Northern Territory.

#### *Location*

Longitude 132.606742°E, Latitude -13.586228°S; 1:250 000 map sheet: Mount Evelyn (SD 53–05), 1:100 000 map sheet: Stow (5470); ~230 km southeast of Darwin.

#### *Geological province*

Pine Creek Orogen, Northern Territory.

#### *Resources*

Indicated Resource of 3.49 Mt @ 5.12 g/t Au, 0.21 g/t Pt, 0.56 g/t Pd; Inferred Resource of 2.87 Mt @ 7.25 g/t Au, 0.35 g/t Pt, 1.31 g/t Pd (Mernagh et al., 1994). In 1986, the Coronation Hill Joint Venture (CHJV), which comprised BHP Gold Mines Ltd, Pioneer Mineral (Gold) Pty Ltd, and Norgold Limited, announced that Coronation Hill had inferred resources of more than 34 t of Au, and about 2.5 t of Pt, and 5.3 t of Pd. The mineralisation is open to the south, east, and persists to at least 300 m vertical depth.

### *Current status and exploration history*

Undeveloped U-Au-PGE deposit. The discovery of the Coronation Hill deposit by a BMR geologist in 1953 coincided at the time with the coronation of Queen Elizabeth II. The discovery focussed large-scale exploration programs in the South Alligator River region. Intensive prospecting by private companies located another 13 small U deposits and some 15 prospects, most of which occur in a northwest-trending structural belt 24 km-long and 3 km-wide (Figure 6.51). Between 1956 and 1964 some 874 t of  $U_3O_8$  was mined from these deposits. Uranium-gold ore from Coronation Hill was mined in 1961 and 1962 with a small open cut, and glory hole methods. The average grade of ore mined was an estimated 0.26%  $U_3O_8$  and 10.4 g/t Au. The CHJV carried out an exploration program for Au in the South Alligator Valley from 1984 to 1989. Exploration and drilling by the CHJV defined the Au-Pt-Pd orebody at Coronation Hill in 1984 (McKay and Mieзитis, 2001). The mineralisation lies beneath, and to the east of, the old Coronation Hill U open-cut mine. A number of other similar  $U \pm Pt \pm Pd \pm Au$  prospects were subsequently discovered in the South Alligator Valley Uranium Field by the CHJV and the BMR.

### *Economic significance*

In Australia, unconformity-related  $U \pm Au$  deposits and occurrences are located in the Northern Territory, Western Australia and South Australia (Maas, 1989; McKay and Mieзитis, 2001; Lambert et al., 2005; Ahmad and Munson, 2013; AIMR, 2013). The Pine Creek Orogen in Northern Territory contains the world-class unconformity-related U deposits in the Alligator Rivers field, as well as the Rum Jungle and South Alligator Valley fields (Ahmad and Munson, 2013). Other unconformity-related U deposits are present in the Rudall Complex (WA) and in the Turee Creek area (WA). Minor unconformity-related U occurrences are present in the Granites–Tanami Inlier (WA and NT), Halls Creek area (WA), Tennant Creek area (NT), and Eyre Peninsula (SA). Coronation Hill is generally regarded as the type example in Australia of an unconformity-related U-Au deposit that contains significant concentrations of PGEs (Mernagh et al., 1988). Such deposits (e.g., Coronation Hill–Pine Creek Orogen, NT; Kintyre–Paterson Province, WA) are generally associated with volcanic-sedimentary rock sequences in Proterozoic orogenic provinces. The Coronation Hill Au-PGE deposit has added significance in that the PGEs show no clear association with, or derivation from, mafic-ultramafic rocks.

### *Geological setting*

The Coronation Hill U-Au-PGE deposit is located on a prominent northwest-trending mineralised corridor that defines the South Alligator Valley Uranium Field in the Pine Creek Orogen (Figure 6.51). All the major U-Au-Pt-Pd prospects in this field lie within, or near, the Rockhole-Palette Fault System, and close to major regional unconformities between Proterozoic volcanic-sedimentary rock sequences. The geological setting consists of folded and faulted Paleoproterozoic metasedimentary rocks that overlie an Archean basement of metasedimentary and felsic meta-igneous rocks. The Paleoproterozoic assemblage consists of basal carbonaceous shale, siltstone and carbonate overlain by chloritised volcanoclastics, and carbonaceous shale; these units are intruded by quartz feldspar porphyry and quartz diorite and all these rock types are unconformably overlain by a regionally extensive, shallow-dipping sequence of hematitic quartz sandstone and minor interbedded volcanics belonging to the Kombolgje Subgroup. The Coronation Hill deposit occupies a zone of complex faulting in a large-scale dilational off-set on the Palette Fault System (Valenta, 1990). The U ore in the old open cut occurs in debris flow breccia and altered rhyolites of the Coronation Sandstone (Needham and Stuart-Smith, 1987). Uranium mineralisation is associated with faulted blocks of carbonaceous shale (Koolpin Formation) within the conglomerate and also with areas where the conglomerate contains abundant clasts of carbonaceous shale (Needham, 1987). The ore zone forms

a vertical cylindrical body about 20 m across and consists of pitchblende mineralisation with narrow veinlets and dissemination of Au. Carville and others (1991) noted that the debris flow breccia (referred to as type 'A' and type 'B' breccias) is in fault contact with the adjoining lithologies and is younger than the sandstones of the Kombolgie Subgroup.

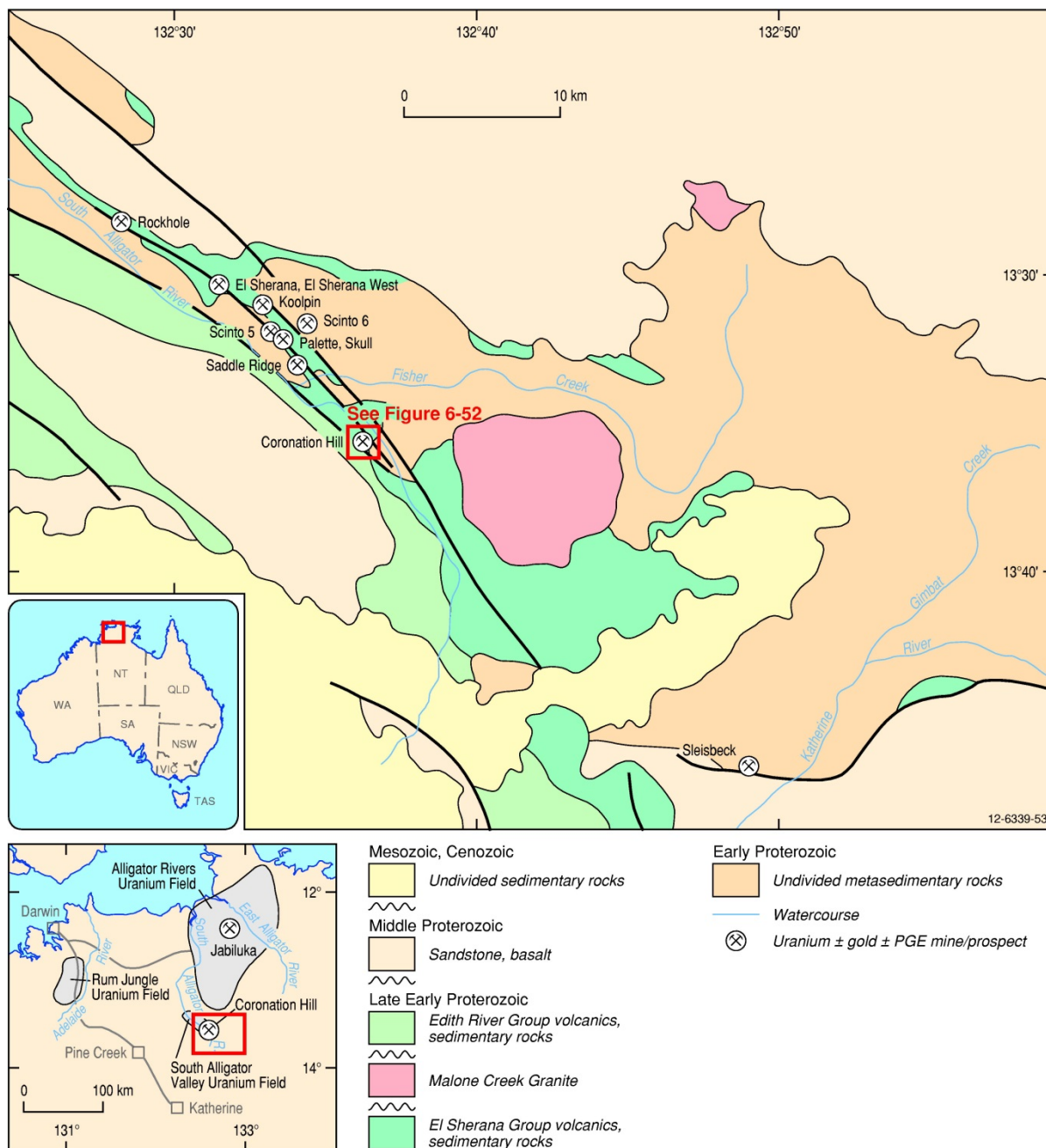


Figure 6.51 Geological setting of the Coronation Hill U-Au-PGE deposit and associated unconformity-related deposits in the South Alligator River Valley Uranium Field, Pine Creek Orogen, Northern Territory. Modified from Needham and Stuart-Smith (1987).

### *Mineralisation environment*

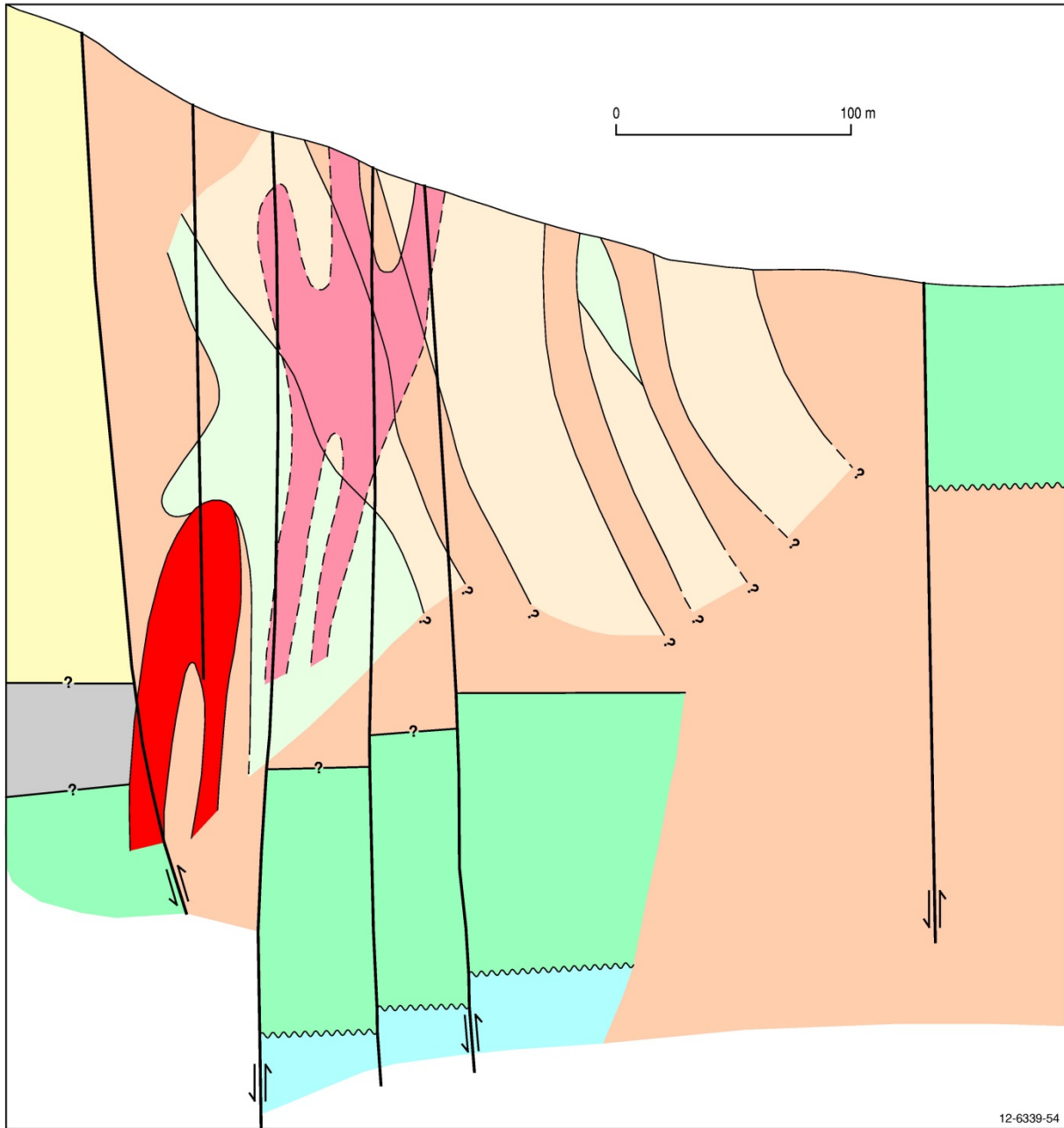
The geology and structural setting of the Au-Pt-Pd mineralisation at Coronation Hill have been described by Carville et al. (1990), Wyborn et al. (1990, 1994b), Wyborn (1992), and Mernagh et al. (1998). The Au-Pt-Pd orebody occurs in a variety of lithologies and is structurally controlled located close to the unconformity between the Coronation Sandstone and older pre-1870 Ma basement sequences and two pre-mineralisation fault systems (Figure 6.52). East-trending reverse faults have vertical movements and dip 70° to the south, whereas west-northwest-trending vertical faults postdate the reverse faults, and have an east-block-up sense of movement. The Au-Pt-Pd mineralisation is adjacent to, but separate from, the U-rich zones. The mineralisation occurs in narrow quartz–carbonate–chlorite veins forming a series of sub-vertical bodies that cut across lithological boundaries. The mineralised zone contains altered felsic volcanics, tuff, sandstone, and felsic porphyry of the Coronation Sandstone, carbonaceous shale of the Koolpin Formation, and altered mafic rocks possibly belonging to the Zamu Dolerite. The mineralised zone has a pipe-like geometry, with a strike length of about 250 m, and is 50- to 100-m-wide (Figure 6.52). Drill-holes have intersected mineralisation at depths in excess of 600 m. Detailed drilling has outlined a mineralised resource, some 240 m in length, up to 80-m-wide and to a depth of 250 m. Mineralisation comprises several narrow (10 m width) tabular bodies that are sub-parallel to north-northwest-trending faults. Mineralisation occurs along microfractures, as quartz-carbonate-haematite microveinlets and as disseminations within the alteration matrix of the host rocks.

McKay and Mieztis (2001) describe two general types of mineralisation that form separate ore zones at Coronation Hill: (1) Au-Pt-Pd; and (2) high-grade U-Au (minor Pt and Pd) approximately 120 m below the old open cut. The ore zone is located in an area of complex faulting and occurs within brecciated chloritic tuffaceous siltstone and carbonaceous siltstones and brecciated quartz feldspar porphyry. The high-grade U-Au mineralisation is best developed where a major fault intersects the unconformity at the base of the Capping Sandstone (Kombolgie sandstone equivalent). *In situ* indicated resources were estimated to be 344 170 t averaging 0.537% U<sub>3</sub>O<sub>8</sub> (1850 t U<sub>3</sub>O<sub>8</sub>) and 9.95 g/t Au. The ore zone is open (untested) to the north and at depth (McKay, 1990). Significant amounts of Pt and Pd are also associated with U±Au mineralisation at a number of other deposits and prospects in the South Alligator Valley Uranium Field (Hoatson and Glaser, 1989).

The precise nature of the spatial association of the most economically important metals (Au, U, PGEs) for other U-dominant deposits in the Pine Creek Orogen has not been established, but in many cases the Au is separate from the U mineralisation (Hoatson and Glaser, 1989). At Palette, one sample yielded 0.3 ppm Pt, 0.64 ppm Pd, and 0.015 ppm Au, with other grab samples returned Au contents of 20.85 ppm, and 61.0 ppm. Of 250 reconnaissance rock chip samples from El Sherana and El Sherana West, 10 samples exceeded 1.0 ppm Au. Composite chip sampling (2 m intervals) from the walls of the El Sherana West open pit returned average grades of 0.38 ppm Pt, 0.66 ppm Pd, and 6.37 ppm Au. At El Sherana and Palette, the felsic volcanics of the El Sherana Group, as seen at Coronation Hill, are absent from the mineralised U-Au fracture zones worked by early miners. Samples from adit dumps and tailings at Rockhole have returned Au levels up to 16 ppm. The prospects in the South Alligator Valley Uranium Field are surrounded by sericite-chlorite-hematite alteration haloes that may extend over 1 km (Wyborn et al., 1990). The proximity, and similar geological settings and metallic associations, suggest these prospects may be similar to Coronation Hill and potentially may host substantial amounts of precious metals. The South Alligator Valley Uranium Field clearly represents a Au-U-PGE province of considerable potential.

Table 6.13 summarises significant PGE-bearing intersections at Coronation Hill.

Cross-section



12-6339-54

- |  |   |  |
|--|---|--|
| <p><b>Komblongie Subgroup</b></p> <ul style="list-style-type: none"> <li><span style="display: inline-block; width: 15px; height: 15px; background-color: yellow; border: 1px solid black; margin-right: 5px;"></span> 'Capping Sandstone'<br/>Sandstone, conglomerate</li> <li><span style="display: inline-block; width: 15px; height: 15px; background-color: grey; border: 1px solid black; margin-right: 5px;"></span> Complex zone: Brecciated quartz-feldspar<br/>porphyry, chloritic tuffaceous siltstone</li> </ul> <p><b>El Sherana Group</b></p> <ul style="list-style-type: none"> <li><span style="display: inline-block; width: 15px; height: 15px; background-color: lightgreen; border: 1px solid black; margin-right: 5px;"></span> Sedimentary breccia</li> </ul> <p><b>Zamu Dolerite</b></p> <ul style="list-style-type: none"> <li><span style="display: inline-block; width: 15px; height: 15px; background-color: lightgreen; border: 1px solid black; margin-right: 5px;"></span> Quartz diorite, dolerite</li> </ul> | <p><b>Gerowie Tuff equivalent</b></p> <ul style="list-style-type: none"> <li><span style="display: inline-block; width: 15px; height: 15px; background-color: orange; border: 1px solid black; margin-right: 5px;"></span> Quartz-feldspar porphyry</li> </ul> <p><b>Shovel Billabong Andesite</b></p> <ul style="list-style-type: none"> <li><span style="display: inline-block; width: 15px; height: 15px; background-color: lightorange; border: 1px solid black; margin-right: 5px;"></span> Chloritic tuffaceous siltstone</li> </ul> <p><b>Koolpin Formation</b></p> <ul style="list-style-type: none"> <li><span style="display: inline-block; width: 15px; height: 15px; background-color: cyan; border: 1px solid black; margin-right: 5px;"></span> Dolomite, siliceous dolomite</li> </ul> | <ul style="list-style-type: none"> <li><span style="display: inline-block; width: 15px; height: 15px; background-color: pink; border: 1px dashed black; margin-right: 5px;"></span> Au-Pt-Pd mineralisation-<br/>boundaries are diagrammatic</li> <li><span style="display: inline-block; width: 15px; height: 15px; background-color: red; border: 1px solid black; margin-right: 5px;"></span> U-Au-Pt-Pd mineralisation</li> <li><span style="display: inline-block; width: 15px; border-bottom: 1px solid black; margin-right: 5px;"></span> Fault zone</li> <li><span style="display: inline-block; width: 15px; border-bottom: 1px wavy black; margin-right: 5px;"></span> Unconformity</li> </ul> |
|--|---|--|

Figure 6.52 Schematic cross-section of the Coronation Hill U-Au-PGE deposit. Modified from Carville et al. (1991).

Table 6.13 Significant drill-hole intersections at Coronation Hill.

Drill-hole	Interval (m)	Pt (ppm)	Pd (ppm)	Au (ppm)	Pt/Pd
CHDDH 6	12.0–26.0	2.07	4.22	13.78	0.49
CHDDH 8	48.0–54.0	0.78	1.52	14.52	0.51
CHDDH 8	98.0–100.0	3.54	6.33	3.63	0.56
CHDDH 10	96.0–100.0	2.41	4.77	12.57	0.51
CHDDH 11	30.0–34.0	1.35	3.56	14.25	0.38
CHDDH 17	90.0–94.0	1.46	4.65	13.20	0.32
CHDDH 18	142.0–160.0	0.81	2.66	14.01	0.30
CHDDH 23	18.0–34.0	1.02	3.46	13.69	0.30
CHDDH 29	70.0–80.0	0.79	2.48	7.54	0.32
CHDDH 53	352.0–364.0	0.17	0.47	3.91	0.36
CHDDH 94	188.0–204.0	0.32	1.52	11.95	0.21
CHDDH 103	298.0–314.0	0.84	2.49	14.78	0.34

Source: Number of sources listed in Hoatson and Glaser (1989).

### PGE mineralisation

There is a positive correlation between microscopic (3.5  $\mu\text{m}$ –332  $\mu\text{m}$ ) Au and the dominant PGEs, Pt and Pd, with the latter metals contributing 10% to 20% of the precious-metal gross value of the deposit. Sulphides are generally rare and include pyrite and trace amounts of marcasite, pyrrhotite, sphalerite, chalcopyrite, and galena. The average grade of 163 samples with more than 1 ppm Au is 0.61 ppm Pt, 1.15 ppm Pd, and 7.72 ppm Au. The Pt/Pd ratios for high Au samples range from 0.30 to 0.88, with nearly 50% of the samples falling in the range 0.5 to 0.65. Metallurgical studies from a mineralised surface sample identified native platinum (Pt), native palladium (Pd), stibiopalladinite ( $\text{Pd}_5\text{Sb}_2$ ), and possible porpezite (a variety of Au which contains up to 10% Pd) in gravity concentrates. Smith (2007) documented the following minerals in fine-grained disseminated Au-PGE mineralisation (invisible to the naked eye): stibiopalladinite, sudburyite (PdSb), native palladium, Pt-Pd selenide ( $(\text{Pt},\text{Pd})\text{Se}_2$ ), Pt-Pd-Fe alloy, very fine electrum, uraninite, pitchblende, and minor pyrite. Other selenide minerals, including clausenthalite (PbSe, PdSbSe), palladseite ( $\text{Pd}_{17}\text{Se}_{15}$ ), tiemannite (HgSe), and Ni-Co and Bi-Pd selenides are also present (Gilbert 1986, 1987; Mernagh et al., 1994). The Au and Pt-group mineral phases show a distinct selenide association. Another association is also present where gold/clausenthalite/stibiopalladinite is associated with pyrite in some of the altered igneous rocks. The ore minerals appear to have no lithological control, occurring in quartz-dolomite-calcite-hematite veinlets and breccias and as disseminations in all of the rock types which lie below the Kombolgie unconformity. Mineralisation was accompanied by hematite alteration of variable intensity that affected all rock types, including the hematitic quartz sandstone above the unconformity. Highly oxidised fluids are indicated by complete oxidation of chlorite to hematite. Drill intersections at Coronation Hill represent some of the best Au intervals reported in the Pine Creek Orogen, e.g., DDH 6: 78.4 m @ 12.3 ppm Au (Table 6.13).

### Age of mineralisation

Like many other U deposits, the geochronology of the Coronation Hill deposit appears to be complex, with multiple apparent ages of mineralisation. As described by Orth et al. (2014), the maximum

depositional age of the sandstone interbedded with ore-bearing volcanic rocks is  $1867 \pm 16$  Ma (LA-ICPMS age of detrital zircons). This age should be considered the maximum age possible for mineralisation. Orth et al. (2014) also reported an upper intercept discordia age for uraninite of  $1607 \pm 26$  Ma (also LA-ICPMS analysis), which they interpreted as the age of primary mineralisation. However, they also interpreted crystallisation or re-crystallisation ages between 1400 Ma and 800 Ma. Given this complexity the  $\sim 1607$  Ma age should be interpreted as a minimum age for mineralisation. This minimum age is consistent with many of the ages (McKay and Miezitis, 2001) obtained by other workers on the South Alligator Valley and East Alligator River deposits. For example, Maas (1989) has documented Sm-Nd ages for mineralisation at Jabiluka 2, Nabarlek, and Koongarra deposits as ranging from 1600 Ma to 1650 Ma. Ludwig et al. (1987) provide a U-Pb isotope age of  $1737 \pm 20$  Ma for mineralisation at Ranger.

### *Genesis*

Dahlkamp (1993), Ruzicka (1995), and Mernagh et al. (1998) have summarised various mineral-system components (e.g., source, transport, formation) of unconformity-related U±Au±PGE deposits in Australia and in the Athabasca Basin, Canada. The following synthesis of these contributions and by others is from McKay and Miezitis (2001). The following meteoric and diagenetic models are proposed for ore formation occurring after the deposition of the cover sandstones:

1. **The 'meteoric model'** (Johnston and Wall, 1984; Wilde et al., 1989; Jaireth, 1992; Mernagh et al., 1994; Solomon and Groves, 1994; Komninou and Sverjensky, 1996) proposes that highly oxidised acidic and Ca-rich meteoric brines (groundwater or sea water, based on isotopic data) transported Pt, Pd, Au, and U in chloride complexes (Figure 6.53). Fluid inclusion data indicates that the fluids transported metal-chloride complexes at  $160^\circ\text{C}$  to  $225^\circ\text{C}$ . As the fluids migrated through the quartz sandstone aquifer in a neutral cover sequence above the Kombolgie unconformity, they maintained a high oxidation state by progressively oxidising  $\text{Fe}^{2+}$  minerals in the sandstone (magnetite, silicates). This pushed a redox interface deeper into the aquifer and successively leached and redeposited Pt, Pd, Au, and U as it flowed down faults and dilational structures. Upon reaching strong redox barriers in feldspar-, magnetite-, and graphite-bearing sedimentary rocks, or fluids containing methane or hydrocarbons beneath the unconformity, the chloride complexes became unstable, experienced chemical reduction, and precipitated ore minerals at  $150^\circ\text{C}$  to  $170^\circ\text{C}$  in open-space fractures in host rocks (Jaireth, 1992). Fluid interaction with feldspathic or calcareous rocks at Coronation Hill caused only a moderate increase in pH and a decrease in the oxidation state ( $f\text{O}_2$ ), leading to precipitation of Au and PGEs, but little or no precipitation of U (Figure 6.53). Mernagh et al. (1994) emphasised that the ore-forming process at Coronation Hill were genetically different from epithermal deposits that have resulted from ascending, deeper level, more reduced hydrothermal fluids.

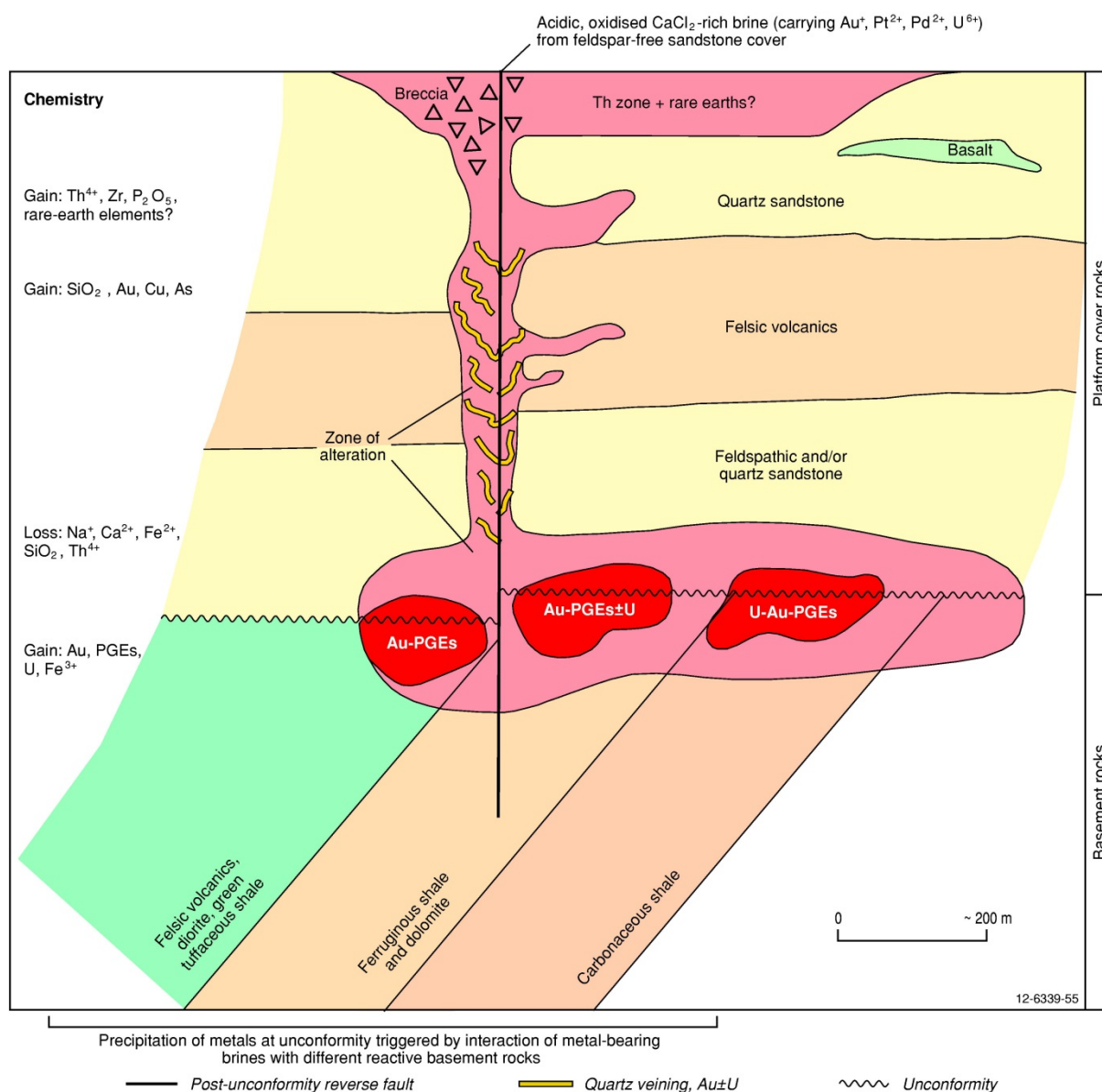


Figure 6.53 Conceptual section of the Coronation Hill U-Au-PGE deposit. Distinctive precious metal-uranium assemblages along the unconformity reflect the chemical interaction of descending acidic and oxidised metal-bearing fluids/brines with basement rocks of different composition. Redox fronts are important in this mineral system with the interaction and reduction of the ore-forming fluids at depth by graphite and/or ferrous iron-bearing biotite being a possible mechanism for ore precipitation. Modified from Wyborn et al. (1994b).

2. **The 'diagenetic model'** (Hoeve et al., 1980; Sibbald and Quirt, 1987; Ruzicka, 1993) largely evolved from the unconformity-related U deposits in the Athabasca Basin of Canada and has been applied to the Pine Creek Orogen of the Northern Territory. Hancock et al. (1990) considered that a similar diagenetic model may be applicable to Jabiluka (see next Deposit Type 8.G). According to these authors, oxidised ore-bearing fluids formed within the sedimentary cover during high-temperature prograde diagenesis. Some of the fluids entered the basement and were reduced before ascending again along faults and fractures, where they mixed with laterally moving oxidised fluids. Precipitation of U and other metals took place at the interface between the oxidising and reducing fluids (i.e., at the redox front). High-grade U or polymetallic mineralisation formed directly at, or slightly above, the unconformity (e.g.,

Cigar Lake and McArthur River (Canada)). Medium-grade U mineralisation may have formed below the unconformity (e.g., Rabbit Lake (Canada); Jabiluka) and low-grade U mineralisation may have formed some distance above the unconformity (e.g., Maurice Bay (Canada)). The Cigar Lake-style high-grade unconformity-related deposits at the unconformity have not been found in the Pine Creek Orogen to date although such deposits could be completely concealed by the cover sandstones. Two models have also been proposed for ore formation prior to the deposition of cover sandstones. Mapping and geochronology data suggest that the cover sandstones of the overlying Kombolgie Subgroup are older than 1720 Ma and may be 1750 Ma, or older (Sweet et al., 1999). These cover sandstones are older than the Jabiluka, Koongarra, and Nabarlek deposits and may also predate the Ranger deposit ( $1737 \pm 20$  Ma). It is still possible that the Ranger deposit is older, in which case it may be possible that at least part of the U mineralisation commenced shortly before the deposition of the overlying sandstones and continued as the sandstones were being deposited. The following supergene (#3) and hypogene (#4) models describe the scenario of ore formation before the deposition of cover sandstones.

3. **The 'supergene model'** (Ruzicka, 1975; Crick and Muir, 1980; Donnelly and Ferguson, 1980; Ferguson et al., 1980; Ewers et al., 1984; Needham, 1988) describes syngenetic enrichment of U in pre-1870 Ma sedimentary rocks, followed by subsequent supergene enrichment. Subsequent to the regional metamorphism a prolonged period of erosion and weathering imposed a saprolitic profile as much as 100 m deep, and peneplaned the early Paleoproterozoic rocks. Uranium and other metals were leached from Paleoproterozoic rocks and the weathering-profile by surface waters, and precipitated in reducing environments. Breccia ore zones at Ranger and Jabiluka formed in carbonate-rich sequences during peneplanation of the Paleoproterozoic strata and before the cover rocks were deposited. Downward percolating meteoric waters transporting uranyl complexes were met by reducing conditions in breccia zones where U oxide was precipitated. It is presumed that this happened during formation of the regolith at the unconformity and before the deposition of the cover sandstones. Maas (1989) noted that Sr and Nd found in U ores from Nabarlek, Jabiluka, and possibly Koongarra, are isotopically sufficiently different from measured isotope signatures in both the late Archean and the Nabarlek Granite to render these rock types the most unlikely U-source rocks. Maas (1989) also argued that his data did not support derivation of radiogenic Nd from remobilisation of pre-Kombolgie concentrations of colluvial U.
4. **The 'hypogene model'** (Hegge and Rowntree, 1978; Binns et al., 1980) proposes that a heat-generating granite was the major driver of a convective cell of metalliferous fluids. The source of the fluids is considered to have been deep-seated and generated during the metamorphic event preceding deposition of the overlying sedimentary rocks. Ludwig et al. (1987) proposed that the first high-grade concentration took place after the peak of regional metamorphism, but at a time when early post-metamorphic igneous bodies were still being emplaced. However, later studies suggest that these igneous bodies are older. Some of the high-grade mineralisation may be an enrichment of earlier low-grade syngenetic concentrations in the lower Cahill Formation. This model cannot satisfactorily account for the spatial association of mineralisation with the unconformity between basement and overlying sediments.

One enigmatic feature of the hydrothermal U mineral systems that operated in the Pine Creek Orogen is the absence of an apparent source rock for the PGEs. No substantial bodies of mafic-ultramafic rocks crop out in the region to indicate an obvious mafic igneous derivation or association. Possible sources (Hoatson and Glaser, 1989) include:

- hydrothermal remobilisation of a fossil PGE placer that could occur at a Proterozoic unconformity, or be related to the high-energy clastic sedimentary units;
- an epithermal origin related to felsic volcanism, as suggested by the close spatial association of the disseminated Au–PGE mineralisation with alteration and felsic volcanics;
- hydrothermal remobilisation of a PGE-enriched phase of the Zamu Dolerite, or a subsurface mafic-ultramafic igneous body;
- leaching from country rocks by sedimentary brines; and
- carbonaceous shales that are prominent in the Early Proterozoic Masson and Koolpin Formations.

### *Key references*

- Needham and Stuart-Smith (1987): regional geological setting; stratigraphy of Coronation Hill; structure; U-Au-PGE mineralisation; epigenetic sandstone-type deposit; debris-flow conglomerate.
- Wilde et al. (1989): unconformity-related U deposits; transport and deposition of Au, U, and PGEs; paragenesis of U-Au-PGE deposits.
- Carville et al. (1990): exploration history; indicated resource; regional geology; stratigraphy and structure of Coronation Hill; alteration; ore mineralogy; Au-PGE-selenide-sulphide association.
- Carville et al. (1991): geology of Coronation Hill; stratigraphy, alteration, structure, gold-PGE mineralisation; mineralogy; PGMs; unconformity deposit model.
- Bloom et al. (1992): South Alligator Mineral Field; Coronation Hill-type deposits; hydrothermal fluid pathways; Au-PGE mineralisation; fluid activity; petrogenesis.
- Wyborn (1992): regional geological setting; Coronation Hill stratigraphy; structure; U-Au-PGE mineralisation.
- Mernagh et al. (1994): geological setting; stratigraphy; structure; mineralogy; geochemistry; PGEs; fluid inclusions; alteration; microthermometry; Raman spectroscopy; stable isotopes; low-temperature hydrothermal Au-PGE-U mineralising system; petrogenesis.
- Wyborn et al. (1994b): geology of Coronation Hill; geochemistry; Au and PGEs; exploration signature and techniques, mineralisation potential.
- Mernagh et al. (1998): unconformity U-Au-PGE deposits; regional geological criteria; Pine Creek Orogen; mineralisation; Coronation Hill deposit; alteration; geochemical and geophysical criteria; fluid chemistry and source; genesis.
- McKay and Mieztis (2001): comprehensive summary of U industry in Australia; historical mining, descriptions of U deposit types; classification, resources, geology and genesis of Coronation Hill deposit; exploration programs, development and production; U and nuclear electricity; economic potential.
- Smith (2007): hydrothermal Au-PGE deposits; carbonaceous shale-hosted PGE mineralisation; unconformity-related PGE-Au deposits; mineral systems at Coronation Hill; comparison of overseas and Australian deposits.
- Orth et al. (2014): geochronology of Coronation Hill mineralisation; LA-ICPMS dating of uraninite; paragenesis of Coronation Hill; geochronology of South Alligator Valley and East Alligator River U-Au deposits.

#### **6.4.8.7 Deposit Type 8.G: U-Au-Pd-Pt mineralisation associated with graphitic schist and carbonaceous sedimentary rocks**

##### *Overview*

Mineral systems associated with the PGE-enrichment of carbonaceous rocks are very similar to that operated for unconformity U-Au-PGE deposits (Deposit Type 8F), except they have a much wider age distribution, extending from the Archean to the Phanerozoic, and the host rocks are invariably carbon rich, i.e., carbonaceous sediments or graphitic schists. Important global examples include the Kupferschiefer Cu-Ag deposits in central Europe where significant concentrations of Pt and Pd are associated with redox fronts in carbonaceous shales and the Beaverlodge U deposits in Canada (Kucha and Pawlikowski, 1986; McDonald, 1988). Anomalous PGE concentrations characterise these rock types from a number of geological settings in Australia ranging from Archean greenstone successions of komatiites-felsic volcanics-chemical sediments, Proterozoic unconformity U-Au-PGE deposits, mylonite zones in roof pendants, to basal sedimentary units in Paleoproterozoic basins (Appendix K).

The Jabiluka unconformity-related U deposit (207 000 t of  $U_3O_8$  and 1.1 Mt @ 10.7 g/t Au, with significant Pd credits in the Jabiluka 2 orebody) in the Alligator Rivers Uranium Field is the type example of this deposit type since it is well documented and it contains significant concentrations of Au and Pd (up to 100 ppm). The host rocks of the mineralisation are Early Proterozoic metasediments of the Cahill Formation, which consist of chlorite and/or graphite schist and their brecciated equivalents. An angular unconformity separates these rocks from overlying Middle Proterozoic clastic and carbonate sediments with minor volcanic interbeds. Mineralisation consists of open-space-filling pitchblende and uraninite, with lesser disseminated material. Gold is closely associated with U and forms inclusions or veins in uraninite, and occurs with Pb- and Ni-tellurides. Palladium values are associated with the U-Au mineralisation. Various origins have been proposed for the unconformity U-Au-PGE mineral systems that operated in the Pine Creek Orogen—these are summarised in Deposit Type 8.F. The Lindeman's Bore Au-Pd prospect is hosted by metamorphosed carbonaceous shales of the Birrindudu Group, which forms the base of the Proterozoic Birrindudu Basin in the Northern Territory. A 1 m-thick drill-hole (LBD2) interval of 0.45 g/t Pd and 5.32 g/t Au was part of a 7 m-interval grading 1.1 g/t Au in pyritic and graphitic black shales of the Birrindudu Group. This Au-Pd intersection is approximately 80 m below an unconformable contact with the Limbunya Group. Other nearby holes identified hydrothermal systems with chlorite-hematite alteration and quartz-carbonate sulphide mineralisation. The PM Cu-Ag-Au-PGE Prospect in the Rudall Complex, Western Australia, is a Proterozoic vein deposit in dolomitic, carbonaceous and graphitic chlorite schist. Polymetallic mineralisation occurs in dilational structural jogs, with surface samples assaying up to 11% Cu, 3.5% Ag, 0.23% Au, 0.49% Pd, and 0.34% Pt. The Gold Ridge prospect in the Pine Creek Orogen, Northern Territory, is a roof pendant of ~2019 Ma Wildman Siltstone within ~1835 Ma Fenton Granite. Precious metals are largely localised in a graphite±pyrite-bearing mylonite structurally above a quartz breccia unit. An inferred resource of 32 000 t grading 4.5 g/t Au, 0.3 g/t Pt and 0.5 g/t Pd has been defined (Table 6.2). Anomalous PGE concentrations associated with carbonaceous units have also been reported (Appendix K; Hoatson and Glaser, 1989) at the Sidewinder and Camel Bore Ni-Cu-PGE prospects (Yilgarn Craton, WA), and with the Marimo Slate (Mount Isa Orogen, Qld). Anomalous PGE concentrations have been documented overseas in Permian carbonaceous Kupferschiefer shales at Zechstein, Poland (Kucha, 1975, 1982, 1985; Kucha and Pawlikowski, 1986; Banas et al., 1978), in bituminous coal in Kentucky (Chyi, 1982), and in base-metal deposits of the central African Copper Belt in Zambia and Zaire, which are associated with organic C and U in black shale and dolomitic siltstone (Mertie, 1969; Freeman, 1983). The Cu-rich Zechstein rocks include thucholites (a

carbonaceous clastic rock with an anomalously high U content) containing electrum and various Pd arsenides. Similarly, the South Alligator River mineralisation is associated with black shale and schist containing unusually high U, Au, Pd, and Pt. Moreover, the Pd-enriched character of the mineralisation at Coronation Hill-EI Sherana-Palette is consistent with the dominance of Pd over the other PGMs in the thucholites.

The Polish Kupferschiefer shows no evidence of igneous activity, i.e. no intrusions, dykes, or volcanic rocks. Hydrological processes acting at redox barriers and the catalytic activity of organic matter appear to be important mineralising mechanisms. Stumpfl (1986) notes that PGE values of more than 10 ppm in a cm-thick precious-metal-shale horizon at the contact of sandstone (oxidising conditions) and black shale (reducing conditions), extend over tens of thousands of square metres. Values exceeding 200 ppm Pt do occur over limited areas. The Pd and Pt in the thucholites are believed by Kucha (1975) to have been derived by the decomposition of Pd- and Pt-bearing organic compounds during diagenesis, and remobilised by circulating brines enriched in dissolved organic complexes and redeposited as arsenides, sulpharsenides, and bismuthides in the shales, or rocks directly below the shales. Kucha and Pawlikowski (1986) suggested brines that percolated downward from overlying anhydrites into underlying redbeds where, upon heating, they leached the PGEs from interbedded volcanics. The hotter metalliferous brines interacted with descending colder brines in shallower parts of the basin and deposition of the base and precious metals resulted.

#### *Australian deposits/prospects/hosts*

Jabiluka, Gold Ridge (Pine Creek Orogen, NT); Lindeman's Bore (Birrindudu Basin, NT); Marimo Slate-Cloncurry (Mount Isa Orogen, Qld); ?Nairne (Delamerian Orogen, SA); PM Prospect-Copper Hills PM (Rudall Province, WA); Sidewinder, Camel Bore, (Yilgarn Craton, WA).

#### *Significant global example(s)*

Kupferschiefer (Germany-Poland); Lubin-Zechstein (Poland); Zambian Copperbelt (Zambia); Kalahari Copperbelt (Namibia); Athabasca Basin, (Canada); Sukhoi Log (Siberia).

#### *Type example in Australia*

Jabiluka, Northern Territory.

#### *Location*

Longitude 132.9029°E, Latitude -12.4994°S; 1:250 000 map sheet: Alligator River (SD 53-01), 1:100 000 map sheet: Cahill (5472); ~220 km east of Darwin.

#### *Geological province*

Pine Creek Orogen, Northern Territory.

#### *Resources*

Unknown. Palladium is the dominant PGE associated with U and Au. The total U resources for Jabiluka No. 1 Orebody at a cut-off grade of 0.05% U<sub>3</sub>O<sub>8</sub> are 1.3 Mt averaging 0.25% U<sub>3</sub>O<sub>8</sub>, which represents 3400 t of U<sub>3</sub>O<sub>8</sub> (Pancontinental Mining Ltd, 1979). The total U resources for the Jabiluka No. 2 Orebody at a cut-off grade of 0.2% U<sub>3</sub>O<sub>8</sub> are 31.1 Mt averaging 0.53% U<sub>3</sub>O<sub>8</sub>, which represents 163 000 t of U<sub>3</sub>O<sub>8</sub> (ERA Ltd, 2000).

### *Current status and exploration history*

Undeveloped U-Au-PGE deposit with JORC-compliant resources. The Alligator Rivers Uranium Field in the Pine Creek Orogen contains a number of major U±Au±PGE deposits (Ranger 1, Koongarra, Nabarlek, and Jabiluka). The mineral potential of the area was recognised in 1967, when BMR published a revised 1:500 000 geological map of the Darwin–Katherine region which showed probable Archean basement in the Alligator Rivers area (McKay and Mieizitis, 2001). The Archean rocks were shown to be unconformably overlain by deformed and metamorphosed Paleoproterozoic rocks, which were in turn overlain by Mesoproterozoic sandstones of the McArthur Basin. This map highlighted similarities to the U deposits in the Archean–Paleoproterozoic–Mesoproterozoic setting at Rum Jungle. Uranium exploration in the Alligator Rivers and Arnhem Land regions of the Northern Territory was restricted for many years because of political and environmental factors. Much of this prospective region has only been subjected to first pass exploration designed to detect outcropping deposits and extensions of known deposits. There has been little exploration to locate deeply concealed deposits lying near the unconformity similar to those in Canada. A detailed ground radiometric survey over the Jabiluka area was carried out by Pancontinental Mining Ltd in 1971 (Rowntree and Mosher, 1975). The small Jabiluka 1 deposit was detected as a weak ground radiometric anomaly; it was not recognised in earlier airborne radiometric surveys. The very large Jabiluka 2 deposit was found in 1973 by drilling along strike to the east of Jabiluka 1, through the overlying barren Kombolgie sandstone (McKay and Mieizitis, 2001). The Jabiluka mine site is surrounded by, but not part of, the World Heritage-listed Kakadu National Park.

### *Economic significance*

Unconformity-related U-Au deposits account for about 20% of Australia's total U resources, mainly in the Alligator Rivers Uranium Field (Ranger 1, Jabiluka, Koongarra), and possibly in one prospect in the Rudall Province, Western Australia (Kintyre).

### *Geological setting*

McKay and Mieizitis (2001) have shown that the Jabiluka 1 and 2 deposits occur in the lower member of the Early Proterozoic Cahill Formation, at the northeastern margin of the Nanambu Complex. Jabiluka 1 lies just west of a large outlier of the Kombolgie Subgroup, but Jabiluka 2 (~800 m east of Jabiluka 1) is concealed by up to 200 m of Kombolgie sandstone (Figure 6.54 and Figure 6.55). Both the Jabiluka 1 and 2 deposits occur within an open asymmetric flexure, striking east-southeast and dipping to the south. The Jabiluka 1 deposit measures about 400 m in a northwesterly direction and 200 m in a northeasterly direction (Hegge, 1977). It dips south at 15–30°, and in the Main Mine Series the ore zone is up to 35 m-thick. Jabiluka 2 deposit extends for at least 1000 m in a west-northwest direction and at least 400 m north–south. It dips south in a series of flexures at between 30° and 60°. The deposit is still open to the south and east at depth. In the Main Mine Series the ore zones are up to 135 m-thick. Hancock et al. (1990) consider that the mineralised sequence of the Cahill Formation is overturned and the orebodies are situated along the lower limb of a recumbent fold. The metasedimentary sequence at Jabiluka consists of alternating quartz–muscovite–chlorite schist, quartz–chlorite schist, quartz–graphite schist and magnesite–dolomite. Some units are feldspathic, locally containing garnet, sillimanite, and zircon. In the vicinity of the deposits, retrograde metamorphism has resulted in chloritisation of biotite and garnet, together with sericitisation of feldspar, sillimanite, and cordierite.

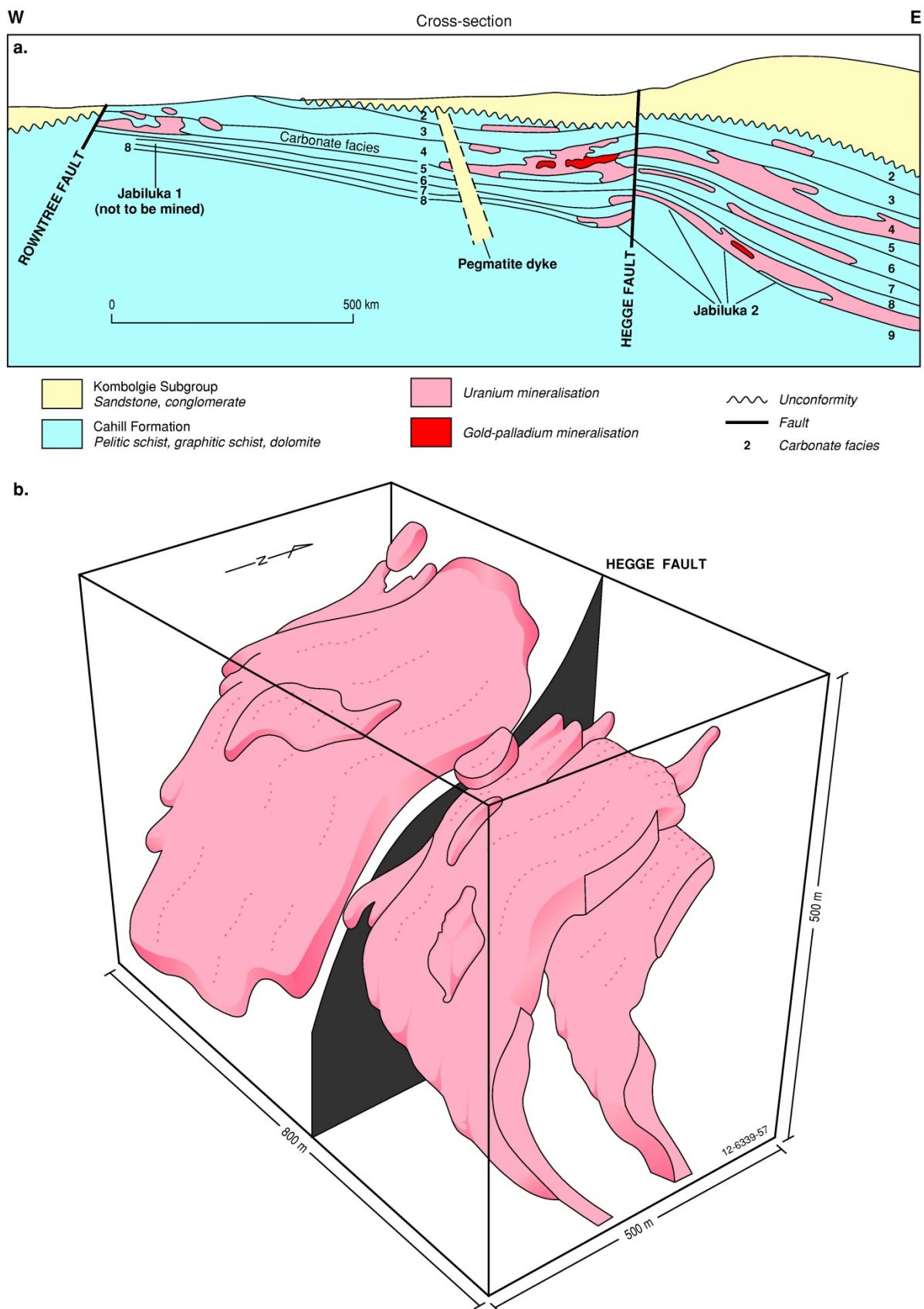


Figure 6.54 (a). Generalised east-west long-section of Jabiluka 1 and 2 U-Au-Pd orebodies, and (b). conceptual 3-D perspective of the Jabiluka 2 deposit. Modified from Kinhill (1996).

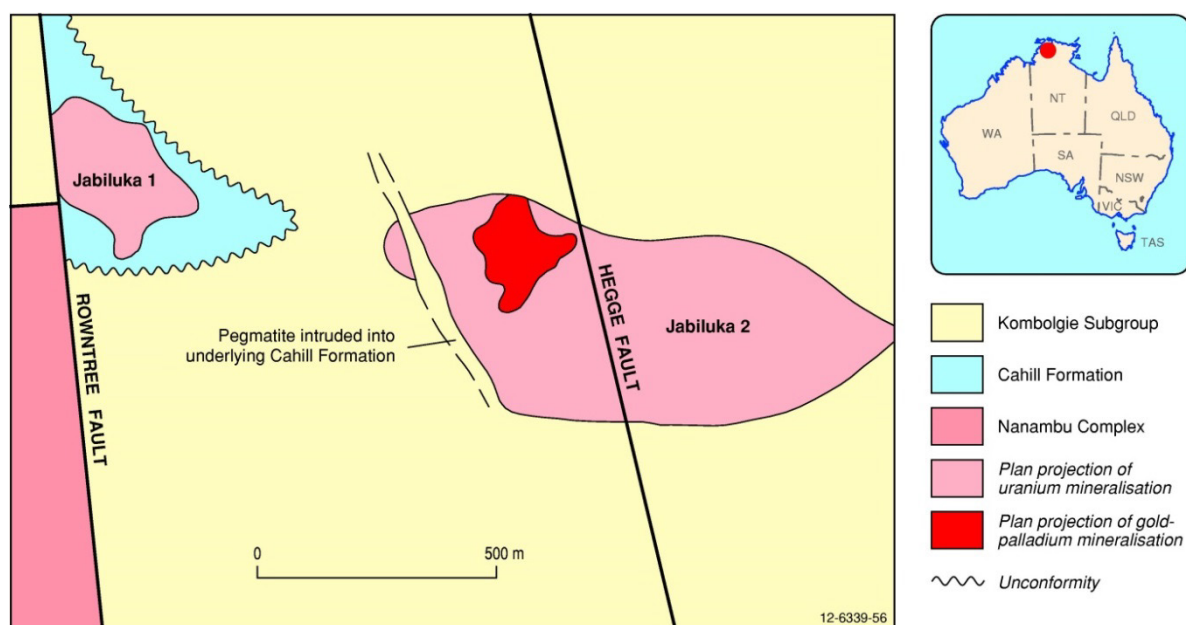


Figure 6.55 Geological plan of Jabiluka 1 and 2 U-Au-Pd orebodies, Pine Creek Orogen, Northern Territory. Modified from Needham (1982).

### Mineralisation environment

The Jabiluka deposits occur in four separate horizons in the lower member of the Cahill Formation: the Upper Graphite Series, Main Mine Series, Lower Mine Series 1, and Lower Mine Series 2. An angular unconformity separates these mineralised rocks from overlying Middle Proterozoic clastic and carbonate sediments with minor volcanic interbeds. Sixty-seven percent of the U mineralisation is in the Main Mine Series, and most of the economic mineralisation occurs in breccia zones (Hancock et al., 1990). The host rocks largely consist of chlorite and/or graphite schist and their brecciated equivalents. Wilde (1988) showed that chloritic alteration associated with mineralisation is extensive parallel to the unconformity, but appears to decrease with depth below the unconformity. The deposit extends for more than 500 m below the unconformity and remains open at depth. Mineralisation is in three main forms: breccias; veins adjacent to breccias; and as disseminations within schist. Primary U mineralisation consists of open-space-filling pitchblende and uraninite, with minor coffinite, brannerite, and organo-U minerals (Binns et al., 1980). Associated sulphides include pyrite with lesser chalcopyrite and galena. Major gangue minerals are chlorite, quartz, sericite, and graphite.

### PGE mineralisation

Palladium-bearing Au-U mineralisation occurs in graphite horizons in the western part of the Jabiluka 2 orebody (Figure 6.54, Figure 6.55, and Figure 6.56). The Au-bearing zone contains 2.392 Mt ore averaging 3.7 g/t Au and 0.47%  $U_3O_8$ , but there are no resource figures on the PGEs (ERA Ltd, 1992). The Au is mainly in breccia zones of the Main Mine Series and the ore has an average thickness of 2 m (Hegge, 1977). Gold is closely associated with U, chlorite, pyrite, and quartz, and it forms inclusions or veins in uraninite, and occurs with Pb- and Ni-tellurides. Palladium values are generally associated with the U-Au mineralisation, but the PGMs have not been recognised. In detail though, Figure 6.56 shows that Pd enrichment is slightly decoupled from the U and Au peaks, occurring at slightly different stratigraphic levels in white mica schist. The U-Au-Pd mineralisation at Jabiluka typically has low abundances of Pt. It is believed that structural preparation with low-pressure conditions was significant during mineralisation.

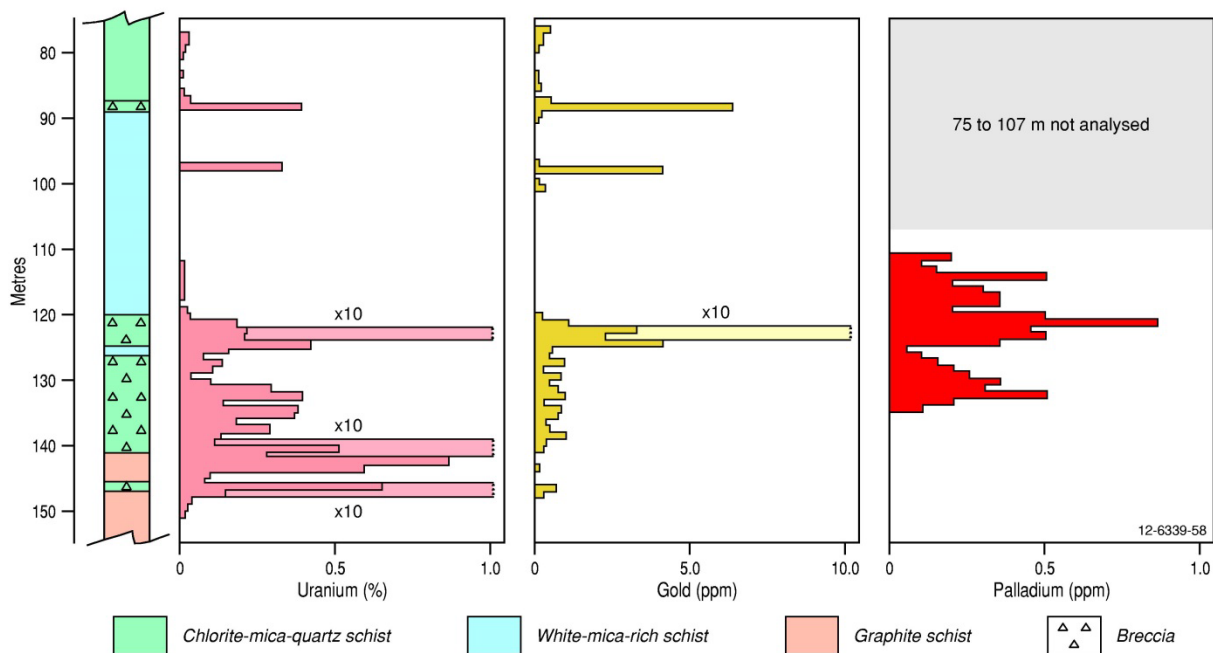


Figure 6.56 Relationship of uranium (%), gold (ppm), and palladium (ppm) abundances in different types of schist and breccia in a typical intersection through the Jabiluka 2 orebody. Platinum is not enriched in this deposit. Modified from Wilde et al. (1989).

### Age of mineralisation

Ludwig et al. (1987) reported an age of  $1437 \pm 40$  Ma for U mineralisation at Jabiluka, however, more recent geochronological data indicates this determination is significantly too young. The age of mineralisation at Jabiluka is considered to be  $\sim 1685$  Ma. LA-ICPMS data reveal initial uraninite precipitation occurred in the basement rocks at  $\sim 1680 \pm 17$  Ma. The oldest  $^{207}\text{Pb}/^{206}\text{Pb}$  ages are coincident with a  $^{40}\text{Ar}/^{39}\text{Ar}$  age of  $1683 \pm 11$  Ma from one S11 illite sample from above the deposit (Polito et al., 2005).

### Genesis

Various origins have been proposed for the origin of the unconformity-related U deposits of the Alligator Rivers region (see previous Type Deposit 8.F, but thermodynamical modelling has shown that oxidised, low-pH and chloride-rich brine solutions possibly derived in the terrestrial, hematitic, or evaporitic sediments of the Middle Proterozoic cover rocks could be favourable for the transport of Au, U, and Pd as chloride complexes. Reduction of the ore-forming solutions by the interaction of the solutions with graphite and/or ferrous iron-bearing biotite may have been a mechanism for ore precipitation. For this model, Nd and Sr isotopic data indicate the U and probably also the Au and Pd at Jabiluka were derived from within the cover rocks.

### Key references

- Ayres and Eadington (1975): regional geology; South Alligator U and Jabiluka deposits; host rock and geochemistry; mineralisation; carbonaceous shale; sandstone aquifer; reduction; structural-chemical traps.
- Rowntree and Mosher (1975): stratigraphy; geological setting; Jabiluka uranium mineralisation.
- Hegge (1977): stratigraphy; structure; mineralisation; geological setting; Jabiluka deposit.

- Gustafson and Curtis (1983): geology; stratigraphy; lithology; structure; depositional environment; alteration; brecciation; chemistry; metasomatism processes; genesis.
- Ludwig et al. (1987): geological setting of the Jabiluka U deposit; U/Pb, Rb/Sr, and K/Ar geochronology; isotopic disturbance.
- Nutt (1989): geological setting; chloritisation and associated alteration; whole-rock chemistry; mineralogy; genesis.
- Hancock et al. (1990): regional geology, exploration history; structure; mineralisation; local geological setting; Jabiluka deposit.
- Mernagh et al. (1998): unconformity U-Au-PGE deposits; regional geological criteria; Pine Creek Orogen; mineralisation; Jabiluka deposit; alteration; geochemical and geophysical criteria; fluid chemistry and source; genesis.
- McKay and Mieozitis (2001): summary of U industry in Australia; historical mining, descriptions of U deposit types; classification, resources, geology and genesis of Jabiluka deposit; exploration programs, development and production; U and nuclear electricity; economic potential.
- Beaufort et al. (2005): regional geology; clay minerals; mineralogy and morphology; hydrothermal alteration; alteration zonation; progressive fluid-rock pathways; interaction of descending fluids with basinal brines and basement rocks.
- Polito et al. (2005): geochronology of Proterozoic Jabiluka unconformity-related U deposit; LA-HR-ICPMS uraninite and  $^{207}\text{Pb}/^{206}\text{Pb}$  ages; petrogenesis.
- Smith (2007): hydrothermal Au-PGE deposits; carbonaceous shale-hosted PGE mineralisation; unconformity-related PGE-Au deposits; comparison of overseas and Australian deposits.

#### **6.4.8.8 Deposit Type 8.H: Mineralisation formed along mid-oceanic ridges**

No confirmed examples documented in Australia.

### **6.4.9 Mineral-System Class 9: Regolith-Laterite**

#### **6.4.9.1 Deposit Type 9.A: PGE-bearing regolith developed on ultramafic-mafic igneous rocks**

##### *Overview*

Australia's PGE-bearing laterites show a spatial and genetic association with olivine-bearing ultramafic igneous rocks in four geological settings. In order of decreasing economic importance they are:

1. Paleozoic 'Alaskan-type' mafic-ultramafic intrusions, Lachlan Orogen, NSW (Syerston, Owendale, Bulbodney Creek, Gilgai);
2. Archean layered mafic-ultramafic intrusions, Yilgarn Craton, WA (Weld Range, Yarawindah Brook, Carr Boyd Rocks);
3. Archean ultramafic-mafic intrusive sills, Yilgarn Craton, WA (Ora Banda Sill, Mount Thirsty Sill); and
4. Archean komatiites and high-MgO basalts, Yilgarn Craton, WA (many occurrences associated with greenstone successions: see examples in Butt et al., 2006 and Elias, 2006).

A genetic correlation between the metal associations in the laterite profile and the underlying ultramafic lithologies is apparent for the group 1 'Alaskan-type' intrusions of central New South Wales.

Weathering profiles above the Tout (formerly the Flemington Intrusion), Owendale, and Bulbodney Creek intrusions record: Pt-Cu mineralisation with variable Ni, Co, and Au credits above dunite-wehrlite rocks; Co-Ni mineralisation with Pt credits above olivine pyroxenite; and elevated Cr and Sc concentrations occur above dunite-wehrlite lithologies. Tectonically emplaced Paleozoic 'Alpine- and ophiolitic-type' ultramafic-mafic intrusions that form anastomosing north-trending linear serpentinite belts in the Lachlan and New England orogens of eastern Australia have associated Ni-Co±Sc laterites in Tasmania (Beaconsfield), New South Wales (Lake Innes, Widgegongs–Homeville–Collerina), and Queensland (Greenville, Lucknow, Kokomo, Rockhampton). However, limited precious metal data for these Ni-bearing laterites indicate they generally have low PGE (tens of ppb) concentrations. Travis et al. (1976) showed that indurated ferruginous products, developed above magnesium-rich rocks in the Yilgarn Craton, have elevated Pd (up to 48 ppb) and Ir (up to 32 ppb) concentrations. Background levels for both Pd and Ir are about 2 ppb. Palladium generally follows the trend of Mn, Cu, and to a lesser degree Ni, Co, and Zn, but Ir correlates with Fe and Al oxides. This suggests that Ir is largely residual in the upper sections of the laterite profile, while Pd appears to have been mobilised from other parts of the profile. No PGE-bearing laterite has been mined in Australia.

The most advanced laterite PGE prospects in Australia are associated with the Paleozoic 'Alaskan-type' mafic-ultramafic intrusions (group 1 above), in particular, the Syerston laterite prospect in the Tout Intrusion, and the Cincinnati–Milverton–Owendale North prospects in the Owendale Intrusion. The Syerston deposit contains the largest resource with an estimated Total Resource of 137 Mt @ 0.24 g/t Pt, and 96 Mt @ 0.69% Ni and 0.12% Co, and a global metal resource of 32.9 t of Pt (Black Range Minerals NL (2000). Indicated Resources for the Owendale group of mineralised laterites range from 1 Mt to 10 Mt @ 0.5 g/t to 0.6 g/t Pt, 0.2% Ni, and 0.05% Co (Helix Resources Ltd, 2004b; Platina Resources Ltd, 2012, 2013a, 2014b). Laterites at Mount Carnage, Weld Range, and Yarawindah Brook in the Yilgarn Craton of Western Australia also have small-tonnage resources of PGEs. Table 6.2 summarises the PGE resources of Australia's laterite deposits.

The enrichment of Sc in Australian laterites appears to be a feature of the younger Phanerozoic ultramafic bodies of eastern Australia (Hoatson et al., 2011; Jaireth et al., 2014), whereas the Ni-Co±PGE laterites superimposed over Archean ultramafic rocks in the Yilgarn Craton of Western Australia appear to have much lower concentrations of Sc. Australian laterites overlying ultramafic-mafic sequences typically contain low-grade PGE deposits (3 to 15 Mt @ ~1 g/t PGEs) that can be potentially brought into production quickly during periods of favourable metal prices. However, low grades and metallurgical issues have inhibited mining.

#### *Australian deposits/prospects/hosts*

Syerston–Owendale–Bulbodney Creek–Gilgai (all Lachlan Orogen, NSW); Weld Range–Gilgarna Rocks–Carr Boyd Rocks–Yarawindah Brook–Youangarra–Ora Banda–Mount Carnage (all Yilgarn Craton, WA).

#### *Significant global example(s)*

Yubdo (Ethiopia); Bahia (Brazil); Guma Water–Sierra Leone (Africa); Falcondo (Dominican Republic); Pirogues (New Caledonia); Andriamena (Madagascar).

#### *Type example in Australia*

Syerston, New South Wales.

### *Location*

Longitude 147.419586°E, Latitude -32.756687°S; 1:250 000 map sheet: Narromine (SI 55–03), 1:100 000 map sheet: Boona Mount (8332); ~8 km northwest of Fifield, New South Wales.

### *Geological province*

Lachlan Orogen, New South Wales.

### *Resources*

The Syerston Pt-Ni-Co prospect, located in the central-eastern part of the Tout Intrusion is one of the most advanced lateritic prospects in the Fifield-Nyngan region. It contains a measured-indicated-inferred resource of 137 Mt @ 0.24 g/t Pt, with associated credits of 96 Mt @ 0.69% Ni and 0.12% Co (Black Range Minerals NL, 2000).

### *Current status and exploration history*

Prospect with advanced exploration. Several junior exploration companies followed up regional aeromagnetic surveys conducted by the BMR in the Fifield region with geophysical-geochemical surveys and shallow drilling programs to penetrate the alluvium that covers the flat-relief countryside. Exploration programs in the Owendale Intrusion initially focussed on primary concentrations of Pt in ultramafic lithologies, but the importance of such commodities as Pt-Sc-bearing laterites and vermiculite became more apparent with further exploration. In 1991, a major vermiculite orebody was discovered in the small Hillview intrusion (see intrusion number 35 in Figure 6.35), near Tottenham. Published resources are 12.4 Mt at 32% vermiculite (Helix Resources NL, 1993b; Martin, 1998; NSW DPI, post-2005). Additional inferred resources of 4.8 Mt at 34% vermiculite have been reported in another body at Tigers Creek, about 14 km southwest of Hillview (Platinum Search NL, 1994). In addition to the Owendale and Bulbodney Creek intrusions, the other well explored PGE-enriched laterite profile is associated with the Tout Intrusion. Drilling programs by Black Range Minerals NL have determined a measured-indicated-inferred Pt-Ni-Co resource at the Syerston prospect (see Resources above). Platinum Search NL has established that laterites above the Gilgai Intrusion, 25 km west of Nyngan (Appendix Figure K.36), attain thicknesses up to 45 m over dunite and pyroxenite. The intrusion is zoned about an olivine-rich dunite core similar to the Owendale Intrusion. The Pt geochemical anomaly in the laterite has grades up to 2 g/t Pt and covers an area of 250 m by 350 m. Nickel and Cr are also enriched, but Pd is low (Jones, 1991). Low-grade Pt mineralisation in the range 0.1 g/t to 0.4 g/t, and reaching peaks of between 1 and 2 g/t Pt over 1-m-thick intervals, characterise dunite and olivine pyroxenite below the mineralised laterite. It is assumed the principal PGM is isoferroplatinum as is the case for the Kars Intrusion (Appendix Figure K.35), and other deposits near Fifield. In 2013, Platina Resources Limited (2013c) reported some of the highest Pt intersections in the Owendale Intrusion that included 9 m @ 0.82 g/t Pt and 331 g/t Sc from 10 m (laterite), and 1 m @ 24 g/t Pt from 26 m (primary).

### *Economic significance*

Since their discovery in 1887, the placer Pt deposits near Fifield in central New South Wales were Australia's first producer of Pt metal, and the only significant producer of Pt as a primary product. Total production from the Platina Lead, Gillenbine Tank Lead, and the Fifield Lead near the Murga, Tout, and Owendale intrusions amounted to about 633 kg Pt and 178 kg of Au (see Section 5.2.2). More recent exploration has also focussed on hard-rock (see Deposit Type 6.A) and laterite sources of Pt associated with the intrusions. Two such high-profile laterite projects are managed by Black Range

Minerals NL and Platina Resources Limited at the Tout and Owendale intrusions, respectively. In regard to the laterite environment at Owendale, Platina Resources Limited (2014b) have estimated a total contained metal resource for the Owendale Platinum-Nickel-Cobalt-Scandium Project of 519 000 ounces of Pt and 9100 t of Sc. Platina Resources Limited (2014b, p. 9) maintains this represents Australia's newest Pt resource, and is the world's largest and most high-grade Sc deposit.

### *Geological setting*

The Tout and Owendale intrusions are two prominent examples within a group of more than sixty 'Alaskan-type' mafic-ultramafic complexes that intrude Cambro-Devonian Girilambone Group metasediments in central western New South Wales (Figure 6.35, Figure 6.36, Figure 6.37). The intrusions occur along the Parkes Terrace—an 80 km-wide and 500 km-long north-trending belt of gravity highs (Suppel and Barron, 1986a). The Parkes Terrace represents a regional zone of crustal thinning that possibly contained deep penetrative crustal structures (sutures, detachments, etc) which facilitated the emplacement of the 'Alaskan-type' intrusions during the late Ordovician to late Silurian into mid-crustal levels from source areas in upwelling lithospheric mantle (Derrick, 1991). Elliott and Martin (1991) note that the late Paleozoic period in the Fifield area was dominated by deep erosion that exposed the 'Alaskan-type' complexes. Erosion continued during the Mesozoic, and the Cenozoic Era witnessed intense weathering that resulted in the development of thick laterite profiles over many of the complexes. The present-day thickness of the laterite profile varies from 10 m to 80 m. The present topography of the Fifield region is flat to gently undulating with slight depressions over the complexes (Elliott and Martin, 1991).

### *Mineralisation environment*

The Tout Intrusion (Agnew et al., 1987; Derrick, 1991; Teluk, 2001) is an elongate ultramafic-mafic-alkaline body, 16 km-long in a west-northwest direction, and up to 6.5 km-wide (Figure 6.57a). Less than 1% of the intrusion is exposed. Drilling has defined several alkaline mafic lithologies in the west of the intrusion that have been grouped into four series: hornblende quartz monzonite, hornblende melamonzonite-meladiorite, hornblende pyroxenite, and clinopyroxene quartz monzonite-diorite. Of greater economic importance in the eastern half of the intrusion are gabbro, pyroxenite, olivine pyroxenite, and dunite that form a crude concentric zonation comprising a central core of primitive ultramafic lithologies surrounded by more fractionated mafic lithologies. The series of rocks are interpreted to represent individual magma pulses that were emplaced into an expanding magma chamber that progressively became more ultramafic with time. Steeply plunging Pt-bearing chromitite lenses and schlieren are hosted by the most primitive lithologies, such as dunite (Derrick, 1991). These chrome-rich bodies are sometimes truncated at the interface of the primary zone and overlying laterite zone, other bodies persist upwards to higher levels in the laterite profile. This is an important distinction with the nearby mineralised Owendale Intrusion, which has no known chromitites or localised concentrations of chromite. The Pt-bearing laterites in the Tout Intrusion form a crude concentric pattern outlining the olivine-rich ultramafic lithologies. In plan view, the individual laterite bodies are irregularly shaped. The mineralised laterites are concentrated above dunite, olivine pyroxenite, pyroxenite, and more rarely gabbroic rock types, and they are absent from the alkaline monzonite, diorite, and hornblende pyroxenite units that constitute the western half of the intrusion.

### *PGE mineralisation*

Parts of the Tout Intrusion are overlain by a thick, ?Cenozoic laterite profile (Figure 6.57b) comprising pisolitic laterite and massive to cavernous limonitic and siliceous laterite units (Derrick, 1991). Nodular masses of magnesite locally invade goethitic clays in the laterite profile. The profile attains maximum

development (>30 m) over the more weathered dunite rock types. Intensive drilling programs by Black Range Minerals NL in the late 1990s defined anomalous Pt grades (>2 g/t Pt) over an area of ~2000 m length by 200 m to 400 m width, indicating an underlying primary zone of mineralisation. Some of the higher Pt grades in the laterite profile include: 12 m @ 8.0 g/t, 4 m @ 8.0 g/t, 1 m @ 32 g/t, 14 m @ 3.3 g/t, 24 m @ 4.2 g/t, and 24 m @ 2.9 g/t. Metallurgical investigations indicate the Pt grain size varies from ultra-fine to coarse (nuggetty), and the dominant mineral is isoferroplatinum (alloy comprising ~80% Pt, 10% other PGEs, and 10% Fe).

Immediately to the north of the Tout Intrusion, is the extensively explored Owendale Intrusion, which has a very similar PGE-enriched laterite profile to that at Tout. Residual enrichment of PGE mineralisation at Owendale is exclusively associated with deep lateritisation of ultramafic lithologies, and in particular, olivine-rich rocks in discordant dunite-wehrlite bodies. The thickness and completeness of the laterite profile varies depending upon the topography prevalent during weathering and the depth of subsequent erosion. This mineralisation is best developed in the Cincinnati and North Owendale areas along the eastern side of the intrusion. Drilling has defined broad parallel high-grade laterite zones parallel to these ultramafic bodies that comprise a elongate central zone some tens of metres wide and hundreds of metres long surrounded by a broad halo of low-grade mineralisation. Platinum grades are generally 0.1 to 1.5 g/t, with lesser Pd, and minor Os, Ir, and Rh (Elliott and Martin, 1991). The Pt/Pd ratio is usually greater than 10:1, which is similar to most other forms of PGE mineralisation in the intrusion. Local high grades of up to 8 g/t Pt over a 1 m vertical interval occur in the Cincinnati area. The laterite profile at Owendale is typical of most laterite profiles that involved the enrichment of iron at the expense of magnesium and silica, which were lost during weathering. Manganese, Ni, Co, Cu, and Cr are also enriched to varying degrees. The regolith profile consists of an upper, iron-rich zone that overlies a mottled zone and sparolite. Platinum in the profile is concentrated over thicknesses from a few metres up to 40 m, with peak values usually occurring at the base of, or immediately below, the ferricrete zone. Metallurgical research showed the PGMs in the laterite are much finer grains than those in the placer deposits, with few grains exceeding 100 µm and most being less than 50 µm (Elliott and Martin, 1991). Bowles (1989) noted the dominant mineral species is Pt-Fe alloy, with one such grain containing a small inclusion of osmiridium.

### *Age of mineralisation*

The laterite profile in the Tout Intrusion was interpreted to have evolved during the ?Early and Late Cenozoic (Derrick, 1991). These events are approximately coeval with the formation of the mineralised paleochannel systems in the nearby Owendale Intrusion which eroded the Early- to Mid-Cenozoic regolith, thus indicating a post mid-Miocene age for its mineral systems. The crystallisation ages of the Tout and other Fifield region intrusions are generally poorly defined. The ages, which appear to be dependent on the dating method used, extend from the late Ordovician to late Devonian. The most recent and robust geochronological methods involving the dating of zircon indicate a late Ordovician to late Silurian age (e.g., 450 to 420 million years) for the Fifield intrusions. Early whole-rock K-Ar geochronology studies by Thomson (1974) indicated that the Tout and Hylea intrusions were coeval at  $397 \pm 16$  Ma and  $397 \pm 12$  Ma, respectively. Pogson and Hilyard (1981) recorded a within error K-Ar age of 405 Ma for the same two intrusions. Barron et al. (2004) compiled whole-rock Rb-Sr ages of  $428 \pm 4$  Ma for the Tout Intrusion (Stojanovic, 1995), and  $446.1 \pm 10.8$  Ma and  $365 \pm 10$  Ma for the Owendale Intrusion (both ages pers. comm., Whitford, 1991). SHRIMP U-Pb zircon ages of  $445 \pm 6$  Ma and  $448 \pm 4$  Ma were obtained for the Honeybugle and Bulbodney Creek intrusions, respectively (pers. comm., R.I. Hill, Australian National University, Canberra, in Elliott and Martin, 1991). More recent ICPMS zircon ages of  $424 \pm 11$  Ma (pers. comm., A.J., Crawford, 2001),  $436 \pm 12$  Ma and  $444 \pm 3$  Ma were reported for the Owendale Intrusion in Barron et al. (2004).

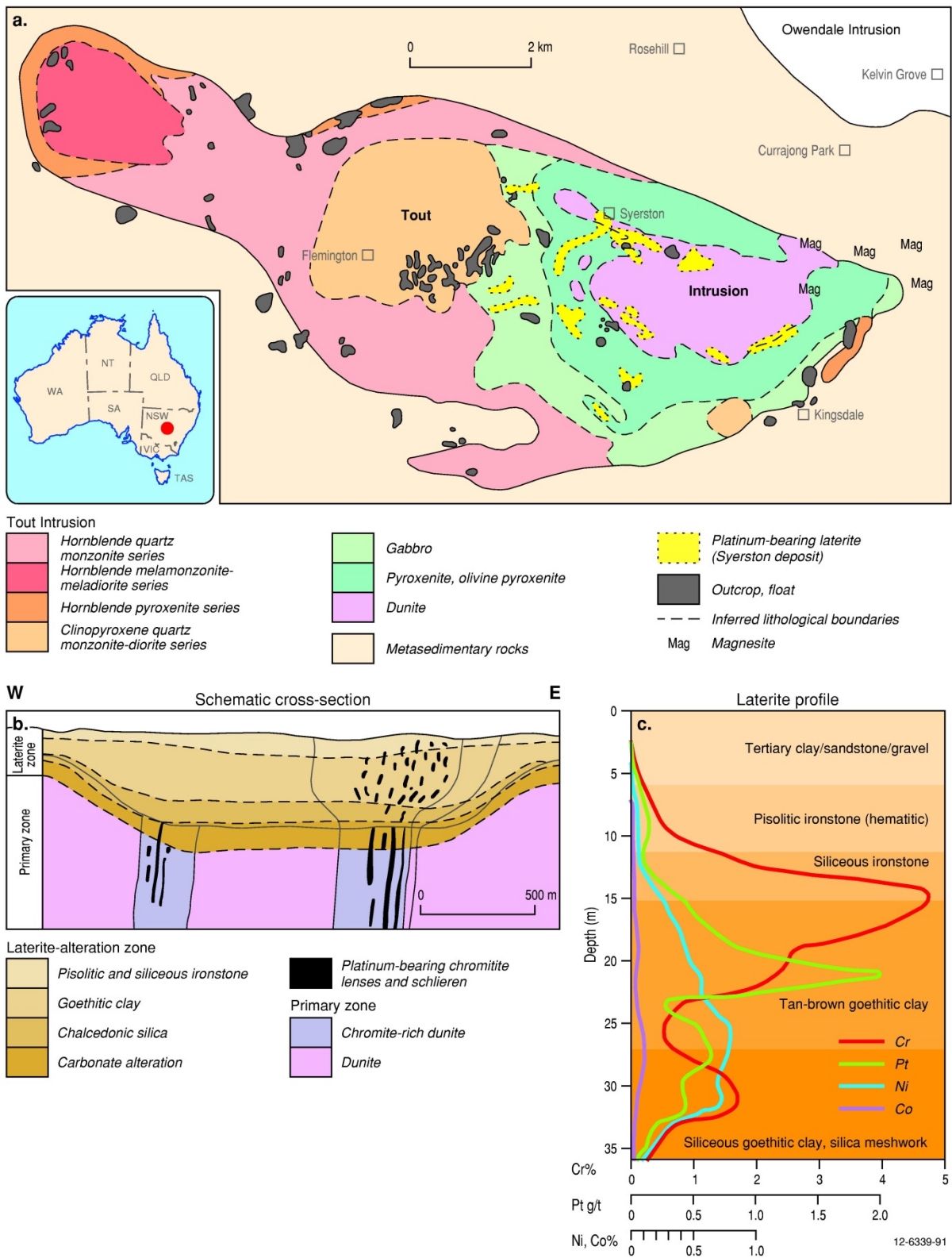


Figure 6.57 (a). Interpreted geological setting of the Tout 'Alaskan-type' mafic-ultramafic intrusion, Lachlan Orogen, central New South Wales. The Syerston PGE-enriched laterite preferentially overlies olivine-dominant ultramafic lithologies in the eastern half of the zoned intrusion. (b). Schematic east-west cross-section across the eastern part of the Tout Intrusion. (c). Geochemistry of laterite profile overlying dunite. Modified from Derrick (1991).

## Genesis

Derrick (1991) recognised at least two geological periods of lateritisation in the Tout Intrusion which resulted in residual enrichment of clays in different mobile metals (e.g., Cr, Ni, Co, and Pt: Figure 6.57c). A moist period in the ?Early Cenozoic resulted in the development of various zones of hematite-rich pisolite, siliceous ironstone, goethitic clay, and silicification at, or above, a high-level water table. A later phase of lateritisation in the ?Late Cenozoic witnessed more arid conditions and a falling water table level. As a result of these changing conditions, Ni and Co were taken into solution and redeposited low down in the profile, chrome remained high in the profile, but Pt was not redistributed by supergene processes. The schematic section of the weathering profile in Figure 6.57c shows the maximum concentrations for Pt of about 2 g/t occur in a tan-brown goethitic clay layer (~22 m depth) below a well-defined ~4.7% Cr peak located near the interface of the goethitic clay and overlying siliceous ironstone layers (15 m depth). Maximum Ni concentrations of ~0.8% and a subtle Co peak of ~0.2% occur in siliceous goethitic clay near the base of the mineralised profile (32 m to 25 m depth). The mineralised weathering profiles overlying the ultramafic-mafic intrusions in the Fifield region, including the Tout complex, are exceptionally well-developed and well-preserved. A spatial and genetic correlation is seen between the metal associations in the laterite profile and the underlying lithologies. Weathering profiles at Tout, Owendale, and Bulbodney Creek reveal that: Pt-Cu mineralisation generally overlies dunite-wehrlite rocks with variable Ni, Co, and Au contents; Co-Ni mineralisation with Pt credits are associated with underlying olivine pyroxenite; and elevated Cr and Sc concentrations occur above dominant dunite-wehrlite lithologies.

Elliott and Martin (1991) state that there is no direct evidence to suggest large-scale supergene remobilisation of PGEs in the lateritic environment at North Owendale although a supergene origin for at least some of the lateritic PGEs was proposed by Turvey (1990) and Bowles (1989). Brill and Keays's (1989a,b) study of laterites in the Bulbodney Creek Intrusion concluded the PGE mineralisation was probably the result of largely residual concentration during weathering.

Shi's (1995) field, textural, and geochemical data support a chemical weathering origin for the mineralised laterite profiles overlying the Fifield intrusions, including the Owendale Intrusion. Meteoric water with intermediate Eh and pH and negligible dissolved species permeated the laterite profile, the Eh increased and pH decreased to conditions typical of lateritic soils. At this point, PGEs and Au went into solution as a part of the process of lateritisation, and were transported to a chemical interface between the ferruginous and saprolite zones that had lower Eh and neutral pH, causing deposition of PGEs and Au, and the formation of PGE-Fe alloys. Some of these alloys frequently become strongly magnetic with larger size. It is assumed that the temperature of the hydrothermal solution is in the range of 300°C–500°C (Bowles, 1986; Shi, 1995).

The PGE mineral systems that operated in the primary rocks and laterite profiles of the intrusions near Fifield are a good example of multi-stage mineralisation processes that involved primary high-temperature magmatic formation, low-temperature postmagmatic hydrothermal alteration, residual lateritic enrichment, and alluvial-placer deposition and preservation.

A number of studies have documented the genesis of PGE-bearing laterites in Australia and overseas. Witt and Barnes (1991), Gray et al. (1996), and Butt and Robertson (2003) describe the enrichment of PGEs in the regolith above the Ora Banda mafic-ultramafic sill in the Yilgarn Craton, and Cornelius (2005) studied the Yarawindah Brook PGE-Ni-Cu laterite deposit. Butt et al. (1992, 2006), Brand et al. (1998), and Elias (2002, 2006) review the geochemical expression of Ni-Co-PGE laterite deposits in different environments in Australia as a guide to developing appropriated exploration procedures.

Bowles (1986) describes examples of Pt-Fe alloy nuggets in laterite associated with the zoned Yubdo ultramafic massif in western Ethiopia, and alluvial-eluvial PGE nuggets believed to be derived from laterite overlying anorthosite of the Freetown Peninsula layered complex in Sierra Leone. Davies and Bloxam (1979) noted Pt levels up to 100 ppb in the Freetown laterites. Derkmann and Jung (1986) have reported anomalous Pt and Pd levels in Ni-laterite in Burundi, and Ahmad and Morris (1978) reported PGE-enriched A and B horizons from lateritic profiles in New Caledonia, Guatemala, and Indonesia. These studies have indicated the transport of PGEs and Au in solution is aided by conditions prevalent in the development of laterite, particularly where humic or fulvic acids are present. Bowles (1985, 1986) has shown that PGEs are mobile in laterite under very acid, chloride-rich conditions with a high Eh. The PGEs may also be mobilised by thiosulphate and sulphite complexes in neutral to alkaline solutions or as chloro-complexes in acid solutions during oxidation of sulphides (Plimer and Williams, 1987). Augé and Legendre (1994) showed that PGE oxides associated with the New Caledonia ophiolite complex may be derived from the alteration of magmatic PGM alloys and from primary crystallisation of oxides in laterite conditions. Their presence indicates the existence of mechanisms of transport and crystallisation of PGE (as oxide) in surface conditions, mechanisms contributing to the redistribution and enrichment of PGE in laterite.

### *Key references*

- Emerson et al. (1979): petrophysical and petrological study of the Flemington (Tout) Intrusion.
- Suppel and Barron (1986a,b); Suppel et al. (1987): regional geological setting, lithologies; PGE mineralisation; alluvial deposits; primary and secondary mineralisation; mineralogy of PGMs.
- Agnew et al. (1987): Tout and Owendale intrusions; petrology; geochemistry; mineralisation.
- Bowles (1989): preliminary mineralogy of platinum-bearing nuggets; Fifield nuggets; laterite profile at Owendale Intrusion.
- Johan et al. (1989, 1990a,b): Pt mineralisation; Fifield intrusions; characteristics; mineralised clinopyroxenite; placer deposits; laterite deposits; mineralogy of PGMs; isoferroplatinum nuggets; Milverton prospect; Owendale Intrusion.
- Derrick (1991): geological setting of the Tout Intrusion; mineralogy and geochemistry, primary and regolith-related mineralisation; regolith profile; Pt resources and potential.
- Elliott and Martin (1991): geology and mineralisation; Alaskan-type intrusions; Tout Intrusion; tectonic setting; alluvial deposits; Pt nuggets; petrogenesis and metallogenesis; lateritisation; geochemistry; geophysics; economic potential.
- Shi (1995): geochemistry of Fifield intrusions; stratigraphy; Syerston Intrusion; primary and secondary PGEs; Alaskan-type complexes; laterite mineralisation.
- Stojanovic (1995): petrology; geochemistry; isotope geochemistry; host rocks; PGE mineralisation.
- Teluk (2001): regional geological setting of Alaskan-type intrusions; geophysics; lithologies; mineralisation; exploration potential.
- Barron et al. (2004): geology of Fifield Alaskan-type intrusions; lithologies; stratigraphy, zonation; primary and secondary PGE mineralisation.
- Butt et al. (2006): laterites derived from Archean ultramafic rocks; petrogenesis; exploration.
- Elias (2006): lateritic Ni-deposits; Yilgarn Craton; economic potential.

## 6.4.10 Mineral-System Class 10: Placer

### 6.4.10.1 Deposit Type 10.A: Alluvial placers derived from 'Alaskan- and Urals-type' mafic-ultramafic intrusions

#### Overview

Historically, alluvial placer deposits (Colombia, Ecuador, Peru, Ural Mountains-Russia, western American states, and British Columbia: Weiser, 2002) dominated the world production of PGEs; this changed in the early 20<sup>th</sup> century when hard-rock deposits in South Africa and Russia commenced mining (see Section 1.3.1). Paleoplacer concentrations of PGEs are restricted to the Phanerozoic terranes of eastern Australia. They show a clear genetic and spatial association with 'Alaskan- and Urals-type' and 'Alpine- and ophiolitic-type' intrusions. No significant PGE-bearing placer, where the PGEs are sourced from Proterozoic or Archean age rocks, has been identified in Australia. Individual detrital PGM grains have been documented from drainage systems that incise Archean rocks in the Roebourne district of the west Pilbara Craton (Hudson and Horwitz, 1985), however, no placer deposits are known in these older terranes. This may simply be due to the poor preservation history of these old mineral systems, or it may reflect the dominant association of PGMs in the Archean being associated with sulphide assemblages. Such associations readily break down by chemical-physical processes in the weathering cycle, compared to the more resistant and refractory PGM-chromite associations that characterise the relatively younger alluvial systems of eastern Australia.

Paleozoic 'Alaskan-type' mafic-ultramafic intrusions in the Fifield district of central New South Wales (see Deposit Type 6.A) and the tectonically emplaced Paleozoic 'Alpine- and ophiolitic-type' ultramafic-mafic intrusions of western Tasmania (Deposit Type 5.A) have accounted for the majority of Australia's historical (pre-1960s) production of alluvial Pt and 'osmiridium', respectively. Deep leads near the township of Fifield, NSW, have been the most important source of Pt in eastern Australia. Total production from the three most significant leads—Platina, Fifield, and Gillenbine Tank—was 633 kg Pt and 178 kg of Au, with 75.8 kg of Pt obtained in the most productive year of 1896. Alluvial Pt and Au grains are found in Cenozoic gravels, buried leads, and recent alluvium derived from both gravels and leads. A typical gravel sequence consists of thick units of reddish loam and clay interspersed with patches of quartz rock and fragments of schistose and dolomitic rocks. The Pt- and Au-bearing gravels were concentrated in physical traps (gutters, depressions, gouges, etc) in the erosional surface of the basement Girilambone Group metasedimentary rocks. The mineralised gravels are considered to be of post mid-Miocene age. The principal PGM is isoferroplatinum, but the source(s) of the Pt-alloys is unknown. It is likely that a considerable amount of the precious metals were originally derived from the nearby Murga, Tout, and/or Owendale 'Alaskan-type' intrusions, and the Pt grains experienced a complex history of multiple transport and depositional events. Recent exploration in the Fifield region has also focussed on low-grade Pt (and Au) mineralisation in three major paleochannel systems—Owendale Lead, Milverton Lead, and Cincinnati Lead—associated with the Owendale Intrusion (Figure 6.37). The three paleochannels have entrenched and partially stripped the early- to mid-Cenozoic regolith, thus indicating a post mid-Miocene age.

#### *Australian deposits/prospects/hosts*

Owendale Intrusion (Lachlan Orogen, NSW); Wateranga (New England Orogen, Qld).

#### *Significant global example(s)*

Nizhny Tagil Complex, Katchkanar Complex, Konder Complex, Inagli Complex (all Russia); Goodnews Bay–Salmon River (Alaska); Tulameen Complex (Canada).

### *Type example in Australia*

Owendale Intrusion, New South Wales.

#### *Location*

Longitude 147.469850°E, Latitude -32.69219°S; 1:250 000 map sheet: Narromine (SI 55–03), 1:100 000 map sheet: Boona Mount (8332); ~15 km north of Fifield, New South Wales.

#### *Geological province*

Lachlan Orogen, New South Wales.

#### *Resources*

No resources have been published for alluvial PGE deposits associated with Alaskan- and Urals-type mafic-ultramafic intrusions in central New South Wales. However, junior exploration companies have defined Pt resources (Table 6.2) for laterite deposits associated with these intrusions, namely: Owendale North Prospect—31 Mt @ 0.52 g/t Pt, 0.15% Ni, 0.05% Co (Total Mineral Resource: Platina Resources Ltd (2014); Cincinnati Prospect—9 Mt @ 0.5 g/t Pt (Inferred Resource), 2.6 Mt @ 0.7 g/t Pt (Indicated Resource), 2.2 Mt @ 0.7 g/t Pt (Inferred Resource: Helix Resources Ltd., 2004b; Platina Resources Ltd., 2012; 2013a); and Milverton Prospect—1.3 Mt @ 0.6 g/t Pt (Inferred Resource: Platina Resources Ltd., 2013a).

#### *Current status and exploration history*

Prospects with advanced exploration. Most of the 'Alaskan-type' mafic-ultramafic intrusions of the Fifield region outcrop poorly, or not at all, many having been only discovered after the 1960s by the drilling of aeromagnetic anomalies. Prior to this period only a few intrusions had been recognised. The identification of the intrusions was facilitated by the release in 1961 of the first regional airborne magnetic survey by the Bureau of Mineral Resources (BMR: now called Geoscience Australia). The survey delineated many mafic and ultramafic intrusions concealed under shallow alluvium and laterite cover. Several junior exploration companies followed up these new findings with ground geophysical-geochemical surveys and shallow drilling programs. The hard-rock potential of the Fifield intrusions was initially highlighted in 1966 during a four-hole diamond-drill program of the Owendale Intrusion by Anaconda Australia Incorporated. High-grade Pt abundances (over 14 g/t Pt+Pd) in fresh pyroxenite from these drill-holes were confirmed some 20 years later by reanalysing of the core by New South Wales government geologists (Suppel and Barron, 1986a). It was during the 1980s that the Fifield–Nyngan belt of 'Alaskan-type' intrusions, which contain PGEs of geochemical significance, and in some cases of economic significance, was formally recognised (Elliott and Martin, 1991). Exploration programs in the Fifield region have since focussed on primary concentrations of Pt in ultramafic lithologies, alluvial deep leads of Pt, and Pt-Sc-bearing laterites.

In 1969–70, Platina Developments and Mines Search carried out an extensive drilling program on the Platina and Gillenbine Tank deep leads and the Cenozoic conglomeratic paleoplacer at Jack's Lookout. A total of 211 holes were drilled into the Platina Lead, but results were equivocal due to sampling problems associated with clay. CRAE in the late 1970s undertook a geomorphological, auger and RAB drilling program that defined a large subeconomic platiniferous zone associated with the Platina Lead. Gold Shamrock Mines Limited in the mid 1980s commenced the most comprehensive phase on the Fifield alluvials. Sampling programs evaluated areas outside and within the known leads.

During the mid-2000s, Rimfire Pacific Mining NL undertook extensive soil sampling, subsoil auger drilling, and trenching programs throughout the Platina and Gillenbine Tank lead region. They demonstrated the co-existence of coarse-grained Pt and Au in several locations and some platinum grains had a ragged form indicating derivation from local proximal sources of metal. Soil programs at the 'Ebenezer' prospect located ~500 m southeast of the Platina and Gillenbine Tank deep lead area, indicated that the Pt is derived from residual or semi-residual soils, not alluvium. Similar Pt anomalies were reported in residual soils at the 'Eastern Shear Zone' prospect near the Gillenbine Tank deep lead. The Pt anomaly at this prospect is continuous over 1 km and is parallel to the northeast-trending Gillenbine Tank Lead. Rimfire Pacific Mining NL has also investigated the bedrock source(s) for the Pt and Au near the deep-lead systems southeast of Fifield. Further details of the exploration history of the 'Alaskan-type' intrusions in the Fifield region can be found in Chapter 5.

### *Economic significance*

The Fifield district in central New South Wales was Australia's first significant producer of alluvial Pt in Australia. Platinum was found in 1887, but there was little production until the discovery of the Platina Lead in 1893. The three most important deep leads, the Platina Lead, Gillenbine Tank Lead, and the Fifield Lead, are located near the Tout and Murga mafic-ultramafic intrusions, about 15 km south of the Owendale Intrusion. Total production from the deep leads amounted to about 633 kg Pt and 178 kg of Au, with 75.8 kg of Pt obtained in the most productive year of 1896 (Appendix K).

### *Geological setting*

Sixty-four ovoid-shaped 'Alaskan-type' mafic-ultramafic intrusions have been recorded in a north-northwest-trending belt that extends from Fifield to just north of Nyngan in central New South Wales (Figure 6.35). This belt correlates with the Girilambone Anticlinorial Zone—one of the earliest tectonostratigraphic provinces of the Lachlan Orogen. The oldest outcropping unit of this province is the late Cambrian to Early Ordovician Girilambone Group, a northerly-trending metamorphosed flysch sedimentary sequence comprising slate, schist, phyllite, quartz greywacke, and quartzite, with minor basaltic amphibolite and calc-silicate amphibolite (Bowman et al., 1982; Elliott and Martin, 1991). The Girilambone Group is bounded to the east by late Silurian to early Devonian felsic volcanic and sedimentary rocks and to the west, middle Devonian sedimentary rocks of the Tullamore and Murga synclines. The 'Alaskan-type' intrusions typically form composite steep-sided plug-like bodies comprising a variety of alkaline mafic and ultramafic rocks. Linear alpine serpentinite bodies thought to represent the remains of a subduction zone active during the Ordovician are spatially associated with some of the larger zoned intrusions (e.g., Honeybugle). The 'Alaskan-type' intrusions were emplaced into the Girilambone Anticlinorial Zone during the late Ordovician to late Silurian. Elliott and Martin (1991) state the late Paleozoic period in the Fifield area was dominated by deep erosion that exposed the 'Alaskan-type' complexes. The Cenozoic Era was a period of intense weathering that resulted in the development of thick laterite profiles and erosional drainage incisions over some of the complexes. Soils, eluvium, sheet wash, and buried drainage channels containing gravel, sand, and clay overly most lithologies. The present topography of the Fifield region is flat to gently undulating, with rare outcrop and slight depressions over the 'Alaskan-type' complexes (Elliott and Martin, 1991).

A number of deep leads surrounding the township of Fifield have been the most important source of Pt in eastern Australia (Figure 6.37, Figure 6.58, and Figure 6.59).

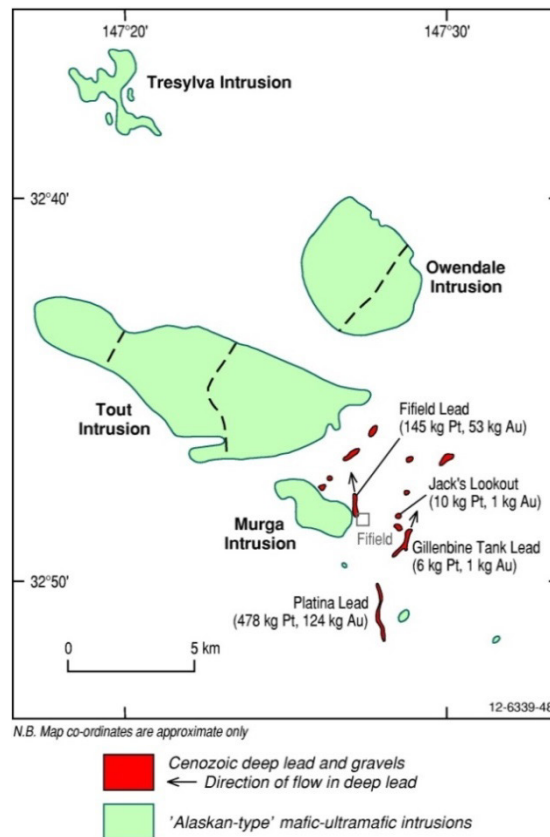


Figure 6.58 Cenozoic Platina Lead, Fifield Lead, and the Gillenbine Tank Lead, and the major 'Alaskan-type' mafic-ultramafic intrusions near Fifield, central New South Wales. Modified from Slansky et al. (1991).

Bowman et al. (1982) notes that the alluvial Pt and Au occurred in Cenozoic gravels, buried leads, and recent alluvium derived from both gravels and leads. The most important paleo-drainage system, the Platina Lead, 5 km south of Fifield, produced approximately 478 kg of Pt at grades of 5 g/t–13 g/t and 124 kg of Au at grades of 1.5 g/t–4.6 g/t (Teluk, 2001). The deep lead extended for approximately 3 km in a north-south direction, with the paleo-drainage direction towards the south. After its apparent confluence with the Un-Named Deep Lead from the west, the Platina Lead changed direction towards the south-southeast (Figure 6.58). The Pt- and Au-bearing gravels were less than 1 m-thick and occurred in traps in the erosional surface of the basement Girilambone Group metasedimentary rocks. The gravels outcrop at the northern end of the lead, but towards the south they were covered by up to 22 m of Quaternary cover. A typical sequence consisted of thick units of reddish loam and clay with quartz rock and fragments of schistose and dolomitic rocks. The distribution of the old workings indicates the deep lead varied from 20 m to 30 m in width. The principal PGM in the gravels is isoferroplatinum, but the source of the Pt-alloys and Au is unknown. The metals were probably derived from the Murga, Tout, Owendale intrusions (Figure 6.58) and they experienced a complex history of cycles of transport and deposition. Other platiniferous deep lead systems near Fifield, such as the Fifield Lead and the Gillenbine Tank Lead also produced minor quantities of alluvial Pt and Au. The 1 km-long, north-trending Fifield Lead (145 kg Pt, 53 kg Au) was a broad 200 m-wide channel less than 7 m-deep, whereas the longer Gillenbine Tank Lead (6 kg Pt, 1 kg Au) was about 2.5 km-long, 30 m-wide, and 27 m-deep (Figure 6.58 and Figure 6.59). Waterworn Pt and Au grains occur in ferruginous cement of a quartz-bearing conglomerate of possible Cenozoic age at Jack's Lookout (Flack, 1967). These conglomerates produced about 10 kg of Pt and 1 kg of Au.

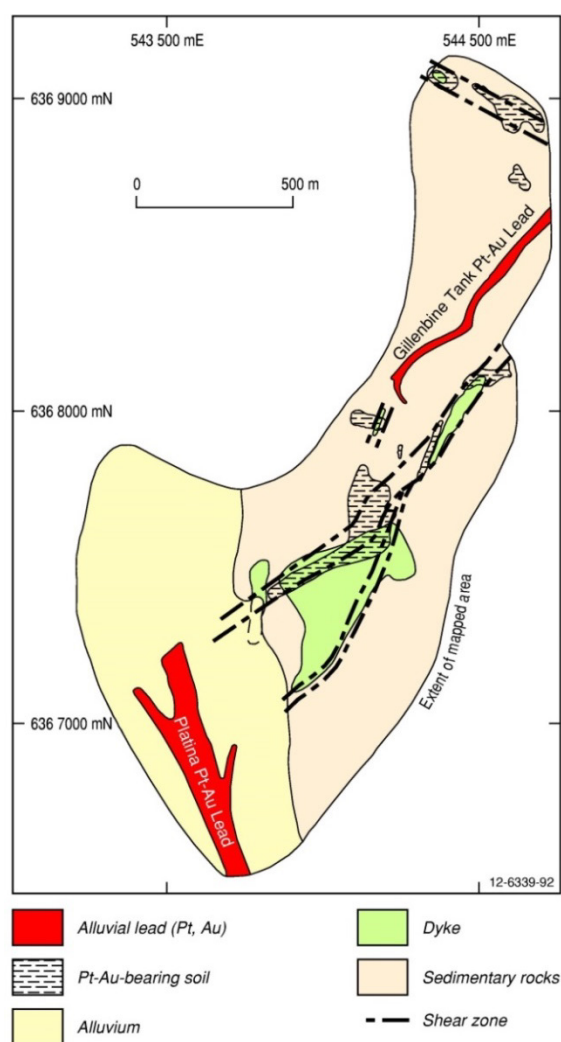


Figure 6.59 Geological setting of platinum-bearing deep leads in the Fifield region. Modified from Rimfire Pacific Mining NL (2006).

Investigations of potential bedrock source(s) for the Pt and Au near the deep-lead systems southeast of Fifield revealed evidence of structurally-controlled alteration and mineralisation events. Structural corridors evident in weathered bedrock coincide with the distribution of the 1920–1930s mining activities for Pt in the soil profile. Examinations of the excavated bedrock pavements and heavy-mineral concentrates from overlying gravels (Figure 6.60) revealed that:

- coarse-grained Pt occurs in bedrock often associated with shear and breccia zones and non-magnetic mafic and possibly ultramafic dykes;
- the breccia zones contain significant alteration and re-brecciation features;
- open stockworks of gossanous and sulphide-carbonate veinlets, and small patches of near massive oxidised sulphides are locally associated with an array of shear and breccia zones;
- the surface features of the Pt (isoferroplatinum) and Au grains from the overlying gravels and soils indicate two different travel distances of 0.1 km to 0.5 km, and 1.5 km to 4 km, respectively;
- the Pt and Au are derived from the same mineralising system;

- the grains are apparently primary as opposed to accreted in the weathering profile (i.e., they are not of supergene chemical origin) despite their coarse grain size (1 to 12 mm, and up to 7.4 g weight); and
- the Pt and Au grains (Figure 6.61 and Figure 6.62) are associated with magnetite, chromite, ilmenite, zircon, monazite, and cassiterite.

### *Mineralisation environment*

The Owendale Intrusion is a steeply plunging, pipe-like body with a surface area of ~55 km<sup>2</sup>. The major lithologies of the intrusion can be broadly subdivided into an: Ultramafic Series, a Mafic-Felsic Series, and a Marginal Series (Raedeke, 1988; Elliott and Martin, 1991). The Ultramafic Series occupies about one-third of the complex, with dunite, wehrlite, and pyroxenite prominent in the eastern and southern parts of the intrusion. The Ultramafic Series hosts several primary hard-rock, residual-laterite, and paleoplacer PGE deposits at North Owendale (northeast), Cincinnati (east), and Kelvin Grove (south). Poorly developed cyclical layering on a scale of several metres to tens of metres show a general increase in olivine from clinopyroxenite to wehrlite towards the centre of the complex. All rocks of the intrusion are weathered to depths from a few metres to 80 m and are covered by a thin veneer of soil and clay/sand/gravel alluvium up to 40 m-deep.



*Figure 6.60 Mining (scoping) operations of platinum-bearing alluvial gravels at the Platina Lead near Fifield, central New South Wales. (a–c). After the removal of overburden, the platinum-bearing alluvial gravels are collected down to the weathered basement rocks in Blocks A, B, C, and D of Pit One. (d). Gravity plant for concentrating platinum and gold from low-clay gravels. All photographs provided by John Kaminsky, Executive Chairman, Rimfire Pacific Mining NL.*

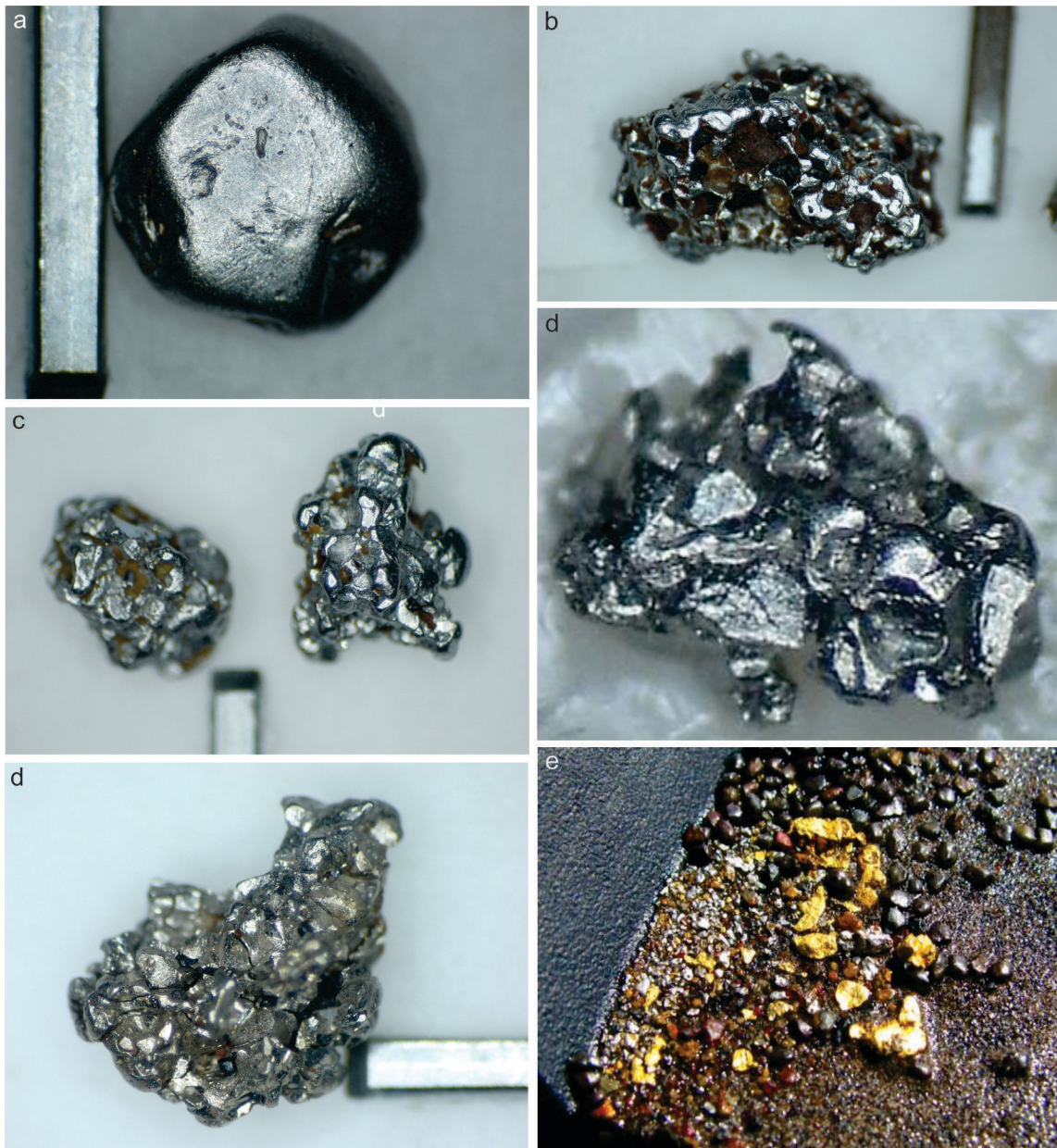


Figure 6.61 Alluvial platinum and gold grains and nuggets from deep leads in the Fifield region, New South Wales. Width of metal bar is ~0.5 mm. (a). Subrounded platinum grain showing abrasion and pitted surface features. (b–d). Angular to indented platinum grains that probably travelled short distances from their source(s). (e). Platinum and gold nuggets recovered from a mixed ironstone concentrate. Additional platinum and gold are also encased within the ironstone. All photographs provided by John Kaminsky, Executive Chairman, Rimfire Pacific Mining NL.



Figure 6.62 Alluvial native gold nuggets from the Fifield region. Field of view is approximately 20 mm wide. Photograph provided by Helix Resources NL.

### *PGE mineralisation*

Low-grade Pt (and Au) mineralisation occurs in poorly sorted gravels in paleochannels overlying and immediately adjacent to the Owendale Intrusion. Three major Pt-Au-bearing paleochannels have been identified (Elliott and Martin, 1991):

- Owendale Lead—northeasterly-trending paleo-valley up to 3 km-wide across the centre of the intrusion;
- Milverton Lead—a 1.5 km-wide sub-parallel paleovalley up to 30 m deep traverses the southeastern corner of the intrusion; and the
- Cincinnati Lead—a smaller 100 m-wide northerly-trending channel along the eastern margin of the intrusion that flows into the main Owendale Lead.

The three mineralised paleochannel systems have entrenched and partially stripped the early- to mid-Cenozoic regolith, thus indicating a post mid-Miocene age. The paleochannels appear to have their headwaters in the Tout Intrusion immediately to the south of the Owendale Intrusion, thus it is possible the source(s) of the alluvial Pt is from the Tout and/or Owendale intrusions. In particular, the Pt could be derived from the residual laterite profiles overlying these complexes. Sediments in the paleochannels comprise clay, sand, and poorly sorted gravel horizons that contain clasts of subrounded to angular vein quartz, goethite, and rare igneous rocks derived from the intrusions. Most clasts are 1 to 2 cm across with rare examples attaining 10 cm. Platinum grains in the deep leads are typically concentrated in gravel horizons overlying erosional unconformities at the base of the channels, or within the channels where a period of deposition has been followed by subsequent erosional and redepositional events. Maximum Pt grades of 0.14 g/loose cubic metres were obtained from bulk sampling of gravels at the Milverton Lead, and alluvial material from RAB holes at the Owendale Lead had grades of up to 0.4 g/t Pt. Typically the Pt grains have a bimodal size distribution, with most grains less than 1 mm, and a coarse fraction from 1 mm to 2 mm, with some examples of centimetre-sized nuggets. The degree of rounding for the grains ranges from angular to subrounded. Over 90% of the grains are isoferroplatinum (Pt<sub>3</sub>Fe). Alloys of Os-Ir-Pt, cuprorhodsite, bowieite-kashinite (Rh, Ir, Pt, Cu, Fe, Os, S, As-bearing minerals), and Pd and Rh-Pd arsenides occurring as inclusions in isoferroplatinum were identified by Johan et al. (1990a,b). Irregular nuggets of Au up to 5 mm-long comprise less than 30% of the precious metals from the Milverton Lead. The Au is probably derived from quartz veins in schist country rocks (Girilambone Group).

### *Age of mineralisation*

The three major mineralised paleochannel systems in the Owendale Intrusion have entrenched and partially stripped the early- to mid-Cenozoic regolith, thus indicating a post mid-Miocene age.

### *Genesis*

Microprobe studies of Fifield Pt and Au nuggets (Figure 6.61 and Figure 6.62) by Johan et al. (1989) indicate they are of primary high-temperature origin (based on iridosmine and osmiridium exsolutions in the isoferroplatinum), and mineralogically are similar to alluvial Pt derived from the Nizhny Tagil Complex in the Urals. Various studies on the Platina, Gillenbine Tank, and Fifield leads indicate that these deep leads are unlikely to be derived from a pre-existing paleo-placer and the nuggets are not of secondary supergene origin. Most results point to an unrecognised source and style of Pt mineralisation.

### *Key references*

- Suppel and Barron (1986a,b); Suppel et al. (1987): regional geological setting, lithologies; PGE mineralisation; alluvial deposits; primary and secondary mineralisation; mineralogy of PGMs.
- Agnew (1987) and Agnew et al. (1987): Tout and Owendale intrusions; petrology; geochemistry; mineralisation; genesis.
- Horwitz (1988b): mineralised alluvial channels; Fifield, Tullamore, Tottenham, and Honeybugle area; geological settings.
- Johan et al. (1989, 1990a,b): Pt mineralisation; Fifield intrusions; characteristics; mineralised clinopyroxenite; placer deposits; laterite deposits; mineralogy of PGMs; isoferroplatinum nuggets; Milverton prospect; Owendale Intrusion.
- Derrick (1991): geological setting of the Tout Intrusion; mineralogy and geochemistry, primary and regolith-related mineralisation; regolith profile; Pt resources and potential.
- Elliott and Martin (1991): geology and mineralisation; Alaskan-type intrusions; Tout Intrusion; tectonic setting; alluvial deposits; Pt nuggets; petrogenesis and metallogenesis; lateritisation; geochemistry; geophysics; economic potential.
- Slansky et al. (1991): geology of Alaskan-type intrusions near Fifield; placer deposits; formation and distribution of PGMs; genesis of alluvial Pt deposits.
- Shi (1995): geochemistry of Fifield intrusions; stratigraphy; Syerston Intrusion; primary and secondary PGEs; Alaskan-type complexes; laterite mineralisation.
- Stojanovic (1995): petrology; geochemistry; isotope geochemistry; host rocks; PGE mineralisation.
- Teluk (2001): regional geological setting of Alaskan-type intrusions; geophysics; lithologies; mineralisation; exploration potential.
- Barron et al. (2004): geology of Fifield Alaskan-type intrusions; lithologies; stratigraphy, zonation; primary and secondary PGE mineralisation.

## **6.4.11 Mineral-System Class 11: Astrobleme-related**

### **6.4.11.1 Deposit Type 11.A: Massive, vein, and disseminated Ni-Cu-PGE sulphides in mafic-ultramafic-felsic rocks and impact melts**

No confirmed examples documented in Australia.

# 7 Principal features of platinum-group-element mineral systems

Subhash Jaireth and David L. Huston

## 7.1 Introduction—what is a mineral system?

Mineral deposits form through the coincidence of favourable geological processes within a given spatial setting and at a specific geological time. By analogy with the concept of a petroleum system (Magoon and Dow, 1991), processes that form a mineral deposit can collectively be termed a mineral system. Wyborn et al. (1994a) defined a mineral system as *'all geological factors that control the generation and preservation of mineral deposits.'* Since this initial definition, the concept of a mineral system has evolved and a number of different formulations of this concept have been developed (e.g., Knox-Robinson and Wyborn, 1997; Barnes et al., 1999; Barnicoat, 2006; McCuaig et al., 2010; Huston et al., 2012). However, all formulations, in one form or another, include geological setting, timing and duration, the source(s) of the mineralising fluid and its components, the pathway upon which the fluid flows, the depositional (or trap) site, and post-depositional modifications. Although the mineral-system concept was developed mainly as a conceptual framework for hydrothermal mineral deposits, most components can be applied to orthomagmatic mineral deposits, which are the major global source of PGEs (see Section 1.3.1).

In recent years, a mineral-system approach has been gaining greater acceptance in mineral exploration. This is particularly apparent given that it is widely recognised that most mineral deposits with prominent surface signatures have been found, and that the future challenges relate to exploring mineralised environments under cover. McCuaig et al. (2010) have suggested three key challenges relating to the translation of the mineral-system approach into an effective exploration targeting system, namely:

1. identifying proxies for system components;
2. applying these at the right scale; and
3. making the transition from prediction to detection.

For many mineral systems, the first process of concentration was the initial chemical differentiation of the Earth (orange box in lower left of Figure 7.1). Based upon the concentration estimates of the core, mantle, and crust of McDonough (2004), Palme and O'Neill (2004), and Rudnick and Gao (2003), many commodities of economic interest (e.g., Sn, W, Ta, Pb, U, and REE) are highly enriched in the crust relative to the bulk Earth, whereas other commodities are only weakly enriched in the crust (e.g., Zn), and others are not significantly fractionated (e.g., Ag). Some elements are fractionated into the mantle and core, either moderately (e.g., Cu) or strongly (e.g., Ni, PGEs: see below). A small number of commodities (e.g., Au and Mo) have a complex distribution, being enriched in the core and crust relative to the mantle.

An unusual characteristic of PGEs and Ni relative to other commodities of economic interest is that bulk Earth concentrations of these elements are of ore grade. The solid Earth concentration of Pt is 1900 ppb and for Ni it is 18 200 ppm (McDonough, 2004). However, most PGEs (and Ni) are

inaccessible, being concentrated in the Earth's core (5700 ppb Pt, 52 000 ppm Ni) and mantle (6.6 ppb Pt, 1860 ppm Ni: McDonough, 2004; Palme and O'Neill, 2004). Platinum-group elements and Ni are highly depleted in the continental crust (1.5 ppb Pt, 59 ppm Ni), particularly in the upper crust (0.5 ppb Pt, 47 ppm Ni: Rudnick and Gao, 2003), making some connection with an ultimate mantle (or core) source imperative in most (or all) PGE-bearing mineral systems and deposits hosted by crustal rocks.

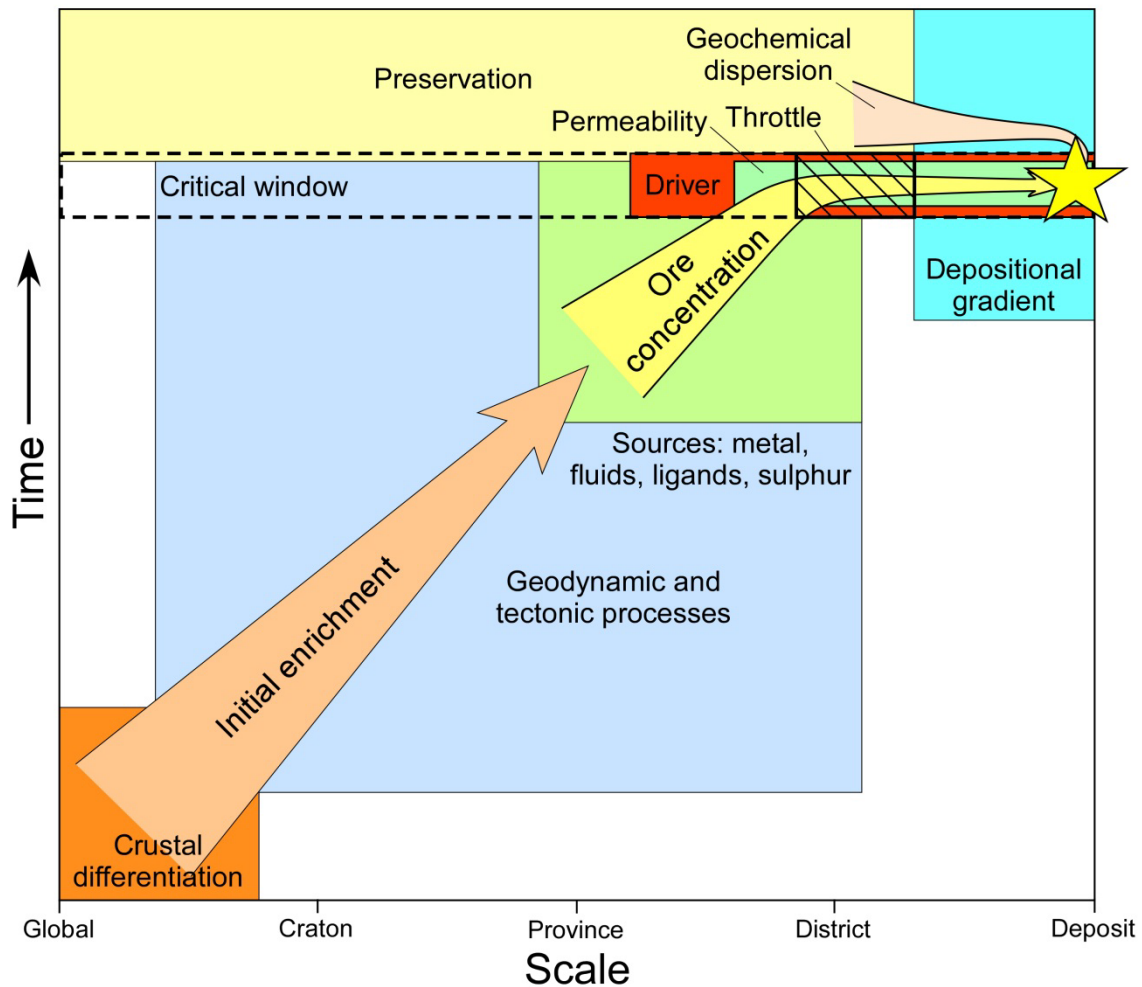


Figure 7.1 Schematic diagram illustrating the evolution of a mineral system in time and in space. Most mineral systems commence through chemical fractionation of metals within the Earth. This happens either through the initial fractionation of the Earth to form the crust, following by further fractionation and enrichment caused by tectonic processes (light-brown arrow). These processes produce a source region (green box) that is enriched in metals. Subsequently, fluids, either generated within the source region (e.g. magmas or metamorphic fluids) or derived externally (e.g., seawater, basinal brines of meteoric waters) extract the metals from the source region and move them to a depositional zone (yellow arrow). This fluid migration occurs along pre-existing permeable zones (faults or aquifers) or structures formed at the time of fluid migration. Fluid migration occurs during a restricted time frame, the “critical window” in response to a driver (red box) than can be tectonic in origin. The fluids are commonly throttled by a restriction in the fluid flow path into the zone of deposition, where chemical and/or physical gradients cause ore deposition. The spent fluid then escapes the site of deposition and can cause geochemical dispersion that aids in exploration. A final, but essential, part of the mineral system is preservation, whereby the mineral deposit formed by the mineral system is preserved from destruction by erosion or tectonic processes.

Following the initial chemical differentiation of the Earth, tectonic processes (blue box in Figure 7.1) further fractionate and enrich commodities (light-brown arrow in Figure 7.1) within the crust and upper mantle. These processes, which operate at the cratonic- to province-scale, generally occur along convergent or divergent margins, and can include processes, such as mantle metasomatism during subduction, the formation of a mafic underplate, and many others. The combination of the initial global chemical differentiation and subsequent tectonic enrichment associated with magmatic and metasomatic processes, along with surficial processes (e.g., weathering and sedimentation) in some cases, produces regions in the upper mantle and crust that act as sources of commodities (green box in Figure 7.1) that are concentrated into mineral deposits by magmatic and/or hydrothermal processes (yellow arrow in Figure 7.1). It is important to note that in many cases, commodity-source regions form millions to hundreds of millions of years prior to the actual mineralisation events in the crust.

The final concentration of commodities by magmatic and/or hydrothermal or magmatic processes generally occurs during a critical window in time during which either magmas or hydrothermal fluids are driven along structures, or other zones of permeability. Drivers of magma/fluid flow (red box in Figure 7.1) are quite diverse, although in many cases they have a tectonic trigger. These drivers can include temperature gradients induced by magmatism (which produce hydrothermal convection), the buoyancy of magmas, the evolution of magmatic-hydrothermal fluids during magma crystallisation, metamorphic devolatilisation during contact or regional metamorphism, formation and expulsion of basinal brines, or hydraulic pressure gradients caused by contractional or extensional deformation. The magma/fluid-flow pathways commonly form synchronous with, or prior to, magma/fluid movement during emplacement of magma, or during development of the rock package through which the fluids move.

In addition to these mineral-system requirements, formation of significant mineral and ore deposits requires features that can cause deposition or trapping of the commodities of economic interest. For PGE-Ni-Cu deposits these features are closely related to sulphide saturation of magma and separation of sulphide liquid.

Figure 7.2 illustrates one of the several conceptual models for the functioning of a mineral system related to the formation of PGE deposits (Mungall and Naldrett, 2008). As shown by this schematic diagram, a mineral system involves the concentration of mineral commodities through a number of different processes to the point at which the concentration is sufficient to consider exploitation. When the commodities can be extracted economically, the product of a mineral system is an ore deposit (it must be borne in mind that most mineral systems do not form ore deposits). Processes that concentrate mineral commodities operate at scales that range from global to the microscopic and can involve crustal differentiation; magmatism including melting of the mantle, fractionation, crystallisation, crustal contamination, sulphide saturation, immiscibility, and magmatic-hydrothermal fluid evolution; hydrothermal leaching and deposition processes; physical processes of density separation; and post-depositional enrichment and preservation.

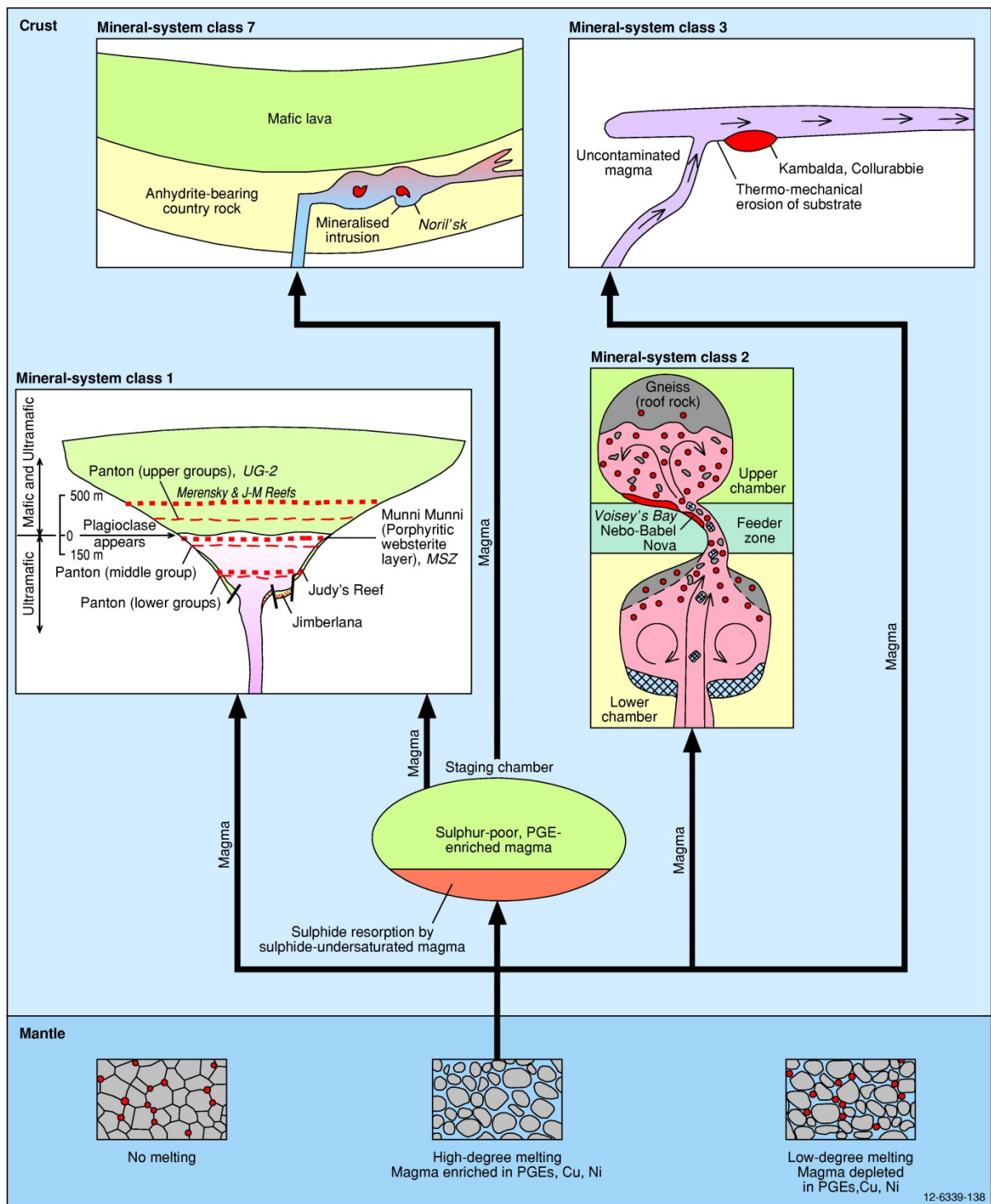


Figure 7.2 Schematic diagram showing significant processes for generating platinum-group elements, nickel, copper mineral systems. Fertile magmas are produced from high-degrees of partial melting of the mantle. PGE-enriched systems require production of sulphur-poor, PGE-enriched magma in a deep-seated staging chamber. Red filled circles and zone represent sulphide liquid and/or mineralised zones. Mineral-system class 1: Layered tholeiitic mafic-ultramafic intrusions; Mineral-system class 2: Massive to poorly layered tholeiitic mafic-dominated intrusions; Mineral-system class 3: Komatiitic flows and related sill-like intrusions; Mineral-system class 7: Continental flood basalts with associated sub-volcanic sills. Modified from Lesher (1989); Li and Naldrett (1999); Hoatson et al. (2006); and Mungall and Naldrett (2008).

In many orthomagmatic and hydrothermal mineral systems, the mineralising processes produce zones (or haloes) of anomalous geochemistry that extend well beyond the economic limits of the ore zones. Such zones of anomalous chemical properties are extremely useful as exploration indicators since they can significantly increase the 'footprint' signature of the mineral deposit. These zones can involve enrichment of ore and related elements or, in some cases, zones depleted in other metals. The zones can extend vertically above and below, or laterally away from, mineral deposits and are integral parts of the mineral systems. In addition, the chemical alteration that produces these zones can significantly change the physical properties of the affected rocks. This most commonly involves changes to the magnetic or electrical properties of the affected rock, although it can also change density. Hypogene geochemical dispersion and physical property changes are also useful in exploration as they potentially increase the detection dimensions of individual mineral deposits.

The last aspects of a mineral system, which are often not considered in prospectivity analyses, are post-depositional processes that can have major effects on the preservation and economic viability of mineral deposits. Post-depositional processes, such as metamorphism and supergene processes, can upgrade mineral deposits to form ore deposits. Either metamorphism coarsens ore minerals to allow greater recovery of commodities, or supergene processes enrich certain commodities (e.g., Cu, Pb, Ag, and Au) during weathering. Weathering processes can also enhance geochemical dispersion, increasing the detectable surface 'footprint' of mineral deposits.

## 7.2 Stages in the formation of platinum-group element and nickel-copper mineral systems

The geochemical behaviours of PGEs are described in Chapter 3. Section 3.3 of that chapter highlighted the fact that the PGEs are highly chalcophile elements, being significantly more chalcophile than Cu and Ni. However, the Pd-subgroup of PGEs (Pd, Pt, Rh) are slightly more chalcophile than the Ir-subgroup (Ir, Ru, Os), which is thought to explain a closer association of Ir-subgroup elements with chromite relative to sulphide. As PGEs are very chalcophile, the origin of PGE-bearing mineral systems is largely controlled by the geochemical behaviour of S through the evolution of the mafic-ultramafic magmatic cycle (i.e., partial melting, interaction of magma with crustal rocks during ascent, and crystallisation of host magma). A fertile PGE-mineral system requires favourable conditions at each of the following three stages of magma evolution (Figure 7.2):

1. **Partial melting of mantle:** The degree of partial melting and the depth at which melting of mantle occurs can influence the S and metal (PGEs, Ni, Cu) contents of magma (Arndt et al., 2005). Metal-bearing mafic or ultramafic parental magmas from the mantle generally represent high degrees of partial melting (>30%), have relatively high-MgO contents, and are sulphide undersaturated during their ascent to the crust. The depth of partial melting is important because the solubility of S in mafic magma decreases with increasing pressure. As a result, most magmas become sulphide undersaturated as they ascend through the lithosphere. Tholeiitic picrites are generated from moderate degrees of partial melting (~30%) at intermediate depths of ~100 km. This degree of partial melting is sufficient to remove all the sulphide in the source and therefore almost all PGEs, Cu, and some Ni. The magma is sulphide undersaturated at the source and becomes more undersaturated as it reaches the crust. Alkali picrites on the other hand are formed from very low degrees (<5%) of partial melting, and hence most sulphides and thereby PGEs, Cu, and Ni remain trapped in the source residue. Tholeiitic basalts are also produced from low degrees of partial melting

(<10%), but from shallower depths (<50 km). They too leave most of the sulphides and ore-forming elements (PGEs, Ni, Cu) in the residual material at the site of melting.

Al-depleted komatiites (Barberton-type) are formed from a moderate degree (~30%) of partial melting of a mantle source enriched, or slightly depleted, in Ca-Al at depths exceeding 200 km (Arndt et al., 2005) or 300 km (Maier et al., 2009). Their Al-depletion is caused by retention of majorite garnet in the source (Maier et al., 2009). These magma-types are known to have lower contents of PPGE-subgroup elements because at moderate degrees of partial melting, some of the sulphides are retained in the source rock. Al-undepleted komatiite (Munro-type) magmas, on the other hand, are produced from a higher degree (~50%) of partial melting of the mantle at relatively shallower depths (<200 km). These magmas are able to consume most of the sulphide in the mantle source and therefore they have higher abundances of PPGE-subgroup elements. The contents of IPGE-subgroup elements in both types of komatiitic magmas are similar. Thus both tholeiitic picrites and komatiitic magmas have the potential to generate fertile PGE, Ni, and Cu mineral systems.

2. **Ascent of magma and assimilation of crustal material:** As the solubility of S in mafic magmas increases with a decrease in pressure, magmas generated in the upper mantle become progressively sulphide undersaturated as they rise through the crust. Assimilation of felsic and/or S-bearing rocks can cause sulphide saturation, triggering removal of PGEs, Cu, and Ni from the magma. Assimilation of crustal material in a deep-staging chamber has been argued for large PGE-bearing mineral systems, such as Merensky Reef and Noril'sk (Naldrett et al., 2008, 2009, 2011; Li et al., 2009). Interaction of sulphide liquid generated from sulphide saturation of mafic magma in the staging chamber with successive batches of sulphide-undersaturated mafic magma can produce PGE-rich (>~200 ppb) magma, thought to be essential for forming PGE-enriched zones in the main magma chamber (Bushveld Intrusion) and in intrusions located in the feeder zones of mafic volcanics (Noril'sk). According to the multistage-dissolution upgrading model proposed by Kerr and Leitch (2005), sulphide-undersaturated magma on reaction with sulphide liquid in the staging chamber begins to dissolve the sulphide liquid. As a result, PGEs, Cu, and Ni, which are more chalcophile than FeS, remain in the sulphide melt, gradually enriching it with these metals and depleting it in S.
3. **Crystallisation of magma and sulphide saturation:** In order to form a PGE deposit it is essential that fertile magmas become saturated with sulphide at, and/or close to, the site of mineralisation (large magma chambers favourable for mixing of magmas or feeder zones of intrusions). The timing of sulphide saturation (early or late) is not so critical for Ni-Cu deposits because Ni and Cu are far less chalcophile and more abundant than the PGEs. Sulphide saturation can occur due to thermal erosion of sulphidic sediments (komatiitic deposits), assimilation of evaporites (perhaps Noril'sk), fractional crystallisation and mixing of various pulses of magma (Bushveld, Stillwater, Munni Munni, Panton). A common feature of all giant PGE mineral deposits is that they result from dynamic and relative open-magmatic systems, which involved several pulses of magma emplacement and magma mixing as evidenced by the presence of chromitite layers (in layered intrusions) and multiple generations of co-magmatic lavas and intrusions.

The grade and size of the PGE deposit can vary depending on the quantity of immiscible sulphide liquid, and on the site of its accumulation. Segregation of very small quantities of sulphide can produce zones of low-tonnage ore with low grades. On the other hand, very large quantities of sulphide may result in the formation of relatively large sulphide-rich zones with low grades of PGEs. Therefore the generation of small quantities of sulphide layers enriched in PGEs requires a delicate balance to attain

the right amount of excess sulphide liquid (Mungall and Naldrett, 2008). Accumulation of sulphide liquids at the base of the body of silicate melt, or within flattened parts of magma conduits, are thought to be more favourable to form economic concentrations of PGEs (Mungall and Naldrett, 2008).

Nickel-Cu mineral systems associated with komatiites (Kambalda- and Mount Keith-style) and with massive to poorly layered tholeiitic intrusions (Voisey's Bay-style) generally do not contain economic-grade concentrations of PGEs, although their magmas generally undergo late (close to the site of mineralisation) sulphide saturation. This may be partly related to the fact that the geodynamic setting of magmatic systems is such that it does not allow generation of staging chamber(s) thought to be essential in producing PGE-enriched (>~200 ppb) deposits by S-depleted magmas. Genetic models for Ni-Cu deposits associated with massive to poorly layered tholeiitic intrusions (Voisey's Bay-style) postulate sulphide saturation in a mid-crustal chamber (Naldrett, 2004). It is possible that most PGEs are stripped from mafic magmas in this chamber, and conditions in the chamber are such that the multistage-dissolution upgrading model proposed by Kerr and Leitch (2005) does not operate effectively to form PGE-enriched magma.

### 7.3 Mineral-system features of platinum-group element and nickel-copper mineral deposits

A classification of PGE mineral occurrences in Australia based on a general mineral-systems framework was used in Chapter 6. In that chapter, the type example of nineteen PGE deposit types was described in detail. In this chapter we summarise the principal features of significant PGE-forming mineral systems using global and Australian examples. The mineral-system concept is presented consistently under a series of headings (i.e., template) to cover the geological setting (including architectural and tectonic setting); age and duration of mineralisation; source(s) of melts and/or fluids; commodities and driving energy; the magma and/or fluid pathway; the trap or depositional site; and preservation. As timing of sulphide saturation is one of the most important constraints for the formation of economic-grade mineralisation, information about this mineral-system component is also included.

Although there are a large range of mineral systems that can or have produced economically viable PGE concentrations around the world, we have concentrated upon those we consider to be most likely to form economic PGE-Ni-Cu and Ni-Cu-PGE deposits (the PGEs either as the major product, a co-product, or a by-product) in Australia. The potential mineral systems described in this chapter are associated with:

- layered tholeiitic mafic-ultramafic intrusions (Section 7.3.1);
- massive to poorly layered tholeiitic mafic-dominated intrusions (Section 7.3.3);
- komatiitic flows and related sill-like intrusions (Section 7.3.5);
- 'Alpine- and ophiolitic-type' ultramafic-mafic intrusions (Section 7.3.7);
- 'Alaskan- and Urals-type' mafic-ultramafic intrusions (Section 7.3.9);
- hydrothermal-metamorphic fluids (Section 7.3.11); and
- sub-volcanic sills associated with continental flood basalts (Section 7.3.13).

Each of the above sections is followed by assessment criteria (regional- and local-scales), which can be used in association with the exploration guidelines summarised in Chapter 8 for delineating areas prospective for these mineral systems in Australia. An important step for that analysis will be to identify regional- and local-scale datasets in which the presence or absence of the critical criteria can be

mapped. For each assessment criteria section, regional-scale criteria generally apply to whole provinces; while local-scale criteria apply to the scale of an individual intrusion or complex.

The challenges of identifying unique features that characterise world-class or giant mineral systems are involved and complex, and only in recent years has some significant progress been made in defining these features (Naldrett, 1991, 1994, 2008, 2011; Li et al., 2001; Zhang et al., 2008; Schulz et al., 2010; Zientek, 2012; Barnes and Fiorentini, 2012).

### **7.3.1 Mineral-system features of platinum-group-element deposits associated with layered tholeiitic mafic-ultramafic intrusions**

**(Deposit Types: 1.A—Stratabound PGE-bearing sulphide layers; 1.B—Stratabound PGE-bearing chromitite layers; and 2.B—Stratabound PGE-bearing magnetite layers)**

#### ***Geological setting***

- Stabilised intracratonic and Proterozoic orogenic zones; some complexes may be related to mantle plumes.
- Large, differentiated, layered mafic-ultramafic intrusions emplaced at mid- to upper-crustal levels. Generally unmetamorphosed to partially metamorphosed (intrusions in the Baltic Shield are metamorphosed to amphibolite facies).
- High proportion of ultramafic to mafic rocks in the layered complex.
- The PGEs are associated with predominantly disseminated sulphides (1%–3% pyrrhotite, chalcopyrite, and pentlandite), massive chromite, and more rarely with massive Fe-Ti-V oxides. Mineralisation occurs in laterally extensive stratabound sulphide-, chromite-, and magnetite-bearing layers.
- The economically most important sulphide- and chromite-bearing layers are commonly located near the contact between the ultramafic and gabbroic zones of the intrusion; the PGE-bearing magnetite layers are hosted by evolved gabbroic rocks from high stratigraphic levels in the intrusion.

#### ***Age and duration of mineralisation***

- Any age from Archean to Mesozoic. However, large economic deposits are generally associated with Archean (<2700 Ma) and Early Proterozoic (>1800 Ma) complexes.
- Duration: Between 5 million and 10 million years.

#### ***Source (melt/fluid, metal, energy)***

##### **Melt**

Two types of melts can be involved (U-type and T-type):

1. **U-type:** High-magnesian basalt (or siliceous high-magnesian basalt: SHMB): The magma is thought to be formed either by two-stage melting in the mantle, or by assimilation of crustal material by a mantle-derived magma; and
2. **T-type:** Tholeiitic: partial melting of mantle.

## **Metals and sulphur**

- PGEs: Predominantly high-magnesian basalt or SHMB (at Bushveld, this magma contains nearly 3 times more S and 1.5 to 2 times more PGEs than the tholeiitic magma).
- Cu, Ni: Both high-magnesian basalt and tholeiitic basalt.
- S: Both high-magnesian basalt and tholeiitic basalt. Some S can be sourced from crustal rocks.

## **Melt/fluid pathway**

For igneous complexes: Major deep crustal (lithospheric?) structures. At shallow level, complexes controlled by ring fractures (e.g., Thabazimbi–Murchison lineament at Bushveld). Stillwater Intrusion may have been emplaced along an unconformity or a fault zone. Layered intrusions in the Baltic Shield are located along the boundaries of Proterozoic rifts.

## **Trap**

### **Structural**

- Minor role. Shape of the magma chamber can influence mixing of magma pulses in the chamber, thereby determining R-factor (magma/sulphide ratio: see Section 3.4.2).

### **Chemical**

Attainment of sulphide saturation is the most critical factor. It can be achieved in the following ways.

- In closed-magma chamber (closed system), such as the Skaergaard Complex.
  - Sulphide-saturation can be caused by extensive fractional crystallisation. Build-up of S concentration in the magmas is thought to be caused by a drop in pressure inside the chamber which increases S solubility (Andersen et al., 2002).
- In open-magma chamber (open system), such as the Bushveld Complex.
  - Mixing of successive pulses of magma (SHMB magma in the chamber mixing with fresh pulses of hot, buoyant tholeiitic magma). Fractionation of plagioclase in the tholeiitic magma increases the density of the melt in the chamber which results in instability and wide-scale magma mixing in the chamber that creates conditions for a high R-factor.
  - For PGEs in sulphides associated with chromitite layers (such as UG-2), mixing Cr-rich mafic magma with relatively more felsic magma triggers crystallisation of chromite. This can also cause sulphide saturation and accumulation of PGEs.
  - Introduction of new pulses of magma in the chamber can cause temporary increase in pressure inside the chamber causing lowering of S solubility in the magma already in the chamber. This can trigger sulphide-saturation and separation of sulphide liquid capable of concentrating PGEs (Cawthorn, 2005b).

## **Relative timing of sulphide saturation**

Magma intrudes the chamber in a sulphide unsaturated state and undergoes sulphide saturation in the chamber.

## **Preservation**

Post-emplacement tectonic history is important to expose mineralised layers to shallower depths. Many complexes are faulted and deformed (layers steep dipping and overturned).

## **Key references**

Schissel et al. (2002); Barnes and Maier (2002); Naldrett (2004); Cawthorn (2005a,b); Naldrett et al. (2011); Maier et al. (2013).

## **7.3.2 Assessment criteria for layered tholeiitic mafic-ultramafic intrusions**

### **Regional scale**

- Central portions of stable cratons (most deposits are located within ~50 km inboard from the craton margin) and within Proterozoic Orogenic zones (particularly for stratabound PGE-bearing chromitite layers) bordering stable Archean cratons.
- Proximity to deep-seated large faults and lineaments.
- Large layered mafic-ultramafic complexes (area >~10 km<sup>2</sup>; thickness >~5 km).
- High ultramafic/mafic rock ratio.
- Layered complex showing injection of several magma pulses (several chromitite layers in the lower parts of the complex and magnetitite layers in the higher parts).
- Siliceous high-magnesian basalt or high-magnesian basalts or boninitic rocks.
- Rock representing parent magma (from chilled rock at the margin, if accessible) with MgO >10%.
- Signs of late (inside magma chamber or in the staging magma chamber) sulphide saturation. An approximate estimate can be determined using S concentrations in unaltered mafic and ultramafic rocks. Presence of rocks with both >400 ppm and <400 ppm S. If all rocks in the complex show values >400 ppm S, it may indicate sulphide saturation throughout the complex and potential for Ni-Cu-Co-PGE mineralisation (see Section 7.3.3). Presence of disseminated sulphides in some, but not all rocks may also be indicative of late sulphide saturation.
- Presence of S-rich country rocks intruded by the complex.

### **Local scale**

- Appearance of plagioclase cumulates near the contact between mafic-ultramafic (at the base) and mafic rocks (at the top).
- Presence of olivine and bronzitite pegmatoid rock at the base of mineralised cyclic unit.
- Evidence of magma mixing in the chamber:
  - cryptic variation/reversals in the normal fractional crystallisation sequence of rock indicated by changes in the Mg# of orthopyroxene, An-number of plagioclase, <sup>87</sup>Sr/<sup>86</sup>Sr ratio of rocks.
- Signs of late (within magma chamber) sulphide saturation:
  - variation (sharp discontinuities) in the concentrations of Cu, Ni, Pd, Pt, Au, S, Se, and Sr with stratigraphic depth/height in the complex;
  - variation (sharp discontinuities) in Cu/Pd, Cu/Pt, Cu/Zr, Cu/(Cu+Ni), (Pt+Pd)/S ratios with stratigraphic depth/height in the complex. According to Maier and Barnes (2002), if the Cu/Pd ratio throughout an intrusion is higher than primitive mantle levels (7700), it is likely that sulphide saturation occurred at the site of partial melting in the source and hence the PGEs were stripped out early; if the Cu/Pd ratio throughout the intrusion is at the primitive mantle level, it is likely that the magma did not reach sulphide saturation during ascent and emplacement, and hence the intrusion is unlikely to contain economic concentrations of

PGEs; if the Cu/Pd ratio in the intrusion is variable, and spans values below and above the mantle level, it is likely that sulphide saturation was achieved at the site of emplacement (magma chamber). The Cu/Pt ratio can also be used in a similar way to the Cu/Pd ratio. The Cu/Zr ratio can also indicate timing of sulphide saturation although this ratio is less sensitive because the difference between the chalcophile affinity of Cu and Zr is less than that between Cu and Pd;

- variation (sharp discontinuities) in Ni content in olivine and pyroxene ( $D_{\text{olivine-basalt}} \sim 2\text{--}15$  and  $D_{\text{opx-basalt}} \sim 1\text{--}3$  and  $D_{\text{cpx-basalt}} \sim 2$ ); and
- decrease in the Cr/Fe ratio of chromite with depth (stratigraphic level) in the layered complex. This can be useful for PGE mineralisation associated with chromite.
- Signs of crustal contamination of magma. Note, these signs are unable to show if the contamination occurs at the site of intrusion emplacement, in a staging chamber deeper in the lithosphere, or at the site of partial melting. Sr, Nd, and S isotope compositions can be used, but the information is not unequivocal. Oxygen isotope compositions of rocks or minerals (e.g., chromite) can be a useful indicator of crustal contamination.  $\delta^{18}\text{O} > 8\text{‰}$  may indicate crustal contamination, whereas values between  $+5\text{‰}$  and  $+8\text{‰}$  may indicate mantle source.

### ***Distinguishing features of large mineral systems***

More than 75% of known global PGE resources are hosted by three large layered intrusions, the Bushveld, Great Dyke, and Stillwater. These intrusions crystallised from the mixing of two magma types: a U-type magma enriched in  $\text{SiO}_2$ , MgO, and Cr, but low in  $\text{Al}_2\text{O}_3$ —this magma is S-poor and PGE rich; and a normal (PGE-poor and relatively S-rich) tholeiitic magma. Large and open-magma chambers are thought to be critical in generating a sufficiently high R-factor to form PGE-rich mineralisation. High R-factors are achieved by the introduction and mixing of fresh pulses of tholeiitic magma. Layered intrusions formed in such magma chambers are characterised by:

- The presence of cyclic units of chromitite, harzburgite, and pyroxenite. The Upper Critical Zone in the Bushveld Complex contains at least seven chromitite layers. Multiple chromitite units are also mapped in the Stillwater Intrusion and in the Great Dyke. Less mineralised intrusions (Munni Munni Intrusion, Skaergaard Intrusion, Sonju Lake Intrusion) represent crystallisation from relatively closed chambers and do not show multiple chromitite layers.
- Signs of magmatic reversals are indicated by reversals in An% of plagioclase, Mg# of pyroxene and olivine within the intrusion. Such reversals are characteristic features of highly mineralised systems, such as the Bushveld Complex.
- Presence of a deep-staging magma chambers. In a number of experimental studies, Naldrett et al. (2008a, 2009, and 2011) have suggested that silicate magmas with 1 ppb–2 ppb Pt (the value estimated from extrapolation of experimental data on the solubility of Pt in mafic magmas) will require extraction from a magma column of the thickness of ~2500 m, a condition difficult to achieve. The same magma with a higher solubility of Pt (~200 ppb) can reduce the thickness of the column to 25 m. Naldrett et al. (2008a) reviewed available experimental solubility data of Pt and Pd in mafic melts and concluded that *'for reasons that are not fully understood, silicate magmas can carry much higher concentrations of PGEs than the experimental study on dry, S- and Fe-free diopside-anorthite melts have demonstrated.'*

A model to generate PGE-rich ( $> \sim 200$  ppb) magma has been proposed by Kerr and Leitch (2005). The multistage-dissolution upgrading model is based on the assumption that fresh pulses of tholeiitic magma are sulphide undersaturated. When this magma reacts with sulphide liquid already separated

during fractionation and/or magma mixing, it begins to dissolve sulphide. Since PGEs, Cu, and Ni are more chalcophile than FeS, they remain in the sulphide melt, gradually enriching it with PGEs, Cu, and Ni, but depleted in S. Calculations using this model suggest that a PGE-enriched (~200 ppb) and S-poor magma can be generated by this process of dissolution and upgrading (Naldrett et al., 2009). According to Naldrett et al. (2008a, 2011) and Li et al. (2009), dissolution and upgrading described above can occur in a deep staging chamber located below the main chamber. The PGE mineralisation in the layered intrusion is thought to result by mixing of this PGE-enriched, but S-poor magma with sulphide-saturated magma in the main chamber. Unusually low Cu/Pd ratios recorded in some sulphide-absent zones in the Bushveld Complex are cited as possible indicators of the dissolution and upgrading process occurring in the staging chamber (Naldrett et al., 2009).

### **Key references**

Andersen et al. (2002); Barnes and Maier (2002); Cawthorn (2005a, 2005b); Li et al. (2009); Maier et al. (2013); Naldrett (2004, 2008a); Naldrett et al. (2009) Naldrett et al. (2011); Schissel et al. (2002).

## **7.3.3 Mineral-system features of platinum-group element deposits associated with massive to poorly layered tholeiitic mafic-dominated intrusions**

**(Deposit Type: 2.A—Segregations of Ni-Cu-Co-PGE sulphides in feeder conduits and basal contacts)**

### **Geological setting**

- Zones of rifting (incipient rifting of continental crust; rifting along continental margin).
- Prominent lithospheric-scale structures on or near craton margins (Voisey's Bay: Abloviak shear zone separating Proterozoic Churchill Province from the Archean Nain Province; Jinchuan: southwest margin of Sino–Korean Craton).
- Regional-scale faults and their lower-order fault offshoots.
- Tholeiitic mafic-ultramafic complexes, dominated by mafic rocks (troctolite-anorthosite-granite suite at Voisey's Bay), but ultramafic intrusions can be equally important (Jinchuan).
- Parental magmas (Table 8.2) range from high-Al basalt (Voisey's Bay: ~8%–9% MgO), high-MgO basalt (Jinchuan: ~11%–13% MgO), siliceous high-Mg basalt (Kabanga: ~13% MgO), to ferropicrite (Pechenga: ~17% MgO), that are possibly related to mantle plumes.
- Magma emplaced in reactive sulphide-rich (Voisey's Bay), or sulphide-poor (Jinchuan) rocks, assimilation of which can trigger sulphide saturation.
- Cu-Ni mineralisation spatially associated with feeder intrusions (dykes or sills).
- Sulphide (massive, disseminated, and vein) mineralisation in various types of troctolites sheathed in mineralised breccia. PGE concentrations are generally low (total PGEs = 0.26 ppm for Jinchuan and 0.19 ppm for Voisey's Bay).

### **Age and duration of mineralisation**

- Mineralisation can be of any age, but economically important large deposits are generally of Proterozoic age (<2000 Ma).
- Duration: Unknown.

## **Source (melt/fluid, metal, energy)**

### **Melt**

- Plume-generated melting of mantle with contamination by SCLM (Sub-Continental Lithospheric Mantle) and continental crust.

### **Metals and sulphur**

- Cu, Ni, PGEs: Picritic and/or high-MgO basaltic magma formed from low degrees (<~30%) of partial melting of mantle.
- S: Crustal (sulphides from country rocks) and/or mantle.

### **Melt/fluid pathway**

For igneous complexes: emplacement along large regional-scale lithospheric faults (expressed as lineaments). Intrusions (sills and dykes) are thought to have crystallised in feeder zones.

### **Trap**

#### **Structural**

- Shape and size of feeder zones (richest ore zone at Voisey's Bay is located in the widest part of the feeder zone). Mineralised breccias also occur in the mineralised environments of the Voisey's Bay deposit. The widening of the funnel-shaped structure at the Jinchuan deposit is thought to have created a favourable trap for sulphide liquid.

#### **Chemical**

- Attainment of sulphide saturation is the most critical factor. It can occur in two stages and in two chambers: (i) in the mid-crustal chamber primarily due to assimilation of felsic material. The sulphide liquid formed in the chamber can strip PGEs from the magma; and (ii) in a relatively shallow chamber closer to the site of mineralisation, where sulphide saturation may be caused by assimilation of sulphide-rich felsic (Voisey's Bay) or calcareous (Jinchuan) rocks.
- High R-factor (magma/sulphide mass ratio: see Section 3.4.2) sulphides at the site of mineralisation can be achieved in the feeder zone by interaction of sulphide liquid with successive batches of mafic magma enriched in Cu and Ni. PGE enrichment can occur in the staging chamber as well as in the feeder zone.

### **Relative timing of sulphide saturation**

Sulphide saturation is thought to occur early at mid-crustal level, which may explain the relatively low PGE concentrations in the ores at Voisey's Bay and Jinchuan. Magma enters the site of mineralisation either sulphide saturated or close to the level of sulphide saturation.

### **Preservation**

Post-emplacement tectonic history can be important. Mineralisation at Jinchuan is thought to represent the root zone of a larger layered intrusion with a sub-vertical feeder to the magma chamber. Hydrothermal remobilisation of PGEs is documented at Jinchuan.

## **Key references**

Li et al. (2001b); Naldrett (2004); Lehmann et al. (2007); Su et al. (2008); Naldrett (2011); Li and Ripley (2011); Ripley and Li (2011).

## **7.3.4 Assessment criteria for massive to poorly layered tholeiitic mafic-dominated intrusions**

### **Regional scale**

- Tholeiitic mafic-ultramafic intrusions including high-Al basalts, on or near craton margins.
- Intrusions may belong to LIPs.
- Regional-scale lithospheric faults (expressed as lineaments) along craton margins. In some areas intrusions may be structurally controlled by faults subsidiary to regional-scale lithospheric faults.
- Intrusions and magma chambers emplaced in felsic, sulphidic, or calcareous wall rocks, assimilation of which can cause sulphide saturation.
- Signs of early sulphide saturation. Early sulphide saturation is commonly recognised in mineralised complexes and may be one of the critical factors, which could determine the low PGE concentrations for these deposit-types. An approximate estimate can be made based on S concentrations in unaltered mafic and ultramafic rocks. High S concentrations (>~400 ppm) throughout the intrusion and the presence of sulphide minerals in the rocks can indicate that the parent magma had arrived at the site of mineralisation already saturated in sulphides. Sulphur concentration in the parent/initial magma can be estimated from abundances of S in chilled marginal rocks.

### **Local scale**

- Sills and dykes of mafic (anorthosite, ferrodiorite, and troctolite) and ultramafic rocks (dunite to olivine pyroxenite).
- Sites of changes in the shape and size of feeder zones (zone of widening and/or flattening).
- Presence of breccias containing fragments of assimilated country rocks.
- Signs of sulphide saturation and un-mixing of sulphide liquid:
  - variation/reversals in the normal fractional crystallisation sequence of rock indicated by changes in the Mg# of orthopyroxene, An-number of plagioclase, and  $^{87}\text{Sr}/^{86}\text{Sr}$  ratio of rocks; and
  - variation in S, Cu, Ni, PGEs along stratigraphic sections can indicate stratigraphic level of sulphide saturation.
- Ni depletion trends indicated by variations in whole-rock S/MgO, S/Mg#, Ni/MgO, Ni/Mg#, and Cu/Zr ratios. Instead of ratios, variations in the concentrations of S, Cu, Ni, PGEs and of Mg# along type stratigraphic sections can also be useful indicators of mineralisation.
- Signs of crustal contamination of magma. Assimilation of crustal material has been shown for several mineralised complexes by using one or several of the following trace-element and isotope criteria:
  - La/Sm and Th/Nb ratios on La/Sm–Th/Nb plot;
  - Cu/Zr (marked discontinuity can indicate separation of sulphide liquid);

- Re/Os trend on (gamma Os versus Re/Os plot (Naldrett, 2004);
- S isotope composition (Jinchuan:  $\delta^{34}\text{S}$  of -2‰ to +4‰; Voisey's Bay:  $\delta^{34}\text{S}$  of -4‰ to +2‰). At Voisey's Bay calculations based on S isotope composition show that up to 30% of the S was derived from the assimilation of country rocks (Li et al., 2001); and
- Nd, Pb, and Sr isotope data. At the Voisey's Bay deposit investigations by Amelin et al. (2000) show that the primary magmas for the Voisey's Bay Intrusion were either derived from an enriched continental mantle, or were contaminated by a small amount of crustal material during their ascent and then by a minor (probably 8%–13%) amount of sulphide-bearing country rocks.

### ***Distinguishing features of large mineral systems***

Li et al. (2001) compared critical mineralising factors of the Voisey's Bay deposit with the Pants Lake occurrences in Canada and concluded that the following factors were important to form large mineral systems, such as Voisey's Bay.

- Contamination of mafic magma with sulphide-bearing country rock (large mineral systems require higher levels of contamination). An approximate estimate of the degree of contamination can be made by S isotope composition of sulphides in ores and of sulphides in country rocks. Li et al. (2001) also used mineral compositions of hercynite (Fe-spinel), plagioclase, Ni (in olivine), and mol % Fo (in olivine) to estimate Ni upgrading.
- Presence of a dynamic magmatic system, such as magma conduits, which can transport large volumes of sulphide liquids.
- Presence of efficient, but limited number of physical/structural sites in conduits (flattening, widening, etc) to trap the sulphide liquid.
- Upgrading of Ni and Cu by reaction of sulphide liquid with successive batches of chalcophile-undepleted magma (high R-factor).

### ***Key references***

Amelin et al. (2000); Lehmann et al. (2007); Li and Ripley (2011); Li et al. (2001b); Naldrett (2004, 2011); Ripley and Li (2011); Su et al. (2008).

## **7.3.5 Mineral-system features of platinum-group-element deposits associated with komatiitic flows and related sill-like intrusions**

**(Deposit Types: 3.A—Massive, matrix, and disseminated Ni-Cu-PGE sulphides in preferred lava pathways; 3.B—Disseminated Ni-Cu-PGE sulphides in central parts of thick dunite bodies; and 3.C—PGE-enriched Ni-Cu sulphides associated with komatiitic and tholeiitic rocks)**

### ***Geological setting***

- Belts of ultramafic-mafic volcanics and associated intrusions (minor), felsic volcanics, and chemical sediments formed in plume-related rift setting. Most mineralised rocks belong to Archean greenstone and Proterozoic supracrustal terranes and are thought to be parts of LIPs.
- Two geochemical types of komatiites: ADK (Barberton-type; Al-depleted;  $\text{Al}_2\text{O}_3/\text{TiO}_2 < 15$ ) and AUDK (Munro -type; Al-undepleted;  $\text{Al}_2\text{O}_3/\text{TiO}_2 = 15\text{--}25$ ).

- Komatiites are formed from MgO-rich primary magmas (>18% MgO; Fo component of olivine = 90–95). Komatiite magmas with MgO values of 25% and higher are present in all terranes, but the proportion of the high-MgO-types appear to be more dominant in mineralised terranes.
- Volcanic sequences are characterised by the presence of coeval komatiite/tholeiite and komatiite/basalt/felsic-intermediate rocks.
- Two types of ore deposits: (a) Kambalda-type (massive and disseminated sulphide ore bodies in preferred pathways (channelised sheet) at the base of mesocumulate dunitic flows and dunite lenses; and (b) Mount Keith-type (disseminated sulphide ore bodies in thick (several hundreds of metres) lenticular adcumulate dunite bodies).
- Ni-Cu mineralisation associated with komatiites is generally poor in PGEs (PGEs extracted only as by-product). For example, the Kambalda and Mount Keith deposits are estimated to contain less than ~130 t of total PGEs.

### ***Age and duration of mineralisation***

- Komatiite-associated Ni-Cu deposits are of specific Archean and Proterozoic ages with the largest deposits formed at ~2705 Ma (Kambalda, Mt Keith, Abitibi Belt–Canada) and ~1920–1880 Ma (Thompson and Cape Smith belts–Canada). Barren komatiites are widespread in the early Archean (e.g., ~3200–3500 Ma, South Africa; 2880 Ma to <3460 Ma Pilbara Craton; >3000 Ma Aldan Craton, Siberia; 2520 Ma Gawler Craton) and, rarely, in the Phanerozoic (270 Ma, Song Da, Vietnam; 89 Ma, Gorgona Island, Colombia: Hoatson et al., 2006).
- Duration: Unknown.

### ***Source (melt/fluid, metal, energy)***

#### **Melt**

- Source magma is produced by plume-generated melting of depleted mantle. Al-depleted magmas are formed by moderate-degree (~30%) partial melting at extreme depths (>300 km), whereas Al-undepleted magmas are produced by high-degree (~50%) partial melting of depleted mantle at relatively shallower depths (<300 km).

#### **Metals and sulphur**

- Cu, Ni, PGEs: Depleted mantle. Abundance of Pt and Pd in most komatiites varies between ~3 ppb and ~12 ppb. The mantle source rock is estimated to have ~5.7 ppb each of Pt and Pd (Puchtel et al., 2004).
- S: Source magmas of komatiites formed from partial melting of mantle are thought to be sulphide undersaturated. As magmas ascend through the lithosphere, the degree of sulphide-undersaturation increases. Sulphide saturation occurs late and can be caused by assimilation of S from the country rocks through thermal and/or physical erosion.

### ***Melt/fluid pathway***

In Archean provinces, komatiitic rocks form part of granite-greenstone belts bound by a network of linear faults and shear zones. These faults may have provided pathways for komatiitic volcanism and associated intrusive.

## **Trap**

### **Structural**

- Base of preferred lava pathways (Kambalda-type) and within lensoidal erosional lava pathways (Mount Keith -type: Barnes, 2006; Hoatson et al., 2006). Changes in the shape, slope, size, and flow direction in lava pathways can favour the segregation of sulphide liquid.

### **Chemical**

- Sulphide saturation caused by assimilation of sulphidic and felsic country rocks. Sulphur isotope compositions of sulphides in ore zones ( $\delta^{34}\text{S}$  of -0.5‰ to +3.8‰ at Kambalda deposit) match those in the substrate rocks.
- R-factor (magma-liquid sulphide ratio) estimated for these systems are of the order of a few hundred (Kerr and Leitch, 2005).

### **Relative timing of sulphide saturation**

Sulphide saturation is thought to occur late (within lava flows or in sub-volcanic feeders, underlying the flows).

### **Preservation**

Post-emplacement tectonic history can be important. Remobilisation of mineralisation caused by deformation and metamorphism has been documented in many deposits.

### **Key references**

Leshner (1989); Dowling and Hill (1998); Leshner et al. (2001); Naldrett (2004); Maier et al. (2009); Fiorentini et al. (2010; 2012); Barnes and Fiorentini (2012).

## **7.3.6 Assessment criteria for komatiitic flows and related sill-like intrusions**

The PGE content of Ni-Cu sulphide mineralisation associated with komatiites is generally very low. The PGEs are recovered only as by-products. Studies have shown that komatiitic magmas are produced from moderate- to high-degrees of partial melting of depleted mantle at extreme depths. Therefore, they are sulphide undersaturated at the site of origin. As they ascend through the lithosphere, the decrease in pressure makes them more sulphide undersaturated. Assimilation of sulphidic substrate at the site of eruption is thought to cause sulphide saturation and separation of sulphide liquid, which selectively traps Ni and Cu. The late sulphide saturation should also favour accumulation of PGEs in sulphides. The low PGE grades of Ni-Cu sulphide mineralisation can be explained by a combination of the following three factors:

1. very low concentrations of PGEs (<~10 ppb) in primary komatiitic magma possibly related to equally low abundance of PGEs in the depleted mantle from which komatiitic magmas are sourced (Maier et al., 2009);
2. relatively low R-factors (~a few hundred) compared to PGE-enriched layered mafic-ultramafic intrusions (R-factor  $>10^5$ : Kerr and Leitch, 2005); and
3. absence of geodynamic conditions suitable to produce PGE-enriched magma. It has been suggested that PGE-enriched mafic-ultramafic systems (mafic-ultramafic intrusions associated with continental flood basalt and layered mafic-ultramafic tholeiitic intrusions) require special

conditions (achieved in relatively deep staging chambers) to generate a PGE-enriched (>~200 ppb) melt (Naldrett et al., 2008, 2009; Naldrett, 2011). Sulphide ores with economic PGE concentration are thought to form from such magmas when they reach sulphide saturation by assimilation of S from country rocks or by mixing with S-rich magma.

### **Regional scale**

- Regionally extensive belts of komatiitic sequences (volcanics and associated intrusions), which contain thick olivine cumulate flow units.
- Volcanic sequences are characterised by the presence of coeval komatiite/tholeiite and komatiite/basalt/felsic-intermediate rocks.
- Komatiite magmas with MgO >25%.
- Volcanic facies dominated by compound sheet flows with internal flow units and dunitic compound sheet flows.
- Presence of sulphidic rocks as substrates to lava flows.
- Signs of late sulphide saturation caused by physical and/or thermal erosion of sulphidic substrate. Assimilation of sulphidic substrate can be judged by S isotope composition of sulphides ( $\delta^{34}\text{S} = -8\text{‰}$  to  $+6\text{‰}$ ). An approximate estimate can be made based on the S concentrations in unaltered mafic and ultramafic rocks. The presence of rocks with both >400 ppm and <400 ppm S. If all rocks in the komatiitic sequence show values >400 ppm S, it may indicate that sulphide saturation occurred throughout the complex. Presence of disseminated sulphides in some, but not all, rocks may also be indicative of late sulphide saturation. In the Mount Keith ultramafic complex, S concentrations vary from <1000 ppm to >10 000 ppm (Hill et al., 2001). In the Lake Harris Greenstone Belt (Gawler Craton) S concentrations in komatiites range between 175 ppm and 1225 ppm (Hoatson et al., 2005).

### **Local scale**

- Komatiitic flow units containing identifiable lava pathways filled with olivine-rich cumulates.
- Transgressive embayments at the base of lava pathways showing evidence of thermal and/or physical erosion.
- Geochemical signatures of substrate/crustal assimilation. Elevated concentrations of light REEs, and Nd, Zr, Y, Ti, Al, Fe have been used as evidence for assimilation. Ratios of La/Sm, Nb/La, Th/Yb, and Nb/Th have been applied as indicators of assimilation (Leshner et al., 2001).
- Signs of sulphide saturation and un-mixing of sulphide liquid:
  - Sharp variations in the S concentration of komatiitic sequence (Hill et al., 2001); and
  - Nickel- and Pd-depletion trends are good indicators of sulphide saturation. Leshner et al. (2001) used Ni-MgO and Pd-MgO plots to illustrate sulphide-saturation events.

### **Distinguishing features of large mineral systems**

- Komatiite magmas with MgO values of 25% and higher are present in all terranes, but the proportion of the high-MgO-types appear to be more dominant in mineralised terranes (Barnes and Fiorentini, 2012).
- Terranes with large deposits also show a much larger abundance of strongly adcumulus-textured olivine-rich ultramafic rocks (Barnes and Fiorentini, 2012).

- Komatiitic sequences with large deposits are dominated by Al-undepleted komatiites (AUDK-type: Hoatson et al., 2006; Maier et al., 2009).
- Volcanic facies of komatiites associated with large deposits are dominated by compound sheet flows and dunitic compound sheet flows (Hill et al., 2001; Barnes et al., 2004; Hoatson et al., 2006).
- Proximity of komatiitic and felsic volcanic system sharing common crustal pathways (Barnes and Fiorentini, 2012).
- Komatiites in all mineralised terranes show signs of assimilation and contamination, but the scale of contamination appears to be much higher in terranes that contain large deposits (Barnes and Fiorentini, 2012).
- Large deposits require high-flux magma dynamics where komatiitic and felsic magma follow the same plumbing system. They also require juxtaposition of high-flux magma with sources of S. Such conditions can be created in translithospheric zones of permeability located in proximity to craton margins (Begg et al., 2010; Barnes and Fiorentini, 2012).

### ***Key references***

Barnes (2006); Barnes et al. (2004a); Barnes et al. (2012); Begg et al. (2010); Dowling and Hill (1998); Fiorentini et al. (2011); Hill et al. (2001); Hoatson et al. (2005b); Hoatson et al. (2006); Kerr and Leitch (2005); Leshner et al. (2001); Maier et al. (2009); Naldrett (2004, 2011); Naldrett et al. (2008b); Naldrett et al. (2009); Puchtel et al. (2004).

### **7.3.7 Mineral-system features of platinum-group-element deposits associated with 'Alpine- and ophiolitic-type' ultramafic-mafic intrusions**

**(Deposit Types: 5.A—Podiform and stratiform chromitite, with associated Deposit Type: 10.B—Alluvial placers)**

#### ***Geological setting***

- Belts of ophiolites in orogens. Ophiolites are thought to be formed in active plate margin settings (mid-oceanic ridge, back-arc basin, island arc).
- PGEs are closely associated with podiform and stratiform chromite in ultramafic rocks (dunite, harzburgite, peridotite, pyroxenite).
- Concentrations of Ir-(Ir, Ru, Os) and Pd-(Pd, Pt, Rh) subgroups of PGEs are closely associated with the chemical composition of chromites. High-Cr chromites have higher abundance of Ir-subgroup and Rh than high Al chromites. Both types have similar Pt and Pd contents.

#### ***Age and duration of mineralisation***

- Mineralisation can be of any age, but most major podiform chromitite deposits associated with ophiolites in the world are Phanerozoic in age ranging from 500 Ma (Thetford, Canada) to 10 Ma (New Caledonia) (Stowe, 1987, 1994; Mosier et al., 2012).
- Duration: Unknown.

## **Source (melt/fluid, metal, energy)**

### **Melts**

- Generally ophiolites have rocks of two different origins: an upper unit of cumulates (dunites with chromitite bands and lenses); and a lower unit consisting mainly of harzburgite, showing tectonite fabrics and interpreted to represent bodies of deformed solid mantle rocks from the uppermost oceanic lithosphere.
- High-Cr (Type I) and high-Al (Type II) chromitites are produced as a result of interaction of either boninites, or tholeiitic magmas with depleted upper mantle harzburgite. They can also form with cumulus phases during early stages of crystallisation of boninitic magma.

### **Metals and sulphur**

- PGEs and Cr: Sourced from depleted upper mantle harzburgite, and boninitic or tholeiitic magmas.
- S: As the PGE mineralisation is associated with chromite, the magmas are either sulphide undersaturated, or reach saturation after fractionation of chromite. Most sulphides, sulphosalts, and arsenides in these deposits are thought to have been formed from hydrothermal fluids of diverse origin (Distler et al., 2008; El Ghorfi et al., 2008).

### **Melt/fluid pathway**

Mafic-ultramafic intrusions are located within ophiolitic belts which follow regional-scale structural corridors. They are often deformed and altered (serpentinised).

### **Trap**

#### **Structural**

- Faults and fractures (post-magmatic/hydrothermal chromite veinlets).

#### **Chemical**

- Fractional crystallisation of chromite which preferentially extracts IPGE-subgroup. The PGE mineralisation is hosted by chromitite veinlets, schlieren, and networks of schlieren in dunite and harzburgite.
- Sulphide liquid formed after attainment of sulphide saturation.

### **Relative timing of sulphide saturation**

PGE mineralisation is formed from sulphide-undersaturated magmas. Sulphide saturation, if reached, occurs after fractionation of chromite.

### **Preservation**

As intrusives form part of ophiolitic belts in active plate-margin settings (mid-oceanic ridge, island arc, back-arc basin), they are commonly deformed and altered. Hydrothermal remobilisation during serpentinisation has been reported in many deposits. Remobilisation of mineralisation by basinal brines has been suggested at the Proterozoic Bou Azzer deposit (Morocco: El Ghorfi et al., 2008).

### ***Key references***

Stowe (1987, 1994); Peck et al. (1992); Arai (1997); Zhou et al. (1998); Distler et al. (2008); El Ghorfi et al. (2008); Mosier et al. (2012).

## **7.3.8 Assessment criteria for 'Alpine- and ophiolitic-type' ultramafic-mafic intrusions**

### ***Regional scale***

- Belts of ophiolites formed in active plate margin settings (mid-oceanic ridge, back-arc basin, island arc).
- Distribution of belts are structurally controlled with ultramafic-mafic bodies invariably fault-bounded and strongly serpentinised.
- Podiform chromites in ultramafic rocks (dunite, harzburgite, peridotite, pyroxenite).
- Signs of sulphide undersaturation of magmas/rocks. Low S content of mafic-ultramafic rocks can be a favourable signature. For example, S content of ultramafic rocks in the Heazelwood River Complex (Tasmania) is less than 90 ppm (Peck and Keays, 1990).
- Pd/Ir versus Ni/Cu plots for ultramafic-mafic rocks can distinguish ophiolites with mineralised chromitites (Barnes et al., 1988).
- Concentration of detrital PGMs (Pt alloys and native metals are prominent) in heavy-mineral fractions (alluvial).

### ***Local scale***

- Zones of intensive serpentinisation of ultramafic rocks.
- Chromitite seams located generally within dunite and harzburgite.
- Mg# ( $100\text{Mg}/(\text{Mg}+\text{Fe}^{2+})$ ) and Cr# ( $100\text{Cr}/(\text{Cr}+\text{Al})$ ) can distinguish high-Cr and high-Al chromites associated with mineralisation.

### ***Distinguishing features of large mineral systems***

As indicated by many studies overseas (Augé, 1986; Page et al., 1986; Prichard et al., 1996; Bai et al., 2000; Mosier et al., 2012; Singh et al., 2013), podiform chromite deposits generally contain low concentrations of associated PGEs. Such deposits have been mined for their metallurgical-grade Cr throughout the world, but there are only a few examples where the PGEs have been exploited. As most deposits are relatively small it is not possible to define signatures of large mineral systems.

### ***Key references***

Arai (1997); Barnes et al. (1987); Distler et al. (2008); El Ghorfi et al. (2008); Page et al. (1986); Peck and Keays (1990b); Peck et al. (1992); Singh et al. (2013); Stowe (1987, 1994); Zhou et al. (1998); Mosier et al. (2012).

### 7.3.9 Mineral-system features of platinum-group-element deposits associated with 'Alaskan- and Urals-type' mafic-ultramafic intrusions

(Deposit Types: 6.A—PGE mineralisation in concentrically zoned mafic-ultramafic intrusions, with associated Deposit Type: 10.A—Alluvial placers)

#### ***Geological setting***

- Convergent plate margin (a system of subduction zone, arcs, troughs, and rises). Some may occur in tectonically stable terranes (e.g., Aldan Craton near the margins of the Siberian Platform).
- Linear belts of mafic-ultramafic (dunite, clinopyroxenite, gabbro), alkaline to sub-alkaline complexes emplaced near the boundary of large mobile belts and older tectonically stable terranes (continental shield).
- Most bodies consist of ultramafic rocks (cumulates) rimmed by gabbroic rocks (older or metasomatic).
- Two types of PGE mineral systems: S-deficient (Urals); and S-rich (Duke Island Complex, Alaska).
- PGE mineralisation hosted by chromitite units (Urals) or in clinopyroxenite (Duke Island Complex).
- High enrichment in Pt, and low Ru/Ir (<1) ratio. Pt/(Pt+Pd) ratios vary from 0.06 (S-rich systems) to 0.59 (S-poor systems).
- Source of PGE-bearing placers.

#### ***Age and duration of mineralisation***

- Mineralisation can be of any age, but most known deposits are Phanerozoic (Devonian, Cretaceous). Proterozoic age rocks in Ethiopia and Egypt.
- Duration: Unknown.

#### ***Source (melt/fluid, metal, energy)***

##### **Melts**

Parental melts may have formed from partial melting of mantle wedge; magma is enriched in volatiles and is relatively more oxidised. Other possible modes of origin include: (a) fractionation of a single ultramafic melt; (b) assimilation of peridotites by felsic magma; and (c) fractionation of basaltic magma in the feeder pipes of volcanoes.

##### **Metals and sulphur**

- PGEs: Mafic-ultramafic magma.
- S: Sulphides in mafic-ultramafic complexes and/or sulphide-rich country rocks. Sulphur in parent magma may have been derived from subducted sediments.

##### ***Melt/fluid pathway***

- Most plutons are thought to represent the roots (deeper levels) of volcanic systems.
- Concentric shape of pipe-like bodies may be controlled by concentric faults.

## ***Trap***

### **Structural**

- Faults and fractures (postmagmatic/hydrothermal chromite veinlets).

### **Chemical**

- Fractional crystallisation of chromite (PGE mineralisation is hosted by chromite veinlets, schlieren, and networks of schlieren in dunite).
- Sulphide liquid formed after attainment of sulphide saturation.

### ***Relative timing of sulphide saturation***

- In S-poor deposits (Urals): sulphide saturation either not achieved or obtained late, after removal of the PGEs in chromite.
- In S-rich deposits: late sulphide saturation thought to occur when clinopyroxene begins to fractionate.

### ***Preservation***

Most plutons of Phanerozoic age are preserved mainly because they are formed in deeper parts of arc-related volcanic structures. For older arc settings preservation can be an important factor.

### ***Key references***

Johan (2002); Naldrett (2004); Thakurta et al. (2008; 2014).

## **7.3.10 Assessment criteria for 'Alaskan- and Urals-type' mafic-ultramafic intrusions**

### ***Regional scale***

- Linear belts of ultramafic, alkaline to subalkaline plutons formed in convergent margin settings.
- Absence of orthopyroxene and plagioclase in ultramafic cumulates.
- Ultramafic cumulates with chromite seams, veinlets, and schlieren.
- Pegmatitic facies in pyroxenite and hornblendite.
- Signs of late sulphide saturation in sulphide-rich systems. An approximate estimate can be made based on the S concentrations in unaltered mafic and ultramafic rocks. Presence of rocks with both >400 and <400 ppm S is considered favourable. If all rocks in the complex show values >400 ppm S it may indicate that sulphide saturation occurred throughout the complex. Presence of disseminated sulphides in some, but not all rocks may be indicative of late sulphide saturation.
- For sulphide-rich systems, interaction with, and assimilation of, reduced country rocks may be important to create conditions favourable for sulphide saturation.
- In sulphide-poor systems, ultramafic rocks may not show S concentrations required for sulphide saturation. These rocks may have low abundance of sulphides.
- Concentration of detrital PGMs (Pt alloys and native metals are prominent) in heavy-mineral fractions (alluvial).

### **Local scale**

- Zones of intensive serpentinisation of ultramafic rocks.
- Negative trends on  $\text{Fe}^{+3}/\text{M}^{+3}$  versus  $\text{Cr}^{+3}/\text{M}^{+3}$  plots of chromite, where  $\text{M}^{+3}$  represents total of trivalent cations (Johan, 2002).
- $\text{Mg}/(\text{Mg}+\text{Fe}^{+2})$  versus  $\text{TiO}_2$  plots of chromite can distinguish Alaskan-type complexes from other similar ultramafic complexes (Johan, 2002).
- V versus Cr plots of clinopyroxenite can distinguish mineralised rocks from barren clinopyroxenite (Johan, 2002).

### **Distinguishing features of large mineral systems**

In most mineralised systems of this type, economic grade mineralisation is present in the form of alluvial placers. In sulphide-rich systems in Alaska, the total amount of PGEs mined from primary sulphide ores is <1.4 t. As most deposits are relatively small, it is not possible to define signatures of large mineral systems.

### **Key references**

Johan (2002); Naldrett (2004); Thakurta et al. (2008, 2014).

## **7.3.11 Mineral-system features of hydrothermal-metamorphic platinum-group-element deposits of primary and remobilised origin**

(various Deposit Types: 8.A to 8.H, represented by Carr Boyd Rocks; Juan Shoot–Kambalda; Elizabeth Hill; Mulga Springs; Copper Hill; Coronation Hill; Jabiluka; Bushveld dunite pipes; Thompson; Lac des Iles; New Rambler; Ingerbelle; Beaverlodge; Kupferschiefer)

### **Geological setting**

- PGE-enriched zones formed either by remobilisation of PGEs from the primary magmatic mineralisation or from non-economic PGEs in mafic-ultramafic source rocks. Mineralisation can result from fluids of diagenetic, metamorphic, and magmatic origin.
- Geological setting similar to that described for layered tholeiitic mafic-ultramafic intrusions (Section 7.3.1); picritic and gabbro-dolerite intrusions associated with continental flood basalts (Section 7.3.13); massive to poorly layered mafic-dominated intrusions (Section 7.3.3); komatiitic flows and related sill-like intrusions (Section 7.3.5).
- Felsic rocks broadly coeval with mafic-ultramafic complexes.
- Geological setting of unconformity-related U (PGE-Au) deposits (diagenetic-hydrothermal) is defined by the presence of an unconformity between Proterozoic oxidised sandstones (lying above the unconformity) and Proterozoic reduced (carbonaceous) metasedimentary basement rocks.
- Geological setting of the Kupferschiefer sediment-hosted Cu deposits (diagenetic-hydrothermal) is defined by a continental rift package of carbonaceous shales (host rocks) underlain by permeable, red (hematite-rich) sandstones. The rift sequence contains evaporites.
- PGE mineralisation is characterised by high Pd/Pt ratios.

### ***Age and duration of mineralisation***

- Mineralisation can be of any age, but most known large deposits are of Archean (Lac des Iles: 2736 Ma) and Proterozoic ages (Platreef: 2060 Ma). Kupferschiefer sediment-hosted deposits are distinctly younger at 264 Ma.
- Duration: Unknown.

### ***Source (melt/fluid, metal, energy)***

#### **Fluids**

- Felsic intrusions for generating high-temperature (>300°C) fluids.
- Felsic to intermediate intrusive-volcanic complexes for generating epithermal fluids.
- Diagenesis of sediments (in relatively oxidised conditions).
- Metamorphism of intrusions and country rocks.

#### **Metals, sulphur, and ligands**

- Cu, Ni, PGEs: Mafic-ultramafic complexes.
- S: Sulphides in mafic-ultramafic complexes and/or sulphide-rich country rocks.
- Ligands: Basinal, metamorphic or metamorphic fluids.

### ***Melt/fluid pathway***

- Major faults.
- Irregular floor topography of mafic-ultramafic intrusion (Platreef).
- Unconformity surface. Paleoregolith. Permeable sandstone.

### ***Trap***

#### **Structural**

- For unconformity-related systems: unconformity surface, breccia zones, fault and shear zones.
- For sediment-hosted Cu systems: structures at the basin margin (thinning of red-bed sequence, faults, permeability contrasts, paleo-topographic surface).
- For epithermal systems: jogs and constrictions within fault zones.

#### **Chemical**

- For unconformity-related and sandstone-hosted copper (Kupferschiefer) systems: reaction with reduced rocks (carbonaceous, and/or Fe<sup>+2</sup>-bearing silicates). Mobile reductant (hydrocarbons) can be important.
- Lac des Iles deposit: sulphide liquid formed due to sulphide saturation of partial melt.
- Thompson deposit: reduced deformed pelitic schist.

### ***Relative timing of sulphide saturation***

Late. Relevant for deposits such as Lac des Iles, where partial melt undergoes sulphide saturation by dissolution of sulphides in mafic-ultramafic rocks.

## ***Preservation***

Preservation can be important for hydrothermal systems formed at shallow levels (epithermal and unconformity related).

## ***Key references***

Naldrett (2004); Wilde (2005); Kinnaird et al. (2005); Barnes and Gomwe (2011).

## **7.3.12 Assessment criteria for hydrothermal-metamorphic PGE mineralisation**

### ***Regional scale***

As large mineral systems of this type show close spatial and temporal relations with the orthomagmatic PGE, Ni, and Cu mineral systems, regional-scale criteria for the latter (see Sections 7.3.1, 7.3.3, 7.3.5, and 7.3.12) are applicable to these systems.

- Felsic intrusions broadly coeval with mafic-ultramafic complexes, emplaced when the complex is still hot.
- For unconformity-related systems, presence of unconformity between Proterozoic oxidised rocks above, and reduced (carbonaceous) metasedimentary rocks below the unconformity.
- For sediment-hosted copper (Kupferschiefer) systems, presence of rift sequence of carbonaceous sedimentary and oxidised (red-bed) rocks. The presence of evaporitic sediments in rift basins can be critical.
- For unconformity-related systems, the thickness of the sandstone package can be important to generate diagenetic fluids of temperatures >200°C.
- Mafic-ultramafic complexes either containing primary orthomagmatic PGE, Ni, and Cu mineralisation or characterised by anomalous abundances of PGEs, Ni, and Cu.

### ***Local scale***

- Felsic dykes, sills, and veins.
- Zones of intensive serpentinisation of mafic-ultramafic rocks.
- Zones of other hydrothermal alteration (characteristic of epithermal-, porphyry-, unconformity-related- and skarn-systems).

### ***Distinguishing features of large mineral systems***

Lac des Iles and Platreef are the largest mineral deposits of this type of mineral system. Critical features of these deposits are:

- primary (orthomagmatic) PGE, Ni, and Cu mineralisation in mafic-ultramafic complexes; and
- emplacement of felsic intrusions when rocks of the mafic-ultramafic complexes are still hot. This facilitates generation of hot volatile-rich fluids which can cause partial melting of wall rocks and produce sulphide-undersaturated magma.

## ***Key references***

Barnes and Gomwe (2011); Kinnaird et al. (2005); Naldrett (2004); Wilde (2005).

### 7.3.13 Mineral-system features of platinum-group-element deposits associated with continental flood basalts and sub-volcanic sills

(Deposit Type: 7.A—Ni-Cu-PGE sulphides in sub-volcanic picritic-gabbroic sills with associated flood basalts)

#### ***Geological setting***

- LIP, commonly hundreds of thousands km<sup>2</sup>, of continental flood basalts (predominantly tholeiitic) with co-magmatic intrusions.
- Magmatism in the LIP is either related to mantle plumes or to lithosphere rifting/extension at craton boundaries.
- Flood basalts include sequences with relatively primitive composition (Mg# ~0.55).
- At Noril'sk, flood basalts are underlain by a thick package of sediments containing evaporites and coal-bearing strata.
- Mineralisation is closely associated with picritic and gabbro-dolerite intrusions (sills and pipe-like bodies).
- PGE-mineralised zone with massive and disseminated sulphide mineralisation is spatially and genetically associated with intrusions. Economic grade PGEs are also recorded in sulphide-poor, disseminated mineralisation.

#### ***Age and duration of mineralisation***

- Mineralisation can be of any age, but large deposits generally occur in LIPs of Phanerozoic age (Permian/Triassic for Noril'sk, and Jurassic for Karoo flood basalts).
- Duration of magmatism in Phanerozoic LIPs is thought to be between 1 million and 2 million years. The time span of Proterozoic flood basalt LIPs is much longer (~15 million years).

#### ***Source (melt/fluid, metal, energy)***

##### **Melt**

Plume-generated melting of mantle with contamination by continental crust, during evolution of plume generated partial melts of lithospheric mantle (possibly metasomatically enriched).

##### **Metals and sulphur**

- PGEs: Picritic magma.
- Cu, Ni: Picritic and tholeiitic basalt.
- S: Picritic and tholeiitic magma; evaporite from crustal sedimentary sequence. If evaporitic S is involved, a reductant may be required to convert sulphate S to sulphide S.

##### ***Melt/fluid pathway***

For igneous complexes: emplacement of lavas and intrusion along large regional-scale lithospheric faults (expressed as lineaments). Intrusions are thought to represent feeder zones for lavas.

## **Trap**

### **Structural**

- The exact role of faults is not clear, but emplacement of mineralised intrusives appears to be controlled by major faults.
- Some faults become feeder zones for intrusives; the sulphide liquid can scavenge PGEs, Ni, and Cu from magma passing through the feeder zone.

### **Chemical**

- Attainment of sulphide saturation is the most critical factor. It can occur in two stages: (i) in the deep crustal staging chamber due to assimilation of felsic crustal material; and (ii) at shallow crustal level due to assimilation of anhydrite-bearing evaporitic rocks. Elevated  $\delta^{34}\text{S}$  values of sulphides between 10‰ to 12‰ at Noril'sk indicate assimilation of sulphate S. The presence of coal-rich sedimentary rocks can be significant because they can reduce sulphate S derived from evaporites.
- High R-factor (magma/sulphide mass ratio: see Section 3.4.2) requires PGE enrichment in the staging chamber as well as in the feeder zone.

### ***Relative timing of sulphide saturation***

Magma intrudes the staging chamber in a sulphide-unsaturated state and undergoes sulphide saturation due to assimilation of felsic crustal material. Sulphide saturation can also occur at shallow crustal level caused by assimilation of anhydrite-bearing evaporitic rocks.

### ***Preservation***

Post emplacement tectonic history is important to expose mineralised layers to shallower depths. Many complexes are faulted and deformed (layers steeply dipping and overturned).

### ***Key references***

Arndt et al. (2003, 2005); Naldrett (2004, 2011); Arndt (2011).

## **7.3.14 Assessment criteria for continental flood basalts and sub-volcanic sills**

### ***Regional scale***

- LIP of continental flood basalts (predominantly tholeiitic) with lavas and co-magmatic intrusions.
- LIP formed by injection of several magma pulses (volcanic and intrusive).
- Large regional-scale lithospheric faults (expressed as lineaments). Some faults penetrating to mantle depths show signs of activation and reactivation during rifting.
- Flood basalts and intrusions emplaced in a thick package of sediments containing evaporites and coal-bearing strata or (meta)sedimentary rocks with sulphides.
- Some flows and intrusions of picritic composition ( $\text{Mg\#} > \sim 0.55$ ).
- A large thickness of lavas showing depletion in chalcophile elements (Ni, Cu, and PGEs).
- Signs of late sulphide saturation (inside feeder conduits or in the staging magma chamber). An approximate estimate can be made based on S concentrations in unaltered mafic and ultramafic rocks. Presence of rocks with both  $>400$  and  $<400$  ppm S is considered favourable. If all rocks

in the complex show values >400 ppm S it may indicate that sulphide saturation occurred throughout the stratigraphy. Presence of disseminated sulphides in some, but not all, rocks may be indicative of late sulphide saturation.

- Concentration of detrital PGMs in heavy-mineral fractions (alluvial).

### **Local scale**

- A combination of major regional-scale faults and their subsidiary-fault splays. Economic mineralisation at Noril'sk is controlled by the Noril'sk–Kharaelakh fault, which is a splay off the North Kharaelakh fault (Naldrett, 2004).
- Mineralisation is closely associated with feeder intrusions. Mineralisation is concentrated in the wider parts of the conduit at the base of the volcanic pile.
- Signs of late sulphide saturation:
  - chalcophile metal (Ni, Cu, PGE) depletion trends in intrusions and volcanics. Low values of Ni at Noril'sk are decoupled from Mg# and are therefore not caused by magmatic differentiation, but probably due to sulphide segregation. The chalcophile metal depletion is characteristic of volcanic units interpreted to be penecontemporaneous with ore-bearing intrusions (Naldrett, 2004, 2011); and
  - abrupt changes in Ni-content of olivine in different rock units of the intrusion also rule out crystallisation caused by differentiation of a parental magma. The trends are more easily explained by crystallisation from separate pulses of magma (Li et al., 2003).
- Signs of crustal contamination of magma:
  - La/Sm versus SiO<sub>2</sub> for volcanics at Noril'sk has been used to distinguish between contaminated and uncontaminated volcanics (Naldrett, 2004);
  - Nd, Os, and Sr isotopic compositions of intrusives have been used to model different contamination histories of mineralised and poorly-mineralised intrusions at Noril'sk (Arndt et al., 2003);
  - sulphides showing enrichment in <sup>34</sup>S. At Noril'sk, δ<sup>34</sup>S of sulphides range from +5 ‰ to +15 ‰; and
  - presence of anhydrite (xenolith, hydrothermal, and magmatic) in intrusions (Li et al., 2009). At Noril'sk, δ<sup>34</sup>S of magmatic anhydrite range from +19 ‰ to +22 ‰: Li et al., 2009).

### **Distinguishing features of large mineral systems**

Zhang et al. (2008) compared geochemical data from ten LIPs to establish chemical signatures favourable for Ni-PGE mineralisation. The study shows that fertile LIPs (hosting mineralisation of various type, size, and grade):

- are emplaced within Archean-Proterozoic cratonic blocks (located either inside, or close to, their margins);
- generally show a relatively high abundance of primitive melts that are high in MgO and Ni, and are low in Al<sub>2</sub>O<sub>3</sub> and Na<sub>2</sub>O;
- are highly enriched in most of the strongly incompatible elements (K, P, Ba, Sr, Pb, Th, Nb, and light REE); and
- have relatively high Os contents (≥0.3 ppb to 10 ppb) and low Re/Os ratios (<10).

Geological and geochemical signatures of fertile LIPs, which form large mineral systems are not discussed by Zhang et al. (2008). Naldrett (2004) noted that although mafic-ultramafic rocks in the Lake Superior region have several features (tectonic setting, abundance of basalts, chalcophile depletion trends in basalts) similar to the highly mineralised system at Noril'sk, large deposits of the size known at Noril'sk have yet to be found. However, some of the most critical features missing (or yet to be identified) in the Lake Superior region are: major mantle-penetrating structures that could have served as the pathways for ore-bearing magma(s); networks of feeder conduits; and post-mineralisation tectonic movement which could have exhumed mineralised intrusions formed at the base of volcanic sequences.

The giant size of the Noril'sk Ni-Cu-PGE mineral system is thought to be the result of a number of critical processes that occurred in conjunction. These include:

- an open, more dynamic, magmatic system characterised by the injection of several pulses of magma. It is important to note that highly mineralised layered intrusions such as the Bushveld Complex, the Great Dyke, and the Stillwater Intrusion also represent crystallisation in an open system;
- emplacement of magmas in country rocks which contain both evaporite and coal seams. Assimilation of evaporite can facilitate formation of large quantities of sulphide liquid because relatively more oxidised mafic magma can dissolve more S as sulphate S (see Chapter 3). Concurrent assimilation of carbonaceous material of the coal seams can provide favourable reductants to convert sulphate S to sulphide S;
- network of feeder conduits filled with multiple intrusions;
- presence of deep-staging chamber that is critical in generating PGE-rich magmas (Arndt et al., 2003; Li et al., 2009; Arndt, 2011). A similar staging chamber is postulated to explain the genesis of PGE mineralisation in the Bushveld Complex (see Section 7.3.1); and
- contamination of magma with large amounts of crustal material in the staging chamber as well as during its passage to the surface. Arndt et al. (2003) highlighted both scale and timing of contamination as possible controls on mineralisation. At Noril'sk, the Lower Talnakh intrusions with disseminated sulphide mineralisation, poor in Cu, Ni, and PGEs, crystallised from magmas which became strongly contaminated, probably with granitoid crust, in an intermediate-level magma chamber. This caused segregation of sulphides, stripping magmas of chalcophile elements. The main ore-bearing intrusions on the other hand (Noril'sk-type) were formed from magmas which underwent less contamination in the intermediate-level magma chambers, and did not segregate sulphides and therefore retained high concentrations of chalcophile elements. These magmas became sulphide saturated by assimilating evaporite in subvolcanic settings which led to the separation of ore-bearing sulphide liquids.

### **Key references**

Arndt (2011); Arndt et al. (2003); Arndt et al. (2005); Li et al. (2003, 2009); Naldrett (2004, 2011); Zhang et al. (2008).

# 8 Summary of exploration strategies, prospectivity, and guidelines

Dean M. Hoatson and Subhash Jaireth

## 8.1 What is the status of Australia's exploration record?

Platinum-group elements have been explored in Australia for more than one and half centuries (see Chapter 5). Despite this protracted period of time, the skilful efforts of explorers and many hardened prospectors, the activities of large mining companies with substantial exploration expenditures, and the rapid development of exploration technologies and concepts, a significant hard-rock deposit in which the PGEs are the main economic product has yet to be found in Australia. Australia's PGE production record comprises historical contributions from small-scale alluvial deposits that were mined in eastern Australia one hundred years ago, and in more recent times as by-products derived from Archean Ni sulphide deposits in Western Australia. The latter deposits have been the only source of Australia's current modest production of PGEs since their discovery in the late 1960s. In contrast to these early successes, albeit on a small-scale, recent exploration endeavours have failed to make Australia a significant contributor to the global supply of PGEs.

The major aims of this summary chapter are to determine the possible reasons for the apparent poor performance of the Australian PGE exploration industry by reviewing past failures and successes, and to assess the local and global factors that have impacted on PGE exploration in Australia. The potential for recognising a major PGE mineral system in Australia is examined at different scales (continent, province, and local), and the chapter concludes with suggested exploration strategies and guidelines for the more prospective mineral systems, i.e., a framework for successful low-risk exploration. These exploration strategies and guidelines that are focussed on Australia should be used in association with the more 'generic' mineral-system templates (Sections 7.3.1 to 7.3.13) and regional-local assessment criteria for delineating areas of prospective PGE mineralisation in Australia. Chapter 8 will also draw on many of the important conclusions highlighted in the previous 7 chapters.

So what elements of PGE exploration has the Australian industry done well? One of the most successful periods of Australia's PGE industry was from the late 1800s to the early 1900s, when prospectors exploited small commercial quantities of alluvial Pt and 'osmiridium', in central New South Wales and western Tasmania, respectively (see Chapter 5). One of the major reasons why this embryonic phase of the industry was successful was the invaluable early scientific contributions provided by a number of prominent statesmen that had personal interests in geology, and in particular, Au and the PGEs. From 1850 to 1900, the perceptive observations of such identities as the state geological surveyor Samuel Stutchbury and Reverend William Branwhite Clarke (considered the 'father of Australian geology') highlighted the geology and mineral potential of New South Wales. Stutchbury explored the uncharted inland parts of the state, and is acknowledged to have made the first discovery of Pt in Australia, near Orange, central New South Wales in 1851 (see Section 5.1). Reverend Clark was a prolific scientific writer, producing some 80 papers, and his geological sketches formed the basis of the first geological maps of New South Wales. He was the first to discover tin (Sn) in Australia in 1849, and announce the first occurrence of diamonds. Clark also documented many new finds of Pt and Au throughout the state, including in 1860, Pt grains from the goldfields of New

South Wales. Similarly, the Deputy Surveyor-General of Tasmania, Charles Percy Sprent, credited with the first discovery of 'osmiridium' in Tasmania, played a pivotal role in highlighting the mineral potential of his state. His expeditions of 1876 and 1876–1877 and his findings (Sprent, 1876, 1877: Appendix I) that documented many occurrences of alluvial 'osmiridium', were the catalysts that ultimately led to the discovery of alluvial and hard-rock 'osmiridium' deposits throughout Tasmania (see Section 5.2.3). The early documentation of PGEs by these individuals provided timely information for the prospector to become involved in exploration and contribute to Australia's PGE production. In addition, most of the earliest bench-mark bulletins by Twelvetrees (1914), Brown (1919), Reid (1921), Nye (1929, 1930), and Nye and Blake (1938) that described the geology of Tasmanian PGE deposits were published prior to, and during, the main production phases of mining. The timely release of this information provided added momentum to the Tasmanian 'osmiridium' industry.

The early examples of successful alluvial PGE mining in western Tasmania and New South Wales illustrate that some fundamental elements of a mineral system (see Chapter 7), such as the recognition of source rocks, geographical clustering of deposits, and the concentration of heavy minerals by alluvial processes and physical traps, were being used by the prospector more than 100 years ago. The prospectors recognised the spatial association of the PGEs with certain types of altered ultramafic igneous rocks in intrusions (later to be recognised as 'alpine- and ophiolitic-type'), and these prospective fault-bounded bodies defined linear geographical belts throughout western Tasmania. In addition, they noted that PGM grains were often concentrated with other indicator heavy metals, such as chromite and Au, in physical traps along the creek beds, such as cavities and gutters in the erosional surface of the basement rocks. The recognition of these basic mineral-system elements was fundamental to the success of their existing mining operations and the delineation of new targets. Basic mining techniques included tracing the alluvial grains in the drainage systems to their hard-rock source, panning, shallow scrapings and costeaning, hand shovelling the prospective alluvium into riffled sluice boxes, cradles, or puddling machines for heavy-mineral separation. During the mid-1920s, Tasmania was recognised as the largest producer of 'osmiridium' in the world (Reid, 1921; Geary et al. 1956).

The komatiite-hosted Ni sulphide deposits in the Yilgarn Craton of Western Australia have also been successful in providing by-products of Pd and Pt that since the early 1970s have represented the sole contributor to Australia's PGE production. In 2013, these deposits collectively produced 786 kg of Pd and Pt that equates to only ~0.2% of global supply (see Section 1.3.3). Hronsky and Schodde (2006) show that the Yilgarn Craton experienced a major peak in exploration activity between 1966 and 1971—'the nickel boom'—which accounted for more than half of all the Ni sulphide deposits, and all of the large world-class deposits so far discovered in the Yilgarn Craton. Many of these deposits contain significant quantities of by-product PGEs. The most successful period of exploration was therefore at the beginning when a major new search space was opened. About 70% of these discoveries were related to direct-discovery prospecting methods that identified the surface expression of Ni mineralisation (e.g., detailed stratigraphic mapping, gossan geochemistry) and were often based on the recognition of magnetic ultramafic rocks (e.g., komatiites) as favourable hosts, and in particular gossans along the contacts of ultramafic units (Hronsky and Schodde, 2006). Komatiites also made their first appearance in the geological literature in the late 1960s, with the recognition of ultramafic lava flows in the Komati River Valley of the Barberton greenstone belt (Viljoen and Viljoen, 1969). Komatiites are commonly defined as ultramafic rocks with >18% MgO on an anhydrous basis (Arndt and Nisbet, 1982). Barnes (2006) states that examples of spinifex-textured ultramafic flows were also recognised at about the same time in Western Australia, and several landmark papers on komatiites in this state (McCall and Leishman, 1971; Williams, 1971; Hallberg and Williams, 1972) were published

shortly after the Viljoen paper. The increased scientific exposure of these unusual high-MgO rocks at a similar time to the discovery of Kambalda in 1966 immediately increased the regional prospectivity of the Archean greenstone belts in the Yilgarn Craton. The dominant discovery methods for Ni sulphide deposits after the 'the nickel boom' period were follow-up exploration around significant existing deposits (e.g., brownfields environments) and electromagnetic (EM) surveying. An improved understanding of geological processes and controls has also sustained exploration success since the early, surface-prospecting phase of exploration. Such understandings included (Hronsky, 2007; Hronsky and Schodde, 2006): deposits were associated with the basal contact of ultramafic horizons that were locally of an anomalously magnesian nature; capability to map ultramafic rocks through obscuring regolith—in particular, the application of magnetics; capability to discriminate Ni-bearing gossans from other ironstones based on relict textures and geochemistry; 'trough-flank' model first developed at Kambalda (Ross and Hopkins, 1975) and then ultimately expanded in modified form to all sulphide deposits; and the recognition that in more highly strained environments, massive sulphide orebodies can occur dislocated (up to 100 m) from their host ultramafic unit.

Hronsky and Schodde (2006) described the Ni-discovery record of the Yilgarn Craton as having many characteristics typical of an emerging exploration province, namely the early discovery of the both the largest deposits and most of the metal, and generally increasing discovery costs as the province matures. So why did it take more than 70 years for the discovery of Ni deposits in the centre of a major Au-mining region? Hronsky (2007) proposed four reasons for this delay, namely:

1. nickel was a relatively unknown commodity in a Au-rich Western Australia (the first Ni explorers were the North American companies, Newmont and INCO);
2. prior to the 1960s the Ni price was very stable so there were no price booms to drive interest;
3. geological thinking and exploration strategies were dominated by the Sudbury model (large Proterozoic mafic intrusion associated with an impact event) of Canada; and
4. the effect of the regolith in obscuring sulphide deposits and even their ultramafic hosts.

The genetic models proposed for Kambalda-type Ni-Cu-(PGE) mineralisation (see Section 6.4.3.1) in more recent years have incorporated some important mineral-system components that are applicable to many other magmatic Ni-Cu-PGE ore deposits. For example:

- metal source—fertile komatiitic magma that was generated by high-degree partial melting of the mantle and was strongly undersaturated in sulphide in the source;
- S source—S-rich country rocks (sulphide-bearing sediments and volcanic rocks) that can be readily melted and assimilated by high-temperature komatiitic magma. Nickel, Cu, Co, and the PGEs are strongly chalcophilic and will preferentially partition from the silicate melt into the sulphide melt;
- dynamic magmatic system—dynamic high magma-flux environments, such as compound sheet flows with internal pathways facies (Kambalda-type) or dunitic compound sheet flow facies (Mount Keith-type). The metal tenors (metal contents normalised to 100% sulphide) are enhanced by the flushing of voluminous komatiitic melt across the sulphide accumulation; and
- physical trap—depressions in the footwall rocks that may represent structural-deformational features, or volcanic topographic irregularities modified by thermomechanical erosion. Sulphides within the komatiite lava flows are denser than the silicate melt and tend to pool within topographic lows, which may be enhanced in the linear lava channel. Such traps are important for the accumulation of high Ni-bearing massive sulphides that may determine the economic status of the deposit.

Australia has been frustratingly close on several occasions to acquiring its first major economic hard-rock PGE deposit. Most of these high-profile deposits have common parameters in that they generally occur in the Precambrian cratonic and orogenic provinces of Western Australia, represent orthomagmatic mineral systems associated with mafic-ultramafic intrusions (e.g., PGE-enriched sulphide and/or chromitite layers, basal segregations of massive sulphides, PGE-enriched oxides), they have protracted histories of resource evaluation, and in some cases have JORC-compliant resources of PGEs, Ni, and Cu (Table 6.2). Such high-profile examples include: Panton, Lamboo, and Eastman Bore (Halls Creek Orogen); Munni Munni (west Pilbara Craton); Nebo–Babel and Haran (Musgrave Orogen); Weld Range, Jimberlana, Windimurra, Narndee, and Collurabbie (Yilgarn Craton). Nebo–Babel (and Collurabbie) is strictly a Ni-Cu-Co sulphide deposit with associated PGEs, but it contains the largest inventory of PGEs compared with the other prospects listed above. Similarly, the recently discovered Nova–Bollinger Ni-Cu-Co deposit in the Albany-Fraser Orogen has low-level PGEs associated with the sulphides (e.g., DDH SFRC0026: 8 m @ 5.81% Ni, 2.26% Cu, 0.16% Co, 0.12 g/t Pd, 0.12 g/t Pt; Appendix K). Using the PGE resource statistics in Table 6.2, the descending order of global PGE metal resources is Nebo–Babel (70.6 t), Panton (65.6 t), and Munni Munni (63.7 t), followed by the laterite mineral systems of Syerston (32.9 t) and Owendale (17.7 t), both in New South Wales. Despite the commitment of considerable financial resources and multiple phases of intensive exploration by different explorers, none of these prospects have been mined. Koek et al. (2010) estimated that it is most likely that several A\$100 million have been committed to the PGE exploration and development of Australia's major PGE projects. One of the major limitations to the mining of these deposits has been the low PGE grades that typically range from 0.2 g/t to 2.5 g/t. Most mining operations overseas exploit deposits with PGE grades from 2 g/t to 20 g/t (Cawthorn et al., 2005). The Panton Intrusion in the East Kimberley, which contains a total JORC Resource of 14.32 Mt @ 2.19 g/t Pt, 2.39 g/t Pd, 0.27% Ni, 0.07% Cu, 0.31 g/t Au (Platinum Australia Ltd., 2005), has been regularly promoted in the media as representing Australia's first PGE mine. However, issues that have impacted on its economic status since its discovery in 1962 include: the structural disruption of the PGE-bearing chromitite layers along strike (by high-angle faults); rapid variations in the thicknesses (0.1 m to 2.4 m) of the chromitites (by post-magmatic slumping); developing an efficient metallurgical-recovery process for the separation of the PGEs from its refractory Cr-rich host ores; and unfavourable global Pt and Pd prices. The first two factors need to be considered when assessing stratabound mineralised layers hosted by tectonised intrusions in the Proterozoic orogenic belts of Australia. In contrast, mineralised layers in large Archean intrusions of more stable cratonic terranes (e.g., Munni Munni, Jimberlana, Windimurra, Weld Range, Narndee) generally show greater lateral continuity of grades and widths which are important physical parameters for determining economic resources.

Most interest in the Phanerozoic provinces of eastern Australia has been generated by the 'Alaskan-type' intrusions in the Fifield region of New South Wales, and in particular, the PGE±Sc potential of laterite profiles in the Owendale and Tout intrusions (Lachlan Orogen), and structurally-controlled hydrothermal mineralisation in ultramafic-mafic intrusions at Mulga Springs (Curnamona Craton, NSW), Thomson River (Lachlan Orogen, Vic), and Westwood (New England Orogen, Qld). The total mineral resource estimate for the Owendale Platinum and Scandium Project is 519 000 ounces of Pt and 9100 t of Sc, which according to Platina Resources Limited (2014a,b) represents one of the most recently defined PGE resources in Australia and is the world's largest, highest-grade Sc resource. Advances in the processing of Sc could unlock the potential of this metal to contribute toward an economically viable project that exploits both Pt and Sc.

Koek et al. (2009, 2010) have attempted to identify the recent factors that have impacted on the Australian PGE industry, and assess the main risks associated with PGE exploration in Australia. These authors point out that PGE exploration in Australia is largely undertaken by junior companies with their PGE projects forming part of a larger, more diverse project portfolio. Companies that are only dedicated to PGE exploration are rare in Australia. At least several A\$100 of millions were committed to PGE exploration and development projects during the successful 1960 to 1990 period when several significant prospects were identified in Western Australia (see above), but none of these advanced to the mining phase. Koek et al. (2009, 2010) maintain that the viability of Australian PGE projects is very sensitive to: metal prices, the US\$/A\$ exchange rate, and the large capital expenditure requirements relative to the small size of Australian PGE-only deposits. Most PGE-dominant projects were invariably initiated at times of high PGE prices, however, advanced exploration, feasibility studies, and project generation always lags behind the price booms. The Australian Institute of Geoscientists (AIG) in 2014 (AIG, 2014) stated that it takes between 8 years to 13 years for a new mineral discovery to become a mine. Another complicating factor is that South Africa contains most of the world's economic resources of PGEs with 63 000 t (~95%), followed by Russia with 1100 t (~1.7%), and the USA has about 900 t (~1.4%) (USGS, 2014). This very narrow resource inventory has a negative effect on the Australian PGE industry as the well-endowed nations dominate the major share of exploration expenditure and the acquisition of new projects.

The evolution of Australia's PGE industry has witnessed a number of trends relating to the discoveries of the individual PGE deposits and mineral fields. Table 8.1 summarises various characteristics of these discoveries including the major exploration method(s) considered responsible for the discovery of the deposit. This table shows that from the earliest discoveries of the 'osmiridium' fields in northwestern Tasmania in 1876 to the more recent Ni sulphide deposits in the 2000s, there is an overall discovery trend that starts with alluvial deposits (western Tasmania, Fifield), to various hard-rock deposits that crop out (Panton, Lamboo, Kambalda, Jimberlana, Eastman Bore, Munni Munni), to residual-laterite deposits (Owendale, Syerston), and concluding with the discovery of 'blind' deposits found in mafic-ultramafic bodies under shallow cover (Owendale, Nebo–Babel, Collurabbie, Nova–Bollinger). More unconventional PGE settings (unconformity-related, breccia-hosted, alkaline intrusions) feature late in the evolution of the industry. This record of deposit-type discovery reflects such factors as the ease of discovery, advancements of technical and scientific knowledge, and some exploration focus on greenfields environments. Exploration methods that led to the discovery of the deposits (Table 8.1) included the early activities by Government state-territory geological surveys, explorers, and prospectors; gossan search, stratigraphic mapping, and soil-rock-stream geochemical programs that gained momentum from the 1960s; and in more recent decades, airborne geophysical techniques (electromagnetics, aeromagnetics, gravity, etc) in association with ground and down-hole geophysics, and deep-drilling have located deposits under cover and at greater depths. The future discovery of such deposits will require an innovative multidisciplinary approach, that involves an understanding of the different components of a mineral-system concept (see Chapter 7), integrated with cutting-edge geochemical, geophysical, and deep-drilling exploration techniques.

Table 8.1 Significant platinum-group-element discoveries and exploration methodologies in Australia.

Deposit(s) <sup>1</sup>	Type of mineralisation <sup>2</sup>	Discovered	Discovery–mining methods	References
Wilson River–Mount Stewart–Savage River, Delamerian Orogen, Tas	Alluvial: 10.B (deep leads)	1876	Government geological survey–panning, trenching, sluice boxes, cradles, puddling	Twelvvetrees (1914); Brown (1919); Reid (1921)
Fifield, Lachlan Orogen, NSW	Alluvial: 10.A	1887	?Prospector activities–horse-drawn scrapers, panning, trenching, costeans, puddling	Hoatson and Glaser (1989); Johan et al. (1990a,b); Elliot and Martin (1991); Slansky et al. (1991); Teluk (2001)
Adamsfield, Delamerian Orogen, Tas	Alluvial: 10.B (deep leads)	1924	Government geological survey–panning, sluice boxes, cradles, puddling	Brown (1919); Reid (1921); Nye (1929); Bacon (1992); Bottrill (1989, 2014); Shree Minerals Ltd (2009)
Panton, Halls Creek Orogen, WA	Hard-rock: 1.B (layered intrusion–chromitites)	1962	Government geological survey, geological mapping, chromitite geochemistry	Perring and Vogt (1991); Hoatson and Blake (2000); Hoatson and Sun (2002); Platinum Australia Ltd (2005)
Lambo, Halls Creek Orogen, WA	Hard-rock: 1.B (layered intrusion–chromitites)	Early 1960s	Geological mapping, chromitite geochemistry	Hoatson and Glaser (1989); Griffin et al. (1998); Hoatson and Blake (2000); Thundelarra Exploration Ltd (2006)
Owendale, Lachlan Orogen, NSW	Hard-rock: 6.A (Alaskan intrusion–‘p-units’)	1966	Government geological survey re-analysing historical company drill core	Agnew et al. (1987); Johan et al. (1989; 1990a,b); Turvey (1990); Elliot and Martin (1991)
Kambalda, Yilgarn Craton, WA	Hard-rock: 3.A and 3.B (komatiitic volcanics–sulphides)	1966–	Gossan search, geological mapping, identification of komatite stratigraphy, diamond drilling–underground mining	Marston (1984); Gresham (1990, 1991); Barnes (2006); Hoatson et al. (2006); Hronsky and Schodde (2006)
Jimberlana, Yilgarn Craton, WA	Hard-rock: 1.A (layered intrusion–sulphides)	~1969	?Drilling of surface gossans and geochemical anomalies	Travis (1975); McClay and Campbell (1976); Keays and Campbell (1981); Campbell (1991); Mallee Gold Corporation Ltd (2007)
Eastman Bore, Halls Creek Orogen, WA	Hard-rock: 1.B (layered intrusion–chromitites)	Late 1960s	Regional base-metal geochemical program, chromitite geochemistry	Hoatson and Glaser (1989); Sanders (1999); Hoatson and Blake (2000); Magma Metals Limited (2006)
Munni Munni, Pilbara Craton, WA	Hard-rock: 1.A (layered intrusion–sulphides)	1983	Assessment of mineral system, analogy with large mineralised intrusions overseas, rock geochemistry	Donaldson (1974); Hoatson (1984); Williams et al. (1990); Hoatson et al. (1992); Barnes and Hoatson (1994)

Deposit(s) <sup>1</sup>	Type of mineralisation <sup>2</sup>	Discovered	Discovery–mining methods	References
Coronation Hill, Pine Creek Orogen, NT	Hard-rock: 8.F (hydrothermal–unconformity)	1984 (Au–PGEs) 1953 (U–Au)	Diamond drilling near contiguous U–Au mineral system	Carville et al. (1990); Mernagh et al. (1994); McKay and Miezitis (2001); Orth et al. (2014)
Windimurra, Yilgarn Craton, WA	Hard-rock: 1.A and 1.B (layered intrusion–chromitites and sulphides)	1987	Regional mapping, stream-sediment geochemical survey	Mathison et al. (1991); Mathison and Ahmat (1996); Apex Minerals NL (2002, 2003); Ivanic (2009); Ivanic et al. (2010)
Elizabeth Hill, Pilbara Craton, WA	Hard-rock: 8.C (hydrothermal–breccia)	1987	Lineament studies for hydrothermal mineral systems, diamond drilling–underground mining	Barnes (1995); Ruddock (1999); Marshall (2000); Hoatson and Sun (2002); Hickman and Van Kranendonk (2008); East Coast Minerals (2009)
Owendale, Lachlan Orogen, NSW	Regolith: 9.A ('Alaskan' intrusion–laterite)	~1980s	Regional geochemical surveys, rotary-air-blast and diamond drilling	Johan et al. (1989; 1990a,b); Elliot and Martin (1991); Shi (1995); Platina Resources Ltd (2013a,b; 2014b)
Syerston, Lachlan Orogen, NSW	Regolith: 9.A ('Alaskan' intrusion–laterite)	~1980s	Regional mapping geochemical surveys, rotary and air-blast and diamond drilling	Derrick (1991); Elliot and Martin (1991); Black Range Minerals NL (2000)
Weld Range, Yilgarn Craton, WA	Hard-rock and regolith: 1.A and 9.A (layered intrusion–sulphides and laterite)	Late 1980s–early 1990s	Geological mapping of intrusion and diamond drilling	Harrison (1993); Parks (1998); Minara Resources Ltd (2005); Dragon Mining Ltd (2009); Ivanic et al. (2010); Van Kranendonk et al. (2010)
Nebo–Babel, Musgrave Province, WA	Hard-rock: 2.A (mafic intrusion–sulphides)	2000	Mineral-system assessment, geophysical-geochemical surveys, aeromagnetic anomalies, gossan-lag sampling	Baker and Waugh (1995); Hoatson et al. (2006); Seat et al. (2007, 2009, 2011); Seat (2008); Howard et al. (2009); Godel et al. (2011); Maier et al. (2014a,b)
Mordor, Arunta Orogen, NT	Hard-rock: 4.A (alkaline intrusion–sulphides)	2001	Soil geochemical anomaly, rock geochemistry, diamond drilling	Nelson et al. (1989); Hoatson and Stewart (2001); Rowan et al. (2004, 2005); Hoatson et al. (2005a); Barnes et al. (2008)
Mulga Springs, Curnamona Craton, NSW	Hard-rock: 8.D (hydrothermal–sulphides)	<2001	Gossans near contacts of ultramafic bodies, auger drilling of geochemical anomalies	Hoatson and Glaser (1989); Impact Minerals Ltd (2013); Golden Cross Resources (2014)
Collurabbie, Yilgarn Craton, WA	Hard-rock: 3.C (komatiitic volcanics–sulphides)	2004	Aircore drilling; aeromagnetic anomalies, favourable komatiitic facies	Falcon Minerals Ltd (2004; 2005; 2009a,b,c; 2010; 2012); Fiorentini et al. (2010, 2011); Locmelis et al. (2011, 2013); Barnes and Fiorentini (2012)

Deposit(s) <sup>1</sup>	Type of mineralisation <sup>2</sup>	Discovered	Discovery–mining methods	References
Nova–Bollinger, Albany-Fraser Orogen, WA	Hard-rock: 2.A (mafic intrusion– sulphides)	2012 (Nova) 2013 (Bollinger)	Diamond drilling of regional aeromagnetic anomaly ('Eye') and electromagnetic conductor	Smithies et al. (2011); Sirius Resources NL (2012a,b,c,d; 2013a,b)

<sup>1</sup> Includes those deposits where the PGEs are the dominant commodity, to others where the PGEs constitute by-products of other mineral commodities (e.g., Ni, Cu, Co, Au). Resource statistics for most of these deposits/prospects are shown in Table 6.2.

<sup>2</sup> The type of mineralisation is from the mineral systems (deposit type) outlined in Table 6.1, namely: 1.A = Stratabound PGE-bearing sulphide layers; 1.B = Stratabound PGE-bearing chromitite layers; 2.A = Segregations of Ni-Cu-Co-PGE sulphides in feeder conduits and basal contacts; 3.A = Massive, matrix, and disseminated Ni-Cu-PGE sulphides in preferred lava pathways; 3.B = Disseminated Ni-Cu-PGE sulphides in central parts of thick dunite bodies; 3.C = PGE-enriched Ni-Cu sulphides associated with komatiitic and tholeiitic rocks; 4.A = Stratabound and disseminated Cu-Au-PGE sulphides; 5.A = Podiform and stratabound chromitites; 6.A = Concentrically zoned mafic-ultramafic intrusions; 8.C = Magmatic breccias involving mafic, ultramafic, and felsic igneous rocks; 8.D = Structurally-controlled remobilised Ni-Cu-PGE sulphides in mafic±ultramafic±felsic dykes/veins in shear zones; 8.F = Unconformity-type U-Au-PGEs; 9.A = PGE-bearing regolith developed on ultramafic-mafic igneous rocks; 10.A = Alluvial platinum derived from 'Alaskan- and Urals-type' mafic-ultramafic intrusions and 10.B = Alluvial placers derived from 'alpine- and ophiolitic-type' ultramafic-mafic intrusions.

## 8.2 Temporal distribution of platinum-group-element mineral systems

Knowledge of the temporal and spatial distribution of ore deposits is important in exploration, particularly in target generation (Hronsky and Groves, 2008; Naldrett, 2010; Goldfarb et al., 2010; Maier and Groves, 2011). It is rather surprising that Australia does not have a significant economic PGE deposit given the long history of exploration (see Chapter 5) and the wide variety of igneous, sedimentary, and metamorphic rock types in this continent that record an almost continuous geological evolution from the Archean (~3730 Ma) to the present (see Section 1.5). In addition, many different types of geotectonic settings (e.g., continental rifts, continental rifted margins, continental LIPs, mid-ocean ridges and mid-continent anorogenic provinces) hosting different mineral systems characterise the geological record of this country. The prospectivity of Australia is also highlighted by more than 500<sup>26</sup> occurrences of PGEs described from a variety of geological settings in Appendix K. If a major PGE resource is to be found in Australia, it is likely that after many decades of prospecting and company exploration it would have little, if any, obvious surface expression (e.g., large gossans), and it is probably covered by younger alluvium deposits or rock sequences. These are the future challenges confronting the PGE industry in Australia.

The protracted geological evolution of Australia is also indicated by the different PGE mineral systems that have operated in this continent. The geological time scale of Figure 8.1 shows the temporal distribution of the most major PGE occurrences in Australia. A wide time distribution is evident for the occurrences, extending from the Neoproterozoic to the present—a period of ~3000 million years. The early Archean (pre-3000 Ma) and Neoproterozoic (1000 Ma to 542 Ma) are the only time intervals not represented by a major PGE occurrence in Figure 8.1. As a preliminary exploration criterion, Australia's PGE mineral systems occur during distinct periods of geological time. For example:

- PGE-bearing sulphide and chromite orthomagmatic associations in tholeiitic mafic-ultramafic intrusions occur in both the Neoproterozoic and Paleoproterozoic;
- a time-line extending from the Neoproterozoic to the Mesoproterozoic is represented by PGE-enriched sulphide accumulations in mafic-dominant intrusions;
- mineralised komatiitic sequences in Australia are restricted to the Neoproterozoic; unconformity-type U-Au-PGE deposits are most prominent in the late Paleoproterozoic;
- rare PGE associations of alkaline affinity occur in the Mesoproterozoic and mid-Paleozoic igneous complexes;
- 'alpine- and ophiolitic-type' intrusions of western Tasmania are early-middle Cambrian (although this is based on limited geochronology data);
- 'Alaskan-type' intrusions in central New South Wales were emplaced in the late Ordovician;
- hydrothermal associations appear to have no geological time constraints, with a wide distribution throughout the Archean, Proterozoic, and Phanerozoic; and
- placer and regolith associations occur over similar time periods during the Cenozoic.

It should be emphasised that further geochronological data are required to confirm the temporal trends shown in Figure 8.1.

---

<sup>26</sup> This is a minimum number of occurrences since some of the larger mineralised fields described in Appendix K contain multiple spatially close entries (e.g., the Adamsfield Osmiridium Field in Tasmania comprises 49 unnamed alluvial and 42 other occurrences) not individualised in the national compilation.

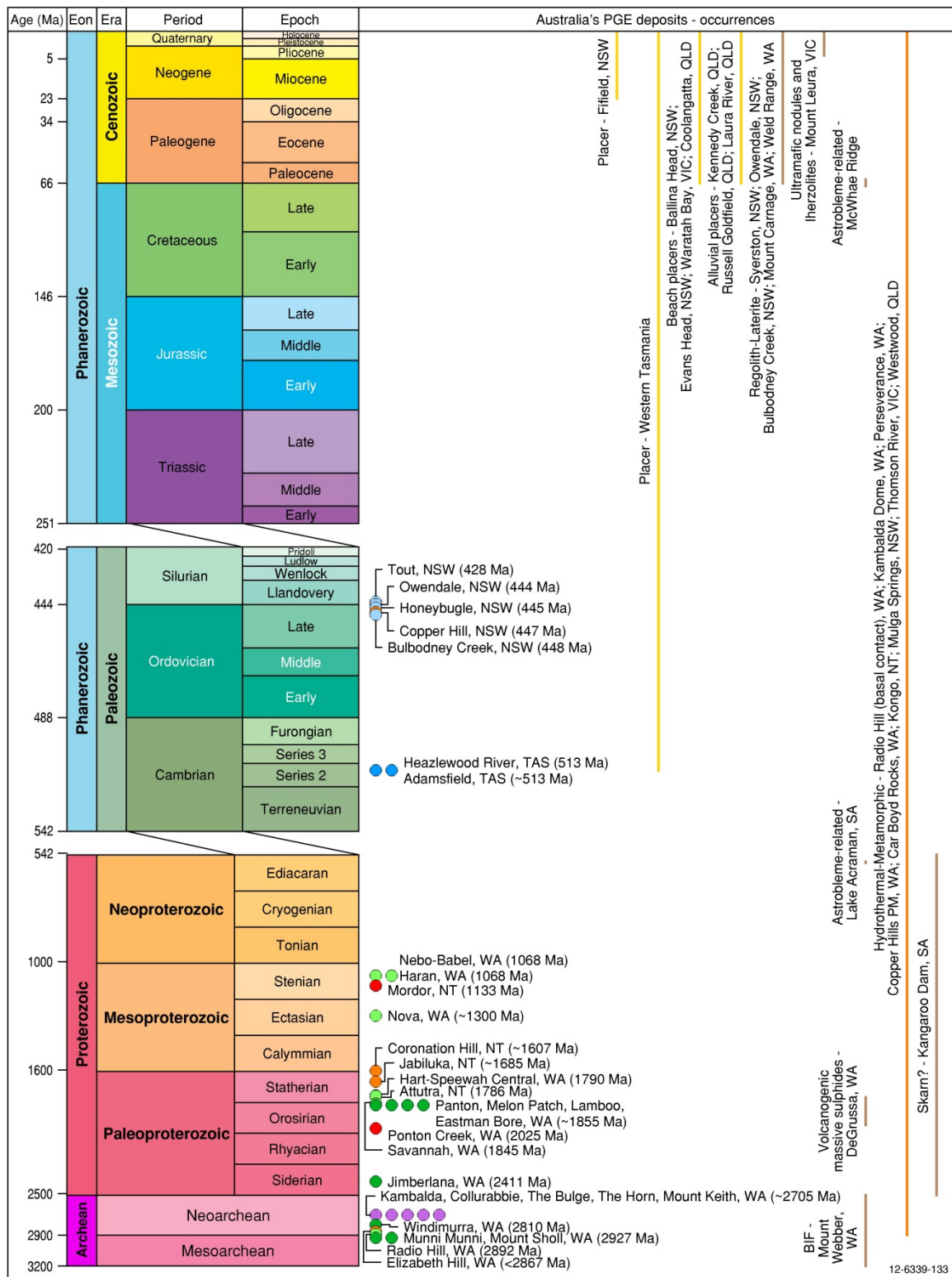


Figure 8.1 Geological time scale and formation of the major platinum-group-element deposits and occurrences in Australia. The geological time lines of some of the major PGE deposit types are also shown. The age data for the various deposits and prospects are largely from the type examples of PGE occurrences described in Chapter 6. The geological time scale is based on Gradstein et al. (2004). Ma = million years before present.

From an exploration point of view, it would be useful to know if Australia's major PGE-Ni deposits have similar coeval deposits from other parts of the world, and if so, are they a manifestation of global-scale metallogenic events that could have been initiated by major crustal-scale and/or superplume events? Figure 8.2 is a time–metallogenic event plot showing the ages and relative sizes of PGE-Ni-Cu and Ni-Cu-PGE-sulphide deposits, and mining camps/provinces in the world. These two major groups of deposits are concentrated in different periods of geological time. The large PGE-Ni-Cu deposits (in the Bushveld, Great Dyke, Stillwater, Penikat, Stella, Munni Munni, and Panton intrusions) are all older than 1800 Ma, with potentially only one significant deposit (Skaergaard–Greenland) being younger at 55 Ma. The 2927 Ma Munni Munni Intrusion contains the oldest PGE deposit in Australia (Hoatson and Sun, 2002), and the oldest on Earth is the uneconomic 3200 Ma Baula deposit in India (Augá et al., 1993). In contrast, Ni-Cu-PGE deposits have a wider time distribution occurring at ~2700 Ma (Kambalda, Abitibi Belt, Zimbabwe Craton), ~1920 Ma to ~1850 Ma (Cape Smith and Thompson belts, Sudbury), ~1400 Ma to ~1330 Ma (Kabanga, Voisey's Bay), ~1100 Ma to ~830 Ma (Duluth, Nebo–Babel, Jinchuan), and ~250 Ma (Noril'sk). It is apparent from Figure 8.2 that the ~2705 Ma Kambalda and Mount Keith komatiitic-hosted Ni-Cu-PGE deposits have coeval komatiitic analogues in the Abitibi Belt (Canada) and Zimbabwe Craton, and are the same age as the 2705 Ma Stillwater Complex (USA) and the 2694 Ma Lorraine basal sulphide deposit (Canada). The 1856 Ma Panton Intrusion is of similar age to the globally significant 1850 Ma deposits of the Sudbury Complex in Canada. Major basal Ni-Cu sulphide deposits (Radio Hill, Savannah, Platreef, Nova, Kabanga, Voisey's Bay, Jinchuan) do not appear to be age dependent, although the larger deposits are younger than ~2060 Ma. Super-large deposits that occur in large mining camps at Sudbury in Canada (Pye et al., 1984; Naldrett, 1997) and in the Noril'sk–Talnakh region of Russia (Kozyrev et al., 2002; Diakov et al., 2002) are in many respects anomalous or 'unique' in the geological record. These globally significant deposits are associated with astrobleme-crustal melting (Sudbury) and continental flood basalt (Noril'sk, Duluth) events at ~1850 Ma and ~250 Ma, respectively. The Sudbury and Noril'sk mineralising events appear to have a very restricted representation in the geological record with the closest time analogue to Noril'sk being the slightly older ~264 Ma PGE-enriched carbonaceous basinal shales in the vast Kupferschiefer deposits of Europe (Kucha, 1985; Kucha and Pawilowski, 1986). There are currently no known occurrences of PGEs in Australia that are contemporaneous or have a similar style to the Sudbury and Noril'sk mineralising events. The concentration of different types of PGE-Ni deposits forming during a particular geological period defines three major global metallogenic events from 1840 Ma to 2060 Ma, 2690 Ma to 2705 Ma, and 2875 Ma to 3000 Ma. These three major metallogenic periods appear to correlate with three superplume events (right column of Figure 8.2) as defined by Abbott and Isley (2002).

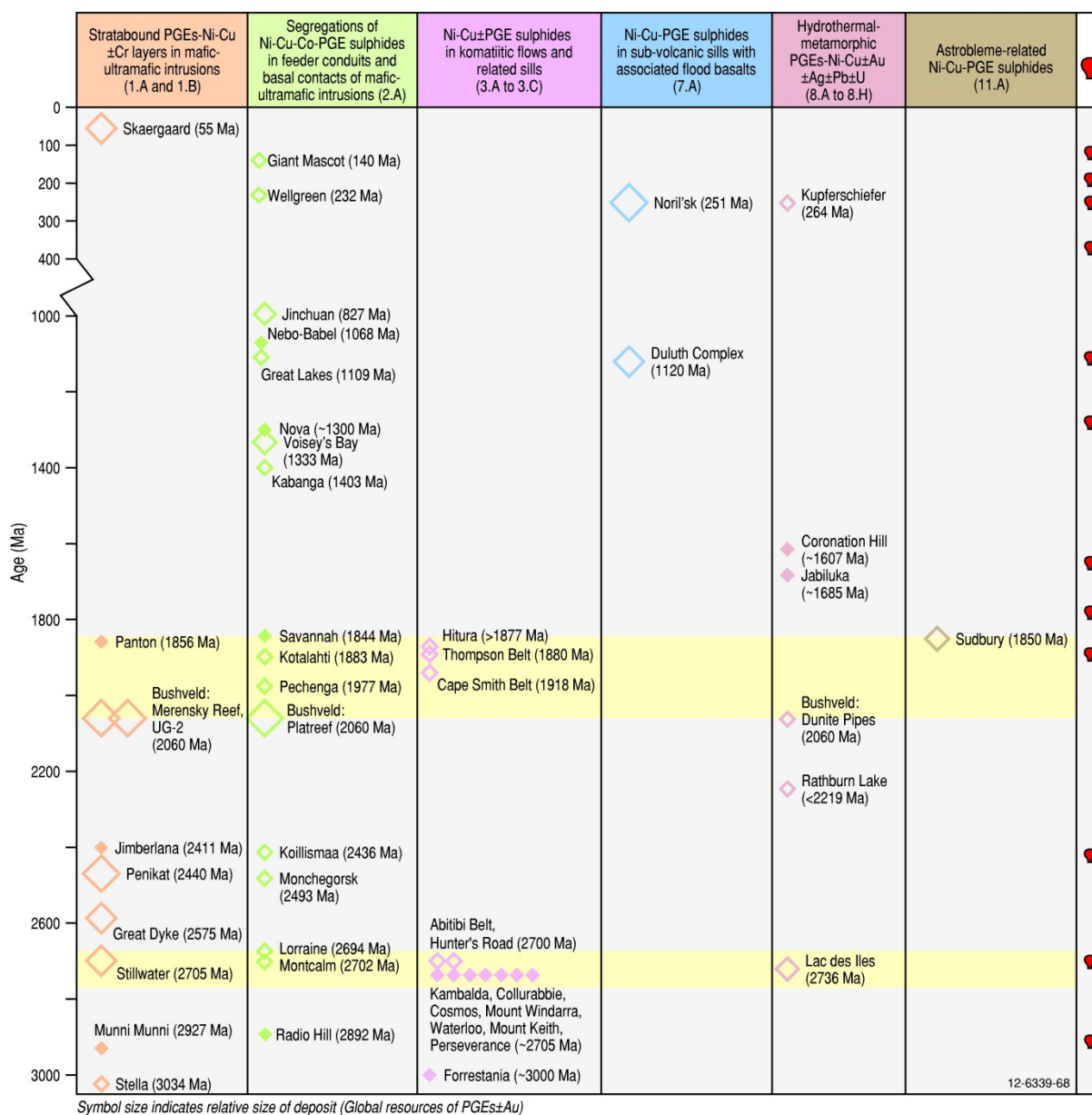


Figure 8.2 Time-PGE metallogenetic event plot showing approximate ages and relative sizes of PGE deposits and PGE camps/provinces in the world. The concentration of different types of PGE and Ni deposits forming during a particular geological period defines three major global metallogenetic events at 1840 Ma to 2060 Ma, 2690 Ma to 2705 Ma, and 2875 Ma to 3000 Ma. The Australian deposits are shown with a filled symbol, and overseas deposits with an open symbol. The size of the symbol indicates the relative size of the deposit (global resources of PGEs±Au). The geological periods of the major superplume events in the right column are from Abbott and Isley (2002).

### 8.3 Fertility status of tholeiitic- and komatiitic-magmatic mineral systems

All the major magmatic PGE-Ni-Cu and Ni-Cu-PGE deposits in the world are genetically and spatially related to bodies of mafic or ultramafic igneous rocks (Naldrett, 1997). This association is almost exclusively related to tholeiitic and komatiitic magma types, with some minor deposits of relatively little economic significance derived from magmas with alkaline affinities. Magmatic PGE sulphide deposits form when mantle-derived mafic and ultramafic magmas become saturated in sulphide and segregate immiscible sulphide liquid, commonly following interaction with crustal rocks (Arndt et al., 2005). The behaviours of important chalcophile ore metals, such as the PGEs, Cu, Ni, and Au are largely controlled by sulphide phases during partial melting and magma evolution due to their high partition coefficients into sulphide melts (see Section 3.3). The crystallised sulphides generally constitute a small volume of the host rock(s) and are dominated by a simple major mineralogy of pyrrhotite ( $\text{Fe}_7\text{S}_8$ ), pentlandite ( $[\text{Fe},\text{Ni}]_9\text{S}_8$ ), and chalcopyrite ( $\text{CuFeS}_2$ ). While a wide range of precious, base, and other metals are recovered from these rocks, the most important products are the PGEs (in particular Pt, Pd, and Rh), and Ni, with Cu, Co, Au, Ag, and Pb being minor associated metals. The other major orthomagmatic mineral system that has considerable economic significance in layered mafic-ultramafic intrusions is stratabound chromitite layers. The global type example is the UG-2 Chromitite of the Bushveld Intrusion, which contains the largest global resource of PGEs (32 730 t; Naldrett, 2004, 2011; Naldrett et al., 2008a) in the world. These deposits are characteristic of large layered bodies of late Archean to early Proterozoic age and where the more primitive ultramafic component of the stratigraphy is dominant relative to the mafic component. An early hypothesis proposed by Irvine (1977) suggests the chromitite layers formed as a consequence of injection and mixing of a chemically relatively primitive magma into a chamber occupied by more evolved magma. This forces supersaturation of the mixture in chromite, which upon crystallisation accumulates on the magma chamber floor to form a nearly monomineralic layer possibly enriched in PGEs. Other origins (Campbell and Turner, 1986) that have been proposed for the formation of chromitite layers include sudden changes in oxygen fugacity (Ulmer, 1969) or pressure (Cameron, 1978), liquid immiscibility (McDonald, 1965), mixing of different composition magmas (Sharpe and Irvine, 1983), and crustal contamination (Irvine, 1975). Naldrett et al. (2012) have more recently reviewed the origin of chromitites and related PGE mineralisation in the Bushveld Complex.

Relative to other mineral deposits, magmatic PGE-Ni-Cu deposits are rare. The metal endowment (PGEs, Ni, and Cu) of 31 deposits/mining camps are shown in Figure 8.3. The global resource data for the PGEs, Ni, and Cu are from Naldrett (2004, 2011), which are compiled in Appendix E. The deposits/mining camps are arranged sequentially down the figure according to the classification scheme used in this study (Table 6.1). Only six such 'deposit-types' have global PGE resources exceeding 5000 t, including the UG-2 (32 730 t), Merensky Reef (26 161 t), Great Dyke (13 946 t), Noril'sk mining camp (12 610 t), Stillwater (6690 t), and the Platreef (6582 t). Three of these (UG-2, Merensky Reef, Platreef) occur in the Bushveld Complex of South Africa. These significant metal endowments not only reflect the large number of individual ore deposits in the mining camps, but also their protracted mining histories, e.g., the Merensky Reef, Platreef, and Noril'sk were discovered in 1924, 1925, and 1926, respectively (Hoatson et al., 2006), and the sulphide ores from Sudbury were exploited from 1886 (Giblin, 1984). The remainder of the deposits and mining camps shown in Figure 8.3 have global PGE resources less than 3000 t of PGEs, with Australia's largest PGE inventories in the Nebo-Babel (70.6 t), Panton (65.6 t), and Munni Munni (63.7 t) mafic-ultramafic intrusions.

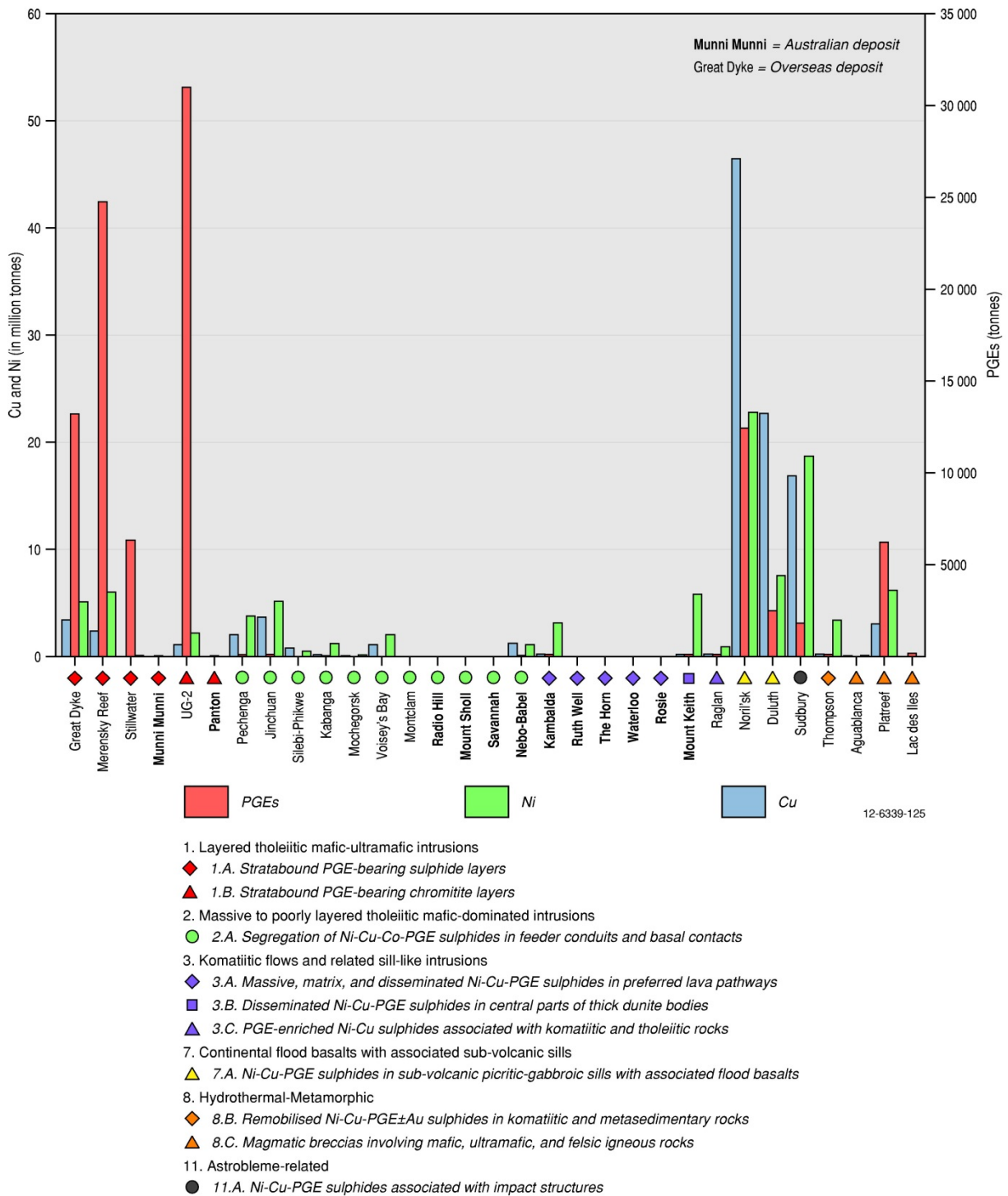


Figure 8.3 Histogram of global resources of PGEs (red), Ni (green), and Cu (blue) metal in the major PGE-Ni-Cu and Ni-Cu-PGE deposits and mining camps of the world. The classification (based on Table 6.1) of the deposit/mining camp is indicated by the coloured symbol on the X axis. Australian deposits are shown in bold font, overseas deposits in normal font. Global resource data from Naldrett (2004, 2011) and Hoatson et al. (2006).

Figure 8.2 and Figure 8.3 provide two important insights into PGE endowment, magmatic associations, and economic potential:

1. Late Archean to early Proterozoic (~2900 Ma to ~1800 Ma) layered tholeiitic mafic-ultramafic intrusions (Deposit Types 1.A and 1.B) contain most of the major PGE deposits in the world, and clearly have a significantly higher PGE endowment relative to all the other PGE mineral systems. The global type example of sulphides in the feeder conduits of mafic-dominant intrusions (Deposit Type 2.A) is Voisey's Bay in Canada, which has a modest PGE endowment of 25.6 t, considerably less than Australia's equivalent type example Nebo–Babel (70.6 t). Other similar Australian deposits include Savannah, Radio Hill, and Mount Sholl, which have PGE credits less than 1 t. The contribution of PGEs in komatiitic deposits (Deposit Types 3.A, 3.B, and 3.C) at Thompson (127 t), Raglan (123 t), and the Kambalda- (130 t) and Mount Keith-type (112 t) deposits of the Eastern Goldfields Province reflects their by-product status, containing at least two orders of magnitude less metal endowment than the large tholeiitic intrusion-hosted deposits described above. Small komatiite-hosted Ni-Cu sulphide deposits at Ruth Well, The Horn, Waterloo, and Rosie all have PGE credits of less than 3 t. Alkaline-magmatic associations, alpine-ophiolitic intrusions, Alaskan-Urals intrusions, hydrothermal-metamorphic, and placer mineral systems have no global economic significance in regard to PGEs and they do not feature in the 31 deposit histograms of Figure 8.3. Using global metal endowment as an exploration criterion, mineral systems (for sulphides or chromite) associated with Precambrian layered tholeiitic mafic-ultramafic intrusions (Deposit Types 1.A and 1.B) would be a high priority, followed by mafic intrusions related to flood basalts (7), and mineral systems related to komatiitic flows (3.A, 3.C) and sill-like intrusions (3.B). The mineral systems shown in Table 6.1 (e.g. 4,5,6,8,9, and 10) that characterise the younger Phanerozoic terranes of eastern Australia provide no contributions to global endowment and therefore have low priority for exploration.
2. With the exception of South Africa, which hosts the three world-class deposit-types (e.g., UG-2, Merensky Reef, and Platreef); all other countries shown in Figure 8.3 contain only a maximum of one world-class geological formation/deposit (e.g., Zimbabwe–Great Dyke; Russia–Noril'sk; Canada–Sudbury; USA–Stillwater). The USA could achieve the rare distinction of having two major PGE deposit-types with the established economic Stillwater Complex, and the Duluth mafic intrusion in Minnesota, which contains a large low-grade resource (4000 Mt @ ~0.65 g/t PGEs, 0.2% Ni, 0.6% Cu: Naldrett, 2011). The rarity of such world-class PGE deposits indicates that efficient and large-scale mineral systems may be limited to one major example per continent, and they do not form geographical clusters of several deposits, as seen for Ni, Cu, Pb, Zn, U, and Au mineral systems. For example, over 140 Ni deposits and camps in the world contain more than 100 000 t of global resources of Ni metal (Hulbert and Eckstrand, 2005). This is further illustrated by five such world-class (i.e., >1 Mt global Ni metal resource) komatiite-associated Ni sulphide deposits in the Eastern Goldfields Province of the Yilgarn Craton, Western Australia (Hoatson et al., 2006). These deposits include Mount Keith (~3.4 Mt global Ni resource), Perseverance (~2.5 Mt), Yakabindie (~1.7 Mt), Honeymoon Well (~1 Mt), and several deposits in the Kambalda Dome region (~1.4 Mt).

The grade and global resource statistics for the major PGE deposits of the world (Figure 8.4: data from Naldrett, 2004, 2011) show that six major mafic-ultramafic complexes are of world-class status (global resources of PGE metal >1000 t) in regard to their PGE endowments. These complexes include the 2060 Ma Bushveld (65 473 t of PGE metal), 2587 Ma Great Dyke (13 946 t), 251 Ma Noril'sk (12 609 t), 2705 Ma Stillwater (6690 t), 1099 Ma Duluth (2621 t), and the 1850 Ma Sudbury (1933 t) complexes. Figure 8.4 also reconfirms that stratabound PGE-Ni-Cu±Cr deposits (UG-2, Merensky Reef, and Platereef in Bushveld, J-M Reef in Stillwater, and Main Sulphide Zone in Great Dyke) hosted by large layered tholeiitic mafic-ultramafic intrusions of Archean-Proterozoic age contain the most significant resources of PGEs. Figure 8.4 highlights that both Stillwater (20.7 g/t PGEs) and Noril'sk (10.0 g/t PGEs) have anomalously high PGE concentrations relative to all other deposits. Australia's PGE deposits have significantly smaller global metal endowments and lower PGE grades by some 1 to 2 orders of magnitude compared to overseas deposits. One notable exception is the PGE-chromite deposit in the East Kimberley's Panton Intrusion, which has relatively high PGE grades of 4.58 g/t.

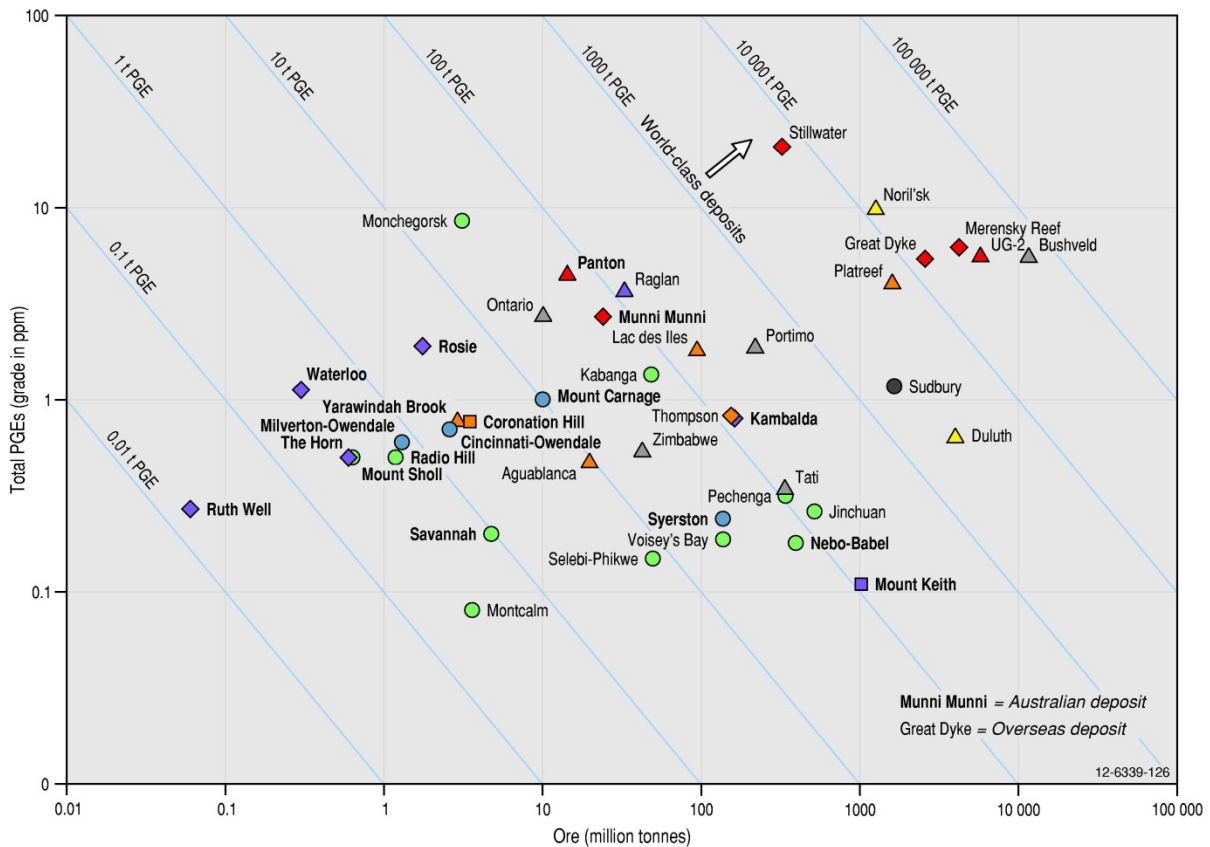
### 8.3.1 Tholeiitic magmatic systems: fertile versus barren

Many studies (Maier, 2005; Markwitz et al., 2010; Naldrett, 1997, 2002, 2011; Maier and Groves, 2011) have examined the question 'what gives magma ore potential?' Naldrett (2002) proposed that the essential ingredients for the formation of world-class deposits are: large magmatic systems involving PGE-bearing magma(s); source of S in rocks traversed by the magma close to its point of final emplacement; reaction with country rocks; and focused magma flow in feeder conduits. Similarly, Arndt et al. (2005) suggested that some of the most important petrogenetic controls include:

- the abundance of ore metals in the magma;
- the sulphide saturation status of the magma; and
- the capacity of the magma to interact with other rocks (e.g., temperature, viscosity, volatile content, dynamics of magma emplacement, nature of wall rocks).

In this respect, hot, low-viscosity primitive tholeiitic picrite and komatiitic magmas have more potential for forming PGE deposits than relative colder, volatile-rich alkali picritic and low-MgO basaltic magmas.

Magmatic PGE-Ni-Cu and Ni-Cu-PGE deposits share many key ore-forming processes, namely they are generally derived from primitive, relatively magnesian, mantle-derived magmas or their differentiates, and they evolve in magma chambers formed at fairly moderate pressures (<~5 kb) and depths (<~18 km) in the crust (Trudu and Hoatson, 1996, 2000). In many cases the parent magmas of the host intrusions have tholeiitic basaltic compositions. Consequently, PGE-Ni-Cu and Ni-Cu-PGE deposits are commonly located in similar geological environments and their characteristics are summarised together in Table 8.2. The following discussion examines some of the more important parameters that are thought to influence the fertility of tholeiitic magmatic systems, and which can be used for target selection during exploration. The brief description of the two major groups of PGE deposits below is partly abridged from Maier and Groves (2011) and Hoatson et al. (2006), and references within.



1. Layered tholeiitic mafic-ultramafic intrusions
    - ◆ 1.A. Stratabound PGE-bearing sulphide layers
    - ▲ 1.B. Stratabound PGE-bearing chromitite layers
  2. Massive to poorly layered tholeiitic mafic-dominated intrusions
    - 2.A. Segregation of Ni-Cu-Co-PGE sulphides in feeder conduits and basal contacts
  3. Komatiitic flows and related sill-like intrusions
    - ◆ 3.A. Massive, matrix, and disseminated Ni-Cu-PGE sulphides in preferred lava pathways
    - 3.B. Disseminated Ni-Cu-PGE sulphides in central parts of thick dunite bodies
    - ▲ 3.C. PGE-enriched Ni-Cu sulphides associated with komatiitic and tholeiitic rocks
  7. Continental flood basalts with associated sub-volcanic sills
    - ▲ 7.A. Ni-Cu-PGE sulphides in sub-volcanic picritic-gabbroic sills with associated flood basalts
  8. Hydrothermal-Metamorphic
    - ◆ 8.B. Remobilised Ni-Cu-PGE±Au sulphides in komatiitic and metasedimentary rocks
    - ▲ 8.C. Magmatic breccias involving mafic, ultramafic, and felsic igneous rocks
    - 8.F. Unconformity-type U-Au-PGEs
  9. Regolith-Laterite
    - 9.A. PGE-bearing regolith developed on ultramafic-mafic igneous rocks
  11. Astrobleme-related
    - 11.A. Ni-Cu-PGE sulphides associated with impact structures
    - ▲ Contains multiple deposit types or deposit type is unknown
- Munni Munni = Australian deposit**  
Great Dyke = Overseas deposit

Figure 8.4 Logarithmic plot of total PGE grade (ppm) versus global resources of PGE ore (production plus reserves and resources in million tonnes) for the major PGE-Ni-Cu and Ni-Cu-PGE deposits of the world. Australian deposits are shown in bold font and foreign deposits in normal font. The grey diagonal lines indicate contained PGE metal in tonnes. World-class deposits are defined as those containing more than one thousand tonnes of contained PGE metal. Data compiled from OZMIN (2014) and Naldrett (2004, 2011).

Table 8.2 Characteristics and indicators of fertility for platinum-group-element deposits hosted by 'tholeiitic' mafic-ultramafic intrusions: Type 1.A, 1.B, and 2.A deposits<sup>1</sup>.

Intrusion <sup>1</sup>	Province	Global PGE metal resources (t) <sup>2</sup>	Global Ni resources (Mt)	Deposit Class. <sup>3</sup>	Age (Ma)	Geodynamic setting	Bulk composition	Parent magma composition	Mineralisation setting	Country rocks	Increasing PGE-Ni fertility of intrusions
Bushveld Complex Merensky Reef <sup>4</sup>	Kaapvaal Craton, South Africa	15 012 Pt, 7790 Pd, 909 Rh, 1891 Ru, 345 Ir, 214 Os)	6.31	1.A	2060	Intra-continental rift	Mafic > ultramafic	Tholeiitic basalt, high-Mg basalt (~7%–14% MgO) Ultramafic-boninite (~9%–17% MgO)	Stratabound reef (Merensky Reef)	Shale, dolomite, quartzite, BIF, conglomerate, felsic volcanics, granite	↑
Great Dyke of Zimbabwe	Zimbabwe Craton, Zimbabwe	13 946 (7130 Pt, 5482 Pd, 335 Rh, 744 Ru, 135 Ir, 120 Os)	5.41	1.A	2590	Intra-continental rift	Ultramafic > mafic	High-Mg tholeiitic basalt (~15% MgO)	Stratabound reef (Main Sulphide Zone)	Granite, gneiss, mafic volcanics, BIF, greenstone	
Stillwater	Wyoming Archean Province, Beartooth Block, USA	6690 (1403 Pt, 5124 Pd, 87 Rh, 32 Ru, 30 Ir, 14 Os)	0.13	1.A	2705	Cratonic	Mafic > ultramafic	Siliceous high-Mg basalt (15% MgO)	Stratabound reef (J-M Reef)	Hornfels, metapelitic rocks, quartzite, BIF	
Jinchuan	Sino-Korean Craton, China	135 (65 Pt, 51 Pd, 3 Rh, 5 Ru, 5 Ir, 6 Os)	5.46	2.A	830	Rifted continental margin	Ultramafic	High-Mg basalt (~11%–13% MgO)	Basal contact, remobilised veins	Migmatite, biotite gneiss, schist, marble	
Pechenga	Baltic Shield, Russia	107 (41 Pt, 59 Pd, 2 Rh, 2 Ru, 1 Ir, 2 Os)	4	2.A	1980	Rifted continental margin	Ultramafic > mafic	Ferropicrite (~17% MgO)	Basal contact, wall-rock contact, fold axes, fault breccia, veins	Gabbro, shale, tuff, sulphur-bearing graphitic sediments, gneiss, schist	
Nebo–Babel	Musgrave Province, Australia	70.6	1.18	2.A	1070	Meso-proterozoic orogenic belt	Mafic	Medium- to low-tholeiite (8% to 9% MgO)	Feeder conduit, basal contact	Granitic gneiss, felsic and mafic granulites, mafic rocks	

Intrusion <sup>1</sup>	Province	Global PGE metal resources (t) <sup>2</sup>	Global Ni resources (Mt)	Deposit Class. <sup>3</sup>	Age (Ma)	Geodynamic setting	Bulk composition	Parent magma composition	Mineralisation setting	Country rocks	Increasing PGE-Ni fertility of intrusions
Panton	Halls Creek Orogen, Australia	65.6	0.04	1.B	1850	Paleo-proterozoic orogenic belt	Ultramafic = mafic	Olivine tholeiitic basalt, quartz tholeiitic basalt (~8%–10% MgO)	Stratabound chromitites	Migmatitic gneiss, schist, granite, mafic granulite	↑
Kabanga	Kibaran Orogenic Belt, Tanzania	65.04 (26.0 Pt, 39.04 Pd)	0.2	?2.A	1400	Meso-proterozoic orogenic belt	Ultramafic > mafic	Siliceous high-Mg basalt (~13% MgO)	Basal contact	Schist, quartzite, granite	
Munni Munni	Pilbara Craton, Australia	63.7	0.02	1.A	2925	Intra-continental rift	Mafic > ultramafic	Siliceous high-Mg, Al-depleted basalt (~9%–12% MgO)	Stratabound reef (Porphyritic Websterite Layer)	Granite, phyllite, schist, psammite, mafic and felsic metavolcanics	
Voisey's Bay	Torngat Orogen, Canada	25.6 (9.6 Pt, 13.7 Pd, 0.7 Rh, 1 Ru, 0.3 Ir, 0.3 Os)	2.17	2.A	1330	Proterozoic orogenic belts	Mafic	High-Al basalt (~8%–9% MgO)	Feeder conduit, basal contact	Biotite orthogneiss, pelitic and psammitic paragneiss, sulphur-bearing paragneiss	
Kotalahti	Svecokarelian Orogenic Belt, Finland	Low tonnage (Ni ore averages 5 ppb Pt, <5 ppb Pd and Rh)	0.16	2.A	1883	Paleo-proterozoic orogenic belt	Mafic > ultramafic	Tholeiitic basalt, ?high-Mg basalt (15% MgO)	Basal contact, wall-rock contact, veins	Granite gneiss, gneiss, graphitic schist, amphibolite, quartzite, calc-silicate rocks	

<sup>1</sup> Sudbury (astrobleme-associated: Canada) and Noril'sk–Talnakh (sub-volcanic sills associated with flood basalts: Russia) are not included in this table since they are large mining camps that contain many deposits that are derived from different mineral systems compared to the 'typical' mineralised mafic-ultramafic intrusions in this table. Naldrett (2004, 2011) estimates that Sudbury has a global metal resource of 1933 t of PGEs (comprising 763 Pt, 961 Pd, 92 Rh, 73 Ru, 31 Ir, 13 Os), and for the Noril'sk–Talnakh region it is 12 607.38 t of PGEs (comprising 2388.3 Pt, 9678.9 Pd, 286.0 Rh, 155.77 Ru, 39.66 Ir, 58.75 Os). The Pechenga deposit has been included in this table, but it does have chemical affinities with both primitive tholeiitic and komatiitic (Table 8.3) magmatic systems.

<sup>2</sup> Global metal resource statistics for the PGEs are from the references cited in Appendix E of this report. Most global metal statistics are from Naldrett (2004, 2011).

<sup>3</sup> For deposit classification see Table 6.1.

<sup>4</sup> The UG-2 Chromitite (32 730 t PGEs) and the Platreef (6580 t PGEs) also contain significant amounts of PGEs in the Bushveld Complex. See Naldrett (2004) for details of their geological settings and resources.

Source: Purvis et al. (1972); Papunen and Gorbunov (1985); Anhaeusser and Maske (1986); Naldrett (1989, 1997, 2002, 2004, 2011); Prendergast and Jones (1989); Hoatson et al. (1992); Eckstrand et al. (1995); Amelin et al. (1999); Hoatson and Blake (2000); Li et al. (2004); Leshner (2004); Maier, (2005); Hoatson et al. (2006); Seat et al. (2007, 2009, 2011); this study; and references cited within these publications.

### **8.3.1.1 PGE-Ni-Cu deposits**

Most economic PGE-dominant deposits in the world occur in stratabound sulphide- and chromite-bearing layers or 'reefs' within extensively differentiated, Precambrian layered mafic-ultramafic intrusions. Notable global examples of these magmatic sulphide deposits (Hoatson et al., 2006) include the UG-2 Chromitite and Merensky Reef in the 2060 Ma Bushveld Complex, the J-M Reef in the 2705 Ma Stillwater Complex, the Main Sulphide Zone in the 2587 Ma Great Dyke, and the Sompujärvi–Ala–Penikka–Paasivaara reefs in the 2440 Ma Penikat Intrusion, Finland (Halkoaho et al., 1990). The most metal endowed and laterally extensive layers generally occur in the largest intrusions (e.g., Bushveld, Great Dyke, Stillwater), whereas less continuous and more irregular layers characterise relatively smaller intrusions (Portimo–Finland; Skaergaard–Greenland; Rincon Del Tigre–Bolivia; and Panton, Weld Range, Munni Munni, Australia). Important factors common to these mineralised layers include: they are hosted by large differentiated intrusions several km in thickness (>3 km); host rocks form texturally distinctive horizons at particular stratigraphic levels within thick, cyclically layered cumulate sequences; the laterally continuous mineralised layers contain a few percent of disseminated magmatic sulphides; and their formation is often related to crustal contamination, crystal fractionation, and magma-mixing processes between primitive PGE-bearing resident magmas and influxes of tholeiitic magmas saturated with sulphides into an evolving and expanding magma chamber (Hoatson and Keays, 1989). A strong correlation is evident between the size of the intrusion and metal endowment, with the largest PGE resources occurring in the three largest intrusions, namely the Bushveld (65 473 t of metal), Great Dyke (13 946 t), and Stillwater (6690 t). The mineralised stratabound layers or 'reefs' in these intrusions vary in thickness from a few centimetres to metres. As an exploration indicator, the thinnest reefs generally have the highest PGE grades, and are located internally within large intrusions. Lower PGE grades characterise thicker reefs which are more abundant near the base, or the margins, of the intrusions.

The economically most important layers (Merensky Reef, UG-2, J-M Reef, Main Sulphide Zone) and similar uneconomic examples in Australia (PWL–Munni Munni, MCL–Panton, Parks Reef–Weld Range: see Chapter 6 and Appendix K) are generally located at, or near, major compositional interfaces in the intrusion that involved the crystallisation of cumulus plagioclase (i.e., near major contacts between ultramafic and mafic sequences). Exploration for PGE-enriched stratabound layers should therefore initially focus on the ~650-m thick stratigraphic interval from ~150 m below the contact between the ultramafic and mafic sequences, and up to 500 m above this contact. The PGMs in the mineralised layers are spatially associated with small volumes (1% to 3%) of disseminated magmatic sulphides (pyrrhotite–pentlandite–chalcopyrite), and in chromitite layers where the PGMs are hosted by chromite and/or minor sulphides. The sulphide components of the mineralised layers have high-metal tenors of up to hundreds of parts per million PGEs. The host rocks comprise a wide range of mafic and ultramafic lithologies, ranging from dunite, harzburgite, pyroxenite, norite–gabbro, gabbro, troctolite, anorthosite, chromitite, and magnetite. Coarse grained, pegmatoidal, and porphyritic textures are a common feature of PGE-bearing sulphide layers (Merensky Reef, J-M Reef, and the PWL at Munni Munni), and disseminated and massive cumulus textures characterise the PGE-bearing chromitite layers (UG-2, Sompujärvi Reef–Penikat, and MCL–Panton).

### **8.3.1.2 Ni-Cu-PGE deposits**

Another major group of magmatic sulphide deposits where the PGEs are subordinate in abundance and economic importance to Ni and Cu are found associated with komatiites (Kambalda, Mount Keith, Thompson, Dumont, Raglan: discussed in Section 8.3.2), ultramafic intrusions (Jinchuan–China, Pechenga–Russia, Kabanga–Tanzania), and in mafic-dominant intrusions (Voisey's Bay–Canada,

Sudbury–Canada, Nebo–Babel–Australia). The latter mineralised ultramafic and mafic-dominant intrusions are invariably of Proterozoic age (<2000 Ma), and their geological characteristics are summarised in Table 8.2. The host intrusions generally consist of relatively small stocks, sills, chonoliths, and ovoid bodies, ranging from a few kilometres to hundreds of metres in diameter, and thicknesses are generally less than 3 km. Intrusions in Proterozoic orogenic zones (Voisey’s Bay, Kabanga, Nebo–Babel, Savannah) compared to those in stable Archean cratons have more irregular, fault-bounded shapes, and may be folded. Massive, matrix, and disseminated Fe-Ni-Cu-Co sulphides are most prominent in the lower parts of the stratigraphy, and remobilised vein systems enriched in Cu-Pd-Pt-Au-Ag-bearing sulphides can intrude the country rocks for several metres. The massive sulphides—critical to the economic status of the deposit—are generally confined to structural embayments and depressions in basal contacts below the thickest sequence of cumulates, or in feeder conduits, which are high-priority exploration targets. Massive sulphides commonly contain abundant xenoliths of country rocks or autoliths from other, related intrusive phases indicating the interaction of different magma and rock types may be important processes for inducing sulphide saturation in these mineral systems. The massive sulphides often have overlying haloes of relatively lower-grade matrix and disseminated sulphides (Sudbury, Kabanga, Jinchuan, Pechenga, Nebo–Babel, Radio Hill) thus these deposits represent much more sulphide-rich mineral systems compared to the PGE-Ni-Cu deposits described above. Nickel and Cu tenors of the sulphides typically range from <1% to >20%, whereas PGE abundances are generally much lower (<1 g/t) than for the PGE-dominant deposits. In contrast, ‘unique’ super-large deposits, such as those at Noril’sk–Talnakh in Russia, can have extremely high grades of PGEs of up to 50 g/t. Host rocks range from dunite (Jinchuan), harzburgite (Kabanga), pyroxenite (Selibe Phikwe–Botswana), olivine gabbro (Noril’sk), gabbro-norite (Sudbury, Nebo–Babel, Radio Hill), and troctolite (Voisey’s Bay).

Magmatic Ni-Cu-PGE sulphide deposits often occur in the same geological province, and indeed usually spatially near other magmatic ore deposits. These include PGE-Ni-Cu deposits, PGE-chromite, PGE-magnetite, komatiite-hosted Ni-Cu deposits, Fe-Ti-V, and alluvial placer deposits. In addition, secondary hydrothermal processes can produce associated asbestos, talc, base-metal vein, and native Cu deposits (Schulz et al., 2010). In Australia, this clustering of different deposit types, which can be a useful exploration indicator, is clearly evident in the Musgrave Province, Halls Creek Orogen, west Pilbara Craton, and greenstone belts in the Yilgarn Craton. It is likely such a spatial association of different deposit types will occur in the emerging Albany-Fraser Province of Western Australia and parts of the Gawler Craton in South Australia.

Table 8.2 indicates that intracontinental rifts within cratons or near the margins of Archean cratons are one of the most important geodynamic settings, whereas multiply deformed orogenic belts characterise Proterozoic terranes. Significant global examples of PGE-Ni-Cu deposits are associated with stabilised Archean cratons, and most occur within the central segments of the cratons (e.g., Bushveld–Kaalvaal, Great Dyke–Zimbabwe). In contrast to the PGE deposits, many Ni-Cu-PGE deposits are located near the margins of cratonic blocks (Noril’sk, Voisey’s Bay, Duluth, Thompson, Raglan, Jinchuan, Kabanga, Baltic Shield intrusions). The Yilgarn Craton in Western Australia is unusual in having many Ni-Cu-PGE deposits, but containing no significant PGE-Ni-Cu deposits. Maier and Groves (2011) indicate that particularly well mineralised cratons include Kaapvaal (mainly PGE-Ni-Cu deposits), Zimbabwe (Ni-Cu-PGE and PGE-Ni-Cu), Yilgarn (Ni-Cu-PGE only), Superior (Ni-Cu-PGE and PGE-Ni-Cu), and Svecokarelian (Ni-Cu-PGE and PGE-Ni-Cu). The most endowed PGE-bearing intrusions have either mafic- or ultramafic-dominant bulk compositions, whereas the Ni-dominant intrusions (Voisey’s Bay, Nebo–Babel, Sudbury, Kotalahti) have a stronger association for mafic-dominant intrusions. Parent magmas are generally of evolved basaltic parentage, with

compositions generally ranging from high-Mg basalt (~15% MgO), magnesian basalt (~12% MgO), tholeiitic basalt (~7% MgO), to more silica-rich variants such as boninite and siliceous high-Mg basalt (9% to 15% MgO). Some deposits (e.g., Pechenga: Barnes et al., 2001) that have more primitive ferropicritic parent magmas (~17% MgO) also show some similarities with komatiitic magmatic systems. There is no obvious correlation between mineralisation and composition of basement rock lithologies, or between mineralisation and metamorphic grade of basement lithologies. Low-grade pelitic sedimentary rocks, chemical sediments, and mafic-felsic volcanics are equally represented with the more high-grade migmatitic, gneissic, and granitic country rocks. This is not surprising since what may be more important in regard to the S evolution of the mineralised intrusions are the rocks the magma(s) interacted with during their ascent through the crust rather than those rocks at the final crustal level of emplacement (i.e., the importance of the third dimension).

The timing of the sulphide-saturation event (e.g., through crustal contamination, magma mixing, temperature gradients) and the mechanism of magma emplacement are critical elements for the concentration of massive sulphides in such deposits as Voisey's Bay (Naldrett, 1997). These deposits are favoured by dynamic feeder systems, physical and chemical interaction with S-bearing country rocks, and a structural framework that facilitates the rapid emplacement of voluminous amounts of hot primitive Ni-bearing magmas (Scoates and Mitchell, 2000). Dynamic magmatic systems that involve repeated surges of magma promote the interaction of a sulphide liquid with a sufficiently large volume of silicate magma to concentrate chalcophile elements (Ni, Cu, PGEs) to economic concentrations (Schulz et al., 2010). The dynamics of a focused magma flow (e.g., fast, slow, turbulent, passive, changes from narrow vertical conduits to broad sub-horizontal open-magma chambers) are also important for the deposition of economically significant massive sulphides.

Evans-Lamswood et al. (2000) highlighted the importance of geometric and morphologic changes in the magmatic feeder conduit for mineralisation at Voisey's Bay. Sulphides are preferentially concentrated in traps where physical irregularities and changes in conduit morphology favour the precipitation, capture, and preservation of sulphides as a result of changes in the velocity and viscosity of the ascending magma. Therefore, sulphide deposition at Voisey's Bay is ultimately related to the complex interplay of dyke geometry (i.e., changes in dyke orientation and thickness) and the fluid dynamics of the magma within the conduit system. Evans-Lamswood et al. (2000) also state that the Voisey's Bay deposit does not conform to the traditional model of magmatic sulphide generation within a mafic intrusion (e.g., Sudbury), where sulphides largely accumulate by gravitational settling within a chamber following sulphide saturation of the magma through crustal contamination. In fact, they proposed that little gravitational settling took place at Voisey's Bay, and that the distribution of sulphides was controlled by magma emplacement through multiple braids of a dynamic, channel-like conduit dyke system. An assessment of the critical mineralising elements at Voisey's Bay can be found in a Special Issue of Economic Geology (2000, Volume 95, Number 4).

### **8.3.2 Komatiitic magmatic systems: fertile versus barren**

Australia's PGE production over the past five decades has been exclusively derived from Archean komatiitic-hosted Ni-Cu sulphide deposits in the Yilgarn Craton of Western Australia. More than 24 812 kg of Pd and Pt, representing 94% of Australia's total PGE production (see Section 1.3.3), have been produced as by-products from these deposits. Komatiitic magmatism has been an integral part of the Archean evolution of the Yilgarn (Barnes, 2006), Pilbara (Hickman and Van Kranendonk, 2008) and Gawler cratons (Fanning et al., 2007). Hoatson et al. (2006; 2009a,b) have shown that the favourable age range for mineralised komatiites in the Yilgarn Craton is ~2700 Ma to ~3000 Ma,

whereas the komatiitic sequences in the Pilbara Craton are older (~2880 Ma to ~3460 Ma), thinner, and contain no significant Ni-Cu deposits. The unmineralised ~2520 Ma Lake Harris Komatiite in the central Gawler Craton of South Australia is the youngest and easternmost known occurrence of komatiitic rocks in Australia (Hoatson et al., 2005b). In regard to exploration targeting, and based upon existing data, komatiites in the Yilgarn Craton have significantly higher priority for PGE (and Ni: Hoatson et al., 2006) mineral systems relative to those in the Pilbara and Gawler cratons.

Komatiitic rocks in Australia have high potential for by-product contributions of PGEs. These distinctive ultramafic rocks have played important roles in Australia's Ni and PGE industries, and because they form a significant part of Australia's Archean cratonic areas in Western Australia and to a lesser degree South Australia, the following section focuses on the main characteristics of fertile and barren komatiitic magmatic systems.

A comparison of global resources of Ni-Cu±PGE deposits in the major komatiite provinces of the world reveals significant differences in metal endowment (Table 8.3). The contribution (as by-products) of PGEs in komatiitic-associated Ni-Cu sulphide deposits shows similar trends to the global Ni metal contents of these deposits. For example, the fertility matrix diagram of Table 8.3 indicates that PGEs constitute major by-products in the prospective Eastern Goldfields, Thompson Belt, Abitibi, and Cape Smith provinces, whereas for the relatively Ni-poor Pilbara, Barberton, Gawler, Zimbabwe, Southern Cross, and Crixás provinces the PGEs form minor by-product components, or are not known. The apparent correlation of high Ni endowment with by-product PGEs is reinforced by the deposits in the Eastern Goldfields Province accounting for ~63% of the world's total Ni sulphide resources hosted by komatiites, which is almost twice the collective Ni resources of the Abitibi, Thompson, Cape Smith, Southern Cross, and Zimbabwe greenstone provinces (Hoatson et al., 2006). It is not clear if the variations of Ni and PGE endowment are due to processes at a global (mantle), regional (geodynamic setting), or local (volcanic architecture, magma composition or volume, type of country rocks) scale, or a combination of these factors. Despite the uncertainty surrounding the genesis of komatiite-associated Ni sulphide deposits (see summaries in Lesher and Keays, 2002, Barnes, 2006, Hoatson et al., 2006), there is some consensus about two significant petrogenetic aspects of these deposits: firstly, komatiitic magmas are derived from high degrees of partial melting of mantle material and arrive at the 'eruptive' site sulphide undersaturated; and secondly, physical and chemical assimilation of S-bearing substrate (ground melting or substrate erosion) can potentially initiate sulphide saturation and the precipitation of Ni sulphides (Barnes et al., 2004a).

Lithochemistry of komatiites has been found to be useful in distinguishing between fertile and barren sequences by helping to identify favourable volcanic environments, and more directly through the geochemical characterisation of crustal contamination and sulphide-saturation processes (Barnes et al., 2004a). According to Barnes et al. (2004a) favourable volcanic environments, such as those containing large-volume lava pathways, can be identified on the basis of the distribution and ratios of whole-rock Mg, Fe, Ni, Cr, and Ti abundances. Crustal contamination can be indicated by enriched abundances and abundance ratios of strongly to weakly incompatible lithophile elements in fractionated lavas, but the effects of metamorphism and alteration on the sequences are often significant and may be misleading. Lesher et al. (2001) have also discriminated between komatiites generated from normal igneous crystallisation processes (barren) and those that were formed during ore-forming processes (fertile) by identifying geochemical and isotopic signatures typical of crustal contamination (e.g., Th-U-LREE enrichment, negative Nb-Ta-Ti anomalies) and/or sulphide segregation (e.g., Ni-Cu-Co-PGE depletion).

Table 8.3 Significant characteristics of fertile and barren komatiitic provinces in the world: Type 3.A, 3.B, 3.C, and 8.B deposits.

Geological province	Major deposit/prospect	Deposit Class. <sup>1</sup>	By-product PGEs	Global Ni resources for province (Mt) <sup>2</sup>	Age (Ma)	Geodynamic setting	Magma composition <sup>3</sup>	Dominant volcanic facies <sup>4</sup>	Basement rocks	Intensity of deformation and/or remobilisation	Increasing Ni±PGE fertility of komatiitic provinces
Eastern Goldfields Province, Australia	Kambalda, Cosmos, Mount Keith, Perseverance	3.A, 3.B, 8.B	Major, minor	11.89 (63%)	2705	Plume-related extensional basin, rift (possibly back-arc)	AUDK, ADK	CSF, DCSF	Felsic and mafic volcanics, sulphidic shale, chert	Moderate to high	↑
Thompson Belt, Canada	Thompson, Pipe, Bowden	3.A, 8.B	Minor	4.22 (22%)	1880	Plume-related rifted continental margin	AUDK	?	Graphitic units, sulphide- and silicate-facies iron formation, pillowed basalt	High	
Abitibi Belt, Canada	Dumont, Shebandowan	3.B, 3.A	Major, minor	1.09 (6%)	2700	Plume-related extension with adjacent volcanic arc, rift	AUDK, ADK	CSF	Felsic volcanics, sulphide-facies iron formation	Moderate	
Cape Smith Belt, Canada	Raglan, Expo–Ungava	3.C, 3.A	Major, minor	0.73 (4%)	1920	?Plume-related continental margin, rift	AUDK	?CSF, LLLS	Gabbro, shale, slate, high-Mg basalt	Moderate	
Zimbabwe Craton, Zimbabwe	Hunter's Road, Shangani	3.A, 3.B	?	0.51 (3%)	2700	Plume-related rifting (possibly back-arc)	AUDK	TDF, ?CSF	Sulphide-bearing felsic units, silicate-facies iron formation	Moderate to high	
Southern Cross Province, Australia	Maggie Hays, Emily Ann	3.A, 8.B	Minor	0.44 (2%)	2900–3000	Plume-related extensional basin, rift	ADK, AUDK	TDF, CSF	Volcaniclastics, oxide-facies iron formation	Moderate	
Crixás Belt, Brazil	Boa Vista	?3.A	Minor	No significant resources	2800	Plume-related extensional basin, rift	ADK	?	Iron formation, mafic units	Moderate	

Geological province	Major deposit/prospect	Deposit Class. <sup>1</sup>	By-product PGEs	Global Ni resources for province (Mt) <sup>2</sup>	Age (Ma)	Geodynamic setting	Magma composition <sup>3</sup>	Dominant volcanic facies <sup>4</sup>	Basement rocks	Intensity of deformation and/or remobilisation	Increasing Ni±PGE fertility of komatiitic provinces
Pilbara Craton, Australia	Ruth Well, Beasley, Dalton	?3.A, 3.C	Minor, major	No significant resources	2880–<3460	Plume-related extension, rift	ADK	?LLLS	Felsic volcanics, sulphide-facies iron formation	Moderate	↑
Barberton Belt, South Africa	Bon Accord	?3.A, 8.B	Minor	No significant resources	3500	Plume-related oceanic plateau/ridge, rift	ADK	TDF	Silicified volcanoclastic, chert, schist, conglomerate, serpentinite	Moderate	
Gawler Craton, Australia	Lake Harris, Mount Hope	No deposits	No known PGEs	No resources	2520	Plume-related extension, rift	ADK	LLLS, TDF	Granite, orthogneiss, paragneiss, iron formation	Moderate	

<sup>1</sup> See Table 6.1 for deposit classifications.

<sup>2</sup> Global resources of nickel metal statistics from Hoatson et al. (2006) and Naldrett (2004, 2011), and references within.

<sup>3</sup> AUDK ( $Al_2O_3/TiO_2 = 15-25$ ): Aluminium-undepleted komatiite (Munro-type); ADK ( $Al_2O_3/TiO_2 < 15$ ): Aluminium-depleted komatiite (Barberton-type). Where both types are present, the dominant chemical type is shown first.

<sup>4</sup> TDF: Thin Differentiated Flows; CSF: Compound Sheet Flows with internal pathways; DCSF: Dunitic Compound Sheet Flows; LLLS: Layered Lava Lakes and/or Sills (Hill et al., 1987; Barnes et al., 1991a, 2004a; Barnes, 2006).

Source: Anhaeusser and Maske (1986); Naldrett (1989, 1997, 2002, 2004, 2011); Parrish (1989); Eckstrand et al. (1995); Ernst and Buchan (2001); Ferreira Filho and Leshner (2001); Meisel et al. (2001); Ayer et al. (2002); Leshner and Keays (2002); Barnes et al. (2004); Hoatson et al. (2005b); Hulbert et al. (2005); this study; and references cited within these publications.

Various studies have shown relationships between the fertility, the age of emplacement and the geochemical type of the komatiites (Barnes et al., 2004a; Maier, 2004; Leshner and Keays, 2002; Leshner et al., 2001; Ferreira Filho and Leshner, 2001; Arndt et al., 1997; Perring et al., 1996; Hoatson et al., 2006; Barnes and Fiorentini, 2012). It has been suggested that fertile komatiites were emplaced in the late Archean (~2700 Ma) as part of a global metallogenic event (Figure 8.2 and Table 8.3). The relatively older komatiites (~2900 Ma) in the Yilgarn (Southern Cross Province), Pilbara, and Aldan (Siberia) cratons, and in the Barberton Belt are less fertile or even barren. It is possible that this increase in the fertility of the late Archean komatiites is related to changes in the composition or physical characteristics of the mantle source, but the evidence (e.g., Nd isotopes) for this is ambiguous (Arndt et al., 1997). According to Maier (2004), the apparent infertility of the older (~3500 to 3200 Ma) South African komatiite sequences may be due to the lower sulphide content of the older Archean (meta)sedimentary substrate.

Table 8.3 shows that fertile komatiitic provinces are dominated by late Archean, Al-undepleted komatiites (AUDK) or 'Munro-type' komatiites. Their  $\text{Al}_2\text{O}_3/\text{TiO}_2$  ratios vary between 15 and 25 and they are typically depleted in incompatible trace elements. The less fertile and older (>~2900 Ma) komatiites in the Yilgarn (Southern Cross Province), Pilbara and Aldan cratons, and in the Barberton and Crixás (Brazil) belts are dominated by Al-depleted komatiites (ADK) or 'Barberton-types', with  $\text{Al}_2\text{O}_3/\text{TiO}_2$  ratios of <15 and enrichment of the more incompatible elements.

Cassidy et al. (2005) have described similar scenarios for the petrogenesis of komatiites from the Yilgarn Craton to that of the 'Barberton' and 'Munro-type' komatiites. They suggest that the Al-depleted komatiites of the Yilgarn Craton reflect high-pressure melting of undepleted mantle, possibly during the rise and stalling of a mantle plume against the base of a thick continental lithosphere mantle. In contrast, the more prospective Al-undepleted komatiites, typical of the Eastern Goldfields Province, may indicate limited or thinned lithospheric mantle as they are sourced from high degrees of melting of depleted mantle at moderate pressures.

Another critical factor that may control the fertility of komatiitic magmas at the site of eruption is the composition of the substrate that may be assimilated through thermal erosion. Such assimilation would lead to cooling of the magma, an increase in silica concentration, and the crystallisation of olivine causing a decrease in the solubility of S in the magma leading to sulphide saturation. For example, a major difference between the contrasting Ni endowments of the Southern Cross and Eastern Goldfields provinces may be related to the chemical composition of the substrate (Table 8.3). According to Groves and Batt (1984), the relatively less-fertile komatiites in the Southern Cross Province belong to the so called platform-type greenstones, formed in shallow-water environment under conditions of low-crustal extension dominated by shallow-water volcanoclastics and/or oxide-facies iron formations. The more fertile komatiites of the Eastern Goldfields Provinces, on the other hand, are suggested to represent rift-phase greenstones formed in relatively deep-water environments under conditions of high-crustal extension. Such environments contain abundant sulphidic shales and/or cherts (Perring et al., 1996), the assimilation of which would facilitate rapid sulphide saturation. The fertile komatiites in the Abitibi Belt have been interpreted as part of rift-phase greenstones, and those in the Proterozoic Thompson Belt inferred to have formed on a rifted-continental margin that contained abundant graphitic-sulphide-bearing units and silicate-facies Fe formations (Bleeker and Macek, 1996).

A comparison of significant features of fertile and non-fertile komatiite belts (Table 8.3) shows that various criteria can be used as regional indicators of fertility. In some fertile provinces, Al-undepleted and Al-depleted komatiitic sequences occur together, however, the most significant mineralisation is

invariably associated with the former compositional group (Sproule et al., 2002b; Barnes et al., 2004a). The most endowed provinces (Eastern Goldfields, Thompson, Abitibi, Cape Smith, and Zimbabwe) are all dominated by Al-undepleted komatiites. Therefore, the predominance of Al-undepleted komatiites in a greenstone belt could be used as a broad regional indicator of fertility. There also appears to be a correlation between the age of the komatiite and Ni endowment. Table 8.3 highlights that ~2700 Ma and ~1900 Ma komatiites contain substantially more resources than komatiites of other ages. Within individual greenstone belts, the type of volcanic facies or flow environment appears to be important in determining fertility. Empirical data for fertile and non-fertile komatiitic sequences suggest that thin differentiated flows and layered lava lakes and/or sills are not as prospective as compound sheet flows with internal pathways or dunitic compound sheet flows, although these latter facies are not always mineralised (Barnes et al., 2004a). The compound sheet flow and dunitic compound sheet flow sequences are not only more likely to have well-insulated lava channels, but they will also contain larger volumes of primitive ultramafic magma in more dynamic environments (i.e., unlike a passive lava lake or pond facies). Thermal erosion of any substrate will help saturate the magma with S and the presence of sulphidic sediments in the substrate that can be readily assimilated will substantially accelerate and enhance mineralising processes.

In regard to craton-scale processes, regional Nd and Pb isotope investigations of the Yilgarn Craton by Champion (2014) and Huston et al. (2014) have shown that well-endowed komatiitic Ni provinces are generally characterised by more evolved crust, and the less endowed provinces are located in more juvenile crust (the opposite relationship applies to volcanic-hosted massive sulphide deposits). The spatial Ni association applies to between provinces (i.e., more evolved Yilgarn Craton compared with juvenile components of Abitibi Belt, Canada), and also to within provinces. For example, in the Eastern Goldfields Province of the Yilgarn Craton there is a clear spatial association of komatiitic-hosted Ni deposits with the more evolved parts of the province. Provinces with more evolved crust appear to have a higher exploration potential relative to other provinces with more juvenile crust.

In summary, the following factors (see Chapter 7) are considered significant in defining the fertility of global komatiitic sequences:

- **Age:** Most fertile komatiite sequences are either of late Archean (~2700 Ma) or Paleoproterozoic (~1900 Ma to 1800 Ma) age. Komatiitic sequences outside these ages appear to have low potential for Ni-Cu-PGE mineralisation or are barren.
- **Magma generation and lithospheric architecture:** Fertile primitive komatiitic magmas derived from high degrees of partial melting of mantle material are funnelled towards lithospheric discontinuities (Mole et al., 2010). The development or reactivation of deeply penetrating faults provide zones of dilation along which the magmas can rapidly ascend through the crust and arrive at the 'eruptive' site *sulphide* undersaturated.
- **Maturity of crust:** Isotopic data (Nd and Pb) indicates that provinces with more evolved crust would have a higher exploration priority for Ni-Cu-PGE deposits relative to other provinces with more juvenile crust.
- **Chemical affinity:** Many Precambrian provinces contain Al-undepleted ( $Al_2O_3/TiO_2 = 15-25$ ) and Al-depleted ( $Al_2O_3/TiO_2 < 15$ ) komatiite sequences. However, the most significant mineralisation is associated with the Al-undepleted komatiites. Al-depleted komatiitic sequences are generally poorly mineralised, particularly if associated with Al-undepleted sequences.
- **Volcanic facies:** Mineralisation is predominantly associated with two major facies: compound sheet flows with internal pathways, or dunitic compound sheet flows. In contrast, such passive facies as thin differentiated flows, lava lakes, and sill-like ponded flows are generally

unmineralised. Well-insulated dynamic lava pathways that help focus large volumes (i.e., high-magma flux) of magma flow and facilitate chemical interaction of the magma with the substrate are more likely to occur in the prospective compound sheet flow facies.

- **Thermal erosion of sulphide-bearing substrate:** With a few exceptions, examples of thermal erosion and/or assimilation of substrate have been demonstrated in fertile komatiite sequences. The assimilation of sulphide-bearing substrate can dramatically accelerate the *sulphide* saturation of a primitive ultramafic magma and deposition of sulphides.
- **Intensity of deformation, metamorphism, post-mineralisation remobilisation, and preservation:** Most mineralised komatiite sequences show evidence of variable degrees of deformation, remobilisation, and dislocation of sulphides during post-mineralisation tectonic, metamorphic, and hydrothermal events (Barnes, 2006). In some instances these processes have resulted in local tenor variations of metals, upgrading of metal concentrations, thickening of ore zones, formation of late-stage discordant vein-type ores, and in highly strained environments, massive sulphide orebodies can occur up to 100 m from their host ultramafic unit. The preservation status of the mineralised environment(s) during tectonism, metamorphism, regolith formation, and erosion can determine economic resource capabilities.

## 8.4 Prospectivity analysis of platinum-group-element mineral systems in Australia

It is difficult to provide an unambiguous exploration framework for any specific PGE deposit, and even harder to generalise about the processes producing these fertile mineral systems. However, there appears to be at least four fundamental key events (or criteria) that mark the development of a 'tholeiitic' magmatic PGE-Ni-Cu±Cr or Ni-Cu-PGE sulphide deposit. Exploration programs should integrate the following criteria, which have been synthesised from Naldrett (1989, 1997, 2002, 2004, 2011), Schulz et al. (2010), and the findings of Chapter 7 in this report.

- **Magma generation:** Fertile metal-bearing mafic or ultramafic parental magmas are generated from hotter-than-normal parts of the mantle. These magmas generally form from high degrees of partial melting (>30%), have relatively high-MgO contents (8% to 15% MgO), and are sulphide undersaturated during their rise from the mantle and emplacement into the crust (Keays, 1995). Such magmas characterise LIPs and the mineral systems at Noril'sk, where picrites and high-MgO basalts are generally present early in the magmatic history.
- **Crustal interaction and timing of sulphide-saturation event:** The ascending magma physically and chemically interacts with its wall-rocks in conduits and in staging sub-crustal magma chambers. Such interaction can form hybrid or contaminated magma and results in incorporation of crustal S. Both processes can result in driving the magma to S saturation and the generation or segregation of an immiscible sulphide liquid (Li et al., 2001a; Naldrett, 2011). Although S-bearing crustal rocks, such as black shales, evaporates, or chemical sediments, are proximal to many deposits, they may not be the primary source of S. One important issue is to determine what other potential S-bearing rocks types could have interacted with the magmas during their ascent through the total crustal sequence. The fact that no S-bearing country rocks are observed in proximity to the intrusion does not necessarily down-grade the potential of such a mineral system; therefore one needs to take a more holistic approach (Hoatson et al., 2006). For the efficient accumulation of massive sulphide, it is important that sulphide saturation and sulphide liquid segregation occur early in the crystallisation sequence before abundant silicate

minerals crystallise and trap the sulphides. In addition, early sulphide saturation is necessary to form typical Ni sulphide ores. This is because significant olivine crystallisation prior to formation of an immiscible sulphide liquid will deplete a silicate liquid in Ni, thus limiting the quantity of Ni available to a sulphide liquid (Naldrett, 2004). In regard to the PGE-enriched stratabound layer scenario (e.g., Merensky Reef, UG-2, J-M Reef, PWL–Munni Munni), it is important that the PGE-fertile magma does not experience a sulphide-saturation event early in its evolution (i.e., at deep crustal levels) since it will be rapidly depleted in strongly chalcophile metals that have very large partition coefficients between sulphide liquid and silicate magmas, such as the PGEs (Capobianco and Drake, 1990; Bezmen et al., 1994; Mungall, 2005a,b; see Section 3.3). Sulphide-saturation events that occur in the magma chamber (i.e., by rapid cooling of magma against country rocks, assimilation of country rocks, crystal fractionation, large-scale magma mixing) will facilitate the formation of PGE-enriched stratabound layers relative to Ni-Cu-PGE sulphide ores concentrated near the basal contacts or in the feeder conduits of the intrusion (Hoatson, 1998).

- **Metal upgrading:** The resulting immiscible sulphide liquid has an opportunity to interact dynamically with a much larger mass of silicate magma (high R-factor: see Section 3.4.2), thereby increasing the tenor of the ore metals, particularly for the strong chalcophile metals. The Ni, Cu, and PGE contents of many ores are much higher than would be expected of sulphide separated from the relatively small quantity of magma represented by their host intrusions (Campbell and Naldrett, 1979). Therefore, sulphide liquid must have interacted with, and extracted ore metals from, a much larger volume of silicate magma. Such upgrading is enhanced in magma conduits where sulphide can interact with new pulses of fertile (with Ni, Cu, and PGEs) magma (Naldrett, 2004, 2011).
- **Concentration of sulphides:** Metal-rich sulphide liquid becomes concentrated in a restricted locality in a quantity sufficient to form an economic deposit (Hoatson et al., 2006; Schulz et al., 2010). Fluid dynamics are important for the deposition of massive sulphides, such as where the flow velocity of magma is reduced or changed from turbulent to passive flow. Such a scenario would be where a narrow feeder conduit enters a broad magma chamber, resulting in a decrease in flow velocity and the concentration of heavy descending sulphide droplets (Li and Naldrett, 2000; Hoatson et al., 2006). In addition, structurally-controlled (e.g., fault-bounded) and thermally eroded embayments in the basal footwall contact, where dense sulphide liquids can migrate to and accumulate as massive sulphides, are important elements of the Ni-Cu-PGE mineral system. Such embayments have been documented for several mineralised Paleoproterozoic mafic intrusions in the Halls Creek Orogen (Hoatson, 2000). In contrast, for PGE-enriched stratabound layers, the most significant mineralisation is generally associated with disseminated sulphides or massive chromitite layers near major compositional interfaces, i.e., the contact between the ultramafic zone and gabbroic zone, in large layered differentiated intrusions. In these mineral systems, wide-scale magma mixing between a PGE bearing, high-MgO resident magma that is sulphide undersaturated, and a later, hot and buoyant, sulphide-saturated  $Al_2O_3$ -rich tholeiitic magma, will initiate sulphide saturation in a mineralised hybrid magma near the ultramafic and gabbroic zone contact and provide a potential mechanism for establishing a high R-factor (Hoatson and Keays, 1989; Naldrett, 2011). In this situation, the stratigraphic interval 150 m below to 500 m above this contact is generally the most favourable for PGE-enriched sulphide and chromitite layers (see Chapter 6), as seen for the Merensky Reef and UG-2 (Bushveld Complex), J-M Reef (Stillwater Complex), MSZ (Great Dyke of Zimbabwe), PWL (Munni Munni Intrusion), and MCL (Panton Intrusion).

Chapter 7 and Sections 8.2 and 8.3 of this report have discussed the various factors considered important for the development of fertile PGE mineral systems. Many criteria, such as the metal endowment of global deposits, temporal associations, geotectonic setting, size and composition of the mafic-ultramafic host body, primitive status of ultramafic and mafic rock types, fertility of parent magma, country rocks, crustal contamination, volcanic-intrusive architecture, dynamics of magma emplacement, evolution of S in magmas, magmatic-metamorphic-hydrothermal-regolith processes, and preservation, need to be considered when assessing the appropriate mineral system and prioritising exploration targets. The extensive database of more than 500 documented occurrences of PGEs in Appendix K, indicates that many different types of mineral systems were active in Australia from at least the late Archean (~2930 Ma: Figure 8.1) to present times. These mineral systems obviously have different levels of potential for forming a major economic resource of PGEs.

As discussed in Section 8.3, all the major magmatic PGE-Ni-Cu and Ni-Cu-PGE deposits in the world (UG-2, Merensky Reef, Platreef–Bushveld; J-M Reef–Stillwater; MSZ–Great Dyke; Noril'sk; Sudbury) that dominate global resources and production of PGEs are genetically and spatially related to bodies of mafic and/or ultramafic igneous rocks (Naldrett, 1997). This association is also seen in Australia with the most significant PGE prospects (Panton, Munni Munni, Windimurra, Owendale, Adamsfield) associated with various types of mafic-ultramafic intrusions. Therefore, as a first-order exploration criteria for target generation, the identification of prospective mafic and ultramafic rocks should be the highest priority. With the exception of the 'unique' 251 Ma Noril'sk and 1850 Ma Sudbury Ni-Cu-PGE deposits, and based on existing data, all the major PGE-producing deposits in the world are older than ~1900 Ma. Using the two target criteria of rock association and geological age, exploration programs focussed on Archean and early Proterozoic mafic and ultramafic rocks would have less exploration risk in finding a large-tonnage PGE deposit relative to such programs operating in the younger Phanerozoic terranes of eastern Australia. An abundance of prospective mafic-ultramafic rocks of Archean and Proterozoic age occur in the west of the continent. These rocks are particularly widespread in outcrop and under cover in Archean cratons, Proterozoic orogenic belts, and in sedimentary basins west of the Tasman Line (Shaw et al., 1996; Direen and Crawford, 2003; Glen, 2005). In many respects, the Tasman Line, a controversial zig-zag line that crosses the Australian continent from north to south, divides the continent into different levels of PGE prospectivity. The Tasman Line is interpreted by some researchers as a regional orogenic suture that demarcates the western extent of the break-up of Rodinia, followed by the growth of orogenic belts along the eastern margin of Gondwana. Other investigators have interpreted it as the westernmost limit of deformation associated with the eastern Australian Paleozoic fold belts (e.g., Tasman Foldbelt System). The region east of the Tasman Line, extending across to the east coast (referred to as the Tasmanides of eastern Australia: Glen, 2005), essentially consists of Phanerozoic rocks, and contains no exposed Archean rocks and only a few percent Proterozoic mafic-ultramafic rocks (Hoatson et al., 2008a,b).

Exploration potential can be determined at scales ranging from continent and province scale down to outcrop scale (e.g., surface gossan) of a few metres wide. The sampling in 1939 of some curious green-stained gossanous rocks (0.7% Ni, 0.5% Cu) near Lake Lefroy in Western Australia led to the discovery of one of the great Ni mineral inventories of the world. The full significance and potential of this small outcrop was realised 27 years later, when the world-class Ni-Cu-PGE sulphide ore-bodies at Kambalda were discovered in 1966 (see Section 5.2.4). This seminal event in Australia's Ni history indicates that globally significant mineral deposits can be discovered at the scale of an outcrop.

The following discussion examines prospectivity analysis and exploration strategies at three different geographical scales, namely: Section 8.4.1 Continent Scale; Section 8.4.2. Province Scale: LIPs; and Section 8.4.3 Intrusion Scale.

### 8.4.1 Prospectivity analysis—continent scale

During the periods 2006 to 2009 and 2012 to 2014, Geoscience Australia (GA), in collaboration with the State/Territory geological surveys and other organisations, produced four online resource packages relating to mafic-ultramafic magmatic events in Australia. The first three packages comprised geological maps (at various scales), accompanying GA records, and time-slice maps of magmatic events that summarised the temporal and spatial evolution of Archean and Proterozoic mafic-ultramafic magmatism in Australia. The most recent package release is a national GIS dataset and GA record, which incorporates the results of the Archean and Proterozoic resource packages released between 2006 and 2009 and a recent compilation on the Phanerozoic Eon from 2012 to 2014 (see details below). The different 'Mafic-Ultramafic Magmatic Events' packages focuses attention on the continent-wide extent and volume of certain magmatic systems, and associations with mineralisation. The locations of magmatic units, correlations across the continent, and the relationship of magmatism to the evolving crustal structure of the continent, are all prominent. The mafic-ultramafic magmatic events are based on several hundred published age measurements, and are derived from recent U-Pb dating of zircon and baddeleyite, as well as potassium-argon and argon-argon whole-rock for many of the Phanerozoic aged rock units. Regional solid geology, interpreted basement geology and surface geology base maps are used for the representation of Magmatic Events, made available by the State and Northern Territory geological surveys. Solid-geology maps were favoured over other map types where coverage was available since these maps provide insight into the total areal extent of the magmatic system, which is an important criterion when assessing mineral potential. The 'Mafic-Ultramafic Magmatic Events' products provide a national framework for investigating under-explored and potentially mineralised environments, and assessing the role of mafic-ultramafic magmatism in the development of the Australian continent.

In addition to the above investigations, a related study that focussed on the evolution of Proterozoic LIPs in Australia (see Section 8.4.2) was completed in 2009. The spatial representation of the LIPs indicates continent-scale crustal controls on their regional distribution. An innovative series of time slices also highlight the repeated use during the Proterozoic of certain structural corridors and crustal elements for the emplacement of these voluminous mafic-dominant magmatic systems.

From 2012 to 2014, GA compiled mafic and ultramafic magmatic events in Australia for the Phanerozoic Eon. These results were integrated with the Archean and Proterozoic datasets to produce a national GIS dataset. The chronology of Australian mafic-ultramafic magmatism resolves into 74 magmatic events within resolvable bands of  $\pm 10$  million years. These magmatic events range in age from the Eoarchean ~3730 Ma Manfred Event (ME 1), confined within a small remnant domain within the Yilgarn Craton, to the widespread record of Cenozoic magmatism in eastern Australia (ME 72 to ME 74).

Figure 8.5 and Figure 8.6 are Time–Space–Event charts for Australian Archean and post-Archean Mafic-Ultramafic Magmatic Events, respectively. The national map portraying 74 mafic-ultramafic magmatic events is shown in Figure 8.7.

The national magmatic events digital dataset and derivative charts and maps provide in more detail a framework for the exploration of orthomagmatic and hydrothermal mineral deposits, and for assessing their generation in geodynamic processes that range in scale from the local to the continent-wide. The GIS dataset would be of interest to those explorers identifying particular suites of mafic-ultramafic rocks (by age, geochemistry, metal endowment, mineral system), and/or searching for such commodities as PGEs, Ni, Cu, Cr, Ti, Co, and V associated with these rocks. Users are encouraged to

make use of this fundamental Time–Space–Event framework to overlay and integrate their own datasets, to evaluate:

- the spatial distribution of mafic and ultramafic rocks, their geological settings, the frequency of emplacement and potential coeval relationships;
- the secular variation of mafic and ultramafic magmatism, such as mafic-dominated systems versus ultramafic-dominated systems;
- the magnitude of each magmatic system (including LIPs) which has implications for structural frameworks, tectonic settings, and metallogenesis;
- correlatives of magmatic units that are mineralised elsewhere in the Australian continent, and in other continents;
- relationships with favourable reactive (e.g., carbonaceous, S-bearing) country rocks that may potentially induce contamination and sulphide saturation of mafic-ultramafic magmatic systems during emplacement; and
- the spatial distribution of extrusive versus intrusive magmatic components within each magmatic event, as an indication of erosional levels and potential vectors to favourable mineralised environments, such as feeder conduits and basal contacts of intrusive bodies.

Datasets that should be considered for integration include geochemical and isotopic data for specific magmatic events of interest: these can now be placed within a systematic context of correlation in time and space, and so used to discriminate coeval systems and their potential for mineralisation. The context of other metamorphic and igneous rocks, including alkaline igneous rocks (kimberlite, lamprophyre, etc) can be used to evaluate mantle processes and the wider geodynamic systems of which the mafic-ultramafic magmatism is a part. Integration with the increasing coverage and sophistication of geophysical surveys, including continental seismic traverses, can improve knowledge of the fundamental crustal architecture within which the magmatic systems are emplaced, and enhance the capacity to detect and evaluate mineralised igneous rock units under cover.

Four major Mafic-Ultramafic Magmatic Events resource packages are listed in Section 1.6. Other GA national geophysical datasets that have applications for assessing the potential of mafic-ultramafic rocks and were used for the above 'Mafic-Ultramafic Magmatic Events' resource packages are:

- magnetic anomaly dataset of Australia;
- gravity worm dataset of Australia;
- radiometric dataset of Australia;
- surface geology dataset of Australia;
- national geochemical survey dataset of Australia; and
- the Australian Stratigraphic Units Database.

The details and applications of the first five datasets are summarised in Chapter 5.3 of Hoatson et al. (2011).

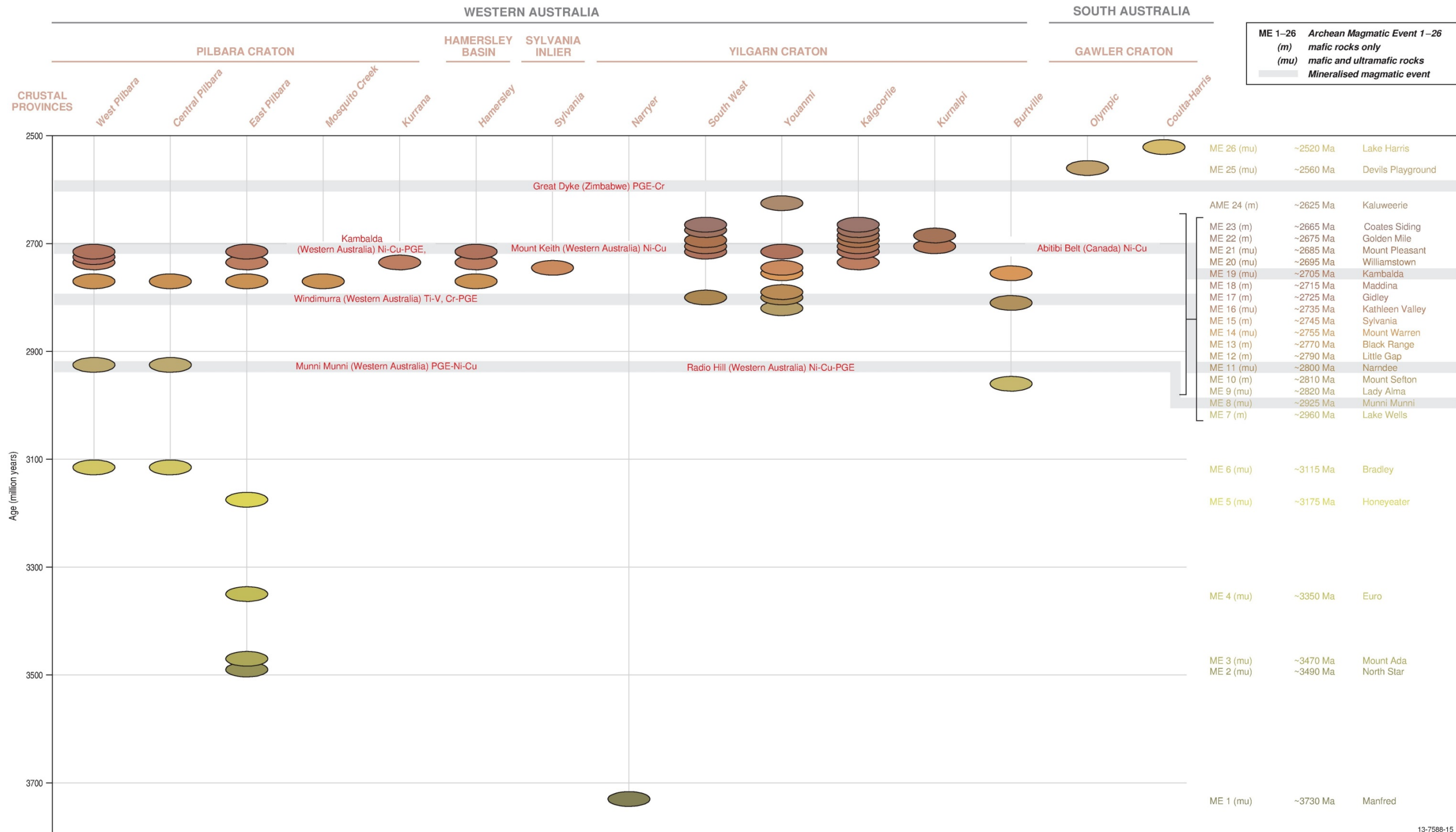


Figure 8.5 Time-Space-Event chart of Australian Archean Mafic-Ultramafic Magmatic Events. From Australian Mafic-Ultramafic Magmatic Events GIS Dataset (Thorne et al., 2014).

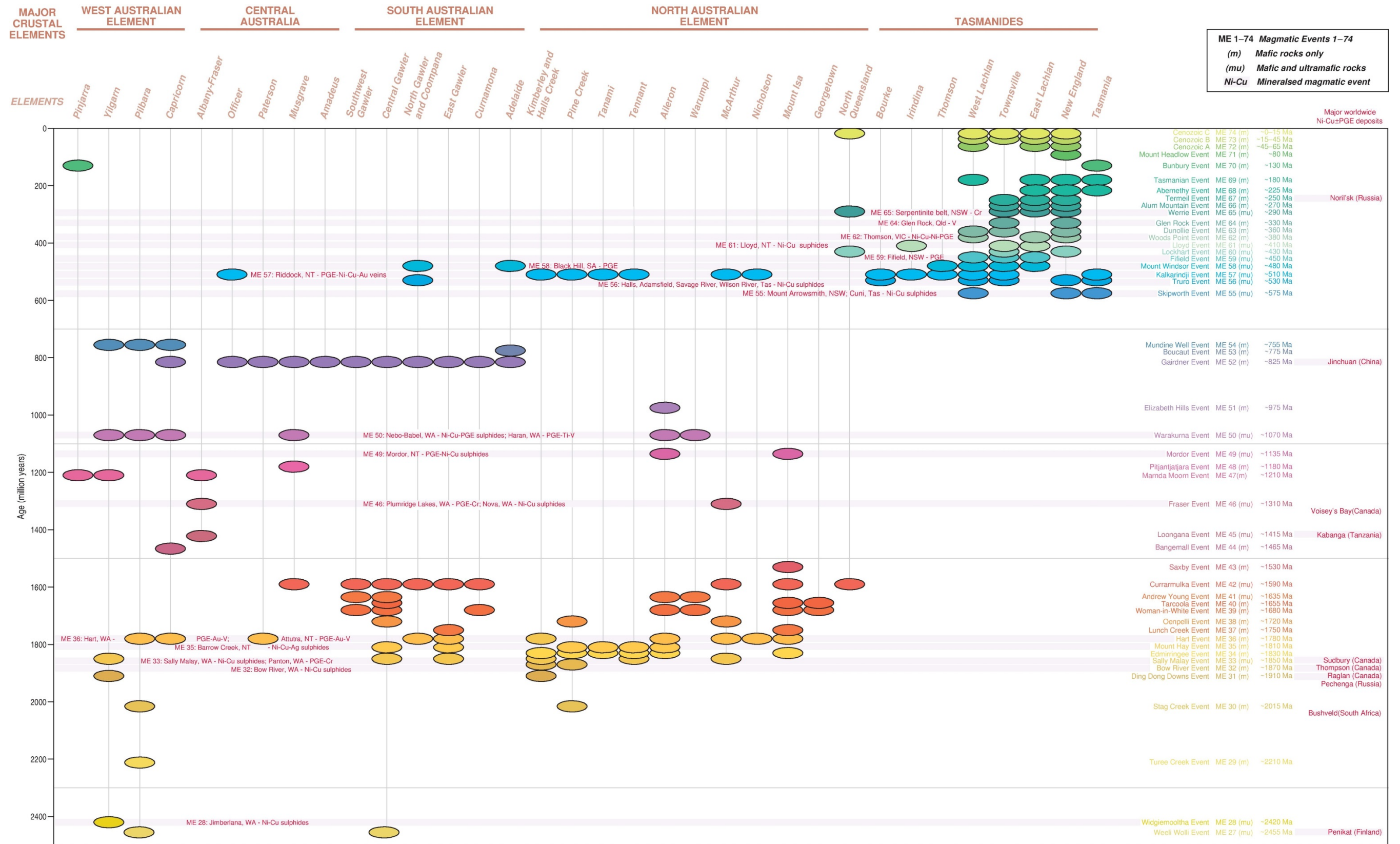


Figure 8.6 Time-Space-Event chart of Australian Proterozoic and Phanerozoic Mafic-Ultramafic Magmatic Events. From Australian Mafic-Ultramafic Magmatic Events GIS Dataset (Thorne et al., 2014).

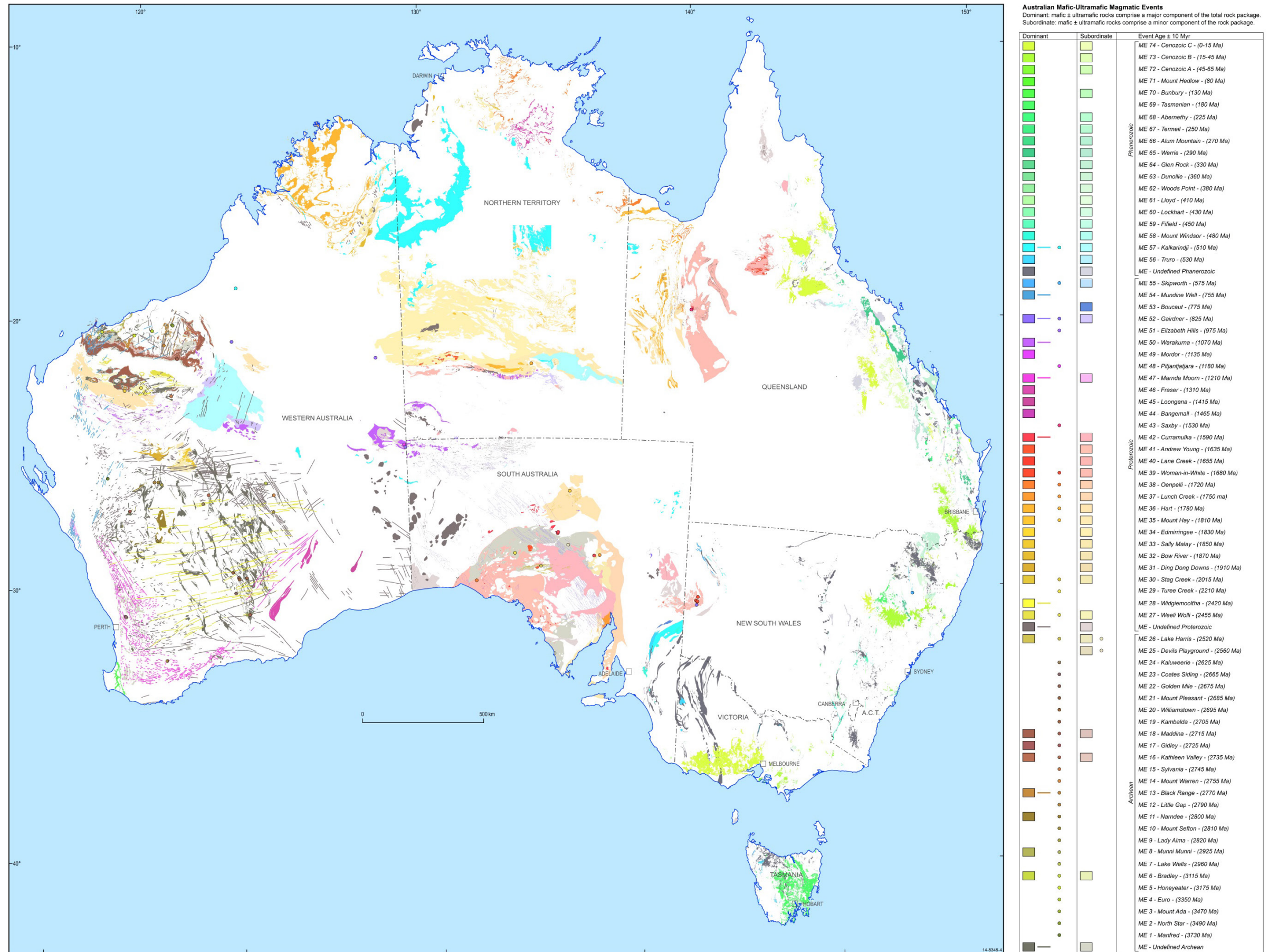


Figure 8.7 Map of Australian Archean, Proterozoic, and Phanerozoic Mafic-Ultramafic Magmatic Events. From Australian Mafic-Ultramafic Magmatic Events GIS Dataset (Thorne et al., 2014).



#### 8.4.2 Prospectivity analysis—province scale: large igneous provinces

Large Igneous Provinces are formed by the rapid and voluminous emplacement of mafic, ultramafic, and/or felsic magmas in intraplate settings (Ernst and Buchan, 2001). These transient magmatic events are believed to be related to large-scale processes in the Earth's upper and/or lower mantle region not related to normal plate margin magmatism (Coffin and Eldholm, 2001). Such 'magmatic environments' as volcanic passive margins, oceanic plateaus, submarine ridges, seamount groups, and ocean basin flood basalts do not originate at seafloor spreading centres. Most LIPs are thought to be associated with mantle upwellings (e.g., mantle plumes), and they are preserved as coeval continental flood basalts, layered mafic-ultramafic intrusions, mafic sills, and large mafic dyke swarms. LIPs typically evolve over extremely short geological time periods of a few million years or less. They play an important role in the geological record, as they represent anomalous conditions when large amounts of mafic and felsic magmas were produced during this short time period. Bryan and Ernst (2008) have redefined LIPs as magmatic provinces with areal extents  $>0.1 \text{ Mkm}^2$ , igneous volumes  $>0.1 \text{ Mkm}^3$ , and maximum lifespans of  $\sim 50$  million years that have intraplate tectonic settings or geochemical affinities, and are characterised by igneous pulse(s) of short duration ( $\sim 1$  to  $5 \text{ Ma}$ ), during which a large proportion ( $>75\%$ ) of the total igneous volume has been emplaced. Sheth (2007) proposed that LIPs have outcrop areas  $>50\,000 \text{ km}^2$ , and they are independent of composition, tectonic setting, or emplacement mechanisms.

The economic importance of LIPs in the genesis of mineral, hydrocarbon, and even ground-water resources has recently been highlighted by Ernst and Jowitt (2013) and Ernst (2014-in press). These authors maintain that LIPs can be a primary host for mineral deposits, as exemplified by LIP-related orthomagmatic Ni-Cu-PGE sulphide, Fe-Ti-V oxide, and Cr deposits, where mineral deposits are formed as a direct consequence of mafic-ultramafic magmatism during a LIP event. The links between LIPs and carbonatites and kimberlites also mean that such commodities associated with these rocks, e.g., REEs, Nb, Ta and diamonds, could be also directly linked with LIP events. In an indirect sense, LIPs may also have the potential to provide a source of energy for circulating hydrothermal systems, such as in Fe-oxide Cu-Au and VMS deposits.

The structural framework of the crust is important for the development of the LIP and associated mineral deposits. Extension, rifting, and the development or reactivation of deeply penetrating faults provide zones of weakness and dilation along which magma can rapidly ascend into the crust (Begg et al. 2010; Pirajno and Hoatson, 2012). These magma-focussing structures facilitate the formation of dynamic subvolcanic feeder systems that typically host Ni-Cu-PGE sulphide deposits (Arndt, 2005; Schulz et al., 2010).

Pirajno and Hoatson (2012) have described Australia's LIPs (Figure 8.8) that cover much of the geological time scale from the Archean to the Recent. Continental flood basalts, fragments of oceanic plateaus, layered mafic-ultramafic intrusions, sill complexes, and dyke swarms are the major components of Australia's mafic-ultramafic LIPs. The discovery of the Nebo–Babel Ni-Cu-PGE sulphide deposit (see Section 6.4) in the Musgrave Province of central Australia in 2000 raised the awareness of the economic potential of LIPs in Australia.

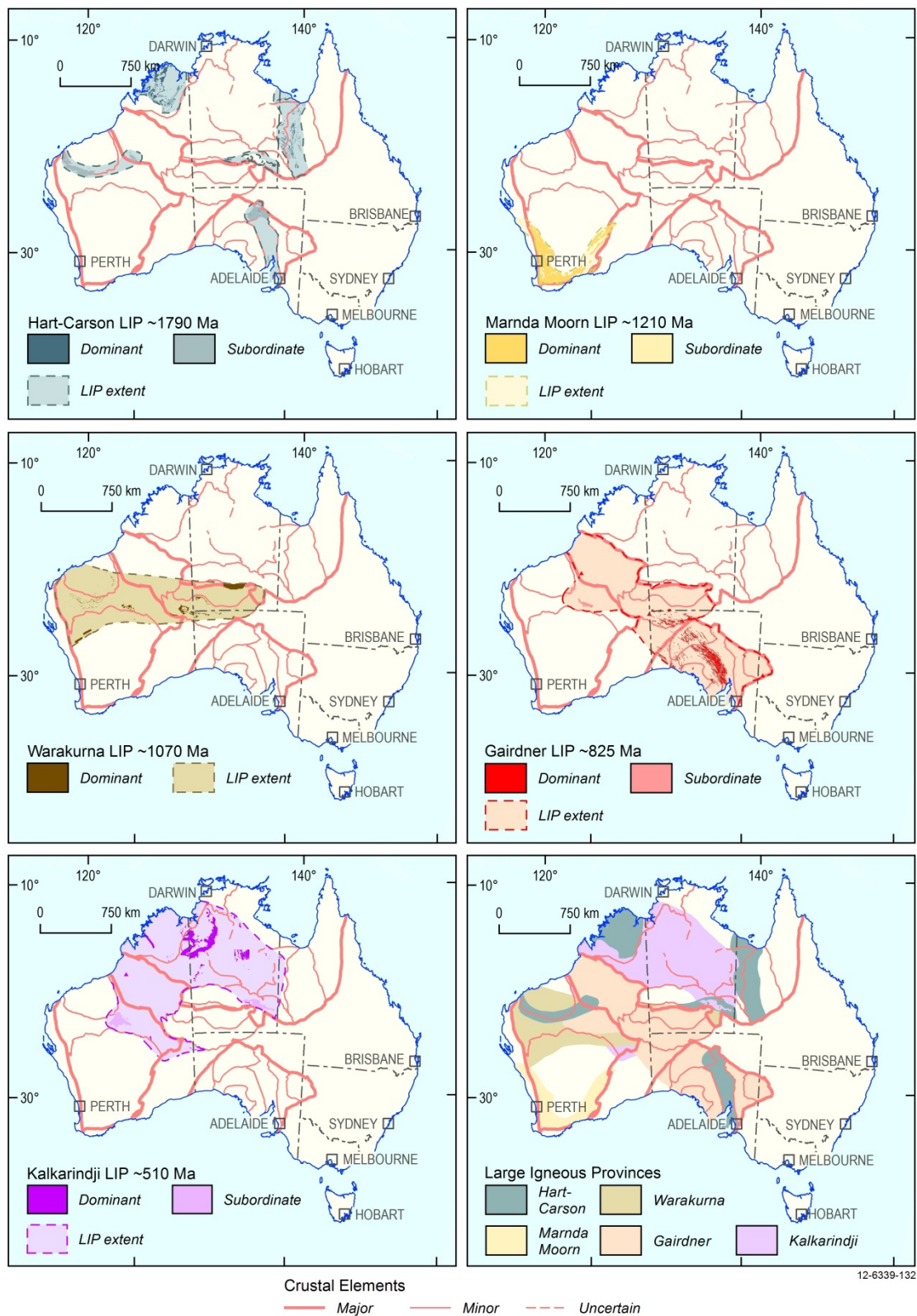


Figure 8.8 Interpreted distributions of some major Large Igneous Provinces in Australia. Those LIPs shown are modified after the following respective authors: Hart–Carson LIP ~1790 Ma (Tyler et al., 2006); Marnda Moorn LIP ~1210 Ma (Wingate and Pidgeon, 2005); Warakurna LIP ~1070 Ma (Wingate et al., 2004); Gairdner LIP ~825 Ma (Zhao et al., 1994); and the Kalkarindji LIP ~510 Ma (Glass and Phillips, 2006). The final figure in the bottom right corner is a composite map of the five LIPs. Dark screens indicate areas of outcrops and light screens indicate the interpreted distribution of the LIP. Modified from Claoué-Long and Hoatson (2009a,b; 2010).

Exploring LIPs can be high risk and present many challenges, such as defining favourable mineralised environments (feeder conduits, lava channels, dynamic magma surges) under cover in extremely large areas; lack of reliable geochronology and geochemical data for identifying different phases of the magmatic system; and a general perception that the global type example—Noril'sk–Talnakh Ni-Cu-PGE sulphide deposits in Russia—may be a 'unique' mineral system. Despite these potential issues, the rewards of discovery could be significant since many of the giant PGE deposits (e.g., Noril'sk, Duluth, Bushveld) are related to rapidly developed LIPs that may have originated from plume-related magmatism. Since Ni has a moderate partition factor with crystallising olivine, the Ni-Cu sulphide-bearing magma needs to reach the crust with minimum olivine fractionation and sulphide segregation (Barnes and Lightfoot, 2005). If the plume does not rise at a plate boundary, Begg et al. (2010) suggest that the plume will rise beneath the thick lithosphere and then be channelled by the lower boundary of the lithosphere to areas of thinner lithosphere adjacent to a cratonic margin where it will be extruded or emplaced. Subject to their history of S evolution, some LIPs may retain their PGEs until reaching appropriate trap sites in crustal reservoirs or lava flows, leading to an ideal situation for clusters of PGE deposits (Green and Peck, 2005). There are also opportunities for hydrothermal PGE deposits, particularly along the major plumbing faults that provided the pathway for the mantle-derived melts through the crust. Other attractions include the potential for large-tonnage Ni-Cu-PGE deposits, associated polymetallic deposits (e.g., PGEs, Ni, Cu, Au, Pb, Zn, Ni, Ti, Mo, Mn), and LIPs in Australia have received very little systematic and thorough exploration exposure.

The geological setting and economic potential of the following five LIPs are discussed in the following sections.

- Section 8.4.2.1: Fortescue LIP: ~2770 Ma (Thorne and Trendall, 2001)
- Section 8.4.2.2: Hart–Carson LIP: ~1790 Ma (Tyler et al., 2006)
- Section 8.4.2.3: Warakurna LIP: ~1070 Ma (Wingate et al., 2004)
- Section 8.4.2.4: Kalkarindji LIP: ~510 Ma (Glass and Phillips, 2006)
- Section 8.4.2.5: Tasmanian Dolerite LIP: ~175 Ma (Hergt and Brauns, 2001)

#### **8.4.2.1 Fortescue large igneous province**

**Age:** ~2770 Ma–2710 Ma (Pirajno and Hoatson, 2012). SHRIMP U-Pb zircon ages for Mount Roe Basalts vary from ~2775 Ma to ~2663 Ma (Thorne and Trendall, 2001). A rhyolite in the Maddina Formation (previously called Mount Jope Volcanics) has a younger age of 2717 Ma. Geochronological studies by Blake et al. (2004) yielded U-Pb zircon ages of felsic and mafic rocks ranging from ~2766 Ma to ~2713 Ma.

**Brief description:** The lower stratigraphic part of the Hamersley Basin in Western Australia—the Fortescue Group—contains a significant thickness of mafic to intermediate and ultramafic volcanic rocks, mafic sills, mafic-ultramafic layered intrusions, and dykes. The mafic volcanics form a stacked sequence of flood basalts that have tholeiitic and calc-alkaline affinities. There are at least eight major episodes of basalt-dominated magmatism in the group ranging in age from ~2770 Ma (Bellary Formation–Mount Roe Basalt) to possibly as young as ~2630 Ma (Jeerinah Formation). With the exception of the  $2775 \pm 10$  Ma Mount Roe Basalt (and its coeval  $2772 \pm 2$  Ma Black Range Dolerite Suite), the  $2741 \pm 3$  Ma Kylena Formation, the  $2715 \pm 2$  Ma Maddina Formation, and their lateral equivalents the Boongal and Bunjinah formations, respectively, very few of these basaltic episodes have reliable crystallisation ages (Hoatson et al., 2009a,b). The mafic rocks of the basin are dominantly continental tholeiitic basalts deposited both subaqueously and subaerially. High-Mg komatiitic lavas (Pyradie Formation) and mafic sills (Jeerinah Formation) also form minor components

in the Fortescue Group. Doleritic sills of the ~2455 Ma Weeli Wolli Formation (Hoatson et al., 2008a,b) are the major mafic component in the upper part of the Hamersley Group that overlies the Fortescue Group (Barley et al., 1997), but these are not included in the Fortescue LIP.

**Size:** The total succession of the Fortescue LIP is about 6.5 km-thick and covers about 40 000 km<sup>2</sup> (Pirajno, 2004; Pirajno and Hoatson, 2012). Significantly, several of the basaltic formations in the Fortescue Group are areally extensive thus appearing to satisfy one of the basic criteria for establishing a LIP. Coeval mafic-ultramafic rocks occur in the west and east Pilbara terranes, Hamersley Basin, and three terranes (South West, Youanmi, Kalgoorlie) of the Yilgarn Craton.

**Feeder zone:** No feeder zones have been identified. However, large north-northeast-trending 2772 ± Ma dolerite dykes of the Black Range Dolerite Suite that traverse the Pilbara Craton are coeval (and possibly comagmatic) with the continental flood basalts in the Fortescue Group of the Hamersley Basin (Wingate, 1999). In addition, the 2747 ± 4 Ma dolerites of the Sylvania dyke swarm (Wingate, 1999) could be feeders to the voluminous 2741 ± 3 Ma basalts in the Kylene Formation of the Fortescue Group (Hoatson et al., 2009a).

**MgO concentration:** The MgO concentration ranges from 2.26% to 8.15% for the Mount Roe Basalt and from 3.78% to 34.05% for the more primitive Maddina Formation (Arndt et al., 2001).

**Sulphur concentration:** Very limited data. Sulphur concentration varies between 80 ppm and 1100 ppm (Mount Roe Basalt; Thorne and Trendall, 2001) and between 220 ppm and 380 ppm (Kylene Formation, Maddina Formation; Thorne and Trendall, 2001).

**Isotope composition:**  $\epsilon_{Nd}$  (T) values for Mount Roe Basalt and Maddina Formation vary between -2.4 and -1.1 and -0.7 and 0.5, respectively (Arndt et al., 2001).

**Pre-eruptive country rocks:** Mafic rocks overlie and intrude Archean granite-greenstone rocks of Pilbara Craton. Some of the greenstones locally contain sulphide- and sulphate-bearing sequences.

**Evidence of crustal contamination:** Geochemical data in Arndt et al. (2001) suggest interaction with and contamination of continental lithosphere. Petrogenetic modelling by Arndt et al. (2001) using Nb and REE concentrations (La, Sm, Nd) indicates that some komatiites may have undergone 30% to 40% contamination of crustal material. These results are consistent with negative  $\epsilon_{Nd}$  data.

**PGE-Ni-Cu occurrences/prospects/anomalies:** A number of Ni-Cu-PGE prospects (Beasley Ni and Bellary Ni) have been reported in association with basaltic komatiites (Pyradie Formation, see Appendix K for more information). The Beasley Ni-Cu-PGE prospect (AusQuest Limited, 2003, 2004, 2006) in the Hamersley Basin contains mineralised komatiite rocks interpreted to be comagmatic with basaltic rocks of the ~2770 Ma Fortescue Group.

**Mineral potential:** Available information suggests that continental tholeiitic basalts and komatiitic basalts are prospective for PGE-Ni-Cu mineralisation associated with komatiitic flows (mineral-system class 3) and with continental flood basalts (mineral-system class 7, Noril'sk-type). The presence of Ni Cu prospects suggests that mafic rocks were able to generate fertile mineral systems. However, the following investigations are required to properly assess the mineral potential of this LIP.

- Detailed geochronological work to establish different phases of lava eruption and emplacement of intrusions.
- Mapping of feeder zones and lava channels. Archean age of rocks and post eruption/emplacement deformation suggests that some deep-seated feeder zones may have

been uplifted to accessible depths. However, it is also possible that many of the feeder zones have been eroded.

- Detailed geochemical studies to establish nature and timing of sulphide saturation and in areas proximal to interpreted feeder zones.
- Detailed geochemical studies to determine the nature and extent of crustal contamination. Areas in proximity to the Archean Sulphur Springs Group may be more promising because the sediments contain both sulphate- and sulphide-bearing sequences (Huston et al., 2001).
- Pirajno and Morris (2005) discuss the possible links of the Fortescue Group basaltic rocks with mantle plumes, and the Ni-Cu-PGE potential of these magmatic systems. The geotectonic setting of these rocks has been variably interpreted as a rift-to-passive margin, to a more complex rift and breakup-shelf subsidence environment (Thorne and Trendall, 2001).

### Major references

Arndt et al. (2001); AusQuest Limited (2003, 2004, 2006); Barley et al. (1997); Blake et al. (2004); Hoatson et al. (2009a, b); Huston et al. (2001); Pirajno (2004); Pirajno and Hoatson (2012); Pirajno and Morris (2005); Thorne and Trendall (2001); Wingate (1999).

#### 8.4.2.2 Hart–Carson large igneous province

**Age:** 1835–1790 Ma. A Rb-Sr isochron age of  $1762 \pm 15$  Ma was reported by Page et al. (1984) for the Hart Dolerite. A more robust estimate of the age is given by a SHRIMP U-Pb zircon age of  $1790 \pm 4$  Ma (R.W. Page, unpublished data, Geoscience Australia). This age is consistent with a SHRIMP U-Pb crystallisation age of  $1797 \pm 11$  Ma for two granophyre samples from the upper part of the Hart Dolerite (Sheppard et al., 2012). No direct age for the Carson Volcanics is available. The volcanics are intercalated with sandstone and siltstone of the Kimberley Group, which unconformably overlies the Speewah Group. A SHRIMP U-Pb zircon age of  $1834 \pm 3$  Ma of the felsic volcanics in the Speewah Group (Page and Sun, 1994) provides a maximum age for the Carson Volcanics. The precise time gap between the eruption of the Carson Volcanics and intrusion of the Hart Dolerite is not known (Tyler et al., 2006).

**Brief description:** The Carson Volcanics outcrop throughout the lower part of the Kimberley Basin and are associated with Proterozoic volcanoclastic and sedimentary rocks. The volcanic rocks consist mainly of tholeiitic basalt. Lava flows include pillowed and amygdaloidal basalts with subordinate pyroclastic rocks and are interlayered with sandstone, siltstone, and chert, with aggregate thicknesses ranging from 200 m to 700 m (Tyler and Griffin, 1993). The Carson Volcanics locally have disseminated pyrite and chalcopyrite (Griffin et al., 1993). The Hart Dolerite consists of a number of mafic sills, with a combined thickness of 3000 m (Griffin et al., 1993). The sills are typically tholeiitic and several contain thick granophyric tops (Griffin and Grey, 1990). The main rock types are dolerite, quartz dolerite, and olivine dolerite, with minor diorite and granophyric dolerite. The granophyre is mainly a monzogranite or syenogranite, but it may also include minor quartz monzonite or quartz syenite. The granophyre is mostly a medium-grained rock comprising pyroxene and plagioclase in a granophyric or micrographic matrix. Pegmatitic granophyre, comprising intergrowths of pyroxene, altered amphibole, and plagioclase, is a minor component (Griffin et al., 1993; Thorne et al., 1999). The granophyre is unlikely to be related to the dolerite by *in situ* crystal fractionation. Although there is a range of rock types from olivine dolerite to felsic granophyre, transitional rock types between dolerite and granophyre are a very minor component of the unit (Gellatly et al., 1975). Contacts between dolerite and granophyre bodies also appear to be sharp (Thorne et al., 1999).

**Size:** The aerial extent of the basaltic and doleritic rocks is probably in excess of 100 000 km<sup>2</sup>, and with an estimated total volume of 250 000 km<sup>3</sup> (Tyler et al., 2006). Figure 8.8 shows that possible extensions of the Hart–Carson LIP to the south and southeast of the Kimberley Province encompasses time-equivalent magmatism in eight other provinces across the West, North, and South Australian Crustal Elements, and in Central Australia (Hoatson et al., 2008a,b). Detailed geochemical and isotopic studies are needed to establish the extent to which they may represent comagmatic systems.

**Feeder zone:** Vertical cylindrical feeder systems in the northeastern part of the Kimberley Basin and offshore in the vicinity of an exploration oil well (Cambridge 1) have been interpreted from regional aeromagnetic data (Meixner and Gunn, 1997).

**MgO concentration:** MgO concentrations range from 6.21% to 9.45% for the Carson Volcanics (3 samples, Ozchem), and from 4.67% to 5.12% for the Hart Dolerite (4 samples, Ozchem).

**Sulphur concentration:** Sulphur concentrations in the Carson Volcanic range from 20 ppm to 327 ppm (3 samples, Ozchem), and in the Hart Dolerite they range from 250 ppm to 700 ppm (4 samples, Ozchem).

**Isotope composition:** Information is not available.

**Pre-eruptive country rocks:** The Carson Volcanics outcrop throughout the lower part of the Kimberley Basin and are associated with volcanoclastic and sedimentary rocks (sandstone, siltstone, and chert units). The Hart Dolerite intruded already lithified sedimentary rocks of the Speewah (metamorphosed sandstone, chloritic and micaceous siltstone, shale, and minor rhyolitic ashstone and tuff) and Kimberley (sandstone and shale) groups.

**Evidence of crustal contamination:** Information is not available.

**PGE-Ni-Cu occurrences/prospects/anomalies:** Vanadiferous PGE-bearing mineralisation occurs within disseminated titanomagnetite (up to 3.98% V<sub>2</sub>O<sub>3</sub>), with most abundant titanomagnetite (up to 20%) located in the basal 15–25 m-thick section of a disseminated magnetite-bearing gabbro. See the Buckman, Speewah Central, Red Hill entries in Appendix K for details and Figure 8.9. Hollis et al. (2013) indicate a combined resource estimate of 4712 Mt @ 0.30% V<sub>2</sub>O<sub>5</sub>. The transition from a basal high-grade mineralised zone (~20 m-thick) to a lower grade zone is marked by a laterally extensive PGE-Au reef (0.1 m-thick) which has a maximum PGE+Au content of ~700 ppb. The oxide-hosted PGE, Au, and Cu mineralisation is similar in style to that hosted by the ~3035 Ma Stella layered intrusion in South Africa (NiPlats, 2009, 2010; Maier et al., 2003). The Carson Volcanics also locally have disseminated pyrite and chalcopyrite (Griffin et al., 1993).

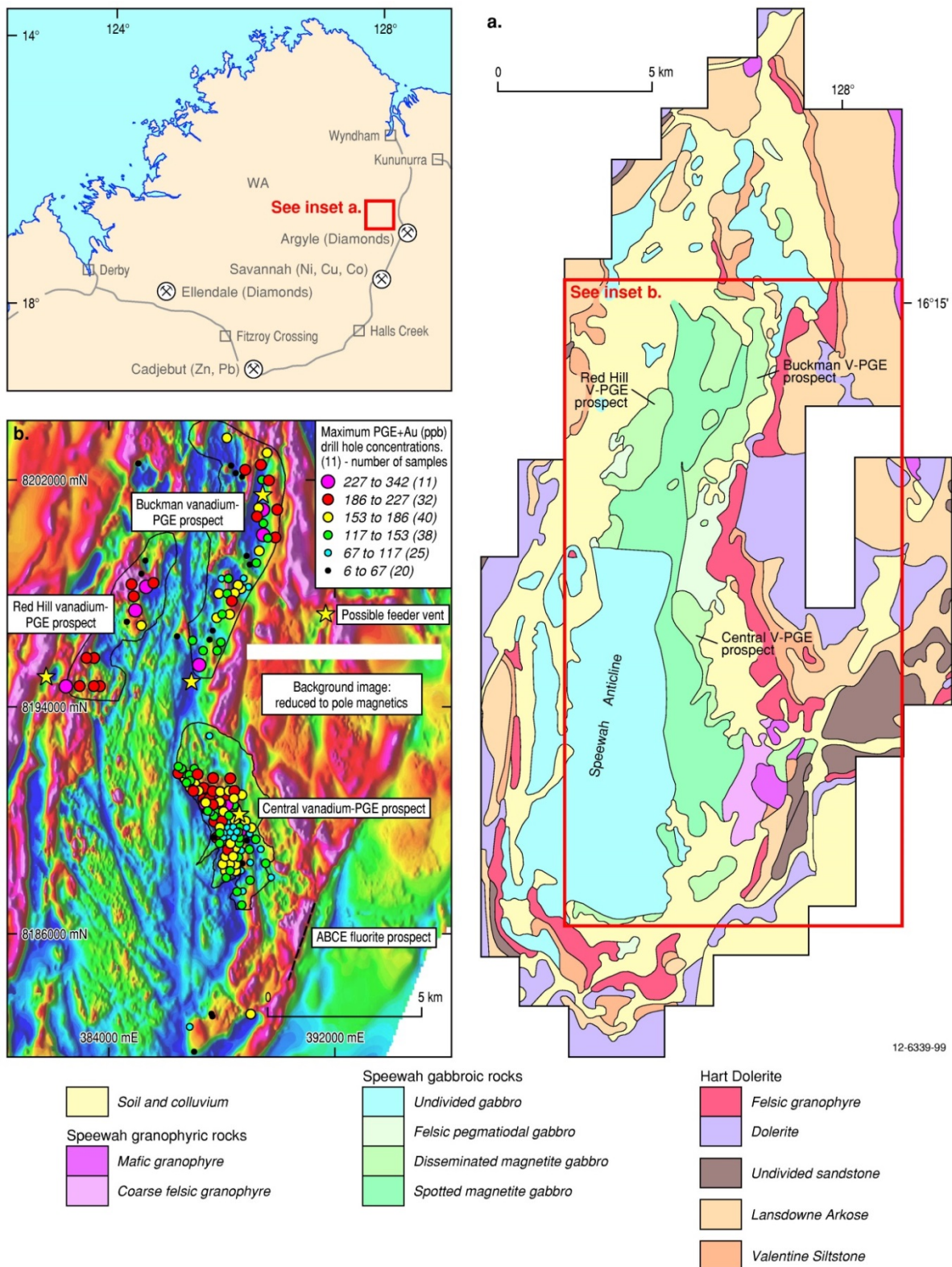


Figure 8.9 (a). Geology of Speewah Dome near the eastern margin of the Kimberley Basin, Western Australia. (b). Aeromagnetic image (reduced to pole) of Speewah Central Ti-V-PGE deposits that are associated with the magnetite-bearing olivine gabbro layer in the Hart Dolerite, Speewah Dome. Modified from NiPlats Australia Limited (2009, 2010a,b).

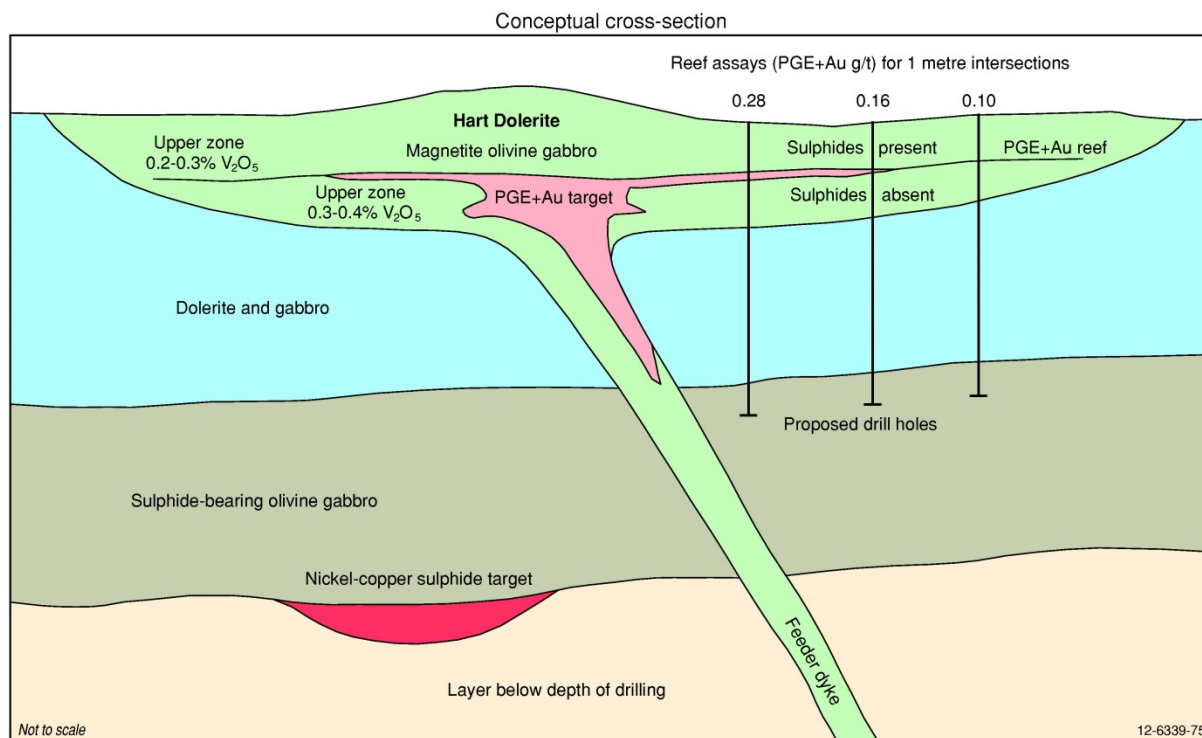


Figure 8.10 Schematic cross-section of Hart Dolerite sill and feeder dyke with conceptual platinum-group-element-gold and nickel-copper sulphide targets associated with the Speewah Central Ti-V-PGE deposits, Western Australia. Modified from NiPlats Australia Limited (2010a).

**Mineral potential:** Mafic rocks in the Hart–Carson LIP are considered prospective for PGE-Au and Ni-Cu deposits (Figure 8.9, Figure 8.10). However, more work is required to understand the temporal and genetic relationships between the Carson Volcanics and the Hart Dolerite. Future studies should focus on the following two possibilities which directly impact on the potential of this mineral system.

1. The basalts of the Carson Volcanics and the intrusions of the Hart Dolerite constitute a co-magmatic system (LIP). In this case, the voluminous mafic system can be considered prospective for PGE-Ni-Cu deposits in Noril'sk-type intrusions. Some intrusive bodies in the Hart Dolerite may represent feeder zones that are potentially mineralised, and some of these prospective feeders may be covered by the Carson Volcanics.
2. The basalts of the Carson Volcanics and the intrusions of the Hart Dolerite do not constitute a single co-magmatic system (LIP). Hanley and Wingate (2000) found that although the MgO% contents are similar in the Carson Volcanics and the Hart Dolerite, the abundances of HFSE (Zr, Hf, and Ti) and of heavy REE were different, suggesting that the two formations were not genetically related. In this scenario, the magmatic system should be assessed separately, namely: tholeiitic basalts of the Carson Volcanics for PGE-Ni-Cu deposits in intrusions associated with continental flood basalts (Noril'sk-type). This will require mapping of both feeder zones; and intrusions of the Hart Dolerite for PGE-deposits associated with Bushveld- or Stella-type intrusions. PGE-mineralisation can be associated with sulphide-rich layers, and/or in more oxidised titanomagnetite layers. The latter type of oxide-hosted mineralisation has already been found in fractionated doleritic sills of the Hart Dolerite in the Speewah Domain (see Buckman, Speewah Central, and Red Hill entries in Appendix K).

## Major references

Gellatly et al. (1975); Griffin and Grey (1990); Griffin et al. (1993); Hanley and Wingate (2000); Hollis et al. (2013); Maier et al. (2003); Meixner and Gunn (1997); NiPlats Australia Limited (2009, 2010); Thorne et al. (1999); Page et al. (1984); Tyler and Griffin (1993); Tyler et al. (2006).

### 8.4.2.3 Warakurna large igneous province

**Age:** ~1070 Ma. Numerous isotopic age determinations (SHRIMP U-Pb zircon and baddeleyite, K-Ar, Rb-Sr: Wingate et al., 2004a,b and references therein) on mafic rocks yield ages ranging from  $1058 \pm 13$  Ma to  $1078 \pm 3$  Ma. Mafic-ultramafic rocks of the Giles intrusions in the Musgrave Province provide U-Pb zircon ages ranging from  $1068 \pm 6$  Ma to  $1058 \pm 14$  Ma (Sun et al., 1996; Glikson et al., 1996). U-Pb zircon ages of rhyolites of the Tollu Group yield  $1075 \pm 2.5$  Ma and  $1078 \pm 5$  Ma; and of  $1051 \pm 22$  Ma and  $1071 \pm 5$  Ma for rapakivi granites (Sun et al., 1996), which are almost identical with the age of the Giles intrusions and the Bangemall mafic sill complexes.

**Brief description:** The ~1070 Ma Warakurna LIP includes time-equivalent mafic-ultramafic magmatism in a ~2000-km-long east-trending belt across the West Australian Crustal Element and the southern margin of the North Australian Crustal Element (Hoatson et al., 2008a,b; Figure 8.8). A significant component of the Warakurna LIP is the Giles Complex, which consists of a suite of layered mafic-ultramafic intrusions, mafic and felsic dykes, and associated volcanic rocks and granites. In addition to the Giles Complex, various swarms of coeval dolerite dykes traverse the Musgrave Province, Edmund Basin, Collier Basin, Hamersley Basin, and Earraheedy Basin. The Warakurna LIP contains up to 20 large- to moderate-sized mafic-ultramafic intrusions, sills, sheets and dykes (dolerite and gabbro). Locally gabbro sheets are associated with rocks of rhyolitic composition, probably representing partial melting of the sedimentary country rocks. The mafic-ultramafic intrusions of the Giles Complex comprise gabbro, anorthosite, troctolite, gabbronorite, norite, pyroxenite (both clin- and ortho-), dunite and peridotite. Granophyres are present as dykes and as masses up to 60 m-thick, and locally form high-level cappings of the layered gabbros (Myers, 1990). Nesbitt et al. (1970) described the Giles mafic-ultramafic intrusions as a series of variably deformed and metamorphosed sheets, which form isolated bodies scattered over an area of some 25 000 km<sup>2</sup>. However, gravity surveys in the West Musgrave Province indicate that at least some of these intrusions may be linked below the surface (Smithies et al., 2009; Evins et al., 2010b). The layered intrusions in some areas are considered as tectonically disrupted parts of a single large intrusion (Smithies et al., 2009). Mafic sills (Glenayle Dolerite and Prenti Dolerite) in Proterozoic sedimentary basins west of the Musgrave Province locally consist of several thin (<2 m) stacked sheets one above the other, separated by sedimentary rocks. The mineralogy of the Glenayle Dolerite is dominated by plagioclase and clinopyroxene with or without orthopyroxene (Pirajno and Hoatson, 2012). The main feature of the Glenayle Dolerite is the presence of well-developed interstitial granophyre. The mafic sills in the Edmund and Collier basins are interpreted to be variably fractionated tholeiites.

**Size:** Pirajno et al. (2002) noted the ~1070 Ma Warakurna LIP potentially covers a large area from the west coast of Australia to the centre of the continent extending, roughly along an E-W trend, for a length of about 2000 km, a width of about 800 km and inferred to cover an area of at least  $1.5 \times 10^6$  km<sup>2</sup>. Figure 8.8 shows that time-equivalent magmatism for the Warakurna LIP occurs in an east-trending belt that includes the Musgrave province and crosses the West Australian Crustal Element, and dolerite dykes in the southern margin of the North Australian Crustal Element (Hoatson et al., 2008a,b).

**Feeder zone:** The mineralised tube-like intrusion (chonolith) at the Nebo–Babel deposit is thought to resemble the feeder troctolite sheet at the Voisey’s Bay Ni-Cu deposit, Canada (Seat et al., 2007). No other feeder zones have been reliably identified in the LIP.

**MgO concentration:** The MgO concentrations of chilled mafic rocks at the margin of the Nebo–Babel body vary between 6.87% and 8.33% (Mg# ranging between 51 and 61: Godel et al., 2011). This chilled margin may not represent the composition of the primary magma, but that of a melt which has undergone fractionation (Godel et al., 2011). The mafic sills in the Edmund and Collier basins have Mg#  $\geq 55$  and show weak light rare-earth-element (LREE) enrichment, with  $(\text{La}/\text{Yb})_{\text{CN}}$  ranging from 3 to 7 and  $\text{La}_{\text{CN}}$  ranging from 30 to 70 (where CN is chondrite normalised).

**Sulphur concentration:** Sulphur isotopic data of sulphides at the Nebo–Babel deposit (see Section 6.4.2.1) show a narrow range of  $\delta^{34}\text{S}$  values from 0.0‰ to 0.8‰ (average of  $0.4\text{‰} \pm 0.2\text{‰}$ ) that are consistent with the S being of mantle origin and similar to other magmatic mineralising systems, e.g., Voisey’s Bay and Jinchuan. At the Nebo–Babel deposit, the S concentrations of chilled mafic rocks at the margin vary between 882 ppm and 1244 ppm (Godel et al., 2011).

**Isotope composition:** Seat et al. (2011) have shown from isotopic and chemical data that units in the Nebo–Babel Ni-Cu-PGE deposit can be related by crystal fractionation of a parental tholeiitic magma and crustal contamination was not a significant process. Mineral  $\delta^{18}\text{O}$  values are of typical mantle values and preclude large-scale crustal contamination of the parental magma with anything other than material with similar values. Although even the least contaminated intrusive units have negative Nb anomalies and enriched  $^{87}\text{Sr}/^{86}\text{Sr}$  initial ratios compared to bulk Earth at the time, the crustal assimilation must have been significantly less than 10% based on mantle-like  $\delta^{18}\text{O}$  values and  $^{143}\text{Nd}/^{144}\text{Nd}$  ratios.

**Pre-eruptive country rocks:** Sills and dykes in the Collier and Edmund basins intrude siliciclastic rocks. Some mafic bodies (such as the Mingol Dolerite) intrude thermally metamorphosed limestone and sandstone of the Paleoproterozoic Earraheedy Group. The Glenayle Dolerite and Prenti Dolerite intruded a succession of siliciclastic sedimentary rocks of the Collier Basin, north of the Earraheedy Basin, as well as parts of the Earraheedy Basin. Mafic intrusions at the Nebo–Babel deposit are emplaced within felsic and mafic granulites and felsic orthogneiss (S abundance of  $\sim 100$  ppm).

**Evidence of crustal contamination:** Isotopic data and trace-element geochemistry of mafic sills in the Edmund and Collier basins, suggest their generation from melting of a subduction-modified mantle source and crustal contamination. A narrow range of  $\delta^{34}\text{S}$  values from 0‰ to +0.8‰ of sulphides at the Nebo–Babel deposit indicates that S had a mantle source and was not derived from the contamination of crustal S. Based on geochemical modelling using major and trace elements and isotopic data, Godel et al. (2011) argue that crustal contamination did not play a major role in the generation and evolution of different magma suites. However, assimilation of felsic orthogneiss could have caused sulphide saturation at the deposit (Godel et al., 2011).

**PGE-Ni-Cu occurrences/prospects/anomalies:** In addition to the Nebo–Babel Ni-Cu-PGE deposit (see Section 6.4.2.1) in the Giles Complex, several Ni-Cu sulphide and lateritic Ni occurrences have been reported in the area of the LIP. These include: Cu-mineralised gabbro and mafic dykes of the Alcurra Suite northwest of Jameson, and stratabound vanadiferous magnetite deposits (Haran) at Jameson Range. Several mafic intrusions are known to contain disseminations of sulphides.

**Mineral potential:** Mafic rocks in the LIP host a world-class Ni-Cu-PGE deposit (Nebo–Babel) and several Ni-Cu-PGE, chromite, and vanadiferous magnetite occurrences. Most of them are closely

associated with the ~1070 Ma Giles Complex in the Musgrave Province. Thus although high mineral potential of the Giles Complex is widely accepted, the potential of other complexes (such as Glenayle Dolerite, Prenti Dolerite, and Mingol Dolerite) has not been fully assessed. Seat (2008), Godel et al. (2011), and Maier et al. (2014) provide useful summaries of known and potential mineralisation associated with the Giles mafic-ultramafic intrusions. More detailed investigations similar to the studies outlined below are required to properly assess the mineral potential of the Warakurna LIP.

- Further geochronological work to define the ages of different phases of intrusions (other than the Giles Complex where nine different phases have been identified).
- Mapping of feeder zones. At this stage feeder zones have only been identified at the Nebo–Babel deposit.
- Detailed geochemical studies to establish nature and timing of sulphide saturation in areas near feeder zones.
- Detailed geochemical studies (isotopic and minor elements) to determine nature and extent of crustal contamination. Sedimentary sequences in the Collier, Edmund, and Earraheedy basins contain sulphidic shales. It is possible that mafic magmas intruded into these rocks could have assimilated S, and consequently be of economic interest.

#### **Major references**

Evins et al. (2010); Glikson et al. (1996); Godel et al. (2011); Maier et al. (2014a,b); Myers (1990); Nesbitt et al. (1970); Pirajno et al. (2002); Pirajno and Hoatson (2012); Seat (2008); Seat et al. (2007); Seat et al. (2011); Smithies et al. (2009); Sun et al. (1996); Wingate (2004a, b).

#### **8.4.2.4 Kalkarindji large igneous province**

**Age:** 510 Ma; U–Pb zircon age of  $510 \pm 2$  Ma (Chen and Liu, 1996). Table Hills Volcanics ( $504.6 \pm 2.5$  Ma). Glass and Phillips (2006) reported  $^{40}\text{Ar}/^{39}\text{Ar}$  ages of  $508 \pm 2$  Ma and  $505 \pm 2$  Ma. The Milliwindi dolerite dyke in the West Kimberley region, which has a U–Pb age of  $513 \pm 10$  Ma, is interpreted as one of the feeders of the Kalkarindji flood basalts (Hanley and Wingate, 2000). These are similar broad ages to the ultramafic-mafic intrusions of western Tasmania (U–Pb zircon age of  $513.6 \pm 5$  Ma for the Heazlewood River Intrusion: Turner and Bottrill, 2001), and to various rock types in the Mt Read, Stavely, and Koonenberry regions of eastern Australia.

**Brief description:** The middle Cambrian Kalkarindji LIP represents an important voluminous mafic magmatic episode that impacted on much of northern and central Australia. Its interpreted spatial extent exceeds all other LIP events in Australia (Figure 8.8), and it provides valuable insights into the geological evolution of Australia during the transitional period from the Neoproterozoic to the middle Cambrian. The Kalkarindji province includes tholeiitic basalt and dolerite dominated by augite, pigeonite, and plagioclase, with accessory ilmenite, titanomagnetite, chlorite, albite, quartz, sphene, and K-feldspar. The lavas are intercalated with thin beds of aeolian sandstone, conglomerate, siltstone, and chert. The volcanic succession is overlain by middle Cambrian limestone. The sedimentary rocks intercalated with the lavas suggest that the environment during the eruption of the Kalkarindji lavas was distinctly continental. Evins (2005) proposed that the middle Cambrian Kalkarindji continental flood basalt event may have had important links to environmental impacts and mass extinctions.

**Size:** Estimated extent greater than  $2.1 \times 10^6$  km<sup>2</sup> (Pirajno and Hoatson, 2012). Figure 8.8 shows the Kalkarindji LIP contains extensive basaltic lavas and associated sills across the North Australian and Central Australia Crustal Elements, as well as intrusions in the Kimberley and Irindina provinces.

**Feeder zone:** Eruptive centres are possibly located in the East Kimberley region, where the lavas reach their maximum thickness. Feeder zones have not been extensively mapped. The Milliwindi dolerite dyke is a possible feeder to the Kalkarindji flood basalts (Hanley and Wingate, 2000). A number of lava channels in the Great Victorian Desert (Vennon and Wanna 1:250 000 map sheets) and the Wave Hill region in the Northern Territory have also been interpreted from aeromagnetic data (Glass, 2002).

**MgO concentration:** MgO concentrations vary between 3% and 9%, and the Mg# (molar  $100 \times \text{Mg}/(\text{Mg} + \text{Fe}^{2+})$ ) ranges from 34 to 72 (Glass, 2002). Isotopic compositions ( $^{87}\text{Sr}/^{86}\text{Sr}$ ,  $\delta^{18}\text{O}$ ) and Ba/Rb ratios show that the crust-like signature of the Kalkarindji basalts was acquired at compositions more primitive than 9% MgO (Marshall and Widdowson, 2013).

**Sulphur concentration:** Sulphur concentrations range from 38 ppm to 330 ppm (38 samples: Ozchem database)

**Isotope composition:** Initial  $^{87}\text{Sr}/^{86}\text{Sr}$  compositions range from 0.707 to 0.723, which indicate enrichment relative to depleted mantle values.  $\epsilon_{\text{Nd}}(t)$  values range from -2.7 to -9.6, with most samples clustering between -3.0 and -4.5 (7.9 to -12.3 for Siberian flood basalts, Noril'sk region);  $\delta^{18}\text{O}$  of whole-rock samples vary from +6.6‰ to +8.5‰ (relative to Standard Mean Ocean Water: Marshall and Widdowson, 2013).

**Pre-eruptive country rocks:** The magma may have intruded at least five Proterozoic Basins (Kimberley, Birrindudu, Victoria River, Wolfe, and Officer).

**Evidence of crustal contamination:** Isotopic compositions and Ba/Rb ratios indicate measurable high-crustal level contamination. A significant enrichment in Th and U, and very high Th/U ratios also indicate contamination by felsic crust. Lavas and intrusions emplaced into Officer Basin sedimentary rocks may have assimilated evaporitic S. Proterozoic Basins in the Tennant Creek region are also known to contain evaporite and/or pseudomorphs after evaporitic minerals.

**PGE-Ni-Cu occurrences/prospects/anomalies:** Gabbroic rocks in the Northwest Officer Basin locally contain chalcopyrite and pyrite (Pirajno and Hoatson, 2012). AusQuest Limited is one of the few companies that assessed the Ni-Cu-PGE potential of parts of the Kalkarindji and Fortescue LIPs in northwest Western Australia. They explored the ~505 Ma mafic-ultramafic rocks of the Table Hill Volcanics, and identified disseminated Ni-Cu-PGE sulphides associated with komatiitic rocks that may belong to the ~2770 Ma Fortescue LIP at the Beasley and Bellary prospects (see Appendix X).

**Mineral potential:** Unknown. The following studies are required to properly assess the mineral potential of this LIP.

- Further geochronological data to establish the different phases of lava eruption and emplacement of intrusions.
- Mapping of feeder zones and lava channels. At this stage only one eruption centre in the Halls Creek region has been interpreted.
- Detailed geochemical studies to establish the nature and timing of sulphide saturation especially in areas proximal to feeder zones.

- Detailed geochemical studies (isotopic and minor elements) to determine the nature and extent of crustal contamination. Areas within the Officer Basin appear more promising because the sediments contain both evaporites and carbonaceous sediments.

### Major references

Chen and Liu (1996); Evins (2005); Evins et al. (2009); Glass (2002, 2006); Glass and Phillips (2006); Glass et al. (2004); Hanley and Wingate (2000); Marshall and Widdowson (2013); Pirajno and Hoatson (2012); Turner and Bottrill (2001).

#### 8.4.2.5 Tasmanian Dolerite large igneous province (part of Karoo–Ferrar–Tasman LIP)

**Age:** Jurassic. The Tasmanian Dolerite has a Re–Os isochron age of ~175 Ma (Hergt and Brauns, 2001) and a recalculated K–Ar age on feldspar and whole rock samples of  $174.5 \pm 8$  Ma (Steiger and Jäger, 1978). The age is similar to the age determined for the Karoo and Ferrar magmatism (zircon and baddeleyite U–Pb ages of 183 Ma: Encarnacion et al., 1996). Everard et al. (2014) provide a comprehensive summary of the geochronology (mainly K/Ar dating techniques) of the Tasmanian Jurassic Dolerites and the coeval basaltic and doleritic rocks of the Ferrar Magmatic Province of Antarctica.

**Brief description:** Geochronological, geological, and tectonic evidence suggest that both the Karoo and Ferrar intraplate magmatism is related to the same thermal and rifting event of Gondwana, and it was accompanied by the voluminous emplacement of coeval mafic and picritic magma. Tasmanian Dolerites are thought to have formed from a large volume of tholeiitic magma that intruded the Tasmanian crust. The dolerite forms individual sills up to 500 m-thick, stepped composite sills, inclined sheets, cone sheets, and dykes. Contact metamorphic aureoles are confined to within a few metres of the intrusion margins. Modal compositions of the dolerites comprise 40% plagioclase ( $An_{65-70}$ ), 20% clinopyroxene, 20% quartz, 5% ilmenite, pigeonite, and small percentages of potassium feldspar and amphibole. Accessory minerals include pyrite, chalcopyrite, biotite, apatite, fluorite, zircon, and various zeolites. The quartz tholeiitic parent magmas underwent marked differentiation that was mainly controlled by the crystallisation of pyroxene (Hergt et al., 1989).

**Size:** The Tasmanian Dolerite LIP is exposed over ~14 500 km<sup>2</sup>, or about 22% of the landmass area of Tasmania, and is present at shallow depths beneath a considerably larger area (Everard et al., 2014). The tholeiitic dolerite body has an estimated volume ranging from more than ~8000 km<sup>3</sup> to 15 000 km<sup>3</sup>, and has a total volume of >35 000 km<sup>3</sup> when allowing for off-shore occurrences and erosion (Hergt et al., 1989; Everard et al., 2014). Dredge samples of dolerite from the northern margin of the South Tasman Rise, 150 km south of Tasmania, have been assigned a Jurassic age on the basis of geochemical similarities. Geological and geochemical studies also postulate that the province may have extended from southern Africa (Karoo province), to East Antarctica (Ferrar Magmatic Province; Transantarctic Mountains), and to Australia (Tasman Province: Pirajno and Hoatson, 2012).

**Feeder zone:** Leaman (1972, in Hergt 1987) used detailed gravity surveys over an area of 2300 km<sup>2</sup> to locate numerous feeders to the dolerite sills. Centres appear to be pipes up to 1.6 km in diameter and up to 11 km–12 km in depth. Some dolerite feeders occupy major fractures in the crust and are spaced 1 km to 10 km apart with an average spacing of ~4 km, and others are often extended and aligned, and appear to be narrow dykes. Some of the feeders have been used multiple times (Everard et al., 2014).

**MgO concentration:** The parent magmas of the Tasmanian and Ferrar (Antarctica) dolerites have low TiO<sub>2</sub> (0.5% at MgO = 9%). Mean compositions of chilled margin samples from many major dolerite intrusions reported in Everard et al. (2014) are of a basaltic andesite composition (normative Q of ~6.5%) with ~55.0% SiO<sub>2</sub> (anhydrous) and ~6.7% MgO. Compared with other continental tholeiites, SiO<sub>2</sub>, CaO (10.7%), and Al<sub>2</sub>O<sub>3</sub> (14.85%) are high, whereas Na<sub>2</sub>O (2.0%), K<sub>2</sub>O (0.89%), total Fe (8.91% as FeO), TiO<sub>2</sub> (0.65%), and P<sub>2</sub>O<sub>5</sub> (0.09%) are low. Everard et al. (2014) summarise the incompatible-trace-element ratios and chondrite-normalised REE patterns of chilled margin samples.

**Sulphur concentration:** Sulphur concentrations in the dolerites vary between 200 ppm and 1100 ppm. Some samples taken from the chilled margin show concentrations greater than 400 ppm (varying between 500 ppm and 1100 ppm: Hergt, 1987). The S contents of the dolerites in the vicinity of feeder conduits are not known.

**Isotope composition:** The average initial <sup>87</sup>Sr/<sup>86</sup>Sr ratios of the dolerites are 0.71153 ± 0.00005. The ratios are not correlated with SiO<sub>2</sub>, K<sub>2</sub>O, Rb, and Sr concentrations, which confirms that they were formed from fractional crystallisation of a homogenous magma (Faure, 1986). Various references in Everard et al. (2014) report similar initial <sup>87</sup>Sr/<sup>86</sup>Sr ratios (at 175 Ma) that range from 0.7094 to 0.7128, which are unusually high for mantle-derived rocks, whereas initial ε<sub>Nd</sub> (-6.4 to -4.9) is unusually low. Both isotope results are akin to crustal rocks. In contrast, O isotope values of the chilled dolerites (δ<sup>18</sup>O ~+1.9‰ to +6.1‰) lie close to, or just below, typical mantle values (5.7‰ ± 0.3‰) and show no influence from crustal rocks (which are usually higher in δ<sup>18</sup>O). The Pb isotope compositions of the Tasmanian dolerite are very uniform with <sup>206</sup>Pb/<sup>204</sup>Pb ~18.91, <sup>207</sup>Pb/<sup>204</sup>Pb ~15.65, and <sup>208</sup>Pb/<sup>204</sup>Pb ~38.77 at 175 Ma.

**Pre-eruptive country rocks:** Late Carboniferous to Triassic Parmeener Supergroup. The Parmeener Supergroup contains coal measures, oil shale, pyritic siltstone, and chemically reactive carbonate rocks. If these rocks are enriched in sulphides they could have supplied external S to the mafic magmatic system, thereby initiating sulphide saturation (Kreuzer, 2009).

**Evidence of crustal contamination:** The Sr, O, and Os isotopic data suggest continental contamination of mantle-derived magmas. However, the data indicates that contamination could not have occurred during intrusion in the crust, but the source from which the melt was derived was itself contaminated (Hergt and Brauns, 2001; Brauns et al., 2000). The possibility of local-scale introduction of S in the magma cannot be ruled out completely because the dolerites intruded sediments of the Lower Parmeener Supergroup which contain pyritic siltstone.

**PGE-Ni-Cu occurrences/prospects/anomalies:** No known occurrences of Cu, Ni, and PGEs have been reported in the area of the Jurassic dolerites. The small low-grade Forster Au-Zn-Ni prospect (Bottrill et al., 1999) in the Glovers Bluff Inlier of southeastern Tasmania is spatially associated with the Jurassic dolerite, but it is unlikely the Ni is directly linked to these dolerites. The Forster prospect is hosted in magnesian skarns and siliceous breccias and may have formed from the metasomatic activity associated with dolerite emplacement, with Au abundances upgraded locally by later supergene weathering (Bottrill et al., 1999).

**Mineral potential:** Available data suggest that the Tasmanian Dolerites are prospective to host PGE-Ni-Cu mineralisation. This conclusion is supported by the following criteria.

- Large size of the Tasmanian Dolerite LIP (volume >35 000 km<sup>3</sup>).
- Evidence of late-sulphide saturation. Sulphur concentrations in the dolerites vary between 200 ppm and 1100 ppm. Some chilled margin samples with elevated S concentrations greater

than 400 ppm (between 500 ppm and 1100 ppm) indicate that the mafic rocks probably reached sulphide saturation, and this event probably occurred late in the evolution of the dolerites.

- Everard et al. (2012) note that the strongly compatible trace elements Cr and Ni are, relative to their chilled margin values (108 ppm and 78 ppm, respectively), enriched in the lower pyroxene-rich cumulates, and are depleted in the upper granophyric parts of the sills.
- Low maximum Ni (~160 ppm), Cu (~155 ppm), Cr (~375 ppm), and V (~260 ppm) values for different dolerite bodies in Tasmania, as indicated in the geochemical fractionation plots of Everard et al. (2014), have little direct economic significance. However, they may provide important indicators to the timing of possible sulphide-saturation events and subsequent metal depletion trends throughout the mafic stratigraphy. Enrichment-depletion metal trends would be useful in determining proximity to potential mineralised source(s), e.g., near a mineralised magma conduit or a structural trap along a basal contact of an intrusive body.
- The presence of primitive picritic rocks have been reported in the Karoo and Ferrar provinces (these rock types have not yet been documented in the Tasmanian Dolerites).
- Presence of feeder zones, although at this stage, feeder zones have been interpreted only in small areas (Hobart 1: 50 000 sheet).
- Signs of crustal contamination, although Sr, O, and Os isotope data suggest that the contamination of the mafic-ultramafic magma could not have occurred during intrusion in the crust. Assimilation of S-rich country rocks is considered a critical factor for fertile systems of this type. This conclusion needs to be confirmed in other areas, because it assigns a significant constraint on the fertility of this magmatic system. Crustal contamination of mafic magma occurs in the crust at the globally significant Ni-Cu-PGE deposits at Noril'sk, Russia.
- Presence of Late Carboniferous to Triassic Permian Supergroup rocks are known to contain coal measures, oil shale, pyritic siltstone, and chemically reactive carbonate rocks, which can provide conditions suitable for late sulphide-saturation.
- No typical magmatic PGE-Ni-Cu occurrences have been reported in the Tasmanian Dolerites. However, one relatively large overseas Ni-Cu deposit (Waterfall Gorge in the Insizwa Complex), associated with the Karoo Flood Basalt, South Africa, has been described (Naldrett, 2004).

The following investigations are required to assess the mineral potential of this LIP.

- Mapping of feeder zones and lava channels. At this stage feeder zones have only been interpreted from a very small area. Geophysical (gravity, magnetics) and structural surveys can be useful in mapping feeder zones.
- Additional geochronological data in areas proximal to feeder zones can help to determine different phases of lava eruption and emplacement of intrusions.
- The areas near feeder zones also require detailed geochemical studies to establish the nature and timing of sulphide saturation events.
- Detailed isotopic and minor element geochemistry can establish more clearly the nature and extent of crustal contamination of mafic magma.

### Major references

Bottrill et al. (1999); Brauns et al. (2000); Encarnacion et al. (1996); Everard et al. (2014); Faure (1986); Hergt (1987); Hergt et al. (1989; 2001); Kreuzer (2009); Naldrett (2004); Pirajno and Hoatson (2012); Steiger and Jäger (1978).

### 8.4.3 Prospectivity analysis—intrusion scale

During this review and analysis of mafic-ultramafic orthomagmatic systems, two complexes in particular, are considered to have considerable potential for PGE-Ni-Cu and Ni-Cu-PGE mineralisation—the Windimurra Igneous Complex (Figure 8.11 and Figure 8.12) and the Andrew Young Hills intrusion (Figure 8.13, Figure 8.14, and Figure 8.15). The ~2800 Ma Windimurra Igneous Complex in the central Yilgarn Craton of Western Australia is the largest mafic-ultramafic intrusion in Australia. It is one of the few intrusions in Australia where two fertile mineral systems have operated:

- in the more primitive lower stratigraphic parts of the body (e.g., stratabound PGE-chromitite, PGE-bearing sulphides); and
- economic resources of Ti and V occur in gabbro-hosted stratabound magnetite layers in the upper stratigraphic levels of the intrusion.

The ~1633 Ma Andrew Young Hills mafic intrusion in the west Arunta Orogen of central Australia is a relatively unexplored body, and like Windimurra, is largely hidden below thin alluvial cover (<10% outcrop). This has important implications in a region of sparse outcrop because a better understanding of the size of the intrusion, the original geometries of deformed bodies, fractionation (younging) directions, and the delineation of basal intrusive contacts are critical elements for defining favourable mineralised environments (e.g., embayments in the basal contact and in feeder conduits) in sulphide-saturated intrusions, such as Andrew Young Hills. The identification of favourable environments in poorly exposed prospective bodies, such as the Windimurra and Andrew Young Hills intrusions, requires an integrated mineral-system approach, high-resolution geophysical modelling (airborne magnetic, airborne electromagnetic, Bouguer gravity), in association with petrological-geochemical information derived from diamond drilling and limited surface exposure.

The Windimurra and Andrew Young Hills intrusions represent typical case studies that highlight the challenges of exploring poorly exposed terranes. These two intrusions are described in this report since the challenges of exploring under cover are increasingly becoming more of a reality with future exploration in Australia.

#### 8.4.3.1 Windimurra (Narndee) layered mafic-ultramafic intrusion

**Age:** Archean mafic-ultramafic rocks in structurally dismembered layered intrusions comprise approximately 40% by volume of greenstones in the Murchison Domain of the Youanmi Terrane, Yilgarn Craton. Ivanic et al. (2010) have divided mafic-ultramafic rocks in the Murchison Domain into five Archean components: ~2810 Ma Meeline Suite (includes the Windimurra Igneous Complex); 2800 ± 6 Ma Boodanoo Suite (includes the Narndee Igneous Complex: Figure 8.11); and the 2792 ± 5 Ma Little Gap Suite. The Murchison Domain of the Youanmi Terrane also contains the ~2750 Ma Gnanagooragoo Igneous Complex and the 2735–2710 Ma Yalgowra Suite of layered gabbroic sills, which are not discussed in this section.

**Brief description:** Meeline Suite, which includes the Windimurra Igneous Complex (Figure 8.12), consists of strongly layered and fractionated bodies (sills, laccoliths, lopoliths) of gabbroic rocks with abundant leucogabbro and magnetite components, including multiple layers of magnetite (Ivanic et al., 2010). The Windimurra Igneous Complex is the largest mafic-ultramafic intrusion in Australia. It is made up of four zones consisting of an ultramafic zone at the base and three overlying mafic zones that collectively have a total thickness of 10 km to 13 km. In general, the complex shows a progression from more mafic rocks in the lower zone to large volumes of anorthositic and leucogabbroic rocks at the top (Ivanic et al., 2010). The complex shows many megacyclic units, over 100 m-thick. Ahmat

(1986) interpreted at least 13 fractionation reversals that represent injections of new magma pulses into the evolving chamber. The parental magma for the lower zone (leucocratic/anorthositic zone) is inferred to be a high-alumina olivine tholeiite with negligible crustal contamination. The Windimurra Igneous Complex may be gently folded about a N-S axis and tilted slightly west, increasing the dips on the eastern side (Mathison et al., 1991). The nearby Narndee Igneous Complex (Figure 8.11) has three zones, consisting of an ultramafic zone (peridotite and pyroxenite) at the base, overlain by a gabbro-norite-dominant lower zone, followed by at least seven megacycles of peridotite-gabbro-norite-anorthosite forming the main upper zone. Scowen (1991, cited in Ivanic et al., 2010) identified several fractionation reversals that indicate an open-magma system with regular new injections of magma.

**Size:** The largest of the layered intrusions is the Windimurra Igneous Complex (Figure 8.12), which outcrops over an area of ~2300 km<sup>2</sup> (85 km N-S by 37 km E-W: Mathison et al., 1991). The nearby Narndee Igneous Complex covers an area of 700 km<sup>2</sup>. Collectively the two complexes occupy an area of 250 km by 400 km, which is similar in extent to the Bushveld Igneous Complex, South Africa (Ivanic et al., 2010). The actual stratigraphic thickness of the Windimurra Igneous Complex is ~10–13 km (Mathison et al., 1991), but the thickness is a maximum of ~6 km from gravity modelling (Mathison and Booth, 1990; Ivanic et al., 2010). The Narndee Igneous Complex has a stratigraphic thickness of >5 km (Ivanic et al., 2010).

**Feeder zone:** Based on the presence of a high-density region (interpreted from gravity data), Ivanic et al. (2010) suggested the presence of a concealed, funnel-shaped basal portion in the central region of the Windimurra Igneous Complex.

**MgO concentration:** MgO concentrations range from 38.9% (Ultramafic rocks) to 3% (anorthositic gabbro-norite: Mathison and Ahmat, 1996). A chilled margin was identified, but it had been metamorphosed.

**Sulphur concentration:** Mathison and Booth (1990) note low S values (~10 ppm) in the Windimurra Igneous Complex rocks and explain these low values by surface oxidation.

**Isotope composition:** Initial <sup>87</sup>Sr/<sup>86</sup>Sr ratios for plagioclase (Mathison and de Laeter, 1994) and for whole-rocks (Ahmat and de Laeter, 1982), and an  $\epsilon_{Nd}$  analysis of 1.3 (Fletcher et al., 1984, cited in Mathison and Ahmat, 1996) collectively suggest a primitive source and lack of contamination, at least with older evolved crust, for the Windimurra Igneous Complex. Mathison and Ahmat (1996) also postulate the existence of two parent magmas for the intrusion.

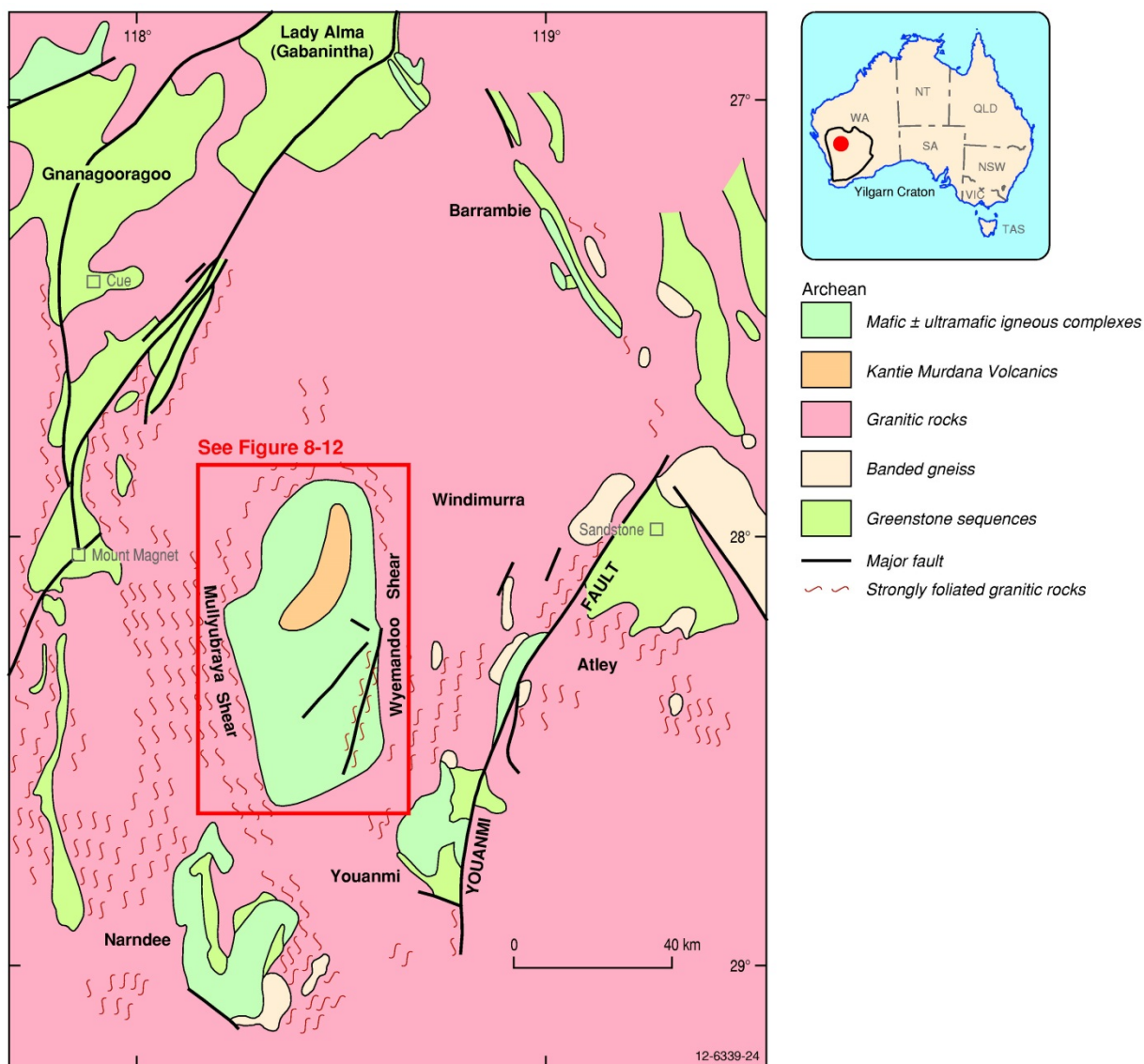


Figure 8.11 Regional geological setting of the Windimurra and Narndee layered mafic-ultramafic intrusions in the Murchison Domain of the Youanmi Terrane, Yilgarn Craton, Western Australia. Modified from Ivanic et al. (2009, 2010).

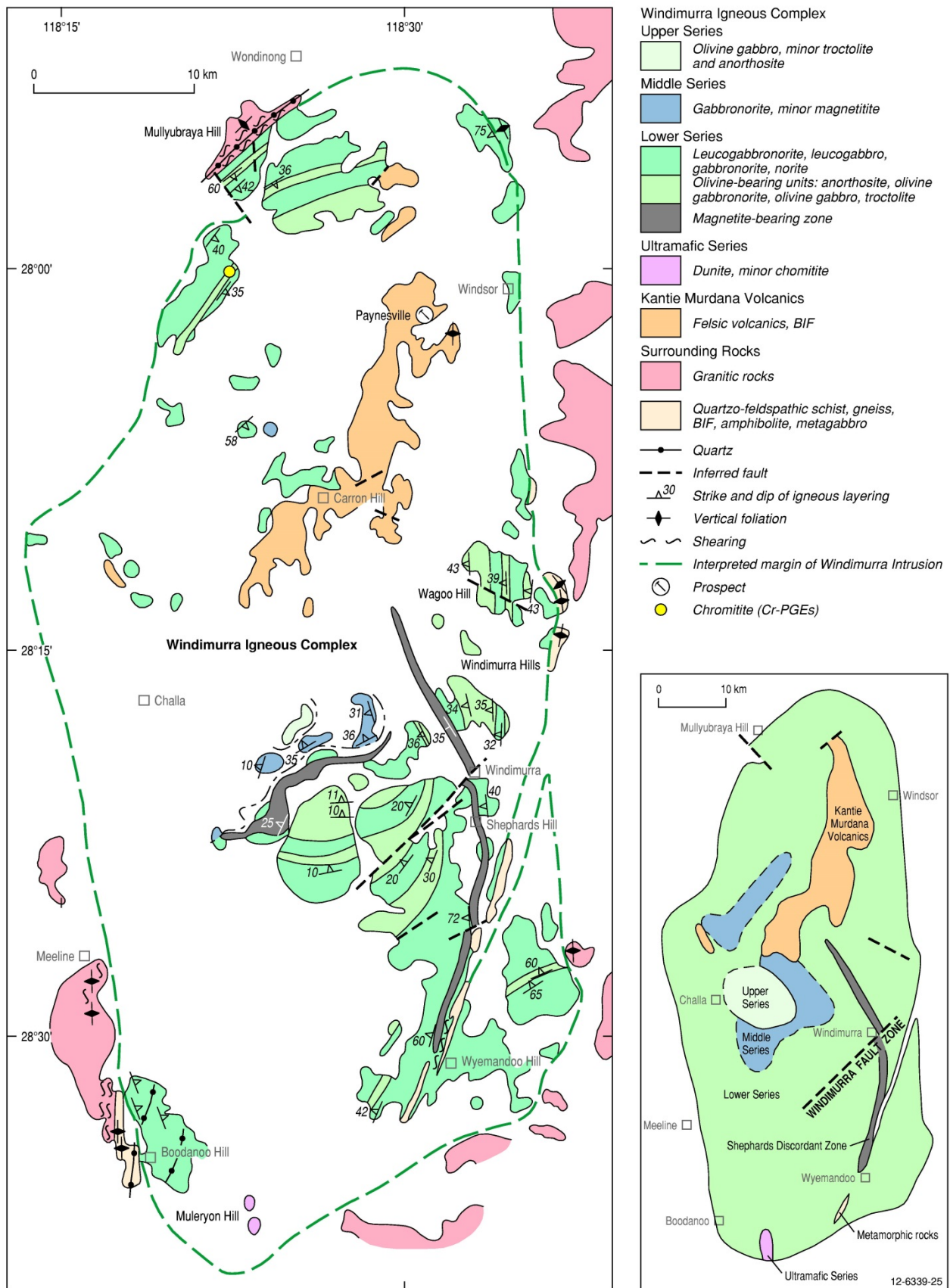


Figure 8.12 Geology of the Windimurra Igneous Complex, showing the main areas of outcrop, PGE-bearing chromitite, and magnetite zones. Modified from Mathison et al. (1991).

**Pre-eruptive country rocks:** Archean granite-greenstone rocks of the Youanmi Terrane.

**PGE-Ni-Cu occurrences/prospects/anomalies:** The Windimurra Igneous Complex is one of the few mafic-ultramafic intrusions in Australia which hosts stratabound PGE-chromitite, PGE-bearing sulphides, and stratabound Ti-V mineralisation associated with magnetite (Mathison et al., 1991; Withall, 2001). With the exception of the latter setting, the two other styles of PGE mineralisation are sub-economic, but indicate fertile mineral systems operated in the Archean. Significant V mineralisation has been identified in association with various complexes in the region, e.g., Barrambie Fe-Ti-V deposit (Ward, 1975). Basal parts of the Meeline, Boodanoo, and Yalgowra Suites also host at least minor Ni-Cu-PGE mineralisation in sulphides (e.g., Milgoo area of the Narndee Igneous Complex; Bunting 2004, cited in Ivanic et al., 2010). There is also minor Ni-Cu-PGE in lateritic formations overlying ultramafic parts of these three suites (Parks, 1998).

**Mineral potential:** The Windimurra and Narndee igneous complexes are considered highly prospective for PGE mineralisation associated with layered complexes as indicated by the following points.

- Large size of both complexes, which are comparable in areal extent and thickness to that of the Bushveld Complex.
- Strongly differentiated stratigraphies that encompass a wide variety of rock types ranging from various primitive ultramafics, chromitite, olivine-bearing gabbro, and troctolite, through various types of leucogabbro and anorthosite, to evolved mafic-hosted magnetitites.
- Presence of layering, fractionation reversals, and chromitite layers representing injection and possible mixing of multiple pulses of magma. Thus like many fertile complexes (Bushveld, Stillwater), these complexes may have formed from an open and dynamic magmatic system.
- Presence of economic V and Ti deposits, Ni-Cu and Cr occurrences.
- PGE-bearing chromitite layers indicate that fertile PGE mineral systems operated in the Windimurra Igneous Complex. Mathison et al. (1991) reported maximum PGE concentrations of 3150 ppb Pt, 4300 ppb Pd, 380 ppb Rh, 340 ppb Ru, 10 ppb Ir, and <8 ppb Os in massive chromitite from the Wondinong area on the northern side of the intrusion. Maximum concentrations in drill-hole intersections were 1 m @ 760 ppb Pt and 1200 ppb Pd.
- Most of the Windimurra Igneous Complex is blanketed by laterite cover, with only ~10% outcrop preserved, mostly along parts of the northern and southeastern margins. The extensive cover has in part prohibited traditional exploration techniques and consequently there are now new opportunities for exploring under shallow cover with more sophisticated 'cutting edge' geophysical and geochemical methods.
- Exploration opportunities exist for potential styles of mineralisation that have received little exposure at Windimurra and Narndee, e.g., stratabound PGE-bearing sulphide horizons high in the mafic stratigraphy (Picket Pin deposit, Stillwater Complex, USA: Boudreau and McCallum, 1986; and Platinova Reef, Skaergaard Intrusion, Greenland: Holwell and Keays, 2014). Stratabound PGE-enriched magnetitite layers in the Stella Intrusion, South Africa (Maier et al., 2003) and the Haran prospect in the Musgrave Province (Appendix K) are also potential targets especially in view of the economic Ti-V-bearing magnetitite layers in the Windimurra Igneous Complex. As the two complexes have undergone several episodes of deformation and metamorphism and have been intruded by dykes and felsic intrusives, the complexes as well as country rocks may be prospective for several types of PGE-Cu-Au-bearing hydrothermal systems.

However, more studies are required to better define prospective areas within the two complexes. The studies should focus on the following issues.

- Pre-metamorphic and pre-deformational geometry and architecture of the complexes. This will help to confirm the presence of a funnel-shaped geometry and delineate possible feeder zones.
- Magmatic evolution of the two complexes. It is important to establish how many parent magmas were involved in the evolution of the complexes and to quantify the geochemical parameters of these magmas, i.e., sulphide-saturation status and are they PGE fertile?
- Behaviour of S during magmatic evolution of the complexes. At this stage there is limited data on the abundance or behaviour of S in the rocks.
- Detailed isotope and trace-element geochemistry aimed to understand nature and timing of potential crustal contamination.
- Detailed geophysical surveys (airborne electromagnetics, magnetics, gravity) should be integrated with new concepts generated by mineral-system modelling that defines the detailed geometry, younging directions, contact relationships, and areas of stratigraphic-structural discordance of the intrusions, and favourable settings (feeder conduits, structural embayments in basal contact, etc) for potential conductive orebodies that may have little or no surface expression.

### Major references

Ahmat (1990); Ahmat and de Laeter (1982); Boudreau and McCallum (1986); Holwell and Keays (2014); Ivanic et al. (2010); Jones et al. (2012); Maier et al. (2003); Mathison and de Laeter (1994); Mathison and Booth (1990); Mathison and Ahmat (1996); Mathison et al. (1991); Parks (1998); Ward (1975); Withall (2001).

#### 8.4.3.2 Andrew Young Hills mafic intrusion

**Age:** 1633 Ma. Gabbro-norite (containing 115 ppm Zr) from the eastern part of the intrusion has an interpreted primary U-Pb zircon crystallisation age of  $1632.9 \pm 2.8$  Ma (Claoué-Long and Hoatson, 2005). This is consistent with quoted U-Pb zircon ages of  $\sim 1625$  Ma for gabbro-norite and  $1635 \pm 9$  Ma for a coarse-grained granite body that is hosted by (and considered to be to coeval with) the mafic rocks, which are unpublished, but are cited in Young et al. (1995a,b).

**Brief description:** The Andrew Young Hills intrusion, located just to the north of the boundary between the Aileron Province and the Warumpi Province in the Arunta Orogen (Figure 8.13), is a high-level fractionated gabbro-norite-tonalite body that was strongly contaminated by felsic crustal material. Outcrop is restricted to five prominent gabbroic hills that have a regional arcuate alignment that swings from east-west in the north to south-southeast in the east (Figure 8.14). This alignment is parallel to macroscopic compositional layering trends in the mafic rocks that are visible on aerial photographs and aeromagnetics, but are not readily seen on the ground. The structure of the intrusion is interpreted to be a broad inclined synform, with the fold axis plunging to the south-southwest. The intrusion consists of a homogeneous mafic sequence of gabbro-norite, magnetite gabbro-norite, biotite gabbro-norite, gabbro, hornblende tonalite, and diorite. Contacts between the rock types are diffuse and gradational, and the absence of distinctive marker layers and compositional layering prohibits subdivision of the mafic rocks in outcrop. The rocks are neither foliated nor strongly recrystallised, and are of possible sub-amphibolite metamorphic facies.

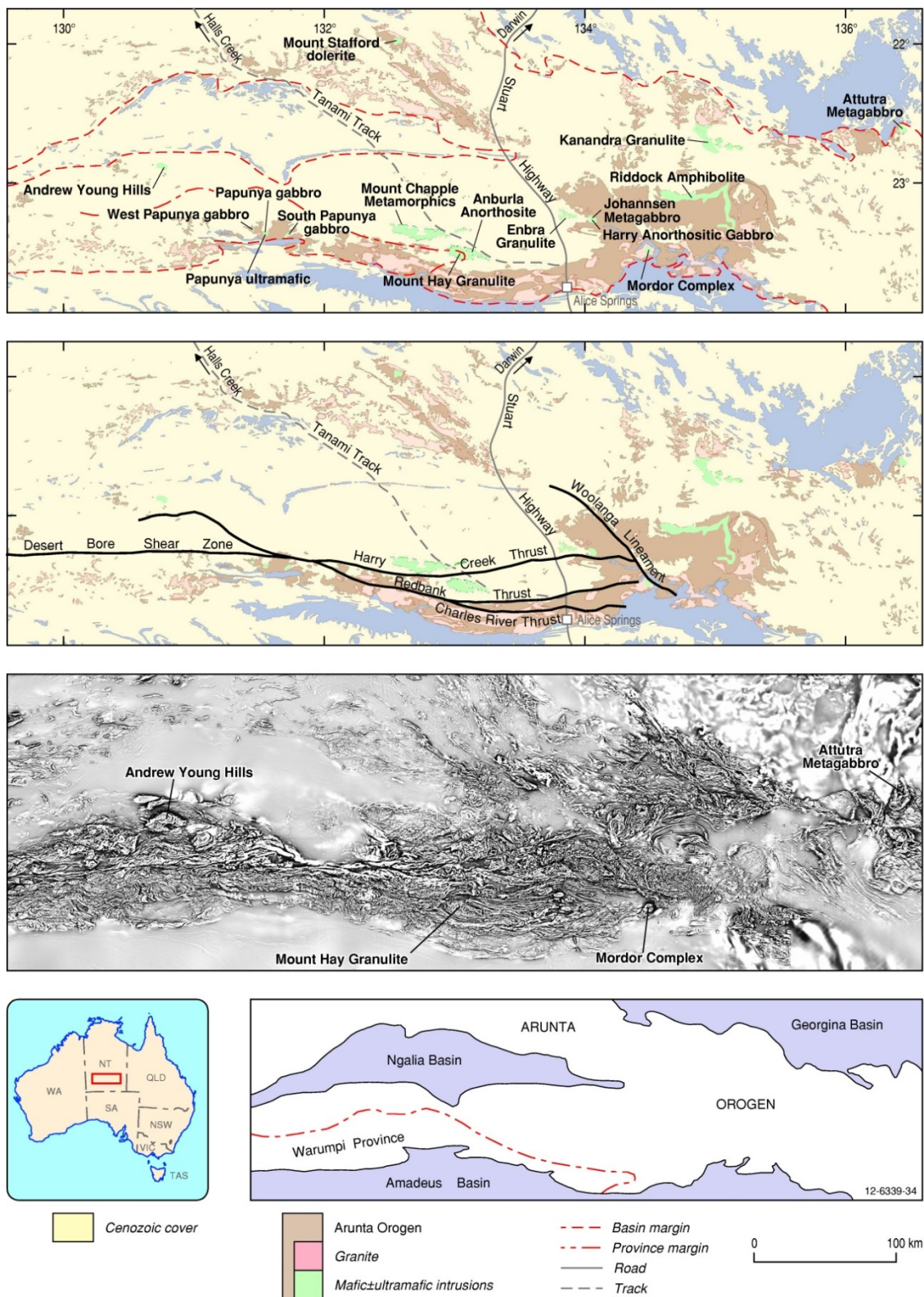


Figure 8.13 (Images from top to bottom). Outcrop map of the Arunta Orogen and surrounding sedimentary basins, central Australia, Northern Territory. The map highlights the Proterozoic mafic-ultramafic intrusions investigated by Hoatson et al. (2005a) and the large areas covered by alluvium. Other maps shown include: regional faults; total magnetic intensity (vertical gradient, reduced to pole; Meixner and Hoatson, 2003); and boundaries of the Aileron, Warumpi, and Irindina provinces (Close et al., 2003b, 2004).

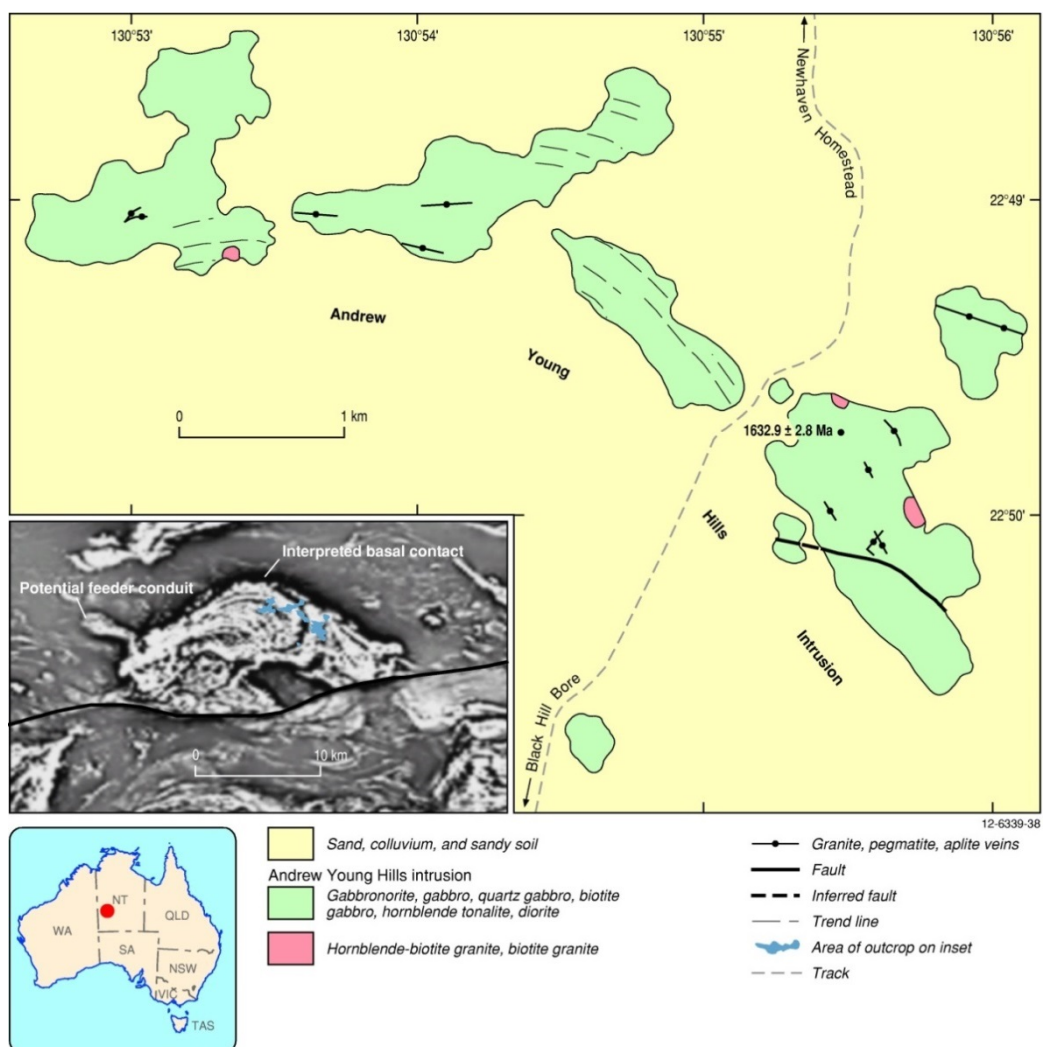


Figure 8.14 Geological map of the Andrew Young Hills intrusion, Arunta Orogen, central Australia. The poorly exposed gabbroic intrusion has a primary U-Pb zircon crystallisation age of  $1632.9 \pm 2.8$  Ma (Claoué-Long and Hoatson, 2005). The vertical gradient of total magnetic intensity image (reduced to pole: processed by T. Meixner, Geoscience Australia) in the bottom left corner shows that outcrop is restricted to the northeastern part of the intrusion and that most of the intrusion extends under shallow alluvial cover. Modified after Hoatson et al. (2005a).

**Size:** The exposed part of the intrusion covers an area of 4.5 km by 6.5 km near the northeastern side of a large arcuate magnetic high (Figure 8.14). Low-metamorphic grade intrusions with minimal deformation like Andrew Young Hills intrusion are characterised by well-defined strong magnetic anomalies related to primary igneous features, such as macroscopic compositional layering. Modelling of this high-amplitude (up to 2000 nT) anomaly by Meixner and Hoatson (2003) indicates a subsurface body measuring ~22 km east-west by ~13 km north-south (Figure 8.15); and that the depths of alluvial cover over the intrusion are generally shallow and not prohibitive for exploration.

**Feeder zone:** A west-northwest trending elongated aeromagnetic anomaly situated at a high angle to the northwestern margin of the body may be a related dyke or feeder conduit to the intrusion (see inset to Figure 8.14, and Figure 8.15).

**MgO concentration:** Twenty gabbroic samples from outcrop have an average MgO content of 5.81% (with a one standard deviation variation of 1.27%).

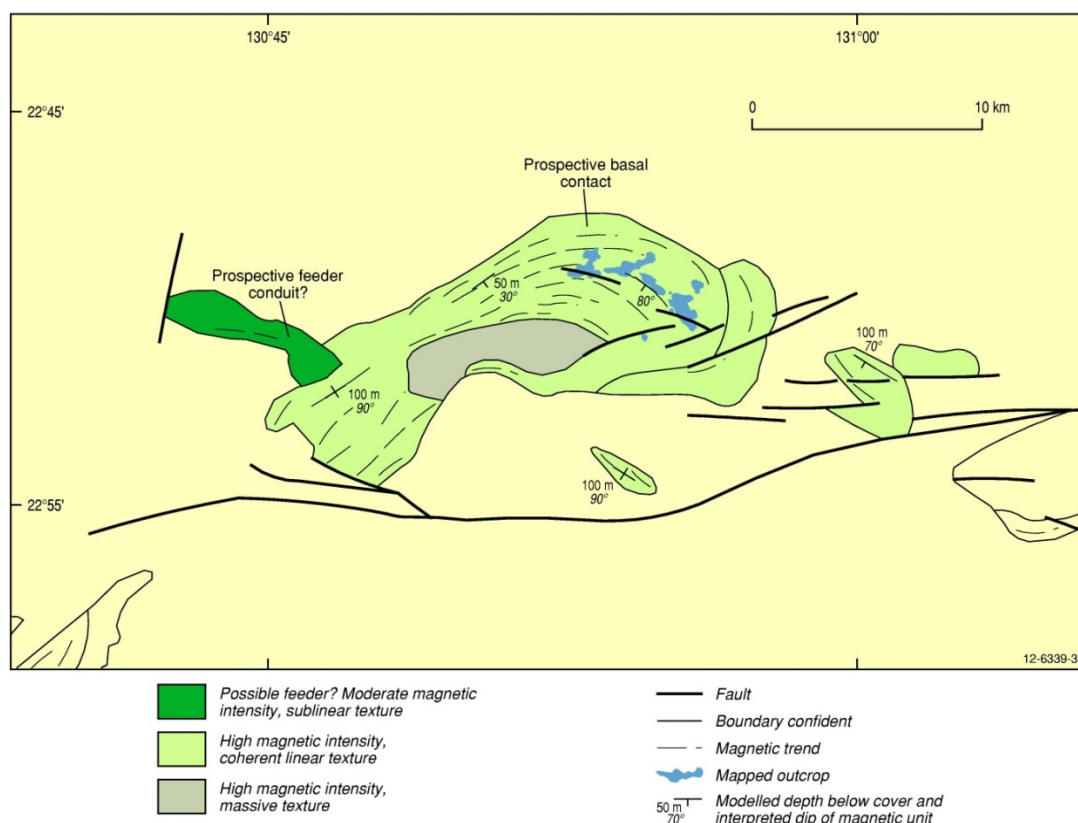


Figure 8.15 Geological interpretation of the Andrew Young Hills intrusion, Arunta Orogen. Solid geology interpretation is based on aeromagnetic and gravity datasets. Modified from Meixner and Hoatson (2003).

**Sulphur concentration:** Andrew Young Hills is one of several S-rich intrusions (~1200 ppm to 300 ppm S: Andrew Young Hills intrusion, Mount Hay Granulite, Mount Chapple Metamorphics) from the western and central Arunta regions that has potential for basal Ni-Cu-Co-sulphide associations (Hoatson, 2001; Hoatson et al., 2005a). Twenty gabbroic samples from outcrop have an average whole-rock S content of 784 ppm (with a one standard deviation variation of 50 ppm).

**Isotope composition:** Gabbroic samples from the intrusion has a  $^{147}\text{Sm}/^{144}\text{Nd}$  ratio of only 0.1207 and the lowest initial  $\epsilon_{\text{Nd}}$  value (-4.7) for all samples analysed by Hoatson et al. (2005a), which is consistent with its strongly contaminated character.

**Pre-eruptive country rocks:** Metasediments with a maximum depositional age of 1860 Ma adjacent to the 1635 Ma Andrew Young Hills intrusion have undergone low-P, high-T metamorphism and partial melting at conditions of 3–4 kb and >750°C. Metamorphic rims on zircons from these metasediments also have a U-Pb age of 1635 Ma, attesting to their contact metamorphic origins (pers. comm. Ian Scrimgeour, NTGS, 2002).

**Evidence of crustal contamination:** Well preserved primary magmatic features, such as mafic pillows with contaminated cusped margins and various xenocrysts, indicate that commingling of mafic and felsic magmas was an important process in this body. Clusters of large (up to 3 cm) resorbed alkali feldspar xenocrysts zoned from cores of alkali feldspar to rims of fine intergrowths of quartz and feldspar, and thin discontinuous trains of quartz xenocryst grains (1 to 5 mm) characterise the hybrid rocks. Large isolated blocks (up to 80 m-wide) and smaller irregular pods of leucocratic biotite-hornblende granite may represent rafts of country rock (Hoatson and Stewart, 2001). Gabbros from

the Andrew Young Hills intrusion have evolved compositions ( $mg_{56-38}$ ) and their elevated  $K_2O$  and  $Na_2O$  contents testify to larger amounts of crustal contamination relative to other Arunta mafic bodies (Hoatson et al, 2005a). The high degree of contamination is indicated by the Andrew Young Hills intrusion having the highest  $(La/Sm)_{MN}$  ratio of  $\sim 3.5$  for all the Arunta intrusions studied by Hoatson et al. (2005a), by the high orthopyroxene content of the gabbroic rocks, enrichment of LREE, and evolved Nd isotopic compositions.

**PGE-Ni-Cu occurrences/prospects/anomalies:** Chalcophile trace-element trends by Hoatson et al. (2005a) show that the Andrew Young Hills intrusion is one of the most S-rich bodies (690 ppm–860 ppm) investigated in the Arunta Orogen, but is depleted in Ni (30 ppm–155 ppm), Cu (25 ppm–65 ppm), and precious metals ( $<0.5$  ppb Pt, Pd;  $<1$  ppb Au).

### Mineral potential

- The major challenge for finding massive Ni-Cu-Co-PGE sulphides in the lower parts of prospective sulphide-saturated Andrew Young Hills intrusion is to determine the pre-deformational geometries of the bodies and to locate favourable mineralised environments, such as embayments in basal contacts and feeder conduits, concealed by thin Cenozoic alluvial deposits.
- Field relationships, petrological, geochemical, and isotopic data from restricted outcrop collectively indicate that crustal contamination played a significant role in the genesis of the Andrew Young Hills intrusion. More representative drill-core samples from other stratigraphic levels in the body are required to determine if crustal contamination was responsible for inducing sulphide saturation in the body.
- The low abundances of chalcophile metals Ni (30–155 ppm), Cu (25–65 ppm), and the precious metals ( $<0.5$  ppb Pt, Pd;  $<1$  ppb Au) in the mafic rocks may be a legacy of the composition of the parent magma(s), or it may indicate a sulphide-saturation event occurred early in the evolution of the intrusion which resulted in these metals being significantly depleted from the melt. From an exploration point of view, it would be important to assess if this possible event took place within the magma chamber, the feeder conduit, or at greater depths in the crust or mantle.
- Preliminary drilling (8 drill-holes: Mithril Resources Ltd, 2005) that tested magnetic and gravity features in the Andrew Young Hills intrusion (or possibly in another covered mafic body to the southeast of the Andrew Young Hills intrusion) defined favourable rock types, but no significant Ni-PGE mineralisation.
- The Andrew Young Hills intrusion received the highest mineral potential rating (5) of all Arunta intrusions investigated (Miezitis et al., 2006) for segregations of Ni-Cu-Co-PGE sulphides in feeder conduits and basal contacts of mafic intrusions (Mineral System Class 2.A).
- The extensive alluvial cover blanketing the Andrew Young Hills body has in part prohibited traditional exploration techniques and consequently there are now new opportunities for exploring under shallow cover with more sophisticated 'cutting edge' geophysical and geochemical methods.

### Major references

Claoué-Long and Hoatson (2005); Hoatson (2001); Hoatson and Stewart (2001); Hoatson et al. (2005a); Meixner and Hoatson (2003); Miezitis et al. (2006); Mithril Resources Ltd (2005); Young et al. (1995a); Young et al. (1995b).

## 8.5 Prospectivity and exploration guidelines for platinum-group-element mineral systems in Australia

Platinum-group elements have been documented from all Australian states and the Northern Territory, with Western Australia and Tasmania accounting for more than 80% of known occurrences.

Appendix K compiles geological information and resource data for over 500 PGE occurrences in many geological settings. On the basis of this comprehensive dataset, the different geological settings of Australia's major PGE occurrences are summarised in Figure 8.16, Figure 8.17, Figure 8.18, and Figure 8.19<sup>27</sup>.

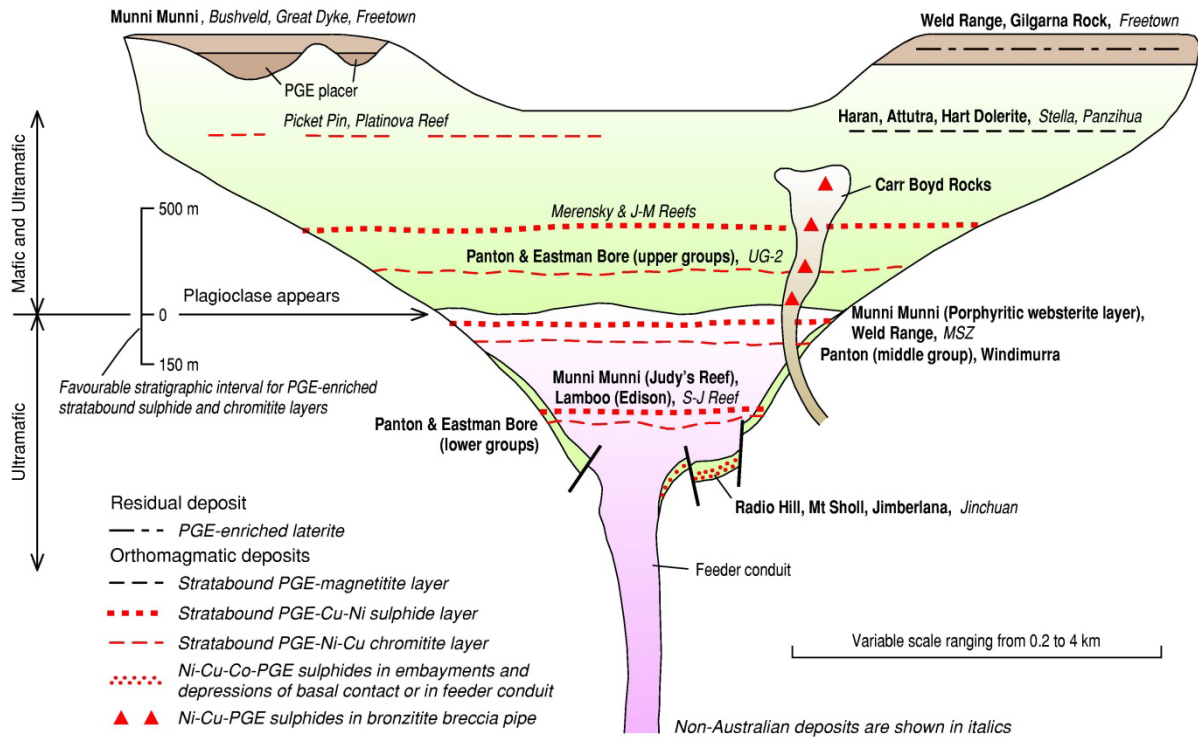
Australia's PGE production since the late 1960s has been exclusively derived from Archean komatiitic-hosted Ni-Cu sulphide deposits in the Yilgarn Craton of Western Australia. More than 24 812 kg of Pd and Pt, representing 94% of Australia's total PGE production, have been produced as by-products from these deposits (see Section 1.3.3). Historical PGE contributions have been derived from placer deposits of Pt, Os, Ir, and Ru alloys spatially associated with Paleozoic 'alpine- and Alaskan-type' mafic-ultramafic intrusions in eastern Australia. Despite this narrow supply base of PGEs, several prospects have highlighted the geological potential of Australia for different styles of economic PGE mineralisation. These prospects, which in some cases have had several decades of exploration and resource assessment, include: Munni Munni and Radio Hill, WA (~2925 Ma layered mafic-ultramafic intrusions); Windimurra, WA (~2800 Ma layered mafic-ultramafic intrusion); Collurabbie, WA (~2705 Ma PGE-enriched komatiite); Jimberlana (~2410 Ma layered mafic-ultramafic intrusion); Weld Range, WA (Archean layered mafic-ultramafic intrusion); Panton, WA (~1855 Ma tectonised layered mafic-ultramafic intrusion); Coronation Hill, NT (~1605 Ma hydrothermal–unconformity related); Nova, WA (~1300 Ma mafic intrusion); Nebo–Babel, WA (~1070 Ma mafic intrusion); Haran, WA (~1070 Ma mafic intrusion); Adamsfield and Heazlewood, Tas (~515 Ma 'alpine-type' ultramafic-mafic intrusions); Owendale, NSW (~430 Ma 'Alaskan-type' mafic-ultramafic intrusion); and Syerston and Owendale, NSW (Cenozoic laterites).

Most of the hard-rock prospects above represent orthomagmatic mineral systems associated with mafic and ultramafic igneous rocks. In these mineral systems, the PGEs mainly occur:

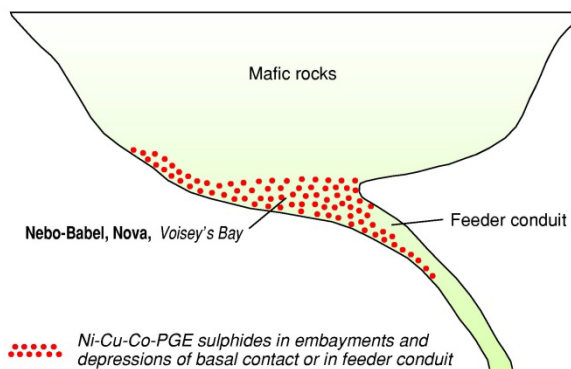
- in laterally extensive sulphide-bearing stratabound layers in large layered Archean and early Proterozoic mafic-ultramafic intrusions;
- as by-products of Ni-Cu sulphides in Archean komatiitic volcanic-intrusive sequences;
- as by-products of Ni-Cu sulphides in massive sulphide accumulations near the basal contacts or in the feeder conduits of Archean and Proterozoic mafic-dominant intrusions;
- in laterally extensive sulphide-bearing chromitite layers in dismembered mafic-ultramafic intrusions of Proterozoic orogenic zones;
- in stratabound magnetitite layers hosted by evolved gabbroic rocks in the upper parts of fractionated mafic-dominated Proterozoic layered intrusions; and
- with chromite in Paleozoic 'alpine-type' ultramafic-mafic intrusions and related placers.

<sup>27</sup> It should be emphasised that the diagrams of Figure 8.16 to Figure 8.19 are not to scale and are only a schematic representation of the mineral system shown.

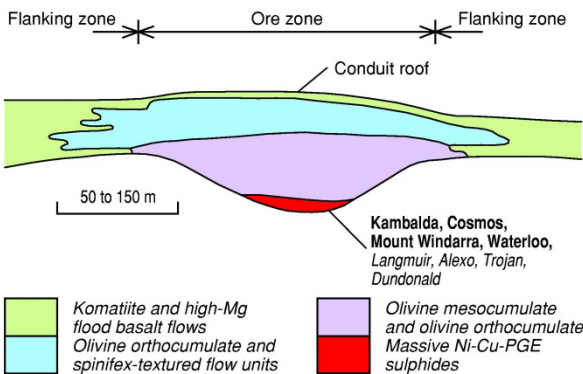
**a. Tholeiitic Mafic-Ultramafic Intrusion (1.A, 1.B, 2.A, 2.B, 8.A, 9.A, 10.C)**



**b. Tholeiitic Mafic Intrusion (2.A)**



**c. PGE-Bearing Komatiite (3.A)**



**d. PGE-Enriched Komatiite (3.C)**

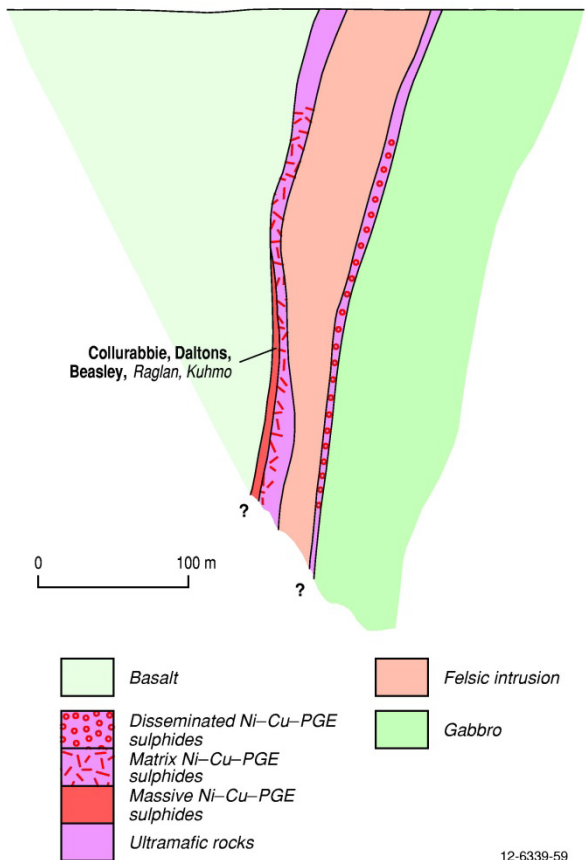
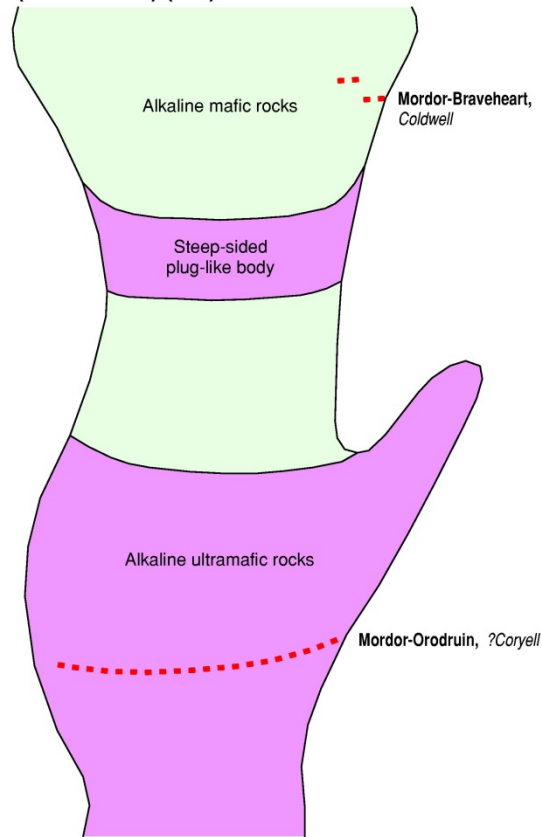


Figure 8.16 Schematic diagrams a–d showing the different geological settings of PGE mineralisation in Australia. Australian deposits are indicated by bold font; overseas deposits are indicated by italicised font. Figures modified from Hoatson and Sun (2002), Hoatson et al. (2005a, 2006), and Barnes (2006).

**e. Alkaline Mafic-Ultramafic Intrusion (Proterozoic) (4.A)**



**f. 'Alpine- and Ophiolitic-type' Ultramafic-Mafic Intrusion (Eastern Australia) (5.A, 10.B)**

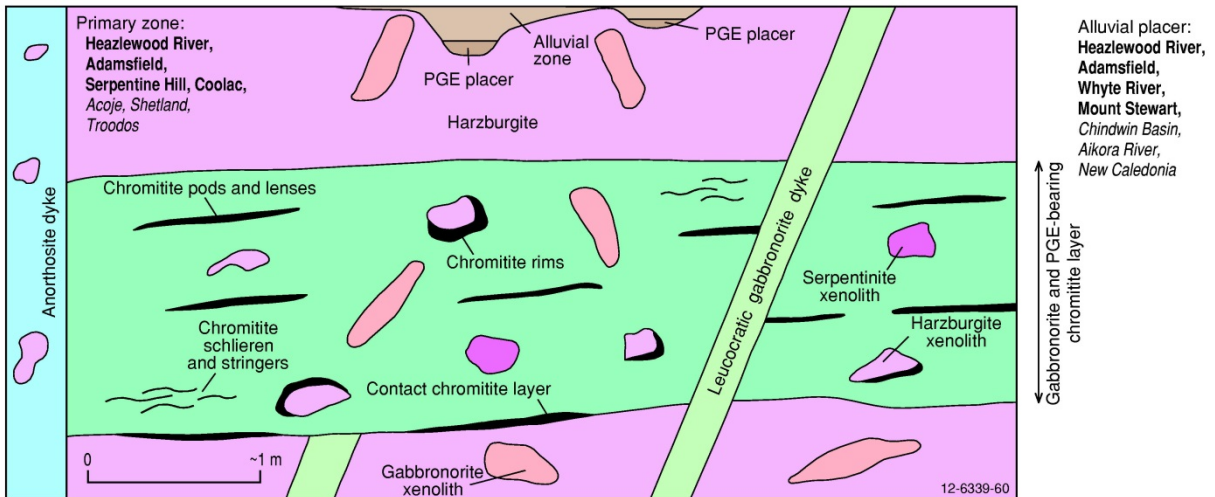
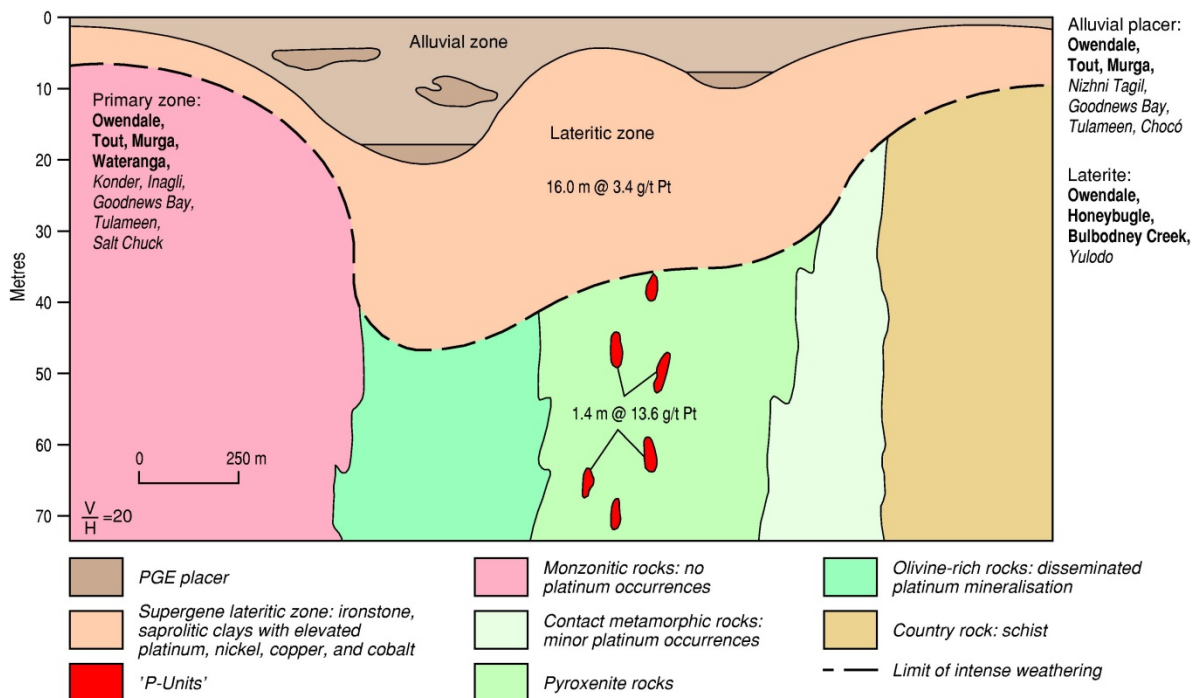


Figure 8.17 Schematic diagrams e–f showing the different geological settings of PGE mineralisation in Australia. Australian deposits are indicated by bold font; overseas deposits are indicated by italicised font. Figure modified from Hoatson (unpublished, 2014), and Peck and Keays (1990a).

**g. 'Alaskan- and Urals-type' Mafic-Ultramafic Intrusion (6.A, 9.A, 10.A)**



**h. Hydrothermal-Metamorphic-Remobilised (8.C, 8.D)**

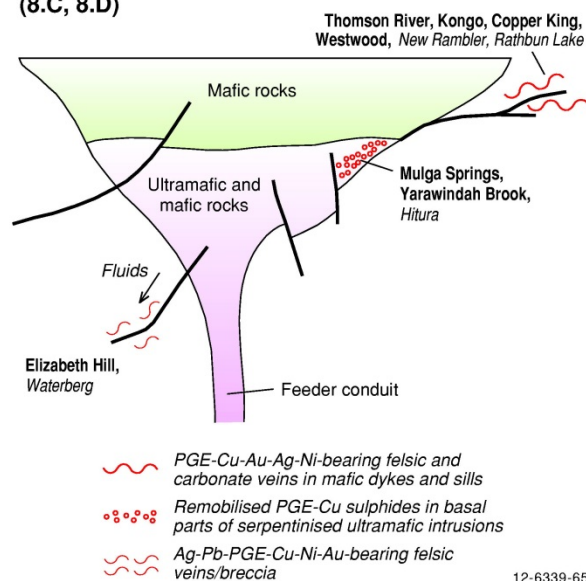
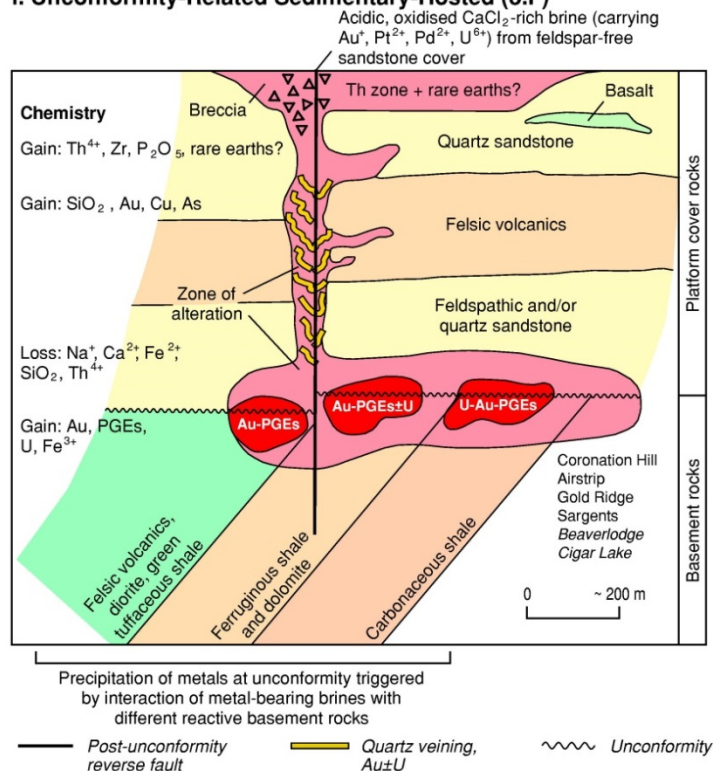


Figure 8.18 Schematic diagrams g–h showing the different geological settings of PGE mineralisation in Australia. Australian deposits are indicated by bold font; overseas deposits are indicated by italicised font. Figures modified from Elliot and Martin (1991), Hoatson and Sun (2002), and Hoatson et al. (2005a, 2006).

**i. Unconformity-Related Sedimentary-Hosted (8.F)**



**j. Carbonaceous Shale-Hosted (8.G)**

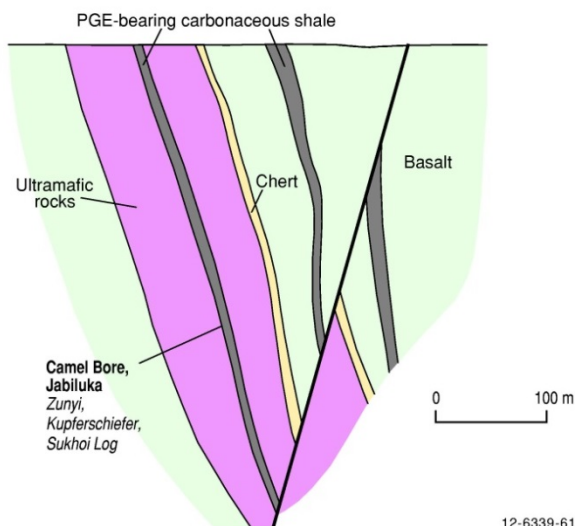


Figure 8.19 Schematic diagrams i–j showing the different geological settings of PGE mineralisation in Australia. Australian deposits are indicated by bold font; overseas deposits are indicated by italicised font. Figures modified from Mernagh et al. (1994, 1998) and Hoatson (unpublished, 2014).

This distribution reflects the secular variation of the PGEs to be associated with sulphides, Cr-oxides and Ti-V oxides, and Cr-oxides from the Archean to the Proterozoic to the Phanerozoic. Platinum-group mineralisation associated with most Paleozoic concentrically zoned 'Alaskan-type' intrusions in eastern Australia does not appear to show any clear affinity with sulphides or chromite. However, PGEs in hydrothermal settings are commonly associated with Cu and Ni in the Archean, Au and U in

the Proterozoic, and with Au, Ag, Cu, Ni, Pb, and As in Phanerozoic terranes. The temporal and frequency distributions of Australia's PGE occurrences are described in more detail by Hoatson and Glaser (1989), Hoatson (1990), and Koek et al. (2009, 2010).

Mineralised layered mafic-ultramafic intrusions are most common in the Archean Yilgarn and Pilbara cratons and the Proterozoic Halls Creek, Musgrave, Albany-Fraser, and Litchfield orogenic zones. PGE-sulphide associations are usually characteristic of Archean intrusions (Munni Munni, Weld Range), whereas PGE-chromite associations are more common in Proterozoic intrusions (Panton, Eastman Bore, Lamboo, Salt Creek). Coobina (Sylvania Dome, WA) and Windimurra (Yilgarn Craton, WA) are two obvious examples where PGE-chromite associations are also important in the Archean. Stratabound mineralised PGE layers occur in large, differentiated mafic-ultramafic bodies, where the PGEs are associated with disseminated Ni-Cu sulphides and/or chromite at particular stratigraphic levels in the intrusion (see below). Komatiite-hosted Ni-Cu deposits enriched in PGEs characterise the eastern parts of the Yilgarn Craton where dynamic high magma-flux environments, such as compound sheet flows with internal pathways facies (Kambalda-type), or dunitic compound sheet flow facies (Mount Keith-type), are well developed. Hard-rock occurrences related to alpine-ophiolite- and Alaskan-type intrusions are of early Cambrian to Permian and late Ordovician to Silurian age, respectively, and are largely confined to north-trending linear geographic belts in the Lachlan Orogen of eastern Australia.

Australian PGE occurrences related to hydrothermal-metamorphic mineral systems are not restricted to any time period and cover a wide spectrum of geological settings, ranging from deposits which are largely due to primary magmatic processes and having a minor hydrothermal overprint (Juan, WA; Radio Hill, WA; Thomson River, Vic), to those involving late-stage hydrothermal remobilisation of PGEs derived from a nearby mafic-ultramafic rock source (Mulga Springs, NSW; Melba Flat, Tas), to deposits which are strictly hydrothermal in origin (Coronation Hill, NT; Jabiluka, NT), i.e., the PGEs show no spatial association with, or obvious derivation from mafic-ultramafic rocks, and fluid movement has been the dominant mechanism for PGE transport. In some of these latter deposits graphitic horizons may have provided an important source of PGEs for subsequent remobilisation by magmatic-hydrothermal processes. The recognition of the importance of late and post-magmatic processes in the transport and concentration of PGEs (Stumpfl, 1986, 1987; Stumpfl and Ballhaus, 1986; Kucha and Pawlikowski, 1986; Bloom et al., 1992; Gammons and Bloom, 1993; Mernagh et al., 1994; Gammons, 1995; Kucha and Przybyowicz, 1999; Hanley, 2005; Wilde, 2005; Pašava et al., 2007; Barnes and Liu, 2012) has seriously questioned preconceived views that PGEs are exclusively associated with the early stages of mafic-ultramafic magma evolution.

Precambrian layered mafic-ultramafic intrusions in Australia are considered to have high potential for the discovery of a large economic PGE resource. Stratabound sulphide- and chromite-bearing layers in these intrusions are attractive targets since they generally display great lateral continuity (60 km in the Munni Munni Intrusion), have uniform grades (1 g/t to 6 g/t Pt+Pd+Au) and thicknesses (0.5 m to 3 m), contain a significant component of the more valuable precious metals (Pt, Rh, Au), and have potential for large tonnage (up to 30 Mt) multi-element deposits (PGEs, Cr, Cu, Ni, Co, Au). However, the Australian PGE examples are currently subeconomic with the largest deposits, Panton (65.6 t global resource) and Munni Munni (63.7 t), containing one to two orders of magnitude less PGE metal than the major economic deposits overseas. In addition, stratabound PGE-enriched sulphide layers can be difficult targets to explore in poorly exposed terranes because they typically form narrow targets (e.g., Merensky Reef is a 0.8-m-thick layer within the ~9000-m-thick Bushveld Complex) and they have weak geophysical and geochemical signatures due to their low disseminated sulphide content (typically 1% to 3%).

Prospective layered mafic-ultramafic intrusions hosting stratabound PGE mineralisation (Munni Munni Weld Range, Jimberlana, Panton, Lamboo: Deposit Types 1.A and 1.B) in Australia are generally 2940 Ma to 1840 Ma in age, were emplaced into the upper crust at pressures <5 kb (Trudu and Hoatson, 2000), exceed 5 km in thickness, are strongly differentiated, have a significant ultramafic component relative to the mafic component, contain multiple magma pulses, and have experienced late S and/or Cr saturation in the magma chamber by crustal contamination, crystal fractionation, magma mixing, constitutional zone refining, and/or hydrothermal processes. The economically important global examples of mineralised layers—Merensky Reef (Bushveld Complex, Republic of South Africa: Viljoen, 1999), Main Sulphide Zone (Great Dyke of Zimbabwe: Prendergast and Jones, 1989), and J-M Reef (Stillwater Complex, Montana, USA: Czamanske and Zientek, 1985)—show textural and stratigraphic similarities that are useful indicators for exploration. They are often coarse-grained, porphyritic, and/or pegmatoidal, and occur within the stratigraphic interval from 20 m below (MSZ—Great Dyke, PWL—Munni Munni) to 500 m above (Merensky Reef, J-M Reef) the stratigraphic level where plagioclase first becomes a cumulus mineral, i.e., the stratigraphic level first dominated by gabbroic rather than ultramafic cumulates (Hoatson, 1998). In some Australian examples (e.g., PWL), the mineralised layer truncates the layering and structural features of the underlying ultramafic stratigraphy. This magmatic unconformity was interpreted by Hoatson and Keays (1989) to represent magmatic erosion that occurred during a wide-scale magma mixing event between the ultramafic and gabbroic zones in the magma chamber.

Small, mafic-dominant tholeiitic intrusions that experienced sulphide saturation earlier in their evolution relative to the PGE-dominant deposits described above, typically contain small-tonnage Ni-Cu-Co-PGE sulphide deposits (2 Mt to 5 Mt @ 1%–3% Ni, 1%–2% Cu, 0.1%–0.2% Co, <0.6 g/t PGEs) with low PGE/(Ni+Cu) ratios. The Australian type example is the Nebo–Babel Ni-Cu-PGE deposit (392 Mt @ 0.3% Ni, 0.33% Cu, 0.18 g/t PGEs: Phaceas, 2007) in the Musgrave Province, which although sub-economic, contains the largest global resource of PGE metal (70.6 t) in Australia. The discovery of the Voisey's Bay, Canada, and Nebo–Babel Ni-Cu-Co±PGE deposits in the last two decades stimulated exploration in Australia for mafic-intrusive hosted mineralisation. Mineral-system elements, such as long-lived deep crustal-scale structural zones, juxtaposed Archean and Proterozoic blocks, and tectonically reworking of Precambrian rock sequences that were proposed for major overseas Ni provinces (e.g., Voisey's Bay–Nain Plutonic Suite and Thompson Nickel Belt: Naldrett, 1997; Naldrett et al., 1996; Ryan, 1997; Ryan et al., 1995) were incorporated into local exploration programs. Greenfields environments in less traditional provinces were also targeted for mafic-hosted Ni-Cu-Co-PGE mineralisation, e.g., the Fowler Domain along the western margin of the Gawler Craton, South Australia, and the Albany-Fraser Orogen on the southern side of the Yilgarn Craton, Western Australia were interpreted as favourable Archean-Paleoproterozoic suture zones that would facilitate the localisation and rapid ascent of primitive fertile magmas.

Western Australia is relatively well endowed with mineralised mafic-dominant intrusions with several Precambrian provinces having at least one deposit that has been either mined, or at least, contains significant JORC-compliant Ni-Cu-Co-PGE resources. Such examples include Savannah (HCO), Radio Hill and Mount Sholl (Pilbara Craton), Nebo–Babel and Halleys (Musgrave Province), Nova–Bollinger (Albany-Fraser Orogen), and Sandy Creek (Litchfield Province). The host intrusions are typically small- to medium-sized (1 km- to 4 km-thick) mafic-dominant bodies that probably had an early history of sulphide saturation (i.e., in the conduit or prior to their emplacement into the chamber). They are generally composed of a thicker mafic sequence of primitive and fractionated gabbroic and anorthositic rocks that overly a thinner ultramafic sequence dominated by olivine-rich cumulates. The host rocks to the sulphide mineralisation often form a thin (<50-m thick) veneer of gabbroic rocks

located along the basal contact between the country rocks and overlying ultramafic cumulates. Massive and disseminated pyrrhotite-pentlandite-chalcopyrite±pyrite±magnetite assemblages contain low (tens to hundreds of ppb PGEs) to moderate (0.2 ppm to 0.6 ppm) concentrations of Pt, Pd, and lesser Rh. Very rich Pd-Cu-Au remobilised vein-type ores (e.g., Radio Hill) may locally traverse the basal contact and intrude the country rocks for a few metres. The massive Ni-Cu-Co-PGE sulphides in the basal parts of the intrusion are often localised in, or over, structural embayments or depressions in the footwall contact beneath the thickest sequence of cumulates (Radio Hill, Mount Sholl, Savannah), and/or in feeder conduits (Babel, Savannah, Nova-Bollinger, Radio Hill). To attain economic grades, massive sulphides need to be concentrated in structural depressions or embayments of the footwall contact, or in feeder conduits. Crustal assimilation and gravitational settling of dense sulphide melts are important processes concentrating these sulphides. The dynamics of magma flow, e.g., decrease in the velocity of magma flow from narrow vertical conduits to broad open magma chambers, are also considered important for the concentration of heavy massive sulphides into structural traps.

The timing of S saturation in layered intrusions is critical, since if the host magma(s) attain S saturation too early in their evolution (i.e., in the mantle or during its ascent into the crust), the PGEs will be rapidly depleted in the magma due to their extremely high partition coefficients into the sulphide phases (e.g., up to 30 000 for the PGEs: see Table 3.6). Consequently, early S saturation of a magma will inhibit the effectiveness of later concentrating mechanisms, such as crystal fractionation, action of hydrothermal fluids, and the generation of high R-factor sulphides, for the formation of PGE-enriched layers. Therefore one of the most important initial requirements when exploring mafic-ultramafic intrusions is to determine the stratigraphic level of S saturation. If the intrusion is in part S undersaturated, the stratigraphic level of S saturation needs to be determined for potential stratabound PGE-enriched sulphide layers (Munni Munni, Weld Range, Jemberlana), usually located near major compositional interfaces defined by the appearance of cumulus plagioclase in the intrusion; if the intrusion is S saturated throughout its total stratigraphy, the basal contact region and feeder conduit should be initially investigated for massive and disseminated Ni-Cu-Co-PGE sulphides (Radio Hill, Mount Sholl, Savannah, Nova). In general, most evolved mafic rocks containing >1000 ppm S are sulphide saturated. As described in Chapter 3, the most important variables that control the solubility of S in mafic magmas are temperature, pressure, FeO content, and fugacities of O<sub>2</sub> and S<sub>2</sub> (Haughton et al., 1974). Sulphur solubility in a silicate melt increases with increasing temperature, FeO content, and fS<sub>2</sub>, and with decreasing pressure and fO<sub>2</sub> (Wendlandt, 1982). To determine whether a cumulate rock formed from a sulphide-saturated magma also requires knowledge of the amount of trapped intercumulus melt as well as the S concentration of the primary magma. Hoatson and Keays (1989) described the various methods for determining the sulphide saturation status of an intrusion by:

- using the compositions of uncontaminated rocks that are chilled near the margins of the intrusion and comparing these results to experimental S-solubility data;
- normalising cumulate rocks to 100% melt components; and
- using S/Se ratios in cumulates with suspected loss of S during low-temperature alteration.

As described above, layered intrusions in Australia and overseas containing significant resources of PGEs are generally large bodies more than 5 km-thick. The average Pt and Pd contents of most unmineralised mafic-ultramafic rocks range from about 1 ppb to 20 ppb and are generally less than 10 ppb. If economic grades of at least ~6 ppm Pt + Pd are to be achieved for a Merensky Reef-type deposit in Australia, concentration factors of about 1000 are required. Such high concentration factors necessitate a large volume of PGE-fertile magma, and/or a very efficient mineralising mechanism. Thus, intrusions that exceed 5 km in thickness are potentially more favourable for stratabound-type

PGE mineralisation (Munni Munni, Windimurra, Narndee) than smaller, thin bodies. For example, a 20-m-thick dolerite sill that has a limited intrusive area has essentially no potential for hosting a Merensky-Reef-type deposit. It should be emphasised that if the parent magma is particularly enriched in PGEs (>~15 ppb Pt, ~20 ppb Pd) and/or voluminous amounts of magma are emplaced over large areas or through narrow conduits (Noril'sk–Talnakh, Russia), intrusions less than 5 km-thick may be still prospective for other styles of PGE mineralisation. The Noril'sk–Talnakh Ni-Cu ores have higher PGE grades than all Australian orthomagmatic PGE deposits, but occur in intrusions less than 200 m-thick that are associated with voluminous comagmatic continental flood basalts. The identification of associated comagmatic components is important to assessing the size of the magmatic system, and therefore the potential of the mineral system.

Does Australia have large, thick, and voluminous Precambrian mafic-ultramafic bodies that appear critical to hosting globally significant PGE deposits? Figure 8.20 summarises the estimated comparative thicknesses of mafic and ultramafic rocks and the stratigraphic distribution of mineralisation for some of the largest mafic-ultramafic intrusions in Australia, including those from the Halls Creek and Musgrave orogens, and the Pilbara and Yilgarn cratons, and major mineralised intrusions from overseas. Australian layered intrusions which are stratigraphically thicker than 5 km, include the Windimurra Igneous Complex (10 km to 13 km thick: Mathison et al., 1991; Ivanic, 2009; Ivanic et al., 2010), Narndee Complex (9 km: Ahmat and Ruddock, 1990; Ivanic, 2009; Ivanic et al., 2010), Munni Munni Complex (>5.5 km: Hoatson and Keays, 1989; Barnes and Hoatson, 1994), Giles Complex (up to 8 km: Glikson, 1995; Ballhaus and Glikson, 1995; Glikson et al., 1996; Evins et al., 2010a,b; Maier et al., 2014), and the McIntosh intrusion (7 km: Mathison and Hamlyn, 1987; Hoatson and Tyler, 1993; Hoatson, 2000). In contrast, the size of the intrusion does not appear as important for those bodies hosting basal segregations of Ni-Cu-Co-PGE sulphides (Deposit Type 2.A). They are typically sheet-like bodies that range in thickness from 0.5 km to 3 km. The LIPs described in Section 8.4.2 represent very large magmatic systems and potentially economic targets. However, there is currently a view in the mineral industry that LIPs are high-risk greenfields environments to explore as identifying prospective feeder zones within large areas is difficult.

It is important when evaluating mafic-ultramafic intrusions to remain open-minded, be observation-driven, and maintain a flexible exploration approach. Avoid being purely model-driven and consider other styles of mineralisation in addition to the widely explored Merensky Reef- and/or UG-2 Chromitite-type scenarios. Such potential settings could include discordant bodies of magmatic and/or hydrothermal origin like the dunite pipes in the Bushveld Complex, and stratabound PGE sulphide horizons high in the mafic stratigraphy as seen for the Picket Pin deposit of the Stillwater Complex, USA (Boudreau and McCallum, 1985, 1986), and the Platinova Reef of the Skaergaard Intrusion, Greenland (Bird et al., 1991; Nielsen and Brooks, 1995; Nielsen et al., 2005; Holwell and Keays, 2014). Stratabound PGE-enriched magnetitite layers as found in the Stella Intrusion, South Africa (Maier et al., 2003) and the Haran prospect in the Musgrave Province (Appendix K) are potential exploration targets that have not been extensively explored for in Australia. Prospective intrusions for Stella- and Platinova-style mineralisation in Australia would include the evolved Fe-rich components of the larger mafic-dominant intrusions (Baxter, 1978; Hoatson, 1984; Collins, 2011), such as the McIntosh (Halls Creek Orogen), Windimurra, Barrambie, Buddadoo, Coates, Gabanintha, Lady Alma, Youanmi (Yilgarn Craton), Balla Balla, Andover (Pilbara Craton), and evolved bodies of the Giles Complex (Musgrave Province). Other potential targets that have received relatively minor exploration exposure in Australia include Lac des Iles-style pegmatoidal mineralisation, Canada (Lavigne et al. 2005; Barnes and Gomwe, 2011; Hanley and Gladney, 2011) and Platreef-type Ni-Cu-PGE deposits, South Africa (McDonald and Holwell, 2011) near the margins of the intrusions.

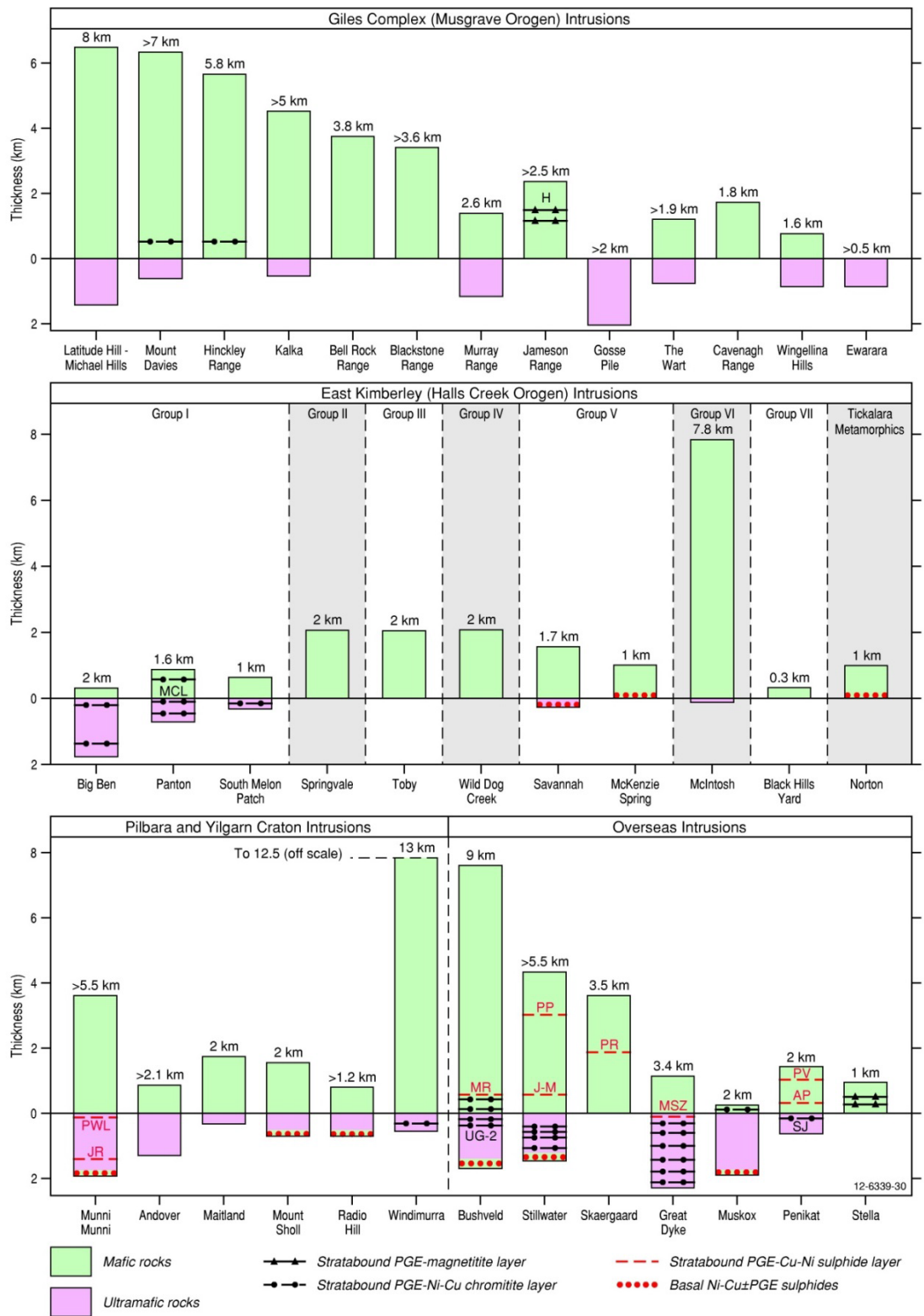


Figure 8.20 Estimated thicknesses of mafic and ultramafic rocks and the stratigraphic distribution of mineralisation for some of the largest mafic-ultramafic intrusions in Australia. Intrusions from the Halls Creek and Musgrave orogens, and the Pilbara and Yilgarn cratons are compared with the major mineralised intrusions from overseas. Mineralised layers shown are: Munni Munni Intrusion: PWL = Porphyritic Websterite Layer, JR = Judy's Reef; Bushveld Intrusion: MR = Merensky Reef, UG-2 = Upper-Group 2 Chromitite; Stillwater Complex: PP = Picket Pen Reef, J-M = Johns-Manville Reef; Skaergaard Intrusion: PR = Platinova Reef; Great Dyke of Zimbabwe: MSZ = Main Sulphide Zone; Penikat Intrusion: PV = Paasivaara Reef, AP = Ala-Penikka Reef, SJ = Sompujärvi Reef.

The Paleoproterozoic layered mafic–ultramafic intrusions in the HCO of the East Kimberley, Western Australia (Figure 8.21), represent one of the most mineralised igneous associations of their type in Australia. Exploration activities over the past five decades have focussed on Cr-PGEs-Ni-Cu±Au (chromite association—Deposit Type 1.B) and Ni–Cu–Co±PGEs (sulphide association—Deposit Type 2.A) mineral systems that have prominent surface signatures defined by chromite outcrop and sulphide gossans. The type examples of these mineral systems are the Panton and Savannah deposits, respectively (see Section 6.4). The regional distribution of the major mineralised intrusions (groups I, II, and V; Hoatson, 2000) in the HCO defines two parallel northeast-trending corridors, which can focus exploration for the two major mineral systems described above. Figure 8.22 summarises the different styles of known mineralisation associated with the intrusions. However, the intrusions also contain a range of mineral commodities (e.g., PGEs, Cr, Ni, Cu, Co, Ti, V, Fe, Au, and fluorite) and have petrological indicators that suggest other mineral systems were active in the Proterozoic. Figure 8.23 considers such potential mineral systems in the intrusions considered to be the most prospective (groups I, II, V, and VI) for PGE and Ni-Cu deposits in the East Kimberley. The Kimberleys have had a protracted history of exploration for largely outcropping deposits. The challenges of today relate to finding ‘new’ styles of mineralisation under shallow cover.

The Munni Munni Complex is another example where companies in the 1970s investigated the basal contact of the intrusion for Ni-Cu-PGE sulphide segregations, but did not initially consider the possibilities of PGE mineralisation at higher stratigraphic levels. The mineralised horizon at Munni Munni crops out over a strike length of 12 km, contains fresh sulphides or evidence of sulphides in places, and occurs at a similar stratigraphic level to the major overseas stratabound PGE horizons; thus it is surprising that the PGE potential of the intrusion was only first confirmed by a mapping-rock geochemical program undertaken by the Bureau of Mineral Resources, Geology and Geophysics in mid-1983 (Hoatson, 1984; see Section 6.4). Another example is from the Fifield district of central New South Wales, where important exploration advancements were achieved with the realisation that different mineral systems could exist, rather than being ‘blinker-visioned’ to a particular model, such as a Bushveld setting, which hindered previous exploration investigations. Accordingly, companies at Fifield employed a more predictive mineral-system approach that assessed various mineralised settings related to ‘Alaskan-type’ mafic-ultramafic intrusions (e.g., mineralised ‘P units’, hydrothermal veins, residual enrichment of PGEs in laterite, and alluvial placer deposits: see Section 6.4).

The Archean komatiite mineral systems of the Yilgarn Craton, in particular, offer considerable potential for by-product PGEs in Australia. Economically the most important komatiite-associated deposits in Australia can be classified into two end-members (Barnes, 2006; Hoatson et al., 2006): Kambalda—Deposit Type 3.A and Mount Keith—Type 3.B. An analysis of the major komatiite provinces of the world (Table 8.3) reveals that the most fertile komatiite sequences are generally of late Archean (~2700 Ma) or Paleoproterozoic (~1900 Ma to 1800 Ma) age, and have dominantly Al-undepleted ( $Al_2O_3/TiO_2 = 15–25$ ) chemical affinities. The younger age group largely feature in Canada (Thompson and Cape Smith belts) with apparently no similar-aged sequences documented in Australia. Compound sheet flows with internal pathways and dunitic compound sheet flows are considered more favourable facies for hosting massive sulphides than thin differentiated flow, lava lake, and sill-like pond facies (Hoatson et al., 2005b; Barnes, 2006). Well-insulated lava pathways that focus large volumes of magma flow and facilitate dynamic interaction of the magma with a S-bearing substrate are more likely to occur in the compound sheet flow facies. The assimilation of such a substrate can accelerate the S saturation of a primitive ultramafic magma and initiate the deposition of sulphides. Suggested exploration strategies and guideline for Type 3.A and 3.B komatiite deposits based on Australian examples are summarised in Table 8.4.



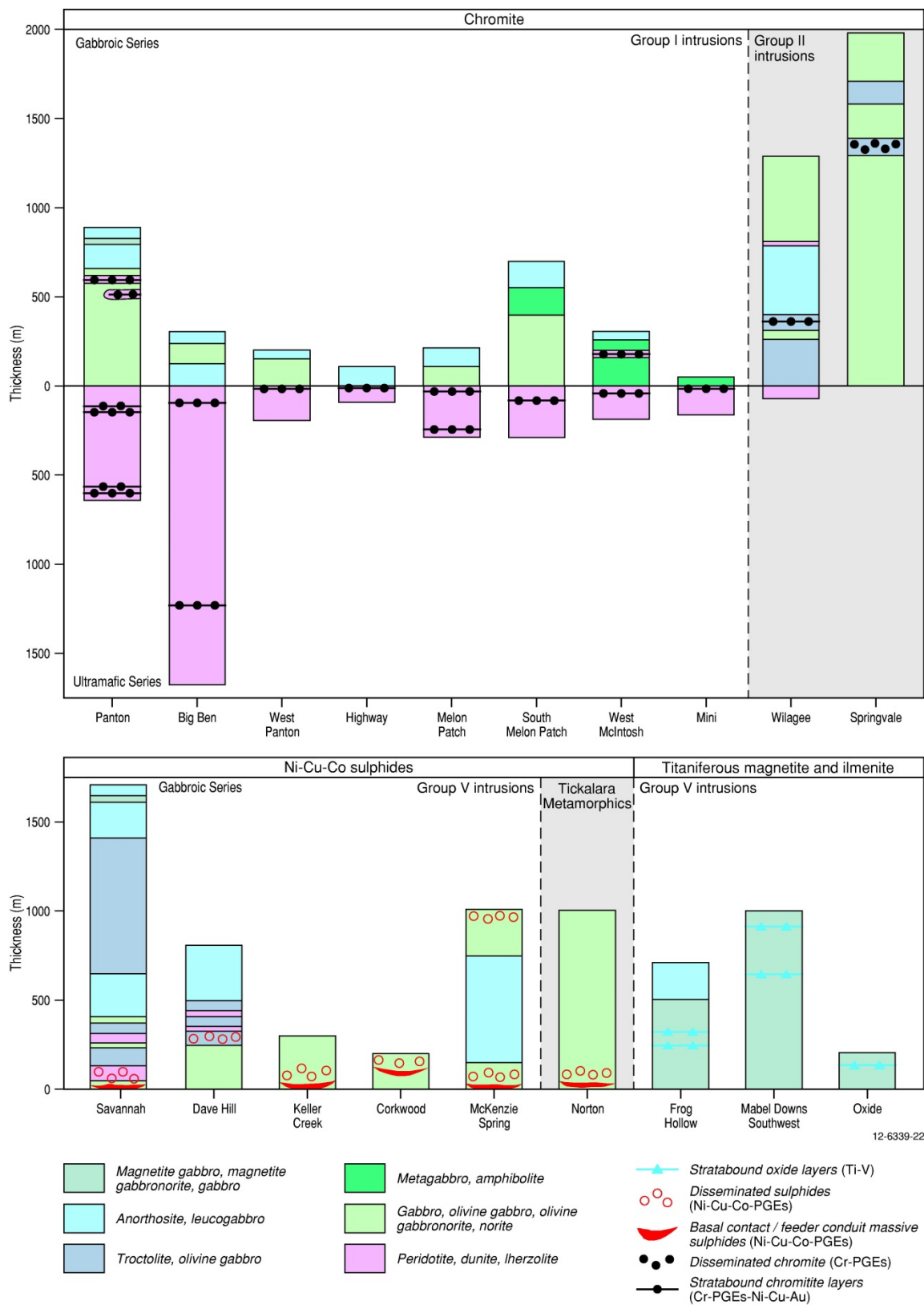


Figure 8.22 Stratigraphic distribution of chromite, Ni-Cu-Co sulphides, and titaniferous magnetite and ilmenite in the layered mafic-ultramafic intrusions of the Hall Creek Orogen, East Kimberley, Western Australia. The vertical axis shows the estimated true thickness of the Ultramafic Series and Gabbroic Series for each intrusion. Modified from Hoatson and Blake (2000).

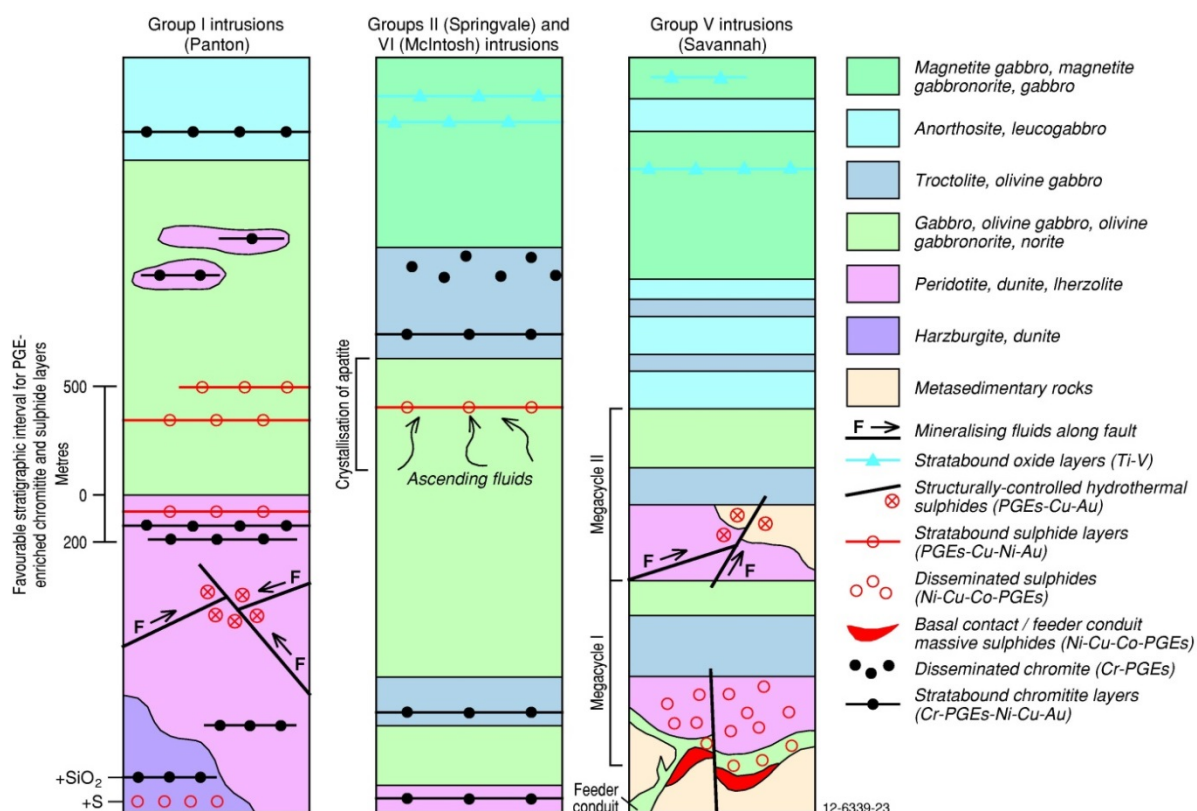


Figure 8.23 Stratigraphic levels of potential orthomagmatic and hydrothermal mineralisation in the groups I, II, V, and VI mafic-ultramafic intrusions of the Halls Creek Orogen, East Kimberley, Western Australia. Modified from Hoatson and Blake (2000).

In addition to the more typical komatiite-associated Ni deposits of the Yilgarn Craton (Types 3.A and 3.B), recent exploration in covered areas and in less traditional environments has defined an increasing number of deposits and prospects that have unusual settings and metal signatures. These include those komatiite deposits and prospects with exceptionally high Ni grades (e.g., Cosmos, Long, Flying Fox-T5), with normal Ni/Cu ratios and high PGE grades (Waterloo), and with low Ni/Cu ratios and high PGE grades (Collurabbie, Collurabbie South, Daltons). This diversity of mineralisation styles, which enhances the prospectivity of this magmatic association, is likely to expand in the future with exploration moving into more greenfields environments.

Proterozoic sedimentary rocks of the Yerrida and Earahedy basins unconformably overlie Archean greenstone sequences on the northern margins of the Yilgarn Craton. Geophysical studies (aeromagnetics and gravity) have shown that narrow, high-amplitude magnetic signatures typical of komatiitic sequences and/or Banded Iron Formations (BIFs) can be traced northwards under these sedimentary sequences for several tens of kilometres strike extent (Whitaker and Bastrakova, 2002). The greenstone sequences between Leinster and Wiluna (Figure 8.24) represent the richest Ni-bearing komatiite belt in the world, with four world-class deposits (Mount Keith, Perseverance, Yakabindie, Honeymoon Well), five of the six largest Ni sulphide deposits in Australia, and a collective global Ni resource of at least 9.2 Mt, equivalent to more than 70% of Australia's known total Ni-sulphide resources (Hoatson et al., 2006). The interpreted extensions of the ultramafic sequences beneath the Proterozoic rocks north of Wiluna have considerable potential for Ni-Cu-PGE mineralisation, especially in view of the significant metal endowment of the greenstones immediately to the south of Wiluna and the discovery of massive sulphides (0.3 m @ 6.6% Ni: Agincourt

Resources Limited, 2005) at Bodkin north of Wiluna (inset of Figure 8.24). This is the first time massive Ni sulphides have been reported from the northern part of the Perseverance–Wiluna greenstone belt. The presence of thick MgO-rich komatiite channel sequences, massive sulphides in embayment structures, and sulphidic footwall rocks in this part of the belt indicate favourable environments for economic concentrations of Ni sulphides. Significant drill intersections, such as reported at Collurabbie (see Section 6.4.3.3), also highlight the potential of poorly exposed greenstone sequences near the margins of the craton that have experienced little exploration. Similarly, extensions of potentially mineralised komatiitic sequences may also exist under cover for other sections of the Eastern Goldfields, Northeastern Goldfields, and Southern Cross provinces (see Figure 8.24). The Eastern Goldfields and Southern Cross provinces have similar cumulative frequency endowment trends (see Figure 22 in Hoatson et al., 2006), except for the apparent absence of world-class deposits in the latter province. These similar grade-tonnage trends suggest that large deposits remain to be found under cover in the Southern Cross Province.

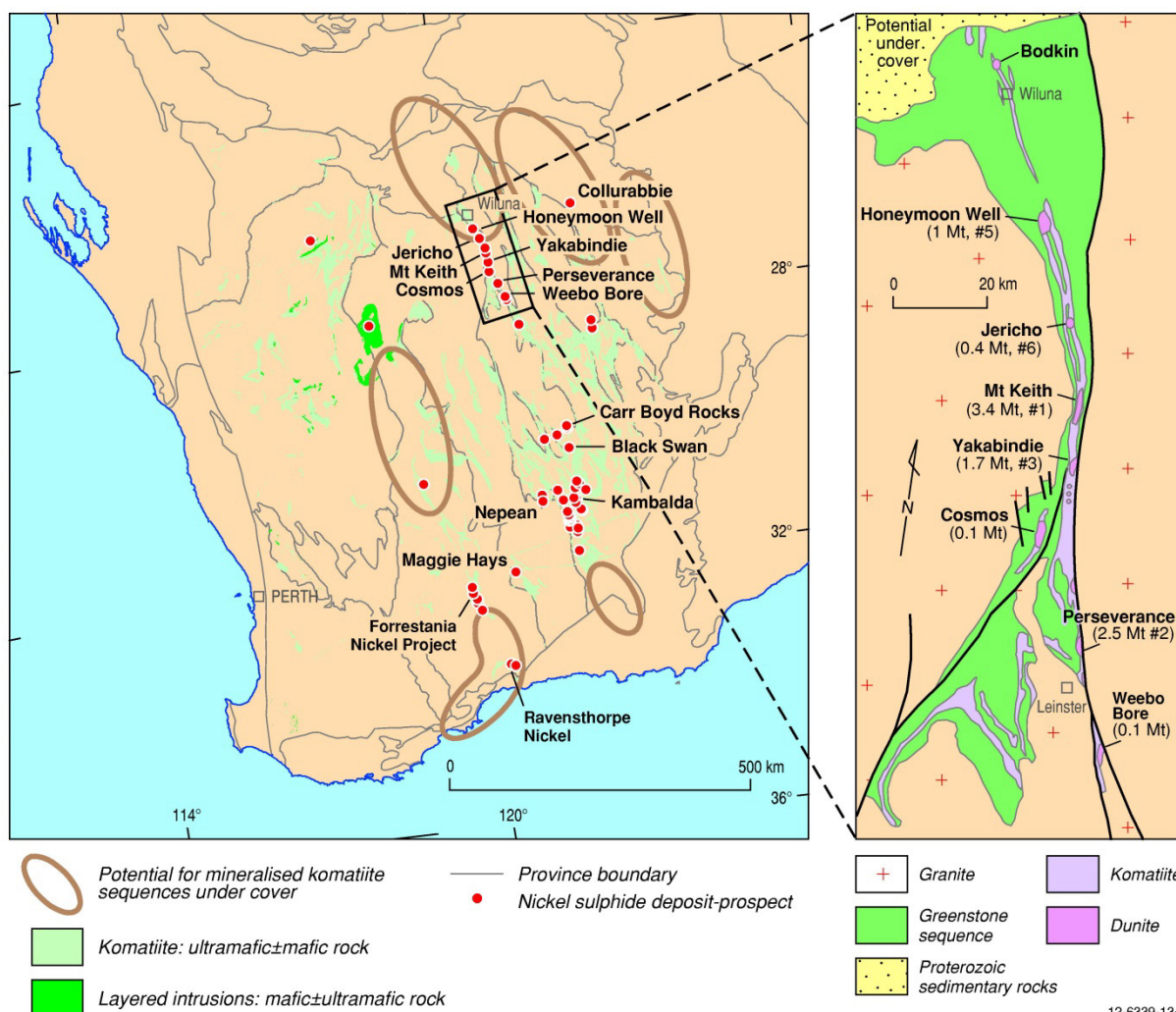


Figure 8.24 Interpreted extensions (brown ellipses) of potentially mineralised komatiite sequences under cover in the Yilgarn Craton, Western Australia. Proterozoic sedimentary rocks (Yerrida and Earaheedy basins) unconformably overlie Archean greenstone sequences along the northern margins of the craton. Magnetic signatures typical of komatiitic sequences and/or BIFs can be traced northwards under these sequences for tens of kilometres strike extent (Whitaker and Bastrakova, 2002). Inset on right shows major komatiite-associated nickel sulphide deposits in the northern Norseman–Wiluna greenstone belt and their global nickel resources and size ranking relative to Australian nickel sulphide deposits. Modified from Hoatson et al. (2006).

Komatiitic rocks in Australia have previously been considered to be confined to the older Archean components of the West Australian Craton (Myers et al., 1996), namely the Yilgarn and Pilbara cratons. However, the confirmation of primitive komatiitic rocks near Lake Harris and Mt Hope in the Gawler Craton (Hoatson et al., 2005b) now extend their regional distribution much further east on the Australian continent. The wider distribution of the komatiites has implications for further discoveries of Ni-Cu-PGE deposits and the geodynamic reconstruction of Australia's Precambrian crustal architecture (Betts and Giles, 2006).

The recognition of several PGE occurrences related to hydrothermal mineral systems in the Pine Creek Orogen, Northern Territory, has defined a province where PGE+Au±U mineralisation shows no clear spatial association with, or derivation from, mafic-ultramafic rocks. This unusual style of unconformity-related mineralisation is prominent in the Proterozoic Alligator Rivers region, and possibly in the Rudall area of the Paterson Province, Western Australia (see PM Cu-Ag-Au-PGE Prospect in Appendix K). With further research on the physico-chemical conditions of ore formation in these deposits (e.g., source rocks, chemical mobility, transport, and chemical traps for PGEs, Au, and U), it is likely that similar occurrences will be found elsewhere. The bench-mark mineral-system studies undertaken for the Coronation Hill U-Au-PGE deposit by Wyborn et al. (1994) and Mernagh et al. (1994, 1998) need to be applied to other Proterozoic terranes that have similar PGE-bearing unconformity-related deposits.

Placer deposits related to 'alpine- and ophiolitic-type' intrusions in eastern Australia have scope for small-scale operations where production can be quickly brought on stream during periods of favourable metal prices, and mining methods are cost-effective. However, these types of intrusions generally have low potential for a major hard-rock resource of PGEs since they: have been extensively explored by the prospector; are confined to well-defined ~north-trending geographic belts along major fault zones and thus have a high degree of predictability about their distribution; often crop out well; are spatially associated with earlier discovered alluvial placer or beach deposits (thus facilitating recognition); and the PGE mineralisation associated with chromite generally has an erratic, unpredictable distribution often overprinted by hydrothermal-remobilisation processes (Hoatson, 1984; Franklin et al., 1992). The shallow hard-rock deposits overseas are commonly mined by open pits or quarries and the deeper extensions by underground workings. When developed, the deposits are quickly mined out, and exploration drilling around these deposits has had limited success (Mosier et al., 2012). Although chromite pods tend to be found in clusters, and chances for discovery of additional ore bodies are greater around known deposits, there are no proven geological guidelines for finding additional ore bodies (Mosier et al., 2012). As indicated by many studies overseas (Augé, 1986; Page et al., 1986; Prichard et al., 1996; Bai et al., 2000; Mosier et al., 2012; Singh et al., 2013), podiform chromite deposits generally contain low concentrations of associated PGEs. Such deposits have been mined for their metallurgical-grade Cr throughout the world, but there are only a few examples where the PGEs have been exploited. Page et al. (1986) documented PGE concentrations for 280 podiform chromite deposits of Paleozoic to Mesozoic age in California and Oregon: maximum concentrations were 2.53 ppm Pt, 0.2 ppm Pd, 0.14 ppm Rh, 4.93 ppm Ru, and 2.93 ppm Ir. They concluded that the low grades of the PGEs and the relatively low volumes of total PGEs indicate that the potential supply of by-product PGEs from hard-rock mining of podiform chromite in ophiolitic intrusions is small. The United States Geological Survey study (Mosier et al., 2012) of 1124 podiform chromite deposits from around the world showed that the vast majority (>98%) of the chromitites (major, minor, and banded) had concentrations less than: ~70 ppb Rh, ~250 ppb Ir, ~400 ppb Ru, ~30 ppb Pd, and ~130 ppb Pt. They also concluded that for most of the podiform chromite deposits they studied, the chromite mineralisation appeared to be randomly distributed within the ultramafic

rocks, which makes for difficult exploration. Although podiform chromite deposits are largely associated with dunite, not all dunite bodies contain chromite, and the dunite bodies themselves appear to be randomly distributed in the peridotite host. The regional geochemical studies of Page et al. (1986) and Mosier et al. (2012) indicate that 'alpine- and ophiolitic-type' intrusions in general have low potential for a major hard-rock resource of PGEs. Mosier et al. (2012), and references within, summarise some exploration case studies that involved drilling 'blind' deposits, electromagnetic and gravitational geophysical surveys, and geochemical methods for podiform chromite deposits. They conclude from their exhaustive study of over 1100 global deposits that because of the complexity of geological factors, no single method of exploration can be universally applied to finding these deposits.

Table 8.4 provides a summary of exploration strategies, guidelines, and target geological provinces relevant to Australia for those mineral systems considered to have high potential for large-tonnage PGE resources (Deposit Types 1.A and 1.B), and those deposits where the PGEs constitute a significant by-product component of other metals as indicated by historical production trends (Deposit Types 2.A, 3.A, 3.B and 3.C). The latter deposit types have been included since their contributions to Australia's PGE production record indicates these mineral systems have been operative and efficient, and Australia is well represented with these particular mineral systems (e.g., komatiites and mafic-dominated intrusions).

Table 8.4 Exploration guidelines for Australian PGE deposits (based on Australian examples).

<b>Stratabound PGE-bearing sulphide and chromitite layers</b> (e.g., Type 1.A: Munni Munni, Weld Range, Jimberlana, Windimurra) and stratabound PGE-bearing chromitite layers (e.g., Type 1.B: Panton, Eastman Bore, Coobina, Mount Davies, Windimurra) in layered tholeiitic mafic-ultramafic intrusions)	
<b>Regional geological criteria</b>	Tholeiitic-dominated intrusions emplaced in rift zones in Archean-Proterozoic cratons (Pilbara, Yilgarn, Gawler) or in Proterozoic orogenic belts (Halls Creek, Albany-Fraser, Musgrave, Fowler) near the margins of stable cratons.
	Cratonic settings: dominantly postorogenic intrusions associated with sinuous greenstone sequences of coeval komatiitic-basaltic-felsic volcanics, metasediments, elongate to ovoid granitic bodies; anastomosing to linear tectonic patterns. Orogenic settings: tectonised orogenic to postorogenic bodies associated with fault-bounded linear belts of metasediments and metavolcanics, elongate granitic bodies; linear tectonic patterns.
	Emplacement ages: ~2925 Ma to ~2700 Ma in the Pilbara and Yilgarn (Munni Munni, Weld Range, Windimurra, Nardee), ~1850 Ma in the East Kimberleys (Panton, Eastman Bore, Lamboo, Big Ben), ~1080 Ma in the Musgraves (Mount Davies).
	Large and thick (>3 km) differentiated layered mafic-ultramafic and ultramafic intrusions that display open-fractionation systems involving large pulses of primitive S-undersaturated magma (source of PGEs) and younger, more evolved S-saturated mafic magma (source of S).
	Fertile PGE-bearing primitive magmas (not depleted by early S-saturation events) that achieve late S saturation (in the magma chamber) through magma mixing, crystal fractionation, crustal contamination, and/or movement of fluids.
<b>Local geological criteria</b>	Macrorhythmic cycles of ultramafic (ol-opx-cpx-chr) and mafic (pl-cpx-opx-ol-mt-ap) rocks that show considerable lateral continuity; most mineralised layers are stratabound, although some may be discordant to the underlying stratigraphy (Munni Munni); the mineralised layers need to maintain uniform thicknesses and constant metal grades over considerable strike distance (km's) to be economic.
	The most PGE-enriched mineralised layers generally occur at, or near, major compositional interfaces in the intrusion that involved the cumulus crystallisation of plagioclase (i.e., near major contacts between ultramafic and mafic sequences). Exploration should initially focus on the stratigraphic interval from 150 m below the contact between ultramafic and mafic sequences up to 500 m above this contact.
	PGE-enriched layers either show no spatial relationship with cyclic units (Munni Munni), or occur at the base or within cyclic units (Panton) that are tens to hundreds of metres thick.
	High tenor PGEs are associated with either minor (1 vol.%–3 vol.%) disseminated magmatic Fe-Ni-Cu sulphides (chalcopyrite-pentlandite-pyrrhotite±magnetite) and/or with chromite, at some appreciable height above the base of the intrusion. Ores are often associated with reappearance in stratigraphy of high-temperature, primitive cumulus minerals (olivine, chromite, orthopyroxene); orthopyroxene and/or olivine cumulates are more favourable than clinopyroxene cumulates for hosting stratabound chromitite layers because of the relative high partitioning of Cr into clinopyroxene (inhibits precipitation of chromite).
	Chemical and isotopic indicators of sulphide contamination and assimilation processes: $\delta^{34}\text{S}$ values distinctly different from those of the mantle; Se/S ratios much lower than those of the mantle; anomalously high Zn contents in chromite indicative of the assimilation of Zn-bearing sulphidic metasedimentary rocks.
	Textures of ultramafic rocks: cumulus (adcumulate, mesocumulate, orthocumulate), foliated, massive; textures of gabbroic rocks: intergranular, subophitic, laminated.
	Textures of sulphide ore layers: porphyritic, pegmatoidal, coarse-grained (host rocks: plagioclase-bearing pyroxenite, gabbro); textures of chromitite ore layers: disseminated, massive, cumulus (host rocks: dunite, troctolite, orthopyroxenite).
	Wide-scale turbulent and efficient mixing of resident with new primitive magma in the chamber and/or rapid turbulent flow through a narrow conduit is required so that sulphides equilibrate with a large volume of magma to achieve significant PGE enrichment.
	Aeromagnetic and gravity surveys to determine regional extent, geometries, major compositional interfaces (ultramafic versus mafic), igneous layering, and major structures of poorly exposed bodies; ground magnetics to define lithological contacts, magmatic unconformities, and magnetite-bearing reefs; gravity for determining the sub-surface extent and volume of mafic and ultramafic igneous rocks of variable density; electromagnetic and induced polarisation methods to delineate large concentrations of disseminated sulphides-electrical responses are subtle; 3-D seismic surveys have been used to identify faults, slumps, and potholes in the Merensky Reef. Satellite hyperspectral imagery and gamma-ray spectrometry are useful for discriminating broad packages of ultramafic, mafic, and felsic rock types.
<b>Exploration methods</b>	Soil and stream geochemistry: used in the discovery of several major deposits, e.g., the J-M Reef of the Stillwater Complex was discovered by analysing soil and talus fines; soil geochemistry was used for the delineation of mineralisation in the Platreef; the Merensky Reef was discovered from detrital PGMs in panned concentrates from river alluvials; and glacial-till geochemical surveys were used in the Duluth Complex (Zientek, 2012).
	Detailed geological mapping and close-spaced rock sampling (10 m to 20 m intervals) through the entire stratigraphic succession to assess the stratigraphic level of S saturation.
	Marked discontinuities in lithochemical profiles of S, Cu, Zr, Rb, Sr, Cs, Cu/Pd, Pd/Zr, Pd/Ir, Cu/Zr, and mg number indicate stratigraphic levels of new magma pulses and S saturation, and mineralised layers formed by magma mixing. For example, the stratigraphic level of a stratabound PGE layer/reef may be indicated by a sharp increase in Cu/Pd up the stratigraphy.
	The economically most important layers (Merensky Reef, UG-2, J-M Reef, Main Sulphide Zone) and uneconomic examples in Australia (PWL–Munni Munni, MCL–Panton, Parks Reef–Weld Range) are located at, or near, major compositional interfaces in the intrusion that involved the cumulus crystallisation of plagioclase (i.e., near major contacts between ultramafic and gabbroic sequences). Therefore exploration should initially focus on the ~650-m thick stratigraphic interval from ~150 m below the contact between the ultramafic and mafic sequences, and up to 500 m above this contact. If the intrusion is S saturated throughout the total stratigraphy, Ni-Cu-Co±PGE sulphides along the basal contact, or in the feeder conduit, (Type 2.A deposit below) should be investigated.
	Important mineralising processes, such as mixing of primitive magma with more fractionated magma, are indicated by: rapid changes in compositions of cumulus minerals and the volume of intercumulus melt; presence of sulphides, chromite, Al-spinel, graphite, and halogen-bearing minerals (apatite, biotite, amphibole); transitions from Fe-rich to Cu-rich sulphide assemblages; development of porphyritic, pegmatoidal, and orthocumulus textures; presence of hybrid rocks, xenoliths in slump deposits, lateral variations of rock types; and unconformities that indicate magmatic erosion/disruption of footwall units.
	High Mg, high-Cl, primitive 'basaltic' parent magmas (e.g., contaminated komatiitic, picritic, siliceous high-magnesian, boninitic types) with Pt and Pd concentrations of greater than 10 ppb are favoured for the formation of PGE-sulphide deposits.
	Stratabound PGE-sulphide layers are difficult targets to explore because they are generally narrow (~1–2 m thick layers in up to 10-km-thick sequences), and they have weak geophysical (only 2–3 vol. % disseminated sulphides) signatures; in contrast, chromitite layers often crop out, are readily identified, and are defined by elevated contents of pathfinder elements Cr, Pt, Pd, Ni, Cu, Co, Au, Mg, As, and Hg.

<b>Segregations of Ni-Cu-Co-PGE sulphides in feeder conduits and basal contacts of tholeiitic mafic-dominated intrusions</b> (e.g., Type 2.A: Nebo–Babel, Radio Hill, Mount Sholl, Nova, Savannah)	
<b>Regional geological criteria</b>	Tholeiitic mafic-dominated intrusions emplaced in rift zones in Archean-Proterozoic cratons (Pilbara, Yilgarn, Gawler) or in Proterozoic orogenic belts (Halls Creek, Albany-Fraser, Fowler). Province boundaries, rifts, and deeply penetrating faults that can allow for efficient and rapid ascent of magma through the crust. Intrusions often occur in clusters and as stacked bodies at different levels in the crust (Musgrave Province, Halls Creek Orogen).
	Cratonic settings: postorogenic intrusions associated with sinuous greenstone sequences of coeval komatiitic basaltic-felsic volcanics, metasediments, elongate to ovoid granitic bodies; anastomosing to linear tectonic patterns.
	Orogenic settings: tectonised orogenic to postorogenic bodies associated with fault-bounded linear belts of metasediments and metavolcanics, elongate granitic bodies; linear tectonic patterns.
	Emplacement ages: ~2925 to ~2700 Ma in the Pilbara and Yilgarn (Radio Hill, Mount Sholl, Windimurra); ~1865 Ma to ~1850 Ma in the Halls Creek Orogen (Savannah, Corkwood, Keller Creek, Bow River, Copernicus, Norton); ~1633 Ma in the Arunta Orogen (Andrew Young Hills); ~1300 Ma in the Albany-Fraser Orogen (Nova); ~1070 Ma in the Musgrave Province (Nebo–Babel, Halleys–Saturn).
	Small- to medium-sized (<3 km-thick), differentiated mafic and mafic-ultramafic intrusions as dipping sheets, sills, dykes, funnels, chonoliths, and plug-like bodies. Intrusions maybe associated with comagmatic volcanic sequences and sub-volcanic feeder conduits that may have been removed through deformation and/or erosion. Deposits are generally not hosted in thick, large-layered intrusions that have had protracted and passive evolutions.
	Ni-bearing magmas (Ni not depleted by early-crystallising olivine or early S-saturation events) that achieve rapid S saturation by contamination and/or turbulent mixing in a dynamic magma chamber in the middle to upper crust.
<b>Local geological criteria</b>	Mafic-dominated tholeiitic intrusions with ultramafic rocks, if present, generally forming thin cyclically layered sequences in the lower parts of the stratigraphy.
	Massive or more rarely layered bodies consisting of cumulus (adcumulate, mesocumulate, orthocumulate)-, equigranular-, intergranular-, subophitic-textured rocks. Intergranular and ophitic textures are more prominent in the evolved mafic rocks in the upper parts of the intrusion.
	Sulphur-bearing (sulphide and/or sulphate) crustal rocks.
	Presence of massive, matrix, and disseminated Fe-Ni-Cu-Co sulphides in lower parts of stratigraphy, and remobilised and fractionated Cu-Pd-Pt-Au-Ag-enriched sulphides in vein systems in the basal contact region of the intrusion and in the country rocks.
	Massive sulphides—critical to the economic status of deposit—are confined to structural embayments and depressions in basal contacts below the thickest sequence of cumulates. They are generally hosted by thin (metres to tens of metres thick) basal 'veneers' of evolved gabbroic rocks located between the country rocks, and an overlying, more primitive ultramafic-mafic cumulate sequence (Savannah, Radio Hill, Mount Sholl). Massive, disseminated, and breccia sulphides also hosted in narrow feeder conduits (Nova, Nebo–Babel, Radio Hill, Savannah).
	Preservation of basal contacts and feeder conduits (not sheared out or overprinted by younger intrusions).
	Dynamic, open-magmatic systems (periodically replenished magma chambers, subvolcanic feeder sills and dykes, volcanic vents, extensive interaction of hot primitive magma(s) with S-bearing country rocks, brecciation, turbulent magma mixing) rather than passive, slowly evolving magmatic systems. Dynamics of focussed magma flow and conduit geometry (slow, fast, or turbulent flow; changes from narrow vertical conduits to subhorizontal broad magma chambers; physical traps) are important considerations for the precipitation and capture of massive sulphides. Significant changes in dip and width along strike of an intrusion, indicating sites of possible changes in magma flow dynamics.
	Reversals in fractionation indicators (abrupt increases in Fo contents of olivine, resetting of mg numbers of pyroxenes); changes in chalcophile element contents and rock porosity; magma mixing; hybrid rocks; lateral variation of different rock types that show interfingering, thinning, and thickening features; magmatic unconformities; presence of chrome and aluminous spinels reflecting changing fO <sub>2</sub> conditions; and localised concentrations of magmatic breccias all indicate dynamic, open-magmatic systems that involve regular new pulses of magma into the chamber.
<b>Exploration methods</b>	Geophysics: regional aerial magnetic and gravity surveys to determine total extent, pre-deformational geometries, and fractionation (younging) directions of intrusions, and locate favourable mineralised environments (basal contacts, feeder conduits); ground magnetics to define lithological contacts and small-scale mineralised structures (embayments); airborne-ground electromagnetics and induced polarisation to delineate conductive sulphides.
	Geochemical profiling (S, Cu, Ni, PGEs, Cu/Pd, mg number) along type stratigraphic sections to determine stratigraphic level and effectiveness of S-saturation event(s).
	Evidence for thermal-chemical interaction of magma(s) with S-bearing country rocks (fractionated compositions of marginal rocks, xenoliths of country rock, xenocrysts, hybrid rocks, association of sulphides and alkalis, elevated Zr, Y, Ti, Al, Fe, Nd contents).
	Composition of olivine (Ni content versus mg number) is a useful indicator of Ni depletion in the magma from which olivine crystallised from.
	Chemistry of gossans of massive sulphides as defined by coincident high Ni, Cu, and Pt, Pd, Ir, and Bi contents; regolith and geobotanical mapping since many deposits are covered by alluvium, laterite, or lacustrine sediments.
	Close-spaced core drilling of basal contact and feeder conduit (especially entry point region into magma chamber) regions. Down-hole geophysics, e.g., time-domain electromagnetics and radio-imaging, of these favourable mineralised environments.

**Komatiite-associated Ni-Cu-PGEs sulphides in preferred lava pathways**

(e.g., Types 3.A, 3.C: Kambalda, Prospero, Cosmos, Flying Fox, Waterloo, Collurabbie) and in central parts of thick dunite bodies (e.g., Type 3.B: Mount Keith, Perseverance, Honeymoon Well, Yakabindie, Black Swan)

<b>Regional geological criteria</b>	Komatiitic magmas emplaced in rift zones in granite-greenstone belts in Archean cratons (Yilgarn, Pilbara, Gawler).
	Granite-greenstone belts: sub-parallel linear and sinuous greenstone sequences; elongate, ovoid, and domal granitic bodies; coeval komatiitic, basaltic (tholeiitic), and felsic volcanics; metasedimentary rocks; province wide shear systems; and linear tectonic patterns.
	Intracratonic-extensional rift environments (Groves and Batt, 1984): (a) rift-phase greenstone sequences formed in deep-water under conditions of high-crustal extension; abundant sulphidic shale and chert (e.g., Kambalda and Mount Keith districts); or (b) platform-phase greenstone sequences formed in relatively shallow water under conditions of low-crustal extension; volcanoclastic rocks and oxide-facies iron formation (e.g., Forrestania district).
	Regionally extensive (10's to 100's km strike extent) komatiite sequences containing thick olivine cumulate units. Cumulates proportionally thicker relative to more evolved komatiitic rocks from upper parts of sequences.
	Emplacement ages: ~2700 Ma, and ~2900 Ma to ~3000 Ma in the Yilgarn (Kambalda, Mount Keith, Maggie Hays); ~2880 Ma to ~3460 Ma in the Pilbara (Ruth Well, East Pilbara); and ~2520 Ma in the Gawler (Lake Harris, Mount Hope) cratons.
	Although most mineralised provinces contain both Al-undepleted ( $Al_2O_3/TiO_2 = 15-25$ ) and Al-depleted ( $Al_2O_3/TiO_2 < 15$ ) komatiitic sequences, the most significant mineralisation is generally associated with the former type. Provinces with only Al-depleted sequences are generally poorly mineralised or barren.
<b>Local geological criteria:</b>	Presence of outcropping gossans and primitive komatiitic rocks: spinifex, quenched, breccia, and aphyric textures for komatiitic basalts and low- to high-Mg komatiites (15% MgO to 32% MgO whole-rock compositions), and cumulus (orthocumulate, mesocumulate, adcumulate) textures for more primitive (32% MgO to 50% MgO whole-rock and $>Fo_{85}$ olivine compositions) sequences.
	Massive and matrix ores concentrated in basal part of stacked sequence of relatively thin (few metres up to tens of metres) compound sheet flows with internal pathways (Kambalda-type), or disseminated ores within thick (up to 800 m) olivine cumulate dunite lenses with transgressive basal contacts (Mount Keith-type).
	Preserved lava pathways or lava tubes (i.e., focussed flow) within thick inflated flows.
	Presence of sulphide-bearing substrate lithologies (chemical-exhalative sediments, volcanics) that have relatively low melting points to facilitate thermal erosion.
	Presence of transgressive embayments and structural traps along footwall contacts of channel facies to concentrate massive sulphides.
	Evidence of S saturation (e.g., presence of Ni-enriched magmatic sulphides, Ni depletion trends in olivine compositions, depletion of PGEs).
<b>Exploration methods</b>	Regional aerial magnetic and gravity surveys to define potential host komatiitic rocks (generally, but not always strongly magnetic) and lava pathways; ground magnetics to identify lithological contacts and small-scale structures; airborne-surface electromagnetics to delineate electrically conductive Fe-Ni-Cu sulphides (can be hampered by barren sulphide-bearing sediments and saline groundwaters). Down-hole electromagnetics are becoming more effective due to greater depth of penetration and they avoid problems related to conductive regolith. New 'Geoferrit' electromagnetic technology is able to detect orebodies <500 m below the surface.
	Need to identify physical or chemical haloes which are much larger than the orebodies themselves. Gossans of massive sulphides defined by coincident high Ni, Cu, and PGEs; most deposits are covered by alluvium, laterite, or lacustrine sediments thus regolith and geobotanical mapping to interpret subsurface geology and supergene geochemistry (Sheard and Robertson, 2002).
	Determine magmatic environments (volcanic, subvolcanic, intrusive) and facies (flood sheet flows, compound flows, ponded lakes: Dowling and Hill, 1998).
	Chemical evidence of substrate erosion and crustal contamination (enrichment in Zr, La, Th, U, Y, Nd, Ti, Al, Fe, negative Nb-Ta-Ti anomalies: Barnes et al., 1999; Leshner, 2004); depletion trends in chalcophile trace element ratios (Pd/S, Cu/Pd) along basal flows to indicate location of S saturation and mineralisation.
	Close-spaced core drilling of most primitive parts of komatiite sequences.

ap = apatite, chr = chromite, cpx = clinopyroxene, hb = hornblende, mt = magnetite, ol = olivine, opx = orthopyroxene, pl = plagioclase.

Sources of data for the following exploration guidelines include: Leshner (1989); Naldrett (1989, 2002, 2004, 2008a,b; 2011); Groves and Hudson (1990); Dowling and Hill (1998); Hoatson (1998, 2001); Hoatson and Keays (1989); Hoatson and Blake (2000); Hoatson and Sun (2002); Hronsky, pers. commun. (2004); Hoatson et al. (2005a,b; 2006); Barnes (2006); Fiorentini et al. (2010, 2012), and this study.



There is a profusion of published information that describes the exploration strategies and techniques used for different PGE deposits overseas. However, it is beyond the scope of this report to describe these applications and case studies and it is recommended the reader refers to the following publications for further details, namely:

- **General exploration methods for PGEs**—Naldrett (1981, 1989, 1997, 1999, 2002, 2004, 2011); Duke (1988); Hoatson et al. (1992); Barrie (1995); Duke (1995); Eckstrand (1995); McLeod and Morison (1995); Lee (1996); Maier et al. (1998, 2001, 2014a,b); Hoatson and Blake (2000); Leshner (2004); Maier (2005); Green and Peck (2005); Ames and Farrow (2007); Eckstrand and Hulbert (2007); Mungall and Naldrett (2008); Causey et al. (2009); Markwitz et al. (2010); Schulz et al. (2010); Maier and Groves (2011); Zientek (2012); and Mosier et al. (2012).
- **Economic Geology Bulletins devoted to PGEs and Ni**—these contain many papers describing exploration techniques and case exploration histories of new PGE and Ni-Cu-PGE deposits. These issues include: 1976—volume 71—number 7 (theme of PGEs); 1981—76—6 (Ni deposits in Western Australia); 1982—77—6 (PGEs); 1985—80—4 (Bushveld Complex); 1986—81—5 (PGEs); 2000—95—4 (Voisey's Bay); 2002—97—7 (Sudbury Basin); 2008—103—6 (Abitibi Greenstone Belt); 2012—107—5 (komatiites); and 2013—108—8 (China).
- **Geophysical signatures**—Pridmore et al. (1984); Elliott and Staltari (1985); Peters and de Angelis (1987); Dentith et al. (1994); Emerson et al. (1999); Bourne (1996); Guo and Dentith (1997); Craven et al. (2000); Stolz (2000); Peters and Buck (2000); Wolfram and Golden (2001); Meixner and Hoatson (2003); Mutton and Peters (2004); Balch (2005); Mortimer (2005); Peters (2006); and Ford et al. (2007).
- **Geochemical exploration**—Bachmann et al. (1987); Hamlyn et al. (1988); Gunn (1989); Prendergast and Keays (1989); Groves and Hudson (1990); Salpeteur and Jezequel (1992); Boudreau (1995); Maier et al. (1996, 2002, 2003); Prendergast et al. (1998); Brand (1999); Cameron (2001); Li et al. (2001a); Moroni et al. (2001); Wood (2002); Diakov et al. (2002); Barnes et al. (2004a); Cornelius (2005); Baker and Waugh (2005); Cameron and Hattori (2005); Li and Ripley (2005); Maier and Barnes (2005); Mieztis et al. (2006); and Godel et al. (2011).
- **Regolith and supergene PGE exploration**—McGoldrick and Keays (1981); Butt et al. (1992, 2001, 2006); Gray et al. (1996); Williams (2001); Elias (2002, 2006); Wilde (2005); Oberthür and Melcher (2005); and Marsh and Anderson (2011).
- **Biochemical exploration**—Dunn (1986, 1992); Hall et al. (1990); and Rencz et al. (1992).

There are very few publications that describe in detail the applications of PGE model types and exploration techniques specific to Australia. Koek et al. (2010) outline the various 'mineral-system' stages of four PGE deposit models they consider to have relevance to Australia, namely PGEs in layered mafic to ultramafic intrusions, PGEs as by-products in magmatic Ni-Cu deposits, late magmatic and hydrothermal PGEs, and alluvial placer PGEs. Hoatson and Glaser (1989) and Hoatson (1998) provide the most comprehensive summaries of exploration techniques and case-histories relating to PGE mineral systems in Australia, including: regional geophysical (aeromagnetism, gravity, AEM, radiometrics, remote sensing) and geochemical programs; effectiveness of geological mapping and different types of drilling at different scales; and the applications of soil-stream sediment-geobotanical studies. The applications of these exploration methods in various geological provinces have been described for: the Halls Creek Orogen (Wallace and Hoatson, 1990; Sun et al., 1991; Hoatson, 1995; Hoatson et al., 1997; Sanders, 1999; Hoatson and Blake, 2000; Sproule et al., 2002a); Pilbara Craton (Hickman, 1983; Marston, 1984; Simpson et al., 1988; Harrison and Blockley, 1990;

Wallace and Hoatson, 1990; Sun et al., 1991; Hoatson et al., 1992; Ruddock, 1999); Yilgarn Craton (Keays et al., 1981a; Marston, 1984; Harrison, 1986; Harrison and Blockley, 1990; Elias, 2002, 2006; Huston et al., 2002; Barnes, 2006); Collier Basin and Edmund Basin (Morris and Pirajno, 2005); Gawler Craton (Sheard and Robertson, 2002; Hoatson et al., 2005b); Arunta Orogen (Hoatson, 2001; Hoatson and Stewart, 2001; Meixner and Hoatson, 2003; Hoatson et al., 2005a; Mieziitis et al., 2006); Musgrave Province (Morris and Pirajno, 2005; Maier et al., 2014a,b); Delamerian Orogen (Bacon, 1992; Brown, 1992, 1998; Bottrill, 2014); Lachlan Orogen (Elliott and Martin, 1991; Teluk, 2001); and for the continent (Hoatson, 1984, 1990, 1998; Hamlyn et al., 1988; Butt et al., 1992, 2006; Solomon and Groves, 1994; Brand et al., 1998; Hoatson et al., 2006; Koek et al., 2010).

During the last few years there has been an increasing trend of 'less traditional' innovative exploration methods being considered for exploring mineralised environments in mafic and ultramafic rocks at depth and/or under cover. This apparent paradigm shift in exploration is partly being driven by the demand for elusive world-class deposits and the dramatic decrease in the discovery rate of major mineral deposits globally during the last decade (Schodde, 2010). Future exploration success will depend on continuing to develop the new technologies and concepts that will stimulate and challenge exploration thinking. Such innovative techniques include: mapping bedrock lithologies through *in situ* regolith using discriminant element ratios and large high-quality, multi-element datasets (Barnes et al., 2014); mineral deposit density regression models to estimate the number of undiscovered deposits (Mamuse et al., 2010); *in situ* analysis of Os, Ir, and Ru in chromite (Locmelis et al., 2011, 2013; Pagé et al., 2012) and trace-element concentrations of Fe-oxides in massive sulphides (Dare et al., 2012) as petrogenetic indicators; high-resolution X-ray computed tomography of the three-dimensional distribution of sulphide minerals in spaces between silicate crystals in natural and synthetic rock samples (Godel, 2013); multiple S and Fe isotopes (Hiebert et al., 2013); Pt-Os geochronology for dating PGE-mineralisation events (Coggon et al., 2012); seismic-reflection imaging of mafic-ultramafic intrusions (Jones et al., 2012); regional-scale geochemical prospectivity analysis (González-Álvarez et al., 2010; Porwal et al., 2010; Lisitsin et al., 2013); craton-margin geodynamic models for the genesis of large magmatic Ni-Cu-PGE deposits and a predictive framework for mineral exploration (Begg et al., 2010). Ames and Farrow (2007) have observed that the early successful geophysical tools for locating Ni-Cu-PGE sulphide deposits in the Sudbury district of Canada, such as magnetic and EM methods, have now been integrated with non-traditional geophysical methods, such as 3-D seismic, audio-magnetotellurics, seismic velocity/cross-hole tomography, and radar-imaging of orebodies. Cross-hole radio imaging (RIM) were instrumental in the discovery of two of the most Cu-Ni-PGE-rich deposits discovered in recent years (e.g., Ni Rim South, Levack Footwall deposits). Although numerous airborne and ground geophysical techniques have been applied in the Sudbury camp, both surficial cultural influences and the increasing depth of new discoveries have rendered modern borehole electromagnetic surveys as most effective in the delineation of highly conductive, pyrrhotite-rich Ni-Cu-PGE orebodies (Ames and Farrow, 2007).

Figure 8.25 summarises the potential relationships between the discovery rates of PGE-Ni-Cu and Ni-Cu-PGE deposits in Australia and Pt, Pd, and Ni metal prices. One of the striking features of the trends shown in this figure is that despite the historically high Pt, Pd, and Ni prices for the two-decade period since 1995, there have been no discoveries of PGE-dominant deposits (i.e., orthomagmatic deposits associated with layered mafic-ultramafic intrusions). The only major discoveries during this period pertain to by-product PGE contributions related to komatiitic associations (several deposits) and mafic intrusions (Nebo-Babel and Nova). Figure 8.25 indicates that a sustained period of relatively high-metal prices has failed to stimulate the discovery of a major PGE resource in Australia.

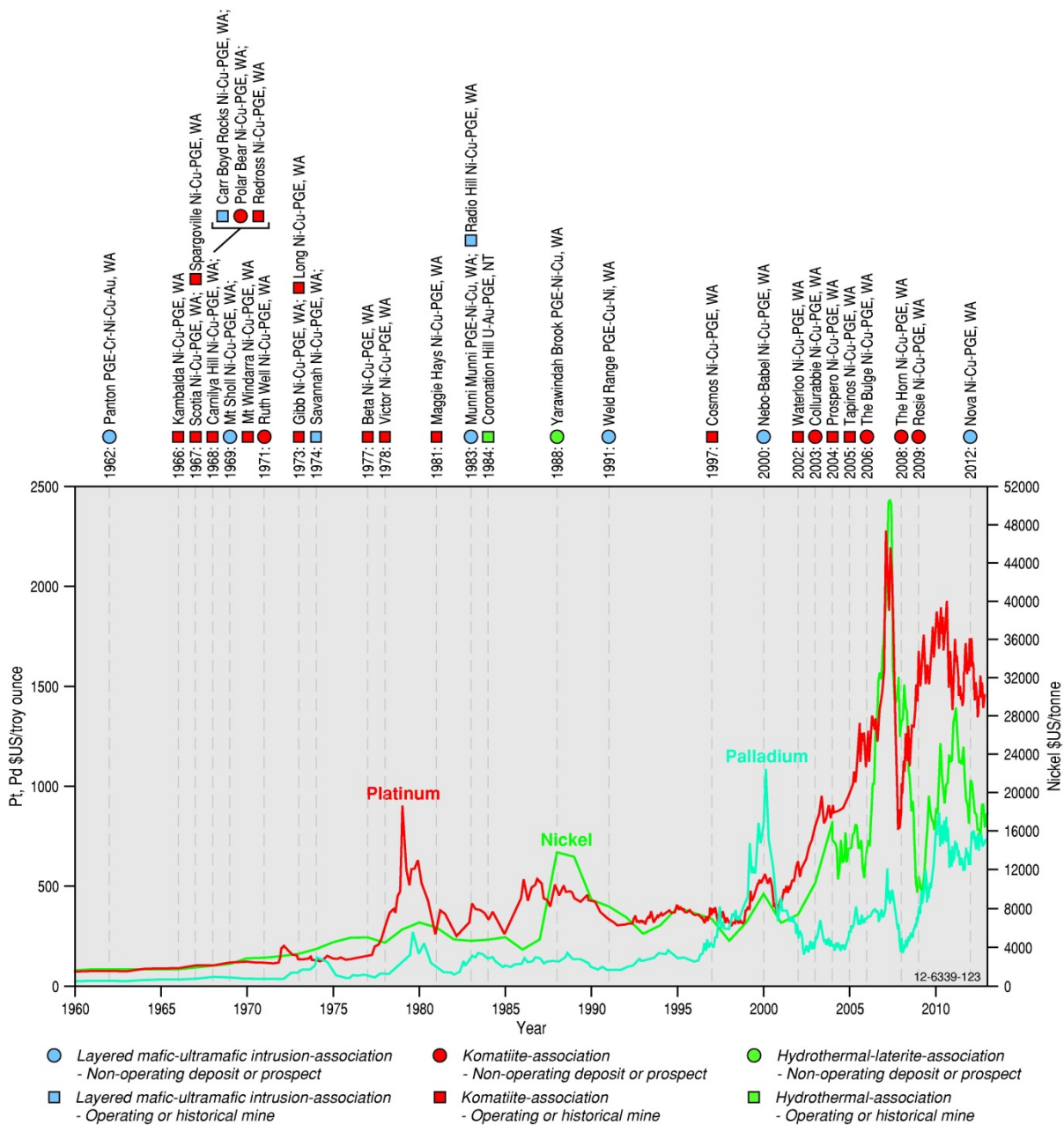


Figure 8.25 Relationships of exploration discoveries in Australia and platinum, palladium, and nickel prices from 1960 to 2013. Discovery data of deposits are from references within Hoatson et al. (2006). Metal price data from Johnson Matthey at <http://www.platinum.matthey.com/prices/price-tables>; BASF (2014); and USGS (2014).

The discovery and assessment of any potential PGE deposit-type, particularly those under cover, requires the integration of different exploration techniques over a protracted period of time. The J-M Reef in the Stillwater Complex, Montana (Czamanske and Zientek, 1985), is a good example where in a well-exposed terrain, a combination of mapping, soil and silt geochemistry, magnetics, IP, low-frequency EM surveys, trenching, and diamond drilling successfully delineated a major PGE resource. The reef was discovered in 1974 by a soil and talus fines geochemical survey that involved analysing 10 900 samples for Pt and Pd (Zientek, 2012). The delineation of the resource over a 1 km-strike-length of the J-M Reef required a grid spacing of less than 15 m from at least 575 drill-holes. Despite the success of these techniques, 20 years of exploration and evaluation were

required to bring the J-M Reef into production. Another example of persistence in exploration is the relatively recent discovery and assessment of the significant Au–PGE-bearing layer—the Platinova Reef in the Skaergaard Intrusion, Greenland (Holwell and Keays, 2014)—an intrusion which has been investigated in great detail by many geoscientists and exploration companies over 60 years. Thus, the early recognition of mineral potential, a thorough understanding of the mineral system(s), a flexible multidisciplinary approach supported by careful observations, exploration persistence, and in some cases, significant capital investment and elements of serendipity will be required for the discovery of a major PGE deposit in Australia.

# References

- ABARE, 2006. Australian Mineral Statistics. Australian Bureau of Agricultural and Resource Economics, June Quarter 2006, Canberra, 339–341.
- Abbott, D.H. and Isley, A.E., 2002. The intensity, occurrence, and duration of superplume events and eras over geological time. *Journal of Geodynamics*, 34, 265–307.
- Agincourt Resources Limited, 2005. Agincourt Resources Limited Annual Report, 84 pp.
- Agiorgitis, G. and Wolf, R., 1978. Aspects of osmium, ruthenium and iridium contents in some Greek chromitites. *Chemical Geology*, 23, 267–272.
- Agnew, P.D., 1987. The petrology and geochemistry of the Tout and Owendale Complexes, Fifield, NSW. BSc Honours thesis, University of New South Wales, Department of Applied Geology.
- Agnew, P.D., Hensen, B.J. and Dunlop, A.C., 1987. The petrology and geochemistry of the Tout and Owendale complexes, Fifield, NSW. In: *Platiniferous Horizons in Layered Intrusions, Abstracts, Symposium on Sydney, 21 October 1987*. University of New South Wales and Geological Society of Australia.
- Ahmad, M. and Munson, T.J. (compilers), 2013. *Geology and mineral resources of the Northern Territory*. Northern Territory Geological Survey, Special Publication 5, ~1086 pp.
- Ahmad, M., Wygralak, A.S, Ferenczi, P.A. and Scrimgeour, I.R., 2009. *Gold deposits of the Northern Territory, second edition*. Northern Territory Geological Survey Report 11, 131 pp.
- Ahmad, S. and Morris, D.F.C., 1978. Geochemistry of some lateritic nickel-ores with particular reference to the distribution of noble metals. *Mineralogical Magazine*, 42, Abstract, 143, Text M4 to M8.
- Ahmat, A.L., 1990. Yilgarn Craton; Windimurra Complex. *Geology and Mineral Resources of Western Australia, Memoir 3*. Geological Survey of Western Australia, 119–124.
- Ahmat, A.L., 1993. Mafic/ultramafic rocks of the Gindalbie Terrane: a review of the Bulong and Carr Boyd Complexes. In: *An International Conference on Crustal Evolution, Metallogeny and Exploration of the Eastern Goldfields. Extended Abstracts*. AGSO Record 1993/54, 23–27.
- Ahmat, A.L. and de Laeter, J.R., 1982. Rb-Sr isotopic evidence for Archaean-Proterozoic crustal evolution of part of the central Yilgarn Block, Western Australia; constraints on the age and source of the anorthositic Windimurra Gabbroid. *Journal of the Geological Society of Australia*, 29, 177–190.
- Ahmat, A.L. and Ruddock, I., 1990. Windimurra and Narndee layered complexes. In: *Geology and Mineral Resources of Western Australia*. Western Australia Geological Survey, Memoir 3, 119–126.
- AIG, 2014—[Web page]. Australian Geoscientist Unemployment Soars, March 13<sup>th</sup> 2014. <http://www.aig.org.au/australian-geoscientist-unemployment-soars/> (last accessed 10 October 2014).
- AIMR, 2013. *Australia's Identified Mineral Resources 2012* (published 2013). Geoscience Australia, Canberra, 162 pp. [http://www.ga.gov.au/metadata-gateway/metadata/record/gcat\\_75326](http://www.ga.gov.au/metadata-gateway/metadata/record/gcat_75326) (last accessed 10 October 2014).
- Aitchison J.C. and Ireland T.R., 1995. Age profile of ophiolitic rocks across the late Palaeozoic New England Orogen, New South Wales: implications for tectonic models. *Australian Journal of Earth Sciences*, 42, 11–23.
- Alapieti, T.T. and Lahtinen, J.L., 2002. Platinum-group element mineralization in layered intrusions of northern Finland and the Kola Peninsula, Russia. In: Cabri, L.J. (editor), *The Geology, Geochemistry, Mineralogy and Mineral Beneficiation of Platinum-Group Elements*. Canadian Institute of Mining, Metallurgy and Petroleum, Special Volume 54, 507–546.

- Amelin, Y., Li, C. and Naldrett, A.J., 1999. Geochronology of the Voisey's Bay intrusion, Labrador, Canada by precise U-Pb dating of coexisting baddeleyite, zircon, and apatite. *Lithos*, 47, 33–51.
- Amelin, Y.V., Li, C., Valeyev, O. and Naldrett, A.J., 2000. Nd-Pb-Sr isotope systematics of crustal assimilation in the Voisey's Bay and Mushuau intrusions, Labrador, Canada. *Economic Geology*, 95, 815–830.
- Ames, D.E. and Farrow, C.E.G., 2007. Metallogeny of the Sudbury mining camp, Ontario. In: Goodfellow, W.D. (editor), *Mineral Deposits of Canada: A Synthesis of Major Deposit-Types, District Metallogeny, the Evolution of Geological Provinces, and Exploration Methods*. Geological Association of Canada, Mineral Deposits Division, Special Publication No. 5, 329–350.
- Andersen, J.C.O., Power, M.R. and Momme, P., 2002. Platinum-group elements in the Palaeogene North Atlantic igneous province. Special Volume, Canadian Institute of Mining and Metallurgy, 54, 637–667.
- Andersen, P., Bottrill, R.S. and Davidson, P., 2002. Famous mineral localities: The Lord Brassey mine, Tasmania. *Mineralogical Record*, 33, 321–332.
- Andrews, E.C., 1922. The geology of the Broken Hill district. Memoir, Geological Survey of New South Wales, *Geology*, 8, 432 pp.
- Anhaeusser, C.R. and Maske, S. (editors), 1986. *Mineral Deposits of Southern Africa, Volumes I, II*. Geological Society of South Africa, 2376 pp.
- Apex Minerals NL, 2002. Apex Minerals NL Prospectus 2002. Australian Securities Exchange, 100 pp.
- Apex Minerals NL, 2003. Apex Minerals NL Annual Report 2003. Australian Securities Exchange.
- Arai, S., 1997. Origin of podiform chromitites. *Journal of Asian Earth Sciences*, 15, 303–310.
- Arndt, N.T., 2005. The conduits of magmatic ore deposits. In: Mungall, J.E. (editor), *Exploration for Platinum-Group Element Deposits*. Mineralogical Association of Canada Short Course 35, Oulu, Finland, 181–201.
- Arndt, N.T., 2011. Insights into the geologic setting and origin of Ni-Cu-PGE sulfide deposits of the Norilsk-Talnakh region, Siberia. *Reviews in Economic Geology* 17, 199–215.
- Arndt, N.T. and Jenner, G.A., 1986. Crustally contaminated komatiites and basalts from Kambalda, Western Australia. *Chemical Geology*, 56, 229–255.
- Arndt, N.T. and Nisbet, E.G., 1982. What is a komatiite? In: Arndt, N.T. and Nisbet, E.G. (editors), *Komatiites*. George Allen and Unwin, London, 19–28.
- Arndt, N.T., Naldrett, A.J., and Pyke, D.R., 1977. Komatiitic and iron-rich tholeiitic lavas of Munro Township, northeast Ontario. *Journal of Petrology*, 18, 319–369.
- Arndt, N.T., Nelson, D.R., Compston, W., Trendall, A.F. and Thorne, A.M., 1991. The age of the Fortescue Group, Hamersley Basin, Western Australia, from ion microprobe zircon U-Pb results. *Australian Journal of Earth Sciences*, 38, 261–281.
- Arndt, N.T., Bruzak, G. and Reischmann, T., 2001. The oldest continental and oceanic plateaus; geochemistry of basalts and komatiites of the Pilbara Craton, Australia. *Special Paper Geological Society of America* 352, 359–387.
- Arndt, N.T., Czamanske, G.K., Walker, R.J., Chauvel, C. and Fedorenko, V.A., 2003. Geochemistry and origin of the intrusive hosts of the Noril'sk-Talnakh Cu-Ni-PGE sulfide deposits. *Economic Geology*, 98, 495–515.
- Arndt, N.T., Leshner, C.M. and Czamanske, G.K., 2005. Mantle-derived magmas and magmatic Ni-Cu-(PGE) deposits. In: Hedenquist, J.W., Thompson, J.F.H., Goldfarb, R.J. and Richards, J.P. (editors), *Economic Geology One Hundredth Anniversary Volume 1905–2005*. Society of Economic Geologists, Littleton, Colorado, 5–24.
- Arrowhead, 2012. Arrowhead Business and Investment Decisions Due Diligence and Valuation Report, 24 April 2012, 33 pp.
- Augé, T., 1986. Platinum-group-mineral inclusions in chromitites from the Oman ophiolite. *Bulletin Minéralogy*, 109, 301–304.

- Augé, T. and Legendre, O., 1994. Platinum-group element oxides from the Pirogues ophiolitic mineralization, New Caledonia: origin and significance. *Economic Geology*, 89, 1454–1468.
- Augé, T., Cocherie, A., Genna, A., Armstrong, R., Guerrot, C., Mukherjee, M.M. and Patra, R.N., 1993. Age of the Baula PGE mineralisation (Orissa, India) and its implications concerning the Singbhum Archaean nucleus. *Precambrian Research*, 121, 85–101.
- AusQuest Limited, 2003. AusQuest Prospectus 2003, 63 pp.
- AusQuest Limited, 2004. Quarterly Report for period ended 30 June 2004. AusQuest Limited, 6 pp.
- AusQuest Limited, 2006. AusQuest Limited announcement to the Australian Securities Exchange, 17 October 2006, 2 pp.
- Ayer, J.A., Amelin, Y., Corfu, F., Kamo, S., Ketchum, J., Kwok, K. and Trowell, N., 2002. Evolution of the southern Abitibi greenstone belt based on U-Pb geochronology: autochthonous volcanic construction followed by plutonism, regional deformation and sedimentation. *Precambrian Research*, 115, 63–95.
- Ayres, D.E. and Eadington, P.J., 1975. Uranium mineralization in the South Alligator River Valley. *Mineralium Deposita*, 10, 27–41.
- Bachmann, H.G., Graham, J.M., Meares, R.M.D. and Collin, A.R., 1987. Exploration techniques for platinum group metals in Papua New Guinea. In: *Proceedings Pacific Rim Congress 87*. Australasian Institute of Mining and Metallurgy, Melbourne, 21–24.
- Bacon, C.A., 1992. Notes on the history of mining and exploration at Adamsfield. *Mineral Resources Tasmania Report 1992/20*, 33 pp.
- Bacon, C.A. and Lynch, J., 1993. Partial inventory of sites in rainforest used for mining or exploration purposes. *Mineral Resources Tasmania Report 1993/31*, 32 pp.
- Bai, W., Robinson, P.T., Fang, Q., Yang, J., Yan, B., Zhang, Z., Hu, X., Zhou, M. and Malpas, J., 2000. The PGE and base-metal alloys in the podiform chromitites of the Luobusa ophiolite, Southern Tibet. *Canadian Mineralogist*, 38, 585–598.
- Baker, P.M. and Waugh, R.S., 2005. The role of surface geochemistry in the discovery of Babel and Nebo magmatic nickel-copper-PGE deposits. *Geochemistry: Exploration, Environment, Analysis*, 5, 195–200.
- Balch, S.J., 2005. The geophysical signatures of platinum-group element deposits. In: Mungall, J.E. (editor), *Exploration for Platinum-Group Element Deposits*. Mineralogical Association of Canada Short Course 35, Oulu, Finland, 275–285.
- Ball, L.C., 1905. Gold, platinum, tinstone, and monazite in the beach sands on the south coast of Queensland. *Queensland Government Mining Journal*, 6, 62–67.
- Ballhaus, C. and Glikson, A.Y., 1995. The petrology of layered mafic-ultramafic intrusions of the Giles Complex, western Musgrave Block, Western Australia. *AGSO Journal*, 16, 69–89.
- Ballhaus, C.G. and Stumpfl, E.F., 1986. Sulfide and platinum mineralization in the Merensky Reef: evidence from hydrous silicates and fluid inclusions. *Contributions to Mineralogy and Petrology*, 94, 193–204.
- Ballhaus, C.G., Cornelius, M. and Stumpfl, E.F., 1988. The upper critical zone of the Bushveld Complex and the origin of Merensky-type ores; a discussion. *Economic Geology*, 83, 1082–1085.
- Ballhaus, C., Ryan, C.G., Mernagh, T.P. and Green, D.H., 1994. The partitioning of Fe, Ni, Cu, Pt, and Au between sulfide, metal, and fluid phases: a pilot study. *Geochimica et Cosmochimica Acta*, 58, 811–826.
- Banas, M., Jarosz, J. and Salamon, W., 1978. Thucholite from Permian copper-bearing rocks in Poland. *Mineralogia Polonica*, 9, 3–22.
- Barley, M.E., Pickard, A.L. and Sylvester, P.J., 1997. Emplacement of a large igneous province as a possible cause of a banded iron formation 2.45 billion years ago. *Nature*, 385, 55–58.
- Barnes, G.B., 1995. Silver mineralisation at Elizabeth Hill, Munni Munni Complex, Western Australia. In: Ho, S.E. and Amann, W.J. (editors), *Recent Developments in Base Metal Geology and Exploration*. Australian Institute of Geoscientists, Bulletin 16, 89–94.

- Barnes, R., Jaireth, S., Mieziitis, Y. and Suppel, D., 1999. Regional mineral potential assessments for land use planning; GIS-based examples from eastern Australia. Publication Series, Australasian Institute of Mining and Metallurgy 4–99, 601–605.
- Barnes, S.J., 2004a. How nickel took off. *Earthmatters*. CSIRO Exploration, Mining Quarterly Magazine, 4, 16–19.
- Barnes, S.J., 2004b. Introduction to nickel sulfide orebodies and komatiites of the Black Swan area, Yilgarn Craton, Western Australia. *Mineralium Deposita*, 39, 679–683.
- Barnes, S.J. (editor) 2006. *Nickel Deposits of the Yilgarn Craton: Geology, Geochemistry, and Geophysics Applied to Exploration*. Economic Geology Special Publication Number 13, 210 pp.
- Barnes, S.J., 2007. Cotectic precipitation of olivine and sulfide liquid from komatiite magma, and the origin of komatiite-hosted disseminated nickel sulfide mineralization at Mt Keith and Yakabindie, Western Australia. *Economic Geology*, 102, 299–304.
- Barnes, S.J. and Fiorentini, M.L., 2008. Iridium, ruthenium and rhodium in komatiites: Evidence for iridium alloy saturation. *Chemical Geology*, 257, 44–58.
- Barnes, S.J. and Fiorentini, M.L., 2012. Komatiite magmas and sulfide nickel deposits: a comparison of variably endowed Archean terranes. *Economic Geology*, 107, 755–780.
- Barnes, S.J. and Hoatson, D.M., 1994. The Munni Munni Complex, Western Australia: stratigraphy, structure and petrogenesis. *Journal of Petrology*, 35, 715–751.
- Barnes, S.J. and Jones, S., 2013. Deformed chromitite layers in the Coobina Intrusion, Pilbara Craton, Western Australia. *Economic Geology*, 108, 337–354.
- Barnes, S.J. and Liu, W., 2012. Pt and Pd mobility in hydrothermal fluids: Evidence from komatiites and from thermodynamic modelling. *Ore Geology Reviews*, 44, 49–58.
- Barnes, S.J. and Zhong-Li, T., 1999. Chrome spinels from the Jinchuan Ni-Cu sulfide deposit, Gansu province, People's Republic of China. *Economic Geology*, 94, 343–356.
- Barnes, S.J., Gole, M.J. and Hill, R.E.T., 1988a. The Agnew nickel deposit, Western Australia: Part I. Structure and stratigraphy. *Economic Geology*, 83, 524–536.
- Barnes, S.J., Gole, M.J. and Hill, R.E.T., 1988b. The Agnew nickel deposit, Western Australia: Part II. Sulfide geochemistry, with emphasis on the platinum-group elements. *Economic Geology*, 83, 537–550.
- Barnes, S.J., McIntyre, J.R., Nisbet, B.W. and Williams, C.R., 1990. Platinum group element mineralisation in the Munni Munni Complex, Western Australia. *Mineralogy and Petrology*, 42, 141–164.
- Barnes, S.J., Hill, R.E.T., Hoatson, D.M., Perring, R.J., Witt, W.K., Mathison, C.I. and Bunting, J.A., 1991a. Chapter 1: Layered mafic-ultramafic complexes of Western Australia: Introduction. In: Barnes, S.J. and Hill, R.E.T. (editors), *Mafic-Ultramafic Complexes of Western Australia*, Excursion Guidebook No. 3. Sixth International Platinum Symposium, July 1991, Perth, Western Australia. IAGOD and the Geological Society of Australia, 1–13 pp.
- Barnes, S.J., Hoatson, D.M. and McIntyre, J.R., 1991b. Chapter 6: The Munni Munni Complex. In: Barnes, S.J. and Hill, R.E.T. (editors), *Mafic-Ultramafic Complexes of Western Australia*, Excursion Guidebook No. 3. Sixth International Platinum Symposium, July 1991, Perth, Western Australia. IAGOD and the Geological Society of Australia, 77–96.
- Barnes, S.J., Keays, R.R. and Hoatson, D.M., 1992. Distribution of sulphides and PGE within the porphyritic websterite zone of the Munni Munni Complex, Western Australia. *Australian Journal of Earth Sciences*, 39, 289–302.
- Barnes, S.J., Leshner, C.M. and Keays, R.R., 1995. Geochemistry of mineralised and barren komatiites from the Perseverance nickel deposit, Western Australia. *Lithos*, 34, 209–234.
- Barnes, S.J., Hill, R.E.T., Perring, C.S. and Dowling, S.E., 1999. Komatiite flow fields and associated Ni-sulphide mineralisation with examples from the Yilgarn Block, Western Australia. In: Keays, R.R., Leshner, C.M. and Lightfoot, P.C. (editors), *Dynamic Processes in Magmatic Ore Deposits and their Applications in Mineral Exploration*. Geological Association of Canada Short Course 13, 159–194.

- Barnes, S.J., Hill, R.E.T., Perring, C.S. and Dowling, S.E., 2004a. Lithogeochemical exploration for komatiite-associated Ni-sulfide deposits: strategies and limitations. *Mineralogy and Petrology*, 82, 259–293.
- Barnes, S.J., Smith, T., Anderson, J. and Kavanagh, M., 2004b. PGE mineralisation related to cyclic layering in the Mordor Complex, Northern Territory: an unusual association of PGE-enriched magmatic sulfides with cumulates from an ultrapotassic hydrous magma. 17th Australian Geological Convention. *Dynamic Earth: Past, present and future*, 8-13 February 2004, Hobart, Tasmania. Abstracts 73, 51.
- Barnes, S.J., Anderson, J.A.C., Smith, T.R. and Bagas, L., 2008. The Mordor alkaline igneous complex, Central Australia: PGE-enriched disseminated sulfide layers in cumulates from a lamprophyric magma. *Mineralium Deposita*, 43, 641–662.
- Barnes, S.J., Godel, B.M., Locmelis, M., Fiorentini, M.L. and Ryan, C.G., 2011a. Extremely Ni-rich Fe-Ni sulfide assemblages in komatiitic dunite at Betheno, Western Australia: results from synchrotron X-ray fluorescence mapping. *Australian Journal of Earth Sciences*, 58, 691–709.
- Barnes, S.J., Fiorentini, L.F., Duuring P., Grguric, B.A. and Perring, C.S., 2011b. The Perseverance and Mount Keith deposits of the Agnew-Wiluna Belt, Yilgarn Craton, Western Australia. In: Li, C, and Ripley, E. (editors), *Magmatic Ni-Cu and PGE Deposits: Geology, Geochemistry, and Genesis*. *Reviews Economic Geology*, 17, 51–88.
- Barnes, S.J., Fiorentini, M.L. and Fardon, M.C., 2012. Platinum group element and nickel sulfide ore tenors of the Mount Keith nickel deposit, Yilgarn Craton, Australia. *Mineralium Deposita*, 47, 129–150.
- Barnes, S.J., Heggie, G.J. and Fiorentini, M.L., 2013. Spatial variation in platinum group element concentrations in ore-bearing komatiite at the Long-Victor Deposit, Kambalda Dome, Western Australia: Enlarging the footprint of nickel sulfide orebodies. *Economic Geology*, 108, 913–933.
- Barnes, S.J., Fisher, L.A., Anand, R. and Uemoto, T., 2014. Mapping bedrock lithologies through in situ regolith using retained element ratios: a case study from the Agnew-Lawlers area, Western Australia. *Australian Journal of Earth Sciences*, 61, 269–285.
- Barnes, S-J. and Gomwe, T.S., 2011. The Pd deposits of the Lac des Iles Complex, northwestern Ontario. *Reviews in Economic Geology* 17, 351–370.
- Barnes, S-J. and Lightfoot, P.C., 2005. Formation of magmatic nickel sulfide deposits and processes affecting their copper and platinum group element contents. In: Hedenquist, J.W., Thompson, J.F.H., Goldfarb, R.J. and Richards, J.P. (editors), *Economic Geology One Hundredth Anniversary Volume 1905–2005*. Society of Economic Geologists, Littleton, Colorado, 179–214.
- Barnes, S-J. and Maier, W.D., 1999. The fractionation of Ni, Cu and the noble metals in silicate and sulphide liquids. In: Keays, R.R. (editor), *Dynamic Processes in Magmatic Ore Deposits and their Applications in Mineral Exploration*. Geological Association of Canada Short Course Notes, 13, 69–106.
- Barnes, S-J. and Maier, W.D., 2002. Platinum-group element distributions in the Rustenburg layered suite of the Bushveld Complex, South Africa. *Special Volume - Canadian Institute of Mining and Metallurgy (1982)* 54, 431–458.
- Barnes, S-J., Naldrett, A.J. and Gorton, M.P., 1985. The origin of the fractionation of platinum group elements in terrestrial magmas. *Chemical Geology*, 53, 303–323.
- Barnes, S-J., Boyd, R., Korneliussen, A., Nilsson, L.P., Often, M., Pedersen, R.B. and Robins, B., 1987. The use of mantle normalization and metal ratios in discriminating between the effects of partial melting, crystal fractionation and sulphide segregation on platinum-group elements, gold, nickel and copper; examples from Norway. In: Prichard, H.M., Potts, P.J., Bowles, J.F.W. and Cribb, S.J. (editors), *Geo-Platinum 87*. Elsevier Scientific Publishing, Essex, United Kingdom, 113–144.
- Barnes, S-J., Couture, J-F., Sawyer, E.W. and Bouchaib, C., 1993. Nickel-copper occurrences in the Belleterre-Angliers Belt of the Pontiac Subprovince and the use of Cu-Pd Ratios in interpreting platinum-group element distributions. *Economic Geology*, 88, 1402–1418.

- Barnicoat, A.C., 2006. Science, the 5 questions and exploration. Barnicoat, A.C. and Korsch, R.J. (editors), Predictive Mineral Discovery Cooperative Research Centre, Extended Abstracts from the April 2006 Conference, 2006. *Geoscience Australia Record* 2006/07, 5–8.
- Barrett, F.M., Binns, R.A., Groves, D.I., Marston, R.J. and McQueen, K.G., 1977. Structural history and metamorphic modification of Archean volcanic-type nickel deposits, Yilgarn Block, Western Australia. *Economic Geology*, 77, 1195–1223.
- Barrie, C.T., 1995. Magmatic platinum group elements. In: Eckstrand, O.R., Sinclair, W.D. and Thorpe, R.I. (editors), *Geology of Canadian Mineral Deposit Types. The Geology of North America Series*, Geological Society of America, volume P-1. Geological Survey of Canada, *Geology of Canada* 8, 605–614.
- Barrie, C.T. and Naldrett, A.J., 1989. Geology and tectonic setting of the Montcalm Gabbroic Complex and Ni-Cu deposit, Western Abitibi Subprovince, Ontario, Canada. In: Prendergast, M.D. and Jones, M.J. (editors), *Magmatic Sulphides—The Zimbabwe Volume*. The Institution of Mining and Metallurgy, London, 151–163.
- Barrie, J., 1965. Platinum group metals. In: McLeod, I.R. (editor), *Australian Mineral Industry: The Mineral Deposits*. Bureau of Mineral Resources, Australia, *Bulletin* 72, 487–494.
- Barron, L.M., Suppel, D.W., Johan, Z. and Ohnenstetter, M., 1987. The petrology and geochemistry of a platinum prospect in the Owendale intrusive complex. In: *Abstracts: Platiniferous Horizons in Layered Intrusions*, Abstracts, Symposium, Sydney, 21 October 1987. University of New South Wales and Geological Society of Australia.
- Barron, L.M., Ohnenstetter, M., Barron, B.J., Suppel, D.W., Johan, Z. and Falloon, T., 2004. Geology of the Fifield Alaskan-type complexes, New South Wales, Australia. *New South Wales Geological Survey Report* GS2004/323, 36 pp.
- BASF, 2014—[Web page]. Metal price history charts. <http://apps.catalysts.basf.com/apps/EIBPrices/mp/YearlyCharts.aspx> (last accessed 10 October 2014).
- Baxter, J.L., 1978. Molybdenum, tungsten, vanadium and chromium in Western Australia. *Western Australia Geological Survey, Mineral Resources Bulletin* 11, 140 pp.
- Beaufort, D., Patrier, P., Laverret, E., Bruneton, P. and Mondy, J., 2005. Clay alteration associated with Proterozoic unconformity-type uranium deposits in the East Alligator Rivers Uranium Field, Northern Territory, Australia. *Economic Geology*, 100, 515–536.
- Begg, G.C., Hronsky, J.A.M., Arndt, N.T., Griffin, W.L., O'Reilly, S.Y. and Hayward, N., 2010. Lithospheric, cratonic, and geodynamic setting of Ni-Cu-PGE sulfide deposits. *Economic Geology*, 105, 1057–1070.
- Bekker, A., Barley, M.E., Fiorentini, M., Rouxel, O.J., Rumble, D. and Beresford, S.W., 2009. Atmospheric sulfur in Archaean komatiite-hosted nickel deposits. *Science*, 326, 1086–1089.
- Bennett, V.C., 2003. Compositional Evolution of the Mantle. In: Holland, H.D. and Turekian, K.K. (editors), *Treatise on Geochemistry*. Pergamon, Oxford, 493–519.
- Beresford, S.W. and Stone, W.E., 2004. Komatiite-hosted Ni-Cu-PGE deposits of the Kambalda nickel camp—an overview. In: Neumayr, P., Harris, M. and Beresford, S.W. (compilers), *Gold and Nickel Deposits in the Archaean Norseman-Wiluna Greenstone Belt, Yilgarn Craton, Western Australia. A Field Guide: Predictive Mineral Discovery under Cover, Western Australia*. Geological Survey of Western Australia, *Record* 2004/16, 5–8.
- Beresford, S.W., Cas, R., Lahaye, Y. and Jane, M., 2002. Facies architecture of an Archean komatiite-hosted Ni-sulphide ore deposit, Victor, Kambalda, Western Australia: Implications for komatiite lava emplacement. *Journal of Volcanology and Geochemical Research*, 118, 57–75.
- Beresford, S.W., Stone, W.E., Cas, R., Lahaye, Y. and Jane, M., 2005. Volcanology controls on the localization of the komatiite-hosted Ni-Cu-(PGE) Coronet deposit, Kambalda, Western Australia. *Economic Geology*, 100, 1457–1467.
- Berry, R.F. and Crawford, A.J., 1988. The tectonic significance of Cambrian allochthonous mafic-ultramafic complexes in Tasmania. *Australian Journal of Earth Sciences*, 35, 523–533.

- Bertuch, D.I., 2004. The komatiitic basalt-hosted Ni–Cu–(PGE) occurrences of the Collurabbie ultramafics, Gerry Well Greenstone Belt, Western Australia. Honours thesis, Monash University, Victoria, Australia.
- Betts, P.G. and Giles, D., 2006. The 1800–1100 Ma tectonic evolution of Australia. *Precambrian Research*, 144, 92–125.
- Bezmen, N.I., Asif, M., Brugmann, G.E., Romanenko, I.M. and Naldrett, A.J., 1994. Distribution of Pd, Rh, Ru, Ir, Os, and Au between sulfide and silicate metals. *Geochimica et Cosmochimica Acta*, 58, 1251–1260.
- Binns, R.A., McAndrew, J. and Sun, S.S., 1980. Origin of uranium mineralization at Jabiluka. In: Ferguson, J. and Goleby, A.B. (editors), *Uranium in the Pine Creek Geosyncline*. International Atomic Energy Agency, Vienna, 543–562.
- Bird, D.K., Brooks, C.K., Gannicott, R.A. and Turner, P.A., 1991. A gold-bearing horizon in the Skaergaard intrusion, East Greenland. *Economic Geology*, 86, 1083–1092.
- Black, L.P. and Gulson, B.L., 1978. The age of the Mud Tank Carbonatite, Strangways Range, Northern Territory. *BMR Journal of Australian Geology and Geophysics*, 3, 227–232.
- Blackburn, C.E., Johns, G.W., Ayer, J. and Davis, D.W., 1992. Wabigoon subprovince. *Ontario Geological Survey Special Volume 4, Part 2*, 303–381.
- Blake, T.S., Buick, R., Brown, S.J.A. and Barley, M.E., 2004. Geochronology of a late Archaean flood basalt province in the Pilbara Craton, Australia; constraints on basin evolution, volcanic and sedimentary accumulation, and continental drift rates. *Precambrian Research*, 133, 143–173.
- Bleeker, W. and Macek, J., 1996. Evolution of the Thompson Nickel Belt, Manitoba. Setting of the Ni–Cu Deposits in the Western Part of the Circular Superior Boundary Zone—Filed Trip Guidebook A1, Geological Association of Canada/Mineralogical Association of Canada Annual Meeting, Winnipeg, Manitoba, May 27–19, 1996, 44 pp.
- Blevin, P.L., 2002. The petrographic and compositional character of variably K-enriched magmatic suites associated with Ordovician porphyry Cu–Au mineralization in the Lachlan Fold Belt, Australia. *Mineralium Deposita*, 37, 87–99.
- Blewett, R.S. (editor), 2012. *Shaping a Nation: A geology of Australia*. Geoscience Australia and ANU E Press, Canberra, 571 pp.
- Bloom, M.S., Gilbert, D.J., Gammons C.H. and Wilde, A.R., 1992. Reaction path models for hydrothermal Au–PGE mineralization at Coronation Hill and similar deposits of the South Alligator mineral field, Australia. In: Kharaka, Y.K. and Maest, A.S. (editors), *Water-rock Interaction*. Rotterdam, Balkema, 2, 1569–1573.
- Bottrill, R.S., 1989. Appendix A—Economic Geology, in Huntley, Geological Survey Explanatory Report by Brown et al., Geological Atlas 1:50 000 Series Sheet 73 (8112N). Tasmania Department of Mines, 100–106.
- Bottrill, R.S., 2014. Mineral deposits associated with the mafic-ultramafic complexes. In: Corbett, K.D., Quilty, P.G. and Calver, C.R. (editors), Section 4.4.7. *Geological Evolution of Tasmania*. Geological Society of Australia Special Publication 24, Geological Society of Australia (Tasmania Division), 141–145.
- Bottrill, R.S., Taheri, J. and Calver, C.R., 1999. The nature and origin of gold mineralisation at the Forster Prospect, Glovers Bluff/Weld River area. *Record Tasmanian Geological Survey 1999/06*, 87 pp.
- Boudreau, A.E., 1995. Some geochemical considerations for platinum-group-element exploration in layered intrusions. *Exploration Mining Geology*, 4, 215–225.
- Boudreau, A.E. and Hoatson, D.M., 2004. Halogen variations in the Paleoproterozoic layered mafic-ultramafic intrusions of East Kimberley, Western Australia: Implications for platinum-group element mineralization. *Economic Geology*, 99, 1015–1026.
- Boudreau, A.E. and McCallum, I.S., 1985. Features of the Picket Pin Pt–Pd deposit. In: Czamanske, G.K. and Zientek, M.L. (editors), *The Stillwater Complex, Montana: Geology and Guide*. Montana Bureau of Mines and Geology, Special Publication 92, IGCP Project 161, 346–357.

- Boudreau, A.E. and McCallum, I.S., 1986. Investigations of the Stillwater Complex: III. The Picket Pin Pt/Pd Deposit. *Economic Geology*, 81, 1953–1975.
- Boudreau, A.E. and McCallum, I.S., 1992. Infiltration metasomatism in layered intrusions - an example from the Stillwater Complex, Montana. *Journal of Volcanology and Geothermal Research*, 52, 171–183.
- Boudreau, A.E., Mathez, E.A. and McCallum, I.S., 1986. Halogen geochemistry of the Stillwater and Bushveld Complexes: Evidence for transport of the platinum-group elements by Cl-rich fluids. *Journal of Petrology*, 27, 967–986.
- Boudreau, A.E., Love, C. and Hoatson, D.M., 1993. Variation in the composition of apatite in the Munni Munni Complex and associated intrusions of the West Pilbara Block, Western Australia. *Geochimica et Cosmochimica Acta* 57, 4467–4477.
- Bourne, B.T., 1996. Geophysics of the Honeymoon Well nickel deposits, Western Australia. Nickel '96. Australasian Institute of Mining and Metallurgy, Publication Series, 6, 159–166.
- Bowles, J.F.W., 1985. A consideration of the development of platinum-group minerals in laterite. In: Fourth International Platinum Symposium, Program and Abstracts. Mineralogical Association of Canada and Society of Economic Geologists, IGCP Project 161, University of Toronto, 1985, 296.
- Bowles, J.F.W., 1986. The development of platinum-group minerals in laterites. *Economic Geology*, 81, 1278–1285.
- Bowles, J.F.W., 1989. Mineralogical study of platinum-rich nuggets from the Fifield area: Initial examination October–December, 1989. Mineral Sciences Limited.
- Bowles, J.F.W., Gize, A.P., Vaughan, D.J. and Norris, S.J., 1993. Organic controls on supergene weathering of platinum-group element (PGE) deposits and the development of platinum-group minerals in placers. *Institution of Mining and Metallurgy, Transactions, Section B: Applied Earth Science*, 102, 192–193.
- Bowles, J.F.W., Gize, A.P. and Cowden, A., 1994. The mobility of the platinum-group elements in the soils of the Freetown Peninsula, Sierra Leone. *Canadian Mineralogist*, 32, 957–967.
- Bowman, H.N., Richardson, S.J. and Dolanski, J., 1982. Narromine 1:250 000 Metallogenic Map SI 55–3, Mine Data Sheets and Metallogenic Study. New South Wales Geological Survey, 337 pp.
- Bradbrook, C., 2006. Advancing the New Afton copper-gold project – world class grades next to the Trans-Canada Highway: Roundup, Association for Mineral Exploration BC, 2006, Abstract Volume, 38–39.
- Brand, N.W., 1999. Element ratios in nickel sulfide exploration: vectoring towards ore environments. *Journal of Geochemical Exploration*, 67, 145–165.
- Brand, N.W., Butt, C.R.M. and Elias, M., 1998. Nickel laterites: classification and features. *AGSO Journal of Australian Geology and Geophysics*, 17, 81–88.
- Brauns, C.M., Hergt, J.M., Woodhead, J.D. and Maas, R., 2000. Os isotopes and the origin of the Tasmanian dolerites. *Journal of Petrology*, 41, 905–918.
- Breakaway Resources Limited, 2008a. Breakaway Resources Limited announcement to the Australian Securities Exchange, 29 January 2008, 3 pp.
- Breakaway Resources Limited, 2008b. Breakaway Resources Limited announcement to the Australian Securities Exchange, 5 February 2008, 3 pp (unpublished).
- BREE, 2013—[Web page]. Annual resource statistics, 2013. [http://www.bree.gov.au/sites/default/files/files//publications/res/annual\\_res\\_2013.pdf](http://www.bree.gov.au/sites/default/files/files//publications/res/annual_res_2013.pdf) (last accessed 10 October 2014).
- Brenan, J.M., 2008. The platinum-group elements: "admirably adapted" for science and industry. *Elements*, 4, 227–232.
- Brenker, F.E., Meibom, A. and Frei, R., 2003. On the formation of peridotite-derived Os-rich PGE alloys. *American Mineralogist*, 88, 1731–1740.
- Brill, B.A. and Keays, R.R., 1989a. Fifield Project Report: January–March, 1989. University of Melbourne, Department of Geology, Research Report.

- Brill, B.A. and Keays, R.R., 1989b. Fifield Project Report: May-August, 1989. University of Melbourne, Department of Geology, Research Report.
- Brill, B.A. and Keays, R.R., 1990. Fifield Project Report: May 1990. University of Melbourne, Department of Geology, Research Report.
- Brookins, D.G., 1988. Eh-pH diagrams for geochemistry. Springer-Verlag, Berlin, Federal Republic of Germany.
- Brown, C., 1919. A review of the osmiridium mining industry of Tasmania. John Vail, Government Printer, Tasmania, 24 pp.
- Brown, A.V., 1986. Geology of the Dundas–Mount Lindsay–Mount Youngbuck Region. Geological Survey of Tasmania Bulletin 62, 221 pp.
- Brown, A.V., 1992. Platinum group elements and their host rocks in Tasmania: A summary review. Tasmanian Geological Survey Bulletin 70, 48–55.
- Brown, A.V., 1998. Platinum group elements and their host rocks in Tasmania: A summary review. Tasmanian Geological Survey Record 1998/04, 7 pp.
- Brown, A.V. and Jenner, G.A., 1989. Geological setting, petrology and chemistry of Cambrian boninite and low-Ti tholeiite lavas in western Tasmania. In: Crawford, A.J. (editor), Boninites. Unwin Hyman, London, United Kingdom, 232–263.
- Brown, A.V., Rubenach, M.J. and Varne, R., 1979. Geological environment, petrology and tectonic significance of the Tasmanian Cambrian ophiolitic and ultramafic complexes. In: Panayiotou, A. (editor), Ophiolites. Proceedings, International Ophiolite Symposium, Cyprus, 1979. Geological Survey Department, Ministry of Agriculture and Natural Resources, Republic of Cyprus, 649–659.
- Brown, A.V., Page, N.J. and Love, A.H., 1988. Geology and platinum-group-element geochemistry of the Serpentine Hill Complex, Dundas Trough, western Tasmania. Canadian Mineralogist, 26, 161–175.
- Brown, M.A.N., Jolly, R.J.H., Stone, W. and Coward, M.P., 1999. Nickel ore troughs in Archaean volcanic rocks, Kambalda, Western Australia: Indications of early extension. Geological Society Special Publication 155, 197–221.
- Brugmann, G.E., Arndt, N.T., Hofmann, A.W. and Tobschall, H.J., 1987. Noble metal abundances in komatiite suites from Alexo, Ontario, and Gorgona Island, Colombia. Geochimica et Cosmochimica Acta, 51, 2159–2169.
- Bryan, S.E. and Ernst, R.E., 2008. Revised definition of Large Igneous Provinces (LIPs). Earth-Science Reviews, 86, 175–202.
- Buchanan, D.L. and Nolan, J., 1979. Solubility of sulfur and sulfide immiscibility in synthetic tholeiitic melts and their relevance to Bushveld-complex rocks. Canadian Mineralogist, 17, 483–494.
- Bunting, J. and MacDonald, F., 2004. The Yarrabubba Structure, Western Australia—Clues to identifying impact events in deeply eroded ancient cratons, 17th Australian Geological Convention. Dynamic Earth: Past, present and future, 8-13 February 2004, Hobart, Tasmania. Abstracts 73, 227.
- Butler, J., 2012. Precious Metal Handbook. Johnson Matthey Public Limited Company, London, Platinum Metals Review, 56, 267–270.
- Butt, C.R.M. and Nickel, E.H., 1981. Mineralogy and geochemistry of the weathering of the disseminated nickel sulfide deposit at Mt Keith, Western Australia. Economic Geology, 76, 1736–1751.
- Butt, C.R.M. and Robertson, I.D.M., 2003. Ora Banda sill platinum prospect. CRC LEME 2003, 1–3.
- Butt, C.R.M., Williams, P.A., Gray, D.J., Robertson, I.D.M., Schorin, K.H., Churchward, H.M. and Tenhaeff, M.F.J., 1992. Geochemical exploration for platinum group elements in lateritic terrain. Report No 332R, CSIRO Australia, Division of Exploration Geoscience, 3 Volumes, 413 pp.
- Butt, C.R.M., Robertson, I.D.M., Schorin, K.H. and Churchward, H.M., 2001. Geochemical dispersion of platinum group elements in lateritic regolith, Ora Banda sill. In: Geochemical Exploration for Platinum Group Elements in Weathered Terrain. CRC LEME Open File Report 85, Volume IIA, 80 pp.

- Butt, C.R.M., Nickel, E.H. and Brand, N.W., 2006. The weathering of nickel sulfide deposits and implications for geochemical exploration. In: Barnes, S.J. (editor), *Nickel Deposits of the Yilgarn Craton: Geology, Geochemistry, and Geophysics Applied to Exploration*. Economic Geology Special Publication Number 13, 139–165.
- Cabri, L.J. (editor), 1981. *Platinum-Group Elements: Mineralogy, Geology, Recovery*. Canadian Institute of Mining and Metallurgy, Special Volume 23, 267 pp.
- Cabri, L.J. (editor), 2002. *The Geology, Geochemistry, Mineralogy and Mineral Beneficiation of Platinum-Group Elements*. Canadian Institute of Mining, Metallurgy and Petroleum, Special Volume 54, 852 pp.
- Cabri, L.J. and Harris, D.C., 1975. Zoning in Os-Ir alloys and the relation of the geological and tectonic environment of the source rocks to the bulk Pt: Pt+Ir+Os ratio for placers. *Canadian Mineralogist*, 13, 266–274.
- Cabri, L.J. and Laflamme, J.H.G., 1976. The mineralogy of the platinum-group elements from some copper-nickel deposits of the Sudbury area, Ontario. *Economic Geology*, 71, 1159–1195.
- Cabri, L.J., Harris, D.C. and Weiser, T.W., 1996. Mineralogy and distribution of platinum-group mineral (PGM) placer deposits of the world. *Exploration and Mining Geology*, 5, 73–167.
- Cameco Australia, 2014—[Web page]. Kintyre summary. <http://www.cameco.com/australia/kintyre/> (last accessed 10 October 2014).
- Cameron, E.N., 1978. The lower zone of the Eastern Bushveld Complex in the Olifants River trough. *Journal of Petrology*, 19, 437–462.
- Cameron, E.M. and Hattori, K.H., 2005. Platinum group elements in geochemical exploration. In: Mungall, J.E. (editor), *Exploration for Platinum-Group Element Deposits*. Mineralogical Association of Canada Short Course 35, Oulu, Finland, 287–307.
- Campbell, I.H., 1991. The Jimberlana Intrusion. In: Barnes, S.J. and Hill, R.E.T. (editors), *Mafic-Ultramafic Complexes of Western Australia*, Excursion Guidebook No. 3. Sixth International Platinum Symposium, July 1991, Perth, WA. IAGOD and the Geological Society of Australia, 15–18.
- Campbell, I.H. and Naldrett, A.J., 1979. The influence of silicate:sulfide ratios on the geochemistry of magmatic sulfides. *Economic Geology*, 74, 1503–1506.
- Campbell, I.H. and Turner, J.S., 1986. The role of convection in the formation of platinum and chromitite deposits in layered intrusions. In: Scarfe, C.M. (editor), *Short Course in Silicate Melts*. Mineralogical Association of Canada: Ottawa, Canada, 236–278.
- Campbell, I.H., Naldrett, A.J. and Barnes, S.J., 1983. A model for the origin of the platinum-rich sulphide horizons in the Bushveld and Stillwater Complexes. *Journal of Petrology*, 24, 133–165.
- Campbell, I.H., Griffiths, R.W. and Hill, R.I., 1989. Melting in an Archaean mantle plume: Heads it's basalts, tails its komatiites. *Nature*, 339, 697–699.
- Capobianco, C.J. and Drake, M.J., 1990. Partitioning of ruthenium, rhodium, and palladium between spinel and silicate melt and implications for platinum group element fractionation trends. *Geochimica et Cosmochimica Acta*, 54, 869–874.
- Carey, S.W., 1952. Adamsfield report for Lipscombe. TCR 52–0115.
- Carr, G.R., Dean, J.A., Suppel, D.W. and Heithersay, P.S., 1995. Precise lead isotope fingerprinting of hydrothermal activity associated with Ordovician and Carboniferous metallogenic events in the Lachlan Fold Belt of New South Wales. *Economic Geology*, 90, 1467–1505.
- Carville, D.P., Leckie, J.F., Moorhead, C.F., Rayner, J.G. and Durbin, A.A., 1990. Coronation Hill gold-platinum-palladium deposit. In: Hughes, F.E. (editor), *Geology of Mineral Deposits of Australia and Papua New Guinea*. Australasian Institute of Mining and Metallurgy, Melbourne, Monograph 14, 759–762.
- Carville, D.P., Leckie, J.F., Moorhead, C.F. and Rayner, J.G., 1991. Coronation Hill unconformity related gold-platinum-palladium prospect, Northern Territory. In: *Proceedings World Gold '91*, Cairns, April 21–25, 1991, AusIMM, Parkville, Victoria, 287–293.

- Cas, R., Self, S. and Beresford, S., 1999. The behaviour of the fronts of komatiite lavas in medial to distal settings. *Earth and Planetary Science Letters*, 172, 127–139.
- Cassidy, K.F., Champion, D.C. and Huston, D.L., 2005. Crustal evolution constraints on the metallogeny of the Yilgarn Craton. In: Mao, J. and Bierlein, F.P. (editors), *Mineral Deposit Research: Meeting the Global Challenge. Proceedings of the Eighth Biennial SGA Meeting Beijing, China, 18–21 August 2005, Volume 2*, 901–904.
- Causey, J.D., Galloway, J.P. and Zientek, M.L., 2009. An index to PGE-Ni-Cr deposits and occurrences in selected mineral-occurrence databases. United States Geological Survey Open-File Report 2009–1045, 16 pp.
- Cawthorn, R.G., 1999. The platinum and palladium resources of the Bushveld Complex. *South African Journal of Sciences*, 95, 481–489.
- Cawthorn, R.G., 2001. A stream sediment geochemical re-investigation of the discovery of the Bushveld Complex. *Journal of Geochemical Exploration*, 72, 59–69.
- Cawthorn, R.G., 2005a. Stratiform platinum group element deposits in layered intrusions. *Short Course Series—Mineralogical Association of Canada* 35, 57–73.
- Cawthorn, R.G., 2005b. Pressure fluctuations and the formation of the PGE-rich Merensky and chromitite reefs, Bushveld Complex. *Mineralium Deposita*, 40, 231–235.
- Cawthorn, R.G., 2010. The platinum group element deposits of the Bushveld Complex in South Africa. *Platinum Metals Review*, 54, 205–215.
- Cawthorn, R.G., Barnes, S.J., Ballhaus, C. and Malitch, K.N., 2005. Platinum group element, chromium, and vanadium deposits in mafic to ultramafic rocks. In: Hedenquist, J.W., Thompson, J.F.H., Goldfarb, R.J. and Richards, J.P. (editors), *Economic Geology One Hundredth Anniversary Volume 1905–2005*. Society of Economic Geologists, Littleton, Colorado, 215–249.
- Challis, G.A., 1989. Platinum group metals in New Zealand. In: Kear, D. (editor), *Mineral Deposits of New Zealand*. Australasian Institute of Mining and Metallurgy, Monograph 13, 25–29.
- Champion, D.C., 2014. Neodymium depleted mantle model age map of Australia: explanatory notes and user guide. *Geoscience Australia Record* 2013/044, 209 pp.
- Chen, Y.D. and Liu, S.F., 1996. Precise U–Pb zircon dating of a post-D2 metadolerite: constraints on rapid tectonic development of the southern Adelaide Fold Belt during the Cambrian. *Journal of the Geological Society of London*, 153, 83–90.
- Chivas, A.R. and Nutter, A.H., 1975. Copper Hill porphyry copper prospect. In: Knight, C.L. (editor), *Economic Geology of Australia and Papua New Guinea, I, Metals: Australasian Institute of Mining and Metallurgy Monograph* 5, 716–720.
- Chivas, A.R., 1976. The porphyry copper district at Copper Hill, New South Wales. *Economic Geology*, 71, 942–944.
- Christie, T. and Challis, G.A., 1995. Mineral Commodity Report 5—Platinum group metals. *New Zealand mining*, 15, 7 pp.
- Chyi, L. L., 1982. The distribution of gold and platinum in bituminous coal. *Economic Geology*, 77, 1592–1597.
- Claoué-Long, J.C. and Hoatson, D.M., 2005. Proterozoic mafic-ultramafic intrusions in the Arunta Region, central Australia. Part 2: Event chronology and regional correlations. *Precambrian Research*, 142, 134–158.
- Claoué-Long, J.C. and Hoatson, D.M., 2009a. Guide to using the Map of Australian Proterozoic Large Igneous Provinces. *Geoscience Australia Record* 2009/44, 38 pp.
- Claoué-Long, J.C. and Hoatson, D.M., 2009b. Australian Proterozoic Large Igneous Provinces, Sheets 1 and 2 (1:5 000 000, 1:7 500 000, and 1:15 000 000 scale maps), *Geoscience Australia, Canberra, GeoCat* 69213. [http://www.ga.gov.au/metadata-gateway/metadata/record/gcat\\_69213](http://www.ga.gov.au/metadata-gateway/metadata/record/gcat_69213) (last accessed 10 October 2014).
- Claoué-Long, J.C. and Hoatson, D.M., 2010. Australian LIPs and the Australian Precambrian 'barcode'. *October 2010 LIP of the Month*, 19 pp.

- Close, D.F., Scrimgeour, I.R. and Edgoose, C.J., 2003a. Compilation of geochronological data from the northwestern Musgrave Block, Northern Territory: Northern Territory Geological Survey, Technical Report 2003–006, 39 pp.
- Close, D., Scrimgeour, I., Edgoose, C., Cross, A., Claoué-Long, J., Kinny, P. and Meixner, T., 2003b. Defining the Warumpi Province. Annual Geoscience Exploration Seminar (AGES) Alice Springs, 25–26 March, 2003, Abstracts. Northern Territory Geological Survey Record 2003–001.
- Close, D., Scrimgeour, I., Edgoose, C., Frater, M. and Cross, A., 2004. New insights into geology and prospectivity of the southwestern Arunta Region. Annual Geoscience Exploration Seminar (AGES) Alice Springs, 23–24 March, 2004, Abstracts. Northern Territory Geological Survey Record 2004–001.
- Cochrane, G.W., 1982. Copper, lead, zinc and barium deposits of Victoria. Geological Survey of Victoria, Bulletin 61, 109–122.
- Coffin, M.F. and Eldholm, O., 2001. Large igneous provinces: progenitors of some ophiolites? In: Ernst, R.E. and Buchan, K.L. (editors), *Mantle Plumes: Their Identification Through Time*. The Geological Society of America Incorporated, Geological Society of America Special Paper 352, 59–70.
- Coggon, J.A., Nowell, G.M., Pearson, D.G., Oberthür, T., Lorand, J.-P., Melcher, F. and Parman, S.W., 2012. The  $^{190}\text{Pt}$ – $^{186}\text{Os}$  decay system applied to dating platinum-group element mineralization of the Bushveld Complex, South Africa. *Chemical Geology*, 302–303, 48–60.
- Collins, J.E., Barnes, S.J., Hagemann, S.G., McCuaig, T.C. and Frost, K.M., 2012. Postmagmatic variability in ore composition and mineralogy in the T4 and T5 ore shoots at the high-grade Flying Fox Ni-Cu-PGE deposit, Yilgarn Craton, Western Australia. *Economic Geology*, 107, 859–879.
- Collins, P.L.F., 2011. Orthomagmatic Fe-Ti-V mineralisation in Archaean-Proterozoic layered mafic intrusive complexes in Australia. In: Barr, F. (editor), *Let's Talk Ore Deposits*. Proceedings of the 11<sup>th</sup> Biennial Meeting SGA. Society for Geology Applied to Mineral Deposits, Antofagasta, Chile, 26–29 September 2011, 3 pp.
- Connah, T.H., 1961. Beach sand heavy mineral deposits of Queensland. Publication no. 302, Geological Survey of Queensland, Brisbane.
- Connolly, R.R., 1959. Iron ores in Western Australia: Western Australia Geological Survey, Mineral Resources Bulletin 7, 103 pp.
- Cooke, D.R., Wilson, A.J., House, M.J., Wolfe, R.C., Walshe, J.L., Lickfold, V. and Crawford, A.J., 2007. Alkalic porphyry Au-Cu and associated mineral deposits of the Ordovician to Early Silurian Macquarie Arc, New South Wales. *Australian Journal of Earth Sciences*, 54, 445–463.
- Corbett, K.D., Berry, R.F., Everard, J.L., Calver, C.R., Crawford, A.J., Vickary, M.J. and Bottrill, R.S., 2014. Cambrian Tasmania. In: Corbett, K.D., Quilty, P.G. and Calver, C.R. (editors), *Geological Evolution of Tasmania*. Geological Society of Australia Special Publication 24, Geological Society of Australia (Tasmania Division), 95–240.
- Core Exploration Limited, 2013. Core Exploration Limited announcement to the Australian Securities Exchange, 11 June 2013, 7 pp.  
[http://coreexploration.com.au/user\\_files/reports/20130611\\_CXO\\_Large\\_Scale\\_Copper\\_Nickel\\_PGE\\_Target\\_-\\_Albarta\\_Project\\_NT.pdf](http://coreexploration.com.au/user_files/reports/20130611_CXO_Large_Scale_Copper_Nickel_PGE_Target_-_Albarta_Project_NT.pdf) (last accessed 10 October 2014).
- Cornelius, M., 2005. Yarawindah Brook PGE-Ni-Cu deposit, New Norcia, Western Australia. In: Butt, C.R.M., Robertson, I.D.M., Scott, K.M. and Cornelius, M. (editors), *Regolith Expression of Australian Ore Systems*. Cooperative Research Centre for Landscape Environments and Mineral Exploration (CRC LEME), Perth, 124–126.
- Coveney Jr, R.M., Murowchick, J.B., Grauch, R.I., Glascock, M.D. and Denison, J.R., 1992. Gold and platinum in shales with evidence against extraterrestrial sources of metals. *Chemical Geology*, 99, 101–114.
- Cowden, A. and Roberts, D.E., 1990. Komatiite hosted nickel sulphide deposits, Kambalda. In: Hughes, F.E. (editor), *Geology of the Mineral Deposits of Australia and Papua New Guinea*. Australasian Institute of Mining and Metallurgy, Melbourne, Monograph 14, 567–581.

- Cowden, A., Donaldson, M.J., Naldrett, A.J. and Campbell, I.H., 1986. Platinum-group elements and gold in the komatiite-hosted Fe-Ni-Cu sulfide deposits at Kambalda, Western Australia. *Economic Geology*, 81, 1226–1235.
- Cozens, B. and Rangott, M.F., 1972. Ore control in the Thomson River copper mine. *Mines Department of Victoria, Mining and Geological Journal*, 7, 23–30.
- Craven, B., Rovira, T., Grammer, T. and Styles, M., 2000. The role of geophysics in the discovery and delineation of the Cosmos nickel sulfide deposit, Leinster. 14<sup>th</sup> Geophysical Conference, *Exploration Geophysics*, 31, 201–209.
- Crawford, A.J. and Berry, R.F., 1992. Tectonic implications of Late Proterozoic–Early Palaeozoic igneous rock associations in western Tasmania. In: Ferguson, C.L. and Glen, R.A. (editors), *The Palaeozoic Eastern Margin of Gondwanaland: Tectonics of the Lachlan Fold Belt, southeastern Australia and Related Orogens*. *Tectonophysics*, 214, 37–56.
- Crawford, A.J., Falloon, T.J. and Green, D.H., 1989. Classification, petrogenesis and tectonic setting of boninites. In: Crawford, A.J. (editor), *Boninites*. Unwin Hyman, London, United Kingdom, 1–49.
- Crick, I.H. and Muir, M.D., 1980. Evaporites and uranium mineralization in the Pine Creek Geosyncline. In: Ferguson, J. and Goleby, A.B. (editors), *Uranium in the Pine Creek Geosyncline*. International Atomic Energy Agency, Vienna, 531–542.
- Crocket, J., 1979. Platinum group elements in mafic and ultramafic rocks: a survey. *Canadian Mineralogist*, 17, 391–402.
- Crocket, J.H., 2000. PGE in fresh basalt, hydrothermal alteration products, and volcanic incrustations of Kilauea volcano, Hawaii. *Geochimica et Cosmochimica Acta*, 64, 1791–1807.
- Crocket, J.H., 2002. platinum-group elements in basalts from Maui, Hawai'i: low abundances in alkali basalts. *Canadian Mineralogist*, 40, 595–609.
- Czamanske, G.K. and Zientek, M.L. (editors), 1985. *The Stillwater Complex, Montana: Geology and Guide*. Montana Bureau of Mines and Geology, Special Publication 92, IGCP Project 161, Montana Bureau of Mines, USA. 396 pp.
- Dahlkamp, F.J., 1993. *Uranium Ore Deposits*. Springer-Verlag. Berlin Heidelberg.
- Daniels, J.L., 1974. *The Geology of the Blackstone region. Western Australia: Geological Survey of Western Australia, Bulletin 123*, 257 pp.
- Dare, S.A.S., Barnes, S-J. and Beaudoin, G., 2012. Variation in trace element content of magnetite crystallized from a fractionating sulfide liquid, Sudbury, Canada: Implications for provenance discrimination. *Geochimica et Cosmochimica Acta*, 88, 27–50.
- Davies, G. and Tredoux, M., 1985. The platinum-group element and gold contents of the marginal rocks and sills of the Bushveld Complex. *Economic Geology*, 80, 838–848.
- Davies, T.C. and Bloxam, T.W., 1979. Heavy metal distribution in laterites, southwest of Regent, Freetown Igneous Complex, Sierra Leone. *Economic Geology*, 74, 638–644.
- Dayah, M., 1997. Dynamic Periodic Table (Ptable), 1 October 1997. <http://www.ptable.com/> (last accessed 10 October 2014).
- de Angelis, M., Hoyle, M.W.H., Peters, W.S. and Wightman, D., 1987. The nickel–copper deposit at Radio Hill, Karratha, Western Australia: Australasian Institute of Mining and Metallurgy, *Bulletin and Proceedings*, 292, 61–74.
- de Angelis, M., Hoyle, M.W.H. and Voermans, F.M., 1988. The Radio Hill Ni-Cu deposit and the Mt Sholl-Munni Munni mafic-ultramafic metallogenic province: A case of integrated exploration technique. In: *The Second International Conference On Prospecting In Arid Terrain, April 1988, Perth, Western Australia*. The Australasian Institute of Mining and Metallurgy, 51–58.
- de Laeter, J.R. and Trendall, A.F., 1971. The age of the Gidley Granophyre: Western Australia Geological Survey, *Annual Report, 1970*, 62–67.
- Delta Gold NL, 2006. *Delta Gold NL 2006 Annual Report*.

- DMITRE, 2014—[Web page]. Musgrave Economic Geology.  
[http://www.pir.sa.gov.au/minerals/geological\\_survey\\_of\\_sa/geology/geological\\_provinces/musgrave\\_province/musgrave\\_economic\\_geology](http://www.pir.sa.gov.au/minerals/geological_survey_of_sa/geology/geological_provinces/musgrave_province/musgrave_economic_geology) (last accessed 10 October 2014).
- Denaro, T.J., Randall, R.E. and Smith, R.J., 2013. Chapter 10, Mineral and Energy Resources. Section 10.3.13 Platinum Group Metals. In: Jell, P.A. (editor), *Geology of Queensland*. Geological Survey of Queensland, 712–716.
- Dentith, M.C., Frankcombe, K.F. and Trench, A., 1994. Geophysical signatures of Western Australian mineral deposits: an overview. *Exploration Geophysics*, 25, 103–160.
- De Paolo, D.J. and Wasserburg, G.J., 1979. Sm-Nd age of the Stillwater Complex and the mantle evolution curve for neodymium. *Geochimica et Cosmochimica Acta*, 43, 999–1008.
- Derkmann, K. and Jung, R., 1986. Assessing the potential of Burundi's nickel laterites. *Economic and Mining Journal*, July 1986, 8–9.
- Derrick, G.M., 1991. Geology and economic potential of the Tout Complex, NSW. In: Elliott, S.J. and Martin, A.R (editors), *Geology and Mineralisation of the Fifield Platinum Province, New South Wales*. Sixth International Platinum Symposium, Perth, Western Australia. Guidebook for the Pre-Symposium Field Excursion. Geological Society of Australia, 24–34.
- Diakov, S., West, R., Schissel, D., Krivtsov, A., Kochnev-Pervoukhov, V. and Migachev, I., 2002. Recent advances in the Noril'sk model and its application for exploration of Ni-Cu-PGE sulfide deposits. In: Goldfarb, R.J. and Nielsen, R.L. (editors), *Integrated Methods for Discovery: Global Exploration in the Twenty-first Century*. Society of Economic Geologists Inc, Special Publication 9, 203–226.
- Dill, H.G., 2010. The “chessboard” classification scheme of mineral deposits: Mineralogy and geology from aluminium to zirconium. *Earth-Science Reviews*, 100, 1–420.
- Direen, N.G. and Crawford, A.J., 2003. The Tasman Line: where is it, what is it, and is it Australia's Rodinian breakup boundary? *Australian Journal of Earth Sciences*, 50, 491–502.
- Distler, V.V. and Yudovskaya, M.A., 2005. Chapter 21: Polymetallic platinum-group element (PGE)-Au mineralization of the Sukhoi Log deposit, Russia. In: Mungall, J.E. (editor), *Exploration for Platinum-Group Element Deposits*. Mineralogical Association of Canada Short Course 35, Oulu, Finland, 457–485.
- Distler, V.V., Kryachko, V.V. and Yudovskaya, M.A., 2008. Ore petrology of chromite-PGE mineralization in the Kempirsai ophiolite complex. *Mineralogy and Petrology*, 92, 31–58.
- Donaldson, M.J., 1974. Petrology of the Munni Munni Complex, Roebourne, Western Australia. *Journal of the Geological Society of Australia*, 21, 1–16.
- Donaldson, M.J., Leshner, C.M., Groves, D.I. and Gresham, J.J., 1986. Comparison of Archean dunites and komatiites associated with nickel mineralisation in Western Australia. *Mineralium Deposita*, 21, 266–305.
- Donnelly, T.H. and Ferguson, J., 1980. A stable isotope study of three deposits in the Alligator Rivers Uranium Field, NT. In: Ferguson, J. and Goleby, A.B. (editors), *Uranium in the Pine Creek Geosyncline*. International Atomic Energy Agency, Vienna, 397–406.
- Douch, C.J., 1987. Platinum-group-metal occurrence in New Zealand. In: *Proceedings Pacific Rim Congress 87*, Australasian Institute of Mining and Metallurgy, Melbourne, 109–114.
- Dow, D.B. and Gemuts, I., 1967. Dixon Range, Western Australia, 1:250 000 Geological Series Explanatory Notes, Sheet SE 52–6. Bureau of Mineral Resources, Canberra, ACT, Australia, 15 pp.
- Dow, D.B. and Gemuts, I., 1969. Geology of the Kimberley region, Western Australia: the East Kimberley. Bureau of Mineral Resources, Australia, Bulletin 106; and the Geological Survey of Western Australia, Bulletin 120, 135 pp.
- Dowling, S.E. and Hill, R.E.T., 1992. The distribution of PGE in fractionated Archean komatiites, Western and Central Ultramafic Units, Mt. Keith region, Western Australia: *Australian Journal of Earth Sciences*, 39, 349–364.

- Dowling, S.E. and Hill, R.E.T., 1998. Komatiite-hosted nickel sulphide deposits, Australia. Special Jubilee Issue of Australian Geological Survey Organisation Journal of Australian Geology, Geophysics, 17, 121–127.
- DPIPWE, 2014—[Web page]. Surveyors General of Tasmania: 1825-1887. <http://dPIPWE.tas.gov.au/Documents/Honour-Board.pdf> (last accessed 10 October 2014).
- Dragon Mining Limited, 2009. Dragon Mining Limited Annual Report 2009.
- Duke, J.M., 1988. Magmatic segregation deposits of chromite. In: Roberts, R.G. and Sheahan, P.A. (editors), Ore Deposit Models. Geoscience Canada, Reprint Series 3, 133–143.
- Duke, J.M., 1995. Mafic-ultramafic-hosted chromite. In: Eckstrand, O.R., Sinclair, W.D. and Thorpe, R.I. (editors), Geology of Canadian Mineral Deposit Types. The Geology of North America Series, Geological Society of America, volume P-1. Geological Survey of Canada, Geology of Canada 8, 615–624.
- Dundas, A., 2004. WMC Nickel, Business development potential. WMC Resources Limited report, 28 October 2004, 31 pp.
- Dunn, C.E., 1986. Biogeochemistry as an aid to exploration for gold, platinum and palladium in the northern forests of Saskatchewan, Canada. Journal of Geochemical Exploration, 25, 21–40.
- Dunn, C.E., 1992. Biogeochemical exploration for deposits of the noble metals. In: Brooks, R.R. (editor), Noble Metals and Biological Systems. CRC Press, Boca Raton, 47–89.
- Dunstan, B., 1913. Queensland mineral index and guide. Geological Survey of Queensland, Publication 241, 826.
- Dunstan, B., 1917. Queensland mineral deposits. A review of occurrences, production, values, and prospects. 14. Platinum. Queensland Government Mining Journal, 18, 556–562.
- Dunstan, B., 1920. Platinum group metals. Article 5 in Industrial Minerals, Queensland Geological Survey, Department of Mines, 268 (in part).
- Dunstan, B., 1921. Queensland industrial minerals, review of occurrences, treatment, uses, values, and production. V. Platinum. Queensland Government Mining Journal, 22, 17–20, 51–55, 95–100.
- Dunstan, B., 1926. Queensland industrial minerals Part 1: a review of occurrences, uses, values, and production with special reference to Queensland resources in salt, asbestos, mica, molybdenite, platinum, nickel, graphite, manganese, and arsenic. Publication 268, Geological Survey of Queensland, Brisbane.
- Duuring, P., Cassidy, K.F. and Hagemann, S.G., 2007. Granitoid-associated orogenic, intrusion-related, and porphyry style metal deposits in the Archean Yilgarn Craton, Western Australia. Ore Geology Reviews, 32, 157–186.
- Eales, H.V. and Cawthorn, R.G., 1996. The Bushveld Complex. In: Cawthorn, R.G. (editor), Layered Intrusions. Elsevier, Amsterdam, 181–230.
- Earp, G.B., 1852. The gold colonies of Australia: comprising their history, territorial divisions, produce, and capabilities, how to get to the gold mines, and every advice to emigrants. Routledge and Co, London, 216 pp.
- East Coast Minerals NL, 2009. East Coast Minerals NL announcement to the Australian Securities Exchange, 15 May 2009, 6 pp. <http://www.infomine.com/index/pr/Pa756862.PDF> (last accessed 10 October 2014).
- Eckstrand, O.R., 1995. Nickel-copper-sulfide. In: Eckstrand, O.R., Sinclair, W.D. and Thorpe, R.I. (editors), Geology of Canadian Mineral Deposit Types. The Geology of North America Series, Geological Society of America, vol. P-1. Geological Survey of Canada, Geology of Canada 8, 584–605.
- Eckstrand, O.R., 2005. Ni-Cu-Cr-PGE mineralization types: Distribution and classification. In: Mungall, J.E. (editor), Exploration for Platinum-Group Element Deposits. Mineralogical Association of Canada Short Course 35, Oulu, Finland, 487–493.
- Eckstrand, O.R. and Hulbert, L., 2007. Magmatic nickel-copper-platinum group element deposits. Mineral deposits of Canada: a synthesis of major deposit-types, district metallogeny, the evolution of geological provinces, and exploration methods. In: Goodfellow, W.D. (editor), Mineral Deposits

- of Canada. Geological Association of Canada, Mineral Deposits Division, Special Publication 5, 205–222.
- Eckstrand, O.R., Yakubchuk, A., Good, D.J. and Gall, Q., 2003. World Minerals Geoscience Database Project Beta Release 3.5.
- Economou-Eliopoulos, M., 2005. Platinum-group element potential of porphyry deposits. In: Mungall, J.E. (editor), *Exploration for Platinum-Group Element Deposits*. Mineralogical Association of Canada Short Course 35, Oulu, Finland, 203–245.
- Edgoose, C.J., Close, D.F. and Scrimgeour, I.R., 2004a. Musgrave Block, Northern Territory, 1:500 000 geological special, First edition Northern Territory Geological Survey 1v Map.
- Edgoose, C.J., Scrimgeour, I.R. and Close, D.F., 2004b. *Geology of the Musgrave Block, Northern Territory*. Northern Territory Geological Survey, Report 15, 44 pp.
- El Ghorfi, M., Melcher, F., Oberthuer, T., Boukhari, A.E., Maacha, L., Maddi, A. and Mhaili, M., 2008. Platinum group minerals in podiform chromitites of the Bou Azzer Ophiolite, Anti Atlas, central Morocco. *Mineralogy and Petrology*, 92, 59–80.
- Elhaddad, M.A., 1996. The first occurrence of platinum group minerals (PGM) in a chromite deposit in the eastern Desert, Egypt. *Mineralium Deposita*, 31, 439–445.
- Elias, M., 2002. Nickel laterite deposits—geological overview, resources and exploitation. In: Cooke, D.R. and Pongratz, J. (editors), *Giant Ore Deposits: Characteristics, Genesis, and Exploration*. Centre for Ore Deposit Research Special Publication 4, University of Tasmania, Hobart, 205–220.
- Elias, M., 2006. Lateritic nickel mineralization of the Yilgarn Craton. In: Barnes, S.J. (editor), *Nickel Deposits of the Yilgarn Craton: Geology, Geochemistry, and Geophysics Applied to Exploration*. Economic Geology Special Publication Number 13, 195–210.
- Eliopoulos, D.G. and Economou-Eliopoulos, M., 2000. Geochemical and mineralogical characteristics of Fe-Ni- and bauxitic-laterite deposits of Greece. *Ore Geology Reviews*, 16, 41–58.
- Elliott, P.J. and Staltari, G., 1985. The Mt Keith south nickel sulfide deposit—A TEM case study. 4<sup>th</sup> Geophysical Conference, *Exploration Geophysics*, 16, 210–216.
- Elliott, S.J. and Martin, A.R. (editors), 1991. *Geology and mineralisation of the Fifield platinum province, New South Wales*. Sixth International Platinum Symposium, Perth, Western Australia. Guidebook for the Pre-Symposium Field Excursion. Geological Society of Australia, 43 pp.
- Elliston, J., 1953. Platinoids in Tasmania. In: Edwards, A.B. (editor), *Geology of Australian Mineral Deposits*, 5<sup>th</sup> Empire Mining and Metallurgical Congress. Australasian Institute of Mining and Metallurgy, Melbourne, 1250–1254.
- Emerson, D.W., Embleton, B.J.J. and Clark, D., 1979. The Flemington intrusion, Fifield, NSW—petrophysical and petrological notes. *Australian Society of Exploration Geophysicists, Bulletin* 10, 67–78.
- Emerson, D.W., Martin, K. and Williams, P.K., 1999. 'The rock doctor'—electrical, magnetic and mass properties of the nickeliferous komatiite sequence near Leinster, Western Australia. *Preview*, 81, 13–21.
- Encarnacion, J., Fleming, T.H., Elliot, D.H. and Eales, H.V., 1996. Synchronous emplacement of Ferrar and Karoo dolerites and the early breakup of Gondwana. *Geology*, 24, 535–538.
- ERA Limited, 2000. *Energy Resources of Australia Ltd. Annual Report 2000*.
- Erceg, M., 1992. Copper Hill Exploration Licence 2290, Annual Report to 13 November, 1991. Cyprus Gold Australia Corporation. NSW GS1992/083, 529.
- Ernst, R.E., (2014-in press). *Large Igneous Provinces*. Cambridge University Press.
- Ernst, R.E. and Buchan, K.L., 2001. Large mafic magmatic events through time and links to mantle-plume heads. In: Ernst, R.E. and Buchan, K.L. (editors), *Mantle Plumes: Their Identification Through Time*. Geological Society of America Special Paper 352, 483–575.
- Ernst, R.E. and Jowitt, S.M., 2013. Large Igneous Provinces (LIPs) and Metallogeny. October 2013 LIP of the Month, 12 pp.

- Eupene Exploration Enterprises Pty Ltd., 1989. Platinum group metals in the Northern Territory. Department of Mines and Energy, Northern Territory Geological Survey, 16 pp.
- European Commission, 2010. Critical raw materials for the EU. Report of the Ad-hoc Working Group on defining critical raw materials, July 2010. [http://ec.europa.eu/enterprise/policies/raw-materials/files/docs/report-b\\_en.pdf](http://ec.europa.eu/enterprise/policies/raw-materials/files/docs/report-b_en.pdf) (last accessed 10 October 2014).
- Evans-Lamswood, D.M., Butt, D.P., Jackson, R.S., Lee, D.V., Muggridge, M.G. and Wheeler, R.I., 2000. Physical controls associated with the distribution of sulfides in the Voisey's Bay Ni-Cu-Co deposit, Labrador. *Economic Geology*, 95, 749–769.
- Everard, J.L., Leaman, D.E., Calver, C.R. and Morrison, K.C., 2014. Jurassic dolerite and associated minor lavas and sedimentary rocks. In: Corbett, K.D., Quilty, P.G. and Calver, C.R. (editors), *Geological Evolution of Tasmania*. Geological Society of Australia Special Publication 24, Geological Society of Australia (Tasmania Division), 385–407.
- Evins, L.Z., 2005. The Late Early Cambrian Kalkarindji continental flood basalt province: a link to mass extinction. October 2005 LIP of the Month, 9 pp.
- Evins, L.Z., Jourdan, F. and Phillips, D., 2009. The Cambrian Kalkarindji Large Igneous Province: Extent and characteristics based on new  $^{40}\text{Ar}/^{39}\text{Ar}$  and geochemical data. *Lithos*, 110, 294–304.
- Evins, P.M., Smithies, H.R., Howard, H.M., Kirkland, C.L., Wingate, M.T.D. and Bodorkos, S., 2010a. Redefining the Giles Event within the setting of the 1120–1020 Ma Ngaanyatjarra Rift, west Musgrave Province, central Australia. *Geological Survey of Western Australia Record* 2010/6, 36 pp.
- Evins, P., Smithies, H., Howard, H., Kirkland, C., Wingate, M.T.D. and Bodorkos, S., 2010b. Devil in the detail; the 1150–1000 Ma magmatic and structural evolution of the Ngaanyatjarra Rift, West Musgrave province, Central Australia. *Precambrian Research*, 183, 572–588.
- Ewers, G.R., Ferguson, J., Needham, R.S. and Donnelly, T.H., 1984. Pine Creek Geosyncline NT. In: Ferguson, J. (editor), *Proterozoic Unconformity and Stratabound Uranium Deposits*. International Atomic Energy Agency, Vienna, Tecdoc, 315, 135–206.
- Falcon Minerals Limited, 2004. Falcon Minerals Limited second quarter activity report to 31 March 2004, 11 pp.
- Falcon Minerals Limited, 2005. Falcon Minerals Limited second quarter activity report to 31 December 2004, Collurabbie WA and Cargo NSW, 18 pp.
- Falcon Minerals Limited, 2006. Falcon Minerals Limited announcement to the Australian Securities Exchange 15 May 2006, 3 pp.
- Falcon Minerals Limited, 2009a. Falcon Minerals Limited fourth quarterly activity report to 30 June 2009, 19 pp.
- Falcon Minerals Limited, 2009b. Falcon Minerals Limited announcement to the Australian Securities Exchange 14 December 2009, 4 pp.
- Falcon Minerals Limited, 2009c. Falcon Minerals Limited announcement to the Australian Securities Exchange, 17 December 2009, 31 pp.
- Falcon Minerals Limited, 2010. Falcon Minerals Limited announcement to the Australian Securities Exchange, 26 November 2010, 6 pp.
- Falcon Minerals Limited, 2012. Falcon Minerals Limited Annual Report 2012, 65 pp.
- Falcon Minerals Limited, 2014—[Web page]. Collurabbie Project-Western Australia. [http://www.falconminerals.com.au/projects/collurabbie\\_wa.phtml](http://www.falconminerals.com.au/projects/collurabbie_wa.phtml) (last accessed 10 October 2014).
- Farrow, C.E.G., 1994. Geology, alteration, and the role of fluids in Cu-Ni-PGE mineralization of the footwall rocks to the Sudbury Igneous Complex, Levack and Morgan Townships, Sudbury District, Ontario. PhD thesis, Carleton University, Ottawa, Ontario.
- Faure, G., 1986. Principles of isotope geology. John Wiley and Sons, New York, NY, United States, 589 pp.
- Ferguson, J., Ewers, G.R. and Donnelly, T.H., 1980. Model for the development of economic uranium

- mineralisation in the Alligator Rivers Uranium Field. In: Ferguson, J. and Goleby, A.B. (editors), Uranium in the Pine Creek Geosyncline. International Atomic Energy Agency, Vienna, 563–574.
- Ferguson, K.M., 1999. Lead, zinc and silver deposits of Western Australia: Western Australia Geological Survey, Mineral Resources Bulletin 15, 314 pp.
- Ferguson, W.H., 1936. Turtons Creek Goldfield. Geological Survey of Victoria, Records 5, 249–252.
- Ferreira Filho, C.F. and Leshner, C.M., 2001. The komatiite-associated Ni-sulfide deposit of Boa Vista, Brazil. In: Cassidy, K.F., Dunphy, J.M. and Van Kranendonk, M.J. (editors), 4<sup>th</sup> International Archaean Symposium 2001, Extended Abstracts. AGSO–Geoscience Australia, Record 2001/37, 429–431.
- Fiorentini, M.L., Barley, M.E., Pickard, A., Beresford, S.W., Rosengren, N.M., Cas, R.A.F. and Duuring, P., 2005. Age constraints of the structural and stratigraphic architecture of the Agnew-Wiluna greenstone belt: Implications for the age of komatiite-felsic association and interaction in the Eastern Goldfields Province, Western Australia: Perth, Minerals and Energy Research Institute of Western Australia, MERIWA Final Report no. 255, Project M356, 39 pp.
- Fiorentini, M.L., Beresford, S.W., Grguric, B., Barnes, S.J. and Stone, W.E., 2007a. Atypical stratiform sulfide-poor platinum-group element mineralisation in the Agnew–Wiluna belt komatiites, Wiluna, Western Australia. *Australian Journal of Earth Sciences*, 54, 801–824.
- Fiorentini, M.L., Rosengren, N., Beresford, S.W., Grguric, B. and Barley, M.E., 2007b. Controls on the emplacement and genesis of the MKD5 and Sarah's Find Ni–Cu–PGE deposits, Mount Keith, Agnew–Wiluna Greenstone Belt, Western Australia. *Mineralium Deposita*, 42, 847–877.
- Fiorentini, M.L., Barnes, S.J., Leshner, C.M., Heggie, G.J., Keays, R.R. and Burnham, O.M., 2010. Platinum-group element geochemistry of mineralized and non-mineralized komatiites and basalts. *Economic Geology*, 105, 795–823.
- Fiorentini, M.L., Barnes, S.J., Maier, W.D., Burnham, O.M. and Heggie, G.J., 2011. Global variability in the platinum-group element contents of komatiites. *Journal of Petrology*, 52, 83–112.
- Fiorentini, M.L., Beresford, S.W., Barley, M.E., Duuring, P., Bekker, A., Rosengren, N.M., Cas, R.A.F. and Hronsky, J., 2012. District to camp controls on the genesis of komatiite-hosted nickel sulfide deposits, Agnew-Wiluna Greenstone Belt, Western Australia: Insights from the multiple sulfur isotopes. *Economic Geology*, 107, 781–796.
- Fitton, M.J., Horwitz, R.C. and Sylvester, G., 1975. Stratigraphy of the early Precambrian in the west Pilbara, Western Australia: Commonwealth Scientific and Industrial Research Organisation, Minerals Research Laboratories, Report FP11, 41 pp.
- Flack, D.S., 1967. Platinum. Mineral Industry of New South Wales, Geological Survey of New South Wales, Department of Mines, Summary Report Series 33, 16 pp.
- Flint, D.J., Searston, S.M., Cooper, R.W. and Abeyasinghe, P.B., 2005. Nickel-cobalt in Western Australia commodity review for 2003. Western Australia Geological Survey Record 2005/3, 38 pp.
- Ford, K., Keating, P. and Thomas, M.D., 2007. Overview of geophysical signatures associated with Canadian ore deposits. In: Goodfellow, W.D. (editor), Mineral Deposits of Canada. Geological Association of Canada, Mineral Deposits Division, Special Publication 5, 939–970.
- Ford, R.J., 1981. Platinum-group minerals in Tasmania. *Economic Geology*, 76, 498–504.
- Foster, J.G., 2003. The Noril'sk-Talnakh ore deposits: Russia. New Frontiers in Research on Magmatic NiS-PGE Mineralisation. Short Course Notes, Centre for Global Metallogeny, University of Western Australia, Perth, Western Australia, February 2003, 129–136.
- Foster, J.G., Lambert, D.D., Frick, L.R. and Maas, R., 1996. Re-Os isotopic evidence for genesis of Archaean nickel ores from uncontaminated komatiites. *Nature*, 382, 703–705.
- Fox Resources Limited, 2007. Fox Resources Limited Annual Report 2007, 98 pp.
- Franklin, B.J., Marshall, B., Graham, L.T. and McAndrew, J., 1992. Remobilization of PGE in podiform chromitite in the Coolac Serpentinite Belt, southeastern Australia. *Australian Journal of Earth Sciences*, 39, 365–371.
- Freeman, M.J., 1986. Huckitta, Northern Territory—1:250 000 geological map (Sheet SF 53–11). Northern Territory Geological Survey, Darwin (second edition).

- Freeman, P.V., 1983. Mining in Zambia today: Exploration and mining in Zambia. Proterozoic '83 Conference, Lusaka, Zambia, Geological Society of Zambia.
- Frey, F.A., 1984. Rare earth element abundances in upper mantle rocks, in: Henderson, P. (editor), Rare Earth Element Geochemistry. Elsevier Scientific Publishing Company, Amsterdam, Netherlands, 153–203.
- Frick, L.R., Lambert, D.D. and Hoatson, D.M., 2001. Re-Os dating of the Radio Hill Ni-Cu deposit, west Pilbara Craton, Western Australia. *Australian Journal of Earth Sciences*, 48, 43–47.
- Froude, D.O., Ireland, T.R., Kinny, P.D., Williams, I.S., Compston, W., Williams, I.R. and Myers, J.S., 1983. Ion-microprobe identification of 4100–4200 Myr old terrestrial zircons. *Nature*, 304, 616–618.
- Galahad Gold PLC, 2005. Skaergaard Project Resource Estimates Announced. Galahad Gold PLC media release, 28 October 2005. <http://www.galahadgold.com/mediacentre/article.html?id=73> (last accessed 10 October 2014).
- Gammons, C.H., 1995. Experimental investigations of the hydrothermal geochemistry of platinum and palladium: IV. The stoichiometry of Pt(IV) and Pd(II) chloride complexes at 100 to 300°C. *Geochimica et Cosmochimica Acta*, 59, 1655–1667.
- Gammons, C.H., 1996. Experimental investigations of the hydrothermal geochemistry of platinum and palladium: V. Equilibria between platinum metal, Pt(II), and Pt(IV) chloride complexes at 25 to 300°C. *Geochimica et Cosmochimica Acta*, 60, 1683–1694.
- Gammons, C.H. and Bloom, M.S., 1993. Experimental investigation of the hydrothermal geochemistry of platinum and palladium; II, The solubility of PtS and PdS in aqueous sulfide solutions to 300 degrees C. *Geochimica et Cosmochimica Acta*, 57, 2451–2467.
- Gammons, C.H., Bloom, M.S. and Yu, Y., 1992. Experimental investigation of the hydrothermal geochemistry of platinum and palladium: I. Solubility of platinum and palladium sulfide minerals in NaCl/H<sub>2</sub>SO<sub>4</sub> solutions at 300°C. *Geochimica et Cosmochimica Acta*, 56, 3881–3894.
- Geary, J.K., Barrie, J., Haycraft, J.A., Morgan, J.W. and Kalix, Z., 1956. Platinum group metals. Bureau of Mineral Resources, Geology and Geophysics, Australia, Summary Report 39, 25 pp.
- Gellatly, D.C., Derrick, G.M. and Plumb, K.A., 1975. The geology of the Lansdowne 1:250,000 Sheet area, Western Australia. Bureau of Mineral Resources, Geology and Geophysics, Canberra, ACT, Report 152, 100 pp.
- German, C.R., Thurnherr, A.M., Knoery J., Charlou, J.-L., Jean-Baptiste, P. and Edmonds, H.N., 2010. Heat, volume and chemical fluxes from submarine venting: A synthesis of results from the Rainbow hydrothermal field, 36°N MAR. *Deep-Sea Research I*, 57, 518–527.
- Giblin, P.E., 1984. History of exploration and development, of geological studies and development of geological concepts. In: Pye, E.G., Naldrett, A.G. and Giblin, P.E. (editors), *The Geology and Ore Deposits of the Sudbury Structure*. Ontario Geological Survey Special Volume 1, 3–23.
- Gilbert D.J., 1986. Mineralogy and texture of a wet table gravity gold concentrate from Coronation Hill, NT, with notes on the occurrence of platinum and florencite. Broken Hill Proprietary Co Ltd, Exploration Department. Northern Territory Geological Survey, Open File Company Report CR1986–0324.
- Gilbert D.J., 1987. Mineralogical occurrence and texture of gold, platinum group minerals and other phases in heavy liquid fractions and diamond drill core samples, from Coronation Hill, Northern Territory. BHP Minerals Exploration. Northern Territory Geological Survey, Open File Company Report CR1987–0337.
- Giralia Resources NL, 2004. Giralia Resources NL Annual General Meeting presentation 25 November 2004.
- Girvan, S.W., 1992. Geology and mineralisation of the Copper Hill Porphyry Copper-Gold Deposit, near Molong, NSW. BSc (Hons.) thesis, Australian, 75 pp.
- Glass, L.M., 2002. Petrogenesis and geochronology of the North Australian Kalkarindji low-Ti continental flood basalt province. PhD thesis, Australian National University, Canberra, 325 pp.
- Glass, L.M., 2006. The Kalkarindji continental flood basalt province: a new large igneous province in Australia. October 2006 lip of the month, 3 pp.

- Glass, L.M. and Phillips, D., 2006. The Kalkarindji continental flood basalt province: A new Cambrian large igneous province in Australia with possible links to faunal extinctions. *Geology*, 34, 461–464.
- Glass, L.M., Bennett, V.C. and Phillips, D., 2004. A new flood basalt province from northern Australia: geochronology and petrogenesis of the Cambrian Kalkarindji low-Ti basalts. 2004 Goldschmidt Conference, Abstracts. *Geochimica et Cosmochimica Acta*, 68, Issue 11, Supplement 1, A585.
- Glen, R.A., 2005. The Tasmanides of eastern Australia. In: Vaughan, A.P.M., Leat, P.T. and Pankhurst, R.J. (editors), *Terrane Processes at the Margins of Gondwana*. The Geological Society of London Special Publication 246, 23–96.
- Glen, R.A., Crawford, A.J. and Cooke, D.R., 2003. Tectonic setting of porphyry copper-gold mineralisation in the Macquarie Arc. In: Blevin, P. Jones, M. and Chappell, B. (editors), *Magma to Mineralisation: The Ishihara Symposium*. *Geoscience Australia Record* 2003/14, 65–68.
- Glikson, A.Y. (editor), 1995. The Giles mafic–ultramafic complex and environs, western Musgrave Block, central Australia: Thematic issue. *AGSO Journal of Geology and Geophysics*, 16, 193 pp.
- Glikson, A.Y., Stewart, A.J., Ballhaus, C.G., Clarke, G.L., Feecken, E.H.J., Leven, J.H., Sheraton, J.W. and Sun, S.-S., 1996. Geology of the western Musgrave Block, central Australia, with particular reference to the mafic–ultramafic Giles Complex. Australian Geological Survey Organisation, Bulletin 239, 206 pp.
- Godel, B., 2013. High-resolution x-ray computed tomography and its application to ore deposits: from data acquisition to quantitative three-dimensional measurements with case studies from Ni-Cu-PGE deposits. *Economic Geology*, 108, 2005–2019.
- Godel, B., Seat, Z., Maier, W.D. and Barnes, S.-J., 2011. The Nebo-Babel Ni-Cu-PGE sulfide deposit (West Musgrave Block, Australia): Part 2. Constraints on parental magma and processes, with implications for mineral exploration. *Economic Geology*, 106, 557–584.
- Gold Fields Resources, 2006—[Web page]. Mineral Resources and ore reserves. Gold Fields Resources media release. [http://www.goldfields.co.za/book\\_index.asp?bookmark=resources.asp](http://www.goldfields.co.za/book_index.asp?bookmark=resources.asp) (last accessed 10 October 2014).
- Golden Cross Resources, 2011 —[Web page]. Copper Hill Summary, Golden Cross Resources, February 2011. <http://www.goldencross.com.au/projects/copper-hill/> (last accessed 10 October 2014).
- Golden Cross Resources, 2013. IIR's 7<sup>th</sup> Annual Mining NSW Conference, Orange, 26–27 June 2013, PowerPoint Presentation. <http://www.goldencross.com.au/wp-content/uploads/260613.pdf> (last accessed 10 October 2014).
- Golden Cross Resources, 2014a—[Web page]. Golden Cross Resources, Projects-Broken Hill. <http://www.goldencross.com.au/projects/australian-projects/broken-hill/> (last accessed 10 October 2014).
- Golden Cross Resources, 2014b—[Web page]. The Copper Hill Story – from 1845. [www.goldencross.com.au/copper-hill-story-from-1845/](http://www.goldencross.com.au/copper-hill-story-from-1845/) (last accessed 10 October 2014).
- Goldfarb, R.J., Bradley, D. and Leach, D.L., 2010. Secular variation in economic geology. *Economic Geology*, 105, 459–465.
- Goldstream Mining NL, 2005a. Report for the quarter ended March 2005. Goldstream Mining NL announcement to the Australian Securities Exchange, 11 pp.
- Goldstream Mining NL, 2005b. Annual Report 2005. Australian Securities Exchange, 78 pp.
- Goldstream Mining NL, 2005c. Report for the quarter ended December 2005. Goldstream Mining NL announcement to the Australian Securities Exchange, 15 pp.
- Gole, M.J., Robertson, J. and Barnes, S.J., 2013. Extrusive origin and structural modification of the komatiitic Mount Keith ultramafic unit. *Economic Geology*, 108, 1731–1752.
- González-Álvarez, I., Porwal, A., Beresford, S., McCuaig, T.C. and Maier, W., 2010. Hydrothermal Ni prospectivity analysis of Tasmania, Australia. *Ore Geology Reviews Special Issue* 38, 168–183.
- Gostin, V.A., Keays, R.R. and Wallace, M.W., 1989. Iridium anomaly from the Acraman impact ejecta horizon—impacts can produce sedimentary iridium peaks. *Nature*, 340, 542–544.

- Gradstein, F.M., Ogg, J. and Smith, A.G., 2004. *A Geological Time Scale, 2004*, Cambridge University Press, New York.
- Gray, D.J., Schorin, K.H. and Butt, C.R.M., 1996. Mineral associations of platinum and palladium in lateritic regolith, Ora Banda Sill, Western Australia. *Journal of Geochemical Exploration*, 57, 245–255.
- Gray, F., Page, N.J., Carlson, C.A., Wilson, S.A. and Carlson, R.R., 1986. Platinum-group element geochemistry of zoned ultramafic suites, Klamath mountains, California and Oregon. *Economic Geology*, 81, 1252–1260.
- Green, T. and Peck, D., 2005. Platinum group elements exploration: Economic considerations and geological criteria. In: Mungall, J.E. (editor), *Exploration for Platinum-Group Element Deposits. Mineralogical Association of Canada Short Course 35*, Oulu, Finland, 247–274.
- Gresham, J.J., 1990. Nickel sulphide deposits of Western Australia—the discovery of the Kambalda nickel deposits. In: Glasson, K.R. and Rattigan, J.H. (editors), *Geological Aspects of the Discovery of some Important Mineral Deposits in Australia*. Australasian Institute of Mining and Metallurgy, Monograph 17, 395–396.
- Gresham, J.J., 1991. Kambalda, history of a mining town. Western Mining Corporation Limited, 114 pp.
- Gresham, J.J. and Loftus-Hills, G.D., 1981. The geology of the Kambalda nickel field, Western Australia. *Economic Geology*, 76, 1373–1416.
- Grguric, B.A., 2003. Minerals of the MKD5 nickel deposit, Mount Keith, Western Australia. *Australian Journal of Mineralogy*, 9, 55–71.
- Grguric, B.A., Rosengren, N.M., Fletcher, C.M. and Hronsky, J.M.A., 2006. Type 2 Deposits: Geology, mineralogy, and processing of the Mount Keith and Yakabindie orebodies, Western Australia. In: Barnes, S.J. (editor), *Nickel Deposits of the Yilgarn Craton: Geology, Geochemistry, and Geophysics Applied to Exploration*. Economic Geology Special Publication Number 13, 119–138.
- Griffin, T.J. and Grey, K., 1990. Kimberley Basin. In: *Geology and Mineral Resources of Western Australia*. Geological Survey of Western Australia, Memoir 3, 293–304.
- Griffin, T.J., Tyler, I.M., Playford, P.E. and Lewis, J.D., 1993. Lennard River, Western Australia, 1:250 000 Geological Series Explanatory Notes, Sheet SE 51–8. Third edition. Geological Survey of Western Australia, Perth, Western Australia, Australia, 56 pp.
- Griffin, T.J., Tyler, I.M., Orth, K. and Sheppard, S., 1998. Geology of the Angelo sheet. Western Australia Geological Survey, 1:100 000 Geological Series Explanatory Notes, 27 pp.
- Griffith, W.P., 2003. Bicentenary of four platinum group metals. Part I: Rhodium and palladium—events surrounding their discoveries. Johnson Matthey Public Limited Company, London, *Platinum Metals Review*, 47, 175–183.
- Griffith, W.P., 2004. Bicentenary of four platinum group metals. Part II: Osmium and iridium—events surrounding their discoveries. Johnson Matthey Public Limited Company, London, *Platinum Metals Review*, 48, 182–189.
- Groves, D.I. and Batt, W.D., 1984. Spatial and temporal variations of Archaean metallogenic associations in terms of evolution of granitoid-greenstone terrains with particular emphasis on the Western Australian Shield. In: Kroner, A., Hanson, G.N. and Goodwin, A.M. (editors), *Archean Geochemistry*. Springer-Verlag, Berlin, 73–98.
- Groves, D.I. and Hudson, D.R., 1990. Nickel sulphide deposits of Western Australia—exploration for nickel sulphide ores. In: Glasson, K.R. and Rattigan, J.H. (editors), *Geological Aspects of the Discovery of some Important Mineral Deposits in Australia*. Australasian Institute of Mining and Metallurgy, Monograph 17, 421–428.
- GSWA, 1991. Semi-quantitative platinum and gold analyses from Western Australia. Geological Survey of Western Australia, Record 1991/2, 39 pp.
- Gunn, A.G., 1989. Drainage and overburden geochemistry in exploration for platinum-group element mineralization in the Unst ophiolites, Shetland, United Kingdom. *Journal of Geochemical Exploration*, 31, 209–236.

- Guo, W.W. and Dentith, M.C., 1997. Geophysical signature of the Jinchuan Ni-Cu-PGE deposit, Gansu Province, China. *Exploration and Mining Geology*, 6, 223–231.
- Gustafson L.B. and Curtis, L.W., 1983. Post-Kombolgie metasomatism at Jabiluka, Northern Territory, Australia, and its significance in the formation of high-grade uranium mineralization in Lower Proterozoic rocks. *Economic Geology*, 78, 26–56.
- Halkoaho, T.A.A., Alapieti, T.T. and Lahtinen, J.J., 1990. The Sompujärvi PGE Reef in the Penikat layered intrusion, northern Finland. *Mineralogy and Petrology*, 42, 39–55.
- Hall, G.E.M., Pelchat, J.-C. and Dunn, C.E., 1990. The determination of Au, Pd, and Pt in ashed vegetation by ICP-mass spectrometry and graphite furnace atomic absorption spectrometry. *Journal of Geochemical Exploration*, 37, 1–23.
- Hallberg, J.A. and Williams, D.A.C., 1972. Archaean mafic and ultramafic rock associations in the Eastern Goldfields region, Western Australia. *Earth and Planetary Science Letters*, 15, 191–200.
- Hamlyn, P.R., 1975. Chromite alteration in the Panton sill, East Kimberley region, Western Australia. *Mineralogical Magazine*, 40, 181–192.
- Hamlyn, P.R., 1977. Petrology of the Panton and McIntosh layered intrusions, Western Australia, with particular reference to the genesis of the Panton chromite deposits. PhD thesis, University of Melbourne, Australia.
- Hamlyn, P.R., 1980. Equilibration history and phase chemistry of the Panton Sill, Western Australia. *American Journal of Science*, 280, 631–668.
- Hamlyn, P.R. and Keays, R.R., 1979. Origin of chromite compositional variation in the Panton Sill, Western Australia. *Contributions to Mineralogy and Petrology* 69/1, 75–82.
- Hamlyn, P.R., Keays, R.R., Peck, D.C. and Reeves, S.J., 1988. Geochemical criteria for platinum metal exploration. Australian Mineral Industries Research Association Limited, Final Report 85/P228, 215 pp.
- Hancock, M.C., Maas, R. and Wilde A.R., 1990. Jabiluka uranium-gold deposits. In: Hughes, F.E. (editor), *Geology of Mineral Deposits of Australia and Papua New Guinea*. Australasian Institute of Mining and Metallurgy, Melbourne, Monograph 14, 785–793.
- Hanley, J.J., 2005. The aqueous geochemistry of the platinum group elements (PGE) in surficial, low-T hydrothermal and high-T magmatic-hydrothermal environments. Short Course Series - Mineralogical Association of Canada 35, 35–56.
- Hanley, J.J. and Gladney E.R., 2011. The Presence of Carbonic-Dominant Volatiles during the Crystallization of Sulfide-Bearing Mafic Pegmatites in the North Roby Zone, Lac des Iles Complex, Ontario. *Economic Geology*, 106, 33–54.
- Hanley, J.J. and Mungall, J.E., 2002. Experimental constraints on platinum-group element solubility in hypersaline aqueous fluids at temperatures above 600 degrees C; preliminary results and application to fluid-modified deposits. Program with Abstracts - Geological Association of Canada; Mineralogical Association of Canada: Joint Annual Meeting 27, 45.
- Hanley, L.M. and Wingate, M.T.D., 2000. SHRIMP zircon age for an Early Cambrian dolerite dyke: An intrusive phase of the Antrim Plateau Volcanics of northern Australia. *Australian Journal of Earth Sciences*, 47, 1029–1040.
- Hanski, E., Huhma, H., Smolkin, V.F. and Vaasjoki, M., 1990. The age of the ferropicritic volcanics and comagmatic Ni-bearing intrusions at Pechenga, Kola Peninsula, USSR. *Bulletin of the Geological Society of Finland* 62, 123–133.
- Haoma Mining NL, 2012. Bamboo Creek and Mt Webber contains significant commercial quantities of gold and platinum group metals (PGM). Haoma Mining NL Report to the Australian Securities Exchange, 18 June 2012, 4 pp.
- Haoma Mining NL, 2014. Haoma Mining NL, announcement to the Australian Securities Exchange, 30 April 2014, 16 pp.
- Harris, D.C. and Cabri, L.J., 1973. The nomenclature of the natural alloys of osmium, iridium, and ruthenium based on new compositional data of alloys from world wide occurrences. *Canadian Mineralogist*, 12, 104–112.

- Harris, D.C. and Cabri, L.J., 1991. Nomenclature of platinum-group-element alloys: review and revision. *Canadian Mineralogist*, 29, 231–237.
- Harrison, B.C., 1993. Precious metals in the supergene environment, Weld Range, Western Australia, BSc Honours thesis, The University of Western Australia, Perth.
- Harrison, P.H., 1986. The mineral potential of layered igneous complexes within The Western Gneiss Terrain: Western Australian Geological Survey, Report 19, Professional Papers for 1984, 37–54.
- Harrison, P.H. and Blockley, J.G., 1990. Platinum and chromium. In: *Geology and Mineral Resources of Western Australia*. Western Australia Geological Survey Memoir 3, 724–726.
- Hattori, K. and Cabri, L.J., 1992. Origin of platinum-group mineral nuggets inferred from an osmium-isotope study. *Canadian Mineralogist*, 30, 289–301.
- Haughton, D.R., Roeder, P.L. and Skinner, B.J., 1974. Solubility of sulfur in mafic magmas. *Economic Geology*, 69, 451–467.
- Haxel, G.B., Hedrick, J.B. and Orris, G.J., 2005. Rare Earth Elements—critical resources for high technology. United States Geological Survey Fact Sheet 087–02, 4 pp. <http://pubs.usgs.gov/fs/2002/fs087-02/> (last accessed 10 October 2014).
- Hayward, N., 2004. Structural geology of the Mount Keith mine area, Belmont, Western Australia, WMC Resources Ltd internal memorandum, 51 pp.
- Hegge, M.R., 1977. Geologic setting and relevant exploration features of the Jabiluka uranium deposits. *Proceedings of the Australasian Institute of Mining and Metallurgy*, 264, 19–32.
- Hegge, M.R. and Rowntree, J.C., 1978. Geologic setting and concepts of the origin of main deposits in the East Alligator River Region, NT, Australia. *Economic Geology*, 73, 1420–1429.
- Helix Resources Limited, 1993a. Helix Resources Limited 8<sup>th</sup> Annual Report, 36 pp.
- Helix Resources NL, 1993b. Hillview vermiculite project. *Minfo—New South Wales Mining and Exploration Quarterly*, 39, 6–8.
- Helix Resources Limited, 2004a. Helix Resources Limited Annual Report 2004, 4.
- Helix Resources Limited, 2004b. Helix Resources Limited Quarterly Report, Quarter ending 31 March 2004.
- Hergt, J.M., 1987. The origin and evolution of the Tasmanian Dolerites. PhD thesis, Australian National University.
- Hergt, J.M. and Brauns, C.M., 2001. On the origin of Tasmanian dolerites. *Australian Journal of Earth Sciences*, 48, 543–550.
- Hergt, J.M., Chappell, B.W., McCulloch, M.T., McDougall, I. and Chivas, A.R., 1989. Geochemical and isotopic constraints on the origin of the Jurassic dolerites of Tasmania. *Journal of Petrology*, 30, 841–883.
- Hickman, A.H., 1983. Geology of the Pilbara Block and its environs. Geological Survey of Western Australia, Bulletin 127, 268 pp.
- Hickman, A.H., 1997. A revision of the stratigraphy of Archaean greenstone successions in the Roebourne-Whundo area, west Pilbara. *Geological Survey of Western Australia Annual Review, 1996–97*, 76–81.
- Hickman, A.H. and Van Kranendonk, M.J., 2008. Archean crustal evolution and mineralization of the northern Pilbara Craton—a field guide. Geological Survey of Western Australia. *Record*, 2008/13, 79 pp.
- Hiebert, R.S., Bekker, A., Wing, B.A. and Rouxel, O.J., 2013. The role of paragneiss assimilation in the origin of the Voisey's Bay Ni-Cu sulfide deposit, Labrador: Multiple S and Fe isotope evidence. *Economic Geology*, 108, 1459–1469.
- Hill, R.E.T., Gole, M.J. and Barnes, S.J., 1987. Physical volcanology of komatiites. Excursion Guidebook Number 1. Geological Society of Australia, Western Australia, 74 pp.
- Hill, R.E.T., Barnes, S.J. and Perring, C.S., 1996. Komatiite volcanology and the volcanogenic setting of associated magmatic nickel deposits. In: Grimsey, E.J. and Neuss, I. (editors), *Nickel '96 Mineral*

- to Market. Kalgoorlie, 27–29 November 1996. Australasian Institute of Mining and Metallurgy, Publication Series 6/96, 91–95.
- Hill, R.E.T., Barnes, S.J. and Dowling, S.E., 2001. Komatiites of the Norseman-Wiluna greenstone belt, Western Australia; a field guide. Geological Survey of Western Australia, Perth, West. Aust., Australia.
- Hinchev, J.G., Hattori, K.H. and Lavigne, M.J., 2005. Geology, petrology, and controls on PGE mineralization of the southern Roby and Twilight Zones, Lac des Iles mine, Canada. *Economic Geology*, 100, 43–61.
- Hirschmann, M.M., Renne, P.R. and McBirney, A.R., 1997.  $^{40}\text{Ar}/^{39}\text{Ar}$  dating of the Skaergaard Intrusion. *Earth and Planetary Science Letters*, 146, 645–658.
- Hoatson, D.M., 1984. Potential for platinum group mineralisation in Australia. A review. Bureau of Mineral Resources Australia Record 1984/1, 84 pp.
- Hoatson, D.M., 1986. Geology of the Munni Munni layered intrusion: Preliminary Edition 1:20 000 BMR Australia Geology Geophysics geological map.
- Hoatson, D.M., 1990. Platinum group element mineralisation and potential in Australia. In: Hughes, F.E. (editor), *Geology of Mineral Deposits of Australia and Papua New Guinea*. Australasian Institute of Mining and Metallurgy, Melbourne, Monograph 14, 85–98.
- Hoatson, D.M., 1991a. The petrology and platinum-group element geochemistry of the Munni Munni and Mount Sholl layered mafic-ultramafic intrusions of the west Pilbara Block, Western Australia. PhD thesis, University of Melbourne, Australia, 510 pp.
- Hoatson, D.M., 1991b. Layered Archaean mafic-ultramafic intrusions of the west Pilbara Block, Western Australia. BMR Map 1:20 000 scale (includes the Munni Munni, Mount Sholl, Maitland, and Radio Hill layered intrusions).
- Hoatson, D.M., 1992. Field relationships, petrography, mineralogy, and geochemistry of the Munni Munni Complex. In: Hoatson, et al., *Petrology and Platinum-Group-Element Geochemistry of Archaean Layered Mafic-Ultramafic Intrusions, West Pilbara Block, Western Australia*. Australian Geological Survey Organisation Bulletin 242, 19–91.  
[http://www.ga.gov.au/corporate\\_data/5/Bull\\_242.pdf](http://www.ga.gov.au/corporate_data/5/Bull_242.pdf) (last accessed 10 October 2014).
- Hoatson, D.M., 1993a. Summary of geoscientific information for the East Kimberley, Western Australia, with specific reference to the Dixon Range 1:250 000 Sheet (SE 52–6) and Gordon Downs 1:250 000 Sheet (SE 52–10). Australian Geological Survey Organisation, Record 1993/32, 76 pp.
- Hoatson, D.M., 1993b. Correlation of structurally disrupted layered ultramafic-mafic intrusions in the East Kimberley: Is Big Ben part of the Panton intrusion? *AGSO Research Newsletter*, 19, 9–10.
- Hoatson, D.M., 1995. New mineral discoveries in the East Kimberley. *AGSO Research Newsletter*, 22, 9–11.
- Hoatson, D.M., 1998. Platinum-group element mineralisation in Australian Precambrian layered mafic-ultramafic intrusions. Special Jubilee Issue of Australian Geological Survey Organisation *Journal of Australian Geology, Geophysics*, 17, 139–151.
- Hoatson, D.M., 2000. Chapter 5. Geological setting, petrography, and geochemistry of the mafic-ultramafic intrusions. In: Hoatson, D.M. and Blake, D.H. (editors), *Geology and Economic Potential of the Palaeoproterozoic Layered Mafic-Ultramafic Intrusions in the East Kimberley, Western Australia*. Australian Geological Survey Organisation Bulletin 246, 99–162.
- Hoatson, D.M., 2001. Metallogenic potential of mafic-ultramafic intrusions in the Arunta Province, central Australia: Some new insights. *AGSO Research Newsletter*, 34, 29–33.
- Hoatson, D.M., 2008—[Web page]. New products from Geoscience Australia to assist nickel and platinum explorers: 2008. [http://www.ga.gov.au/corporate\\_data/70278/70278.pdf](http://www.ga.gov.au/corporate_data/70278/70278.pdf) (last accessed 10 October 2014).
- Hoatson, D.M. and Barnes, S.J., 1991. Mafic-ultramafic intrusions of the west Pilbara Block. In: Barnes, S.J. and Hill, R.E.T. (editors), *Mafic-ultramafic Complexes of Western Australia*. Excursion

- Guidebook No. 3. Sixth International Platinum Symposium, July 1991, Perth, WA. IAGOD and the Geological Society of Australia, 7–10.
- Hoatson, D.M. and Blake, D.H. (editors), 2000. Geology and economic potential of the Palaeoproterozoic layered mafic-ultramafic intrusions in the East Kimberley, Western Australia. Australian Geological Survey Organisation Bulletin 246, 476 pp. [http://www.ga.gov.au/corporate\\_data/34432/Bull\\_246.pdf](http://www.ga.gov.au/corporate_data/34432/Bull_246.pdf) (last accessed 10 October 2014).
- Hoatson, D.M. and England, R.N., 1986. Platinum group minerals from a layer in the Munni Munni Complex of the Pilbara Block. BMR Research Newsletter, 5, 1–2.
- Hoatson, D.M. and Glaser, L.M., 1989. Geology and economics of platinum-group metals in Australia. Bureau of Mineral Resources, Australia, Resource Report 5, 81 pp. [http://www.ga.gov.au/corporate\\_data/22202/Res\\_Rep\\_05.pdf](http://www.ga.gov.au/corporate_data/22202/Res_Rep_05.pdf) (last accessed 10 October 2014).
- Hoatson, D.M. and Keays, R.R., 1987a. Platinum group geochemistry of the Munni Munni layered intrusion, west Pilbara Block, Western Australia: An example of the formation of platiniferous sulphide horizons by crystal fractionation and magma mixing. In: von Gruenewaldt, G., Keays, R.R. and Hoatson, D.M. (compilers), Platinum-Group Element Deposits. Sydney 6-8 October 1987. The Earth Resources Foundation Workshop, University of Sydney, 50 pp.
- Hoatson, D.M. and Keays, R.R., 1987b. Platinum group geochemistry of the Munni Munni layered intrusion, west Pilbara Block, Western Australia: An example of the formation of platiniferous sulphide horizons by crystal fractionation and magma mixing. In: Platiniferous Horizons in Layered Intrusions. Abstracts. Sydney, 21 October 1987. University of New South Wales and Geological Society of Australia Symposium, 1–5.
- Hoatson, D.M. and Keays, R.R., 1989. Formation of platiniferous sulfide horizons by crystal fractionation and magma mixing in the Munni Munni layered intrusion, west Pilbara Block, Western Australia. *Economic Geology*, 84, 1775–1804.
- Hoatson, D.M. and Stewart, A.J., 2001. Field investigations of Proterozoic mafic-ultramafic intrusions in the Arunta Province, central Australia. *Geoscience Australia Record* 2001/39, 87 pp.
- Hoatson, D.M. and Sun, S.-S., 2002. Archean layered mafic-ultramafic intrusions in the west Pilbara Craton, Western Australia: a synthesis of some of the oldest orthomagmatic mineralizing systems in the world. *Economic Geology*, 97, 847–872.
- Hoatson, D.M. and Tyler, I., 1993. Prospective layered mafic-ultramafic intrusions in the East Kimberley. *AGSO Research Newsletter*, 18, 8–9.
- Hoatson, D.M., Wallace, D.A., Sun, S.-S., Macias, L.F., Simpson, C.J. and Keays, R.R., 1992. Petrology and platinum-group-element geochemistry of Archaean layered mafic-ultramafic intrusions, west Pilbara Block, Western Australia. Australian Geological Survey Organisation Bulletin 242, 320 pp. [http://www.ga.gov.au/corporate\\_data/5/Bull\\_242.pdf](http://www.ga.gov.au/corporate_data/5/Bull_242.pdf) (last accessed 10 October 2014).
- Hoatson, D.M., Sproule, R.A. and Lambert, D.D., 1997. Are there Voisey's Bay-type Ni-Cu-Co sulphide deposits in the East Kimberley of Western Australia? *AGSO Research Newsletter*, 27, 17–19.
- Hoatson, D.M., Sun, S.-S. and Clauoué-Long, J.C., 2005a. Proterozoic mafic-ultramafic intrusions in the Arunta Region, central Australia. Part 1: Geological setting and mineral potential. *Precambrian Research*, 142, 93–133.
- Hoatson, D.M., Sun, S.-S., Duggan, M.B., Davies, M.B., Daly, S.J. and Purvis, A.C., 2005b. Late Archean Lake Harris Komatiite, central Gawler Craton, South Australia: geologic setting and geochemistry. *Economic Geology*, 100, 349–374.
- Hoatson, D.M., Jaireth, S. and Jaques, A.L., 2006. Nickel sulfide deposits in Australia: Characteristics, resources, and potential. *Ore Geology Reviews*, 29, 177–241.
- Hoatson, D.M., Clauoué-Long, J.C. and Jaireth, S., 2008a. Guide to Using the 1:5 000 000 Map of Australian Proterozoic Mafic-Ultramafic Magmatic Events. *Geoscience Australia Record* 2008/15, 140 pp. [http://www.ga.gov.au/corporate\\_data/66624/Rec2008\\_015.pdf](http://www.ga.gov.au/corporate_data/66624/Rec2008_015.pdf) (last accessed 10 October 2014).

- Hoatson, D.M., Claoué-Long, J.C. and Jaireth, S., 2008b. Australian Proterozoic Mafic-Ultramafic Magmatic Events, Sheets 1 and 2 (1:10 000 000 scale maps), Geoscience Australia, Canberra, GeoCat 66114. [http://www.ga.gov.au/metadata-gateway/metadata/record/gcat\\_a05f7892-f7ac-7506-e044-00144fdd4fa6/Australian+Proterozoic+Mafic-Ultramafic+Magmatic+Events%3A+Map+Sheets+1+and+2](http://www.ga.gov.au/metadata-gateway/metadata/record/gcat_a05f7892-f7ac-7506-e044-00144fdd4fa6/Australian+Proterozoic+Mafic-Ultramafic+Magmatic+Events%3A+Map+Sheets+1+and+2) (last accessed 10 October 2014).
- Hoatson, D.M., Jaireth, S., Whitaker, A.J., Champion, D.C. and Claoué-Long, J.C., 2009a. Guide to Using the Australian Archean Mafic-Ultramafic Magmatic Events Map. Geoscience Australia Record 2009/41, 135 pp.
- Hoatson, D.M., Jaireth, S., Whitaker, A.J., Champion, D.C. and Claoué-Long, J.C., 2009b. Australian Archean Mafic-Ultramafic Magmatic Events, Sheet 1 (1:5 000 000 scale map) and Sheet 2 (1:3 000 000 and 1:6 000 000 scale maps), Geoscience Australia, Canberra, GeoCat 69347. [http://www.ga.gov.au/metadata-gateway/metadata/record/gcat\\_69347](http://www.ga.gov.au/metadata-gateway/metadata/record/gcat_69347) (last accessed 10 October 2014).
- Hoatson, D.M., Jaireth, S. and Miezitis, Y., 2011. The Major Rare-Earth-Element Deposits of Australia: Geological Setting, Exploration, and Resources. Geoscience Australia, Monograph, 204 pp.
- Hoeve J., Sibbald T.I.I., Ramaekers P. and Lewry J.F., 1980. Athabasca Basin unconformity-type uranium: a special type of sandstone-type deposits? In: Ferguson, J. and Goleby, A.B. (editors), Uranium in the Pine Creek Geosyncline. International Atomic Energy Agency, Vienna, 575–594.
- Hollis, J.A., Orth, K., Tyler, I.M., Kirkland, C.L. and Wingate, M.T.D., 2013. Setting and prospectivity of a large igneous province: the 1800 Ma Hart Dolerite, Kimberley Region. GSWA 2013 extended abstracts: promoting the prospectivity of Western Australia. Geological Survey of Western Australia, Record 2013/2, 9–13.
- Holwell, D.A. and Keays, R.R., 2014. The formation of low-volume, high-tenor magmatic PGE-Au sulfide mineralization in closed systems: evidence from precious and base metal geochemistry of the Platinova Reef, Skaergaard Intrusion, East Greenland. *Economic Geology*, 109, 387–406.
- Hopf, S. and Head, D.L., 1998. Mount Keith nickel deposit. In: Berkman, D.A. and Mackenzie, D.H. (editors), *Geology of Australian and Papua New Guinean Mineral Deposits*. Australasian Institute of Mining and Metallurgy, Melbourne, Monograph 22, 307–314.
- Horwitz, R.C., 1988a. Contributed discussion to 'The nickel-copper deposit at Radio Hill, Karratha, Western Australia' by de Angelis, Hoyle, Peters and Wightman. *Australasian Institute of Mining and Metallurgy, Bulletin and Proceedings*, 293, 57–58.
- Horwitz, R.C., 1988b. The buried alluvial channels of the Fifield, Tullamore, Tottenham and Honeybugle areas of New South Wales. Notes to accompany generalised geological maps. Helix Resources NL Report.
- Howard, H.M., Smithies, H.R., Kirkland, C.L., Evins, P.M. and Wingate, M.T.D., 2009. Age and geochemistry of the Alcurra suite in the West Musgrave province and implications for orthomagmatic Ni-Cu-PGE mineralization during the Giles event. *Geological Survey of Western Australia Record* 2009/16, 16 pp.
- Hronsky, J.M.A., 2007. The history of nickel exploration in the Yilgarn Craton of Western Australia. Western Mining Services LLC. MEGWA PowerPoint presentation, 15 August 2007.
- Hronsky, J.M.A. and Groves, D.I., 2008. Science of targeting: definition, strategies, targeting and performance measurements. *Australian Journal of Earth Sciences*, 55, 3–12.
- Hronsky, J.M.A. and Schodde, R.C., 2006. Nickel exploration history of the Yilgarn Craton: From the nickel boom to today. In: Barnes, S.J. (editor), *Nickel Deposits of the Yilgarn Craton: Geology, Geochemistry, and Geophysics Applied to Exploration*. *Economic Geology Special Publication Number 13*, 1–11.
- Hudson, D.R., 1986. Platinum-group minerals from the Kambalda nickel deposits, Western Australia. *Economic Geology*, 81, 1218–1225.
- Hudson, D.R. and Donaldson, M.J., 1984. Mineralogy of platinum group elements in the Kambalda nickel deposits, Western Australia. In: Buchanan, D.L. and Jones, M.J. (editors), *Sulphide Deposits in Mafic and Ultramafic Rocks*. The Institution of Mining and Metallurgy, London, 55–61.

- Hudson, D.R. and Horwitz, R.C., 1985. Mineralogy and geological setting of a new occurrence of platinum group minerals, between Roebourne and Karratha, Western Australia. Commonwealth Scientific and Industrial Research Organisation, Division of Mineralogy and Geochemistry, Research Review, 1985, 79–80.
- Hudson, D.R., Elias, M. and Barnes, S.J., 1991. Chapter 3: Komatiite-hosted nickel sulphide deposits of the Kambalda-Widgiemooltha region. In: Barnes, S.J. and Hill, R.E.T. (editors), *Mafic-Ultramafic Complexes of Western Australia*, Excursion Guidebook No. 3. Sixth International Platinum Symposium, July 1991, Perth, Western Australia. IAGOD and the Geological Society of Australia, 19–25.
- Hughes, T.D., 1965. Nickel mineralization in Tasmania. In: McAndrew, J. (editor), *Geology of Australian Ore Deposits*. Proceedings Eighth Commonwealth Mining and Metallurgical Congress, 1, 523–524.
- Hulbert, L.J. and Eckstrand, R., 2005. Magmatic nickel-copper-platinum group element deposits. Abstract. Prospectors and Developers Association of Canada Convention 2005, Toronto, Canada, March 6-9, 2005 (C-D Rom).
- Hulbert, L.J., Duke, J.M., Eckstrand, O.R., Lydon, J.W., Scoates, R.F.J., Cabri, L.J. and Irvine, T.N., 1988. Geological environments of the platinum group elements. Geological Survey of Canada, Open File 1440, 148 pp.
- Hulbert, L.J., Hamilton, M.A., Horan, M.F. and Scoates, R.F.J., 2005. U-Pb zircon and Re-Os isotope geochronology of mineralized ultramafic intrusions and associated nickel ores from the Thompson nickel belt, Manitoba, Canada. *Economic Geology*, 100, 29–41.
- Huppert, H.E. and Sparks, R.S.J., 1985. Komatiites I: Eruption and flow. *Journal of Petrology*, 26, 694–725.
- Huppert, H.E., Sparks, R.S.J., Turner, J.S. and Arndt, N.T., 1984. Emplacement and cooling of komatiite lavas. *Nature*, 309, 19–22.
- Huston, D.L., Blewett, R.S., Sweetapple, M., Brauhart, C., Cornelius, H. and Collins, P.L.F., 2001. Metallogensis of the north Pilbara granite-greenstones, Western Australia—a field guide. Geological Survey of Western Australia Record 2001/11, 87 pp.
- Huston, D.L., Sun, S.-S., Blewett, R., Hickman, A., Van Kranendonk, M., Phillips, D., Baker, D. and Brauhart, C., 2002. The timing of mineralization in the Archean North Pilbara Terrain, Western Australia. *Economic Geology*, 97, 733–755.
- Huston, D.L., Blewett, R.S., Skirrow, R., McQueen, A., Wang, J., Jaques, L., Waters, D. and Bierlein, F., 2012. Foundations of wealth; Australia's major mineral provinces. In: Blewett, R.S. (editor), *Shaping a Nation: A Geology of Australia*. Geoscience Australia and ANU E Press, Canberra, 380–431.
- Huston, D.L., Champion, D.C. and Cassidy, K.F., 2014. Tectonic controls on the endowment of Neoproterozoic cratons in volcanic-hosted massive sulfide deposits: evidence from lead and neodymium isotopes. *Economic Geology*, 109, 11–26.
- Impact Minerals Limited, 2013. Impact Minerals Limited Annual Report 2013, 100 pp, <http://www.impactminerals.com.au/userfiles/file/Impact%20Annual%20Report%202013.pdf> (last accessed 10 October 2014).
- Impact Minerals Limited, 2014a—[Web page]. Yarrabubba and Quinns Lake Projects: Nickle – Copper – PGE. <http://www.impactminerals.com.au/?page=92> (last accessed 10 October 2014).
- Impact Minerals Limited, 2014b. Impact Minerals Limited announcement to the Australian Securities, 21 May 2014, 9 pp.
- INAL Staff, 1975. Nickeliferous laterite deposits of the Rockhampton area, Queensland. In: Knight, C.L. (editor), *Economic Geology of Australia and Papua New Guinea*. 1. Metals. Australasian Institute of Mining and Metallurgy, Monograph 5, 1001–1006.
- Independence Group NL., 2010. Independence Group NL Quarterly Report for the Three Months ended 31 March 2010, 28 pp.

- Info Comm., 2009—[Web page]. UNCTAD: United Nations Conference on Trade and Development. Info comm., metals minerals, characteristics. [http://www.unctad.info/en/Infocomm/Metals\\_Minerals/Platinum2/Characteristics/](http://www.unctad.info/en/Infocomm/Metals_Minerals/Platinum2/Characteristics/) (last accessed 10 October 2014).
- Irvine, T.N., 1974. Petrology of the Duke Island Ultramafic Complex, southeastern Alaska. Geological Society of America, Memoir 138, 240 pp.
- Irvine, T.N., 1975. Crystallization sequences in the Muskox intrusion and other layered intrusions, II. Origin of chromitite layers and similar deposits of other magmatic ores. *Geochimica et Cosmochimica Acta*, 39, 991–1020.
- Irvine, T.N., 1977. Origin of chromitite layers in the Muskox intrusion and other stratiform intrusions: a new interpretation. *Geology*, 5, 273–277.
- Irvine, T.N., 1982. Terminology for layered intrusions. *Journal of Petrology*, 23, 127–162.
- Ivanic, T.J., 2009. The Windimurra and Narndee mafic-ultramafic intrusions: mineralization and geological context. *Geological Survey of Western Australia, Record 2009/2*, 4–6.
- Ivanic, T.J., Wingate, M.T.D., Kirkland, C.L., Van Kranendonk, M.J. and Wyche, S., 2010. Age and significance of voluminous mafic-ultramafic magmatic events in the Murchison Domain, Yilgarn Craton. *Australian Journal of Earth Sciences*, 57, 597–614.
- Jackson, D.G. and Andrew, R.L., 1988. The Kintyre uranium deposit: An exploration case history. In: *The Second International Conference on Prospecting in Arid Terrain, Perth, Western Australia*. The Australasian Institute of Mining and Metallurgy, 79–82.
- Jackson D.G. and Andrew R.L., 1990. Kintyre uranium deposit. In: Hughes, F.E. (editor), *Geology of the Mineral Deposits of Australia and Papua New Guinea*. Australasian Institute of Mining and Metallurgy, Melbourne, Monograph 14, 653–658.
- Jaireth, S., 1992. The calculated solubility of platinum and gold in oxygen-saturated fluids and the genesis of platinum-palladium and gold mineralization in the unconformity-related uranium deposits. *Mineralium Deposita*, 27, 42–54.
- Jaireth, S., Hoatson, D.M. and Mieziotis, Y., 2014. Geological setting and resources of the major rare-earth-element deposits in Australia. *Ore Geology Reviews*, 62, 72–128.
- Jaquet, J.B., 1893. Progress report, appendix 4C. New South Wales Department of Mines Annual Report 1892, 142–145.
- Jaquet, J.B., 1896. Platinum in New South Wales. *Record Geological Survey of New South Wales* 5, 33–39.
- Jefferson, C.W., Thomas, D.J., Gandhi, S.S., Ramaekers, P., Delaney, G., Brisbin, D., Cutts, C., Quirt, D., Portella, P. and Olson, R.A., 2007. Unconformity-associated uranium deposits of the Athabasca Basin, Saskatchewan and Alberta. In: Goodfellow, W.D. (editor), *Mineral Deposits of Canada: A Synthesis of Major Deposit-Types, District Metallogeny, the Evolution of Geological Provinces, and Exploration Methods*. Geological Association of Canada, Mineral Deposits Division, Special Publication No. 5, 273–305.
- Johan, Z., 2002. Alaskan-type complexes and their platinum-group element mineralization. In: Cabri, L.J. (editor), *The Geology, Geochemistry, Mineralogy and Mineral Beneficiation of Platinum-Group Elements*. Canadian Institute of Mining, Metallurgy and Petroleum, Special Volume 54, 669–719.
- Johan, Z., Ohnenstetter, M., Slansky, E., Barron, L. M. and Suppel, D., 1989. Platinum mineralization in the Alaskan-type intrusive complexes near Fifield, New South Wales, Australia. Part I. Platinum-group minerals in clinopyroxenites of the Kelvin Grove prospect, Owendale intrusion. *Mineralogy and Petrology*, 40, 289–309.
- Johan, Z., Slansky, E., Ohnenstetter, M., Barron, L.M. and Suppel, D., 1990a. Platinum mineralization in the Alaskan-type intrusive complexes near Fifield, N.S.W., Australia: Platinum-group minerals in placer deposits at Fifield. *Geological Survey of New South Wales Department of Mineral Resources, Unpublished Mineralogical Report 90/19, Geological Survey Report Number GS1990/282*, 36 pp.

- Johan, Z., Slansky, E. and Ohenstetter, M., 1990b. Platinum mineralization in the Alaskan-type intrusive complexes near Fifield, N.S.W., Australia: Isoferroplatinum nuggets from Milverton. Geological Survey of New South Wales Department of Mineral Resources, Unpublished Mineralogical Report 90/21, Geological Survey Report Number GS1990/351, 11 pp.
- Johnson Matthey, 1985. Platinum 1985. Johnson Matthey Public Limited Company, London.
- Johnson Matthey, 2001. Platinum 2001. Johnson Matthey Public Limited Company, Hertfordshire, England, 52 pp. <http://www.platinum.matthey.com/media/820449/pt2001.pdf> (last accessed 10 October 2014).
- Johnson Matthey, 2002. Platinum 2002. Johnson Matthey Public Limited Company, Hertfordshire, England, 56 pp. [http://www.platinum.matthey.com/media/820439/pt\\_2002.pdf](http://www.platinum.matthey.com/media/820439/pt_2002.pdf) (last accessed 10 October 2014).
- Johnson Matthey, 2003. Platinum 2003. Johnson Matthey Public Limited Company, Hertfordshire, England, 48 pp. <http://www.platinum.matthey.com/media/820425/pt2003-fullreport.pdf> (last accessed 10 October 2014).
- Johnson Matthey, 2004. Platinum 2004. Johnson Matthey Public Limited Company, Hertfordshire, England, 56 pp. [http://www.platinum.matthey.com/media/820401/04\\_contents.pdf](http://www.platinum.matthey.com/media/820401/04_contents.pdf) (last accessed 10 October 2014).
- Johnson Matthey, 2005. Platinum 2005. Johnson Matthey Public Limited Company, Hertfordshire, England, 56 pp. [http://www.platinum.matthey.com/media/820378/05\\_full\\_report\\_3.3mb.pdf](http://www.platinum.matthey.com/media/820378/05_full_report_3.3mb.pdf) (last accessed 10 October 2014).
- Johnson Matthey, 2006. Platinum 2006. Johnson Matthey Public Limited Company, Hertfordshire, England, 56 pp. [http://www.platinum.matthey.com/media/820350/06\\_full\\_report.pdf](http://www.platinum.matthey.com/media/820350/06_full_report.pdf) (last accessed 10 October 2014).
- Johnson Matthey, 2007. Platinum 2007. Johnson Matthey Public Limited Company, Hertfordshire, England, 56 pp. [http://www.platinum.matthey.com/media/820326/complete\\_publication.pdf](http://www.platinum.matthey.com/media/820326/complete_publication.pdf) (last accessed 10 October 2014).
- Johnson Matthey, 2008. Platinum 2008. Johnson Matthey Public Limited Company, Hertfordshire, England, 60 pp. [http://www.platinum.matthey.com/media/820291/08\\_complete\\_publication.pdf](http://www.platinum.matthey.com/media/820291/08_complete_publication.pdf) (last accessed 10 October 2014).
- Johnson Matthey, 2011. Johnson Matthey 2011 Interim Review. Supply and Demand Tables. [http://www.platinum.matthey.com/uploaded\\_files/Int\\_2011/platinum\\_book\\_complete\\_publication.pdf](http://www.platinum.matthey.com/uploaded_files/Int_2011/platinum_book_complete_publication.pdf) (last accessed 10 October 2014).
- Johnson Matthey, 2013a—[Web page]. Platinum Today. Market data tables: supply and demand for platinum, palladium, rhodium, iridium, and ruthenium. <http://www.platinum.matthey.com/publications/market-data-tables/> (last accessed 10 October 2014).
- Johnson Matthey, 2013b. Platinum 2013. Johnson Matthey Public Limited Company, Hertfordshire, England, 57 pp. [http://www.platinum.matthey.com/media/1614079/platinum\\_2013.pdf](http://www.platinum.matthey.com/media/1614079/platinum_2013.pdf) (last accessed 10 October 2014).
- Johnston J.D. and Wall V.J., 1984. Why unconformity-related U deposits are unconformity related. Geological Society of Australia; Abstracts 12, 285–287.
- Joly, A., Aitken, A.R.A., Dentith, M., Porwal, A.K. and Smithies, R.H., 2013. Mineral prospectivity analysis of the West Musgrave Province, GSWA Report. Geological Survey of Western Australia, Perth.
- Jones, G.J., 1991. The Kars and Gilgai intrusive complexes and associated PGM mineralisation, Fifield, NSW. In: Elliott, S.J. and Martin, A.R (editors), Geology and Mineralisation of the Fifield Platinum Province, New South Wales. Sixth International Platinum Symposium, Perth, Western Australia. Guidebook for the Pre-Symposium Field Excursion. Geological Society of Australia, 35–40.

- Jones, L.E.A., Ivanic, T.J. and Costello, R.D., 2012. Seismic reflection imaging of the mafic-ultramafic Windimurra Igneous Complex, Yilgarn Craton, Western Australia. 22nd ASEG International Geophysical Conference and Exhibition, 26–29 February 2012, Brisbane, Australia, 4 pp.
- Jubilee Mines NL., 2005. Jubilee Mines NL announcement to the Australian Securities Exchange Media, 9 June 2005, 3 pp.
- Jugo, P.J., Luth, R.W. and Richards, J.P., 2005. Experimental data on the speciation of sulfur as a function of oxygen fugacity in basaltic melts. *Geochimica et Cosmochimica Acta*, 69, 497–503.
- Kalix, Z., Fraser, L.M. and Rawson, R.I., 1966. Platinum group metals. In: Kalix, Z., Fraser, L.M. and Rawson, R.I. (editors), *Australian Mineral Industry: Production and Trade, 1842–1964*. Bureau of Mineral Resources, Australia, Bulletin 81, 343–348.
- Kamo, S.L., Czamanske, G.K., Amelin, Y., Fedorenko, V.A., Davis, D.W. and Trofimov, V.R., 2003. Rapid eruption of Siberian flood-volcanic rocks and evidence for coincidence with the Permian-Triassic boundary and mass extinction at 251 Ma. *Earth and Planetary Science Letters*, 214, 75–91.
- Keays, R.R., 1995. The role of komatiitic and picritic magmatism and S-saturation in the formation of ore deposits. *Lithos*, 34, 1–18.
- Keays, R.R. and Campbell, I.H., 1981. Precious metals in the Jimberlana Intrusion, Western Australia: Implications for the genesis of platiniferous ores in layered intrusions. *Economic Geology*, 76, 1118–1141.
- Keays, R.R. and Davison, R.M., 1976. Palladium, iridium and gold in the ores and host rocks of nickel-sulfide deposits in Western Australia. *Economic Geology*, 71, 1214–1228.
- Keays, R.R. and Green, A.H., 1974. Geology and gold mineralisation in the Wood's Point dyke swarm. Geological Survey of Victoria Report 1974/12.
- Keays, R.R. and Kirkland, M.C., 1972. Hydrothermal mobilization of gold from copper-nickel sulphides and ore genesis at the Thomson River copper mine, Victoria, Australia. *Economic Geology*, 67, 1263–1275.
- Keays, R.R., Ross, J.R. and Woolrich, P., 1981a. Precious metals in volcanic peridotite-associated nickel sulfide deposits in Western Australia. II: Distribution within the ores and host rocks at Kambalda. *Economic Geology*, 76, 1645–1674.
- Keays, R.R., Sewell, D.K.B. and Mitchell, R.H., 1981b. Platinum and palladium minerals in upper mantle-derived lherzolites. *Nature*, 294, 646–648.
- Kerr, A. and Leitch, A.M., 2005. Self-destructive sulfide segregation systems and the formation of high-grade magmatic ore deposits. *Economic Geology*, 100, 311–332.
- Kimbrough, D. and Brown, A.V., 1992. Zircon Pb/U age of 520 Ma for tonalite associated with the Heazlewood Ultramafic/Mafic Complex, western Tasmania. Tasmania Department of Mines Report, 1992/24.
- Kinhill, 1996. Jabiluka Project. Draft Environmental Impact Statement. Unpublished report.
- Kinloch, E.D., 1982. Regional trends in the platinum-group mineralogy of the critical zone of the Bushveld Complex, South Africa. *Economic Geology*, 77, 1328–1347.
- Kinnaird, J.A., Hutchinson, D., Schurmann, L., Nex, P.A.M. and de Lange, R., 2005. Petrology and mineralization of the southern Plat Reef; northern limb of the Bushveld Complex, South Africa. *Mineralium Deposita*, 40, 576–597.
- Kinny, P.D., Williams, I.S., Froude, D.O., Ireland, T.R. and Compston, W., 1988. Early Archaean zircon ages from orthogneisses and anorthosites at Mount Narryer, Western Australia. *Precambrian Research*, 38, 325–341.
- Kinny, P.D., Wijbrans, J.R., Froude, D.O., Williams, I.S. and Compston, W., 1990. Age constraints on the geological evolution of the Narryer Gneiss Complex, Western Australia. *Australian Journal of Earth Sciences*, 37, 51–69.
- Knutson, J. and Currie, K., 1990. The Mud Tank Carbonatite, Northern Territory: an example of metasomatism at mid-crustal levels. *BMR Research Newsletter*, 12, 11–12.

- Knox-Robinson, C.M. and Wyborn, L.A.I., 1997. Towards a holistic exploration strategy: using geographic information systems as a tool to enhance exploration. *Australian Journal of Earth Sciences*, 44, 453–463.
- Koek, M., Kreuzer, O.P., Maier, W.D., Porwal, A.K., Thompson, M. and Guj, P., 2009. Australian platinum group metal (PGM) exploration in the context of the global PGM industry. *Specialist Group in Economic Geology. SGEF Newsletter* 3, July 2009, 4–10.
- Koek, M., Kreuzer, O.P., Maier, W.D., Porwal, A.K., Thompson, M. and Guj, P., 2010. A review of the PGM industry, deposit models and exploration practices: Implications for Australia's PGM potential. *Resources Policy*, 35, 20–35.
- Komninou, A. and Sverjensky, D.A., 1996. Geochemical modelling of the formation of an unconformity type uranium deposit. *Economic Geology*, 91, 590–606.
- Korsch, M.J. and Gulson, B.L., 1986. Nd and Pb isotopic studies of an Archaean layered mafic-ultramafic complex, Western Australia, and implications for mantle heterogeneity. *Geochimica et Cosmochimica Acta*, 50, 1–10.
- Kositcin, N., Brown, S.J.A., Barley, M.E., Krapez, B., Cassidy, K.F. and Champion, D.C., 2008. SHRIMP U-Pb zircon age constraints on the Late Archaean tectonostratigraphic architecture of the Eastern Goldfields Superterrane, Yilgarn Craton, Western Australia. *Precambrian Research*, 161, 5–33.
- Kozyrev, S.M., Komarova, M.Z., Emelina, L.N., Oleshkevich, O.I., Yakovleva, O.A., Lyalinov, D.V. and Maximov, V.I., 2002. The mineralogy and behaviour of PGM during processing of the Noril'sk-Talnakh PGE-Cu-Ni ores. In: Cabri, L.J. (editor), *The Geology, Geochemistry, Mineralogy and Mineral Beneficiation of Platinum-Group Elements*. Canadian Institute of Mining, Metallurgy and Petroleum, Special Volume 54, 757–791.
- Kreuzer, O., 2009. Boldjet Proprietary Limited, Final report for the period 08 September 2008 to 30 January 2009, EL 04/2008 (Poatina), 5 pp.
- Krogh, T.E., Davis, D.W. and Corfu, F., 1984. Precise U-Pb zircon and baddeleyite ages for the Sudbury area. In: Pye, E.G., Naldrett, A.J. and Giblin, P.E. (editors), *The Geology and Ore Deposits of the Sudbury Structure*. Ontario Geological Survey, Special Volume 1, 431–446.
- Krstic, S. and Tarkian, M., 1997. Platinum-group minerals in gold-bearing placers associated with the Veluce Ophiolite complex, Yugoslavia. *Canadian Mineralogist*, 35, 1–21.
- Kruger, F.J., Cawthorn, R.G., Meyer, P.S. and Walsh, K.L., 1986. Sr-isotopic, chemical and mineralogical variations across the pyroxenite marker and in the Upper Zone of the western Bushveld Complex. *Geo-congress '86, 21st Congress, Johannesburg*. Geological Society of South Africa, Abstracts, 609–612.
- Kucha, H., 1975. Preliminary report on the occurrence of palladium minerals in Zechstein rocks of the Fore-Sudetic Monocline. *Mineralogia Polonica*, 6, 87–91.
- Kucha, H., 1982. Platinum-group minerals in the Zechstein copper deposits, Poland. *Economic Geology*, 77, 1578–1591.
- Kucha, H., 1985. Platinum-group metals in the Zechstein copper deposits, Poland—A reply. *Economic Geology*, 80, 519–520.
- Kucha, H. and Pawlikowski, M., 1986. Two-brine model for the genesis of strata-bound Zechstein deposits (Kupferschiefer type), Poland. *Mineralium Deposita*, 21, 70–80.
- Kucha, H. and Przybyowicz, W., 1999. Noble metals in organic matter and clay-organic matrices, Kupferschiefer, Poland. *Economic Geology*, 94, 1137–1162.
- Kwitko, R.R., Cabral, A.R., Lehmann, B., Laflamme, J.H.G., Cabri, L.J., Criddle, A.J. and Galbiatti, H.F., 2002. Hongshiite, Pt-Cu, from itabirite-hosted Au-Pd-Pt mineralization (jacutinga), Itabira District, Minas Gerais, Brazil. *The Canadian Mineralogist*, 40, 711–723.
- Lambert, D.D., Foster, J.G., Frick, L.R., Hoatson, D.M. and Purvis, A.C., 1998. Application of the Re-Os isotopic system to the study of Precambrian magmatic sulfide deposits of Western Australia. *Australian Journal of Earth Sciences*, 45, 265–284.

- Lambert, I., Jaireth, S., McKay, A. and Mieziitis, Y., 2005. Why Australia has so much uranium. AGSO News, December 2005, 80, 7–11.
- Langworthy, A.P. and Black, L.P., 1978. The Mordor Complex: a highly differentiated potassic intrusion with kimberlitic affinities in central Australia. *Contributions to Mineralogy and Petrology*, 67, 51–62.
- Lavigne, M.J. and Michaud, M.J., 2001. Geology of North American Palladium Limited's Roby Zone deposit, Lac des Iles. *Exploration and Mining Geology*, 10, 1–17.
- Lavigne, M.J., Michaud, M.J. and Rickard, J., 2005. Discovery and geology of the Lac des Iles palladium deposits. In: Mungall, J.E. (editor), *Exploration for Platinum-Group Element Deposits*. Mineralogical Association of Canada Short Course 35, Oulu, Finland, 369–390.
- Lazarenkov, V.G., Tikhomirov, I.N., Zhidkov, A. Ya. and Talovina, I.V., 2005. Platinum group metals and gold in supergene nickel ores of the Moa and Nikaro deposits (Cuba). *Lithology and Mineral Resources*, 40, 527–532.
- Lee, C.A., 1996. A review of mineralization in the Bushveld Complex and some other layered intrusions. In: Cawthorn, R.G. (editor), *Layered Intrusions*, Amsterdam, The Netherlands, Elsevier, 103–145.
- Lehmann, J., Arndt, N., Windley, B., Zhou, M., Wang, C.Y. and Harris, C., 2007. Field relationships and geochemical constraints on the emplacement of the Jinchuan Intrusion and its Ni-Cu-PGE sulfide deposit, Gansu, China. *Economic Geology*, 102, 75–94.
- Leitch, E.C., 1980. The Great Serpentine Belt in New South Wales: Diverse mafic-ultramafic complexes set in a Palaeozoic arc. In: Panayiotou, A. (editor), *Ophiolites*. Proceedings International Ophiolite Symposium, Cyprus 1979. Geological Survey Department, Republic of Cyprus, 637–648.
- Leshner, C.M., 1983. Localisation and genesis of komatiite-associated Fe-Ni-Cu sulfide mineralization of Kambalda, Western Australia. PhD thesis, University of Western Australia, Australia, 318 pp.
- Leshner, C.M., 1989. Komatiite-associated nickel sulfide deposits. In: Whitney, J.A. and Naldrett, A.J. (editors), *Ore Deposition Associated with Magmas*. Society of Economic Geologists, University of Texas, El Paso, USA, *Reviews in Economic Geology Volume 4*, 45–101.
- Leshner, C.M., 2004. Footprints of magmatic Ni-Cu(-PGE) systems. In: Muhling, J., Goldfarb, R., Vielreicher, N., Bierlein, F., Stumpfl, E., Groves, D.I. and Kenworthy, S. (editors), *SEG 2004: Predictive Mineral Discovery under Cover*. Extended Abstracts. Centre of Global Metallogeny, The University of Western Australia, Publications No. 33, 27 September-1 October 2004, Perth, Western Australia, 117–120.
- Leshner, C.M. and Keays, R.R., 1984. Metamorphically and hydrothermally mobilized Fe-Ni-Cu sulphides at Kambalda, Western Australia. In: Buchanan, D.L. and Jones, M.J. (editors), *Sulphide Deposits in Mafic and Ultramafic Rocks*. The Institution of Mining and Metallurgy, London, 62–69.
- Leshner, C.M. and Keays, R.R., 2002. Komatiite-associated Ni-Cu-PGE deposits: geology, mineralogy, geochemistry, and genesis. In: Cabri, L.J. (editor), *The Geology, Geochemistry, Mineralogy and Mineral Beneficiation of Platinum-Group Elements*. Canadian Institute of Mining, Metallurgy and Petroleum, Special Volume 54, 579–617.
- Leshner, C.M., Arndt, N.T. and Groves, D.I., 1984. Genesis of komatiite-associated nickel sulphide deposits at Kambalda, Western Australia: A distal volcanic model. In: Buchanan, D.L. and Jones, M.J. (editors), *Sulphide Deposits in Mafic and Ultramafic Rocks*. The Institution of Mining and Metallurgy, London, 70–80.
- Leshner, C.M., Burnham O.M., Keays, R.R., Barnes, S.J. and Hulbert, L., 2001. Geochemical discrimination of barren and mineralized komatiites associated with magmatic Ni-Cu-(PGE) sulphide deposits. *Canadian Mineralogist*, 39, 673–696.
- Lewis, D.G., 2011. The early life of Smithson Tennant FRS (1761–1815). *Platinum Metals Review*, 55, 196–200.
- Li, C. and Naldrett, A.J., 1999. Geology and petrology of the Voisey's Bay intrusion: reaction of olivine with sulfide and silicate liquids. *Lithos*, 47, 1–31.

- Li, C. and Naldrett, A.J., 2000. Melting reactions of gneissic inclusions with enclosing magma at Voisey's Bay: Implications with respect to ore genesis. *Economic Geology*, 95, 801–814.
- Li, C. and Ripley, E.M., 2005. Empirical equations to predict the sulfur content of mafic magmas at sulfide saturation and applications to magmatic sulfide deposits. *Mineralium Deposita*, 40, 218–230.
- Li, C. and Ripley, E.M., 2011. The giant Jinchuan Ni-Cu-(PGE) deposit; tectonic setting, magma evolution, ore genesis, and exploration implications. *Reviews in Economic Geology* 17, 163–180.
- Li, C., Maier, W.D. and de Waal, S.A., 2001a. Magmatic Ni-Cu versus PGE deposits; contrasting genetic controls and exploration implications. *South African Journal of Geology*, 104, 309–318.
- Li, C., Naldrett, A.J. and Ripley, E.M., 2001b. Critical factors for the formation of a nickel-copper deposit in an evolved magma system: lessons from a comparison of the Pants Lake and Voisey's Bay sulfide occurrences in Labrador, Canada. *Mineralium Deposita*, 36, 85–92.
- Li, C., Ripley, E.M. and Naldrett, A.J., 2003. Compositional variations of olivine and sulfur isotopes in the Noril'sk and Talnakh Intrusions, Siberia: Implications for ore-forming processes in dynamic magma conduits. *Economic Geology*, 98, 69–86.
- Li, C., Ripley, E.M. and Naldrett, A.J., 2009. A new genetic model for the giant Ni-Cu-PGE sulfide deposits associated with the Siberian flood basalts. *Economic Geology*, 104, 291–301.
- Li, X., Su, L., Song, B. and Liu, D., 2004. SHRIMP U-Pb zircon age of the Jinchuan ultramafic intrusion and its geological significance. *Chinese Science Bulletin* 49, 420–422.
- Lightfoot, P.C., Keays, R.R., Evans-Lamswood, D. and Wheeler, R., 2012. S saturation history of Nain Plutonic Suite mafic intrusions: origin of the Voisey's Bay Ni-Cu-Co sulfide deposit, Labrador, Canada. *Mineralium Deposita*, 47, 23–50.
- LionOre International Mining Limited, 2004. LionOre Mining International Limited Approval for Waterloo Nickel Project, News Release, 1 pp.  
<http://www.thefreelibrary.com/LIONORE+MINING+INTERNATIONAL+LTD+-+Approval+for+Waterloo+Nickel...-a0131805576> (last accessed 10 October 2014).
- Lisitsin, V., González-Álvarez, I. and Porwal, A., 2013. Regional prospectivity analysis for hydrothermal-remobilised nickel mineral systems in western Victoria, Australia. *Ore Geology Reviews Special Issue* 52, 100–112.
- Locmelis, M., Barnes, S.J., Pearson, N.J. and Fiorentini, M.L., 2009. Anomalous sulfur-poor platinum-group element mineralization in komatiitic cumulates, Mount Clifford, Western Australia. *Economic Geology*, 104, 841–855.
- Locmelis, M., Pearson, N.J., Barnes, S.J. and Fiorentini, M.L., 2011. Ruthenium in komatiitic chromite. *Geochimica et Cosmochimica Acta*, 75, 3645–3661.
- Locmelis, M., Fiorentini, M.L., Barnes, S.J. and Pearson, N.J., 2013. Ruthenium variation in chromite from komatiites and komatiitic basalts—a potential mineralogical indicator for nickel sulfide mineralization. *Economic Geology*, 108, 355–364.
- Lorand, J.P., 1990. Are spinel lherzolite xenoliths representative of the abundance of sulfur in the upper mantle? *Geochimica et Cosmochimica Acta*, 54, 1487–1492.
- Lorand, J. P., Luguët, A. and Alard, O., 2008. Platinum-group elements: a new set of key tracers for the Earth's interior. *Elements*, 4, 247–252.
- Ludwig, K.R., Grauch, R.I., Nutt, C.J., Nash, J.T., Frishman, D. and Simmons, K.R., 1987. Age of uranium mineralization at the Jabiluka and Ranger deposits, Northern Territory, Australia: New U-Pb Isotope Evidence. *Economic Geology*, 82, 857–874.
- Maas, R., 1989. Nd–Sr isotope constraints on the age and origin of unconformity-type uranium deposits in the Alligator Rivers uranium field, Northern Territory, Australia. *Economic Geology*, 84, 64–90.
- Macdonald, A.J., 1988. The platinum group element deposits: classification and genesis. In: Roberts, R.G. and Sheahan, P.A. (editors), *Ore Deposit Models*. Geoscience Canada, Reprint Series 3, 117–131.

- Macias, L.F. and Simpson, C.J., 1990. Image processing of TM data over ultramafic complexes. Proceedings of the 5th Australasian Remote Sensing Conference, 1. Committee of the 5th Australasian Remote Sensing Conference Incorporated 1990, Western Australia, 616–627.
- MacNevin, A.A., 1975a. The Great Serpentinite Belt. In: Markham, N.L. and Basden, H. (editors), The Mineral Deposits of New South Wales. Geological Survey of New South Wales, New South Wales Department of Mines, Sydney, 392–403.
- MacNevin, A.A., 1975b. The Gordonbrook Serpentinite Belt. In: Markham, N.L. and Basden, H. (editors), The Mineral Deposits of New South Wales. Geological Survey of New South Wales, New South Wales Department of Mines, Sydney, 420–427.
- Magma Metals Limited, 2006. Magma Metals Limited 2006 Prospectus, 132 pp.
- Magoon, L.B. and Dow, W.G., 1994. The petroleum system. AAPG Memoir 60, 3–24.
- Maier, W.D., 2004. Magmatic Ni-Cu-PGE sulfide deposits in southern and central Africa: recent exploration activities Abstract. Geological Society of Australia Abstracts 73, 9.
- Maier, W.D., 2005. Platinum-group element (PGE) deposits and occurrences: Mineralization styles, genetic concepts, and exploration criteria. *Journal of African Earth Sciences*, 41, 165–191.
- Maier, W.D. and Barnes, S.-J., 2005. Application of lithochemistry to exploration for PGE deposits. In: Mungall, J.E. (editor), *Exploration for Platinum-Group Element Deposits*. Mineralogical Association of Canada Short Course 35, Oulu, Finland, 309–341.
- Maier, W.D. and Groves, D.I., 2011. Temporal and spatial controls on the formation of magmatic PGE and Ni-Cu deposits. *Mineralium Deposita*, 46, 841–857, DOI 10.1007/s00126-011-0339-6.
- Maier, W.D., Barnes, S.-J., De Klerk, W.J., Teigler, B. and Mitchell, A.A., 1996. Cu/Pd and Cu/Pt of silicate rocks in the Bushveld Complex: Implications for platinum-group element exploration. *Economic Geology*, 91, 1151–1158.
- Maier, W.D., Barnes, S.-J. and De Waal, S.A., 1998. Exploration for magmatic Ni-Cu-PGE sulphide deposits: a review of recent advances in the use of geochemical tools, and their application to some South African ores. *South African Journal of Geology*, 101, 165–182.
- Maier, W.D., Li, C. and De Waal, S.A., 2001. Why are there no major Ni-Cu sulfide deposits in large layered mafic-ultramafic intrusions? *Canadian Mineralogist*, 39, 547–556.
- Maier, W.D., Marsh, J.S. and Barnes, S.-J., 2002. The distribution of PGE in the Insizwa lobe, Mount Ayliff Complex, South Africa: implications for Ni-Cu-PGE sulfide exploration in the Karoo Igneous Province. *Economic Geology*, 97, 1293–1306.
- Maier, W.D., Barnes, S.-J., Gartz, V. and Andrews, G., 2003. Pt-Pd reefs in magnetitites of the Stella layered intrusion, South Africa: A world of new exploration opportunities for platinum group elements. *Geology*, 31, 885–888.
- Maier, W.D., Peltonen, P. and Livesey, T., 2007. The ages of the Kabanga North and Kapalagulu intrusions, western Tanzania: A reconnaissance study. *Economic Geology*, 102, 147–154.
- Maier, W.D., Barnes, S.J., Campbell, I.H., Fiorentini, M.L., Peltonen, P., Barnes, S.-J. and Smithies, R.H., 2009. Mantle magmas reveal progressive mixing of meteoritic veneer into the early Earth's deep mantle. *Nature*, 460, 620–623.
- Maier, W.D., Barnes, S.J. and Groves, D.I., 2013. The Bushveld Complex, South Africa; formation of platinum-palladium, chrome- and vanadium-rich layers via hydrodynamic sorting of a mobilized cumulate slurry in a large, relatively slowly cooling, subsiding magma chamber. *Mineralium Deposita*, 48, 1–56.
- Maier, W.D., Howard, H.M. and Smithies, R.H., 2014a. Mafic-ultramafic intrusions of the Giles Event, Western Australia: Prospectivity for magmatic ore deposits. March 2014 LIP of the Month, 31 pp.
- Maier, W.D., Howard, H.M., Smithies, R.H., Yang, S., Barnes, S.-J., O'Brien, H., Huhma, H. and Gardoll, S., 2014b. Mafic-ultramafic intrusions of the Giles Event, Western Australia: petrogenesis and prospectivity for magmatic ore deposits. Geological Survey of Western Australia Report 134, 82 pp.
- Makovicky, E., 2002. Ternary and quaternary phase systems with PGE. Special Volume - Canadian Institute of Mining and Metallurgy (1982) 54, 131–175.

- Mallee Gold Corporation Limited, 2007. Mallee Gold Corporation Limited, 2007 Prospectus 79 pp.
- Mamuse, A., Beresford, S., Porwal, A. and Kreuzer, O.P., 2010. Assessment of undiscovered nickel sulphide resources, Kalgoorlie terrane, Western Australia: Part 1. Deposit and endowment density models. *Ore Geology Reviews*, 37, 141–157.
- Markwitz, V., Maier, W.D., González-Álvarez, I., McCuaig, T.C. and Porwal, A., 2010. Magmatic nickel sulfide mineralization in Zimbabwe: Review of deposits and development of exploration criteria for prospectivity analysis. *Ore Geology Reviews*, 38, 139–155.
- Marsh, E.E. and Anderson, E.D., 2011. Ni-Co laterites deposits. United States Geological Survey Open-File Report 2011–1259, 9 pp.
- Marshall, A.E., 2000. Low temperature-low pressure ('epithermal') siliceous vein deposits of the North Pilbara granite-greenstone terrane, Western Australia. AGSO Record 2000/1, 40 pp.
- Marshall, P. and Widdowson, M., 2013. A review of the Kalkarindji—the oldest Phanerozoic flood basalt province. September 2013 LIP of the Month, 6 pp.
- Marston, R.J., 1979. Copper mineralization in Western Australia. Western Australia Geological Survey, Mineral Resources Bulletin 13, 208 pp.
- Marston, R.J., 1984. Nickel mineralization in Western Australia. Geological Survey of Western Australia, Mineral Resources Bulletin 14, 271 pp.
- Marston, R.J. and Kay, B.D., 1980. The distribution, petrology, and genesis of nickel ores at the Juan Complex, Kambalda, Western Australia. *Economic Geology*, 75, 546–565.
- Martin A.R., 1998. Hillview vermiculite deposit. In: Berkman, D.A. and Mackenzie, D.H. (editors), *Geology of Australian and Papua New Guinean Mineral Deposits*. Australasian Institute of Mining and Metallurgy, Melbourne, Monograph 22, 651–654.
- Mathison, C.I. and Ahmat, A.L., 1996. The Windimurra Complex, Western Australia. In: Cawthorn, R.G. (editor), *Layered Intrusions*. Elsevier, Amsterdam, 485–510.
- Mathison, C.I. and Booth, R.A., 1990. Macrorhythmically layered gabbro-norites in the Windimurra gabbroid complex, Western Australia. *Lithos*, 24, 171–180.
- Mathison, C.I. and de Laeter, J.R., 1994. Geological Note. Strontium isotope initial ratios in the Windimurra layered gabbroid complex, Western Australia: A test for Bushveld-type magma mixing. *Australian Journal of Earth Sciences*, 41, 281–284.
- Mathison, C.I. and Hamlyn, P.R., 1987. The McIntosh layered troctolite-olivine gabbro intrusion, east Kimberley, Western Australia. *Journal of Petrology*, 28, 211–234.
- Mathison, C.I. and Marshall, A.E., 1981. Ni-Cu sulfides and their host mafic-ultramafic rocks in the Mt. Sholl intrusion, Pilbara region, Western Australia. *Economic Geology*, 76, 1581–1596.
- Mathison, C.I., Perring, R.J., Vogt, J.H., Parks, J., Hill, R.E.T. and Ahmat, A.L., 1991. The Windimurra Complex. In: Barnes, S.J. and Hill, R.E.T. (editors), *Mafic-Ultramafic Complexes of Western Australia*, Excursion Guidebook No. 3. Sixth International Platinum Symposium, July 1991, Perth, WA. IAGOD and the Geological Society of Australia, 45–76.
- Mavrogenes, J.A. and O'Neill, H.S.C., 1999. The relative effects of pressure, temperature and oxygen fugacity on the solubility of sulfide in mafic magmas. *Geochimica et Cosmochimica Acta*, 63, 1173–1180.
- McCall, G.J.H. and Leishman, J., 1971. Clues to the origin of Archaean eugeosynclinal peridotites and the nature of serpentinisation. *Geological Society of Australia Special Publication* 3, 281–299.
- McClay, K.R. and Campbell, I.H., 1976. The structure and shape of the Jimberlana Intrusion, Western Australia, as indicated by an investigation of the Bronzite Complex. *Geological Magazine*, 113, 129–139.
- McCuaig, T.C., Beresford, S. and Hronsky, J., 2010. Translating the mineral systems approach into an effective exploration targeting system: *Ore Geology Reviews*, 38, 128–138.
- McDonald, D. and Hunt, L.B., 1982. *A History of Platinum and its Allied Metals*. Johnson Matthey, Hatton Garden, London, 450 pp.

- McDonald, I. and Holwell, D.A., 2011. Geology of the Northern Bushveld Complex and the Setting and Genesis of the Platreef Ni-Cu-PGE Deposit. *Economic Geology*, 17, 297–327.
- McDonald, J.A., 1965. Liquid immiscibility as one factor in chromite seam formation in the Bushveld Complex. *Economic Geology*, 60, 1674–1685.
- McDonough, W.F., 2004. Compositional model for the Earth's core. In: Carlson, R.W. (editor), *The Mantle and Core*. Elsevier, Oxford, United Kingdom, 547–568.
- McDonough, W.F. and Sun, S.-S., 1995. The composition of the Earth. *Chemical Geology*, 120, 223–253.
- McDonough, W.F., Sun, S.-S., Ringwood, A.E., Jagoutz, E. and Hofmann, A.W., 1992. Potassium, rubidium, and cesium in the Earth and Moon and the evolution of the mantle of the Earth. *Geochimica et Cosmochimica Acta*, 56, 1001–1012.
- McGoldrick, P.J. and Keays, R.R., 1981. Precious and volatile metals in the Perseverance nickel deposit gossan: implications for exploration in weathered terrains. *Economic Geology*, 76, 1752–1763.
- McKay, A.D., 1990. Evaluation of the uranium mineralisation and uranium resource potential at Coronation Hill. In: Curtis R.E.S. (editor), *Assessment of the Identified Resource at Coronation Hill and its Possible Extensions*. BMR Geological and Mineral Resource Studies, Resource Assessment Commission Kakadu Conservation Zone Inquiry Consultancy Series, Australian Government Publishing Service, Canberra.
- McKay, A.D. and Mieziotis, Y., 2001. Australia's uranium resources, geology and development of deposits. AGSO–Geoscience Australia, Mineral Resource Report 1, 184 pp.
- McKenzie, C.B. (compiler), 2000. A special issue on the Voisey's Bay Ni-Cu-Co deposit, Labrador, Canada. *Economic Geology*, 95, 673–915.
- McLeod, C.R. and Morison, S.R., 1995. Placer gold, platinum. In: Eckstrand, O.R., Sinclair, W.D. and Thorpe, R.I. (editors), *Geology of Canadian Mineral Deposit Types*. The Geology of North America Series, Geological Society of America, volume P-1. Geological Survey of Canada, Geology of Canada 8, 23–32.
- Meisel, T., Moser, J. and Wegscheider, W., 2001. Recognizing heterogeneous distribution of platinum group elements (PGE) in geological materials by means of the Re-Os isotope system. *Fresenius J Anal Chem*, 370, 566–572.
- Meixner, A.J. and Gunn, P.J., 1997. Three-dimensional kinematic modelling of the magnetic field of the southern Joseph Bonaparte Gulf. *Exploration Geophysics*, 28, 260–264.
- Meixner, T. and Hoatson, D.M., 2003. Geophysical interpretation of Proterozoic mafic-ultramafic intrusions in the Arunta Region, central Australia. *Geoscience Australia Record 2003/29*, 125 pp.
- Mernagh, T.P. and Hoatson, D.M., 1995. A Laser Raman microprobe study of platinum-group minerals from the Munni Munni layered intrusion, west Pilbara Block, Western Australia. *Canadian Mineralogist*, 33, 409–417.
- Mernagh, T.P. and Hoatson, D.M., 1997. Raman spectroscopic study of pyroxene structures from the Munni Munni layered intrusion, Western Australia. *Journal of Raman Spectroscopy*, 28, 647–658.
- Mernagh, T.P., Heinrich, C.A., Leckie, J.F., Carville, D.P., Gilbert, D.J., Valenta, R.K. and Wyborn, L.A.I., 1994. Chemistry of low-temperature hydrothermal gold, platinum, and palladium ( $\pm$ uranium) mineralisation at Coronation Hill, Northern Territory, Australia. *Economic Geology*, 89, 1053–1073.
- Mernagh, T.P., Wyborn, L.A.I. and Jagodzinski, E., 1998. 'Unconformity-related' U $\pm$ Au $\pm$ platinum-group-element deposits. *AGSO Journal of Australian Geology and Geophysics*, 17, 197–205.
- Mernagh, T.P., Trudu, A.G. and Hoatson, D.M., 2000. Chapter 13. A Laser Raman and electron probe microanalysis study of chromite from Precambrian layered mafic-ultramafic intrusions in northern Western Australia. In: Hoatson, D.M. and Blake, D.H. (editors), *Geology and Economic Potential of the Palaeoproterozoic Layered Mafic-Ultramafic Intrusions in the East Kimberley, Western Australia*. Australian Geological Survey Organisation Bulletin 246, 265–277.
- Mertie, J.B. Jr., 1969. Economic geology of the platinum metals. United States Geological Survey Professional Paper 630, 120 pp.

- Miele, T., Moser, J. and Wegscheider, W., 2001. Recognizing heterogeneous distribution of platinum group elements (PGE) in geological materials by means of the Re-Os isotope system. *Analytical Chemistry*, 370, 566–572.
- Miezitis, Y., Jaireth, S. and Hoatson, D.M., 2006. Mineral potential modelling of Proterozoic mafic-ultramafic intrusions in the Arunta Region, central Australia. *Geoscience Australia Record 2006/14*, 56 pp.
- Miller, L.J. and Smith, M.E., 1975. Sherlock Bay nickel-copper. In: Knight, C.L. (editor), *Economic Geology of Australia and Papua New Guinea*. 1. Metals. Australasian Institute of Mining and Metallurgy, Monograph 5, 168–174.
- Minara Resources Limited, 2005. Minara Resources Limited announcement to the Australian Securities Exchange, 16 June 2005.
- Mindat, 2014—[Web page]. Otter Shoot Nickel mine. <http://www.mindat.org/loc-227.html> (last accessed 10 October 2014).
- MINOCC 2011 (available for purchase from the Geological Survey of Queensland: <http://mines.industry.qld.gov.au/geoscience/default.htm>). (last accessed 10 October 2014).
- Mithril Resources Ltd, 2005. Report for the quarter ending 31 March 2005. Quarterly Report by Mithril Resources Limited, 7 pp.
- MMC Norilsk, 2007. MMC Norilsk Nickel Annual Report 2007, 352 pp. [http://www.nornik.ru/upload/report2007\\_eng.pdf](http://www.nornik.ru/upload/report2007_eng.pdf) (last accessed 10 October 2014).
- Mole, D.R., Fiorentini, M.L., Thebaud, N., McCuaig, T.C., Cassidy, K.F., Barnes, S.J., Belousova, E., Mudrovskaya, I. and Doublier, M.P., 2010. Lithospheric controls on the localization of komatiite-hosted nickel-sulfide deposits, 5th International Archean Symposium. *Geological Survey of Western Australia Record 2010/18*, Perth, 101–103.
- Mondal, S.K. and Mathez, E.A., 2007. Origin of the UG2 chromitite layer, Bushveld Complex. *Journal of Petrology*, 48, 495–510.
- Moroni, M., Girardi, V.A. and Ferrario, A., 2001. The Serra Pelada Au-PGE deposit, Serra dos Carajás (Para State, Brazil): geological and geochemical indications for a composite mineralising process. *Mineralium Deposita*, 36, 768–785.
- Morris, P.A. and Pirajno, F., 2005. Mesoproterozoic sill complexes in the Bangemall Supergroup, Western Australia: geology, geochemistry, and mineralization potential. *Western Australia Geological Survey Report 99*, 75 pp.
- Morrison, G.W., 1998. Copper Hill magmatic-hydrothermal evolution: Magmatic and hydrothermal evolution of intrusive related gold deposits. AMIRA P245 Final Report, Section 15A.
- Morrison, M., 1928. Platinum. *Mineral Industry of New South Wales*. Geological Survey of New South Wales, 119.
- Mortimer, R.M., 2005. The role of downhole TEM in the discovery of the Daybreak, Daybreak Deeps and Flying Fox T1 to T5 nickel sulphide deposits. *Australian Society of Exploration Geophysicists, Preview*, 117, 22–25.
- Mosier, D.L., Singer, D.A., Moring, B.C. and Galloway, J.P., 2012. Podiform chromite deposits—database and grade and tonnage models: United States Geological Survey Scientific Investigations Report 2012-5157, 45 pp. [http://pubs.usgs.gov/sir/2012/5157/sir2012-5157\\_text.pdf](http://pubs.usgs.gov/sir/2012/5157/sir2012-5157_text.pdf) (last accessed 10 October 2014).
- Mukasa, S.B., Wilson, A.H. and Carlson, R.W., 1998. A multielement geochronologic study of the Great Dyke, Zimbabwe: significance of the robust and reset ages. *Earth and Planetary Science Letters*, 164, 353–369.
- Mungall, J.E., 2005a. Platinum-group elements; petrology, geochemistry, mineralogy. In: Mungall, J.E. (editor), *The Canadian Mineralogist*. Mineralogical Association of Canada, Ottawa, ON, Canada, Ottawa, 694.
- Mungall, J.E., 2005b. Magmatic geochemistry of the platinum-group elements. In: Mungall, J.E. (editor), *Exploration for Platinum-Group Element Deposits*. Mineralogical Association of Canada Short Course 35, Oulu, Finland, 1–34.

- Mungall, J.E. and Naldrett, A.J., 2008. The platinum-group elements: Ore deposits of the platinum-group elements, *Elements*, 4, 253–258.
- Murphy, R., 2000 (editor). Register of Australian Mining, 2000/2001: Resource Information Unit Ltd, Perth, 672 pp.
- Mutton, P. and Peters, B., 2004. The Waterloo and Amorac nickel deposits, Western Australia: A geophysical case history. ASEG Conference, Extended Abstracts, 2004, Sydney, 1–8.
- Myers, J.S., 1985. The Fraser Complex: a major layered intrusion in Western Australia, Professional papers for 1983: Geological Survey of Western Australia, Report 14, 57–66.
- Myers, J.S., 1990. Wingelina Complex and Bentley Supergroup: Geological Survey of Western Australia. Memoir 3, 283–290.
- Myers, J.S., Shaw, R.S. and Tyler, I.M., 1996. Tectonic evolution of Proterozoic Australia. *Tectonics*, 15, 1431–1446.
- Naldrett, A.J., 1981. Nickel sulfide deposits: classification, composition, and genesis. *Economic Geology*, 75<sup>th</sup> Anniversary Volume, 628–685.
- Naldrett, A.J., 1989. *Magmatic Sulfide Deposits*. Clarendon Press, New York, 186 pp.
- Naldrett, A.J., 1997. Key factors in the genesis of Noril'sk, Sudbury, Jinchuan, Voisey's Bay and other world-class Ni–Cu–PGE deposits: implications for exploration. *Australian Journal of Earth Sciences*, 44, 283–315.
- Naldrett, A., 1999. World-class Ni-Cu-PGE deposits: key factors in their genesis. *Mineralium Deposita*, 34, 227–240.
- Naldrett A.J., 2002. Requirements for forming giant Ni-Cu sulfide deposits. In: Cooke, D.R. and Pongratz, J. (editors), *Giant Ore Deposits: Characteristics, Genesis, and Exploration*. Centre for Ore Deposit Research Special Publication 4. University of Tasmania, Hobart, 195–204.
- Naldrett, A.J., 2004. *Magmatic Sulfide Deposits: Geology, Geochemistry and Exploration*. Springer Verlag, Berlin, 728 pp.
- Naldrett, A.J., 2010. Secular variation of magmatic sulfide deposits and their source magmas. *Economic Geology*, 105, 669–688.
- Naldrett, A.J., 2011. Fundamentals of magmatic sulfide deposits. In: Li, C. and Ripley, E.M. (editors), *Magmatic Ni-Cu and PGE Deposits: Geology, Geochemistry, and Genesis*. Society of Economic Geologists Incorporated, Colorado, USA. *Reviews in Economic Geology* Volume 17, 1–50.
- Naldrett, A.J. and Cabri, L.J., 1976. Ultramafic and related mafic rocks: their classification and genesis with special reference to the concentration of nickel sulfides and platinum group elements. *Economic Geology*, 71, 1131–1158.
- Naldrett, A.J. and Turner, A.R., 1977. The geology and petrogenesis of a greenstone belt and related nickel sulfide mineralization at Yakabindie, Western Australia. *Precambrian Research*, 3, 43–103.
- Naldrett, A.J., Hoffman, E.L., Green, A.H., Chou, C.L., Naldrett, S.R. and Alcock, R.A., 1979. The composition of Ni-sulfide ores, with particular reference to their content of PGE and Au. *The Canadian Mineralogist*, 17, 403–415.
- Naldrett, A.J., Keats, H., Sparkes, K. and Moore, R., 1996. Geology of the Voisey's Bay Ni–Cu–Co deposit, Labrador, Canada. *Journal of Exploration of Mining and Geology*. Canadian Institute of Mining, Metallurgy, and Petroleum, 5, 169–179.
- Naldrett, A.J., Kinnaird, J., Stanley, C., Wilson, A. and Chunnett, G., 2008a. Origin of PGE in the UG-2 unit of the Bushveld Complex, South Africa. Abstract Volume (Geological Association of Canada) 33, 120–121.
- Naldrett, A.J., Kinnaird, J., Wilson, A. and Chunnett, G., 2008b. The concentration of PGE in the earth's crust with special reference to the Bushveld Complex. *Earth Sciences Frontiers*, 15, 264–297.
- Naldrett, A.J., Wilson, A., Kinnaird, J. and Chunnett, G., 2009. PGE tenor and metal ratios within and below the Merensky Reef, Bushveld Complex; implications for its genesis. *Journal of Petrology*, 50, 625–659.

- Naldrett, A.J., Kinnaird, J., Wilson, A., Yudovskaya, M. and Chunnett, G., 2011. Genesis of the PGE-enriched Merensky Reef and chromitite seams of the Bushveld Complex. *Reviews in Economic Geology* 17, 235–296.
- Naldrett, A.J., Wilson, A., Kinnaird, J., Yudovskaya, M. and Chunnett, G., 2012. The origin of chromites and related PGE mineralization in the Bushveld Complex: new mineralogical and petrological constraints. *Mineralium Deposita*, 47, 209–232.
- Needham R.S., 1982. Cahill Northern Territory (Sheet 5472). Bureau of Mineral Resources, Australia; 1:100 000 Geological Map Commentary.
- Needham, R.S., 1987. A review of mineralisation in the South Alligator Conservation Zone. Bureau of Mineral Resources, Australia, Record 1987/52, 28 pp.
- Needham, R.S., 1988. Geology of the Alligator Rivers Uranium Field, Northern Territory. Bureau of Mineral Resources, Australia Bulletin 224, 177 pp.
- Needham, R.S. and Stuart-Smith, P.G., 1987. Coronation Hill U-Au mine, South Alligator Valley, Northern Territory: an epigenetic sandstone-type deposit hosted by debris-flow conglomerate. *BMR Journal of Australian Geology and Geophysics*, 10, 121–131.
- Needham, R.S., Stuart-Smith, P.G. and Page, R.W., 1988. Tectonic evolution of the Pine Creek Inlier, Northern Territory. *Precambrian Research*, 40/41, 543–564.
- Nelson, D.R., 1997. Evolution of the Archaean granite-greenstone terranes of the Eastern Goldfields, Western Australia: SHRIMP U-Pb constraints. *Precambrian Research*, 83, 57–81.
- Nelson, D.R., 1998. Compilation of SHRIMP U-Pb zircon geochronology data 1997. Western Australia Geological Survey Record 1998/2, 242 pp.
- Nelson, D.R., 2001. Compilation of geochronology data, 2000. Western Australia Geological Survey, Record 2001/2, 81–86.
- Nelson, D.R., Black, L.P. and McCulloch, M.T., 1989. Nd-Pb isotopic characteristics of the Mordor complex, Northern Territory: Mid-Proterozoic potassic magmatism from an enriched mantle. *Australian Journal of Earth Sciences*, 36, 541–551.
- Neradovsky, Y.N., Borisova, V.V. and Sholokhnev, V.V., 1997. The Monchegorsk layered complex and related mineralization. In: Mitrofanov, F., Torokhov, F., Iljina, M. (editors), *Ore Deposits of the Kola Peninsula, Northwestern Russia*. 4th Biennial SGA Meeting, August 11-13, 1997, Turku, Finland, Geological Survey of Finland Guide 45, Excursion Guidebook B4.
- Nesbitt, R.W., Goode, A.D.T., Moore, A.C. and Hopwood, T.D., 1970. The Giles Complex, central Australia: a stratified sequence of mafic and ultramafic intrusions. In: Visser, D.J.L. and Von Gruenewaldt, G. (editors), *Symposium on the Bushveld Igneous Complex and Other Layered Intrusions*. Geological Society of South Africa Special Publication 1, 547–564.
- Neuendorf, K.K.E., Mehl, J.P.Jr. and Jackson, J.A. (editors), 2005. *Glossary of Geology*, Fifth Edition. American Geological Institute, Alexandria, Virginia, 779 pp.
- Nevada Outback Gems, 2014—[Web page]. Part 1: Placers and Deposits. [http://nevada-outback-gems.com/placer\\_gold/Platinum\\_placers\\_P1.htm](http://nevada-outback-gems.com/placer_gold/Platinum_placers_P1.htm) (last accessed 10 October 2014).
- Newsom, H.E. and Sims, K.W.W., 1991. Core formation during early accretion of the Earth. *Science*, 252, 926–933.
- Nickel, E.H. and Wildman, J.E., 1981. Hydrohonessite a new hydrated Ni-Fe hydroxy sulphate mineral- its relationship to honessite, carrboydite and minerals of the pyroaurite group, *Mineralogical Magazine*, 44, 333–337.
- Nickel, E.H. and Robinson, B.W., 1985. Kambaldaite a new hydrated Ni-Na carbonate mineral from Kambalda Western Australia. *American Mineralogist*, 70, 419–422.
- Nielsen, T.F.D. and Brooks, C.K., 1995. Precious metals in magmas of East Greenland: Factors important to the mineralization in the Skaergaard Intrusion. *Economic Geology*, 90, 1911–1917.
- Platina Resources Limited announcement to the Australian Securities Exchange, 26 April 2012, 12 pp.

- Nielsen, T.F.D., Andersen J.C.O. and Brooks, C.K., 2005. The Platinova Reef of the Skaergaard Intrusion. In: Mungall, J.E. (editor), *Exploration for Platinum-Group Element Deposits*. Mineralogical Association of Canada Short Course 35, Oulu, Finland, 431–455.
- NiPlats Australia Limited, 2009. NiPlats Australia Limited announcement to the Australian Securities Exchange, 1 December 2009, 8 pp.
- NiPlats Australia Limited, 2010a. NiPlats Australia Limited Quarterly Activities Report for the period ended 10 February 2010, Australian Securities Exchange, 5 pp.
- NiPlats Australia Limited, 2010b. NiPlats Australia Limited Quarterly Activities Report for the period ended 31 March 2010, Australian Securities Exchange, 10 pp.
- Nisbet, E.G. and Chinner, G.A., 1981. Controls on the eruption of mafic and ultramafic lavas, Ruth Well Ni-Cu prospect, West Pilbara. *Economic Geology*, 76, 1729–1735.
- Nixon, G.T. and Hammack, J.L., 1991. Metallogeny of ultramafic-mafic rocks in British Columbia with emphasis on the platinum-group elements. *Ore Deposits, Tectonics and Metallogeny in the Canadian Cordillera*. Province of British Columbia, Paper 1991-4, 125–161.
- NSW DPI post-2007 Chromite.  
[http://www.resourcesandenergy.nsw.gov.au/\\_\\_data/assets/pdf\\_file/0009/237816/Chromite.pdf](http://www.resourcesandenergy.nsw.gov.au/__data/assets/pdf_file/0009/237816/Chromite.pdf) (last accessed 10 October 2014).
- NSW DPI post-2005 Vermiculite.  
[http://www.resourcesandenergy.nsw.gov.au/\\_\\_data/assets/pdf\\_file/0020/238214/Vermiculite.pdf](http://www.resourcesandenergy.nsw.gov.au/__data/assets/pdf_file/0020/238214/Vermiculite.pdf) (last accessed 10 October 2014).
- Nutt, C.J., 1989. Chloritisation and associated alteration at the Jabiluka unconformity-type uranium deposit, Northern Territory, Australia. *Economic Geology*, 27, 41–58.
- Nye, P.B., 1929. The Osmiridium deposits of the Adamsfield district. *Tasmania Department of Mines Geological Survey Bulletin* 39, 70 pp.
- Nye, P.B., 1930. Report of the Osmiridium “lode” at the head of Main Creek, Adamsfield. *Tasmania Department of Mines Geological Survey Report*.
- Nye, P.B. and Blake, F., 1938. The geology and mineral deposits of Tasmania. *Tasmania Department of Mines Geological Survey Bulletin* 44, 112 pp.
- Oberthür, T. and Melcher, F., 2005. PGE and PGM in the supergene environment: a case study of persistence and redistribution in the Main Sulphide Zone of the Great Dyke, Zimbabwe. In: Mungall, J.E. (editor), *Exploration for Platinum-Group Element Deposits*. Mineralogical Association of Canada Short Course 35, Oulu, Finland, 97–111.
- Oberthür, T., Davis, D.W., Blenkinsop, T.G. and Höhn-Dorf, A., 2002. Precise U-Pb mineral ages, Rb-Sr and Sm-Nd systematics for the Great Dike, Zimbabwe – constraints on late Archean events in the Zimbabwe Craton and Limpopo Belt. *Precambrian Research*, 113, 293–305.
- Oberthür, T., Weiser, T., Melcher, F., Gast, L. and Wöhr, C., 2013. Detrital platinum-group minerals in rivers draining the Great Dyke, Zimbabwe. *The Canadian Mineralogist*, 51, 197–222.
- Och, D.J., Leitch, E.C. and Caprarelli, G., 2007. Geological units of the Port Macquarie–Tacking Point tract, north-eastern Port Macquarie Block, Mid North Coast region of New South Wales. *Quarterly Notes, Geological Survey of New South Wales*, October 2007, 126. 1–19.  
[http://www.resources.nsw.gov.au/\\_\\_data/assets/pdf\\_file/0015/203712/00126-quarterly-notes-oct-07.pdf](http://www.resources.nsw.gov.au/__data/assets/pdf_file/0015/203712/00126-quarterly-notes-oct-07.pdf) (last accessed 10 October 2014).
- Olivo, G.R. and Gammons, C.H., 1996. Thermodynamic and textural evidence for at least two stages of Au-Pd mineralization at the Caue iron mine, Itabira District, Brazil. *The Canadian Mineralogist*, 34, 547–557.
- Organ, M.K., 1998. “...a small fish in a small pond...” The Reverend W.B. Clarke (1798-1878): 200 Years on. University of Wollongong Research Online. [Parts I & II], *Journal and Proceedings of the Royal Society of New South Wales*, 131–1998 and 132–1999, 26 pp.  
<http://ro.uow.edu.au/cgi/viewcontent.cgi?article=1021&context=asdpapers> (last accessed 10 October 2014).

- Orth, K., Meffre, S. and Davidson, G., 2014. Age and paragenesis of mineralisation at Coronation Hill uranium deposit, Northern Territory, Australia. *Mineralium Deposita*, DOI 10.1007/s00126-013-0501-4, 1–29.
- Oshin, I.O. and Crocket, J.H., 1982. Noble metals in Thetford Mines ophiolites, Quebec, Canada. Part I: Distribution of gold, iridium, platinum, and palladium in the ultramafic and gabbroic rocks. *Economic Geology*, 77, 1556–1570.
- Ostwald, J., 1979. Porpezite (PdAu) from Westwood, Queensland, Australia. *Australian Mineralogist*, 27, 129–131.
- OZMIN, 2014. Geoscience Australia's national mineral deposits database. Geoscience Australia, Canberra.
- Paces, J.B. and Miller, J.D. Jr., 1993. Precise U-Pb ages of Duluth Complex and related mafic intrusions, northeastern Minnesota; geochronological insights to physical, petrogenetic, paleomagnetic, and tectonomagnetic processes associated with the 1.1 Ga Midcontinent Rift System. *Journal of Geophysical Research, B, Solid Earth and Planets* 98; 8, 13 997–14 013.
- Page, N.J., Singer, D.A., Moring, B.C., Carlson, C.A., McDade, J.M. and Wilson, S.A., 1986. Platinum-group element resources in podiform chromitites from California and Oregon. *Economic Geology*, 81, 1261–1271.
- Pagé, P., Barnes, S.-J., Bédard, J.H. and Zientek, M.L., 2012. In situ determination of Os, Ir, and Ru in chromites formed from komatiite, tholeiite and boninite magmas: Implications for chromite control of Os, Ir and Ru during partial melting and crystal fractionation. *Chemical Geology*, 302–303, 3–15.
- Page, R.W. and Hoatson, D.M., 1997. SHRIMP U-Pb geochronology of Palaeoproterozoic layered mafic-ultramafic intrusions, East Kimberley, Western Australia. Abstract GAC/MAC Annual Meeting Ottawa '97, 9–21 May, A 111.
- Page, R.W. and Hoatson, D.M., 2000. Chapter 6. Geochronology of the mafic-ultramafic intrusions. In: Hoatson, D.M. and Blake, D.H. (editors), *Geology and Economic Potential of the Palaeoproterozoic Layered Mafic-Ultramafic Intrusions in the East Kimberley, Western Australia*. Australian Geological Survey Organisation Bulletin 246, 163–172.
- Page, R.W., McCulloch, M.T. and Black, L.P., 1984. Isotopic record of major Precambrian events in Australia. *International Geological Congress, Abstracts. Congres Geologique International, Resumes*, 27, 365.
- Page, R.W., Hoatson, D.M., Sun, S.-S. and Foudoulis, C., 1995. High-precision geochronology of Palaeoproterozoic layered mafic-ultramafic intrusions in the East Kimberley. *AGSO Research Newsletter*, 22, 7–8.
- Palme, H. and O'Neill, H.S.C., 2004. Cosmochemical Estimates of Mantle Composition. In: Holland, H.D. and Turekian, K.K. (editors), *Treatise on Geochemistry*, Pergamon, Oxford, 1–38.
- Pancontinental Mining Limited, 1979. Jabiluka Project. Environmental Impact Statement, July 1979.
- Panoramic Resources Limited, 2014—[Web page]. Panton PGM Project. <http://www.panoramicresources.com/display/index/panton> (last accessed 10 October 2014).
- Papunen, H. and Gorbunov, G.I. (editors), 1985. Nickel-copper deposits of the Baltic Shield and Scandinavian Caledonides. *Geological Survey of Finland Bulletin* 333, 394 pp.
- Parks, J., 1998. Weld Range platinum group element deposit. In: Berkman, D.A. and Mackenzie, D.H. (editors), 1998. *Geology of Australian and Papua New Guinean Mineral Deposits*. The Australasian Institute of Mining and Metallurgy, Melbourne, Monograph 22, 279–286.
- Parrish, R.R., 1989. U-Pb Geochronology of the Cape Smith Belt and Sugluk Block, Northern Quebec. *Geoscience Canada*, 16, 126–130.
- Pašava, J., 1993. Anoxic sediments; an important environment for PGE; an overview. *Ore Geology Reviews*, 8, 425–445.
- Pašava, J., Vymazalová, A. and Petersen, S., 2007. PGE fractionation in seafloor hydrothermal systems: examples from mafic- and ultramafic-hosted hydrothermal fields at the slow-spreading Mid-Atlantic Ridge. *Mineralium Deposita*, 42, 423–431.

- Pearson, R.G., 1963. Hard and soft acids and bases. *Journal of the American Chemical Society*, 85, 3533–3539.
- Peck, D.C., 1990. Platinum-group element geochemistry and petrogenesis of the Heazlewood River mafic-ultramafic complex, Tasmania. PhD thesis, University of Melbourne, Australia.
- Peck, D.C. and Keays, R.R., 1990a. Geology, geochemistry and origin of platinum group element chromitite occurrences in the Heazlewood River Complex, Tasmania. *Economic Geology*, 85, 765–793.
- Peck, D.C. and Keays, R.R., 1990b. Insights into the behavior of precious metals in primitive, S-undersaturated magmas; evidence from the Heazlewood River complex, Tasmania. *The Canadian Mineralogist*, 28, 553–577.
- Peck, D.C., Keays, R.R. and Ford, R. J., 1992. Direct crystallization of refractory platinum-group element alloys from boninitic magmas: evidence from western Tasmania. *Australian Journal of Earth Sciences*, 39, 373–387.
- Perkins, C, Walshe, J.L. and Morrison, G.W., 1995. Metallogenic episodes of the Tasman Fold Belt System, eastern Australia. *Economic Geology*, 90, 1443–1466.
- Perring, C.S., Barnes, S.J. and Hill, R.E.T., 1996. Geochemistry of Archaean komatiites from the Forrestania Greenstone Belt, Western Australia: evidence for supracrustal contamination. *Lithos*, 37, 181–197.
- Perring, R.J. and Vogt, J.H., 1991. The Panton Sill. In: Barnes, S.J. and Hill, R.E.T. (editors), *Mafic-Ultramafic Complexes of Western Australia. Excursion Guidebook 3. Sixth International Platinum Symposium, July 1991, Perth, Western Australia. IAGOD and the Geological Society of Australia*, 97–106.
- Peters, B. and Buck, P., 2000. The Maggie Hays and Emily Ann nickel deposits, Western Australia: a geophysical case history. *Exploration Geophysics*, 31, 210–221.
- Peters, W.S., 2006. Geophysical exploration for nickel sulfide mineralization in the Yilgarn Craton. In: Barnes, S.J. (editor), *Nickel Deposits of the Yilgarn Craton: Geology, Geochemistry, and Geophysics Applied to Exploration. Economic Geology Special Publication Number 13*, 167–193.
- Peters, W.S. and de Angelis, M., 1987. The Radio Hill Ni-Cu massive sulphide deposit. A geophysical case history. *Exploration Geophysics*, 18, 160–166.
- Peyerl, W., 1982. The influence of the Driekop dunite pipe on the platinum-group mineralogy of the UG-2 Chromitite in its vicinity. *Economic Geology*, 77, 1432–1438
- Phaceas, J., 2007. BHP dusts off plans for Nebo and Babel. *West Australian Business News* article, 10/2/2007, 69 and 72.
- Pidgeon, R.T., 1984. Geochronological constraints on early volcanic evolution of the Pilbara Block, Western Australia. *Australian Journal of Earth Sciences*, 31, 237–242.
- Pioneer Nickel Limited, 2008. Pioneer Nickel Limited announcement to the Australian Securities Exchange, 24 November 2008, 2 pp.
- Pirajno, F., 2004. The Fortescue Group, Western Australia; an Archean (2.7 Ga) Large Igneous Province. December 2004 LIP of the Month, 11 pp.
- Pirajno, F. and Hoatson, D.M., 2012. A review of Australia's Large Igneous Provinces and associated mineral systems: Implications for mantle dynamics through geological time. *Ore Geology Reviews*, 48, 2–54.
- Pirajno, F. and Morris, P., 2005. Large igneous provinces in Western Australia: implications for Ni-Cu and Platinum Group Elements (PGE) mineralization. In: Mao, J. and Bierlein, F.P. (editors), *Mineral Deposit Research: Meeting the Global Challenge. Proceedings of the Eighth Biennial SGA Meeting Beijing, China, 18–21 August 2005, Volume 2*, 1049–1052.
- Pirajno, F., Morris, P.A. and Wingate, M.T.D., 2002. A possible large igneous province (LIP) in central western Australia: implications for mineralization models. *Geological Society of Australia Abstracts*, 67, 140.
- Pirajno, F., Smithies, F. and Howard, H.M., 2006. Mineralisation associated with the 1076 Ma Giles mafic-ultramafic intrusions, Musgrave Complex, central Australia: a review. *SGA News*, 20, 1–20.

- Platina Resources Limited, 2012. Platina Resources Limited announcement to the Australian Securities Exchange, 26 April 2012, 12 pp.
- Platina Resources Limited, 2013a. Platina Resources Limited announcement to the Australian Securities Exchange, 16 July 2013, 10 pp.
- Platina Resources Limited, 2013b. Platina defines Arctic gem. MiningNews.net article, 23/7/2013. Aspermont Limited, Perth, Western Australia, 1 pp.
- Platina Resources Limited, 2013c. Platina Resources Limited presentation 2013 Diggers and Dealers Mining Forum. PowerPoint presentation by Mark Dugmore, 6 August 2013, Kalgoorlie, Western Australia, 19 pp.
- Platina Resources Limited, 2014a—[Web page]. Munni Munni, Western Australia, and Owendale, New South Wales Projects. <http://www.platinaresources.com.au/projects/munni-munni/> (last accessed 10 October 2014).
- Platina Resources Limited, 2014b. Platina Resources Limited announcement to the Australian Securities Exchange, 26 February 2014, 9 pp. [http://new.platinaresources.com.au/files/announcements/26\\_02\\_2014\\_-\\_Project\\_Update\\_Activities.pdf](http://new.platinaresources.com.au/files/announcements/26_02_2014_-_Project_Update_Activities.pdf) (last accessed 10 October 2014).
- Platinum Australia Limited, 2005. Platinum Australia Limited announcement to the Australian Securities Exchange, 7 December 2005, 2 pp.
- Platinum Australia Limited, 2014—[Web page]. Kalplats Project. Platinum Australia Limited, Resources media release. <http://www.platinumaus.com.au/viewStory/Kalplats%20Project> (last accessed 10 October 2014).
- Platinum Australia Limited, 2014—[Web page]. Pantom PGM Recovery Process. <http://www.platinumaus.com.au/viewStory/Pantom+PGM+Recovery+Process> (last accessed 10 October 2014).
- Platinum Search NL, 1994. First annual exploration report EL 4454, Tottenham area. New South Wales Geological Survey, File GS1994/055.
- Playford, P.E., McLaren, D.J., Orth, C.J., Gilmore, J.S. and Goodfellow, W.D., 1984. Iridium anomaly in the Upper Devonian of the Canning Basin, Western Australia. *Science*, 226, 437–439.
- Plimer, I.R. and Williams, P.A., 1987. Mechanisms for the mobilization of PGE in oxide zones. Abstract Geoplatinum '87 Symposium, The Open University, UK.
- Pogson, D.J. and Hilyard, D., 1981. Results of isotopic age dating related to Geological Survey of New South Wales investigations, 1974–1978. *New South Wales Geological Survey Records* 20, 251–273.
- Polito, P., Kurt Kyser, T., Thomas, D., Marlatt, J. and Drever, G., 2005. Re-evaluation of the petrogenesis of the Proterozoic Jabiluka unconformity-related uranium deposit, Northern Territory, Australia. *Mineralium Deposita*, 40, 257–288.
- Poltock, R., 2001. Internal report to Golden Cross Resources Limited on the Copper Hill Project, 10 pp.
- Porwal, A., González-Álvarez, I., Markwitz, V., McCuaig, T.C., Mamuse, A., 2010. Regional-scale nickel sulfide prospectivity mapping of the Yilgarn Craton, Western Australia. *Ore Geology Reviews Special Issue* 38, 184–196.
- Power-Fardy, D., 1986. Commodity review: platinum group element occurrences in Papua New Guinea. Geological Survey of Papua New Guinea Report 86/25.
- Power-Fardy, D., Meares, R.M.D., Collins, A.R. and Goldner, P.T., 1990. Platinum group element mineralisation in Papua New Guinea. In: Hughes, F.E. (editor), *Geology of the Mineral Deposits of Australia and Papua New Guinea*. Australasian Institute of Mining and Metallurgy, Melbourne, Monograph 14, 1703–1705.
- Premo, W.R., Helz, R.T., Zientek, M.L. and Langston, R.B., 1990. U-Pb and Sm-Nd ages for the Stillwater Complex and its associated sills and dikes, Beartooth Mountains, Montana. Identification of a parent magma? *Geology*, 18, 1065–1068.

- Prendergast, M.D., 2003. The nickeliferous Late Archean Reliance Komatiitic Event in the Zimbabwe Craton—Magmatic architecture, physical volcanology, and ore genesis. *Economic Geology*, 98, 865–891.
- Prendergast, M.D. and Jones, M.J. (editors), 1989. *Magmatic Sulphides—The Zimbabwe Volume*. The Institution of Mining and Metallurgy, London, 254 pp.
- Prendergast, M.D. and Keays, R.R., 1989. Controls of platinum-group element mineralisation and the origin of the PGE-rich main sulphide zone in the Wedza subchamber of the Great Dyke, Zimbabwe: implications for the genesis of, and exploration for, stratiform PGE mineralisation in layered intrusions. In: Prendergast, M.D. and Jones, M. J. (editors), *Magmatic Sulphides—The Zimbabwe Volume*. Institution of Mining and Metallurgy, London, 21–69.
- Prendergast, M.D., Bennett, M. and Henicke, G., 1998. Platinum exploration in the Rincon del Tigre Complex, eastern Bolivia. *Transactions of the Institute of Mineralogy and Metallurgy*, 107, B39–B47.
- Prichard, H.M., Lord, R.A. and Neary, C.R., 1996. A model to explain the occurrence of platinum- and palladium-rich ophiolite complexes. *Journal of Geological Society of London*, 153, 323–328.
- Pridmore, D.F., Coggon, J.H., Esdale, D.J. and Lindemann, F.W., 1984. Geophysical exploration for nickel sulfide deposits in the Yilgarn Block, Western Australia. In: Buchanan, D.L. and Jones, M.L. (editors), *Sulfide Deposits in Mafic and Ultramafic Rocks*. Institute of Mining and Metallurgy, London, 22–34.
- Puchtel, I.S., Humayun, M., Campbell, A.J., Sproule, R.A. and Leshner, C.M., 2004. Platinum group element geochemistry of komatiites from the Alexo and Pyke Hill areas, Ontario, Canada. *Geochimica et Cosmochimica Acta*, 68, 1361–1383.
- Purvis, A.C., Nesbitt, R.W. and Hallberg, J.A., 1972. The geology of part of the Carr-Boyd Rocks complex, and its associated nickel mineralisation, Western Australia. *Economic Geology*, 67, 1093–1113.
- Pye, E.G., Naldrett, A.G. and Giblin, P.E. (editors), 1984. *The Geology and Ore Deposits of the Sudbury Structure*. Ontario Geological Survey, Special Volume 1, 603 pp.
- Raedeke, L.D., 1988. Owendale Complex, Fifield Platinum Prospect, New South Wales, Australia. Chevron Oil Field Research Company Report.
- Redstone Resources Limited, 2010. Redstone Resources Limited NL announcement to the Australian Securities Exchange, 5 March 2010, 4 pp.
- Regis Resources NL., 2007a. Regis Resources NL announcement to the Australian Securities Exchange, 28 June 2007, 3 pp.
- Regis Resources NL., 2007b. Regis Resources NL Annual Report 2007, 88 pp.
- Reid, A.M., 1921. Osmiridium in Tasmania. Tasmania Department of Mines Geological Survey Bulletin 32, 123 pp.
- Reid, K.D., Ansdell, K., Jiricka, D., Witt, G. and Card, C., 2014. Regional setting, geology, and paragenesis of the Centennial unconformity-related uranium deposit, Athabasca Basin, Saskatchewan, Canada. *Economic Geology*, 109, 539–566.
- Rencz, A.N. and Hall, G.E.M., 1992. Platinum group elements and Au in arctic vegetation growing on gossans, Keewatin District, Canada. *Journal of Geochemical Exploration*, 43, 265–279.
- Richard, A., Rozsypal, C., Mercadier, J., Banks, D.A., Cuney, M., Boiron, M-C. and Cathelineau, M., 2012. Giant uranium deposits formed from exceptionally uranium-rich acidic brines. *Nature Geoscience*, 5, 142–146.
- Richards, J.R. and Blockley, J.G., 1984. The base of the Fortescue Group, Western Australia: further galena lead isotope evidence on its age. *Australian Journal of Earth Sciences*, 31, 257–268.
- Rimfire Pacific Mining NL, 2006. Rimfire Pacific Mining NL AGM November 29<sup>th</sup> 2006. Exploration Activity Presentation by Colin Plumridge, 48 pp.  
<http://www.rimfire.com.au/PDF/Exploration%20Project%20Presentation%20AGM%2029%20Nov%202006.pdf> (last accessed 10 October 2014).

- Rimfire Pacific Mining NL, 2009. Fifield regional geology and mineralisation. Combination of Geological Survey of New South Wales data and Rimfire Pacific Mining NL interpretation, July 2009, AMG55, 1:100 000 Geological Map.
- Ripley, E.M. and Li, C., 2011. A review of conduit-related Ni-Cu-(PGE) sulfide mineralization at the Voisey's Bay Deposit, Labrador, and the Eagle Deposit, northern Michigan. *Reviews in Economic Geology* 17, 181–197.
- Rödsjö, L., 1999. The alteration history of the Agnew-Wiluna Greenstone Belt, Western Australia, and the impacts on nickel sulfide mineralization. PhD thesis, University of Western Australia, Perth, Western Australia, 185 pp.
- Rollinson, H., 1993. *Using Geochemical Data: Evaluation, Presentation, Interpretation*. Longman Group Limited, Essex, England, 352 pp.
- Rosengren, N.M., 2004. Architecture and emplacement origin of an Archean komatiite dunite and associated NiS mineralisation: Mt Keith, Agnew-Wiluna greenstone belt, Yilgarn craton, Western Australia. PhD thesis, Monash University, Victoria, Australia, 216 pp.
- Rosengren, N.M., Beresford, S.W., Grguric, B.A. and Cas, R.A.F., 2005. An intrusive origin for the komatiitic-dunite hosted Mount Keith disseminated nickel sulfide deposit, Western Australia. *Economic Geology*, 100, 149–156.
- Rosengren, N.M., Grguric, B.A., Beresford, S.W., Fiorentini, M.L. and Cas, R.A.F., 2007. Internal stratigraphic architecture of the komatiitic dunite-hosted MKD5 disseminated nickel sulfide deposit, Mount Keith Domain, Agnew-Wiluna Greenstone Belt, Western Australia. *Mineralium Deposita*, 126, 821–845.
- Ross, J.R. and Hopkins, G.M.F., 1975. Kambalda nickel sulphide deposits. In: Knight, C.L. (editor), *Economic Geology of Australia and Papua New Guinea*. 1. Metals. Australasian Institute of Mining and Metallurgy; Monograph 5, 100–121.
- Ross, J.R. and Keays, R.R., 1979. Precious metals in volcanic-type nickel sulphide deposits in Western Australia. I: Relationship with the composition of the ores and their host rocks. *Canadian Mineralogist*, 17, 417–435.
- Rowan, L.C., Simpson, C.J. and Mars, J.C., 2004. Hyperspectral analysis of the ultramafic complex and adjacent lithologies at Mordor, NT, Australia. *Remote Sensing of Environment*, 91, 419–431.
- Rowan, L.C., Mars, J.C. and Simpson, C.J., 2005. Lithologic mapping of the Mordor, NT, Australia, ultramafic complex by using the Advanced Spaceborne Thermal Emission and Reflection Radiometer (ASTER). *Remote Sensing of Environment*, 99, 105–126.
- Rowntree, J.C. and Mosher, D.V., 1975. Jabiluka uranium deposits. In: Knight, C.L. (editor), *Economic Geology of Australia and Papua New Guinea*. 1. Metals. Australasian Institute of Mining and Metallurgy; Monograph 5, 321–326.
- Royal Resources Limited, 2006. Royal Resources Limited 2006 Prospectus, 28 February 2006, 85 pp.
- RSG Global Proprietary Limited, 2006. Independent Geologist's Report. 3D Resources Prospectus 2006, 27–68.  
<http://globaldocuments.morningstar.com/documentlibrary/document/457f6b5c4a1bff57.msdoc/original> (last accessed 10 October 2014).
- Rubenach, M.J., 1973. The Tasmanian ultramafic-gabbro and ophiolite complexes. PhD thesis, University of Tasmania, Australia.
- Rubenach, M.J., 1974. The origin and emplacement of the Serpentine Hill ultramafic complex, western Tasmania. *Journal of Geological Society of Australia*, 21, 91–106.
- Ruddock, I., 1999. Mineral occurrences and exploration potential of the west Pilbara. Western Australia Geological Survey Report 70, 63 pp.
- Rudnick, R.L. and Gao, S., 2003. Composition of the Continental Crust. In: Holland, H.D. and Turekian, K.K. (editors), *Treatise on Geochemistry*, Volume 3.01. Pergamon, Oxford, 1–64.
- Ruzicka, V., 1975. Some metallogenic features of the 'D' uranium deposit at Cluff Lake, Saskatchewan. Geological Survey of Canada; Paper 75-1C: 279–283.

- Ruzicka, V., 1993. Unconformity-associated uranium deposits. In: Kirkham, R.V., Sinclair, W.D., Thorpe, R.I. and Duke, J.M. (editors), *Mineral Deposit Modelling*. Geological Association of Canada; Special Paper 40, 125–149.
- Ruzicka, V., 1995. Unconformity-associated uranium deposits. In: Eckstrand, O.R., Sinclair, W.D. and Thorpe, R.I. (editors), *Geology of Canadian Mineral Deposit Types*. Geological Survey of Canada, *Geology of Canada*, No. 8, 197–210.
- Ruzicka, V. and Thorpe, R.I., 1996. Arsenide vein silver, uranium. In: Eckstrand, O.R., Sinclair, W.D. and Thorpe, R.I. (editors), *Geology of Canadian Mineral Deposit Types*. Geological Survey of Canada, *Geology of Canada*, No. 8, 287–322.
- Ryan, B., 1997. The Mesoproterozoic Nain Plutonic Suite in eastern Canada, and the setting of the Voisey's Bay Ni-Cu-Co sulphide deposit. *Geoscience Canada*, 24, 173–188.
- Ryan, B., Wardle, R.J., Gower, C.F. and Nunn, G.A.G., 1995. Nickel–copper sulphide mineralization in Labrador: The Voisey Bay discovery and its exploration implications. Current Research Newfoundland and Labrador Department of Natural Resources, Geological Survey, Report 95-1, 177–204.
- Salpeteur, I. and Jezequel, J., 1992. Platinum and palladium stream sediment geochemistry downstream from PGE-bearing ultramafics, west Andriamena area, Madagascar. *Journal of Geochemical Exploration*, 43, 43–65.
- Sanders T.S., 1999. Mineralization of the Halls Creek Orogen, east Kimberley region, Western Australia. Geological Survey of Western Australia, Report 66 and Appendix, 44 pp.
- Sandfire Resources NL, 2009. Sandfire Resources NL announcement to the Australian Securities Exchange, 9 June 2009, 3 pp.  
<http://clients2.weblink.com.au/clients/sandfire/article.asp?asx=SFR&view=6449154> (last accessed 10 October 2014).
- Sandfire Resources NL, 2011a. DeGrussa: Approved for development, from concept to cash. Sandfire Resources NL Global Investor Presentation, March 2011, 25 pp.
- Sandfire Resources NL, 2011b. Sandfire Resources NL, March 2011 Quarterly Report highlights, 10 pp.
- Schiffries, C.M., 1982. The petrogenesis of a platinumiferous dunite pipe in the Bushveld Complex: infiltration metasomatism by a chloride solution. *Economic Geology*, 77, 1439–1453.
- Schissel, D., Tsvetkov, A.A., Mitrofanov, F.P. and Korchagin, A.U., 2002. Basal platinum-group element mineralization in the Federov Pansky layered mafic intrusion, Kola Peninsula, Russia. *Economic Geology*, 97, 1657–1677.
- Schodde, R., 2010. Global discovery trends 1950-2009: What, where and who found them. PowerPoint presentation at PDAC 2010, 7 March 2010, Toronto, Canada, 31 pp.  
<http://www.minexconsulting.com/publications/Global%20Discovery%20Trends%201950-2009%20PDAC%20March%202010.pdf> (last accessed 10 October 2014).
- Schulte, R.F., Taylor, R.D., Piatak, N.M. and Seal, R.R.II, 2010. Stratiform chromite deposit model. United States Geological Survey Open-File Report 2010–1232, 7 pp.
- Schultz, K., 1975. Carr-Boyd Rocks, nickel-copper deposits. In: Knight, C.L. (editor), *Economic Geology of Australia and Papua New Guinea*. 1. Metals. Australasian Institute of Mining and Metallurgy, Monograph 5, 125–128.
- Schulz, K.J., Chandler, V.W., Nicholson, S.W., Piatak, N., Seal, R.R., Woodruff, L.G. and Zientek, M.L., 2010. Magmatic sulfide-rich nickel-copper deposits related to picrite and (or) tholeiitic basalt dike-like-sill complexes: a preliminary deposit model. United States Geological Survey Open-File Report 2010–1179, 25 pp.
- Scoates, J.S. and Mitchell, J.N., 2000. The evolution of troctolite and high Al basaltic magmas in Proterozoic anorthosite plutonic suites and implications for the Voisey's Bay massive Ni-Cu sulfide deposit. *Economic Geology*, 95, 677–701.

- Scoon, R.N. and Mitchell, A.A., 2004. The platiniferous dunite pipes in the eastern limb of the Bushveld Complex: review and comparison with unmineralized discordant ultramafic bodies. *South African Journal of Geology*, 107, 505–520.
- Scott, D.A. and Bray, W., 1980. Ancient platinum technology in South America. Its use by the Indians in pre-Hispanic times. *Platinum Metals Review*, Johnson Matthey and Company Limited, London, October 1980, 24, 147–157.
- Scott, K.M., 1978. Geochemical aspects of the alteration-mineralization at Copper Hill, New South Wales, Australia. *Economic Geology*, 73, 966–976.
- Scott, K.M., 1988. The mineralogy of weathered profiles within the porphyritic Copper Hill Cu-Au deposit, central NSW. CSIRO Division of Exploration Geoscience Restricted Investigation Report 1772R, 13 pp.
- Scott, K.M. and Torrey, C.E., 2003. Copper Hill porphyry Cu-Au prospect, central NSW. CRC LEME 2003, 3 pp. <http://crcleme.org.au/RegExpOre/CopperHill.pdf> (last accessed 10 October 2014).
- Seabrook, C.L., Prichard, H.M. and Fisher, P.C., 2004. Platinum-group minerals in the Raglan Ni-Cu-(PGE) sulfide deposit, Cape Smith, Quebec, Canada. *Canadian Mineralogist*, 42, 485–497.
- Seat, Z., 2008. Geology, petrology, mineral and whole-rock chemistry, stable and radiogenic isotope systematics and Ni-Cu-PGE mineralisation of the Nebo-Babel intrusion, West Musgrave, Western Australia. PhD thesis, University of Western Australia, Australia, 479 pp.
- Seat, Z., Beresford, S.W., Grguric, B.A., Waugh, R.S., Hronsky, J.M.A., Gee, M.A.M., Groves, D.I. and Mathison, C.I., 2007. Architecture and emplacement of the Nebo-Babel gabbro-hosted magmatic Ni-Cu-PGE sulphide deposit, West Musgrave, Western Australia. *Mineralium Deposita*, 42, 551–581.
- Seat, Z., Beresford, S.W., Grguric, B.A., Gee, M.A.M. and Grassineau, N.V., 2009. Reevaluation of the role of external sulfur addition in the genesis of Ni-Cu-PGE deposits: Evidence from the Nebo-Babel Ni-Cu-PGE Deposit, West Musgrave, Western Australia. *Economic Geology*, 104, 521–538.
- Seat, Z., Gee, M.A.M., Grguric, B.A., Beresford, S.W. and Grassineau, N.V., 2011. The Nebo-Babel Ni-Cu-PGE sulfide deposit (West Musgrave, Australia): Pt. 1. U/Pb zircon ages, whole-rock and mineral chemistry, and O-Sr-Nd isotope compositions of the intrusion, with constraints on petrogenesis. *Economic Geology*, 106, 527–556.
- Secombe, P.K., Groves, D.I., Marston, R.J. and Barrett, F.M., 1981. Sulfide paragenesis and sulphur mobility in Fe-Ni-Cu sulfide ores at Lunnon and Juan main shoots, Kambalda: Textural and sulphur isotopic evidence. *Economic Geology*, 76, 1675–1685.
- Sehr, U. and Grehl, M. (editors), 2012. *Precious Materials Handbook*. Umicore AG and Co KG, Hanau-Wolfgang, Germany, 576 pp.
- Seymour, A.R., 2006. Nickel prospectivity in Victoria. Geological Survey of Victoria Technical Record 2006/3. Geological Survey of Victoria, 76 pp.
- Seymour, D.B., Green, G.R. and Calver, C.R., 2007. The geology and mineral deposits of Tasmania: a summary. *Mineral Resources Tasmania. Geological Survey Bulletin 72*, 29 pp.
- Shannon, R.D., 1976. Revised effective ionic radii and systematic studies of interatomic distances in halide and chalcogenides. *Acta Crystallographica Section A*, 32, 751–767.
- Sharpe, M.R. and Irvine, T.N., 1983. Melting relations of two Bushveld chilled margin rocks and implications for the origin of chromitite. *Carnegie Institute of Washington Year Book*, 82, 295–300.
- Shaw, R.D. and Black, L.P., 1991. The history and tectonic implications of the Redbank Thrust Zone, central Australia, based on structural, metamorphic and Rb-Sr isotopic evidence. *Australian Journal of Earth Sciences*, 38, 307–332.
- Shaw, R.D., Wellman, P., Gunn, P., Whitaker, A.J., Tarlowski, C. and Morse, M., 1996. Guide to using the Australian Crustal Elements Map. Australian Geological Survey Organisation, Record, 1996/30, 44 pp.
- Sheard, M.J. and Robertson, I.D.M., 2002. Regolith morphology and geochemistry over greenstones; what works and what does not? Gawler Craton, South Australia: Gawler Craton 2002: State of Play

- Workshop, Regional concepts and data for targeting ore systems in the Gawler Craton, 5-6 December 2002, Adelaide, (CD Rom): Minerals and Energy Resources of South Australia.
- Sheppard, S., Griffin, T.J. and Tyler, I.M., 1995. Geochemistry of felsic igneous rocks from the southern Halls Creek Orogen. Geological Survey of Western Australia, Record 1995/4, 81 pp.
- Sheppard, S., Tyler, I.M. and Hoatson, D.M., 1997. Geology of the Mount Remarkable 1:100 000 sheet: Western Australia Geological Survey, 1:100 000 Geological Series Explanatory Notes, 27 pp.
- Sheppard, S., Page, R.W., Griffin, T.J., Rasmussen, B., Fletcher, I.R., Tyler, I.M., Kirkland, C.L., Wingate, M.T.D., Hollis, J. and Thorne, A.M., 2012. Geochronological and isotopic constraints on the tectonic setting of the c. 1800 Ma Hart Dolerite and the Kimberley and Speewah Basins, northern Western Australia. Geological Survey of Western Australia Record 2012/7, 28 pp.
- Sheth, H.C., 2007. 'Large Igneous Provinces (LIPs)': definitions, recommended terminology, and a hierarchical classification. *Earth-Science Reviews*, 85, 117–124.
- Shi, B., 1995. Geochemistry and mineralisation of primary and secondary platinum-group elements in the ultramafic "Alaskan-type" Owendale complex and laterites in the Fifield Region, New South Wales, Australia. PhD thesis, School of Earth Sciences, The University of Melbourne, 392 pp.
- Shima, H. and Naldrett, A.J., 1975. Solubility of sulfur in an ultramafic melt and the relevance of the system Fe-S-O. *Economic Geology and the Bulletin of the Society of Economic Geologists*, 70, 960–967.
- Shree Minerals Limited, 2009. Prospectus, 2009 (dated 19 November 2009), 132 pp. <http://www.shreeminerals.com/Scripts/default.asp> (last accessed 10 October 2014).
- Sibbald, T.I.I. and Quirt, D., 1987. Uranium deposits of the Athabasca Basin. Saskatchewan Research Council, Publication #R-855-5G-87, 72 pp.
- Simpson, C.J., Macias, L.F. and Moore, R.F., 1988. Differentiation of mafic and ultramafic rocks in the Pilbara of Western Australia, using remote sensing techniques: The Second International Conference on Prospecting in Arid Terrain, Perth, Western Australia, April 1988, 127–128b.
- Simpson, E.S., 1914. The rare metals and their distribution in Western Australia. *Western Australia Geological Survey*, Article 59, 31–56.
- Sinclair, W.D., 2007. Porphyry deposits. In: Goodfellow, W.D. (editor), *Mineral Deposits of Canada: A Synthesis of Major Deposit-Types, District Metallogeny, the Evolution of Geological Provinces, and Exploration Methods*. Geological Association of Canada, Mineral Deposits Division, Special Publication No. 5, 223–243.
- Singh, A.K., Devi, L.D., Singh, N.I., Subramanyam, K.S.V., Singh, R.K.B. and Satyanarayanan, M., 2013. Platinum-group elements and gold distributions in peridotites and associated podiform chromitites of the Manipur Ophiolitic Complex, Indo-Myanmar Orogenic Belt, northeast India. *Chemie der Erde-Geochemistry*, 73, 147–161.
- Sirius Resources NL, 2010. Sirius Resources NL Explorers 2010 Freemantle presentation, 22 pp. <http://www.siriusresources.com.au/documents/SiriusASXannouncement-100225-Explorers2010conferencepresentation.pdf> (last accessed 10 October 2014).
- Sirius Resources NL, 2012. Sirius Resources NL announcement to the Australian Securities Exchange, 26 July 2012, 5 pp.
- Sirius Resources NL, 2012b. Sirius Resources NL announcement to the Australian Securities Exchange, 20 August 2012, 5 pp.
- Sirius Resources NL, 2012c. Sirius Resources NL announcement to the Australian Securities Exchange, 10 September 2012, 8 pp.
- Sirius Resources NL, 2012d. Sirius Resources NL announcement to the Australian Securities Exchange, 26 September 2012, 5 pp.
- Sirius Resources NL, 2013a. Sirius Resources NL announcement to the Australian Securities Exchange, 6 March 2013, 13 pp.
- Sirius Resources NL, 2013b. Sirius Resources NL announcement to the Australian Securities Exchange, 18 March 2013, 11 pp.

- Sirius Resources NL, 2013c. Sirius Resources NL announcement to the Australian Securities Exchange, 15 July 2013, 31 pp.
- Skirrow, R.G., Huston, D.L., Mernagh, T.P., Thorne, J.P., Dulfer, H. and Senior, A.B., 2013. Critical commodities for a high-tech world: Australia's potential to supply global demand. Geoscience Australia, Canberra, 118 pp. [http://www.ga.gov.au/corporate\\_data/76526/76526.pdf](http://www.ga.gov.au/corporate_data/76526/76526.pdf) (last accessed 10 October 2014).
- Slansky, E., Johan, Z., Ohnenstetter, M., Barron, L.M. and Suppel, D., 1991. Platinum mineralization in the Alaskan-type intrusive complexes near Fifield, New South Wales, Australia. Part 2. Platinum-group minerals in placer deposits in Fifield. *Mineralogy and Petrology*, 43, 161–180.
- Smith, C.L., 2007. El Capitan precious metals, Incorporated. Report on El Capitan gold-platinum project, including measured resource calculation, Lincoln County, New Mexico. Consulting Geologist Report, April 16, 2007, 13 pp. [http://www.elcapitanpmi.com/sites/default/files/gold\\_platinum\\_report.pdf](http://www.elcapitanpmi.com/sites/default/files/gold_platinum_report.pdf) (last accessed 10 October 2014).
- Smithies, R.H., 1998. Geology of the Sherlock 1:100 000 sheet. Western Australia Geological Survey, 1:100 000 Geological Series Explanatory Notes, 29 pp.
- Smithies, R.H., Hickman, A.H. and Nelson, D.R., 1999. New constraints on the evolution of the Mallina Basin, and their bearing on relationships between the contrasting eastern and western granite-greenstone terranes of the Archaean Pilbara Craton, Western Australia. *Precambrian Research*, 94, 11–28.
- Smithies, R.H., Howard, H.M., Evins, P.M., Kirkland, C.L., Bodorkos, S. and Wingate, M.T.D., 2009. West Musgrave Complex—new geological insights from recent mapping, geochronology and geochemical studies. *Geological Survey of Western Australia Record* 2008/19, 20 pp.
- Smithies, R.H., Spaggiari, C.V., Kirkland, C.L., Howard, H.M. and Maier, W.D., 2011. Petrogenesis of gabbros of the Mesoproterozoic Fraser Zone: constraints on the tectonic evolution of the Albany-Fraser Orogen. *Geological Survey of Western Australia, Record* 2013/5, 29 pp.
- Solomon, M. and Groves, D.I., 1994. *The Geology and Origin of Australia's Mineral Deposits*. Oxford Monographs on geology and geophysics, 24, Clarendon Press, Oxford, 951 pp.
- South Boulder Mines Limited, 2009. South Boulder Mines Limited announcement to the Australian Securities Exchange, 16 November 2009, 5 pp.
- Sprent, C.P., 1876. Mount Bischoff. Mr Sprent's report on country round. Table Cape, 3<sup>rd</sup> May, 1876, 6 pp.
- Sprent, C.P., 1877. Western country. Reports by the Hon. J.R. Scott and Mr C.P. Sprent. *Government Geologist*, New Town, 22<sup>nd</sup> May 1877, 12 pp.
- Sproule, R.A., 1999. Genesis of Palaeoproterozoic mafic-ultramafic intrusions and associated PGE–Cr and Ni–Cu–Co mineralisation in the East Kimberley, Western Australia. PhD thesis, Monash University, Australia, 320 pp.
- Sproule, R.A., Lambert, D.D. and Hoatson, D.M., 2002a. Decoupling of the Sm–Nd and Re–Os isotopic systems in sulphide-saturated magmas in the Halls Creek Orogen, Western Australia. *Journal of Petrology*, 43, 375–402.
- Sproule, R.A., Leshner, C.M., Ayer, J.A., Thurston, P.C. and Herzberg, C.T., 2002b. Spatial and temporal variations in the geochemistry of komatiites and komatiitic basalts in the Abitibi greenstone belt. *Precambrian Research*, 115, 153–186.
- Squire, R.J., Cas, R.A.F., Clout, J.M.F. and Behets, R., 1995. Volcanology of the Archaean Lunnon Basalt and its relevance to nickel sulphide-bearing trough structures at Kambalda, Western Australia. *Australian Journal of Earth Sciences*, 45, 695–715.
- Starkey, L., 1994. Geophysical signature of the Balla Balla titaniferous magnetite deposit, Western Australia. In: Dentith, M.C., Frankcombe, K.F., Ho, S.E., Shepherd, J.M., Groves, D.I. and Trench, A. (editors), *Geophysical Signatures of Western Australian Mineral Deposits*. Geology and Geophysics Department and UWA Extension, University of Western Australia, 26, 385–389.

- Steiger, R.H. and Jäger, E., 1978. Subcommittee on Geochronology; convention on the use of decay constants in geochronology and cosmochronology. *Studies in Geology* (Tulsa), 67–71.
- Stevens, B.P.J., Barnes, R.G. and Lishmund, S.R., 1975. Adelaide Fold Belt. In: Markham, N.L. and Basden, H. (editors), *The Mineral Deposits of New South Wales*. Geological Survey of New South Wales, 41–86.
- Stockman, H.W. and Hlava P.F., 1984. Platinum-group minerals in alpine chromitites from southwestern Oregon. *Economic Geology*, 79, 491–508.
- Stojanovic, M., 1995. Petrology, geochemistry and isotope geochemistry of host rocks to platinum mineralisation at Fifield, New South Wales. MSc thesis, University of New South Wales, Australia, 186 pp.
- Stolz, E.M., 2000. Electromagnetic methods applied to exploration for deep nickel sulfides in the Leinster area. 14<sup>th</sup> Geophysical Conference, *Exploration Geophysics*, 31, 222–238.
- Stone, W.E. and Archibald, N.J., 2004. Structural controls on nickel sulphide ore shoots in Archaean komatiite, Kambalda, WA; the volcanic trough controversy revisited. *Journal of Structural Geology*, 26, 1173–1194.
- Stone, W.E. and Masterman, E.E., 1998. Kambalda nickel deposits. In: Berkman, D.A. and Mackenzie, D.H. (editors), *Geology of Australian and Papua New Guinean Mineral Deposits*. Australasian Institute of Mining and Metallurgy, Melbourne, Monograph 22, 347–356.
- Stone, W.E., Heydari, M. and Seat, Z., 2004. Nickel tenor variations between Archaean komatiite-associated nickel sulphide deposits, Kambalda ore field, Western Australia. The metamorphic model revisited. *Mineralogy and Petrology*, 82, 295–316.
- Stone, W.E., Beresford, S.W. and Archibald, N.J., 2005. Structural setting and shape analysis of nickel sulfide shoots at the Kambalda Dome, Western Australia: Implications for deformation and remobilization. *Economic Geology*, 100, 1441–1455.
- Stowe, C.W. (editor), 1987. *Evolution of Chromium Ore Fields*. Evolution of Ore Fields Series, Van Nostrand Reinhold Company, New York, 340 pp.
- Stowe, C.W., 1994. Compositions and tectonic settings of chromite deposits through time. *Economic Geology*, 89, 528–546.
- Stumpfl, E.F., 1986. Distribution, transport and concentration of platinum group elements. In: Gallagher, M.J., Ixer, R.A., Neary, C.R. and Prichard, H.M. (editors), *Metallogeny of Basic and Ultrabasic Rocks*. The Institution of Mining and Metallurgy, London, 3379–3394.
- Stumpfl, E.F., 1987. The mobility of platinum group elements. In: Campbell, A. (editor), *Abstract and Field Guide, 5th Magmatic Sulphides Field Conference*, Harare, Zimbabwe, 3–13 August, 1987. Geological Society of Zimbabwe, IGCP Project 161, 20.
- Stumpfl, E.F. and Ballhaus, C.G., 1986. Stratiform platinum deposits: New data and concepts. *Fortschritte der Mineralogie*, 64, 205–214.
- Su, S., Li, C., Zhou, M.-F., Ripley, E.M. and Qi, L., 2008. Controls on variations of platinum-group element concentrations in the sulfide ores of the Jinchuan Ni-Cu deposit, western China. *Mineralium Deposita*, 43, 609–622.
- Sun, S.-S., Wallace, D.A., Hoatson, D.M., Glikson, A.Y. and Keays, R.R., 1991. Use of geochemistry as a guide to platinum group element potential of mafic-ultramafic rocks: examples from the west Pilbara Block and Halls Creek Mobile Zone, Western Australia. *Precambrian Research*, 50, 1–35.
- Sun, S.-S., Sheraton, J.W., Glikson, A.Y. and Stewart, A.J., 1996. A major magmatic event during 1050–1080 Ma in central Australia, and an emplacement age for the Giles Complex. *AGSO Journal of Australian Geology and Geophysics*, 24, 13–15.
- Suppel, D.W. and Barron, L.M., 1986a. Platinum in basic to ultrabasic intrusive complexes at Fifield: A preliminary report. *New South Wales Geological Survey Quarterly Notes*, 65, 1–8.
- Suppel, D.W. and Barron, L.M., 1986b. New data on the occurrence of platinum at Fifield. In: *Geological Setting of Precious Metals in New South Wales*. Abstracts 18. Geological Society of Australia, Sydney, 1986, 1–5.

- Suppel, D.W., Barron, L.M., Spencer, R., Slansky, E., Johan, Z. and Ohnenstetter, M., 1987. Platinum in basic to ultrabasic intrusive complexes at Fifield, New South Wales. In: *Platiniferous Horizons in Layered Intrusions, Abstracts, Symposium, Sydney, 21 October 1987*. University of New South Wales and Geological Society of Australia.
- Sutton, J., 2008. The history and applications for platinum. *Ezine Articles*, submitted 29 September 2008, 3 pp. <http://ezinearticles.com/?The-History-and-Applications-For-Platinum&id=1538868> (last accessed 10 October 2014).
- Sweet, I.P., Brakel, A.T. and Carson, L., 1999. The Kombolgie Subgroup—a new look at an old 'formation'. *AGSO Research Newsletter*, 30, 26–28.
- Sydney Morning Herald, 2014—[Web page]. Gem found on Australian sheep ranch is the oldest known piece of Earth, scientists find. <http://www.smh.com.au/technology/sci-tech/gem-found-on-australian-sheep-ranch-is-the-oldest-known-piece-of-earth-scientists-find-20140227-hvdkd.html> (last accessed 10 October 2014).
- Talusani, R.V.R., Sivell, W.J. and Ashley, P.M., 2005. Mineral chemistry, petrogenesis, and tectonic setting of the Wateranga layered intrusion, southeast Queensland, Australia. *Canadian Journal of Earth Sciences*, 42, 1967–1985.
- Tarkian, M. and Stribny, B., 1999. Platinum-group elements in porphyry copper deposits: a reconnaissance study. *Mineralogy and Petrology*, 65, 161–183.
- Taylor, S.R. and McLennan, S.M., 1985. *The Continental Crust: its Composition and Evolution. An Examination of the Geochemical Record Preserved in Sedimentary Rocks*. The Continental Crust: its Composition and Evolution. An Examination of the Geochemical Record Preserved in Sedimentary Rocks, Blackwell, Oxford, United Kingdom, 312 pp.
- Taylor, S.R. and McLennan, S.M., 1995. The geochemical evolution of the continental crust. *Reviews of Geophysics*, 33, 241–265.
- Taylor, S.R. and McLennan, S.M., 2009. *Planetary Crust: Their Composition, Origin, and Evolution*. Cambridge University Press, Cambridge, United Kingdom, 378 pp.
- Teluk, A.J., 2001. Fifield platinum project, New South Wales, Australia. *Platinum metallogenesis, Ural-Alaskan type complexes*. Rimfire Pacific Mining NL Technical Report, 71 pp.
- Thakurta, J., Ripley, E.M. and Li, C., 2008. Pre-requisites for sulphide-poor PGE and sulphide-rich Cu-Ni-PGE mineralisation in Alaskan-type complexes. *Journal Geological Society of India*, 72, 611–622.
- Thakurta, J., Ripley, E.M. and Li, C., 2014. Platinum group element geochemistry of sulfide-rich horizons in the Ural-Alaskan-type ultramafic complex of Duke Island, southeastern Alaska. *Economic Geology*, 109, 643–659.
- Thebaud, N., Fiorentini, M.L., McCuaig, C., Miller, J., Barnes, S.J., Joly, A. and Doublier, M., 2009. Tectonostratigraphic controls on the localization of Archaean komatiite-hosted nickel-sulphide deposits and camps in the Yilgarn Craton: *Geochimica et Cosmochimica Acta*, Supplement 1, 73, A1323.
- Thompson, J.F.H., Lang, J.R. and Stanley, C.R., 2001. Platinum group elements in alkaline porphyry deposits, British Columbia. *Exploration and Mining in British Columbia, Mines Branch, Part B*, 57–64.
- Thomson, J., 1974. Results of radiometric dating programme, 1971–1973. *New South Wales Geological Survey Records* 16, 141–147.
- Thorne, J.P., Cooper, M., Claoué-Long, J.C., Hight, L., Hoatson, D.M., Jaireth, S., Huston, D.L. and Gallagher, R., 2014. Guide to Using the Australian Mafic-Ultramafic Magmatic Events GIS Dataset. Record 2014/039. *Geoscience Australia*, Canberra. [http://www.ga.gov.au/metadata-gateway/metadata/record/gcat\\_78742](http://www.ga.gov.au/metadata-gateway/metadata/record/gcat_78742) (last accessed 10 October 2014).
- Thorne, A.M. and Trendall, A.F., 2001. *Geology of the Fortescue Group, Pilbara Craton, Western Australia*. Geological Survey of Western Australia, Bulletin 144, 249 pp.

- Thorne, A.M., Sheppard, S. and Tyler, I.M., 1999. Lissadell, Western Australia, 1:250 000 Geological Series Explanatory Notes, Sheet SE 52–2. Geological Survey of Western Australia, Perth, Western Australia, Australia, 68 pp.
- Thornett, J.R., 1981. The Sally Malay deposit: gabbroid associated nickel-copper sulfide mineralization in the Halls Creek Mobile Zone, Western Australia. *Economic Geology*, 76, 1565–1580.
- Thundelarra Exploration Limited, 2001. Thundelarra Exploration Limited 2001 Annual Report, 62 pp.
- Thundelarra Exploration Limited, 2006a. Thundelarra Exploration Limited announcement to the Australian Securities Exchange, 17 August 2006, 21 pp.
- Thundelarra Exploration Limited, 2006b. Thundelarra Exploration Limited announcement to the Australian Securities Exchange, 1 December 2006, 3 pp.
- Todd, S.G., Keith, D.W., Le Roy, L.W., Schissel, D.J., Mann, E.L. and Irvine, T.N., 1982. The J-M platinum-palladium reef of the Stillwater Complex, Montana: I. Stratigraphy and petrology. *Economic Geology*, 77, 1454–1480.
- Tolstykh, N.D., Sidorov, E.G. and Krivenko, A.P., 2005. Platinum-group element placers associated with Urals-Alaska type complexes. In: Mungall, J.E. (editor), *Exploration for Platinum-Group Element Deposits*. Mineralogical Association of Canada Short Course 35, Oulu, Finland, 113–143.
- Torres-Ruiz, J., Garuti, G. Gazzoti, M., Gervilla, F. and Fenoll Hach-Ali, P., 1996. Platinum group minerals in chromites from the Ojen Iherzolite massif (Serrania de Ronda, Betic Cordillera, Southern Spain). *Mineralogy and Petrology*, 56, 25–50.
- Torrey, C.E., 1990. Copper Hill project, Exploration Licence 2290, review and exploration proposal. Cyprus Gold Australia Corporation. NSW GS1990/225, 192.
- Traka Resources Limited, 2010a. Musgrave Project—Strongly anomalous rock-chip and auger geochemical results on the ‘Jamieson Prospect’. Traka Resources Limited Report to the Australian Securities Exchange, 30 June 2010, 3 pp.
- Traka Resources Limited, 2010b. Quarterly activities report for the three months ended 30 September 2010. Traka Resources Limited Report to the Australian Securities Exchange, 30 September 2010, 12 pp.
- Traore, D., Beauvais, A., Chabaux, F., Peiffert, C., Parisot, J.-C., Ambrosi, J.-P. and Colin, F., 2008. Chemical and physical transfers in an ultramafic rock weathering profile: Part 1. Supergene dissolution of Pt-bearing chromite. *American Mineralogist*, 93, 22–30.
- Travis, G.A., 1975. Nickel-copper sulphide mineralisation in the Jimberlana intrusion. In: Knight, C.L. (editor), *Economic Geology of Australia and Papua New Guinea*. 1. Metals. Australasian Institute of Mining and Metallurgy, Monograph 5, 75–78.
- Travis, G.A., Keays, R.R. and Davison, R.M., 1976. Palladium and iridium in evaluation of nickel gossans in Western Australia. *Economic Geology*, 71, 1229–1243.
- Trudu, A.G., 1994. First report on the Copper Hill Porphyry Cu-Au-Pd Prospect, Molong, NSW. Report to MIMEX, 39 pp.
- Trudu, A. and Hoatson, D.M., 1996. Depths of emplacement of Precambrian layered intrusions in the East Kimberley. *AGSO Research Newsletter*, 25, 10–12.
- Trudu, A. and Hoatson, D.M., 2000. Chapter 9. Depths of emplacement of the mafic-ultramafic intrusions. In: Hoatson, D.M. and Blake, D.H. (editors), *Geology and Economic Potential of the Palaeoproterozoic Layered Mafic-Ultramafic Intrusions in the East Kimberley, Western Australia*. Australian Geological Survey Organisation Bulletin 246, 201–219.
- Turner, N.J. and Bottrill, R.S., 2001. Blue amphibole, Arthur Metamorphic Complex, Tasmania: composition and regional tectonic setting. *Australian Journal of Earth Sciences*, 48, 167–181.
- Turner, N.J., Black, L.P. and Kamperman, M., 1998. Dating of Neoproterozoic and Cambrian orogenies in Tasmania. *Australian Journal of Earth Sciences*, 45, 789–806.
- Turvey, D.J., 1990. Primary platinum mineralisation review; Owendale intrusion. Unpublished report.

- Twelvetrees, W.H., 1914. The Bald Hill Osmiridium Field. Tasmania Department of Mines Geological Survey Bulletin 17, 39 pp.
- Tyler, I.M., 1991. The geology of the Sylvania Inlier and the southeast Hamersley Basin, Geological Survey of Western Australia. Bulletin, 138, 108 pp.
- Tyler, I.M. and Griffin, T.J., 1993. Yampi, Western Australia, 1:250 000 Geological Series Explanatory Notes, Sheet SE 51–3. Second edition. Geological Survey of Western Australia, Perth, Western Australia, Australia, 32 pp.
- Tyler, I.M., Griffin, T.J., Page, R.W. and Shaw, R.D., 1995. Are there terranes within the Lamboo Complex of the Halls Creek Orogen? Western Australia Geological Survey, Annual Review 1993–94, 37–46.
- Tyler, I.M., Sheppard, S., Pirajno, F. and Griffin, T.J., 2006. Hart-Carson LIP, Kimberley region. August 2006 LIP of the Month, 8 pp. <http://www.largeigneousprovinces.org/06aug> (last accessed 10 October 2014).
- Ulmer, G.C., 1969. Experimental investigations of chromite-spinels. In: Wilson, H.D.B. (editor), Magmatic Ore Deposits. Economic Geology Monograph 4, 114–131.
- USGS, 2014—[Web page]. Mineral Commodity Summaries, 2014, 196 pp. <http://minerals.usgs.gov/minerals/pubs/mcs/2014/mcs2014.pdf> (last accessed 10 October 2014).
- United States National Academy of Sciences, 2008. Minerals, critical minerals, and the U.S. economy. [http://www.nap.edu/catalog.php?record\\_id=12034](http://www.nap.edu/catalog.php?record_id=12034) (last accessed 10 October 2014).
- Valenta, R.K., 1990. Structural setting of unconformity-related U-Au-platinoid mineralisation in the South Alligator Valley, NT. In: Gondwana Terranes and Resources. Geological Society of Australia, Abstracts, 25, 173.
- Valley, J.W., Cavosie, A.J., Ushikubo, T., Reinhard, D.A., Lawrence, D.F., Larson, D.J., Clifton, P.H., Kelly, T.F., Wilde, S.A., Moser, D.E. and Spicuzza, M.J., 2014. Hadean age for a post-magma-ocean zircon confirmed by atom-probe tomography: Nature Geoscience 7, 3, 219–223.
- VandenBerg, A.H.M., Cayley, R.A., Willman, C.E., Morand, V.J., Seymon, A.R., Osborne, C.R., Taylor, D.H., Haydon, S.J., McLean, M., Quinn, C., Jackson, P. and Sandford, A.C., 2006. Walhalla-Woods Point-Tallangalook special map area geological report. Geological Survey of Victoria Report 127. Geoscience Victoria. Department of Primary Industries, 448 pp.
- Van Kranendonk, M.J. and Ivanic, T.J., 2010. A new lithostratigraphic scheme for the northeastern Murchison Domain, Yilgarn Craton. In: Annual Review 2007–08, Western Australia Geological Survey, 35–53.
- Van Kranendonk, M.J., Hickman, A.H., Smithies, R.H. and Nelson, D.R., 2002. Geology and tectonic evolution of the Archean North Pilbara Terrain, Pilbara Craton, Western Australia. Economic Geology, 97, 695–732.
- Varne, R. and Brown, A.V., 1978. The geology and petrology of the Adamsfield Ultramafic Complex, Tasmania. Contributions to Mineralogy and Petrology, 67, 195–207.
- Viljoen, M.J., 1999. The nature and origin of the Merensky Reef of the western Bushveld Complex based on geological facies and geological data. South African Journal of Geology, 102, 221–239.
- Viljoen, M.J. and Viljoen, R.P., 1969. Evidence for the existence of a mobile extrusive peridotitic magma from the Komati Formation of the Onverwacht Group. Geological Society of South Africa Special Publication 2, 87–112.
- Vulcan Resources Limited, 2005. Vulcan Resources Limited Annual Report 2005, 65 pp.
- WA Department of Mines and Petroleum (2014)—[Web page]. Quantity and Value 2013 Tables. <http://www.dmp.wa.gov.au/1521.aspx> (last accessed 10 October 2014).
- Wallace, D.A., 1992a. Andover mafic-ultramafic complex, West Pilbara, Western Australia: Chemical and petrographic data, and summary of geology. Bureau of Mineral Resources, Geology and Geophysics, Australia, Record 1992/13, 29 pp.
- Wallace, D.A., 1992b. Field relationships, petrography, mineralogy, and geochemistry of the Andover Complex. In: Hoatson et al., Petrology and Platinum-Group-Element Geochemistry of Archaean

- Layered Mafic-Ultramafic Intrusions, west Pilbara Block, Western Australia. Australian Geological Survey Organisation Bulletin 242, 126–140.
- Wallace, D.A. and Hoatson, D.M., 1990. Petrology and whole-rock geochemistry of selected mafic and ultramafic suites from the Pilbara Block and Halls Creek Mobile Zone, Western Australia. Bureau of Mineral Resources, Australia, Record 1990/46, 69 pp.
- Ward, H.J., 1975. Barrambie iron-titanium-vanadium deposit. Monograph Series - Australasian Institute of Mining and Metallurgy, 207–210.
- Washington Resources Limited, 2005. Washington Resources Limited Prospectus 2005, 39 pp.
- Washington Resources Limited, 2006. Washington Resources Limited announcement to the Australian Securities Exchange, 18 July 2006, 4 pp.
- Weiser, T.W., 1998. Platinum-group minerals in placer deposits from Papua New Guinea. Geological Society of South Africa and South African Institute of Mining and Metallurgy, Symposium ser S 18, 439–441.
- Wedepohl, K.H., 1995. The composition of the continental crust. *Geochimica et Cosmochimica Acta*, 59, 1217–1232.
- Weiser, T.W., 2002. Platinum-group minerals (PGM) in placer deposits. In: Cabri, L.J. (editor), *The Geology, Geochemistry, Mineralogy and Mineral Beneficiation of Platinum-Group Elements*. Canadian Institute of Mining, Metallurgy and Petroleum, Special Volume 54, 721–756.
- Wendlandt, R.F., 1982. Sulfide saturation of basalt and andesite melts at high pressures and temperatures. *American Mineralogist*, 67, 877–885.
- Western Mining Corporation Limited, 1993. Western Mining Corporation Limited Corporation 1993 Annual Report.
- Western Mining Corporation Limited, 2003. WMC Exploration: Geological setting of Ni-Cu-PGE mineralisation at the West Musgrave, MEGWA January 2003 PowerPoint Presentation.
- White, R.M.S., Collins, S., Denne, R., Hee, R. and Brown, P., 2001. A new survey design for 3D IP inversion modelling at Copper Hill. *Exploration Geophysics*, 32, 152–155.
- Whitaker, A.J. and Bastrakova, I.V., 2002. Yilgarn Craton aeromagnetic interpretation. 1:1 500 000 scale colour map. Geoscience Australia, Canberra.
- Wilde, A., 2005. Descriptive ore deposit models: hydrothermal and supergene Pt and Pd deposits. In: Mungall, J.E. (editor), *Exploration for Platinum-Group Element Deposits*. Mineralogical Association of Canada Short Course 35, Oulu, Finland, 145–161.
- Wilde, A.R., 1988. On the origin of unconformity-type uranium deposits. PhD thesis, Monash University, Victoria, Australia.
- Wilde, A., 2005. Descriptive ore deposit models; hydrothermal and supergene Pt Pd deposits. Short Course Series—Mineralogical Association of Canada 35, 145–161.
- Wilde, A.R., Bloom, M.S. and Wall, V.J., 1989. Transport and deposition of gold, uranium, and platinum-group elements in unconformity-related uranium deposits. *Economic Geology Monograph* 6, 637–650.
- Wilde, S.A. and Spaggiari, C., 2007. The Narryer Terrane, Western Australia: a review. In: Van Kranendonk, M.J., Smithies, R.H. and Bennett, V.C. (editors), *Earth's Oldest Rocks*. Developments in Precambrian Geology 15, Elsevier, The Netherlands, 275–304.
- Wilde, S.A., Valley, J.W., Peck, W.H. and Graham, C.M., 2001. Evidence from detrital zircons for the existence of continental crust and oceans on the Earth 4.4 Gyr ago. *Nature*, 409, 175–178.
- Williams, C.R., Nisbet, B.W. and Hoatson, D.M., 1990. Munni Munni Complex platinum group mineralisation. In: Hughes, F.E. (editor), *Geology of the Mineral Deposits of Australia and Papua New Guinea*. Australasian Institute of Mining and Metallurgy, Monograph 14, Melbourne, Volume 1, 145–150.
- Williams, D.A.C., 1971. Determination of primary mineralogy and textures of ultramafic rocks from Mount Monger, Western Australia, *Society of Australia Special Publication* 3, 259–268.
- Williams, E., 1978. Tasman Fold Belt System in Tasmania. *Tectonophysics*, 48, 159–205.

- Williams, G.E. and Gostin, V.A., 2005. The Acraman–Bunyeroo impact event (Ediacaran), South Australia, and environmental consequences: 25 years on. *Australian Journal of Earth Sciences*, 52, 607–620.
- Williams, G.E. and Gostin, V.A., 2010. Geomorphology of the Acraman impact structure, Gawler Ranges, South Australia. *Cadernos Lab. Xeolóxico de Laxe Coruña*, 35, 209–220.
- Williams, L., 2012. Duluth sets Bechtel parameters for 100 year copper-nickel-pgm mine PFS. Mineweb article posted 22 March 2012. <http://www.mineweb.com/mineweb/view/mineweb/en/page36?oid=147766&sn=Detail> (last accessed 10 October 2014).
- Williams, P.A., 2001. Chemical behavior of the platinum group elements during weathering. In: *Geochemical Exploration for Platinum Group Elements in Weathered Terrain*. CRC LEME Open File Report 85, Volume I, 8–29.
- Wilson, A.H. and Tredoux, M., 1990. Lateral and vertical distribution of platinum-group elements and petrogenetic controls on the sulfide mineralization in the P1 pyroxenite layer of the Darwendale subchamber of the Great Dyke, Zimbabwe. *Economic Geology*, 85, 556–584.
- Wilson, A.H., Naldrett, A.J. and Tredoux, M., 1989. Distribution and controls of platinum group element and base metal mineralization in the Darwendale subchamber of the Great Dyke, Zimbabwe. *Geology*, 17, 649–652.
- Wingate, M.T.D., 1999. Ion microprobe baddeleyite and zircon ages for Late Archaean mafic dykes of the Pilbara Craton, Western Australia. *Australian Journal of Earth Sciences*, 46, 493–500.
- Wingate, M.T.D. and Pidgeon, R.T., 2005. The Marnda Moorn LIP, a late Mesoproterozoic large igneous province in the Yilgarn craton, Western Australia. July 2005 LIP of the month. <http://www.largeigneousprovinces.org/05jul> (last accessed 10 October 2014).
- Wingate, M.T.D., Campbell, I.H., Compston, W. and Gibson, G.M., 1998. Ion microprobe U-Pb ages for Neoproterozoic basaltic magmatism in south-central Australia and implications for the breakup of Rodinia. *Precambrian Research*, 87, 135–159.
- Wingate, M.T.D., Pirajno, F. and Morris, P.A., 2004a. *Geology*, 32, 105–108.
- Wingate, M.T.D., Pirajno, F. and Morris, P.A., 2004b. Warakurna large igneous province: a new Mesoproterozoic large igneous province in west-central Australia. January 2004 LIP of the month. <http://www.largeigneousprovinces.org/04jan> (last accessed 10 October 2014).
- Withall, J., 2001. Windimurra vanadium mine. Archean granite–greenstones of the central Yilgarn Craton, Western Australia—a field guide. *Geological Survey of Western Australia Record 2001/14*.
- Witt, W.K. and Barnes, S.J., 1991. The Ora Banda Sill. In: Barnes, S.J. and Hill, R.E.T. (editors), *Mafic-Ultramafic Complexes of Western Australia*, Excursion Guidebook No. 3. Sixth International Platinum Symposium, July 1991, Perth, WA. IAGOD and the Geological Society of Australia, 31–35. WMC Limited, 2003. Geological setting of Ni-Cu-PGE mineralisation at the West Musgrave. WMC Limited Mining and Exploration Group, Western Australia–January 2003. WMC PowerPoint presentation.
- Wolfram, P. and Golden, H., 2001. Airborne EM applied to sulfide nickel-examples and analysis. *Exploration Geophysics*, 32, 136–140.
- Wollaston, W. 1805. On the Discovery of Palladium; With Observations on Other Substances Found with Platina. *Philosophical Transactions of the Royal Society of London*. 95, 316–330. <https://archive.org/details/philtrans00739436> doi:10.1098/rstl.1805.0024 (last accessed 10 October 2014).
- Wood, S.A., 1990. The interaction of dissolved platinum with fulvic acid and simple organic acid analogues in aqueous solutions. *The Canadian Mineralogist*, 28, 665–673.
- Wood, S.A., 2002. The aqueous geochemistry of the platinum-group elements with applications to ore deposits. In: Cabri, L.J. (editor), *The Geology, Geochemistry, Mineralogy and Mineral Beneficiation of Platinum-Group Elements*. Special Volume, Canadian Institute of Mining and Metallurgy, 54, 211–249.

- Wyborn, D., 1988. Ordovician magmatism, gold mineralisation, and an integrated tectonic model for the Ordovician and Silurian history of the Lachlan Fold Belt in NSW. *BMR Research Newsletter*, 8, 13–14.
- Wyborn, D., 1990. High platinum potential in the Lachlan Fold Belt. *BMR Research Newsletter*, 13, 8.
- Wyborn, D. and Cameron, W., 1990. Ordovician magmatism in the central Lachlan Fold Belt and precious metal potential. In: *Gondwana: Terranes and Resources*. Geological Society of Australia, Tenth Australian Geological Convention, Hobart, Abstracts 25.
- Wyborn, L., 1992. Au-Pt-Pd-U mineralisation in the Coronation Hill-EI Sherana region, Northern Territory. *AGSO Research Newsletter*, 16, 1–3.
- Wyborn, L.A.I., Valenta, R.K., Needham, R.S., Jagodzinski, E.A., Whitaker, A. and Morse, M.P., 1990. A review of the geological, geophysical and geochemical data of the Kakadu Conservation Zone as a basis for assessing the resource potential. In: *BMR Geological and Mineral Resource Studies, Resource Assessment Commission Kakadu Conservation Zone Inquiry Consultancy Series*, Australian Government Publishing Service, Canberra.
- Wyborn, L.A.I., Heinrich, C.A. and Jaques, A.L., 1994a. Australian Proterozoic mineral systems; essential ingredients and mappable criteria. Publication Series, Australasian Institute of Mining and Metallurgy Annual Conference, Darwin, 5-9 August 1994, 109–115.
- Wyborn, L., Jagodzinski, E.A., Morse, M.P., Whitaker, A., Cruikshank, B.I. and Pyke, J.G., 1994b. The exploration signature of the Coronation Hill gold, palladium and platinum deposit. Australasian Institute of Mining and Metallurgy Annual Conference, Darwin, 5-9 August 1994, 51–55.
- Young, D.N., Edgoose, C.J., Blake, D.H. and Shaw, R.D., 1995a. Mount Doreen, Northern Territory, 1:250 000 Geological Series Explanatory Notes, Sheet SF 52–12. Second edition. Northern Territory Geological Survey, Darwin, Australia, 55 pp.
- Young, D.N., Fanning, C.M., Shaw, R.D., Edgoose, C.J., Blake, D.H., Page, R.W. and Camacho, A., 1995b. U–Pb zircon dating of tectonomagnetic events in the northern Arunta Inlier, central Australia. In: Collins, W.J. and Shaw, R.D. (editors), *Time Limits on Tectonic Events and Crustal Evolution using Geochronology: some Australian Examples*. *Precambrian Research*, 71, 45–68.
- Yu, H., 1985. Skarns in the Xujiachong picrite body, Jingshan County, Hubei. *Acta Petrologica Mineralogica et Analytica*, 4, 108–113.
- Zhang, M., O'Reilly, S.Y., Wang, K.-L., Hronsky, J. and Griffin, W.L., 2008. Flood basalts and metallogeny: the lithospheric mantle connection. *Earth-Science Reviews*, 86, 145–174.
- Zhao, J.-x., McCulloch, M.T. and Korsch, R.J., 1994. Characterisation of a plume-related ~800 Ma magmatic event and its implications for basin formation in central-southern Australia. *Earth and Planetary Science Letters*, 121, 349–367.
- Zhou, M.-F., Sun, M., Keays, R.R. and Kerrich, R.W., 1998. Controls on platinum-group elemental distributions of podiform chromitites: a case study of high-Cr and high-Al chromitites from Chinese orogenic belts. *Geochimica et Cosmochimica Acta*, 62, 677–688.
- Zientek, M.L., 2012. Magmatic ore deposits in layered intrusions-Descriptive model for reef-type PGE and contact-type Cu-Ni-PGE deposits. United States Geological Survey Open-File Report 2012–1010, 48 pp.
- Zientek, M.L., Cooper, R.W., Corson, S.R. and Geraghty, E.P., 2002. Platinum-group element mineralization in the Stillwater Complex, Montana. In: Cabri, L.J. (editor), *The Geology, Geochemistry, Mineralogy and Mineral Beneficiation of Platinum-Group Elements*. Canadian Institute of Mining, Metallurgy and Petroleum, Special Volume 54, 459–481.

# Appendix A Chemical elements

Modified from <http://periodic.lanl.gov/list.shtml>

Appendix Table A.1 Alphabetical listing of chemical elements.

Symbol	Element	Atomic number	Symbol	Element	Atomic number
Ac	Actinium	89	Md	Mendelevium	101
Al	Aluminum	13	Hg	Mercury	80
Am	Americium	95	Mo	Molybdenum	42
Ar	Argon	18	Nd	Neodymium	60
As	Arsenic	33	Ne	Neon	10
At	Astatine	85	Np	Neptunium	93
Ba	Barium	56	Ni	Nickel	28
Bk	Berkelium	97	Nb	Niobium	41
Be	Beryllium	4	N	Nitrogen	7
Bi	Bismuth	83	No	Nobelium	102
Bh	Bohrium	107	<b>Os</b>	<b>Osmium</b>	<b>76</b>
B	Boron	5	O	Oxygen	8
Br	Bromine	35	<b>Pd</b>	<b>Palladium</b>	<b>46</b>
Cd	Cadmium	48	P	Phosphorus	15
Ca	Calcium	20	<b>Pt</b>	<b>Platinum</b>	<b>78</b>
Cf	Californium	98	Pu	Plutonium	94
C	Carbon	6	Po	Polonium	84
Ce	Cerium	58	K	Potassium	19
Cs	Cesium	55	Pr	Praseodymium	59
Cl	Chlorine	17	Pm	Promethium	61
Cr	Chromium	24	Pa	Protactinium	91
Co	Cobalt	27	Ra	Radium	88
Cn	Copernicium	112	Rn	Radon	86
Cu	Copper	29	Re	Rhenium	75
Cm	Curium	96	<b>Rh</b>	<b>Rhodium</b>	<b>45</b>
Ds	Darmstadtium	110	Rg	Roentgenium	111
Db	Dubnium	105	Rb	Rubidium	37
Dy	Dysprosium	66	<b>Ru</b>	<b>Ruthenium</b>	<b>44</b>
Es	Einsteinium	99	Rf	Rutherfordium	104
Er	Erbium	68	Sm	Samarium	62

Symbol	Element	Atomic number	Symbol	Element	Atomic number
Eu	Europium	63	Sc	Scandium	21
Fm	Fermium	100	Sg	Seaborgium	106
F	Fluorine	9	Se	Selenium	34
Fr	Francium	87	Si	Silicon	14
Gd	Gadolinium	64	Ag	Silver	47
Ga	Gallium	31	Na	Sodium	11
Ge	Germanium	32	Sr	Strontium	38
Au	Gold	79	S	Sulfur	16
Hf	Hafnium	72	Ta	Tantalum	73
Hs	Hassium	108	Tc	Technetium	43
He	Helium	2	Te	Tellurium	52
Ho	Holmium	67	Tb	Terbium	65
H	Hydrogen	1	Tl	Thallium	81
In	Indium	49	Th	Thorium	90
I	Iodine	53	Tm	Thulium	69
<b>Ir</b>	<b>Iridium</b>	<b>77</b>	Sn	Tin	50
Fe	Iron	26	Ti	Titanium	22
Kr	Krypton	36	W	Tungsten	74
La	Lanthanum	57	U	Uranium	92
Lr	Lawrencium	103	V	Vanadium	23
Pb	Lead	82	Xe	Xenon	54
Li	Lithium	3	Yb	Ytterbium	70
Lu	Lutetium	71	Y	Yttrium	39
Mg	Magnesium	12	Zn	Zinc	30
Mn	Manganese	25	Zr	Zirconium	40
Mt	Meitnerium	109			

*Platinum-group elements are shown in bold font.*

## Appendix B Glossary

Modified from Cassidy et al. (1997), Neuendorf et al. (2005), and Barnes (2006).

**adcumulate**—a textural term describing an igneous rock consisting of at least 90% accumulated liquidus crystals.

**aeolian**—sand sized material picked up, transported, and deposited by wind.

**airborne geophysical data**—geophysical information (e.g., gravity, gamma-ray spectrometric, and magnetic data) collected by instruments specially fitted to and being transported by an aircraft.

**alkaline**—igneous rock that contains more sodium and/or potassium than is required to form feldspar with the available silica.

**alkaline rock**—any of various rocks in which the chemical content of the alkalis (potassium oxide and sodium oxide) is great enough for alkaline minerals to form, e.g., the feldspathoids, aegirine pyroxene, and riebeckite.

**alluvial sediments**—sediments deposited, usually in stream channels, by flowing water.

**aplite**—a light-coloured igneous rock characterised by a fine-grained granular texture and consisting predominantly of quartz, potassium feldspar, and sodium-calcium feldspar.

**Archean**—the term, meaning ancient, has been generally applied to the oldest rocks of the Precambrian (older than 2500 million years).

**base metal**—generally referring to the elements, copper, lead, zinc and sometimes nickel.

**basement**—the lowest mappable rocks, generally with complex structure, that underlies other major rock sequences of a region.

**blebby ore**—disseminated ore variety consisting of spherical blebs of sulphide, in at least some cases showing evidence for forming within segregation vesicles.

**breccia**—a coarse-grained clastic rock, composed of angular broken rock fragments held together by a mineral cement or in a fine-grained matrix.

**brownfields**—exploration that is delineating or proving up an existing deposit, including extensions and infill, which has been classified as an Inferred Mineral Resource or higher.

**Cambrian**—see Paleozoic.

**carbonaceous**—rock or sediment that is rich in carbon or organic matter.

**Cenozoic**—the era of geological time from 65.5 million years to present; divided into three Periods: Paleogene, Neogene, and Quaternary, which in turn are divided into seven Epochs: Paleocene, Eocene, Oligocene, Miocene, Pliocene, Pleistocene, and Holocene (present). See Figure 8.1 for details of the geological time scale.

**concordant**—structurally conformable; strata displaying parallelism of bedding or structure.

**conglomerate**—a coarse-grained clastic sedimentary rock, composed of rounded to subangular fragments larger than 2 mm in diameter set in a fine-grained matrix of sand or silt.

**craton**—a part of the Earth's crust that has attained stability and has been little deformed for a prolonged period, and generally restricted to continents.

**deep lead mining**—occurred in regions where alluvial deposits in ancient stream beds are buried beneath younger sediments or lava flows. The process involved sinking a main shaft and extending tunnels from this underneath the old buried riverbeds (called leads) to extract the precious metal-bearing gravels.

**discordant**—structurally unconformable; strata lacking conformity or parallelism of bedding or structure.

**disseminated ore**—olivine-rich cumulate containing a few percent interstitial magmatic sulphides.

**dunite**—a dark, intrusive ultramafic igneous rock comprising at least 90% olivine, with or without other minor minerals spinel (e.g., chromite) and pyroxene.

**dyke**—a tabular igneous intrusion that cuts across the bedding or foliation of the country rock.

**element**—one of a class of substances which consist entirely of atoms of the same atomic number.

**exploration**—phase in which a company or organisation searches for mineral resources by carrying out geological and geophysical surveys, followed up where appropriate by drilling and other evaluation of the most prospective sites.

**extrusive rock**—an igneous rock that crystallised from a magma that is poured out or ejected at the Earth's crust. Extrusive rocks are usually distinguished from intrusive rocks on the basis of their texture (usually fine-grained or glassy) and mineral composition. Lava flows and pyroclastic debris (fragmented volcanic material) are extrusive; they are commonly glassy (e.g., obsidian) or finely crystalline (basalt, rhyolite, dacite). Common extrusive rocks include basalt, rhyolite, rhyodacite, dacite, scoria, tuff, and pumice.

**felsic**—a descriptive term applied to the composition of an igneous rock containing abundant light coloured and few dark-coloured minerals.

**fractionation**—the process by which a magma changes chemical composition as a result of crystallisation and preferential removal of a liquidus phase, such as olivine.

**gneiss**—a foliated rock formed by regional metamorphism, in which bands or lenticles of granular minerals alternate with bands or lenticles in which minerals having flaky or elongate prismatic habits. Varieties include augen gneiss, granite gneiss, feldspar gneiss, and aplitic gneiss.

**granite, granitic**—broadly applied, any holocrystalline, quartz-bearing plutonic (intrusive) igneous rock.

**greenfields**—exploration on previously unknown mineralisations or known mineralisations yet to be classified as an Inferred Mineral Resource or higher. They include: (1) exploration resulting in finding mineralisation that was previously unknown; (2) exploration on previously known mineralisation that has not been subjected to modern exploration; and (3) exploration within an existing mining tenement for the purpose of finding new sources of mineralisation that have not already been classified as at least an Inferred Mineral Resource.

**greenstone**—a field term applied to any compact dark-green altered or metamorphosed mafic igneous rock (e.g., basalt, gabbro, diorite) that owes its colour to the presence of chlorite, amphibole or epidote.

**Heavy-Mineral (HM) sands**—a concentration of heavy minerals (rutile, zircon, ilmenite, monazite) on a contemporary or ancient beach, or along a coastline.

**Holocene**—see Cenozoic.

**holocrystalline**—texture of an igneous rock composed entirely of crystals.

**hydrothermal**—of or pertaining to hot water or other mineral-bearing fluids, to the action of hot water-fluids or to the products of this action, such as a mineral deposit precipitated from a hot aqueous solution, with or without demonstrable association with igneous processes.

**hydrothermal deposit**—a mineral deposit formed by precipitation of ore and gangue minerals in fractures, faults, breccia openings, or other spaces, by replacement or open-space filling, from fluids generally ranging in temperature from 50oC to 700oC and ranging in pressure from less than 4 kilobars.

**igneous complex**—an assemblage of intimately associated and roughly contemporaneous igneous rocks differing in form or in petrographic type; it may consist of plutonic rocks, volcanic rocks, or both.

**igneous rocks**—a rock or mineral that solidified from molten or partly molten material, i.e., from a magma; also, applied to processes leading to, related to, or resulting from, the formation of such rocks. Igneous rocks can be divided into intrusive rocks or extrusive rocks and they constitute one of the three main classes into which rocks are divided, the others being metamorphic and sedimentary.

**inlier**—an area or group of rocks surrounded by rocks of younger age.

**intermediate**—an igneous rock that is transitional between felsic and mafic, generally having a silica content of 54% to 65%.

**intrusive rock**—an igneous rock that crystallised from a magma forced into older rocks at depths within the Earth's crust, which then slowly solidifies below the Earth's surface, though it may later be exposed by

erosion of the Earth. Intrusive rocks are usually distinguished from extrusive rocks on the basis of their texture (usually coarser-grained) and mineral composition. Common intrusive rocks include gabbro, anorthosite, granite, and syenite.

**JORC Code**—the Australasian Code for Reporting of Exploration Results, Mineral Resources and Ore Reserves, prepared by the Joint Ore Reserves Committee. This is a principal-based code, which sets out recommended minimum standards and guidelines on classification and public reporting. Companies listed on the Australian Securities Exchange are required to report exploration outcomes, resources, and reserves in accordance with the JORC Code standards and guidelines. See Appendix G for more details.

**komatiite**—strictly, a distinctive volcanic rock commonly having a spinifex texture, formed from a high-temperature ultramafic lava containing more than 18% MgO on an anhydrous basis; more loosely a volcanic (or possibly hyperbyssal) rock with or without spinifex texture.

**komatiitic rock**—derived from a komatiitic ultramafic magma containing more than 18% MgO, or from the fractionation product of a komatiite magma, e.g., komatiitic basalt.

**laterite**—a term for a highly weathered red subsoil or material rich in secondary oxides of iron and/or aluminium. It develops in a tropical or forested warm to temperate climate, and is a residual product of weathering.

**lava channel**—a high-volume lava pathway open to the air or seawater as distinct to a pathway confined within a roofed lava tube.

**lava tube**—a lava pathway confined by solidification products of the flanking and overlying crust, as distinct from an open lava channel.

**limonite**—a general field term for a group of brown, amorphous, naturally occurring hydrous ferric oxides whose real identities are unknown. Common secondary material formed by oxidation (weathering) of iron or iron-bearing minerals.

**Ma**—million years.

**massive ore**—ore consisting of 80% or more of magmatic sulphide.

**mafic**—a descriptive term applied to the composition of an igneous rock (intrusive or extrusive) containing abundant ferromagnesian, dark coloured minerals, such as olivine, orthopyroxene, clinopyroxene, and lighter coloured minerals, such as plagioclase. Common mafic rocks include gabbro, gabbro-norite, basalt, and dolerite.

**magma**—naturally occurring mobile ‘rock’ material, generated within the Earth and capable of intrusion and extrusion, from which igneous rocks are thought to have been derived through solidification and related processes.

**matrix ore**—ore consisting of a touching open-framework of olivine crystals (or their pseudomorphs) in a continuous matrix of magmatic sulphides.

**mesocumulate**—a textural term for an igneous rock that is intermediate between adcumulate and orthocumulate in terms of cumulus and intercumulus components.

**Mesozoic**—the era of geological time from the end of the Paleozoic (251 million years) to the beginning of the Cenozoic (65.5 million years). The Mesozoic is divided into the Triassic, Jurassic, and Cretaceous time Periods.

**metals**—are chemical elements that have a characteristic lustre, are good conductors of heat and electricity, and are opaque, fusible, and generally malleable or ductile. Most metals occur in nature as compounds within minerals although some important metals such as gold, copper and platinum also occur naturally in elemental (native) form. Among metals there are several subgroups, including transition metals (such as iron, zinc, copper), noble metals (such as gold, platinum, palladium), alkaline earth metals, etc. Semi-metals have characteristics that are transitional between metals and non-metals, such as semi-conductance of electricity.

**metamorphic grade**—the intensity or rank of metamorphism, measured by the amount or degree of difference between the original parent rock and the metamorphic rock. It indicates in a general way the pressure-temperature environment or facies in which the metamorphism took place. For example, conversion of shale to slate or phyllite would be low-grade metamorphism, whereas continued

transformation to a garnet-sillimanite schist would be very high-grade metamorphism.

**metamorphic rocks**—any rock derived from pre-existing rocks by mineralogical, chemical, and/or structural changes, essentially in the solid state, in response to marked changes in temperature, pressure, shear stress, and chemical environment, generally at depth in the Earth's crust.

**metasomatic**—pertaining to the process of metasomatism and to its results. The term is especially used in connection with the origin of ore deposits.

**metasomatism**—the processes by which one mineral is replaced by another of different chemical composition owing to reactions set up by the introduction of material from external sources.

**migmatite**—a composite rock composed of igneous or igneous-appearing and/or metamorphic materials, which are generally distinguishable megascopically.

**mineral**—a naturally occurring inorganic element or compound having a periodically repeating arrangement of atoms, and characteristic chemical composition, resulting in distinctive physical properties.

**mineral deposit**—a mass of naturally occurring mineral material, e.g., metal ores or non-metallic minerals, usually of economic value, without regard to mode of origin.

**mineral system**—all geological factors that control the generation and preservation of mineral deposits.

**Mt**—million tonnes.

**net-textured ore**—North American synonym for matrix ore (see above).

**orthocumulate**—a textural term for an igneous rock that consists of at least 30%, and less than 70%, accumulated crystals originally formed at or near the liquidus of the parent magma.

**orthomagmatic mineral deposit**—a mineral deposit formed from primary magmatic processes (i.e., magmas), and are hosted by the igneous rocks in which they have formed. Most of the world's Ni, Cr, PGEs, Ti, V, and diamonds are derived from these deposits. They are associated with mantle-derived magmas that have undergone a high degree of partial melting, and occur in various tectonic settings, including continental rifts, continental rifted margins, continental LIPs mid-ocean ridges and mid-continent anorogenic provinces.

**Paleozoic**—the era of geological time from the end of the Precambrian (542 million years) to the beginning of the Mesozoic (251 million years). The Paleozoic is divided into Cambrian, Ordovician, Silurian, Devonian, Carboniferous, and Permian time Periods.

**pathway**—the locus of prolonged magma flow within a flow field or subvolcanic plumbing system.

**pegmatite**—an exceptionally coarse-grained igneous rock, with interlocking crystals, usually found as irregular dykes, lenses, or veins, especially at the margins of large granitic igneous bodies. Pegmatites have gross compositions generally similar to that of granite.

**(per)alkaline**—igneous rock in which the molecular proportion of aluminium oxide is less than that of sodium and potassium oxides combined; a general chemical class of igneous rocks.

**peridotite**—a dark, intrusive ultramafic igneous rock comprising 40 to 90% olivine, with or without other minor mafic minerals pyroxene, amphibole, mica, and spinel.

**PGEs**—the platinum-group elements (PGEs) comprise the six closely related metallic elements: platinum (Pt), palladium (Pd), rhodium (Rh), iridium (Ir), osmium (Os), and ruthenium (Ru). The PGEs possess unique physical and chemical properties that make them critical to many emerging technologies. The PGEs are sometimes referred to as precious metals due to their rarity and desirability and also as strategic metals due to their specialised applications (e.g., automotive, aerospace, military). Also see PGMs.

**PGMs—platinum-group minerals**—in the literature, the abbreviation PGMS can also refer to platinum-group metals and also to platinum-group elements. This definition needs to be clearly defined near the start of any publication to avoid confusion. Also see PGEs.

**pyroxenite**—a dark, intrusive ultramafic igneous rock comprising dominantly of clinopyroxene and/or orthopyroxene, 5 to 40% olivine, with or without minor hornblende and biotite.

**placer**—a surficial mineral deposit formed by mechanical concentration of mineral particles from weathered debris. The common types are beach placers and alluvial placers. The mineral concentrated is usually a heavy mineral, such as gold, cassiterite, chromite, magnetite, zircon, rutile, and monazite.

**Pleistocene**—see Cenozoic.

**Pliocene**—see Cenozoic.

**Precambrian**—all geological time, and its corresponding rocks, before the beginning of the Paleozoic; it is equivalent to about 90% of geological time and includes the Proterozoic and Archean Eons.

**Precambrian basement**—basement rocks belonging to the Precambrian.

**production**—the phase at which operations produce mined product.

**prospect**—a potential accumulation of minerals that is sufficiently well defined to represent a viable drilling target.

**Proterozoic**—the era of geological time from the end of the Archean (about 2500 million years) to the beginning of the Phanerozoic (542 million years).

**puddling**—early mining process that involved the physical separation of PGMs and gold grains from alluvium. Puddling machines ranged from elaborate wooden structures powered by horses to a simple water-filled container stirred by a wooden stake.

**pyroclastic**—pertaining to clastic rock material formed by volcanic explosion or aerial expulsion from a volcanic vent; also, pertaining to rock texture of explosive origin.

**Quaternary**—see Cenozoic.

**regolith**—the unconsolidated material, both weathered in place and transported, which overlies consolidated rocks (bedrock).

**resources**—a concentration of naturally occurring solid, liquid, or gaseous materials in or on the Earth's crust in such form and amount that its economic exploitation is currently or potentially feasible.

**rift, rift basins**—a long, narrow continental trough that is bounded by normal faults; a graben of regional extent that marks a zone along which the entire thickness of the lithosphere has ruptured under extension.

**sedimentary rocks**—a rock resulting from the consolidation of loose sediment that has accumulated in layers; e.g., a clastic rock (such as conglomerate or sandstone) consisting of mechanically formed fragments of older rock transported from its source and deposited in water or from air or ice; or a chemical rock (such as rock salt or gypsum) formed by precipitation from solution; or an organic rock (such as certain limestones) consisting of the remains or secretions of plants and animals.

**shale**—a fine-grained detrital sedimentary rock, formed by the consolidation (especially by compression) of clay, silt, or mud. It is characterised by finely laminated structure, which imparts a fissility approximately parallel to the bedding, along which the rock breaks readily into thin layers and that is commonly most conspicuous on weathered surfaces.

**siliceous high-magnesian basalt (SHMB)**—a volcanic rock of basaltic andesite composition, having in excess of 52% SiO<sub>2</sub> and 10% MgO.

**sill**—a tabular igneous intrusion that parallels the planar structure of the surrounding rock.

**skarn**—a general term for silicate gangue (amphibole, pyroxene, garnet, etc) of certain iron-ore and sulphide deposits, particularly those that have replaced limestone and dolomite, and experienced introduction of large amounts of silicon, aluminium, iron, and magnesium by hydrothermal fluids.

**slate**—a compact, fine-grained metamorphic rock that possesses slaty cleavage and hence can be split into slabs and thin plates.

**supergene**—mineral deposit or enrichment process formed near the surface, commonly by descending solutions.

**spinifex texture**—a suite of distinctive primary igneous textures defined by extreme dendritic growth of olivine and/or pyroxene; typically developed within the upper few metres of komatiitic lava flows in response to supercooling and rapid nucleation processes.

**tectonic**—said of, or pertaining to, the rock structure and external forms resulting from the deformation of the Earth's crust; broad architecture of the outer part of the Earth.

**tholeiitic rock**—any of a series of igneous rocks that are similar in composition to basalt, but are richer in silica and iron and poorer in aluminum than basalt is. Tholeiites often contain plagioclase, feldspar

(labradorite), clinopyroxene (augite with pigeonite), and iron ore (magnetite and ilmenite), and tholeiitic volcanics form especially at mid-ocean ridges and in continental rift areas.

**tuff**—a general term for all consolidated pyroclastic rocks associated with a volcano.

**ultramafic**—a descriptive term applied to the composition of an igneous rock (intrusive or extrusive) containing abundant ferromagnesian, dark-coloured minerals, such as olivine, orthopyroxene, and clinopyroxene. Common ultramafic rocks include dunite, pyroxenite, peridotite, orthopyroxenite, clinopyroxenite, and websterite.

**volcanic**—pertaining to the activities, structures, or rock types of a volcano.

**volcanic rocks**—a generally finely crystalline or glassy igneous rock resulting from volcanic action at or near the Earth's surface, either ejected explosively or extruded as lava (e.g., basalt, andesite, dacite, rhyolite).

**weathered rock**—bedrock which has had its composition and appearance changed by weathering.

**weathering**—the destructive process or group of processes by which earthy and rocky materials on exposure to atmospheric agents at or near the Earth's surface are changed in colour, texture, composition, firmness, or form, with little or no transport of the loosened or altered material; specifically the physical disintegration and chemical decomposition of rock that produce an in situ mantle of waste and prepare sediments for transportation.

## Appendix C Platinum-group minerals

Sources detailed in table footnote.

*Appendix Table C.1 Platinum-group minerals documented in Australia.*

Platinum-group mineral	Formula
Adnuoite	$\text{RuAs}_2$
Arsenopalladinite	$\text{Pd}_8\text{As}_{2.5}\text{Sb}_{0.5}$
Atheneite	$(\text{Pd,Hg})_3\text{As?}$
Braggite	$(\text{Pt,Pd})\text{S}$
Cherepanovite	$(\text{Rh,Pt,Ni,Fe})(\text{As,S})$
Chrisstanleyite (and its Cu-analogue)	$\text{Ag}_2\text{Pd}_3\text{Se}_4$
Clausthalite	$(\text{PbSe, PdSbSe})$
Cooperite	$\text{PtS}$
Erlichmanite	$\text{OsS}_2$
Ferronickelplatinum	$\text{Pt}_2\text{Fe}(\text{Ni,Cu})$
Germanium-bearing atokite	$\text{PdSnCu}$ (minor Pt, As, Ge)
Geversite	$\text{PtSb}_2$
Hollingworthite	$((\text{Rh,Ir})\text{AsS})$
Irarsite	$((\text{Ir,Ru,Rh,Pt})\text{AsS})$
Iridarsenite	$(\text{IrAs}_2)$
Iridosmine	$(\text{Os,Ir})$
Isoferroplatinum, ferroisoplatinum	$\text{Pt}_3\text{Fe}$
Kashinite	$(\text{Ir}_2\text{S}_3)$
Kotulskite	$\text{PdTe}$
Laurite	$\text{RuS}_2$
?Luberoite	$\text{Pt}_5\text{Se}_4$
Merenskyite	$\text{PdTe}_2$
Michenerite	$\text{PdBiTe}$
Malanite	$\text{Cu}(\text{Pt,Ir})_2\text{S}_4$
Moncheite	$\text{PtTe}_2$ ; $\text{Pt}(\text{Te,Bi})_2$ ; $(\text{Pt,Pd})\text{Te}_2$
Native metals (PGEs)	Pt, Pd, Ir, Os, Ru
Naumannite	$\text{Ag}_2\text{Se}$ (plus Pt, Hg, Cu)
Oosterboschite	$(\text{Pd,Cu})_7\text{Se}_5$

Platinum-group mineral	Formula
Osmiridium	(Ir,Os,Ru)
Palladium-bearing sperrylite	PtAsPd
Palladseite	(Pd <sub>17</sub> Se <sub>15</sub> )
Palladoarsenide	Pd <sub>2</sub> As
Platarsite	PtAsS
Platiniridium	(Ir,Pt)
Porpezite	(Au,Pd)
Potarite	PdHg
Ruarsite	RuAsS
Ruthenarsenite	RuAs
Rutheniridosmine	(Os,Ir,Ru)
?Safflorite	((Co,Ru,Ni)As <sub>2</sub> )
Sperrylite	PtAs <sub>2</sub>
Stibiopalladinite	Pd <sub>5+x</sub> Sb <sub>2-x</sub> ?
Stillwaterite	Pd <sub>8</sub> As <sub>3</sub>
Stumpflite	Pt (Sb,Bi)
Sudburyite	PdSb
?Taimyrite	(Pt,Pd,Cu) <sub>3</sub> (Sn,Sb)
Tetraferroplatinum	PtFe
Temagamite	Pd <sub>3</sub> HgTe <sub>3</sub>
Tulameenite	Pt <sub>2</sub> FeCu
Umangite	Cu <sub>3</sub> Se <sub>2</sub> (plus Pt, Pd, Hg, Ag)
Vysotskite	PdS

*Hudson and Donaldson (1984); Hudson and Horwitz (1985); Hudson (1986); Hoatson and England (1986); Barron et al. (1987); Hoatson and Glaser (1989); Johan et al. (1989, 1990a,b); Hudson et al. (1991); Marshall (2000); Grguric et al. (2006); Smith (2007); Bottrill (2014).*

## Appendix D World supply and demand for platinum-group elements

All data as published by Johnson Matthey PLC.

Appendix Table D.1 World supply and demand statistics (tonnes) for the platinum-group elements.

		2000	2001	2002	2003	2004	2005	2006	2007	2008	2009	2010	2011	2012	2013
<b>Platinum supply</b>	South Africa	118.2	127.5	138.4	144.0	155.8	159.1	164.7	157.7	140.4	144.2	144.2	151.2	127.4	128.1
	Russia	34.2	40.4	30.5	32.7	26.3	27.7	28.6	28.5	25.2	24.4	25.7	26.0	24.9	24.3
	North America	8.9	11.2	12.1	9.2	12.0	11.3	10.7	10.1	10.1	8.1	6.2	10.9	9.2	9.8
	Others	3.3	3.1	4.7	7.0	7.8	8.4	8.4	9.0	9.2	10.8	12.1	13.7	14.0	16.3
	<i>Total Supply</i>	164.5	182.3	185.7	192.8	201.9	206.5	212.4	205.3	184.9	187.5	188.2	201.8	175.5	178.5
<b>Platinum demand</b>	Autocatalyst <sup>1</sup>	44.2	61.9	63.0	81.6	87.1	94.2	94.7	99.8	80.2	52.4	95.6	99.1	100.8	97.2
	Chemical	9.2	9.0	10.1	10.0	10.1	10.1	12.3	13.1	12.4	10.9	13.7	14.6	14.0	16.8
	Electrical	14.2	12.0	9.8	8.1	9.3	11.2	11.2	7.9	7.0	5.4	7.2	7.2	5.1	6.4
	Glass	7.9	9.0	7.3	6.5	9.0	11.2	12.6	14.6	10.0	1.1	12.0	16.0	5.6	7.3
	Investment	1.9	2.8	2.5	0.5	1.4	0.5	1.2	5.3	17.3	19.6	20.4	14.3	14.2	23.8
	Jewellery	88.0	80.6	87.7	78.1	67.2	61.1	51.0	45.2	42.4	76.2	75.3	77.0	86.5	85.2
	Petroleum	3.4	4.0	4.0	3.7	4.7	5.3	5.6	6.5	7.5	6.4	5.3	6.5	6.2	4.8
	Others	11.7	14.5	16.8	14.6	14.6	14.8	15.2	15.4	15.6	12.0	16.5	17.2	17.9	20.4
	<i>Total Demand</i>	180.5	193.8	201.2	203.1	203.4	208.1	203.8	207.8	192.4	184.0	246.0	251.9	250.3	261.9
	<b>Palladium supply</b>	South Africa	7.9	62.5	67.2	72.2	77.1	81.0	86.3	86.0	75.6	78.7	82.1	79.6	72.5
Russia		161.7	135.0	60.0	91.8	149.3	143.7	121.9	141.2	113.8	110.8	115.7	108.2	89.6	84.0

		2000	2001	2002	2003	2004	2005	2006	2007	2008	2009	2010	2011	2012	2013
<b>Palladium supply cont.</b>	North America	19.8	26.4	30.8	29.1	32.2	28.3	30.6	30.8	28.3	23.3	18.4	28.0	28.1	28.9
	Others	3.3	3.7	5.3	7.6	8.2	8.4	8.4	8.9	9.6	10.4	12.6	13.0	13.3	14.0
	<i>Total Supply</i>	242.6	227.7	163.3	200.6	266.9	261.4	247.2	266.9	227.3	223.2	228.8	228.8	203.5	200.0
<b>Palladium demand</b>	Autocatalyst <sup>1</sup>	168.3	149.6	83.4	94.6	101.4	100.8	99.9	109.8	104.0	91.6	173.6	191.4	205.7	216.8
	Chemical	7.9	7.8	7.9	8.2	9.6	12.9	13.7	11.7	11.0	10.7	11.5	13.7	16.5	16.5
	Dental	25.5	22.6	24.4	25.7	26.4	25.3	19.3	19.7	19.5	18.8	18.5	16.8	16.5	15.9
	Electrical	67.2	20.8	23.6	28.0	28.6	30.2	37.5	38.6	34.2	31.1	43.9	42.8	37.3	32.8
	Investment	0.0	0.0	0.0	0.9	6.2	6.8	1.5	8.1	26.6	28.6	34.1	-17.6	14.6	2.3
	Jewellery	7.9	7.5	8.4	8.1	28.9	44.5	30.9	22.1	13.1	19.8	18.5	15.7	13.8	12.1
	Others	1.9	2.0	2.8	3.4	2.8	8.2	2.6	2.6	2.3	2.2	2.8	3.4	3.3	3.1
	<i>Total Demand</i>	278.7	210.3	150.5	168.9	204.0	228.7	205.4	212.6	210.7	202.8	302.8	266.2	307.7	299.5
	<b>Rhodium supply</b>	South Africa	14.2	14.1	15.2	16.9	18.3	19.5	21.5	21.6	17.8	19.3	19.7	19.9	17.9
Russia		9.0	3.9	2.8	4.4	3.1	2.8	3.0	2.8	2.6	2.0	2.2	2.2	2.8	2.6
North America		0.5	0.7	0.8	0.8	0.5	0.6	0.6	0.6	0.6	0.4	0.3	0.7	0.7	0.7
Others		0.1	0.1	0.3	0.4	0.5	0.5	0.6	0.6	0.6	0.7	0.7	1.0	1.0	1.2
<i>Total Supply</i>		23.9	18.8	19.1	22.5	22.4	23.5	25.6	25.6	21.6	22.4	22.8	23.8	22.4	22.4
<b>Rhodium demand</b>	Autocatalyst <sup>1</sup>	22.2	14.9	15.6	16.7	19.2	21.5	21.7	21.6	16.8	13.6	22.6	22.2	24.3	24.9
	Chemical	1.2	1.4	1.2	1.2	1.3	1.5	1.5	2.0	2.1	2.1	2.1	2.2	2.5	2.5
	Electrical	0.2	0.2	0.2	0.2	0.2	0.3	0.3	0.1	0.1	0.1	0.1	0.2	0.2	0.2
	Glass	1.3	1.3	1.2	0.8	1.4	1.8	2.0	1.8	1.1	0.7	2.1	2.4	1.0	1.2
	Others	0.3	0.3	0.3	0.4	0.4	0.6	0.7	0.7	0.7	0.6	0.6	1.2	2.1	2.8
	<i>Total Demand</i>	25.3	18.0	18.4	19.3	22.7	25.7	26.2	26.2	20.8	17.1	27.6	28.2	30.1	31.6

		2000	2001	2002	2003	2004	2005	2006	2007	2008	2009	2010	2011	2012	2013
<b>Iridium demand</b>	Chemical	NA	NA	0.3	0.6	0.8	0.8	1.0	0.7	0.7	0.7	0.6	0.6	0.6	0.6
	Electrical	0.6	0.7	0.7	0.7	0.8	1.0	0.9	0.8	0.5	0.2	6.3	6.1	1.3	1.1
	Electrochemical	1.8	0.9	0.7	1.0	0.9	0.9	1.1	0.7	0.8	1.0	2.5	2.4	2.2	1.8
	Others	1.5	1.1	0.8	0.9	1.1	1.3	1.1	1.0	1.2	0.9	1.2	1.3	1.5	2.6
	<i>Total Demand</i>	3.9	2.7	2.5	3.2	3.6	4.0	4.1	3.2	3.2	2.8	10.5	10.4	5.6	6.1
<b>Ruthenium demand</b>	Chemical	2.5	1.9	3.1	4.4	3.8	5.1	6.9	4.7	4.3	2.8	3.1	8.5	3.1	3.2
	Electrical	3.0	2.9	3.6	3.7	3.0	18.1	39.6	24.1	12.8	10.5	21.1	16.7	11.7	16.5
	Electrochemical	7.2	4.2	4.4	8.6	12.1	3.0	4.2	1.9	2.9	2.9	3.9	4.0	4.0	3.9
	Others	1.1	1.9	2.0	2.4	2.1	1.5	1.7	2.2	1.7	1.7	1.3	1.8	2.3	2.1
	<i>Total Demand</i>	13.8	10.9	13.1	19.1	21.0	27.7	52.5	32.9	21.7	17.9	29.4	31.0	21.12	25.8

All data as published by Johnson Matthey. Note that for the latter years of reporting there are minor (less than a few percent) adjustments of previous year supply and demand statistics for some applications (e.g., especially autocatalysts<sup>1</sup>).

The tables above generally record the supply and demand statistics for that year of publication, i.e., updates from later years to supply and demand data have not been recorded here. Similarly, the data shown in the supply and demand plots of Figure 1.3 to Figure 1.6 are for the year of publication and have not been updated by later adjustments.

NA = Not Available.

Platinum, palladium, and rhodium supply and demand data for 2000 to 2009: [http://www.platinum.matthey.com/uploaded\\_files/Int\\_2009/pt\\_00\\_to\\_09.xls](http://www.platinum.matthey.com/uploaded_files/Int_2009/pt_00_to_09.xls)

[http://www.platinum.matthey.com/uploaded\\_files/Int\\_2009/pd\\_00\\_to\\_09.xls](http://www.platinum.matthey.com/uploaded_files/Int_2009/pd_00_to_09.xls) [http://www.platinum.matthey.com/uploaded\\_files/Int\\_2009/rh\\_00\\_to\\_09.xls](http://www.platinum.matthey.com/uploaded_files/Int_2009/rh_00_to_09.xls)

Iridium and ruthenium demand data for 2000 to 2009 from David Jollie, Publications Manager, Johnson Matthey, February, 2010

Platinum, palladium, and rhodium supply and demand data, and iridium and ruthenium demand data for 2010 to 2011: [http://www.platinum.matthey.com/uploaded\\_files/Int\\_2011/pt\\_02\\_to\\_11.xls](http://www.platinum.matthey.com/uploaded_files/Int_2011/pt_02_to_11.xls)

[http://www.platinum.matthey.com/uploaded\\_files/Int\\_2011/pd\\_02\\_to\\_11.xls](http://www.platinum.matthey.com/uploaded_files/Int_2011/pd_02_to_11.xls) [http://www.platinum.matthey.com/uploaded\\_files/Int\\_2011/rh\\_02\\_to\\_11.xls](http://www.platinum.matthey.com/uploaded_files/Int_2011/rh_02_to_11.xls)

[http://www.platinum.matthey.com/uploaded\\_files/Int\\_2011/ir\\_05\\_to\\_11.xls](http://www.platinum.matthey.com/uploaded_files/Int_2011/ir_05_to_11.xls) [http://www.platinum.matthey.com/uploaded\\_files/Int\\_2011/ru\\_05\\_to\\_11.xls](http://www.platinum.matthey.com/uploaded_files/Int_2011/ru_05_to_11.xls)

Platinum, palladium, and rhodium supply and demand data, and iridium and ruthenium demand data for 2012: [http://www.platinum.matthey.com/media/816528/pt\\_03\\_to\\_12b.pdf](http://www.platinum.matthey.com/media/816528/pt_03_to_12b.pdf)

[http://www.platinum.matthey.com/media/816540/pd\\_03\\_to\\_12b.pdf](http://www.platinum.matthey.com/media/816540/pd_03_to_12b.pdf) [http://www.platinum.matthey.com/media/816552/rh\\_03\\_to\\_12b.pdf](http://www.platinum.matthey.com/media/816552/rh_03_to_12b.pdf)

[http://www.platinum.matthey.com/media/816560/ir\\_05\\_to\\_12b.pdf](http://www.platinum.matthey.com/media/816560/ir_05_to_12b.pdf) [http://www.platinum.matthey.com/media/816564/ru\\_05\\_to\\_12b.pdf](http://www.platinum.matthey.com/media/816564/ru_05_to_12b.pdf)

Platinum, palladium, and rhodium supply and demand data, and iridium and ruthenium demand data for 2013: [http://www.platinum.matthey.com/media/816528/pt\\_04\\_to\\_13.pdf](http://www.platinum.matthey.com/media/816528/pt_04_to_13.pdf)

[http://www.platinum.matthey.com/media/816540/pd\\_04\\_to\\_13.pdf](http://www.platinum.matthey.com/media/816540/pd_04_to_13.pdf) [http://www.platinum.matthey.com/media/816552/rh\\_04\\_to\\_13.pdf](http://www.platinum.matthey.com/media/816552/rh_04_to_13.pdf) [http://www.platinum.matthey.com/media/816560/ir\\_05\\_to\\_13.pdf](http://www.platinum.matthey.com/media/816560/ir_05_to_13.pdf)

[http://www.platinum.matthey.com/media/816564/ru\\_05\\_to\\_13.pdf](http://www.platinum.matthey.com/media/816564/ru_05_to_13.pdf)



# Appendix E Platinum-group-element resources of world deposits

Major sources of data Naldrett (2004, 2011).

Appendix Table E.1 Platinum-group element resources of the major deposits and mining camps in the world.

Geological formation, country; geotectonic region	Formation/ deposit	Deposit type	Discovered	Age <sup>2</sup> (Ma)	Reference (for age)	Ore resource (Mt)	Average grade PGEs±Au (g/t)	Contained PGEs±Au metal (t)	Resource category	Reference (for resource)
Bushveld, South Africa; Kaapvaal Craton, Transvaal Basin	Merensky Reef	Strata	1924	2060 ± 3	Kruger et al. (1986)	2160	8.1 PGEs+Au	17 496 PGEs+Au	Rv	Barrie (1995)
	UG-2 Chromitite	Strata	post ~1924	2060 ± 3	Kruger et al. (1986)	3700	8.7 PGEs+Au	32 190 PGEs+Au	Rv	Barrie (1995)
	Platreef	Basal <sup>3</sup>	1925	2060 ± 3	Kruger et al. (1986)	1700	7.3 PGEs+Au	12 410 PGEs+Au	Rv	Barrie (1995)
	Total Bushveld					7560	NA	62 096 PGEs+Au	Rv	Barrie (1995)
	Total Bushveld					NA	NA	6293 Pt, 3596 Pd	Prv+Prob Rv	Cawthorn (1999)
	Total Bushveld					NA	NA	29 047 Pt, 22 010 Pd	R	Cawthorn (1999)
	Merensky Reef	Strata				4359	NA	12 400 Pt, 6851 Pd	R	Barnes and Maier (2002)
	UG-2 Chromitite	Strata				5105	NA	12 493 Pt, 10 974 Pd	R	Barnes and Maier (2002)
	Platreef	Basal				2117	NA	4216 Pt, 4216 Pd	R	Barnes and Maier (2002)
	Total Bushveld					11 581	NA	51 150 Pt+Pd	R	Barnes and Maier (2002)
	Bushveld Dunite Pipes	Hydro	1924	2060 ± 3	Kruger et al. (1986)	NA	NA	~1.162 Pt	Production (1927–1929)	Scoon and Mitchell (2004)
	Merensky Reef					4210	6.21 PGEs: 3.57 Pt, 1.85 Pd, 0.216 Rh, 0.449 Ru, 0.082 Ir, 0.051 Os	26 161 PGEs: 15 012 Pt, 7790 Pd, 909 Rh, 1891 Ru, 345 Ir, 214 Os	Glob R	Naldrett (2004, 2011)
	UG-2 Chromitite					5743	5.70 PGEs: 2.66 Pt, 1.71 Pd, 0.428 Rh, 0.710 Ru, 0.131 Ir, 0.062 Os	32 730 PGEs: 15 279 Pt, 9809 Pd, 2457 Rh, 4077 Ru, 752 Ir, 356 Os	Global Res	Naldrett (2004, 2011)
	Platreef					1597	4.12 PGEs: 1.77 Pt, 2.01 Pd, 0.114 Rh, 0.165 Ru, 0.038 Ir, 0.033 Os	6582 PGEs: 2820 Pt, 3204 Pd, 182 Rh, 263 Ru, 60 Ir, 53 Os	Global Res	Naldrett (2004, 2011)
	Total Bushveld					9815	4.0 Pt+Pd	39 260 Pt+Pd	R	Eckstrand and Hulbert (2007)
	Total Bushveld					11 550	5.67 PGEs: 2.87 Pt, 1.80 Pd, 0.307 Rh, 0.539 Ru, 0.100 Ir, 0.054 Os	65 473 PGEs: 33 111 Pt, 20 803 Pd, 3548 Rh, 6231 Ru, 1157 Ir, 623 Os	Global Res	Naldrett (2004, 2011)
	Merensky Reef					3733	2.91 Pt, 1.43 Pd, 0.20 Rh, 0.27 Au		Rv+Total R	Zientek (2012)
	UG-2 Chromitite					6636	2.70 Pt, 1.83 Pd, 0.50 Rh, 0.06 Au		Rv+Total R	Zientek (2012)
Platreef					2274	2.20 Pt, 2.22 Pd		Prv+Prob Rv+Inf R	Zientek (2012)	
Duluth, USA; Mid-Continent Rift System		Flood Basalt	1948	1099±0.7	Paces and Miller (1993)	NA	NA	?279 Pt, ?992 Pd	R	Cawthorn (1999)
						4000	0.66 PGEs: 0.15 Pt, 0.49 Pd, 0.007 Rh, 0.007 Ru, 0.003 Ir, 0.003 Os	2621 PGEs: 585 Pt, 1959 Pd, 27 Rh, 27 Ru, 11 Ir, 12 Os	Global Res	Naldrett (2004, 2011)
						550	0.66 Pt+Pd+Au	NA	Ind R	Williams (2012)
						274	0.685 Pt+Pd+Au	NA	Inf R	Williams (2012)

Geological formation, country; geotectonic region	Formation/ deposit	Deposit type	Discovered	Age <sup>2</sup> (Ma)	Reference (for age)	Ore resource (Mt)	Average grade PGEs±Au (g/t)	Contained PGEs±Au metal (t)	Resource category	Reference (for resource)
Great Dyke, Zimbabwe; Zimbabwe Craton		Strata	1925	2575.4±0.7	Oberthür et al. (2002)	NA	4.7 PGEs+Au	7900 PGEs+Au	R	Hulbert et al. (1988)
						1680	4.7 PGEs+Au	7896 PGEs+Au	Rv	Barrie (1995)
						2615	NA	4433 Pt, 2697 Pd	R	Cawthorn (1999)
						2574	5.42 PGEs: 2.77 Pt, 2.13 Pd, 0.130 Rh, 0.289 Ru, 0.052 Ir, 0.047 Os	13 946 PGEs: 7130 Pt, 5482 Pd, 335 Rh, 744 Ru, 135 Ir, 120 Os	Global Res	Naldrett (2004, 2011)
						2136	1.79 Pt, 1.43 Pd, 0.15 Rh, 0.30 Au		Rv+Total R	Zientek (2012)
		Hartley Complex				168.2	4.9 PGEs	NA	R	Delta Gold NL (?2006)
						50.9	2.6 Pt, 1.81 Pd, 0.21 Rh, 0.47 Au	NA	Rv	Delta Gold NL (?2006)
Jinchuan, China; Sino-Korean Craton		Basal	1958	827±8	Li et al. (2004)	508	NA	186 Pt, 93 Pd	R	Cawthorn (1999)
						515	0.26 PGEs: 0.13 Pt, 0.10 Pd, 0.005 Rh, 0.010 Ru, 0.010 Ir, 0.011 Os	135 PGEs: 65 Pt, 51 Pd, 3 Rh, 5 Ru, 5 Ir, 6 Os	Global Res	Naldrett (2004, 2011)
Kambalda, Australia; Eastern Goldfields Province, Yilgarn Craton		Komatiite	1966	2705±4	Nelson (1997)	67	1.13 PGEs: 0.30 Pt, 0.42 Pd, 0.065 Rh, 0.197 Ru, 0.047 Ir, 0.097 Os	75 PGEs: 20 Pt, 28 Pd, 4 Rh, 13 Ru, 3 Ir, 7 Os	Global Res	Naldrett (2004)
Kabanga, Tanzania; Kinaran Orogenic Belt		?Basal	1976	1403±14	Maier et al. (2007)	48.2	1.35 PGEs: 0.54 Pt, 0.81 Pd	65.04 PGEs: 26.0 Pt, 39.04 Pd	Global Res	Naldrett (2011)
Lac des Iles, Canada; Wabigoon Belt, Superior Province		Hydro	1963	2692 +4, -2	Blackburn et al. (1992)	6.7	5.4 PGEs+Au	36 PGEs+Au	Rv	Barrie (1995)
		Roby Zone				232	1.72 Pt+Pd	399 Pt+Pd	Meas+Ind+ Inf R	Lavigne and Michaud (2001)
						NA	NA	20.8 Pt+Pd	Production (1993–2001)	Lavigne and Michaud (2001)
						63.8	0.23 Pt, 2.54 Pd	15 Pt, 162 Pd	R	Nth American Palladium press release 29/3/2004
						94.1	1.85 PGEs: 0.18 Pt, 1.66 Pd, 0.008 Rh	174 PGEs: 17 Pt, 156 Pd, 1 Rh	Global Res	Naldrett (2004, 2011)
						88	1.51 Pd, 0.17 Pt, 0.12 Au	132.9 Pd, 15 Pt, 10.6 Au	Prov+Prob Rv	Hinchey et al. (2005)
						65	1.58 Pd, 0.17 Pt, 0.11 Au	102.7 Pd, 11 Pt, 7.1 Au	Meas+Ind R	Hinchey et al. (2005)
Monchegorsk, Russia; Baltic Shield, Kola Peninsula	NKT orebody	Basal	pre-1935	2493±7	Neradovsky et al. (1997)	3.1	8.590 PGEs: 1.460 Pt, 6.920 Pd, 0.210 Rh	26.6 PGEs: 4.5 Pt, 21.45 Pd, 0.65 Rh	Global Res	Naldrett (2011)
Montcalm, Canada; Abitibi Belt		Basal	1976	2702±2	Barrie and Naldrett (1989)	3.6	0.0772 PGEs: 0.048 Pt, 0.014 Pd, 0.0002 Rh, 0.013 Ru, 0.002 Ir	0.27 PGEs: 0.20 Pt, 0.05 Pd, 0.01 Ru, 0.01 Ir	Global Res	Naldrett (2011)
Narkaus, Finland; Baltic Shield (Fennoscandian Shield),	Siika-Kämä Reef	Strata	?	2440	Zientek (2012)	43.1	0.72 Pt, 2.7 Pd, 0.11 Au		Meas+Ind+ Inf R	Zientek (2012)
Noril'sk (N)–Talnakh (T), Russia; Siberian Platform		Flood Basalt	~1926 (N), 1960 (T)	251±0.3	Kamo et al. (2003)	NA	3.8 PGEs	6200 PGEs	R	Hulbert et al. (1988)
						1671	NA	2759 Pt, 9734 Pd	R	Cawthorn (1999)
						1500	2.5 Pt, 9.7 Pd	NA	Rv+ Production	Diakov et al. (2002)
						2100	1.5 Pt, 2.9 Pd	3100 Pt, 6200 Pd	R	Foster (2003)
		Noril'sk Region				2125	1.1 Pt, 4.5 Pd	2393 Pt, 9507 Pd	R	MMC Noril'sk (2004) in Table 11.1 of Green and Peck (2005)

Geological formation, country; geotectonic region	Formation/deposit	Deposit type	Discovered	Age <sup>2</sup> (Ma)	Reference (for age)	Ore resource (Mt)	Average grade PGEs±Au (g/t)	Contained PGEs±Au metal (t)	Resource category	Reference (for resource)
						88.7 (mass sulph)	5–100 PGEs (mass sulph)	NA	Meas+Ind+Inf R	Eckstrand and Hulbert (2007)
						108.4 (Cu breccia)	5–50 PGEs (Cu breccia)	NA	Meas+Ind+Inf R	Eckstrand and Hulbert (2007)
						1706.3 (diss sulph)	2–10 PGEs (diss sulph)	NA	Meas+Ind+Inf R	Eckstrand and Hulbert (2007)
						1257	10.031 PGEs: 1.90 Pt, 7.70 Pd, 0.228 Rh, 0.124 Ru, 0.032 Ir, 0.047 Os	12 608.9 PGEs: 2388.3 Pt, 9678.9 Pd, 286.6 Rh, 155.9 Ru, 40.2 Ir, 59.1 Os	Global Res	Naldrett (2011)
	Tamiyr Peninsula					329	7.9 PGEs: 5.98 Pd, 1.56 Pt	2594 PGEs: 1966 Pd, 512 Pt	Prv+Prob Rv	MMC Norilsk (2007)
						1414	4.12 PGEs: 3.06 Pd, 0.88 Pt	5831 PGEs: 4333 Pd, 1239 Pt	Meas+Ind R	MMC Norilsk (2007)
						474	5.81 PGEs: 4.45 Pd, 1.13 Pt	2755 PGEs: 2106 Pd, 537 Pt	Inf R	MMC Norilsk (2007)
	Kola Peninsula					137	0.07 PGEs: 0.04 Pd, 0.03 Pt	10 PGEs: 5.1 Pd, 4.1 Pt	Prv+Prob Rv	MMC Norilsk (2007)
						497	0.06 PGEs: 0.04 Pd, 0.02 Pt	32 PGEs: 20 Pd, 11 Pt	Meas+Ind R	MMC Norilsk (2007)
					221	0.06 PGEs: 0.04 Pd, 0.02 Pt	15 PGEs: 8.8 Pd, 4.9 Pt	Inf R	MMC Norilsk (2007)	
Pechenga, Russia; Baltic Shield, Kola Peninsula		Basal	1912	1977±55	Hanski et al. (1990)	339	0.32 PGEs: 0.12 Pt, 0.17 Pd, 0.005 Rh, 0.007 Ru, 0.004 Ir, 0.006 Os	107 PGEs: 41 Pt, 59 Pd, 2 Rh, 2 Ru, 1 Ir, 2 Os	Global Res	Naldrett (2004, 2011)
Penikat, Finland; Baltic Shield (Fennoscandian Shield)		Strata	~1982	2440	Alapieti and Lahtinen (2002)	NA	NA	?2883 Pt, ?7688 Pd	R	Cawthorn (1999)
	Arctic Platinum Projects					168.3	2.3 PGE + Au	391 PGE + Au	R	Gold Fields Resources (2006)
	Sompujärvi Reef					6.7	3.08 Pt, 5.36 Pd, 0.38 Rh, 0.1 Au			Zientek (2012)
	Paasivaara Reef					5.0	4.04 Pt, 2.58 Pd, 0.08 Rh, 0.61 Au			Zientek (2012)
Portimo, Finland; Baltic Shield (Fennoscandian Shield)			~1982	2440	Alapieti and Lahtinen (2002)					
	Konttijarvi	Strata				43.4	1.42 Pd, 0.39 Pt, 0.1 Au	61.6 Pd, 16.9 Pt, 4.3 Au	R	Alapieti and Lahtinen (2002)
	Ahmavaara	Strata				74.1	1.05 Pd, 0.22 Pt, 0.1 Au	77.8 Pd, 16.3 Pt, .8.1 Au	R	Alapieti and Lahtinen (2002)
	Portimo Area					218.6	1.92 PGEs: 0.38 Pt, 1.54 Pd	420 PGEs: 83 Pt, 337 Pd	Global Res	Naldrett (2004, 2011)
Raglan, Canada; Capte Smith Belt		Komatiite	~1931	?1918+9,-7	Parrish (1989)	32.8	3.76 PGEs: 0.82 Pt, 2.27 Pd, 0.150 Rh, 0.374 Ru, 0.065 Ir, 0.080 Os	123.35 PGEs: 27.10 Pt, 74.32 Pd, 4.92 Rh, 12.26 Ru, 2.13 Ir, 2.62 Os	Global Res	Naldrett (2011)
Skaergaard, Greenland; North Atlantic Igneous Province		Strata	1987	55.7±0.3	Hirschmann et al. (1997)	NA	~2 PGEs+Au	NA	Rv	Barrie (1995)
						1520	0.61 Pd, 0.04 Pt, 0.21 Au	927 Pd, 61 Pt, 319 Au	Inf R	Galahad Gold PLC (2005)
	Platinova 7 Reef	Strata				23	2.3 Au, 0.7 Pd, 0.1 Pt	48 Au, 14 Pd, 1.1 Pt	Inf R	Platina Resources Ltd (2013b)
	Combined Reefs H0 + H3 + H5					202.2	1.33 Pd, 0.11 Pt, 0.88 Au	269.0 Pd, 22.2 Pt, 178.0 Au	Ind+Inf R	Platina Resources Ltd (2013b, 2014)
Stella (Kalplats), South Africa; Kraaipan Greenstone Belt	South Africa	Strata	~1990	3033.5±0.3	Maier et al. (2003)	76.4	1.42 Pt+Pd+Au	103.5 Pt+Pd+Au	R	Platinum Australia (2007)

Geological formation, country; geotectonic region	Formation/ deposit	Deposit type	Discovered	Age <sup>2</sup> (Ma)	Reference (for age)	Ore resource (Mt)	Average grade PGEs±Au (g/t)	Contained PGEs±Au metal (t)	Resource category	Reference (for resource)
	Main Reef Package					133.3	0.68 Pt, 0.78 Pd, 0.04 Au		Rv+Total R	Zientek (2012)
Stillwater, USA; Beartooth Mountains, Archean Craton	J-M Reef	Strata	1973	2705±4	Premo et al. (1990)	NA	22.3 PGEs+Au	1100 PGEs+Au	R	Hulbert et al. (1988)
						325	NA	1116 Pt, 4030 Pd	R	Cawthorn (1999)
						421.4	18.8 Pt+Pd	7915 Pt+Pd	R	Zientek et al. (2002)
						32.3	24.91 PGEs: 5.30 Pt, 19.11 Pd, 0.27 Rh, 0.10 Ru, 0.096 Ir, 0.043 Os	804 PGEs: 172 Pt, 616 Pd, 9 Rh, 3 Ru, 3 Ir, 1 Os	Global Res	Naldrett (2004)
						154.5	3.9 Pt, 14.07 Pd	604 Pt, 2174 Pd	R	SMC AR (2004) in Table 11.1 of Green and Peck (2005)
						323.2	20.699 PGEs: 4.34 Pt, 15.85 Pd, 0.27 Rh, 0.10 Ru, 0.096 Ir, 0.043 Os	6689.9 PGEs: 1402.7 Pt, 5122.7 Pd, 87.3 Rh, 32.3 Ru, 31.0 Ir, 13.9 Os	Global Res	Naldrett (2011)
						149.4	3.68 Pt, 12.88 Pd		Rv+ Min material	Zientek (2012)
Sudbury, Canada; Superior-Southern-Grenville Provinces		Astro	1856	1850±1	Krogh et al. (1984)	NA	0.9 PGEs+Au	394 PGEs+Au	R	Hulbert et al. (1988)
						434	NA	279 Pt, 341 Pd	R	Cawthorn (1999)
						1648	1.17 PGEs: 0.46 Pt, 0.58 Pd, 0.056 Rh, 0.044 Ru, 0.019 Ir, 008 Os	1933 PGEs: 763 Pt, 961 Pd, 92 Rh, 73 Ru, 31 Ir, 13 Os	Global Res	Naldrett (2004, 2011)
Thompson, Canada; Thompson Nickel Belt		?Komatiite	1956	1880±5	Hulbert et al. (2005)	154.0	0.83 PGEs: 0.10 Pt, 0.54 Pd, 0.046 Rh, 0.072 Ru, 0.033 Ir, 0.041 Os	127.33 PGEs: 15.4 Pt, 82.43 Pd, 7.07 Rh, 11.03 Ru, 5.01 Ir, 6.39 Os	Global Res	Naldrett (2011)
Troia Unit: Cruzeta Complex, Brazil; Tróia Massif, Borborema Province	Pedra Branca		?	2.7–3.0 Ga	Zientek (2012)	6.6	2.27 Pt+Pd+Au		Inf R	Zientek (2012)
Voisey's Bay, Canada; Torngat Orogen		Basal	1993	1333±1	Amelin et al. (1999)	127	NA	?62 Pt, ?62 Pd	R	Cawthorn (1999)
						136.7	0.19 PGEs: 0.07 Pt, 0.10 Pd, 0.005 Rh, 0.007 Ru, 0.002 Ir, 0.002 Os	25.6 PGEs: 9.6 Pt, 13.7 Pd, 0.7 Rh, 1 Ru, 0.3 Ir, 0.3 Os	Global Res	Naldrett (2004, 2011)
Yilgarn Craton, Australia; Eastern Goldfields Province, Yilgarn Craton		Komatiite								
	Kambalda (type 1)-type		post-1966	2705±4	Nelson (1997)	161.8	0.803 PGEs: 0.214 Pt, 0.300 Pd, 0.046 Rh, 0.140 Ru, 0.034 Ir, 0.069 Os	129.94 PGEs: 34.60 Pt, 48.48 Pd, 7.50 Rh, 22.74 Ru, 5.42 Ir, 11.20 Os	Global Res	Naldrett (2011)
	Mount Keith (type 2)-type		post-1968	2705±4	Nelson (1997)	1021.9	0.109 PGEs: 0.016 Pt, 0.039 Pd, 0.006 Rh, 0.021 Ru, 0.012 Ir, 0.015 Os	111.91 PGEs: 16.70 Pt, 40.32 Pd, 5.93 Rh, 21.91 Ru, 12.04 Ir, 15.01 Os	Global Res	Naldrett (2011)
<b>World Total:</b>						<b>NA</b>	<b>NA</b>	<b>47 337 Pt, 51 181 Pd</b>	<b>R</b>	<b>Cawthorn (1999)</b>

<sup>1</sup> Strata = stratabound PGE-Ni-Cu sulphides in mafic-ultramafic intrusion; Basal = basal Ni-Cu-PGE sulphides in mafic-ultramafic intrusion; Hydro = hydrothermal-remobilised; Flood Basalt = Ni-Cu-PGE sulphides in intrusions related to flood basalts; Komatiite = Ni-Cu-PGE sulphides in komatiite; Astro = astrobleme-associated Ni-Cu-PGE sulphides.

<sup>2</sup> Age can refer to the age of a specific PGE deposit (e.g., 2440 Ma Penikat), or the general age of the metallogenic province containing other PGE deposits that are similar to a dated deposit (e.g., 2440 Ma PGE deposits, such as Portimo, in the Fennoscandian Shield).

<sup>3</sup> Some deposits may not be representative, sensu stricto, of the indicated deposit type (e.g., Platreef is not a basal sulphide deposit similar to Voisey's Bay, but for convenience it is included in this category).

Many of the deposits listed in this table have significant credits of nickel, copper, chromium, cobalt, titanium, vanadium, and gold. The reader should refer to the relevant references for details of these commodities.

General information on deposits compiled from Cabri (2002), Green and Peck (2005), Maier (2005), and Hoatson et al. (2006)

R = Resource; Prelim R = Preliminary Resource; Meas R = Measured Resource; Ind R = Indicated Resource; Inf R = Inferred Resource; Total Min R = Total Mineral Resource; Global Res = Global Resource; Rv = Reserves; Prob Rv = Probable Reserves; Prv = Proven.

## Appendix F Production and value of platinum-group elements in Australia

Data from the Government of Western Australia Department of Mines and Petroleum Resources Data Files—Quantity and Value Tables

Appendix Table F.1 Annual production (kg) and value (A\$) of platinum-group elements in Australia from 1894 to 2013.

Year	Pt	Pt	Pt	Pd	Pt+Pd <sup>1</sup>	Os <sup>2</sup>	Total Pt+Pd+Os <sup>2</sup>	Cumulative Pt+Pd+Os <sup>2</sup>	Pt Value <sup>3</sup> (A\$)	Pd Value <sup>3</sup> (A\$)	Pt+Pd Value <sup>3</sup> (A\$)
	NSW	WA	VIC	WA	WA	TAS					
1894	33.0						33.0	33.0			
1895	12.8						12.8	45.8			
1896	75.8						75.8	121.6			
1897	61.1						61.1	182.7			
1898	38.9						38.9	221.6			
1899	19.8						19.8	241.4			
1900	16.5						16.5	257.9			
1901	12.1						12.1	270.0			
1902	11.7						11.7	281.7			
1903	16.5						16.5	298.2			
1904	16.6						16.6	314.8			
1905	12.4						12.4	327.2			
1906	6.4						6.4	333.6			
1907	8.6						8.6	342.2			
1908	4.2						4.2	346.4			
1909	13.7						13.7	360.1			

Year	Pt	Pt	Pt	Pd	Pt+Pd <sup>1</sup>	Os <sup>2</sup>	Total Pt+Pd+Os <sup>2</sup>	Cumulative Pt+Pd+Os <sup>2</sup>	Pt Value <sup>3</sup> (A\$)	Pd Value <sup>3</sup> (A\$)	Pt+Pd Value <sup>3</sup> (A\$)
1910	10.3					3.7	14.0	374.1			
1911	14.6		5.7			8.5	28.8	402.9			
1912	19.0					24.2	43.2	446.1			
1913	13.7		3.9			39.2	56.8	502.9			
1914	7.6					31.7	39.3	542.2			
1915	1.7					7.7	9.4	551.6			
1916	2.5					6.9	9.4	561.0			
1917	8.0					10.3	18.3	579.3			
1918	18.8					50.0	68.8	648.1			
1919	6.6					51.9	58.5	706.6			
1920	24.8					62.5	87.3	793.9			
1921	7.7					54.4	62.1	856.0			
1922	2.5					36.5	39	895.0			
1923	18.2					20.9	39.1	934.1			
1924	20.1					11.3	31.4	965.5			
1925	17.8					104.7	122.5	1088.0			
1926	12.3					99.6	111.9	1199.9			
1927	7.0					19.7	26.7	1226.6			
1928	11.0					50.6	61.6	1288.2			
1929	4.0					41.2	45.2	1333.4			
1930	4.8					29.6	34.4	1367.8			
1931	8.8					39.8	48.6	1416.4			
1932	10.4					24.4	34.8	1451.2			

Year	Pt	Pt	Pt	Pd	Pt+Pd <sup>1</sup>	Os <sup>2</sup>	Total Pt+Pd+Os <sup>2</sup>	Cumulative Pt+Pd+Os <sup>2</sup>	Pt Value <sup>3</sup> (A\$)	Pd Value <sup>3</sup> (A\$)	Pt+Pd Value <sup>3</sup> (A\$)
1933	3.5					17.0	20.5	1471.7			
1934	5.6					15.2	20.8	1492.5			
1935	3.0					7.3	10.3	1502.8			
1936	1.5					8.7	10.2	1513.0			
1937	1.4					18.2	19.6	1532.6			
1938	0.2					5.9	6.1	1538.7			
1939	0.2					8.8	9.0	1547.7			
1940	0.4					14.4	14.8	1562.5			
1941	0.7					6.4	7.1	1569.6			
1942	0.1					4.4	4.5	1574.1			
1943	0.1					2.8	2.9	1577.0			
1944	0.1					3.3	3.4	1580.4			
1945	0.1					3.4	3.5	1583.9			
1946						2.9	2.9	1586.8			
1947						3.1	3.1	1589.9			
1948						2.9	2.9	1592.8			
1949						1.2	1.2	1594.0			
1950	0.5					1.4	1.9	1595.9			
1951	0.3					1.0	1.3	1597.2			
1952						1.6	1.6	1598.8			
1953						1.8	1.8	1600.6			
1954	0.7					0.5	1.2	1601.8			
1955	0.2					0.7	0.9	1602.7			

Year	Pt	Pt	Pt	Pd	Pt+Pd <sup>1</sup>	Os <sup>2</sup>	Total Pt+Pd+Os <sup>2</sup>	Cumulative Pt+Pd+Os <sup>2</sup>	Pt Value <sup>3</sup> (A\$)	Pd Value <sup>3</sup> (A\$)	Pt+Pd Value <sup>3</sup> (A\$)
1956	0.6					0.8	1.4	1604.1			
1957	0.5					2.0	2.5	1606.6			
1958	0.7					1.3	2.0	1608.6			
1959						0.1	0.1	1608.7			
1960	0.1						0.1	1608.8			
1961	0.1						0.1	1608.9			
1962	0.1						0.1	1609.0			
1963	0.1						0.1	1609.1			
1964							0	1609.1			
1965							0	1609.1			
1966	0.4						0.4	1609.5			
1967							0	1609.5			
1968						0.4	0.4	1609.9			
1969		14.6		10			24.6	1634.5	\$36 931	\$9 656	
1970		45					45	1679.5	\$155 454		
1971			2.5				2.5	1682			
1972							0	1682			
1973		7		23			30	1712	\$23 900	\$41 000	
1974		60		164			224	1936	\$227 200	\$428 700	
1975		45		108.2			153.2	2089.2	\$178 236	\$267 240	
1976		98		247			345	2434.2	\$394 553	\$301 930	
1977		114.9		298.2			413.1	2847.3	\$527 666	\$499 599	
1978		92.1		229.7			321.8	3169.1	\$557 698	\$418 136	

Year	Pt	Pt	Pt	Pd	Pt+Pd <sup>1</sup>	Os <sup>2</sup>	Total Pt+Pd+Os <sup>2</sup>	Cumulative Pt+Pd+Os <sup>2</sup>	Pt Value <sup>3</sup> (A\$)	Pd Value <sup>3</sup> (A\$)	Pt+Pd Value <sup>3</sup> (A\$)
1979		85.9		213.9			299.8	3468.9	\$862 865	\$625 772	
1980		63.6		328.2			391.8	3860.7	\$954 184	\$1 834 614	
1981		65.1		401.1			466.2	4326.9	\$868 736	\$1 254 422	
1982		74.3		416.1			490.4	4817.3	\$933 357	\$1 112 023	
1983		52		449			501	5318.3	\$863 905	\$1 963 478	
1984		66		523			589	5907.3	\$1 010 176	\$2 693 559	
1985		95		476			571	6478.3	\$1 405 304	\$2 382 702	
1986		115		482			597	7075.3	\$2 459 690	\$2 557 435	
1987		84		450			534	7609.3	\$2 150 013	\$2 980 875	
1988		73		360			433	8042.3	\$1 584 833	\$2 118 657	
1989		61		323			384	8426.3	\$1 275 979	\$1 917 445	
1990		96		435			531	8957.3	\$1 235 806	\$1 185 127	
1991		82		351			433	9390.3	\$1 494 173	\$1 260 296	
1992		143		539			682	10072.3	\$1 249 742	\$1 372 039	
1993		79		405			484	10 556.3	\$1 142 319	\$2 035 430	
1994		113		450			563	11 119.3	\$1 266 118	\$2 904 466	
1995		74		528			602	11 721.3	\$1 734 790	\$3 065 446	
1996		119		559			678	12 399.3	\$1 584 578	\$2 416 416	
1997		315		429			744	13 143.3	\$2 419 386	\$3 227 915	
1998		155		827			982	14 125.3	\$2 852 073	\$10 096 972	
1999		90		816			906	15 031.3	\$1 700 645	\$10 566 069	
2000		171		812			983	16 014.3	\$4 976 316	\$28 280 483	
2001		174		828			1002	17 016.3	\$5 302 472	\$32 267 391	

Year	Pt	Pt	Pt	Pd	Pt+Pd <sup>1</sup>	Os <sup>2</sup>	Total Pt+Pd+Os <sup>2</sup>	Cumulative Pt+Pd+Os <sup>2</sup>	Pt Value <sup>3</sup> (A\$)	Pd Value <sup>3</sup> (A\$)	Pt+Pd Value <sup>3</sup> (A\$)
2002		122		810			932	17 948.3	\$2 945 218	\$16 146 791	
2003		133		477			610	18 558.3	\$4 306 903	\$4 002 358	
2004		196		846			1042	19 600.3	\$3 717 783	\$6 849 997	
2005		58		603			661	20 261.3	\$1 740 018	\$4 280 093	
2006					959		959	21 220.3			\$12 505 294
2007					742		742	21 962.3			\$10 162 872
2008					710		710	22 672.3			\$8 753 701
2009					1034		1034	23 706.3			\$10 001 145
2010					781		781	24 487.3			\$8 225 481
2011					445		445	24 932.3			\$8 185 694
2012					706		706	25 638.3			\$15 679 998
2013					786		786	26 424.3			\$20 442 434
<b>Total (kg)</b>	<b>633.5</b>	<b>3431.5</b>	<b>12.1</b>	<b>15 217.4</b>	<b>6163.0</b>	<b>966.8</b>	<b>26 424.34</b>		<b>\$56 139 020</b>	<b>\$153 364 532</b>	<b>\$93 956 619</b>

<sup>1</sup> From 2006 onwards the Government of Western Australia Department of Mines and Petroleum did not report individual production statistics for platinum and palladium in Western Australia.

<sup>2</sup> Os = 'osmiridium'

<sup>3</sup> Total value for palladium and platinum produced in Western Australia from the start of State records at 1886 to 1979 inclusive was \$4 426 647 (Pd) and \$3 918 687 (Pt). These amounts are not included in this Table.

<sup>4</sup> This total of 26 424.3 kg does not include 32 kg (\$51 640) of ruthenium produced in Western Australia sometime from 1886 to 1979 inclusive. In addition, minor historical quantities of Pt, Pd, Os, and Ir were produced prior to 1894 (see Table 5.1), and these unofficial amounts are not included in this Table.

Source: Geary et al. (1956); Kalix et al. (1966); Government of Western Australia Department of Mines and Petroleum Resources Data Files—Quantity and Value Tables (<http://www.dmp.wa.gov.au/1521.aspx>); Australian Mineral Industry Annual Reviews; pers. comm. D. Flint and P. Abeysinghe (GSWA, 2007, 2012).

# Appendix G Australia's national classification system for identified mineral resources

From JORC Code 2009 (<http://www.jorc.org/>)

## G.1 Introduction

Australia's mineral resources are an important component of its wealth, and a long-term perspective of what is likely to be available for mining is a prerequisite for formulating sound policies on resources and land access.

In 1975, Australia (through the Bureau of Mineral Resources, now Geoscience Australia) adopted, with minor changes, the McKelvey resource classification system used in the USA by the then Bureau of Mines and the United States Geological Survey (USGS). Australia's national system remains comparable with the current USGS system, as published in its Mineral Commodity Summaries.

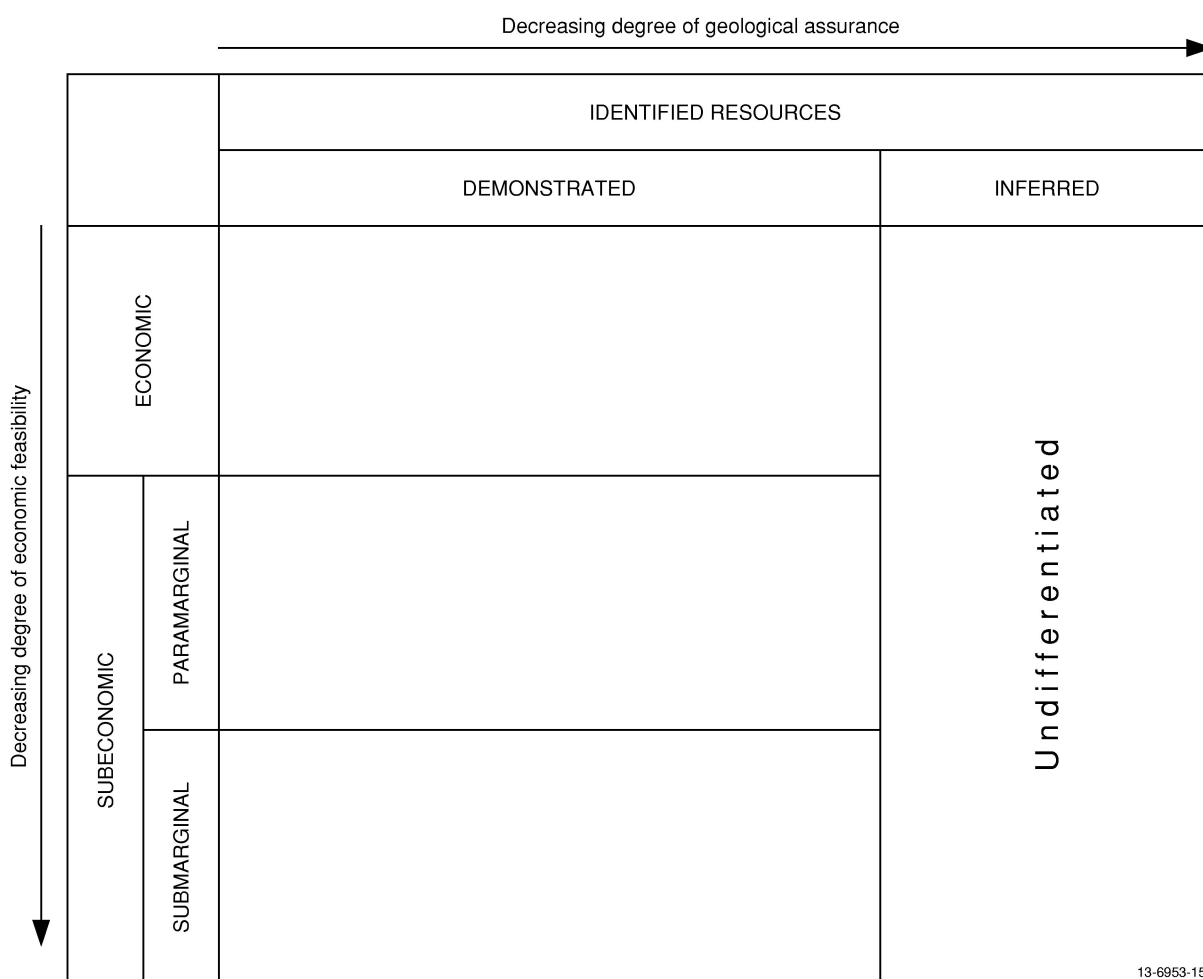
Companies listed on the Australian Securities Exchange are required to report publicly on ore reserves and mineral resources under their control, using the Joint Ore Reserves Committee (JORC) Code (2009, see <http://www.jorc.org/>). This has also evolved from the McKelvey system, so the national system and JORC Code are compatible. Data reported for individual deposits by mining companies are compiled in Geoscience Australia's national mineral resources database and used in the preparation of the annual national assessments of Australia's mineral resources.

Estimating the total amount of each commodity likely to be available for mining in the long term is not a precise science. For mineral commodities, the long-term perspective takes account of the following:

- JORC Code Reserves will all be mined, but they only provide a short term view of what is likely to be available for mining;
- most current JORC Code Measured and Indicated Resources are also likely to be mined;
- some current JORC Code Inferred Resources will also be transferred to Measured Resources and Indicated Resources and Reserves; and
- new discoveries will add to the resource inventory.

## G.2 Classification principles

The national system for classification of Australia's identified mineral resources is illustrated in Appendix Figure G.1. It classifies Identified (known) Mineral Resources according to two parameters, the degree of geological assurance and the degree of economic feasibility of exploitation. The former takes account of information on quantity (tonnage) and grade while the latter takes account of economic factors such as commodity prices, operating costs, capital costs, and discount rates.



Appendix Figure G.1 Australia's national classification system for mineral resources.

Resources are classified in accordance with economic circumstances at the time of estimation. Resources that are not available for development at the time of classification because of legal and/or land access factors are classified without regard to such factors, because circumstances could change in the future. However, wherever possible, the amount of resource affected by these factors is stated.

Because of its specific use in the JORC Code, the term 'Reserve' is not used in the national inventory, where the highest category is 'Economic Demonstrated Resources' (EDR, Appendix Figure G.1). In essence, EDR combines the JORC Code categories 'Proved Reserves', Probable Reserves', plus 'Measured Resources' and 'Indicated Resources'. This is considered to provide a reasonable and objective estimate of what is likely to be available for mining in the long term.

### G.3 Terminology and definitions

**Resource:** A concentration of naturally occurring solid, liquid or gaseous material in or on the Earth's crust in such form and amount that economic extraction of a commodity from the concentration is currently or potentially (within a 20-25 year timeframe) feasible.

The definition does not intend to imply that exploitation of any such material will take place within that time span, but that exploitation might reasonably be considered. It should be applied also on a

commodity by commodity basis to take account of prevailing and prospective technologies. The term includes, where appropriate, material such as tailings and slags. Mineralisation falling outside the definition of 'Resource' is referred to as an 'occurrence' and is not included in the national inventory.

**Identified Resource:** A specific body of mineral-bearing material whose location, quantity and quality are known from specific measurements or estimates from geological evidence for which economic extraction is presently or potentially (within a 20–25 year timeframe) feasible.

## G.4 Categories based on degree of geological assurance of occurrence

To reflect degrees of geological assurance, Identified Resources are divided into Demonstrated Resources and Inferred Resources:

1. **Demonstrated Resource:** A collective term used in the national inventory for the sum of 'Measured Mineral Resources', 'Indicated Mineral Resources' 'Proved Ore Reserves' and 'Probable Ore Reserves', which are all defined according to the JORC Code:
  - A '**Measured Mineral Resource**' is that part of a Mineral Resource for which quantity, grade (or quality), densities, shape and physical characteristics are estimated with confidence sufficient to allow the application of Modifying Factors to support detailed mine planning and final evaluation of the economic viability of the deposit.

Geological evidence is derived from detailed and reliable exploration, sampling and testing gathered through appropriate techniques from locations such as outcrops, trenches, pits, workings and drill-holes, and is sufficient to confirm geological and grade (or quality) continuity between points of observation where data and samples are gathered.

A Measured Mineral Resource has a higher level of confidence than that applying to either an Indicated Mineral Resource or an Inferred Mineral Resource. It may be converted to a Proved Ore Reserve or, under certain circumstances, to a Probable Ore Reserve.

- An '**Indicated Mineral Resource**' is that part of a Mineral Resource for which quantity, grade (or quality), densities, shape and physical characteristics are estimated with sufficient confidence to allow the application of Modifying Factors in sufficient detail to support mine planning and evaluation of the economic viability of the deposit.

Geological evidence is derived from adequately detailed and reliable exploration, sampling and testing gathered through appropriate techniques from locations such as outcrops, trenches, pits, workings and drill-holes, and is sufficient to assume geological and grade (or quality) continuity between points of observation where data and samples are gathered.

An 'Indicated Mineral Resource' has a lower level of confidence than that applying to a Measured Mineral Resource and may only be converted to a Probable Ore Reserve.

- A '**Proved Ore Reserve**' is the economically mineable part of a Measured Mineral Resource. A Proved Ore Reserve implies a high degree of confidence in the Modifying Factors.

A Proved Ore Reserve represents the highest confidence category of reserve estimate and implies a high degree of confidence in geological and grade continuity, and the consideration

of the Modifying Factors. It includes diluting materials and allowances for losses that may occur when the material is mined. Appropriate assessments and studies have been carried out, and include consideration of and modification by realistically assumed mining, metallurgical, economic, marketing, legal, environmental, social and governmental factors. These assessments demonstrate at the time of reporting that extraction could reasonably be justified.

- A '**Probable Ore Reserve**' is the economically mineable part of an Indicated, and in some circumstances, a Measured Mineral Resource. The confidence of the Modifying Factors applying to a Probable Ore Reserve is lower than that applying to a Proved ore Reserve.

A Probable Ore Reserve has a lower level of confidence than a Proved Ore Reserve but is of sufficient quality to serve as the basis for a decision on the development of the deposit. It includes diluting materials and allowances for losses which may occur when the material is mined. Appropriate assessments and studies have been carried out, and include consideration of and modification by realistically assumed mining, metallurgical, economic, marketing, legal, environmental, social and governmental factors. These assessments demonstrate at the time of reporting that extraction could reasonably be justified.

2. An **Inferred Mineral Resource** is that part of a Mineral Resource for which quantity and grade (or quality) are estimated on the basis of limited geological evidence and sampling. Geological evidence is sufficient to imply but not verify geological and grade (or quality) continuity. It is based on exploration, sampling and testing information gathered through appropriate techniques from locations such as outcrops, trenches, pits, workings and drill-holes.

An Inferred Mineral Resource has a lower level of confidence than that applying to an Indicated Mineral Resource and must not be converted to Ore Reserves. It is reasonably expected that the majority of Inferred Mineral Resources could be upgraded to Indicated Mineral Resources with continued exploration.

By definition, Inferred Mineral Resources are classified as such for want of adequate knowledge and therefore it may not be feasible to differentiate between economic and subeconomic Inferred Resources. Where the economics cannot be determined, these Inferred Resources are shown as 'undifferentiated'.

## G.5 Categories based on economic feasibility

Identified resources include economic and subeconomic components.

1. **Economic:** Implies that, at the time of determination, profitable extraction or production under defined investment assumptions has been established, analytically demonstrated, or assumed with reasonable certainty.
2. **Subeconomic:** Refers to those resources which do not meet the criteria of economic; Subeconomic Resources include Paramarginal and Submarginal categories:
  - **Paramarginal:** That part of Subeconomic Resources which, at the time of determination, could be produced given postulated limited increases in commodity prices or cost-reducing advances in technology. The main characteristics of this category are economic uncertainty and/or failure (albeit just) to meet the criteria for economic.

- **Submarginal:** That part of Subeconomic Resources that would require a substantially higher commodity price or major cost-reducing advance in technology, to render them economic.

The definition of 'economic' is based on the important assumption that markets exist for the commodity concerned. All deposits that are judged to be exploitable economically at the time of assessment are included in the economic resources category irrespective of whether or not exploitation is commercially practical. It is also assumed that producers or potential producers will receive the 'going market price' for their production.

The information required to make assessments of the economic viability of a particular deposit is commercially sensitive. Geoscience Australia's assessment of what is likely to be economic over the long term must take account of postulated price and cost variations. Economic resources include resources in enterprises that are operating or are committed, plus undeveloped resources that are judged to be economic on the basis of a realistic financial analysis, or compare with similar types of deposits in operating mines.

# Appendix H Useful links for information about platinum-group elements

All weblinks current as at 10 October 2014

## H.1 Reports, maps, and statistical data relating to PGEs from Geoscience Australia:

- Australian Mineral Exploration—A review of exploration for the year 2013:  
[http://www.ga.gov.au/corporate\\_data/78620/78620.pdf](http://www.ga.gov.au/corporate_data/78620/78620.pdf)
- Australian Mineral Exploration, a review of exploration—Archived issues from 2000 to 2012:  
<http://www.ga.gov.au/cedda/publications/1200>
- Australian Mines Atlas: Interactive mapping tool for displaying known mineral and energy assets, mines, and production/processing centres; an aid to industry research:  
<http://www.australianminesatlas.gov.au/index.jsp>
- Australia's Identified Mineral Resources 2012  
[http://www.ga.gov.au/corporate\\_data/79672/79672.pdf](http://www.ga.gov.au/corporate_data/79672/79672.pdf)
- Australia's Identified Mineral Resources—Archived issues from 1992 to 2011:  
<http://www.ga.gov.au/cedda/publications/1201>
- New products from Geoscience Australia to assist nickel and platinum explorers—2008 flyer:  
[http://www.ga.gov.au/corporate\\_data/70278/70278.pdf](http://www.ga.gov.au/corporate_data/70278/70278.pdf)
- Platinum-Group Elements—General description of PGEs and references:  
<http://www.ga.gov.au/minerals/mineral-resources/platinum.html>

## H.2 Australian supply, demand, and price statistics of PGEs:

- Australian Bureau of Statistics:  
<http://www.abs.gov.au>
- Bureau of Resources and Energy Economics:  
<http://www.bree.gov.au>
- Western Australia production statistics of PGEs. Government of Western Australia Department of Mines and Petroleum; Commodity statistics (historical and current production and value data for calendar and financial years occur under Quantity and Value heading):  
<http://www.dmp.wa.gov.au/1521.aspx>

## H.3 Global supply, demand, and price statistics of PGEs:

- Johnson Matthey Platinum Today—Price Charts of PGEs (1992 to 2014):  
<http://www.platinum.matthey.com/pgm-prices/price-charts/>

- Johnson Matthey Platinum Today—Market Data Tables of PGE Supply and Demand (1975 to 2013):  
<http://www.platinum.matthey.com/publications/market-data-tables/>
- Kitco Metals Incorporated—Current and historical PGE metal price charts (1960 to 2012):  
<http://www.kitco.com/charts/>
- London Metal Exchange—Trading and pricing of metals:  
<http://www.lme.com/>
- Metal Prices.com—Prices and Marketing News of PGEs and Other Metals:  
<http://www.metalprices.com/FreeSite/index.asp>
- Reserve Bank of Australia—Exchange Rates:  
<http://www.rba.gov.au/statistics/frequency/exchange-rates.html>
- United States Geological Survey—Historical PGE prices (1880 to 1998):  
<http://minerals.usgs.gov/minerals/pubs/commodity/platinum/550798.pdf>

## H.4 Naming PGEs and PGE-bearing minerals:

- A History of Platinum and its Allied Metals by McDonald and Hunt (1982: Johnson Matthey, London, 450 pp):  
<http://www.platinummetalsreview.com/resources/history-of-platinum-2/>
- History of the origin of the chemical elements and their discoverers by Holden (2001):  
<http://www.nndc.bnl.gov/nndc/history/origindc.pdf>
- Development of the chemical symbols and the Periodic Table:  
[http://elements.vanderkrogt.net/chemical\\_symbols.php](http://elements.vanderkrogt.net/chemical_symbols.php)
- Elementymology and Elements Multidict:  
<http://elements.vanderkrogt.net/index.php>
- Mineral information—Mindat.org:  
<http://www.mindat.org/>
- The history and applications for platinum by Jude Sutton (2008):  
<http://ezinearticles.com/?The-History-and-Applications-For-Platinum&id=1538868>
- Thomas Jefferson National Accelerator Facility—Periodic Table of Elements:  
<http://education.jlab.org/itselemental/>
- Water Treatment Solution Lenntech—Periodic Table of Elements:  
<http://www.lenntech.com/periodic/periodic-chart.htm>
- Periodic Elements Spiral—Wikipedia:  
<http://en.wikipedia.org/wiki/File:Elementspiral.svg>
- Periodic Table of Elements—Chemical Elements:  
<http://www.chemicalelements.com/>
- Periodic Table of Elements—Environmental Chemistry:  
<http://environmentalchemistry.com/yogi/periodic/#periodic%20table%20sorted%20by>
- Periodic Table of Elements—Chemicool:  
<http://www.chemicool.com/>
- Periodic Table of Elements—WebElements:  
<http://www.webelements.com/>

- Photographic Periodic Table of Elements:  
<http://periodictable.com/>
- Ptable—Dynamic Periodic Table:  
<http://www.ptable.com/>

## H.5 Government organisations involved with PGE research

- Australian Nuclear Science and Technology Organisation Minerals (ANSTO):  
<http://www.ansto.gov.au/home>
- Commonwealth Scientific and Industrial Research Organisation (CSIRO):  
[http://www.csiro.au/csiro/channel/\\_ca\\_dch2t.html](http://www.csiro.au/csiro/channel/_ca_dch2t.html)
- General Portal for State and Territory Geological Surveys:  
<http://www.geoscience.gov.au/>
- Geoscience Australia (GA):  
[www.ga.gov.au](http://www.ga.gov.au)
- British Geological Survey:  
<http://www.bgs.ac.uk/>
- United States Geological Survey (USGS):  
<http://www.usgs.gov>

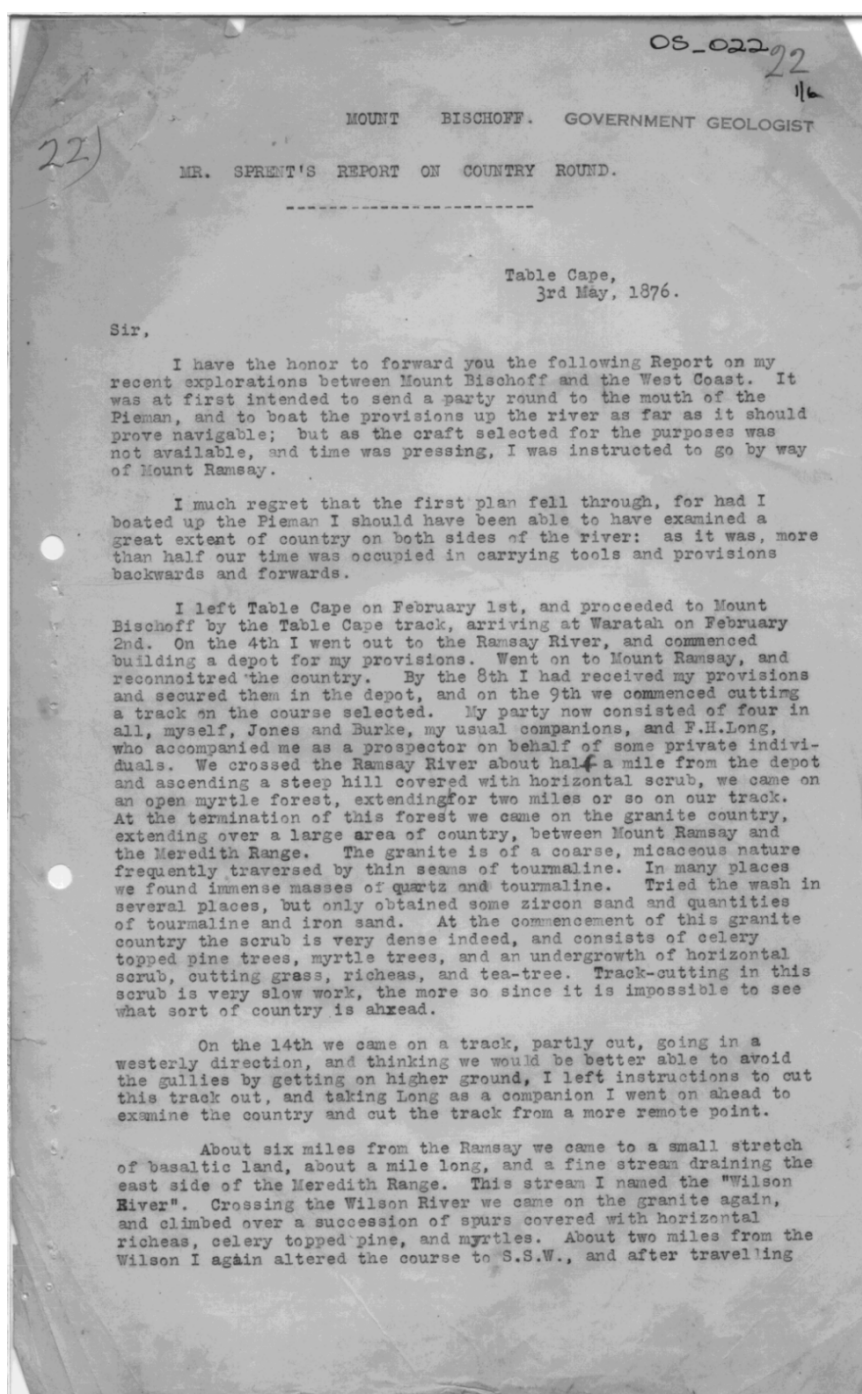
## H.6 General information on PGEs:

- About.com Chemistry—Multiple articles about the elements:  
<http://chemistry.about.com/>
- Australian Shares—Database of Australian mining and energy shares:  
<http://www.australian-shares.com>
- Australian company reporting—Australian Securities Exchange:  
<http://www.asx.com.au/>
- International Union of Pure and Applied Chemistry (IUPAC):  
[http://old.iupac.org/dhtml\\_home.html](http://old.iupac.org/dhtml_home.html)
- Johnson Matthey Platinum Metals Review:  
<http://www.platinummetalsreview.com/>
- Johnson Matthey Platinum Today—PGE applications and image gallery:  
<http://www.platinum.matthey.com/applications/>
- The PGM Database—published information and data:  
<http://www.pgmdatabase.com/jmpgm/index.jsp>
- United States Geological Survey (USGS)—Platinum-group-metals: statistics and information:  
<http://minerals.usgs.gov/minerals/pubs/commodity/platinum/>
- Wikipedia, the free encyclopedia about platinum-group elements:  
[http://en.wikipedia.org/wiki/Platinum\\_group\\_elements](http://en.wikipedia.org/wiki/Platinum_group_elements)
- Wikimedia Commons: Historical photographs, explorers, chemists, metallurgists:  
[http://commons.wikimedia.org/wiki/Main\\_Page](http://commons.wikimedia.org/wiki/Main_Page)

# Appendix I Exploration reports by Sprent

Expedition results of Deputy Surveyor-General of Tasmania, Charles Percy Sprent in 1876 and 1877

Appendix Figure I.1 'Mr Sprent's report on country round' Table Cape 3<sup>rd</sup> May, 1876. Yellow shaded sections show references to 'osmiridium' and platinum.



four miles through the same description of country to that just mentioned, we came on a change in the shape of gum timber, tea-tree richeas, bauera, and cutting grass. This sort of country extended for about a mile in our course, and was very wearisome travelling. Amongst this bauera scrub we found a fine stream running, and along its banks quantities of large pine trees of the Macquarie Harbour species. Some of these trees were upwards of three feet through, but all of them were dead, killed by some fire many years ago. Half a mile from this river we came on a long narrow plain of button grass. This plain which I named the "Yellow-band Plain," is about five miles long, and about half a mile in its widest place. It is drained by several streams, one of which the "Yellow Stream" is a fair size river, difficult to cross in winter. The plain is fringed with peppermint trees, and contains several belts of timber: the walking is good, the plain having been burnt off some two years ago.

The bare tops of the Meredith Range are close to this plain on the west and south-east sides. Made a camp on the plain, and started up the Meredith Plain. Just as we reached the summit a heavy storm of rain came on and obscured the view, so that we were forced to return. The following day I proceeded down the plain for about three miles, and finding an opening towards the "Parson's Hood" determined to go up and obtain a view. Accordingly we selected a route where the fire had cleared off the scrub and button grass and made for one of the peaks on the Meredith Range. Following up the bed of a creek, I noticed that the granite is traversed by many veins of finer granite, frequently containing much iron pyrites, and in one instance the grey granite was cut by a wide vein of red granite containing small seams of iron ore. We reached the summit of the Meredith Range without much difficulty and had a fair view for a few moments, when, as on the previous day, fierce storms of wind and rain came on, and completely obscured the view; indeed so strong was the wind that one could not stand upright on the bare granite rocks, and for an hour or more we stayed under the lee of the pinnacle waiting for the wind to moderate.

By the 29th the track was cut from the Ramsay River to the top of Meredith Range and leaving Jones and Burke to carry out provisions, I went on again with Long to examine the Parson's Hood.

The Meredith Range, so named by the late Mr. Gordon Burgess extends from the Parson's Hood in a northerly direction up to Wombat Hill. As far as I could see the rock is all granite, slate might be found on the north and west side, and I think sandstone on the North-west. The summits are covered with tea-tree and bauera scrub, with occasional patches of button grass, easily got rid of by firing in summer. This range is well worthy the attention of prospectors.

By the 16th March we had cut our track through a dense scrub of tea-tree and bauera and reached the Parson's Hood where we camped for a time. I found the Parson's Hood to be a long flat-topped mountain, the southern bluff of the Meredith Range. Approaching it from the north, we ascended a steep granite spur burnt off by Mr. Joseph Harman some two years ago, and found ourselves on a bare granite top. Going along the top of the mountain found the granite ~~to~~ and tea-tree scrub continued for about a quarter of a mile, then changed into a hard metamorphic rock, and an open forest of myrtle and tall richeas? Another quarter of a mile further on the granite showed again, and a nasty scrub of horizontal, tea-tree, cutting grass and richeas, then we lost the granite altogether, and came on hard slate rock, in some places containing iron pyrites. The travelling was now much better being through myrtle forest and ferns with here and there stringy-bark and blackwood trees. This sort of country continued to the base of the "Hood". From the Yellow-band Plain to the top of the "Hood" the total rise is about 1500 feet, and from the top to the base on the south west the fall is 1770 feet. In the vicinity we obtained zircon sand and a little platinum. The platinum might be worth examination, but I am afraid that the place is too difficult of access to offer much encouragement to prospectors.

On the west side of the Parson's Hood I am informed the formation is quite different, and consists of serpentine, diallage, hypersthene, with iron ores, asbestos, copper, and platinum, and in some places gold. A large creek drains the south-west side of the Parson's Hood. On the north side of this creek the rock is slate, on the south side sandstone and quartz. About a quarter of a mile from the base of the "Hood" we came on a complete change of country in the shape of low hills covered with button grass and heath. The formation here is slate, of all degrees of hardness and quartz veins.

On March 10th we set fire to the open country and succeeding in getting a very good burn. On the 11th showers of rain checked the fire, so we went through it, and made out way to a long, narrow ridge of hills, which extended for a great distance in a south-west course. Towards evening the smoke cleared off, and we saw the Pieman River just beneath us; heavy rain came on, and we camped in a bauera and tea-tree scrub.

On Monday 13th, we started again, and followed the ridge until we came close to the river; then, cutting through about twenty chains of bauera, tea-tree and horizontal scrub we pitched out tent, on the north bank of the Pieman, some 2100 feet below the ~~xx~~ summit ~~below~~ of the Parson's Hood and about seven miles of walking from its base.

The Pieman River, where we crossed it, is about 80 feet wide, flowing very gently and almost without any sound. At its lowest level shallow bars appear, and rapid water for short distances but, as a general rule the water is deep and quiet. The banks are scrubby and the edge of the river is lined with snags and logs. I am almost certain a light could be brought up from the Coast to a point about south of the Parson's Hood; possibly it might be taken much further if it were lifted over the bars. The Pieman is subject to heavy floods. I have seen fifteen feet in as many hours; at such times the current is very rapid indeed, and it would be impossible to cross or navigate the river. Very fine eels are to be obtained in the river, also native trout and lobsters, but I never caught any blackfish. I never saw any kangaroo in the vicinity and only the traces of wombats.

Our provisions were exhausted the day after we reached the Pieman so on the 14th we started back again. The day being warm and windy, we set the button grass on fire and made a line of fire about four miles long. Reached the Yellow-band Plain that night, almost exhausted. Meanwhile Jones and Burke had been carrying out provisions from the Ramsay River to the Yellow-band Plains, and by making frequent trips had brought out all the stores. I cannot imagine any work more tiring than carrying heavy loads over such rough country day after day. It was by far the hardest part of our work.

On the 18th March I went into Bischoff and obtained the services of Mr. F. R. Lampriers, so that I might divide my company into two parties. After various delays, caused by wet weather, we reached the Pieman again on the 25th.

Long had incurred a violent attack of dysentery, through drinking bad water at Mount Bischoff, and on the journey out was very ill indeed, so much so that I feared he would die of exhaustion; however he managed to reach the Yellow-band Plains where we had some chlorodyne and a few doses set him right again. He joined us at the Pieman on the 29th.

On the 29th heavy rain set in and the river rose rapidly. The night of the 30th was very rough; rain came down in torrents and a heavy gale set in, which sent the limbs of trees flying in all directions; one tree struck the guy rope at the corner of the tent. Rain continued up to the 7th of April, and as it was im-

possible to cross the river we did some prospecting on the north side. As all the gullies were flooded we could not try the best places, but whenever we managed to reach the bed rock we obtained gold. The wash is mostly quartz and slate; in some places a kind of micaceous cement. The gold is scaly, similar to that obtained on the Hellyer. The rocks in the vicinity are soft slates, micaceous slates, and quartz.

Seeing that we should run a great risk if we crossed the Pieman I determined to fetch up more provisions, and leave some on the south side in case of floods cutting off our return. Took Burke with me and went to the Wilson River for flour. On the way met Jones and Lempriere, who were travelling in a westerly direction. Returned to the Pieman on the 12th, and crossed it on the 13th.

Found the country on the south side of the Pieman to be similar to that on the north side, but not so hilly. About half a mile from the river tried some of the creeks and obtained gold in every instance. In one spot obtained about five specs to the dish, and about an ounce of tin. The wash is quartz, tourmaline and slate, very much waterworn, apparently a former bed of the river.

Continued our course in the direction of Mount Heemskirk and found the walking very good. The gullies are very deep and filled with bawera and small gum trees; but by keeping on the high ground these are avoided and time saved.

On the 14th we reached Mount Heemskirk and went up one of the peaks. Found Mount Heemskirk to be a group of hills some of them slate and others granite, quartz, and tourmaline - a very promising locality for minerals. Finding that we were now about five miles from the beach and the country all flat between us and the sea, and thinking we were now in well-known ground, I determined to devote my attention to examining the country north and south of the Pieman in its immediate vicinity. Camped near the foot of Mount Heemskirk intending to go in the direction of Mount Dundas. During the day observed that Lemprier and Jones had fired the country west of the Parson's Hood and that the fire was travelling rapidly, in a south-west direction; during the night the reflection was very bright.

On the morning of the 15th found that the barometer was falling fast and the wind coming in strong gusts from the north west. Fearing a flood I determined to go back to the Pieman, and pushed on so as to reach there by evening. Set fire to the country as we went along. Sunday, 16th was wet, and the river began to rise, but towards evening it fell again, and although rain fell on Monday it did not prevent us from recrossing the Pieman and examining the south side. On Monday night rain fell in earnest and a heavy flood came down the river. Rain continuing the river rose nearly twenty feet; and, thinking it was too late in the season for further work, I determined to return to Mount Bischoff on the first opportunity.

On the 20th April we struck our camp on the Pieman, and went as far as the summit of the Parson's Hood the most wretched journey I ever made in my life. Rain set in as we went up the Hood, and when we reached the summit we encountered a perfect hurricane of wind and rain; everything was wet through and we spent a weary night sitting in a tent full of smoke. I never remember such a gale in Tasmania. Reached our tent on the

Yellow-band on the 21st. and managed to get our things dried. Furious squalls of wind and rain continued, and we were obliged to remain until the 23rd. Arrived at my cottage, Waratah, early on the 24th.

Messrs Lempriere and Jones, after separating from my party, proceeded to examine the country in a westerly direction, and in the first stage of their journey ascended the peak to the west of the Parson's Hood. This peak is about the same height as the Hood, of slate formation, although the junction of the slate and granite is not far to the northward. The button grass was fired and a great extent of country cleared, but rain prevented the fires extending as far as they might have done in fine weather. Leaving the ranges they then followed the button grass hills in a westerly direction and found that the country was precisely similar to that already described.

Approaching the Pieman the course was altered to southwest, and after passing through some four miles of forest, the river was struck at a point where a large tributary joins it. At this point they report the water slightly brackish, and the river very deep and wide, with no current to speak of. The formation in the vicinity is talcose and micaceous schists, quartz veins, and iron ore. One mass of iron ore was found weighing between four and five tons. The weather was too wet for prospecting and accordingly they returned to Bischoff, arriving there on the 26th.

The entire country from the Ramsay River to the west coast is utterly worthless for agricultural or pastoral purposes, not do I think there is any large quantity of valuable timber. The Macquaries Harbour pine grows in the vicinity of the Pieman and a few of its tributaries, but the trees are few and far between.

There are, however, sure indications that this part of Tasmania abounds in mineral wealth although it may be that the search will be arduous and slow. As in the case of the Hellyer River so it is with the Pieman; wherever the softer schists occur gold is found in small quantities and I have not the slightest doubt but that in both rivers gold will be found in paying quantities both alluvial and reef gold. Tin and gold occurring together in some spots near the Pieman in what is called "made" ground would indicate that the country higher up the river is worthy of examination, and I would recommend prospectors to try the vicinity of Mount Murchison and the Murchison River.

I do not think it advisable to open up horse-tracks into the west country until there is something to warrant the expenditure, but I would advise the Government to cut tracks fit for men to travel with loads on their backs. The route I adopted presents so many difficulties that I cannot recommend its adoption; but would suggest a route to the westward of the Merédith Range.

To completely open up the west coast to prospectors three tracks are required.

First,- Burgess's track from Khole Plain to a point west of Mount Cleveland. This track would not require much clearing, as it has been partly opened on various occasions.

Second,- A track from the termination of Emmett's track from Circular Head to the Arthur to join Burgess's track. This track to be continued in a southerly direction towards Macquarie Harbour.

Third,- A track from Lake St. Clair to some point on the west coast crossing track by river two. This track is of importance since a prospector might be on the south side of the Pieman and un-

able to cross on account of floods be obliged to make out in another direction.

These tracks would not be expensive affairs as they would pass through open country. They could all be out and marked by a good party during the next summer.

I would respectfully suggest that a party be fitted out early next summer and sent round to the mouth of the Pieman by sea. Proceeding up the Pieman in a boat, the party would establish a depot on the open country and search out and cut a track towards the Arthur River and towards Macquarie Harbour. A couple of men from Mount Bischoff could then cut out Burgess' track so as to meet the other party. Time permitting, the party would push on towards Lake St. Clair by way of the King River and Collingwood Valley. It would be useless to call for tenders to cut tracks in such a country and further examination is not required.

A good party would examine the route and cut the necessary tracks, at the same time furnishing much valuable information on the topography and resources of the country.

Prospectors will find it extremely difficult work to examine the western country by "swagging" from Mount Bischoff, and I would strongly advise them not to attempt it at present. Four days would be spent in reaching the Pieman and three in coming back so that a party encumbered with tools, bedding, tents &c. could not carry sufficient provisions to enable them to make a systematic search. By boating up the Pieman the work would be easy and pleasant.

I may conclude with mentioning as an inducement to prospecting the western country that over three hundred ounces of gold have been obtained in one season from the Hellyer River, and that a party of Chinamen have done exceedingly well there during the past season. Copper has been discovered on the Arthur in several places; and copper lead, tin, gold, and platinum have been found in the vicinity of the Parson's Hood, and the Pieman, not to mention the discoveries at Mount Bischoff and Mount Ramsay.

I append a sketch map to illustrate the above Report.

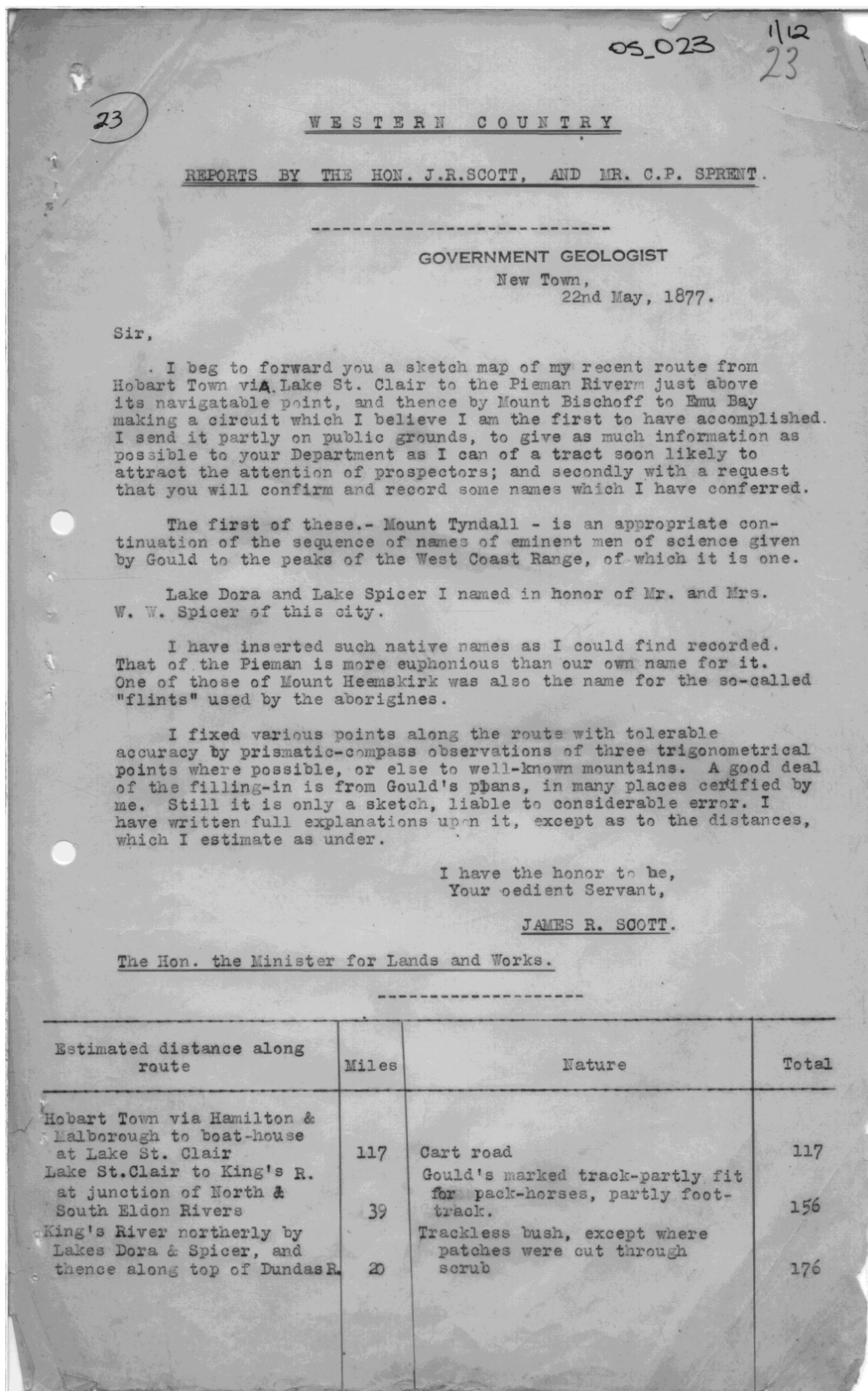
I have the honor to be,  
Sir,  
Your obedient Servant.

CHAS. P. SPRENT,  
District Surveyor

The Hon. the Minister for Lands and Works,  
Hobart Town.

-----

Appendix Figure I.2 Reports by the Hon. J.R. Scott and Mr C.R. Sprent, New Town 22<sup>nd</sup> May, 1877. Yellow shaded sections show references to 'osmiridium' and platinum.



Top of Dundas Range down to nearest open country in direction of Mount Heemkirk .	5	Foot-track cut through forest and scrub.	181
Across open country to Donnelly's track near bend of Pieman River south of Mount Livingstone	10	Trackless bush- part recently burnt	191
Along Donnelly's track to his main depot at head of navigation.	12	Foot-track cut through scrub-unmarked across about four miles of open country	203
-----			
Donnelly's depot to Sprent's track of 1876, S.W. of Parson's Hood	12	Part cut track through scrub-rest trackless bush	12
Along Sprent's track of 1876 to Knole Plain.	25	Rough foot-track cut & marked to Mt Ramsay Rd. then horse track.	37
Knole Plain to Emu Bay	48	By cart road.	85

Lands and Works Office,  
19th June, 1877.

Sir,

I have the honor to acknowledge the receipt of your letter of the 22nd May last, accompanied by a sketch map illustrative of your route through Western Tasmania via Lake St. Clair to the Pieman River and via Mount Bischoff to Emu Bay, and desire to thank you on behalf of the Government for the very valuable information it contains.

The names suggested by you for various mountains, &c shall be adopted; and when Mr. Sprent furnishes me with a map of the various routes he has accomplished in that country, it is my intention to have a lithographic plan issued for the public benefit, more especially prospectors, whose researches will be materially assisted by the information you have each contributed.

I have the honor to be,  
Sir,  
Your obedient Servant,

C.O'REILLY,  
Minister for Lands & Works

The Honorable James Reid Scott, New Town.

Hobart Town,  
May, 1877.

Sir,

During the past five months I have been employed cutting tracks and exploring in the vicinity of the Pieman and Arthur Rivers, and I now have the honor to furnish you with the following Report.

The members of the party besides myself were C.W.Lord, F.H. Long, D.Jones, and J.Burke, Leaving Table Cape on the 21st December.

1876, we arrived at Circular Head the same day, and immediately sent our baggage out to the starting point selected. On the invitation of Mr. S.B. Emmett we established our head-quarters at his farm, close to the south boundary of the Circular Head estate.

The first work to be undertaken was the re-opening of Emmett's track to the Arthur. This track was cut by Mr. Emmett for the Government years ago and has several times been re-opened at private expense, but at the time of my visit it was much blocked up by fallen timber.

After leaving the cultivated farms the track follows a direction as nearly south as the nature of the country permits and for a distance of about one mile passes through some good agricultural land, after that it enters the usual description of myrtle forest, almost universal in the back parts of the Country of Wellington. This description of country continues for about two miles, save where the locality a stretch of about one mile of bauera scrub and gum trees lends a by no means pleasing variety to the travelling. The forest is very broken and intersected by numerous creeks, but the ~~hills~~ hills do not rise to any great height above the surrounding country. The rock is in most places basalt, but here and there quartz gravels shows out, and a soil, composed apparently of decomposed slate. In fact it would appear that this country, as well as the Campbell Range, is but a thin overlap of basalt upon a Silurian formation.

About nine miles from Emmett's farm there is a branch track going to Kay's hut, at the junction of the Arthur and Hellyer Rivers. We followed this track for about half a mile then left it and cut a few chains of new track on to Gibson's Plains. North of Gibson's Plain there is some extent of good land, heavily timbered with myrtle, stringy bark, sassafras and fern trees. The creeks show quartz in abundance, and patches of white clay occur. This clay is plentiful, and may some day be used for pottery purposes, although it is not "kaolin" as many have supposed, but rather a decomposed slate, kaolin being a decomposed felspar largely used in the manufacture of china.

Gibson's Plain is about two miles long from north to south, extending for about the same distance westward from the track. Mr. Emmett states that there are other plains on the west side divided from Gibson's Plain by a narrow belt of timber. The plain is covered with button grass and coarse herbage, here and there a few peppermint and gum trees. The soil is very wet and cold, being a spongy white clay, unfit for cultivation. In fact the plain is so boggy as to be dangerous for horses, and we subsequently had some difficulty in inducing anyone to risk horses upon it. The south end of the plain, being higher, is dry and more gravelly, exhibiting quartz veins and slate rock.

After leaving Gibson's Plain the track passes over some very broken country, frequently covered with thick patches of horizontal scrub. Several creeks are crossed, one large one known as the Gunn River. The rock in this vicinity is a dark slate or g flag. One more narrow belt of button grass is crossed and the track then follows the course of a creek, passing over rough ground with cutting grass, tea tree, and bauera of and emerging on a small extent of open ground close to the Arthur River.

As Emmett's track finishes up on a steep bank of the river we cut a fresh track so as to strike a ford lower down, and by making some slight side cuttings we managed to get a fair crossing place for the horses.

The country in the vicinity of the Arthur is very broken and rough, abounding in bauera and horizontal scrubs. The rocks are sandstones, quartzites, and slates. The slates in many places are flat, splitting into flags; they have been classified as Cambrian, but I am inclined to think they are Silurian. The locality is not a promising one for minerals; a little fine gold is found in the river, but it is evidently derived from sources higher up the river. The occurrence of blocks of granite in the river has led many people to imagine that a granite country would be found higher up, but I am of opinion that the granite is derived from conglomerates of Campbell's Range, and that the original site is Hampshire Hills and Mount Bischoff. To the west of Emmett's track the country is entirely unexplored, and I would suggest it to Circular Head prospectors as the field of future operations. It would not be difficult to take out a punt sufficiently strong to carry a party down the river; fish, lobsters and eels are plentiful and there is a fair chance of success in the vicinity of Mount Balfour and the country to the south of the Duck River settlements.

To provide against any interception of our communications by floods, we carried out the boards for a light punt; these we put together at the river, and at our departure left the punt in a small gully on the south side close to our depot.

By the 13th January we had finished clearing out Emmett's track and established our headquarters on the Arthur River, seventeen miles from Mr. Emmett's farm. On the 15th I sent Jones back to Circular Head to fetch out pack-horses, and with the rest of the party started off to examine the country to the south.

After crossing the Arthur we passed through a few chains of timber and found ourselves on a narrow belt of open ground; striking a southerly course, we travelled for four miles over button grass and heath until we came abreast of the Blue Peaked Hill. This hill is, I suppose the one from which Mr. Wedge examined the country in 1828, although I fancy that the "Blue Peaked Range" as Hellyer calls it, was further to the west. The hill itself is a small one of three peaks, not very high in fact not so high as some of the surrounding country. Turning towards the east we crossed a large creek running through a belt of timber and then resumed our southerly course. Another three miles over button grass hills brought us to a fine large creek running through a forest towards the S.W. Seeing a lofty forest in front of us I sent Lord and Burke back to the creek and Arthur to complete the track, whilst Long and I examined the ground ahead. After crossing the creek and travelling for another mile we came to the Rapid River, and immediately on crossing it got into very rough country indeed. After two days tumbling about in bauera and horizontal scrub I determined to strike a course more to the westward, and on making over in that direction we soon came on to extensive button grass plains. Finding that a tongue of these ~~xxx~~ plains extended back nearly to the Rapid River we crossed that river and marked a route back to our former track from the Arthur.

From a high rise near the Rapid River we had a capital view of the country, and saw Mount Cameron, Cape Grim, and other points on the Woolnorth estate. The country between us and Woolnorth appears to be low but very broken, with here and there patches of button grass and bauera scrubs.

We returned to the Arthur on the 20th January, and found the depot completed, and a good supply of provisions fetched out by the pack-horses. On the 22nd we carried out a load of provisions to the Rapid River and commenced cutting a pack horse track across the valley. The Rapid River runs through a deep gorge the banks are very precipitous and covered with horizontal scrub. To make a safe road for horses we were obliged to make side cuttings, and remove immense logs and rocks. This occupied us until the 27th when we again reached the open ground on the south side of the river. Finding that the open ground some distance south we determined to shift our depot our as far as the horses could be got.

The Rapid River is well named running as it does very swiftly over a bed of hard red slate; immense cliffs of slate rock, of the metamorphic variety occur all along its banks. In these cliffs small veins of iron occur, and the crevices and protected parts are frequently covered with crystals of alum. All the button grass country on both sides of the river is composed of slates, quartzites and sandstones, no appearance of gold or black sand, occasionally a few zircons.

On the 29th January Jones went to Circular Head to fetch out the pack horses, the rest of us crossed the Rapid River and struck out in a S.S.W. direction over the open ground. We found the travelling very good, and as we proceeded the open ground extended further to the westward to the eastward being a high forest. The button grass was short and scanty having been burnt off not many years previously consequently our fires did not make much progress. Crossing several small creeks we continued our route over level ground until we came to a large creek running through a narrow band of timber. After crossing this belt the open ground widens out very much, extending for more than a mile to the east whilst to the westward veins of forest and button grass plains extended as far as the eye could see. The plains hereabouts are studded with trees and present a very pleasing appearance, and from a distance would be mistaken for a fine grassy country. Continuing our course about S.W. we passed over open rises until we came to a river running round the base of a wooded hill. This river is no doubt the one Wedge named the Arthur mistaking it for the Arthur named by Hellyer, a river which unites with the Hellyer many miles to the east. At the place where we struck the river it flows over flat flags, the water being shallow but here and there deep holes occur and frequent falls. Higher up the stream is gravelly impeded by timber and abounds in large blackfish and lobsters. We established out camp on this river, two of the party returning to stake out the route we had taken, whilst Long and I examined the forest in front. On entering the forest we found that it was very good agricultural land, timbered with gums, myrtles, fern trees, pepper, &c. the soil being derived from a dark blue slate. Clay-slates abounded some of them splitting well but containing too much iron pyrites to be of any value. There must be a large extent of fair land in this locality and it appears to extent some miles to the west. On examination we found that the button grass country extended farther in a S.E. direction; accordingly we struck our camp and returning about a mile on our track, altered our course to S.E. and travelled over button grass rises for some three ~~or four~~ miles or four miles further, the latter part of the route being south again. We now found that a narrow forest divided us from a high range of open hills and that there were several branches of the river flowing from them.

After cutting a track through the forest and crossing two branches of the river, we came out on some wet button grass plains extending up to the foot of the high hills. As these plains had never been burnt we lost no time in setting them on fire, and soon had the satisfaction of seeing the high button grass swept clean away. Travelling over this country for a couple of miles we pitched our camp at a creek close to the foot of a spur leading into the high hills, having determined to establish a depot here.

Reckoning the Rapid River as eight miles from the Arthur we had now travelled about eighteen miles from the latter river and with the exception of about a mile and a quarter of forest at the Rapid River and the half mile of forest dividing ~~this country from the~~ the plains, the whole of this route was over button grass country, of slate and quartzite formation.

Meanwhile Jones had hired pack horses and fetched them out thirteen miles south of the Arthur. They might easily have come on another five miles, but their owners were afraid of the boggy nature of parts of the plain.

Leaving Jones and Burke to carry the provisions from the place where the horses left them to our new depot, I started out with Long and Lord to make a route over the hills. After setting fire to the button grass we climbed up some steep rises covered with tall button grass and tea tree and with some difficulty got on to the ridge. To the east of us appeared a deep gully separating us from a range of bare mountains running north and south for many miles; to the westward were deep gullies full of bauera scrub and thick tea-tree, and beyond them again bare hills connected with the Norfolk range. Travelled for four miles over this high ridge and then finished up with a high peak which we named the "Pyramid Hill". From this hill we observed a deep valley in front of us, and open ground on beyond apparently extending right up to Mount Norfolk.

By this time the country was on fire in all directions, and completely obscured by the smoke; but on another occasion from this same hill we saw Mount Bischoff, Mount Cleveland, Meredith Range, Mount Heemskirk, and the whole of the Norfolk Range. On coming down off this peak we entered the forest and commenced cutting out a track. The edge of the forest as usual was very thick bauera, tea-tree, and cutting grass then changing into thick horizontal.

(Continued on next page)

After cutting about half a mile we came on a very rapid stream, not very large, but very rocky and very troublesome to get across in wet weather. In this river I noticed waterworn boulders of granite showing mica and iron pyrites. Climbing up a steep bank we cut our way through horizontal and tea tree and in a short distance came on another river but much larger than the last one. This river also showed granite, and we procured a few specs of scaly gold from the gravel. On the south side of the river an open spur came close down to the bank so that we lost no time in getting across and setting fire to the button grass, and we soon had the satisfaction of seeing an extensive fire.

The belt of forest we had cut through would be about a mile and a half wide, and appears to be the valley of the Savage River, as indicated on Mr. Gordon Burgess's map.

We now took a course nearly S.S.E., and travelled for a mile or so over open rises covered with button grass, then over wet flats of tea-tree and button grass for another mile, arriving at the foot of some steep quartzite hills. Here we established our camp for a few days whilst we burnt off the surrounding country.

Provisions being exhausted we returned to our last depot and obtained a fresh supply, and on the 15th February carried out a heavy load each, just in time to escape a perfect deluge of rain. The weather was now very wet and stormy and hindered our operations very much; but as our present camp was almost flooded out we were obliged to get further on to obtain shelter and firewood. We accordingly climbed up the steep hills and saw in front of us an immense timbered gorge evidently containing several streams. By this time I was getting tired of the barren and useless sort of country we had been travelling over and thinking that if I got nearer the Granite Range I might come across a more promising country for minerals, I altered the course E.S.E., not gone a quarter of mile before the quartzites gave place to limestones, and the forest proved to be more open than usual. We prospected one large creek and obtained a few specs of scaly gold. After crossing several creeks about a mile and a half from the open ground, we came on the River Donaldson and camped there for a few days. Noticing some pebbles of iron ore in the creeks we traced the gullies up and soon came to an immense quantity of iron ore, thousands of tons strewn the surface of the ground. The ore is sometimes magnetite ore sometimes brown ore and hematites here and there veins of iron pyrites. The most abundant rock in the vicinity is mica schist; but limestones are abundant on the west side of the river. The iron is all on the east side, and is associated with a quartz conglomerate and veins of granite.

Metalliferous veins abound, but I could not find any valuable ones, although I am of opinion that copper pyrites would be found along with the veins of iron pyrites. We traced the iron over some half a mile of country up the river, and also examined the river for gold but on account of the immense quantity of iron sand in every dish we had not much success. On going down the river we lost the iron and came on mica schists and metamorphic slates, obtained gold wherever we managed to bottom a hole, but there is very little wash dirt in the river. Large boulders of granite abound derived probably from dykes of granite penetrating the slates. Altogether this is a country well worth prospecting.

Leaving the Donaldson, we went over a steep rise and found another valley before us, this we had to cut our way across, and we found the horizontal very thick indeed. The soil had now changed to quartz gravel. After cutting through about three miles of scrub we again came on to open button grass country.

By this time our work was getting very heavy as we had our provisions some distance, two men being constantly at work going and returning with loads. I now saw very plainly that we should not be able to fetch out our provisions from Circular Head but must communicate with Mount Bischoff. We therefore established a depot on the open plains we had just reached, and after stowing away our baggage shaped a course in the direction of Mount Cleveland to try and find Burgess's track. For about three miles we travelled over a spur of the Button Grass Hills, and then came to a thick scrub of tea-tree and bauera. Here we picked up Burgess's marks, and followed them as far as we could trace them. Passing through the bauera scrub we went down a deep gully of slate formation, where we had to encounter some bad horizontal scrub; missing the marked-track we came on a large stream, most probably the Whyte River. Here I noticed a clay-slate containing carbonate of copper amongst the boulders in the river. At a late period we discovered this same rock in situ; it will be described further on.

The geological nature of the country now changed entirely for after crossing the Whyte a second time we came on rocks which appeared to me to be chlorite and hornblende schists gradually giving place to a dense hornblende rock. Further on we came on rocks which I think are serpentines; frequently narrow veins of asbestos traverse these rocks. Other rocks, which are altogether strange to me, occur, and until I have had them properly classified it would be useless to describe them.

After leaving the Whyte River for the second time we went up a steep spur covered with tea-tree, cutting grass and bauera, very slow travelling indeed, and it cost us much hard labour to gain the button grass beyond. Another three miles of steep bare hills succeeded, when we found ourselves stopped by a dense scrub of bauera, tea-tree, and cutting grass. This piece of scrub was the worst I have ever been in; and although there was not a quarter of a mile of it, we were nearly four hours tearing our way through it to the Hazlewood River. After some hours tumbling about on rocky hills covered with dense scrub we came on a blazed line going in an easterly direction. After crossing the Hazlewood River the hornblende rocks were replaced by schists and patches of basalt and quartzites. Making our way along the blazed line over some very steep hills and gullies we came down on the Whyte River again, and crossed it three times before we got clear from the valley. The track now led up a very steep spur of the Magnet Range very fair travelling, but blocked up by much fallen timber. For the past two days we had been on very short allowance of provisions and when we reached the Magnet we were reduced to small cakes amongst five of us so that we had to make the best speed we could to Bischoff. Climbing up the spur of the Magnet Range we at length came on some open ground - a gum forest with a slight undergrowth of bauera. The track was now more distinct having been cut through in 1866, and though much timber has fallen across it, it is still a great assistance to travellers.

After crossing a large creek running into the Arthur we came on the granite country at the back of the Wombat Hill. Passed over a large button grass plain and came on a man prospecting for silver. This man informed us of our distance from Bischoff, and by stepping out briskly we managed to get there the same night, March 8th.

From my experience of Burgess's track I saw that it would be too rough and hilly for use to carry heavy loads over ~~the~~ ~~little~~ in the little time we had left; I therefore decided to make use of the track I had cut in the previous summer from the Ramsay River to the Parson's Hood.

By March 13th I had sent out about seven hundred pounds weight of baggage to the Ramsay River, and we had now to carry it on our backs to the Parson's Hood. On our way out with the first load I was taken ill with diarrhoea and obliged to stop for a day. I sent Long and Lord ahead, with instructions to mark a track from the Parson's Hood to our depot near the Whyte River, Burke and Jones remaining with me to carry out the provisions. By the 23rd March we had all the provisions on the Yellband Plain, but on account of heavy rain and hail it was not until the 2nd April that we got them to the south side of the Hood.

In my Report of last year I have fully described the nature of the country from the Ramsay River to the Parson's Hood: I will now describe the country from the Hood to our depot at the Whyte River.

After leaving the camp at the foot of the Parson's Hood we followed the Pieman track on the open ground, and at the foot of the first bare rise we struck off in a westerly direction to make our way round the south end of the Meredith Range. The route led us over the ground burnt off by us last summer, consequently the travelling was very good. About a mile from the end of the forest we crossed the Stanley River and found ourselves at the foot of a steep bare hill composed of quartz and slate. Climbing these hills and following the ridge round until we could see up the west side of the Meredith Range, we took a course N.10°W., and travelling over spurs covered with short button grass and stunted honeysuckles. Close to us on the east was the steep slope of the Meredith Range, slate and sandstone formation, very barren, and worthless. In every direction the country was intersected by deep and steep gullies, full of bauera cutting grass, and other detestable scrubs. The first creek we came to was in an almost inaccessible gully. Just as we arrived there a furious storm of hail and rain set in, and we were obliged to camp. So steep and rough was the ground that we could not even find a spot flat enough to sleep on, and we were obliged to build a wooden floor for our tent to stand on. In this miserable camp we were obliged to stop for several days, the hail and rain being something to be remembered. The force of the wind on these bare and exposed hills is very great indeed, and a few hours' rain floods all the creeks and renders the ground so soft and pulpy as to make travelling very laborious.

On the 9th April Lord and Long returned, and reported having marked a trackthrough to the depot and examined the country near the Whyte River. They had found the locality of the copper previously noticed by us in the Whyte, and had also procured in a little gold and platinum. They had been on short allowance for some days and were almost in rags.

On the 10th April I sent Long and Jones back to Bischoff with instructions to examine the country between Hadfield Plain and Mount Sophia and to fire the button grass if the weather should clear up. The rest of us went on with the track.

On the 12th we managed to get a start again, and were in hopes of finishing before bad weather came on again. The same barren sandstone hills continued for another couple of miles until we came to a very steep gorge running across our course.

On the east of us the Meredith Range now showed a bare and rugged tier of granite, the junction of the sandstones, slates and granites being within a few chains of the track. Our fires had made a clean sweep of the scrub and button grass, except in the deep gorges.

After crossing two deep gorges we got into a dense scrub of bauera, tea-tree, and cutting grass and our progress

became very slow indeed, every inch having to be cut out. On the 16th we came to the forest and a complete change of country. In place of granites, quartzites, and sandy slates we now had micaceous schists and quartz, the latter sometimes in veins, but more frequently inter-mixed with the schists. All the quartz contains sulphides of iron, and ought to be examined for gold. No reefs occur nor could I find any alluvial gold. Sometimes the micaceous disappear and their places are supplied by clay-slates and white quartz the quartz in the micaceous schists being all rusty. Some two miles of rough ups and downs brought us to the Whyte River, a large and rapid stream, running over a rocky bottom. In the boulders of this river I detected many traces of copper ores, carbonate and sulphurets, but on account of the rush of flood-water could not examine the river for gold.

After crossing the White River we went up a long spur of horizontal scrub, large tea-tree and stringy barks, and again got into the micaceous schists, quartz, and talcose schist.

Veins in clay-slate filled <sup>with</sup> the calcareous matter, are numerous; some of them I think contain lead; but they are of no value at present.

As we approached the open country the quartzites and slates reappear, and would seem to be the general formation of the button grass hills.

On the 26th we came on burnt ground again and finished the track, reaching our depot at sundown. Having a day to spare we went down to the Whyte and examined the rocks. Noticed clay-slates metamorphic slates, mudstone, and masses of decomposed vein-stone, oxides of iron; obtained some very fine gold, but could not find much wash in the river.

As our ~~xxxx~~ rations were getting low we determined to make a start for Mount Bischoff. Stowed all the superfluous baggage away in the hopes of being able to make use of it at some other time, and on the 28th were on the way home.

Camped at the Whyte for a day whilst we examined the place where Long and Lord found gold. The river being high were unable to sink in a promising place, so had to content ourselves with surfacing. The spot where we tried was on a small beach of the river. We obtained gold and platinum in every dish; quite enough to pay if there were any quantity of dirt, but unfortunately there is not. The bed rock appeared to be a chloritic slate, very soft and greasy. If my rations had not been so low I might have further examined the river for gold, and also tested the terraces round about. After getting a sample of the gold and platinum we went higher up the river to where the copper shows out. Close to the bank of the river was an immense quantity of a reddish clay-slate everywhere impregnated with carbonate of copper, apparently the outcrop of a large lode. Traced the copper for some three or four chains across the face of the hill and about the same distance up. Found some large masses of "gossan" in a creek, and a very much decomposed veinstone. The red clay-slate invariably contained copper, but there was none in an adjoining yellow clay-slate.

As it was impossible to make any impression on this mass of rock with our used-up pick we crossed the river and proceeding on our journey. A short distance from the river I noticed the red slate again, and on examination it proved to contain carbonate of copper. The red slate was succeeded by black clay-slates, hornblended slates, and finally hornblende rock, this bringing us on to the country I have already described in this Report as being the route we took to Bischoff.

We arrived at Bischoff on the 7th May, Long and Jones arriving at the same hour from Hatfield Plain.

The season being now too far advanced to permit much more exploration, I sent our Burke with Long and Jones, instructing them to cut a track from Hatfield Plain as far in the direction of Mount Sophia as circumstances would permit. I have not yet received any report from them, nor so I think they will be able to get very far in the present weather. Mr. Lord and myself left the party and came on to town.

The result of my explorations on this occasion more than ever confirm my often expressed opinion that the western country is rich in minerals, and will ultimately become an important part of the colony. Utterly worthless for agricultural or pastoral purposes it has hitherto been but little explored and ~~even now when so much has hitherto been but little explored and~~ even now when so much ~~attention is directed~~ attention is directed to the search for minerals, the west offers few attractions for prospectors. The country is exceedingly rough and what scrubs there are grow so thick that a whole day is sometimes occupied in getting across a single river gully.

At Mount Heemskirk the presence of tin, reported by me in my last year's Report has been conclusively proved by the discoveries of the Messrs Meredith, and I have little fear that the ore will be found in large quantities. The specimens exhibited to me by the Messrs Meredith are black oxide of tin, similar to the ore of Mount Bischoff; and as slate and granites are together at the Mount Heemskirk, it is more probable that lodes will be found there. The discovery is an important one, and will do much towards opening up the west coast.

The Meredith Range another great granite formation deserves a more careful examination. I do not think much alluvial tin will be found there, nor indeed any mineral veins in the central portion; at the north and south end, where the granite and metamorphic rocks join the indications are very promising indeed. As noticed in my last year's Report, Mr. Harman discovered on the east side of the Parson's Hood copper in small quantities in connection with serpentine rock, gold, and osmiridium. These minerals occur precisely the same on the north end of the range.

The east side of the Meredith is occupied largely by sandstones and granite, with tourmaline; and this is exactly the formation of the tin country in the island of Banca, where the ore occurs with peroxide of iron at the junction of sandstones and granites.

Gold occurs in small quantities almost everywhere. In two instances it occurs with osmiridium (a metal of the platinum class) in the vicinity of serpentine. Instances of serpentine being the mother rock of gold are by no means rare in Australia.

Dykes of diorite are often met with; and as these dykes in Victoria are frequently auriferous prospectors should pay them particular attention.

Much of the quartz, particularly that found in connection with micaceous schists, contains much sulphide of iron. I am not aware of any of it having been tested for gold. The Rev. W. B. Clarke I think, states that sulphide of iron is the matrix of gold in Tasmania; and he also explains how gold is often contained in the sulphide though invisible to the sight. This statement is fully borne out by recent tests of the pyrites of Mount Ramsay which yielded both gold and cobalt. The best authorities agree that where the pyrites are abundant the gold is scanty; where the pyrites are scanty the gold occurs more freely; in the absence of pyrites the gold is not general found. It seems then that some

attention should be directed to the sulphides of iron so abundant in many parts of the colony, more especially to the arsenical pyrites. The common cubic pyrites is not often auriferous.

Most of the gullies in the western country are very steep and the creeks very rapid consequently there is not much wash-dirt, and prospecting for tin or gold is rendered difficult; whilst other minerals, such as copper, silver, bismuth, &c. require rather more careful examination than most prospectors are able or willing to devote to them.

I am of opinion that copper will ultimately be found in large quantities on the western country. It has already been found in many localities, but as yet the extreme roughness of the country has deterred speculators from testing the value of the discoveries. As a proof of the large area over which it is to be found, I may mention a few localities that occur to my remembrance: - Port Davey, Eldon Ranges, Parson's Hood, Meredith Ranges, Mount Ramsay, Hampshire Hills, Campbell's Range, Duck River, Duniam River, Mount Balfour, besides many localities in the County of Devon.

An immense area of the western country is occupied by button grass hills of quartzite slate, and quartz formations as far as my observations go, entirely destitute of useful minerals. A few specimens of zircon, corundum, rubies, &c. are to be obtained; none of them sufficiently large or clear to be of any value.

Although the season was the finest I have ever known we were not able to do nearly so much work as I expected. Much of our time was expended in carrying provisions and baggage, in fact two of the party were almost constantly employed in that extremely laborious work.

My operations were entirely confined to the country north side of the Pieman, there being plenty of prospectors cutting tracks on the south side.

To complete the examination of the country I would strongly recommend the continuance of the track from Knole Plains to Lake St. Clair so as to open up the granite country near Mount Sophia and Granite Tor.

A track from Knole Plains to the west side of the Meredith is much required. Burgess's track is too rough; a better one might be had more to the south.

The two tracks would not cost more than £300 and they would be of immense assistance to prospectors.

I hope to be in a position to communicate further information respecting the geology of the country after my specimens have been examined by a competent authority.

A map is in preparation to illustrate this Report.

I have the honor to be

Sir,

Your obedient Servant,

CHARLES P. SPRENT,  
District Surveyor

The Hon. the Minister for ~~Miner~~ Lands and Works

# Appendix J Summary of Australian platinum-group-element deposits and occurrences

Yanis Mieзитis and David L. Huston

Appendix Table J.1 Tabulated summary of Australian platinum-group-element deposits and occurrences. Full descriptions shown in Appendix K.

Name <sup>1</sup>	State <sup>2</sup>	Longitude °E	Latitude °S	Operating status	Commodities <sup>3</sup>	Mineral-system class	Deposit type	100 K map name	100 K map number
Abrahams Find	WA	118.490402	-20.914459	Prospect–unspecified	PGEs	?8, ?1	?8.D	Yule	2556
Airstrip Cr Pt	WA	124.903823	-29.58224	Prospect–unspecified	Cr, Pt	1	1.B	Bowden	3838
Alice Downs 3	WA	127.87442	-17.69359	Occurrence–unspecified	PGEs, Cr	1	1.B	McIntosh	4462
Alice Downs 4	WA	127.88967	-17.66656	Occurrence–unspecified	PGEs	1	1.B	McIntosh	4462
Anomaly 11–Blair	WA	121.715897	-30.96147	Prospect–drill-hole	Ni, PGEs, Au	3		Kanowna	3236
Antlion Intrusion Baggaley Hills*	WA	128.85	-26.28	Occurrence–outcrop	Cu, PGEs	?2		Bell Rock	4645
Babel	WA	127.696899	-26.107121	Deposit–unspecified	Ni, Cu, PGEs, Co, Au	2	2.A	Cooper	4445
Bakers Target	WA	121.010722	-28.4608	Prospect–drill-hole	Ni, Cu, Pt, Pd	?3		Weebo	3141
Balla Balla*	WA	117.775703	-20.766041	Mineral deposit	Ti, V, Fe, PGEs	?1		Sherlock	2456
Bamboo Creek Plant*	WA	120.209396	-20.92528	Processing plant	Au, Ag, PGEs	12	12.E	Muccan	2956
Barlee Environmental Group	WA	119.095398	-29.475519	Mine–open pit	Au, PGEs, Ni	8		Barlee	2739
Beadell South East**	WA	122.252402	-22.996441	Occurrence–outcrop	Cr, PGEs	1	?1.B	Connaughton	3452
Beasley Nickel	WA	117.292099	-22.705959	Occurrence–drill-hole	Ni, Cu, Pt, Pd	?3, ?1	?3.C	Rocklea	2352
Bellary Nickel	WA	117.6593	-23.040435	Occurrence–outcrop	Ni, Cu, Pt, Pd	?3, ?1		Paraburdoo	2451

Name <sup>1</sup>	State <sup>2</sup>	Longitude °E	Latitude °S	Operating status	Commodities <sup>3</sup>	Mineral-system class	Deposit type	100 K map name	100 K map number
Big Ben*	WA	127.83752	-17.93196	Prospect-outcrop	Pt, Pd, Au, Ni, Cu	1	1.B	McIntosh	4462
Black Oak Creek Cr Pt	WA	124.880971	-29.540224	Prospect–unspecified	Cr, Pt	1	1.B	Bowden	3838
Blackadder	WA	126.585899	-18.72513	Prospect–unspecified	Pt, Pd, PGEs, Au	1	1.B	Ramsay	4260
Black Swan–Gosling*	WA	121.648804	-30.393431	Historic mine	Ni, PGEs	3	3.B	Gindalbie	3237
Boddington–Darkan*	WA	116.3581	-32.7509	Prospect-outcrop	Au, PGEs	3	3.A	Dwellingup	2132
Bodkin	WA	120.157997	-26.56485	Deposit–unspecified	Ni, Cu, Pt, Pd	3	3.A	Wiluna	2944
Bodkin North	WA	120.15752	-26.56314	Prospect–drill-hole	Ni, Cu, Pd, Pt	3	3.A	Wiluna	2944
Bodkin North	WA	120.15752	-26.56314	Prospect–drill-hole	Ni, Co, Pd, Pt	9	9.A	Wiluna	2944
Bond	WA	127.316101	-18.418961	Prospect–drill-hole	Pt, Pd, Au	?1		Angelo	4361
Bond (WAMIN)	WA	127.31977	-18.41714	Prospect–unspecified	PGEs, Au	?1		Angelo	4361
Breakaway PGEs	WA	117.181297	-29.0385	Prospect–drill-hole	Pt, Pd, Cu	?1	?1.A	Ninghan	2339
Bronzite Ridge*	WA	121.302531	-32.177997	Prospect	Ni, Cu, Co, Pd	1, 9	1.A, 9.A	Bronzite Ridge	3133
Brumby PGEs	WA	126.608002	-18.707439	Prospect–unspecified	Pt, Pd, PGEs, Au	1	1.B	Ramsay	4260
Buckman	WA	127.958451	-16.294041	Deposit–unspecified	V, Ti, Mag, PGEs, Au	2	2.B	Elgee	4465
Bullock PGEs	WA	126.636101	-18.702801	Prospect–unspecified	Pt, Pd, PGEs, Au	1	1.B	Ramsay	4260
Byro East	WA	116.387001	-26.037849	Deposit–unspecified	Ni, Cu, Au, Pt, Pd, Cr	?2	?2.A	Byro	2145
Cabernet	WA	118.761703	-28.803129	Occurrence–drill-hole	Ni, Cu, PGEs, Co	?1		Youanmi	2640
Camel Bore*	WA	120.682838	-28.062266	Prospect	Ni, Cr, Cu, Zn, Pt, Pd	?8	?8.G	?Wildara	3041
Camp Oven	WA	121.969704	-27.499701	Occurrence–outcrop	Cu, Ni, Pt, Pd, Au	3	3.A	Tate	3243
Canaan*	WA	127.554802	-25.62096	Prospect	Ni, Cu, Co, PGEs, Mag	2	?2.B	Finlayson	4446
Carnilya Hill*	WA	121.862099	-31.05271	Dormant mine	Ni, Cu, Pd	3	3.A	Lake Lefroy	3235
Carr Boyd Rocks*	WA	121.626099	-30.065901	Active mine	Ni, Cu, PGEs	8	8.A	Gindalbie	3237
Cattle Creek–Wills Creek	WA	128.088104	-17.467331	Prospect–drill-hole	Ni, Cu, PGEs, Co	2	2.A	Turkey Creek	4563
Chromite Creek	WA	124.866611	-29.635844	Prospect–unspecified	Cr, Pt	1	1.B	Bowden	3838

Name <sup>1</sup>	State <sup>2</sup>	Longitude °E	Latitude °S	Operating status	Commodities <sup>3</sup>	Mineral-system class	Deposit type	100 K map name	100 K map number
Coglia Well	WA	123.045998	-29.18631	Deposit–unspecified	Ni, Co, Pt, Pd	3, 9	3.A, 9.A	Lightfoot	3539
Collurabbie–Achilles	WA	122.171866	-26.799402	Prospect–drill-hole	Ni, Cu, PGEs	3	3.C	Collurabbie	3344
Collurabbie–Agora	WA	122.205701	-26.862562	Prospect–drill-hole	Ni, Cu, Co, Pt, Pd	3	3.C	Collurabbie	3344
Collurabbie–Argos	WA	122.21046	-26.880884	Prospect–drill-hole	Ni, Cu, Co, Pt, Pd	3	3.C	Collurabbie	3344
Collurabbie–Leros	WA	122.225688	-26.915386	Prospect–drill-hole	Ni, Cu, Co, Pt, Pd	3	3.C	Collurabbie	3344
Collurabbie–Olympia	WA	122.216003	-26.88645	Prospect–drill-hole	Ni, Cu, Co, Pt, Pd, PGEs	3	3.C	Collurabbie	3344
Collurabbie–Rhodes	WA	122.217903	-26.90855	Prospect–drill-hole	Ni, Cu, Co, Pt, Pd	3	3.C	Collurabbie	3344
Collurabbie–Spartacus	WA	122.18575	-26.835971	Prospect–drill-hole	Ni, Cu, PGEs	3	3.C	Collurabbie	3344
Collurabbie–Troy	WA	122.175833	-26.810311	Prospect–drill-hole	Ni, Cu, PGEs	3	3.C	Collurabbie	3344
Collurabbie South	WA	122.1903	-27.231871	Prospect–drill-hole	Ni, Co, Cu, PGEs	3	3.C	Urarey	3343
Collurabbie North*	WA	121.969398	-26.57699	Prospect–drill-hole	Ni, Au, PGEs	3	3.C	Yelma	3244
Collurabbie Paros*	WA	122.217122	-26.859707	Prospect–drill-hole	Ni, Cu, Co, Pd, Pt	3	3.C	Collurabbie	3344
Constantine	WA	118.936013	-28.530065	Prospect–drill-hole	Pd, Pt, Ni, Cu, Co	12, ?1		Youanmi	2640
Cooya Pooya Gossan	WA	117.55846	-20.99848	Occurrence–unspecified	Pd, Pt, Au	2	?2.A	Sherlock	2456
Copernicus Deeps	WA	127.990501	-17.653231	Prospect–drill-hole	Ni, Cu, Co, Pt, Pd	2	2.A	McIntosh	4462
Copernicus North	WA	127.990954	-17.654519	Prospect–drill-hole	Ni, Cu, Co, Pt, Pd	2	2.A	McIntosh	4462
Corkwood	WA	128.187698	-17.295031	Deposit–unspecified	Ni, Cu, Co, Pt, Pd	2	2.A	Turkey Creek	4563
Corner Well	WA	118.483716	-28.557727	Prospect–outcrop	PGEs, Ni, Cu	1	1.A	Coolamaninu	2540
Cosmos	WA	120.575699	-27.60014	Mine–open pit	Ni, Cu, Co, Pt, Pd	3	3.A	Sir Samuel	3042
Cosmos Deeps	WA	120.575875	-27.596973	Mine–decline	Ni, Cu, Co, Pt, Pd	3	3.A	Sir Samuel	3042
Cosmos Group	WA	120.575875	-27.596973	Mine–decline	Ni, Cu, Co, Pt, Pd	3	3.A	Sir Samuel	3042
Cosmos Resource Group	WA	120.575699	-27.60014	Mine–open pit	Ni, Cu, Co, Pt, Pd	3	3.A	Sir Samuel	3042

Name <sup>1</sup>	State <sup>2</sup>	Longitude °E	Latitude °S	Operating status	Commodities <sup>3</sup>	Mineral-system class	Deposit type	100 K map name	100 K map number
Crabman–Crabman South–Buddy	WA	119.0896	-29.48103	Prospect–drill-hole	Au, PGEs, Ni	8		Barlee	2739
Cundeelee	WA	123.274454	-30.534756	Prospect–drill-hole	REE, PGEs, Ni, Cu, Zn, Ap	4	4.A	Cundeelee	3536
Cunig	WA	117.00914	-21.00138	Occurrence–outcrop	Cu, Ni, PGEs, Au	8	8.D	Cooya Pooya	2355
Curlew PGE	WA	117.18364	-29.03936	Prospect–drill-hole	Pd, Pt, Ni, Cu	?1	?1.A	Ninghan	2339
Daltons–Kingsway*	WA	119.164761	-21.494564	Prospect–drill-hole	Ni, Cu, PGEs	?3	?3.C	North Shaw	2755
Davyhurst Nickel	WA	120.56264	-29.782452	Prospect–drill-hole	Ni, Cu, Pt, Pd	3		Riverina	3038
DeGrussa Environmental Group	WA	119.328132	-25.540623	Mine–open pit	Cu, Au, Ag, Zn, Pd, Cu	12	12.A	Doolgunna	2746
DeGrussa Operations Group	WA	119.328132	-25.540623	Mine–open pit	Cu, Au, Ag, Zn, Pd, Cu	12	12.A	Doolgunna	2746
DeGrussa Open Pit	WA	119.328132	-25.540623	Mine–open pit	Cu, Au, Ag, Zn, Pd, Cu	12	12.A	Doolgunna	2746
DeGrussa Resource Group	WA	119.328132	-25.540623	Mine–open pit	Cu, Au, Ag, Zn, Pd, Cu	12	12.A	Doolgunna	2746
DeGrussa Underground	WA	119.328128	-25.54063	Mine–decline	Cu, Au, Ag, Zn, Pd	12	12.A	Doolgunna	2746
Dingo	WA	116.80078	-20.95088	Occurrence–unspecified	PGEs	?1		Dampier	2256
Doolena Gap	WA	119.75	-20.91417	Occurrence–outcrop	Cu, Ni, PGEs	?8		Coongan	2856
Dragonfly–Murray Hills*	WA	128.357	-25.548	Prospect–drill-hole	Ni, Cu, Co, Zn, PGEs	9	?9.A	Holt	4546
Dugite–Gum Creek	WA	119.563103	-27.32159	Occurrence–outcrop	Cu, Ni, PGEs	12	?12.A	Montagu	2843
Dundas Gossan	WA	121.850788	-31.919874	Prospect–outcrop	Cu, Pd, Pt, PGEs, Ni	3		Cowan	3234
Durkin*	WA	121.662804	-31.167589	Historic mine	Ni, Cu, PGEs	3	3.B	Lake Lefroy	3235
Dusty Bore 2	WA	127.38326	-18.41333	Occurrence–unspecified	PGEs	1	?1.B	Angelo	4361
East Alpha	WA	121.697998	-31.23901	Mine–decline	Ni, Cu, Co, Pt, Pd	3	3.A	Lake Lefroy	3235
Eastman Bore (Cu 4)	WA	126.63036	-18.70372	Occurrence–outcrop	Cu, PGEs	1	1.B	Ramsay	4260
Eastman Bore PGEs 1	WA	126.58822	-18.72035	Occurrence–unspecified	PGEs, Cr, Au	1	1.B	Ramsay	4260

Name <sup>1</sup>	State <sup>2</sup>	Longitude °E	Latitude °S	Operating status	Commodities <sup>3</sup>	Mineral-system class	Deposit type	100 K map name	100 K map number
Eastman Bore PGEs 10	WA	126.61503	-18.70176	Occurrence–unspecified	PGEs, Cr	1	1.B	Ramsay	4260
Eastman Bore PGEs 11	WA	126.6114	-18.70279	Occurrence–unspecified	PGEs, Cr	1	1.B	Ramsay	4260
Eastman Bore PGEs 12	WA	126.61397	-18.70244	Occurrence–unspecified	PGEs, Au, Cr	1	1.B	Ramsay	4260
Eastman Bore PGEs 13	WA	126.61324	-18.70093	Prospect–unspecified	PGEs, Cr	1	1.B	Ramsay	4260
Eastman Bore PGEs 14	WA	126.61214	-18.70442	Occurrence–unspecified	PGEs, Cr	1	1.B	Ramsay	4260
Eastman Bore PGEs 15	WA	126.62744	-18.6963	Occurrence–unspecified	PGEs, Cr	1	1.B	Ramsay	4260
Eastman Bore PGEs 16	WA	126.63042	-18.7048	Occurrence–unspecified	PGEs, Au, Cr	1	1.B	Ramsay	4260
Eastman Bore PGEs 17	WA	126.61108	-18.70433	Prospect–unspecified	PGEs, Cr	1	1.B	Ramsay	4260
Eastman Bore PGEs 18	WA	126.61261	-18.70342	Prospect–unspecified	PGEs, Cr	1	1.B	Ramsay	4260
Eastman Bore PGEs 2	WA	126.6098	-18.70381	Prospect–unspecified	PGEs, Au, Cr	1	1.B	Ramsay	4260
Eastman Bore PGEs 3	WA	126.60876	-18.7041	Prospect–unspecified	PGEs, Au, Cr	1	1.B	Ramsay	4260
Eastman Bore PGEs 4	WA	126.60741	-18.70503	Occurrence–unspecified	PGEs, Au, Cr	1	1.B	Ramsay	4260
Eastman Bore PGEs 5	WA	126.62229	-18.70473	Occurrence–unspecified	PGEs, Cr	1	1.B	Ramsay	4260
Eastman Bore PGEs 6	WA	126.63866	-18.70099	Prospect–unspecified	Cr, PGEs	1	1.B	Ramsay	4260
Eastman Bore PGEs 7	WA	126.63586	-18.70302	Occurrence–unspecified	Cr, PGEs	1	1.B	Ramsay	4260
Eastman Bore PGEs 8	WA	126.62794	-18.70379	Occurrence–unspecified	PGEs, Cr	1	1.B	Ramsay	4260
Eastman Bore PGEs 9	WA	126.61195	-18.7071	Occurrence–unspecified	PGEs, Cr	1	1.B	Ramsay	4260
Eastman VMS	WA	126.560997	-18.71044	Deposit–unspecified	Zn, Pb, Cu, Ag, Au, PGEs, Ni	?12	?12.A	Ramsay	4260
Edison	WA	127.330795	-18.461251	Prospect–unspecified	Pt, Pd, Au	1, 8	1.B	Angelo	4361
Eileen Bore	WA	127.95864	-17.72297	Prospect–unspecified	Ni, Cu, PGEs	2	2.A	McIntosh	4462
El Cortez–Murray Hills*	WA	128.403	-25.577	Prospect–drill-hole	Ni, Co, PGEs, Au	9	9.A	Holt	4546
Elizabeth Hill*	WA	116.874901	-21.090031	Historic mine	Cu, Pb, Zn, Ag, PGEs, Ni, Au	8	8.C	Pinderi Hills	2255

Name <sup>1</sup>	State <sup>2</sup>	Longitude °E	Latitude °S	Operating status	Commodities <sup>3</sup>	Mineral-system class	Deposit type	100 K map name	100 K map number
Emily Ann*	WA	120.49208	-32.202863	Historic mine	Ni, PGEs	8	8.B	Roundtop	2933
Emu Lake–Binti Binti Gossan Zone*	WA	121.956802	-30.28853	Occurrence	Ni, Co, Cu, PGEs	3		Gindalbie	3237
Erong Hill	WA	116.695099	-25.634029	Prospect–unspecified	Pt, Pd	12	12.E	Erong	2246
Evans Decline–DeGrussa	WA	119.329808	-25.545412	Mine–decline	Cu, Au, Ag, Zn, Pd	12	12.A	Doolgunna	2746
Far West–Camel Hills	WA	116.363529	-25.898385	Occurrence–outcrop	Ni, Cr, Cu, Zn, Pt, Pd	1		Yalbra	2146
Flying Fox T4, T5*	WA	119.689003	-32.417782	Mine	Ni, Cu, Co, PGEs	3, 8	3.A, 8.B	Holland	2833
Freemans	WA	121.43811	-27.47757	Prospect–unspecified	PGEs	?3		Wanggannoo	3143
Giles	WA	122.227443	-27.001175	Prospect–drill-hole	Ni, Cu, Pt, Pd	9, ?3	9.A	Urarey	3343
Giles North	WA	122.227984	-26.995761	Prospect–drill-hole	Ni, Cu, Pt, Pd	9, ?3	9.A	Collurabbie	3344
Goliath North*	WA	120.589203	-27.44562	Deposit	Ni, PGEs	3	3.B	Mount Keith	3043
Green Dam	WA	122.713699	-30.53718	Prospect–drill-hole	Ni, Cu, PGEs, Co	?3		Roe	3436
GSP	WA	121.455597	-30.18314	Deposit–unspecified	Ni, PGEs, Co	3, 8		Bardoc	3137
Halleys–Blackstone	WA	128.043304	-26.163589	Prospect–drill-hole	Cu, Ni, PGEs, Au, Cr	2	?2.A	Blackstone	4545
Halleys Channel	WA	119.091482	-29.475134	Prospect–drill-hole	Au, PGEs, Ni	8	?8.B	Barlee	2739
Halleys East–Barlee	WA	119.095398	-29.475519	Mine–open pit	Au, PGEs, Ni	8	?8.B	Barlee	2739
Halleys Northeast	WA	119.097165	-29.47324	Prospect–drill-hole	Au, PGEs, Ni	8	?8.B	Barlee	2739
Halls Knoll Gossan	WA	121.847761	-31.915991	Prospect–drill-hole	Pt, Pd, Au, Ni	3	3.A	Cowan	3234
Haran*	WA	127.528702	-25.7173	Prospect	Ni, Cu, Co, PGEs, Mag	2	2.B	Finlayson	4446
Heron Well*	WA	121.3762	-29.0973	Prospect–drill-hole	Pt, Pd, Cu, Ni	1, 12	12.E	Melita	3139
Honeymoon Well Group*	WA	120.380699	-26.92182	Deposit	Ni, PGEs	3, 8	3.B, 8.B	Wiluna	2944
Hunters Reef East	WA	116.86636	-21.12275	Occurrence–unspecified	PGEs, Au, Cu	1	1.A	Pinderi Hills	2255
Hunters Reef West	WA	116.81177	-21.11818	Occurrence–unspecified	PGEs, Au, Cu	1	1.A	Pinderi Hills	2255
Jamieson Prospect*	WA	127.57361	-25.79778	Prospect–outcrop	Ni, Cu, Co, PGEs, Mag	2	2.B	Finlayson	4446

Name <sup>1</sup>	State <sup>2</sup>	Longitude °E	Latitude °S	Operating status	Commodities <sup>3</sup>	Mineral-system class	Deposit type	100 K map name	100 K map number
Jacks Hill	WA	124.465612	-16.938638	Prospect–outcrop	Cu, Ni, Au, Ag, PGEs	8	?8.D	Tarraji	3764
Jason	WA	122.2267	-22.56976	Prospect–unspecified	PGEs	?8		Rudall	3352
Jillian–Wills Creek	WA	128.028702	-17.600031	Prospect–drill-hole	Ni, Cu, PGEs	2	2.A	Dixon	4562
Jilbadgie	WA	119.260418	-31.570516	Occurrence	Ni, Cu, PGEs, Au, Pb, Zn	12	12.E	Holleton	2734
Jimberlana South*	WA	121.95	-32.157	Occurrence	Ni, Cu, Pd, Pt	?1, ?8		Norseman	3233
Joshua	WA	118.524002	-20.91054	Prospect–unspecified	PGEs	1		Wallaringa	2656
Joshua East	WA	118.5336	-20.905939	Prospect–unspecified	PGEs	1		Wallaringa	2656
J Reef	WA	116.8805	-21.10076	Prospect–unspecified	Pd, Cu, Au, Ni, Ag	1, ?8	1.A, ?8.C	Pinderi Hills	2255
Judys Reef	WA	116.873596	-21.091749	Prospect–unspecified	Pt, Pd, Cu, Ni, Ag	1, ?8	1.A, ?8.C	Pinderi Hills	2255
Kambalda–Braemore	WA	121.675003	-31.18424	Deposit–unspecified	Ni, Ag, Co, Pd, Cu, Pt	3	3.A	Lake Lefroy	3235
Keller Creek	WA	127.97129	-17.30187	Prospect–drill-hole	Ni, Cu, Pt	2, ?8	2.A	Mount Remarkable	4463
Killaloe Nickel*	WA	121.940651	-31.977496	Prospect–outcrop	Cu, Pd, Pt, PGEs, Ni	3		Cowan	3234
Kintyre Group*	WA	122.079596	-22.33543	Deposit	U, Bi, Cu, Pb, Au, PGEs	8	8.F	Broadhurst	3353
Koondooloo Yard	WA	127.93162	-17.42548	Occurrence–unspecified	PGEs	2		Mount Remarkable	4463
Kurnalpi* (Acra South-Kurnalpi Nickel)	WA	122.091301	-30.538799	Prospect–outcrop	Ni, Cu, Pd, Ir	12	12.E	Kurnalpi	3336
Lake Giles Nickel	WA	119.928902	-29.822241	Occurrence–outcrop	Ni, Cu, Pt, Pd, PGEs, Au	?3		Lake Giles	2838
Lamboo (Cr 2)	WA	127.31782	-18.46883	Prospect–unspecified	Cr, Zn, PGEs	1	1.B	Angelo	4361
Lamboo (Cr 5)	WA	127.35284	-18.42666	Occurrence–unspecified	Cr, PGEs	1	1.B	Angelo	4361
Lamboo (Cr 7)	WA	127.32712	-18.45135	Occurrence–unspecified	Cr, PGEs	1	1.B	Angelo	4361
Lamboo (Cr 21)	WA	127.34067	-18.46051	Occurrence–unspecified	Cr, PGEs	1	1.B	Angelo	4361

Name <sup>1</sup>	State <sup>2</sup>	Longitude °E	Latitude °S	Operating status	Commodities <sup>3</sup>	Mineral-system class	Deposit type	100 K map name	100 K map number
Lamboo (Cr 22)	WA	127.35466	-18.4955	Prospect–unspecified	Cr, PGEs	1	1.B	Angelo	4361
Lamboo (Cr 23)	WA	127.34364	-18.50963	Prospect–unspecified	Cr, PGEs	1	1.B	Dockrell	4360
Lamboo (Cr 27)	WA	127.35926	-18.48265	Occurrence–unspecified	Cr, PGEs	1	1.B	Angelo	4361
Lamboo (PGEs 1)	WA	127.33032	-18.47556	Prospect–unspecified	PGEs, Cr, Ni	1	?1.B	Angelo	4361
Lamboo (PGEs 2)	WA	127.3298	-18.47484	Prospect–unspecified	PGEs	1	?1.B	Angelo	4361
Lamboo (PGEs 3)	WA	127.32936	-18.47411	Prospect–unspecified	PGEs, Au	1	?1.B	Angelo	4361
Lamboo (PGEs 4)	WA	127.32067	-18.46177	Prospect–unspecified	PGEs, Cr	1	?1.B	Angelo	4361
Lamboo (PGEs 5)	WA	127.33407	-18.46907	Prospect–unspecified	PGEs, Cr	1	?1.B	Angelo	4361
Lamboo (PGEs 6)	WA	127.34129	-18.43673	Prospect–unspecified	PGEs, Cr	1	?1.B	Angelo	4361
Lamboo (PGEs 7)	WA	127.34422	-18.43413	Prospect–unspecified	PGEs, Cr	1	?1.B	Angelo	4361
Lamboo (PGEs 8)	WA	127.31281	-18.48201	Prospect–unspecified	PGEs, Au, Ni	1	?1.B	Angelo	4361
Lamboo (PGEs 9)	WA	127.31953	-18.48498	Prospect–unspecified	PGEs, Cr	1	?1.B	Angelo	4361
Lamboo (PGEs 10)	WA	127.32384	-18.45908	Prospect–unspecified	PGEs, Au, Ni, Cr	1	?1.B	Angelo	4361
Lamboo (PGEs 11)	WA	127.32348	-18.45821	Prospect–unspecified	PGEs, Cr	1	?1.B	Angelo	4361
Lamboo (PGEs 12)	WA	127.32946	-18.44908	Prospect–unspecified	PGEs, Cr	1	?1.B	Angelo	4361
Lamboo (PGEs 13)	WA	127.34839	-18.42793	Prospect–unspecified	PGEs, Au, Ni, Cr	1	?1.B	Angelo	4361
Lamboo (PGEs 14)	WA	127.30936	-18.48436	Prospect–unspecified	PGEs, Cr	1	?1.B	Angelo	4361
Leo Dam	WA	121.725854	-30.893884	Prospect–drill-hole	Ni, Cu, PGEs	3		Kanowna	3236
Limestone Spring–Maiwa Reward	WA	124.460297	-16.94095	Mine–decline	Cu, Ni, Au, Ag, PGEs	12	12.E	Tarraji	3764
Longhorn	WA	126.499397	-18.731911	Prospect–unspecified	Pt, Pd, PGEs, Au	1	?1.B	Bohemia	4160
Loongana	WA	126.42265	-30.776866	Occurrence–unspecified	Ni, Pt, Pd	2	2.A	Turner	4136
Louisa	WA	126.6138	-18.702641	Prospect–unspecified	Pt, Pd, PGEs	1	1.B	Ramsay	4260
Malbec	WA	118.766502	-28.80541	Prospect–drill-hole	Ni, Cu, PGEs, Co	?1		Youanmi	2640

Name <sup>1</sup>	State <sup>2</sup>	Longitude °E	Latitude °S	Operating status	Commodities <sup>3</sup>	Mineral-system class	Deposit type	100 K map name	100 K map number
Malbec–Wills Creek	WA	128.001999	-17.641041	Prospect–drill-hole	Ni, Cu, PGEs	2	2.A	Dixon	4562
Manchego*	WA	127.48939	-25.677728	Prospect	Fe, Ti, V, PGEs, Au	2	2.B	Bentley	4346
Marriott*	WA	120.9916	-28.451361	Prospect	Ni, PGEs	3	3.B	Wildara	3041
McWhae Ridge*	WA	126.083	-18.733	No economic significance	Ir, Pt, V, Co, Ni, Cu, As, Sb, Pb, Th	12	12.B	Bohemia	4160
Medusa–Peninsula	WA	125.016396	-29.665268	Prospect–unspecified	Cr, Ni, Cu, Au, Pt, Pd, HM	1	1.B	Plumridge	3938
Melon Patch 1	WA	127.93577	-17.6031	Occurrence–unspecified	Cu, Ni, PGEs	1	1.B	McIntosh	4462
Melon Patch 3	WA	127.93121	-17.64049	Prospect–unspecified	PGEs, Cr	1	1.B	McIntosh	4462
Melon Patch 4	WA	127.93698	-17.637	Prospect–unspecified	PGEs, Cr	1	1.B	McIntosh	4462
Melon Patch 5	WA	127.91808	-17.64593	Occurrence–unspecified	PGEs, Cr	1	1.B	McIntosh	4462
Melon Patch 6	WA	127.94077	-17.63521	Prospect–unspecified	Au, PGEs, Cr	1	1.B	McIntosh	4462
Melon Patch 7	WA	127.94266	-17.63432	Prospect–unspecified	PGEs	1	1.B	McIntosh	4462
Melon Patch 9	WA	127.9294	-17.64019	Occurrence–unspecified	PGEs, Cr	1	1.B	McIntosh	4462
Melon Patch 10	WA	127.91242	-17.64952	Occurrence–unspecified	PGEs, Cr	1	1.B	McIntosh	4462
Melon Patch 11	WA	127.93189	-17.64064	Occurrence–unspecified	PGEs, Cr	1	1.B	McIntosh	4462
Melon South	WA	127.87435	-17.70443	Occurrence–unspecified	PGEs, Cr	1	1.B	McIntosh	4462
Merlot	WA	118.745796	-28.809441	Prospect–drill-hole	Ni, Cu, PGEs, Co	?1		Youanmi	2640
Milgoo	WA	118.126388	-28.8946	Prospect–drill-hole	Pt, Pd	1	1.A	Coolamaninu	2540
Millipede–Capricorn	WA	120.09495	-23.452418	Prospect–drill-hole	Ni, Cu, Pt	12	12.E	Murramunda	2951
Mineral Patch Hill	WA	122.984596	-29.0369	Deposit–unspecified	Ni, Cu, Co, Pt, Pd	9	9.A	Mount Celia	3439
Mini M (Cr PGEs) 1	WA	127.85841	-17.69169	Occurrence–unspecified	Cr, PGEs	1	1.B	McIntosh	4462
Mini M (Cr PGEs) 2	WA	127.86157	-17.69788	Occurrence–unspecified	Pt, Pd, Cr	1	1.B	McIntosh	4462
Monarch Nickel	WA	121.724503	-32.101521	Prospect–drill-hole	Ni, Cu, Pt, Pd, PGEs	?2, ?1	?2.A, ?1.A	Norseman	3233

Name <sup>1</sup>	State <sup>2</sup>	Longitude °E	Latitude °S	Operating status	Commodities <sup>3</sup>	Mineral-system class	Deposit type	100 K map name	100 K map number
Moonborough	WA	116.158997	-26.06307	Prospect–drill-hole	Cu, Au, Pd, Pt, Ni	?2, ?8		Byro	2145
Moonborough Northeast	WA	116.202247	-26.027051	Prospect–outcrop	Cu, Pd, Au	?2, ?8		Byro	2145
Mt Alexander–Cathedrals	WA	120.275929	-28.838262	Prospect–drill-hole	Ni, Cu, PGEs	?3		Mount Alexander	2940
Mt Carnage	WA	120.963729	-30.352919	Prospect–drill-hole	Pt, Pd	1, 2	?1.A, ?2.A	Davyhurst	3037
Mt Carnage	WA	120.963729	-30.352919	Prospect–drill-hole	Pt, Pd, Co	9	9.A	Davyhurst	3037
Mt Cumming	WA	123.352303	-27.759359	Prospect–outcrop	Au, Ag, Pd, Pt, PGEs, Cr, Ni, Cu	1	1.A	Jutson	3542
Mt Fisher East–Musket*	WA	121.554149	-26.810276	Prospect	Ni, PGEs	3	3.A	Yelma	3244
Mt Fisher East–Cannonball*	WA	121.553732	-26.803501	Prospect	Ni, PGEs	3	3.A	Yelma	3244
Mt Fisher East–Camelwood*	WA	121.550206	-26.793617	Prospect	Ni, PGEs	3	3.A	Yelma	3244
Mt Holland Nickel	WA	119.726696	-32.317986	Occurrence–drill-hole	Ni, Au, PGEs	3	3.A	Holland	2833
Mt Keith*	WA	120.54174	-27.229599	Mine	Ni, PGEs	3	3.B	Mount Keith	3043
Mt Thirsty*	WA	121.647797	-32.101891	Prospect	Ni, Co, PGEs	1		Norseman	3233
Mt Venn	WA	123.5056	-28.09704	Prospect–drill-hole	Cu, Ni, PGEs	8	8.D	Dorothy Hills	3641
Mt Warren	WA	123.308502	-27.777611	Prospect–outcrop	Au, Ag, Pd, Pt, PGEs, Cr, Ni, Cu	1	1.A	Jutson	3542
Mt Webber*	WA	119.29855	-21.543976	Mine	Fe, Au, Ag, Pt, Pd, Ir, Ru	12	12.C	Tambourah	2754
Mt Windarra	WA	122.238466	-28.486819	Deposit, historic mine	Ni, Pd, Pt	3	3.A	Mount Varden	3341
Mulga Tank*	WA	123.20849	-29.930099	Prospect–drill-hole	Ni, Cr, Cu, Co, PGEs, Pd	3, 8	3.A, 8.B	Minigwal	3538
Muleryon Hill	WA	118.383496	-28.573454	Prospect–outcrop	PGEs, Ni, Cu	1	1.A	Coolamaninu	2540
Munni Munni Central Zone	WA	116.828769	-21.12037	Deposit–unspecified	Pt, Pd, Rh, Au, Ni, Cu	1	1.A	Pinderi Hills	2255
Munni Munni Pinderi*	WA	116.818966	-21.123186	Prospect–unspecified	Pt, Pd, Rh, Au, Ni, Cu	1	1.A	Pinderi Hills	2255
Munni Munni South (PGEs)	WA	116.82713	-21.20779	Prospect–unspecified	PGEs	1	1.A	Pinderi Hills	2255

Name <sup>1</sup>	State <sup>2</sup>	Longitude °E	Latitude °S	Operating status	Commodities <sup>3</sup>	Mineral-system class	Deposit type	100 K map name	100 K map number
Nanadie Well–Western Lode*	WA	118.948502	-27.159941	Prospect–unspecified	Cu, Au, Ni, Co, PGEs, REE	12		Nowthanna	2643
Narndee	WA	118.12511	-28.89542	Prospect–unspecified	Ni, Cu, PGEs	1	1.A	Coolamaninu	2540
Natalies Hill	WA	116.874298	-21.09063	Prospect–unspecified	Pt, Pd, Cu, Ni	1	1.A	Pinderi Hills	2255
Nebo	WA	127.727402	-26.095381	Deposit–unspecified	Ni, Cu, PGEs, Co, Au	2	2.A	Cooper	4445
Nebo–Babel Group	WA	127.696899	-26.107121	Deposit–unspecified	Ni, Cu, PGEs, Co, Au	2	2.A	Cooper	4445
Nepean*	WA	121.084198	-31.164789	Historic mine	Ni, Cu, Pd	3, 8	3.A, 8.B	Yilmia	3135
Netty*	WA	118.968903	, -33.876919	Historic mine	Cu, Ni, Au, Ag, PGEs	?1		Jerramungup	2630
Nickol River East (PGEs)	WA	116.99172	-20.74434	Occurrence–unspecified	Os, Ir, Pt, Pd	10	10.C	Dampier	2256
Nicholsons Find PGE	WA	127.35802	-18.41676	Occurrence–unspecified	PGEs, Cr	1	?1.B	Angelo	4361
Nova–Bollinger*	WA	123.192413	-31.819886	Deposit–undeveloped	Ni, Cu, Co, PGEs, Au, Ag	2	2.A	Symons Hill	3534
Nova–Bollinger*	WA	123.192413	-31.819886	Deposit–undeveloped	Ni, Cu, Co	9	9.A	Symons Hill	3534
Odysseus	WA	120.575875	-27.596973	Deposit–unspecified	Ni, Cu, Co, Pt, Pd	3	?3.A	Sir Samuel	3042
Odysseus North	WA	120.575875	-27.596973	Deposit–unspecified	Ni, Cu, Co, Pt, Pd	3	?3.A	Sir Samuel	3042
Ora Banda Sill	WA	121.0583	-30.4	Prospect–drill-hole	Pt, Pd	1, 2	?1.A, ?2.A	Bardoc	3137
Ora Banda Sill	WA	121.0583	-30.4	Prospect–drill-hole	Pt, Pd, Co	9	9.A	Bardoc	3137
Otter–Juan*	WA	121.651802	-31.166599	Deposit	Ni, PGEs	8	8.B	Lake Lefroy	3235
Palamino–Wills Creek	WA	128.003204	-17.638849	Prospect–outcrop	Ni, Cu, PGEs	2	2.A	Dixon	4562
Panton	WA	127.831596	-17.75153	Deposit	Pt, Pd, Au, Ni, Cu	1	1.B	McIntosh	4462
Panton Environmental Group	WA	127.831596	-17.75153	Mine–decline	Pt, Pd, Au, Ni, Cu	1	1.B	McIntosh	4462
Panton North 1	WA	127.84969	-17.72778	Prospect–unspecified	PGEs, Cr	1	1.B	McIntosh	4462
Panton North 2	WA	127.84869	-17.73682	Prospect–unspecified	PGEs, Cr	1	1.B	McIntosh	4462
Panton North 3	WA	127.85352	-17.71877	Occurrence–unspecified	PGEs, Cr	1	1.B	McIntosh	4462

Name <sup>1</sup>	State <sup>2</sup>	Longitude °E	Latitude °S	Operating status	Commodities <sup>3</sup>	Mineral-system class	Deposit type	100 K map name	100 K map number
Peninsula HA2*	WA	124.961513	-29.755636	Occurrence–identified	Pd, Pt	1	1.B	Bowden	3838
Perseverance*	WA	120.705597	-27.818119	Mine	Ni, Cu, PGEs	3, 8	3.B, ?8.B	Sir Samuel	3042
Phenoclast Hill	WA	122.680603	-24.630911	Occurrence–outcrop	Cu, Au, Ni, PGEs, Ba	12	12.E	Nicholls	3448
Phil North and South	WA	119.092707	-29.459506	Deposit–unspecified	Au, PGEs, Ni	8	?8.B	Barlee	2739
Pindar SE 1	WA	117.6805	-27.24711	Occurrence–drill-hole	Pt, Pd	?8		Cue	2443
Pindar SE 2	WA	117.68125	-27.25343	Occurrence–drill-hole	Pt, Pd	?8		Cue	2443
Pioneer JH	WA	121.64313	-31.974787	Deposit–unspecified	Ni, Cu, PGEs	3	3.A	Cowan	3234
PM Prospect	WA	123.221901	-22.92333	Prospect–costean/trench	Pt, Pd, Au, Cu	8		Blanche	3552
Pokali–Charlies Find Zone	WA	128.35072	-22.94455	Prospect–drill-hole	Cu, Ag, Au, Pd	8		Webb	4552
Pokali North	WA	128.326513	-22.931827	Prospect–outcrop	Cu, Au, Ag, Pd	?8		Webb	4552
Pokali South	WA	128.346971	-22.948116	Prospect–drill-hole	Cu, Au, Ag, Pd	?8		Webb	4552
Polar Bear*	WA	121.84	-31.92	Prospect	Ni, PGEs	3	3.A	Cowan	3234
Poona North	WA	117.442076	-27.087218	Prospect–drill-hole	PGEs	?1		Noondie	2343
Priors	WA	120.970634	-31.039413	Prospect–drill-hole	Ni, Cu, Pt, Pd, Au	3		Woolgangie	3035
Python–Gum Creek	WA	119.525803	-27.27706	Prospect–drill-hole	Cu, Ni, PGEs	12	?12.A	Montagu	2843
Radio Hill*	WA	116.8694	-20.984421	Historic mine	Ni, Cu, Co, PGEs	2	2.A	Dampier	2256
Range Well (Cr PGEs)	WA	117.761597	-26.832279	Deposit–unspecified	Cr, Pt, Pd, Au	9	9.A	Madoonga	2444
Range Well Group	WA	117.726997	-26.854521	Deposit–unspecified	Pt, Pd, Au	1	1.A	Madoonga	2444
Ravensthorpe*	WA	120.0691	-33.8466	Occurrence	Au, PGEs	12, 10	12.E, 10.C	Ravensthorpe	2930
Red Bull (VI)*	WA	123.079504	-32.117727	Prospect–drill-hole	Ni, Cu, Co, Pd, Pt, Cr	2, 9	?2.A, 9.A	Harms	3533
Red Hill*	WA	127.924427	-16.299675	Prospect–drill-hole	PGEs, Au	2	2.B	Elgee	4465
Red Rock*	WA	127.6167	-26.0333	Prospect	Ni, Co, PGEs	2	2.A	Cooper	4445
Redross*	WA	121.648903	-31.683241	Historic mine	Ni, Co, Cu, PGEs	3	3.A	Lake Lefroy	3235
Reynolds Creek	WA	115.61982	-23.74662	Occurrence–unspecified	Pt, Pd, Au, Cu, Ni	12	12.E	Mangaroon	2050

Name <sup>1</sup>	State <sup>2</sup>	Longitude °E	Latitude °S	Operating status	Commodities <sup>3</sup>	Mineral-system class	Deposit type	100 K map name	100 K map number
Ringlock	WA	121.410103	-30.143431	Prospect–drill-hole	Ni, PGEs	3, 8		Bardoc	3137
Robertsons East	WA	119.167661	-31.077497	Prospect–drill-hole	Pt, Pd, PGEs, Cr, Ni	1	1.A	Southern Cross	2735
Rocky's Reward*	WA	120.697197	-27.791439	Historic mine	Ni, Cu, PGEs	8	8.B	Sir Samuel	3042
Rocky Well–Irwin Hills	WA	123.028099	-29.154739	Deposit–unspecified	Ni, Co, Pt, Pd	3, 9	3.A, 9.A	Lightfoot	3539
Rosie	WA	122.014331	-27.624587	Deposit–unspecified	Ni, Cu, Pt, Pd, Au, Co, As, S	3	3.A	Duketon	3342
Rosie Boxcut	WA	122.01364	-27.619055	Mine–decline	Ni, Cu, Pt, Pd	3	3.A	Duketon	3342
Ruth Well*	WA	116.865501	-20.86838	Deposit	Ni, Cu, Co, Pd	3		Dampier	2256
RX1892	WA	127.99394	-17.6533	Occurrence–unspecified	PGEs, Cu, Ni	2	2.A	McIntosh	4462
Sally Malay Bore 1	WA	128.1628	-17.32471	Prospect–unspecified	Cu, Ni, PGEs	2	2.A	Turkey Creek	4563
Savannah*	WA	128.027695	-17.3526	Mine	Ni, Cu, Co, PGEs	2, 8	2.A	Turkey Creek	4563
Scotia Broad Arrow*	WA	121.274064	-30.198942	Mine	Ni, Cu, Pd, Ir	3	3.A	Bardoc	3137
Sherlock Bay Extended*	WA	117.612964	-20.763744	Prospect	Ni, Cu, Ag PGEs	?1		Sherlock	2456
Spargoville 1A	WA	121.491699	-31.32065	Historic mine	Ni, PGEs	3	3.A	Yimia	3135
Spargoville 2 or 5B	WA	121.505321	-31.36704	Mine–open pit	Ni, Cu, Au, Pt, Pd	3	3.A	Lake Lefroy	3235
Spargoville 5A	WA	121.505898	-31.35313	Mine–open pit	Ni, Cu, Co, Pt, Pd	3	3.A	Lake Lefroy	3235
Spargoville Environmental Group M15/395	WA	121.505898	-31.35313	Mine–open pit	Ni, Cu, Co, Pt, Pd	3	3.A	Lake Lefroy	3235
Sparrow–Wills Creek	WA	128.068405	-17.473551	Prospect–outcrop	Ni, Cu, PGEs	2	2.A	Turkey Creek	4563
Speewah Central*	WA	127.949538	-16.361424	Prospect–outcrop	V, Fe, Ti, PGEs, Au	2	2.B	Elgee	4465
Springvale 1	WA	127.62827	-17.76612	Prospect–unspecified	Cr, PGEs	1	1.B	McIntosh	4462
Springvale 2	WA	127.61282	-17.75156	Prospect–unspecified	Cr, PGEs	1	1.B	McIntosh	4462
Springvale 3	WA	127.65219	-17.78256	Prospect–unspecified	PGEs, Cr	1	1.B	McIntosh	4462
Springvale A	WA	127.74256	-17.80937	Prospect–unspecified	Ni, Cu, PGEs	1	?1.B	McIntosh	4462

Name <sup>1</sup>	State <sup>2</sup>	Longitude °E	Latitude °S	Operating status	Commodities <sup>3</sup>	Mineral-system class	Deposit type	100 K map name	100 K map number
Stripeys*	WA	128.3	-25.5952	Prospect	Cu, PGEs, Au	?1		Holt	4546
Symons Hill*	WA	123.174116	-31.900285	Prospect	Ni, Cu, Co, Pt, Pd	?2	?2.A	Symons Hill	3534
The Bulge C2	WA	121.996104	-27.611774	Prospect–drill-hole	Ni, Cu, Pt, Pd	3	3.A	Banjiwarn	3242
The Horn	WA	120.916603	-28.167379	Deposit–unspecified	Ni, Cu, PGEs, Pd, Pt	3	?3.A	Wildara	3041
Tickalara Bore 4	WA	128.01721	-17.40269	Occurrence–unspecified	Ni, Cu, Ag, Au, Pt	9, 8	9.A	Turkey Creek	4563
Toby South	WA	127.69026	-17.60614	Occurrence–unspecified	Cr, PGEs	1	1.B	McIntosh	4462
Togo 5A	WA	127.87754	-17.69516	Occurrence–unspecified	Cr, V, Ti, Pt, Pd	1	1.B	McIntosh	4462
Tom Tit	WA	122.23087	-22.59002	Prospect–unspecified	PGEs	?8		Rudall	3352
Tregurtha*	WA	121.617	-30.083	Prospect	Ni, Cu, PGEs	8	8.A	Gindalbie	3237
Vidure*	WA	118.756729	-28.812851	Prospect	Ni, Cu, Co, Pd, Pt, Au	?1		Youanmi	2640
Voyager 2 SE*	WA	128.064614	-26.185918	Prospect	Au, Cu, PGEs	8		Blackstone	4545
Wannaway*	WA	121.521103	-31.606319	Historic mine	Ni, Cu, Co, PGEs	8	8.B	Cowan	3234
Waterloo	WA	120.977997	-28.14377	Mine–decline	Ni, Cu, Pd, Pt	3	3.A	Wildara	3041
Weld Range East PGEs	WA	117.81858	-26.82856	Deposit–unspecified	PGEs	1	1.A	Madoonga	2444
Weld Range PGEs	WA	117.726997	-26.854521	Deposit–unspecified	Pt, Pd, Au	1	1.A	Madoonga	2444
Weld Range West PGEs	WA	117.70129	-26.86983	Prospect–unspecified	PGEs	1	1.A	Madoonga	2444
White Rock Well 3	WA	127.9596	-17.63531	Occurrence–unspecified	Ni, Cu, PGEs	12	12.E	McIntosh	4462
Wildcat–Baron	WA	117.43556	-29.058092	Prospect	Pd, Pt	1, 9	?1.A, 9.A	Ninghan	2339
Wondinong PGEs	WA	118.360294	-28.008045	Occurrence–outcrop	PGEs, Pt, Pd, Cr	1	1.A, 1.B	Challa	2541
Yamarna PGE 1	WA	123.6465	-28.172034	Prospect–drill-hole	Pd, Pt, Cr	?1, ?3	?1.B	Dorothy Hills	3641
Yamarna PGE 2	WA	123.645767	-28.170621	Prospect–drill-hole	Pd, Pt, Cr	?1, ?3	?1.B	Dorothy Hills	3641
Yarawindah (PMA)	WA	116.23324	-31.11557	Occurrence–unspecified	PGEs	8	8.C	Chittering	2135
Yarawindah 2	WA	116.26644	-31.09501	Prospect–unspecified	PGEs, Cu	8	8.C	Chittering	2135
Yarawindah Brook	WA	116.261597	-31.090179	Deposit–unspecified	Pt, Pd, Cu, Ni	9, 8	9.A, 8.C	Chittering	2135

Name <sup>1</sup>	State <sup>2</sup>	Longitude °E	Latitude °S	Operating status	Commodities <sup>3</sup>	Mineral-system class	Deposit type	100 K map name	100 K map number
Yellowdine*	WA	119.6616	-31.2863	Prospect	Au, Pt, Pd	?3		Yellowdine	2835
Yornup South (Cr)	WA	116.18604	-34.09709	Occurrence–unspecified	Cr, PGEs	?3	?3.B	Manjimup	2129
Zanthus HMS	WA	123.544985	-31.781826	Prospect–drill-hole	HM, Au, PGEs	10	10.C	Noondiana	3634
Zen*	WA	127.505402	-25.67057	Prospect	Ni, Cu, Co, PGEs, Mag	2	?2.B	Finlayson	4446
Airstrip	NT	132.497843	-13.492111	Mineral occurrence	U, Pd, Pt, Au	8	8.F	Mundogie	5371
Baldrick	NT	135.452889	-23.276653	Mineral occurrence	Cu, Ag, Au, Pd, Pt, Ni	8	8.D	Quartz	5951
Blackadder	NT	135.443717	-23.288268	Mineral occurrence	Cu, Pd, Pt, Co, Ni	8	8.D	Quartz	5951
Braveheart (Mordor)*	NT	134.48132	-23.46178	Mineral occurrence	Cu, Pd, Pt, Au	4	4.A	Laughlen	5751
Casper* (Attutra)	NT	136.3672	-22.64564	Mineral occurrence	V, Pt, Pd, Au	2	2.B	Jervis Range	6152
Casper	NT	133.515542	-13.046285	Mineral occurrence	U, Pt, Pd	8	8.F	Mann River	5671
Coco*	NT	136.36768	-22.63453	Mineral occurrence	V, Fe, Pt, Pd, Au	2	2.B	Jervis Range	6152
Copper King	NT	134.65344	-23.126378	Mineral occurrence	Cu, Pt, Pd, Au	8		Riddoch	5851
Copper Queen*	NT	134.66991	-23.15368	Mineral occurrence	Cu, Au, Pd, Pt	8		Riddoch	5851
Coronation Hill Gold	NT	132.606742	-13.586228	Prospect	Au, U, Pd, Pt	8	8.F	Stow	5470
Devils Elbow	NT	133.54603	-12.612384	Mineral occurrence	U, Pd, Au	8	8.F	Liverpool	5672
Edmund	NT	135.517749	-23.446801	Mineral occurrence	Cu, Ag, Au, Pd, Pt, Ni	8		Brahma	6051
Flying Ghost	NT	133.323329	-13.290478	Mineral occurrence	U, Pd, Pt	8	8.F	Gilruth	5571
Gold Ridge	NT	131.27927	-13.685805	Mineral occurrence	Au, Pt, Pd	8	8.F, 8.G	Tipperary	5170
Goldeneye	NT	131.49869	-13.572102	Mineral occurrence	U, Au, Pd, Pt	8	8.F	Tipperary	5170
Hardtop	NT	130.998983	-13.209242	Mineral occurrence	Au, Pd, Pt	8	8.F	Reynolds River	5071
Jabiluka 2*	NT	132.9029	-12.4994	Deposit	U, Au, Pd, Pt	8	8.G	Cahill	5472
Kongo	NT	134.647732	-23.120448	Mineral occurrence	Cu, Pt, Pd, Au	8	8.D	Riddoch	5851
Lindeman's Bore*	NT	130.12832	-17.46228	Mineral occurrence	Au, Cu, Co, Pd	?8	?8.G	Gregorys Depot	4963
Orodruin (Mithril)*	NT	134.48134	-23.43826	Mineral occurrence	Ni, Cu, Pt, Pd, Au	4	4.A	Laughlen	5751

Name <sup>1</sup>	State <sup>2</sup>	Longitude °E	Latitude °S	Operating status	Commodities <sup>3</sup>	Mineral-system class	Deposit type	100 K map name	100 K map number
Ranger 3*	NT	132.915	-12.6751	Mine	U, Au, Pd, Pt	8	8.F	Cahill	5472
RD	NT	136.34023	-22.60659	Mineral occurrence	V, Ti, Fe, Au, Pt, Pd	2	2.B	Jervois Range	6152
Sargent	NT	131.024633	-13.173089	Mineral occurrence	Au, Pd, Pt	8	8.F	Batchelor	5171
Sargent North	NT	131.026342	-13.157775	Mineral occurrence	Au, Pd, Pt	8	8.F	Batchelor	5171
Stevens	NT	133.525089	-12.339486	Abandoned mine	Au, U, Pt, Pd	8	?8.F	Goomadeer	5673
Cooper Hill	SA	132.681356	-31.782785	Prospect	Ni, PGEs	?2	?2.A	Bookabie	5434
Kangaroo Dam	SA	134.90932	-29.376471	Prospect	PGEs	?8		Cooper Pedy	5839
Lake Acraman*	SA	135	-32.417	Occurrence	PGEs	12	12.B	Everard	5934
Michael Hills Copper Prospect*	SA	129.025	-26.2583	Occurrence	Au, Pd, Pt, Cu, Ni, Co, Cr	?2		Davies	4745
Mount Alvey	SA	130.10757	-26.262251	Prospect	Ni, Cu, PGEs	?2		Hanging Knoll	4945
Nairne*	SA	139.005043	-35.044923	Deposit	Cu, Pb, S, Pd	8		Mobilong	6727
Taurus	SA	135.623673	-29.654006	Prospect	Cu, PGEs	8		Millers Creek	6038
Wishbone	SA	134.562695	-32.916184	Prospect	Cu, PGEs	12	12.E	Cungena	5832
Alma and Great New Zealand	QLD	152.668636	-26.186317	Mine–abandoned	Au, Pt	8		Gympie	9445
Broadbeach	QLD	153.434422	-28.022886	Mine–abandoned	Rt, Zrn, Ilm, Mnz, Pt, Os	10	10.D	Murwillumbah	9541
Coopa	QLD	145.739411	-17.422392	Mine–abandoned	Au, Pt	10	10.B	Bartle Frere	8063
Coopooroo	QLD	145.737789	-17.384425	Mine–abandoned	Au, Pt, Sn	10	10.B	Bartle Frere	8063
Copper Canyon*	QLD	140.527406	-20.928331	Occurrence	Au, Cu, Pd, Pt	?8, ?10	?8.G, ?10.C	Cloncurry	7056
Currumbin	QLD	153.500108	-28.149039	Occurrence–identified	Rt, Zrn, Ilm, Mnz, Pt, Os	10	10.D	Tweed Heads	9641
Di	QLD	144.413761	-15.560711	Prospect–inactive	Au, Pt	10	10.C	Laura	7766
Goldfind Creek	QLD	143.323581	-18.786697	Mine–abandoned	Au, Pt	10	10.C	North Head	7560

Name <sup>1</sup>	State <sup>2</sup>	Longitude °E	Latitude °S	Operating status	Commodities <sup>3</sup>	Mineral-system class	Deposit type	100 K map name	100 K map number
Goondicum Crater	QLD	151.409117	-24.843981	Mine	Ilm, Ap, FeI, Mag, Pt, Pd	10, 6		Monto	9148
Gympie Goldfield Alluvial Group	QLD	152.659364	-26.191397	Mine–abandoned	Au, Ag, Pt	10	10.C	Gympie	9445
Hawkwood	QLD	150.873261	-25.788553	Prospect–active	Mag, Pt, Pd, Cu, Ilm, V <sub>2</sub> O <sub>5</sub>	?2	2.B	Auburn	9046
Hawkwood North	QLD	150.856642	-25.778861	Prospect–active	Mag, Pt, Pd, Ilm, V <sub>2</sub> O <sub>5</sub>	?2	2.B	Auburn	9046
Jack Goody	QLD	151.4196	-24.919981	Prospect–inactive	Ilm, Au, Pt, Pd	10	10.C	Monto	9148
Kennedy Creek	QLD	144.527908	-15.67765	Prospect–abandoned	Au, Pt, Sn	10	10.C	Butchers Hill	7866
Kokomo	QLD	145.171214	-18.552506	Prospect–active	Ni, Co, Sc, Pt	9	9.A	Valley Of Lagoons	7960
Koppany	QLD	140.021294	-20.761642	Prospect–abandoned	Cu, Au, Ag, Ni, Co, Pt, Pd	8		Marraba	6956
Lady Mary North	QLD	152.668394	-26.183472	Mine–abandoned	Au, Ag, Pt, Pb	8		Gympie	9445
Laura River	QLD	144.459158	-15.582017	Prospect–active	Au, Pt, Pd	10	10.C	Laura	7766
Lucknow	QLD	152.662189	-26.183908	Mine–abandoned	Ag, Te, Au, Cu, Pt	8		Gympie	9445
Magdalene	QLD	150.149131	-23.619622	Prospect–active	Pd, Cu, Au	8		Mount Morgan	8950
Palm Beach	QLD	153.468381	-28.113044	Occurrence–identified	Rt, Zrn, Ilm, Mnz, Pt, Os	10	10.C	Murwillumbah	9541
Prospect Bore	QLD	142.251575	-18.892753	Prospect–abandoned	Ilm, Pt, Au, Mag, V <sub>2</sub> O <sub>5</sub> , Pd	?2, ?8	2.B	Prospect	7360
Saint George River	QLD	144.026075	-15.632575	Occurrence–identified	Au, Pt	10	10.C	Laura	7766
Saxby	QLD	140.88015	-19.188533	Prospect–active	Ni, Cu, Pt	1	1.A	Canobie	7059
Unnamed 309578	QLD	143.187528	-18.455942	Occurrence–identified	Zn, Pd, Mn	9	9.A	Forest Home	7561
Wairambar	QLD	145.72535	-17.413717	Mine–abandoned	Au, Pt	10	10.C	Bartle Frere	8063
Walkers Road Prospect	QLD	150.891914	-25.810578	Prospect–active	Cu, Pt, Pd	?1	?1.A	Auburn	9046

Name <sup>1</sup>	State <sup>2</sup>	Longitude °E	Latitude °S	Operating status	Commodities <sup>3</sup>	Mineral-system class	Deposit type	100 K map name	100 K map number
Wateranga	QLD	151.836164	-25.317061	Prospect–active	Fel, Ilm, Ap, Sc, Mica, Zrn, Rt, Pt, Mag	10, ?6	?10.A, ?6.A	Mount Perry	9247
West Coast Creek Alluvials	QLD	152.2865	-26.102358	Mine–abandoned	Au, Pt	10	10.C	Goomeri	9345
Westwood Palladium	QLD	150.144203	-23.625581	Mine–abandoned	Cu, Pd, Au, Ag	8	8.D	Mount Morgan	8950
Yanky Franks	QLD	143.286542	-18.782639	Mine–abandoned	Au, Pt	10	10.C	North Head	7560
Avondale Ni-Co-Pt Prospect	NSW	147.492138	-32.923527	Prospect	Ni, Pt, Co	9	9.A	Boona Mount	8332
Ballina Beach Workings	NSW	153.599824	-28.854498	Historic mine	Au, Sn, Pt	10	10.D	Ballina	9640
Boonoo Boonoo River	NSW	152.119219	-28.873261	Historic mine	Au, Sn, Pt	10	10.C	Drake	9340
Buchanans Head	NSW	153.344806	-29.549638	Occurrence–identified	Pt	10	10.D	Bare Point	9538
Bulbodney Platinum Prospect	NSW	147.332505	-32.287812	Prospect–active	Pt, Ni, Cr, Co	6	6.A	Tottenham	8333
Burra Alluvial	NSW	147.368203	-32.678206	Prospect	Sn, Au, Pt	10	10.A	Boona Mount	8332
Cincinnati (Pt) Prospect	NSW	147.468662	-32.709922	Deposit	Pt, Sc	9	9.A	Boona Mount	8332
Cincinnati Lead	NSW	147.46644	-32.713448	Prospect–active	Au, Pt	10	10.A	Boona Mount	8332
Coolac*	NSW	148.222536	-34.962046	Prospect–active	Cr, Pt	5	5.A	Cootamundra	8528
Copper Hill Mine	NSW	148.867931	-33.052192	Historic mine	Cu, Au, Pd	8	8.E	Molong	8631
Fifield Lead	NSW	147.451648	-32.795454	Historic mine	Au, Pt	10	10.A	Boona Mount	8332
Fifield Project	NSW	147.469331	-32.83216	Unknown	Au, Pt, Ag	10	10.A	Boona Mount	8332
Flemington	NSW	147.417555	-32.756017	Prospect	Pt	6	6.A	Boona Mount	8332
Forners Prospect	NSW	141.634443	-31.83906	Occurrence–identified	Cu, Ni, Pt, Pd, Au	8	8.D	Taltingan	7234
Gallaghers Claim	NSW	153.447212	-29.12767	Occurrence–identified	Au, Zr, Rt, Pt	10	10.D	Woodburn	9539
Gilgai Prospect	NSW	146.995927	-31.610977	Prospect–active	Pt	6, 9	6.A, 9.A	Hermidale	8234
Gillenbine Lead	NSW	147.479795	-32.816232	Historic mine	Pt, Au	10	10.A	Boona Mount	8332
Honeybugle North Prospect	NSW	146.907159	-31.820258	Prospect–active	Fe, Pt	9	9.A	Hermidale	8234

Name <sup>1</sup>	State <sup>2</sup>	Longitude °E	Latitude °S	Operating status	Commodities <sup>3</sup>	Mineral-system class	Deposit type	100 K map name	100 K map number
Honeybugle Yarran	NSW	146.913476	-31.844622	Prospect–active	Pt	9	9.A	Hermidale	8234
Hylea Tiger Creek	NSW	147.226548	-32.364998	Prospect–active	Pt	6	6.A	Tottenham	8333
Jacks Lookout	NSW	147.475583	-32.805604	Historic mine	Pt, Au	10	10.A	Boona Mount	8332
Kars Prospect	NSW	147.500925	-33.021362	Prospect–active	Pt, Cr, Ni	6, 9	6.A, 9.A	Bogan Gate	8431
Keens Prospect, RAB hole BCR122	NSW	147.30041	-32.297364	Unknown	Pt	12	12.E	Tottenham	8333
Kelvin Grove	NSW	147.446903	-32.722134	Prospect–active	Pt, Cu, Ni, Vrm	6, 9	6.A	Boona Mount	8332
Little Darling Creek Ultrabasic	NSW	141.604612	-31.964156	Prospect–active	Pt, Cu	8	8.D	Taltingan	7234
Mallee Valley	NSW	146.94626	-31.811259	Prospect	Pt	12	12.E	Hermidale	8234
McAuleys Lead	NSW	153.351035	-29.259729	Occurrence–identified	Au, Zr, Rt, Pt	10	10.D	Woodburn	9539
Milverton Lead	NSW	147.476408	-32.72198	Deposit	Au, Pt	10	10.A	Boona Mount	8332
Milverton Residual Pt Deposit	NSW	147.472163	-32.712916	Deposit	Pt	9	9.A	Boona Mount	8332
Mineral Claim MC127	NSW	141.986633	-29.430069	Occurrence–identified	Cu, Au, Pb, Pt, Ag, S, Sn, Zn	12	12.E	Olive Downs	7239
Minnie Water	NSW	153.295904	-29.769785	Occurrence–identified	Au, Pt, Sn	10	10.D	Bare Point	9538
Monkey Hill Deep Lead	NSW	149.585781	-33.041563	Occurrence–identified	Au, Pt, Dmdg	10	10.C	Bathurst	8831
Mount Derriwong	NSW	147.35333	-32.982178	Prospect	Pt	6	6.A	Boona Mount	8332
Mount Mary Mines	NSW	148.259338	-35.005049	Historic mine	Cr, Pt	5, 8	5.A, 8.D	Tumut	8527
Mulga Springs	NSW	141.665109	-31.885816	Prospect–active	Cu, Pt, Pd, Ni, Re, Au	8	8.D	Taltingan	7234
Murga	NSW	147.432519	-32.793041	Prospect–active	Pt	6	6.A	Boona Mount	8332
New Zealanders claim	NSW	153.450343	-29.13849	Prospect	Au, Pt	10	10.D	Woodburn	9539
Nyngan Nickel Deposit	NSW	147.039105	-31.498191	Prospect–active	Ni, Co, Sc, Pt	9	9.A	Canonba	8335
Nyngan Scandium Deposit*	NSW	146.994	-31.612	Prospect–active	Ni, Co, Sc, Pt	9	9.A	Hermidale	8234

Name <sup>1</sup>	State <sup>2</sup>	Longitude °E	Latitude °S	Operating status	Commodities <sup>3</sup>	Mineral-system class	Deposit type	100 K map name	100 K map number
Owendale Lead	NSW	147.461007	-32.694525	Prospect–active	Au, Pt	10	10.A	Boona Mount	8332
Owendale North Pt-Cu prospect	NSW	147.469849	-32.692192	Prospect	Pt	6	6.A	Boona Mount	8332
Owendale North Residual Pt-Cu-Ni-Co Prospect	NSW	147.470062	-32.692147	Prospect–active	Pt, Co, Ni, Cu, Sc	9	9.A	Boona Mount	8332
Platina Lead	NSW	147.468196	-32.845142	Historic mine	Pt, Au	10	10.A	Boona Mount	8332
RAB hole BCR58	NSW	147.316884	-32.300301	Unknown	Pt	12	12.E	Tottenham	8333
Red Hill Silver Mining Company	NSW	141.58735	-32.045341	?Historic mine	Cu, Pt, Ni, Zn, Pb, Ag	8	8.D	Redan	7233
Reynolds Tank	NSW	147.458502	-32.776125	Prospect	Pt, Au	10	10.A	Boona Mount	8332
drill-hole SMR2 Sampsons Tank Magnetic Anomaly	NSW	147.26722	-32.097884	Unknown	Pt	12	12.E	Tottenham	8333
Shellharbour Alluvials	NSW	150.869994	-34.583405	Occurrence–identified	Sn, Au, Pt	10	10.D	Kiama	9028
Studwick's Lead	NSW	147.48127	-32.772838	Prospect	Pt, Au	10	10.A	Boona Mount	8332
Syerston	NSW	147.419586	-32.756687	Prospect–active	Ni, Co, Pt, Cr, REE	9	9.A	Boona Mount	8332
Talbragar River Alluvials	NSW	148.757326	-32.174353	Occurrence–identified	Sn, Pt	10	10.C	Dubbo	8633
The Diggings	NSW	149.129705	-32.350376	Occurrence–identified	Au, Pt, Ir, Os	10	10.C	Cobbora	8733
Tree Point	NSW	153.290792	-29.790553	Occurrence–identified	Au, Pt	10	10.D	Bare Point	9538
Unnamed 102277	NSW	147.468777	-32.807326	Occurrence	Pt, Au	10	10.A	Boona Mount	8332
Unnamed 102524	NSW	147.412433	-32.802941	Occurrence	Pt	6	6.A	Boona Mount	8332
Unnamed 102552	NSW	147.52382	-32.854844	Occurrence	Pt	6	6.A	Tullamore	8432
Unnamed 102555	NSW	147.423968	-32.7578	Occurrence	Pt, Co, Ni, Cr	9	9.A	Boona Mount	8332
Unnamed 102556	NSW	147.381239	-32.751623	Occurrence	Cu, Au, Pd	12	12.E	Boona Mount	8332
Unnamed 181767	NSW	141.63369	-31.837169	Occurrence	Cu, Pt, Ni	8	8.D	Taltingan	7234
Wellington Alluvials	NSW	149.106546	-32.633495	Unknown	Au, Dmdi, Dmdg	10	10.C	Euchareena	8732

Name <sup>1</sup>	State <sup>2</sup>	Longitude °E	Latitude °S	Operating status	Commodities <sup>3</sup>	Mineral-system class	Deposit type	100 K map name	100 K map number
Wylie Creek	NSW	152.121318	-28.622812	Historic mine	Sn, W, Bi, Au, Dmdg, Zrn, Toz, Pt	10	10.C	Drake	9340
Yarran Park Prospect	NSW	146.917706	-31.842821	Prospect	Pt	12	12.E	Hermidale	8234
East Walhalla Copper and Platinum Mine	VIC	146.46208	-37.93866	Occurrence	Cu, Ag, Au, Cu, Pt	8	8.D	Matlock	8122
Errinundra*	VIC	148.88805	-37.44593	Historic mine	Au, Ag, Pt, Os,	8		Bendoc	8623
Hunts*	VIC	146.19006	-37.48214	Occurrence	Au, Pt	8	8.D	Mansfield	8123
Loch Fyne	VIC	146.2308	-37.61228	Prospect	Au, Pt	8	8.D	Matlock	8122
Maynards Gully*	VIC	146.4164	-37.7363	Historic mine	Au, Pt	8	8.D	Matlock	8122
Morning Star*	VIC	146.2456	-37.5686	Historic mine	Au, Pt	8	8.D	Matlock	8122
Mt Leura*	VIC	143.15	-38.25	Scientific interest	Ni, Cu, Pd, Pt	12	12.D	Corangamite	7521
Shamrock	VIC	146.26983	-37.58742	Historic mine	Au, Cu, Pt	8	8.D	Matlock	8122
Thomson River Copper Mine	VIC	146.42765	-37.98594	Historic mine	Cu, Ag, Au, Ni, Pd, Pt	8	8.D	Matlock	8122
Unnamed (Stockyard Creek)	VIC	146.20024	-38.65323	Occurrence	Au, Pt	10	10.C	Foster	8120
Unnamed (Turtons Creek*)	VIC	146.24144	-38.55228	Occurrence	Au, Pt	10	10.C	Foster	8120
Unnamed* 962400	VIC	145.99697	-38.85524	Occurrence	Au, PGEs	10	10.D	Wonthaggi	8020
Unnamed* 962401	VIC	146.00576	-38.87722	Occurrence	Au, PGEs	10	10.D	Foster	8120
Walhalla Copper Mining Co.	VIC	146.42676	-37.98676	Historic mine	Cu, Pt	8	8.D	Matlock	8122
Adamsfield Osmiridium Field	TAS	146.329555	-42.727892	Mineral Field	Os, Cr, PGEs	10, 5	10.B, 5.A	Wedge	8112
Ahearne Creek	TAS	145.38912	-41.723363	Alluvial workings	Os, Au, PGEs	10	10.B	Pieman	7914
Alfred River	TAS	145.40788	-41.693903	Alluvial workings	Os, Au, PGEs	10	10.B	Pieman	7914
Andersons Creek	TAS	146.768788	-41.196675	Mineral occurrence	Os, PGEs	10	10.B	Tamar	8215
Bald Hill	TAS	145.309981	-41.439411	Mineral field	PGEs, Os	10	10.B	Arthur River	7915

Name <sup>1</sup>	State <sup>2</sup>	Longitude °E	Latitude °S	Operating status	Commodities <sup>3</sup>	Mineral-system class	Deposit type	100 K map name	100 K map number
Bealey Creek	TAS	145.43433	-41.742903	Alluvial workings	Os, Au, PGEs	10	10.B	Pieman	7914
Berkery Creek	TAS	145.390119	-41.731483	Alluvial workings	Os, Au, PGEs	10	10.B	Pieman	7914
Boyes River Mineral Field	TAS	146.257452	-42.628386	Mineral field	Os, PGEs	10	10.B	Wedge	8112
Brassy North	TAS	145.32317	-41.457168	Mine or prospect	PGEs, Pt	10	10.B?	Arthur River	7915
Burgess	TAS	145.328274	-41.444902	Mine or prospect	Os, PGEs	10	10.B?	Arthur River	7915
Burgess Creek	TAS	145.325444	-41.44324	Alluvial workings	PGEs, Os	10	10.B	Arthur River	7915
Carpenter Creek	TAS	145.435597	-41.740218	Alluvial workings	Os, Au, PGEs	10	10.B	Pieman	7914
Castra River	TAS	145.308273	-41.505137	Alluvial workings	PGEs, Au, Os, Sn	10	10.B	Pieman	7914
Caudrys Creek	TAS	145.269519	-41.457634	Alluvial workings	PGEs, Os	10	10.B	Arthur River	7915
Caudrys Prospect	TAS	145.27214	-41.458123	Mine or prospect	PGEs, Os	5	5.A	Arthur River	7915
Chromite Creek	TAS	145.440907	-41.719575	Alluvial workings	Os, PGEs	10	10.B	Pieman	7914
Cuni (Five Mile) Mineral Field	TAS	145.391115	-41.835974	Mineral field	Ni, Cu, Pd, PGEs, Pt	8		Pieman	7914
Dundas Osmiridium Field	TAS	145.434343	-41.890611	Alluvial workings	Au, Os, PGEs	10	10.B	Pieman	7914
Fenton Creek B	TAS	145.304524	-41.437529	Alluvial workings	PGEs, Os	10	10.B	Arthur River	7915
Fenton Creek A	TAS	145.304494	-41.434106	Alluvial workings	PGEs, Os	10	10.B	Arthur River	7915
Fentons Prospect	TAS	145.299093	-41.43925	Mine or prospect	PGEs, Os	10	10.B	Arthur River	7915
Florentine Valley	TAS	146.427518	-42.701407	Alluvial workings	Os, PGEs	10	10.B	Wedge	8112
Fourteen Mile Creek	TAS	146.524504	-42.791906	Alluvial workings	Os, Au, PGEs	10	10.B	Tyenna	8212
Fowler Creek	TAS	145.411155	-41.756094	Alluvial workings	Os, Cr, PGEs	10	10.B	Pieman	7914
Gold Creek	TAS	145.423708	-41.734651	Alluvial workings	Os, Au, PGEs	10	10.B	Pieman	7914
Gould Creek	TAS	145.378371	-41.72051	Alluvial workings	Os, Au, PGEs	10	10.B	Pieman	7914
Gravelly Beach Prospect	TAS	145.398559	-42.384553	Mineral occurrence	Cr, Au, PGEs, Os	10	?10.B, ?10.C	Cape Sorell	7913

Name <sup>1</sup>	State <sup>2</sup>	Longitude °E	Latitude °S	Operating status	Commodities <sup>3</sup>	Mineral-system class	Deposit type	100 K map name	100 K map number
Greens Creek	TAS	146.642364	-43.553243	Mine or prospect	Os, PGEs	10	10.B	South East Cape	8210
Halls O/C	TAS	146.35452	-42.723443	Mine or prospect	Os, PGEs, Cr	10	10.B	Wedge	8112
Harman River	TAS	145.356954	-41.678775	Alluvial workings	Os, Au, PGEs	10	10.B	Pieman	7914
Harrison and Brandstater	TAS	146.33777	-42.759459	Alluvial workings	Os, PGEs	10	10.B	Wedge	8112
Hatchet Creek	TAS	145.298017	-41.434641	Alluvial workings	PGEs, Os	10	10.B	Arthur River	7915
Humphries Creek	TAS	145.309808	-41.529028	Alluvial workings	PGEs, Os	10	10.B	Pieman	7914
Joint Creek	TAS	145.299499	-41.437455	Alluvial workings	PGEs, Os	10	10.B	Arthur River	7915
Jones Creek A	TAS	145.338099	-41.416402	Alluvial workings	Os, PGEs	10	10.B	Arthur River	7915
Jones Creek B	TAS	145.325976	-41.422531	Alluvial workings	PGEs, Os	10	10.B	Arthur River	7915
Jones Creek C	TAS	145.355927	-41.421162	Alluvial workings	Os, PGEs	10	10.B	Arthur River	7915
Keegan Creek	TAS	145.357931	-41.578813	Alluvial workings	Sn, Os, PGEs	10	10.B	Pieman	7914
Keenan Creek	TAS	145.367971	-41.656415	Alluvial workings	Os, Au, PGEs	10	10.B	Pieman	7914
Kershaw Creek	TAS	145.402427	-41.744265	Alluvial workings	Os, Au, PGEs	10	10.B	Pieman	7914
King Creek	TAS	145.43817	-41.743225	Alluvial workings	Os, Au, PGEs	10	10.B	Pieman	7914
Limestone Creek	TAS	145.386212	-41.695402	Alluvial workings	Os, Au, PGEs	10	10.B	Pieman	7914
Melba Flats	TAS	145.399543	-41.836092	Alluvial workings	Sn, Au, PGEs, Os	8		Pieman	7914
Merton Creek	TAS	145.414424	-41.721013	Alluvial workings	Os, PGEs	10	10.B	Pieman	7914
Newall Creek	TAS	145.54119	-42.163019	Alluvial workings	Au, PGEs, Os	10	10.B	Franklin	8013
Nickel Reward	TAS	145.39024	-41.84686	Mine or prospect	Ni, Cu, Pd, PGEs, Pt	8		Pieman	7914
Nineteen Mile Creek A	TAS	145.30338	-41.435531	Alluvial workings	PGEs, Os	10	10.B	Arthur River	7915
Nineteen Mile Creek B	TAS	145.299105	-41.434206	Alluvial workings	PGEs, Os	10	10.B	Arthur River	7915
Nineteen Mile Creek C	TAS	145.306816	-41.432249	Alluvial workings	PGEs, Os	10	10.B	Arthur River	7915
Osmiridium Beach	TAS	146.627436	-43.564901	Mine or prospect	Os, PGEs	10	10.D	South East Cape	8210
Osmiridium Creek	TAS	145.414225	-41.729117	Alluvial workings	Os, Au, PGEs	10	10.B	Pieman	7914

Name <sup>1</sup>	State <sup>2</sup>	Longitude °E	Latitude °S	Operating status	Commodities <sup>3</sup>	Mineral-system class	Deposit type	100 K map name	100 K map number
Pine Creek	TAS	145.341075	-41.581273	Alluvial workings	Sn, Os, PGEs	10	10.B	Pieman	7914
Pollards Shaft	TAS	146.354286	-42.722451	Mine or prospect	Os, PGEs	10	?10.B	Wedge	8112
Purcells Prospect	TAS	145.277913	-41.457129	Mine or prospect	PGEs, Os	10	?10.B	Arthur River	7915
Purcells South Workings	TAS	145.27811	-41.458753	Mine or prospect	PGEs, Os	10	?10.B	Arthur River	7915
R. J. Stacey No. 9468	TAS	146.332181	-42.756365	Alluvial workings	Os, PGEs	10	10.B	Wedge	8112
Ramsay`s	TAS	145.302823	-41.530276	Alluvial workings	PGEs, Os	10	10.B	Pieman	7914
Renison Osmiridium Field	TAS	145.41051	-41.782205	Alluvial workings	PGEs, Au	10	10.B	Pieman	7914
Riley Creek	TAS	145.416142	-41.748958	Alluvial workings	Os, Cr, PGEs	10	10.B	Pieman	7914
Roberts Creek	TAS	145.389917	-41.739587	Alluvial workings	Os, Au, PGEs	10	10.B	Pieman	7914
Rocky Boat Harbour	TAS	146.611368	-43.560345	Mine or prospect	Os, PGEs	10	10.D	South East Cape	8210
Rocky Boat Harbour (Surprise Rivulet*)	TAS	146.648633	-43.539756	Alluvial workings	Os, PGEs	10	10.B	South East Cape	8210
Rocky Boat Plain	TAS	146.628707	-43.559502	Mine or prospect	Os, PGEs	10	?10.B	South East Cape	8210
Savage River Section 11663	TAS	145.081819	-41.626776	Alluvial workings	Au, Os, PGEs, Sn	10	10.B	Pieman	7914
Savage River Dredge	TAS	145.098908	-41.617152	Alluvial workings	Au, Os, PGEs, Sn	10	10.B	Pieman	7914
Spero River	TAS	145.348777	-42.6333	Alluvial workings	Os, PGEs	10	?10.B, ?10.C	Spero	7912
Stacey Bros No. 20	TAS	146.335316	-42.760346	Alluvial workings	Os, PGEs	10	10.B	Wedge	8112
Stacey Bros No. 21	TAS	146.335324	-42.759625	Alluvial workings	Os, PGEs	10	10.B	Wedge	8112
Stanton and Loughnan	TAS	145.305408	-41.523109	Alluvial workings	PGEs, Os	10	10.B	Pieman	7914
Star Creek	TAS	145.454457	-41.806222	Alluvial workings	Sn, Au, PGEs, Os	10	10.B	Pieman	7914
Strongs Creek–Tylers Creek	TAS	146.623738	-43.562187	Mine or prospect	Os, PGEs	10	10.B	South East Cape	8210
Sweeney Creek	TAS	145.419811	-41.726852	Alluvial workings	Os, Au, PGEs	10	10.B	Pieman	7914

Name <sup>1</sup>	State <sup>2</sup>	Longitude °E	Latitude °S	Operating status	Commodities <sup>3</sup>	Mineral-system class	Deposit type	100 K map name	100 K map number
Three Mile Creek	TAS	145.401748	-41.747408	Alluvial workings	Os, Cr, PGEs	10	10.B	Pieman	7914
Tin Creek	TAS	145.432319	-41.726663	Alluvial workings	Os, Au, PGEs	10	10.B	Pieman	7914
Tributary Creek	TAS	145.470811	-41.715743	Mine or prospect	Os, PGEs	10	10.B	Pieman	7914
Trinder Creek A	TAS	145.416031	-41.75346	Alluvial workings	Os, Cr, PGEs	10	10.B	Pieman	7914
Trinder Creek B	TAS	145.405232	-41.75241	Alluvial workings	Os, Cr, PGEs	10	10.B	Pieman	7914
Tunbridge and Kellys	TAS	145.302965	-41.524874	Alluvial workings	PGEs, Os	10	10.B	Pieman	7914
Unnamed	TAS	145.305747	-41.44115	Alluvial workings	PGEs, Os	10	10.B	Arthur River	7915
Unnamed	TAS	145.316883	-41.468785	Alluvial workings	PGEs, Os	10	10.B	Arthur River	7915
Unnamed	TAS	146.369474	-42.718213	Alluvial workings	Os, PGEs	10	10.B	Wedge	8112
Unnamed	TAS	146.331504	-42.717007	Alluvial workings	Os, PGEs	10	10.B	Wedge	8112
Unnamed	TAS	146.340249	-42.721561	Mine or prospect	Os, PGEs	10	10.B	Wedge	8112
Unnamed	TAS	146.304788	-42.725313	Alluvial workings	Os, PGEs	10	10.B	Wedge	8112
Unnamed	TAS	146.33581	-42.725497	Alluvial workings	Os, PGEs	10	10.B	Wedge	8112
Unnamed	TAS	146.342655	-42.736614	Alluvial workings	Os, PGEs	10	10.B	Wedge	8112
Unnamed	TAS	146.320624	-42.740357	Alluvial workings	Os, PGEs	10	10.B	Wedge	8112
Unnamed	TAS	146.254959	-42.632873	Alluvial workings	Os, PGEs	10	10.B	Wedge	8112
Unnamed	TAS	146.732858	-43.04779	Mine or prospect	Os, PGEs	10	?10.B	Huon	8211
Unnamed	TAS	146.354058	-42.720829	Mine or prospect	Os, PGEs	10	10.B	Wedge	8112
Unnamed	TAS	146.32566	-42.726609	Alluvial workings	Os, PGEs	10	10.B	Wedge	8112
Unnamed	TAS	146.326223	-42.731025	Alluvial workings	Os, PGEs	10	10.B	Wedge	8112
Unnamed	TAS	146.327049	-42.733731	Alluvial workings	Os, PGEs	10	10.B	Wedge	8112
Unnamed	TAS	146.317242	-42.736825	Alluvial workings	Os, PGEs	10	10.B	Wedge	8112
Unnamed	TAS	146.33157	-42.722231	Alluvial workings	Os, PGEs	10	10.B	Wedge	8112
Unnamed	TAS	146.300824	-42.730242	Mine or prospect	Os, PGEs	10	10.B	Wedge	8112

Name <sup>1</sup>	State <sup>2</sup>	Longitude °E	Latitude °S	Operating status	Commodities <sup>3</sup>	Mineral-system class	Deposit type	100 K map name	100 K map number
Unnamed	TAS	146.311072	-42.731385	Alluvial workings	Os, PGEs	10	10.B	Wedge	8112
Unnamed	TAS	146.32609	-42.732015	Alluvial workings	Os, PGEs	10	10.B	Wedge	8112
Unnamed	TAS	146.258214	-42.62578	Alluvial workings	Os, PGEs	10	10.B	Wedge	8112
Unnamed	TAS	146.335124	-42.721171	Alluvial workings	Os, PGEs	10	10.B	Wedge	8112
Unnamed	TAS	146.370733	-42.714438	Alluvial workings	Os, PGEs	10	10.B	Wedge	8112
Unnamed	TAS	146.334383	-42.733324	Alluvial workings	Os, PGEs	10	10.B	Wedge	8112
Unnamed	TAS	146.325972	-42.720397	Alluvial workings	Os, PGEs	10	10.B	Wedge	8112
Unnamed	TAS	146.340681	-42.738493	Alluvial workings	Os, PGEs	10	10.B	Wedge	8112
Unnamed	TAS	146.317054	-42.742858	Mine or prospect	Os, PGEs	10	10.B	Wedge	8112
Unnamed	TAS	146.342424	-42.770022	Alluvial workings	Os, PGEs	10	10.B	Wedge	8112
Unnamed	TAS	146.265541	-42.645729	Alluvial workings	Os, PGEs	10	10.B	Wedge	8112
Unnamed	TAS	145.228636	-41.472864	Alluvial workings	Au, Os, PGEs	10	10.B	Arthur River	7915
Unnamed	TAS	146.314823	-42.734649	Alluvial workings	Os, PGEs	10	10.B	Wedge	8112
Unnamed	TAS	145.296726	-41.442818	Alluvial workings	PGEs, Os	10	10.B	Arthur River	7915
Unnamed	TAS	145.302819	-41.438675	Alluvial workings	PGEs, Os	10	10.B	Arthur River	7915
Unnamed	TAS	145.177842	-41.499091	Alluvial workings	PGEs, Au, Os	10	10.B	Arthur River	7915
Unnamed	TAS	146.333069	-42.719178	Mine or prospect	Os, PGEs	10	10.B	Wedge	8112
Unnamed	TAS	146.308652	-42.729299	Alluvial workings	Os, PGEs	10	10.B	Wedge	8112
Unnamed	TAS	146.332397	-42.736284	Alluvial workings	Os, PGEs	10	10.B	Wedge	8112
Unnamed	TAS	146.253815	-42.626562	Alluvial workings	Os, PGEs	10	10.B	Wedge	8112
Unnamed	TAS	146.56713	-42.81639	Mine or prospect	Os, PGEs	10	?10.B	Tyenna	8212
Unnamed	TAS	146.732743	-43.045989	Mine or prospect	Os, PGEs	10	?10.B	Huon	8211
Unnamed	TAS	145.288413	-41.444856	Alluvial workings	PGEs, Os	10	10.B	Arthur River	7915
Unnamed	TAS	146.337211	-42.720102	Mine or prospect	Os, PGEs	10	10.B	Wedge	8112

Name <sup>1</sup>	State <sup>2</sup>	Longitude °E	Latitude °S	Operating status	Commodities <sup>3</sup>	Mineral-system class	Deposit type	100 K map name	100 K map number
Unnamed	TAS	146.336392	-42.728202	Alluvial workings	Os, PGEs	10	10.B	Wedge	8112
Unnamed	TAS	146.307909	-42.730195	Alluvial workings	Os, PGEs	10	10.B	Wedge	8112
Unnamed	TAS	146.732777	-43.038244	Mine or prospect	Os, PGEs	10	?10.B	Huon	8211
Unnamed	TAS	145.1364	-41.565527	Alluvial workings	Au, Os, PGEs	10	10.B	Pieman	7914
Unnamed	TAS	146.372724	-42.710756	Alluvial workings	Os, PGEs	10	10.B	Wedge	8112
Unnamed	TAS	146.338474	-42.727674	Alluvial workings	Os, PGEs	10	10.B	Wedge	8112
Unnamed	TAS	146.309818	-42.734349	Alluvial workings	Os, PGEs	10	10.B	Wedge	8112
Unnamed	TAS	146.352602	-42.71992	Mine or prospect	Os, PGEs	10	10.B	Wedge	8112
Unnamed	TAS	146.253869	-42.622059	Alluvial workings	Os, PGEs	10	10.B	Wedge	8112
Unnamed	TAS	146.349831	-42.716302	Alluvial workings	Os, PGEs	10	10.B	Wedge	8112
Unnamed	TAS	146.346725	-42.721328	Alluvial workings	Os, PGEs	10	10.B	Wedge	8112
Unnamed	TAS	146.325679	-42.724898	Alluvial workings	Os, PGEs	10	10.B	Wedge	8112
Unnamed	TAS	145.414101	-41.831791	Mine or prospect	Ni, PGEs	8		Pieman	7914
Unnamed	TAS	146.310926	-42.722469	Alluvial workings	Os, PGEs	10	10.B	Wedge	8112
Unnamed	TAS	146.325938	-42.723548	Alluvial workings	Os, PGEs	10	10.B	Wedge	8112
Unnamed	TAS	146.348754	-42.737549	Alluvial workings	Os, PGEs	10	10.B	Wedge	8112
Unnamed	TAS	146.31851	-42.743767	Mine or prospect	Os, PGEs	10	10.B	Wedge	8112
Unnamed	TAS	146.257596	-42.605963	Alluvial workings	Os, PGEs	10	10.B	Wedge	8112
Unnamed	TAS	146.322686	-42.719297	Alluvial workings	Os, PGEs	10	10.B	Wedge	8112
Warners Creek A	TAS	145.307902	-41.431904	Alluvial workings	PGEs, Os	10	10.B	Arthur River	7915
Warners Creek B	TAS	145.309547	-41.433099	Alluvial workings	PGEs, Os	10	10.B	Arthur River	7915
Warners Creek C	TAS	145.309606	-41.435442	Alluvial workings	PGEs, Os	10	10.B	Arthur River	7915
Warners Creek D	TAS	145.314141	-41.435959	Alluvial workings	PGEs, Os	10	10.B	Arthur River	7915
Warners Creek E	TAS	145.317686	-41.437722	Alluvial workings	PGEs, Os	10	10.B	Arthur River	7915

Name <sup>1</sup>	State <sup>2</sup>	Longitude °E	Latitude °S	Operating status	Commodities <sup>3</sup>	Mineral-system class	Deposit type	100 K map name	100 K map number
Westerway Creek	TAS	145.429824	-41.927476	Alluvial workings	Au, Os	10	10.B	Pieman	7914
Whyte River	TAS	145.183959	-41.623031	Alluvial workings	Au, Os, PGEs, Sn	10	10.B	Pieman	7914
Williams Creek	TAS	146.33603	-42.750714	Alluvial workings	Os, PGEs	10	10.B	Wedge	8112
Wilson River A	TAS	145.379276	-41.684496	Alluvial workings	Os, Au, PGEs, Cr	10	10.B	Pieman	7914
Wilson River B	TAS	145.373996	-41.6556	Alluvial workings	Os, Au, PGEs, Cr	10	10.B	Pieman	7914
Wilson River C	TAS	145.371005	-41.678975	Alluvial workings	Os, Au, PGEs, Cr	10	10.B	Pieman	7914

<sup>1</sup> The PGE deposits and occurrences marked with an asterisk indicate those entries which were not identified in the State and Northern Territory databases listed in the introduction to Appendix K as having PGEs, and the information on these deposits and occurrences was obtained from other sources.

<sup>2</sup> WA = Western Australia; NT = Northern Territory; SA = South Australia; QLD = Queensland; NSW = New South Wales; VIC = Victoria; TAS = Tasmania.

<sup>3</sup> Ag = silver; Ap = apatite; Au = gold; Bi = bismuth; Co = cobalt; Cr = chromium; Cu = copper; Dmdg = Diamond-gem; Dmdi = Diamond-industrial; Fe = iron; Fel = feldspar; HM = Heavy minerals; Ilm = ilmenite; Ir = iridium; Mag = magnetite; Mnz = monazite; Ni = nickel; Pb = lead; Pd = palladium; PGEs = platinum-group elements; Pt = platinum; Re = rhenium; REE = rare-earth elements; Rt = rutile; Ru = ruthenium; S = sulphur; Sb = antimony; Sc = scandium; Sn = tin; Th = thorium; Ti = titanium; Toz = topaz; U = uranium; V = vanadium; Vrm = vermiculite; W = tungsten; Zrn = zircon; Zn = zinc.

# Appendix K Australian platinum-group-element deposits and occurrences

Yanis Mieзитis and David. L. Huston

Geological information and locational co-ordinates for PGE deposits and occurrences in this Appendix are derived from Geoscience Australia's Mineral Location (MINLOC) database, which is based on the following State and Northern Territory databases available online in 2014:

- Geological Survey of Queensland website at:  
<https://webgis.dme.qld.gov.au/webgis/webqmin/viewer.htm>
- New South Wales Department of Trade and Investment, Resources and Energy MinView website for minerals at:  
<http://minview.minerals.nsw.gov.au/mv2web/mv2?cmd=MainMapandtopic=min>
- Victoria Energy and Earth Resources GeoVic–Explore Victoria website at: [http://er-info.dpi.vic.gov.au/sd\\_weave/anonymous.html](http://er-info.dpi.vic.gov.au/sd_weave/anonymous.html)
- Mineral Resources Tasmania TIGER website at:  
<http://www.mrt.tas.gov.au/portal/database-searches?inheritRedirect=true>
- The South Australian resources geoserver SARIG at:  
<https://sarig.pir.sa.gov.au/Map>
- Geological Survey of Western Australia MINEDEX (Mines and Mineral Deposits) at:  
<http://www.dmp.wa.gov.au/3970.aspx>
- The Northern Territory Geological Survey NT STRIKE website at:  
[http://geoscience.nt.gov.au/GeosambaU/strike\\_gs\\_webclient/default.aspx](http://geoscience.nt.gov.au/GeosambaU/strike_gs_webclient/default.aspx)

Additional information regarding PGE deposits and occurrences has also been sourced from relevant geological reports and maps published by Geoscience Australia in addition to State and Northern Territory publications and exploration company reports on open files accessible from the above databases (<http://www.geoscience.gov.au/>). Company reports to the Australian Securities Exchange (<http://www.asx.com.au/>) and scientific research publications were also consulted.

The PGE deposits and occurrences marked with an asterisk in this Appendix indicate those entries which were not identified in the above databases as having PGEs and the information on these deposits and occurrences was obtained from other publications that are listed after each deposit and occurrence in this Appendix. Although a number of operating Ni mines in Western Australia produce by-products of PGEs (collectively ~300 kg to ~850 kg of Pd and ~50 kg to ~320 kg of Pt produced annually: see Appendix F), companies generally do not publish PGE resource statistics, nor the PGE contents of individual Ni deposits. As a consequence, the amount of detail summarised for the PGE deposits and occurrences in this Appendix do not necessarily reflect the relative significance of these entries since the descriptions are simply based on the available information in the public domain.

Descriptions of PGE deposits and occurrences are presented in a standard format that includes the following headings of a template:

- **PGE deposit and occurrence:** Name of PGE deposit or occurrence. The order of states/territories compiled in Appendix K is organised from the west to the east and from the north to south is Western Australia; Northern Territory; South Australia; Queensland; New South Wales; Victoria; and Tasmania.
- **Geological province:** Name of geological province hosting the PGE occurrence sourced from Geoscience Australia's province database at Australian Geological Provinces 2013.01 at <http://www.ga.gov.au/products-services/data-applications/australian-geological-provinces.html>. Province names derived from relevant State/Northern Territory sources.
- **Location:** Longitude and latitudes co-ordinates for the relevant PGE deposit and occurrence as in GA's MINLOC database which is populated from relevant State/Northern Territory databases. The 1:250 000 and 1:100 000 map sheets and codes are also indicated.
- **Classification:** Based on the classification scheme shown in Table 6.1.
- **Geological setting:** Description of the regional geology hosting the PGE deposit and occurrence.
- **PGE mineralisation:** Description of PGE mineralisation in the deposit and occurrence.
- **Age of mineralisation:** If available, otherwise a general comment on the age of the host rock.
- **Current status:** Historical or currently active exploration site or mine.
- **Economic significance:** A general indication of whether the deposit has a resource, or is an active or historical mine, and whether the occurrence is minor, has no economic significance, or is only of scientific significance.
- **Major references:** Available sources of information.
- **Relevant figure(s):** If available, maps and sections included in this report.

The descriptions are arranged alphabetically by State or Territory.

## K.1 WESTERN AUSTRALIA

### K.1.1 Abrahams Find–Joshua prospects

#### ***Geological province***

Pilbara Craton.

#### ***Location***

Abrahams Find: 118.490402°E, -20.914459°S; Roebourne (SF 50–03), Yule (2556); ~62 km south-southwest of Port Hedland.

Joshua: 118.524°E, -20.91054°S; Port Hedland (SF 50–04), Wallaringa (2656); ~3.5 km east of Abrahams Find.

Joshua East: 118.5336°E, -20.90594°S; Port Hedland (SF 50–04), Wallaringa (2656); ~5.5 km east of Abrahams Find.

Mt Dove\*: Now renamed as Abrahams Find?

#### ***Classification***

- ?1. Layered tholeiitic mafic-ultramafic intrusions. (Joshua, Joshua East, ?Mt Dove).
- ?8. Hydrothermal-Metamorphic, 8.D. Structurally-controlled remobilised Ni-Cu-PGE±Au. (Abrahams Find).

#### ***Geological setting***

De Grey Mining Limited (2005) investigated a number of PGE prospects (Abrahams Find, Joshua, Joshua East) from 2002 at its Three Kings Platinum Project in the Archean greenstone belts of the west Pilbara Craton. The Abrahams Find PGE prospect occurs in peridotite lenses within the Tabbata Tabbata Shear Zone. It was first identified as a geochemical anomaly (Location 13) in 1974. The PGE and Au mineralisation at the Joshua prospect, ~3.5 km along an easterly strike from Abrahams Find, was discovered in 2002. Mineralisation is hosted by a large differentiated mafic-ultramafic dyke-like body of the Archean Millindinna Intrusion and occurs near the contact between pyroxenite and peridotite. According to Smithies (1999: p. 9) the Millindinna Intrusion appears to be intruded by the Peawah Granodiorite and therefore cannot be significantly older than ~2950 Ma. The mineralised mafic-ultramafic intrusion near Mt Dove was recognised during Cu-Ni orientated exploration by Utah in 1972–1974. The mineralised intrusion is a deformed sill-like body strongly differentiated from dunite, peridotite, pyroxenite, to gabbro and granophyre (Hoatson and Glaser, 1989). The Mt Dove occurrence may coincide with the Abrahams Find prospect.

#### ***PGE mineralisation***

Anomalous PGEs are associated with mafic-ultramafic rocks (gabbro, pyroxenite, peridotite) at Abrahams Find. Sub-vertical mineralisation has been traced by drilling over a strike length of 12 km immediately south of the Mt Dove Granite with higher-grade intersections over a 4.5 km-long zone that includes:

- 6 m @ 1.58 g/t PGEs from 75 m;
- 15 m @ 1.39 g/t PGEs from 28 m; and

## Western Australia

- 14 m @ 1.32 g/t PGEs from 58 m.

A 9 km-strike length of the ultramafic body extends to the east of Joshua. Another 13 km-strike length of linear magnetic anomalies interpreted to be similar differentiated dykes lie beneath shallow transported cover to the west.

Drilling at the Mt Dove prospect tested low-order PGE soil anomalies and delineated minor PGE levels of 1 m @ 0.25 ppm Pt+Pd+Au in the mineralised mafic-ultramafic intrusion (Hoatson and Glaser, 1989)

### ***Age of mineralisation***

Archean.

### ***Current status***

Exploration site.

### ***Economic significance***

Occurrence.

### ***Major references(s)***

De Grey Mining Limited, 2007. De Grey Mining Limited Annual Report, 72 pp.

De Grey Mining Limited, 2005. De Grey intercepts outstanding wide zone of platinum, palladium and gold at Joshua East. De Grey Mining Limited announcement to the Australian Securities Exchange, 14 March 2005, 3 pp.

Hoatson, D.M. and Glaser, L.M., 1989. Geology and economics of platinum-group metals in Australia. Bureau of Mineral Resources, Australia, Resource Report 5, 81 pp.

Smithies, R.H., 1999. Geology of the Yule 1:100 000 sheet. Western Australia Geological Survey, 1:100 000 Geological Series Explanatory Notes, 15 pp.

Smithies, R.H., Champion, D.C. and Blewett, R.S., 2002. Geology of the Wallaringa 1:100 000 sheet. Western Australia Geological Survey, 1:100 000 Geological Series Explanatory Notes, 27 pp.

### ***Relevant figure(s)***

## **K.1.2 Adder\***

(see Dugite–Gum Creek group)

## **K.1.3 Airstrip Cr Pt, Black Oak Creek Cr Pt, Chromite Creek, Medusa-Peninsula, (Plumridge group), Peninsula HA2\* (previously known as Plumridge)**

### ***Geological province***

Albany-Fraser Orogen.

### ***Location***

This group of prospects is about 350 km east-northeast of Kalgoorlie and comprises five occurrences:

Airstrip Cr Pt: 124.90382°E, -29.58224°S; Plumridge (SH 51–08), Bowden (3838);

Black Oak Creek Cr Pt: 124.88097°E, -29.54022°S; Plumridge (SH 51–08), Bowden (3838);

## Western Australia

Chromite Creek: 124.86661°E, -29.63584°S; Plumridge (SH 51–08), Bowden (3838);

Medusa-Peninsula: 125.0164°E, -29.66527°S; Plumridge (SH 51–08), Plumridge (3938); and

Peninsula HA2\*, 124.961513°E, -29.755636°S; Plumridge (SH 51–08), Bowden (3838). Previously known as Plumridge.

### **Classification**

- 1. Layered tholeiitic mafic-ultramafic intrusions; 1.B. Stratabound PGE-bearing chromitite layers.

### **Geological setting**

The five prospects are located along the western side of a major aeromagnetic anomaly within the Albany-Fraser Orogen referred to as the Plumridge magnetic complex (Kelly, 2004; Baulch, 2003) which was initially interpreted as a major mafic-ultramafic complex due to:

- indications of mafic and ultramafic rocks intersected in previous drilling (although of limited extent) across the complex;
- large, intense (~50 mgal) gravity anomaly, suggesting the presence of a significant mass of more dense rocks, most likely mafic and/or ultramafic rocks; and
- existence of PGE-bearing chromitite layers in felsic gneiss on the western side of the magnetic anomaly.

Although drilling confirmed the existence of mafic and ultramafic intrusive rocks within the complex, the vast majority of rocks underlying the Plumridge magnetic complex are not related to a layered mafic-ultramafic intrusive sequence. The tectonised remnants of igneous mafic-ultramafic rocks are of limited extent. Lithologies include pyroxenite, dunite, and mafic granulite, with interleaved tectonic slices of felsic and mafic granulite, and metamorphosed granitic-gneissic rocks (Kelly, 2004).

### **PGE mineralisation**

Chromitite layers in a layered mafic-ultramafic complex, 30 km west of Plumridge Lakes include surface samples with Cr contents of 46% and 28%, and traces of Pt (Hoatson and Glaser, 1989; Western Areas NL, 2000). Other historical surface sampling yielded Cr analyses of up to 34% Cr and 0.8 g/t Pt (Baulch, 2003; Western Areas NL, 2003).

Orion Gold NL (2014) reported an assay result from a 1 m drill-hole sample of 0.08 g/t Pt and 0.28 g/t Pd from a drill-hole depth of 12 m (OPRC008) at the Peninsula HA2 prospect.

### **Age of mineralisation**

Proterozoic?

### **Current status**

Exploration sites.

### **Economic significance**

Occurrences.

### **Major references(s)**

Baulch, J., 2003. Plumridge Project. Final technical report. In: Kelly, G.R., 2004. Plumridge Project: Mt. Margaret and Warburton Mineral Fields–WA, Combined annual technical report for period

- 29/03/2003 to 28/03/2004 exploration completed on active tenements E39/904, E39/905, E39/906, E39/909, E39/915, E69/982, E69/983, E69/1252, E69/1550 and E69/1721. Western Areas NL, 176 pp.
- Hoatson, D.M. and Glaser, L.M., 1989. Geology and economics of platinum-group metals in Australia. Bureau of Mineral Resources, Australia, Resource Report 5, 81 pp.
- Orion Gold NL, 2014. Wide intersections of nickel-copper mineralisation, Fraser Range, WA. Orion Gold NL announcement to the Australian Securities Exchange, 17 March 2014, 19 pp.
- Western Areas NL, 2000. Information release. Extended exploration project for nickel-copper-platinum-chromite. Western Areas NL announcement to the Australian Securities Exchange, 7 December 2000, 3 pp.
- Western Areas NL, 2003. Update on Flying Fox and expansion of nickel-copper and PGE exploration activities. Western Areas NL announcement to the Australian Securities Exchange, 10 October 2003, 4 pp.

### ***Relevant figure(s)***

## **K.1.4 Alice Downs 3, 4; Togo 5A, Melon South (West McIntosh Group)**

### ***Geological province***

Halls Creek Orogen.

### ***Location***

Alice Downs 3: 127.87442°E, -17.69359°S, occurs in the southern half of a group of mafic-ultramafic intrusions abutting the large 1830 ± 3 Ma McIntosh Intrusion; Dixon Range (SE 52–06), McIntosh (4462); ~62 km north-northeast of Halls Creek.

Alice Downs 4: 127.88967°E, -17.66656°S; Dixon Range (SE 52–06), McIntosh (4462).

Togo 5A: 127.87754°E, -17.69516°S; Dixon Range (SE 52–06), McIntosh (4462).

Melon South: 127.87435°E, -17.70443°S; Dixon Range (SE 52–06), McIntosh (4462).

### ***Classification***

- 1. Layered tholeiitic mafic-ultramafic intrusions; 1.B. Stratabound PGE-bearing chromitite layers.

### ***Geological setting***

The West McIntosh Intrusion is a steeply dipping sheet, 8 km-long by 500 m-wide, 500 m-thick mafic-ultramafic body along the western margin of the 1830 ± 3 Ma McIntosh Intrusion. It youngs to the east, with foliation in amphibolite and metagabbro dipping steeply (60°–75°) east and parallel to lithological contacts. Basal serpentinitised foliated peridotite, tremolite-anthophyllite-chlorite schist (200 m-thick), and chromitite layers are overlain to the east by strongly foliated amphibolite and metagabbro (200 m). Thin peridotite lenses (50 m) host thin chromitite layers. Discontinuous outcrops of mottled anorthosite and minor gabbro (50 m) define the top of the intrusion. The West McIntosh Intrusion is separated from the McIntosh Intrusion in the east by thin screens of poorly-exposed migmatised metasediments of Tickalara Metamorphics and alluvium. Contacts with the Tickalara Metamorphics to the west are generally obscured by alluvium. Peridotite consists of chromite-bearing adcumulate and mesocumulate, which have a pervasive foliation defined by aligned ovoid olivine grains (1 mm by 2 mm) parallel to closely spaced secondary veinlets of serpentine, iddingsite, and magnetite. Olivine and rare intercumulus orthopyroxene contain small chromite subhedra. Chromitite

consists of fine-grained (0.1 mm–0.3 mm) disseminated chromite grains enclosing subrounded serpentinised olivine ('doughnut' texture). The margins of chromite grains are irregular and embayed, owing to blades of serpentine minerals in the groundmass. Fine-grained anorthosite mesocumulates contain small (<1.5 mm) aligned plagioclase ( $An_{62}$ ) laths enclosed by intercumulus clinopyroxene which has been replaced by hornblende (Hoatson, 2000). The West McIntosh Intrusion is similar in stratigraphy, lithology, and mineralisation to the nearby comagmatic group I Panton and South Melon Patch intrusions.

### ***PGE mineralisation***

Stacked chromitite layers (2 cm- to 10 cm-thick), some more than 3 km-long, occur in the upper 20 m of the basal ultramafic sequence, and in peridotite lenses in the foliated mafic sequence. Chromitite in upper part of ultramafic sequence contains anomalous Pt (333 ppb and 662 ppb), Pd (79 ppb and 488 ppb), and Au (2 ppb and 6 ppb).

Analyses for samples from a chromitite layer in the West McIntosh Intrusion are shown in Appendix Table K.1 (Hoatson, 2000).

*Appendix Table K.1 Geochemical data of the West McIntosh Intrusion chromitite layer. Data from Hoatson (2000).*

Sample number	Lithology	Pt (ppb)	Pd (ppb)	Au (ppb)	Cu (ppm)	Ni (ppm)	S (ppm)	Cr (ppm)	Pt/Pd	Pdx10 <sup>3</sup> /S
92522354	Chromitite	662	488	6	54	1263	20	>99 999	1.36	24.4
92522359	Chromitite	333	79	2	145	1088	90	>99 999	4.21	0.88

### ***Age of mineralisation***

Correlated with the  $1856 \pm 2$  Ma Panton mafic-ultramafic intrusion.

### ***Current status***

Dormant exploration site.

### ***Economic significance***

Occurrence.

### ***Major references(s)***

Hoatson, D.M., 2000. Geological setting, petrography, and geochemistry of the Palaeoproterozoic layered mafic-ultramafic intrusions. In: Hoatson, D.M. and Blake, D.H. (editors), *Geology and economic potential of the Palaeoproterozoic layered mafic-ultramafic intrusions in the East Kimberley, Western Australia*. Canberra: Australian Geological Survey Organisation Bulletin 246, 99–162.

### ***Relevant figure(s)***

Figure 6.13 and Figure 8.21.

## **K.1.5 Anomaly 11–Blair**

### ***Geological province***

Yilgarn Craton.

### ***Location***

Anomaly 11–Blair: 121.715897°E, -30.961470°S (drill-hole AMRC014); Kurnalpi (SH 51–10), Kanowna (3236); ~28 km north of Kambalda.

### ***Classification***

- 3. Komatiitic flows and related sill-like intrusions.

### ***Geological setting***

Disseminated Ni mineralisation in ultramafic sequence (shown as serpentinite on Kanowna 1:100 000 map) near its contact with occasionally sulphidic metasediments.

### ***PGE mineralisation***

Analyses of drill-hole intersections on the Anomaly 11—Blair deposits are listed below as follows (Australian Mines Limited, 2004a,b):

- AMRC014—7 m @ 1.19% Ni and 0.35 g/t 'PGEs' (Pt+Pd+Au), including 1 m @ 1.79% Ni and 0.57 g/t 'PGEs' (Pt+Pd+Au);
- AMRC015—5 m @ 1.87% Ni and 0.51 g/t 'PGEs' (Pt+Pd+Au), including 1 m @ 2.89% Ni and 0.72 g/t 'PGEs' (Pt+Pd+Au); and
- AMRC017—5 m @ 0.65% Ni and 0.16 g/t 'PGEs' (Pt+Pd+Au), including 1 m @ 1.09% Ni and 0.26 g/t 'PGEs' (Pt+Pd+Au).

### ***Age of mineralisation***

Archean?

### ***Current status***

Exploration site.

### ***Economic significance***

Occurrence.

### ***Major references(s)***

Australian Mines Limited, 2004a. Managing director's presentation, 25 November 2004, 26 pp.

Australian Mines Limited, 2004b. Australian Mines Limited announcement to the Australian Securities Exchange, 13 December 2004, 4pp.

### ***Relevant figure(s)***

Figure 6.21.

### **K.1.6 Antlion Intrusion Baggaley Hills\***

#### ***Geological province***

Musgrave Province.

#### ***Location***

Antlion Intrusion Baggaley Hills\*: 128.85°E, -26.28°S; Cooper (SG 52–10), Bell Rock (4645).

#### ***Classification***

- ?2. Massive to poorly layered tholeiitic mafic-dominated intrusions.

#### ***Geological setting***

A 5 km-diameter intrusion.

#### ***PGE mineralisation***

Surface samples from the western portion of the Antlion Intrusion analysed with a handheld XRF instrument (Niton) defined a trend of anomalous Cu values (523 ppm, 421 ppm, 369 ppm, and 251 ppm) over a length of 2.5 km. Associated with this Cu anomaly are peak values of 284 ppb, 252 ppb, 200 ppb, and 64 ppb PGEs+Au. Twenty-one rock-chip samples analysed with handheld XRF instrument yielded two peak values of 0.29% Cu and 0.14% Cu.

#### ***Age of mineralisation***

Proterozoic?

#### ***Current status***

Exploration site.

#### ***Economic significance***

Occurrence.

#### ***Major references(s)***

Redstone Resources Limited, 2006. Redstone Resources Limited Prospectus 2006, 99 pp.  
Redstone Resources Limited project webpage ([http://www.redstone.com.au/contents\\_projects.html](http://www.redstone.com.au/contents_projects.html))

#### ***Relevant figure(s)***

### **K.1.7 Babel**

(see Nebo–Babel)

### **K.1.8 Bakers Target, Mount Clifford\***

#### ***Geological province***

Yilgarn Craton.

### **Location**

Bakers Target: 121.010722°E, -28.460800°S; Leonora (SH 51–01), Weebo (3141); ~55 km northwest of Leonora. Site location is that of Breakaway Resources Limited drill-hole 07BMCC007.

Mount Clifford (37)\*: 121.058800°E, -28.462740°S; Leonora (SH 51–01), Weebo (3141). Location of Mount Clifford for the Ni-Cu-PGE occurrence is uncertain. There are several mineral occurrences ~4.7 km east of Bakers Target, which are labelled variously as Mount Clifford, but all are Au occurrences rather than Ni or PGEs.

### **Classification**

The mineralisation at Bakers Target is recorded in MINEDEX as in komatiitic or dunitic host rocks:

- ?3. Komatiitic flows and related sill-like intrusions.

### **Geological setting**

The occurrence is located within a dominantly metamorphosed ultramafic sequence in the Agnew–Wiluna greenstone belt, the Kalgoorlie Terrane of the Eastern Goldfields Superterrane.

### **PGE mineralisation**

Breakaway Resources Limited reported assay results for a drill-hole intersection in 07BMCC007, located 2 km southwest of the Marriott's Ni deposit. The assays of this drill-hole originally drilled and reported in 2007 returned values of 8 m @ 0.43% Ni, 608 ppm Cu, and 136 ppb Pt+Pd (Breakaway Resources Limited, 2007, 2011a). In 2011, Breakaway Resources drilled another hole, 08BMCD008, 80 m down-dip from 07BMCC007, which intersected 3 m of vein and breccia sulphides (pyrrhotite, pyrite, and chalcopyrite) at a drill-hole depth of 257 m. The sulphides intersected in 08BMCD008 were reported to occur within a zone of strong shearing at the base of an ultramafic unit and were interpreted to be equivalent to the mineralisation intersected in 07BMCC007. Analyses for drill samples returned 4.33 m @ 0.37% Ni, 0.12% Cu, 161 ppb Pt+Pd from 246 m in 08BMCD008, and 0.38 m @ 0.44% Ni, 0.16% Cu, 81 ppb Pt+Pd from 280.95 m in 08BMCD009 (Breakaway Resources Limited, 2011b).

The quarterly report for September 2007 also mentioned the occurrence of Ni sulphide and PGE mineralisation at the nearby Randal's Find with drill-hole intersections of 0.75 m @ 5.12% Ni and 5.49 g/t PGEs.

Maximum PGE contents for gossan samples as reported by Keays and Davison (1976) and Travis et al. (1976) including Mount Clifford returned 1.70 ppm Pd (2.52% Ni, 1.40% Cu). There are three Au occurrences ~4.7 km east of Bakers Target, which have been labelled variously as Mount Clifford, but none of these have recorded Ni or PGE values.

### **Age of mineralisation**

Archean.

### **Current status**

Inactive exploration site.

### **Economic significance**

Occurrence.

### **Major references(s)**

Breakaway Resources Limited, 2007. Activity report for the quarter ended 30 September 2007, 20 pp.

Breakaway Resources Limited, 2011a. Nickel drilling update—Leinster District. Breakaway Resources Limited announcement to the Australian Securities Exchange, 30 March 2011, 2 pp.

Breakaway Resources Limited, 2011b. Leinster District nickel drilling returns highly promising results. Breakaway Resources Limited announcement to the Australian Securities Exchange, 4 July 2011, 3 pp.

### **Relevant figure(s)**

## **K.1.9 Balla Balla\***

### **Geological province**

Pilbara Craton.

### **Location**

Balla Balla\*: 117.775703°E, -20.766041°S; Roebourne (SF 50–03), Sherlock (2456); ~10 km northwest of Whim Creek.

### **Classification**

- ?1. Layered tholeiitic mafic-ultramafic intrusions.

### **Geological setting**

The Balla Balla vanadiferous titanomagnetite deposit is located within the Sherlock mafic-ultramafic intrusion. The rock sequence extending over a 15 km-strike length and 1 km- to 2 km-thickness, consists of lower norite, anorthosite, and minor pyroxenite units, overlain by gabbro, granophyre, and vanadiferous-titanomagnetite units.

### **PGE mineralisation**

Anomalous PGE and Au values have been delineated in a reconnaissance rock-sampling program from the poorly-exposed intrusion. The precious metals coincide with anomalous Cu and Ni concentrations in soil samples along a geologically favourable horizon within the lower half of the stratigraphy (Hoatson and Glaser, 1989).

### **Current status**

Historical PGE exploration site.

### **Economic significance**

Trace PGEs associated with Fe-V-Ti mineralisation?

### **Major references(s)**

Hoatson, D.M. and Glaser, L.M., 1989. Geology and economics of platinum-group metals in Australia. Bureau of Mineral Resources, Australia, Resource Report 5, 81 pp.

### **Relevant figure(s)**

Figure 6.3.

### **K.1.10 Bamboo Creek Plant\***

#### ***Geological province***

Pilbara Craton.

#### ***Location***

Bamboo Creek Plant: 120.209396°E, -20.925280°S; Yarrie (SF 51–01), Muccan (2956); ~55 km east-northeast of Marble Bar.

#### ***Classification***

Gold, Ag, and PGEs in tailings.

- 12. Others (minor or unknown economic importance); 12.E. Others (unknown geological setting).

#### ***Geological setting***

Tailings from nearby historical mines.

#### ***PGE mineralisation***

PGE resources are in tailings at the Bamboo Creek treatment plant, but trace Au, Ag, and PGEs in the Mt Webber banded-Fe ore deposit are also being investigated. Haoma Mining NL (2012, 2014a,b) is investigating the feasibility of extracting PGEs, Au, and Ag from up-graded concentrate derived from tailings at the Bamboo Creek processing plant.

#### ***Age of mineralisation***

Precambrian.

#### ***Current status***

Haoma Mining NL is investigating the feasibility of upgrading concentrates from the tailings stockpiles for export to overseas refiners for extraction of Au, Ag, and PGEs.

#### ***Economic significance***

Economic significance being assessed.

#### ***Major references(s)***

Haoma Mining NL, 2012. Bamboo Creek and Mt Webber contains significant commercial quantities of gold and platinum group metals (PGM). Report to the Australian Securities Exchange, 18 June 2012, 4 pp.

Haoma Mining NL, 2014a. Activities report for the quarter ended December 31, 2013–Highlights, 23 pp.

Haoma Mining NL, 2014b. Activities report for the quarter ended March 31, 2014–Highlights, 22 pp.

#### ***Relevant figure(s)***

### **K.1.11 Barlee Environmental Group**

(see Halleys East–Barlee)

## **K.1.12 Beadell South East**

### ***Geological province***

Paterson Province.

### ***Location***

Beadell South East: 122.852402°E, -22.996441°S; Rudall (SF 51–10), Connaughton (3452); ~155 km south-southeast of Telfer.

### ***Classification***

- Layered tholeiitic mafic-ultramafic intrusions; ?1.B. Stratabound PGE-bearing chromitite layers.

### ***Geological setting***

The Beadell prospect is located in the Connaughton Terrane. Elevated Cu-Au-Co-U soil values associated with a west-northwest fault cutting magnetic basement with an outcropping layered mafic-ultramafic complex.

### ***PGE mineralisation***

It was reported in a company prospectus that at least two separate mafic and ultramafic intrusions are present within the Beadell project tenements. Both intrusions show indications of layering and the presence of chromitite bands has been reported by the Geological Survey of Western Australia. Geochemical sampling returned low anomalous PGE values, up to 15 ppb Pt, in the south of the project area.

A 4.5 km-long, west-northwest-trending shear zone returned anomalous Cu-Au and some U-Co (Scimitar Resources Limited Prospectus, 2004).

### ***Age of mineralisation***

Archean?

### ***Current status***

Exploration site.

### ***Economic significance***

Occurrence.

### ***Major references(s)***

Scimitar Resources Limited, 2004. Scimitar Resources Limited 2004 Prospectus.

### ***Relevant figure(s)***

## **K.1.13 Beasley Nickel**

### ***Geological province***

Fortescue Basin.

## **Location**

Beasley Nickel: 117.292099°E, -22.705959°S; Mount Bruce (SF 50–11), Rocklea (2352); ~52 km west of Tom Price.

## **Classification**

- ?3. Komatiitic flows and related sill-like intrusions; ?3.C. PGE-enriched Ni-Cu sulphides associated with komatiitic and tholeiitic rocks.
- ?1. Layered tholeiitic mafic-ultramafic intrusions.

## **Geological setting**

The Beasley Nickel prospect is located on the northern side of the Rocklea Dome where the upper volcanic members of the Boongal, Pyradie, and Bunjinah formations of the Archean Fortescue Group are exposed on the flank of the dome. The Boongal and Bunjinah formations are composed mostly of basaltic andesite lavas and volcanic breccias, whereas the Pyradie Formation is composed of a range of rocks formed from basaltic komatiite magmas with additional relatively abundant interflow sedimentary rocks including tuff, sandstone, and sulphidic black shale (Thorne and Tyler, 1996; Thorne and Trendall, 2001; Donaghy and Ascough, 2006).

## **PGE mineralisation**

The Beasley Ni-Cu-PGE prospect (AusQuest Limited, 2003, 2004, 2006) in the Fortescue Basin that unconformably underlies the Hamersley Basin, contains mineralised komatiite rocks interpreted to be comagmatic with basaltic rocks of the Late Archean (~2770 Ma) Fortescue Group—an extensive platform sequence on the southern margin of the Pilbara Craton. The mineralised basaltic komatiite sequence is associated with andesitic basalt and gabbroic sills. A Ni gossan sample returned assay values of 0.42% Ni, 0.52% Cu, 0.32 g/t Pt, and 0.73 g/t Pd.

Magmatic Ni-Cu-PGE sulphides were intersected in holes BRD06-02 and BRD06-01 within an ultramafic sequence, over thicknesses of 52 m and 9 m, respectively. The drill-holes were collared 400 m and 800 m west of drill-hole BNDH07, which intersected similar mineralisation over a 14 m-wide section. Assays, over 1 m-intervals, range up to 0.25% Ni, 550 ppm Cu, and 0.18 g/t PGEs. The company reports did not report the stratigraphic position of the ultramafic sequence hosting the drill-hole intersections, but the Beasley Nickel prospect appears to be hosted in the Pyradie Formation (AusQuest Limited, 2006).

## **Age of mineralisation**

Age of Pyradie Formation is  $2715 \pm 6$  Ma (Thomas and Trendall, 2001).

## **Current status**

Historical exploration site.

## **Economic significance**

Occurrence.

## **Major references(s)**

AusQuest Limited, 2003. AusQuest Prospectus 2003, 63 pp.

AusQuest Limited, 2004. Beasley nickel project exploration update. AusQuest Limited announcement to the Australian Securities Exchange, 6 July 2004, 1 pp.

## Western Australia

- AusQuest Limited, 2006. Magmatic Ni-Cu-PGE sulphides intersected at Beasley. AusQuest Limited announcement to the Australian Securities Exchange, 17 October 2006, 2 pp.
- Donaghy, A. and Ascough, G., 2006. Beasley-Bellary project. Exploration Licence E47/1426 Western Australia.
- Thorne, A.M. and Trendall, A.F., 2001. Geology of the Fortescue Group, Pilbara Craton, Western Australia. Geological Survey of Western Australia, Bulletin 144, 249 pp.
- Thorne, A.M. and Tyler, I.M., 1996. Geology of the Rocklea 1:100 000 sheet. Western Australia Geological Survey, 1:100 000 Geological Series Explanatory Notes, 15 pp.

### **Relevant figure(s)**

Figure 6.24.

## **K.1.14 Bellary Nickel**

### **Geological province**

Pilbara Craton, Hamersley Basin.

### **Location**

Bellary Nickel: 117.659300°E, 23.040435°S; Turee Creek (SF 50–15), Paraburdoo (2451); ~18 km north of Paraburdoo.

### **Classification**

- ?3. Komatiitic flows and related sill-like intrusions.
- ?1. Layered tholeiitic mafic-ultramafic intrusions.

### **Geological setting**

The Bellary Ni prospect is located on the northeast side of the Bellary Dome and three other Ni-Cu-PGE prospects have been marked on a map in AusQuest Limited quarterly report for December 2004. The upper volcanic members of the Boongal, Pyradie, and Bunjinah formations of the Archean Fortescue Group are exposed on the flank of the Bellary Dome. The Boongal and Bunjinah formations are composed mostly of basaltic andesite lavas and volcanic breccias whereas the Pyradie Formation comprises a range of rocks formed from basaltic komatiite magmas with additional relatively abundant interflow sedimentary rocks including tuff, sandstone, and sulphidic black shale (Jackson, 2009; Thorne and Trendall, 2001).

### **PGE mineralisation**

Stream-sediment sampling assays up to 569 ppm Ni, 223 ppm Cu, 83 ppm Co, 34 ppb Pt, and 20 ppb Pd (AusQuest, 2005).

Drill-hole DDH07 (at the Hardey prospect) intersected anomalous PGEs (2 m @ 1.0 g/t), which are confined to a thin ultramafic flow unit (AusQuest Limited, 2008).

### **Age of mineralisation**

Age of Pyradie Formation is  $2715 \pm 6$  Ma (Thomas and Trendall, 2001).

### **Current status**

Exploration site.

**Economic significance**

Occurrence.

**Major references(s)**

- AusQuest Limited, 2005. Quarterly report for the period ended 31 December 2004, 11 pp.  
 AusQuest Limited, 2008. Quarterly report for the period ended 31 December 2007, 15 pp.  
 Jackson, D.G., 2009. Bellary Ni-Cu-PGE project. Annual and final report for Exploration Licence E47/1040, Western Australia, 27 pp.  
 Thorne, A.M. and Tyler, I.M., 1994. Geology of the Paraburdoo 1:100 000 sheet. Western Australia Geological Survey, 1:100 000 Geological Series Explanatory Notes, 18 pp.

**Relevant figure(s)****K.1.15 Big Ben\*****Geological province**

Halls Creek Orogen.

**Location**

Big Ben\*: 127.837520°E, -17.931960°S; Dixon Range (SE 52–06), McIntosh (4462); ~38 km north-northeast of Halls Creek.

**Classification**

- 1. Layered tholeiitic mafic-ultramafic intrusions; 1.B. Stratabound PGE-bearing chromitite layers.

**Geological setting**

The Big Ben Intrusion is a fault-bounded block considered to have originally been part of the southern end of the Panton Intrusion. It was displaced 15 km to the south by the sinistral strike-slip Panton Fault. The Big Ben Intrusion is considered to represent part of the Panton Intrusion because of its similar rock types, stratigraphy, layering, and PGE-chromitite mineralisation.

**PGE mineralisation**

The geochemistry of chromitite layers in the Big Ben Intrusion is shown in Appendix Table K.2 (Hoatson, 2000).

*Appendix Table K.2 Geochemical data of the Big Ben Intrusion. Data from Hoatson (2000).*

Sample	Lithology	Pt (ppb)	Pd (ppb)	Au (ppb)	Cu (ppm)	Ni (ppm)	S (ppm)	Cr (ppm)	Pt/Pd	Pd $\times 10^3$ /S
93522026	Chromitite	583	1080	8	44	664	70	>99 999	0.54	15.4
BB1	Chromitite	520	580	7	20	640		140 000	0.9	
BB3	Chromitite	450	760	15	40	540		175 000	0.59	
BB2	Pyroxenite	40	33	13	130	440		4400	1.21	
93522029	Peridotite	2.4	1.9	2	88	343	410	1901	1.26	0.005

### ***Age of mineralisation***

The Big Ben Intrusion is correlated with the  $1856 \pm 2$  Ma Panton mafic-ultramafic intrusion.

### ***Current status***

Exploration site.

### ***Economic significance***

Occurrence.

### ***Major references(s)***

Hoatson, D.M., 2000. Geological setting, petrography, and geochemistry of the Palaeoproterozoic layered mafic-ultramafic intrusions. In: Hoatson, D.M. and Blake, D.H. (editors), *Geology and economic potential of the Palaeoproterozoic layered mafic-ultramafic intrusions in the East Kimberley, Western Australia*. Canberra: Australian Geological Survey Organisation Bulletin 246, 99–162.

### ***Relevant figure(s)***

Figure 6.14 and Figure 8.21.

## **K.1.16 Blackadder**

(see Eastman Bore–Louisa group)

## **K.1.17 Black Oak**

(see Airstrip Cr Pt, Black Oak Creek Cr Pt, Chromite Creek, and Medusa-Peninsula (Plumridge group) Peninsula HA2\* (previously known as Plumridge)).

## **K.1.18 Black Swan-Gosling\*, Silver Swan\* (Cygnet and Gosling lodes)**

### ***Geological province***

Yilgarn Craton.

### ***Location***

Black Swan\*: 121.648804°E, -30.393431°S; Kurnalpi (SH 51–10), Gindalbie (3237); ~42 km northeast of Kalgoorlie.

Silver Swan\*: 121.640404°E, -30.392349°S; Kurnalpi (SH 51–10), Gindalbie (3237); ~42 km northeast of Kalgoorlie.

### ***Classification***

- 3. Komatiitic flows and related sill-like intrusions; 3.B. Disseminated Ni-Cu-PGE sulphides in central parts of thick dunite bodies.

### ***Geological setting***

The Black Swan komatiite sequence, in the Eastern Goldfields Superterrane of the Archean Yilgarn Craton in Western Australia consists of dominantly olivine-rich cumulates with lesser volumes of

spinifex-textured rocks, interpreted as a section through an extensive komatiite lava flow field. The sequence hosts a number of Ni-sulphide orebodies, including the Silver Swan massive shoot and the Cygnet and Black Swan disseminated orebodies (Barnes, 2004).

### **PGE mineralisation**

Barnes (2004) researched the Ni-sulphide ores in the Black Swan deposits and a modified table of results is presented below in Appendix Table K.3.

Median composition of individual ore samples from the various massive and disseminated orebodies and standard deviation (SD) over indicated number of samples (modified after Barnes, 2004).

*Appendix Table K.3 Geochemical data of Ni-sulphide ores in the Black Swan deposits (modified from Barnes, 2004).*

	Massive ores								Disseminated ores			
	Black Duck		Gosling		Silver Swan		White Swan		Black Swan		Cygnet	
	Median	SD	Median	SD	Median	SD	Median	SD	Median	SD	Median	SD
S (%)	10.36	4.76	17.91	10.44	29.65	15.14	32.50	15.23	1.41	1.67	4.01	7.35
Ni (%)	4.95	3.38	6.98	3.66	11.70	6.66	10.10	4.83	1.70	2.22	3.19	3.60
Cu (%)	0.02	0.05	0.19	0.19	0.28	0.10	0.39	0.51	0.06	0.04	0.16	0.10
Os (ppb)	223	140	53	95	125	159	245	152	37	61	12	14
Ir (ppb)	124	100	21	24	102	113	213	123	19	12	12	12
Ru (ppb)	470	288	37	135	130	294	640	395	31	43	19	25
Rh (ppb)	106	78	46	39	96	76	188	101	15	17	15	11
Pt (ppb)	163	906	113	85	220	220	127	209	52	37	70	51
Pd (ppb)	147	480	187	3188	327	728	148	4482	95	148	210	159
Au (ppb)	6	2	8	10	49	55			9	6	30	50
Total sulphide	41.6	19.6	48.7	25.5	80.7	41.1	86.8	40.5	3.5	4.2	11.5	20.2
<b>In 100% sulphide</b>												
Ni (%)	15.0	3.7	14.2	2.6	16.8	8.5	11.8	1.9				
Os (ppb)	500	243	176	106	199	488	261	146				
Ir (ppb)	322	147	52	25	167	345	226	115				
Ru (ppb)	855	696	131	154	371	777	681	370				
Rh (ppb)	199	240	95	48	137	181	199	90				
Pt (ppb)	419	3003	185	340	387	1736	269	257				
Pd (ppb)	304	1624	312	12581	761	4859	261	22446				
Au (ppb)	12	2	11	38	109	556						
Cu (%)	0.3	0.3	0.4	0.7	0.5	2.7	0.7	3.8				
Number of samples	8		17		181		17		21		18	

Barnes (2004) concluded that '*... the massive sulfide orebodies of the Black Swan Succession are pervasively depleted in all PGEs, particularly Pt and Pd, despite very high Ni contents. This depletion cannot be explained by R-factor variations, which would also require relatively low Ni tenors. The PGE depletion could be explained in part if the ores are enriched in a monosulfide solid solution*

*(MSS) cumulate component, but requires some additional fractional segregation of sulfide melt upstream from the site of deposition. The Silver Swan orebody shows a remarkably consistent vertical zonation in PGE contents, particularly in Ir, Ru, Rh, Os, which increase systematically from very low levels at the stratigraphic base of the sulfide body to maxima corresponding roughly with the top of a lower layer of the orebody rich in silicate inclusions. Platinum shows the opposite trend, but is somewhat modified by remobilisation during talc carbonate alteration. A similar pattern is also observed in the adjacent White Swan orebody. This zonation is interpreted and modelled as the result of fractional crystallisation of MSS from the molten sulfide pool. The strong IPGE (Ir, Os and Ru) depletion towards the base of the orebody may be a consequence of sulfide liquid crystallisation in an inverted thermal gradient, between a thin rapidly cooling upper rind of komatiite lava and a hot substrate.'*

### **Age of mineralisation**

Archean host rocks.

### **Current status**

Historical mines on care and maintenance.

### **Economic significance**

Remnant Ni ores.

### **Major references(s)**

Barnes, S.J., 2004. Komatiites and nickel sulfide ores of the Black Swan area, Yilgarn Craton, Western Australia. 4. Platinum group element distribution in the ores, and genetic implications. *Mineralium Deposita*, 39, 752–765.

### **Relevant figure(s)**

Figure 6.21.

## **K.1.19 Boddington–Darkan\***

### **Geological province**

Yilgarn Craton.

### **Location**

Boddington Au mine\*: 116.3581°E, -32.7509°S; Pinjarra (SI 50–02), Dwellingup (2132).

### **Classification**

- 3. Komatiitic flows and related sill-like intrusions; 3.A. Massive, matrix, and disseminated Ni-Cu-PGE sulphides in preferred lava pathways.

### **Geological setting**

The Archean Saddleback greenstone belt is a north-northwest-trending zone that extends from Mount Wells southeast to Mount Saddleback. The Saddleback belt includes rocks similar to the Eastern Goldfields Superterrane, which hosts Au, Au-Cu, Cu-Zn, and Ni-Cu deposits. The Boddington South greenstone sequence contains basalt, gabbro, andesite, and associated sedimentary units permeated by quartz-vein stockworks.

### ***PGE mineralisation***

Rock-chip sampling has defined anomalous Au, PGEs, and base-metal concentrations (Hoatson and Glaser, 1989).

### ***Age of mineralisation***

Archean host rocks.

### ***Current status***

Historical exploration site.

### ***Economic significance***

Occurrence.

### ***Major references(s)***

Hoatson, D.M. and Glaser, L.M., 1989. Geology and economics of platinum-group metals in Australia. Bureau of Mineral Resources, Australia, Resource Report 5, 81 pp.

### ***Relevant figure(s)***

## **K.1.20 Bodkin, Bodkin North**

### ***Geological province***

Yilgarn Craton.

### ***Location***

Bodkin: 120.157997°E, -26.564850°S; Wiluna (SG 51–09), Wiluna (2944); ~7.5 km west-northwest of Wiluna.

Bodkin North (previously Wiluna M53/457): 120.157520°E, -26.563140°S; Wiluna (SG 51–09), Wiluna (2944); ~7.5 km north-northwest of Wiluna.

### ***Classification***

- 3. Komatiitic flows and related sill-like intrusions.
- 9. Regolith-Laterite also developed at Bodkin North.

### ***Geological setting***

The Bodkin and Bodkin North prospects are located at the northern end of the exposed Agnew–Wiluna greenstone belt, in the Eastern Goldfields Superterrane of the Yilgarn Craton. These prospects are geologically on strike north from the Honeymoon Well Ni deposit. An ultramafic sequence comprising olivine adcumulates, mesocumulates, and orthocumulates with associated spinifex-textured flows occurs within the felsic volcanic and sedimentary units. The ultramafic rocks have been totally serpentinitised and the metamorphic grade increases southward from prehnite-pumpellyite facies near Wiluna to lower amphibolite facies in the Agnew area (Johansen and Bourne, 1995).

### ***PGE mineralisation***

Reverse circulation drilling at the Bodkin prospect intersected Ni-Cu-PGE mineralisation at the base of an ultramafic sequence as follows:

- 1 m @ 6.38% Ni, 0.5% Cu, and 2.5 g/t Pt+Pd (WILRC001 from 72 m); and
- 1 m @ 2.67% Ni, 0.38% Cu, and 1.42 g/t Pt+Pd (WILRC002 from 92 m).

At the Bodkin North prospect, anomalous Ni, Co, Pt, and Pd concentrations were reported in olivine orthocumulate in reverse circulation drill-hole 95WJVP251:

- 74–76 m @ 2.15% Ni, 388 ppb Pt, and 614 ppb Pd; and
- in diamond drill-hole 96WJVD008, with maximum values of 4958 ppm Ni, 118 ppm Co, 103 ppb Pt, and 168 ppb Pd reported at the 63–65 m level within a lateritic section.

### ***Age of mineralisation***

The Ni-Co-Co and associated PGE mineralisation in the primary rocks is associated with ~2705 Ma komatiites.

### ***Current status***

Exploration site.

### ***Economic significance***

Occurrence.

### ***Major references(s)***

Independence Group NL, 2007. Quarterly report 31 March 2007. Independence Group NL announcement to the Australian Securities Exchange, 31 pp.

Johansen, P. and Bourne, B., 1995. Annual technical report for the period ending 14/10/95 on E53/400, Wiluna South SG51–09 Wiluna Western Australia. CRA Exploration Pty. Limited. WAMEX report A46128, 90 pp.

### ***Relevant figure(s)***

Figure 6.21 and Figure 8.24.

## **K.1.21 Bond, Bond (WAMIN)**

### ***Geological province***

Halls Creek Orogen.

### ***Location***

Bond: 127.316101°E, -18.418961°S; Mount Ramsay (SE 52–09), Angelo (4361); ~44 km west-southwest of Halls Creek.

Bond (WAMIN): 127.319770°E, -18.417140°S; Mount Ramsay (SE 52–09), Angelo (4361).

### ***Classification***

- ?1. Layered tholeiitic mafic-ultramafic intrusions.

### ***Geological setting***

Occurrence located in the Central Zone of the Halls Creek Orogen.

### ***PGE mineralisation***

At the Bond occurrence, a drill-hole intersection returned 9 m @ 0.78 g/t PGEs+Au from a drill-hole depth of 26 m, including 1 m @ 2.49 g/t PGEs+Au from a drill-hole depth of 27 m (Northern Star Resources Limited, 2006a).

At the Bond North prospect, PGE mineralisation is associated with a weak NE-trending magnetic anomaly. Best drill-hole intersections reported from drill-hole RBC-014 were 1 m @ 0.29 ppm Pt and 0.66 ppm Pd, from a drill-hole depth of 44 m, and 3 m @ 2.2 ppm Au from 67 m (Northern Star Resources Limited, 2006a).

### ***Age of mineralisation***

Proterozoic host rocks.

### ***Current status***

Exploration site.

### ***Economic significance***

Occurrence.

### ***Major references(s)***

Griffin, T.J., Tyler, I.M., Orth, K. and Sheppard, S., 1998. Geology of the Angelo 1:100 000 sheet. Western Australia Geological Survey, 1:100 000 Geological Series Explanatory Notes, 27 pp.  
Northern Star Resources Limited, 2006a. Quarterly report for the period ended 30 June 2006.  
Northern Star Resources Limited announcement to the Australian Securities Exchange, 13 pp.  
Northern Star Resources Limited, 2006b. Northern Star Resources Limited Annual Report 2006, 60 pp.

### ***Relevant figure(s)***

## **K.1.22 Breakaway, Curlew, Shrike\* (see also Wildcat–Baron)**

### ***Geological province***

Yilgarn Craton.

### ***Location***

Breakaway PGE: 117.181297°E, -29.038500°S; Ninghan (SH 50–07), Ninghan (2339); ~55 km west-northwest of Paynes Find and ~92 km west of Narndee/Milgoos prospects.

Curlew PGE: 117.18364°E, -29.03936°S; Ninghan (SH 50–07), Ninghan (2339); ~55 km west-northwest of Paynes Find.

### ***Classification***

- ?1. Layered tholeiitic mafic-ultramafic intrusions; ?1.A. Stratabound PGE-bearing sulphide layers.

### ***Geological setting***

The Fields Find intrusive complex in the Warriedar greenstone belt, is a zoned mafic-ultramafic body with maximum dimensions of 3 km by 12 km and covering an area of ~30 km<sup>2</sup> (Appendix Figure K.1). The Warriedar greenstone belt comprises predominantly mafic greenstone sequences of mafic volcanics, interflow BIF units, dolerite and gabbro sills, and ultramafic intrusives. Granitoid bodies are present in the northern and southern parts of the project area and granitoid and porphyry dykes intrude the greenstone sequence. The Fields Find Intrusion is largely covered by laterite and transported sands, with limited exposure of the igneous rocks in the erosional windows around the margins of the complex. Interpretation of aeromagnetics reveals a major east-west-trending fault that bisects the intrusion near the Breakaway, Weiro, and Shrike prospects. A 1998 CSIRO research report (cited in Royal Resources Limited Prospectus, 2006) concluded that the 'Fields Find ultramafic/mafic rocks are layered cumulates forming an intrusive complex, with two possible intrusions, which crystallised from a relatively high-Mg magma with ~12% MgO. Identified rock types include olivine cumulates, augite cumulates, and olivine-augite cumulates, and gabbros containing augite, plagioclase, and ± quartz. Brown hornblende, magnetite, ilmenite, and phlogopite are accessory phases' (Royal Resources Limited, 2006).

### ***PGE mineralisation***

Breakaway PGE: Soil sampling over a 2.2 km strike length defined a PGE anomalous zone of 1.8 km-strike length; 100 m–500 m in width; with Pt+Pd values ranging from 20 ppb to 456 ppb and Cu to 963 ppm. Rock chips in the mineralised zone contain up to 1.83 ppm Pt+Pd and 0.2% Cu. Drill-hole intersections for BAB006 included 25 m @ 0.61 g/t Pt+Pd and 0.16% Cu from surface (Royal Resources Limited, 2006).

Curlew: 5 RAB drill-holes were completed. Broad intercepts of elevated Cu, Ni, and PGEs, including 11 m @ 0.24% Cu, 0.24% Ni, and 0.18 g/t Pt+Pd from 14 m depth. There is potential to host Cu-Ni±PGE±Au and PGE-Ni-Cu sulphide deposits.

Shrike: ~5 km east of Breakaway PGE—soil-geochemical program outlined a 1600 m-long anomaly with values of 63 ppb Pt and 163 ppb Pd. Rock-chip sampling in the prospect area recorded values of 900 ppm Cu, 118 ppb Pt, and 76 ppb Pd (Royal Resources Limited, 2006).

Cormorant: ~7 km north-northwest of the Breakaway prospect and lies in the same stratigraphic position. The prospect has a surface anomaly up to 1020 ppm Cu with coincident values of 26 ppb Pt and 43 ppb Pd (Royal Resources Limited, 2006).

### ***Age of mineralisation***

Unknown.

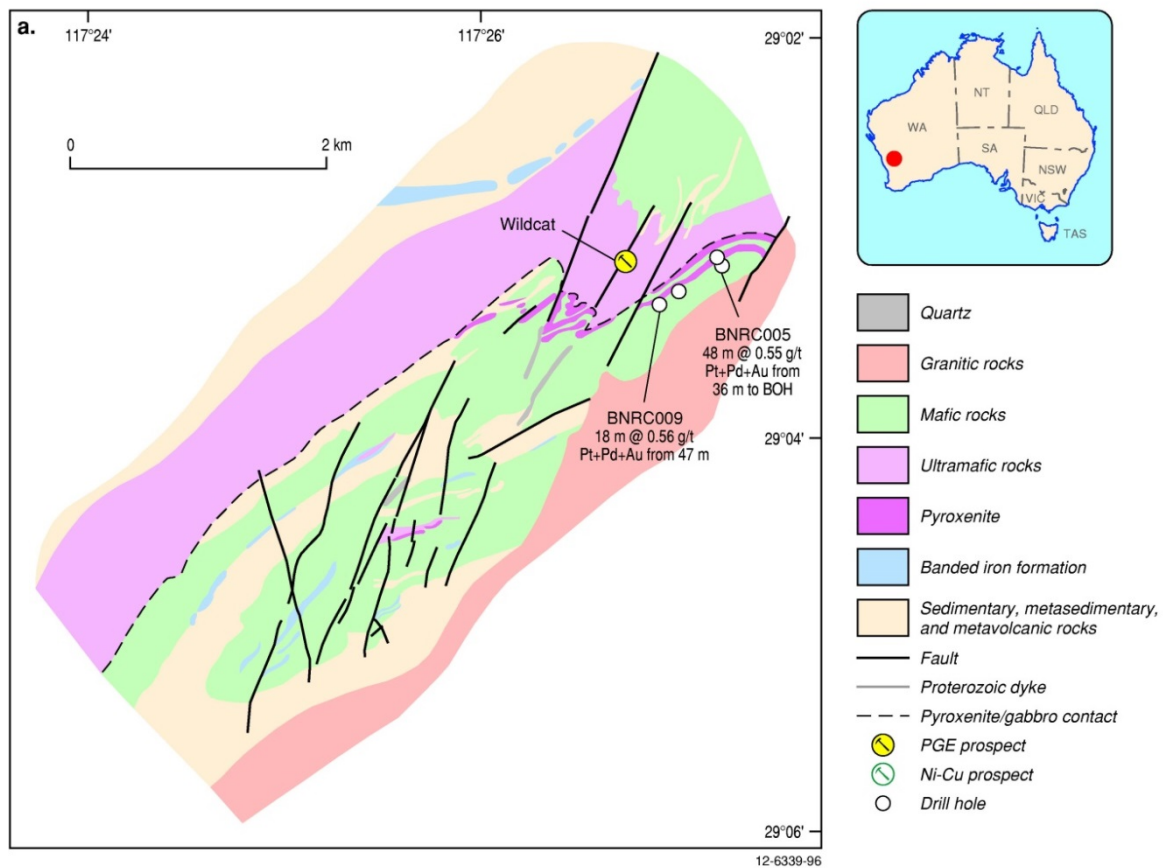
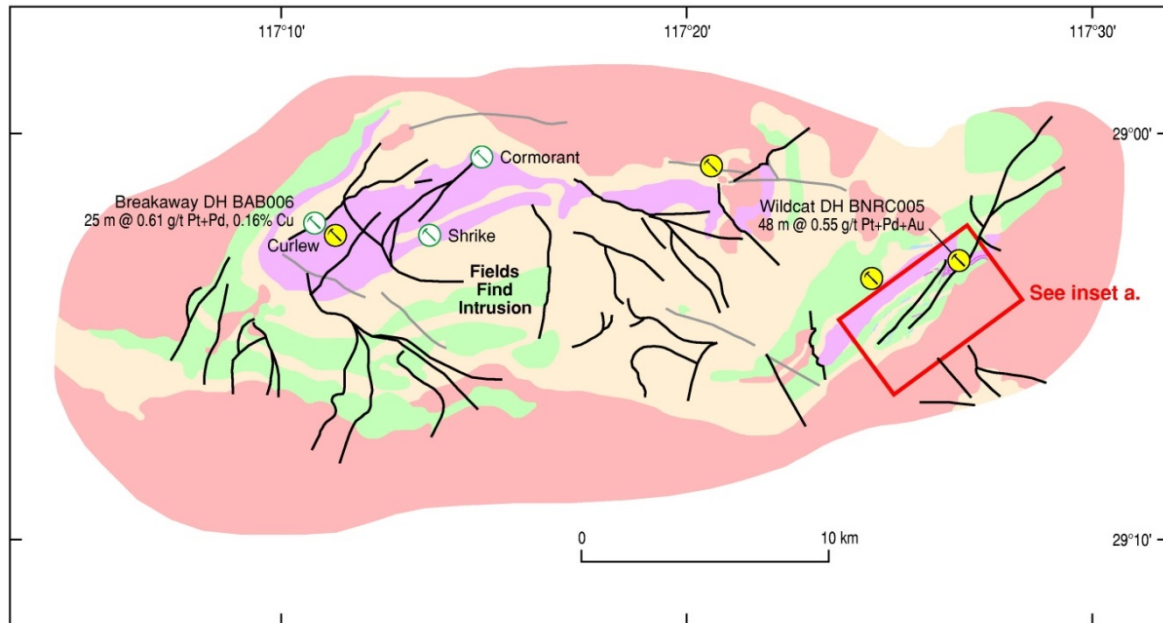
### ***Current status***

Exploration site.

### ***Economic significance***

Occurrences.

Western Australia



Appendix Figure K.1 Geological setting of the Breakaway, Cormorant, Shrike, Curlew, and Wildcat PGE Ni-Cu and Ni-Cu-PGE prospects in the Fields Find Intrusion, Yilgarn Craton, Western Australia. Inset (a). Detailed geology of the Wildcat PGE-Ni-Cu prospect region. Both figures are modified from Royal Resources Limited (2006).

**Major references(s)**

Royal Resources Limited, 2006. Royal Resources Limited 2006 Prospectus, 28 February 2006, 85 pp.

## ***Relevant figure(s)***

Appendix Figure K.1.

### **K.1.23 Bronzite Ridge\***

#### ***Geological province***

Yilgarn Craton.

#### ***Location***

Bronzite Ridge\*: 121.302531°E, -32.177997°S; Lake Johnston (SI 51–01), Bronzite Ridge (3133).

#### ***Classification***

- 9. Regolith-Laterite.

#### ***Geological setting***

Unknown, but considered to be hosted by the 2411 Ma Jimberlana Dyke. The Jimberlana Dyke (Keays and Campbell, 1981) is the best-documented example of a group of Paleoproterozoic (~2410 Ma) dykes that trend west-southwest across the southern part of the Yilgarn Craton in Western Australia. Other prominent examples include Binneringie Dyke and Celebration Dyke. Mafic-ultramafic and mafic types have been the focus of exploration for PGE-Ni-Cu and Ni-Cu-PGE mineral systems. Massive Ni-Cu sulphide-bearing breccia pipes within off-set dykes (or satellite dykes) adjacent to the Jimberlana Dyke in the Yilgarn Craton contain PGEs. The breccia pipes are located below the PGE-enriched stratabound sulphide layers in the upper part of the Ultramafic Series and are sub-parallel to the basal intrusive contact of the intrusion. Exploration by Avoca Resources Limited on the Jimberlana Dyke includes the research and identification of a magma chamber to the south of the dyke and below the main base of the dyke.

#### ***PGE mineralisation***

Maximum PGE contents for gossan samples near Bronzite Ridge (see Jimberlana South and its accompanying Appendix Figure K.9 and Appendix Figure K.10) as reported by Keays and Davison (1976) and Travis et al. (1976) recorded 2.49 ppm Pd, 1.25% Ni, and 0.35% Cu. The deposit has been recorded as a lateritic Ni deposit in the MINEDEX database, but PGEs have not been recorded for this deposit in the database.

#### ***Age of mineralisation***

The Jimberlana Dyke has identical Rb-Sr isochron and Sm-Nd model ages of  $2411 \pm 50$  Ma (Turek, 1966; Fletcher et al., 1987; Myers, 1995).

#### ***Current status***

A small undeveloped Ni-Cu-Co deposit.

#### ***Economic significance***

An Inferred Resource of 4.31 Mt of ore at 1.02% Ni and 0.063% Co has been recorded in the MINEDEX database.

### **Major references(s)**

- Fletcher, I.R., Libby, W.G. and Rosman, K.J.R., 1987. Sm-Nd dating of the 2411 Ma Jimberlana dyke, Yilgarn Block, Western Australia. *Australian Journal of Earth Sciences*, 34, 523–525.
- Keays, R.R. and Campbell, I.H., 1981. Precious metals in the Jimberlana Intrusion, Western Australia: Implications for the genesis of platiniferous ores in layered intrusions. *Economic Geology*, 76, 1118–1141.
- Keays, R.R. and Davison, R.M., 1976. Palladium, iridium and gold in the ores and host rocks of nickel-sulphide deposits in Western Australia. *Economic Geology*, 71, 1214–1228.
- MINEDEX database.
- Myers, J.S., 1995. Geology of the Esperance 1:1 000 000 sheet. Geological Survey Western Australia, 1:100 000 Geological Series Explanatory Notes, 10 pp.
- Travis, G.A., Keays, R.R. and Davison, R.M., 1976. Palladium and iridium in evaluation of nickel gossans in Western Australia. *Economic Geology*, 71, 1229–1243.
- Turek, A., 1966, Rubidium-strontium isotopic studies in the Kalgoorlie–Norseman area, Western Australia. PhD thesis, Australian National University, Canberra, Australia.

### **Relevant figure(s)**

See Jimberlana South and its accompanying Appendix Figure K.9 and Appendix Figure K.10.

### **K.1.24 Brumby**

(see Eastman Bore group)

### **K.1.25 Buckman, Speewah Central\*, Red Hill\***

#### **Geological province**

Halls Creek Orogen, Speewah Basin.

#### **Location**

Buckman: 127.958451°E, -16.294041°S; Lissadell (SE 52–02), Elgee (4465); ~92 km south of Wyndham.

Speewah Central\*: 127.949538°E, -16.361424°S.

Red Hill\*: 127.924427°E, -16.299675°S.

#### **Classification**

- 2. Massive to poorly layered tholeiitic mafic-dominated intrusions; 2.B. Stratabound PGE-bearing magnetitite layers.

#### **Geological setting**

The Speewah Central V-Ti-PGE magnetite deposit, and the Red Hill and Buckman prospects occur in the Hart Dolerite, which forms a large dome in the Speewah Basin located near the easterly margin of the Kimberley Basin and the underlying Halls Creek Orogen.

### ***PGE mineralisation***

The PGE+Au mineralisation in the Speewah deposits occurs in multiple reefs in up to 3 different stratigraphic levels and are associated with a vanadiferous magnetite unit with the best grades at the top of the thickest and highest grade V mineralisation.

Samples from 17 drill-holes in the Buckman prospect returned values ranging from 104 ppb to 245 ppb PGEs+Au (Niplats Australia NL, 2010).

The Speewah Central deposit has an Indicated and Inferred Resource of 851 Mt @ 0.32% V<sub>2</sub>O<sub>5</sub>, 14.9% raw magnetite and 2.1% Ti. PGE values from 43 samples with ≥100 ppb PGEs+Au from about 42 reverse circulation drill-holes in the Speewah Central deposit ranged from 100 ppb to 228 ppb PGEs+Au.

Eight samples with ≥100 ppb PGEs+Au from six drill-holes from the Red Hill prospect have PGEs+Au ranging from 139 ppb to 342 ppb PGEs+Au.

### ***Age of mineralisation***

Age of Hart Dolerite about 1790 Ma (Thorne et al., 1999; Hoatson et al., 2008a,b).

### ***Current status***

Undeveloped deposit, exploration sites.

### ***Economic significance***

Speewah Central is a large deposit currently undergoing pre-feasibility scoping studies. Vanadium mineralisation at the Buckman prospect is reported to extend over an area of 9 km by 2 km and is up to 80 m-thick, and over 6 km by 1.5 km at the Red Hill prospect (Niplats Australia NL 2009).

### ***Major references(s)***

Niplats Australia Limited, 2009. Drilling extends vanadium at Red Hill and Buckman. Announcement to the Australian Securities Exchange, 1 December 2009, 10 pp.

Niplats Australia Limited, 2010. New platinum results at Speewah. Niplats Australia Limited announcement to the Australian Securities Exchange, 10 February 2010, 5 pp.

Thorne, A.M., Sheppard, S. and Tyler, I.M., 1999. Lissadell, Western Australia, 1:250 000 Geological Series Explanatory Notes, Sheet SE 52–2. Geological Survey of Western Australia, Perth, Western Australia, Australia, 68 pp.

### ***Relevant figure(s)***

Figure 8.9 and Figure 8.10.

## **K.1.26 Bullock PGE**

(see Eastman Bore–Louisa Downs group)

## **K.1.27 Byro East**

### ***Geological province***

Yilgarn Craton.

**Location**

Byro East: 116.387001°E, -26.037849°S; Byro (SG 50–10), Byro (2145); ~365 km north-northeast of Geraldton.

**Classification**

- ?2. Massive to poorly layered tholeiitic mafic dominated intrusions; ?2.A. Segregations of Ni-Cu-Co-PGE sulphides in feeder conduits and basal contacts.

**Geological setting**

The Byro East ultramafic complex, within the Narryer Terrane, consists of four zones with a total exposed area of 6 km<sup>2</sup> and a combined basal contact length of 29 km. The intrusion trends north-northwest and a long, narrow 'tail' and smaller intrusions on the southern end of the body of the main intrusion may be part of the 'feeder zone'.

**PGE mineralisation**

The ultramafic rocks of the intrusion have been serpentinised and petrological analyses have identified lizardite, antigorite as well as sulphide minerals pentlandite, millerite, chalcopyrite, native copper, and traces of chrome spinel. Analyses of rock-chip samples collected from the Byro East prospect, 2 km north of the Byro Homestead, are listed in Appendix Table K.4 below.

*Appendix Table K.4 Geochemical data of rock-chip samples from the Byro East prospect.*

Sample	Cu (%)	Au (ppb)	Pt (ppb)	Pd (ppb)	Ni (ppm)
MBCR186	25.5	200	38	28	287
MBCR187	0.002	18	2	1	440
MBCR188	0.0004	1	11	4	2070
MBCR190	0.003	2	3	6	238
MBCR191	7.49	468	2	10	936
MBCR192	0.01	3	45	3	1290
MBCR193	0.004	1	4	1	2380
MBCR194	2.23	382	1	2	894
MBCR195	3.28	27	3	3	954
MBCR196	0.58	18	2	1	297

The anomalous Cu, Au, and PGE mineralisation is hosted by sheared metagabbro, bounded to the west by pyroxenite, and lateritised cumulus-textured ultramafic rock (Athena Resources Limited, 2009). Analyses of drill-hole samples of a reverse circulation drill-hole AHRC0027, which was deepened by diamond drill-hole AHDH0001 are shown in Appendix Table K.5.

Appendix Table K.5 Geochemical data of AHRC0027 and AHDH0001 drill-hole samples from the Byro East prospect.

Drill-hole	Interval (m)	Pt (ppb)	Ni (%)	Mg (%)	Cr (%)	Cu (%)	S (%)	Zone
AHRC0027	0–24	6.7	0.2156	0.4	0.1125	0.0020	0.0166	Laterite
AHRC0027	24–40	5.0	0.1887	19.8	0.0712	0.0008	0.0075	UM; Saprock Zone
AHRC0027	40–44	27.5	0.2590	25.2	0.2860	0.0012	0.0400	Anomalous PGEs, also includes 37.5 ppb Pd; shear at top of serpentinised UM Zone
AHRC0027	44–88	13.3	0.2658	26.2	0.1760	0.0043	0.1950	Serpentinised UM zone with anomalous Ni, PGEs, Cr, and S
AHRC0027	88–149.7	5.0	0.2809	26.2	0.0820	0.0013	0.0791	Serpentinised UM zone
AHDH0001	149.7–152.2	5.0	0.3136	24.2	0.0972	0.0373	0.1630	Serpentinised UM zone with anomalous Ni, Cr, and S, including 0.8 m @ 0.33% Ni from 151.4 m and 1.73 m @ 0.31% Ni from 157.4 m
AHDH0001	152.2–208.4	5.0	0.2872	26.3	0.0821	0.0020	0.0543	Serpentinised UM zone
AHDH0001	208.4–212.4		0.3043	26.3	0.0940	0.0024	0.1025	Serpentinised UM zone with anomalous Ni, Cr, and S, including 4 m @ 0.30% Ni from 208.4 m

UM = Ultramafic.

The diamond drill-hole was deepened to 500 m and analyses of drill-hole samples included intersections of:

- 22.7 m @ 0.30% Ni from 232.3 m;
- 10.5 m @ 0.61% Cr from 354 m;
- 10 m @ 561 ppm Cu from 346.5 m; and
- 0.5 m @ 0.31% S from 254.5 m.

### **Age of mineralisation**

Archean?

### **Current status**

Exploration site.

### **Economic significance**

Occurrences.

### **Major references(s)**

Athena Resources Limited, 2009. Copper mineralisation at Byro East. Athena Resources Limited announcement to the Australian Securities Exchange, 3 December 2009, 4 pp.

Athena Resources Limited, 2012. Byro nickel-copper-PGE project. Athena Resources Limited announcement to the Australian Securities Exchange, 2 February 2012, 18 pp.

**Relevant figure(s)****K.1.28 Cabernet**

(see Malbec-Cabernet, Merlot, Vidure)

**K.1.29 Camel Bore\***

(not in MINEDEX as a PGE occurrence)

**Geological province**

Yilgarn Craton.

**Location**

Camel Bore: original location ~20 km southeast of Lawlers in the East Murchison Goldfields, but no longer recorded in this area due to possible change of name. Exact location uncertain, but appears to be in the general area of the Lawlers Ni group of occurrences and deposits at about 120.682838°E, -28.062266°S; Leonora (SH 51–01), Wildara (3041), which is the location for the Lawlers Ni group in MINEDEX database.

**Classification**

- ?8. Hydrothermal-Metamorphic; ?8.G. U-Au-Pd-Pt mineralisation associated with graphitic schist and carbonaceous shale.

**Geological setting**

Yilgarn Craton.

**PGE mineralisation**

Anomalous Cu, Pb, Zn, and PGE concentrations are associated with Archean mafic-ultramafics with carbonaceous shale and exhalative chert horizons. Drilling in 1970 by Mines Administration Pty Limited reported anomalous Pt (up to 3.4 ppm) and Pd (3 ppm) in four holes north of Camel Bore. Outside Kambalda, these are some of the best PGE intersections reported for the Yilgarn Craton. The PGEs are associated with relatively high Cr analyses (see table below) indicating the PGEs may be associated with disseminated chromite in the ultramafic rocks rather than a carbonaceous shale-PGE association. Further investigations are required to confirm the geological setting of the PGEs. Composite bulk samples of Cr-bearing zones for the best two drill-holes are shown in Appendix Table K.6.

*Appendix Table K.6 Geochemical data of composite bulk samples of chromium-bearing zones in CBP 5 and T3 drill-holes in the Camel Bore prospect.*

Drill-hole	Interval (m)	Cr (%)	Ni (%)	Pt (ppm)	Pd (ppm)
CBP 5	0.0–7.6	0.44	0.42	1.7	3.0
CBP 5	7.6–15.2	0.40	0.27	3.0	2.0
CBP 5	15.2–22.9	1.72	0.40	3.4	0.9
CBP 5	22.9–30.5	1.03	0.52	0.5	0.3

## Western Australia

Drill-hole	Interval (m)	Cr (%)	Ni (%)	Pt (ppm)	Pd (ppm)
CBP 5	30.5–38.1	0.49	0.22	0.3	0.5
T3	0.0–7.6	0.80	0.91	2.2	0.02
T3	7.6–15.2	1.32	0.70	1.3	0.02
T3	15.2–22.9	1.04	0.57	0.5	0.02
T3	22.9–30.5	0.39	0.59	1.8	0.03

(Louthean and Seidel, 1988; Hoatson and Glaser, 1989)

### **Age of mineralisation**

Archean host rocks?

### **Current status**

Historical exploration site.

### **Economic significance**

Occurrences.

### **Major references(s)**

Hoatson, D.M. and Glaser, L.M., 1989. Geology and economics of platinum-group metals in Australia. Bureau of Mineral Resources, Australia, Resource Report 5, 81 pp.

Louthean, R. and Seidel, H., 1988. Platinum. In: Louthean, R. (editor), Register of Australian Mining, 1987. Resource Information Unit Limited, Perth, 217–232.

### **Relevant figure(s)**

Figure 8.19.

## **K.1.30 Camp Oven**

(see The Bulge C2, Rosie and Camp Oven)

## **K.1.31 Canaan**

(see Haran)

## **K.1.32 Carnilya Hill**

(see Kambalda Group)

## **K.1.33 Carr Boyd Rocks\*, Tregurtha\***

### **Geological province**

Yilgarn Craton.

## **Location**

Carr Boyd Rocks: 121.626099°E, -30.065901°S; Kurnalpi (SH 51–10), Gindalbie (3237); ~72 km northeast of Kalgoorlie.

Tregurtha: Approximately 2.5 km south-southwest of Carr Boyd Rocks, this location for Tregurtha is derived from Yilgarn Mining Limited 2005 Annual Report and is not in MINEDEX database.

## **Classification**

- 8. Hydrothermal-Metamorphic; 8.A. Discordant-brecciated bronzite pipes in mafic-ultramafic, and felsic igneous rocks.

## **Geological setting**

The Carr Boyd Rocks Complex intrudes mafic volcanic and sedimentary rocks of the Archean Morelands Group and is itself intruded by Archean granites on the northern side in the Eastern Goldfields Superterrane of the Yilgarn Craton. The geological setting of complex is poorly understood due to limited exposure. This ~2700 Ma body is lobate in outline and mafic-ultramafic rocks types with an aggregate thickness of up to 3000 m cover an area of 75 km<sup>2</sup>. The western, southern, and eastern lobes contain ultramafic rocks, while the centre and north are characterised by overlying mafic and minor ultramafic units. Purvis et al. (1972) subdivided the stratigraphy into five units (I to V) of which three are ultramafic and two are mafic. Rock types in most units (except unit IV) display cyclic layering and are partly to completely altered to metamorphic assemblages of serpentine, magnetite, chlorite, talc, tremolite-actinolite, anthophyllite, and cummingtonite. Rock types in the five units are:

- Unit V—troctolite, olivine anorthosite, norite, and minor dunite, bronzitite, augite norite (approximate thickness 1000 m<sup>+</sup>);
- Unit IV—dunite (250 m);
- Unit III—dunite-harzburgite-bronzitite cycles (200 m), dunite (50 m), and bronzitite (~200 m);
- Unit II—norite, augite norite, olivine norite, harzburgite, and dunite (200 m to 800 m); and
- Unit I—dunite harzburgite-bronzitite cycles (50 m), bronzitite (150 m), dunite-harzburgite-bronzitite cycles (50 m), and bronzitite (150 m).

## **PGE mineralisation**

Most samples in the four ore shoots generally have a similar range of Pt concentrations that range from 6 ppb to ~300 ppb for Ni grades up to ~5%. Ore shoots 1 and 4 have marginally higher Pt concentrations relative to the other two shoots. Greater variations are observed for the Ni grades, which range from ~5% for ore shoots 2 and 4, down to maximum grades of ~3.5% for shoots 1 and 3. Anomalous Pt and Pd concentrations have also been detected from a pyroxenite unit near the base of the mafic-ultramafic stratigraphy and also in stream sediments distant from the mine.

Yilgarn Mining Limited (2005) shows a drill-hole location at a prospect labelled Tregurtha, about 2.5 km south-southwest of the Carr Boyd Rocks decline with a drill-hole intersection of 12 m @ 1% Ni, 0.4% Cu, and 1.2 g/t PGEs in drill-hole RC96CB015. The company reported that this mineralisation is above the basal contact and the hole did not reach that contact.

## **Age of mineralisation**

The age of the complex is tentatively assigned to ~2700 Ma (major mafic-ultramafic magmatic event in the Eastern Goldfields Superterrane), which provides a maximum age constraint for the discordant sulphide-bearing pipe-like bodies.

### ***Current status***

Historical Ni-Cu mine.

### ***Economic significance***

Carr Boyd Rocks is the only non-komatiitic-hosted Ni-Cu-PGE sulphide-deposit that has been mined in the Yilgarn Craton. Anomalous PGEs are associated with Ni-Cu sulphides in discordant breccia pipes of hydrothermal origin, but mining-refining operations have focussed on Ni and Cu, and details of PGE resources are unknown. A drill program in 1969 defined an initial resource of 1.361 Mt @ 1.65% Ni and 0.57% Cu in three shoots numbered 1, 2, and 3 (Marston, 1984). The deposit also contains unquantified additional low-grade mineralisation. The first phase of mining commenced in about 1971 and ceased in 1977 followed by periods of intermittent evaluation, development, and mining. The Carr Boyd Rocks deposit is currently reported to have an Indicated and Inferred Resource of 618 000 t of ore @ 1.375% Ni and 0.478% Cu (Yilgarn Mining Limited, 2006). The economic significance of the PGEs is unknown.

### ***Major references(s)***

- Marston, R.J., 1984. Nickel mineralization in Western Australia. Geological Survey of Western Australia, Mineral Resources Bulletin 14, 271 pp.
- Purvis, A.C., Nesbitt, R.W. and Hallberg, J.A., 1972. The geology of part of the Carr-Boyd Rocks complex, and its associated nickel mineralisation, Western Australia. *Economic Geology*, 67, 1093–1113.
- Yilgarn Mining Limited, 2005. Yilgarn Mining Limited Annual Report 2005, 58 pp.
- Yilgarn Mining Limited, 2006. New Carr Boyd resource estimate. Yilgarn Mining Limited announcement to the Australian Securities Exchange, 10 November 2006, 4 pp.

### ***Relevant figure(s)***

Figure 6.41, Figure 6.42, Figure 6.43, Figure 6.44, and Figure 8.16a.

## **K.1.34 Cattle Creek–Wills Creek**

(see Copernicus group)

## **K.1.35 Chromite Creek**

(see Airstrip Cr Pt group)

## **K.1.36 Cobra\***

(see Dugite–Gum Creek group)

## **K.1.37 Coggia Well, Rocky Well–Irwin Hills**

### ***Geological province***

Yilgarn Craton.

### **Location**

Coglia Well: 123.045998°E, -29.18631°S; Minigwal (SH 51–07), Lightfoot (3539); ~90 km southeast of Laverton.

Rocky Well-Irwin Hills: 123.028099°E, -29.15474°S; Minigwal (SH 51–07), Lightfoot (3539); 89 km southeast of Laverton.

### **Classification**

- 3. Komatiitic flows and related sill-like intrusions; 3.A. Massive, matrix, and disseminated Ni-Cu-PGE sulphides in preferred lava pathways.
- 9. Regolith-laterite; 9.A. PGE-bearing regolith developed on ultramafic-mafic igneous rocks.

### **Geological setting**

Located in the Merolia greenstone belt, in ultramafic rocks underlying lateritic Ni deposits (Abeysinghe and Flint, 2007).

### **PGE mineralisation**

Thick zones of olivine cumulate rocks in the Rocky Well and Matilda-Coglia Well prospect may represent komatiitic lava channels. Laterally extensive areas containing highly elevated Ni-Cu-PGE geochemistry have been defined by the drilling of the laterite deposits, with assay results (from limited sampling) of over 1.0 g/t Pt+Pd recorded from several holes. Maximum assays of 3.58 g/t Pt+Pd have been reported from Coglia Well, 1.95 g/t Pt+Pd from Rocky Well, and 1.2 g/t Pt+Pd from Rocky Well North.

### **Age of mineralisation**

Archean host rocks for mineralisation in primary zone. Cenozoic host rocks for the mineralisation in the lateritic profile.

### **Current status**

Dormant exploration site.

### **Economic significance**

PGE occurrences, Rocky Well occurrence coincides with the undeveloped Rocky Well–Irwin Hills lateritic Ni-Co deposit with a JORC code compliant Indicated Resource of 8.8 Mt of ore @ 1.04% Ni and 0.11% Co, plus 1 Mt of Inferred Resources at 1.08 Mt @ 1.06% Ni and 0.12% Co. No PGE values were reported for this deposit.

### **Major references(s)**

Abeysinghe, P.B. and Flint, D.J., 2007. Nickel and cobalt in Western Australia: commodity review for 2005. Western Australia Geological Survey, Record 2007/12, 46 pp.

Brockman Resources Limited, 2008. Brockman Resources Limited Annual Report 2008, 83 pp.

### ***Relevant figure(s)***

## **K.1.38 Collurabbie, Achilles, Troy, Spartacus, Agora, Paros, Argos, Olympia, Rhodes, Leros, Collurabbie North, Collurabbie South**

### ***Geological province***

Yilgarn Craton.

### ***Location***

Collurabbie–Achilles: 122.171866°E, -26.799402°S; Kingston (SG 51–10), Collurabbie (3344); ~205 km north of Laverton;

Collurabbie–Troy: 122.175833°E, -26.810311°S;

Collurabbie–Spartacus: 122.185750°E, -26.835971°S;

Collurabbie–Agora: 122.205701°E, -26.862562°S;

Collurabbie–Paros: 122.217122°E, -26.859707°S;

Collurabbie–Argos: 122.210460°E, -26.880884°S;

Collurabbie–Olympia: 122.216003°E, -26.886450°S;

Collurabbie–Rhodes: 122.217903°E, -26.908550°S;

Collurabbie–Leros: 122.225688°E, -26.915386°S;

Collurabbie North: 121.969398°E, -26.576990°S; Kingston (SG 51–10), Yelma (3244); ~175 km east of Wiluna;

Collurabbie South: 122.190300°E, -27.231871°S; Duketon (SG 51–14), Urarey (3343); ~155 km north of Laverton.

### ***Classification***

- 3. Komatiitic flows and related sill-like intrusions; 3.C. PGE-enriched Ni-Cu sulphides associated with komatiitic and tholeiitic rocks.
- The mineralisation styles at the Collurabbie prospects have been labelled in GSWA MINEDEX database as 'orthomagmatic mafic and ultramafic–layered mafic intrusions'.

### ***Geological setting***

The Collurabbie prospects are located ~170 km east-northeast of the Mount Keith Ni mine. They occur in the poorly exposed Archean greenstone sequences of the Gerry Well (Duketon) greenstone belt, near the northeastern margin of the Yilgarn Craton. The Olympia Prospect consists of a parallel series of narrow ribbon-like bands of komatiitic and ultramafic rocks that dip steeply towards the west within a dominantly basaltic sequence. Narrow zones of massive sulphides, often structurally remobilised and containing the highest grades of Ni, Cu, Co, Au, and PGEs are spatially associated with matrix and disseminated sulphides near the contacts of the ultramafic rocks.

**PGE mineralisation**

Initially reported by WMC Limited in November 2004 of Ni-Cu-PGE drill-hole intersection (5.8 m @ 3% Ni, 2% Cu, 5.3 g/t PGEs) at the Olympia prospect in greenstones at the northeastern margin of the Yilgarn Craton. Ongoing drilling confirmed Ni-Cu-PGE mineralisation at 6 prospects along a greenstone strike length of 20 km. In addition, Paros–Naxos and Zeus are located at two separate greenstone belts east of Agora and Olympia. From south to north the prospects are Leros, Rhodes, Olympia, Argus, Agora, Spartacus, Troy, and Achilles. Massive Ni-Cu-PGE sulphides have been intersected at Olympia and Rhodes (Falcon Minerals Limited, 2009c). Drill-hole intercepts showing some analyses at Collurabbie-Olympia are listed in Appendix Table K.7 below (Falcon Minerals Limited, 2009a,b; 2010). Detailed analytical results for each PGE metal in some of the holes in the previous table are shown in Appendix Table K.8 below (Falcon Minerals Limited, 2005).

*Appendix Table K.7 Select geochemical data from the Collurabbie-Olympia prospects (Falcon Minerals Limited, 2009a,b; 2010).*

Drill-hole	Thickness (m)	From (m)	Ni (%)	Cu (%)	Total PGEs (g/t)	Style of mineralisation
CLD122	0.08	200.18	2.93	2.60	2.24	Massive
CLD125	8.00	64.00	1.23	1.62	3.82	
CLD127	4.00	82.00	1.00	0.55	0.97	
CLD136	1.90	176.00	3.64	2.77	6.95	Massive
CLD136	1.10	184.90	3.67	3.12	7.78	Massive
CLD137	2.00	136.00	2.85	1.77	2.52	Massive
CLD139	12.86	131.64	1.33	0.95	2.69	Massive, matrix, and disseminated
CLD159	5.77	279.43	3.00	1.96	5.29	Massive and matrix
CLD197	1.42	268.27	1.13	0.73	1.34	
CLD199	5.32	226.27	1.05	0.89	1.74	
CLD201	3.74	163.75	1.47	1.59	4.43	
CLD201	1.42	163.75	2.72	2.13	7.49	
CLD202	3.82	153.88	1.74	1.05	2.37	
CLD203	4.38	376.10	0.82	0.30	0.76	
CLD203	0.80	379.10	1.22	0.31	1.14	
CLD211	3.75	189.8	2.21	1.82	3.53	
CLD211	5.05	232.95	0.51	0.37	0.54	
CLD213	0.45	319.95	0.94	0.66	1.89	
CLD215	0.6	215.6	0.36	0.14	0.25	
CLD217	8.4	233.4	0.43	0.13	0.23	
CLD218	12.3	190.8	0.43	0.20	0.33	
CLD219	5.2	188.8	0.38	0.10	0.13	

Appendix Table K.8 Detailed geochemical data for selected drill-holes from the Collurabbie-Olympia prospects (Falcon Minerals Limited, 2005).

Drill-hole	Interval (m)	Thickness (m)	Ni (%)	Cu (%)	Pt (g/t)	Pd (g/t)	Ru (g/t)	Rh (g/t)	Ir (g/t)	Os (g/t)	Total PGEs (g/t)	Au (g/t)
CLD122	200.18–200.26	0.08	2.93	0.27	0.04	0.18	0.92	0.71	0.17	0.21	2.24	
CLD125	64–72	8.00	1.21	1.62	1.64	2.00	0.07	0.09	0.02	0.02	3.34	0.23
CLD136	176–177.9	1.90	3.64	2.77	2.42	3.97	0.23	0.22	0.05	0.06	6.95	0.33
CLD136	184.9–186	1.10	3.67	3.12	3.47	3.38	0.42	0.32	0.09	0.10	7.78	0.57
CLD139	131.64–144.5	12.86	1.33	0.95	0.92	1.32	0.12	0.11	0.04	0.04	2.55	0.13
CLD159	279.43–285.2	5.77	3.00	1.96	1.72	2.83	0.32	0.26	0.09	0.07	5.29	0.26

Drilling results from some of the other Collurabbie prospects are summarised below:

- Agora prospect, 3.5 km north-northwest of Olympia, where drill-hole CLAC14 intersected 12 m @ 0.6% Ni, 0.2% Cu, and 0.46 g/t PGEs from 12 m (Falcon Minerals Limited, 2004).
- widespread disseminated Ni-Cu-PGE sulphides were intersected in four drill-holes at the Spartacus Prospect located ~5 km north-northwest of Olympia, included:
  - CLD219: 20.25 m @ 0.38% Ni, 0.10% Cu, and 0.13 g/t PGEs (Pt+Pd) from 188.75 m;
  - CLD218: 5.20 m @ 0.43% Ni, 0.20% Cu, and 0.33 g/t PGEs (Pt+Pd) from 190.8 m;
  - CLD217: 12.25 m @ 0.43% Ni, 0.13% Cu, and 0.23 g/t PGEs (Pt+Pd) from 233.4 m; and
  - CLD215: 8.4 m @ 0.36% Ni, 0.14% Cu, and 0.25 g/t PGEs (P t+ Pd) from 215.6 m.
- the Troy Prospect north of Spartacus, where broad disseminated sulphide zones were intersected, including 20 m @ 0.68% Ni, 0.28% Cu, and 0.62 g/t PGEs from 145 m in CLD040, as well as matrix sulphides along the basal contact (e.g., 0.6 m @ 2.21% Ni, 0.98% Cu, and 0.81 g/t PGEs from 347.10 m in CLD053).

Falcon Minerals were planning to examine the potential for a large, bulk tonnage low-grade Ni-Cu-PGE deposit at the Spartacus and Troy prospects.

Falcon Minerals reported in their 2012 Annual Report that their drilling defined two zones of mineralisation:

- a small high-grade pod of massive to matrix style mineralisation located above a felsic porphyry intrusion (an 'Exploration Target' of the order of 150 000–200 000 t at 1.5%–2.0% Ni, 1.1%–2.0% Cu, 2 g/t–3 g/t PGEs); and
- a larger low-grade zone of disseminated mineralisation located immediately below a felsic porphyry intrusion (an 'Exploration Target' of the order of 600 000–700 000 t at 0.45%–0.55% Ni, 0.3%–0.4% Cu, 0.4 g/t–0.6 g/t PGEs).

### **Age of mineralisation**

Komatiitic host rocks probably Archean (~2705 Ma) by analogy with similar mineralised greenstone belts and Ni-sulphide deposits in the Eastern Goldfields Superterrane that have been dated (Nelson, 1997; Hoatson et al., 2009; Locmelis et al., 2013).

### **Current status**

Exploration sites.

### ***Economic significance***

Occurrences.

#### ***Major references(s)***

- Falcon Minerals Limited, 2004. Second quarter activity report to 31 March 2004, 11 pp.
- Falcon Minerals Limited, 2005. Second quarter activity report to 31 December 2004, Collurabbie WA and Cargo NSW, 18 pp.
- Falcon Minerals Limited, 2009a. Fourth quarterly activity report to 30 June 2009, 19 pp.
- Falcon Minerals Limited, 2009b. Falcon Minerals Limited announcement to the Australian Securities Exchange 14 December 2009, 4 pp.
- Falcon Minerals Limited, 2009c. Updated projects presentation. Submitted to the Australian Securities Exchange, 17 December 2009, 31 pp.
- Falcon Minerals Limited, 2010. Exploration update for Collurabbie project, Western Australia. Falcon Minerals Limited announcement to the Australian Securities Exchange, 26 November 2010, 6 pp.
- Falcon Minerals Limited, 2012. Falcon Minerals Limited Annual Report 2012, 51 pp.
- Hoatson, D.M., Jaireth, S., Whitaker, A.J., Champion, D.C. and Claoué-Long, J.C., 2009. Guide to using the Australian Archaean Mafic-Ultramafic magmatic events map. *Geoscience Australia Record* 2009/41, 135 pp.
- Locmelis, M., Fiorentini, M.L., Barnes, S.J. and Pearson, N.J., 2013. Ruthenium variation in chromite from komatiites and komatiitic basalts—a potential mineralogical indicator for nickel sulfide mineralization. *Scientific Communications, Economic Geology*, 108, 355–364.
- Nelson, D.R., 1997. Evolution of the Archaean granite-greenstone terranes of the Eastern Goldfields, Western Australia: SHRIMP U-Pb constraints. *Precambrian Research*, 83, 57–81.

#### ***Relevant figure(s)***

Figure 6.26, Figure 6.27, and Figure 8.24.

## **K.1.39 Constantine**

### ***Geological province***

Yilgarn Craton.

#### ***Location***

Constantine: 118.93601°E, -28.53007°S; Youanmi (SH 50–04), Youanmi (2640); ~70 km south-southwest of Sandstone.

#### ***Classification***

- 12. Others (minor or unknown to no economic importance).
- ?1. Layered tholeiitic mafic-ultramafic intrusions.

#### ***Geological setting***

The Constantine prospect occurs in the eastern part of the Youanmi greenstone belt which adjoins the Youanmi Igneous Complex in the East Murchison Mineral Field of Western Australia (Van Kranendonk and Ivanic, 2009). This greenstone belt consists of a lower succession of metamorphosed tholeiitic basalt and ultramafic intrusives, with lesser BIFs, felsic volcanics, and porphyry intrusions.

### ***PGE mineralisation***

Platinum-Pd mineralisation was located in drill-hole intersections in two horizons of a major layered mafic-ultramafic intrusion. This latter body forms part of the Yuinmery syncline and is traceable for 13 km along strike on the regional magnetics (Empire Resources Limited, 2012). Drill-hole intersections include:

- YRC10-15: 80 m @ 0.49 g/t Pt+Pd and 0.22% Ni from 28 m in ultramafic rocks containing abundant magnetite and 1%–2% disseminated sulphides. YRC10-16: 28 m @ 0.44 g/t Pt+Pd and 0.16% Ni from 4 m; and 28 m @ 0.31 g/t Pt+Pd and 0.15% Ni from 128 m, both in ultramafic rocks (Empire Resources Limited, 2011a); and
- one RC drill-hole tested a coincident EM and RAB drilling anomaly 500 m north of the Constantine prospect. From 96 m this drill-hole intersected 8 m @ 0.15% Cu, 0.27% Ni, and 0.61 g/t Pt+Pd associated with traces of pyrite in an ultramafic sequence. A subsequent down-hole EM survey detected a weak off-hole conductor at 100 m. (Empire Resources Limited, 2011b).

### ***Age of mineralisation***

Archean host rocks?

### ***Current status***

Dormant exploration site.

### ***Economic significance***

Occurrence, drill-hole intersection.

### ***Major references(s)***

- Empire Resources Limited, 2011a. New dual campaign on Yuinmery after test show December's pgm-nickel discovery is in sulphides. Empire Resources Limited announcement to the Australian Securities Exchange, 2 March 2011, 5 pp.
- Empire Resources Limited, 2011b. Quarterly report for the period ending 30 September 2011, 13 pp.
- Empire Resources Limited, 2012. Quarterly report for the period ending 30 June 2012, 15 pp.
- Van Kranendonk, M.J. and Ivanic, T.J., 2009. A new lithostratigraphic scheme for the northeastern and Murchison Domain, Yilgarn Craton. Technical Papers, Geological Survey of Western Australia, 20 pp.

### ***Relevant figure(s)***

## **K.1.40 Cooya Pooya Gossan**

### ***Geological province***

Pilbara Craton.

### ***Location***

Cooya Pooya: 117.558460°E, -20.998480°S; Roebourne (SF 50–03), Sherlock (2456); ~35 km west-southwest of Whim Creek.

**Classification**

- 2. Massive to poorly layered tholeiitic mafic-dominated intrusions; ?2.A. Segregations of Ni-Cu-Co-PGE sulphides in feeder conduits and basal contacts.

**Geological setting**

The Cooya Pooya Dolerite is a large sill complex which crops out over a strike length of 85 km in the northwest Pilbara sub-basin (Thorne and Trendall, 2001). The PGE occurrence is located at the base of the Cooya Pooya Dolerite where gossanous outcrops occur over differentiated olivine cumulate (Ruddock, 1999).

**PGE mineralisation**

PGE occurrence located by Duval Mining (Australia) Limited in 1984 and re-examined by Hunter Resources NL in 1988. Appendix Table K.9 summarises the PGE data for the Cooya Pooya gossan (McIntyre, 1988).

Appendix Table K.9 Geochemical data of the Cooya Pooya gossan (McIntyre, 1988).

Sample	Au <sup>1</sup> (ppb)	Pt (ppb)	Pd (ppb)	Ru (ppb)	Rh (ppb)	Ir (ppb)	Os (ppb)
304754	170	190	1200	24	55	8.5	4
304758	210	220	830	24	110	12	4
Detection limits	2	0.5	0.5	0.5	0.5	0.5	2

<sup>1</sup> Au not quantitative in NiS fire assay.

One sample of Cooya Pooya 'dolerite' has 2% fresh pyrrhotite and trace chalcopyrite contains 810 ppb Pt+Pd+Au, indicating high PGE tenors in the sulphides.

**Age of mineralisation**

Archean host rocks. No direct ages, maximum age based on U-Pb zircon age range of 2768 Ma to 2752 Ma for the Hardey Formation (SHRIMP U-Pb zircon: Thorne and Trendall, 2001) which the Cooya Pooya Dolerite intrudes (Hoatson et al., 2009).

**Current status**

Historical exploration site.

**Economic significance**

Occurrence.

**Major references(s)**

- Alston, T., 1984. West Pilbara Project, final report on Prospecting Licences 47/21, 47/22, 47/41, 47/122–127 and Exploration Licences 47/68, 47/69, 47/81, 47/173 and 47/174. December 31, 1984. Duval Mining (Australia) Limited. 76 Thomas Street, West Perth. WAMEX report A15241, 1087 pp.
- Hoatson, D.M., Jaireth, S., Whitaker, A.J., Champion, D.C. and Claoué-Long, J.C., 2009. Guide to using the Australian Archean Mafic-Ultramafic magmatic events map. Geoscience Australia Record 2009/41, 135 pp.
- McIntyre, J.R., 1988. Sherlock–Mt Fraser Project. EL47/233, 47/284, 47/307. Hunter Resources NL 1988 Annual Report. Hunter Resources NL WAMEX report A28771.

Ruddock, I., 1999. Mineral occurrences and exploration potential of the west Pilbara: Western Australia Geological Survey Report 70, 63 pp.

Thorne, A.M. and Trendall, A.F., 2001. Geology of the Fortescue Group, Pilbara Craton, Western Australia. Geological Survey of Western Australia, Bulletin 144, 249 pp.

### ***Relevant figure(s)***

## **K.1.41 Copernicus North, Copernicus Deeps, RX1892, Malbec–Wills Creek, Palamino–Wills Creek, Jillian–Wills Creek, Sparrow–Wills Creek, Cattle Creek–Wills Creek, Eileen Bore**

### ***Geological province***

Halls Creek Orogen.

### ***Location***

Copernicus North: 127.990954°E, -17.654519°S; Dixon Range (SE 52–06), McIntosh (4462); ~72 km north-northeast of Halls Creek.

RX1892: 127.990954°E, -17.654519°S; Dixon Range (SE 52–06), McIntosh (4462); ~72 km north-northeast of Halls Creek.

Cattle Creek–Wills Creek: 128.0881°E, -17.46733°S; Dixon Range (SE 52–06), Turkey Creek (4563); ~96 km north-northeast of Halls Creek.

Palamino–Wills Creek: 128.0023°E, -17.63885°S; Dixon Range (SE 52–06), Dixon (4562); ~96 km north-northeast of Halls Creek.

Eileen Bore: 127.99394°E, -17.6533°S; Dixon Range (SE 52–06), McIntosh (4462); ~64 km north-northeast of Halls Creek.

### ***Classification***

- 2. Massive to poorly layered tholeiitic mafic-dominated intrusions; 2.A. Segregations of Ni-Cu-Co-PGE sulphides in feeder conduits and basal contacts.

### ***Geological setting***

The Copernicus North mineralisation is hosted in pyroxenite, probably related to the pyroxenite unit within a small gabbro complex located 200 m to the southwest at the Copernicus Ni-Cu deposit. Company mapping and magnetic surveys indicate that the Copernicus and Salk pyroxenites are part of the one intrusion displaced by ~400 m by a northeast-trending fault.

The Malbec–Wills Creek and Palamino–Wills Creek PGE occurrences are about 2 km northeast of the Copernicus North occurrence, the Jillian–Wills Creek is about 8 km northeast and the Sparrow–Wills Creek and the Cattle Creek–Wills Creek occurrences are 23 km northeast of Copernicus North. Eileen Bore lies 8 km southwest of Copernicus North. Apart from Copernicus North, there is very little information on this group of PGE occurrences.

### ***PGE mineralisation***

No information apart from a rock-chip sample of a pyroxenite (RX1892), which assayed 1.34 ppm Pt+Pd+Au, 0.8% Cu, and 0.9% Ni (Thundelarra Exploration Limited, 2003). The sample was reported to occur within the interpreted Copernicus Intrusion and is located about 500 m northeast of

## Western Australia

Copernicus North. Eight km southwest of Copernicus North, drill intercepts of ultramafic-hosted Ni-Cu mineralisation at Eileen Bore, include 116 m @ 0.9 g/t Pt+Pd+Au, 0.78% Cu, and 0.30% Ni.

Rock-chip samples at from Palamino–Wills Creek prospect returned 1% Ni, 0.7% Cu, and 0.9 g/t PGEs (Navigator Resources Limited, 2004 March QR, ASX, 29 April 2004).

### ***Age of mineralisation***

Proterozoic host rocks.

### ***Current status***

Historical exploration site.

### ***Economic significance***

Occurrences.

### ***Major references(s)***

Abeyasinghe, P.B. and Flint, D.J., 2008. Nickel-cobalt in Western Australia. Geological Survey of Western Australia commodity review for 2006. Geological Survey of Western Australia Record 2008/3, 48 pp.

Navigator Resources Limited, 2004. Quarterly report March 2004, 13 pp.

RSG Global Proprietary Limited, 2003. Independent consulting geologist's report. In: Navigator Resources Limited Prospectus, 21–64.

Thundelarra Exploration, Limited, 2003. Activities report for the quarter ended 30 June 2003.

### ***Relevant figure(s)***

Figure 8.21.

## **K.1.42 Corkwood, Sally Malay Bore 1**

### ***Geological province***

Halls Creek Orogen.

### ***Location***

Corkwood: 128.187698°E, -17.295031°S; Dixon Range (SE 52–06), Turkey Creek (4563); ~118 km north-northeast of Halls Creek.

Sally Malay Bore 1: 128.162800°E, -17.324710°S; Dixon Range (SE 52–06), Turkey Creek (4563); ~4.2 km south-southwesterly of Corkwood.

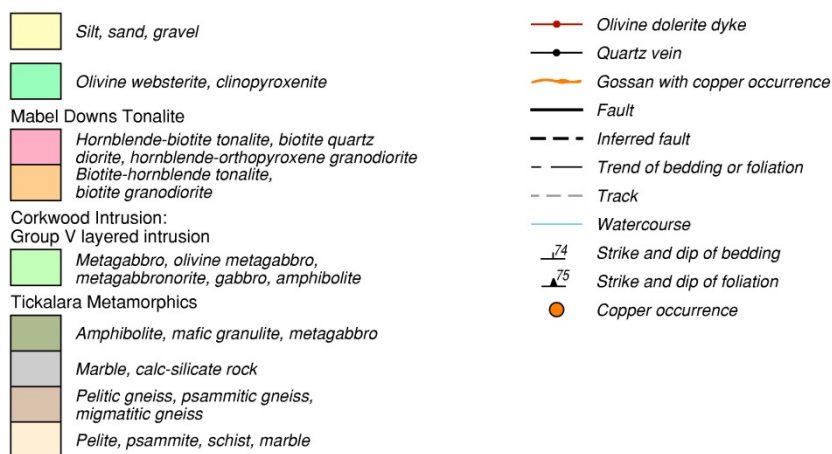
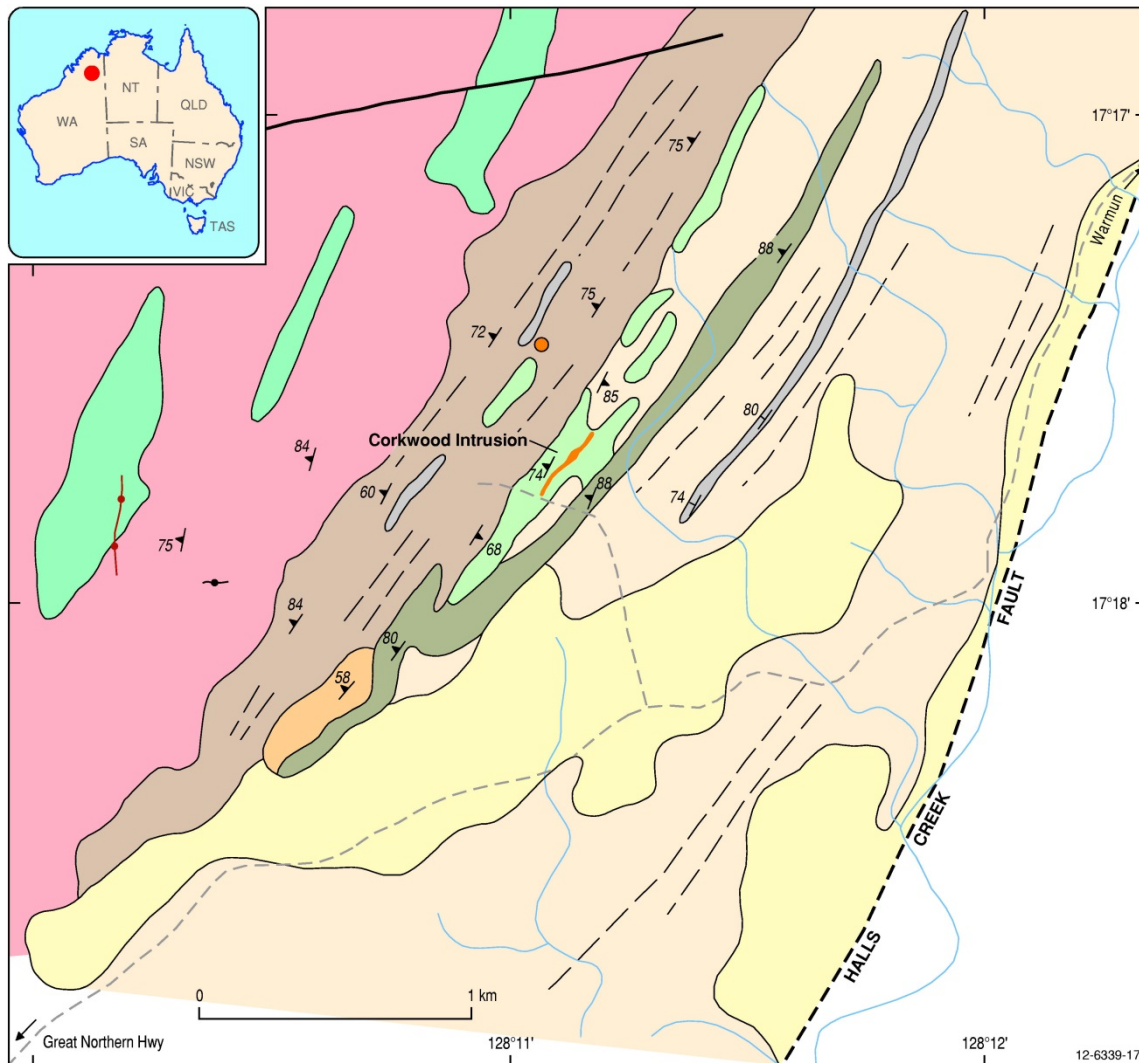
### ***Classification***

- 2. Massive to poorly layered tholeiitic mafic-dominated intrusions; 2.A. Segregations of Ni-Cu-Co-PGE sulphides in feeder conduits and basal contacts.

### ***Geological setting***

Steeply dipping mafic sheet, 2.2 km-long by 0.2 km-wide and 200 m-thick, in a north-northeast-striking narrow zone of high-grade Tickalara Metamorphics bounded by the Halls Creek Fault to the east and the Mabel Downs Tonalite to the west (Appendix Figure K.9). The penetrative foliation in the intrusion dips steeply to the northwest, which is generally concordant with the foliation in the country

rocks (58°–88°) of the Tickalara Metamorphics. The Corkwood body consists of a weakly foliated to massive homogeneous sequence of metagabbro, olivine metagabbro, and metagabbronorite, with no marked compositional layering or ultramafics. Metagabbros are fine- to medium-grained (1 mm–2 mm), weakly foliated uralitised rocks, containing plagioclase, clinopyroxene, orthopyroxene, and minor Fe–Ti oxides, rutile, sulphides, quartz, and biotite. Sulphides occur as thin bands of massive pyrrhotite, pyrite, pentlandite, and chalcopyrite, and as a matrix to silicates. The concentration of the sulphides typically varies markedly over a few centimetres. Pyrrhotite contains exsolved pentlandite, which is altered to violarite, pyrite is secondary after pyrrhotite, and chalcopyrite forms small grains and fine stringers in fractures and cleavages of silicates (Hoatson, 2000).



Appendix Figure K.2 Geological setting of the Corkwood Intrusion, Halls Creek Orogen, Western Australia. A copper gossan near the centre of the intrusion is hosted by massive, weakly foliated metagabbro indicating possible metamorphic remobilisation of sulphides towards low-strain regions. Modified from Hoatson (2000).

**PGE mineralisation**

A recessive limonitic gossan, 220 m by 10 m, with fine boxwork textures and malachite and chrysocolla staining characterises the lower part of the intrusion. Small pods of gossan occur along

strike for most of the length of the intrusion. The main sulphide body plunges 10° towards 35° with sulphide bands below the main gossan generally subparallel to the regional north-northeast-trending foliation. The sulphides are concentrated in massive and weakly foliated metagabbro, indicating possible metamorphic remobilisation and partitioning of sulphides into low-strain regions. BHP Minerals reported in an exploration report in 1996 that the best assays for Cu, Ni, Au, and Pd came from the Corkwood gossan and were 6.5%, 1.34%, 64 ppb, and 41 ppb, respectively, no other details are available.

Results from two gossan (?) samples from the Sally Malay Bore 1 area are shown in Appendix Table K.10 (Dampier Mining Company, 1973):

*Appendix Table K.10 Geochemical for the Sally Malay Bore 1 gossan (Dampier Mining Company, 1973).*

Sample	Cr (ppm)	Co (ppm)	Ni (ppm)	Cu (ppm)	Zn (ppm)	Pt (ppm)	Pd (ppm)
KMB387	2050	104	1400	3000	74	0.82	0.19
KMB388	450	68	1500	9.1%	32	0.06	0.26

### **Age of mineralisation**

Correlated with the 1844 ± 3 Ma Savannah Intrusion, but may be older (>1850 Ma), or possibly coeval with deformed metamorphosed mafic bodies in the Tickalara Metamorphics (Hoatson et al., 2006).

### **Current status**

Historical exploration site.

### **Economic significance**

Occurrences.

### **Major references(s)**

BHP Minerals Proprietary Limited, 1996. BHP Minerals Proprietary Limited Annual Report for period 01/08/1995–01/08/1996. M9061/1: Kimberley Region diamond/gold/base metals exploration. WAMEX report reference A49625.

Dampier Mining Company, 1973. Mineral claims 80/4159–4161, 80/4166, 80/4167, 80/4258–4264. Kimberleys, Western Australia. Dampier Mining Company Annual Report 1973. Geological Survey Western Australia, WAMEX Report A4813, 83 pp.

Hoatson, D.M., 2000. Geological setting, petrography, and geochemistry of the Palaeoproterozoic layered mafic-ultramafic intrusions. In: Hoatson, D.M. and Blake, D.H. (editors), *Geology and economic potential of the Palaeoproterozoic layered mafic-ultramafic intrusions in the East Kimberley, Western Australia*. Canberra: Australian Geological Survey Organisation Bulletin 246, 99–162.

Hoatson, D.M., Jaireth, S. and Jaques, A.L., 2006. Nickel sulfide deposits in Australia: Characteristics, resources, and potential. *Ore Geology Reviews*, 29, 177–241.

### **Relevant figure(s)**

Figure 8.21 and Appendix Figure K.10.

## **K.1.43 Corner Well**

(see Wondinong, Corner Well, Narndee/Milgo)

### **K.1.44 Cosmos, Cosmos Deeps, Cosmos Group, Cosmos Resources Group, Prospero\***

#### ***Geological province***

Yilgarn Craton.

#### ***Location***

Cosmos: 120.575699°E, -27.600140°S; Sir Samuel (SG 51–13), Sir Samuel (3042); ~38 km north-northwest of Leinster.

Cosmos Deeps–Alec Mairs: 120.575875°E, -27.596973°S; Sir Samuel (SG 51–13), Sir Samuel (3042); ~38 km north-northwest of Leinster.

Mercury–Cosmos: 120.576936°E, -27.573572°S; Sir Samuel (SG 51–13), Sir Samuel (3042).

Venus–Cosmos: 120.576479°E, -27.583623°S; Sir Samuel (SG 51–13), Sir Samuel (3042); ~40 km north northwest of Leinster.

Cosmos–North: 120.571282°E, -27.592189°S; Sir Samuel (SG 51–13), Sir Samuel (3042); ~40 km north northwest of Leinster.

Cosmos–West: 120.575699°E, -27.500140°S; Sir Samuel (SG 51–13), Sir Samuel (3042); ~38 km north northwest of Leinster.

Prospero Nickel\*: 120.581727°E, -27.638546°S; Sir Samuel (SG 51–13), Sir Samuel (3042); ~4.5 km south of Cosmos.

#### ***Classification***

- 3. Komatiitic flows and related sill-like intrusions; 3.A. Massive, matrix, and disseminated Ni-Cu-PGE sulphides in preferred lava pathways.

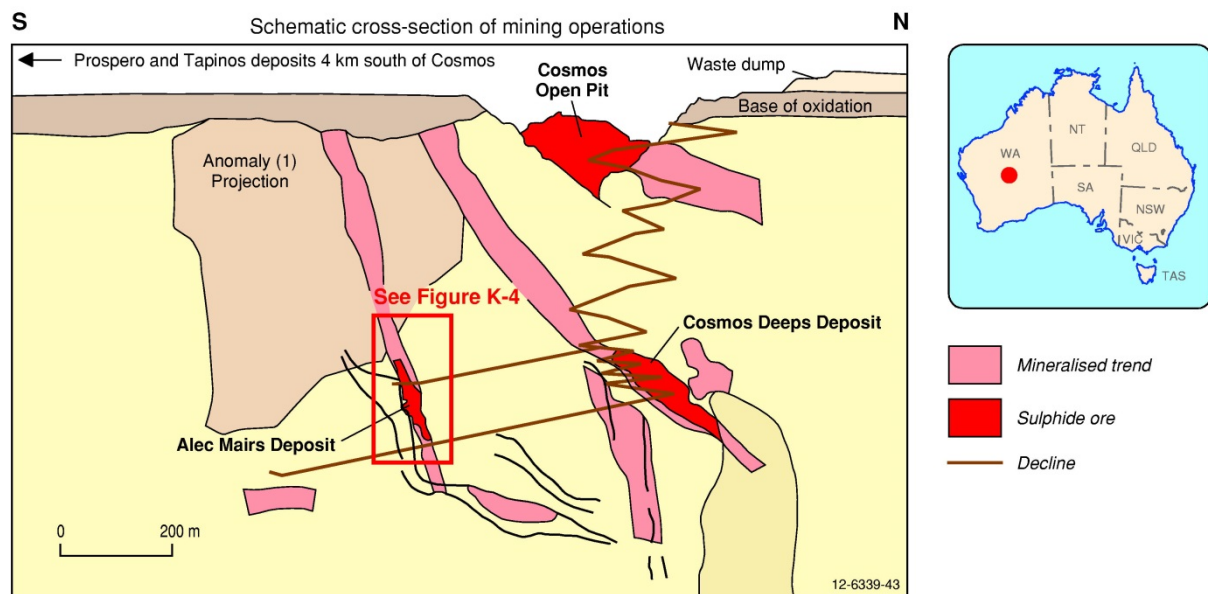
#### ***Geological setting***

The following description is modified after Langworthy (2004). Cosmos is situated within the Agnew–Wiluna portion of the Norseman–Wiluna greenstone belt in the northern part of the Eastern Goldfields Superterrane (Figure 6.21). The location of the deposits is near the junction of the northwestern-trending Keith–Kilkenny Tectonic Zone and the north-trending Miranda Shear. The area is divided into three geological zones, locally termed the Western, Central, and Eastern Zones. The Western Zone consists of a northeast-striking and southeast-facing sequence of tholeiitic lavas, differentiated gabbroic sills, and ultramafic chloritic schists, metamorphosed to upper greenschist facies. The Eastern Zone comprises a northerly striking, east-dipping sequence of felsic, mafic, and ultramafic volcanic and sedimentary rocks, with an upper greenschist to mid-amphibolite metamorphic grade. The ultramafic rocks consists of a series of komatiitic lava flows containing primary igneous textures, including spinifex and cumulus textures, which have been variably hydrothermally altered. The ultramafic rocks in the Eastern Zone contain the Ni-sulphide deposits at Perseverance, Yakabindie, Mount Keith, and Honeymoon Well (all type 3.B. deposits), and, before the discovery of Cosmos, were historically the target for most Ni exploration in the district. The Western and Eastern zones are separated by the Central Zone, which is a mixed package of rocks comprising the heterogeneous Jones Creek Conglomerate; felsic, mafic, and ultramafic volcanic rocks; felsic volcanoclastic sedimentary rocks; and doleritic and felsic porphyry intrusions. The Cosmos and Cosmos Deeps deposits are hosted within the Central Zone, and the Alec Mairs deposit is located 450 m further south (Appendix Figure K.3 and Appendix Figure K.4).

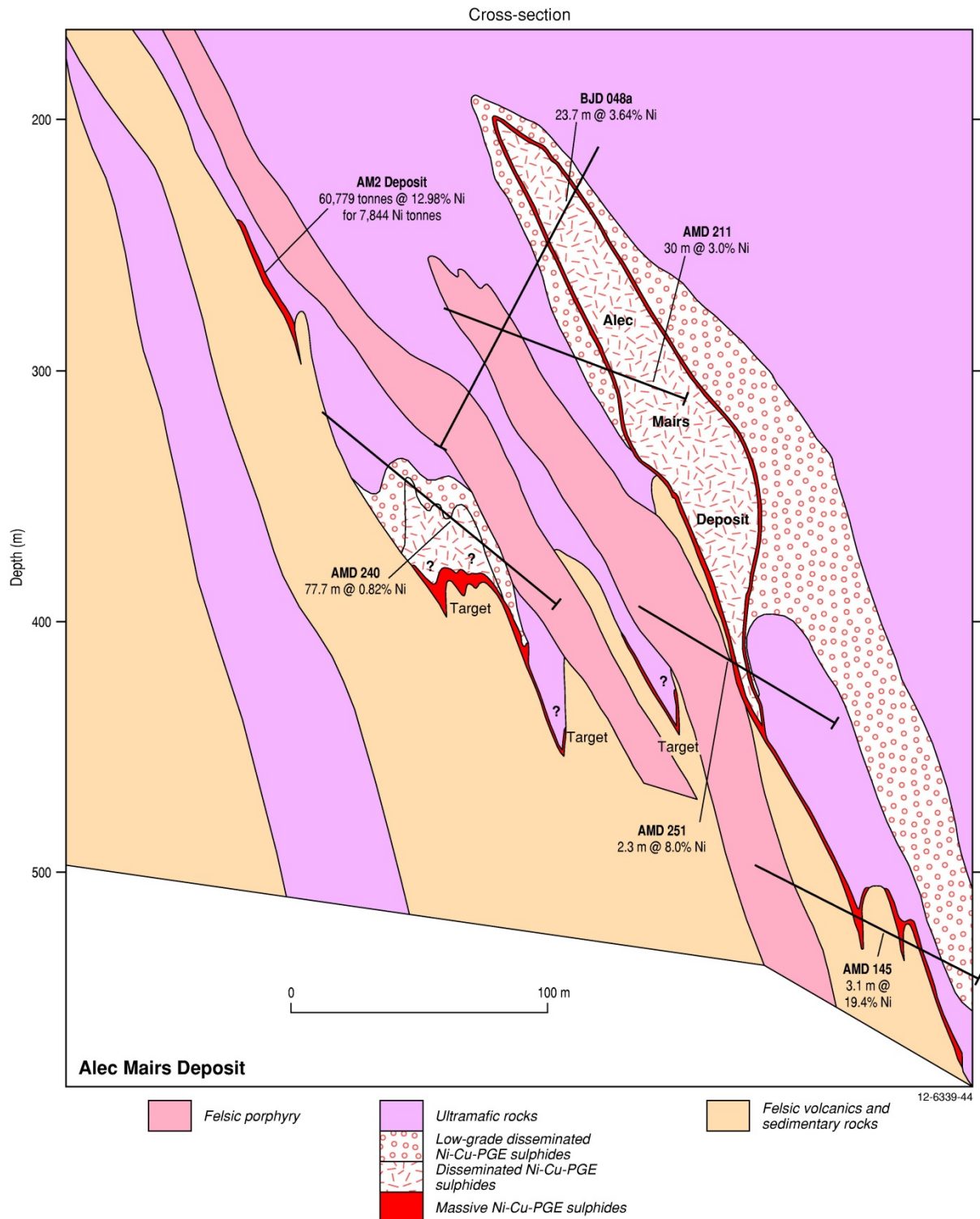
**PGE mineralisation**

Two Ni-sulphide deposits with Cosmos near surface at 100 m- to 150 m-deep and about 200 m-long, and Cosmos Deeps deposit at 400 m–600 m below the surface. The Cosmos deposits represent an essentially *in situ* accumulation of primary magmatic Ni–Fe sulphides. Mineralisation is dominated by massive and semi-massive (breccia and stringer) Ni–Fe sulphides located at the base of an ultramafic unit hosted within the Central Zone (Langworthy, 2004).

Underlying the ultramafic unit and, in most areas, forming the footwall to the Cosmos massive sulphide mineralisation is a mixed sequence of felsic breccia, volcanic and sedimentary rocks, and porphyries. The Cosmos Deeps mineralisation, which consists of several zones of massive, breccia, and stringer Ni–Fe sulphides, is contained entirely within this package of rocks.



Appendix Figure K.3 Schematic north-south cross-section of the Cosmos Open Pit, Cosmos Deeps, and Alec Mairs Ni-Cu-PGE deposits, Yilgarn Craton, Western Australia. Modified from Jubilee Mines NL (2005).



Appendix Figure K.4 Detailed cross-section of the Alec Mairs Ni-Cu-PGE deposit, Yilgarn Craton, Western Australia. Modified from Jubilee Mines NL.

A feasibility study for the Cosmos deposit in June 1998 announced an ore reserve of 420 000 t @ 7.5% Ni. Similarly, an ore reserve of 520 000 t at 7.2% Ni was announced for the Cosmos Deeps deposit in April 2001.

Jubilee Mines NL in their 2002/03 Annual Report published the resource data of the Cosmos Deeps deposit as in Appendix Table K.11 below.

Appendix Table K.11 PGE resource data of the Cosmos Deeps deposit (Jubilee Mines NL, 2003).

Mineral Resource Category	Zone	Tonnes	Density	Ni (%)	Cu (%)	Co (%)	Pt (ppm)	Pd (ppm)
Measured Resource	Main Zone	270 000	3.4	8.7	0.39	0.13	0.3	0.55
Indicated Resource	Main Zone	180 000	3.4	9.9	0.43	0.15	0.34	0.62
Inferred Resource	Hanging Wall Zones	110 000	3.4	3.9	0.19	0.05	0.21	0.26
<b>Total Mineral Resources</b>		<b>560 000</b>	<b>3.4</b>	<b>8.2</b>	<b>0.36</b>	<b>0.12</b>	<b>0.29</b>	<b>0.52</b>

### **Age of mineralisation**

Archean host rocks ~2900 Ma–2700 Ma (Hoatson et al., 2006; Hoatson et al., 2009).

### **Current status**

Historical mine on care and maintenance.

### **Economic significance**

The Cosmos group of Ni-sulphide deposits includes AM5, AM6, Odysseus, Odysseus North, and Mt Goode. Cosmos went into care and maintenance status in 2012, and Xstrata Nickel Australasia Pty Limited, the owner of the Cosmos group of deposits during this time, stated that there were no plans for further exploration or resource conversion to reserve until post-2013 pending the completion of scoping and feasibility studies assessing the viability of the Odysseus deposits.

### **Major references(s)**

- Hoatson, D.M., Jaireth, S. and Jaques, A.L., 2006. Nickel sulfide deposits in Australia: Characteristics, resources, and potential. *Ore Geology Reviews*, 29, 177–241.
- Hoatson, D.M., Jaireth, S., Whitaker, A.J., Champion, D.C. and Claoué-Long, J.C., 2009. Guide to using the Australian Archean Mafic-Ultramafic Magmatic Events Map. *Geoscience Australia Record 2009/41*, 135 pp.
- Jubilee Mines NL, 2003. Jubilee Mines NL Annual Report for the year ended 30 June 2003.
- Langworthy, P., 2004. Cosmos Nickel Project, Kathleen Valley. *Geological Survey Western Australia Record 2004/16*. In: Neumayr, P., Harris, M. and Beresford, S.W.W. (compilers), *Gold and Nickel Deposits in the Norseman–Wiluna Greenstone Belt, Yilgarn Craton, Western Australia—a field guide: Western Australia Geological Survey, Record 2004/16*, 109–115.

### **Relevant figure(s)**

Figure 6.21, Figure 8.24, Appendix Figure K.3, and Appendix Figure K.4.

## **K.1.45 Crabman—Crabman South**

(see Halleys East–Barlee)

## **K.1.46 Cundeelee (now known as Ponton Creek)**

### **Geological province**

Yilgarn Craton.

## **Location**

Cundeelee: 123.274454°E, -30.534756°S; Cundeelee (SH 51–11), Cundeelee (3536); ~235 km northeast of Norseman.

## **Classification**

- 4. Alkaline mafic-ultramafic intrusions; 4.A. Stratabound and disseminated Cu-Au-PGE sulphides.

## **Geological setting**

The ~2025 Ma (Re-Os isochron, Graham et al., 2003, 2004) complex is located at the southeastern margin of the Archean Yilgarn Craton near the intersection of a shear system associated with the Albany-Fraser Orogen to the southeast and the southern extensions of the Laverton Tectonic Zone. The Cundeelee intrusive complex (also known as Ponton Creek) is a deep-seated concealed ultramafic alkaline complex that has carbonatite affinities. It was identified as a distinctive doughnut-shaped aeromagnetic feature. Exploration commenced in the Cundeelee Mission region in the 1970s targeting sandstone-hosted U mineralisation. In 1986, a hole drilled by Union Oil intersected serpentinised pyroxenite at 557 m. In 1994, aerial and ground magnetic and radiometric surveys undertaken by Herald Resources Limited outlined a strong radiometric anomaly in addition to several magnetic anomalies. Surface sampling and small pits dug over the radiometric anomaly in 1995 produced strongly anomalous results up to 23% Rare-Earth Oxides (REO). Galaxy Resources Limited reported in 2011 ([http://www.galaxyresources.com.au/projects\\_ponton.shtml](http://www.galaxyresources.com.au/projects_ponton.shtml)) that Herald Resources completed an aircore-drilling program with the best drill REO intersections being: 16 m @ 14.48% REO (all lanthanide elements plus Y), and 28 m @ 10.50% REO, including 8 m @ 13.12% REO (Hoatson et al., 2011). Further drilling identified a 10 km-wide central core of alkaline ultramafic cumulates. One of the main lithologies intersected in drill-holes in the pre-Permian basement was magnetite-olivine pyroxenite (Union Oil Development Corporation, 1987). In contrast to the nearby economic Mount Weld Carbonatite, there is no development of a paleo-regolith profile due to the scouring of the complex by Permian glaciations.

The main basement lithologies to the carbonatite comprise granitic gneiss, migmatite, and intrusives overprinted by the northeast-trending tectonic fabrics of the Proterozoic Albany-Fraser Orogen. The complex is overlain by 350 m to 550 m of Permian tillite. The 10 km-wide central core of alkaline ultramafic cumulates is cut by veins of primary apatite-rich rauhaugite (hypabyssal dolomitic carbonatite), secondary calcite-magnetite-bearing rocks, and pods and veins of pegmatitic aegirine syenite (Hoatson et al., 2011).

## **PGE mineralisation**

Western Areas NL (2002) reported that analyses of drill samples, presumably of Union Oil Development Corporation diamond drill-hole PC2, analysed by BHP produced anomalous PGEs of up to 89 ppb Pt, 81 ppb Pd, and 70 ppb Au associated with anomalous Ni (up to 1800 ppm), Cu (up to 1000 ppm), Zn (up to 1500 ppm), and up to 1.5% P. Drill-hole PC2 is located in the core area of the Cundeelee complex labelled as 'Unit A'—a reversely magnetised picrite intrusion.

## **Age of mineralisation**

Paleoproterozoic host rock dated at ~2025 Ma (Graham et al., 2003, 2004; Hoatson et al., 2011).

## **Current status**

Exploration site.

### ***Economic significance***

Occurrence.

#### ***Major references(s)***

- Graham, S., Lambert, D. and Shee, S., 2003. Geochemical and isotopic evidence of a kimberlite melonite-carbonatite genetic link. 8th International Kimberlite Conference, Long Abstract, Victoria, British Columbia, Canada, June 22–27, 2003, 5 pp.
- Graham, S., Lambert, D. and Shee, S., 2004. The petrogenesis of carbonatite, melonite and kimberlite from the Eastern Goldfield Province, Yilgarn Craton. *Lithos*, 76, 519–533.
- Hoatson, D.M., Jaireth, S. and Mieziotis, Y., 2011. The Major Rare-Earth-Element Deposits of Australia: Geological Setting, Exploration, and Resources. *Geoscience Australia*, 204 pp.
- Union Oil Development Corporation, 1986. Union Oil Development Corporation Annual Report on exploration EL28/131 Ponton Creek 1986. Submission to WA Mines Department for the period 31.10.85 to 30.10.86, 26 pp. WAMEX report A19987.
- Union Oil Development Corporation, 1987. Union Oil Development Corporation Final Report on exploration EL28/131 Ponton Creek 1987. Submission to WA Mines Department for the period 31.10.85 to 30.10.86, 26 pp. WAMEX report A21981.
- Western Areas NL, 2002. Cundeelee project: Annual technical report for E28/522, Cundeelee for the period 23 December 2000 to 22 December 2001, 23 pp. WAMEX report A64685

#### ***Relevant figure(s)***

### **K.1.47 Cunig**

#### ***Geological province***

Pilbara Craton.

#### ***Location***

Cunig: 117.009140°E, -21.001380°S; Pyramid (SF 50–07), Cooya Pooya (2355); ~30 km south-southwest of Roebourne.

#### ***Classification***

- 8. Hydrothermal-Metamorphic; 8.D. Structurally-controlled remobilised Ni-Cu-PGE±Au.

#### ***Geological setting***

The regional geological framework consists of the 2770 Ma–2717 Ma volcanic and sedimentary rocks of the Fortescue Group which unconformably overlie: (1) folded and faulted 3240 Ma–2930 Ma greenschist to amphibolite facies rocks of the West Pilbara Granite–Greenstone Terrane (volcanic rocks of the ~3130 Ma–3115 Ma Whundo Group and 3240 Ma–2930 Ma granitic rocks of the Cherratta Granitoid Complex); and (2) greenschist facies rocks of the 3010 Ma–2930 Ma Mallina Basin (volcanic and sedimentary rocks of the Whim Creek, Buckingarra, and De Grey groups: Hickman, 2004a). Metabasalts which host the Cunig prospect are part of the Whundo Group.

#### ***PGE mineralisation***

At the Cunig prospect, Ni–Cu mineralisation occupies a shear zone in metabasalt close to a gabbro contact, and two samples of gossan contained very high concentrations of Pd, Pt, and Au. One sample contained 4400 ppb Pd, 980 ppb Pt, and 1.25 g/t Au, in addition to anomalous Ni (720 ppm), Cr (2750 ppm), and Cu (2900 ppm). According to Hickman (2004a) these results are indicative of

potential for gabbro-hosted Ni-Cu-PGE-Au mineralisation, as associated with sanukitoid intrusions in the Mallina Basin (Hickman, 2004b).

### ***Age of mineralisation***

Unknown.

### ***Current status***

Unknown.

### ***Economic significance***

Occurrence.

### ***Major references(s)***

Hickman, A.H., 2004a. Geology of the Cooya Pooya 1:100 000 sheet. Western Australia Geological Survey, 1:100 000 Geological Series Explanatory Notes, 33 pp.

Hickman, A.H., 2004b. Using new-generation maps of the Pilbara to guide mineral exploration. Western Australia Geological Survey, Record 2004/5, 1–3.

### ***Relevant figure(s)***

## **K.1.48 Curlew**

(see Breakaway PGE group)

## **K.1.49 Daltons–Kingsway\***

### ***Geological province***

Pilbara Craton.

### ***Location***

Daltons–Kingsway: 119.164761°E, -21.494564°S; Marble Bar (SF 50–08), North Shaw (2755); ~70 km west-southwest of Marble Bar.

### ***Classification***

- ?3. Komatiitic flows and related sill-like intrusions; ?3.C. PGE-enriched Ni-Cu sulphides associated with komatiitic and tholeiitic rocks.

### ***Geological setting***

The Daltons–Kingsway prospect is located along the basal contact of the Daltons ultramafic complex in the eastern Pilbara Craton.

### ***PGE mineralisation***

Giralia Resources NL reported on 28 January 2003 that historical records from 1971 relating to the Daltons ultramafic complex showed drill intersections of high-grade massive Ni-Cu sulphides at a serpentinite-sedimentary rock contact:

- DDH 3: 3.5 m @ 2.55% Ni and 1.16% Cu, including 0.9 m @ 9.29% Ni and 3.59% Cu; and
- DDH 4: 3.7 m @ 2.41% Ni and 0.61% Cu, including 0.7 m @ 11.81% Ni and 3.11% Cu.

## Western Australia

Rock-chip samples from gossans in the vicinity of the high-grade drill intersections returned up to 13.5% Ni, 17.5% Cu, and 10.5 g/t PGEs.

Later rock-chip sampling along the contact zones of the Daltons Intrusion identified another zone of strongly Ni-Cu-PGE-enriched gossans approximately 400 m north of the original prospect, with >1 g/t PGEs reported over 360 m of strike of malachite-rich gossans along an ultramafic-sedimentary rock contact, with rock-chip samples containing the following high grades (Giralia Resources, 2003a):

- 7.0% Ni, 0.52% Cu, and 52.2 g/t PGEs;
- 6.8% Ni, 12.5% Cu, and 28.3 g/t PGEs; and
- 6.2% Ni, 1.8% Cu, and 13.23 g/t PGEs.

Additional assays of gossans along the basal ultramafic contact in the northern portion of the Daltons ultramafic intrusion returned strongly anomalous Ni, Cu, and PGE values, including (Giralia Resources, 2003b):

- 5.7% Ni, 9.43% Cu, and 7.1 g/t Pt+Pd+Au;
- 1.86% Ni, 3.36% Cu, and 4.7 g/t Pt+Pd+Au; and
- 4.92% Ni, 1.55% Cu, and 3.2 g/t Pt+Pd+Au.

The Kingsway prospect at Daltons comprises a 400 m-long basal contact segment at the northern tip of the 5 km-long Daltons ultramafic body. Follow-up drilling intersected significant Ni as shown in Appendix Table K.12 below. At the Kingsway prospect, drill-hole RDDN029 intersected 3.5 m @ 1.61% Ni, 0.85% Cu, and 0.81 g/t PGEs. Mineralisation is hosted by metasedimentary rocks in the immediate footwall of a thick serpentinised ultramafic body. The sulphides form fine disseminations and fracture-controlled remobilised veinlets (Abeyinghe and Flint, 2007; Giralia Resources NL, 2005a,b,c).

Appendix Table K.12 Geochemical data from the Kingsway Prospect, Daltons.

Drill-hole	Width of intercept (m)	Depth of intercept from (m)	Ni (%)	Cu (%)	PGEs (g/t)
RDDN022	0.50	353.00	1.98	0.97	0.42
RDDN023	0.50	248.10	0.47	0.04	0.12
RDDN027	0.25	317.00	0.4	0.4	0.63
RDDN029	3.50	282.80	1.61	0.85	0.81

The Daltons Ni-Cu-PGE prospect in the southeast Pilbara Craton has distinctive Ni and PGE geochemistry for a komatiite-hosted Ni-Cu-PGE deposit (Giralia Resources NL, 2004; Hoatson et al., 2006). High-Mg ultramafic lithologies have metal grades of up to 13.5% Ni, 17.5% Cu, and 52 g/t PGEs+Au. A narrow basal layer of massive and disseminated sulphides in peridotite and remobilised sulphides in a footwall chert unit have elevated PGEs and low Ni/Cu ratios (<4) similar to the Collurabbie–Olympia prospects in the northeast Yilgarn Craton.

### **Age of mineralisation**

Archean host rocks.

### **Current status**

Historical exploration site.

### ***Economic significance***

Occurrence.

### ***Major references(s)***

- Abeyasinghe, P.B. and Flint, D.J., 2007. Nickel and cobalt in Western Australia: commodity review for 2005. Western Australia Geological Survey, Record 2007/12, 46 pp.
- Giralia Resources NL, 2003a. New nickel, PGE project. Giralia Resources NL announcement to the Australian Securities Exchange, 28 January 2003, 1 pp.
- Giralia Resources NL, 2003b. Giralia Resources NL Annual Report 2003. Report to the Australian Securities Exchange, 55 pp.
- Giralia Resources NL, 2005a. Daltons Project: High grade nickel-copper mineralization confirmed and extended. Report to Australian Securities Exchange, 6 January 2005, 2 pp.
- Giralia Resources NL, 2005b. Daltons nickel Project—significant nickel-copper-PGE intersection at Kingsway Zone. Report to Australian Securities Exchange, 27 October 2005, 2 pp.
- Giralia Resources NL, 2005c. Giralia Resources NL Annual Report 2005. Report to the Australian Securities Exchange, 69 pp.

### ***Relevant figure(s)***

## **K.1.50 Davyhurst Nickel**

### ***Geological province***

Yilgarn Craton.

### ***Location***

Davyhurst Nickel: 120.562640°E, -29.782452°S; Menzies (SH 51–05), Riverina (3038); ~138 km northwest of Kalgoorlie.

### ***Classification***

- 3. Komatiitic flows and related sill-like intrusions.

### ***Geological setting***

The Davyhurst Ni occurrence is located in the Mount Ida greenstone belt in the Eastern Goldfields Superterrane of the Yilgarn Craton. The prospect comprises mafic to ultramafic volcanic rocks in the eastern segment and is dominated by a thick sequence of tholeiitic basalt with units of BIF (Painter et al., 2003).

### ***PGE mineralisation***

Analyses of drill-hole samples identified PGE values in ultramafics as follows:

- NDA 087: 36 m @ 0.65% Ni, 229 ppm Cu, and 34 ppb (Pt+Pd) from 24 m, including 12 m @ 1.1% Ni, 367 ppm Cu, and 58 ppb (Pt+Pd) from 28 m;
- NDA 005: 26 m @ 0.4% Ni, 447 ppm Cu, and 52 ppb (Pt+Pd) from 24 m;
- NDA 003: 16 m @ 0.19% Ni, 1045 ppm Cu, and 126 ppb (Pt+Pd) from 36 m (Nickel Australia Limited, 2005a,b); and
- NDA 009: 1 m @ 1.06% Ni, 241 ppm Cu, and 90 ppb (Pt+Pd) from 21 m; Hole NDA 025: 1 m @ 1.21% Ni, 1360 ppm Cu, and 120 ppb (Pt+Pd) from 32 m; NDA 084: 1 m @ 1.15% Ni, 273 ppm Cu, and 45 ppb (Pt+Pd) from 29 m (Nickel Australia Limited, 2005a,b).

### ***Age of mineralisation***

Archean host rocks.

### ***Current status***

Historical exploration site.

### ***Economic significance***

Occurrence.

### ***Major references(s)***

- Nickel Australia Limited, 2005a. New nickel sulphide targets identified at Davyhurst project.
- Nickel Australia Limited announcement to the Australian Securities Exchange, 7 September 2005, 4 pp.
- Nickel Australia Limited, 2005b. Quarterly activity report for the period ended 30 September 2005, 7 pp.
- Painter, M.G.M., Groenewald, P.B. and McCabe, M., 2003. East Yilgarn Geoscience Database, 1:100 000 geology of the Leonora–Laverton region, Eastern Goldfields Granite–Greenstone Terrane—an explanatory note. Western Australia Geological Survey, Report 84, 45 pp.

### ***Relevant figure(s)***

## **K.1.51 Dead Bullock Well\***

### ***Geological province***

Pilbara Craton.

### ***Location***

Dead Bullock Well\*: ~90 km southwest of Marble Bar; exact location unknown.

### ***Classification***

- ?1. Layered tholeiitic mafic-ultramafic intrusions.

### ***Geological setting***

The rock types at Dead Bullock Well include interbedded mafic-ultramafics, metasediments, BIFs, and amphibolite schists flanked to the southwest by gneiss, granite, and pegmatite dykes. The amphibolite schists are believed to be metamorphosed gabbroic rocks, forming the major part of a layered complex up to 330 m-wide, while the ultramafics represent a differentiated portion of the complex. Intruding the complex is a coarse-grained altered chrysotile pyroxenite body, which has a circular outcrop and has been interpreted as a pipe.

### ***PGE mineralisation***

Drilling 4 km southeast of the pipe in the layered complex delineated anomalous Pd values in chromiferous ultramafic rocks (Hoatson and Glaser, 1989).

### ***Age of mineralisation***

Archean host rocks?

### ***Current status***

Historical exploration site.

### ***Economic significance***

Occurrence.

### ***Major references(s)***

Hoatson, D.M. and Glaser, L.M., 1989. Geology and economics of platinum-group metals in Australia. Bureau of Mineral Resources, Australia, Resource Report 5, 81 pp.

### ***Relevant figure(s)***

## **K.1.52 DeGrussa**

(PGEs recorded for DeGrussa Environmental Group, DeGrussa Operations Group, DeGrussa Open Pit, DeGrussa Resource Group, DeGrussa Underground, Evans Decline)

### ***Geological province***

Bryah Basin.

### ***Location***

DeGrussa open pit: 119.328132°E, -25.540623°S; Peak Hill (SG 50–08), Doolgunna (2746); ~148 km northwest of Wiluna.

### ***Classification***

- 12. Others (minor or unknown to no economic importance); 12.A. PGE enrichment in volcanogenic-massive sulphides.

### ***Geological setting***

The DeGrussa volcanogenic sulphide deposits are located at the boundary zone between the Archean Marymia Inlier and the Proterozoic Bryah Basin, and are hosted within the Narracoota Volcanics of the Bryah Group (Geological Survey of Western Australia, 2010; Sandfire, 2011a,b).

### ***PGE mineralisation***

PGE mineralisation was reported in the drill-holes of the DeGrussa deposit in the earlier drilling programs as indicated below:

- DGRC101: 22 m (96 m to 118 m) @ 3.6% Cu, 3.8 g/t Au, and 13.4 g/t Ag (includes 5 m @ 17.4 g/t Au from 115 m), and 18 m (126 m to 144 m) @ 2.9% Cu, 13.0 g/t Ag, 2.1% Zn, and 1.0 g/t Pd;
- DGRC104: 26 m (117 m to 143 m) @ 3.2% Cu, 2.9 g/t Ag, 1.3% Zn, and 2.4 g/t Pd, and 75 m (160 m to 235 m) @ 2.4% Cu and 10.9 g/t Ag;
- DGRC105: 47 m (93 m to 140 m) @ 5.3% Cu, 20.1 g/t Ag, and 1.0% Zn; and
- DGRC106: 22 m (106 m to 128 m) @ 4.9% Cu, 15.4 g/t Ag, and 0.5% Zn (Sandfire Resources NL, 2009).

### ***Age of mineralisation***

Proterozoic host rocks.

### ***Current status***

Operating mine.

### ***Economic significance***

The deposit was discovered in May 2009. Reserves, Measured, Indicated, and Inferred Resources announced in March 2011 were collectively 14.3 Mt @ 4.6% Cu and 1.6 g/t Au. Open pit and underground mine development commenced in June 2011 (Sandfire Resources NL, 2011).

### ***Major references(s)***

Geological Survey of Western Australia, 2010. Geological Survey of Western Australia Annual Review 2008–09. Geological Survey of Western Australia, 119 pp.

Sandfire Resources NL, 2009. DeGrussa prospect–update. Sandfire Resources NL announcement to the Australian Securities Exchange, 9 June 2009, 3 pp.

Sandfire Resources NL, 2011a. DeGrussa: Approved for development, from concept to cash. Global Investor Presentation, March 2011, 25 pp.

Sandfire Resources NL, 2011b. March 2011 quarterly report highlights, 10 pp.

### ***Relevant figure(s)***

## **K.1.53 Dingo**

### ***Geological province***

Pilbara Craton.

### ***Location***

Dingo: 116.800780°E, -20.950880°S; Dampier (SF 50–02), Dampier (2256); ~25 km south-southwest of Karratha.

### ***Classification***

- ?1. Layered tholeiitic mafic-ultramafic intrusions.

### ***Geological setting***

The Dingo Complex is a group of small isolated ultramafic-mafic bodies 6 km west of the Mount Sholl Intrusion in the west Pilbara Craton. The bodies cover an area of 1.5 km by 5 km and form part of the altered, differentiated Toorare Pool Intrusion, which intrudes Archean Warrawoona Group amphibolites and the Cherratta Batholith. Peridotite, pyroxenite, gabbro, and hybridised gabbroic units are interlayered with felsic and mafic metavolcanics. The intrusive bodies are poorly layered, and the mafic rocks are extensively uralitised to fine-grained assemblages of tremolite-actinolite. One of these bodies contains minor weakly PGE-enriched disseminated sulphides in irregular gabbroic units (McIntyre et al., 1986). Interpretations for the origin of the Dingo intrusions range from rafts in underlying granite gneiss to a sequence of sills, possibly related (?slowly cooled lateral equivalents) to the extrusive komatiites in the Ruth Well Synclinorium, 8 km to the north. This major east- to northeast-trending structure, which is truncated to the south by the Sholl Shear Zone, contains a mineralised bimodal spinifex-textured komatiite and komatiitic basalt suite and associated mafic-ultramafic intrusives, chert, and BIF. At Ruth Well, subeconomic concentrations of disseminated and

minor massive and matrix Ni-Cu sulphides, together with massive magnetite layers, occur in peridotite which has been altered to antigorite, tremolite, chlorite, talc, and carbonate (Nisbet and Chinner, 1981; Hoatson et al., 1992).

### ***PGE mineralisation***

Rock-chip sampling located a small area of anomalous PGE mineralisation near the eastern margin of the intrusion with the highest value of 1.62 ppm Pt+Pd. Ten of the rock-chip samples exceeded 0.5 ppm Pt+Pd (see Appendix Table K.13). The PGEs are associated with minor disseminated chalcopyrite-pyrrhotite-pentlandite in a gabbro pod. One diamond hole was drilled, but failed to intersect significant PGE mineralisation. An intensive rock-chip sampling program was carried out to test for further mineralised pods. No significant PGE or Au mineralisation was recorded (McIntyre et al., 1986).

*Appendix Table K.13 Geochemical data of rock-chip samples from the eastern margin of the Dingo Complex.*

Sample	Lithology	Cu (ppm)	Ni (ppm)	Cr (ppm)	Pt (ppb)	Pd (ppb)	Au (ppb)
62301	Feldspathic pyroxenite	1200	1800	140	410	350	82
62302	Feldspathic pyroxenite	1800	2100	140	490	370	120
62303	Feldspathic pyroxenite	2300	2400	80	810	520	180
62303	Repeat assay	2400	2600	140	120	490	370
62304	Feldspathic pyroxenite	1500	1000	120	150	84	98
62305	Feldspathic pyroxenite	1300	1400	100	310	230	91
62306	Feldspathic pyroxenite	79	200	380	9.5	7.5	7
62307	Coarse-grained gabbro	12	190	260	5.5	4.5	4
62308	Feldspathic pyroxenite	1300	1100	340	310	220	63
62309	Feldspathic pyroxenite	2600	2000	60	690	530	150
62310	Feldspathic pyroxenite	2600	3200	140	930	690	150
62310	Repeat assay	2300	2900	160	760	630	160
62311	Feldspathic pyroxenite	3600	2500	180	770	590	130
62312	Feldspathic pyroxenite	2600	2100	240	560	430	120
62313	Feldspathic pyroxenite	2100	1900	60	260	170	130
62314	Siliceous material	88	94	180	12	8	9
62315	Melagabbro	530	280	280	15	14	28

### ***Age of mineralisation***

Archean host rocks.

### ***Current status***

Historical exploration site.

### ***Economic significance***

Occurrence.

### **Major references(s)**

- Hoatson, D.M., Wallace, D.A., Sun, S.-S., Macias, L.F., Simpson, C.J. and Keays, R.R., 1992. Petrology and platinum-group-element geochemistry of Archaean layered mafic-ultramafic intrusions, west Pilbara Block, Western Australia. Australian Geological Survey Organisation, Bulletin 242, 320 pp.
- McIntyre, J., Parks, J. and Lemmon, T.C., 1986. Toorare Pool Prospect. Hunter Resources Limited, 26 pp.
- Nisbet, E.G. and Chinner, G.A., 1981. Controls on the eruption of mafic and ultramafic lavas, Ruth Well Ni-Cu prospect, West Pilbara. Economic Geology, 76, 1729–1735.

### **Relevant figure(s)**

Figure 6.3.

## **K.1.54 Doolena Gap**

### **Geological province**

Pilbara Craton.

### **Location**

Doolena Gap: 119.750000°E, -20.914170°S; Port Hedland (SF 50–04), Coongan (2856); ~30 km north of Marble Bar.

### **Classification**

- Unknown. The Doolena Gap occurrence is classified in the GSWA MINEDEX database as Cu-Pb-Zn in veins and shears, 'vein and hydrothermal–undivided'.
- ?8. Hydrothermal-Metamorphic.

### **Geological setting**

The Doolena Gap prospect with reported Cu-Pb-Zn mineralisation, occurs in felsic volcanoclastic rocks of the Duffer Formation in the western part of the Doolena Gap greenstone belt of the Pilbara Craton (Van Kranendonk, 2010). The outcrop sampled by Mithril appears to be located about 1 km to the east of the Doolena Gap prospect in mafic and ultramafic rocks of the Warrawoona Group (Mithril Resources Limited, 2010).

### **PGE mineralisation**

Surface samples assayed 0.7% Cu, 0.1% Ni, and 42 ppb Pt+Pd (Mithril Resources Limited, 2010).

### **Age of mineralisation**

Archean host rocks?

### **Current status**

Historical exploration site.

### **Economic significance**

Occurrence.

### **Major references(s)**

Mithril Resources Limited, 2010. New mineralisation identified on the East Pilbara project. Mithril Resources Limited announcement to the Australian Securities Exchange, 19 October 2010, 3 pp.  
Van Kranendonk, M, J., 2010. Geology of the Coongan 1:100 000 sheet. Geological Survey of Western Australia, 1:100 000 Geological Series Explanatory Notes, 67 pp.

### **Relevant figure(s)**

## **K.1.55 Dragonfly–Murray Hills\***

(not in MINEDEX as a PGE occurrence)

### **Geological province**

Musgrave Province.

### **Location**

Dragonfly–Murray Hills: 128.357°E, -25.548°S; Scott (SG 52–06), Holt (4546); ~75 km northwest of Wingellina lateritic Ni deposit and ~4 km northwest of the El Cortez prospect.

### **Classification**

- 9. Regolith-Laterite; ?9.A. PGE-bearing regolith developed on ultramafic-mafic igneous rocks.

### **Geological setting**

Dragonfly is a Ni-Cu-Co-Zn anomaly with peak values of 2.2% Ni, 2.9% Co, 866 ppm Cu, and 1654 ppm Zn. The anomaly is in sand-dune country with sporadic gabbro outcrops. The coincident geochemical and EM anomalies are situated in a flexure in the regional magnetics.

### **PGE mineralisation**

RAB drilling yielded peak results of 1 m @ 0.54% Ni, 0.62% Co, 0.30 g/t PGEs+Au, and 0.33% Cu (Redstone Resources Limited, 2008).

### **Age of mineralisation**

Cenozoic/Proterozoic?

### **Current status**

Historical exploration site.

### **Economic significance**

Occurrences.

### **Major references(s)**

Redstone Resources Limited, 2006. Redstone Resources Limited 2006 Prospectus, 99 pp.  
Redstone Resources Limited, 2008. Redstone Resources Limited 2008 Annual Report, 72 pp.  
Redstone Resources Limited project webpage ([http://www.redstone.com.au/contents\\_projects.html](http://www.redstone.com.au/contents_projects.html))

### **Relevant figure(s)**

Figure 6.16.

### K.1.56 Dugite–Gum Creek, Python–Gum Creek, Sidewinder\*, Cobra\*, Adder\* (Bungarra igneous complex)

#### **Geological province**

Yilgarn Craton.

#### **Location**

Dugite–Gum Creek: 119.563103°E, -27.321590°S; Sandstone (SG 50–16), Montagu (2843); ~82 km north-northeast of Sandstone.

Python–Gum Creek: 119.525803°E, -27.277060°S; Sandstone (SG 50–16), Montagu (2843); ~78 km north-northeast of Sandstone.

#### **Classification**

- 12. Others (minor to no economic importance); ?12.A. PGE enrichment in volcanogenic-massive sulphides.

Volcanic massive-sulphide hosted? Classified in GSWA MINEDEX database as 'volcanogenic Cu-Zn, Stratabound volcanic and sedimentary-volcanic-hosted sulphide'.

#### **Geological setting**

The Ni-Cu-PGE prospects are reported to occur as gossans with coincident EM conductors along the basal margin of the layered Bungarra igneous complex (Legend Mining Limited, 2007a).

#### **PGE mineralisation**

PGE mineralisation first discovered from sampling of gossans at the Python and Dugite prospects in the Bungarra igneous complex (Legend Mining Limited, 2007a). Additional prospects were located, all of which are from north to south as follows–Cobra, Python, Sidewinder, Dugite, and Adder. Results of the initial rock-chip sampling of the gossans at Python and Dugite are listed in Appendix Table K.14 below (Legend Mining Limited, 2007b).

*Appendix Table K.14 Geochemical data of rock-chip sampling from the Python and Dugite gossans. Data from Legend Mining Limited (2007b).*

Prospect	Cu (%)	Ni (%)	Pt (ppb)	Pd (ppb)	Rh (ppb)	Ru (ppb)	Os (ppb)	Ir (ppb)
Python	0.10	0.41	137	1530	548	66	12	56
Python	0.10	0.27	213	242	403	53	8	40
Python	0.21	0.04	22	154	6	<1	<1	<1
Python	0.04	0.02	18	296	65	4	<1	2
Python	0.33	0.22	113	415	85	10	2	6
Python	5.70	0.99	146	500	43	2	3	2
Python	2.10	0.51	91	404	65	7	3	6
Python	0.15	0.55	108	41	316	34	<1	26
Python	0.14	0.55	95	87	200	20	2	18
Python	0.21	0.42	108	221	79	12	4	7
Python	0.38	0.34	387	305	324	13	2	19

Western Australia

Prospect	Cu (%)	Ni (%)	Pt (ppb)	Pd (ppb)	Rh (ppb)	Ru (ppb)	Os (ppb)	Ir (ppb)
Python	0.05	0.08	197	77	31	2	<1	4
Dugite	0.10	0.17	3	170	2	<1	<1	<1
Dugite	0.07	0.10	58	104	12	3	<1	<1
Dugite	0.20	0.11	8	976	8	<1	<1	1
Dugite	0.09	0.23	5	266	2	1	<1	1
Dugite	0.05	0.23	27	101	9	2	<1	1
Dugite	0.02	0.08	105	13	7	1	<1	1
Dugite	0.26	0.45	14	80	5	2	<1	1
Dugite	0.11	0.36	22	111				

The rock-chip sampling was followed by ground EM and high-resolution aeromagnetic surveys. Follow-up drilling provided additional data for the Cobra, Python, Sidewinder, Dugite, and Adder prospects. Analyses of drill-hole samples are tabulated below in Appendix Table K.15 (Legend Mining Limited, 2007b, 2008, 2009).

*Appendix Table K.15 Geochemical data for drill-hole samples from the Cobra, Python, Sidewinder, Dugite, and Adder prospects. Data from Legend Mining Limited (2007b, 2008, 2009).*

Prospect	Drill-hole	From (m)	To (m)	Interval (m)	Ni (%)	Cu (%)	Cr (%)	Pt (ppb)	Pd (ppb)	Zn (%)
Cobra	LGCA178 (AC)	0	6*	6	0.13	0.02	0.26	38	102	
Cobra	LGCA179	0	5*	5	0.14	0.03	0.3	60	115	
Cobra	LGCA180	0	6*	6	0.28	0.08	0.26	70	227	
Cobra	LGCA181	12	15*	3	0.11	0.03	0.15	60	170	
Cobra	LCBC001 (RC)	0	88	88	0.12	0.06	0.20	39	128	0.02
Cobra	including	52	56	4	0.26	0.29	0.19	105	470	0.02
Cobra	LCBC002	20	44	24	0.11	0.05	0.22	35	103	0.01
Python	LPYC001 (RC)	56	84	28		0.17				
Python		76	80	4	0.16	0.41		175	225	
Python		140	165*	25	0.02	0.01		138	59	
Python	LPYC003	80	104	24		0.11				
Python	LPYC004	12	16	4	0.10	0.14		20	45	
Python		64	80*	16	0.03	0.01		165	55	
Python	LPYC005	76	80	4	0.15	0.25		40	255	
Python	LPYC006	28	44	16	0.08	0.12		29	130	
Python	LGCD001 (DDH)	7	15	8	0.1	0.21		35	256	
Python		40.7	41.2	0.5	0.25	0.29		150	511	
Python		51.4	57	5.6	0.16	0.15		49	268	
Python		69	70	1	0.03	0.08		159	212	
Python		138	140	2	0.07	0.14		108	62	
Sidewinder	LSWC001 (RC)	52	100	48 (CM)	0.02	0.07	0.02	5	5	0.22

Prospect	Drill-hole	From (m)	To (m)	Interval (m)	Ni (%)	Cu (%)	Cr (%)	Pt (ppb)	Pd (ppb)	Zn (%)
Sidewinder		132	156*	24 (MP)	0.12	0.07	0.18	50	169	0.02
Sidewinder	including	136	140	4	0.16	0.12	0.17	85	320	0.02
Sidewinder	LSWC002	56	80	24 (CM)	0.02	0.09	0.03	5	<5	0.27
Sidewinder		120	156*	36 (MP)	0.10	0.05	0.15	35	145	0.02
Sidewinder	including	140	144	4	0.17	0.1	0.16	80	350	0.02
Dugite	LGCC001 (RC)	104	132	28	0.02	0.10	0.02	5	10	0.21
Dugite	LGCC002	184	201*	17	0.02	0.06	0.02	<5	<5	0.20
Adder	LGCC003	52	68	16	0.03	0.01	0.14	215	68	0.02

\* = end of hole.

DDH = Diamond Drill-Hole; RC – Reverse Circulation drill-hole ; AC = Air Core drill-hole.

CM = carbonaceous metasediment; MP = metapyroxenite.

### **Age of mineralisation**

Archean host rocks?

### **Current status**

Exploration site.

### **Economic significance**

Occurrence.

### **Major references(s)**

Legend Mining Limited, 2007a. Legend discovers outcropping copper-nickel-platinum group element mineralisation at Gum Creek. Legend Mining Limited announcement to the Australian Securities Exchange, 10 April 2007, 6 pp.

Legend Mining Limited, 2007b. Legend Mining Limited announcement to the Australian Securities Exchange, 6 August 2007, 6 pp.

Legend Mining Limited, 2008. Legend Mining Limited announcement to the Australian Securities Exchange, 11 February 2008, 9 pp.

Legend Mining Limited, 2009. Legend Mining Limited 2009 Annual Report, 82 pp.

### **Relevant figure(s)**

## **K.1.57 Dundas Gossan, Killaloe Nickel**

### **Geological province**

Yilgarn Craton.

### **Location**

Dundas Gossan: 121.850788°E, -31.919874°S; Widgiemooltha (SH 51–14), Cowan (3234); ~32 km north-northeast of Norseman.

Killaloe Nickel: 121.940651°E, -31.977496°S; Widgiemooltha (SH 51–14), Cowan (3234); ~30 km north-northeast of Norseman.

## **Classification**

- 3. Komatiitic flows and related sill-like intrusions.

## **Geological setting**

The Dundas Gossan and the Halls Knoll Gossan (see Halls Knoll Gossan, Polar Bear), both of the Polar Bear Project, occur on the Polar Bear Peninsula which protrudes northwards into Lake Cowan. The dominant rocks are a sequence of northwest-trending metakomatiite with minor metasiltstone, metagabbro, and dolerite sills. The ultramafic sequence at Polar Bear is locally complexly folded and thick and appears to be structurally thickened by thrust faulting (Sirius Resources NL, 2014b). This is also known to occur at Kambalda and Widgiemooltha and creates opportunities for the repetition of the prospective basal horizon on parallel trends. Such thrusting can also cause remobilisation of Ni sulphide mineralisation and create discrete high-grade massive sulphide deposits (e.g., Flying Fox, Spotted Quoll, and Emily Ann). The ultramafic sequence is extensively concealed with recent sediments of Lake Cowan.

## **PGE mineralisation**

The Dundas Gossan, which occurs beneath a thin layer of salt-lake sediments and surface samples, averaged 2.8% Cu, 0.8% Ni, and 13.3 g/t PGEs, including 2.8 g/t Pt, 5.6 g/t Pd, and 1.0 g/t Rh. The Dundas Gossan is located 550 m to the southeast of the Halls Knoll gossan where Sirius Resources NL has previously reported outcrop grades averaging 1% Cu, 0.75% Ni, and 12.5 g/t PGEs (Sirius Resources NL, 2011a). A drill-hole SPBD0004 near the Dundas Gossan intersected 5 m @ 0.27% Ni, 341 ppm Cu, 0.13 g/t Pd, and 0.06 g/t Pt from 18 m (Sirius Resources NL, 2011b).

Sirius Resources NL (2014a) announced high-grade Ni sulphide mineralisation in the reconnaissance diamond drill-hole SPBD0046 at the Taipan prospect, Polar Bear Project region. The intersection at the Taipan prospect demonstrated the presence of both massive and disseminated Ni-Cu-Co sulphides and the enrichment of PGEs. The intersection was 4.10 m (from 104.4 m) @ 3.8% Ni, 2.45% Cu, 0.08% Co, 0.9 g/t Pt, and 1.6 g/t Pd, including 2.15 m (from 106.0 m) @ 5.84% Ni, 3.73% Cu, 0.12% Co, 1.1 g/t Pt, and 1.65 g/t Pd. Nickel-Cu-PGE-sulphide mineralisation has been identified over 5 km along the Halls Knoll–Taipan trend demonstrating the prospectivity of this underexplored region (Sirius Resources NL, 2014b). The Taipan geology shows similarities to that at Halls Knoll region, some 3 km to the southeast, where previous drilling by Sirius Resources NL and others has intersected disseminated Ni sulphides.

At the Killaloe Ni prospect, the presence of highly anomalous Ni, Cu, and PGEs in gossans developed over the ultramafic units, is recorded in the MINEDEX database.

## **Age of mineralisation**

Archean host rocks?

## **Current status**

Dormant exploration site.

## **Economic significance**

Occurrence.

## **Major references(s)**

Sirius Resources NL, 2011a. New nickel gossan at Polar Bear. Sirius Resources NL announcement to the Australian Securities Exchange, 11 January 2011, 4 pp.

## Western Australia

Sirius Resources NL, 2011b. Further nickel-copper-platinum-palladium mineralisation intersected at Polar Bear. Sirius Resources NL announcement to the Australian Securities Exchange, 16 August 2011, 4 pp.

Sirius Resources NL, 2014a. Nickel exploration update. Sirius Resources NL announcement to the Australian Securities Exchange, 16 July 2014, 27 pp.

Sirius Resources NL, 2014b. Polar Bear nickel exploration update. Sirius Resources NL announcement to the Australian Securities Exchange, 21 July 2014, 12 pp.

### ***Relevant figure(s)***

See Appendix Figure K.7 and Appendix Figure K.8 accompanying Halls Knoll Gossan, Polar Bear.

### **K.1.58 Durkin\***

(see Mt Keith\*)

### **K.1.59 Dusty Bore 2**

(see Lamboo group)

### **K.1.60 East Alpha**

(see Kambalda group)

### **K.1.61 Eastman Bore–Louisa (Eastman Bore (PGE 1 to 18), Eastman Bore (Cu 4), Blackadder, Brumby, Louisa, Bullock PGE, Longhorn)**

#### ***Geological province***

King Leopold Orogen.

#### ***Location***

Eastman Bore 1: 126.588220°E, -18.720350°S; Mount Ramsay (SE 52–09), Ramsay (4260); ~122 km east-southeast of Fitzroy Crossing.

Louisa Downs: 126.6138°E, -18.702641°S; Mount Ramsay (SE 52–09), Ramsay (4260); ~122 km east-southeast of Fitzroy Crossing.

Bullock PGE: 126.6361°E, -18.7028°S; Mount Ramsay (SE 52–09), Ramsay (4260); ~122 km west-southwest of Halls Creek.

Longhorn: 126.499397°E, -18.731911°S; Mount Ramsay (SE 52–09), Bohemia (4160); ~114 km east-southeast of Fitzroy Crossing.

#### ***Classification***

Most of the PGE mineralisation associated with stratabound PGE-bearing chromitite layers:

- 1. Layered tholeiitic mafic-ultramafic intrusions; 1.B. Stratabound PGE-bearing chromitite layers.

Anomalous PGE mineralisation also associated with shear zones:

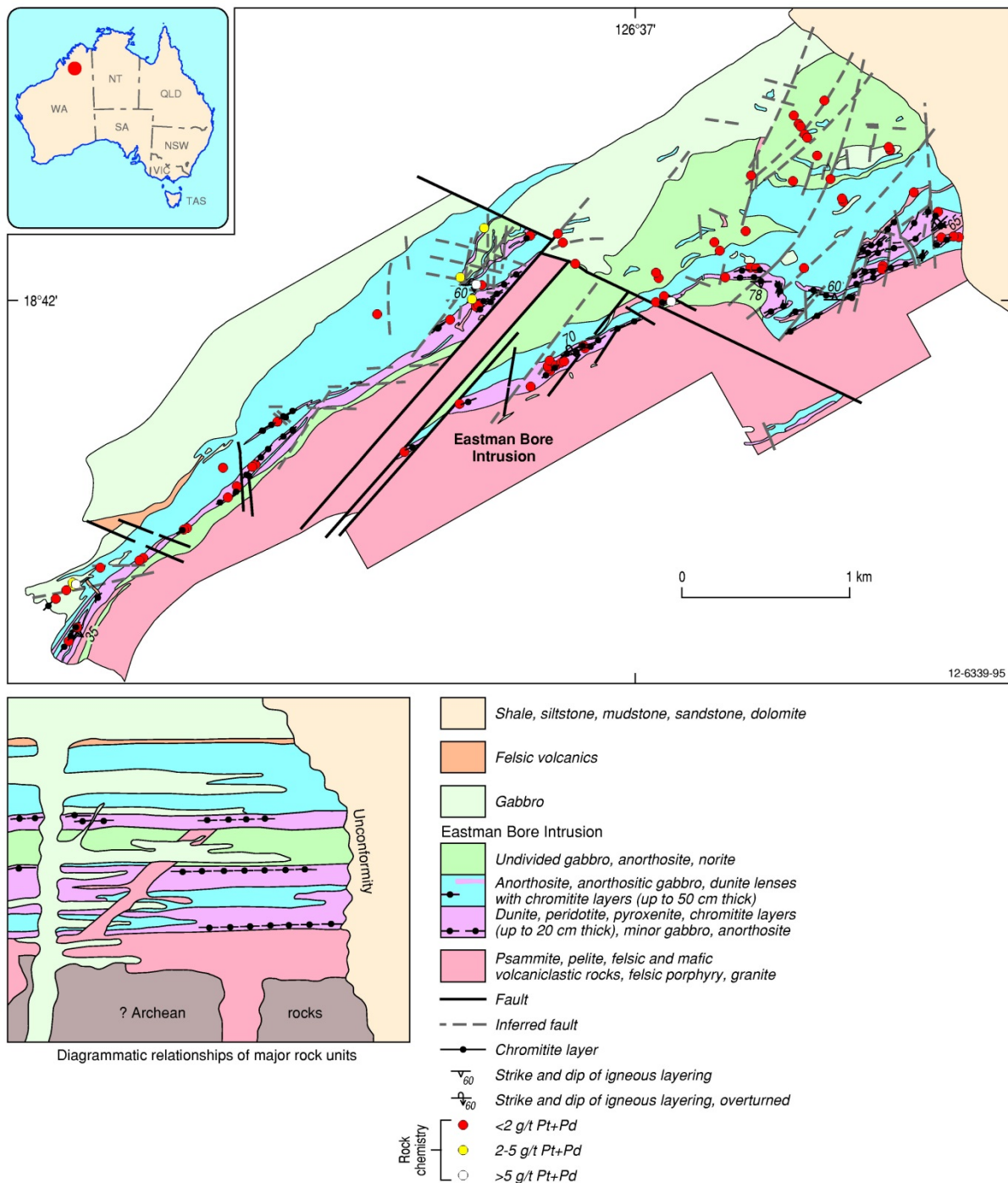
- ?8. Hydrothermal-Metamorphic; 8.D. Structurally-controlled remobilised Ni-Cu-PGE±Au.

### ***Geological setting***

The Eastman Bore Intrusion lies within the southwest extension of the Central Zone of the Halls Creek Orogen (HCO), close to the junction between the north-northeast-trending HCO and the northwest-trending King Leopold Orogen (Appendix Figure K.5). The intrusive mafic-ultramafic body is a steeply dipping folded sill 950 m-thick and has a strike length of approximately 10 km which contains the Bullock–Eastman, Louisa, Brumby, and Blackadder prospects. The western end of the intrusion appears to be truncated by the Eastman Granite. Airborne magnetic trends and minor outcrops of magnetite gabbro and chromite-bearing ultramafic rock with anomalous PGE values suggest that the layered intrusive extends for another 8 km west of the Eastman Granite where it hosts the Longhorn prospect. The eastern portion of the Eastman Bore Intrusion consists of three main zones comprising a basal or lower zone (250 m-thick) of dunite, peridotite, orthopyroxenite, with several thin PGE-bearing chromitites, overlain by an anorthosite and norite middle zone (350 m) containing lenses of chromite-bearing ultramafics, and an upper zone comprising a thick sequence (350 m) of gabbro. Country rocks include felsic volcanics and metasediments of Paleoproterozoic age.

### ***PGE mineralisation***

Exploration has identified laterally persistent PGE mineralisation within the exposed eastern portion of the Eastman Bore Intrusion over a 6 km strike length. The most significant PGE mineralisation is hosted by multiple stacked chromitite seams and variably sheared chromite-bearing ultramafic rocks in the lower and middle zones. Rock-chip sampling of the chromitite seams has generated widespread results up to 7.5 g/t Pt+Pd+Au. Both zones show a coincident Pt-Pd-Au-Cr-Ni-Cu anomaly in systematic soil-sampling program, with peak results including 150 ppb Pt, 600 ppb Pd and 140 ppb Au. The most significant PGE mineralisation identified to date occurs within the middle zone. At the Louisa prospect, twelve trenches between 2 m and 6 m in length and distributed over 1000 m, generated results exceeding 1 g/t Pt+Pd, indicating good continuity of mineralisation, with the best interval being 5 m @ 3.26 g/t PGEs+Au, that included 1 m @ 6.2 g/t PGEs+Au. However, RC drilling completed by Navigator Resources Limited at the Louisa prospect generated a best result of 3 m @ 1.07 g/t PGEs+Au. The Pt+Pd+Au grades from rock-chip sampling of multiple chromitite seams in the lower ultramafic zone, which have returned up to 4.9 g/t Pt+Pd, show no systematic variation in abundance with stratigraphic position within the intrusion. Localised soil sampling at the Bullock Yard prospect returned maximum results of 335 ppb Pt, 2950 ppb Pd, and 370 ppb Au. These highly anomalous results are consistent with nearby rock chip and trench sampling, and the Bullock Yard prospect also returned the best interval from Navigator Resource Limited drilling of 6 m @ 2.37 g/t PGEs+Au. Drilling also returned consistently anomalous intersections averaging 1 g/t to 2 g/t PGEs+Au over intervals of 1 m to 3 m at the Brumby, Blackadder, and Longhorn prospects. Field observations suggest that the chromite-rich layers may be discontinuous at a detailed scale, although the mineralised horizon can readily be traced as a continuous envelope, approximately 3 m to 5 m in thickness, containing both disseminated and massive chromite.



Appendix Figure K.5 Geological setting of the Eastman Bore Intrusion, Halls Creek Orogen, Western Australia. The structurally-disrupted PGE-enriched chromitite layers occupy different stratigraphic levels in the lower ultramafic rock types of the intrusion.

Within the middle zone, significantly elevated PGE abundances occur within variably sheared chromite-bearing ultramafic rocks adjacent to the chromitite horizons. Anomalous PGEs (up to 2.1 g/t Pt+Pd) are also evident within rock-chip samples of chromite-bearing ultramafic rocks sampled throughout the intrusion.

Secondary Cu mineralisation is locally developed near the base of the intrusion, within both shear zones and ultramafic units containing megacrysts of orthopyroxene. Rock-chip sampling of these zones detected up to 16.7% Cu, as secondary Cu minerals, 0.6 g/t Au, 0.34 g/t Pd, 0.21 g/t Pt, and

3.1% Cr. Mapping suggests that this mineralisation may represent weathering of disseminated magmatic sulphide mineralisation, some of which may be remobilised by late-shearing events.

### ***Age of mineralisation***

Proterozoic.

### ***Current status***

Exploration sites.

### ***Economic significance***

Significant PGE deposit in Australia which contains several PGE-bearing chromitite layers. The intrusion has been a focus for exploration over several decades by many companies.

### ***Major references(s)***

Hoatson, D.M., 2000. Exploration history of the East Kimberley, Western Australia. In: Hoatson, D.M. and Blake, D.H. (editors), *Geology and economic potential of the Palaeoproterozoic layered mafic-ultramafic intrusions in the East Kimberley, Western Australia*. Canberra: Australian Geological Survey Organisation Bulletin 246, 13–34.

Magma Metals Limited, 2006. *Magma Metals Limited 2006 Prospectus*, 132 pp.

Sanders, T.S., 1999. Mineralization of the Halls Creek Orogen, east Kimberley region, Western Australia. Geological Survey of Western Australia, Report 66 and Appendix, 44 pp.

### ***Relevant figure(s)***

Appendix Figure K.5.

## **K.1.62 Eastman VMS\***

### ***Geological province***

King Leopold Orogen.

### ***Location***

Eastman VMS: 126.560997°E, -18.710447°S; Mount Ramsay (SE 52–09), Ramsay (4260); ~120 km east-southeast of Fitzroy Crossing.

### ***Classification***

- A volcanic massive sulphide deposit with PGEs mentioned in the suite of commodities in the MINEDEX database for this occurrence, but PGEs were not reported in drill-hole assays.
- ?12. Others (minor or unknown to no economic importance); ?12.A. PGE enrichment in volcanogenic-massive sulphides.

### ***Geological setting***

Drilling has defined Pb-Zn mineralisation within altered carbonate rocks above felsic fragmental rocks with disseminated and stringer Cu mineralisation. Gossans and malachite stained rock at surface; tested by 7 diamond, and 12 percussion drill-holes.

### ***PGE mineralisation***

Base-metal mineralisation reported in drill-hole assays, but no mention of PGEs in the reports which were examined. Drill-hole intersections include:

- ERC021
  - 17 m @ 3.27% Zn, 0.99% Pb, 0.23% Cu, and 26.7 g/t Ag from 38 m; and
  - 12 m @ 5.69% Zn, 1.86% Pb, 3.2% Cu, and 26.5 g/t Ag from 65 m.

Mineralisation in drill-holes include disseminated and massive sulphide together with a zone of Au anomalism that returned a best assay of 1 m @ 2.65 g/t Au within a Cu-Ag-rich zone that assayed 4 m @ 7.91% Cu, 0.9 g/t Au, and 54 g/t Ag.

- ERC 43 intersected 52 m @ 1.8% Zn from 125 m, including 5 m @ 5.76 g/t Au, 45.7 g/t Ag, 0.9% Cu, 6.7% Pb, and 5.8% Zn from 125 m (Magma Metals Limited, 2006a,b).

### ***Age of mineralisation***

Uncertain.

### ***Current status***

Exploration site.

### ***Economic significance***

Undeveloped deposit.

### ***Major references(s)***

Magma Metals Limited, 2006a. Magma Metals Limited 2006 Prospectus, 132 pp.

Magma Metals Limited 2006b. Wide zone of zinc mineralisation intersected at Eastman Cu-Zn-Pb-Au-Ag prospect, East Kimberley. Magma Metals Limited announcement to the Australian Securities Exchange, 14 September 2006, 5 pp.

### ***Relevant figure(s)***

#### **K.1.63 Edison, Edison (Wamin)\***

(see Lamboo group)

#### **K.1.64 Eileen Bore**

(see Copernicus group)

#### **K.1.65 El Cortez—Murray Hills\***

(not in MINEDEX as a PGE occurrence)

### ***Geological province***

Musgrave Province.

### **Location**

El Cortez—Murray Hills: 128.403°E, -25.577°S; Scott (SG 52–06), Holt (4546); ~72 km northwest of Wingellina lateritic Ni deposit.

### **Classification**

- 9. Regolith-Laterite; 9.A. PGE-bearing regolith developed on ultramafic-mafic igneous rocks.

### **Geological setting**

Broad zones of low-grade Ni were intersected with anomalous Cu and PGEs and the anomalous values may be related to an ultramafic layer within the Murray Range body. The Ni enrichment may be related to the weathering profile of an olivine-rich unit. The anomalous PGE and Cu results are generally on the margin of the nickeliferous enrichment and may be related to PGE reef-type mineralisation at depth.

### **PGE mineralisation**

Vertical RAB drilling at the El Cortez Prospect in May 2008 intersected significant Ni-Co-PGE mineralisation over a strike length of 800 m, with peak values of 0.55% Ni, 0.23% Co, and 0.373 g/t PGEs+Au. (Redstone Resources Limited, 2008).

### **Age of mineralisation**

Cenozoic/Proterozoic?

### **Current status**

Exploration site.

### **Economic significance**

Occurrence.

### **Major references(s)**

Redstone Resources Limited, 2006. Redstone Resources Limited 2006 Prospectus, 99 pp.  
Redstone Resources Limited, 2008. Redstone Resources Limited 2008 Annual Report, 72 pp.  
Redstone Resources Limited project webpage ([http://www.redstone.com.au/contents\\_projects.html](http://www.redstone.com.au/contents_projects.html))

### **Relevant figure(s)**

Figure 6.16.

## **K.1.66 Elizabeth Hill**

(see Munni Munni group)

## **K.1.67 Emily Ann\***

(see Otter–Juan Kambalda\* group)

## **K.1.68 Emu Lake–Binti Binti Gossan Zone\***

### ***Geological province***

Yilgarn Craton.

### ***Location***

Emu Lake–Binti Binti Gossan Zone\*: 121.956802°E, -30.288530°S; Kurnalpi (SH 51–10), Gindalbie (3237); ~70 km northeast of Kalgoorlie.

### ***Classification***

- 3. Komatiitic flows and related sill-like intrusions.

### ***Geological setting***

The Emu Lake prospect is associated with a 15 km strike-length north northwest-trending unit of komatiitic ultramafic flows. Historical exploration has identified several high-grade thin (0.1 m–0.3 m) massive Ni-sulphide horizons, notably along the Binti gossan zone (Heron Resources Limited, 2013, 2014).

### ***PGE mineralisation***

The Ni sulphides in the Emu Lake area are associated with the east-dipping overturned contact between a younger ultramafic flow and an older sulphidic felsic volcanic substrate. A best result of 2 m @ 6.2% Ni, 1.78% Cu, and 2.17 g/t PGEs occurred in hole ELD015 (Emu Nickel NL, 2011; Heron Resources Limited, 2013).

### ***Age of mineralisation***

Archean host rocks.

### ***Current status***

Exploration site.

### ***Economic significance***

Occurrence.

### ***Major references(s)***

Emu Nickel NL, 2011. Quarterly report for the quarter ended 30 June 2011. Announcement to the Australian Securities Exchange, 5 pp.

Heron Resources Limited, 2013. Exploration update–Emu Lake nickel sulphide targets. Heron Resources Limited announcement to the Australian Securities Exchange, 26 November 2013, 5 pp.

Heron Resources Limited, 2014. Quarterly report. Summary and Highlights. Announcement to the Australian Securities Exchange, March 2014, 31 pp.

### ***Relevant figure(s)***

## **K.1.69 Erong Hill**

### ***Geological province***

Yilgarn Craton.

### **Location**

Erong Hill: 116.695099°E, -25.634029°S; Glenburgh (SG 50–06), Erong (2246); ~400 km north-northeast of Geraldton.

### **Classification**

- 12. Others (minor or unknown economic importance); 12.E. Others (unknown geological setting).

### **Geological setting**

#### **PGE mineralisation**

#### **Age of mineralisation**

#### **Current status**

Exploration site?

#### **Economic significance**

Occurrences?

#### **Major references(s)**

There is no information on this prospect apart from an entry in the GSWA MINEDEX database stating that the location of this prospect was sourced from a quarterly report in 2004 (quarter not specified) by Platinum Australia Limited submitted to the Australian Securities Exchange. The Erong Prospect is located about 44 km northeast of the Far West–Camel Hills prospect (see Far West–Camel Hills prospect).

#### **Relevant figure(s)**

### **K.1.70 Evans Decline**

(see DeGrussa group)

### **K.1.71 Far West–Camel Hills**

#### **Geological province**

Yilgarn Craton.

#### **Location**

Far West: 116.363529°E, -25.898385°S; Glenburgh (SG 50–06), Yalbra (2146); ~365 km northeast of Geraldton.

#### **Classification**

- ? 1. Layered tholeiitic mafic-ultramafic intrusions.

#### **Geological setting**

The Camel Hills prospect occurs in the northwest margin of the Archean Yilgarn Craton and the adjacent Errabiddy Shear zone (Desert Energy Limited, 2010). The anomalous PGE values are in the

## Western Australia

Far West ultramafic complex. Far West—Camel Hills project is 15 km north-northwest of Byro East and 27 km northeast of the Moonborough prospect.

### **PGE mineralisation**

The Far West ultramafic complex occurs over an area of 9 km<sup>2</sup> and surface rock-chip samples returned up to 5.2% Cr, 4260 ppm Ni, 818 ppm Cu, 1920 ppm Zn, 29 ppb Pt, and 14 ppb Pd (Desert Energy Limited, 2010).

### **Age of mineralisation**

Archean?

### **Current status**

Exploration site.

### **Economic significance**

Occurrences.

### **Major references(s)**

Desert Energy Limited, 2010. Exploration update, Camel Hills joint venture, Western Australia, 5 pp.

### **Relevant figure(s)**

## **K.1.72 Flying Fox T4, T5\***

### **Geological province**

Yilgarn Craton.

### **Location**

Flying Fox T4\*: 119.689003°E, -32.417782°S; Hyden (SI 50–04), Holland (2833); ~260 km northwest of Esperance and ~135 km south-southeast of Southern Cross.

### **Classification**

- 3. Komatiitic flows and sill-like intrusions; 3A. Massive, matrix, and disseminated Ni-Cu-PGE sulphides in preferred lava pathways.
- 8. Hydrothermal-Metamorphic.

### **Geological setting**

A comprehensive study by Collins et al. (2012b) states that ‘... the high-grade Flying Fox komatiite-hosted Ni sulfide deposit, located in the Forrestania greenstone belt of the Archean Yilgarn Craton, Western Australia, is hosted in a deformed and metamorphosed volcano-metasedimentary succession. Post-mineralisation events have sheared and modified the texture and composition of the original massive sulphide ore, creating up to 11 distinct ore shoots including massive, stringer/vein, and breccia sulfides composed of pyrrhotite, pentlandite, chalcopyrite, and variable abundances of pyrite ranging up to 40% volume. Nickel and PGE tenor variations were investigated in two ore shoots, T4 and T5. All mineralisation styles show considerable variability in Ni tenor. PGEs show strong linear correlations between Ir, Os, Ru, and Rh, but poor correlation between Pt, Pd, and Cu.’

The Forrestania greenstone belt also hosts the Spotted Quoll komatiite-hosted Ni deposit (7 km south) and the Mt Holland Ni-PGE occurrence (12 km northeast). The host volcanosedimentary succession has been metamorphosed to amphibolite facies (Abeyasinghe and Flint, 2006; Collins et al., 2012a,b).

### **PGE mineralisation**

Collins et al. (2012a) published an extensive analysis of the post-magmatic variability in ore composition and mineralogy in the T4 and T5 ore shoots of the Flying Fox Ni-Cu-PGE deposit. Their study included a comprehensive whole-rock geochemical analysis of the PGE concentrations of 65 selected samples and Appendix Table K.16 below provides a summary of this data.

*Appendix Table K.16 Summary of whole-rock geochemical data for the T4 and T5 shoots of the Flying Fox Ni-Cu-PGE deposit. Data from Collins et al. (2012a).*

<b>Element</b>	<b>Minimum concentration (style of mineralisation, host rock)<sup>1</sup></b>	<b>Maximum concentration (style of mineralisation, host rock)<sup>1</sup></b>
Ni (%)	0.5 (B, S)	13.9 (M, -)
Cu (%)	0.0 (SV, G)	0.8 (M, -)
Co (%)	0.0 (B, G)	0.4 (SV, G)
Cr (ppm)	30.0 (B, S)	6060.0 (M, -)
Zn (ppm)	22.0 (SV, G)	2700.0 (B, G)
As (ppm)	2.0 (B, S)	475.0 (B, S)
Bi (ppm)	0.2 (SV, S)	139.0 (M, -)
Mn (ppm)	270.0 (B, S)	4330.0 (B, S)
Pb (ppm)	4.0 (B, S/G)	2320.0 (B, G)
Au (ppb)	7.0 (B, G)	3740.0 (SV, G)
Os (ppb)	0.5 (B, S)	296.0 (M, -)
Ir (ppb)	0.5 (B, S)	287.0 (M, -)
Ru (ppb)	1.1 (B, S)	1130.0 (M, -)
Rh (ppb)	0.4 (B, S)	208.0 (M, -)
Pd (ppb)	26.0 (B, S)	1060.0 (M, -)
Pt (ppb)	4.0 (B, G)	2070.0 (M, -)

<sup>1</sup> Style of Ni sulphide mineralisation: B = breccia, S = stringer, M = massive, SV = stringer/vein.  
Host rock: S = footwall sedimentary rock, G = granitic rock.

Collins et al. (2012a) stated that a high proportion of the 55 representative samples plot within the characteristic compositional field for typical magmatic sulphides, and these samples have komatiitic Ni sulphide tenors of around 9% Ni, which is considered to be in the middle of the typical range for komatiite-hosted ores. However, the wide Ni sulphide tenor variation cannot be explained via primary magmatic processes, such as R-factor variability, or the fractional crystallisation of an immiscible sulphide melt. Secondary processes such as structural relocation, metamorphism, magmatism, and hydrothermal-fluid activity may have played a significant role in modifying the Ni distribution throughout the Flying Fox deposit.

### **Age of mineralisation**

Archean host rocks.

### **Current status**

Operating Ni-Cu-Co mine.

### **Economic significance**

A significant medium-sized Ni-Cu-Co mine. In 2013, the Flying Fox and the adjoining Lounge Lizard deposit contained a total Measured, Indicated, and Inferred Resource of 6.625 Mt at 2% Ni containing 133 677 t of Ni metal. The total production since commencement of mining in 2007 to 31 March 2014, amounted to 91 069 t of Ni metal.

### **Major references(s)**

- Abeyinghe, P.B. and Flint, D.J., 2006. Nickel–cobalt in Western Australia: commodity review for 2004. Western Australia Geological Survey, Record 2006/6, 57 pp.
- Collins, J.E., Hagemann, S.G., McCuaig, T.C. and Frost, K.M., 2012a. Structural controls on sulfide mobilization at the high-grade Flying Fox Ni-Cu-PGE sulfide deposit, Forrestania greenstone belt, Western Australia. *Economic Geology*, 107, 1433–1455.
- Collins, J.E., Barnes, S.J., Hagemann, S.G., Campbell, T., McCuaig, T.C. and Frost, K.M., 2012b. Postmagmatic variability in ore composition and mineralogy in the T4 and T5 ore shoots at the high-grade Flying Fox Ni-Cu-PGE deposit, Yilgarn Craton, Western Australia. *Economic Geology*, 107, 859–879.
- Hoatson, D.M., Jaireth, S., Whitaker, A.J., Champion, D.C. and Claoué-Long, J.C., 2009. Guide to using the Australian Archean Mafic-Ultramafic Magmatic Events Map. *Geoscience Australia Record 2009/41*, 135 pp.

### **Relevant figure(s)**

Figure 6.21.

## **K.1.73 Freemans**

### **Geological province**

Yilgarn Craton.

### **Location**

Freemans: 121.438110°E, -27.477570°S; Sir Samuel (SG 51–13), Wanggannoo (3143); ~80 km northeast of Leinster.

### **Classification**

- ?3. Komatiitic flows and related sill-like intrusions.

### **Geological setting**

The prospect is reported to occur in an Archean greenstone belt, comprising an apparently south-easterly plunging, tightly-folded sequence of BIFs and ferruginous chert horizons, with fine-grained amphibolites to the west, and quartz porphyries, ultramafics and medium-grained amphibolites to the east (Whitfield, 1986).

### **PGE mineralisation**

Ultramafic-peridotite unit east of Mt Mundy reported to have yielded anomalous Pt and Pd values over a strike length of 10 km. The highest PGE concentrations of a Mn-bearing epidote-rich ultramafic rock were reported to be 3 g/t Pt and 4 g/t Pd. Another six samples yielded 2 g/t Pd (Whitfield, 1986).

### ***Age of mineralisation***

Archean host rocks? ~2900 Ma–2700 Ma (Hoatson et al., 2006).

### ***Current status***

Active prospect.

### ***Economic significance***

Occurrence.

### ***Major references(s)***

Hoatson, D.M., Jaireth, S. and Jaques, A.L., 2006. Nickel sulfide deposits in Australia: Characteristics, resources, and potential. *Ore Geology Reviews*, 29, 177–241.

Whitfield, G.B., 1986. Mt Mundy geology and economic potential. Epoch Minerals Exploration NL, 19 pp.

### ***Relevant figure(s)***

## **K.1.74 Giles, Giles North**

### ***Geological province***

Yilgarn Craton.

### ***Location***

Giles: 122.227443°E, -27.001175°S; Duketon (SG 51–14), Urarey (3343); ~180 km north of Laverton.

Giles North: 122.227984°E, -26.995761°S; Kingston (SG 51–10), Collurabbie (3344); the Giles prospects are ~10 km south of the Collurabbie group of prospects.

### ***Classification***

- The oxidised mineralisation is classified as: 9. Regolith-Laterite; 9.A. PGE-bearing regolith developed on ultramafic-mafic igneous rocks.
- Type of mineralisation is uncertain for deeper intersections in unweathered rock. Regis Resources Limited (2009) has investigated the western ultramafic zone of Mocha–Batavia magnetite-sulphide intrusive bodies. Possible type of mineralisation is as for the Collurabbie Ni-Cu-PGE prospects to the north.
- ?3. Komatiitic flows and related sill-like intrusions.

The mineralisation styles at the Giles prospects have been labelled in GSWA MINEDEX database as 'orthomagmatic mafic and ultramafic-layered mafic intrusions'.

### ***Geological setting***

The Giles and Giles North prospects are located in the continuation of the Archean Gerry Well (Duketon) greenstone belt south of the Collurabbie prospects, near the northeastern margin of the Yilgarn Craton.

### ***PGE mineralisation***

Drilling of the oxidised rock above the base of weathering at the Giles prospect intersected anomalous zones of mineralisation including:

## Western Australia

- CRAC2053: 4 m @ 0.11% Ni, 0.04% Cu and 145 ppb Pt+Pd from a depth of 20 m;
- CRAC2057: 54 m @ 0.73% Ni, 0.01% Cu and 21 ppb Pt+Pd; and
- CRAC2059: 8 m @ 0.24% Ni, 0.08 Cu and 203 ppb Pt+Pd from a depth of 48 m.

Regis Resources Limited reported that the drilling was carried out in the western ultramafic zone of the Mocha–Batavia magnetite-sulphide intrusive bodies (Regis Resources Limited, 2009).

At the Giles North prospect, drill-hole CRAC2092 intersected 9 m @ 0.1.2% Ni, 0.1% Cu, and 35 ppb Pt+Pd (Regis Resources Limited, 2009).

### ***Age of mineralisation***

Mineralisation of possible Cenozoic age hosted in the weathered zone above Archean bedrock. Mineralisation in underlying bedrock probably hosted in Archean host rocks.

### ***Current status***

Historical exploration sites.

### ***Economic significance***

Occurrences.

### ***Major references(s)***

Regis Resources Limited, 2009. Quarterly report to 31 December 2008, to the Australian Securities Exchange, 15 pp.

### ***Relevant figure(s)***

## **K.1.75 Goliath North\***

(see Mt Keith\*)

## **K.1.76 Green Dam**

### ***Geological province***

Yilgarn Craton.

### ***Location***

Green Dam: 122.713699°E, -30.537180°S; Kurnalpi (SH 51–10), Roe (3436); ~122 km east-northeast of Kalgoorlie.

### ***Classification***

- ?3. Komatiitic flows and related sill-like intrusions.

### ***Geological setting***

The Green Dam prospect occurs at the northern end of a greenstone belt informally referred to as the 'eastern greenstone belt' in the Edjudina Domain on the Roe 1:100 000 map sheet (Smithies, 1994). The ultramafic rocks are totally serpentinitised, however, olivine adcumulus to (more commonly) mesocumulus textures are commonly recognisable. The rocks comprise serpentine (-Fe-hydroxide-

?goethite) pseudomorphs after euhedral olivine, and an intercumulus assemblage of serpentine-magnetite-chlorite(-quartz).

### ***PGE mineralisation***

Drilling at the Green Dam prospect intersected several anomalous PGE zones in the eastern greenstone belt, and include:

- YRC009: 16 m @ 0.74% Ni, 0.37% Cu, 49 ppb Pt, and 113 ppb Pd from 145 m, including
  - 2 m @ 2.20% Ni, 1.41% Cu, 48 ppb Pt, and 304 ppb Pd from 145 m (Magma Metals Limited, 2007a);
- YRC034: 20 m @ 0.41% Ni, 0.47% Cu, 0.14 g/t Pt+Pd, and 0.05% Co from 88 m;
- YRC027: 6 m @ 0.93% Ni, 0.27% Cu, 0.29 g/t Pt+Pd, and 0.02% Co from 89 m (Magma Metals Limited, 2007b), including
  - 1 m @ 3.34% Ni, 0.17% Cu, 0.82 g/t Pt+Pd, and 0.07% Co; and
- YRC030: 13 m @ 0.61% Ni, 0.16% Cu, 0.17 g/t Pt+Pd, and 0.02% Co from 103 m (Magma Metals Limited, 2007c), including
  - 5 m @ 1.14% Ni, 0.29% Cu, 0.31 g/t Pt+Pd, and 0.03% Co.

### ***Age of mineralisation***

Mineralisation hosted in Archean ultramafics.

### ***Current status***

Exploration site.

### ***Economic significance***

Occurrence.

### ***Major references(s)***

- Magma Metals Limited, 2007a. Drilling intersects nickel-copper sulphide mineralisation at Roe. Magma Metals Limited announcement to the Australian Securities Exchange, 21 February 2007, 6 pp.
- Magma Metals Limited, 2007b. Drilling update—Green Dam Ni-Cu prospect. Magma Metals Limited announcement to the Australian Securities Exchange, 7 September 2007, 4 pp.
- Magma Metals Limited, 2007c. Exploration update Roe project. Magma Metals Limited announcement to the Australian Securities Exchange, 11 October 2007, 6 pp.
- Smithies, R.H., 1994. Geology of the Roe 1:100 000 sheet. Western Australia Geological Survey, 1:100 000 Geological Series Explanatory Notes, 22 pp.

### ***Relevant figure(s)***

## **K.1.77 GSP, Ringlock**

(location of GSP occurrence coincides with the Mt Jewell Ni deposit)

### ***Geological province***

Yilgarn Craton.

## **Location**

GSP: 121.4556°E, -30.18314°S; Kalgoorlie (SH 51–09), Bardoc (3137); ~64 km north of Kalgoorlie.

Ringlock: 121.410103°E, -30.143431°S; ~68 km north of Kalgoorlie and 6 km northwest of the GSP Jewell prospect.

## **Classification**

- 3. Komatiitic flows and related sill-like intrusions.
- 8. Hydrothermal-Metamorphic.

## **Geological setting**

The GSP and Ringlock prospects occur within a narrow belt of northwest-trending greenstones along the boundary of the Boorara and Gindalbie domains in the northeast corner of the Bardoc 1:100 000 map sheet (Groenewald et al., 2000).

## **PGE mineralisation**

A zone of disseminated Ni-Cu-PGE mineralisation occurs along the base of a komatiite unit and encloses a small body of inferred resource, at the base of the ultramafics, of 86 000 t at a grade of about 2% Ni. The delineated resource occupies a small portion of the much more extensive and lower grade disseminated Ni-Cu-PGE zone. Historical drill-hole intersections in this resource include 1.83 m @ 1.62% Ni and 6.7 m @ 1.62% Ni, including 2.13 m @ 3.55% Ni (Magma Metals Limited, 2006a,b). A thin (remobilised?) zone of mineralisation occurs subparallel to the komatiite base within the underlying volcanic and sedimentary rocks with historical drill intercepts of 0.65 m @ 5.5% Ni, 1.4% Cu, 0.5 g/t Pt, and 0.97 g/t Pd (Magma Metals Limited, 2006a,b).

Later drilling of the disseminated zone included some drill sections which were assayed for PGEs as follows:

- MJD 13: 7 m @ 0.70% Ni and 0.19 g/t Pt+Pd from 128 m, including
  - 2 m @ 1.33% Ni and 0.42 g/t Pt+Pd from 128 m (Magma Metals Limited, 2006c);
- MJRC042: 19 m @ 0.78% Ni, 115 ppb Pt, and 301 ppb Pd from 84 m (Magma Metals Limited, 2007);
- MJRC047: 3 m @ 2.85% Ni, 54 ppb Pt and 206 ppb Pd from 104 m (Magma Metals Limited, 2007a,b); and
- Oxide (laterite) Ni mineralisation overlies the sulphide mineralisation as in MJRC043: 8 m @ 0.66% Ni and 0.03% Co from 13 m (Magma Metals Limited, 2007a,b).

Drilling at the Ringlock prospect, located 6 km northwest of the GSP prospect intersected 2.2 m @ 1.32% Ni and 0.55 ppb Pt+Pd in MJD16 (Magma Metals Limited, 2006c).

## **Age of mineralisation**

Mineralisation is hosted in Archean komatiites.

## **Current status**

Historical exploration site.

### ***Economic significance***

A small shallow Inferred Resource of 86 000 t at 2% Ni has been delineated within the GSP prospect and is sometimes referred to as the Mt Jewell Ni deposit (Magma Metals Limited, 2006a).

### ***Major references(s)***

- Groenewald, P.B., Painter, M.G.M., Roberts, F.I., McCabe, M. and Fox, A., 2000. East Yilgarn Geoscience Database, 1:100 000 geology Menzies to Norseman—an explanatory note. Western Australia Geological Survey, Report 78, 53 pp.
- Magma Metals Limited, 2006a. Quarterly report for the period ended 30 June 2006, 7 pp.
- Magma Metals Limited, 2006b. Magma Metals Limited Annual Report 2006, 52 pp.
- Magma Metals Limited, 2006c. Mt Jewell nickel project—drilling update. Magma Metals Limited announcement to the Australian Securities Exchange, 2 October 2006, 7 pp.
- Magma Metals Limited, 2007a. Drilling results confirm nickel potential at GSP. Magma Metals Limited announcement to the Australian Securities Exchange, 12 December 2007, 7 pp.
- Magma Metals Limited, 2007b. Drilling intersects nickel-copper sulphide mineralisation at Roe. Magma Metals Limited announcement to the Australian Securities Exchange, 21 February 2007, 6 pp.

### ***Relevant figure(s)***

## **K.1.78 Halleys–Blackstone**

### ***Geological province***

Musgrave Province.

### ***Location***

Halleys–Blackstone: 128.043304°E, -26.163589°S; Cooper (SG 52–10), Blackstone (4545).

Voyager 2 SE\*: 128.064614°E, -26.185918°S; Cooper (SG 52–10), Blackstone (4545); ~150 km east of Warburton.

### ***Classification***

- The Halleys group of prospects along the Saturn complex: ?2. Massive to poorly layered tholeiitic mafic-dominated intrusions; ?2.A. Segregations of Ni-Cu-Co-PGE sulphides in feeder conduits and basal contacts.
- The available reports on the Tollu prospect suggest a hydrothermal style of mineralisation,
- ?8. Hydrothermal-Metamorphic.

### ***Geological setting***

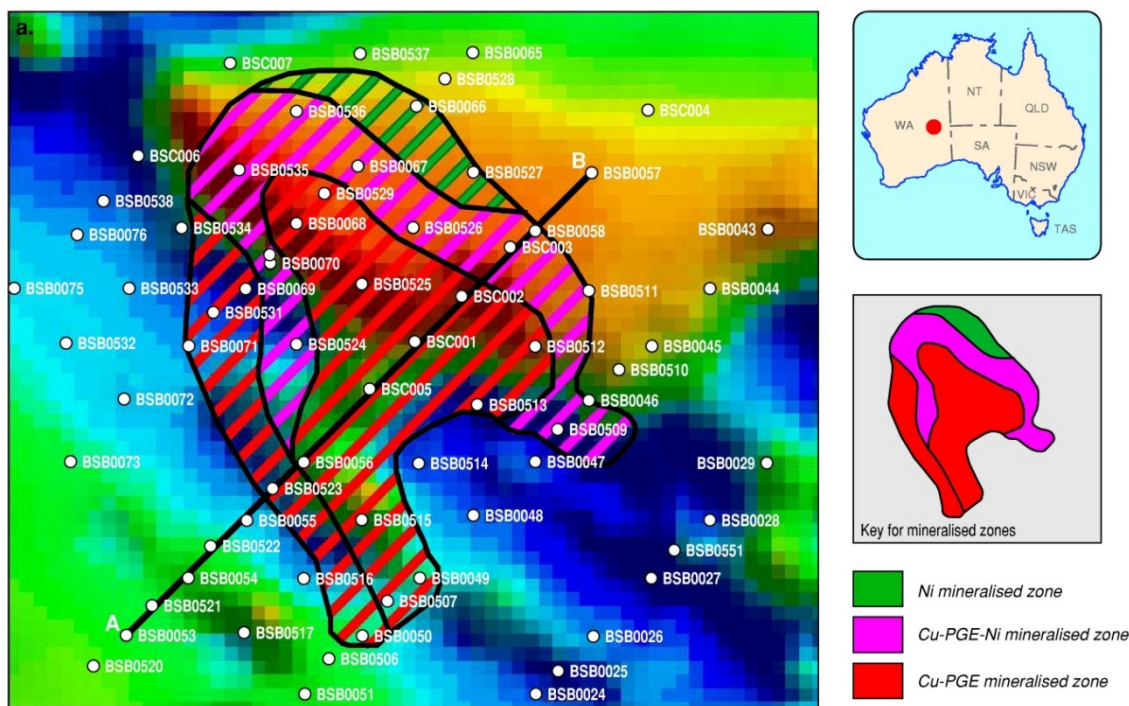
A 12 km-diameter elliptical ring complex named the Saturn complex, is interpreted to be a mafic cone-shaped feeder of the ~1070 Ma Giles Complex.

### ***PGE mineralisation***

A 12 km-long PGE anomaly from surface geochemical samples was delineated along the southwest margin of the Saturn complex. The Halleys Cu-Ni-PGE (Appendix Figure K.6), Halleys NW PGE, and Halleys NW Ni-Cr prospects occur along this PGE anomaly (Redstone Resources Limited, 2006).

**Western Australia**

The prospect was first drilled in 2007 and a >100 m-thick mineralised zone was defined with a peak intercept of 74 m of 0.33% Cu, and 0.24 g/t PGEs+Au, including 20 m @ 0.56% Cu, 0.14% Ni, and 0.32 g/t PGEs+Au (from 16 m). Drilling intercepts in 2008 included 9 m @ 0.67% Cu, 0.1% Ni, and 0.76 g/t PGEs along the eastern margin from an overall intercept of 43 m @ 0.31% Cu, 0.06% Ni, and 0.30 g/t PGEs+Au, and 16 m @ 0.50% Cu, 0.11% Ni, and 0.53 g/t PGEs+Au; and along the western margin 11 m @ 0.56% Cu, 0.25% Ni, and 0.16 g/t PGEs from an overall intercept of 35 m @ 0.29% Cu, 0.12% Ni, and 0.16 g/t PGEs+Au (Redstone Resources Limited, 2008).



**Halleys Cu-PGE-Ni pipe-like body** over total magnetic image.

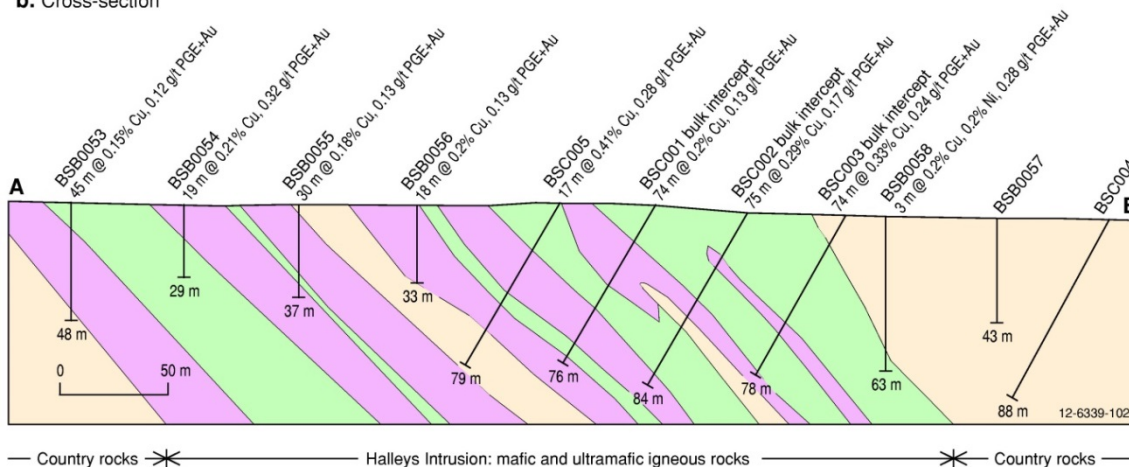
RAB drilling has highlighted a pipe geometry to the mineralised body with a diameter of approximately 300 metres with best grades on margins.

Large thickness of disseminated Cu-Ni-PGE sulphide mineralisation.

Additional intersections:

- 26 m @ 0.44% Cu, 0.08% Ni, 0.39 g/t PGE+Au (BSB512)
- 16 m @ 0.50% Cu, 0.11% Ni, 0.53 g/t PGE+Au (BSB524)
- 19 m @ 0.44% Cu, 0.19% Ni, 0.15 g/t PGE+Au (BSB536)

**b. Cross-section**



**Appendix Figure K.6 Total Magnetic Intensity Aeromagnetic image and schematic northeast-southwest cross-section A-B for the Halleys Cu-PGE-Ni body.** Both figures modified from Redstone Resources Limited (2010).

## Western Australia

The Ni-Cu-PGE mineralisation at the Halleys prospect comprises disseminated sulphides with significant Cu-PGE grades (>0.1% Cu and 200 ppb PGEs) and occur within an ovoid shaped pipe 300 m by 230 m in size. The body is zoned, with a central core of Cu-PGEs and an outer zone richer in Ni with Cu and PGEs. The pipe is coincident with an elongate magnetic high defined by ground magnetics.

Broad zones of Cu-PGE (Pt+Pd+Au) mineralisation intersected in separate holes at Voyager I and Voyager II, with down-hole intersections including: 14 m @ 0.27 g/t PGEs+Au and 0.05% Cu at Voyager II (including 1 m @ 0.61 g/t PGEs+Au); and 28 m @ 0.1 g/t PGEs+Au and 0.1% Cu at Voyager I (including 2 m @ 0.31 g/t PGEs+Au, 0.19% Cu) (West Musgrave Mining Limited, 2002; Traka Resources Limited, 2012).

Copper-PGE mineralisation is hosted in gabbro and leucogabbro rock types containing disseminated sulphides and magnetite.

### ***Age of mineralisation***

Proterozoic mafic host rocks.

### ***Current status***

Exploration site.

### ***Economic significance***

Occurrences.

### ***Major references(s)***

Redstone Resources Limited, 2006. Redstone Resources Limited Prospectus 2006, 99 pp.

Redstone Resources Limited, 2008. New Halleys drill results extend Cu-Ni-PGE mineralised zone in Saturn complex, West Musgraves. Redstone Resources Limited announcement to the Australian Securities Exchange, 14 July 2008, 4 pp.

Redstone Resources Limited, 2013. Redstone Resources Limited Annual Report 2013, 78 pp.

Traka Resources Limited, 2012. Investor presentation. Traka Resources Limited announcement to the Australian Securities Exchange, 11 July 2012, 31 pp.

West Musgrave Mining Limited, 2002. Drilling program confirms copper/PGE mineralisation at two prospects. West Musgrave Mining Limited announcement to the Australian Securities Exchange, 20 December 2002, 3 pp.

### ***Relevant figure(s)***

Appendix Figure K.6.

## **K.1.79 Halleys East–Barlee, Halleys Channel, Halleys Northeast, Crabman–Crabman South–Buddy**

### ***Geological province***

Yilgarn Craton.

### ***Location***

Halleys East–Barlee: 119.095398°E, -29.475519°S; Barlee (SH 50–08), Barlee (2739); ~196 km north of Southern Cross.

## Western Australia

Halleys Channel: 119.091482°E, -29.475134°S; Barlee (SH 50–08), Barlee (2739);

Halleys Northeast: 119.097165°E, -29.473240°S; Barlee (SH 50–08), Barlee (2739);

Crabman–Crabman South–Buddy: 119.089600°E, -29.481030°S; Barlee (SH 50–08), Barlee (2739).

### Classification

- Uncertain. Published company reports refer to structurally controlled mesothermal Au mineralisation suggesting a possible hydrothermal origin for the deposit (Beacon Minerals Limited, 2007a).
- 8. Hydrothermal-Metamorphic; ?8.B. Remobilised Ni-Cu-PGE±Au in komatiitic and metasedimentary rocks.

### Geological setting

The Au-PGE-Ni prospects are located in the northern Archean Southern Cross greenstone belt. All greenstones have been metamorphosed, with grades varying from lower greenschist to amphibolite. Past and current exploration activity has been mainly for Au, which shows a strong association with shearing in the area, often at sheared contacts between ultramafic units and either basalt or high-Mg basalt (Bloem et al., 1994; Hilko and Ridley, 1995; Beacon Minerals Limited, 2007a).

### PGE mineralisation

The area contains a number of small Au deposits with an initial JORC Code compliant Au resource announced in December 2009 totalling 384 000 t @ 6.0 g/t Au for 74 000 ounces Au (Beacon Minerals Limited, 2009). A prefeasibility study of the Halleys East deposit in 2013 estimated a Probable Reserve of 58 500 t @ 10.6 g/t Au containing 20 000 ounces Au, but analyses for PGEs were not published. The mining of the Halleys East deposit commenced at the end of 2013 (Beacons Minerals Limited, 2014). A number of exploration drill-holes returned elevated PGEs as tabulated below in Appendix Table K.17 (Beacon Minerals Limited, 2007b,c).

*Appendix Table K.17 Drill-hole intersections for the Halleys deposits where PGE analyses are available. Data from Beacon Minerals Limited, (2007b,c).*

Prospect	Drill-hole Number (BRB)	From (m)	To (m)	Major intersections
Russel (Halleys Northeast)	005	12	17	5 m @ 0.14 g/t PGEs, 0.12% Ni, 200 ppm Cu
Russel (Halleys Northeast)	015	12	14	2 m @ 0.21 g/t PGEs, 0.2% Ni, 300 ppm Cu
Russel (Halleys Northeast)	20	16	24	8 m @ 0.1 g/t PGEs, 0.2% Ni, 500 ppm Cu
Halleys East	055	8	16	8 m @ 0.1 g/t PGEs, 0.22% Ni, 600 ppm Cu
Halleys East	062	4	12	8 m @ 0.21 g/t PGEs, 0.1% Ni
Halleys East	081	16	28	12 m @ 0.11 g/t PGEs
Halleys East	082	12	24	12 m @ 0.3 g/t Au, 0.15 g/t PGEs, 0.2% Ni, 300 ppm Cu
Halleys East	083	12	20	8 m @ 2.5 g/t Au, 0.12 g/t PGEs, 0.15% Ni
Halleys East	087	16	24	8 m @ 1.3 g/t Au, 0.15 g/t PGEs, 0.1% Ni, 0.1% Cu
Halleys (Halleys Channel)	095	20	28	8 m @ 0.15 g/t PGEs, 0.15% Ni, 400 ppm Cu

Only drill-holes with analyses for PGEs are shown in the above table. Drill intersections in the Halleys East Au deposit included 6 m @ 63.53 g/t Au (Beacon Minerals Limited, 2011).

### ***Age of mineralisation***

Archean host rocks of unassigned basaltic and high-Mg basaltic units (Hoatson et al., 2009).

### ***Current status***

Halleys East is an operating Au mine in 2014.

### ***Economic significance***

PGE occurrence, operating Au mine.

### ***Major references(s)***

- Beacon Minerals Limited, 2007a. Beacon Minerals Limited Prospectus, 100 pp.
- Beacon Minerals Limited, 2007b. Beacon Minerals Limited announcement to the Australian Securities Exchange, 20 March 2007, 6 pp.
- Beacon Minerals Limited, 2007c. Quarterly report to the Australian Securities Exchange, March 2007, 19 pp.
- Beacon Minerals Limited, 2009. Beacon Minerals Limited announcement to the Australian Securities Exchange, 11 December 2009, 6 pp.
- Beacon Minerals Limited, 2011. Barlee gold project, Western Australia. Gold Coast Resources Showcase, June 2011, 14 pp.
- Beacon Minerals Limited, 2014. December 2013 Quarterly activities and cash flow report, 11 pp.
- Bloem, J.M., Hilko, J.D., Groves, D.I. and Ridley, J.R., 1994. Metamorphic and structural setting of Archean amphibolite-hosted gold deposits near Southern Cross, Southern Cross province, Yilgarn Block, Western Australia. *Ore Geology Reviews*, 9, 183–208.
- Hilko, J.D. and Ridley, J.R., 1995. Structural and metamorphic controls on gold mineralisation in the Southern Cross and Marda Diemals Greenstone Belts, Yilgarn Block, Western Australia. *Key Centre for Strategic Mineral Deposits*, UWA.
- Hoatson, D.M., Jaireth, S., Whitaker, A.J., Champion, D.C. and Claoué-Long, J.C., 2009. Guide to Using the Australian Archean Mafic-Ultramafic Magmatic Events Map. *Geoscience Australia Record* 2009/41, 135 pp.

### ***Relevant figure(s)***

## **K.1.80 Halls Knoll Gossan, Polar Bear\***

### ***Geological province***

Yilgarn Craton.

### ***Location***

Halls Knoll Gossan: 121.847761°E, -31.915991°S; Widgiemooltha (SH 51–14), Cowan (3234); ~32 km north-northeast of Norseman.

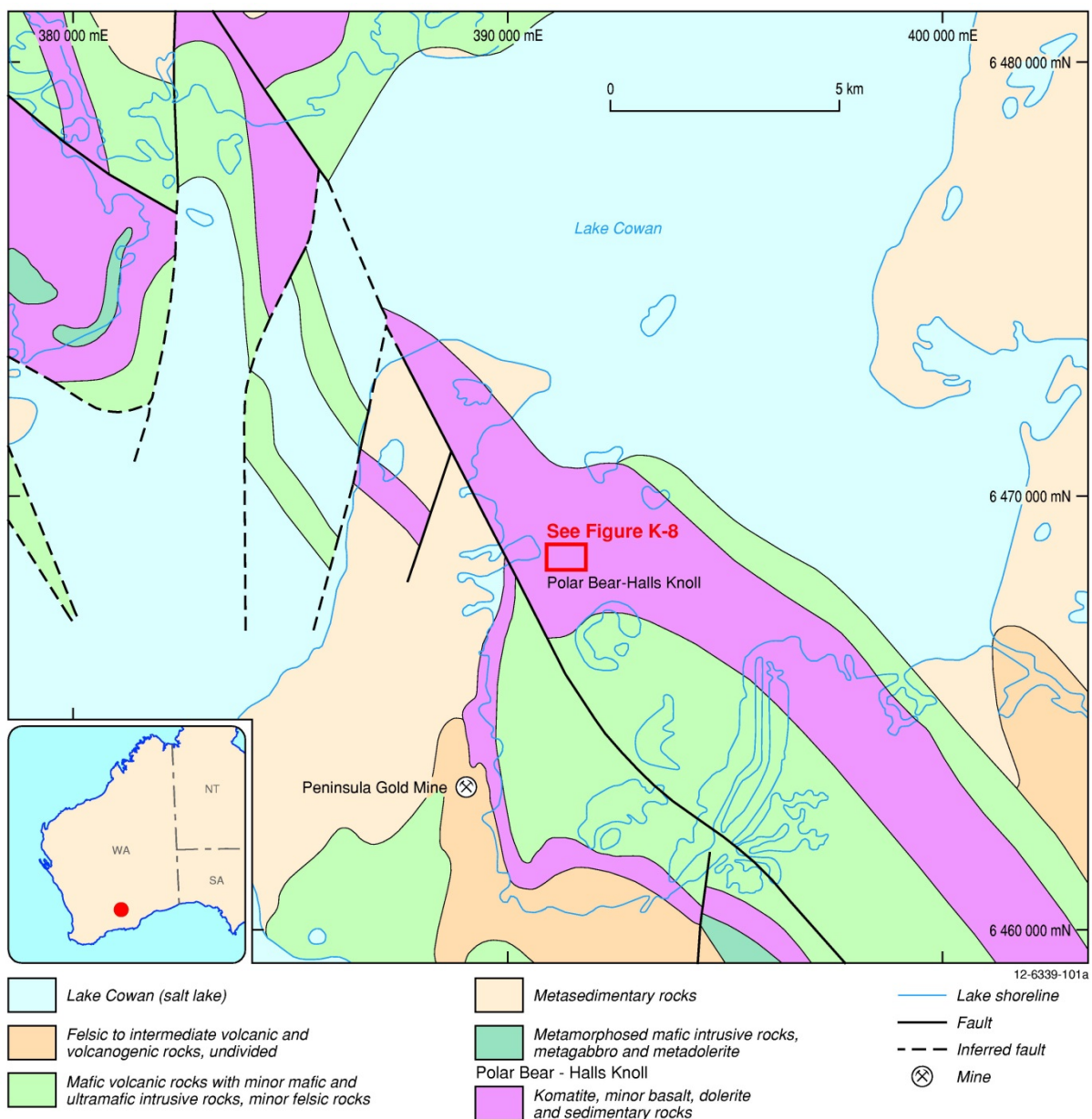
Polar Bear\*: 121.84°E, -31.92°S; Widgiemooltha (SH 51–14), Cowan (3234).

### ***Classification***

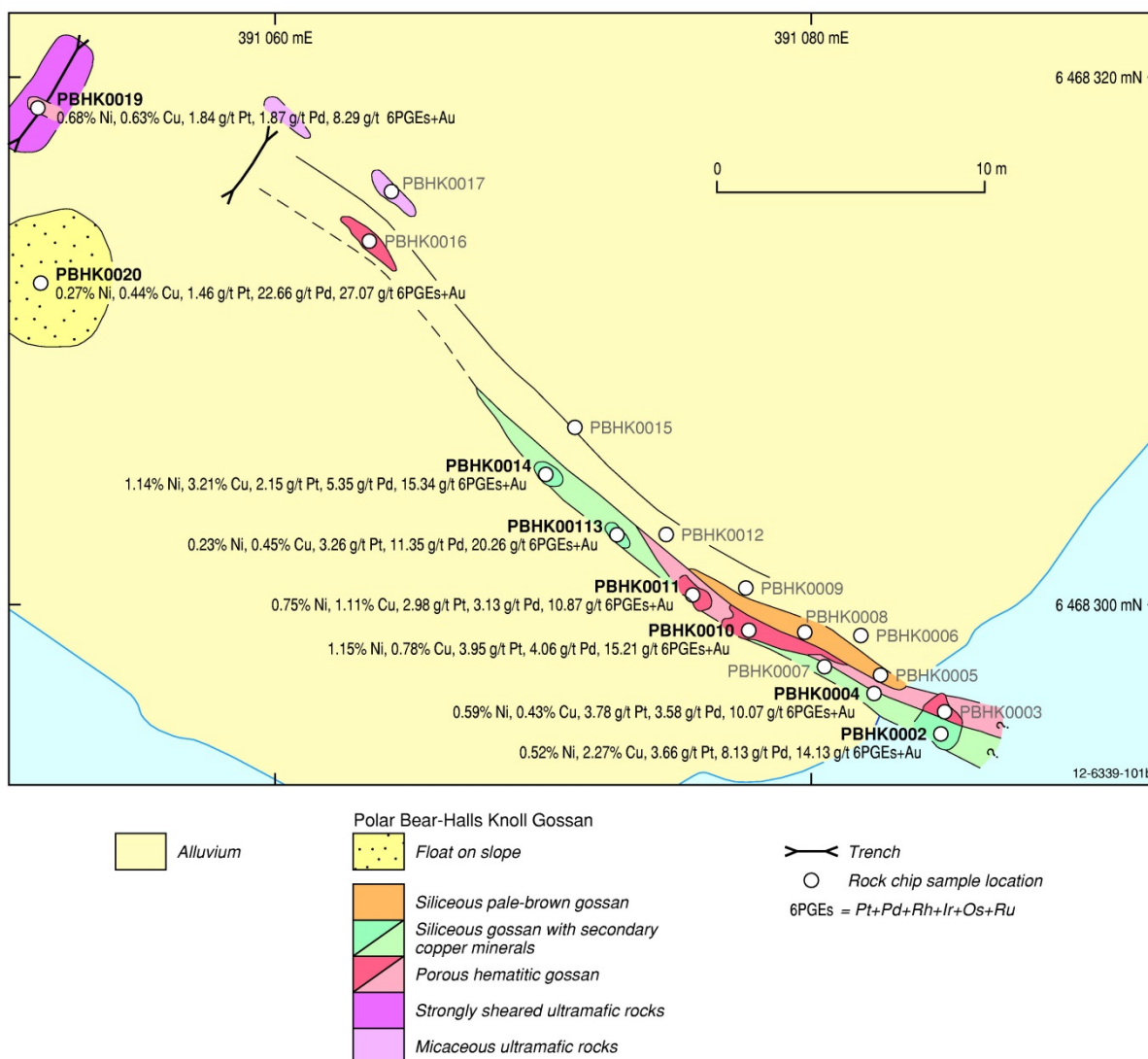
- 3. Komatiitic flows and related sill-like intrusions; 3.A. Massive, matrix and disseminated Ni-Cu-PGE sulphides in preferred lava pathways.

### Geological setting

The Halls Knoll and Polar Bear prospects occur on the Polar Bear Peninsula which protrudes northwards into Lake Cowan of the Yilgarn Craton (Appendix Figure K.7 and Appendix Figure K.8). The dominant rocks are a sequence of northwest-trending metakomatiite with minor metasilstone, metagabbro, and dolerite sills. The ultramafic sequence in the Polar Bear region is locally complexly folded and thick and appears to be structurally thickened by thrust faulting (Sirius Resources NL, 2014b). This is also known to occur at Kambalda and Widgiemooltha and creates opportunities for the repetition of the prospective basal horizon on parallel trends. Such thrusting can also cause remobilisation of Ni sulphide mineralisation and create discrete high-grade massive sulphide deposits (e.g., Flying Fox, Spotted Quoll, and Emily Ann). The sequence is extensively concealed with recent sediments of Lake Cowan. The sequence is extensively concealed with recent sediments of Lake Cowan.



Appendix Figure K.7 Geological setting of the Polar Bear and Halls Knoll Ni-Cu-PGE prospects, Yilgarn Craton, Western Australia. Modified from Sirius Resources Limited (2010).



Appendix Figure K.8 Detailed geology and Ni-Cu-PGE geochemistry of the Polar Bear and Halls Knoll Ni-Cu-PGE prospects, Yilgarn Craton, Western Australia. Modified from Sirius Resources Limited (2010).

### PGE mineralisation

Rock chip and soil sample analyses over the mineralised zones are tabulated in Appendix Table K.18 with a maximum result of 27 g/t PGEs+Au (Platina Resources Limited 2007; Sirius Resources NL, 2010).

Appendix Table K.18 Geochemical data for rock chip and soil samples from mineralised zones of the Halls Knoll and Polar Bear prospects. Data from Platina Resources Limited (2007) and Sirius Resources NL (2010).

Sample	Type	Ni (%)	Cu (%)	Co (%)	Pt (g/t)	Pd (g/t)	Os (g/t)	Ir (g/t)	Ru (g/t)	Rh (g/t)	Au (g/t)	PGEs+Au (g/t)
PBHK0002	Gossan	0.52	2.27	0.03	3.66	8.13	0.20	0.20	1.07	0.73	0.15	14.13
PBHK0004	Gossan	0.59	0.43	0.03	3.78	3.58	0.17	0.27	1.23	1.00	0.04	10.07
PBHK0007	Gossan	1.09	0.29	0.04	3.51	1.55	0.15	0.19	1	0.75	0.02	7.17
PBHK0013	Gossan	0.23	0.45	0.02	3.26	11.35	0.43	0.37	3.29	1.45	0.1	20.26
PBHK0014	Gossan	1.14	3.21	0.03	2.15	5.35	0.61	0.64	4.54	1.76	0.28	15.34

Sample	Type	Ni (%)	Cu (%)	Co (%)	Pt (g/t)	Pd (g/t)	Os (g/t)	Ir (g/t)	Ru (g/t)	Rh (g/t)	Au (g/t)	PGEs+Au (g/t)
PBHK0020	Gossan	0.27	0.44	0.01	1.46	22.66	0.19	0.25	1.69	0.79	0.02	27.07
PBHK0003	Gossan	0.69	0.71	0.03	1.97	2.16	0.26	0.43	2.42	1.6	0.01	8.86
PBHK0010	Gossan	1.15	0.78	0.05	3.95	4.06	0.46	0.61	4.16	1.93	0.03	15.21
PBHK0011	Gossan	0.75	1.11	0.1	2.98	3.13	0.26	0.39	3.09	1	0.01	10.87
PBHK0016	Gossan	1.19	0.32	0.02	0.13	0.52	0.01	0.01	0.04	0.02	0.03	0.75
PBHK0019	Gossan	0.68	0.63	0.03	1.84	1.87	0.24	0.38	2.71	1.23	0.02	8.29
PBHK0006	Ultramafic	0.40	0.49	0.02	0.1	0.27	0.01	0.01	0.06	0.05	0.03	0.55
PBHK0009	Ultramafic	0.43	0.65	0.01	0.11	0.24	0.01	0.01	0.04	0.03	0.07	0.52
PBHK0015	Ultramafic	0.87	0.25	0.04	0.16	0.73	0.01	0.01	0.03	0.02	0.01	0.97
PBHK0017	Ultramafic	0.54	0.07	0.02	0.28	0.57	0.01	0.01	0.02	0.01	0.02	0.91
PBHK0005	Caprock	0.1	0.07	Nil	0.58	0.86	0.03	0.09	0.32	0.44	Nil	2.33
PBHK0008	Caprock	0.10	0.2	Nil	0.37	0.67	0.02	0.02	0.16	0.13	0.01	1.39
PBHK0012	Soil rubble	0.67	8.2	0.02	0.5	0.73	0.01	0.03	0.17	0.1	0.01	1.69

Drill-hole KNUTD3 intersected 0.5 g/t Pd+Pt+Au and 0.41% Ni from 32 m (Appendix Table K.19). The mineralisation is hosted in komatiite that had undergone extensive hydrothermal alteration (Platina Resources Limited, 2008).

*Appendix Table K.19 Drill-hole intersections and geochemical results from the Polar Bear and Halls Knoll prospects. Data from Platina Resources Limited (2008).*

Drill-hole	Lithology	Depth (m)	Analyses
KNUTD1	Komatiite, schist	156–172	0.11 g/t Pd+Pt+Au, 0.17% Ni
KNUTD2	Komatiite, schist		No significant results
KNUTD3	Komatiite, schist	32–36	0.5 g/t Pd+Pt+Au, 0.41% Ni
KNUTD4	Komatiite, schist	133–148	0.15 g/t Pd+Pt+Au, 0.18% Ni
KNUTD5	Metasediments		No significant results
KNUTD6	Komatiite, shear zone		No significant results
KNUTD7	Komatiite, schist	250–254	0.26 g/t Pd+Pt+Au, 0.55% Ni
KNUTD7	Komatiite, schist	257–260	0.22 g/t Pd+Pt+Au, 0.45% Ni
KNUTD7	Komatiite, schist	263–266	0.33 g/t Pd+Pt+Au, 0.77% Ni (Including 1 m @ 1.27% Ni and 0.52 g/t PGEs from 264 m–265 m)

Sirius Resources NL (2014a) announced high-grade Ni sulphide mineralisation in the reconnaissance diamond drill-hole SPBD0046 at the Taipan prospect, Polar Bear Project region. The intersection at the Taipan prospect demonstrated the presence of both massive and disseminated Ni-Cu-Co sulphides and the enrichment of PGEs. The intersection was 4.10 m (from 104.4 m) @ 3.8% Ni, 2.45% Cu, 0.08% Co, 0.9 g/t Pt, and 1.6 g/t Pd, including 2.15 m (from 106.0 m) @ 5.84% Ni, 3.73% Cu, 0.12% Co, 1.1 g/t Pt, and 1.65 g/t Pd. Nickel-Cu-PGE-sulphide mineralisation has been identified over 5 km along the Halls Knoll–Taipan trend demonstrating the prospectivity of this underexplored region (Sirius Resources NL, 2014b). The Taipan geology shows similarities to that at Halls Knoll region, some 3 km to the southeast, where previous drilling by Sirius Resources NL and others has intersected disseminated Ni sulphides.

### ***Age of mineralisation***

Archean host rocks.

### ***Current status***

Dormant exploration site.

### ***Economic significance***

Occurrence, drill-hole site.

### ***Major references(s)***

Platina Resources Limited, 2007. September 2007 Quarterly Report, to the Australian Securities Exchange, 19 October 2007, 7 pp.

Platina Resources Limited, 2008. December 2007 Quarterly Report to the Australian Securities Exchange, 31 Jan 2008a, 4 pp.

Platina Resources Limited, 2008. March 2008 Quarterly Report to the Australian Securities Exchange, 17 April 2008b, 9 pp.

Sirius Resources NL, 2010. Nickel sulphides identified at Polar Bear. Sirius Resources NL announcement to the Australian Securities Exchange, 14 July 2010, 4 pp.

Sirius Resources NL, 2014a. Nickel exploration update. Sirius Resources NL announcement to the Australian Securities Exchange, 16 July 2014, 27 pp.

Sirius Resources NL, 2014b. Polar Bear nickel exploration update. Sirius Resources NL announcement to the Australian Securities Exchange, 21 July 2014, 12 pp.

### ***Relevant figure(s)***

Figure 6.21, Appendix Figure K.7, and Appendix Figure K.8.

## **K.1.81 Haran\*, Jamieson Prospect\*, Canaan\*, Zen\***

### ***Geological province***

Musgrave Province.

### ***Location***

Haran: 127.528702°E, -25.717300°S; Scott (SG 52–06), Finlayson (4446); ~108 km east-northeast of Warburton.

Jamieson Prospect: 127.57361°E, -25.79778°S; ~10 km southeast of Haran.

Canaan: 127.554802°E, -25.620960°S; ~12 km north of Haran.

Zen\*: 127.505402°E, -25.670570°S; ~3 km northeast of Haran.

### ***Classification***

- 2. Massive to poorly layered tholeiitic mafic-dominated intrusions; 2.B. Stratabound PGE-bearing magnetite layers.

### ***Geological setting***

Hosted in magnetite bands interlayered with gabbro and anorthositic gabbro of the Jameson Range Intrusion. The Jameson Range Intrusion is composed of approximately 2500 m of layered Fe-rich

troctolite, gabbroic troctolite, and anorthosite adcumulates, with disseminated magnetite (Gliksen et al., 1996; WMC, 2003).

### ***PGE mineralisation***

The Haran Ti-V-PGE-Cu prospect occurs in the upper part of the Jameson Range Intrusion in PGE-bearing massive Fe-Ti oxide layers in anorthosite and troctolite. A significant drill-hole intersection is 2.8 m @ 20% TiO<sub>2</sub>, 0.8% V<sub>2</sub>O<sub>5</sub>, 50% Fe<sub>2</sub>O<sub>3</sub>, 0.6 g/t Pt+Pd+Au, and 0.2% Cu.

The Jamieson Prospect, ~10 km southeast of Haran, is another titaniferous magnetite horizon that has a strike length of over 10 km. Rock-chip samples contain 0.1 g/t to 2.1 g/t Pt+Pd+Au. The average combined grade was 1.3 g/t with the Pt component comprising 0.96 g/t Pt. The average V and Ti oxide compositions were reported to be 1.18% V<sub>2</sub>O<sub>5</sub> and 23.2% TiO<sub>2</sub>, and the Fe content of the rock averages 44% Fe with 442 ppm Cu and 280 ppm Ni (Traka Resources Limited, 2010a,b).

The Canaan prospect is underlain by a basal troctolite, and more dominantly, magnetite-bearing gabbro. A unit of olivine-bearing gabbro, with a small lens of wehrlite on the northeastern margin, coincides with a geochemical anomaly and both these units occur within the broader magnetite-bearing gabbro. A thin quartz-bearing gabbro lens occurs near the southwestern boundary of the Canaan prospect. The Canaan anomaly is a Ni-Cu target with less consistent associated PGEs. One diamond drill-hole obtained the following intersections (AXG Mining Limited, 2004):

- 6 m (191m to 197 m) @ 0.60 g/t Pt+Pd+Au; and
- 3 m (212 m to 245 m) @ 0.68 g/t Pt+Pd+Au.

The Zen prospect occurs in a laterally extensive (along strike) PGE mineralised layer. It is defined by elevated Pt values in the regional geochemical data and a shallow strike oriented AEM conductor, perhaps showing deeper weathering of a sulphide-bearing horizon (AXG Mining Limited, 2004).

### ***Age of mineralisation***

Proterozoic.

### ***Current status***

Exploration sites.

### ***Economic significance***

Undeveloped deposit.

### ***Major references(s)***

AXG Mining Limited, 2004. AXG Mining Limited 2004 Prospectus. Prospectus submitted to the Australian Securities Exchange, 9 March 2004, 71 pp.

Gliksen, A.Y., Stewart, A.J., Ballhaus, C.G., Clarke, G.L., Feeken, E.H.J., Leven, J.H., Sheraton, J.W. and Sun, S.-S., 1996. Geology of the western Musgrave Block, central Australia, with particular reference to the mafic-ultramafic Giles Complex. Australian Geological Survey Organisation Bulletin 239, 206 pp.

Traka Resources Limited, 2010a. Musgrave Project—Strongly anomalous rock-chip and auger geochemical results on the 'Jamieson Prospect'. Report to the Australian Securities Exchange, 30 June 2010, 3 pp.

Traka Resources Limited, 2010b. Quarterly activities report for the three months ended 30 September 2010. Report to the Australian Securities Exchange, 30 September 2010, 12 pp.

WMC, 2003. Geological setting of Ni-Cu-PGE mineralisation at the West Musgrave. Mining and Exploration Group Western Australia—January 2003. WMC PowerPoint presentation.

### ***Relevant figure(s)***

Figure 6.16, Figure 6.20, and Figure 8.16a.

### **K.1.82 Harmony\***

(see Otter–Juan Kambalda\* group)

### **K.1.83 Heron Well\***

#### ***Geological province***

Yilgarn Craton.

#### ***Location***

Heron Well\*: 121.3762°E, -29.0973°S; Leonora (SH 51–01), Melita (3139); ~24 km south-southeast of Leonora.

#### ***Classification***

- Unknown.

#### ***Geological setting***

The Heron Well Ni-Cu-PGE prospect is located in a north-south-trending greenstone belt, which contains pillowed tholeiitic basalts, felsic volcanics, and shale horizons. Two large gabbroic bodies intrude the greenstone sequence—the western Boxies Bore complex, and an eastern gabbro body. A differentiated peridotite sequence defines the western margin of the Boxies Bore gabbro and has a strike length of about 1500 m. Massive and disseminated Ni-Cu sulphide mineralisation containing PGE concentrations occurs along the basal contact of the peridotites with the underlying felsic volcanics (Hoatson and Glaser, 1989).

#### ***PGE mineralisation***

The mineralisation consists of chalcopyrite, pentlandite, chromite, cobaltite, and michenerite. The most encouraging intersections have been: HWDD-2, 2.1 m @ 6.51 ppm Pd, 1.55 ppm Pt, 0.44 ppm Au, 0.79% Cu, and 1.14% Ni; HWP-9, 2.0 m @ 0.63 ppm Pd, 0.45 ppm Pt, 0.99% Cu, and 0.65% Ni. Minor Pd and Pt enrichment also occurs in the oxidised zone of the peridotite, with Pd+Pt around 0.5 ppm (Hoatson and Glaser, 1989).

#### ***Age of mineralisation***

Archean host rocks?

#### ***Current status***

Dormant exploration site.

#### ***Economic significance***

Occurrence, drill-hole intersection.

### **Major references(s)**

Hoatson, D.M. and Glaser, L.M., 1989. Geology and economics of platinum-group metals in Australia. Bureau of Mineral Resources, Australia, Resource Report 5, 81 pp.

### **Relevant figure(s)**

#### **K.1.84 Honeymoon Well Group\***

(see Mt Keith\*, Otter–Juan Kambalda\* group)

#### **K.1.85 Hunters Reef East**

(see Munni Munni)

#### **K.1.86 Hunters Reef West**

(see Munni Munni)

#### **K.1.87 Jacks Hill**

##### **Geological province**

King Leopold Orogen.

##### **Location**

Jacks Hill: 124.465612°E, -16.938638°S; Yampi (SE 51–03), Tarraji (3764); ~98 km east-northeast of Derby.

##### **Classification**

- Mineralisation in gossans and in sheared ?dolerite dyke.
- 8. Hydrothermal-metamorphic; ?8.D. Structurally-controlled remobilised Ni-Cu-PGE sulphides in mafic-felsic dykes/veins in shear zones.

##### **Geological setting**

The Jacks Hill prospect lies within Paleoproterozoic rocks of the King Leopold Orogen, and include altered sedimentary units of the Marboo Formation, which have been intruded by the Ruins Dolerite and coarse-grained granitic bodies. The regional stratigraphy and foliation trend is northwest. A gossan has developed at Jacks Hill over chloritic mica schists and minor quartzite adjacent to the contact between the Ruins Dolerite and the Marboo Formation (Tyler and Griffin, 1993; Al Maynard and Associates Pty Limited, 2012).

##### **PGE mineralisation**

In 2007, 29 samples from a drilling program of seven reverse circulation holes returned assay values of up to 3.7% Cu, 1.14 g/t Au, 0.48% Ni, 0.73 g/t Pt, and 14.4 g/t Ag. From 2007 to 2011, 67 rock-chip samples were collected from four gossans and 25 samples returned values >1% Cu, five returned values of >1% Ni, 33 samples had values >1 g/t Ag, 3 samples >0.5 g/t Pt (maximum of 1.16 g/t Pt), 15 samples >0.5 g/t Pd (maximum of 1.22 g/t Pd), and 5 samples >0.3 g/t Au (Al Maynard and Associates Pty Limited, 2012).

## Western Australia

Assays of a drilling program, announced in 2013, indicated broad Ni sulphide mineralisation and intersections include: 47 m @ 0.15% Ni from 36 m, including 11 m @ 0.30% Ni and 0.11% Cu from 52 m; and 42 m @ 0.22% Ni from 14 m, including 5 m @ 0.39% Ni and 0.16% Cu from 38 m. Host rock for the Ni-Cu mineralisation is interpreted to be a dolerite dyke which is bounded on both sides by a muscovite mica schist (Victory Mines Limited, 2013).

### ***Age of mineralisation***

Mineralisation in host rocks belonging to the Proterozoic Ruins Dolerite.

### ***Current status***

Exploration site.

### ***Economic significance***

Occurrence. Discovered in 1902, the Jacks Hill Prospect is reported to have produced small tonnages of gossan material containing high-grade Cu carbonate/oxide during the ~mid-1900s (Al Maynard and Associates Pty Limited, 2012).

### ***Major references(s)***

Al Maynard and Associates Proprietary Limited, 2012. Independent Geologists's report. In: Victory Mines Limited 2012 Prospectus, 35–77.

Tyler, I.M. and Griffin, T.J., 1993. Yampi, Western Australia, 1:250 000 Geological Series Explanatory Notes, Sheet SE 51–3. Second edition. Geological Survey of Western Australia, Perth, Western Australia, Australia, 32 pp.

Victory Mines Limited, 2013. Broad zones of nickel sulphide mineralisation discovered and Clara Hills. Victory Mines Limited announcement to the Australian Securities Exchange, 16 January 2013, 3 pp.

### ***Relevant figure(s)***

## **K.1.88 Jameson Range\***

(see Manchego)

## **K.1.89 Jamieson Prospect\***

(see Haran\*)

## **K.1.90 Jason**

(see Tom Tit, Jason)

## **K.1.91 Jilbadgie**

### ***Geological province***

Yilgarn Craton.

### **Location**

Jilbadgie: 119.260418°E, -31.570516°S; Southern Cross (SH 50–16), Holleton (2734); ~38 km south-southwest of Southern Cross.

### **Classification**

- Unknown.

### **Geological setting**

Unknown.

### **PGE mineralisation**

At Jilbadgie, programmes of infill MAGLAG soil samples have defined three areas of ultramafic rocks with coherent anomalies defined by Ni, base metals, PGEs, and Au geochemistry (Westonia Mines Limited, 2004). Drilling in 2008 did not reveal significant Ni values (Catalpa Resources Limited, 2008).

### **Age of mineralisation**

Unknown.

### **Economic significance**

Occurrence.

### **Major references(s)**

Catalpa Resources Limited, 2008. Catalpa Resources Limited 2008 Annual Report. Report to the Australian Securities Exchange, October 2008, 84 pp.

Westonia Mines Limited, 2004. Quarterly report for three months ended 31 March 2004. Report to the Australian Securities Exchange, April 2004, 11 pp.

### **Relevant figure(s)**

## **K.1.92 Jillian–Wills Creek**

(see Copernicus group)

## **K.1.93 Jimberlana South\***

### **Geological province**

Yilgarn Craton.

### **Location**

Jimberlana South: 121.95°E, -32.157°S; Sir Samuel (SI 51–02), Norseman (3233); ~8 km east of Norseman.

### **Classification**

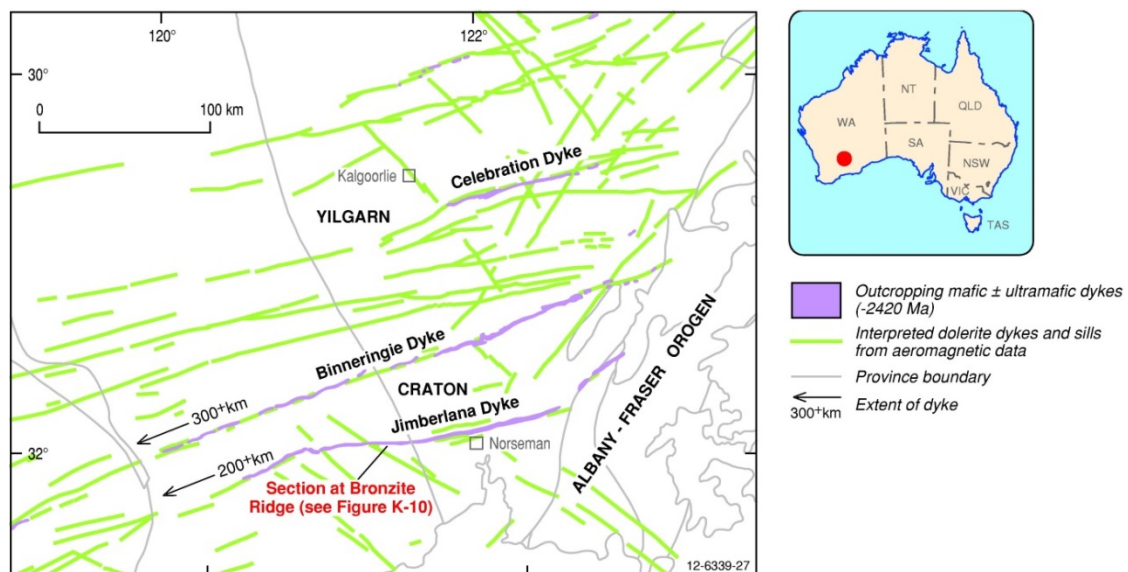
- ?1. Layered tholeiitic mafic-ultramafic intrusions.
- ?8. Hydrothermal-Metamorphic.

## Geological setting

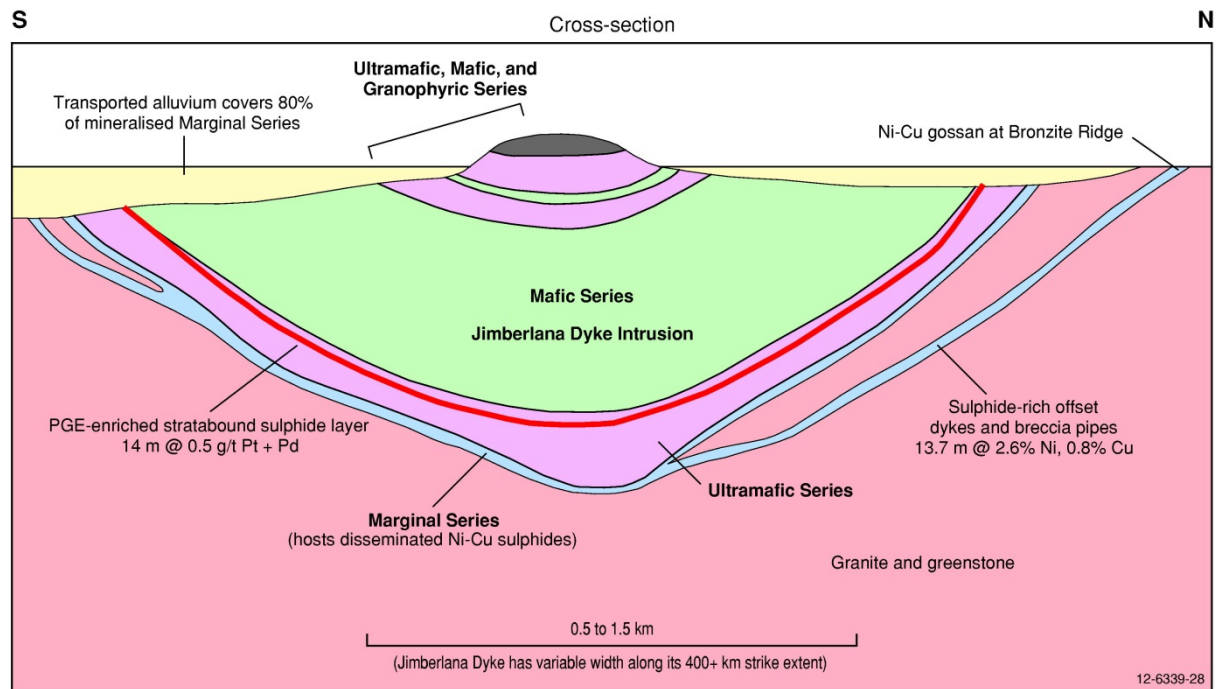
The Jimberlana Dyke (Keays and Campbell, 1981) is the best-documented example of a group of large Paleoproterozoic (~2420 Ma) dykes that trend west-southwest across most of the Yilgarn Craton in Western Australia (Appendix Figure K.9 and Appendix Figure K.10). Other prominent examples include Binneringie Dyke and Celebration Dyke. Mafic-ultramafic and mafic rock types have been the focus of exploration for PGE-Ni-Cu and Ni-Cu-PGE mineral systems. Massive Ni-Cu sulphide-bearing breccia pipes occur within off-set dykes (or satellite dykes) adjacent to the Jimberlana Dyke. The breccia pipes are located below PGE-enriched stratabound sulphide layers in the upper part of the Ultramafic Series and are sub-parallel to the basal intrusive contact of the intrusion. Exploration by Avoca Resources Limited on the Jimberlana Dyke includes the research and identification of a magma chamber to the south of the dyke and below the main base of the dyke.

## PGE mineralisation

A 13.7 m drill-hole intersection, which defined massive Ni sulphides associated with a sulphidic breccia in an offset dyke near the basal contact of the Jimberlana Dyke assayed 2.6% Ni and 0.8% Cu (no PGE data). Geological mapping at Dundas Hills has confirmed that surface PGE anomalism is directly associated with a major lithology change at depth. The anomalism occurs just below an ultramafic/mafic stratigraphic contact. The surface anomaly has been traced along the magmatic horizon for over 2.5 km at the 30 ppb Pd+Pt concentration level. The anomaly peaks at 1010 ppb Pt and 765 ppb Pd, and is open to the east along the Norcott complex. Drilling has shown that a PGE-enriched stratabound sulphide layer (14 m @ 0.5 g/t Pt+Pd) is laterally persistent in the upper part of the Ultramafic Series just below the interface with the overlying Mafic Series (Appendix Figure K.9).



Appendix Figure K.9 Distribution of different generations of mafic-ultramafic and dolerite dykes in the Kalgoorlie–Norseman region, southern part of the Yilgarn Craton, Western Australia. Most of the larger mafic-ultramafic dykes (Jimberlana Dyke, Binneringie Dyke, Celebration Dyke) are Paleoproterozoic (~2420 Ma) in age, trend west-southwest, and have strike extents of more than ~500 km across the craton. They have created considerable exploration interest for Ni-Cu-PGE sulphides similar to that seen in the Great Dyke of Zimbabwe. The large dykes are part of the ~2420 Ma Widgiemooltha Magmatic Event. The section at Bronzite Ridge in the Jimberlana Dyke is shown in Appendix Figure K.10. Modified from Hoatson et al. (2008a,b).



Appendix Figure K.10 Schematic north-south cross-section of the Bronzite Ridge region of the Jimberlana Dyke. The location of the section is indicated on Appendix Figure K.9.

### Age of mineralisation

The Jimberlana Dyke has identical Rb-Sr isochron and Sm-Nd model ages of  $2411 \pm 50$  Ma (Turek, 1966; Fletcher et al., 1987; Myers, 1995).

### Current status

Exploration.

### Economic significance

Occurrence.

### Major references(s)

- Fletcher, I.R., Libby, W.G. and Rosman, K.J.R., 1987. Sm-Nd dating of the 2411 Ma Jimberlana dyke, Yilgarn Block, Western Australia. *Australian Journal of Earth Sciences*, 34, 523–525.
- Keays, R.R. and Campbell, I.H., 1981. Precious metals in the Jimberlana Intrusion, Western Australia: Implications for the genesis of platiniferous ores in layered intrusions. *Economic Geology*, 76, 1118–1141.
- Mallee Gold Corporation Limited, 2007. Mallee Gold Corporation Limited 2007 Prospectus. 79 pp.
- Myers, J.S., 1995. Geology of the Esperance 1:1 000 000 sheet. Geological Survey Western Australia, 1:100 000 Geological Series Explanatory Notes, 10 pp.
- Turek, A., 1966. Rubidium-strontium isotopic studies in the Kalgoorlie–Norseman area, Western Australia. PhD thesis, Australian National University, Canberra, Australia.

### Relevant figure(s)

Appendix Figure K.9 and Appendix Figure K.10.

### **K.1.94 Joshua and Joshua East**

(see Abrahams Find–Joshua)

### **K.1.95 J Reef**

(see Munni Munni group)

### **K.1.96 Judys Reef**

(see Munni Munni group)

### **K.1.97 Kambalda Group, Kambalda/Braemore, East Alpha, Carnilya Hill\***

#### ***Geological province***

Yilgarn Craton.

#### ***Location***

Kambalda Group: 121.649101°E, -31.180241°S; Widgiemooltha (SH 51–14), Lake Lefroy (3235); ~3 km northwest of Kambalda.

Kambalda/Braemore: 121.675003°E, -31.184240°S; Widgiemooltha (SH 51–14), Lake Lefroy (3235); ~2 km north-northeast of Kambalda.

East Alpha: 121.697998°E, -31.239010°S; Widgiemooltha (SH 51–14), Lake Lefroy (3235); ~5 km southeast of Kambalda.

Carnilya Hill\*: 121.862099°E, -31.052710°S; Widgiemooltha (SH 51–14), Lake Lefroy (3235); ~25 km northeast of Kambalda.

#### ***Classification***

- 3. Komatiitic flows and related sill-like intrusions; 3.A. Massive, matrix and disseminated Ni-Cu-PGE sulphides in preferred lava pathways.

#### ***Geological setting***

The Kambalda Ni-Cu-PGE-sulphide deposits occur in the southern part of the Kalgoorlie Terrane forming the western fault-bounded tectonostratigraphic unit of the Eastern Goldfields Superterrane of the Yilgarn Craton. Nickel sulphide mineralisation is primarily hosted within the volcanic sequences exposed along the flanks of granitic intrusions that post-date the sulphide mineralisation and form the core of a doubly plunging anticline known as the Kambalda Dome (Gresham and Loftus-Hills, 1981; Cassidy et al., 2006). The Ni sulphide mineralisation is mostly localised at the contact between the Lunnon Basalt and Silver Lake Member of the Kambalda Komatiite Formation (Fiorentini, 2010). The Ni-Cu-PGE deposits form elongate sulphide bodies contained in thick sequences of metamorphosed komatiitic flows, tholeiitic basalts, and carbonaceous and pyritic sediments (Hoatson and Glaser, 1989). Following magmatic emplacement, the mineralised sequences have been multiply deformed, metamorphosed to lower amphibolite facies, and intruded by felsic dykes (Stone et al., 2005; Hoatson et al., 2006).

### **PGE mineralisation**

Ni-Cu ores (2.96% Ni, 0.22% Cu) have PGE concentrations of approximately 325 ppb Pt, 425 ppb Pd, 110 ppb Os, 60 ppb Ir, 50 ppb Rh, and 220 ppb Ru. The major PGMs are sperrylite, moncheite, sudburyite, stibiopalladinite, and palladoarsenide (Appendix C). The Ni-Cu matte (73% Ni, 5.5% Cu) produced in treating the ore contains about 4.2 ppm Pt, 10.9 ppm Pd, 1.2 ppm Rh, and 4.1 ppm Ru (Hudson and Donaldson, 1984). A summary of variation in average composition of Kambalda Ni deposits (100% sulphides) is provided by Cowden and Roberts (1990) in Appendix Table K.20 below.

*Appendix Table K.20 Summary of variation in average composition of Kambalda Ni deposits (100% sulphides) from Cowden and Roberts (1990).*

Element	Composition (%)	Element	Composition (ppb)
Fe	38–54	Pt	500–1500
Ni	8–22	Pd	1100–3000
S	35–39	Os	250–1000
Cu	0.6–1.3	Ir	120–500
Co	0.2–0.3	Rh	200–700
Cr	0.18–0.4	Ru	400–2000
Zn	0.02–0.04	Au	100–400
Pb	15–25 ppm	Ag	2–4 ppm

The Ni and PGE tenors of the sulphide ores on the Kambalda Dome vary considerably both between, and within, ore shoots. Neighbouring ore shoots such as the Victor and Long shoots have markedly contrasting tenor. Barnes (2006) attributes the different metal grades to variable fluid dynamic conditions determining the extent of equilibration between the komatiite lava and the sulphide-bearing ore magma.

Maximum PGE contents for some of the Kambalda-type 3.A deposits as reported by Keays and Davison (1976) and Travis et al. (1976), including Carnilya Hill, are 1.50 ppm Pd (10.4% Ni, 1.22% Cu), and 1.50 ppm Pd (0.35% Ni, 0.27% Cu) in Ni gossan.

Other Ni gossans in the region have anomalous concentrations of PGEs, and these include:

Kurnalpi: 3.63 ppm Pd (2.70% Ni, 5.05% Cu).

### **Age of mineralisation**

Age of komatiitic host rock is Archean (~2705 Ma) from the direct dating of komatiitic rocks and associated rocks in the Kambalda region (Nelson, 1997; Hoatson et al., 2006; Kositcin et al., 2008).

### **Current status**

Current and historical mines in the Kambalda Dome include Otter–Juan, Durkin, Fisher, Gibb, Long–Victor, McLeay, Lunnon, and Hunt.

### **Economic significance**

Major economic significance.

### **Major references(s)**

- Cassidy, K.F., Champion, D.C., Krapez, B., Barley, M.E., Brown, S.J.A., Blewett, R.S., Groenewald, P.B. and Tyler, I.M., 2006. A revised geological framework for the Yilgarn Craton, Western Australia. Geological Survey of Western Australia, Record 2006/8, 8 pp.
- Cowden, A. and Roberts, D.E., 1990. Komatiite hosted nickel sulphide deposits, Kambalda. In: Hughes, F.E. (editor), *Geology of the Mineral Deposits of Australia and Papua New Guinea*. Australasian Institute of Mining and Metallurgy, Melbourne, Monograph 14, 567–581.
- Florentini, M.L., 2010. Chapter 4—The Kambalda Nickel Camp. In: McCuaig, T.C., Miller, J. and Beresford, S. (compilers), *Controls on Giant Minerals Systems in the Yilgarn Craton—a Field Guide: Geological Survey of Western Australia, Record 2010/26*, 164 pp.
- Gresham, J.J. and Loftus-Hills, G.D., 1981. The geology of the Kambalda nickel field: *Economic Geology*, 76, 1373–1416.
- Hoatson, D.M. and Glaser, L.M., 1989. Geology and economics of platinum-group metals in Australia. Bureau of Mineral Resources, Australia, Resource Report 5, 81 pp.
- Hoatson, D.M., Jaireth, S. and Jaques, A.L., 2006. Nickel sulfide deposits in Australia: Characteristics, resources and potential. *Ore Geology Reviews*, 29, 177–241.
- Hudson, D.R. and Donaldson, M.J., 1984. Mineralogy of platinum group elements in the Kambalda nickel deposits, Western Australia. In: Buchanan, D.L. and Jones, M.J. (editors), *Sulphide Deposits in Mafic and Ultramafic Rocks*. The Institution of Mining and Metallurgy, London, 55–61.
- Keays, R.R. and Davison, R.M., 1976. Palladium, iridium and gold in the ores and host rocks of nickel-sulphide deposits in Western Australia. *Economic Geology*, 71, 1214–1228.
- Kositcin, N., Brown, S.J.A., Barley, M.E., Krapez, B., Cassidy, K.F. and Champion, D.C., 2008. SHRIMP U–Pb zircon age constraints on the Late Archaean Tectonostratigraphic architecture of the Eastern Goldfields Superterrane, Yilgarn Craton, Western Australia: *Precambrian Research*, 161, 5–33.
- Nelson, D.R., 1997. Evolution of the Archaean granite–greenstone terranes of the Eastern Goldfields, Western Australia: SHRIMP U–Pb zircon constraints. *Precambrian Research*, 83, 57–81.
- Stone, W.E., Beresford, S.W. and Archibald, N.J., 2005. Structural Setting and Shape Analysis of Nickel Sulfide Shoots at the Kambalda Dome, Western Australia: Implications for Deformation and Remobilization. *Economic Geology*, 100, 1441–1455.
- Travis, G.A., Keays, R.R. and Davison, R.M., 1976. Palladium and iridium in evaluation of nickel gossans in Western Australia. *Economic Geology*, 71, 1229–1243.

### **Relevant figure(s)**

Figure 6.21, Figure 6.22, Figure 6.23, Figure 6.24, and Figure 8.24.

## **K.1.98 Keller Creek**

### **Geological province**

Halls Creek Orogen.

### **Location**

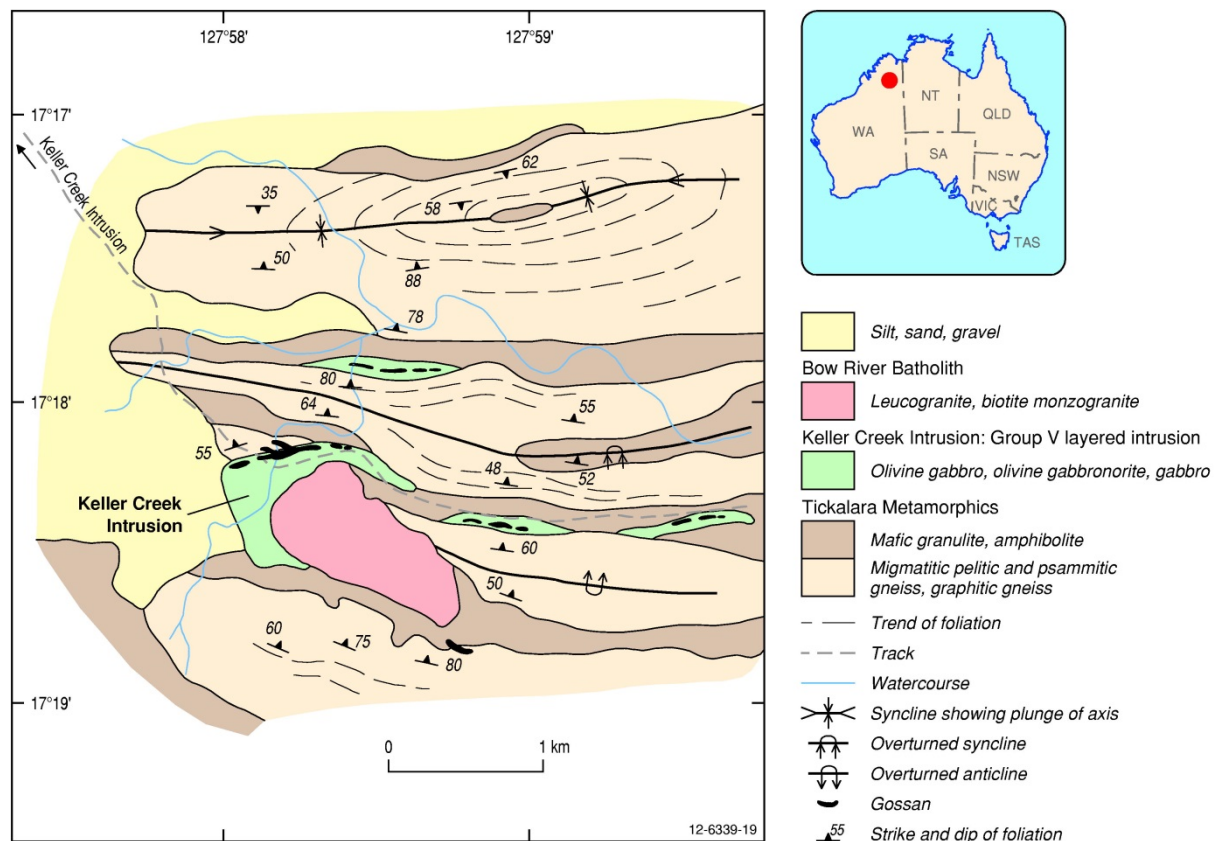
Keller Creek: 127.971290°E, -17.301870°S; Dixon Range (SE 52–06), Mount Remarkable (4463); ~108 km north-northeast of Halls Creek.

### **Classification**

- 2. Massive to poorly layered tholeiitic mafic-dominated intrusions; 2.A. Segregations of Ni-Cu-Co-PGE sulphides in feeder conduits and basal contacts.
- Some remobilisation of sulphide at intrusive contacts with granite.
- ?8. Hydrothermal-Metamorphic.

## Geological setting

The Keller Creek PGE occurrence is located within the Keller Creek Intrusion which forms a gabbroic lens, 0.3 km-wide by 1.5 km-long with an estimated thickness of 0.3 km (Appendix Figure K.11). The intrusion is folded around the northwestern end of a small elongate biotite monzogranite stock ('Misery Hill granite'). The folded western part of the intrusion occupies the hinge of a regional east-trending overturned anticline that extends eastwards towards the Savannah Intrusion and is generally concordant with adjacent mafic granulite and paramigmatite of the Tickalara Metamorphics. The main rock types are massive and weakly layered olivine gabbro, melagabbro, and minor leucogabbro. An unrelated coarse-grained amphibole-spotted melagabbro locally present below base of the intrusion, and no ultramafics have been identified (Sanders, 1999; Hoatson, 2000).



Appendix Figure K.11 Geological setting of the Keller Creek Intrusion, Halls Creek Orogen, Western Australia. Disseminated low-grade Ni-Cu-PGE sulphides persist along the northern basal contact beneath the thickest part of the mafic sequence and sulphides are also locally remobilised into structurally favourable sites in adjacent paragneiss and the contact aureole of the monzogranite stock. Modified from Hoatson (2000).

## PGE mineralisation

Disseminated low-grade Ni-Cu sulphide mineralisation persists along the northern basal contact beneath the thickest part of the mafic sequence. A 100 m-long lens of disseminated pyrrhotite, chalcopyrite, and pentlandite beneath a limonitic gossan crops out for about 400 m along strike (Appendix Figure K.11). The sulphide mineralisation is locally remobilised into structurally favourable sites in adjacent paragneiss and the contact aureole of the monzogranite stock. The best drill-hole intersection of 7.8 m @ 1.0% Ni and 0.26% Cu is in a marginal apophysis to the granite. Thin gossans cut paramigmatites of the Tickalara Metamorphics near the southeast end of the felsic stock indicating that the granitic stock may have been an important source of heat and fluids for remobilisation of the

Ni-Cu sulphides into the country rocks (as observed at the base of the nearby Savannah Intrusion). Thin gossans also occur in small gabbroic lenses 1.5 km and 2.5 km along strike to the east of the Keller Creek Intrusion. The best intersection for PGEs was in D5 from 24.5 m, 0.5 m @ 0.55 ppm Pt, 0.024 ppm Au, 0.63% Cu, 1.38% Ni; and 0.5 m @ 0.14 ppm Pd, 0.18 ppm Au, 0.34% Cu, 0.85% Ni from 25 m (Broken Hill Proprietary Co Limited, 1975).

### ***Age of mineralisation***

The Keller Creek Intrusion is tentatively correlated with the  $1844 \pm 3$  Ma Savannah Intrusion, but it may represent part of the older Tickalara Metamorphics ( $>1850$  Ma) (Hoatson, 2000).

### ***Current status***

Historical exploration site.

### ***Economic significance***

Occurrence.

### ***Major references(s)***

Broken Hill Proprietary Co Limited, 1975. Drill logs to accompany final report—TR Mabel Downs and MCs Keller Creek. WAMEX report A6140.

Hoatson, D.M., 2000. Geological setting, petrography, and geochemistry of the Palaeoproterozoic layered mafic-ultramafic intrusions. In: Hoatson, D.M. and Blake, D.H. (editors), *Geology and economic potential of the Palaeoproterozoic layered mafic-ultramafic intrusions in the East Kimberley, Western Australia*. Canberra: Australian Geological Survey Organisation Bulletin 246, 99–162.

Sanders, T.S., 1999. Mineralization of the Halls Creek Orogen, east Kimberley region, Western Australia. Geological Survey of Western Australia, Report 66 and Appendix, 44 pp.

### ***Relevant figure(s)***

Figure 8.21 and Appendix Figure K.11.

## **K.1.99 Killaloe\***

(see Dundas group)

## **K.1.100 Kintyre Group\***

### ***Geological province***

Paterson Orogen.

### ***Location***

Kintyre Group\*: 122.079596°E, -22.335430°S; Rudall (SF 51–10), Broadhurst (3353); ~72 km south-southwest of Telfer.

### ***Classification***

- 8. Hydrothermal-Metamorphic; 8.F. Unconformity-type U-Au-PGEs.

### ***Geological setting***

The Kintyre deposit is located in the Rudall region of the Paterson Province, north Western Australia. It was discovered in 1985 and has a resource estimate of 36 000 t U<sub>3</sub>O<sub>8</sub> with grades of 1.5–4.0 kg/t U<sub>3</sub>O<sub>8</sub> (Jackson and Andrew, 1990). Basement rocks in this region consist of high-grade isoclinally folded metasediments (Rudall Metamorphic Complex), which are unconformably overlain by Neoproterozoic sedimentary rocks (Coolbro Sandstone, Yeneena Group). Unlike the cover sequences for similar types of unconformity-related deposits in the Pine Creek Orogen of the Northern Territory, the overlying Coolbro Sandstone near Kintyre has been tightly folded and sheared.

### ***PGE mineralisation***

The ore is hosted by graphitic schist, and chloritic and carbonaceous schist, chert, pelite, and psammite in the basement Rudall Metamorphic Complex; hematite and carbonates occur immediately around mineralised veins. Mineralisation occurs as colloform uraninite in dolomitic carbonate veins, with lower-grade disseminated uraninite. Accessory to trace native Bi, chalcopyrite, bornite, galena, and Au are associated with uraninite, and PGEs have been detected.

### ***Age of mineralisation***

Mineralisation in Archean host rocks.

### ***Current status***

Undergoing scoping/feasibility studies.

### ***Economic significance***

Medium-sized U deposit.

### ***Major references(s)***

Jackson, D.G. and Andrew, R.L., 1990. Kintyre uranium deposit. In: Hughes, F.E. (editor), *Geology of the Mineral Deposits of Australia and Papua New Guinea*. The Australasian Institute of Mining and Metallurgy, Monograph 14, 653–658.

Mernagh, T.P., Wyborn, L.A.I. and Jagodzinski, E., 1998. 'Unconformity-related' U±Au±platinum-group-element deposits. *AGSO Journal of Australian Geology and Geophysics*, 17, 197–205.

### ***Relevant figure(s)***

## **K.1.101 Koondooloo Yard**

### ***Geological province***

Halls Creek Orogen.

### ***Location***

Koondooloo Yard: 127.931620°E, -17.425480°S; Dixon Range (SE 52–06), Mount Remarkable (4463); ~94 km north-northeast of Halls Creek.

### ***Classification***

- 2. Massive to poorly layered tholeiitic mafic-dominated intrusions.

### ***Geological setting***

The Koondooloo Yard prospect occurs in the southern half of the Spring Creek mafic intrusion in the Halls Creek Orogen of northern Western Australia. Spring Creek is a 2.5 km-thick ovoid mafic body exposed over an area of 4 km by 4 km (Appendix Figure K.12). Cyclic mafic units in the Lower Mafic Zone are parallel to the arcuate trend of the basal contact and dip towards the centre of the intrusion at 50°–65°. Shallower inward dips of 20°–45° characterise the Upper Mafic Zone. Spatial distribution of cyclic units reflects the original basinal geometry of the magma chamber. The intrusion has been divided into two mafic zones:

- Lower Mafic Zone is 1650 m-thick, and comprises interlayered olivine gabbro, olivine gabbro-norite, leucogabbro, and anorthosite. The Lower Mafic Zone consists of two megacyclic units—a lower 900 m-thick megacycle of interlayered mafic units and an upper 750 m-thick homogeneous megacycle; and
- Upper Mafic Zone is 850 m-thick, and comprises poorly layered troctolite, olivine gabbro, and leucogabbro.

Exploration companies have reported rare thin conformable peridotite layers in the lower part of the Upper Mafic Zone south of Spring Creek.

### ***PGE mineralisation***

About 16 samples across the Spring Creek Intrusion yielded low-level concentrations of PGEs no more than 10 ppb Pt or Pd.

### ***Age of mineralisation***

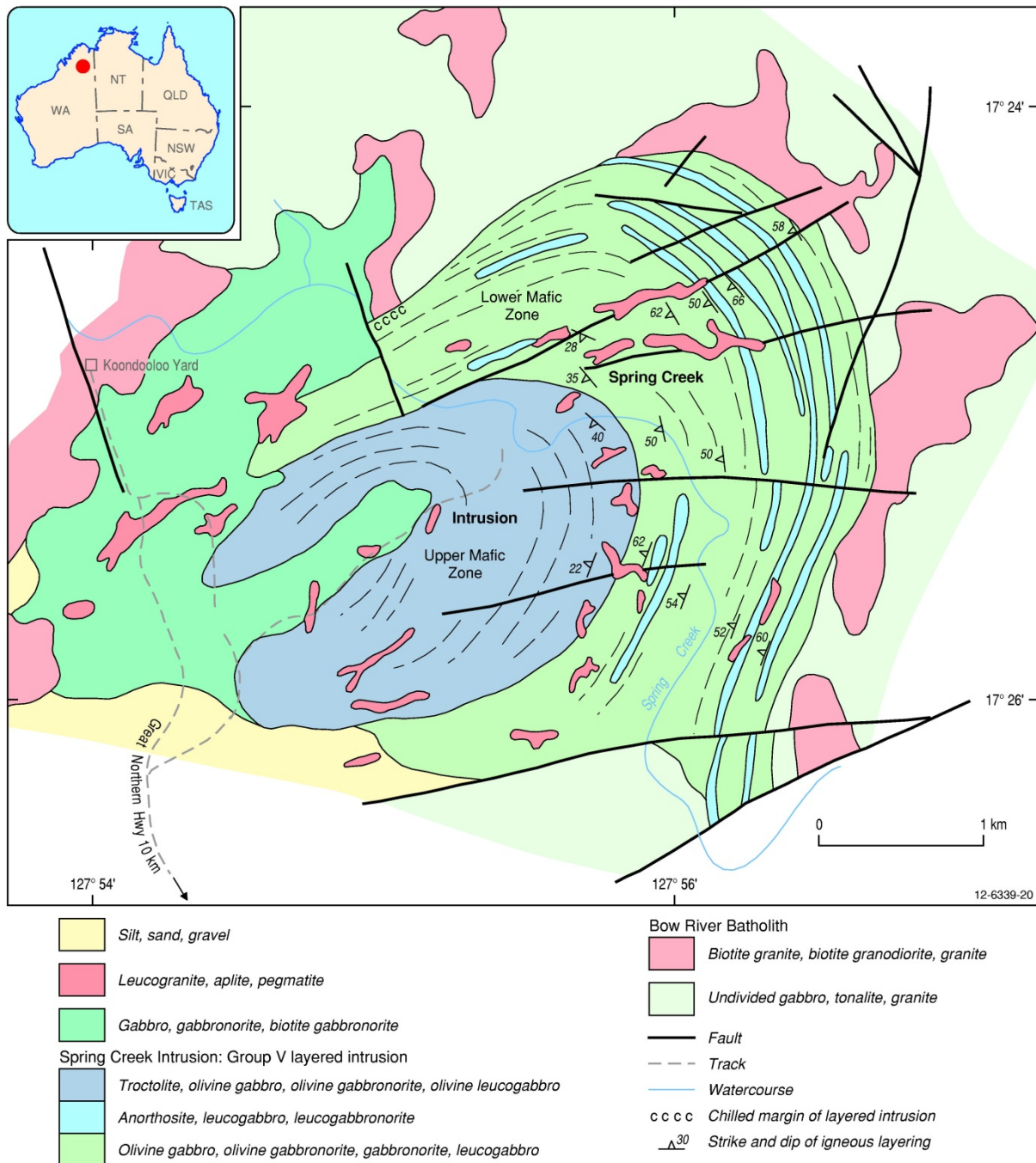
Tentatively correlated with the upper fractionated part of the 1844 ± 3 Ma Savannah Intrusion; however, field relationships described by Sheppard et al. (1997) suggest that it may be younger than 1820 Ma (Hoatson, 2000).

### ***Current status***

Exploration site.

### ***Economic significance***

Occurrence.



Appendix Figure K.12 Geological setting of the Spring Creek Intrusion, Halls Creek Orogen, Western Australia. The Koondooloo Yard prospect is located in the southern half of the Spring Creek mafic intrusion where rare conformable peridotite layers have been located. Modified from Hoatson (2000).

### Major references(s)

- Hoatson, D.M., 2000. Geological setting, petrography, and geochemistry of the Palaeoproterozoic layered mafic-ultramafic intrusions. In: Hoatson, D.M. and Blake, D.H. (editors), *Geology and economic potential of the Palaeoproterozoic layered mafic-ultramafic intrusions in the East Kimberley, Western Australia*. Canberra: Australian Geological Survey Organisation Bulletin 246, 99–162.
- Sanders, T.S., 1999. Mineralization of the Halls Creek Orogen, east Kimberley region, Western Australia. Geological Survey of Western Australia, Report 66 and Appendix, 44 pp.

### **Relevant figure(s)**

Figure 8.21 and Appendix Figure K.12.

## **K.1.102 Kurnalpi\* (?Acra South–Kurnalpi Nickel)**

### **Geological province**

Yilgarn Craton.

### **Location**

Travis et al. (1976) included a Ni-Cu-PGE occurrence named 'Kurnalpi' in their table of assay results of various samples from Ni deposits. All occurrences and deposits called Kurnalpi in the MINEDEX database are for Au. The Ni-Cu-PGE occurrence referred to by Travis et al. (1976) is probably an occurrence now listed in MINEDEX as 'Acra South–Kurnalpi Nickel'.

Acra South–Kurnalpi Nickel\*: 122.091301°E, -30.538799°S; Kurnalpi (SH 51–10), Kurnalpi (3336); ~64 km east-northeast of Kalgoorlie.

### **Classification**

- 12. Others (minor or unknown economic importance); 12.E. Others (unknown geological setting).

### **Geological setting**

Unknown. Pioneer Nickel Limited (2005) reported that drilling of a gossan outcrop included a drill-hole intercept of 7 m (from 202 m to 209 m) @ 0.83% Ni and 569 ppm Cu.

### **PGE mineralisation**

PGE contents for gossan samples as reported by Keays and Davison (1976) and Travis et al. (1976) including Kurnalpi returned 3.63 ppm Pd (2.70% Ni, 5.05% Cu).

### **Age of mineralisation**

Unknown

### **Current status**

Historical exploration site.

### **Economic significance**

Occurrence.

### **Major references(s)**

Keays, R.R. and Davison, R.M., 1976. Palladium, iridium and gold in the ores and host rocks of nickel-sulphide deposits in Western Australia. *Economic Geology*, 71, 1214–1228.

Pioneer Nickel Limited, 2005. Exploration update–November 2005. Pioneer Nickel Limited announcement to the Australian Securities Exchange, 25 November 2005, 2 pp.

Travis, G.A., Keays, R.R. and Davison, R.M., 1976. Palladium and iridium in evaluation of nickel gossans in Western Australia. *Economic Geology*, 71, 1229–1243.

**Relevant figure(s)**

**K.1.103 Lake Giles Nickel**

**Geological province**

Yilgarn Craton.

**Location**

Lake Giles Nickel: 119.928902°E, -29.822241°S; Barlee (SH 50–08), Lake Giles (2838); ~108 km west of Menzies.

**Classification**

- ?3. Komatiitic flows and sill-like intrusions.

**Geological setting**

The Lake Giles prospect occurs within the Archean Yerrilgee greenstone belt, a layered succession of high-Mg basalt, at least 1 km-thick that is intruded by gabbro sills (possibly comagmatic with the upper high-Mg basalts), and overlain by komatiitic ultramafic volcanic rocks, BIF, and other sedimentary rocks. The top of this sequence consists of further high Mg-basalt lavas occasionally with interflow BIF's which are overlain by cherty, silicified and graphitic sedimentary rocks forming the top of the sequence. The ultramafic rocks include metakomatiite and metaperidotite (InterNickel Limited, 2005).

**PGE mineralisation**

Trench geochemical sampling of one of eleven Ni sulphide exploration targets yielded 3 ppb to 24 ppb Pd and 4 ppb to 55 ppb Pt.

**Age of mineralisation**

Archean host rocks.

**Current status**

Historical exploration site.

**Economic significance**

Occurrences, exploration targets.

**Major references(s)**

InterNickel Limited, 2005. InterNickel Limited 2005 Prospectus, 96 pp.

**Relevant figure(s)**

**K.1.104 Lamboo Group (Edison, Edison (Wamin)\*, Western Zone\*, Dusty Bore 2, Nicholsons Find PGE, Lamboo (Cr 2, 5, 7, 21, 22, 23, 27), Lamboo (PGE 1, 2, 3, 4, 5, 6, 7, 8, 9, 10, 11, 12, 13, 14)**

**Geological province**

Halls Creek Orogen.

## **Location**

Lamboos (PGE 1): 127.330320°E, -18.475560°S; Mount Ramsay (SE 52–09), Angelo (4361); ~46 km southwest of Halls Creek.

Lamboos (Cr 23): 127.343640°E, -18.509630°S; Mount Ramsay (SE 52–09), Dockrell (4360); ~48 km southwest of Halls Creek.

Dusty Bore 2: 127.383260°E, -18.413330°S; Mount Ramsay (SE 52–09), Angelo (4361); ~38 km southwest of Halls Creek.

Nicholsons Find PGE: 127.35802°E, -18.41676°S; Mount Ramsay (SE 52–09), Angelo (4361); ~46 km southwest of Halls Creek.

Edison (Wamin): 127.3313°E, -18.46024°S; Mount Ramsay (SE 52–09), Angelo (4361); 44 km southwest of Halls Creek.

## **Classification**

- 1. Layered tholeiitic mafic-ultramafic intrusions; 1.B. Stratabound PGE-bearing chromitite layers.
- 8. Hydrothermal-Metamorphic (e.g., Edison prospect).

## **Geological setting**

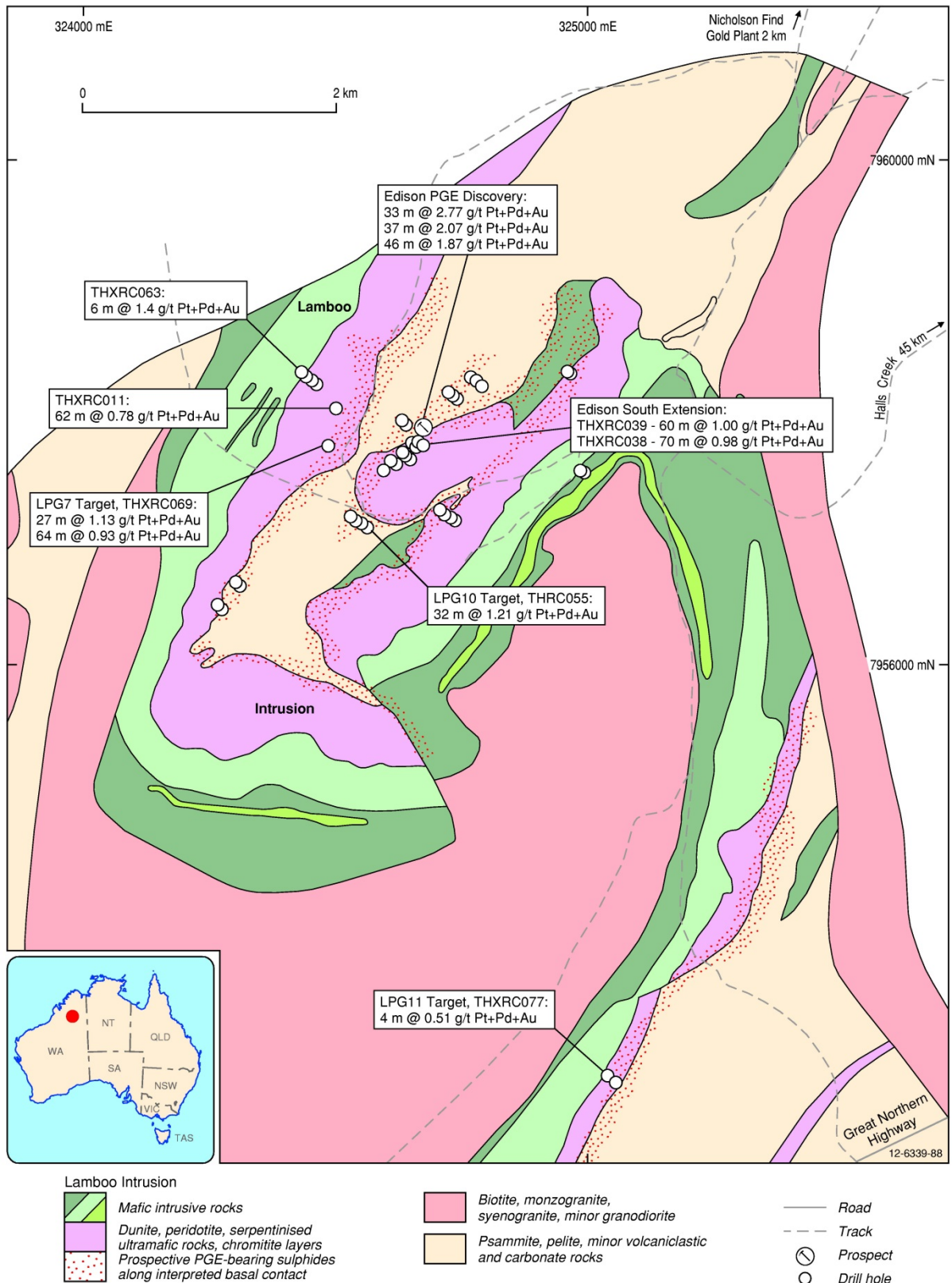
The Edison (Wamin) and Edison prospects covers the irregular basal portion of the Lamboos Igneous Complex (Appendix Figure K.13). The mineralisation is associated with a magnetic, sheared ultramafic unit, the Lamboos Ultramafics that can be traced in geophysical data for more than 800 m in a northeast strike direction. At least another 26 chromitite and PGE prospects are located in the Lamboos Igneous Complex (Griffin et al., 1998).

## **PGE mineralisation**

Two different styles of PGE mineralisation have been recognised in the Lamboos Complex.

The first style comprises the classic chromitite horizons in an oval shaped sill of mafic and ultramafic rock types. Serpentinised peridotite with subordinate pyroxenite and gabbro are the major rock types, with narrow chromitite horizons (up to 15 cm-thick) defining the rhythmic layering. Soil assays up to 1.2 ppm PGEs have been reported and persistent anomalism (>0.1 ppm PGEs) delineates a target zone at the top of a peridotite unit that extends for 14 km. Drilling has indicated that PGE mineralisation is associated with chromite-bearing peridotites at various levels in the intrusion, and in particular in the upper 200 m of the ultramafic series below the gabbro contact. Strike length of mineralisation is 11.5 km. The PGMs occur with chalcopyrite, pyrrhotite, pyrite, pentlandite, chromite, and some silicates. Local high Au values (9.46 ppm in LDH 4) are associated with talc schists. The best drilling results are:

- LDH 1: 1 m @ 0.49 ppm Pt, 0.90 ppm Pd, 0.07 ppm Au;
- LDH 4: 3 m @ 0.02 ppm Pt, 0.03 ppm Pd, 9.46 ppm Au, and 23 m @ 0.11 ppm Pt, 0.30 ppm Pd, 0.03 ppm Au;
- LDH 10: 4 m @ 0.32 ppm Pt, 0.48 ppm Pd, 0.04 ppm Au;
- LDH 16: 3 m @ 0.28 ppm Pt, 0.50 ppm Pd;
- LDH 21: 10 m @ 0.22 ppm Pt, 0.42 ppm Pd, 0.26 ppm Au; and
- LDH 32: 5 m @ 0.46 ppm Pt, 0.81 ppm Pd, 0.02 ppm Au.



Appendix Figure K.13 Geological setting and significant drill-hole PGE+Au intersections in the Lamboo Intrusion, Halls Creek Orogen, Western Australia. Modified from Thundelarra Exploration Limited (2006a,b).

## Western Australia

The potential of the intrusion is enhanced by the wide widths of mineralisation (e.g., up to 15 m in LDH 16), and the high Pt:Pd ratio of 1:1, with some intersections exceeding a 2:1 ratio (Hoatson and Glaser, 1989).

The second style of PGE mineralisation in the Lamboo Complex is typified by the Edison prospect where mineralisation occurs in a sheared ultramafic unit in the basal portion of the Lamboo Igneous Complex. Significant broad drill-hole intersections include 33 m @ 2.77 g/t (Pt+Pd+Au), 46 m @ 1.87 g/t (Pt+Pd+Au), and 37 m @ 2.07 g/t (Pt+Pd+Au) (Thundelarra Exploration Limited, 2006).

Drill-holes in the Western Zone prospect also highlighted broad mineralised zones of 20 m @ 0.37 g/t (Pt+Pd+Au) from THXRC078, and 168 m @ 0.66 g/t (Pt+Pd+Au) from THXRC079 (Thundelarra Exploration Limited, 2006).

### ***Age of mineralisation***

Proterozoic.

### ***Current status***

Historical exploration sites.

### ***Economic significance***

Occurrences.

### ***Major references(s)***

- Griffin, T.J., Tyler, I.M., Orth, K. and Sheppard, S., 1998. Geology of the Angelo sheet: Western Australia Geological Survey, 1:100 000 Geological Series Explanatory Notes, 27 pp.
- Hawthorn Resources Limited, 2008. June quarterly activities report and Appendix 5B cashflow report.
- Hoatson, D.M. and Glaser, L.M., 1989. The geology and economics of platinum-group metals in Australia. Bureau of Mineral Resources, Australia, Resource Report 5, 81 pp.
- Thundelarra Exploration Limited, 2006. Platinum-significant new discovery in the east Kimberley. Thundelarra Exploration Limited announcement to the Australian Securities Exchange, 17 August 2006, 21 pp.

### ***Relevant figure(s)***

Appendix Figure K.13.

## **K.1.105 Leo Dam**

### ***Geological province***

Yilgarn Craton.

### ***Location***

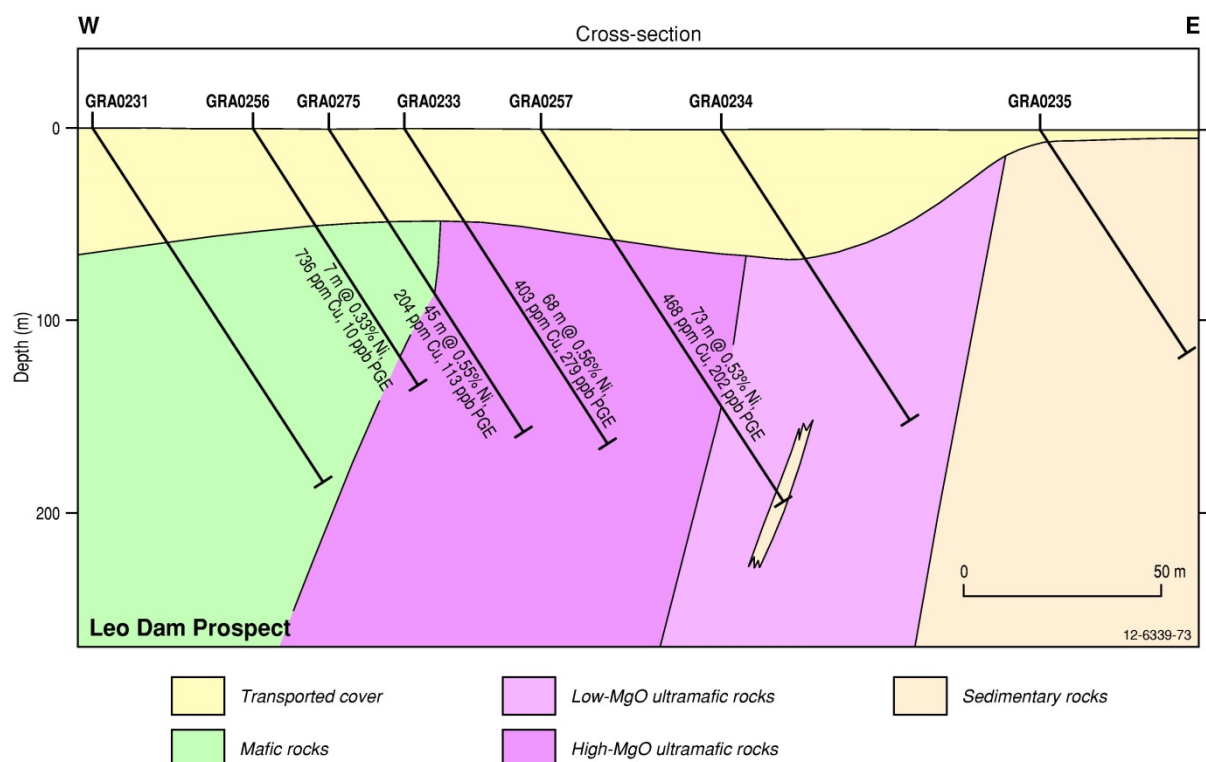
Leo Dam: 121.725854°E, -30.893884°S; Kurnalpi (SH 51–10), Kanowna (3236); ~28 km north of Kambalda.

### ***Classification***

- 3. Komatiitic flows and sill-like intrusions.

## Geological setting

The Leo Dam prospect is located in the Kurnalpi Terrane that comprises tholeiitic and komatiitic basalt lavas, intermediate calcalkaline complexes, feldspathic sedimentary rocks, and mafic to ultramafic intrusive rocks (Barley et al., 2004). Leo Dam is located 1.5 km northeast of the Blair Nickel Mine and is interpreted to lie on the same basal contact. A strong Ni-Cu-(Pd+Pt) anomaly has been defined over a strike of ~350 m, on three drill-hole cross-sections, and the anomalism remains open along strike to the north and south (Australian Mines Limited, 2009). The anomalous mineralisation is located within a weathered high-MgO ultramafic unit located stratigraphically above a footwall basalt (Appendix Figure K.14). One of the best intersections reported by Australian Mines Limited in a broadly spaced aircore program was 47 m at 0.62% Ni, supported by anomalous Cu and PGEs. A number of the geochemical anomalies are coincident with EM conductors as defined by 'SQUID' EM technology.



Appendix Figure K.14 Schematic east-west cross-section of the Leo Dam Ni-Cu-PGE prospect, Yilgarn Craton, Western Australia. Modified from Pioneer Nickel Limited (2008).

## PGE mineralisation

Disseminated Ni-Cu-PGE mineralisation is hosted by weathered high-MgO komatiitic rocks in drill-hole GRA0233, with an intersection of 68 m @ 0.56% Ni, 403 ppm Cu, and 279 ppb Pt+Pd (Australian Mines Limited, 2008).

## Age of mineralisation

Archean (?2715 Ma–2698 Ma) host rocks.

## Current status

Exploration site.

### ***Economic significance***

Occurrence.

### ***Major references(s)***

Australian Mines Limited, 2008. Quarterly report on activities for period ended 30<sup>th</sup> September 2008, 16 pp.

Australian Mines Limited, 2009. Australian Mines Limited Annual Report for the Year ended 30 June 2009, 85 pp.

Barley, M.E., Doyle, M.G., Kositcin, N., Krapez, B., Cassidy, K.F. and Champion, D.C., 2004. Late Archaean arc and seamount volcanism in the Kurnalpi Terrane, Eastern Yilgarn Craton, Western Australia. In: Barnicoat, A.C. and Korsch, R.J. (editors), Predictive Mineral Discovery Cooperative Research Centre—Extended Abstracts from the June 2004 Conference. Geoscience Australia, Record 2004/09, 3–6.

### ***Relevant figure(s)***

Appendix Figure K.14.

## **K.1.106 Limestone Spring–Maiwa Reward**

(see also Jacks Hill)

### ***Geological province***

King Leopold Orogen.

### ***Location***

Limestone Spring–Maiwa Reward: 124.460297°E, -16.940950°S; Yampi (SE 51–03), Tarraji (3764); ~98 km east-northeast of Derby and ~0.6 km southwest of the Jacks Hill prospect.

### ***Classification***

- 12. Others (minor or unknown economic importance); 12.E. Others (unknown geological setting).

### ***Geological setting***

The Limestone Spring–Maiwa Reward prospect lies within Paleoproterozoic rocks of the King Leopold Orogen, which includes altered sediments of the Marboo Formation that have been intruded by the Ruins Dolerite and coarse-grained granitic bodies. The regional stratigraphy and foliation trend is northwest (Tyler and Griffin, 1993; Al Maynard and Associates Pty Limited, 2012).

### ***PGE mineralisation***

Mineralisation for Cu, Ni, Au, Ag, and PGEs was recorded in the WA Department of Mines and Petroleum MINEDEX database for this occurrence in 2014. Copper and Ni mineralisation is hosted in Ruins Dolerite and xenoliths of schists of Marboo Formation within Ruins Dolerite (Masham, 1970). Mineralisation is exposed in a shallow shaft and trenches over 90 m and was tested by 2 diamond drill-holes. Mined for Cu in 1902, but no recorded production.

### ***Age of mineralisation***

Proterozoic?

### ***Current status***

Exploration.

### ***Economic significance***

Occurrence.

### ***Major references(s)***

- Al Maynard and Associates Pty Limited, 2012. Independent Geologists's report. In: Victory Mines Limited 2012 Prospectus, 35–77.
- Masham, J.S., 1970. Limestone Springs drilling program. Pickands Mather and Co International. WAMEX report A523, 31 pp.
- Tyler, I.M. and Griffin, T.J., 1993. Yampi, Western Australia, 1:250 000 Geological Series Explanatory Notes, Sheet SE 51–3. Second edition. Geological Survey of Western Australia, Perth, Western Australia, Australia, 32 pp.
- Victory Mines Limited, 2013. Broad zones of nickel sulphide mineralisation discovered and Clara Hills. Victory Mines Limited announcement to the Australian Securities Exchange, 16 January 2013, 3 pp.

### ***Relevant figure(s)***

## **K.1.107 Lionel\***

### ***Geological province***

Pilbara Craton.

### ***Location***

Lionel\*: ~25 km north of Nullagine; a more accurate location is not available.

### ***Classification***

- ?3. Komatiitic flows and sill-like intrusions.

### ***Geological setting***

Intense serpentinite alteration in the Archean Lionel ultramafic-mafic sequence, which consists of dunite, peridotite, pyroxenite, and gabbro. Banded chert, BIF, felsic agglomerate, tuff, andesite, and basalt are associated with the sill-like intrusive rocks.

### ***PGE mineralisation***

Copper-sulphide vein mineralisation occurs in gabbro and the ultramafics. Copper was mined before World War 2. Drilling in mid-1987 delineated anomalous PGE levels near a contact between gabbro and peridotite (Hoatson and Glaser, 1989).

### ***Age of mineralisation***

Archean host rocks.

### ***Current status***

Exploration site.

### ***Economic significance***

Occurrence.

### ***Major references(s)***

Hoatson, D.M. and Glaser, L.M., 1989. Geology and economics of platinum-group metals in Australia. Bureau of Mineral Resources, Australia, Resource Report 5, 81 pp.

### ***Relevant figure(s)***

## **K.1.108 Longhorn**

(see Eastman Bore–Louisa Downs group)

## **K.1.109 Loongana**

### ***Geological province***

Basement to Eucla Basin.

### ***Location***

Loongana: 126.422650°E, -30.776866°S; Loongana (SH 52–09), Turner (4136); ~255 km west-northwest of Eucla.

### ***Classification***

- 2. Massive to poorly layered tholeiitic mafic-dominated intrusions; 2.A. Segregations of Ni-Cu-Co-PGE sulphides in feeder conduits and basal contacts.

### ***Geological setting***

The Loongana prospect lies within the Madura Crustal Element, immediately east of the Albany-Fraser Province. The principal exploration model at Loongana was for Ni sulphide mineralisation associated with a layered mafic-ultramafic intrusion, which lies beneath 250 m to 350 m of Cenozoic limestone and Mesozoic sedimentary rocks of the Eucla Basin. A vertical drill-hole LNGD1 intersected 77 m of layered gabbro, pyroxenite, and harzburgite immediately below the unconformity at 269 m. The intrusion has an approximate area of 600 km<sup>2</sup>. The layered sequence is truncated by lamprophyric and granitic gneiss sequences at depths below 346 m in LNGD1 (Helix Resources Limited, 2002).

Drill-hole LONRC 1 intersected the intrusive at a depth of between 342 m and 354 m after passing through 97 m of limestone and at least 245 m of intercalated black carbonaceous siltstones and occasional clays. Between 306 m and 342 m, some massive sulphides were intersected in the siltstone. Between 306 m and 308 m the sulphides appeared to be dominantly pyrite and for the balance of the massive sulphide section, at least 50% pyrite. Drill-hole LONRC 2 intersected the intrusion at 299 m, after passing through 132 m of limestone and 167 m of black and grey siltstone. From 299 m to 330 m the intrusion was an olivine peridotite before passing into a pyroxenite to 350 m and then a norite to 372 m. The balance of the drill-hole was logged as a pyroxenite except for two separate felsic intrusions at 372 m–378 m and 390 m–395 m (Richmond Mining Limited, 2009).

### ***PGE mineralisation***

From 275.2 m, 8 m of the drill-hole was anomalous in PGEs with the best result 0.72 m @ 0.11 ppm Pt+Pd from 275.2 m. The best intersection in drill-hole LNGD 2 was 1.4 m @ 53 ppb Pt+Pd for gabbro at 372.1 m.

However, another six drill-holes (LONRC1–6) within the southern bulbous section of the Loongana Intrusion did not intersect Ni-Cu-PGE sulphides. The intrusive rocks below the unconformity, at depths of 258 m to 354 m, are predominantly mafic norites and gabbros while the ultramafic rocks are most likely variably altered metamorphosed mafic rocks (Richmond Mining Limited, 2009). However, LONRC 5 intersected Au mineralisation with associated elevated Cu values. The best intercept was 1 m @ 2.67 g/t Au from 368 m in a quartz–feldspar vein. Further quartz veining between 370 m–372 m contained on average 0.13% Cu and the interval from 371 m–372 m also contained 0.74 g/t Au (Richmond Mining Limited, 2009).

On 4 June 2010, Richmond mining announced that it has been awarded a grant of \$105 000 by the Western Australian State Government for a co-funded drilling programme to test the Loongana prospect. The exploration target for the drill-hole was massive Ni sulphide mineralisation associated with Proterozoic intrusive mafic and ultramafic rocks. The intrusion has been modelled as having a bulbous head region representing a magma chamber and a neck region with a long lenticular tail representing a potential feeder zone (Richmond Mining Limited, 2010).

### ***Age of mineralisation***

The Loongana Intrusion has a U-Pb zircon age of  $1415 \pm 7$  Ma (Bunting, 2007; Hoatson et al., 2008a,b).

### ***Current status***

Exploration site.

### ***Economic significance***

Occurrence.

### ***Major references(s)***

- Bunting, J.A., 2007. Albany-Fraser and sub–Eucla: a new but not-so-remote frontier. PowerPoint presentation at Proterozoic Mineralisation in Western Australia Conference, 11 June 2007. Australian Institute of Geoscientists, Western Australian Branch, 1–8.
- Helix Resources Limited, 2002. Quarterly Report, 31 December 2002, 7 pp.
- Hoatson, D.M., Claoué-Long, J.C. and Jaireth, S., 2008a. Guide to using the 1:5 000 000 map of Australian Proterozoic Mafic-Ultramafic Magmatic Events. Geoscience Australia Record 2008/15, 140 pp.
- Hoatson, D.M., Claoué-Long, J.C. and Jaireth, S., 2008b. Australian Proterozoic Mafic-Ultramafic Magmatic Events, Sheets 1 and 2 (1:10 000 000 scale maps), Geoscience Australia, Canberra, GeoCat 66114.
- Richmond Mining Limited, 2008. Richmond Mining Limited 2008 Prospectus, 120 pp.
- Richmond Mining Limited, 2009. Quarterly Report to December 2009, 7 pp.
- Richmond Mining Limited, 2010. Successful DMP co-funding grant for Loongana Nickel Project. Richmond Mining Limited announcement to the Australian Securities Exchange, 4 June 2010, 1 pp.

## ***Relevant figure(s)***

### **K.1.110 Louisa**

(see Eastman Bore–Louisa Downs group)

### **K.1.111 Malbec—Cabernet, Merlot, Vidure\***

#### ***Geological province***

Yilgarn Craton.

#### ***Location***

Malbec: 118.766667°E, -28.805730°S; Youanmi (SH 50–04), Youanmi (2640); ~105 km south-southwest of Sandstone.

Cabernet: 118.761974°E, -28.803812°S; Youanmi (SH 50–04), Youanmi (2640); ~104 km south-southwest of Sandstone and ~16 km southeast of the Windimurra Igneous Complex.

Merlot: 118.745796°E, -28.809441°S; Youanmi (SH 50–04), Youanmi (2640); ~106 km south-southwest of Sandstone;

Vidure\*: 118.756500°E, -28.8121301°S; Youanmi (SH 50–04), Youanmi (2640); ~106 km south-southwest of Sandstone.

#### ***Classification***

- ?1. Layered tholeiitic mafic-ultramafic intrusions.

#### ***Geological setting***

The three PGE prospects occur along the southern margin of the deformed mafic-ultramafic Youanmi Igneous Complex, which forms part of the ~2810 Ma Meeline Suite. The complex comprises layered gabbro and anorthosite with magnetite and pyroxenite layers (Van Kranendonk and Ivanic, 2009). Some of the prospects appear to be in the adjacent greenstone country rock rather than in the intrusion.

#### ***PGE mineralisation***

Malbec–Cabernet: An auger geochemistry program delineated a previously reported eastern anomaly into a polymetallic zone called the Malbec prospect and a Ni-Cu anomaly about 200 m to the south called the Cabernet prospect. The Cabernet prospect is associated with a historical Ni and Cu gossan prospect, and auger hole intersections returned maximum values of 0.31% Cu, 0.18% Ni, and 11 ppb Au (Ellendale Resources NL 2005a). The Malbec prospect was delineated as a 900-m long geochemical anomaly, located at the contact between a gabbro and an ultramafic with maximum values of 0.25% Ni, 0.31% Cu, 34 ppb Au, 105 ppb Pt, and 90 ppb Pd. Deeper drilling intersected sulphide mineralisation at a contact between talc magnesite and amphibolite in CNRC015 with 7 m @ 0.97% Ni, 0.49% Cu, 0.04% Co, and 1.44 g/t PGEs from 129 m. Drill-hole CNRC018 intersected 7 m @ 0.33% Ni, 0.22% Cu, 0.02% Co, and 0.58 g/t PGEs from 185 m (Ellendale Resources NL, 2004).

Further exploration identified a 700 m-long conductive zone along strike to the north of the Malbec Ni-Cu-PGE-sulphide horizon and results from follow-up drilling are listed in Appendix Table K.21 below (Hawthorn Resources Limited, 2008).

Appendix Table K.21 Geochemical results for the Malbec-Cabernet prospects. Data from Hawthorn Resources Limited (2008).

Dill-hole	From (m)	Interval (m)	Cu (%)	Ni (%)	Pt (ppm)	Pd (ppm)
CWRC023	180	8	0.3	0.57	0.26	0.75
CWRC034	164	4	0.4	0.49	0.09	0.74
CWRC035	128	4	0.37	0.49	0.59	0.63

Merlot: The Merlot prospect overlies an ultramafic sequence covered by shallow transported overburden. The geochemical anomaly is over 800 m-long and returned maximum values of 290 ppb Pd, 115 ppb Pt, 14 ppb Au, 0.15% Ni, and 876 ppm Cu. (Ellendale Resources NL, 2004, 2005b).

Vidure: A soil-sampling geochemical anomaly over the prospect had maximum values of 700 ppb Pd, 195 ppb Pt, 24 ppb Au, 0.18% Ni, and 0.13% Cu. The prospect is located over weathered ultramafics and is coincident with a magnetic low. Limited RAB drilling returned a maximum PGE intersection in the oxide zone of 40 m @ 0.44 g/t Pd and 0.10 g/t Pt from surface to end of hole (including 2 m @ 0.58 g/t Pd, 0.25 g/t Pt to EOH) (Ellendale Resources NL, 2005b).

### **Age of mineralisation**

Murchison Domain age ~2780 Ma? (Van Kranendonk and Ivanic, 2009).

### **Current status**

Exploration sites.

### **Economic significance**

Occurrences.

### **Major references(s)**

Ellendale Resources NL, 2004. Currans Well nickel prospect—holding increased to 100%. Ellendale Resources NL announcement to the Australian Securities Exchange, 10 December 2004, 4 pp.

Ellendale Resources NL, 2005a. Nickel and platinum group anomalies delineated. Ellendale Resources NL announcement to the Australian Securities Exchange, 22 August 2005, 3 pp.

Ellendale Resources NL, 2005b. Ellendale Resources NL Annual Report 2005, 49 pp.

Hawthorn Resources Limited, 2008. Annual Report 2008, 72 pp.

Van Kranendonk, M.J. and Ivanic, T.J., 2010. A new lithostratigraphic scheme for the northeastern Murchison Domain, Yilgarn Craton. In: Western Australia Geological Survey Annual Review 2007–08, 35–53.

### **Relevant figure(s)**

## **K.1.112 Malbec–Wills Creek**

(see Copernicus group)

## **K.1.113 Manchego prospect\***

part of West Musgrave Project (recorded as a Cu, Ni, PGE, Co occurrence in MINLOC)

**Geological province**

Musgrave Province.

**Location**

Manchego prospect: 127.489390°E, -25.677728°S; Bentley (SG 52–05), Bentley (4346).

**Classification**

- 2. Massive to poorly layered tholeiitic mafic-dominated intrusions; 2.B. Stratabound PGE-bearing magnetite layers.

**Geological setting**

The Manchego prospect was detected as an airborne electro-magnetic anomaly in 2012, where it appears to occur over the confluence of two interpreted mafic dykes within the Jameson Range Intrusion, but does not follow the strong northwest-southeast-trending magnetic layers in the complex (Phosphate Australia Limited, 2013a,b). The Jameson Range Intrusion is part of the 1070 Ma Giles mafic-ultramafic complex and is composed of approximately 2500 m of layered Fe-rich troctolite, gabbroic troctolite, anorthosite, and stratabound magnetite layers.

**PGE mineralisation**

Magnetite seams occur as discrete layers within igneous intrusive complexes and show up as linear features on the aeromagnetic images which may be traced for tens of km. Thicknesses of these seams may measure up to 15 m or more. Four samples from a magnetite outcrop were sampled by Phosphate Australia Limited and assayed returning the values in Appendix Table K.22 (Phosphate Australia Limited, 2012).

*Appendix Table K.22 Magnetite outcrop geochemistry data for the Manchego Prospect. Data from Phosphate Australia Limited (2012).*

Drill-hole	Fe (%)	TiO <sub>2</sub> (%)	V <sub>2</sub> O <sub>5</sub> (%)	Pt (ppb)	Pd (ppb)	Rh (ppb)	Ir (ppb)	Au (ppb)	PGEs+Au (g/t)
MR01	46.5	23.9	1.25	2075	780	41	16	58	2.97
MR02	46.9	22.9	1.21	2443	863	38	16	76	3.44
MR03	47.2	23.7	1.29	960	306	70	18	21	1.38
MR05	45.2	27.1	1.11	1280	492	27	12	186	2.00
<b>Average</b>	<b>46.5</b>	<b>24.4</b>	<b>1.22</b>	<b>1690</b>	<b>610</b>	<b>44</b>	<b>16</b>	<b>85</b>	<b>2.44</b>

*Analytical techniques: Fe, TiO<sub>2</sub>, and V<sub>2</sub>O<sub>5</sub> by fused-disk preparation for XRF analysis—analysed by XRF Spectrometry. Pt, Pd, Au, Rh, and Ir by 25 g lead collection fire assay—analysed by Inductively Coupled Plasma Mass Spectrometry. Other PGEs (Os and Ru) were not detected.*

Drilling and analyses of drill-hole samples over the Manchego prospect by Anglo American Plc showed extensive low-grade Cu and Ni mineralised zones, with anomalous PGE values in gabbroic zones as tabulated below in Appendix Table K.23.

Appendix Table K.23 Geochemistry of drill-hole samples across the Manchego Prospect.

Drill-hole	From (m)	To (m)	Interval (m)	Cu (%)	Ni (ppm)	Pt+Pd+Au (ppm)	Pt (ppm)	Pd (ppm)	Au (ppm)	Fe (%)	S (%)	Ti (%)
MRC040	4	8	4	0.09	420	0.06	0.02	0.03	0.01	14.5	0.0	1.2
MRC040	66	100	34	0.21	346	0.11	0.03	0.07	0.01	12.4	>5.0	0.8
MRC041	40	44	4	0.19	507	0.15	0.04	0.10	0.01	11.5	0.9	0.9
MRC041	112	138	26	0.18	233	0.10	0.02	0.07	0.01	10.8	>5.4	0.5
MRC042	66	90	24	0.27	525	0.15	0.03	0.10	0.02	14.4	3.8	1.1
including	71	76	5	0.54	1144	0.28	0.06	0.19	0.03	22.0	5.9	1.4
and	71	72	1	1.65	1080	0.26	0.06	0.18	0.03	22.2	17.0	1.4
MRC043	40	56	16	0.11	220	0.11	0.04	0.06	0.01	12.1	0.4	1.4
MRC043	80	82	2	0.34	457	0.11	0.03	0.07	0.01	15.7	2.0	1.5
MRC044	62	72	10	0.12	211	0.07	0.03	0.04	0.01	8.3	0.2	1.0
MRC044	126	144	18	0.17	163	0.11	0.03	0.07	0.01	11.5	4.1	0.7
MRC044	168	169	1	0.31	492	0.32	0.08	0.21	0.03	10.8	0.5	0.9
MRC048	98	141	43	0.18	658	0.11	0.02	0.08	0.01	17.1	>1.9	1.5
including	114	118	4	0.53	3420	0.37	0.03	0.32	0.01	38.2	>9.3	1.0
MRC0481	235	248	13	0.15	313	0.14	0.03	0.10	0.01	12.4	5.8	
MRC052	22	31	9	0.18	214	0.06	0.02	0.03	0.01	16.1	0.7	
MRC052	55	58	3	0.12	170	0.07	0.02	0.05	0.01	18.6	5.6	
MRC052	88	93	5	0.19	194	0.05	0.02	0.03	0.01	14.6	3.6	
MRC052	97	100	3	0.16	304	0.08	0.02	0.05	0.01	15.2	2.8	
MRC052	105	108	3	0.13	725	0.46	0.16	0.27	0.02	21.3	5.6	
including	105	106	1	0.20	1430	1.00	0.41	0.54	0.05	28.4	11.0	
MRC052	118	119	2	0.16	149	0.06	0.01	0.03	0.01	11.5	5.7	
MRC052	172	174	2	0.12	130	0.08	0.03	0.04	0.01	10.2	0.2	
MRC053	209	212	3	0.11	207	0.07	0.02	0.05	0.00	11.2	3.9	
MRC054	102	128	26	0.16	204	0.10	0.03	0.05	0.01	12.0	1.3	
MRC056	137	144	7	0.11	240	0.08	0.03	0.04	0.01	13.5	0.7	
MRC056	150	157	7	0.25	332	0.12	0.03	0.08	0.01	11.5	2.3	
MRC056	223	225	2	0.10	168	0.24	0.06	0.17	0.00	7.2	5.3	
WB014	102	116	14	0.12	179	0.09	0.03	0.05	0.01	10.9	4.6	
<b>Assay Detection Limits</b>												
Units				ppm	ppm	ppm	ppm	ppm	ppm	%	%	%
Lower Limit of Detection				1	1		0.005	0.001	0.005	0.01	0.01	0.01
Upper Limit of Detection				10 000	10 000					50.0	10.0	10.0

**Age of mineralisation**

Mesoproterozoic.

### ***Current status***

Exploration site.

### ***Economic significance***

Occurrence.

### ***Major references(s)***

Glikson, A.Y., Stewart, A.J., Ballhaus, C.G., Clarke, G.L., Feeken, E.H.J., Leven, J.H., Sheraton, J.W. and Sun, S.-S., 1996. Geology of the western Musgrave Block, central Australia, with particular reference to the mafic-ultramafic Giles Complex. Australian Geological Survey Organisation Bulletin 239, 206 pp.

Phosphate Australia Limited, 2012. Anglo American farm-in agreement for Musgrave Project (WA) secured. Phosphate Australia Limited announcement to the Australian Securities Exchange, 2 April 2012, 3 pp.

Phosphate Australia Limited, 2013a. Phosphate Australia Limited Annual Report 2012, 30 pp.

Phosphate Australia Limited, 2013b. Manhego Prospect, Musgrave WA: Phase 2 drilling to commence late October. Phosphate Australia Limited announcement to the Australian Securities Exchange, 28 October 2013, 7 pp.

Phosphate Australia Limited, 2014. Manhego Prospect, Musgrave WA: Phase 2 drilling results. Phosphate Australia Limited announcement to the Australian Securities Exchange, 3 January 2014, 12 pp.

### ***Relevant figure(s)***

#### **K.1.114 Marriott\***

(see Mt Keith\*)

#### **K.1.115 McWhae Ridge**

##### ***Geological province***

King Leopold Orogen, Canning Basin.

##### ***Location***

McWhae Ridge: 126.083°E, 18.733°S; Mount Ramsay (SE 52–09), Bohemia (4160); on the northern margin of the Canning Basin; ~280 km southeast of Derby.

##### ***Classification***

- 12. Other occurrences; 12.B. Anomalous PGEs in sedimentary rocks related to possible impact structure.

##### ***Geological setting***

Weakly anomalous Ir, with associated elevated concentrations of Pt, V, Co, Ni, Cu, As, Sb, Pb, Th, and rare-earth elements, have been reported in a Late Devonian deep-water limestone sequence in the Canning Basin of Western Australia (Playford et al., 1984; McLaren, 1985). The stratigraphic position of the anomaly appears to coincide with a major global biotic extinction. Similar Ir anomalies have been observed throughout the world in thin clay horizons at the relatively younger Cretaceous-

Cenozoic boundary (Figure 8.1), and have been put forward as evidence that the Ir enrichment and biota extinctions were caused by a large asteroid or comet impact on the Earth.

### ***PGE mineralisation***

The Ir anomaly attains 20 times background levels in the limestones from the Canning Basin, and reaches a maximum of 0.3 ppb. These PGE concentrations have no economic significance.

### ***Age of mineralisation***

Upper Devonian?

### ***Current status***

Unknown.

### ***Economic significance***

Occurrence.

### ***Major references(s)***

Hoatson, D.M. and Glaser, L.M., 1989. Geology and economics of platinum-group metals in Australia. Bureau of Mineral Resources, Australia, Resource Report 5, 81 pp.

McLaren, D.J., 1985. Mass extinction and iridium anomaly in the Upper Devonian of Western Australia: A commentary. *Geology*, 13, 170–172.

Playford, P.E., McLaren, D.J., Orth, C.J., Gilmore, J.S. and Goodfellow, W.D., 1984. Iridium anomaly in the Upper Devonian of the Canning Basin, Western Australia. *Science*, 226, 437–439.

### ***Relevant figure(s)***

## **K.1.116 Medusa—Peninsula**

(see Airstrip Cr Pt group)

## **K.1.117 Melon Patch group (Melon Patch 1, 2, 3, 4, 5, 6, 7, 8, 9 10, 11)**

### ***Geological province***

Halls Creek Orogen.

### ***Location***

Melon Patch 11: 127.93189°E, -17.64064°S, occurs near the centre of the South Melon Patch Intrusion; Dixon Range (SE 52–06), McIntosh (4462); ~70 km north-northeast of Halls Creek.

Melon Patch 7: 127.94266°E, -17.70443°S.

Melon Patch 10: 127.91242°E, -17.64952°S.

Melon Patch 1: 127.93577°E, -17.6031°S.

### ***Classification***

- 1. Layered tholeiitic mafic-ultramafic intrusions; 1.B. Stratabound PGE-bearing chromitite layers.

## Geological setting

The South Melon Intrusion forms a tight southwesterly plunging anticline, 5.5 km-long by 2.5 km-wide, and about 1 km-thick. It is located on the northern side of the McIntosh Intrusion and structurally it appears to be coaxial with the Mini Intrusion to the southwest. A complete, exposed sequence of differentiated mafic and ultramafic rocks, together with roof and floor country rocks, is similar to the nearby Panton Intrusion. The anticlinal axis region of the intrusion consists of basement metasediments of the Tickalara Metamorphics, ovoid bodies of foliated leucogranite, and dolerite dykes. The 300 m-thick basal ultramafic sequence consists of serpentinised peridotite, dunite, chromitite, and minor harzburgite, which is overlain by a 700 m-thick mafic sequence comprising gabbro, gabbronorite, and minor norite (400 m), followed by foliated amphibolite and melagabbro (150 m), and the upper part of the intrusion is represented by mottled anorthosite and leucogabbro (150 m). Thin plagioclase-bearing tremolite–anthophyllite–hercynite schist units occur near the contact between the ultramafic and mafic sequences.

The Melon Patch Intrusion is separated from the South Melon Patch Intrusion by a northwest-trending fault and it consists of two northeast-trending, steeply dipping (65°), elongate bodies that dip and young to the southeast. The southern body is an irregular ultramafic intrusion, 2 km-long by 600 m-wide, and the northern body is a mafic–ultramafic intrusion, 3 km-long by 500 m-wide.

## PGE mineralisation

About nine of 11 Melon Patch PGE occurrences are located in the vicinity of the South Melon Patch Intrusion while Melon Patch 1 is in the northwest portion of the Melon Patch Intrusion. The sequence of peridotite in South Melon Patch Intrusion is well fractionated—(mg78.6–82; 2438 ppm–7235 ppm Cr) melagabbro and gabbro (mg57.4–78.3; 60 ppm–1951 ppm Cr), and leucogabbro (mg42.1; 10 ppm Cr). The PGE-enriched chromitites hosted by serpentinised ultramafic rocks have been a focus for company drilling (Appendix Figure K.15). The PGE and Au mineralisation occurs as chromitite seams up to 3.5 km-long within the South Melon Patch layered mafic-ultramafic intrusion (3D Resources Limited 2006). Chromitite and chromite-bearing peridotite in the upper part of the Ultramafic Zone stratigraphically below the Gabbroic Zone are enriched in Pt (527 ppb and 91.6 ppb), Pd (283 ppb and 179 ppb) and Au (38 ppb and 3 ppb), and the variable S content (40 ppm–1350 ppm) of the mafic and ultramafic cumulates partly reflects serpentinisation and uraltisation alteration. The most PGE-enriched chromitites in the upper parts of the ultramafic stratigraphy is identical to that observed in the nearby Panton Intrusion. Exploration drilling along three lines in 2001 intersected two chromitite seams (Appendix Figure K.15) with analytical results shown in Appendix Table K.24 (Hoatson, 2000; RSG Global Pty Limited, 2006).

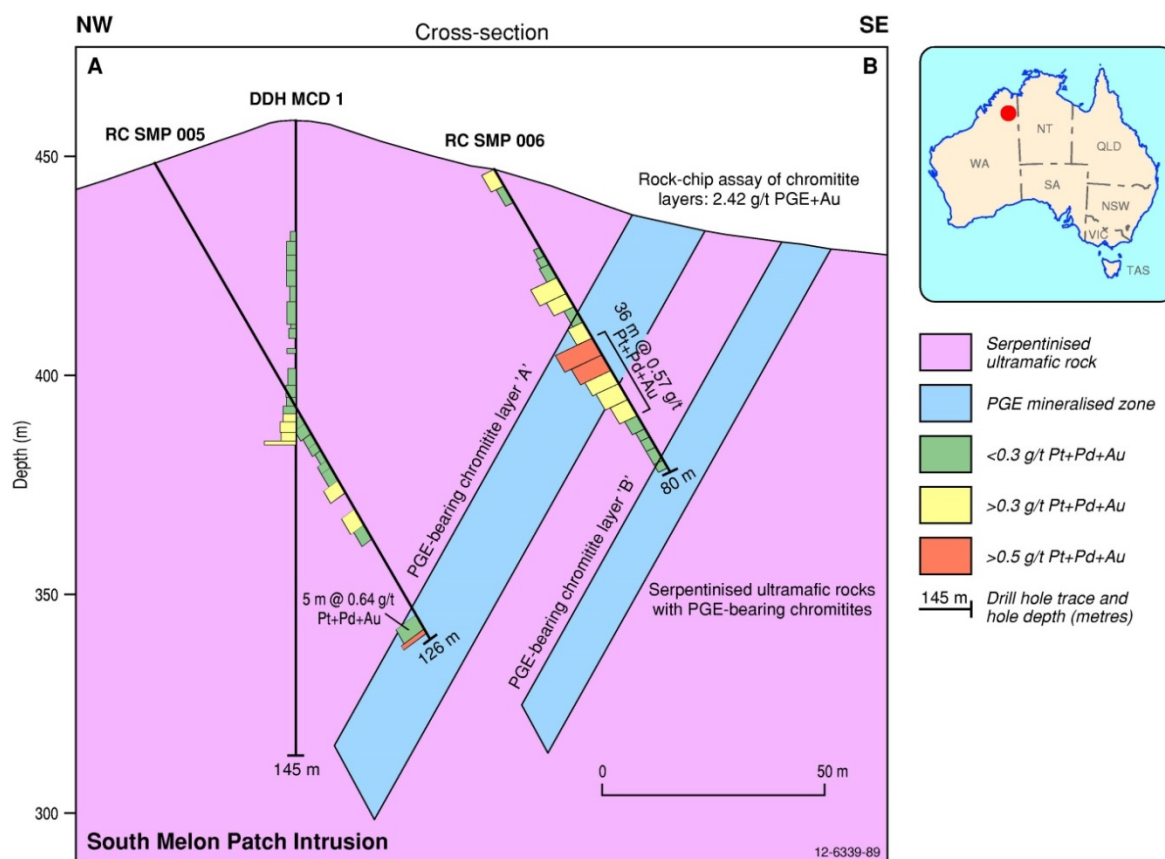
Appendix Table K.24 Geochemical data from 2001 exploration drilling of two chromitite seams in the Melon Patch intrusion. Data from Hoatson (2000) and RSG Global Pty Limited (2006).

Drill-hole	Line number	Depth from (m)	Depth to (m)	Interval (m)	PGEs+Au (ppm)	Cr (%)
SMP 001	1	0	3	3	0.51	0.55
SMP 001	1	5	10	5	0.68	0.75
SMP 001	1	49	52	3	0.93	1.72
SMP 002	1	16	17	1	1.02	2.33
SMP 002	1	59	63	4	0.64	0.78
SMP 002	1	65	67	2	0.97	0.91
SMP 002	1	112	115	3	0.59	1.11

Western Australia

Drill-hole	Line number	Depth from (m)	Depth to (m)	Interval (m)	PGEs+Au (ppm)	Cr (%)
SMP 003	2	1	6	5	0.53	0.48
SMP 003	2	46	51	5	0.9	1.99
SMP 004	2	22	32	10	0.59	0.69
SMP 004	2	38	48	10	0.67	0.65
SMP 004	2	72	80	8	0.43	0.92
SMP 005 <sup>1</sup>	3	121	125	4	0.77	2.2
SMP 006	3	29	35	6	0.68	1.1
SMP 006	3	43	64	21	0.74	2.6
SMP 006	3	44	51	7	1.0	2.93
SMP 006	3	45	50	5	1.07	3.32

<sup>1</sup> Including 1 m @ 0.82 g/t PGEs+Au in dunite at bottom of hole.



Appendix Figure K.15 Schematic northwest-southeast cross-section of PGE-enriched chromitite layers A and B in the South Melon Patch Intrusion, Halls Creek Orogen, Western Australia. Modified from RSG Global Proprietary Limited (2006).

The southern body of the Melon Patch Intrusion contains chromitite layers (1 cm–3 cm-thick) in dunite at different stratigraphic levels at the southwestern end of the southern intrusion and near the contact between dunite and anorthosite in the northern intrusion.

### ***Age of mineralisation***

The Melon Patch intrusions are correlated with the  $1856 \pm 2$  Ma Panton Intrusion.

### ***Current status***

Exploration site.

### ***Economic significance***

Occurrences.

### ***Major references(s)***

Hoatson, D.M., 2000. Geological setting, petrography, and geochemistry of the Palaeoproterozoic layered mafic-ultramafic intrusions. In: Hoatson, D.M. and Blake, D.H. (editors), *Geology and economic potential of the Palaeoproterozoic layered mafic-ultramafic intrusions in the East Kimberley, Western Australia*. Canberra: Australian Geological Survey Organisation Bulletin 246, 99–162.

RSG Global Proprietary Limited, 2006. Independent Geologist's Report. In: *3D Resources Prospectus 2006*, 27–68.

### ***Relevant figure(s)***

Figure 6.13, Figure 8.21, and Appendix Figure K.15.

## **K.1.118 Melon South**

(see Alice Downs 3 group)

## **K.1.119 Merlot**

(see Malbec–Cabernet)

## **K.1.120 Milgoo**

(see Wondinong, Corner Well, Narndee/Milgoo group)

## **K.1.121 Millipede–Capricorn**

### ***Geological province***

Pilbara Craton, Sylvania Dome.

### ***Location***

Milgoo—Capricorn:  $120.094950^{\circ}\text{E}$ ,  $-23.452418^{\circ}\text{S}$ ; Robertson (SF 51–13), Murrumunda (2951); ~40 km east-southeast of Newman and ~19 km west-northwest of the Coobina chromite mine.

### ***Classification***

- Unknown.
- 12. Others (minor or unknown economic importance); 12.E. Others (unknown geological setting).

### ***Geological setting***

The Millipede–Capricorn prospect is located in a layered mafic-ultramafic complex enclosed by Archean granites in the northern part of the Sylvania Dome, which lies on the southern margin of the Pilbara Craton (Hampton Hill Mining NL, 2008).

### ***PGE mineralisation***

Drilling on the Millipede–Capricorn Ni sulphide prospect returned up to 2 m averaging 1.35% Ni and 0.62% Cu within ultramafic units in a layered gabbroic complex (Hampton Hill Mining NL, 2008). Platinum is listed for the Millipede–Capricorn prospect in the MINEDEX database.

### ***Age of mineralisation***

Archean host rocks?

### ***Current status***

Historical exploration site.

### ***Economic significance***

Occurrence.

### ***Major references(s)***

Hampton Hill Mining NL., 2008. Hampton Hill Mining NL Annual Report, 2008, 59 pp.

### ***Relevant figure(s)***

## **K.1.122 Mineral Patch Hill**

### ***Geological province***

Yilgarn Craton.

### ***Location***

Mineral Patch Hill: 122.984596°E, -29.036900°S; Edjudina (SH 51–06), Mount Celia (3439); ~74 km southeast of Laverton.

### ***Classification***

- 9. Regolith-Laterite; 9.A. PGE-bearing regolith developed on ultramafic-mafic igneous rocks.

### ***Geological setting***

The Mineral Patch Hill lateritic Ni deposit overlies ultramafic rocks in the Merolia greenstone belt (Abeyasinghe and Flint, 2007).

### ***PGE mineralisation***

Stratigraphic drilling by Heron Resources Limited indicates an olivine adcumulate target size of 7 km-long by 0.7 km- to 1.4 km-wide. Anomalous PGEs of up to 246 ppb Pt and 111 ppb Pd, and associated 0.04% to 0.09% Cu occur in lateritised profile over the ultramafic rocks (Heron Resources Limited, 2004). The Mineral Patch Hill deposit has a published lateritic resource of 7.5 Mt @ 0.8% Ni% at a 0.75% Ni cut-off (Heron Resources Limited, 2003).

### ***Age of mineralisation***

Cenozoic lateritic Ni-Co deposits, primary Ni mineralisation in Archean host rocks.

### ***Current status***

Historical exploration site.

### ***Economic significance***

Small lateritic Ni deposit.

### ***Major references(s)***

Abeyasinghe, P.B. and Flint, D.J., 2007. Nickel and cobalt in Western Australia: commodity review for 2005. Western Australia Geological Survey, Record 2007/12, 46 pp.

Heron Resources Limited, 2003. Heron Resources Limited Quarterly Report ending 30 June 2003, 16 pp.

Heron Resources Limited, 2004. Heron Resources Limited Annual Report 2004, 68 pp.

### ***Relevant figure(s)***

## **K.1.123 Mini M (Cr-PGE 1), Mini M (Cr-PGE 2)**

### ***Geological province***

Halls Creek Orogen.

### ***Location***

Mini M (Cr-PGE 1): 127.858410°E, -17.691690°S, occurs in the northeast half of an arcuate mafic-ultramafic intrusion west of the West McIntosh Intrusion; Dixon Range (SE 52–06), McIntosh (4462); ~62 km north-northeast of Halls Creek.

Mini M (Cr-PGE 2): 127.861570°E, -17.697880°S: ~760 m south-southeast of Mini M (Cr-PGE 1): Dixon Range (SE 52–06), McIntosh (4462).

### ***Classification***

- Layered tholeiitic mafic-ultramafic intrusions; 1B. Stratabound PGE-bearing chromitite layers.

### ***Geological setting***

Mini M is a 2.5 km-long by 300 m-wide ultramafic sill, folded about a southwest-plunging anticlinal axis on the western margin of the McIntosh Intrusion. The 200 m-thick sill dips 70–82° to the south and southwest, and both ends of the body are displaced by faults. Sheared tremolite–anthophyllite–chlorite schist and serpentinised peridotite are the major ultramafic rocks (180 m-thick), with rare thin (10 m) urutilised gabbro units restricted to the southwestern side of the sill. Codner (1979) described brecciated and variably deformed ultramafic rocks and small ultramafic apophyses in metasediments on the northeastern side of the sill. The sill intrudes, and is concordant with, andalusite-garnet-muscovite-feldspar-quartz schist and gneiss of the Tickalara Metamorphics. The intrusion and country rocks are cut by numerous aplite and dolerite dykes, and minor pegmatite and quartz veins.

### ***PGE mineralisation***

Discontinuous thin chromitite layers crop out on the southern and southwestern sides of the sill (Codner 1979). Sheared massive chromitite layers, 1–10 cm-thick, can be traced along strike for tens

of metres in the tremolite–anthophyllite–chlorite schist and peridotite. Four different stratigraphic levels of chromitites have been recognised and various levels of disseminated chromite also occur within the ultramafic rocks. Codner (1979) found that Pt (0.6→0.7→1.5→2 ppm) and Pd (2→0.15→3→5 ppm) concentrations and Pt/Cr x 10 ratios (0.36→0.44→0.75→1.2) increased upwards (southwards) in the chromitites—these trends and the relative position of the chromitites on the 'upper' side of the sill led Codner to believe that the sill was overturned; however, the most PGE-rich chromitites in other group I intrusions (e.g., Panton) occur high in the ultramafic sequence directly below the Ultramafic Zone and overlying Mafic Zone contact, similar to that observed in the Mini Intrusion. Gossans in shears and quartz veins at northwestern end of sill contain >1% Cu. Chromitites consist of fine-grained (<0.2 mm) disseminated chromite anheda and subhedra in a groundmass of tremolite, anthophyllite, chlorite, and minor serpentine. Disseminated blebs of pyrrhotite with minor exsolved pentlandite, chalcopyrite, and pentlandite occur in the least sheared ultramafic rocks. Chromitites in upper part of Ultramafic Zone directly below the Mafic Zone contain 122 ppb Pd, 43.4 ppb Pt, and 1 ppb Au.

### ***Age of mineralisation***

Correlated with the 1856 ± 2 Ma Panton Intrusion.

### ***Current status***

Historical exploration site.

### ***Economic significance***

Occurrence.

### ***Major references(s)***

Codner, C.C., 1979. Final report on Mini M and Togo 5 prospects. Results of exploration on mineral claims 80/5986 to 80/5992 inclusive. Australian Anglo American Limited internal report for the Department of Minerals and Energy, Western Australia (Item 878, AN8463).

Hoatson, D.M., 2000. Geological setting, petrography, and geochemistry of the Palaeoproterozoic layered mafic-ultramafic intrusions. In: Hoatson, D.M. and Blake, D.H. (editors), *Geology and economic potential of the Palaeoproterozoic layered mafic-ultramafic intrusions in the East Kimberley, Western Australia*. Canberra: Australian Geological Survey Organisation Bulletin 246, 99–162.

### ***Relevant figure(s)***

Figure 6.13 and Figure 8.21.

## **K.1.124 Monarch Nickel**

### ***Geological province***

Yilgarn Craton.

### ***Location***

Monarch Nickel: 121.724503°E, -32.101521°S; Norseman (SI 51–02), Norseman (3233); ~12 km north-northwest of Norseman.

**Classification**

- ?2. Massive to poorly layered tholeiitic mafic-dominated intrusions; ?2.A. Segregations of Ni-Cu-Co-PGE sulphides in feeder conduits and basal contacts.
- ? 1. Layered tholeiitic mafic-ultramafic intrusions; ?1.A. Stratabound PGE-bearing sulphide layers.

**Geological setting**

The Monarch Ni prospect is located within the north-northeast-trending Neoproterozoic Mission Intrusion.

**PGE mineralisation**

In their quarterly report for December 2005, Nickel Australia Limited reported aircore drill-hole intercepts of Pt and Pd as shown in Appendix Table K.25 with maximum individual assay results recorded as 1 m @ 8.34 g/t Pd and 2.4 g/t Pt.

*Appendix Table K.25 Aircore drill-hole intercepts of Pt and Pd by Nickel Australia Limited, December 2005.*

Drill-hole	From (m)	Interval (m)	Pd (g/t)	Pt (g/t)	PGEs (g/t)
NNA 672,	30	25	1.63	0.43	2.06
including	39	13	2.26	0.56	2.82
NNA 673,	33	16	1.29	0.37	1.66
including	33	1	8.34	2.40	10.74
and	48	1	0.88	0.29	1.17

This mineralisation was reported to be part of an extensive zone of strongly anomalous Pt, Pd, Ni, and Cu concentrations in the weathered zone of a layered mafic-ultramafic body known as the Mission Intrusion. The Ni and Cu sulphide mineralisation is hosted within a basal peridotite layer while the PGE mineralisation is within a pyroxenite layer higher up in the intrusion (Nickel Australia Limited, 2005).

**Age of mineralisation**

Neoproterozoic host rock?

**Current status**

Historical exploration site.

**Economic significance**

Occurrence, drill-hole intersection.

**Major references(s)**

Nickel Australia Limited, 2005. Nickel Australia Limited announcement to the Australian Securities Exchange, 30 November 2005, 4 pp.

Nickel Australia Limited, 2006. Quarterly activity report for the period ended 31 December 2005. Announcement to the Australian Securities Exchange, 30 November 2005, 4 pp.

**Relevant figure(s)****K.1.125 Moonborough, Moonborough Northeast****Geological province**

Yilgarn Craton.

**Location**

Moonborough: 116.158997°E, -26.063070°S; Byro (SG 50–10), Byro (2145); ~340 km north-northeast of Geraldton.

Moonborough Northeast: 116.202247°E, -26.027051°S; Byro (SG 50–10), Byro (2145): ~340 km north-northeast of Geraldton.

**Classification**

- ?2. Massive to poorly layered tholeiitic mafic-dominated intrusions.
- ?8. Hydrothermal-Metamorphic.

**Geological setting**

A mafic-ultramafic complex of metagabbro and pyroxenite within the Narryer Gneiss Complex.

**PGE mineralisation**

Analytical results of rock-chip samples collected from the Moonborough prospect, 2 km north of the Byro Homestead, are listed in Appendix Table K.26.

*Appendix Table K.26 Geochemistry of rock-chip samples from the Moonborough prospect.*

Sample	Cu (%)	Pt (ppb)	Pd (ppb)	Au (ppb)
MBCR055	0.61	18	89	482
MBCR056	1.22	93	130	475
MBCR057	1.93	8	3015	525
MBCR058	0.96	84	166	413
MBCR059	0.48	24	118	165
MBCR060	0.55	43	337	272
MBCR061	0.32	53	115	121
MBCR069	0.11	12	130	10
MBCR070	0.47	52	81	329

The anomalous Cu, Au, PGE mineralisation is hosted by sheared metagabbro, bounded to west by pyroxenite, and lateritised cumulus-textured ultramafic rock (Athena Resources Limited, 2008a).

Drilling at the Moonborough prospect returned maximum down-hole assay values in mafic-ultramafic rocks at depth as follows:

## Western Australia

- AHRC0019: 15 ppb Pt, 15 ppb Pd, 10 ppb Au, 96 ppm Cu, and 1010 ppm Ni;
- AHRC0021: 10 ppb Pt, 80 ppb Pd, 17 ppb Au, 620 ppm Cu, and 114 ppm Ni;
- AHRC0022: 31 ppb Pt, 72.86 ppb Pd, 200 ppb Au, 2700 ppm Cu, and 114 ppm Ni; and
- Water-bore hole: 18 ppb Pt, 16 ppb Pd, 3 ppb Au, 140 ppm Cu, and 1350 ppm Ni (Athena Resources Limited, 2010).

A rock-chip sample (MBCR100) from Moonborough Northeast returned an assay of 9.11% Cu, 1.97 g/t Pd, and 40 ppb Au (Athena Resources Limited, 2008b).

### ***Age of mineralisation***

Unknown.

### ***Current status***

Exploration site.

### ***Economic significance***

Occurrence.

### ***Major references(s)***

Athena Resources Limited, 2008a. Soil geochemistry defines copper-PGM anomaly and Byro. Athena Resources Limited announcement to the Australian Securities Exchange, 3 July 2008, 6 pp.

Athena Resources Limited, 2008b. September 2008 quarterly report, 7 pp.

Athena Resources Limited, 2010. Byro nickel-copper-PGE project results: Moonborough. Athena Resources Limited announcement to the Australian Securities Exchange, 9 November 2010, 15 pp.

### ***Relevant figure(s)***

## **K.1.126 Mt Alexander–Cathedrals**

### ***Geological province***

Yilgarn Craton.

### ***Location***

Mt Alexander—Cathedrals: 120.275929°E, -28.838262°S; Leonora (SH 51–01), Mount Alexander (2940); ~110 km south-southwest of Leinster Downs.

### ***Classification***

- ?3. Komatiitic flows and related sill-like intrusions.

### ***Geological setting***

The Mt Alexander–Cathedrals prospect that is located in the Mount Ida greenstone belt in the Eastern Goldfields Superterrane comprises mafic to ultramafic volcanic rocks, tholeiitic basalt, and BIF (Painter et al., 2003).

### ***PGE mineralisation***

Initial drill-hole discovery announced on 2 April 2008, with analytical results of drill-hole samples as outlined in Appendix Table K.27 (Western Areas NL, 2008).

## Western Australia

Appendix Table K.27 Geochemistry of drill-hole samples from the Mt Alexander–Cathedrals prospect. Data from Western Areas NL (2008).

Drill-hole	From (m)	Interval (m)	Ni (%)	Cu (%)	Pd (ppm)	Pt (ppm)	Ir (ppm)	Os (ppm)	Rh (ppm)	Ru (ppm)	Total PGEs (ppm)
MAD012,	81.5	14	1.9	0.8	1.2	0.2	0.02	0.01	0.16	0.18	1.8
including	91.4	4	4.9	1.7	2.4	0.5	0.06	0.04	0.48	0.53	3.9
MAD013,	56.3	3	3.8	1.6	1.9	0.4	0.02	0.01	0.18	0.17	2.7
including	57.6	1.4	7.1	3.0	2.9	0.6	0.04	0.02	0.33	0.33	4.2

Additional analytical results published for 2 m-thick composite samples for drill-hole MARC49 returned 6.0 m @ 3.3% Ni, 1.5% Cu from 60 m, including 2 m @ 4.5%Ni, 1.8% Cu, 2.4 g/t Pd, and 0.6 g/t Pt from 62 m depth (Western Areas NL, 2010).

### **Age of mineralisation**

Archean host rocks.

### **Current status**

Exploration site.

### **Economic significance**

Occurrence.

### **Major references(s)**

Painter, M.G.M., Groenewald, P.B. and McCabe, M., 2003. East Yilgarn Geoscience Database, 1:100 000 geology of the Leonora–Laverton region, Eastern Goldfields Granite–Greenstone Terrane—an explanatory note: Western Australia Geological Survey, Report 84, 45 pp.

Western Areas NL, 2008. Assays confirm high grade nickel/copper/PGE discovery at Mt Alexander Joint Venture. Western Areas NL announcement to the Australian Securities Exchange, 2 April 2008.

Western Areas NL, 2010. Activities report for the period ending 30 September 2010. Western Areas NL announcement to the Australian Securities Exchange, 15 pp.

### **Relevant figure(s)**

## **K.1.127 Mt Carnage**

(see Ora Banda Sill)

## **K.1.128 Mt Cumming, Mt Warren**

### **Geological province**

Yilgarn Craton.

### **Location**

Mt Cumming: 123.352303°E, -27.759359°S; Throssell (SG 51–15), Jutson (3542); ~135 km northeast of Laverton.

Mt Warren: 123.308502°E, -27.777601°S; ~130 km northeast of Laverton.

### **Classification**

- 1. Layered tholeiitic mafic-ultramafic intrusions; 1.A. Stratabound PGE-bearing sulphide layers.

### **Geological setting**

The regional geology is dominated by a north-northwest striking succession of Archean ultramafic, mafic, and felsic extrusive rocks, pyroclastics, and sediments known as the Jutson Rocks greenstone belt. Mafic complexes of thick gabbro and dolerite intrusions are located on the eastern side of the belt, whilst a bimodal sequence of mafic and felsic volcanics with BIF occurs to the west. Within the mafic sequence are two concordant intrusions of pyroxenite, gabbro, and dolerite known as the Mt Warren sill and the Mt Cornell sill, which make up the Mt Cummings mafic complex. A similar, but smaller gabbro north of Jutson Rocks, is known as the Jutson mafic complex.

### **PGE mineralisation**

Soil sampling outlined anomalous PGEs in the Mt Warren and Mt Cornell sills of the Mt Cummings mafic complex (McIntyre, 2003). The Mt Warren PGE anomaly is related to a 25 m-wide stratigraphic horizon dipping at 45° to 55° within the gabbroic portion of the sill, situated between 50 m and 100 m stratigraphically above the gabbro-pyroxenite contact. The sampling defined anomalous PGEs up to 51 ppb Pt+Pd over a 5 km-strike length. In addition, an anomalous (2–3 times background) Cu horizon occurs ~50 m stratigraphically above the PGE horizon and appears to be at the contact between the magnetic gabbro and non-magnetic gabbro. Follow-up rock-chip-channel sampling returned assays up to 226 ppb Pt+Pd over a 1 m-interval within a 3 m- to 11 m-wide PGE-bearing zone for a strike of more than 2 km along the eastern flank of the sill.

The Mt Cornell PGE anomaly is approximately 2 km in strike length and, because of its relatively shallow dip (5° to 10° to south), occurs over a surface width of 500 m. The anomalous horizon defined by values up to 27 ppb Pt+Pd occurs in a similar stratigraphic position to the Mt Warren anomaly, which is within the gabbroic portion of the sill some distance above the pyroxenite.

One line of vacuum drilling, about 6 km south of Mt Warren, tested an interpreted unexposed komatiite sequence. Drill-hole JRVC 691 returned a result of 71 ppb Pt+Pd, coincident with 4840 ppm Cr, 815 ppm Ni, and 104 ppm Cu occurring in ironstone material (possibly a gossan) at shallow depth (Boonjarding Resources Limited, 2005).

### **Age of mineralisation**

Archean host rocks.

### **Current status**

Exploration site.

### **Economic significance**

Occurrences.

### **Major references(s)**

Boonjarding Resources Limited, 2005. Independent Geologist's Report. In: Graynic Metals Limited Prospectus, 19–51.

McIntyre, J., 2003. Final report for the tenements E38/68 and E38/69, Jutson Rocks, for the Period 23/12/01 to 22/12/02: Report by Helix Resources Limited. Combined Reporting Group C123/1995.

### **Relevant figure(s)**

#### **K.1.129 Mt Dove\***

(see Abrahams Find group)

#### **K.1.130 Mt Fisher East\* (Camelwood\*, Cannonball\*, Musket\*)**

##### **Geological province**

Yilgarn Craton.

##### **Location**

Mt Fisher East–Camelwood: 121.550206°E, -26.793617°S; Kingston (SG 51–10), Yelma (3244); ~134 km east of Wiluna.

Mt Fisher East–Cannonball: 121.553732°E, -26.803501°S; Kingston (SG 51–10), Yelma (3244); ~135 km east of Wiluna.

Mt Fisher East–Musket: 121.554149°E, -26.810276°S; Kingston (SG 51–10), Yelma (3244); ~135 km east of Wiluna.

##### **Classification**

- 3. Komatiitic flows and sill-like intrusions; 3.A. Massive, matrix, and disseminated Ni-Cu-PGE sulphides in preferred lava pathways.

##### **Geological setting**

The Mt Fisher East PGE occurrence is located in the Mt Fisher greenstone belt in the northern part of the Kurnalpi Terrane, Yilgarn Craton.

##### **PGE mineralisation**

Rox Resources Limited announced on 19 December 2012 the discovery of Ni sulphides at the Camelwood, which is part of the company's Fisher East Ni project. The company followed up with another announcement on 3 October 2013, which reported an initial Indicated Resource for the Camelwood deposit of 1.6 Mt at 2.2% Ni (Rox Resources Limited, 2013b). The Camelwood Ni-sulphide deposit is located at the basal contact of a komatiitic lava flow and the mineralisation occurs as two main types, massive and matrix/disseminated. The massive ore usually assays between 4% and 7% Ni, while the disseminated ore is usually between 2% Ni and 3.5% Ni (Rox Resources Limited, 2013c).

Significant PGE, Au, and Cu values within massive Ni-sulphide mineralisation were intersected at the Musket prospect, about 1 km south of Camelwood:

## Western Australia

- diamond drill-hole MFED001: 11.4 m @ 2.93% Ni and 0.57 g/t PGEs from 282.6 m, including 6.4 m @ 3.80% Ni and 0.73 g/t PGEs (Rox Resources Limited, 2013a);
- unnamed reverse circulation drill-hole: 2 m @ 5.0 g/t (Pt+Pd+Au) and 0.53% Cu from 227 m in the same interval that contained 2 m @ 8.1% Ni (Rox Resources Limited, 2014).

### ***Age of mineralisation***

Archean host rocks.

### ***Current status***

Exploration sites.

### ***Economic significance***

Occurrences.

### ***Major references(s)***

Rox Resources Limited, 2012. Nickel sulphide discovery at Fishers East. Rox Resources Limited announcement to the Australian Securities Exchange, 19 December 2012, 7 pp.

Rox Resources Limited, 2013a. High grades from Camelwood. Rox Resources Limited announcement to the Australian Securities Exchange, 4 April 2013, 8 pp.

Rox Resources Limited, 2013b. Maiden Camelwood mineral resource. Rox Resources Limited announcement to the Australian Securities Exchange, 3 October 2013, 22 pp.

Rox Resources Limited, 2013c. Rox Resources Limited Annual Report 2013, 79 pp.

Rox Resources Limited, 2014. High grade PGE results. Rox Resources Limited announcement to the Australian Securities Exchange, 27 March 2014, 10 pp.

### ***Relevant figure(s)***

## **K.1.131 Mt Holland Nickel**

### ***Geological province***

Yilgarn Craton.

### ***Location***

Mt Holland: 119.726696°E, -32.317986°S; Hyden (SI 50–04), Holland (2833); ~260 km northwest of Esperance and ~13 km north-northeast of the Flying Fox Ni mine.

### ***Classification***

- 3. Komatiitic flows and sill-like intrusions; 3A. Massive, matrix, and disseminated Ni-Cu-PGE sulphides in preferred lava pathways.

### ***Geological setting***

The Mt Holland Ni prospect is located in the Forrestania greenstone belt of the Yilgarn Craton, which also hosts the Flying Fox and Spotted Quoll komatiite-hosted Ni deposits. The host volcanosedimentary succession has been metamorphosed to amphibolite facies (Abeyasinghe and Flint, 2006; Collins et al., 2012).

### ***PGE mineralisation***

Drill-hole FSTRC17 within the Mount Holland prospect at Forrestania, intersected 14 m of sulphide mineralisation from 202 m to 216 m. Preliminary assays averaged 127 ppm Ni, 39 ppm Cu, 8 ppb Au, and 18 ppb PGEs, and subsequent analyses have indicated large-alteration zones within mafic rocks with Au assays up to 1.01 ppm and anomalous As, but no significant Ni mineralisation (Range Resources Limited, 2004, 2005a,b).

### ***Age of mineralisation***

Archean host rocks.

### ***Current status***

Historical exploration site.

### ***Economic significance***

Occurrence.

### ***Major references(s)***

- Abeysinghe, P.B. and Flint, D.J., 2006. Nickel–cobalt in Western Australia: commodity review for 2004. Western Australia Geological Survey, Record 2006/6, 57 pp.
- Collins, J.E, Hagemann, S.G., McCuaig, T.C. and Frost, K.M., 2012. Structural controls on sulfide mobilization at the high-grade Flying Fox Ni-Cu-PGE sulfide deposit, Forrestania greenstone belt, Western Australia. *Economic Geology*, 107, 1433–1455.
- Hoatson, D.M., Jaireth, S., Whitaker, A.J., Champion, D.C. and Claoué-Long, J.C., 2009. Guide to using the Australian Archean Mafic-Ultramafic Magmatic Events Map. *Geoscience Australia Record 2009/41*, 135 pp.
- Range Resources Limited, 2004. Significant sulphide mineralisation found at Forrestania. Report to Australian Securities Exchange, 29 December 2004, 1 pp.
- Range Resources Limited, 2005a. Sulphide deposit–Forrestania–Preliminary Assays. Range Resources Limited announcement to the Australian Securities Exchange, 10 January 2005, 2 pp.
- Range Resources Limited, 2005b. Forrestania—first campaign drilling results: Report to Australian Securities Exchange, 15 February 2005, 4 pp.

### ***Relevant figure(s)***

#### **K.1.132 Mt Keith\***

(other examples include Ni-Co-PGE deposits at Perseverance, Honeymoon Well Group\*, Yakabindie Group\*, Marriott\*, Durkin\* shoot at Kambalda, Six Mile Well\*, and Goliath North\* (all in Yilgarn Craton, WA)

### ***Geological province***

Yilgarn Craton.

### ***Location***

Mt Keith\*: 120.541740°E, -27.229599°S; Sir Samuel (SG 51–13), Mount Keith (3043); ~80 km north-northwest of Leinster.

Honeymoon Well Group\*: 120.380699°E, -26.921820°S; Wiluna (SG 51–09), Wiluna (2944); ~40 km south-southeast of Wiluna.

Marriotts\*: 120.577003°E, -28.451361°S; Leonora (SH 51–01), Wildara (3041); ~58 km northwest of Leonora.

Yakabindie Group\*: 120.541740°E, -27.428120°S; ~56 km north-northwest of Leinster.

### **Classification**

- 3. Komatiitic flows and related sill-like intrusions; 3.B. Disseminated Ni-Cu-PGE sulphides in central parts of thick dunite bodies.

### **Geological setting**

The most important Type 3.B Ni-sulphide deposits (Mt Keith, Perseverance, Yakabindie, Honeymoon Well Group) occur in the northern part of the Norseman–Wiluna greenstone belt, where they are often spatially associated with the Kambalda Type 3.A deposits. The Mt Keith Ultramafic Complex hosts the Mt Keith Ni-sulphide deposit in a narrow section of the Agnew–Wiluna greenstone belt in the northern part of the Kalgoorlie Terrane of the Yilgarn Craton. The Agnew–Wiluna greenstone belt has a north-northwest to south-southeast trend and is bounded by large terrane-scale faults and granitoid bodies. The Agnew–Wiluna greenstone belt comprises a ~2.7 Ga sequence of felsic-to-intermediate volcanic and volcanoclastic rocks, sulphidic chert, carbonaceous shale, and laterally variable komatiite including cumulates, thin spinifex-textured units, and komatiitic basalts (Barnes et al., 2011). The komatiite stratigraphy of the Mt Keith deposit can be correlated for over 100 km along strike from the Perseverance deposit in the south to the Honeymoon Well deposits in the north of the greenstone belt.

### **PGE mineralisation**

Mount Keith is the type 3B example of a low-grade (0.5–1.5% Ni), large-tonnage disseminated Ni-sulphide deposits hosted by thick dunitic bodies that have relatively low grades (<0.2 to 0.5 g/t) of PGEs. Most of the primary magmatic Ni-Cu ± PGE mineralisation is confined to the central olivine adcumulate zone. The sulphides are typically disseminated and layered, with Ni grades ranging from 0.1% to 1.0% and averaging 0.6%. Pyrrhotite, pentlandite, magnetite, pyrite, chalcopyrite, and chromite are the major phases in ores grading more than 1% Ni, whereas millerite, heazlewoodite, godlevskite, and polydymite occur in ores less than 1% Ni. Supergene minerals often include violarite, pyrite, and marcasite. Magmatic sulphide mineralisation in unit 102 of the MKD5 orebody occurs as discrete pods that appear to plunge steeply and are associated with elevated PGEs (combined 100 ppb to 700 ppb) and Cu (100 ppm to 900 ppm) concentrations. In areas of high arsenic, the PGEs occur in minute amounts as discrete PGMs, namely sperrylite (PtAs<sub>2</sub>) and irarsite (Ir,Ru,Rh Pt)AsS (Grguric, 2003; Grguric et al., 2006). In other parts of the Mount Keith deposit, the PGEs typically constitute a trace component (100 ppb to 200 ppb combined) with the highest concentrations associated with the common sulphide phases. Low levels of Co (100 ppm to 200 ppm) characterise the Mount Keith deposit, where it is hosted predominantly in pentlandite, pyrite, and hypogene violarite. Copper is also a minor component (100 ppm to 600 ppm), and it is represented by chalcopyrite, bornite, native copper, and tochilinite-valleriite series minerals. Nickel enrichment of the sulphides occurred during the re-equilibration of olivine with a residual sulphide-rich melt prior to complete crystallisation, and also during the serpentinisation of olivine that accompanied greenschist-facies metamorphism.

### **Age of mineralisation**

The age of the mineralised komatiitic stratigraphy at Mount Keith is Archean, and is probably of a similar age (~2705 Ma) by analogy with many other Ni-sulphide deposits that have been well dated elsewhere in the Eastern Goldfields Superterrane (Nelson, 1997). Fiorentini et al. (2005, 2012) describe SHRIMP U-Pb ages on magmatic zircon and titanite grains from the Mount Keith Dacite

(which has primary contact relationships with the mineralised Mount Keith ultramafic unit) in the footwall and hanging wall of the unit as, respectively,  $2713 \pm 6$  Ma and  $2706 \pm 6$  Ma. These ages are within error of the Re/Os isotopic age of  $2706 \pm 36$  Ma obtained for the Mount Keith ultramafic unit by Foster et al. (1996). Hoatson et al. (2006, 2009) have compiled U-Pb zircon and baddeleyite ages of komatiite and associated rocks throughout Australia. The ages of these rocks are constrained by felsic units intercalated with komatiitic sequences (i.e., direct age of komatiites), felsic footwall units (maximum age), felsic hanging wall units (minimum age), and felsic dykes cutting the komatiitic sequences (minimum age).

**Current status**

Operating Ni mine.

**Economic significance**

One of the large Ni mining operations in Australia. Original total resource ~3.4 Mt Ni metal, current remaining resource of about ~1 Mt contained Ni metal. Operating Ni mine.

**Major references(s)**

- Barnes, S.J., Godel, B.M., Locmelis, M., Fiorentini, M.L. and Ryan, C.G., 2011. Extremely Ni-rich Fe-Ni sulfide assemblages in komatiitic dunite at Betheno, Western Australia: results from synchrotron X-ray fluorescence mapping. *Australian Journal of Earth Sciences*, 58, 691–709.
- Fiorentini, M.L., Barley, M.E., Pickard, A., Beresford, S.W., Rosengren, N.M., Cas, R.A.F. and Duuring, P., 2005. Age constraints of the structural and stratigraphic architecture of the Agnew-Wiluna greenstone belt: Implications for the age of komatiite-felsic association and interaction in the Eastern Goldfields Province, Western Australia: Perth, Minerals and Energy Research Institute of Western Australia, MERIWA Final Report no. 255, Project M356, 39 pp.
- Fiorentini, M.L., Beresford, S.W., Barley, Duuring, P., Bekker, A., Rosengren, N.M., Cas, R.A.F. and Hronsky, J., 2012. District to camp controls on the genesis of komatiite-hosted nickel sulfide deposits, Agnew-Wiluna Greenstone Belt, Western Australia: Insights from the multiple sulfur isotopes. *Economic Geology*, 107, 781–796.
- Foster, J.G., Lambert, D.D., Frick, L.R. and Maas, R., 1996. Re-Os isotopic evidence for genesis of Archaean nickel ores from uncontaminated komatiites. *Nature*, 382, 703–705.
- Grguric, B.A., 2003. Minerals of the MKD5 nickel deposit, Mt Keith, Western Australia. *Australian Journal of Mineralogy*, 9, 55–71.
- Grguric, B.A., Rosengren, N.M., Fletcher, C.M. and Hronsky, J.M.A., 2006. Type 2 Deposits: Geology, mineralogy, and processing of the Mount Keith and Yakabindie orebodies, Western Australia. In: Barnes, S.J. (editor), *Nickel Deposits of the Yilgarn Craton: Geology, Geochemistry, and Geophysics Applied to Exploration*. *Economic Geology Special Publication Number 13*, 119–138.
- Hoatson, D.M., Jaireth, S. and Jaques, A.L., 2006. Nickel sulphide deposits in Australia: Characteristics, resources and potential. *Ore Geology Reviews*, 29, 177–241.
- Hoatson, D.M., Jaireth, S., Whitaker, A.J., Champion, D.C. and Claoué-Long, J.C., 2009. Guide to Using the Australian Archaean Mafic-Ultramafic Magmatic Events Map. *Geoscience Australia Record 2009/41*, 135 pp.
- Nelson, D.R., 1997. Evolution of the Archaean granite-greenstone terranes of the Eastern Goldfields, Western Australia: SHRIMP U-Pb zircon constraints. *Precambrian Research*, 83, 57–81.

**Relevant figure(s)**

Figure 6.21, Figure 6.24, Figure 6.25, and Figure 8.24.

**K.1.133 Mt Thirsty\*****Geological province**

Yilgarn Craton.

**Location**

Mt Thirsty: 121.647797°E, -32.101891°S; Norseman (SI 51–02), Norseman (3233); ~17 km northwest of Norseman.

**Classification**

- 1. Layered tholeiitic mafic-ultramafic intrusions.

**Geological setting**

The Mount Thirsty and Mission intrusions, west to northwest of Norseman, intrude the Archean mafic-ultramafic sequence along a strike length of about 20 km, and collectively constitute about 1500 m of the total greenstone sequence. These sills comprise lower cumulus-textured serpentinised peridotite and pyroxenite that are overlain by upper units of norite and gabbro, and quartz gabbro with granophyric segregations (Groenewald and Riganti, 2004).

**PGE mineralisation**

Nickel-Cu mineralisation is located near the base of a 50 m-thick flow of olivine-rich ultramafic cumulates. Drilling has intersected a 6-m-thick zone of massive stringer Ni sulphides assaying 3.38% Ni and 0.14% Cu at a down-hole depth of 201 m (interpreted to be a vertical depth of ~190 m) adjacent to the footwall basalt/ultramafic contact, and up to 2 m @ 5.9% Ni in holes MTRC 15 and 22, respectively. The zone of Ni sulphide mineralisation contains visible sulphide minerals, including pyrrhotite, chalcopyrite, pentlandite, pyrite, and magnetite (Fission Energy Limited, 2010).

The Mount Thirsty sill contains 100–300 ppb Pt+Pd+Au in a bronzite (orthopyroxene) cumulate layer (Witt et al., 1991). Nickel-Cu pyrrhotite mineralisation occurs in the mafic-ultramafic rocks. A zone of anomalous Cr, Cu, Ni, Pt, and Pd values was outlined in soils on three adjacent traverses, suggesting bedrock PGE mineralisation may extend over a 1 km-strike length.

Pioneer Nickel Limited (2009) reported that a selection of 255 samples from 20 RAB holes from the Mt Thirsty South prospect (~13 km south of Mt Thirsty) was assayed for Au, Pt, and Pd. RAB drill-holes considered anomalous with coincident Ni-Cu and PGEs are listed in Appendix Table K.28.

*Appendix Table K.28 Drill-hole samples with anomalous geochemistry analyses for Mt Thirsty South prospect. Data from Pioneer Nickel Limited (2009).*

Drill-hole	From (m)	To (m)	Length (m)	PGEs (ppb)	Ni (ppm)	Cu (ppm)
MTB0028	0	4	4	225	2300	230
MTB0037	1	57	56	330	1730	475
MTB0066	20	24	4	535	2800	653
MTB0080	0	14	14	291	1971	154

*Analytical results: KAL Assay Laboratories Pty Limited, 40 g fire assay, 1 ppb lower detection limit for PGEs.*

**Age of mineralisation**

Archean host rock?

### ***Current status***

Exploration site.

### ***Economic significance***

A lateritic Ni-Co-Mn deposit is reported to contain an Indicated and Inferred Resource of 31.94 Mt @ 0.13% Co, 0.55% Ni, and 0.86% Mn. The Ni sulphide prospect adjoins the lateritic deposit to the west (Conico Limited, 2013).

### ***Major references(s)***

- Conico Limited, 2013. 2013 AGM presentation. Conico Limited. Report to the Australian Securities Exchange, 29 November 2013, 20 pp.
- Fission Energy Limited, 2010. High grade nickel sulphides intersected at Mt Thirsty JV. Report to the Australian Securities Exchange, 19 May 2010, 3 pp.
- Groenewald, P.B. and Riganti, A., 2004. East Yilgarn 1:100 000 Geological Information Series—an explanatory note. Western Australia Geological Survey, Report 95, 58 pp.
- Pioneer Nickel Limited, 2009. Quarterly activities report for the period ended 30 June 2009, 5 pp.
- Witt, W.K., Hill, R.E.T., Gole, M.J., Barnes, S.J. and Perring, R.J., 1991. Layered mafic-ultramafic complexes of the Norseman–Wiluna Greenstone Belt. In: Barnes, S.J. and Hill, R. E.T. (editors), Mafic-Ultramafic Complexes of Western Australia. Excursion Guidebook No. 3. Sixth International Platinum Symposium, July 1991, Perth, WA. IAGOD and the Geological Society of Australia, 27–44.

### ***Relevant figure(s)***

## **K.1.134 Mt Venn**

### ***Geological province***

Yilgarn Craton.

### ***Location***

Mt Venn: 123.505600°E, -28.097040°S; Rason (SH 51–03), Dorothy Hills (3641); ~125 km east-northeast of Laverton.

### ***Classification***

- 8. Hydrothermal-Metamorphic; 8.D. Structurally-controlled remobilised Ni-Cu-PGE sulphides in mafic±ultramafic±felsic dykes/veins in shear zones.

### ***Geological setting***

Rock-chip sampling at the Mt Venn mafic-ultramafic intrusion has indicated Ni-Cu- and PGE-rich gossanous horizons along the western margin of the intrusion. The gossans are exposed along 10 km of strike length and overlie the more pyroxenite-rich basal sequence of the intrusion.

### ***PGE mineralisation***

Abeyasinghe and Flint (2007) reported in their summary on Ni and Co exploration in Western Australia that rock-chip samples from these gossans produced significant assay results, including 8.7% Cu, 0.34% Ni, and 0.14 g/t PGEs (Pt+Pd). One gossan sample from a 5 m-wide shear zone in the central part of the Mount Venn Intrusion returned an assay of 24% Cu, 1.9% Ni, 0.4 g/t Au, and 0.1 g/t PGEs. Drilling produced an intersection of 4 m @ 1.3% Cu, including 2 m @ 1.2% Ni from 33 m in drill-hole MVRC10. This drill-hole targeted a late-stage northwestern-trending shear zone where previous

## **Western Australia**

surface sampling identified Ni- and Cu-rich gossans. Several other drill-holes intersected anomalous Cu (up to 1.3%) and Ni (up to 0.5%) associated with massive sulphide horizons (Helix Resources Limited, 2005a,b).

### ***Age of mineralisation***

Archean host rock.

### ***Current status***

Exploration site.

### ***Economic significance***

Occurrence.

### ***Major references(s)***

Abeysinghe, P.B. and Flint, D.J., 2007. Nickel and cobalt in Western Australia: commodity review for 2005. Western Australia Geological Survey, Record 2007/12, 46 pp.

Helix Resources Limited, 2005a. December quarter activities report. Report to Australian Securities Exchange, 18 January 2005, 8 pp.

Helix Resources Limited, 2005b, Quarterly report ending 31 March 2005.

### ***Relevant figure(s)***

## **K.1.135 Mt Warren**

(see Mt Cumming)

## **K.1.136 Mt Webber\***

### ***Geological province***

Pilbara Craton.

### ***Location***

Mt Webber: 119.298550°E, -21.543976°S; Marble Bar (SF 50–08), Tambourah (2754); ~62 km southwest of Marble Bar.

### ***Classification***

- 12. Others (minor or unknown economic importance); 12.C. Anomalous PGEs in banded-iron formations.

### ***Geological setting***

Trace Au, Ag, Pt, Pd, Ir, Ru in banded-Fe ore.

### ***PGE mineralisation***

Au, Ag, Pt, Pd, Ir, and Ru in banded-Fe ore being mined at Mt Webber is being investigated for possible concentration and extraction (Haoma Mining NL, 2012, 2014a,b).

### ***Age of mineralisation***

Archean host rock?

### ***Current status***

Haoma Mining NL is assessing the viability of PGEs, Au, and Ag credits in Fe ore for extraction by European refineries.

### ***Economic significance***

An operating Fe-ore mine. The economic significance of associated Au, Ag, and PGEs is to be confirmed.

### ***Major references(s)***

Haoma Mining NL, 2012. Bamboo Creek and Mt Webber contains significant commercial quantities of gold and platinum group metals (PGM). Report to the Australian Securities Exchange, 18 June 2012, 4 pp.

Haoma Mining NL, 2014a. Activities report for the quarter ended December 31, 2013–Highlights, 23 pp.

Haoma Mining NL, 2014b. Activities report for the quarter ended March 31, 2014–Highlights, 22 pp.

### ***Relevant figure(s)***

## **K.1.137 Mt Windarra\***

### ***Geological province***

Yilgarn Craton.

### ***Location***

Mt Windarra\*: 122.238466°E, -28.486819°S; Laverton (SH 51–02), Mount Varden (3341); ~22 km northwest of Laverton.

### ***Classification***

- 3. Komatiitic flows and related sill-like intrusions; 3.A. Massive, matrix, and disseminated Ni-Cu-PGE sulphides in preferred lava pathways.

### ***Geological setting***

Barnes and Fiorentini (2012) reported that the only mined Ni-Cu-PGE deposit within the eastern terranes is the Mt Windarra deposit, which is associated with an older, ~2.8 Ga komatiite sequence (Barley et al., 2006) in the Burtville terrane associated with abundant oxide-facies (BIFs) that are absent in the Kalgoorlie terrane (Hoatson et al., 2009a,b).

### ***PGE mineralisation***

Western Mining Corporation reported an Indicated Resource of 900 000 t of ore for the F shoot at Mt Windarra at a grade of 0.6% Ni, 0.77 g/t Pd, and 0.15 g/t Pt. According to published reports combined production resulted in more than 7.2 Mt of ore @ 1.59% Ni containing 84 000 t of Ni metal (Niagara Mining Limited, 2005). The PGE content in this Ni ore was not reported.

### ***Age of mineralisation***

Archean host rocks.

### **Current status**

Historical mine that has had a long history of mining since its discovery in 1969. In February 1970, the Mt Windarra deposit featured in one of the most spectacular stock collapses in Australian share-market history—the 'Poseidon Crash'. Uncontrolled speculation drove the 80-cent stock rapidly upwards to a high of ~\$280, until its inevitable crash (see Chapter 5). The mine was advanced to a depth of 550 m below surface and mining ceased in 1990 due to historically low Ni prices. The deposit is currently under a feasibility study.

### **Economic significance**

Small deposit. As at 30 June 2013, the reported resources for the Mt Windarra project amounted to a total Indicated and Inferred Resource of 4.77 Mt @ 1.68% Ni.

### **Major references(s)**

- Barley, M.E., Brown, S.J.A. and Krapez, B., 2006. Felsic volcanism in the eastern Yilgarn Craton, Western Australia: Evolution of a Late Archean convergent margin: *Geochimica et Cosmochimica Acta*, 70, p. A35.
- Barnes, S.J. and Fiorentini, M.L., 2012. Komatiite Magmas and Sulfide Nickel Deposits: A Comparison of Variably Endowed Archean Terranes. *Economic Geology*, 107, 755–780.
- Hoatson, D.M., Jaireth, S., Whitaker, A.J., Champion, D.C. and Claoué-Long, J.C., 2009a. Guide to Using the Australian Archean Mafic-Ultramafic Magmatic Events Map. *Geoscience Australia Record* 2009/41, 135 pp.
- Hoatson, D.M., Jaireth, S., Whitaker, A.J., Champion, D.C. and Claoué-Long, J.C., 2009b. Australian Archean Mafic-Ultramafic Magmatic Events, Sheet 1 (1:5 000 000 scale map) and Sheet 2 (1:3 000 000 and 1:6 000 000 scale maps), Geoscience Australia, Canberra, GeoCat 69347. [http://www.ga.gov.au/metadata-gateway/metadata/record/gcat\\_69347](http://www.ga.gov.au/metadata-gateway/metadata/record/gcat_69347)
- Niagara Mining Limited, 2005. Niagara Mining Limited Annual Report 2005. 65 pp.
- Western Mining Corporation Limited, 1993. Western Mining Corporation Limited 1993 Annual Report.

### **Relevant figure(s)**

Figure 6.21 and Figure 6.23.

## **K.1.138 Muleryon Hill**

(see Wondinong)

## **K.1.139 Mulga Tank\***

### **Geological province**

Yilgarn Craton.

### **Location**

Mulga Tank: 123.208490°E, -29.930099°S; Minigwal (SH 51–07), Minigwal (3538); ~190 km northeast of Kalgoorlie.

### **Classification**

- 3. Komatiitic flows and related sill-like intrusions; 3.A. Massive, matrix, and disseminated Ni-Cu-PGE sulphides in preferred lava pathways, and/or 3.B. Disseminated Ni-Cu-PGE sulphides in central parts of thick dunite bodies.

- 8. Hydrothermal-Metamorphic; 8.B. Remobilised Ni-Cu-PGE±Au sulphides in komatiitic and metasedimentary rocks.

### ***Geological setting***

Impact Minerals Limited have confirmed the widespread presence of Ni-Cu-PGE-sulphide mineralisation over an area of about 15 km<sup>2</sup> within and close to the Mulga Tank Dunite located in the poorly exposed Minigwal greenstone belt. Three different styles of orthomagmatic (disseminated sulphides) and vein-type mineralisation have been defined near the basal contact of the dunite body and in the country rocks. Disseminated Ni sulphide and narrow veins of Ni-Cu sulphides are associated with a komatiite flow channel that probably lies immediately above the Mulga Tank Dunite. Impact Minerals Limited (2014) consider the styles of mineralisation and the geology at Mulga Tank are very similar to the Perseverance Dunite near Leinster in Western Australia that hosts the significant Perseverance deposit (45 Mt at 2% Ni) and the nearby Rocky's Reward deposit (9.6 Mt at 2.4% Ni).

### ***PGE mineralisation***

According to Impact Minerals Limited (2014), the following three styles of mineralisation have been identified at Mulga Tank.

- extensive disseminated Ni sulphides within the Mulga Tank dunite:
  - 2 m @ 1.3% Ni, including 1 m @ 2% Ni;
  - multiple zones of 0.5 m @ 0.5% to 1.2% Ni within an intercept of 115 m @ 0.3% Ni;
  - 21 m @ 0.4% Ni; and
  - 59 m @ 0.3% Ni.
- narrow veins of Ni-Cu-PGE sulphides both within and at the base of the Mulga Tank dunite and which contain textures suggesting they may be remobilised from zones of more massive sulphides:
  - 0.25 m @ 3.8% Ni, 0.7% Cu, 0.7 g/t PGEs; and
  - 0.3 m @ 0.7% Ni.
- disseminated and narrow veins of Ni-Cu-PGE sulphides:
  - 0.75 m @ 0.85% Ni, 0.35% Cu, and 0.28 g/t PGEs (Pt+Pd+Au); and
  - 6.7 m @ 0.5% Ni.

### ***Age of mineralisation***

Archean host rocks.

### ***Current status***

Dormant exploration site.

### ***Economic significance***

New discovery.

### ***Major references(s)***

Impact Minerals Limited, 2014. Assay results confirm extensive nickel at Mulga Tank. Impact Minerals Limited announcement to the Australian Securities Exchange, 29 January 2014, 18 pp.

## ***Relevant figure(s)***

### **K.1.140 Munni Munni, Hunters Reef West, Hunters Reef East, Judys Reef (J Reef), Natalies Hill, Munni Munni South, Elizabeth Hill**

#### ***Geological province***

Pilbara Craton.

#### ***Location***

Munni Munni PGE deposit: 116.828769°E, -21.120370°S; Yarraloola (SF 50–06), Pinderi Hills (2255); ~42 km south of Karratha.

The following PGE prospects located in the area with distances from the Munni Munni deposit are as follows:

Munni Munni South: 116.828140°E, -21.207815°S; ~10 km south of Munni Munni deposit;

Hunters Reef West: 116.811770°E, -21.118180°S; ~2 km west of Munni Munni deposit;

Hunters Reef East: 116.866360°E, -21.122750°S; ~4 km east of Munni Munni deposit;

Natalies Hill: 116.874298°E, -21.090630°S; ~5.3 km northeast of Munni Munni deposit;

Judys Reef (also called J Reef): 116.873596°E, -21.091749°S; ~5.5 km northeast of Munni Munni deposit;

Elizabeth Hill: 116.874901°E, -21.090031°S; Yarraloola (SF 50–06), Pinderi Hills (2255); ~5.8 km northeast of Munni Munni deposit; and

Munni Munni Pinderi\*: 116.818966°E, -21.123186°S; ~1.3 km west-southwest of Munni Munni deposit.

The Toorare Pool occurrence as described by Hoatson and Glaser, (1989) is located near the western margin of the Munni Munni Intrusion.

Descriptions of the Munni Munni Intrusion and its deposits and nearby prospects are largely summarised from Section 6.4.1.1 of this report.

#### ***Classification***

- 1. Layered tholeiitic mafic-ultramafic intrusions; 1.A. Stratabound PGE-bearing sulphide layers (Munni Munni, Hunters Reef West, Hunters Reef East, Judys Reef (J Reef), Natalies Hill, Munni Munni South).
- 8. Hydrothermal-Metamorphic; 8.C. Magmatic breccias involving mafic, ultramafic, and felsic igneous rocks (Elizabeth Hill).

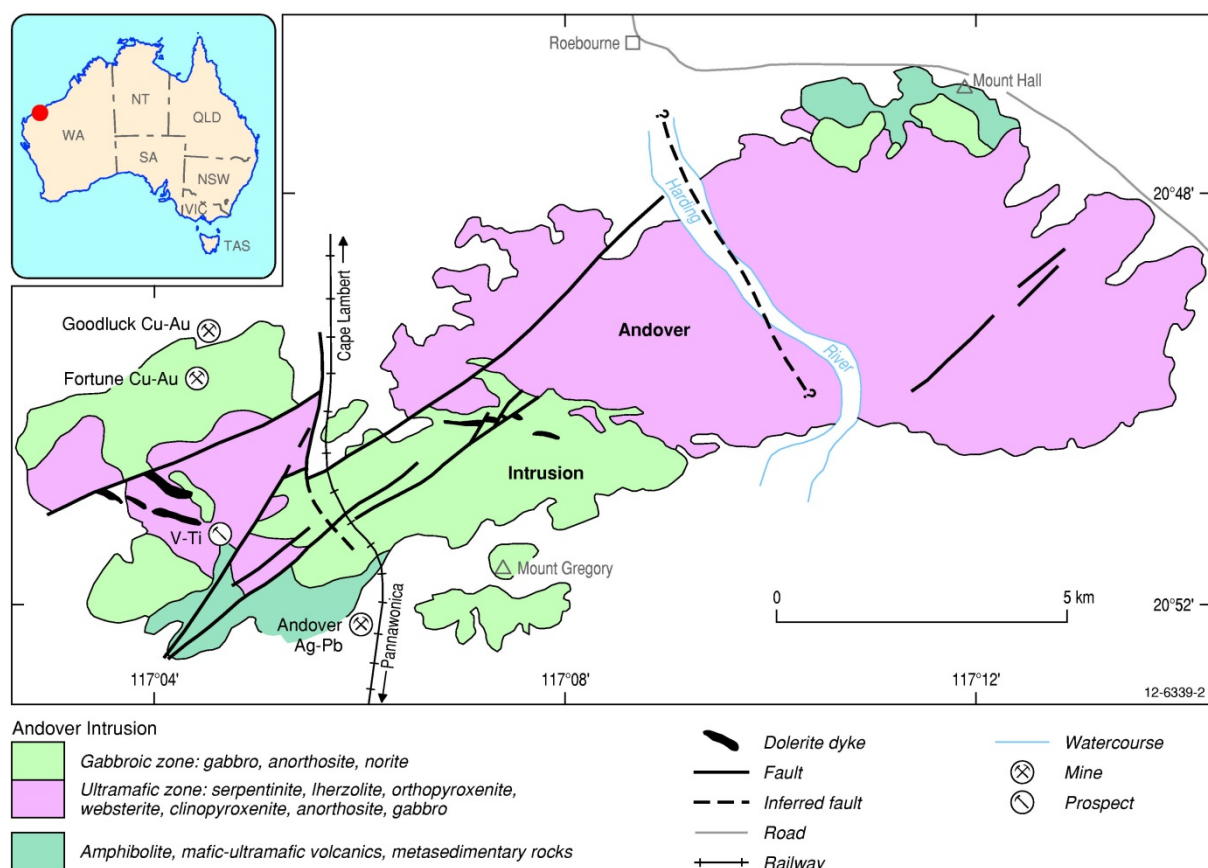
#### ***Geological setting***

The ~2927 Ma Munni Munni Intrusion is an elongated mafic-ultramafic body that crops out over an area of 9 km by 15 km (Hoatson and Keays, 1989; Hoatson et al., 1992; Barnes and Hoatson, 1994). It is one of several mafic-ultramafic intrusions in the west Pilbara Craton (Andover (Appendix Figure K.16), Dingo, Maitland, Mount Sholl, Radio Hill) that have been the focus of sustained PGE-Ni-Cu and Ni-Cu-PGE exploration (Hoatson et al., 1992). The southwestern extension

of the Munni Munni Intrusion is unconformably overlain by ~2.77 Ga sedimentary and volcanic rocks of the Fortescue Group, but near coincident aeromagnetic and gravity highs suggest the overall dimensions of the intrusion are 9 km by 25 km. Hoatson (1991a,b) subdivided the intrusion into a lower 1850 m-thick ultramafic zone and an overlying gabbroic zone which has a minimum thickness of 3630 m. The ultramafic zone consists of nine subzones containing macrorhythmic cycles of olivine-clinopyroxene mesocumulates and adcumulates. Dominant rock types are dunite, lherzolite, wehrlite, olivine websterite, clinopyroxenite, and websterite, with orthopyroxenite, norite, and spinel-bearing xenolithic units prominent in the upper parts of the lower zone.

The upper part of the ultramafic zone contains a distinctive PGE-enriched rock type—porphyritic plagioclase websterite—that forms a 30 m- to 80 m-thick orthocumulate layer which has transitional chemical and mineralogical characteristics between the rock types in the ultramafic and gabbroic zones of the intrusion. The porphyritic plagioclase websterite layer (PWL) is the host rock for the major PGE deposit in the Munni Munni Intrusion.

The intrusion is interpreted as an asymmetric boat-like structure, plunging moderately to the south-southwest, with the cyclic units thickening along the axis of the intrusion. The PWL in the central part of the intrusion generally maintains its thickness and moderate southerly dips to depths of 600 m. An isolated north-trending body of pyroxenite on the northwestern side of the intrusion, referred to as the Cadgerina Dyke, was interpreted by Barnes and Hoatson (1994) to be a feeder conduit to the gabbroic zone and upper parts of the ultramafic zone. The interpreted intersection of this feeder conduit with the intrusion is coincident with a regional gravity-high anomaly indicating a significant vertical thickness of dense rocks at depth.



Appendix Figure K.16 Geological setting of the Andover Intrusion, west Pilbara Craton, Western Australia. Associated V-Ti, Ag-Pb, and Cu-Au prospects are indicated within, and near the margins of, the mafic-ultramafic intrusion. Modified from Wallace (1992a,b).

### ***PGE mineralisation***

Five major styles of PGE mineralisation have been documented in the Munni Munni Intrusion.

1. A thin veneer of gabbro, and plagioclase websterite along the northern basal contact of the ultramafic zone hosts disseminated pyrrhotite, chalcopyrite, and minor pentlandite (up to 6% total sulphides). The mineralised marginal gabbroic rocks are locally at a high-angle to the macrocyclic layering in the ultramafic zone. The basal sulphides generally have low Ni/Cu ratios of 0.4 and Pt and Pd abundances of less than 40 ppb and 60 ppb, respectively.
2. Judy's Reef (also called J Reef) is a 1 m- to 2 m-thick Pd-enriched north-trending layer along the northeastern basal contact of the ultramafic zone (Barnes, 1995). Polymetallic mineralisation occurs 20 m to 30 m above the basal contact for a distance of 2 km south of the Elizabeth Hill Ag deposit. The reef is enriched in Pd, Ni, Cu, Co, and Ag, with Pd constituting about 80% of the total metal content. Typical drill-hole intersections include 1 m to 2 m @ 0.2 ppm to 1.9 ppm Pd+Pt+Au, 0.3% to 2.9% Ni+Cu, and 28 ppm to 260 ppm Ag. Erratic metal grades and ratios and the non-coincident character of Pd and Ag anomalies over several metres suggest a possible hydrothermal origin similar to the nearby Elizabeth Hill Ag deposit.
3. Thin (1 m to a few m) pegmatoidal websterite layers and lenses containing 0.3 ppm to 1 ppm Pd have limited lateral continuity in the ultramafic stratigraphy about one-third of the way up the ultramafic zone of the intrusion (Barnes, 1995).
4. The PWL contains the most significant PGE mineralisation in the intrusion. The PGE enrichment in the PWL occurs at the base of a 5 m- to 15 m-thick interval of disseminated Cu-Ni sulphides generally within 20 m of the overlying ultramafic-gabbroic zone contact. Some of the higher drill-hole intersections include 5.5 m @ 4.3 ppm PGEs+Au. The mineralised horizon averages 2.5 m true thickness and typically grades 2.9 ppm Pt+Pd+Au, 0.2% Ni, and 0.3% Cu. The PWL takes the form of a hybrid layer at the contact of the two zones. Barnes et al. (1990) noted that for about 40% of the mineralised intersections, maximum Pd, Pt, Au, Cu, and Ni grades are coincident, whereas for the remainder the peak PGE grades are offset by about 1 m to 4 m below the Cu and Ni peaks. In the centre of the intrusion, the PWL truncates the arcuate macrocyclic layering in the underlying ultramafic zone, suggestive of an erosional magmatic unconformity formed during magma mixing. This stratigraphic level is also characterised by a variety of hybrid ultramafic and mafic rocks, xenoliths, accidental blocks, and orthopyroxenite lithologies containing aluminous-bearing spinels that represent components of partially mixed magma formed during the main mixing event between the ultramafic and gabbroic zones (Hoatson and Keays, 1989).
5. The Munni Munni South prospect is the location of drill-hole MMS2 which returned analyses of 0.3 g/t–0.7 g/t Pt, 0.3 g/t–0.8 g/t Pd, and 0.1 g/t–0.3 g/t Au from samples at the base of a Cu-Ni mineralised zone within a transitional feldspathic pyroxenite (Lemon, 1987).

Chalcopyrite, pyrrhotite, and pentlandite were reported in a gossan on the same horizon as the Munni Munni deposit (GSWA MINEDEX database).

Visible chalcopyrite in drill-hole chips and adjacent outcrop reportedly along the same horizon as Munni Munni deposit (GSWA MINEDEX database).

The Elizabeth Hill deposit is an Archean hydrothermal polymetallic deposit that has anomalous concentrations of PGEs in the primary and supergene zones. Investigations for structurally controlled precious metal mineralisation at the Munni Munni Intrusion delineated strong hydrothermal Ag

mineralisation along the Munni Munni Fault on the northern margin of the complex. Spectacular assays of 6 m @ 3 478 ppm Ag have been obtained, with associated peak values of 6450 ppm Cu, 3130 ppm Ti, 2180 ppm Ni, 1580 ppm Ba, 1550 ppm Pb, and 494 ppm Mo in the same drill-hole. Another drill-hole intersected 9 m @ 0.21 ppm Au and 0.59 ppm Pd. Primary and supergene silver, chalcopyrite, chalcocite, bornite, pyrrhotite, linarite, pyrite, and marcasite have been recognised for this unusual type of remobilised mineralisation (Hoatson and Glaser, 1989).

### ***Age of mineralisation***

Pooled data for rock samples from the PGE-enriched PWL and the gabbroic zone gave a weighted mean age of  $2927 \pm 13$  Ma ( $2\sigma$ ), which agrees well with the SHRIMP zircon U-Pb age of  $2925 \pm 16$  Ma reported by Arndt et al. (1991) for a ferrogabbro pegmatite near the top of the ultramafic zone. The pegmatite is believed to have been derived from late-crystallising intercumulus liquid, and therefore the age is believed to be a reliable estimate for the crystallisation age of the intrusion and not an inherited age from xenocrystic zircon. The crystallisation ages of  $2927 \pm 13$  Ma and  $2925 \pm 16$  Ma for the Munni Munni Intrusion are also reliable ages for the orthomagmatic PGE mineralisation immediately below the contact of the gabbroic-ultramafic zones.

### ***Current status***

Munni Munni is an undeveloped mineral deposit. Elizabeth Hill is a historical Ag mine.

### ***Economic significance***

Munni Munni is a significant deposit with possible economic potential. A JORC Code compliant Measured, Indicated, and Inferred resource amounts to 23.6 Mt @ 1.1 g/t Pt, 1.5 g/t Pd, 0.1 g/t Rh, 0.15% Cu, 0.09% Ni, 0.2 g/t Au (Platina Resources Limited, 2014). In 2007, a small drilling program of 8 holes and a 2D seismic reflection surveys were carried out in the southwestern portion of the complex to test for extensions of the PWL below the Fortescue Group sediment and volcanic cover. MMPD7 intersected 3 m @ 2.33 g/t (Au+Pd+Pt) mineralisation at a drill-hole depth of 594.5–597.5 m.

Elizabeth Hill was a small underground mine with ~16 800 t of ore grading 2100 g/t Ag (70 ounces/t) mined to produce 1 170 000 ounces of Ag.

### ***Major references(s)***

- Arndt, N.T., Nelson, D.R., Compston, W., Trendall, A.F. and Thorne, A.M., 1991. The age of the Fortescue Group, Hamersley Basin, Western Australia, from ion microprobe zircon U-Pb results. *Australian Journal of Earth Sciences*, 38, 261–281.
- Barnes, G.B., 1995. Silver mineralisation at Elizabeth Hill, Munni Munni Complex, Western Australia. In: Ho, S.E. and Amann, W.J. (editors), *Recent Developments in Base Metal Geology and Exploration*. Australian Institute of Geoscientists, Bulletin 16, 89–94.
- Barnes, S.J. and Hoatson, D.M., 1994. The Munni Munni Complex, Western Australia: Stratigraphy, structure and petrogenesis. *Journal of Petrology*, 35, 715–751.
- Barnes, S.J., McIntyre, J.R., Nisbet, B.W. and Williams, C.R., 1990. Platinum group element mineralisation in the Munni Munni Complex, Western Australia. *Mineralogy and Petrology*, 42, 141–164.
- Hoatson, D.M., 1991a. The petrology and platinum-group element geochemistry of the Munni Munni and Mount Sholl layered mafic-ultramafic intrusions of the west Pilbara Block, Western Australia. PhD thesis, University of Melbourne, Australia, 510 pp.
- Hoatson, D.M., 1991b. Layered Archaean mafic-ultramafic intrusions of the west Pilbara Block, Western Australia. BMR Map 1:20 000 scale (includes the Munni Munni, Mount Sholl, Maitland, and Radio Hill layered intrusions).

## Western Australia

- Hoatson, D.M. and Glaser, L.M., 1989. Geology and economics of platinum-group metals in Australia. Bureau of Mineral Resources, Australia, Resource Report 5, 81 pp.
- Hoatson, D.M. and Keays, R.R., 1989. Formation of platiniferous sulphide horizons by crystal fractionation and magma mixing in the Munni Munni layered intrusion, west Pilbara Block, Western Australia. *Economic Geology*, 84, 1775–1804.
- Hoatson, D.M., Wallace, D.A., Sun, S.-S., Macias, L.F., Simpson, C.J. and Keays, R.R., 1992. Petrology and platinum-group-element geochemistry of Archaean layered mafic-ultramafic intrusions, west Pilbara Block, Western Australia. Australian Geological Survey Organisation Bulletin 242, 320 pp.
- Lemon, T.C., 1987. Munni Munni South EL47/175 1986 report Volume 1. Hunter Resources Limited. GSWA WAMEX report A19793, 172 pp.

### **Relevant figure(s)**

Figure 6.3, Figure 6.4, Figure 6.5, Figure 6.6, Figure 6.7, Figure 6.8, Figure 8.16a, Figure 8.18h, and Appendix Figure K.16.

## **K.1.141 Nanadie Well–Western Lode\***

### **Geological province**

Yilgarn Craton.

### **Location**

Nanadie Well–Western Lode: 118.948502°E, -27.159941°S; Sandstone (SG 50–16), Nowthanna (2643); ~78 km southeast of Meekatharra.

### **Classification**

- 12. Others (minor or unknown to no economic importance).

### **Geological setting**

A Ni-Cu-PGE gossan located ~1.2 km southeast of Nanadie Well Cu deposit has an Inferred Resource of 36.07 Mt @ 0.42% Cu (containing 151 000 t Cu and 74 000 ounces Au: Mithril Resources Limited, 2014). According to a map shown in a report by Mithril Resources Limited to the Australian Securities Exchange, the gossan occurs on the western side of a gabbro-norite body at its contact with metasediments. The gabbro-norite body is adjacent to the Youanmi Shear Zone (Mithril Resources Limited, 2014).

### **PGE mineralisation**

A 300 m-long zone of sub-cropping Ni gossan and Cu mineralisation is characterised by high values of Ni (up to 0.44%), Cu (up to 8.86%), and PGEs (up to 557 ppb Pt+Pd). The Ni-Cu-PGE zone occurs at the contact between a gabbro-norite and a metasedimentary unit (Mithril Resources Limited, 2014).

### **Age of mineralisation**

Unknown.

### **Current status**

Exploration site.

### ***Economic significance***

Occurrence.

### ***Major references(s)***

Mithril Resources Limited, 2014. Nickel gossan identified at Nanadie Well Project, WA. Mithril Resources Limited announcement to the Australia Securities Exchange, 22 April 2014, 10 pp.

### ***Relevant figure(s)***

#### **K.1.142 Narndee**

(see Wondinong group)

#### **K.1.143 Natalies Hill**

(see Munni Munni group)

#### **K.1.144 Nebo–Babel**

##### ***Geological province***

Musgrave Province.

##### ***Location***

Nebo: 127.7274°E, -26.09538°S; Cooper (SG 52–10), Cooper (4445); ~115 km east of Warburton.

Babel: 127.69690°E, -26.10712°S; Cooper (SG 52–10), Cooper (4445); ~112 km east of Warburton, WA.

##### ***Classification***

- 2. Massive to poorly layered tholeiitic mafic-dominated intrusions; 2.A. Segregations of Ni-Cu-Co-PGE sulphides in feeder conduits and basal contacts.

##### ***Geological setting***

The Nebo–Babel Ni-Cu-PGE-sulphide deposit is located in the western part of the Musgrave Province, which consists of a basement of high-grade amphibolite to granulite lithologies overprinted by several major tectonic episodes and intruded by granitoid plutons, layered mafic to ultramafic intrusions of the Giles Complex, and mafic dykes (Ballhaus and Glikson, 1995). The deposit is hosted within a concentrically zoned, olivine-free, tube-like (chonolith), gabbro-norite intrusion that belongs to the ~1070 Ma Giles Complex. Nebo and Babel form two separate mafic bodies of an originally continuous, ~5-km-long gabbro-norite intrusion, which was emplaced into sulphide-free orthogneiss and subsequently offset by the north-trending Jameson Fault. The intrusion is interpreted to have been formed by at least three distinct (but chemically-related) magma pulses, emplaced at depths of 10 km to 12 km, i.e., at a pressure of ~3.5 kbars (Seat et al., 2007; Seat, 2008; Seat et al., 2009; Seat et al., 2011; Godel et al., 2011).

### **PGE mineralisation**

The Nebo–Babel Ni-Cu-PGE deposit was discovered by Western Mining Corporation in mid-2000. It was found using lag sampling and outcropped as scattered gossan, and therefore it is principally a geochemical discovery. However, strong magnetic, EM, and gravity anomalies highlight the massive and disseminated mineralisation within a shallowly WSW-plunging gabbro-norite feeder conduit. The style of mineralisation is similar to the giant Voisey's Bay Ni-Cu-Co sulphide deposit in Canada.

Some of the most significant drill-hole Ni-Cu sulphide intersections in Australia have been reported from this 'world-class' deposit, e.g., 106.5 m @ 2.4% Ni, 2.7% Cu, and 0.2 g/t PGEs. Nebo–Babel has a published preliminary resource of 392 Mt grading 0.3% Ni, 0.33% Cu, and 0.18 g/t PGEs (Seat et al., 2005, 2007), which equates to about 1.2 Mt contained Ni and 1.3 Mt contained Cu, with an in-ground value of A\$25 billion. More than 70% of the resource is contained in the Babel deposit. The deposit was later acquired by BHP Billiton Limited as a result of its takeover of Western Mining Corporation in mid-2005.

Godel et al. (2011) have cited Seat et al. (2007, 2009) for recognising two major types of sulphide mineralisation at Nebo–Babel, namely:

- monoclinic pyrrhotite, pentlandite, chalcopyrite, and trace pyrite predominantly in massive sulphide lenses located close to, or along, the hanging-wall contact; and
- interstitial disseminated sulphides with mineralogy similar to those of the massive sulphides (Seat et al., 2007, 2009). All lithologic units at Nebo–Babel are variably depleted in PGEs, indicating crystallisation from magmas that have experienced various degrees of sulphide segregation prior to emplacement (Seat et al., 2009). The  $\delta^{34}\text{S}$  values (Seat et al., 2009) vary within a narrow range from 0.0‰ to 0.8‰ and are consistent with mantle-derived S. Based on this, Seat et al. (2009) have argued that sulphide saturation did not occur *in situ* and is inferred to have been triggered by a change in magma composition accompanying assimilation of orthogneiss.

Seat (2008) suggests many of the PGMs at Nebo–Babel are tellurides hosted by silicate minerals rather than sulphides. Preliminary scanning electron microscope studies identified moncheite ( $\text{PtTe}_2$ ), merenskyite ( $\text{PdTe}_2$ ), michenerite ( $\text{PdBiTi}$ ), and melonite ( $\text{NiTe}_2$ ) where significant Pd substitutes for Ni. The PGMs typically form small anhedral grains (1  $\mu\text{m}$  to 4  $\mu\text{m}$  and rarely up to 10  $\mu\text{m}$  across) in pyroxene, plagioclase, pyrrhotite, K-feldspar, and quartz. All of the Nebo–Babel rock units are slightly PGE depleted with Cu/Pd ratios higher than primitive mantle, indicating early saturation and segregation of a sulphide and/or PGE removal.

### **Age of mineralisation**

Seat (2008) and Seat et al. (2011) obtained a U-Pb zircon crystallisation age for the intrusion of  $1068.0 \pm 4.3$  Ma by combining the individual  $^{207}\text{Pb}/^{206}\text{Pb}$  ages of the Babel ( $1071.7 \pm 4.7$  Ma) and Nebo ( $1063.7 \pm 8.7$  Ma) bodies. This is consistent with an ion microprobe (SHRIMP) U-Pb zircon age of  $1067 \pm 8$  Ma for a Cu-mineralised dyke that constrains the age of an important magmatic event related to mineralisation (Howard et al., 2009).

### **Current status**

Currently subeconomic with further development on hold.

### **Economic significance**

Large undeveloped Ni-Cu-PGE-sulphide deposit.

### **Major references(s)**

- Ballhaus, C.G. and Glikson, A.Y., 1995. The petrology of layered mafic-ultramafic intrusions of the Giles Complex, western Musgrave Block, Western Australia. In: Glikson, A.Y. (editor), The Giles mafic-ultramafic complex and environs, western Musgrave Block, central Australia. AGSO Journal of Geology and Geophysics, 16:1–2: 69–91, thematic issue.
- Hoatson, D.M., Jaireth, S. and Jaques, A.L., 2006. Nickel sulfide deposits in Australia: Characteristics, resources, and potential. Ore Geology Reviews, 29, 177–241.
- Howard, H.M., Smithies, H.R., Kirkland, C.L., Evins, P. and Wingate, M.T.D., 2009. Age and geochemistry of the Alcurra suite in the West Musgrave province and implications for orthomagmatic Ni-Cu-PGE mineralization during the Giles event. Geological Survey of Western Australia Record 2009/16, 16 pp.
- Seat, Z., 2008. Geology, petrology, mineral and whole-rock chemistry, stable and radiogenic isotopic systematics and Ni-Cu-PGE mineralisation of the Nebo–Babel intrusion, west-Musgrave, Western Australia: Ph.D. thesis, Nedlands, University of Western Australia, Perth, Western Australia, Australia, 479 pp.
- Seat Z., Beresford S.W., Gee M.A.M., Grguric B.A., Groves D.I., Hronsky J.M.A., Mathison C.I. and Waugh R., 2005. Geological and geochemical architecture of the Nebo and Babel Ni-Cu-PGE deposit, West Musgrave, Western Australia. In: Tormanen, T.O. and Alapieti, T. T. (editors), Platinum-Group Elements; from Genesis to Beneficiation and Environmental Impact. 10th International Platinum Symposium, 6-11 August 2005, Geological Survey of Finland, Espoo, Finland, Extended Abstracts, 227–230,
- Seat, Z., Beresford, S.W., Grguric, B.A., Waugh, R.S., Hronsky, J.M.A., Gee, M.M.A., Groves, D.I. and Charter, I.M., 2007. Architecture and emplacement of the Nebo–Babel gabbro-hosted magmatic Ni-Cu-PGE sulfide deposit, West Musgrave, Western Australia: Mineralium Deposita, 42, 551–581.
- Seat, Z., Beresford, S.W., Grguric, B.A., Gee, M.A.M. and Grassineau, N.V., 2009. Reevaluation of the role of external sulfur addition in the genesis of Ni-Cu-PGE deposits: Evidence from the Nebo–Babel Ni-Cu-PGE deposit, West Musgrave, Western Australia. Economic Geology, 104, 521–538.
- Seat, Z., Gee, M.A.M., Grguric, B.A., Beresford, S.W. and Grassineau, N.V., 2011. The Nebo-Babel Ni-Cu-PGE sulfide deposit (West Musgrave, Australia): Pt. 1. U/Pb zircon ages, whole-rock and mineral chemistry, and O-Sr-Nd isotope compositions of the intrusion, with constraints on petrogenesis. Economic Geology, 106, 527–556.

### **Relevant (s)**

Figure 6.16, Figure 6.17, Figure 6.18, and Figure 8.16b.

## **K.1.145 Nepean\***

### **Geological province**

Yilgarn Craton.

### **Location**

Nepean\*: 121.084198°E, -31.164789°S; Boorabbin (SH 51–13), Yilmia (3135); ~60 km southwest of Kalgoorlie and ~18 km southeast of the Priors PGE occurrence.

### **Classification**

- 3. Komatiitic flows and related sill-like intrusions; 3.A. Massive, matrix, and disseminated Ni-Cu-PGE sulphides in preferred lava pathways.
- 8. Hydrothermal-Metamorphic; 8.B. Remobilised Ni-Cu-PGE±Au sulphides in komatiitic and metasedimentary rocks.

### ***Geological setting***

The Nepean Ni deposit is hosted in metamorphosed komatiite and the original magmatic textures and mineralogy have been modified by regional metamorphism and subsequent retrograde effects (Marston, 1984; Roberts, 2004). The Ni deposits in the area appear to be associated with relatively thin metakomatiite flows with massive and disseminated sulphides accumulated in lava-flow channels at the base of the metakomatiite flow (Roberts, 2004).

### ***PGE mineralisation***

Maximum PGE contents for some of the deposits in the Yilgarn Craton, as reported by Keays and Davison (1976) and Travis et al. (1976), include analyses from the historical Nepean Ni mine, e.g., 31.30 ppm Pd (with 19.8% Ni, 0.16% Cu).

### ***Age of mineralisation***

Archean host rocks?

### ***Current status***

Historical Ni mine.

### ***Economic significance***

Historical Ni mine. The Nepean Ni mine produced 1.089 Mt of ore at 2.99% Ni between 1970 and 1987 (Roberts, 2004).

### ***Major references(s)***

- Keays, R.R. and Davison, R.M., 1976. Palladium, iridium and gold in the ores and host rocks of nickel-sulphide deposits in Western Australia. *Economic Geology*, 71, 1214–1228.
- Marston, R.J., 1984. Nickel mineralization in Western Australia. *Geological Survey of Western Australia, Mineral Resources Bulletin 14*, 271 pp.
- Roberts, F.I., 2004. Mineralization of the Woolgongie–Yilmia area, Eastern Goldfields Granite–Greenstone Terrane, Western Australia: Western Australia Geological Survey, Record 2004/6, 58 pp.
- Travis, G.A., Keays, R.R. and Davison, R.M., 1976. Palladium and iridium in evaluation of nickel gossans in Western Australia. *Economic Geology*, 71, 1229–1243.

### ***Relevant figure(s)***

Figure 6.21.

## **K.1.146 Netty\***

### ***Geological province***

Yilgarn Craton.

### ***Location***

Netty\*: 118.968903°E, -33.876919°S; Newdegate (SI 50–08), Jerramungup (2630); ~9 km northeast of Jerramungup.

### ***Classification***

- ?1. Layered tholeiitic mafic-ultramafic intrusions.

### ***Geological setting***

In the Western Gneiss Terrane of the Yilgarn Craton, foliated granitoid and gneissic rocks have been intruded by the mafic Netty dyke, which is probably part of the Widgiemooltha Dyke Swarm that includes the 2411 Ma Jimberlana Dyke, near Norseman. The Netty dyke consists of a leucogabbro core and marginal dolerite, and can be traced for 18 km.

### ***PGE mineralisation***

Sampling of the mullock heaps at the Netty mine revealed anomalous levels of Au, Ag, and PGEs associated with the Cu-Ni mineralisation. Surface samples of gabbroic rocks with disseminated sulphides averaged 1.5 ppm Au (Hoatson and Glaser, 1989).

### ***Age of mineralisation***

Proterozoic host rock?

### ***Current status***

Historical exploration site.

### ***Economic significance***

Occurrence.

### ***Major references(s)***

Hoatson, D.M. and Glaser, L.M., 1989. The geology and economics of platinum-group metals in Australia. Bureau of Mineral Resources, Australia, Resource Report 5, 81 pp.

### ***Relevant figure(s)***

## **K.1.147 Nickol River East**

### ***Geological province***

Pilbara Craton.

### ***Location***

Nickol River East: 116.991720°E, -20.744340°S; Dampier (SF 50–02), Dampier (2256); ~15 km east of Karratha.

### ***Classification***

- 10. Placer; 10.C. Alluvial placers.

### ***Geological setting***

Source for alluvial PGMs may be intrusive ultramafics within the Nickol River Formation of the Warrawoona Group (Ruddock, 1999).

### ***PGE mineralisation***

Osmiridium grains occur in stream sediment and soil samples collected by CSIRO (1983) in the eastern half of the Nickol River goldfield (Hudson and Horwitz, 1985). The Ir, Os, Ru, and Pt alloys, and Au were recovered from stream-sediment samples derived from clastic sedimentary rocks, felsic and mafic volcanics, and chert from a 10 km-strike-length of the Archean Nickol River Formation. The PGMs form

## Western Australia

both flattened and irregular to subhedral grains that vary in diameter from 0.1 mm to 0.4 mm. Associated heavy minerals include gold, ilmenite, chromite, magnetite, rutile, spinel, sphene, garnet, zircon, tourmaline, and epidote. The compositional spread of the PGMs may indicate multiple sources, possibly related to layered mafic-ultramafic intrusions in the Roebourne and Karratha region of the west Pilbara Craton, e.g., Andover, Sherlock River, Maitland (Appendix Figure K.17), Radio Hill, Mount Sholl, and Munni Munni (Hoatson and Blake, 1992). Archean paleoplacers are favoured to account for the present distribution of the mineralisation, although Jurassic or Cenozoic alluvial sediments may be potential host rocks (Minsaco Resources Pty Limited, 1999; Hoatson and Glaser, 1989).

### ***Age of mineralisation***

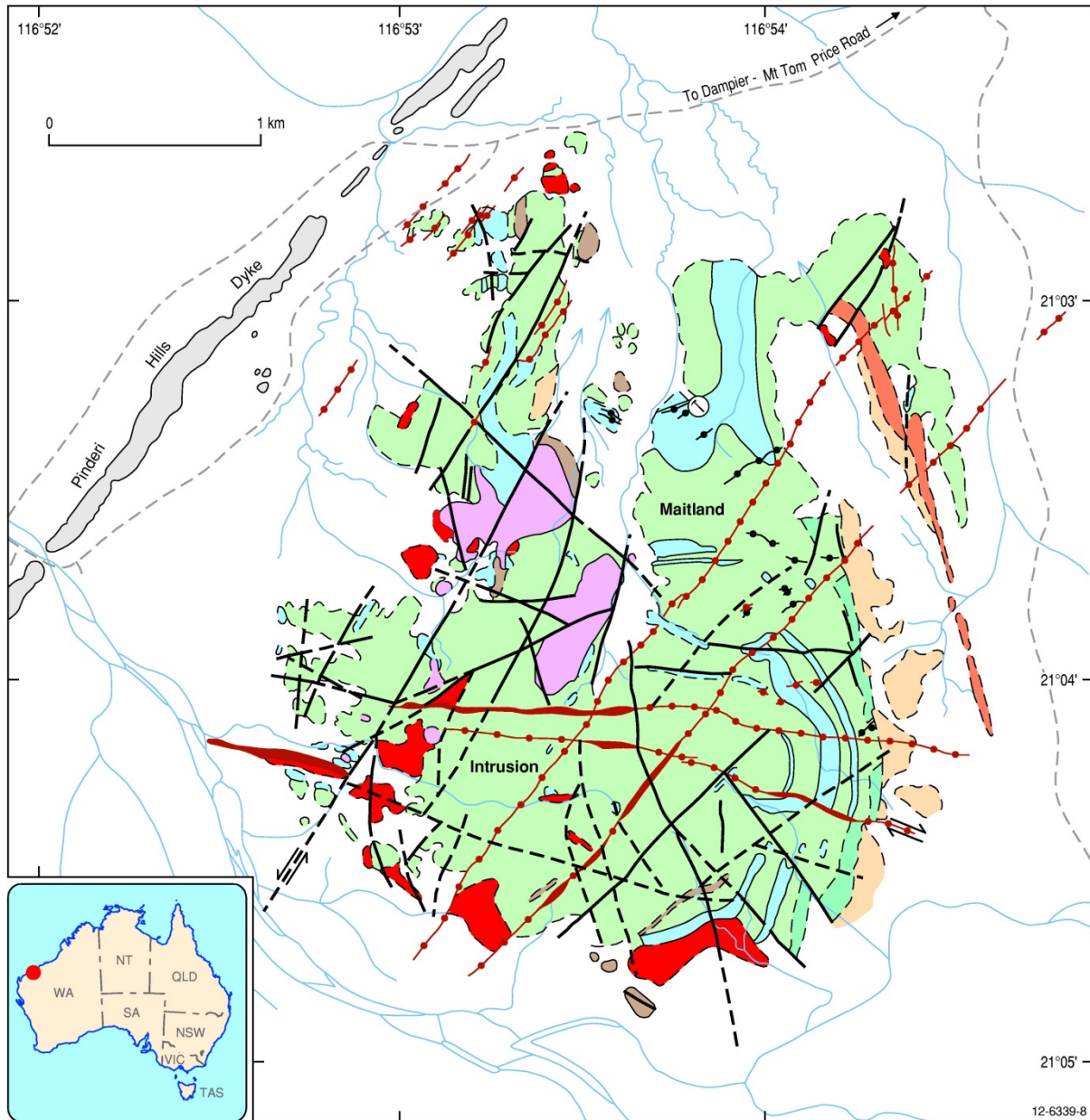
Cenozoic alluvials.

### ***Current status***

Historical exploration site.

### ***Economic significance***

Occurrence.



Maitland Intrusion

- Porphyritic gabbroic dyke
- Discordant plug-like peridotite intrusions containing dunite, lherzolite, olivine websterite, minor pyroxenite
- Clinopyroxenite
- Poorly-layered cyclic units of anorthosite and anorthositic gabbro
- Undivided cyclic mafic sequence of leucogabbro, melagabbro, gabbronorite, olivine gabbronorite, norite, amphibolised gabbro. Pegmatoidal quartz-bearing melagabbro (  ) contains minor disseminated Fe-Cu sulphides along the eastern margin of the intrusion
- Leucocratic aplitic microgranodiorite and granite

Whundo Group

- Intermediate to felsic metavolcanics, minor metabasalt

- Quartz vein
- Metadolerite and pyroxenite dykes
- Pindari Hills Dyke (gabbronorite)
- Fault
- Inferred fault
- Watercourse
- Track
- Copper prospect

Appendix Figure K.17 Geological setting of the Maitland Intrusion, west Pilbara Craton, Western Australia. Minor disseminated Fe-Cu sulphides are hosted by a pegmatoidal quartz-bearing melagabbroic unit along the eastern margin of the mafic-dominated intrusion. Late plug-like ultramafic bodies prominent in the northwestern part of the intrusion appear to be discordant to the mafic stratigraphy. Modified from Hoatson et al. (1992).

### **Major references(s)**

- Hoatson, D.M. and Glaser, L.M., 1989. The geology and economics of platinum-group metals in Australia. Bureau of Mineral Resources, Australia, Resource Report 5, 81 pp.
- Hudson, D.R. and Horwitz, R.C., 1985. Mineralogy and geological setting of a new occurrence of platinum group minerals, between Roebourne and Karratha, Western Australia. Commonwealth Scientific and Industrial Research Organisation, Division of Mineralogy and Geochemistry, Research Review, 1985, 79–80.
- Minsaco Resources Pty Limited, 1986. Final report. M5241/0: Karratha platinum and gold prospect, north-west Pilbara, Western Australia. GSWA WAMEX report A23955, 50 pp.
- Ruddock, I., 1999. Mineral occurrences and exploration potential of the west Pilbara. Western Australia Geological Survey Report 70, 63 pp.

### **Relevant figure(s)**

Figure 6.3 and Appendix Figure K.17.

## **K.1.148 Nicholsons Find PGE**

(see Lamboo group)

## **K.1.149 Nova–Bollinger\***

### **Geological province**

Albany-Fraser Orogen.

### **Location**

Nova: 123.192413°E, -31.819886°S; Zanthus (SH 51–15), Symons Hill (3534); ~95 km northwest of Balladonia.

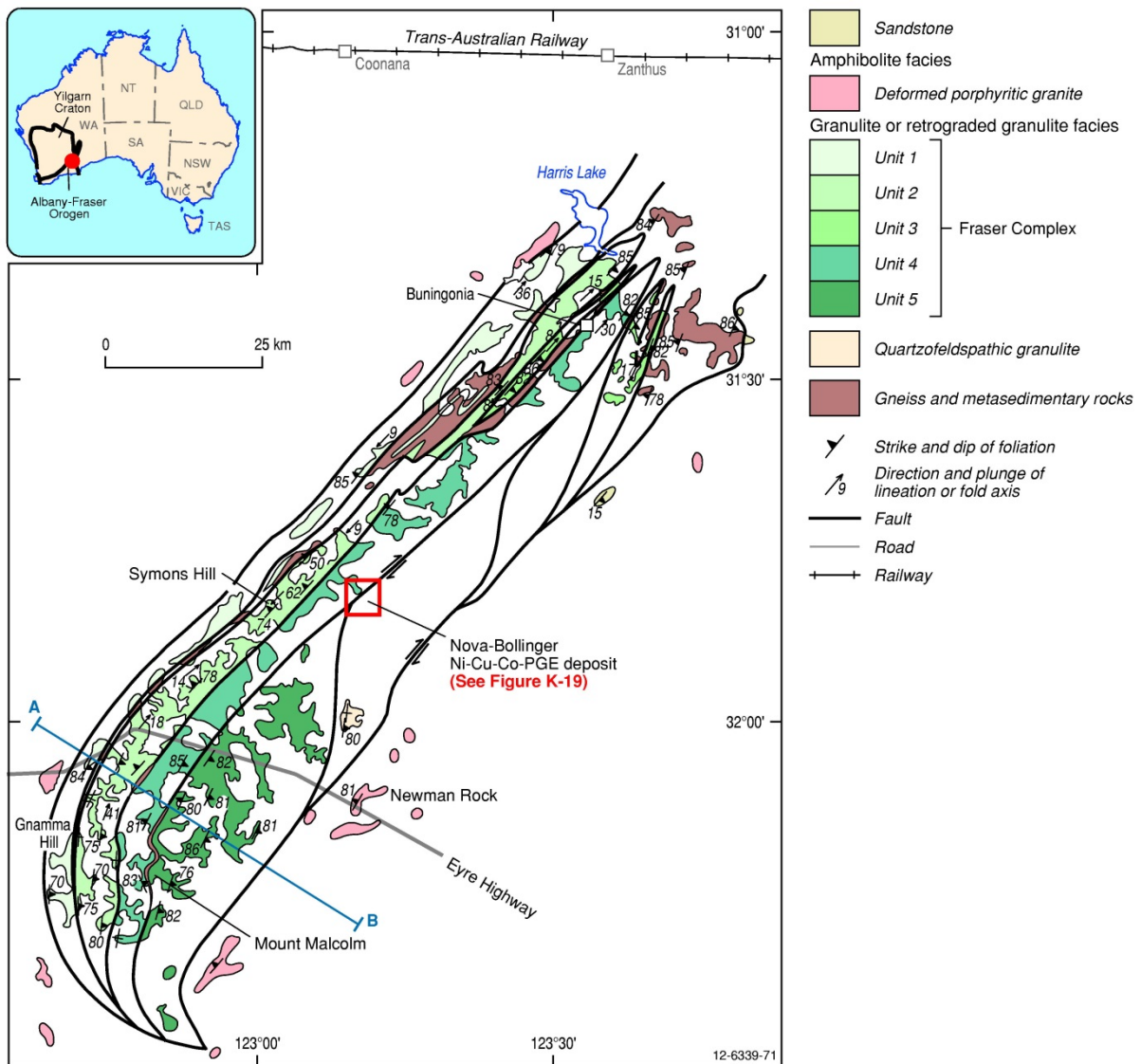
### **Classification**

- 2. Massive to poorly layered tholeiitic mafic-dominated intrusions; 2.A. Segregations of Ni-Cu-Co-PGE sulphides in feeder conduits and basal contacts.
- The Nova–Bollinger Ni-Cu-Co-PGE-sulphide deposit is overlain by a lateritic weathering profile that is enriched in Ni, Cu, and Co. The mineralised zone in the weathering profile corresponds to the mineral-system class: 9. Regolith-laterite; 9.A. PGE-bearing regolith developed on ultramafic-mafic igneous rocks.

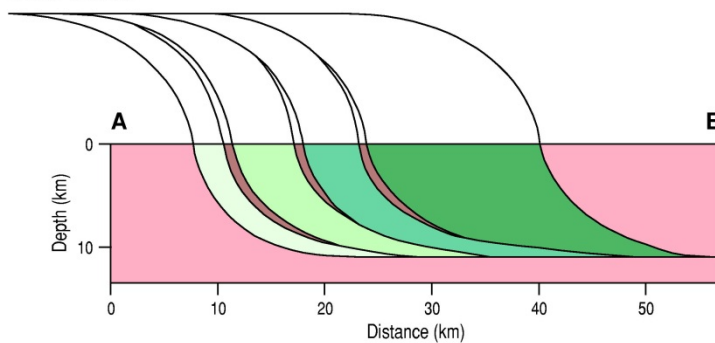
### **Geological setting**

The Nova and Bollinger deposits, discovered in 2012 and 2013, respectively (Sirius Resources NL, 2012a), are located within the northeast Fraser Zone of the Albany-Fraser Orogen (Appendix Figure K.18). The Fraser Zone is a fault-bounded unit approximately ~425 km-long and ~50 km-wide, dominated by metagabbroic rocks. It lies between Paleoproterozoic basement rocks of the Biranup and Nornalup zones (Spaggiari et al., 2013). According to Spaggiari et al. (2013), only the southwestern portion of the Fraser Zone is exposed and it comprises the ~1305 Ma–1290 Ma Fraser Range Metamorphics. The dominant lithologies are sheets of metagabbroic rocks interlayered with monzogranitic to syenogranitic gneiss, pyroxene-bearing granitic gneiss, and, metamorphosed hybrid igneous rocks. The latter rocks are interlayered with amphibolite to granulite facies pelitic, semipelitic to calcic, and Fe-rich metasedimentary rocks of the Mesoproterozoic Arid Basin.

Western Australia



Cross-section



Appendix Figure K.18 Simplified geological outcrop map and schematic cross-section of the Albany-Fraser Orogen. The location of the Proterozoic Nova-Bollinger Ni-Cu-Co-PGE deposit is shown near the centre of the figure. Modified from Myers (1985).

The GSWA has interpreted the Fraser Zone as a structurally modified, lower crustal hot-zone where voluminous gabbroic magmas were variably mixed with contemporaneous granitic magma and country-rock melts. According to the GSWA, the presence of these gabbroic magmas, regional granite magmatism, and previously published peak metamorphic conditions in the metasedimentary

rocks of >800°C and 8–9 kbars are all indicative of a regional thermal anomaly from at least 1305 Ma–1290 Ma that coincided with the formation of the Fraser Zone. The preferred tectonic setting as interpreted by GSWA is either a distal back-arc or an intercontinental rift (Spaggiari et al., 2013).

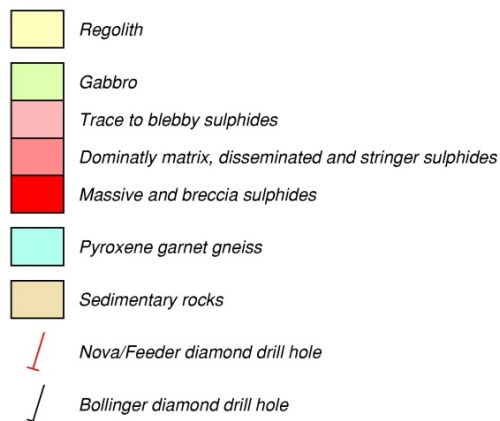
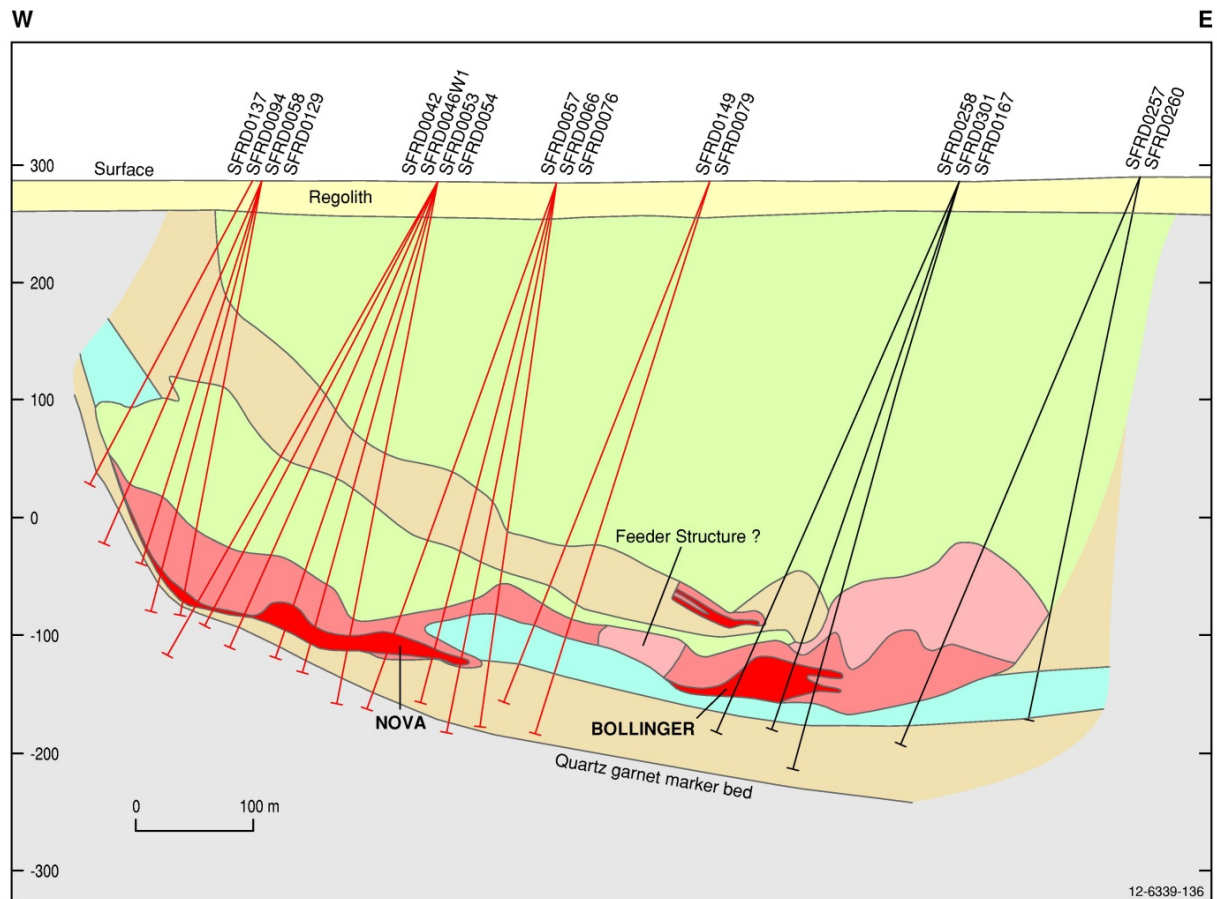
The Nova–Bollinger deposit is defined by a Ni-Cu-Co soil anomaly within a large 'eye-shaped' feature in regional magnetics. The 'eye-shaped' feature was considered to represent coherent ultramafic bodies or layered intrusions within strain shadows giving a greater chance for survival of undisrupted sulphide mineralisation in a high-grade metamorphic environment (Gollan, 2012). The GSWA co-funded drill-hole was also instrumental to the discovery of the Nova–Bollinger deposit, to test the stratigraphy underlying the Ni-Cu-Co soil anomaly within the 'eye-shaped' feature.

### ***PGE mineralisation***

The Ni-Cu-Co mineralisation at the Nova–Bollinger deposit was reported by Sirius Resources NL (2012b,d) as consisting of pyrrhotite, pentlandite, and chalcopyrite. The ore minerals reportedly display typical magmatic textures including massive, matrix, net-textured, breccia, blebby, and disseminated forms although locally mineralisation crosscut garnet-bearing metamorphic layering. The host rocks are dominantly gabbroic granulite, similar to the widespread olivine gabbro to olivine gabbro-norite and hybrid gabbro of the Fraser Zone (Sirius Resources NL., 2012b,d; Spaggiari et al., 2013).

Some PGE concentrations associated with the Ni-Cu sulphides were reported for the early drill-hole assays as tabulated in Appendix Table K.29, but have not been published for the bulk of the more recent analyses of drill-core (Sirius Resources NL, 2012c). Intersections, such as in DDH SFRC0026 (e.g., 8 m @ 5.81% Ni, 2.26% Cu, 0.16% Co, 0.12 g/t Pd, 0.12 g/t Pt: Appendix Table K.29) indicate that some sections of the Nova–Bollinger deposit contain anomalous concentrations of PGEs associated with the Ni-Cu-Co sulphides (Appendix Figure K.19). This PGE-enrichment is a common feature of mafic-intrusive hosted Ni-Cu sulphide deposits in Australia and is observed for the similar deposits in the Savannah Intrusion in the Halls Creek Orogen, Radio Hill Intrusion in the west Pilbara Craton, and the Nebo–Babel Intrusion in the Musgrave Province.

The GSWA has suggested that based on the available geochronological data, metamorphism occurred shortly after magmatism, and may have been a significant secondary ore control on the mineralisation (Spaggiari et al., 2013). Sirius Resources NL (2013) also reported that the two major mineralised zones of Nova and Bollinger may be connected by a (originally magmatic?) feeder structure (Appendix Figure K.19).



<b>SFRD0042:</b>	22.70 m @ 0.91% Ni, 0.73% Cu and 20.93 m @ 1.56% Ni, 0.65% Cu
<b>SFRD0053:</b>	7.30 m @ 2.20% Ni, 0.60% Cu including 1.10 m @ 7.45% Ni, 1.06% Cu and 17.00 m @ 3.68% Ni, 3.82% Cu including 11.10 m @ 4.31% Ni, 5.03% Cu
<b>SFRD0057:</b>	38.90 m @ 3.23% Ni, 1.46% Cu including 24.86 m @ 4.26% Ni, 1.77% Cu including 10.11 m @ 6.00% Ni, 2.75% Cu
<b>SFRD0058:</b>	47.20 m @ 1.86% Ni, 0.57% Cu including 36.00 m @ 2.23% Ni, 0.65% Cu including 3.05 m @ 6.10% Ni, 1.31% Cu
<b>SFRD0076:</b>	3.60 m @ 4.43% Ni, 1.42% Cu
<b>SFRD0167:</b>	102.82 m @ 1.00% Ni, 0.43% Cu including 62.82 m @ 1.41% Ni, 0.57% Cu including 4.78 m @ 4.60% Ni, 1.29% Cu
<b>SFRD0257:</b>	118.0 m of trace to stringer sulphide including 30.2 m of disseminated to stringer sulphide
<b>SFRD0258:</b>	55.10 m @ 3.09% Ni, 1.02% Cu including 17.51 m @ 4.77% Ni, 1.30% Cu and 6.01 m @ 5.18% Ni, 1.74% Cu
<b>SFRD0301:</b>	57.10 m @ 2.73% Ni, 1.14% Cu including 18.22 m @ 5.08% Ni, 2.03% Cu

Appendix Figure K.19 Schematic west-east cross-section of the Proterozoic Nova-Bollinger Ni-Cu-Co-PGE deposit at the 6 479 700 mN line. Drill-hole SFRD0026 (not shown here) indicates the Nova-Bollinger deposit contains minor concentrations of PGEs associated with the sulphides (e.g., 8 m @ 5.81% Ni, 2.26% Cu, 0.16% Co, 0.12 g/t Pd, 0.12 g/t Pt). Sirius Resources NL has suggested the mineralised environment shown in this section represents a feeder structure. Modified from Sirius Resources NL (2013c).

Appendix Table K.29 PGE concentrations associated with the Ni-Cu sulphides for early drill-hole assays in the Nova–Bollinger deposit. Data from Sirius Resources NL (2012c).

Drill-hole	From (m)	Width (m)	Grade
SFRC0024	174	1	0.76% Ni, 1.36% Cu, 0.03% Co, 4.0 g/t Ag, 23 ppb Au, 25 ppb Pd, 6 ppb Pt
SFRC0024	178	3	0.31% Ni, 0.68% Cu, 0.01% Co, 1.4 g/t Ag, 21 ppb Au, 20 ppb Pd, 10 ppb Pt
SFRC0024	191	4	4.02% Ni, 1.41% Cu, 0.12% Co, 2.2 g/t Ag, 44 ppb Au, 68 ppb Pd, 32 ppb Pt
SFRC0026,	123	13	4.30% Ni, 1.83% Cu, 0.12% Co, 3.1 g/t Ag, 36 ppb Au, 90 ppb Pd, 76 ppb Pt
including	128	8	5.81% Ni, 2.26% Cu, 0.16% Co, 3.7 g/t Ag, 39 ppb Au, 0.12 g/t Pd, 0.12 g/t Pt
SFRC0027,	229	9	1.48% Ni, 0.86% Cu, 0.05% Co, 2.5 g/t Ag, 0.15 g/t Au
including	229	3	1.45% Cu, 0.4% Ni, 4.9 g/t Ag, 0.34 g/t Au
SFRC0027,	232	6	1.84% Ni, 0.57% Cu
including	236	1	4.70% Ni, 0.40% Cu, 0.12% Co
SFRC0028	116	4	0.48% Ni, 0.38% Cu, 0.02% Co, 0.09 g/t Ag
SFRC0028	156	8	0.25% Ni, 0.22% Cu, 1.5 g/t Ag
SFRC0029	234	2	0.96% Ni, 0.46% Cu, 1.3 g/t Ag
SFRC0030	188	8	0.41% Ni, 0.40% Cu, 0.02% Co, 1.78 g/t Ag
SFRC0032	60	4	1.47% Ni, 0.17% Cu, 0.05% Co, 0.25 g/t Ag
SFRC0032	80	2	2.11% Ni, 1.12% Cu, 0.07% Co, 4.25 g/t Ag
SFRC0033	165	6	3.16% Ni, 0.49% Cu, 0.10% Co, 1.12 g/t Ag
SFRC0034	200	4	0.22% Ni, 1.07% Cu, 0.01% Co, 2.8 g/t Ag
SFRC0034,	212	7	1.27% Ni, 0.35% Cu, 0.04% Co, 0.84 g/t Ag
including	216	3	2.63% Ni, 0.45% Cu, 0.08% Co, 1.13 g/t Ag
SFRC0034	220	4	0.18% Ni, 0.47% Cu, 1.1 g/t Ag
SFRD0035,	146.70	6.20	1.68% Ni, 0.36% Cu, 0.05% Co, 0.3 g/t Ag
including	149.20	2.90	2.52% Ni, 0.44% Cu, 0.08% Co, 0.5 g/t Ag

### **Age of mineralisation**

The age of host rocks and the metagabbro of the Fraser Zone, according to geochronological data quoted by Smithies et al. (2013), indicate that mafic and felsic magmatism was coeval between ~1310 Ma and ~1283 Ma.

### **Current status**

Pre-feasibility evaluation.

### **Economic significance**

A significant medium-sized Ni-Cu-Co deposit with minor PGE credits. The Nova–Bollinger Ni-Cu-Co resource is held in two ore deposits, Nova and Bollinger, for a combined JORC Code compliant resource amounting to:

## Western Australia

- Indicated Resources of 11.7 Mt at 2.3% Ni, 1.0% Cu, and 0.08% Co; and
- Inferred Resources of 2.9 Mt at 1.1% Ni, 0.5% Cu, and 0.04% Co.

The Nova–Bollinger deposit is currently subject to a pre-feasibility study as part of the process to establish its economic viability.

### **Major references(s)**

- Gollan, M., 2012. Final drilling report 'The Eye'. Cofunded Drilling Agreement DAG2011/00069941. Exploration Licence E28/1724, Fraser Range Project, 24<sup>th</sup> January 2012. Geological Survey of Western Australia. Sirius Gold Pty Limited, WAMEX Report A092733, 14 pp.
- Sirius Resources NL, 2012a. Major nickel-copper discovery. New deposit style, new nickel province, first of three EM targets to be tested at the Eye. Sirius Resources NL announcement to the Australian Securities Exchange, 26 July 2012, 5 pp.
- Sirius Resources NL, 2012b. First diamond hole intersects sulphide where expected at Nova. Sirius Resources NL announcement to the Australian Securities Exchange, 20 August 2012, 5 pp.
- Sirius Resources NL, 2012c. Nova nickel-copper deposit now growing rapidly. Sirius Resources NL announcement to the Australian Securities Exchange, 10 September 2012, 8 pp.
- Sirius Resources NL, 2012d. Best hit yet at Nova. Sirius Resources NL announcement to the Australian Securities Exchange, 26 September 2012, 5 pp.
- Sirius Resources NL, 2013. Drilling at Bollinger confirms potential scale. Sirius Resources NL announcement to the Australian Securities Exchange, 6 March 2013, 13 pp.
- Smithies, R.H., Spaggiari, C.V., Kirkland, C.L., Howard, H.M. and Maier, W.D., 2011. Petrogenesis of gabbros of the Mesoproterozoic Fraser Zone: constraints on the tectonic evolution of the Albany-Fraser Orogen. Geological Survey of Western Australia, Record 2013/5, 29 pp.
- Spaggiari, C.V., Smithies, R.H., Kirkland, C.L., Howard, H.M., Maier, W.D. and Clark, C., 2013. Melting, mixing, and emplacement: evolution of the Fraser Zone, Albany-Fraser Orogen. In: Promoting the Prospectivity of Western Australia. Geological Survey of Western Australia. Extended Abstracts, Record 2013/2, 1–5.

### **Relevant figure(s)**

Appendix Figure K.18 and Appendix Figure K.19.

## **K.1.150 Odysseus, Odysseus North**

(see Cosmos group)

## **K.1.151 Oldham Range\***

(see Phenoclast Hill)

## **K.1.152 Ora Banda Sill, Mt Carnage**

### **Geological province**

Yilgarn Craton.

### **Location**

Ora Banda Sill: 121.0583°E, -30.4°S; Kalgoorlie (SF 51–09), Bardoc (3137), the Ora Banda Pt prospect is on the Ora Banda Sill; ~55 km north-northwest of Kalgoorlie and ~1 km south of Ora Banda townsite.

Mt Carnage: 120.963729°E, -30.352919°S; also known as the Black Range prospect; about 10 km west-northwest of the Ora Banda Sill.

### **Classification**

- Primary mineralisation overlain by a mineralised lateritic profile.
- Classification of primary mineralisation uncertain.
- ?1. Layered tholeiitic mafic-ultramafic intrusions; ?1.A. Stratabound PGE-bearing sulphide layers.

or:

- ?2. Massive to poorly layered tholeiitic mafic-dominated intrusions; ?2.A. Segregations of Ni-Cu-Co-PGE sulphides in feeder conduits and basal contacts.
- 9. Regolith-Laterite; 9A. PGE-bearing regolith developed on ultramafic-mafic igneous rocks.

### **Geological setting**

The Ora Banda Sill is a high-MgO mafic-ultramafic intrusive body, 2 km-thick, emplaced near the contact between tholeiitic volcanic rocks and felsic to intermediate volcanoclastic rocks of the Black Flag Group. The sill comprises six main lithological units as tabulated in Appendix Table K.30. The Ora Banda prospect occurs at the base of the differentiated Ora Banda Sill (Westex Resources Pty Limited, 1999).

*Appendix Table K.30 The six main lithological units of the Ora Banda Sill. Data from Westex Resources Pty Limited (1999).*

Zone	Thickness (m)	Major lithologies
6 (top)	50–100	Pegmatoidal gabbro, granophyre
5	540	Pigeonite-bearing gabbro-norite cumulate
4	315	Bronzite-bearing gabbro-norite cumulate, some mm-scale layering, local lenses of anorthosite
3	90	Norite; massive equigranular plagioclase orthopyroxene adcumulate, grain size 1–2 mm
2	165	Massive equigranular bronzite adcumulate, grain size 1–2 mm
1 (base)	830	Olivine-bronzite peridotite orthocumulate

Peridotites and pyroxenites are generally weathered to 40 m–60 m depth and laterite develops extensively over pyroxenite. Norite is less susceptible to weathering and crops out.

### **PGE mineralisation**

At the Ora Banda Sill prospect, fresh pyroxenite has a broad zone of sulphide, PGEs, and associated Cu (chalcopyrite) enrichment with mean concentrations of 130 ppb Pt (maximum 300 ppb), 80 ppb Pd (215 ppb), and 215 ppm Cu (3940 ppm), with a possible antithetic relationship between PGE and Cu contents suggesting successive cycles of PGE-enriched sulphides. The base of the pyroxenite appears to correspond to the onset of sulphide saturation and the appearance of cumulus sulphides. Peridotite has mean concentrations of 40 ppb Pt (maximum 235 ppb), 55 ppb Pd (429 ppb), and 30 ppm Cu (180 ppm).

## Western Australia

A PGE-enriched zone at the Ora Banda Sill prospect was intersected in RAB holes in saprolite, close to the top of peridotite. See Appendix Table K.31 below.

*Appendix Table K.31 PGE-enriched intersections at the Ora Banda Sill prospect.*

Drill-hole	Depth(m)	Lithology	Pt (ppb)	Pd (ppb)	Pt/Pt+Pd (%)	Ru (ppb)	Rh (ppb)	Os (ppb)	Ir (ppb)
OB 19	0–4	Peridotite	260	475	35	21	11	2	4
OB 20	17–18	Peridotite	820	440	65	34	49	2	10
OB 21	26–27	Peridotite	1800	1200	60	52	114	6	20
DDH 1	106.2–106.5	Pyroxenite	420	360	54	8	15	6	4
DDH 1	106.5–106.7	Peridotite	170	118	59	6	11	4	2

*Detection limits: 2 ppb Pt, 2 ppb Pd, 2 ppb Ru, 1 ppb Rh, 2 ppb Os, and 2 ppb Ir.*

High concentrations of PGEs at Ora Banda occur particularly in lateritic cover over pyroxenite (e.g., 120 ppb–440 ppb Pt, 60 ppb–190 ppb Pd), which are up to 2 to 3 times the PGE content in fresh rock (Butt and Robertson, 2005). See Appendix Table K.32 below.

*Appendix Table K.32 High PGE concentrations recorded at Ora Banda. Data from Butt and Robertson (2005).*

Depth (m)	Lithology	Pt (ppb)	Pd (ppb)	Pt/Pt+Pd (%)	Ru (ppb)	Rh (ppb)	Os (ppb)	Ir (ppb)
1	Calcareous laterite	285	80	78	6	14	2	2
3	Laterite	440	124	78	8	26	4	4
5	Mottled clay	310	82	79	8	16	4	4
9	Mottled clay	170	52	77	8	17	4	6
14	Saprolite	145	64	69	4	7	2	2
20	Saprolite	215	82	72	4	10	2	2
25	Saprolite	300	98	75	4	10	<2	2
30	Saprolite	145	84	63	6	9	4	2
35	Saprolite	116	70	62	4	8	2	2
40	Saprolite	150	90	62	4	10	2	2

*Detection limits: 2 ppb Pt, 2 ppb Pd, 2 ppb Ru, 1 ppb Rh, 2 ppb Os, and 2 ppb Ir.*

At the Mount Carnage prospect the PGE concentrations are higher, mostly 1000 ppb–1950 ppb Pt+Pd over thicknesses of 2 m to 8 m representing an enrichment of 4 to 7 times (wt/wt). A press report dated 1993 reported a non-JORC compliant resource of 10 Mt at about 1 g/t PGEs for the Mount Carnage deposit. A report by Capricorn Resources Australia NL stated that a lateritic resource of 5.0 Mt to 12.0 Mt was determined in the Mount Carnage area. Laterite developed over the pyroxenite layer of the Ora Banda Sill contains up to 1 ppm Pt, whereas the underlying pyroxenite contains 100 ppb–250 ppb Pt.

### **Age of mineralisation**

Archean for hard-rock basement and Cenozoic for lateritic deposits.

### ***Current status***

Exploration site.

### ***Economic significance***

Occurrence.

### ***Major references(s)***

- Butt, C.R.M. and Robertson, I.D.M., 2005. Ora Banda Sill platinum prospect. In: Butt, C.R.M., Robertson, I.D.M., Scott, K.M. and Cornelius, M. (editors), *Regolith Expression of Australian Ore Systems: A Compilation of Exploration Case Histories with Conceptual Dispersion, Process and Exploration Models*. Perth, CRC Leme, 2005, 218–220.
- Capricorn Resources Australia NL, 1991. Mt Carnage platinum prospect Ora Banda region, Western Australia. Capricorn Resources Australia NL 1991 Annual Report, 42 pp.
- Westex Resources Proprietary Limited, 1999. Ora Banda Prospect. P24/3563 - P24/3564 Broad Arrow Mineral Field, Western Australia. Westex Resources Proprietary Limited Annual Report for the period 18/7/ 97 to 17/7/98, 15 pp.

### ***Relevant figure(s)***

## **K.1.153 Otter–Juan Kambalda\***

(other deposits of this type include Perseverance\*, Emily Ann\*, Wannaway\*, Harmony\*, Rocky's Reward\* (all Yilgarn Craton, WA))

### ***Geological province***

Yilgarn Craton.

### ***Location***

Otter–Juan: 121.651802°E, -31.166599°S; Widgiemooltha (SH 51–14), Lake Lefroy (3235); ~4.3 km north-northwest of Kambalda.

Emily Ann: 120.492080°E, -32.202863°S; Lake Johnston (SI 51–01), Roundtop (2933); ~122 km west of Norseman.

Rocky's Reward\*: 120.697197°E, -27.791439°S; Sir Samuel (SG 51–13), Sir Samuel (3042); ~14 km north of Leinster.

Wannaway: 121.521103°E, -31.606319°S; Widgiemooltha (SH 51–14), Cowan (3234); ~48 km south-southwest of Kambalda.

### ***Classification***

- 8. Hydrothermal-Metamorphic; 8.B. Remobilised Ni-Cu-PGE±Au sulphides in komatiitic and metasedimentary rocks.

### ***Geological setting***

The Kambalda Ni-Cu-PGE-sulphide deposits occur in the southern part of the Kalgoorlie Terrane forming the western fault-bounded tectonostratigraphic unit of the Eastern Goldfields Superterrane of the Yilgarn Craton (Wyche et al., 2012). These deposits are located within a 30 km-long by 10 km-wide corridor between the Kambalda Dome and the Tramways Dome near the southern part of the Norseman–Wiluna greenstone belt of the Yilgarn Craton. Nickel sulphide mineralisation is primarily

hosted within the volcanic sequences exposed along the flanks of granitic intrusions that post-date the sulphide mineralisation and form the core of a doubly plunging anticline known as the Kambalda Dome (Gresham and Loftus-Hills, 1981; Cassidy et al., 2006). The Ni sulphide mineralisation is mostly localised at the contact between the Lunnon Basalt and Silver Lake Member of the Kambalda Komatiite Formation (Fiorentini, 2010). The Ni-Cu-PGE deposits form elongate sulphide bodies contained in thick sequences of metamorphosed komatiitic flows, tholeiitic basalts, and carbonaceous and pyritic sediments (Hoatson and Glaser, 1989). Following magmatic emplacement, the mineralised sequence has been multiply deformed, metamorphosed to lower amphibolite facies, and intruded by felsic dykes (Stone et al., 2005; Hoatson et al., 2006).

The Juan–Otter Mine on the northern boundary of the Kambalda Dome has over 60 ore shoots that generally trend northwest-southeast for about 4 km. As is typical of many Kambalda Dome deposits, the shoots lie directly on the Lunnon Basalt. The main ore shoot is called Edwards.

### **PGE mineralisation**

Ni-Cu ores (2.96% Ni, 0.22% Cu) have PGE concentrations of approximately 325 ppb Pt, 425 ppb Pd, 110 ppb Os, 60 ppb Ir, 50 ppb Rh, and 220 ppb Ru. The major PGMs are sperrylite, moncheite, sudburyite, stibiopalladinite, and palladoarsenide. The Ni-Cu matte (73% Ni, 5.5% Cu) produced in treating the ore contains about 4.2 ppm Pt, 10.9 ppm Pd, 1.2 ppm Rh, and 4.1 ppm Ru (Hudson and Donaldson, 1984). A summary of variation in the average composition of Kambalda Ni deposits (100% sulphides) from Cowden and Roberts (1990) is provided in Appendix Table K.33 below.

*Appendix Table K.33 Summary of variation in the average composition of Kambalda Ni deposits (100% sulphides). Data from Cowden and Roberts (1990).*

Element	Values (%)	Element	Values (ppb)
Fe	38–54	Pt	500–1500
Ni	8–22	Pd	1100–3000
S	35–39	Os	250–1000
Cu	0.6–1.3	Ir	120–500
Co	0.2–0.3	Rh	200–700
Cr	0.18–0.4	Ru	400–2000
Zn	0.02–0.04	Au	100–400
Pb	15–25 ppm	Ag	2–4 ppm

Ross and Keays (1979) and Keays et al. (1981) studied the distribution of PGEs and other metals in the different types of sulphide ores and host rocks at Kambalda. Their research showed that:

- palladium was enriched in pentlandite relative to other sulphide phases, whereas Ir occurred in pentlandite, pyrrhotite, pyrite, and chalcopyrite, and Au was enriched in pyrite and chalcopyrite; and
- discrete PGMs were rare in the massive and matrix ores, and the remobilised chalcopyrite-rich footwall stringers were enriched in Pd and Au, owing to the remobilisation of these elements from the massive ores.

Hudson's (1986) study of the PGMs in the Kambalda ores showed that sperrylite was the most abundant PGM in the massive ores, whereas sudburyite, moncheite, merenskyite, michenerite, testibiopalladite, and palladian melonite occur predominantly within veins in the massive and matrix

ores, within stringers of sulphide in the footwall rocks, or in association with post-ore hydrothermal veins and porphyries. These discrete Pd phases appear to have formed as the result of post-magmatic processes, in particular, metamorphic segregation of sulphides and the interaction of Pd-bearing ore sulphides (pentlandite) with younger hydrothermal veins.

### ***Age of mineralisation***

Age of komatiitic host rock is Archean (~2705 Ma) from the direct dating of komatiitic rocks and associated rocks in the Kambalda region (Nelson, 1997; Kositcin et al., 2008). Most Ni-sulphide deposits in the Norseman–Wiluna greenstone belt fall within a very narrow age span centred at 2705 Ma. Therefore the maximum age constraint for the event(s) forming the remobilised Ni-Cu-PGE±Au-bearing sulphides in these komatiitic rocks is 2705 Ma. Since remobilised ores can form through many different processes, e.g., late magmatic-metasomatic-metamorphic-deformational-hydrothermal-regolith, and knowing that the Kambalda ores have undergone a complex history of polyphase deformation and metamorphism (Cowden et al., 1986), it is unlikely that any determined ages could be confidently assigned to a particular post-placement event.

### ***Current status***

Current and historical mines in the Kambalda Dome include Juan, Durkin, Otter, Fisher, Gibb, Long-Victor, McLeay, Lunnon, and Hunt.

### ***Economic significance***

Major economic significance.

### ***Major references(s)***

- Cassidy, K.F., Champion, D.C., Krapez, B., Barley, M.E., Brown, S.J.A., Blewett, R.S., Groenewald, P.B. and Tyler, I.M., 2006. A revised geological framework for the Yilgarn Craton, Western Australia. Geological Survey of Western Australia, Record 2006/8, 8 pp.
- Cowden, A., Donaldson, M.J., Naldrett, A.J. and Campbell, I.H., 1986. Platinum-group elements and gold in the komatiite-hosted Fe-Ni-Cu sulfide deposits at Kambalda, Western Australia. *Economic Geology*, 81, 1226–1235.
- Cowden, A. and Roberts, D.E., 1990. Komatiite hosted nickel sulphide deposits, Kambalda. In: Hughes, F.E. (editor), *Geology of the Mineral Deposits of Australia and Papua New Guinea*. Australasian Institute of Mining and Metallurgy, Melbourne, Monograph 14, 567–581.
- Fiorntini, M.L., 2010. Chapter 4–The Kambalda Nickel Camp. In: McCuaig, T.C., Miller, J. and Beresford, S. (compilers), *Controls on Giant Minerals Systems in the Yilgarn Craton—A Field Guide*. Geological Survey of Western Australia, Record 2010/26, 164 pp.
- Gresham, J.J. and Loftus-Hills, G.D., 1981. The geology of the Kambalda nickel field. *Economic Geology*, 76, 1373–1416.
- Hoatson, D.M. and Glaser, L.M., 1989. Geology and economics of platinum-group metals in Australia. Bureau of Mineral Resources, Australia, Resource Report 5, 81 pp.
- Hoatson, D.M., Jaireth, S. and Jaques, A.L., 2006. Nickel sulfide deposits in Australia: Characteristics, resources, and potential. *Ore Geology Reviews*, 29, 177–241.
- Hudson, D.R. and Donaldson, M.J., 1984. Mineralogy of platinum group elements in the Kambalda nickel deposits, Western Australia. In: Buchanan, D.L. and Jones, M.J. (editors), *Sulphide Deposits in Mafic and Ultramafic Rocks*. The Institution of Mining and Metallurgy, London, 55–61.
- Hudson, D.R., 1986. Platinum-group minerals from the Kambalda nickel deposits, Western Australia. *Economic Geology*, 81, 1218–1225.
- Keays, R.R., Ross, J.R. and Woolrich, P., 1981. Precious metals in volcanic peridotite-associated nickel sulfide deposits in Western Australia. II: Distribution within the ores and host rocks at Kambalda. *Economic Geology*, 76, 1645–1674.

## Western Australia

- Kositcin, N., Brown, S.J.A., Barley, M.E., Krapez, B., Cassidy, K.F. and Champion, D.C., 2008. SHRIMP U–Pb zircon age constraints on the Late Archaean Tectonostratigraphic architecture of the Eastern Goldfields Superterrane, Yilgarn Craton, Western Australia: *Precambrian Research*, 161, 5–33.
- Nelson, D.R., 1997. Evolution of the Archaean granite–greenstone terranes of the Eastern Goldfields, Western Australia: SHRIMP U–Pb zircon constraints. *Precambrian Research*, 83, 57–81.
- Ross, J.R. and Keays, R.R., 1979. Precious metals in volcanic-type nickel sulphide deposits in Western Australia. I: Relationship with the composition of the ores and their host rocks. *Canadian Mineralogist*, 17, 417–435.
- Stone, W.E., Beresford, S.W., Archibald, N.J., 2005. Structural Setting and Shape Analysis of Nickel Sulphide Shoots at the Kambalda Dome, Western Australia: Implications for Deformation and Remobilization. *Economic Geology*, 100, 1441–1455.
- Wyche, S., Fiorentini, M.L., Miller, J.L. and McCuaig, T.C., 2012. Geology and controls on mineralisation in the Eastern Goldfields region, Yilgarn Craton, Western Australia. *Episodes*, 35, 273–281.

### ***Relevant figure(s)***

Figure 6.21, Figure 6.22, Figure 6.45, and Figure 8.24.

## **K.1.154 Palamino–Wills Creek**

(see Copernicus group)

## **K.1.155 Panton, Panton North (1, 2, 3), Panton Environmental Group**

### ***Geological province***

Halls Creek Orogen.

### ***Location***

Panton: 127.831596°E, -17.751530°S; Dixon Range (SE 52–06), McIntosh (4462); ~56 km north-northeast of Halls Creek.

Panton North 3: 127.853520°E, -17.718770°S; Dixon Range (SE 52–06), McIntosh (4462); ~4.4 km north-northeast of the Panton deposit.

### ***Classification***

- 1. Layered tholeiitic mafic-ultramafic intrusions; 1B. Stratabound PGE-bearing chromitite layers.

### ***Geological setting***

The Panton Intrusion is a 10 km by 2.5 km elliptical ultramafic-mafic body that intruded quartz-albite-muscovite schist of the Tickalara Metamorphics in the Central Zone of the Halls Creek Orogen. The intrusion forms a southerly plunging synclinal structure. The igneous sequence consists of a lower 650 m-thick Ultramafic Series (UMS) and an upper 900 m-thick Gabbroic Series (GS). The UMS is made up of a marginal harzburgite facies, overlain by a sequence of medium-grained orthocumulate to mesocumulate dunite containing several PGE-bearing chromitite layers with minor harzburgite and lherzolite near the top of the series. The GS is made up of medium-grained adcumulate to mesocumulate, melanocratic to leucocratic gabbro, gabbro and norite as well as anorthosite and minor dunite and chromitite. Total stratigraphic thickness is in the order of 1550 m (Blake et al., 2000).

Based on the compositions of 'chilled' margins, spinel compositions, and the most primitive olivine compositions in the intrusion (olivine mg number of 85), the estimated mg number of the parent magma to the Panton Intrusion was estimated to be 63, had an estimated MgO content close to 9%, and was of tholeiitic affinity (Sun and Hoatson, 2000).

### ***PGE mineralisation***

Chromitite layers occur at three major stratigraphic levels in the intrusion: (1) Lower Chromitite Group in the basal part of the Ultramafic Series—thin (<10 cm) discontinuous layers in harzburgite and dunite, (2) Middle Chromitite Group about 120 m–150 m below the contact of the Ultramafic and Gabbroic Series—economically important package of PGE-enriched layers in dunite, which includes the Main Chromitite Layer (MCL; also called A chromitite layer by Perring and Vogt (1991)), 0.1 m–2.4 m-thick over a strike length of 12 km, and (3) Upper Chromitite Group in the Middle Mafic Zone of the Gabbroic Series—intensely fractured, locally thickened (up to 0.3 m) layers in a stacked sequence of arcuate dunite lenses that traverse the synclinal axis of the intrusion; in addition thin (millimetre to centimetre) chromitite layers, stringers, and lenses occur throughout the intrusion, particularly in the upper half of the Ultramafic Series.

The focus of the project feasibility studies by Platinum Australia Pty Limited, has been the 'Top Reef' (part of the MLC), which is situated ~150 m below the mafic-ultramafic interface, and the parallel Middle Reef, which is ~15 m below the Top Reef. The average true thickness of the Top Reef is over 1 m, and the average grade is 6.1 g/t PGEs+Au. The Middle Reef averages 0.5 m true thickness and has an average grade of 3.4 g/t PGEs+Au (<http://www.platinumaus.com.au/viewStory/Panton>).

There are at least four PGE-bearing layers located near the middle of the Gabbroic Series (the Upper Chromite Group) that are associated with narrow dunite layers within a sequence of interlayered anorthosite and leucogabbro. These chromitites are generally less than 10 cm-thick and assay up to 1 ppm Pt+Pd.

The published resource for the 'Top' and 'Middle' Reefs amounted to 14.3 Mt at 5.2 g/t 7E PGEs (Pt+Pd+Rh+Ru+Ir+Os+Au) (Platinum Australia Limited, 2005)

### ***Age of mineralisation***

The PGE-chromite mineralisation in the Panton Intrusion is comagmatic with the intrusion, which has a U-Pb zircon age of  $1856 \pm 2$  Ma determined from mottled anorthosite in the Upper Mafic Zone of the intrusion (Page and Hoatson, 1997, 2000; Page et al., 1995).

### ***Current status***

Feasibility study completed.

### ***Economic significance***

Significant PGE deposit in Australia which contains a resource of PGEs (~65.6 t of contained PGE metal) associated with chromitites. Considered by many exploration companies at various times during the past 5 decades as having the highest potential to be Australia's first major economic hard-rock PGE deposit.

### ***Major references(s)***

Blake, D.H., Tyler, I.M. and Page, R.W., 2000. Regional geology of the Halls Creek Orogen. In: Hoatson, D.M. and Blake, D.H. (editors), *Geology and economic potential of the Palaeoproterozoic layered mafic-ultramafic intrusions in the East Kimberley, Western Australia*. Canberra: Australian Geological Survey Organisation Bulletin 246, 35–62.

- Page, R.W. and Hoatson, D.M., 2000. Geochronology of the mafic-ultramafic intrusions. In: Hoatson, D.M. and Blake, D.H. (editors), *Geology and economic potential of the Palaeoproterozoic layered mafic-ultramafic intrusions in the East Kimberley, Western Australia*. Canberra: Australian Geological Survey Organisation Bulletin 246, 163–172.
- Perring, R.J. and Vogt, J.H., 1991. The Panton Sill. In: Barnes, S.J. and Hill, R.E.T. (editors), *Mafic-Ultramafic Complexes of Western Australia. Excursion Guidebook 3. Sixth International Platinum Symposium, July 1991, Perth, Western Australia*. IAGOD and the Geological Society of Australia, 97–106.
- Platinum Australia Limited, 2005. Platinum Australia Limited announcement to the Australian Securities Exchange, 7 December 2005, 2 pp.
- Sun, S.-S. and Hoatson, D.M., 2000. Trace-element geochemical and Nd isotopic study of the mafic-ultramafic intrusions: implications for their petrogenesis and tectonic environment. In: Hoatson, D.M. and Blake, D.H. (editors), *Geology and economic potential of the Palaeoproterozoic layered mafic-ultramafic intrusions in the East Kimberley, Western Australia*. Canberra: Australian Geological Survey Organisation Bulletin 246, 226–249.

### **Relevant figure(s)**

Figure 6.9, Figure 6.10, Figure 6.11, Figure 6.12, Figure 6.13, Figure 8.20, Figure 8.21, Figure 8.22, and Figure 8.23.

## **K.1.156 Peninsula HA2\***

(see Airstrip Cr Pt group)

## **K.1.157 Perseverance\***

### **Geological province**

Yilgarn Craton.

### **Location**

Perseverance: 120.705597°E, -27.818119°S; Sir Samuel (SG 51–13), Sir Samuel (3042); ~11.5 km north of Leinster.

### **Classification**

- 3. Komatiitic flows and related sill-like intrusions; 3.B. Disseminated Ni-Cu-PGE sulphides in central parts of thick dunite bodies.
- 8. Hydrothermal-Metamorphic; ?8.B. Remobilised Ni-Cu-PGE±Au in komatiitic and metasedimentary rocks.

### **Geological setting**

The most important Type 3.B Ni-sulphide deposits (Mount Keith, Perseverance, Yakabindie, Honeymoon Well, Wedgetail Prospect) occur in the northern part of the Norseman–Wiluna greenstone belt, where they are often spatially associated with Type 3.A deposits.

### **PGE mineralisation**

Barnes et al. (1988b; 1995) have documented the PGE geochemistry of the major ore types for the Perseverance and Rocky's Reward Ni deposits (~65 km southeast of Mount Keith), which have similar geological settings to the Mount Keith deposit. The Perseverance deposit consists of a central

dunite lens, ~700 m-thick by ~3 km-wide, flanked by olivine orthocumulate and spinifex-textured komatiite. For massive, matrix, and vein-filling sulphide ores, maximum concentrations (recalculated to 100 weight % sulphides, and all units in ppb) are: 410, 210, 360 Pt; 830, 300, 1200 Pd; 260, 50, 32 Os; 210, 36, 28 Ir; 150, 20, 49 Rh; 590, 92, 110 Ru; and 110, 27, 23 Au, respectively. The chalcophile element (Ni, Ir, Ru, Pt, Pd, Au, and Cu) concentrations in spinifex-textured flows flanking the central dunite (A-zone samples) are typical of komatiites. Komatiites from the Perseverance mineralised units and from Rocky's Reward show evidence of depletion of the more strongly chalcophile PGEs relative to Ni and Cu. This feature is also evident in massive and matrix sulphide ore samples, although less evident in the main Perseverance cloud sulphides. The major element, PGE, and REE chemical data are consistent with derivation by combined assimilation of felsic material and crystallisation of olivine from a primitive komatiitic magma. The geochemical features of mineralised and unmineralised basal komatiite units indicate the effects of crustal assimilation. This is consistent with genetic models for Ni-sulphide deposits, based largely on Kambalda, which emphasise the role of thermal erosion of sulphidic footwall sediments.

It is unclear whether deformation has played any significant role in concentrating or upgrading sulphides, or in localising medium-grade matrix ores, such as at Perseverance, which form the bulk of the economic resource. According to Barnes (2006), there is no compelling evidence that deformation upgraded medium-grade ores, and the PGE chemistry of massive, matrix, and disseminated ores suggest that tectonic upgrading is not an important process, even in areas of severe deformation, such as Perseverance where it might be most likely.

Remobilised sulphide ores have been documented at the Wedgetail prospect at Honeymoon Well, Waterloo–Amorac, Emily Ann, Wannaway, and some of the komatiite-hosted deposits in the Kambalda Dome. In most cases, the sulphides have moved less than 100 m, although in the case of Emily Ann, over 600 m of displacement has been documented.

### ***Age of mineralisation***

Unknown.

### ***Current status***

Care and maintenance.

### ***Economic significance***

A major Ni mine.

### ***Major references(s)***

Barnes, S.J., Gole, M.J. and Hill, R.E.T., 1988. The Agnew nickel deposit, Western Australia: Part II. Sulfide geochemistry, with emphasis on the platinum-group elements. *Economic Geology*, 83, 537–550.

Barnes, S.J., Leshner, C.M. and Keays, R.R., 1995. Geochemistry of mineralised and barren komatiites from the Perseverance nickel deposit, Western Australia. *Lithos*, 34, 209–234.

### ***Relevant figure(s)***

Figure 6.21, Figure 6.23, and Figure 6.24.

## **K.1.158 Phenoclast Hill (Quadrio Lake), Oldham Range\***

### ***Geological province***

Collier Basin.

### ***Location***

Phenoclast Hill: 122.680603°E, -24.630911°S; Trainor (SG 51–02), Nicholls (3448); ~325 km south of Telfer.

### ***Classification***

- 12. Others (minor or unknown economic importance); 12.E. Others (unknown geological setting).

### ***Geological setting***

Two polymetallic prospects, Phenoclast Hill, previously known as Quadrio Lake, and Oldham Range occur within Proterozoic sediments in the Oldham Inlier at the northeast perimeter of the Officer Basin. Both prospects are associated with circular gravity anomalies, which have attracted exploration activity. The Oldham Inlier comprises the Proterozoic Oldham and Cornelia Sandstones, Quadrio Formation, Skates Hill Formation, and northwest-trending dolerite sills and pillow basalts.

### ***PGE mineralisation***

Phenoclast Hill prospect—veins of hematite-barite have been mapped within silicified shale and sandstone in outcropping Quadrio Formation just south of Quadrio Lake. Geochemical sampling at the Phenoclast Hill prospect has defined a widespread zone of Zn and Pb geochemical anomalism. The lag defined anomaly has a maximum Pb value of 237 ppm and maximum Zn value of 498 ppm and appears to be coincident with the interpreted Skates Hill Formation and Quadrio Formation unconformity where it outcrops and trends under sand and alluvial cover. Rock-chip sampling had previously returned Zn values of 1098 ppm and 1413 ppm in the area. A northwest-trending soil anomaly along the northern perimeter of the Phenoclast Hill gravity anomaly was also shown in Genesis Mining Limited Prospectus (p. 29) as having anomalous Pt and Pd values although no assay figures were published (Genesis Minerals Limited, 2007).

Oldham Range prospect—sampling at the Oldham Range Prospect defined three coincident Cu-Ni-PGE-cobalt anomalies which strike northwest. These anomalies are associated with mafic intrusions which strike west to northwest through the prospect area. The strongest of these anomalies has peak values of 740 ppm Cu and 452 ppm Ni (Anomaly B), is up to 1600 m-long, and is associated with an embayment in a mafic intrusion. The southern anomaly (Anomaly C) strikes northwest for over 3000 m and has maximum values of 634 ppm Cu and 266 ppm Ni. Significantly this anomaly is associated with a small gossan which has previously returned values of 899 ppm Cu and 947 ppm Ni. No PGE values have been published (Genesis Minerals Limited, 2008).

### ***Age of mineralisation***

Unknown.

### ***Current status***

Exploration site.

### ***Economic significance***

Occurrence.

### ***Major references(s)***

Genesis Minerals Limited, 2007. Genesis Minerals Limited 2007 Prospectus, 88 pp.

Genesis Minerals Limited, 2008. June quarterly report 2008, 12 pp.

### ***Relevant figure(s)***

## **K.1.159 Phil North and South**

### ***Geological province***

Yilgarn Craton.

### ***Location***

Phil North and South: 119.092707°E, -29.459506°S; Barlee (SH 50–08), Barlee (2739); ~200 km north of Southern Cross.

### ***Classification***

- Published company reports refer to structurally controlled mesothermal Au mineralisation (Beacon Minerals Limited, 2007a).
- 8. Hydrothermal-Metamorphic; ?8.B. Remobilised Ni-Cu-PGE±Au in komatiitic and metasedimentary rocks.

### ***Geological setting***

The Au-PGE-Ni prospects are located in the northern part of the Archean Southern Cross greenstone belt. All greenstones have been metamorphosed, with grades varying from lower greenschist to amphibolite. Past and current exploration activities have been mainly for Au, which shows a strong association with shearing in the area, often at sheared contacts between ultramafic units and either basalt or high-Mg basalt (Beacon Minerals Limited, 2007a; Hilko and Ridley, 1995).

### ***PGE mineralisation***

The area contains a number of small Au deposits with an initial JORC compliant inferred Au resource announced in December 2009 for the Phil North and South deposit totalling 85 000 t at 3.7 g/t Au for 10 000 ounces Au (Beacon Minerals Limited, 2009, 2011). According to the MINEDEX database, PGEs are associated with the Au mineralisation at the Phil North and South deposits, however, analyses for PGEs do not appear to have been published. A number of exploration holes at the Halleys prospects, about 1.6 km to the south, returned elevated PGEs of up to 0.21 g/t PGEs (see Halleys East–Barlee prospects: Beacon Minerals Limited, 2007b,c).

### ***Age of mineralisation***

Archean host rocks.

### ***Current status***

Undeveloped small Au deposit.

### ***Economic significance***

Small Au deposit.

### ***Major references(s)***

- Beacon Minerals Limited, 2007a. Beacon Minerals Limited 2007 Prospectus, 100 pp.
- Beacon Minerals Limited, 2007b. Beacon Minerals Limited announcement to the Australian Securities Exchange, 20 March 2007, 6 pp.
- Beacon Minerals Limited, 2007c. Quarterly report to the Australian Securities Exchange, March 2007, 19 pp.
- Beacon Minerals Limited, 2009. Initial JORC resource for Barlee gold project. Beacon Minerals Limited announcement to the Australian Securities Exchange, 11 December 2009, 6 pp.
- Beacon Minerals Limited, 2011. Barlee gold project, Western Australia. Gold Coast Resources Showcase, June 2011, 14 pp.
- Beacon Minerals Limited, 2014. December 2013 Quarterly activities and cash flow report, 11 pp.
- Hilko, J.D. and Ridley, J.R., 1995. Structural and metamorphic controls on gold mineralisation in the Southern Cross and Marda Diemals Greenstone Belts, Yilgarn Block, Western Australia. Key Centre for Strategic Mineral Deposits, UWA.

### ***Relevant figure(s)***

## **K.1.160 Pindar SE 1, Pindar SE 2**

### ***Geological province***

Yilgarn Craton.

### ***Location***

Pindar SE 1: 117.680500°E, -27.247110°S; Cue (SG 50–15), Cue (2443); ~28 km northwest of Cue.

Pindar SE 2: 117.681250°E, -27.253430°S; Cue (SG 50–15), Cue (2443); ~27.5 km northwest of Cue.

### ***Classification***

- ?8. Hydrothermal-Metamorphic.

### ***Geological setting***

Granite underlies the anomalous PGE-bearing zone in CD5, and also occurs in holes 100 m to the east and west. From this it was inferred that the PGE-bearing zone in CD5 (Pindar SE 1) lies in a raft or xenolith of ultramafic rock in granite. The anomalous PGE values in CD11 (Pindar CD11) appear to occur outside the granite (MIM Exploration Pty Limited, 1993).

### ***PGE mineralisation***

PGE mineralisation in rotary air blast drill-hole intersections in a xenolith or raft of metakomatiite (tremolite-rich ultramafic schist) within granite as follows:

- RAB hole CD5: 6 m (18 m–24 m) @ 0.2 g/t Pt and 0.07 g/t Pd; and 1 m (28 m–29 m) @ 0.15 g/t Pt and 0.06 g/t Pd.
- RAB hole CD11: 8 m (35 m–43 m) @ 0.18 g/t Pt and 0.03 g/t Pd; and 6 m (50 m–56 m) @ 0.28 g/t Pt and 0.02 g/t Pd.

Additional PGE analyses revealed up to 18 ppb Rh, 11 ppb Ru, 5 ppb Ir, and <2 ppb Os.

### ***Age of mineralisation***

Mineralisation in Archean host rocks?

### ***Current status***

Exploration site.

### ***Economic significance***

Occurrence.

### ***Major references(s)***

M.I.M. Exploration Proprietary Limited, 1993. Technical report. Coodardy Exploration Licence 20/153 Annual Report for the year ending July 15, 1993. GSWA WAMEX report A39181, 76 pp.

### ***Relevant figure(s)***

## **K.1.161 Pioneer JH, Spinifex Prospect\***

### ***Geological province***

Yilgarn Craton.

### ***Location***

Pioneer JH: 121.643130°E, -31.974787°S; Widgiemooltha (SH 51–14), Cowan (3234); ~28 km north-northwest of Norseman.

### ***Classification***

- 3. Komatiitic flows and related sill-like intrusions; 3.A. Massive, matrix, and disseminated Ni-Cu-PGE sulphides in preferred lava pathways.

### ***Geological setting***

The Pioneer JH and another small Ni-Cu deposit, the Pioneer BB, are located on the eastern flank of the Pioneer Dome, which consists of a core of granite surrounded by a sequence of extrusive mafic and ultramafic units separated by sediments. The Ni mineralisation is associated with a series of discontinuous to lenticular ultramafic flows, collectively referred to as the western komatiites. The Pioneer JH and Pioneer BB Ni deposits occur in the basal unit of the western komatiite sequence (Pioneer Nickel Limited, 2003).

### ***PGE mineralisation***

The Pioneer JH and Pioneer BB prospects comprise small lenses of Ni-Cu mineralisation in the form of veins and stringers of marcasite after pyrrhotite and violarite after pentlandite. Associated finely disseminated sulphide is less altered and consists of pyrrhotite, pentlandite, and chalcopyrite. Some 32 500 t at 1.1% Ni and 0.1% Cu are reported for the JH Deposit (non-JORC) (Pioneer Nickel Limited, 2003). Drilling returned 3 m @ 4.0% Ni, 0.21% Cu, and up to 1 m @ 3.96 g/t Pt+Pd, associated with the Ni sulphides (Pioneer Nickel Limited, 2005). Soil sampling along the western margin of the Pioneer Dome outlined a coincident Ni-Cu and Pd-Pt anomaly extending over 1.8 km at the Spinifex prospect.

### ***Age of mineralisation***

Archean host rocks.

### ***Current status***

Historical exploration site.

### ***Economic significance***

Occurrence.

### ***Major references(s)***

Pioneer Nickel Limited, 2003. Pioneer Nickel Limited Prospectus. Submitted to the Australian Securities Exchange on 14 November 2003, 72 pp.

Pioneer Nickel Limited, 2005. Exploration update–November 2005. Pioneer Nickel Limited announcement to the Australian Securities Exchange, 25 November 2005, 2 pp.

### ***Relevant figure(s)***

Figure 6.21.

## **K.1.162 PM Prospect (Copper Hills PM)**

(includes the Copper Hills PM and Copper Hills 1 and 2 prospects)

### ***Geological province***

Paterson Orogen.

### ***Location***

PM Prospect: 123.221901°E, -22.923330°S; Tabletop (SF 51–11), Blanche (3552); ~170 km southeast of Telfer.

### ***Classification***

- Bagas and Lubienieckie (2000) described the mineralisation as hosted in graphite-chlorite schist, carbonate rocks, and quartz veins hosted by sheared amphibolite.
- 8. Hydrothermal-Metamorphic.

### ***Geological setting***

The PM Prospect is situated within the Tabletop Terrane, part of the Rudall Complex, in the northwestern part of the Paterson Orogen, a northwesterly trending belt of Paleoproterozoic to Neoproterozoic rocks. The Tabletop Terrane is poorly exposed and forms the eastern portion of the Rudall Complex. The terrane comprises a sequence of mafic schist, amphibolite, and metasedimentary rocks. Widely spaced Cu mineralisation also occurs in the northern part of the northwestern Officer Basin. Mineral occurrences in the region are polymetallic and include Cu associated with various concentrations of Ag, Au, Pb, Zn, Co, Ni, PGEs, and REEs (Bagas and Lubieniecki, 2000).

### ***PGE mineralisation***

The PM Prospect is vein-hosted in dolomitic, carbonaceous and graphitic chlorite schist, on a 2 km-long curvilinear shear zone. The mineralisation occurs in dilational jogs, with surface samples

assaying up to 11% Cu, 3.5% Ag, 0.23% Au, 0.49% Pd, and 0.34% Pt (Bagas and Lubieniecki, 2000: p. 39; Ferguson et al., 2005).

### ***Age of mineralisation***

Mesoproterozoic to Neoproterozoic?

### ***Current status***

Historical exploration site.

### ***Economic significance***

Occurrence.

### ***Major references(s)***

Bagas, L. and Lubieniecki, Z., 2000. Copper and associated polymetallic mineralisation along the Camel–Tabletop Fault Zone in the Paterson Orogen, Western Australia. *Western Australia Geological Survey, Annual Review 1999–2000*, 36–41.

Ferguson, K.M., Bagas, L. and Ruddock, I., 2005. Mineral occurrences and exploration potential of the Paterson area. *Western Australia Geological Survey, Report 97*, 43 pp.

### ***Relevant figure(s)***

## **K.1.163 Point Salvation\***

(see Yamarna PGE 1 and 2)

## **K.1.164 Pokali North, Pokali South, Pokali East, Pokali–Charlies Find Zone**

### ***Geological province***

Arunta Orogen.

### ***Location***

Pokali–Charlies Find Zone: 128.350720°E, -22.944550°S; Webb (SF 52–10), Webb (4552); ~395 km north-northeast of Warburton and ~575 km west of Alice Springs.

Pokali North: 128.326513°E, -22.931827°S; Webb (SF 52–10), Webb (4552); ~395 km north-northeast of Warburton.

Pokali South: 128.346971°E, -22.948116°S; Webb (SF 52–10), Webb (4552); ~395 km north-northeast of Warburton.

### ***Classification***

- The Pokali occurrences are recorded in GSWA MINEDEX database as follows:
  - Cu-Pb-Zn in veins and shears; and
  - Au in shears or faults.
- ?8. Hydrothermal-Metamorphic.

### ***Geological setting***

The Pokali prospects are located in the western part of the Arunta Orogen in Western Australia and contain a complex suite of rock types of Paleoproterozoic to early Mesoproterozoic age. The prospects occur in the vicinity of the Central Australian Suture, a long-lived crustal-scale fault, and its subsidiary structures. Rock types in the area include greenschist facies metamorphic schists variably modified by thermal metamorphism associated with extensive granitoid intrusion including the 1640 ± 5 Ma Mt Webb Granite (Ashburton Minerals Limited, 2009; Wyborn et al., 1998; Budd et al., 2001).

The Pokali prospects are marked by widespread magnetite-silica alteration, outcropping Cu mineralisation in the form of green malachite-bearing rocks, and hematite-quartz breccia veins (Ashburton Minerals Limited, 2009).

### ***PGE mineralisation***

The mineralisation consists of a very strong association between Cu, Au, Ag, Pd, and Bi. Selected analytical results of rock-chip sampling include (Ashburton Minerals Limited, 2008):

- Pokali—Charlies Find Zone (formerly Pokali East):
  - 4.12% Cu, 0.43 g/t Au, 2.81 g/t Ag, 0.78 g/t Pd in sample A0157; and
  - 1.08% Cu, 0.93 g/t Au, 3.97 g/t Ag, 0.18 g/t Pd in sample A0185.
- Pokali North:
  - 7.95% Cu, 0.62 g/t Au, 28.9 g/t Ag, 1.47 g/t Pd in sample A0159.
- Pokali South:
  - 0.05% Cu, 19.08 g/t Au, 9.14 g/t Ag, 1.18 g/t Pd in sample A0149;
  - 13.30% Cu, 0.88 g/t Au, 78.05 g/t Ag, 2.63 g/t Pd in sample A0152;
  - 6.31% Cu, 1.31 g/t Au, 2.91 g/t Ag, 1.10 g/t Pd in sample A0183; and
  - 2.98% Cu, 15.31 g/t Au, 13.30 g/t Ag, 0.61 g/t Pd in sample A0184.
- The Gap (~800 m west-northwest of Pokali North):
  - 2.41% Cu, 0.67 g/t Au, 9.25 g/t Ag, 0.34 g/t Pd in sample A0152.

At the Pokali South prospect the Cu mineralisation (malachite) and alteration comprising silica, magnetite, malachite, and gossan is continuous over 1100 m along strike and reaches 100 m in width. Of the 46 samples collected over this zone, 17 have >0.10% Cu, and average 2.07% Cu, 2.44 g/t Au, 8.20 g/t Ag, and 0.38 g/t Pd.

### ***Age of mineralisation***

Paleoproterozoic or younger.

### ***Current status***

Exploration site.

### ***Economic significance***

Occurrence.

### ***Major references(s)***

Ashburton Minerals Limited, 2008. Ashburton Minerals Limited announcement to the Australian Securities Exchange 17 September 2008, 7 pp.

Ashburton Minerals Limited, 2009. Ashburton Minerals Limited Annual Report 2009, 60 pp.

Budd, A. R., Wyborn, L.A.I. and Bastrakova, I.V., 2001. The metallogenic potential of Australian Proterozoic Granites. *Geoscience Australia Record* 2001/12, 156 pp.

Wyborn, L.A.I., Budd, A.R. and Bastrakova, I.V., 1998. The metallogenic potential of Australian Proterozoic Granites. Seminar, AGSO November 1998, Australian Geological Survey Organisation, 120 pp.

### ***Relevant figure(s)***

#### **K.1.165 Polar Bear\***

(see Halls Knoll Gossan)

#### **K.1.166 Poona North**

##### ***Geological province***

Yilgarn Craton.

##### ***Location***

Poona North: 117.442076°E, -27.087218°S; Cue (SG 50–15), Noondie (2343); ~58 km northwest of Cue.

##### ***Classification***

- ?1. Layered tholeiitic mafic-ultramafic intrusions.

##### ***Geological setting***

Archean serpentinised ultramafic units, ~37 km southwest of Weld Range lateritic Ni-PGE deposit, are defined by gossanous outcrops and aeromagnetic anomalies. Interpreted re-entrant (Kambalda-type) structural settings have been identified in the ultramafic stratigraphy (Hannans Reward NL, 2004).

##### ***PGE mineralisation***

CRA Exploration RC drill-hole WRRC3 tested magnetic anomaly No 3 and intersected Pt and Pd between 76 m and 88 m with the best intersection 0.4 g/t Pt and 0.38 g/t Pd for 2 m from 86 m. Drill-holes intersected overburden up to 46 m. Assay results were supported by anomalous Au values 0.1 g/t from 32 m to 38 m with 0.1%–0.15% Cu. The PGE-host lithology is a serpentinised ultramafic (described as dunite in petrographic description) showing cumulus textures in thin section (Bromley, 1985).

##### ***Age of mineralisation***

Unknown.

##### ***Current status***

Historical exploration site.

##### ***Economic significance***

Occurrence.

### **Major references(s)**

Bromley, G.J., 1985. Final report on E 20/19 Weld Range, Cue, Western Australia. CRA Exploration Pty Limited. WAMEX report A16051, 65 pp.

Hannans Reward NL, 2004. Hannans Reward NL 3<sup>rd</sup> Quarter Activities Report and Cash Flow Statement, 30 April 2004, 14 pp.

### **Relevant figure(s)**

## **K.1.167 Priors**

### **Geological province**

Yilgarn Craton.

### **Location**

Priors: 120.970634°E, -31.039413°S; Boorabbin (SH 51–13), Woolgangie (3035); ~22 km west-southwest of Coolgardie.

### **Classification**

- 3. Komatiitic flows and related sill-like intrusions.

### **Geological setting**

The Priors prospect is located east of the Bullabulling Shear in the Coolgardie Domain which occupies the western portion of the Kalgoorlie Terrane in the Eastern Goldfields Superterrane. The prospect is hosted in metakomatiites within a sequence of greenstones adjoining the southwest flank of the Bali Monzogranite. The greenstone sequence consists of metabasalt and metakomatiite units overlain by metamorphosed felsic volcanic and sedimentary rocks, with layered and differentiated mafic sills at various stratigraphic levels (Roberts, 2004). The Priors prospect is located about 1.6 km northeast of the historical Gibraltar goldmine.

### **PGE mineralisation**

A soil anomaly over a strike length of 500 m was tested with thirteen rotary air-blast holes returning assay values similar to those of the soil anomaly as follows:

- CRN007: 12 m @ 0.74% Ni, 122 ppm Cu, 13 ppb Pt, 11 ppb Pd, 19 ppb Au;
- CRN008: 11 m @ 0.58% Ni, 165 ppm Cu, 15 ppb Pt, 11 ppb Pd, and 211 ppb Au; and
- CRN012: 7 m @ 0.58% Ni, 128 ppm Cu, 10 ppb Pt, 15 ppb Pd, and 9 ppb Au (Sipa Resources Limited, 2004).

### **Age of mineralisation**

Archean host rocks?

### **Current status**

Historical exploration site.

### **Economic significance**

Occurrence.

### **Major references(s)**

- Roberts, F.I., 2004. Mineralization of the Woolgongie–Yilmia area, Eastern Goldfields Granite–Greenstone Terrane, Western Australia: Western Australia Geological Survey, Record 2004/6, 58 pp.
- Sipa Resources Limited, 2004. Quarterly report to the Australian Stock Exchange, 30 July 2004, 19 pp.

### **Relevant figure(s)**

## **K.1.168 Python–Gum Creek**

(see Dugite–Gum Creek group)

## **K.1.169 Radio Hill\***

### **Geological province**

Pilbara Craton.

### **Location**

Radio Hill: 116.869400°E, -20.984421°S; Dampier (SF 50–02), Dampier (2256); ~28 km south of Karratha and ~14 km north of the Munni Munni Intrusion.

### **Classification**

- 2. Massive to poorly layered tholeiitic mafic-dominated intrusions; 2.A. Segregations of Ni-Cu-Co-PGE sulphides in feeder conduits and basal contacts.

### **Geological setting**

The Radio Hill Intrusion is a small mafic-ultramafic body that had the most significant known Ni-Cu-Co sulphide resource in the west Pilbara Craton (Appendix Figure K.20). Covering an area of 3.6 km<sup>2</sup>, this moderately dipping sheet-like body comprises a 330 m-thick basal ultramafic cumulate zone that is overlain by a 440 m-thick sequence of olivine gabbro, which in turn is overlain by a steeply dipping 430 m-thick quartz gabbro sequence. The poorly-exposed ultramafic zone along the northwestern margin of the intrusion is dominated by lherzolite, dunite, olivine websterite, clinopyroxenite, and websterite. The overlying gabbroic zone comprises a homogeneous mafic sequence of olivine gabbro and olivine gabbrobronite, with the highest exposed stratigraphic level of the intrusion comprising quartz-bearing gabbro and gabbrobronite.

Sulphides are largely hosted by thin gabbroic and plagioclase pyroxenite units that persist along the basal contact of the intrusion between the overlying ultramafic cumulates and hornfelsed metavolcanic country rocks. Most mineralisation occurs in structural depressions along the basal contact and in a feeder conduit (Appendix Figure K.20). The confluence of this moderately plunging conduit with the basal contact defines the thickest section of the mineralised host rocks. Massive, disseminated, and stringer vein pyrrhotite-chalcopyrite-pentlandite-magnetite ores form discrete lenses within the structural depressions, and massive chalcopyrite ores enriched in Au, Pd, Pt, Cu, and Ag are prominent in the feeder conduit. Ultramafic and mafic cumulates throughout the intrusion have S contents ranging up to 2000 ppm indicating that the Radio Hill body formed from magmas that were sulphide saturated.

The Radio Hill and nearby Mount Sholl (Appendix Figure K.21) intrusions have very similar geological settings and mineralisation features. The mineralised host rocks are predominantly gabbroic units that form thin marginal envelopes to the overlying ultramafic cumulates, and the massive sulphides are concentrated in structural depressions along the basal intrusive contacts beneath the thickest sequence of overlying mafic-ultramafic cumulates. The localisation of massive sulphides near the entry point of the feeder conduit to the chamber (analogous to Voisey's Bay, Canada) indicates that the dynamics of magma flow, feeder-chamber geometry (e.g., changes from narrow vertical conduits to broad open magma chambers) and physical traps were important for the accumulation of the sulphides (de Angelis, 1987, 1988; Hoatson et al., 1992; Hoatson et al., 2002).

### ***PGE mineralisation***

Intermittent phases of exploration since its discovery in the mid 1980s have defined a global Ni metal resource of ~62 000 t derived from both massive and disseminated sulphide ores. The deposit was also recorded to contain about 68 000 t of Cu and up to 1 million grams of Pd.

### ***Age of mineralisation***

Archean, 2892 ± 34 Ma (Frick et al., 2001).

### ***Current status***

Exploration site.

### ***Economic significance***

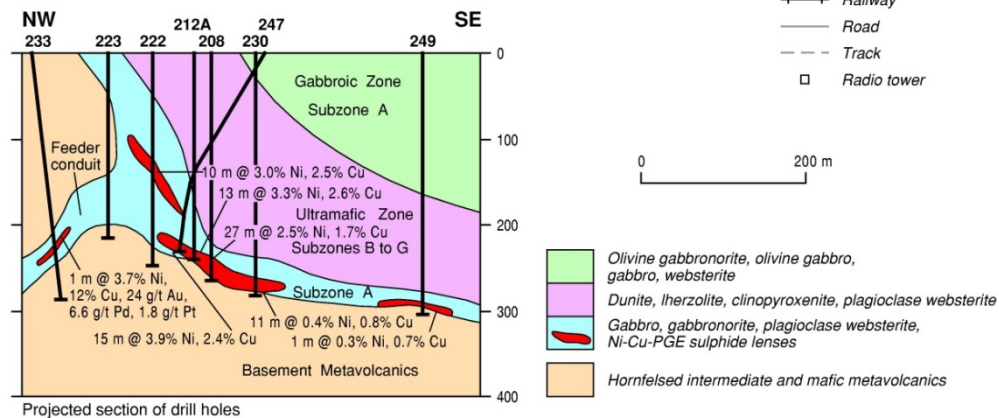
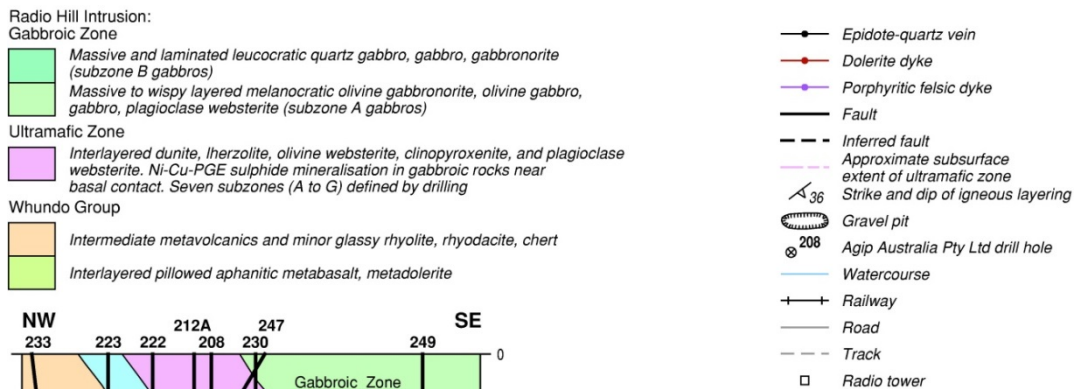
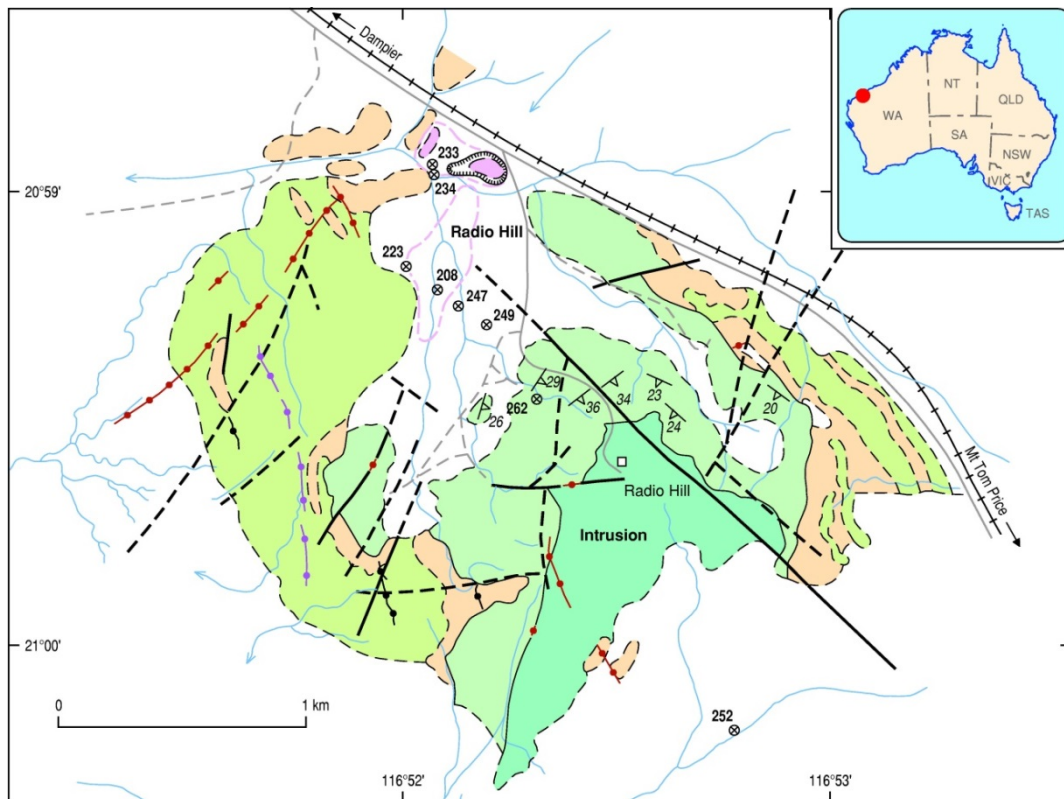
Small deposit.

### ***Major references(s)***

- de Angelis, M., Hoyle, M.W.H., Peters, W.S., Wightman, D., 1987. The nickel–copper deposit at Radio Hill, Karratha, Western Australia: Australasian Institute of Mining and Metallurgy, Bulletin and Proceedings, 292, 61–74.
- de Angelis, M., Hoyle, M. W. H. and Voermans, F.M., 1988. The Radio Hill Ni-Cu deposit and the Mt Sholl–Munni Munni mafic-ultramafic metallogenic province: A case of integrated exploration technique. In: The Second International Conference On Prospecting In Arid Terrain, April 1988, Perth, Western Australia. The Australasian Institute of Mining and Metallurgy, 51–58.
- Frick, L.R., Lambert, D.D. and Hoatson, D.M., 2001. Re-Os dating of the Radio Hill Ni-Cu deposit, west Pilbara Craton, Western Australia. Australian Journal of Earth Sciences, 48, 43–47.
- Hoatson, D.M. and Sun, S.-S., 2002. Archean layered mafic-ultramafic intrusions in the west Pilbara Craton, Western Australia: a synthesis of some of the oldest orthomagmatic mineralizing systems in the world. Economic Geology, 97, 847–872.
- Hoatson, D.M., Wallace, D.A., Sun, S.-S., Macias, L.F., Simpson, C.J. and Keays, R.R., 1992. Petrology and platinum-group-element geochemistry of Archean layered mafic-ultramafic intrusions, west Pilbara Block, Western Australia. Australian Geological Survey Organisation Bulletin 242, 320 pp.

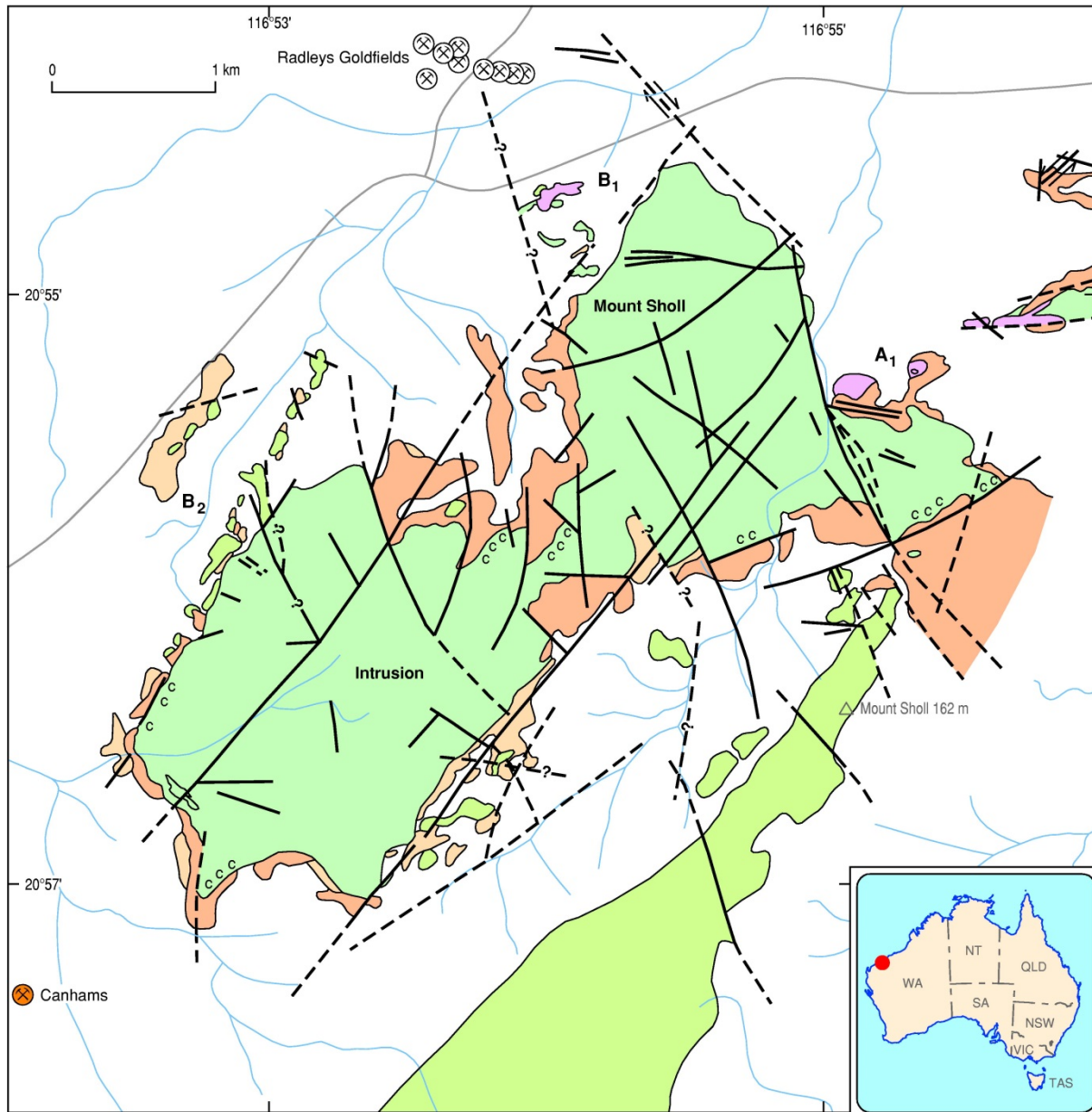
### ***Relevant figure(s)***

Figure 6.3, Appendix Figure K.20, and Appendix Figure K.21.



12-6339-6

Appendix Figure K.20 Geological setting and schematic northwest-southeast cross-section of the Radio Hill Intrusion, west Pilbara Craton, Western Australia. Cross-section is based on a southeastern-trending profile of projected drill-holes shown on the map in the northwest part of the intrusion. Massive Ni-Cu-PGE sulphide lenses are concentrated along the basal contact region below the thickest sequence of overlying mafic-ultramafic cumulates near the entrance of an interpreted feeder conduit into a small magma chamber. Modified from Hoatson et al. (1992).



Mount Sholl Intrusion

- Gabbro, plagioclase clinopyroxenite, minor norite, anorthosite
- Peridotite, dunite, and minor pyroxenite. Disseminated and minor massive Ni-Cu sulphides are hosted by gabbroic rocks along the basal contact

Whundo Group

- Massive rhyolite, rhyodacite, chert, tuff, crystal tuff, ignimbrite, agglomerate
- Intermediate metavolcanics and pyroclastics
- Aphanitic massive pillowed metabasalt, andesite, chert

- c c c c Chilled marginal phase of Mount Sholl gabbro (3-5 m wide)
- Fault
- ⇌ Inferred fault showing horizontal displacement
- Watercourse
- Road
- ⊗ Gold mine
- ⊗ Copper mine
- A<sub>1</sub> Mineralised area

Appendix Figure K.21 Geological setting of the Mount Sholl Intrusion, west Pilbara Craton, Western Australia. Disseminated and minor massive Ni-Cu-PGE sulphides are hosted by gabbroic rocks along the northwestern margin (B<sub>1</sub> and B<sub>2</sub> areas) and with ultramafic rocks on the northeastern margin (A<sub>1</sub>) of the mafic-ultramafic intrusion. Modified from Hoatson et al. (1992).

## **K.1.170 Range Well, Range Well Group**

(see Weld Range PGE)

## **K.1.171 Ravensthorpe\***

### ***Geological province***

Albany-Fraser Orogen.

### ***Location***

Ravensthorpe\*: 120.0691°E, -33.8466°S; Ravensthorpe (SI 51–05), Ravensthorpe (2930); location is very approximate at ~30 km south of Ravensthorpe.

### ***Classification***

- 12. Others (minor or unknown economic importance); 12.E. Others (unknown geological setting).
- 10. Placers; 10.C. Alluvial placers.

### ***Geological setting***

The prospect encompasses Archean ultramafic sills that have intruded metasediments near the boundary between the Yilgarn Craton and the Albany-Fraser Province.

### ***PGE mineralisation***

Surface sampling has defined two lenticular sill-like structures, with Pt levels of up to 1 ppm associated with Cu and As.

Historical exploration prior to 1990s was carried out in the Jerdacuttup and Bandalup Rivers areas, southeast of Ravensthorpe for placer-type Au-PGE mineralisation. The rivers drain a major zone of basement ultramafic and volcanic rocks. The region contains numerous Cenozoic Au placer deposits that consist of partly eroded sequences of fine- to coarse-grained polymictic gravels. Previous investigators have noted the presence of PGEs with the Au (Hoatson and Glaser, 1989).

### ***Age of mineralisation***

Unknown.

### ***Current status***

Historical exploration site.

### ***Economic significance***

Occurrences.

### ***Major references(s)***

Hoatson, D.M. and Glaser, L.M., 1989. Geology and economics of platinum-group metals in Australia. Bureau of Mineral Resources, Australia, Resource Report 5, 81 pp.

### ***Relevant figure(s)***

Figure 6.21.

## **K.1.172 Red Bull (V1)\***

### ***Geological province***

Albany-Fraser Orogen.

### ***Location***

Red Bull (V1): 123.079504°E, -32.117727°S; Balladonia (SH 51–03), Harms (3533); ~83 km west-northwest of Balladonia.

### ***Classification***

The Red Bull prospect is about 20 km southwest of the Nova–Bollinger deposits, and may be of similar deposit type, however there is insufficient information for a definite classification of the mineralisation at the Red Bull prospect.

- 2. Massive to poorly layered tholeiitic mafic-dominated intrusions; ?2.A. Segregations of Ni-Cu-Co-PGE sulphides in feeder conduits and basal contacts.

The samples from the prospect were from aircore drill-holes above the base of the weathering profile which host anomalous Ni-Cu-Co (PGEs, Cr) mineralisation (e.g., at Hook). The mineralised zone in the weathering profile corresponds to:

- 9. Regolith-laterite; 9.A. PGE-bearing regolith developed on ultramafic-mafic igneous rocks.

### ***Geological setting***

The Red Bull prospects are located within the northeast Fraser Zone of the Albany-Fraser Orogen. The Fraser Zone is a fault-bounded unit ~425 km-long and ~50 km-wide, dominated by metagabbroic rocks, and lies between predominantly Paleoproterozoic basement rocks of the Biranup and Nornalup Zones (Spaggiari et al., 2013). According to Spaggiari et al. (2013), only the southwestern portion of the Fraser Zone is exposed and comprise the ~1305 Ma–1290 Ma Fraser Range Metamorphics. The dominant lithologies are voluminous sheets of metagabbroic rocks interlayered with monzogranitic to syenogranitic gneisses, pyroxene-bearing granitic gneisses, and hybrid, metamorphosed igneous rocks. The latter rocks are interlayered with amphibolite to granulite facies pelitic, semipelitic to calcic, and locally Fe-rich metasedimentary rocks of the Mesoproterozoic Arid Basin.

The GSWA has interpreted the Fraser Zone as a structurally modified, lower crustal hot-zone where voluminous gabbroic magmas were variably mixed with contemporaneous granitic magma and country-rock melts. According to the GSWA, the presence of these gabbroic magmas, regional granite magmatism, and previously published peak metamorphic conditions in the metasedimentary rocks of >800°C and 8–9 kbars are all indicative of a regional thermal anomaly from at least 1305 Ma–1290 Ma that coincided with the formation of the Fraser Zone. The preferred tectonic settings as interpreted by GSWA are either a distal back-arc or an intercontinental rift (Spaggiari et al., 2013).

### ***PGE mineralisation***

Sheffield Resources Limited (2014) reported that aircore drilling had identified Ni-Cu-Co-PGE-Cr anomalies at three locations within the Red Bull prospect as indicated by the following intersections:

- Stud:
  - REAC401: 4 m @ 0.31% Ni, 0.11% Cu, 0.05% Co, 7 ppb Pd, 5 ppb Pt, and 0.11% Cr from 56 m;

## Western Australia

- REAC413: 8 m @ 0.37% Ni, 0.01% Cu, 0.01% Co, 4.6 ppb Pd, 4.4 ppb Pt, and 0.18% Cr from 47 m;
- REAC407: 8 m @ 0.30% Ni, 0.03% Cu, 0.04% Co, 5 ppb Pd, 10.5 ppb Pt, and 0.19% Cr from 43 m; and
- REAC423: 4 m @ 0.17% Ni, 0.02% Cu, 0.01% Co, 19 ppb Pd, 5 ppb Pt, and 0.21% Cr from 25 m.
- Earlobe:
  - REAC375: 8 m @ 0.29% Ni, 0.02% Cu, 0.02% Co, 4 ppb Pd, 3.5 ppb Pt, and 0.19% Cr from 36 m; and
  - REAC381: 4 m @ 0.12% Ni, 0.01% Cu, 0.04% Co, 12 ppb Pd, 15 ppb Pt, and 0.57% Cr from 37 m.
- Hook:
  - REAC458: 2 m @ 0.25% Ni, 0.07% Cu, 0.03% Co, 34 ppb Pd, 25 ppb Pt, and 0.64% Cr from 54 m.

The PGE content in general was very low with the highest recorded in drill samples from the Hook anomaly with up to 34 ppb Pd and 25 ppb Pt over a drill-hole length of 2 m from a drill-hole depth of 50 m. All samples were from the saprolite zone above the base of weathered rock.

### ***Age of mineralisation***

Host rocks unknown.

### ***Current status***

Exploration sites.

### ***Economic significance***

Occurrences.

### ***Major references(s)***

- Sheffield Resources Limited, 2014. Large Ni-Cu-Co anomalies identified in the Fraser Range. Sheffield Resources Limited announcement to the Australian Securities Exchange, 11 February 2014, 17 pp.
- Spaggiari, C.V., Smithies, R.H., Kirkland, C.L., Howard, H.M., Maier, W.D. and Clark, C., 2013. Melting, mixing, and emplacement: evolution of the Fraser Zone, Albany-Fraser Orogen. In: Promoting the prospectivity of Western Australia. Geological Survey of Western Australia. Extended Abstracts, Record 2013/2, 1–5.

### ***Relevant figure(s)***

#### **K.1.173 Red Hill\***

(see Buckman group)

#### **K.1.174 Red Rock\***

(not in MINEDEX as a PGE occurrence)

Western Australia

### ***Geological province***

Musgrave Province.

### ***Location***

Red Rock\*: 127.6167°E, -26.0333°S; Cooper (SG 52–10), Cooper (4445); ~4 km northwest of the Nebo–Babel Ni deposit, which is ~125 km west of the South Australia–Northern Territory–Western Australia border junction.

### ***Classification***

- 2. Massive to poorly layered tholeiitic mafic-dominated intrusions; 2.A. Segregations of Ni-Cu-Co-PGE sulphides in feeder conduits and basal contacts.

### ***Geological setting***

The host rocks to the Ni-Co-PGE mineralisation are ultramafic rocks, thought to form a pipe, intruded into the basement gneiss at a major structural intersection on the western edge of the Giles intrusions.

### ***PGE mineralisation***

The semi-precious Ni-bearing silicate mineral chrysoprase was exposed in four small pits. Analyses of rock samples from the pits returned up to 6.86% Ni, 5.74% Co, and 86 ppb PGEs. The chrysoprase occurs over a strike length of 300 m (Redstone Resources Limited, 2006).

### ***Age of mineralisation***

Proterozoic?

### ***Current status***

Exploration site.

### ***Economic significance***

Occurrence.

### ***Major references(s)***

Redstone Resources Limited, 2006. Redstone Resources Limited Prospectus 2006, 99 pp.  
Redstone Resources Limited project webpage ([http://www.redstone.com.au/contents\\_projects.html](http://www.redstone.com.au/contents_projects.html))

### ***Relevant figure(s)***

## **K.1.175 Revolution prospect\***

(see The Horn group)

## **K.1.176 Reynolds Creek**

### ***Geological province***

Gascoyne Province.

### **Location**

Reynolds Creek: 115.619120°E, -25.746620°S; Edmund (SF 50–14), Mangaroon (2050); ~150 km north-northeast of Gascoyne.

### **Classification**

- 12. Others (minor or unknown economic importance); 12.E. Others (unknown geological setting).

### **Geological setting**

Exploration target is a differentiated gabbro covering an area of about 5 km by 2 km, which is represented on maps as a northeast-trending Proterozoic dyke in the central portion of the Gascoyne Complex. A gossanous cap occurs over a 'late-stage gabbroic pegmatoidal unit' along the southern contact between the intrusion and a gneissic country rock.

### **PGE mineralisation**

Mafic intrusion mineralised at the base with maximum values of 2.2 g/t Pt, 2.1 g/t Pd, 0.442 g/t Au, and 1.2% Ni.

### **Age of mineralisation**

Proterozoic host rock.

### **Current status**

Historical exploration site.

### **Economic significance**

Occurrence.

### **Major references(s)**

Barnes, G.B. and Associates, 1987. Regional resources Mangaroon exploration licences. WAMEX report A23712.

### **Relevant figure(s)**

## **K.1.177 Ringlock**

(see GSP)

## **K.1.178 Robertsons East**

### **Geological province**

Yilgarn Craton.

### **Location**

Robertsons East: 119.167661°E, -31.077497°S; Southern Cross (SH 50–16), Southern Cross (2735); ~22 km northwest of Southern Cross.

## **Classification**

- 1. Layered tholeiitic mafic-ultramafic intrusions; 1.A. Stratabound PGE-bearing sulphide layers.

## **Geological setting**

The Robertsons East prospect lies within the Southern Cross greenstone belt, between Southern Cross and Bullfinch in the Southern Cross Domain of the Youanmi Terrane (Bloem et al., 1994; McCuaig et al., 2010). The lower 200 m to 300 m of the greenstone sequence is dominated by ultramafic schist, which is interpreted as part of the Frasers–Corinthia shear zone. The Ghooli granitoid dome adjoins the greenstone belt to the east (Bloem et al., 1994; Witt, 2002). According to Witt (2002), the prospect is hosted in a layered mafic-ultramafic sill-like body comprising five units and a pegmatoidal transition zone. From the base to roof these are:

- basal metaperidotite, comprising an olivine mesocumulate to orthocumulate layer, which is several hundred metres thick;
- coarse-grained tremolitic unit, 50 m–70 m-thick, overlies the basal peridotite. The unit is interpreted to be a metamorphosed magnesian pyroxenite;
- medium-grained metapyroxenite, interpreted to be a metamorphosed relatively Fe-rich pyroxenite, of similar thickness to the underlying unit;
- the transition between the pyroxenite and gabbro units contains metamorphosed pegmatoidal gabbro, either as isolated pods within the metapyroxenite or a semi-continuous layer between metapyroxenite and metagabbro. The pegmatoidal transition zone is probably only a few metres thick;
- medium-grained metagabbro overlies the pyroxenites and is about 200 m-thick; and
- an uppermost, metamorphosed quartz-gabbro overlies the metagabbro unit and is 100 m to 200 m-thick.

The hanging wall of the intrusion consists of pelitic metasedimentary rocks, and the footwall comprises metamorphosed variolitic-textured high-Mg basalt.

## **PGE mineralisation**

Whole-rock sampling indicates PGE-enrichment of the medium-grained, relatively Fe-rich pyroxenite unit of the layered intrusion, and the associated pegmatoidal gabbro. Samples of the coarse-grained, Mg-rich pyroxenite and the gabbro and quartz gabbro all have Pt <50 ppb. Platinum and Pd concentrations increase upwards through the medium-grained pyroxenite, to a maximum of 155 ppb–425 ppb Pt in the pegmatoidal gabbro unit. Samples of medium-grained pyroxenite contain 10 ppb–215 ppb Pt, but most assays lie in the range 50 ppb–100 ppb Pt. Samples with higher Pt (100 ppb–225 ppb Pt) probably have some contamination with pegmatoidal gabbro.

No anomalous Au results were returned apart from some local anomalies in soils, including 7137 ppb Au, over the ultramafic unit that forms a western lobe of the intrusion.

Nickel and Cu values are generally low (<1000 ppm Ni; <100 ppm Cu) although the base of the intrusion was not widely exposed and therefore not systematically sampled.

A ferruginous rock, interpreted as a possible gossan from near the base of the layered intrusion returned 833 ppm Cu, 158 ppm Zn, and 933 ppm Ni. This sample contains around 4000 ppm Mn suggesting that the rock is a ferricrete and that base metals may have been scavenged during Cenozoic ground-water movements.

According to Witt (2002), the layered intrusion at Robertsons prospect is typical of many layered mafic-ultramafic intrusions in the Eastern Goldfields Superterrane (Witt, 1995). These are generally single-pulse intrusions, up to about 2 km-thick, that have crystallised by in situ fractional crystallisation. They differ from the larger (several km-thick), more complex intrusions, such as Windimurra, Weld Range, and Munni Munni, which were more dynamic systems that involved multiple pulses of magma emplacement and turbulent magma-mixing events. Single-pulse Archean layered mafic-ultramafic intrusions commonly contain elevated PGE concentrations at, or about, the pyroxenite layer, however, they rarely attain economic PGE grades.

### ***Age of mineralisation***

Archean host rocks.

### ***Current status***

Historical exploration site.

### ***Economic significance***

Occurrence.

### ***Major references(s)***

- Bloem, J.M., Hilko, J.D., Groves, D.I., Ridley, J.R., 1994. Metamorphic and structural setting of Archean amphibolite-hosted gold deposits near Southern Cross, Southern Cross province, Yilgarn Block, Western Australia. *Ore Geology Reviews*, 9, 183–208.
- McCuaig, T.C., Miller, J. and Beresford, S. (compilers), 2010. Controls on giant minerals systems in the Yilgarn Craton—a field guide: Geological Survey of Western Australia, Record 2010/26, 164 pp.
- Witt, W.K., 1995. Tholeiitic and high-Mg mafic-ultramafic sills in the Eastern Goldfields Province, Western Australia: implications for tectonic settings. *Australian Journal of Earth Sciences*, 42, 407–422.
- Witt, W.K., 2002. Geology of the layered mafic-ultramafic intrusion and potential for PGE, Ni-Cu and Au mineralisation, Gilbeys, Southern Cross JV. In: Mukherji, A., 2003. Southern Cross JV project. Annual Report for the period 01 May 2002–30 April 2003. WAMEX report A66781. Appendix 4, 258–267.

### ***Relevant figure(s)***

#### **K.1.179 Rocky's Reward\***

(see Otter–Juan Kambalda\* group)

#### **K.1.180 Rocky Well-Irwin Hills**

(see Coglia Well)

#### **K.1.181 Rosie**

(see The Bulge C2)

## **K.1.182 Ruth Well\***

### ***Geological province***

Pilbara Craton.

### ***Location***

Ruth Well\*: 116.865501°E, -20.868380°S; Dampier (SF 50–02), Dampier (2256); ~16 km south of Karratha.

### ***Classification***

- 3. Komatiitic flows and sill-like intrusions.

### ***Geological setting***

At Ruth Well, subeconomic concentrations of disseminated and minor massive and matrix Ni-Cu sulphides, together with massive magnetite layers in peridotite units that have been altered to antigorite, tremolite, chlorite, talc, and carbonate (Hoatson et al., 1992). The lavas near Ruth Well are markedly bimodal in composition and consist of komatiite and komatiitic basalt flows. Other important rocks of igneous origin are unusual metamorphosed ultramafic pyroclastics and massive peridotite and pyroxenite presumably cumulates. Sedimentary horizons intercalated in the lava pile are thin cherts and BIFs with chalcopyrite mineralisation. The volcanic pile is host to the only volcanic peridotite-associated Ni deposit known from the Pilbara Craton (Nisbet and Chinner, 1981).

### ***PGE mineralisation***

Fox Resources Limited reported in their 2005 Annual Report a Measured + Indicated Resource for Ruth Well of 18 000 t of ore @ 1.59% Ni, 1.53% Cu, 0.06% Co, and 0.27 g/t Pd, and an additional Inferred Resource of 41 000 t of ore at 0.73% Ni, 0.57% Cu, 0.03% Co, and 0.24 g/t Pd.

### ***Age of mineralisation***

Archean host rocks.

### ***Current status***

Historical exploration site.

### ***Economic significance***

Small subeconomic deposit.

### ***Major references(s)***

Fox Resources Limited, 2006. Annual Report 2005. 84 pp.

Hoatson, D.M., Wallace, D.A., Sun, S.-S., Macias, L.F., Simpson, C.J. and Keays, R.R., 1992. Petrology and platinum-group-element geochemistry of Archean layered mafic-ultramafic intrusions, west Pilbara Block, Western Australia. Australian Geological Survey Organisation, Bulletin 242, 320 pp.

Nisbet, E.G. and Chinner, G.A., 1981. Controls on the eruption of mafic and ultramafic lavas, Ruth Well Ni-Cu prospect, West Pilbara. Economic Geology, 76, 1729–1735.

### ***Relevant figure(s)***

Figure 6.3.

### **K.1.183 RX1892**

(see Copernicus group)

### **K.1.184 Sally Malay Bore 1**

(see Corkwood)

### **K.1.185 Savannah\***

#### ***Geological province***

Halls Creek Orogen.

#### ***Location***

Savannah: 128.027695°E, -17.352600°S; Dixon Range (SE 52–06), Turkey Creek (4563); ~105 km north-northeast of Halls Creek.

#### ***Classification***

- 2. Massive to poorly layered tholeiitic mafic-dominated intrusions; 2.A. Segregations of Ni-Cu-Co-PGE sulphides in feeder conduits and basal contacts.
- 8. Hydrothermal-metamorphic (significant sulphides also occur in offset sulphide breccia zones in the migmatites, which are interpreted to represent fault-remobilised contact sulphides).

#### ***Geological setting***

The Savannah Ni deposit (previously known as the Sally Malay Ni deposit) is located within the Savannah Intrusion (previously known as the Sally Malay Intrusion), which is a multi-chambered body, ~1.5 km by ~3 km in area and ~1.7 km in thickness (Appendix Figure K.22). It comprises four subchambers (A, B, C, D) ranging in thickness from ~150 m to ~800 m that are separated from each other by screens of paramigmatite of the Tickalara Metamorphics. The subchambers may have been emplaced at slightly different levels in the crust and are connected by a network of feeder conduits. Each subchamber had open-fractionation systems, involving regular pulses of mafic-dominated magma. Layering is most prominent in plagioclase-rich rocks in the upper parts of the subchambers and Thornett (1981) described rhythmically layered troctolite with alternating olivine- and plagioclase-rich layers, 0.5–1 cm-thick. Gabbroic rocks show an igneous lamination of aligned plagioclase laths with dips of layers and laminations ranging between subvertical and moderate to the northwest (Hoatson, 2000).

#### ***PGE mineralisation***

The Savannah Intrusion contains the largest Ni-Cu-Co sulphide resource in the East Kimberley with a pre-mining Indicated and Inferred Resource of 3.85 Mt @ 1.79% Ni, 0.73% Cu, and 0.10% Co.

The four major textural types of Ni-Cu-Co sulphides in the intrusion consist of massive basal contact and feeder conduit sulphides; matrix and disseminated sulphides; breccia matrix sulphides; and remobilised vein-type sulphides.

Basal sulphide mineralisation is defined at the surface by a 300 m by 20 m limonite-goethite gossan with oxidation extending to about 30 m depth; primary mineralisation consists of two steeply dipping massive sulphide lenses, which have an overall keel shape at the base of the intrusion (Thornett,

1981; Shedden and Barnes, 1996). The two lenses partially merge, with the thickness of the combined ore horizon ranging from 3 m up to 40 m. Most sulphides are hosted by gabbroic rocks along the basal intrusive contact (Appendix Figure K.23). These host rocks consist largely of microgabbro and norite, which pass upward into peridotite, harzburgite, and lherzolite. The main zone of mineralisation typically consists of interstitial sulphides interspersed with barren zones and sporadically developed massive and matrix sulphides. Massive pyrrhotite-chalcopyrite-pentlandite mineralisation is enveloped by subordinate stringer and matrix chalcopyrite-pyrrhotite-pentlandite mineralisation, which persists into the lower parts of the peridotite units. The grade of the massive sulphides is 2%–2.7% Ni, 0.5%–1.5% Cu, and 0.1%–0.2% Co, whereas the grade of the stringer sulphide is 0.5%–2% Ni, 2.5% Cu, and <0.1% Co.

Significant sulphides also occur in offset sulphide breccia zones in the migmatites, which are interpreted to represent fault-remobilised contact sulphides. Sulphides from higher in the intrusion are restricted to very sparse disseminations, interstitial to olivine and as thin veinlets.

Analyses of PGEs and other elements of sulphides and other rock types from the Savannah Intrusion (Hoatson and Blake, 2000) are shown in Appendix Table K.34. Highest PGE concentrations (336 ppb Pd, 40.5 ppb Pt, 176 ppb Au) for four mineralised core samples are associated with disseminated sulphides rather than massive sulphides.

### **Age of mineralisation**

The Ni-Cu-Co sulphide mineralisation in the Savannah Intrusion is comagmatic with the intrusion, which has a U-Pb zircon age of  $1844 \pm 3$  Ma and a U-Pb baddeleyite age of  $1846 \pm 5$  Ma; both ages are determined from mottled anorthosite in the upper part of sub-chamber A (Page and Hoatson, 1997, 2000; Page et al., 1995).

### **Current status**

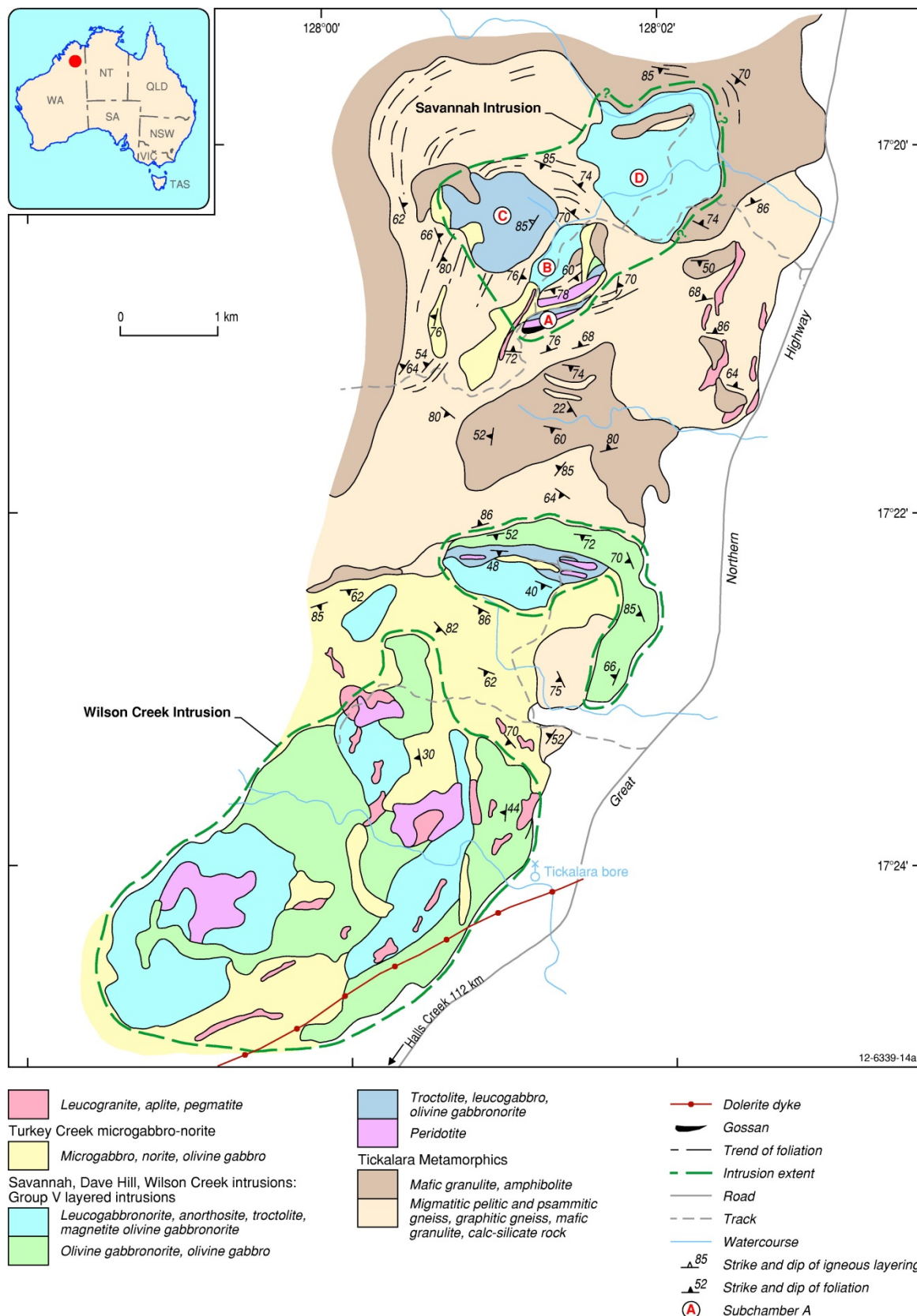
Operating Ni-Cu-Co mine.

### **Economic significance**

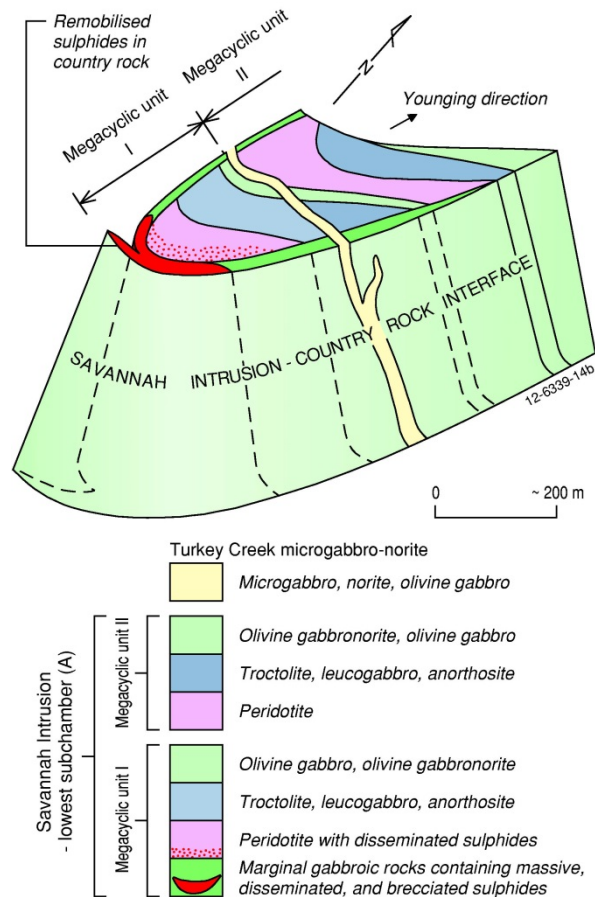
A significant medium-sized Ni-Cu-Co mine with relatively low concentrations of Pt and Pd. Open-pit mining of the Savannah deposit commenced in 2004 and was completed in January 2006, producing 12 120 t of contained Ni from 1.03 Mt of ore @ 1.18% Ni. Current Ni production is from underground operations and exploration is ongoing for extensions of the Savannah deposit below the 900-m level.

*Appendix Table K.34 Analyses of PGEs and other elements for sulphides and other rock types from the Savannah Intrusion. Data from Hoatson and Blake (2000).*

Sample number	Rock type	Pt (ppb)	Pd (ppb)	Au (ppb)	Cu (ppm)	Ni (ppm)	S (ppm)	Cr (ppm)	Pt/Pd	Pd x 103/S
93522064	Olivine websterite	3.1	4.2	2	55	1537	450	1585	0.74	0.009
SMD30/36	Massive sulphides	0.8	102	16					0.008	
SMD30/44	Disseminated sulphides	40.5	336	176					0.12	
SMD88/45.5	Disseminated sulphides	3.7	8.3	10					0.45	



Appendix Figure K.22 Geological setting of the Paleoproterozoic (group V) Savannah, Dave Hill, and Wilson Creek mafic-ultramafic intrusions and the Turkey Creek microgabbro-norite in the Halls Creek Orogen of the East Kimberley, Western Australia. Very minor concentrations of PGEs are associated with massive sulphides in the mafic-dominated Savannah Intrusion (previously known as the Sally Malay Intrusion), which is mined for Ni-Cu-Co sulphides. Mineralisation occurs in an interpreted feeder conduit (subchamber A) on the southern margin of the intrusion (Hoatson et al., 1997). Modified from Hoatson (2000).



Appendix Figure K.23 Schematic diagram of megacyclic units I and II and different mineralisation styles in subchamber A of the Savannah intrusion. The megacyclic units could indicate a prospective dynamic open magmatic system comprising regular surges of new pulses of magma. Massive, disseminated, and brecciated Ni-Cu-Co sulphides are concentrated in gabbroic rocks in the lowest part of the chamber, and remobilised vein-type sulphides intrude the granulite and gneiss country rocks. The mineralised marginal gabbroic rocks form a thin discordant zone along the external contacts of the megacyclic units with the country rocks. They are interpreted by Hoatson (2000) to have formed from rapid cooling and possible contamination of the primary magma. Similar thin 'veneers' of mineralised mafic rocks are observed for other mafic-ultramafic intrusions in the Halls Creek Orogen and west Pilbara Craton. Modified from Thornett (1981).

### Major references(s)

- Hoatson, D.M., 2000. Geological setting, petrography, and geochemistry of the Palaeoproterozoic layered mafic-ultramafic intrusions. In: Hoatson, D.M. and Blake, D.H. (editors), *Geology and economic potential of the Palaeoproterozoic layered mafic-ultramafic intrusions in the East Kimberley, Western Australia*. Canberra: Australian Geological Survey Organisation Bulletin 246, 99–162.
- Shedden, S.H. and Barnes, G.J., 1996. East Kimberley Nickel Province—Characteristics and origin of the Sally Malay Ni-Cu-Co deposit, East Kimberley, Western Australia. In: Grimsey, E.J. and Neuss, I. (editors), *Nickel 96—mineral to market*. Australasian Institute of Mining and Metallurgy, Publication Series 6/96, November 27–29, Kalgoorlie, Western Australia, 145–155.
- Thornett, J.R., 1981. The Sally Malay deposit: gabbroid associated nickel-copper sulfide mineralization in the Halls Creek Mobile Zone, Western Australia. *Economic Geology*, 76, 1565–1580.
- Thornett, J.R., 1986. Evolution of a high-grade metamorphic terrain in the Proterozoic Halls Creek Mobile Zone, Western Australia, PhD. University of Western Australia, Perth, 350 pp.

### **Relevant figure(s)**

Figure 6.9, Figure 8.20, Figure 8.21, Figure 8.22, Figure 8.23, Appendix Figure K.22, and Appendix Figure K.23.

## **K.1.186 Scotia Broad Arrow\***

### **Geological province**

Yilgarn Craton.

### **Location**

Scotia Mine\*: 121.274064°E, -30.198942°S; Kalgoorlie (SH 51–09), Bardoc (3137); ~64 km north of Kalgoorlie.

### **Classification**

- 3. Komatiitic flows and related sill-like intrusions; 3.A. Massive, matrix, and disseminated Ni-Cu-PGE sulphides in preferred lava pathways.

### **Geological setting**

The historical Scotia Broad Arrow mine occurs in the Agnew–Wiluna Domain (northwest of Kalgoorlie) where komatiites are intercalated with a complex assemblage of intermediate and felsic volcanic rocks (Barnes and Fiorentini, 2012). At Scotia Broad Arrow, porphyritic komatiites have been shown to occur between the upper spinifex-textured portion and the lower cumulate part of peridotitic flows. A westward younging is indicated by Ni sulphides at the base of the komatiitic pile at Scotia Broad Arrow (Stolz and Nesbitt, 1981; Witt, 1994).

### **PGE mineralisation**

Samples from the Scotia mine returned 2.35 ppm Pd, 1.09 ppm Ir, 19.0% Ni, and 0.81% Cu (Keays and Davison, 1976; Travis et al., 1976).

### **Age of mineralisation**

Mineralisation is hosted in Archean komatiites.

### **Current status**

Nickel production from the Scotia mine produced 14 628 t of Ni @ 2.17% Ni and 0.15% Cu from between 1969 and 1974 (Marston, 1984; Witt, 1994). The Scotia underground mine stopped production in 1977 when a pillar in the mine workings collapsed.

### **Economic significance**

Historical Ni mine.

### **Major references(s)**

- Barnes, S.J. and Fiorentini, M.L., 2012. Komatiite Magmas and Sulfide Nickel Deposits: A Comparison of Variably Endowed Archean Terranes. *Economic Geology*, 107, 755–780.
- Keays, R.R. and Davison, R.M., 1976. Palladium, iridium and gold in the ores and host rocks of nickel-sulphide deposits in Western Australia. *Economic Geology*, 71, 1214–1228.
- Marston, R.J., 1984. Nickel mineralisation in Western Australia. Western Australia Geological Survey, Mineral Resources Bulletin 14, 271 pp.

- Stolz, G.W. and Nesbitt, R.W., 1981. The komatiite nickel sulphide association at Scotia-A petrochemical investigation of the ore environment. *Economic Geology*, 76, 1480–1502.
- Travis, G.A., Keays, R.R. and Davison, R.M., 1976. Palladium and iridium in evaluation of nickel gossans in Western Australia. *Economic Geology*, 71, 1229–1243.
- Witt, W.K., 1994. Geology of the Bardoc 1:100 000 sheet. Western Australia Geological Survey, 1:100 000 Geological Series Explanatory Notes, 59 pp.

**Relevant figure(s)**

Figure 6.21.

**K.1.187 Sherlock River–Mt Fraser**

(appears to coincide with Sherlock Bay Extended\*)

**Geological province**

Pilbara Craton.

**Location**

Sherlock Bay Extended\*: 117.612964°E, -20.763744°S; Roebourne (SF 50–03), Sherlock (2456); ~24 km west-northwest of Whim Creek.

**Classification**

- ?1. Layered tholeiitic mafic-ultramafic intrusions.

**Geological setting**

Anomalous PGE levels have been defined in a Cu-Ni sulphide gossan at the base of the Sherlock River–Mt Fraser mafic intrusion.

**PGE mineralisation**

Rock-chip samples range up to 0.32 ppm Pt, 1.30 ppm Pd, and 0.51 ppm Au, and are associated with anomalous concentrations of Cu, Ni, and As. The Pt:Pd and Cu:Ni ratios are highly variable indicating different relative chemical behaviours of the precious metals in the weathering profile (Hoatson and Glaser, 1989).

**Age of mineralisation**

Archean (?).

**Current status**

Historical exploration site.

**Economic significance**

Occurrence.

**Major references(s)**

- Hoatson, D.M. and Glaser, L.M., 1989. Geology and economics of platinum-group metals in Australia. Bureau of Mineral Resources, Australia, Resource Report 5, 81 pp.

### ***Relevant figure(s)***

Figure 6.3.

### **K.1.188 Shrike\***

(see Breakaway PGE group)

### **K.1.189 Sidewinder\***

(see Dugite–Gum Creek group)

### **K.1.190 Six Mile Well\***

(see Mt Keith\*)

### **K.1.191 Spargoville 1A, 5A, Spargoville 2 or 5B, Redross\***

#### ***Geological province***

Yilgarn Craton.

#### ***Location***

Spargoville 1A: 121.491699°E, -31.320650°S; Boorabbin (SH 51–13), Yimia (3135); ~21 km southwest of Kambalda.

Spargoville 5A: 121.506405°E, -31.353808°S; Widgiemooltha (SH 51–14), Lake Lefroy (3235); ~23 km southwest of Kambalda.

Spargoville 2 or 5B: 121.505321°E, -31.367040°S; Widgiemooltha (SH 51–14), Lake Lefroy (3235); ~24 km southwest of Kambalda.

Redross\*: 121.648903°E, -31.683241°S; Widgiemooltha (SH 51–14), Lake Lefroy (3235); ~54 km south southwest of Kambalda and ~40 km south southeast of Spargoville 2 or 5B.

#### ***Classification***

- 3. Komatiitic flows and sill-like intrusions; 3A. Massive, matrix, and disseminated Ni-Cu-PGE sulphides in preferred lava pathways.

#### ***Geological setting***

The Spargoville and the Andrews deposits are located in the northern portion of a northwest-trending line of Ni deposits comprising Cooke and Mt Edwards in the south and Spargoville 1A in the north (Appendix Figure K.24). The mineralisation is hosted along the contacts of a southwest-dipping sequence of mafic and ultramafic rocks.



### ***Age of mineralisation***

Archean host rocks.

### ***Current status***

Exploration sites.

### ***Economic significance***

Historical Ni mines.

### ***Major references(s)***

Breakaway Resources Limited, 2008a. Additional high-grade nickel intersected at 1A deposit, West Kambalda. Breakaway Resources Limited announcement to the Australian Securities Exchange, 29 January 2008, 3 pp.

Breakaway Resources Limited, 2008b. Activity report for the quarter ended March 2008. 14 pp.

Keays, R.R. and Davison, R.M., 1976. Palladium, iridium and gold in the ores and host rocks of nickel-sulphide deposits in Western Australia. *Economic Geology*, 71, 1214–1228.

Travis, G.A., Keays, R.R. and Davison, R.M., 1976. Palladium and iridium in evaluation of nickel gossans in Western Australia. *Economic Geology*, 71, 1229–1243.

### ***Relevant figure(s)***

Figure 6.21 and Appendix Figure K.24.

## **K.1.192 Sparrow–Wills Creek**

(see Copernicus group)

## **K.1.193 Speewah Central\***

(see Buckman group)

## **K.1.194 Spinifex Prospect\***

(see Pioneer JH)

## **K.1.195 Springvale Group: Springvale (1, 2, 3), Springvale A**

### ***Geological province***

Halls Creek Orogen.

### ***Location***

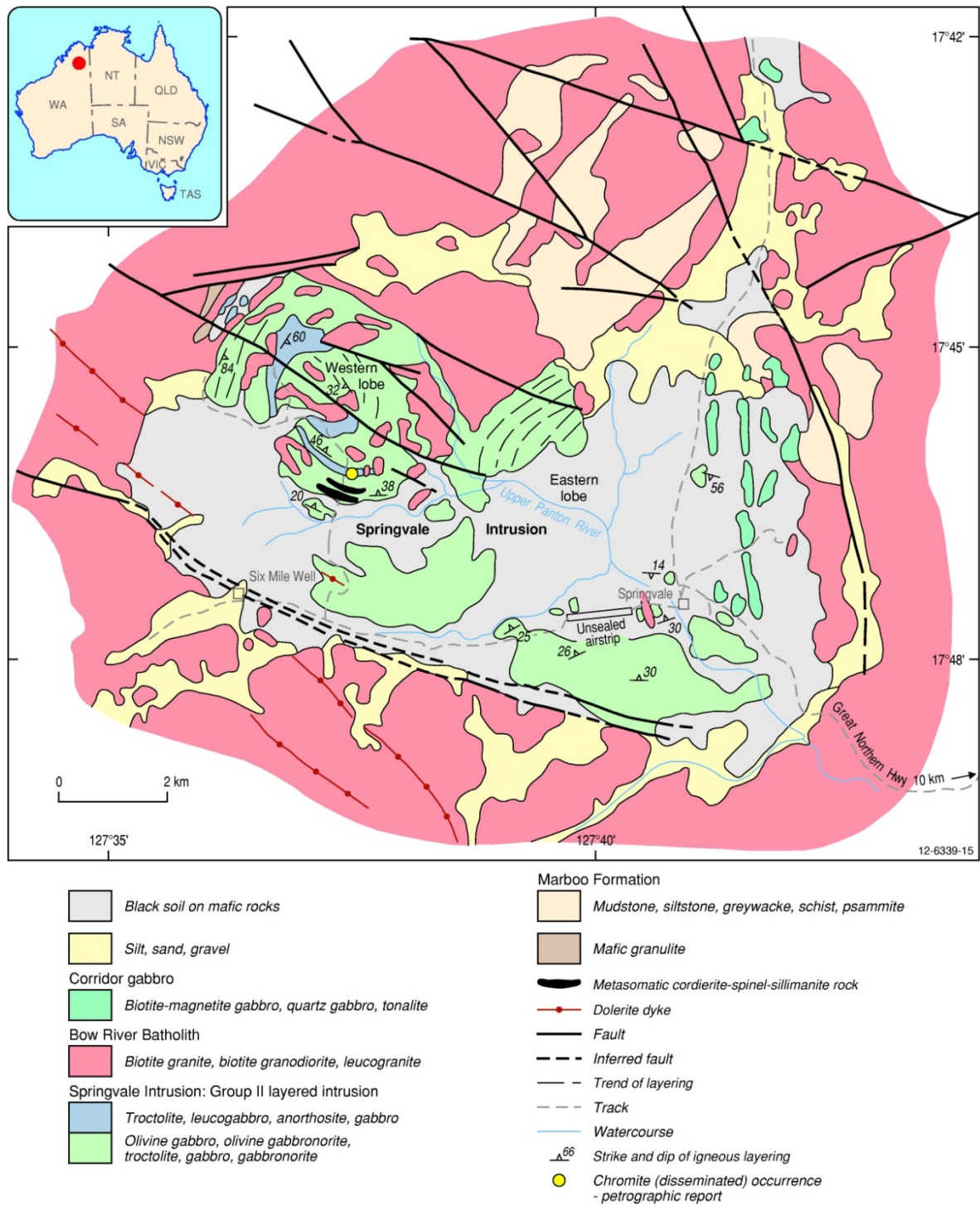
Springvale 1: 127.628270°E, -17.766120°S; Dixon Range (SE 52–06), McIntosh (4462); ~52 km north of Halls Creek.

### ***Classification***

- 1. Layered tholeiitic mafic-ultramafic intrusions; 1B. Stratabound PGE-bearing chromitite layers.

### Geological setting

The intrusions comprise two partly concealed contiguous lobes (western and eastern lobes), which together extend over ~6 km by ~13 km with an estimated thickness of ~2 km and display prominent arcuate cyclic layering (Appendix Figure K.25). The mafic-ultramafic body is faulted against different granite plutons of the Paperbark supersuite.



Appendix Figure K.25 Geological setting of the  $1857 \pm 2$  Ma Springvale Intrusion (group II), Halls Creek Orogen, Western Australia. This mafic intrusion consists of two partly concealed contiguous lobes (western and eastern lobes), with the lower parts of the mafic stratigraphy truncated along a sheared southern basal contact. Modified from Hoatson (2000).

The Western lobe consists mainly of olivine-bearing gabbroic rocks (1200 m-thick) along the southern sheared basal contact, overlain to the north by a well-exposed arcuate cyclic mafic sequence of troctolite and anorthosite (80 m), olivine gabbro (220 m), troctolite (120 m), and olivine gabbro, leucogabbro, and minor troctolite (380 m). Massive porphyritic olivine gabbro and gabbro-norite (containing large poikilitic amphibole grains replacing clinopyroxene) along the southern basal contact are overlain by weakly layered equigranular olivine gabbro and minor magnetite gabbro (Hoatson, 2000). Minor exposures of olivine-bearing gabbroic rocks characterise the Eastern lobe which is largely covered by black soils.

### **PGE mineralisation**

Weakly mineralised Fe-rich gossans (?hydrothermal origin) occur in the shear zone along the southern basal contact. The potential for accumulations of massive magmatic Ni-Cu-Co sulphides in the lower parts of the Springvale Intrusion is downgraded by the sheared nature of the southern basal contact.

Sanders (1999) noted a trend of more primitive composition up the succession, namely: (1) the lowest troctolite cyclic unit of the western lobe is the most evolved based on olivine compositions ( $mg_{63-67}$ ), the presence of magnetite and ilmenite, and the absence of chromite; (2) the central troctolite unit contains more primitive olivine and some low-Cr chromites in addition to ilmenite and magnetite; and (3) the upper chromite-bearing troctolite unit contains the most primitive olivine ( $mg_{74-82}$ ).

The chemistry of two olivine gabbro samples containing minor Cr-spinel from the central part of the Western lobe of the Springvale Intrusion is shown in Appendix Table K.35 below (Hoatson et al., 2000).

*Appendix Table K.35 Geochemistry of olivine gabbro samples from the western lobe of the Springvale Intrusion. Data from Hoatson et al. (2000).*

Sample number	Rock type	Pt (ppb)	Pd (ppb)	Au (ppb)	Cu (ppm)	Ni (ppm)	S (ppm)	Cr (ppm)	Pt/Pd	Pdx10 <sup>3</sup> /S
92522450	Olivine gabbro	1.9	4.2	2	53	314	530	1418	0.45	0.008
92522471	Olivine gabbro	0.5	<0.5	1	111	164	780	1302	>1.0	0.0006

### **Age of mineralisation**

A U-Pb zircon age of  $1857 \pm 2$  Ma was determined for a mottled anorthosite from the upper northwestern part of the Springvale Intrusion (Page and Hoatson, 1997, 2000; Page et al., 1995).

### **Current status**

Historical exploration site.

### **Economic significance**

Occurrences.

### **Major references(s)**

Hoatson, D.M., 2000. Geological setting, petrography, and geochemistry of the Palaeoproterozoic layered mafic-ultramafic intrusions. In: Hoatson, D.M. and Blake, D.H. (editors), *Geology and economic potential of the Palaeoproterozoic layered mafic-ultramafic intrusions in the East Kimberley, Western Australia*. Canberra: Australian Geological Survey Organisation Bulletin 246, 99–162.

## Western Australia

Sanders, T.S., 1999. Mineralisation of the Halls Creek Orogen, east Kimberley region, Western Australia. Geological Survey of Western Australia, Report 66 and Appendix, 44 pp.

### **Relevant figure(s)**

Figure 6.9, Figure 8.20, Figure 8.21, Figure 8.22, Figure 8.23, and Appendix Figure K.25.

### **K.1.196 Stripeys\***

#### **Geological province**

Musgrave Province.

#### **Location**

Stripeys: 128.3°E, -25.5952°S; Scott (SG 52–06), Holt (4546); ~60 km northwest of Wingellina lateritic Ni deposit.

#### **Classification**

- ?1. Layered tholeiitic mafic-ultramafic intrusions.

#### **Geological setting**

Conduit-shaped layered ultramafic intrusion that includes pyroxenite and dunite and four narrow gabbro layers totalling about 2.7 km true thickness.

#### **PGE mineralisation**

A rock-chip sample from near the top of the intrusion returned 0.205 g/t PGEs+Au and anomalous Cu.

#### **Age of mineralisation**

Proterozoic?

#### **Current status**

Exploration.

#### **Economic significance**

Occurrence.

#### **Major references(s)**

Redstone Resources Limited, 2008. Redstone Resources Limited 2008 Prospectus, 99 pp.  
Redstone Resources Limited project webpage ([http://www.redstone.com.au/contents\\_projects.html](http://www.redstone.com.au/contents_projects.html))

### **Relevant figure(s)**

### **K.1.197 Symons Hill\***

#### **Geological province**

Albany-Fraser Orogen.

## **Location**

Symons Hill\*: 123.174116°E, -31.900285°S; Zanthus (SH 51–15), Symons Hill (3534); ~90 km northwest of Balladonia.

## **Classification**

- ?2. Massive to poorly layered tholeiitic mafic-dominated intrusions;
- ?2.A. Segregations of Ni-Cu-Co-PGE sulphides in feeder conduits and basal contacts.

## **Geological setting**

The Symons Hill prospect is located within the Biranup Complex of the northeast Fraser Zone of the Albany-Fraser Orogen. The Fraser Zone is a fault-bounded unit, ~425 km-long and ~50 km-wide, dominated by metagabbroic rocks, and it is located between predominantly Paleoproterozoic basement rocks of the Biranup and Nornalup zones (Spaggiari et al., 2013). According to Spaggiari et al. (2013), only the southwestern portion of the Fraser Zone is exposed and comprises the ~1305 Ma–1290 Ma Fraser Range Metamorphics. The dominant lithologies are voluminous sheets of metagabbroic rocks interlayered with monzogranitic to syenogranitic gneisses, pyroxene-bearing granitic gneisses, and hybrid, metamorphosed igneous rocks. The latter rocks are interlayered with amphibolite to granulite facies pelitic, semipelitic to calcic, and locally Fe-rich metasedimentary rocks of the Mesoproterozoic Arid Basin.

The GSWA have interpreted the Fraser Zone as a structurally modified, lower crustal hot-zone where voluminous gabbroic magmas were variably mixed with contemporaneous granitic magma and country-rock melts. According to the GSWA, the presence of these gabbroic magmas, regional granite magmatism, and previously published peak metamorphic conditions in the metasedimentary rocks of >800°C and 8–9 kbars are all indicative of a regional thermal anomaly from at least 1305 Ma–1290 Ma that coincided with the formation of the Fraser Zone. The preferred tectonic settings as interpreted by GSWA are either a distal back-arc or an intercontinental rift (Spaggiari et al., 2013).

## **PGE mineralisation**

Highest Ni and PGE grades are situated close to the base of the saprolite profile above Ni-rich olivine-bearing gabbro basement rocks. Highest values are listed below:

Drill-hole SHAC040:

- 3 m @ 0.98% Ni, 0.005% Cu, 0.12% Co, 0.015 ppm Pt, and 0.005 ppm Pd from 21 m; including, 1 m @ 1.1% Ni, 0.0035% Cu, 0.045% Co, 0.01 ppm Pt, and 0.006 ppm Pd from 23 m;

Drill-hole SHAC067:

- 1 m @ 0.86% Ni, 0.01% Cu, 0.023% Co, 0.024 ppm Pt, and 0.008 ppm Pd from 40 m.

Bulk residues from all composite air drill-core sample intervals containing greater than 0.1% Ni were resampled at 1 m intervals for a total of 88 samples. Samples were assayed for a 36 element suite, including Pt and Pd. Assay ranges for selected elements are summarised in Appendix Table K.36.

Appendix Table K.36 Assay ranges for selected elements from composite aircore sample intervals from Symons Hill.

Element	Samples	Minimum	Maximum
Ni (ppm)	88	460	11 050
Cu (ppm)	88	9	1440
Co (ppm)	88	19	1870
Pt (ppb)	88	<5	45
Pd (ppb)	88	1	49
Cr (ppm)	88	79	10 005
S (ppm)	88	100	5000
Au (ppb)	88	<1	74
Ag (ppm)	88	<0.5	0.60

**Age of mineralisation**

Archean host rocks.

**Current status**

Exploration site.

**Economic significance**

Occurrence.

**Major references(s)**

Matsa Resources Limited, 2013. High nickel values confirmed at Symons Hill SHG02. Matsa Resources Limited announcement to Australian Securities Exchange, 17 October, 2013, 14 pp.  
 Spaggiari, C.V., Smithies, R.H., Kirkland, C.L., Howard, H.M., Maier, W.D. and Clark, C., 2013. Melting, mixing, and emplacement: evolution of the Fraser Zone, Albany-Fraser Orogen. In: Promoting the prospectivity of Western Australia. Geological Survey of Western Australia. Extended Abstracts, Record 2013/2, 1–5.

**Relevant figure(s)****K.1.198 The Bulge C2, Rosie and Camp Oven****Geological province**

Yilgarn Craton.

**Location**

The Bulge C2: 121.996104°E, -27.611774°S; Duketon (SG 51–14), Banjiwarn (3242); about 120 km north-northwest of Laverton.

Rosie Prospect: 122.014331°E, -27.624587°S; Duketon (SG 51–14), Tate (3243); ~115 km north-northwest of Laverton.

Camp Oven Prospect: 121.969704°E, -27.499701°S; Duketon (SG 51–14), Duketon (3342); ~132 km north-northwest of Laverton and ~15 km northwest along strike of The Bulge Prospect.

## Classification

- 3. Komatiitic flows and related sill-like intrusions; 3.A. Massive, matrix, and disseminated Ni-Cu-PGE sulphides in preferred lava pathways.

## Geological setting

The Archean Duketon greenstone belt is located ~80 km north of Laverton and is dominated by a broad, complex north-northwest-trending fold structure known as the Eristoun syncline. The core of this syncline is occupied by the Ingi-jingi felsic volcanic complex, which consists dominantly of rhyolitic and dacitic tuffs, and represents the youngest rocks in the belt. The western limb of the Eristoun syncline comprises a sequence of mafic and ultramafic volcanics and intrusives, epiclastic and chemical sediments, and minor mafic-felsic rocks known as the Bandy mafics. To the west the Bandy mafics are bounded by the Hootanui Fault and the Granite Hills Batholith. The Ni-Cu-PGE mineralisation at the Rosie Prospect occurs in weathered footwall basalts and komatiites with interbedded siltstone and carbonaceous shale in the western limb of the Eristoun syncline and the mineralisation at the Camp Oven Prospect is in weathered ultramafic olivine cumulates (South Boulder Mines Limited, 2008a,b, 2009b).

## PGE mineralisation

At The Bulge Ni-Cu-PGE prospect (Appendix Figure K.26) mineralisation occurs in three horizons (eastern contact, central, and western contact) and also contains discrete zones of blebby and stringer sulphide mineralisation with grades up to 3.43% Ni. Drill intersections include 22 m @ 0.7% Ni, 2988 ppm Cu, and 975 ppb Pt+Pd. At the Rosie Ni-Cu-PGE prospect (Appendix Figure K.26 and Appendix Figure K.27) mineralisation occurs in the oxide and transition zone overlying footwall basalts at contacts with siltstone and carbonaceous shale. Holes with significant intersections of PGEs at the Rosie and the Bulge prospects are shown in Appendix Table K.37 (Independence Group NL, 2012a,b).

*Appendix Table K.37 Significant PGE intersections in drill-holes at Rosie and The Bulge prospects. Data from Independence Group NL (2012a,b).*

Prospect	Drill-hole <sup>1</sup>	From (m)	To (m)	Interval (m)	Approx. true width (m), or dip	Ni (%)	Cu (%)	Co (%)	Pt+Pd (g/t)	As (ppm)
Rosie	TBRC069	193	194	1	0.4	2.85	0.11		0.11	368
Rosie	TBRC070	186	197	11	3.6	2.04	0.35		2.57	1576
Rosie	including	190	197	7	2.3	2.61	0.42		3.75	1305
Rosie	TBRC073	154	158	4	3.6	1.27	0.10		0.83	402
Rosie	TBRC075	171	176	5	4.3	0.77	0.14		1.30	86
Rosie	TBDD080	205.54	209.13	3.59	2.1	2.27	0.24		3.11	1973
Rosie	TBDD085	301.00	307.86	6.86	3.4	1.61	0.35	0.05	0.97	3669
Rosie	TBDD086	399.31	410.00	10.69	6.0	1.76	0.72	0.06	1.81	610
Rosie	TBDD087	575.31	578.34	3.03		5.28	0.36		3.67	86
Rosie	TBDD093	608.71	610.50	1.79	1.0	1.34	0.12	0.03	0.38	5
Rosie	TBDD098	599.71	604.91	5.20	3.3	9.13	1.09	0.21	3.62	42
Rosie	TBDD130			3.25		1.5	0.8		2.1	
Rosie	TBDD133			8.1		1.2	0.3		1.1	

## Western Australia

Prospect	Drill-hole <sup>1</sup>	From (m)	To (m)	Interval (m)	Approx. true width (m), or dip	Ni (%)	Cu (%)	Co (%)	Pt+Pd (g/t)	As (ppm)
Rosie	TBDD140			3.2		3.0	0.6		3.3	
Rosie	TBAC122	65	72	7	-60°	0.64	0.31		2.42	
Rosie	TBAC124	32	42	10	-60°	0.40	0.49		2.25	
Rosie	TBAC126	32	67	35	-60°	0.40	0.27		1.59	
Rosie	TBAC127	32	44	12	-60°	0.31	0.21		0.77	
Rosie		81	83	2	-60°	0.59	0.13		0.66	
Rosie		91	94	3	-60°	0.59	0.11		0.62	
The Bulge C2	TBRC019	68	90	22	-60°	0.7	0.3		0.98	
The Bulge C2	TBRC020	127	132	5	-60°	1.4	0.2		0.91	
The Bulge C2	TBRC21	172	184	12	-60°	0.76	0.06		0.6	
The Bulge C2	TBRC071	159.84	180.00	20.16	-60°	1.00	0.04		0.08	
The Bulge C2		248.89	263.00	14.11	-60°	0.96	0.07		0.75	
The Bulge C2		267.33	271.83	4.5	-60°	2.04	0.04		0.36	
The Bulge C2	TBDD074	275	325	50	-60°	0.92	0.04		0.08	
The Bulge C2 South	TBAC102	89	92	3	-60°	0.30	0.06		1.74	

<sup>1</sup> Drill-holes include: diamond drill-hole; aircore drill-hole; and reverse circulation drill-hole.

More detailed analysis of the PGEs for sample TBDD098 at the Rosie Prospect is shown below.

Appendix Table K.38 Detailed geochemical analysis of TBDD098.

Prospect	Drill-hole	From (m)	To (m)	Pt (g/t)	Pd (g/t)	Rh (g/t)	Ru (g/t)	Os (g/t)	Ir (g/t)	PGEs (g/t)
Rosie	TBDD098	599.71	604.91	2.22	1.74	0.82	1.79	0.26	0.25	7.09

Analyses of rock-chip samples at the Camp Oven Prospect returned 0.9% Ni, 2.3% Cu, 0.68 g/t Pd, 0.70g/t Pt, and 0.44 g/t Au. Data from South Boulder Mines Limited (2008a,b, 2009a).

### **Age of mineralisation**

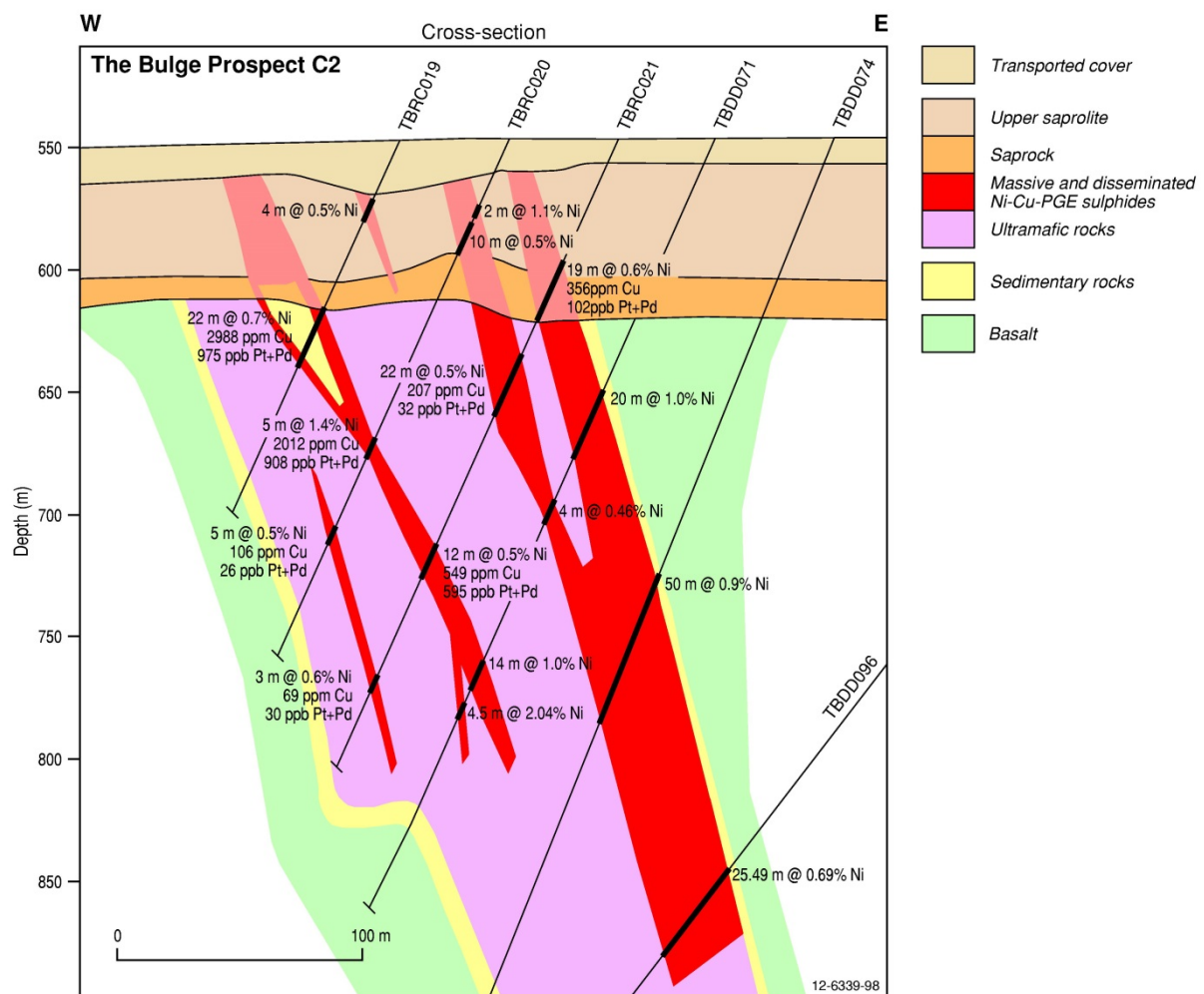
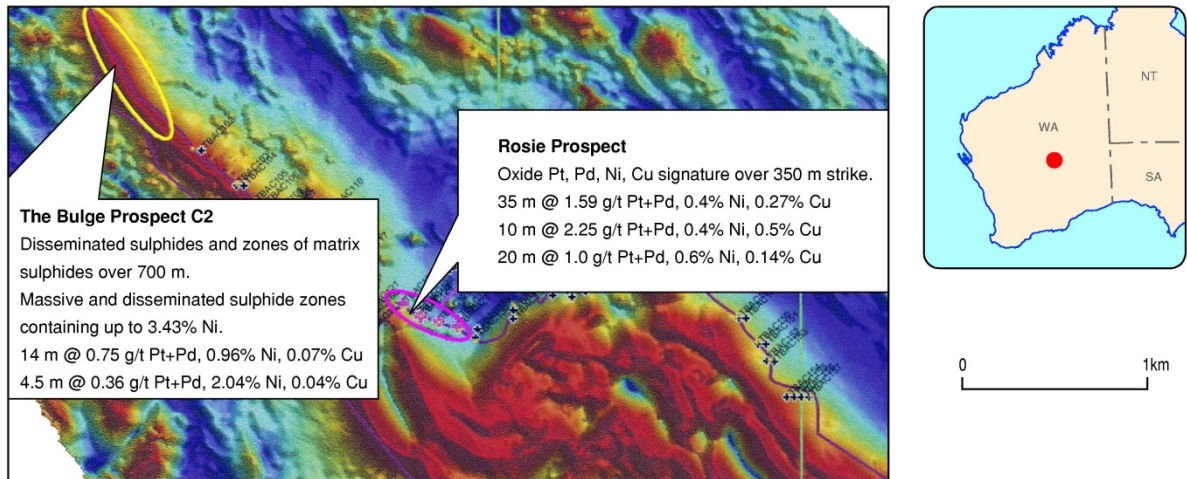
Archean host rocks.

### **Current status**

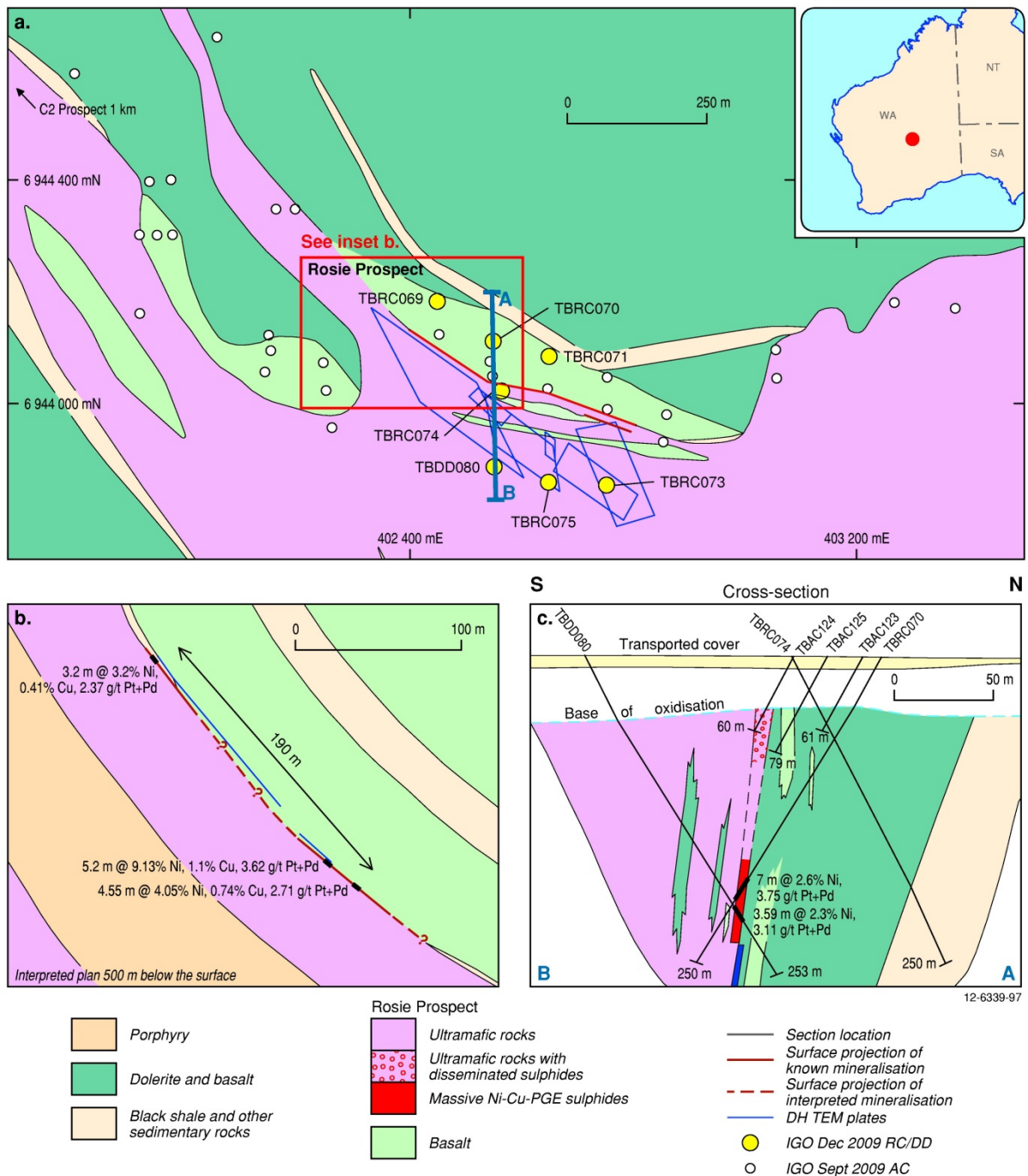
Historical exploration site.

### **Economic significance**

Occurrences with a small deposit at the Rosie deposit. Resources for Rosie as published on 25 January 2012 amounted to Indicated Resources of 715 000 t at 1.9% Ni, 0.4% Cu, 0.8 g/t Pt, and 1.1 g/t Pd, plus an Inferred Resource of 39 000 t at 1.65% Ni, 0.4% Cu, 0.7 g/t Pt, and 1.0 g/t Pd (Independence Group NL, 2012b).



Appendix Figure K.26 Total Magnetic Intensity Aeromagnetic image for The Bulge C2 and Rosie Ni-Cu-PGE prospects, Yilgarn Craton, Western Australia. Schematic east-west cross-section of The Bulge Prospect C2 section 6 945 400 N with geology and significant intersections >0.4% Ni. Precious-metal mineralisation occurs with ultramafic rocks in the primary zone and in the saprolitic weathering zone. Both figures are modified from South Boulder Mines Limited (2009).



Appendix Figure K.27 Rosie Ni-Cu-PGE prospect, Yilgarn Craton, Western Australia. Modified from Independence Group NL (2009, 2010). (a). Geological setting of the Rosie Ni-Cu-PGE prospect. (b). Rosie Prospect Plan approximately 500 m beneath the surface showing significant intercepts down-hole TEM conductors and interpreted location of nickel sulphide mineralisation. (c). Schematic north-south cross-section AB of the Rosie prospect. The location of section A-B is shown in figure (a).

### Major references(s)

Independence Group NL, 2009. Quarterly report for the three months ended 31 December 2009, 24 pp.

Independence Group NL, 2010. Duketon Nickel JV-Rosie prospect drilling results. Independence Group NL announcement to the Australian Securities Exchange, 7 April 2010, 5 pp.

Independence Group NL, 2012a. Duketon Joint Venture. Rosie deposit initial Ni-Cu-PGE mineral resource estimate. Independence Group NL announcement to the Australian Securities Exchange, 25 January 2012, 10 pp.

Independence Group NL 2012b. Quarterly activities report 1 April to 30 June 2012, 28 pp.

South Boulder Mines Limited, 2008a. South Boulder Mines Limited 2008 Annual Report, 60 pp.

South Boulder Mines Limited, 2008b. Duketon nickel JV drilling results provide significant encouragement. South Boulder Mines Limited announcement to the Australian Securities Exchange, 5 November, 2008, 7 pp.

South Boulder Mines Limited, 2009a. Platinum-palladium-nickel-copper mineralisation confirmed at Rosie nickel sulphide prospect. South Boulder Mines Limited announcement to the Australian Securities Exchange, 5 October 2009, 5 pp.

South Boulder Mines Limited, 2009b. June Quarterly Report, 2009, 10 pp.

South Boulder Mines Limited, 2010. Further massive/matrix sulphides intersected at the 'Rosie' nickel sulphide prospect. South Boulder Mines Limited announcement to the Australian Securities Exchange, 22 March 2010, 2 pp.

### ***Relevant figure(s)***

Figure 6.21, Appendix Figure K.26, and Appendix Figure K.27.

## **K.1.199 The Gap prospect\***

(see The Horn group)

## **K.1.200 The Horn**

Also the Revolution prospect\*, about 4 km north-northwest of The Horn; The Gap prospect\* about 2.5 km north-northwest of The Horn; and Horn South\*, about 0.5 km south-southeast of The Horn. The Fly Bore, described by Hoatson and Glaser (1989) appears to be located near The Horn deposit.

### ***Geological province***

Yilgarn Craton.

### ***Location***

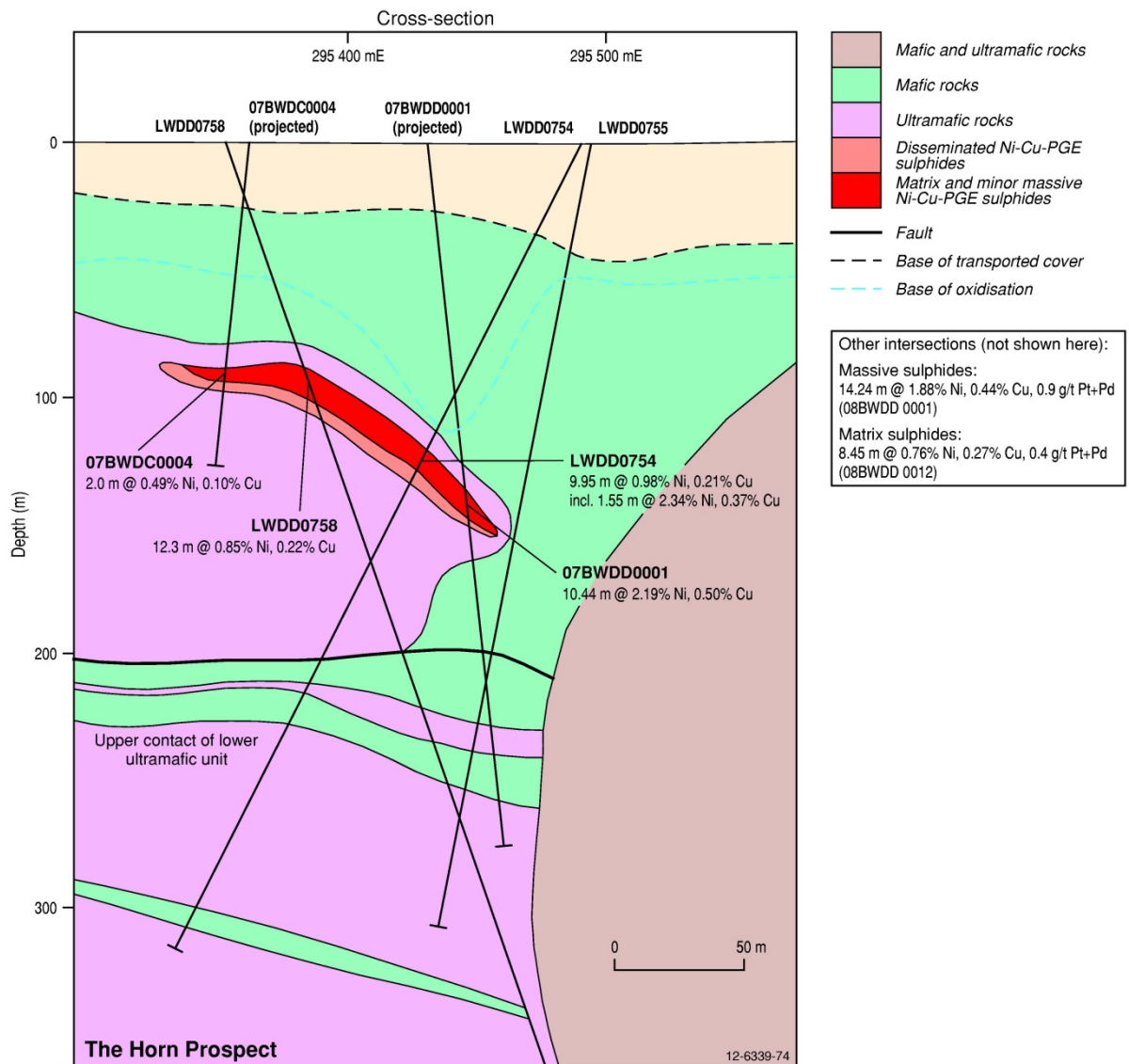
The Horn: 120.916603°E, -28.167379°S; Leonora (SH 51-01), Wildara (3041); ~35 km southeast of Leinster.

### ***Classification***

- 3. Komatiitic flows and related sill-like intrusions; ?3.A. Massive, matrix, and disseminated Ni-Cu-PGE sulphides in preferred lava pathways.

### ***Geological setting***

The Horn Ni-Cu-PGE deposit occurs in the upper ultramafic sequence—the Roadside Ultramafic Belt—within a fault-controlled block in the Agnew–Wiluna greenstone belt (Breakaway Resources Limited, 2010a). The host rocks at The Horn are interpreted to be the southern equivalent of Perseverance ultramafic complex that host the Perseverance Ni deposits (Appendix Figure K.28).



Appendix Figure K.28 Schematic west-east cross-section of The Horn Ni-Cu-PGE prospect, Yilgarn Craton, Western Australia. Modified from Breakaway Resources Limited (2008b).

### PGE mineralisation

The Horn deposit was reported to contain 600 000 t at 1.39% Ni, 0.3% Cu, and 0.5 g/t Pt+Pd.

At the Revolution prospect, about 4 km north-northwest of The Horn deposit, up to 5.1% Ni, 1220 ppm Cu, and 3029 ppb Pt+Pd were recorded in wide-spaced drill-hole samples. The Gap prospect is about 2.5 km north-northwest of The Horn deposit where air-blast drill samples recorded up to about 0.5% Ni, 500 ppm Cu, and 100 ppb PGEs; and gossan samples at the Horn South prospect, about 0.5 km south-southeast of The Horn deposit, recorded 0.09% Ni, 850 ppm Cu, and 63 ppb Pt+Pd (Breakaway Resources Limited, 2010b).

Sampling of gossans at the Hilltop Gossan, about 5 km southwest of The Horn deposit recorded 629 ppm Ni, 345 ppm Cu, and 216 ppb Pt+Pd (Breakaway Resources Limited, 2010a).

### Age of mineralisation

Archean.

### ***Current status***

Exploration site.

### ***Economic significance***

Small deposit.

### ***Major reference(s)***

- Abeyasinghe, P.B. and Flint, D.J., 2008. Nickel-cobalt in Western Australia: commodity review for 2006. Geological Survey of Western Australia, Record 2008/3, 40 pp.
- Breakaway Resources Limited, 2010a. Activity report for the quarter ended 30 June 2010, 511.
- Breakaway Resources Limited, 2010b. Presentation by David Hutton at RIU Explorers Conference 23 February 2010, 24 pp.
- Breakaway Resources Limited, 2008a. Australian Securities Exchange News Release 14 April 2008, 5 pp.
- Breakaway Resources Limited, 2008b. Breakaway Resources Limited 2008 Annual Report, 95 pp.

### ***Relevant figure(s)***

Figure 6.21 and Appendix Figure K.28.

## **K.1.201 Tickalara Bore 4**

### ***Geological province***

Halls Creek Orogen.

### ***Location***

Tickalara Bore 4: 128.017210°E, -17.402690°S; Dixon Range (SE 52–06), Turkey Creek (4563); ~100 km north-northeast of Halls Creek.

### ***Classification***

Mineralisation in gossan:

- 9. Regolith-Laterite; 9.A. PGE-bearing regolith developed on ultramafic-igneous rocks.

PGEs hosted in the unweathered rocks underlying the gossan near the amphibolite-gabbro contact:

- 8. Hydrothermal-Metamorphic.

### ***Geological setting***

The Tickalara Bore 4 prospect is located near the eastern margin of the Wilson Creek Intrusion. The intrusion is a lobate body, 3 km by 6 km, comprising weakly layered mafic sheets intruded by irregular plug-like ultramafic bodies. Stratigraphy is not well defined, although irregular ovoid bodies of massive serpentinitised peridotite appear to cut mottled anorthosite, leucogabbro, and troctolite; ridge-forming units of coarse-grained, locally pegmatitic, amphibole-spotted gabbro, olivine gabbro, and olivine gabbro-norite are interlayered with anorthosite; serpentinitisation and magnesite alteration are intense in peridotite.

### ***PGE mineralisation***

The Tickalara Bore 4 occurrence is a gossan associated with an amphibolite, possibly an altered ultramafic rock. The gossanous material is developed along the contact of the amphibolite with gabbro. A sample analysis of the gossan yielded 0.2 ppm Pt (El-Ansary, 1971). Hoatson (2000) noted that a single olivine gabbro-norite surface sample had low Pd (<0.5 ppb) and Pt (<0.5 ppb) contents.

### ***Age of mineralisation***

The Wilson Creek Intrusion is correlated with the  $1844 \pm 3$  Ma Savannah Intrusion, but may be older (>1850 Ma) (Hoatson, 2000). The mineralisation in the gossan was probably formed during the Cenozoic, possibly over a shear zone between the amphibolite and the gabbro.

### ***Current status***

Occurrence.

### ***Economic significance***

Unknown.

### ***Major references(s)***

- El-Ansary, M., 1971. Geological report Ord Crossing area, Tickalara Bore area. Pickhands Mather and Co. International. WAMEX report A711.
- Hoatson, D.M., 2000. Geological setting, petrography, and geochemistry of the Palaeoproterozoic layered mafic-ultramafic intrusions. In: Hoatson, D.M. and Blake, D.H. (editors), *Geology and economic potential of the Palaeoproterozoic layered mafic-ultramafic intrusions in the East Kimberley, Western Australia*. Canberra: Australian Geological Survey Organisation Bulletin 246, 99–162.

### ***Relevant figure(s)***

Figure 6.9, Figure 8.21, and Appendix Figure K.22.

## **K.1.202 Toby South (Wilagee Intrusion)**

### ***Geological province***

Halls Creek Orogen.

### ***Location***

Toby South: 127.690260°E, -17.606140°S; Dixon Range (SE 52–06), McIntosh (4462); ~70 km north of Halls Creek.

### ***Classification***

- Layered tholeiitic mafic-ultramafic intrusions; 1.B. Stratabound PGE-bearing chromitite layers.

### ***Geological setting***

The Toby South Cr-PGE occurrence is located within the Wilagee Intrusion an arcuate body, 10 km-long by 2 km-wide, with an estimated thickness of 1.3 km (Appendix Figure K.29). The Wilagee Intrusion adjoins the southeastern side of the Toby Intrusion and is divided into southern and northern parts by a northeast-trending fault. The southern part is faulted against the Paperbark Granite of the Paperbark supersuite to the east and fine-grained gabbros of the Toby Intrusion to the west, and the

northern part intrudes and forms chilled margins and net-vein complexes with different granites of the Paperbark supersuite. The southern part contains two differentiated mafic–ultramafic megacycles, each comprising discontinuous basal units, 20 m–50 m-thick, of serpentinised plagioclase peridotite overlain to the southeast by 50 m–500 m-thick units of olivine gabbro, troctolite, anorthosite, and leucogabbro. Primitive cumulates near the base of each megacycle indicate open-fractionation systems that involve magma pulses with olivine and plagioclase on the liquidus. The northern part consists of a homogeneous sequence of troctolite and olivine gabbro similar to the upper parts of megacycles in the southern part (Sanders, 1999; Hoatson, 2000).

### **PGE mineralisation**

A chromitite lens, 15 cm–20 cm-thick, is hosted by pegmatitic troctolite near the middle of the lower megacycle in the southern part (Appendix Figure K.29). This occurrence and the presence of rare disseminated chromite in the Springvale Intrusion to the south are the only known examples of plagioclase-rich cumulates hosting chromite mineralisation in the Halls Creek Orogen. Low-order Pd anomalies near Tobys Dam and the 10–15 cm-thick chromitite were tested by three diamond drill-holes. Low-order PGE anomalies (up to 92 ppb Pt and 240 ppb Pd) were intersected in two holes.

Three samples from the Wilagee Intrusion were assayed for PGEs and trace-element geochemistry as shown in Appendix Table K.39 (Hoatson, 2000).

*Appendix Table K.39 Geochemistry of samples from the Wilagee Intrusion. Data from Hoatson (2000).*

Sample number	Rock type	Pt (ppb)	Pd (ppb)	Au (ppb)	Cu (ppm)	Ni (ppm)	S (ppm)	Cr (ppm)	Pt / Pd	Pd x 103/S
92522499	Chromitite	57.4	148	1	3	1082	<10	>99 999	0.39	>14.8
92522506	Troctolite	6.9	21.7	2	57	1267	240	2256	0.32	0.09
92522533	Gabbro chill	0.5	<0.5	3	95	106	800	389	>1.0	0.0006

### **Age of mineralisation**

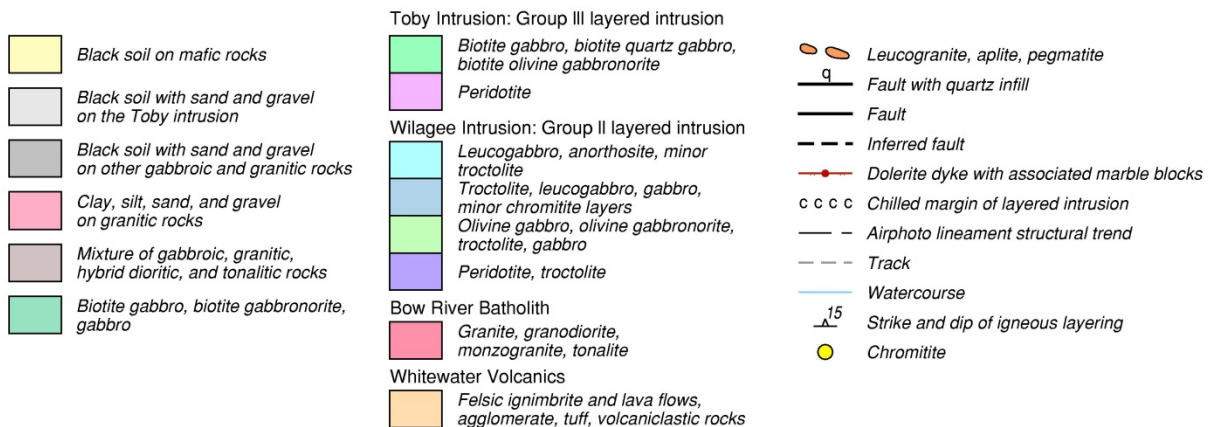
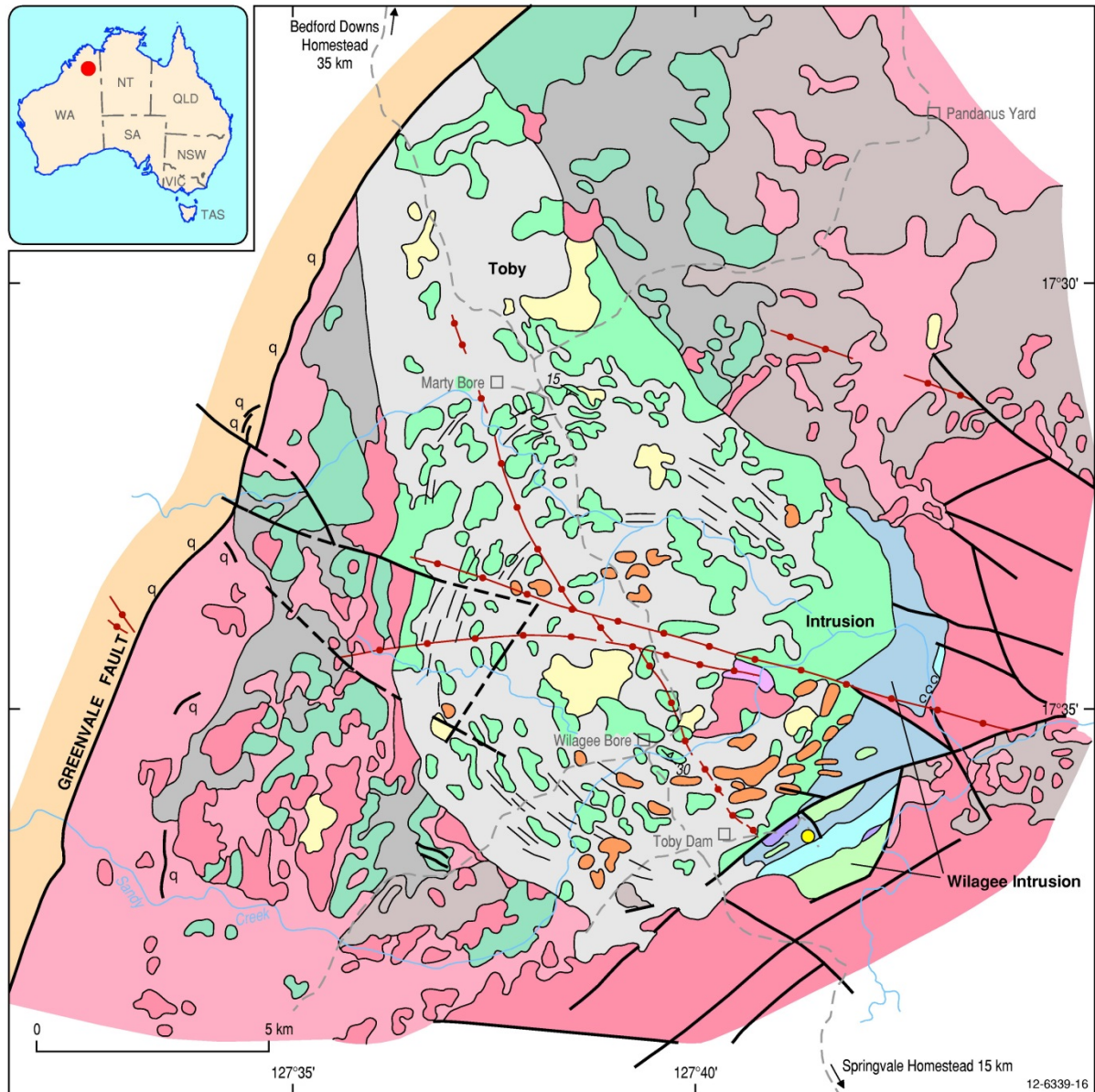
The Wilagee Intrusion is correlated with the  $1857 \pm 2$  Ma Springvale Intrusion (Hoatson, 2000).

### **Current status**

Historical exploration site.

### **Economic significance**

Occurrence.



Appendix Figure K.29 Geological setting of the  $1855 \pm 2$  Ma Toby Intrusion (group III) and Wilagee Intrusion (group II), Halls Creek Orogen, Western Australia. Minor PGE-bearing chromitites are hosted by troctolitic rocks in a cyclic mafic-ultramafic sequence in the Wilagee Intrusion. Modified from Hoatson (2000).

### **Major references(s)**

Hoatson, D.M., 2000. Geological setting, petrography, and geochemistry of the Palaeoproterozoic layered mafic-ultramafic intrusions. In: Hoatson, D.M. and Blake, D.H. (editors), *Geology and economic potential of the Palaeoproterozoic layered mafic-ultramafic intrusions in the East Kimberley, Western Australia*. Canberra: Australian Geological Survey Organisation Bulletin 246, 99–162.

Sanders, T.S., 1999. Mineralization of the Halls Creek Orogen, east Kimberley region, Western Australia. Geological Survey of Western Australia, Report 66 and Appendix, 44 pp.

### **Relevant figure(s)**

Figure 6.9, Figure 8.20, Figure 8.21, Figure 8.22, Figure 8.23, and Appendix Figure K.29.

## **K.1.203 Togo 5A**

(see Alice Downs 3 group)

## **K.1.204 Tollu**

(see Halleys–Blackstone)

## **K.1.205 Tom Tit, Jason**

### **Geological province**

Paterson Orogen.

### **Location**

Tom Tit: 122.230870°E, -22.590020°S; Rudall (SF 51–10), Rudall (3352); ~98 km south-southwest of Telfer.

Jason: 122.226700°E, -22.569760°S; Rudall (SF 51–10), Rudall (3352); ~95 km south-southwest of Telfer.

### **Classification**

- ?8. Hydrothermal-Metamorphic.

### **Geological setting**

Platinum-group-element mineralisation is known at Tom Tit and Jason within fragments of an ultramafic body in the Talbot Terrane of the Rudall Complex. The ultramafic rocks form several small lenses of metamorphosed serpentinite in the Talbot Terrane, and are associated with orthogneiss. The ultramafic rocks appear to represent a dismembered and deformed peridotitic slice of a larger ultramafic body of possible komatiitic affinity (Carr, 1989; Ferguson et al., 2005).

### **PGE mineralisation**

The Tom Tit and Jason PGE prospects are hosted in metaserpentinite reported to contain strongly anomalous Pt (1.99 ppm to 6.65 ppm) in drill-holes (North West Oil and Minerals Co NL, 1971). However, these results could not be reproduced by Blockley (1971). Carr (1989) in his study of the

## Western Australia

ultramafic rocks in the Rudall River area reported a range of Pt and Pd values from a minimum of 0.82 ppb Pt and 0.75 ppb Pd, to a maximum of 151.51 ppb Pt and 261.6 ppb Pd.

### ***Age of mineralisation***

Mineralisation in Archean host rocks.

### ***Current status***

Exploration site.

### ***Economic significance***

Occurrence.

### ***Major references(s)***

Blockley, J.G., 1971. A reported platinum find in the Rudall River area. Geological Survey of Western Australia Annual Report 1971. Geological Survey of Western Australia, 59–60.

Carr, H.W., 1989. The geochemistry and platinum group element distribution of the Rudall River ultramafic bodies, Paterson Province, Western Australia. BSc. Honours thesis, University of Western Australia, Perth, Australia, 126 pp.

Ferguson, K.M., Bagas, L. and Ruddock, I., 2005. Mineral occurrences and exploration potential of the Paterson area. Western Australia Geological Survey, Report 97, 43 pp.

North West Oil Co NL, 1971. Progress report Rudall River platinum. WAMEX report A19707 11 pp.

### ***Relevant figure(s)***

## **K.1.206 Toorare Pool**

(see Munni Munni group)

## **K.1.207 Tregurtha\***

(see Carr Boyd Rocks\*)

## **K.1.208 Vidure\***

(see Malbec—Cabernet)

## **K.1.209 Wannaway\***

(see Otter—Juan Kambalda\* group)

## **K.1.210 Waterloo, Amorac\***

### ***Geological province***

Yilgarn Craton.

### **Location**

Waterloo: 120.977997°E, -28.143770°S; Leonora (SH 51–01), Wildara (3041); ~36 km southeast of Leinster.

Amorac\*: 120.984703°E, -28.149469°S; Leonora (SH 51–01), Wildara (3041); ~38 km southeast of Leinster and 900 m southeast of Waterloo.

### **Classification**

- 3. Komatiitic flows and sill-like intrusions; 3.A. Massive, matrix, and disseminated Ni-Cu-PGE sulphides in preferred lava pathways.

### **Geological setting**

LionOre Mining International Limited reported in their 2004 Annual Report that the Waterloo deposit lies on the eastern limb of a tightly folded ultramafic unit in a synclinal structure at the southern end of the Yandal greenstone belt. The Ni sulphide mineralisation is associated with the basal contact of a serpentinised ultramafic unit, with the footwall region dominated by metasedimentary rocks. The host ultramafic rocks appear to have been truncated at depth by a large flat-dipping shear zone.

The deposit has been outlined over a strike length of almost 900 m and the dip extent ranges from 50 m to 70 m. The basal ultramafic contact generally dips moderately toward the west, steepening with depth and locally dragged back into a flat east dip along the top of the underlying shear zone.

### **PGE mineralisation**

Mineral resources as published by LionOre Mining International Limited in 2004 was 299 000 t of indicated resources @ 3.5% Ni, 0.26% Cu and 1.13 g/t PGEs, and 354 000 t of inferred resources @ 2.2% Ni, 0.14% Cu and 0.63 g/t PGEs. The latest figures published for the deposit by LionOre in 2006 did not give any data on the PGE content. LionOre reported in 2004 that there are four main styles of sulphides at Waterloo: massive, matrix, disseminated, and remobilised stringer and breccia-types. Disseminated sulphides lie stratigraphically above matrix sulphides, while the majority of the high-grade massive sulphides appear to be localised in the vicinity of the fold structure, which plunges shallowly to the south. The tenor of the sulphide typically ranges between 7% and 10% Ni and contains significant concentrations of Cu and PGEs.

### **Age of mineralisation**

Archean host rocks.

### **Current status**

Care and maintenance.

### **Economic significance**

Historical mine with current resources.

### **Major references(s)**

LionOre Mining International Limited, 2004. LionOre Mining International Limited 2004 Annual Report, 50 pp.

LionOre Mining International Limited, 2006. LionOre Mining International Limited 2006 Annual Report, 99 pp.

### **Relevant figure(s)**

Figure 6.21.

## **K.1.211 Weld Range PGE, Weld Range East PGE, Weld Range West PGE, Range Well Group, Range Well (Cr, PGE)**

### **Geological province**

Yilgarn Craton.

### **Location**

Weld Range PGE: 117.726997°E, -26.854521°S; Belele (SG 50–11), Madoonga (2444); ~66 km north-northwest of Cue.

Weld Range East PGE: 117.818510°E, -26.828560°S.

Weld Range West PGE: 117.701290°E, -26.869830°S.

Range Well Group: 117.726997°E, -26.854521°S.

Range Well (Cr, PGE): 117.761597°E, -26.832279°S.

### **Classification**

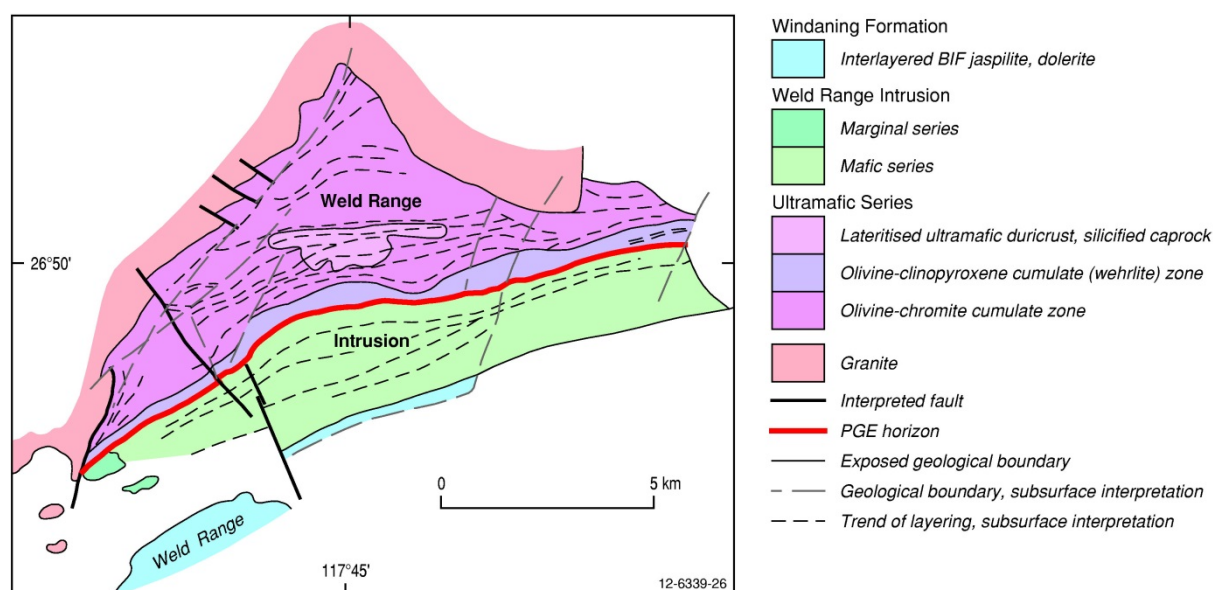
- 1. Layered tholeiitic mafic-ultramafic intrusions; 1A. Stratabound PGE-bearing sulphide layers (Weld Range PGE (has a PGE resource), Weld Range East PGE, Weld Range West PGE);
- 9. Regolith-Laterite; 9A. PGE-bearing regolith developed on ultramafic-mafic igneous rocks (Range Well Cr, PGE).

### **Geological setting**

The Gnanagooragoo Igneous Complex (~2740 Ma) at Weld Range comprises a northeast-trending intrusive mafic-ultramafic intrusion up to 8 km-thick with the sequence younging from north to south. It is located between the Yalgowra Suite to the southeast and the Annean Supersuite to the northwest (Parks, 1998; Van Kranendonk and Ivanic, 2008; Ivanic et al., 2010). The triangular-shaped complex consist of a lower ultramafic series up to 5 km-thick and an overlying mafic series up to 3.5 km-thick (Appendix Figure K.30). The ultramafic series is rhythmically layered, whereas the mafic series appears to be mostly massive. The ultramafic sequence comprises a lower olivine-chromite zone and an overlying wehrlite zone. The first appearance of cumulus clinopyroxene marks the base of the wehrlite zone, which is up to 500 m-thick.

The olivine-chromite zone consists mostly of olivine-chromite cumulates and subordinate chromite-olivine cumulates and olivine adcumulates. No discrete chromitite layers or chromite adcumulates have been observed. Rock types are typically mesocumulate to adcumulate with original interstitial material consisting of orthopyroxene, clinopyroxene, and plagioclase, with rare biotite. The wehrlite zone, which hosts PGE mineralisation, consists of fine- to medium-grained (1 mm–2 mm) olivine- and clinopyroxene-bearing cumulates. Mesocumulate to adcumulate types dominate.

The compositions of olivine and chromite as determined from electron-microprobe analyses of fresh drill-hole samples from near the basal margin of the intrusion do not conclusively determine the parental magma affinities of the complex, but show that it is most closely related to komatiites and layered intrusions.



Appendix Figure K.30 Geological map of the Archean Weld Range Intrusion, Yilgarn Craton, Western Australia. The PGE-enriched sulphide horizon at the contact between the Ultramafic Series and Mafic Series shows similarities in stratigraphic position and lateral continuity to the mineralised porphyritic websterite layer in the Munnii Munnii Intrusion in the west Pilbara Craton (see Figure 6.4). Modified from Parks (1998).

### PGE mineralisation

PGE mineralisation has been identified within a laterally persistent olivine-clinopyroxenite unit with a strike length of 15 km and in the overlying regolith. An inferred resource has been estimated for the supergene part of the deposit. The hard-rock mineralisation remains open at depth and for a further 4 km of strike length.

Primary mineralisation: The primary PGE mineralisation at Weld Range is hosted by a clinopyroxene-olivine cumulate and less commonly by a pegmatoidal clinopyroxene-(olivine) orthocumulate, in the upper part of the wehrlite zone (Appendix Figure K.30). The mineralised zone, as defined by grades in excess of 1 g/t combined precious metals, has a true thickness of 13 m to 18 m with its top 8 m–17 m below the gabbro contact. Widely spaced drilling has determined the persistence of this layer over 11 km of strike length to a depth of 250 m.

The upper part of the mineralised zone contains minor sulphides, but sulphides are absent in the lower part of the zone and the footwall to the mineralisation cannot be identified visually. The sulphides are dominantly chalcopyrite (90%) with subordinate pentlandite (mostly metamorphic), bornite, pyrrhotite, violarite, pyrite, gersdorffite (NiAsS), sphalerite, and possible vallerite [ $2(\text{Fe,Cu})_2\text{S}_2 \cdot 3(\text{Mg,Al})(\text{OH})_2$ ] and millerite.

High-grade mineralisation has also been intersected within a 0.7 m-thick (true thickness) pegmatoidal unit, located near the base of the main mineralised zone in the central part of the intrusion. Values to 10.2 g/t Pd, 8.2 g/t Pt, 1.2 g/t Rh, 0.62 g/t Ir, 0.22 g/t Ru, 0.05 g/t Os, and 230 ppm Cu were obtained. The pegmatoid consists of 60% clinopyroxene and tremolite pseudomorphs after clinopyroxene, which form interlocking tabular grains up to 2 cm-long, containing numerous inclusions of pale-brown hornblende. Ore minerals in the pegmatoid consist mainly of spottily distributed 1-cm diameter intergrowths of bornite with minor magnetite, pyrite, pentlandite, ilmenite, chalcopyrite, tremolite needles and trace amounts of galena, sphalerite, chromite, and PGMs. Qualitative analyses of the PGMs using a scanning-electron microscope identified 10  $\mu\text{m}$  diameter grains of moncheite [ $\text{Pt}(\text{Te,Bi})_2$ ] associated with chalcopyrite-magnetite intergrowths, and possible taimyrite

[(Pt,Pd,Cu)<sub>3</sub>(Sn,Sb)]. The PGMs are largely located within chalcopyrite and less commonly pentlandite. The taimyrite is the most common PGM, and it occurs as stubby tabular grains up to 110 µm in diameter, containing inclusions of bornite and rarely tremolite. Another variety of moncheite [(Pt,Pd)Te<sub>2</sub>], osmium metal, and possible acanthite [(Ag,Cu,Fe)S] were also identified.

Supergene mineralisation: Platinum, Pd, and Au are dispersed into a subhorizontal enrichment zone in the saprolite above the primary wehrlite zone with the depth of weathering 45 m–50 m in the vicinity of the supergene mineralisation.

The residual laterite profile has been eroded and covered by 2 m to 20 m of lateritic gravel over the mineralised zone. Gold is concentrated above a Fe-paleoredox front in the upper saprolite, consistent with the weathering behaviour of Au elsewhere. Platinum and Pd have nearly identical dispersions and are concentrated about 10 m below this front in the lower saprolite above a Mn-paleoredox front, which contains up to 2% Mn oxides. Harrison (1993) attributes the Pt and Pd distribution to chemical adsorption onto the Mn oxides.

### **Age of mineralisation**

Age of host rocks ~2740 Ma from intrusive rock relationships (Van Kranendonk and Ivanic, 1998; Ivanic et al., 2010).

### **Current status**

Historical exploration site.

### **Economic significance**

Parks (1998) published an inferred resource for the supergene PGE mineralisation in the residual laterite profile as outlined in Appendix Table K.40 below.

*Appendix Table K.40 Inferred resource for supergene PGE mineralisation in the residual laterite profile at Weld Range. Data from Parks (1998).*

Cutoff Pt+Pd+Au (g/t)	Pt (g/t)	Pd (g/t)	Au (g/t)	Mt (g/t)	Combined Pt+Pd+Au (g/t)	Combined Pt+Pd+Au (ounces)
0.50	0.6	0.5		14.76	1.1	522 000
0.75	0.8	0.6		9.53	1.4	429 000
1.00	0.9	0.7		6.30	1.6	324 000
2.00	1.5	1.1	0.1	1.38	2.7	120 000

In 2009, Dragon Mining Limited published a chromite resource hosted in the lateritic rocks developed over the Weld Range mafic-ultramafic rocks totalling 63.5 Mt @ 5.2% Cr, 38.1% Fe, and 0.38% Ni (Dragon Mining Limited, 2009).

### **Major references(s)**

- Parks, J., 1998. Weld Range platinum group element deposit. In: Berkman, D.A. and Mackenzie, D.H. (editors), 1998. *Geology of Australian and Papua New Guinean Mineral Deposits*. The Australasian Institute of Mining and Metallurgy, Melbourne, Monograph 22, 279–286.
- Dragon Mining Limited, 2009. *Dragon Mining Limited 2009 Annual Report*, 108 pp.
- Harrison, B.C., 1993. *Precious metals in the supergene environment, Weld Range, Western Australia*. BSc Honours thesis, The University of Western Australia, Perth, Western Australia, Australia.

Ivanic, T.J., M. T. D., Wingate, M.T.D., Kirkland, C.L., Van Kranendonk, M.J. and Wyche, S., 2010. Age and significance of voluminous mafic–ultramafic magmatic events in the Murchison Domain, Yilgarn Craton. *Australian Journal of Earth Sciences*, 57, 597–614.

Van Kranendonk, M.J. and Ivanic, T.J., 2010. A new lithostratigraphic scheme for the northeastern Murchison Domain, Yilgarn Craton. In: *Annual Review 2007–08*, Western Australia Geological Survey, 35–53.

### ***Relevant figure(s)***

Figure 8.11 and Appendix Figure K.30.

## **K.1.212 Western Zone\***

(see Lamboo group)

## **K.1.213 White Rock Well 3**

### ***Geological province***

Halls Creek Orogen.

### ***Location***

White Rock Well 3: 127.959600°E, -17.635310°S; Dixon Range (SE 52–06), McIntosh (4462); ~72 km north-northeast of Halls Creek.

### ***Classification***

- 12. Others (minor or unknown economic importance); 12.E. Others (unknown geological setting).

### ***Geological setting***

This PGE occurrence appears to lie near the northern end of the Wild Dog Creek Gabbro Intrusion comprising large homogeneous sheet-like gabbroic bodies in the central zone of the Halls Creek Orogen (Hoatson, 2000). It is not clear if the prospect is hosted by the Wild Dog Creek Gabbro Intrusion or by another mafic intrusion.

### ***PGE mineralisation***

The occurrence comprises weathered pyroxenite with up to 5% malachite (GSWA MINEDEX database). Some chemical analyses published for magnetite gabbro from the Wild Dog Creek Gabbro Intrusion by Hoatson (2000: p. 124) show only low concentrations of Pd (2.5 ppb) and Pt (2.3 ppb). Freeport (1986) reported that several pyroxene-gabbro sills were located several kilometres south-southeast of the White Rock Well with Cu gossans up to a few hundred metres in length overlying weathered pyroxenite. Chrysocolla, malachite, and sometimes abundant magnetite were reported to occur in weathered pyroxenite. Chip sampling across the Cu gossans and rock samples from basal pyroxenite generally returned PGE values of <0.005 ppm—the detection limit at the time. However, Pd values from the northern end of the sills were in the range of 0.595 ppm to 1.06 ppm (Stadler, 1985).

### ***Age of mineralisation***

The Wild Dog Creek Gabbro Intrusion was probably emplaced between 1843 Ma and 1830 Ma (Hoatson, 2000: p. 124).

### ***Current status***

Historical exploration site.

### ***Economic significance***

Occurrence.

### ***Major references(s)***

Hoatson, D.M., 2000. Geological setting, petrography, and geochemistry of the Palaeoproterozoic layered mafic-ultramafic intrusions. In: Hoatson, D.M. and Blake, D.H. (editors), *Geology and economic potential of the Palaeoproterozoic layered mafic-ultramafic intrusions in the East Kimberley, Western Australia*. Canberra: Australian Geological Survey Organisation Bulletin 246, 99–162.

Stadler, C., 1985. Alice Downs joint venture Annual Report, Exploration Licence E80/122 4 October 1984–3 October 1985. Freeport of Australia Incorporated. Geological Survey Western Australia WAMEX report A16587, 27 pp.

### ***Relevant figure(s)***

## **K.1.214 Wildcat–Baron**

(see also Breakaway, Curlew, Shrike)

### ***Geological province***

Yilgarn Craton.

### ***Location***

Wildcat–Baron: 117.435560°E, -29.058092°S; Ninghan (SH 50–07), Ninghan (2339); ~34 km northwest of Paynes Find.

### ***Classification***

- ?1. Layered tholeiitic mafic-ultramafic intrusions; ?1.A. Stratabound PGE-bearing sulphide layers.
- 9. Regolith-Laterite; 9.A. PGE-bearing regolith developed on ultramafic-mafic igneous rocks.

### ***Geological setting***

The prospect is located on the eastern limb of the Archean Warriedar greenstone belt, a succession of mafic and ultramafic lavas and intrusives, sedimentary rocks, and felsic volcanic and intrusive rocks.

The mafic rock sequences comprise tholeiitic basalt and gabbro, with some units displaying differentiated horizons of peridotite and some clinopyroxenite. Occasional chert, jaspilitic BIF horizons, and sediments indicate that much of the sequence is extrusive. Conformably overlying the mafic sequence is a package of felsic schist and volcanogenic rocks, with lesser intercalated ultramafic horizons and minor BIF.

Detailed geological mapping and aeromagnetic imaging identified the layering of the mafic-ultramafic intrusive—the Baron Intrusive Complex—approximately 9.0 km in length (Royal Resources Limited, 2006).

### ***PGE mineralisation***

Routine analyses for Pt and Pd in drill sampling of Au in a laterite soil anomaly, about 1 km north of the Baron Rothschild Au prospect, returned an intercept of 6 m @ 0.7 g/t Pt+Pd at the bottom of drill-hole PYB009. A number of adjacent holes also returned anomalous PGE values. A more detailed soil sampling program subsequently identified a large amplitude Pt+Pd anomaly extending for a distance of 2.2 km to the east of the discovery hole (Royal Resources Limited, 2006).

The main exploration target is the contact between the ultramafic (pyroxenite) and mafic (gabbro) transition with disseminated PGE mineralisation occurring within the gabbro. The prospective mafic-ultramafic contact extends over a distance of 9 km and has anomalous soil values of up to 185 ppb Pt and 55 ppb Pd. Five reverse circulation drill-holes have tested this prospect identifying strong PGE anomalism in both weathered and fresh gabbro—drill-hole BNRC005 intersected 48 m of 0.55 ppm Pt+Pd (Royal Resources Limited, 2006). Only 800 m of the pyroxenite/gabbro contact has been tested by drilling. A number of areas have been identified for further assessment including an area where airborne magnetics data indicate a zone of folding of the mafic-ultramafic contact and where soil geochemistry has identified a moderate Pt+Pd anomaly.

### ***Age of mineralisation***

#### ***Current status***

Exploration sites.

#### ***Economic significance***

Occurrences.

#### ***Major references(s)***

Royal Resources Limited, 2006. Royal Resources Limited 2006 Prospectus, 28 February, 2006, 85 pp.

#### ***Relevant figure(s)***

Appendix Figure K.1.

## **K.1.215 Windimurra Resources Group\***

(see Wondinong group)

## **K.1.216 Wondinong, Corner Well, Narndee, Milgoo**

(PGE occurrences associated with the Windimurra and Narndee igneous complexes)

### ***Geological province***

Yilgarn Craton.

### ***Location***

Wondinong: 118.360294°E, -28.008045°S; Kirkalocka (SH 50–03), Challa (2541); ~52 km east of Mt Magnet.

Corner Well: 118.483716°E, -28.557727°S; Kirkalocka (SH 50–03), Coolamaninu (2540).

## Western Australia

Muleryon Hill: 118.383496°E, -28.573454°S; Kirkalocka (SH 50–03), Coolamaninu (2540).

Narndee: 118.125110°E, -28.895420°S; Kirkalocka (SH 50–03), Coolamaninu (2540); ~60 km northeast of Paynes Find.

Milgoo: 118.12639°E, -28.8946°S; Kirkalocka (SH 50–03), Coolamaninu (2540).

Windimurra Resources Group\*: 118.529959°E, -28.291621°S.

### **Classification**

- 1. Layered tholeiitic mafic-ultramafic intrusions; 1.A. Stratabound PGE-bearing sulphide layers, and 1.B. Stratabound PGE-bearing chromitite layers.

### **Geological setting**

All of the prospects are located around the Windimurra and Narndee igneous complexes in the northwest region of the Yilgarn Craton (see Section 8.4.3). The Windimurra Igneous Complex measures ~85 km north-south and ~37 km east-west with an area of about 2300 km<sup>2</sup> in the form of a flat-lying lopolith. From base to top the igneous stratigraphy comprises:

- border facies of coarse-grained gabbro interpreted as the chilled margins to the complex;
- basal ultramafic series of poorly exposed serpentinitised olivine and chromite cumulates;
- lower series of layered anorthositic gabbronorite and olivine gabbro. This series is faulted by the 500 m-thick Shephards Discordant Zone, which extends for over 50 km in strike and includes significant vanadiferous magnetite mineralisation;
- middle series of magnetite gabbronorite that shows well-defined igneous layering, and includes the Canegrass layered magnetite zone; and
- upper series of magnetite olivine gabbro.

Layered ultramafic and gabbroic rocks of the Narndee Igneous Complex, southwest of the Windimurra Igneous Complex, are exposed over ~700 km<sup>2</sup> in a broad synclinal keel. The complex comprises two main series, the Milgoo Layered Series (MLS) in the northwest and the Kockalocka layered series (KLS) in the south and east. The MLS consists of a poorly exposed sequence of peridotite, pyroxenite, and gabbronorite extensively intruded by co-magmatic sills and dykes. The MLS dips approximately 50°–70° to the east comprising a 3600 m-thick basal unit of layered olivine-bearing pyroxenite and norite, and an upper unit of 1800 m of gabbronorite. Mafic dykes and sills that are equated with the upper unit extensively intrude the basal unit of the MLS. The KLS is a cyclically layered, ultramafic to mafic series, that defines a north-plunging syncline. The contact between these two series is not exposed, but a primary magmatic relationship, with the KLS forming a stratigraphically higher sequence to the MLS, is inferred from the more evolved mineral compositions in the KLS and higher proportion of ultramafic rocks in the MLS.

The contact between the MLS and the KLS has been interpreted as a low-angle thrust fault, with the MLS thrust south over the KLS. Archean felsic volcanics and granitoids were interpreted to form an upper thrust sheet emplaced over both series (Ivanic, 2009; Ivanic et al., 2010).

### **PGE mineralisation**

PGE-sulphide mineralisation is found in both the Windimurra and Narndee igneous complexes. However, PGE geochemistry reveals that a significant quantity of sulphides have segregated at depth, leaving the higher structural levels of the igneous complexes that are exposed at the surface relatively depleted in Pt and Pd. Copper and Ni are not significantly depleted, but no resources have

been found to date. In the Milgoos area at Narndee, Ni-Cu mineralisation is present in ultramafic lithologies where it is linked to a suite of cross-cutting leucogabbro sheets. Several chromitites and chromite dunites within the Windimurra Igneous Complex are thin and relatively Cr poor (Ivanic, 2009).

Wondinong: located in the northwest end of the Windimurra Igneous Complex. Most significant PGE values are from 7 rock-chip samples of poddy and disseminated chromite mineralisation in dunite units of the lower series with analytical results of up to 3.15 ppm Pt, 4.3 ppm Pd, 380 ppb Rh, and 340 ppb Ru (Apex Minerals NL, 2002). A 1-m-thick intersection in diamond drill-hole WO-2 assayed 1.2 ppm Pd and 0.76 ppm Pt.

Corner Well: located at the southern end of the Windimurra Igneous Complex. Rock-chip sampling indicated high background PGEs in gabbro of 35 ppb Pt, 40 ppb Pd, and one lherzolite sample with 1.3 g/t Pt+Pd+Au.

Milgoos: located in the Narndee Igneous Complex. Sampling and drilling at various locations south of Milgoos yielded up to 20 ppb Pd in stream samples; costean samples with up to 605 ppb Pt, 180 ppb Pd, 0.39% Ni, and 0.56% Cr; trench samples with up to 51 m @ 42 ppb Pt, 309 ppb Pd, 0.21% Ni, 0.18% Cr, and 0.04% Cu; and 1 m @ 0.33% Ni, 0.12% Cu, 5.16 ppm Pd in drill-hole N0005.

### ***Age of mineralisation***

A SHRIMP U-Pb zircon and baddeleyite age of gabbro (Boodanoo Suite; sample 191056) from the Narndee Igneous Complex, which is host to the Narndee–Milgoos prospect, is  $2800 \pm 6$  Ma (Ivanic et al., 2010). In the literature, the Windimurra Igneous Complex has generally been referred to having a crystallisation age of between 2810 Ma to 2800 Ma based on a Sm-Nd age of  $\sim 2.8$  Ga for the Windimurra Igneous Complex (unpublished data: Ahmat and Fletcher) and stratigraphic similarities with the  $2800 \pm 6$  Ma Narndee Igneous Complex.

### ***Current status***

Exploration site.

### ***Economic significance***

Occurrence.

### ***Major references(s)***

Apex Minerals NL, 2002. Apex Minerals NL 2002 Prospectus. Australian Securities Exchange, 100 pp.

Apex Minerals NL, 2003. Apex Minerals NL 2003 Annual Report. Australian Securities Exchange.

Ivanic, T.J., 2009. The Windimurra and Narndee mafic-ultramafic intrusions: mineralization and geological context. Geological Survey of Western Australia, Record 2009/2, 4–6.

Ivanic, T.J., Wingate, M.T.D., Kirkland, C.L., Van Kranendonk, M.J. and Wyche, S., 2010. Age and significance of voluminous mafic–ultramafic magmatic events in the Murchison Domain, Yilgarn Craton. Australian Journal of Earth Sciences, 57, 597–614.

### ***Relevant figure(s)***

Figure 8.11, Figure 8.12, and Figure 8.20.

## **K.1.217 Yakabindie Group\***

(see Mt Keith\*)

## K.1.218 Yamarna PGE 1, Yamarna PGE 2

### ***Geological province***

Yilgarn Craton.

### ***Location***

Yamarna PGE 1: 123.646500°E, -28.172034°S; Rason (SH 51–03), Dorothy Hills (3641); ~132 km east-northeast of Laverton.

Yamarna PGE 2: 123.645767°E, -28.170621°S; Rason (SH 51–03), Dorothy Hills (3641).

The Point Salvation\* occurrence as described by Hoatson and Glaser (1989) appears to be an earlier location name for Yamarna PGE 1 and Yamarna PGE 2.

### ***Classification***

- ?1. Layered tholeiitic mafic-ultramafic intrusions; 1.B. Stratabound PGE-bearing chromitite layers.
- ?3. Komatiitic flows and related sill-like intrusions.

### ***Geological setting***

The Yamarna PGE 1 and 2 prospects occur near the western margin of the Yamarna–Mount Gill greenstone belt near its western boundary marked by the north-northwest-trending regional Yarmana shear zone (Romano et. al., 2008). A map by Eleckra Mines Limited shows an easterly dipping sequence consisting from west to east of plagioclase cumulate, olivine cumulate hosting chromitite seams, followed by metamorphosed sediments and mafic volcanic rocks (Eleckra Mines Limited, 2008). Reports by CRA Exploration Pty Limited noted that the sequence at the prospects from west to east comprised 'plagioclase cumulate, ultramafic (talc chlorite magnetite schist), chromitite, ultramafic (talc chlorite magnetite schist) ultramafic (cumulate texture), chromitite, amphibolite and metasediments, pyroxenite' (Atkinson, 1978).

### ***PGE mineralisation***

Historical drilling targeted chromitite float within an ultramafic unit west of the Yamarna homestead and identified up to six seams of medium- to high-grade chromitite grading up to 30% Cr<sub>2</sub>O<sub>3</sub> over a 2 m-wide interval, and weak PGE mineralisation of up to 0.2 g/t Pt and 0.82 g/t Pd over 0.9 m. More recent analyses of drill-hole samples obtained by CRA Exploration Pty Limited at Yamarna PGE 1 returned 7.5 m @ 8.4% Cr<sub>2</sub>O<sub>3</sub>, including 2 m @ 17.5% Cr<sub>2</sub>O<sub>3</sub>; and 0.9 m @ 0.82 ppm Pd, 0.2 ppm Pt (Eleckra Mines Limited, 2008).

At Yamarna PGE 2, CRA drill-holes intersected 6 chromitite seams with best results of 1.85 m @ 20% Cr<sub>2</sub>O<sub>3</sub>; 0.55 m @ 0.14 ppm Pt; and 2.23 m @ 0.11 ppm Pd (Eleckra Mines Limited, 2008).

### ***Age of mineralisation***

PGE-bearing chromitite seams hosted in metamorphosed Archean ultramafic rocks.

### ***Current status***

Historical exploration site.

### ***Economic significance***

Occurrence.

### **Major references(s)**

- Atkinson, W.J., 1978. Final report on mineral claims 38/7513-7527 Yamarna chromite prospect, Rason, W.A. CRA Exploration Pty Limited, Geological Survey Western Australia, WAMEX A10285, 25 pp.
- Eleckra Mines Limited, 2008. Quarterly activities report for the three months ended 31 December, 2007, 14 pp.
- Hoatson, D.M. and Glaser, L.M., 1989. Geology and economics of platinum-group metals in Australia. Bureau of Mineral Resources, Australia, Resource Report 5, 81 pp.
- Romano, S.S., Pawley, M.J., Hall, C.E., Doublier, M.P., Wingate, M.T.D. and Wyche, S., 2008. Granite-greenstone associations of the Yamarna-Irwin Hills region, northeastern goldfields: the broader context. Geological Survey of Western Australia, Record 2008/2, 20–22.

### **Relevant figure(s)**

## **K.1.219 Yarawindah Brook, Yarawindah 2, Yarawindah PMA**

### **Geological province**

Yilgarn Craton.

### **Location**

Yarawindah Brook: 116.261597°E, -31.090179°S; Perth (SH 50–14), Chittering (2135); ~135 km north-northeast of Perth.

Yarawindah (PMA): 116.233240°E, -31.115570°S; Perth (SH 50–14), Chittering (2135); ~17 km south of New Norcia.

Yarawindah (2): 116.266440°E, -31.095010°S; Perth (SH 50–14), Chittering (2135); ~15 km south-southeast of New Norcia.

### **Classification**

Inferred resource in the residual and supergene zones is classified:

- 9. Regolith-Laterite; 9.A. PGE-bearing regolith developed on ultramafic-mafic igneous rocks.

Mineralisation in the primary zone is classified:

- 8. Hydrothermal-Metamorphic; 8.C. Magmatic breccias involving mafic, ultramafic, and felsic igneous rocks.

### **Geological setting**

A differentiated layered mafic-ultramafic complex has intruded gneiss of the Jimperding metamorphic belt (Appendix Figure K.31). The complex has been interpreted as a composite body comprising several smaller intrusions, several of which also form concordant satellite bodies in the country rocks and along the eastern margin of the main complex (Hoatson and Glaser, 1989). Mineralisation has been defined in the supergene and primary zones of an intensively metamorphosed and structurally dislocated mafic-ultramafic sill (Appendix Figure K.31, Appendix Figure K.32, and Appendix Figure K.33).

Within the prospect area, the mafic-ultramafic body comprises gabbro-norite to harzburgite composition, amphibolite and serpentine rock types. The intrusion strikes north-northwest and is interpreted as being overturned, with a dip to the east of between 20° and 30°. The intrusion can be

divided into three zones—lower mafic, middle ultramafic, and upper mafic (Al Manyard and Associates, 2006). Modelling of the geophysical data suggests that the longest continuous strike of the contact zone is ~7 km, of which 1650 m has been drilled (Washington Resources Limited, 2007).

### ***PGE mineralisation***

An inferred resource was estimated for the Yarawindah Brook deposit in 1989, totalling 2.9 Mt @ 0.79 g/t PGEs in near surface oxidised material (saprolite)—giving a Pt+Pd content of 73 657 ounces (Cornelius 1989). Drilling in 1976 delineated values of up to 3 ppm Pd, 0.4 ppm Pt, and 1.0 ppm Au in sulphide-rich plagioclase cumulate amphibolites and hanging wall metaquartzite. Resampling of the drill-core confirmed anomalous PGEs, e.g., 0.5 m @ 2.6 ppm Pt, 0.36 ppm Pd, and an extended wide zone of 28 m @ 0.35 ppm Pd in the intrusive rocks (Hoatson and Glaser, 1989). Ore minerals recorded in GSWA MINEDEX database were sperrylite and michenerite.

Further drilling was carried out during December 2005 to March 2007 to test the supergene zone at the southern end of the deposit with some of the better drill intersections listed in Appendix Table K.41 (Washington Resources Limited, 2006, 2007).

Sulphides are present throughout the entire mafic-ultramafic sequence, but are most abundant in high-MgO amphibolite and tremolite serpentinite. Relatively high-grade pods of PGEs are present in the fresh rock and appear to lack lateral continuity, although there is insufficient drilling data to allow correlation. Primary magmatic and remobilised sulphides identified include chalcopyrite, pyrrhotite, pyrite, and pentlandite.

### ***Age of mineralisation***

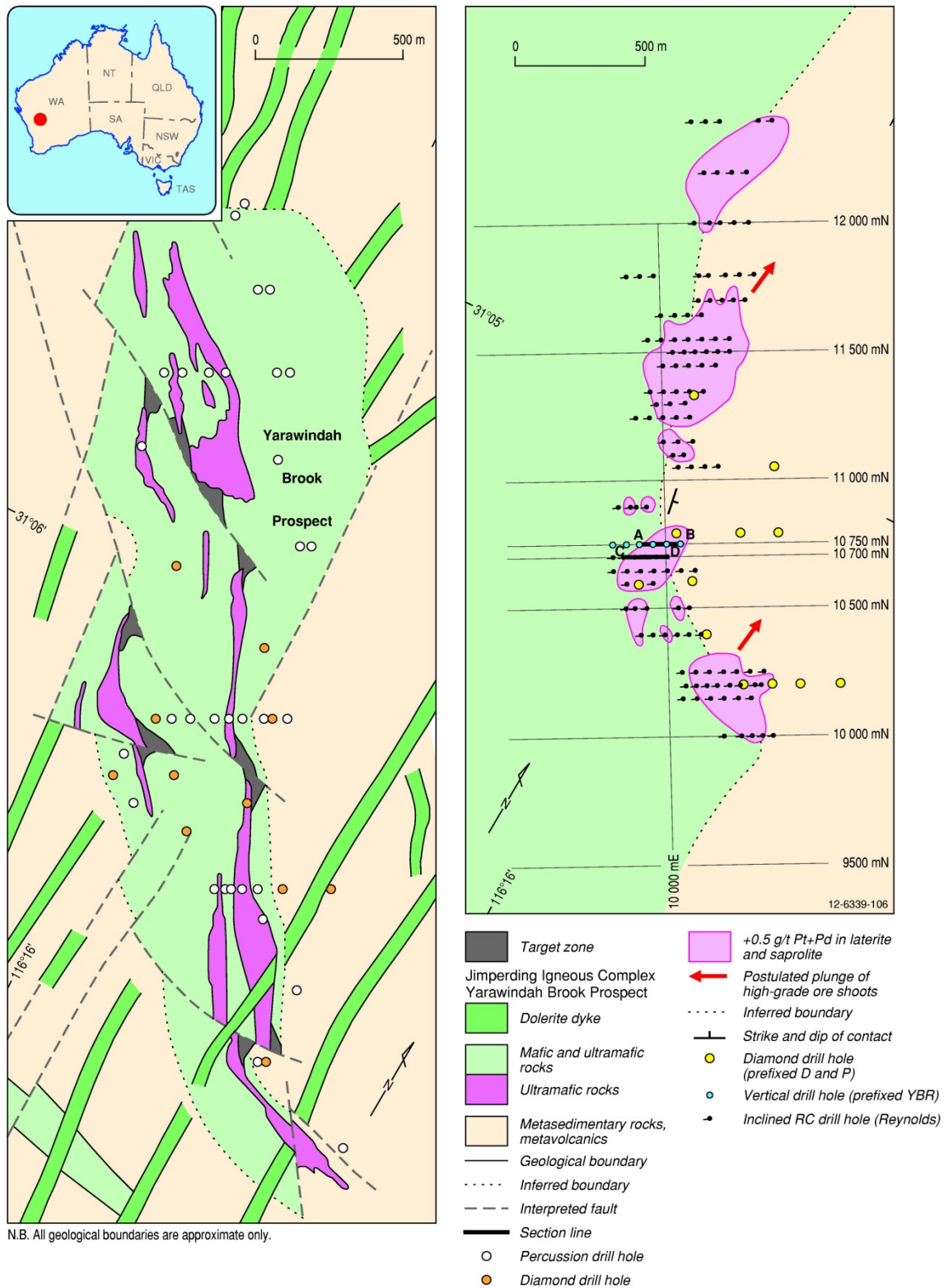
?Archean (primary) and Cenozoic (supergene-laterite).

### ***Current status***

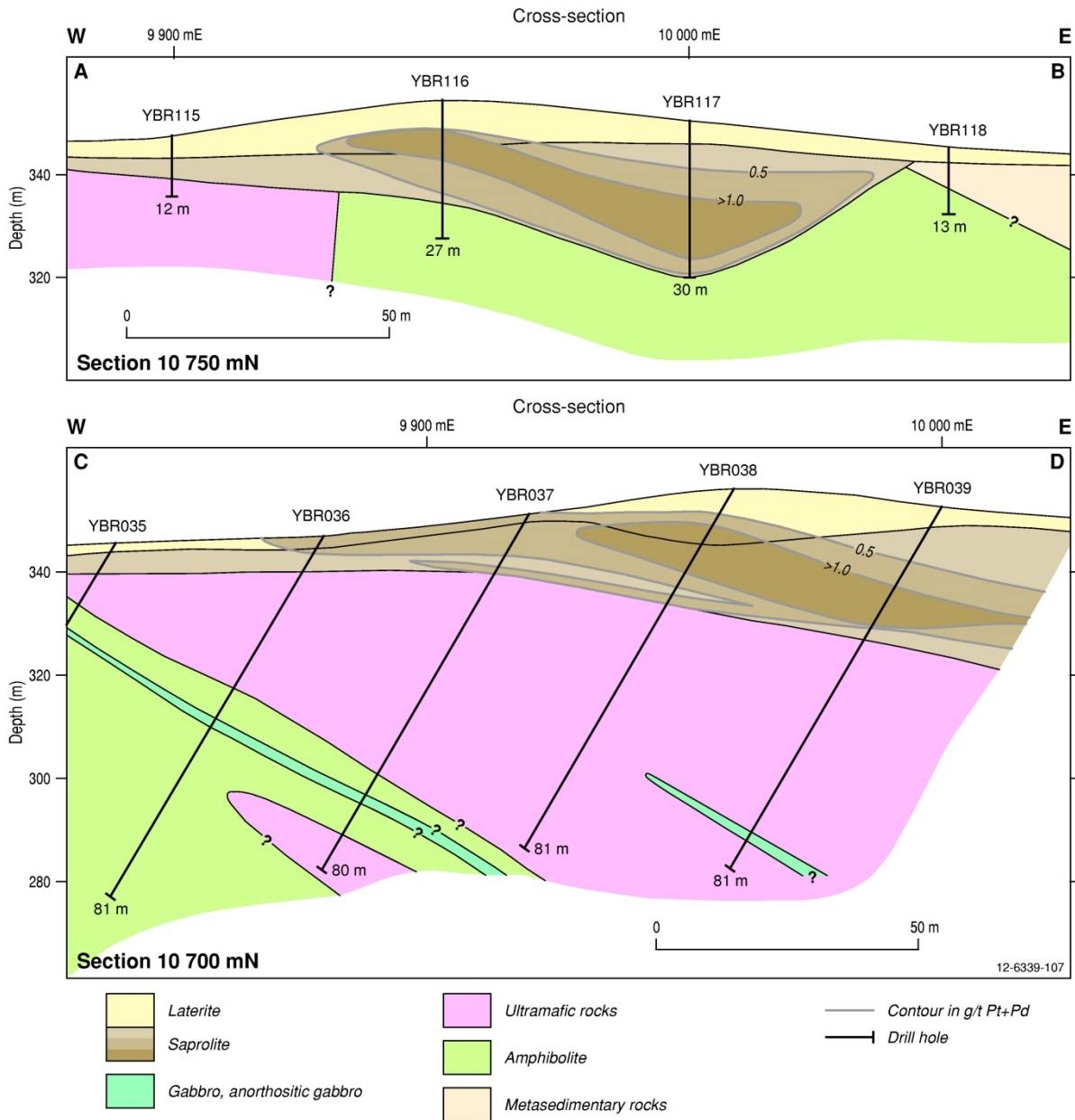
Exploration sites.

### ***Economic significance***

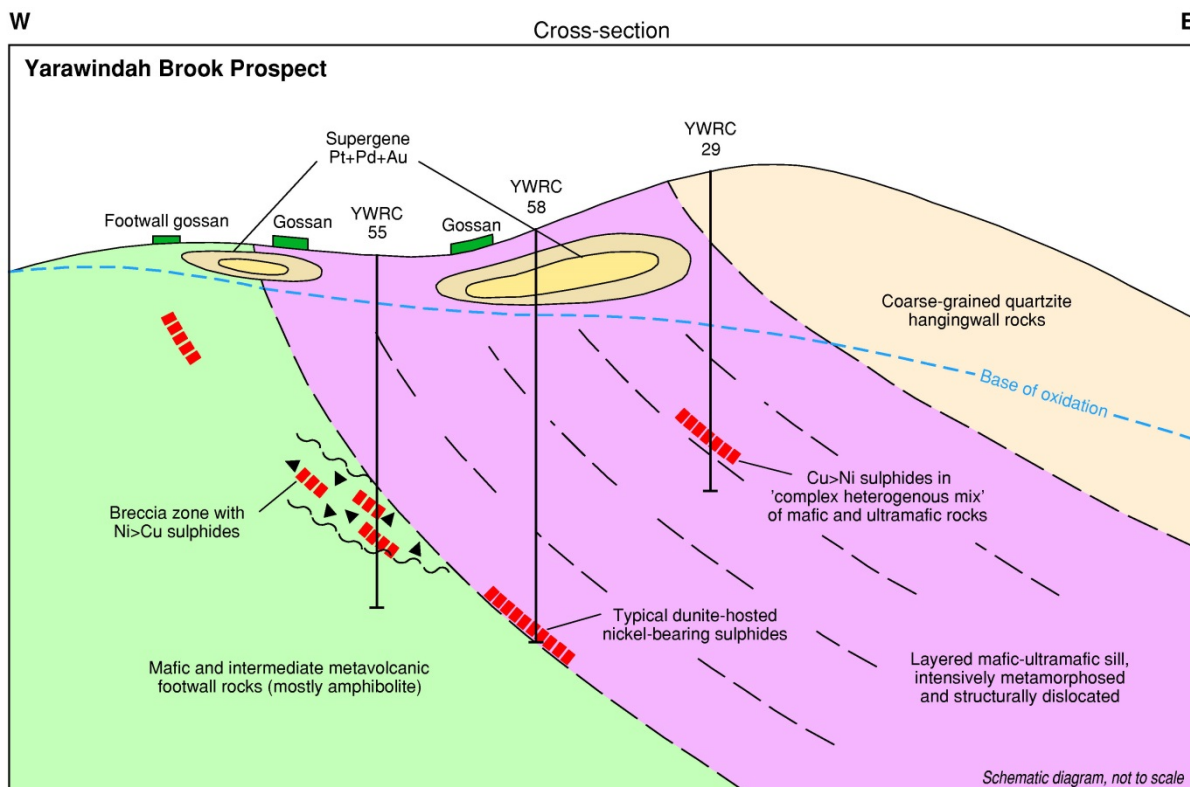
Small deposit.



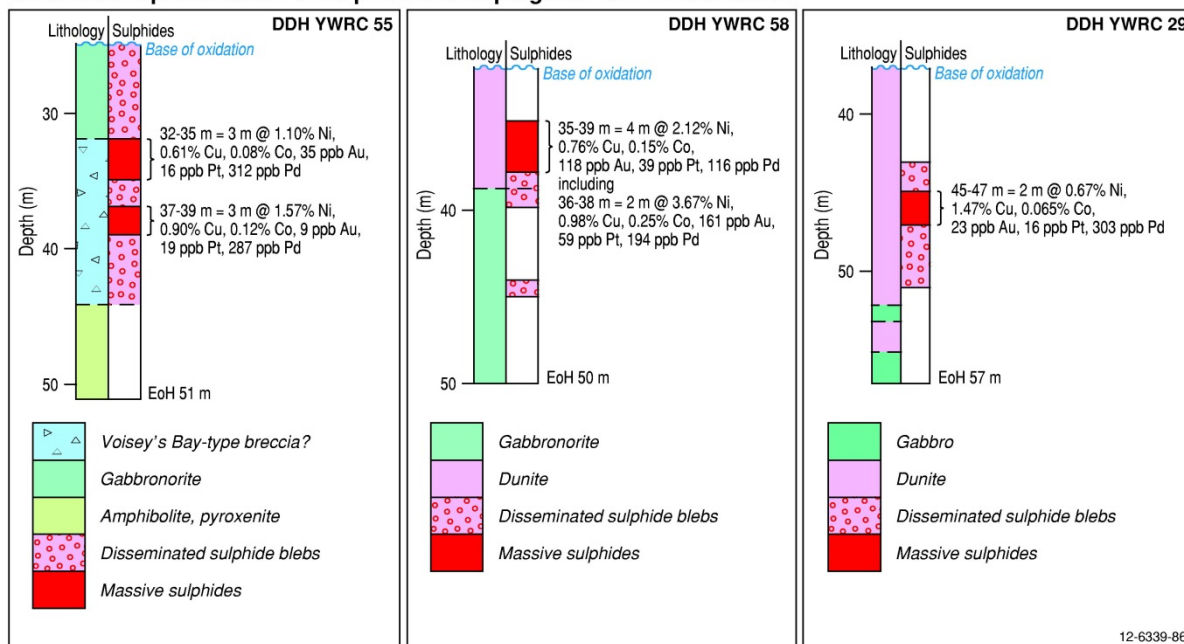
Appendix Figure K.31 Detailed geological setting and mineralised zones of the Yarawindah Brook PGE Ni-Cu prospect, Yilgarn Craton, Western Australia. The mineralised zones shown are from the northern part of the intrusion. Modified from Washington Resources Limited (2005).



Appendix Figure K.32 Schematic cross-sections A–B (Line 10 750 mN) and C–D (Line 10 700 mN) in the Yarawindah Brook PGE Ni-Cu prospect, Yilgarn Craton, Western Australia. Both cross-sections highlight the PGE mineralisation in the saprolite zone of the laterite profile. The locations of sections A–B and C–D are shown in right-hand diagram of Appendix Figure K.31. Modified from Washington Resources Limited (2005).



**Schematic representation of sulphide and supergene PGE mineralisation**



Appendix Figure K.33 Schematic cross-section summarising the spatial distribution of different types of sulphide and supergene PGE-Ni-Cu-Co mineralisation in the Yarawindah Brook prospect, Yilgarn Craton, Western Australia. Bottom figure shows the geology and major intersections for DDH YWRC 55, DDH YWRC 58, and DDH YWRC 29. Modified from Washington Resources Limited (2006).

Appendix Table K.41 Selected drill-hole intersections from the southern Yarawindah Brook deposit. Data from Washington Resources Limited (2006, 2007).

Drill-hole	Interval (m)	Width (m)	Ni (%)	Cu (%)	Co (ppm)	Au+Pd+Pt (ppm)
YWRC1	15–20	5	0.2636	0.2992	514	0.186
YWRC2	25–30	5	0.3352	0.1957	628	0.120
YWRC2	35–40	5	0.3782	0.1761	325	0.083
YWRC3	20–25	5	0.2990	0.3982	3193	0.341
YWRC3	25–30	5	0.3480	0.2743	925	0.342
YWRC10	30–35	5	0.3541	0.2551	476	0.139
YWRC21	15–20	5	0.3253	0.3107	3061	0.308
YWRC22	15–20	5	0.3242	0.1670	628	0.141
YWRC29	45–50	5	0.4767	1.0078	466	0.233
YWRC055	37–39	2	1.57	0.9	1163	0.314
YWRC058	35–39	4	2.12	0.76	1453	0.27
including	from 36 m	2	3.67	0.97		
YWRC83	77–81	4	1.67	0.29	739	0.543
including	78–79	1	2.89	0.54	1274	0.605
YWRC94	76–79	3	0.73	0.52	434	0.630
including	76–77	1	1.23	0.4	735	1.204
YWRC97	95–97	2	0.26	0.9	384	0.927

### Major references(s)

- Al Maynard and Associates, 2006. Independent Geologist's Report. In: Washington Resources Limited Prospectus 2006, 31–58.
- Cornelius, M., 1989. Report on RC drilling programme Yarawindah PGE prospect E 70/320 Western Australia (Volume 1). Reynolds Aust. Metals Limited. WAMEX report A28765.
- Hoatson, D.M. and Glaser, L.M., 1989. The geology and economics of platinum-group metals in Australia. Bureau of Mineral Resources, Australia, Resource Report 5, 81 pp.
- Washington Resources Limited, 2006. Yarawindah drilling progress. Washington Resources Limited announcement to the Australian Securities Exchange, 18 January 2006, 2 pp.
- Washington Resources Limited 2007, Escalating metals portfolio 2007. Exploration portfolio summary sent to shareholders 2 November 2007, 26 pp.

### Relevant figure(s)

Appendix Figure K.31, Appendix Figure K.32 and Appendix Figure K.32.

## K.1.220 Yellowdine\*

### Geological province

Yilgarn Craton.

### Location

Location uncertain.

Yellowdine\*: 119.6616°S, -31.2863°E; Southern Cross (SH 50–16), Yellowdine (2835); ~34 km east-southeast of Southern Cross.

### **Classification**

- ?3. Komatiitic flows and related sill-like intrusions.

### **Geological setting**

The Yellowdine prospect encompasses a Cu-Ni-bearing metaperidotitic segment of a large ultramafic complex along the eastern margin of a granite dome. The layered mafic complex also has potential for by-product Pt, Pd, and Au. Deeply weathered serpentinite, mafic volcanics, tremolite-chlorite schist, BIF, and metasediments are the major rock types (Hoatson and Glaser, 1989).

### **PGE mineralisation**

Minor Au production has been derived from ferruginised serpentinite and quartz veining at the southern end of the prospect. Exceptionally high Pt values, up to 200 ppm, were reported at depths of 30 m, near the base of a 1.5 km-long ultramafic unit (Hoatson and Glaser, 1989).

### **Age of mineralisation**

Archean host rocks.

### **Current status**

Historical exploration site.

### **Economic significance**

Occurrence.

### **Major references(s)**

Hoatson, D.M. and Glaser, L.M., 1989. Geology and economics of platinum-group metals in Australia. Bureau of Mineral Resources, Australia, Resource Report 5, 81 pp.

### **Relevant figure(s)**

## **K.1.221 Yornup South (Cr)**

### **Geological province**

Yilgarn Craton.

### **Location**

Yornup South: 116.186040°E, -34.097090°S; Pemberton (SI 50–10), Manjimup (2129); ~16 km south-southeast of Bridgetown.

### **Classification**

- ?3. Komatiitic flows and related sill-like intrusions; ?3.B. Disseminated Ni-Cu-PGE sulphides in central parts of thick dunite bodies.

### ***Geological setting***

The Yornup South (Cr) prospect is associated with zones of small mafic-ultramafic bodies located within the Balingup metamorphic belt in the South West Terrane of the Yilgarn Craton. In the Yornup area, lensoidal ultramafic rocks are enclosed within felsic paragneiss intercalated with BIF and mafic amphibolite. The metamorphic rocks are multiply deformed and intruded by syn- to post-tectonic granitoids (Morant, 1988). Drilling at Yornup indicated a succession of serpentinised dunite, peridotite, and pyroxenite with subordinate intercalated gabbroic (metagabbro to metanorite) rocks (Cameron, 1990). Rock types described by Cornelius et al. (1987) include lherzolite, harzburgite, dunite, and olivine-gabbro-norite. The basement rocks, including the mafic-ultramafics, are extensively concealed by an eroded laterite profile. The mafic-ultramafic rocks were considered to represent tectonically dismembered bodies of a previously much larger intrusive body which Harrison (1986) interpreted as Bushveld type, however, Cornelius et al. (1987) interpreted them as sills with komatiitic affinities similar to the Dumont sill in the Abitibi greenstone belt of Canada.

### ***PGE mineralisation***

The Yornup South (Cr) prospect was explored in the late 1970s to late 1980s for chromite and for its possible potential for PGEs. Cameron (1990) reported that bleg sampling (bulk leach extractable Au) in the Bridgetown–Yornup area returned values of up to 3.1 ppb Pd and 3.9 ppb Pd. According to Cameron (1990) these values were higher than bleg values from stream samples draining the known PGE mineralised area over the Munni Munni Intrusion, and were considered to be highly anomalous. Morant (1988) noted that diamond drilling of ultramafic bodies in South Yornup area did not reflect chromite-rich segregations similar to those in ultramafic intrusions east of Bridgetown. In the Yornup South area the Cr appears to be dominantly in disseminated Cr-spinels with background levels of ~0.5% Cr in the serpentinites. Anomalous concentrations of Pt and Pd of up to 53 ppb and 80 ppb, respectively, were recorded in weathered ultramafics (Morant, 1988).

### ***Age of mineralisation***

Unknown. According to Hoatson et al. (2009a,b), the ultramafic bodies hosting the Yornup South (Cr) prospect are part of unassigned metamorphosed mafic and ultramafic layered mafic intrusions of the Narndee Magmatic Event (2800 Ma, U-Pb SHRIMP zircon and baddeleyite).

### ***Current status***

Historical exploration site.

### ***Economic significance***

Occurrence.

### ***Major references(s)***

- Cameron, G.H., 1990. Exploration potential of the Bridgetown/Yornup Donnelly River area. Hunter Resources Limited. WAMEX report A29958, 23 pp.
- Cornelius, M., Stumpf, E.F., Gee, D. and Prochaka, W., 1987. Platinum group elements in mafic-ultramafic rocks of the western gneiss terrain, Western Australia. *Mineralogy and Petrology* (1987) 36, 247–265.
- Harrison, P.H., 1986. The mineral potential of the layered igneous complexes within the Western Gneiss Terrain. Geological Survey of Western Australia. Professional Papers for 1984, 19, 37–54.
- Hoatson, D.M., Jaireth, S., Whitaker, A.J., Champion, D.C. and Clauoué-Long, J.C., 2009a. Guide to Using the Australian Archean Mafic-Ultramafic Magmatic Events Map. Geoscience Australia Record 2009/41, 135 pp.

Hoatson, D.M., Jaireth, S., Whitaker, A.J., Champion, D.C. and Claoué-Long, J.C., 2009b. Australian Archean Mafic-Ultramafic Magmatic Events, Sheet 1 (1:5 000 000 scale map) and Sheet 2 (1:3 000 000 and 1:6 000 000 scale maps), Geoscience Australia, Canberra, GeoCat 69347. [http://www.ga.gov.au/metadata-gateway/metadata/record/gcat\\_69347](http://www.ga.gov.au/metadata-gateway/metadata/record/gcat_69347)

Morant, P., 1988. Yornup Prospect. Annual exploration report 1988. West Coast Holdings Limited. WAMEX report A24367, 22 pp.

### ***Relevant figure(s)***

## **K.1.222 Zanthus HMS**

### ***Geological province***

Eucla Basin.

### ***Location***

Zanthus HMS: 123.544985°E, -31.781826°S; Zanthus (SH 51–15), Noondiana (3634); ~80 km north-northwest of Balladonia.

### ***Classification***

- 10. Placers; 10.C. Alluvial placers.

### ***Geological setting***

The prospect is located in a major Cenozoic paleodrainage system which was infilled during transgressive events in the Eocene, Oligocene, and Miocene periods. Lithologies include fluvial and littoral facies sandstones; lignite and lignitic claystones; and marginal marine to marine sediments including claystone, sandstone, and some limestone. A lignite seam averaging about 9 m–12 m in thickness and 400 m to 1000 m in width is inferred to occur over a strike length in excess of ~30 km. Overburden thickness is mostly less than 30 m (Robinson, 1993).

Mineral sand units occur both beneath and above the lignitic zone. The interpreted source area for these sandstones is the ultramafic Fraser Complex several km west of the prospect area which may potentially provide a source for Au and PGEs in addition to a normal suite of heavy minerals (ilmenite, rutile, zircon: Robinson, 1993).

### ***PGE mineralisation***

The target commodity for exploration in the prospect area was lignite, but the sandstone unit (Te11 in report by Robinson, 1993) overlying the lignite zone was investigated for heavy-mineral potential. The sandstone unit formed during the first Eocene transgression and was considered to have the greatest potential for economic placer mineralisation (Robinson, 1993). Drill-hole Z112 assayed 5 m (down-hole depths of 52 m–57 m) @ 3.54% heavy minerals, 5 ppb Au, and 9 ppb Pt; and 2 m (down-hole depths of 57 m–59 m) @ 0.34% heavy minerals, 0.15 g/t–0.18 g/t Au, 4 ppb Pd, and 15 ppb Pt (Robinson, 1993).

### ***Age of mineralisation***

Eocene?

### ***Current status***

Historical exploration site.

Western Australia

***Economic significance***

Occurrence.

***Major references(s)***

Robinson, P.F., 1993. Combined annual reports GSWA REF M 6654/1, Zanthus project. E28/296 and E69/312 to 8/4/93. Sabminco NL, 137 pp.

***Relevant figure(s)***

**K.1.223 Zen\***

(see Haran)

## K.2 NORTHERN TERRITORY

### K.2.1 Airstrip

#### **Geological province**

Pine Creek Orogen.

#### **Location**

Airstrip: 132.49784°E, -13.49211°S; Mount Evelyn (SD 53–05), Mundogie (5371).

#### **Classification**

- 8. Hydrothermal-Metamorphic; 8.F. Unconformity-type U-Au-PGEs.

#### **Geological setting**

The Airstrip occurrence is one of a large number of U-bearing mineral occurrences associated with the Rockhole–El Sherana–Palette fault system in the South Alligator Valley uranium field. The mineralisation occurs as breccia fill and stockwork zones. The host rocks are siltstone and sandstone of the Koolpin Formation. The mineralised zone strikes 315°.

#### **PGE mineralisation**

Platinum, Pd, and Au are reported.

#### **Age of mineralisation**

Unknown. May be contemporaneous with U-Au mineralisation at Coronation Hill dated as  $1607 \pm 26$  Ma (Orth et al., 2014). LA-ICPMS  $^{207}\text{Pb}/^{206}\text{Pb}$  ages from uraninite from El Sherana gave  $1573 \pm 160$  Ma (Chiple et al., 2007).

#### **Current status**

Abandoned mine.

#### **Economic significance**

Occurrence.

#### **Major references(s)**

- Chiple, D., Polito, P. and Kyser, K.T., 2007. Measurement of U-Pb ages of uraninite and davidite by laser ablation-HR-ICP-MS. *American Mineralogist*, 92, 1925–1935.
- Lally, J.H. and Bajwah, Z.U., 2006. Uranium deposits of the Northern Territory. Northern Territory Geological Survey Report 20, 87 pp.
- MODAT (available upon request from the Northern Territory Geological Survey: <http://www.nt.gov.au>)
- Orth, K., Meffre, S. and Davidson, G., 2014. Age and paragenesis of mineralisation at Coronation Hill uranium deposit, Northern Territory, Australia. *Mineralium Deposita*. DOI 10.1007/s00126-013-0501-4.

## **Relevant figure(s)**

### **K.2.2 Baldrick**

#### **Geological province**

Arunta Orogen.

#### **Location**

Baldrick: 135.45289°E, -23.27665°S; Illogwa Creek (SF 53–15), Quartz (5951).

#### **Classification**

- 8. Hydrothermal-metamorphic; 8.D. Structurally-controlled remobilised Ni-Cu-PGE sulphides in mafic-ultramafic±felsic dykes/veins in shear zones.

#### **Geological setting**

Subsequent to the discovery of the Blackadder Ni-Cu-PGE deposit in 2008, regional prospecting identified a number of other similar prospects in the Irindina Province of the Arunta Orogen, including the Baldrick prospect which is located ~1.2 km to the northeast of Blackadder. This prospect is also hosted by gabbroic rocks of the  $409 \pm 9$  Ma Lloyd Gabbro, near a contact with metasedimentary rocks. The Lloyd Gabbro comprises olivine-bearing gabbro and gabbronorite that have high-MgO contents (17% to 24%) with associated anomalous Ni, Cu, Cr, and Co. La/Sm ranges from 1.9 to 2.2 that may indicate a small amount of crustal contamination (Whelan et al., 2009, 2010). Rock-chip samples from Baldrick returned assays of up to 0.78% Ni, 23.2% Cu, 0.8 g/t Pt+Pd+Au, and 25.5 g/t Ag. Reverse circulation drill-holes collared in 2009 returned up to 9 m @ 0.48% Ni and 0.37% Cu.

#### **PGE mineralisation**

The highest reported grade is 0.8 g/t Au+Pt+Pd in a rock chip.

#### **Age of mineralisation**

U-Pb SHRIMP geochronology on magmatic zircons from gabbronorite (Lloyd Gabbro) that hosts the Baldrick and Blackadder Ni-Cu-PGE prospects yield a concordia age of  $409 \pm 9$  Ma. Inherited grains with ages ranging from 1701 Ma to 1760 Ma and  $\epsilon_{Nd} = +0.7$  suggest some crustal contamination (Whelan et al., 2010; Beyer et al., 2013).

#### **Current status**

Exploration site.

#### **Economic significance**

Occurrence.

#### **Major references(s)**

Beyer, E.E., Hollis, J.A., Whelan, J.A., Glass, L.M., Donnellan, N., Yaxley, G., Armstrong, R., Allen, C. and Scherstén, A., 2013. Summary of results. NTGS laser ablation ICPMS and SHRIMP U-Pb, Hf and O geochronology project: Pine Creek Orogen, Arunta Region, Georgina Basin and McArthur Basin, July 2008–May 2011. Northern Territory Geological Survey Record 2012/007.

Whelan, J.A., Close, D.F., Scrimgeour, I.R. and Hallett, L., 2009. Magmatism and mineralisation in the Eastern Arunta, Central Australia: In: Williams P.J. (editor), 'Smart science for exploration and mining.' Proceedings of the 10th Biennial SGA Meeting, Townsville, 20 August 2009. Society for Geology Applied to Mineral Deposits.

Whelan, J.A., Hallett, L., Close, D.F. and Yaxley, G., 2010. Geochemical and isotopic constraints on mafic magmatism in the Irindina Province, eastern Arunta Region: implications for mineral prospectivity. Northern Territory Geological Survey Record 2010/003, 29–32.

**Relevant figure(s)**

### **K.2.3 Blackadder**

**Geological province**

Arunta Orogen.

**Location**

Black Adder: 135.44372°E, -23.28827°S; Illogwa Creek (SF 53–15), Quartz (5951).

**Classification**

- 8. Hydrothermal-metamorphic; 8.D. Structurally-controlled remobilised Ni-Cu-PGE sulphides in mafic-ultramafic±felsic dykes/veins in shear zones.

**Geological setting**

In 2008, follow-up of geological mapping by the Northern Territory Geological Survey in the Irindina Province of the Arunta Orogen identified a Ni-Cu gossan (Blackadder prospect) at the contact between an olivine-bearing gabbroic body and a metasediment. The mineralised host rock is the Lloyd Gabbro, which consists largely of olivine-bearing gabbro and gabbro-norite that have been dated at  $409 \pm 9$  Ma at the nearby Baldrick Ni-Cu-PGE deposit (Whelan et al., 2010; Beyer et al., 2013). These rocks preserve primary igneous textures and appear to be generally undeformed, with the exception of shearing at the contact with granulite-facies metasedimentary rocks of the Irindina Province. The Lloyd Gabbro has high-MgO contents (17% to 24%), with anomalous Ni, Cu, Cr, and Co. La/Sm ranges from 1.9 to 2.2, which may suggest a small amount of crustal contamination (Whelan et al., 2009). Initial rock-chip samples from Blackadder returned assays of up to 1.4% Ni, 4.2% Cu, 165 ppm Co, and 0.258 g/t Pt+Pd+Au. Subsequent rock-chip samples returned assays to 3.8% Ni, 9.8% Cu, and 1.7 g/t Pt+Pd+Au, and two reverse circulation drill-holes collared in 2009 returned up to 3 m @ 0.14% Ni. The first drill-hole at Blackadder (BARC002) intersected the upper contact of the targeted gabbroic body at 22 m and the basal contact at 52 m. Disseminated sulphide mineralisation was noted from 42 m increasing in intensity to 3%–5% stringer sulphides from 50 m to 52 m. The second drill-hole, collared 95 m to the east, intersected the gabbro between 21 m and 54 m. Traces of sulphides were present throughout the gabbro increasing to 3%–5% blebby sulphides (~5 mm in size) on the basal contact between 51 m and 54 m (Mithril Resources Limited, 2009).

**PGE mineralisation**

The highest reported PGE grade is 1.7 g/t Pt+Pd+Au in a rock chip, but typical grades are much lower, at most a few hundred ppb Pt+Pd+Au.

### ***Age of mineralisation***

U-Pb SHRIMP geochronology on magmatic zircons from gabbro (Lloyd Gabbro) that hosts the Baldrick and Blackadder Ni-Cu-PGE prospects yield a concordia age of  $409 \pm 9$  Ma. Inherited grains with ages ranging from 1701 Ma to 1760 Ma and  $\epsilon Nd = +0.7$  suggest some crustal contamination (Whelan et al., 2010; Beyer et al., 2013).

### ***Current status***

Exploration site.

### ***Economic significance***

Occurrence.

### ***Major references(s)***

Beyer, E.E., Hollis, J.A., Whelan, J.A., Glass, L.M., Donnellan, N., Yaxley, G., Armstrong, R., Allen, C. and Scherstén, A., 2013. Summary of results. NTGS laser ablation ICPMS and SHRIMP U-Pb, Hf and O geochronology project: Pine Creek Orogen, Arunta Region, Georgina Basin and McArthur Basin, July 2008–May 2011. Northern Territory Geological Survey Record 2012/007.

Mithril Resources Limited, 2009. Drilling update–Huckitta Project. Mithril Resources Limited announcement to the Australian Securities Exchange, 17 September 2009, 6 pp.

Whelan, J.A., Close, D.F., Scrimgeour, I.R. and Hallett, L., 2009. Magmatism and mineralisation in the Eastern Arunta, Central Australia: In: Williams P.J. (editor), 'Smart science for exploration and mining.' Proceedings of the 10th Biennial SGA Meeting, Townsville, 20 August 2009. Society for Geology Applied to Mineral Deposits.

Whelan, J.A., Hallett, L., Close, D.F. and Yaxley, G., 2010. Geochemical and isotopic constraints on mafic magmatism in the Irindina Province, eastern Arunta Region: implications for mineral prospectivity. Northern Territory Geological Survey Record 2010/003, 29–32.

### ***Relevant figure(s)***

## **K.2.4 Braveheart (Mordor)\***

(Orodrain also occurs within the Mordor Complex)

### ***Geological province***

Arunta Orogen.

### ***Location***

Braveheart: 134.48132°E, -23.46178°S; Alice Springs (SF 53–14), Laughlen (5751).

### ***Classification***

- 4. Alkaline mafic-ultramafic intrusions; 4.A. Stratabound and disseminated Cu-Au-PGE sulphides.

### ***Geological setting***

The Braveheart polymetallic prospect is hosted by porphyritic shonkinite on the southeastern margin of the ~1130 Ma Mordor Igneous Complex. This alkaline complex intrudes Paleoproterozoic tonalitic gneiss (Artunga Gneiss) and has an oval-shape at surface. The ultramafic rocks, which comprise

about 40% of the intrusive complex (eastern part), are dunitic to peridotitic in composition, and include olivine-augite, augite-olivine and augite-phlogopite-apatite-magnetite cumulates. Felsic rocks, which comprise 60% of the complex (western part), are composed mostly of phlogopite-rich syenite and shonkinite.

At Braveheart, the PGEs are hosted by a sulphide-rich zone within porphyritic shonkinite that dips 55° to the northwest and averaged 0.25% Cu over a 30 m-interval. The PGEs are associated with a sulphide assemblage including pyrrhotite, chalcopyrite, and pyrite. Petrophysical studies of core from this interval indicate that the mineralised zone is characterised by a strong EM response, elevated chargeability, and enhanced magnetic susceptibility.

### ***PGE mineralisation***

Grades of up to 0.5 g/t Pt+Pd+Au have been recorded over 1 m-intervals in a 30-m intersection grading 0.25% Cu.

### ***Age of mineralisation***

Claoué-Long and Hoatson (2005) obtained a U-Pb zircon age for a pyroxenite from the northeast corner of the complex of  $1133 \pm 5$  Ma, which is considered the best crystallisation age for the Mordor Igneous Complex. Previous attempts to date the complex include a Rb-Sr whole-rock isochron age of  $1128 \pm 20$  Ma and Rb-Sr mineral isochron age of  $1118 \pm 17$  Ma (Langworthy and Black, 1978, recalculated by Nelson et al., 1989), and a Sm-Nd whole-rock isochron age of  $1100 \pm 280$  Ma (Nelson et al., 1989).

### ***Current status***

Exploration site.

### ***Economic significance***

Occurrence.

### ***Major references(s)***

- Barnes, S.J., Anderson, J.A.C., Smith, T.R. and Bagas, L., 2008. The Mordor Alkaline Igneous Complex, central Australia: PGE-enriched disseminated sulfide layers in cumulates from a lamprophyric magma. *Mineralium Deposita*, 43, 641–662.
- Claoué-Long, J.C. and Hoatson, D.M., 2005. Proterozoic mafic–ultramafic intrusions in the Arunta Region, central Australia. Part 2: Event chronology and regional correlations. *Precambrian Research*, 142, 134–158.
- Langworthy, A.P. and Black, L.P., 1978. The Mordor Complex: a highly differentiated potassic intrusion with kimberlitic affinities in central Australia. *Contributions to Mineralogy and Petrology*, 67, 51–62.
- Nelson, D.R., Black, L.P. and McCulloch, M.T., 1989. Nd-Pb isotopic characteristics of the Mordor Complex, Northern Territory: Mid-Proterozoic potassic magmatism from an enriched mantle source. *Australian Journal of Earth Sciences*, 36, 541–551.

### ***Relevant figure(s)***

Figure 6.28, Figure 8.13, and Figure 8.17e.

## K.2.5 Casper\* (Attutra)

### **Geological province**

Arunta Orogen.

### **Location**

Casper: 136.36720°E, -22.64564°S; Huckitta (SF 53–11), Jervois Range (6152).

### **Classification**

- 2. Massive to poorly layered tholeiitic mafic-dominated intrusions; 2.B. Stratabound PGE-bearing magnetitite layers.

### **Geological setting**

The Casper Ti-V-PGE prospect is hosted by magnetite-bearing horizons within the ~1786 Attutra Metagabbro, which intrudes ~1807 Ma rocks of the Bonya Schist (Appendix Figure K.34). This north-trending body consists mostly of weakly recrystallised gabbro, magnetite-bearing gabbro, and massive stratabound magnetitite. Obvious cyclicity and or compositional layering is lacking.

Anomalous Au and PGE assays at Casper are associated with V-bearing magnetitite layers within the metagabbro. The reported assays (below) are part of a 47 m intersection of 0.13 g/t Pt, 0.43 g/t Pd, and 0.01 g/t Au.

### **PGE mineralisation**

Reported intersections include 32 m @ 0.14 g/t Pt and 0.23 g/t Pd; and 4 m @ 0.17 g/t Pt, 0.43 g/t Pd, and 0.03 g/t Au.

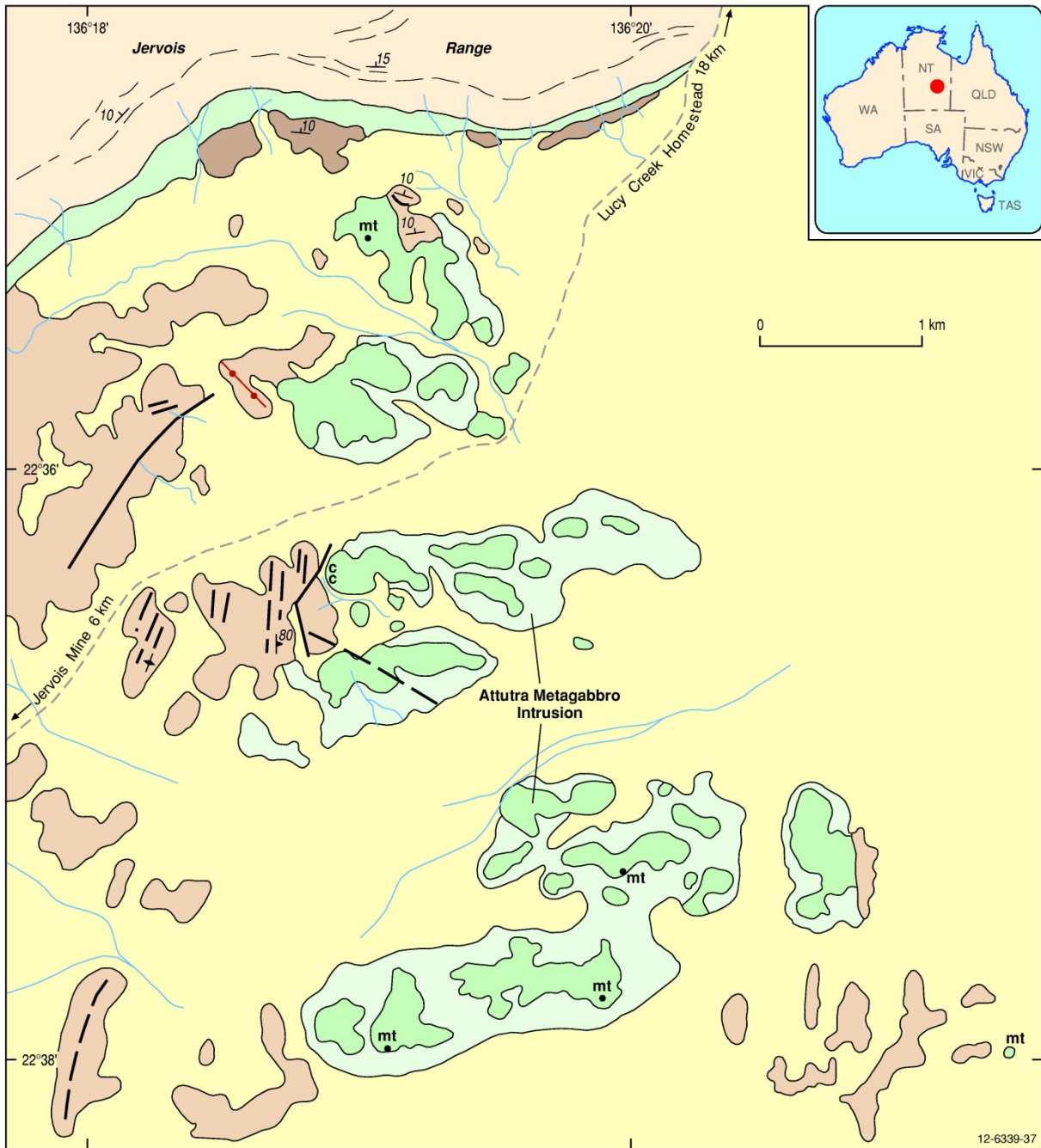
### **Age of mineralisation**

The geochronology sample was a chilled gabbro from the western margin of the intrusion on the basis of its high Zr content (153 ppm Zr) and it was found to contain abundant zircons (Claoué-Long and Hoatson, 2005). The zircons are of uniform appearance, with well defined euhedral crystal shapes and indistinct growth zoning consistent with igneous zircon crystallisation. The concordia diagram in Claoué-Long and Hoatson (2005) shows a homogeneous and concordant population of zircon compositions with only four discordant grains. The 34 concordant grains agree at a weighted mean  $^{207}\text{Pb}/^{206}\text{Pb}$  age of  $1786.4 \pm 4.2$  Ma for the Attutra Metagabbro Intrusion (Claoué-Long and Hoatson, 2005).

Current status: Exploration site.

### **Economic significance**

Occurrence.



- |  |   |   |
|--|---|---|
| <ul style="list-style-type: none"> <li><span style="display: inline-block; width: 15px; height: 10px; background-color: #ffffcc; border: 1px solid black; margin-right: 5px;"></span> Alluvium, colluvium, sandy soil</li> <li><span style="display: inline-block; width: 15px; height: 10px; background-color: #c8e6c9; border: 1px solid black; margin-right: 5px;"></span> Colluvium and scree on escarpment of Georgina Basin</li> <li><span style="display: inline-block; width: 15px; height: 10px; background-color: #e8f5e9; border: 1px solid black; margin-right: 5px;"></span> Ferruginous sandy soil and colluvium derived from Attutra Metagabbro</li> <li><b>Georgina Basin</b></li> <li><span style="display: inline-block; width: 15px; height: 10px; background-color: #ffe0b2; border: 1px solid black; margin-right: 5px;"></span> Grant Bluff Formation: quartz arenite, quartz greywacke</li> <li><span style="display: inline-block; width: 15px; height: 10px; background-color: #d7ccc8; border: 1px solid black; margin-right: 5px;"></span> Elyuah Formation: shale, silty sandstone, pebble conglomerate</li> </ul> | <ul style="list-style-type: none"> <li><b>Attutra Metagabbro Intrusion</b></li> <li><span style="display: inline-block; width: 15px; height: 10px; background-color: #c8e6c9; border: 1px solid black; margin-right: 5px;"></span> Gabbro, pyroxenite, PGE-bearing magnetite lenses (mt), chilled (c) against Bonya Schist</li> <li><span style="display: inline-block; width: 15px; height: 10px; background-color: #d7ccc8; border: 1px solid black; margin-right: 5px;"></span> Bonya Schist: metapelite, metapsammite, calc-silicate rock</li> <li><span style="display: inline-block; width: 15px; height: 10px; background-color: #ff0000; border: 1px solid black; margin-right: 5px;"></span> Dolerite dyke</li> <li><span style="display: inline-block; width: 15px; height: 10px; border-bottom: 1px solid black; margin-right: 5px;"></span> <math>\downarrow</math>10 Strike and dip of bedding</li> <li><span style="display: inline-block; width: 15px; height: 10px; border-bottom: 1px solid black; margin-right: 5px;"></span> <math>\downarrow</math>80 Strike and dip of foliation</li> <li><span style="display: inline-block; width: 15px; height: 10px; border-bottom: 1px solid black; margin-right: 5px;"></span> <math>\uparrow</math> Vertical foliation</li> </ul> | <ul style="list-style-type: none"> <li><span style="display: inline-block; width: 15px; height: 10px; border-bottom: 1px solid black; margin-right: 5px;"></span> Fault</li> <li><span style="display: inline-block; width: 15px; height: 10px; border-bottom: 1px dashed black; margin-right: 5px;"></span> Inferred fault</li> <li><span style="display: inline-block; width: 15px; height: 10px; border-bottom: 1px dotted black; margin-right: 5px;"></span> Trend line</li> <li><span style="display: inline-block; width: 15px; height: 10px; border-bottom: 1px solid blue; margin-right: 5px;"></span> Watercourse</li> <li><span style="display: inline-block; width: 15px; height: 10px; border-bottom: 1px dashed grey; margin-right: 5px;"></span> Track</li> </ul> |
|--|---|---|

Appendix Figure K.34 Geological map of the 1786 ± 4 Ma Attutra Metagabbro Intrusion, Arunta Orogen, Northern Territory. The isolated lenses and pods of magnetitite (mt) hosted in fractionated gabbroic rocks contain anomalous concentrations of PGEs. Modified from Freeman (1986) and Hoatson et al. (2005a).

### **Major references(s)**

- Claoué-Long, J.C. and Hoatson, D.M., 2005. Proterozoic mafic-ultramafic intrusions in the Arunta Region, central Australia. Part 2: Event chronology and regional correlations. *Precambrian Research*, 142, 134–158.
- Hoatson, D.M. and Stewart A., 2001. Field investigations of Proterozoic mafic-ultramafic in the Arunta Province, central Australia. *Geoscience Australia Record* 2001/39, 87 pp.
- Miezitis, Y., Jaireth, S. and Hoatson, D.M., 2006. Mineral potential modelling of Proterozoic mafic-ultramafic intrusions in the Arunta Region, central Australia. *Geoscience Australia Record* 2006/14, 56 pp.
- [www.arafuraresources.com.au](http://www.arafuraresources.com.au) (press release dated 26 April 2012).

### **Relevant figure(s)**

Figure 8.13, Figure 8.16a, and Appendix Figure K.34.

## **K.2.6 Casper**

### **Geological province**

Pine Creek Orogen.

### **Location**

Casper: 133.51554°E, -13.04629°S; Mount Marumba (SD 53–06), Mann River (5671).

### **Classification**

- 8. Hydrothermal-Metamorphic; 8.F. Unconformity-type U-Au-PGEs.

### **Geological setting**

The Casper occurrence is one of several prospects containing anomalous U that have been located in western Arnhem Land. These deposits are hosted by the Gumarrirrbang Sandstone of the Kambolgie Subgroup, close to the contact with the unconformably underlying Gilruth Volcanics. Uranium±PGE-Au enrichment is associated with clay in zones of intense fracturing. Mineralogically, native gold is associated with goethite and lepidocrocite.

### **PGE mineralisation**

The Casper prospect has assays to 236.5 g/t Au, 49.6 g/t Pt, and 8 g/t Pd.

### **Age of mineralisation**

Unknown.

### **Current status**

Exploration site.

### **Economic significance**

Occurrence.

### **Major references(s)**

- Ahmad, M., Wygralak, A.S., Ferenczi, P.A. and Scrimgeour, I.R., 2009. Gold deposits of the Northern Territory, second edition. Northern Territory Geological Survey Report 11, 131 pp.
- Drever, G., Thevissen, J. and Beckitt, G., 1998. Exploration Licences EL 5061 and EL 5062, Deaf Adder Project–Northern Territory, 1997 Annual Report. Cameco Australia Pty Limited. Northern Territory Geological Survey, Open File Company Report CR1998-0426.

### **Relevant figure(s)**

## **K.2.7 Coco\***

### **Geological province**

Arunta Orogen.

### **Location**

Coco: 136.36768°E, -22.63453°S; Huckitta (SF 53–11), Jervois Range (6152).

### **Classification**

- 2. Massive to poorly layered tholeiitic mafic-dominated intrusions; 2.B. Stratabound PGE-bearing magnetitite layers.

### **Geological setting**

The Coco Ti-V-PGE-Au prospect is hosted by magnetite-bearing horizons within the ~1786 Attutra Metagabbro, which intrudes ~1807 Ma rocks of the Bonya Schist. This north-trending body consists mostly of weakly recrystallised gabbro, magnetite-bearing gabbro, and massive stratabound magnetitite. Obvious cyclicity and/or compositional layering is lacking. At Coco, anomalous Au and PGE assays are hosted by V-Ti-rich magnetitite layers within the metagabbro.

### **PGE mineralisation**

The best reported result was 9 m (0 m–9 m) grading 0.14 g/t Pt, 0.17 g/t Pd, and 0.11 g/t Au. This was within a 13 m (0 m–13 m) grading 38.0% Fe, 0.9% V<sub>2</sub>O<sub>5</sub>, and 9.8% TiO<sub>2</sub>.

### **Age of mineralisation**

The geochronology sample was a chilled gabbro from the western margin of the intrusion on the basis of its high Zr content (153 ppm Zr) and it was found to contain abundant zircons (Claoué-Long and Hoatson, 2005). The zircons are of uniform appearance, with well defined euhedral crystal shapes and indistinct growth zoning consistent with igneous zircon crystallisation. The concordia diagram in Claoué-Long and Hoatson (2005) shows a homogeneous and concordant population of zircon compositions with only four discordant grains. The 34 concordant grains agree at a weighted mean <sup>207</sup>Pb/<sup>206</sup>Pb age of 1786.4 ± 4.2 Ma for the Attutra Metagabbro Intrusion (Claoué-Long and Hoatson, 2005).

### **Current status**

Exploration site.

### **Economic significance**

Occurrence.

### **Major references(s)**

- Clauoué-Long, J.C. and Hoatson, D.M., 2005. Proterozoic mafic–ultramafic intrusions in the Arunta Region, central Australia. Part 2: Event chronology and regional correlations. *Precambrian Research*, 142, 134–158.
- Hoatson, D. and Stewart, A., 2001. Field investigations of Proterozoic mafic-ultramafic in the Arunta Province, central Australia. *Geoscience Australia Record* 2001/39, 87 pp.
- Miezitis, Y., Jaireth, S. and Hoatson, D.M., 2006. Mineral potential modelling of Proterozoic mafic-ultramafic intrusions in the Arunta Region, central Australia. *Geoscience Australia Record* 2006/14, 56 pp.
- [www.arafuraresources.com.au](http://www.arafuraresources.com.au) (press release dated 26 April 2012).

### **Relevant figure(s)**

Figure 8.13 and Appendix Figure K.34.

## **K.2.8 Copper King**

### **Geological province**

Arunta Orogen.

### **Location**

Copper King: 134.65344°E, -23.12638°S; Alice Springs (SF 53–14), Riddoch (5851).

### **Classification**

- 8. Hydrothermal-Metamorphic.

### **Geological setting**

The Copper King prospect is one of several hydrothermal Cu-PGE-Au prospects hosted by the Bungintina Metamorphics near the structural contact with the Irindina Province. The Bungintina Metamorphics consist of 1770 Ma–1750 Ma pelitic to psammopelitic gneiss with lesser calc-silicate rock, marble, and quartzite. It is located 800 m to the southeast of the more substantial Kongo prospect.

### **PGE mineralisation**

Rock-chip samples to 0.1 g/t Pt, 4.8 g/t Pd, and 38.5 g/t Au.

### **Age of mineralisation**

Unknown.

### **Current status**

Exploration site.

### **Economic significance**

Occurrence.

### **Major references(s)**

Scrimgeour, I.R., 2013. Aileron Province. In: Ahmad, M. and Munson, T.H. (compilers), *Geology and Mineral Resources of the Northern Territory*. Northern Territory Geological Survey Special Publication 5, 12:1–12:65.

Whelan, J.A., Close, D.F., Scrimgeour, I.R., Beyer, E.E., Kositcin, N. and Armstrong, R.A., 2013. The Cu ± Au potential of the Arunta Region: Links between magmatism, tectonism, regional-scale alteration and mineralisation. *Northern Territory Geological Survey Record 2013/001*, 34–42.

### **Relevant figure(s)**

Figure 8.18h.

## **K.2.9 Copper Queen**

### **Geological province**

Arunta Orogen.

### **Location**

Copper Queen: 134.66991°E, -23.15368°S; Alice Springs (SF 53–14), Riddoch (5851).

### **Classification**

- 8. Hydrothermal-Metamorphic.

### **Geological setting**

Copper Queen is one of several hydrothermal Cu-PGE-Au prospects hosted by the Bungintina Metamorphics near the structural contact with the Irindina Province. The Bungintina Metamorphics consist of 1770 Ma–1750 Ma pelitic to psammopelitic gneiss with lesser calc-silicate rock, marble, and quartzite. Copper Queen is located 4.5 km to the southeast of the Kongo prospect.

The Copper Queen prospect consists of 600 m of semi-continuous malachite outcrop up to 1 m to 2 m in width. It is hosted by metasomatised calc-silicate gneiss containing massive garnet and epidote.

### **PGE mineralisation**

Rock-chip samples to 7.9 g/t Pt, 1.0 g/t Pd, 4.3 g/t Au, and 12% Cu.

### **Age of mineralisation**

Unknown.

### **Current status**

Exploration site.

### **Economic significance**

Occurrence.

### **Major references(s)**

- Scrimgeour, I.R., 2013. Aileron Province. In: Ahmad, M. and Munson, T.H. (compilers), *Geology and Mineral Resources of the Northern Territory*. Northern Territory Geological Survey Special Publication 5, 12:1–12:65.
- Whelan, J.A., Close, D.F., Scrimgeour, I.R., Beyer, E.E., Kositcin, N. and Armstrong, R.A., 2013. The Cu ± Au potential of the Arunta Region: Links between magmatism, tectonism, regional-scale alteration and mineralisation. *Northern Territory Geological Survey Record 2013/001*, 34–42.

### **Relevant figure(s)**

Figure 8.18h.

## **K.2.10 Coronation Hill, Rockhole\***

### **Geological province**

Pine Creek Orogen.

### **Location**

Coronation Hill: 132.60674°E, -13.58623°S; Mount Evelyn (SD 53–05), Stow (5470).

### **Classification**

- 8. Hydrothermal-Metamorphic; 8.F. Unconformity-type U-Au-PGEs.

### **Geological setting**

The Coronation Hill deposit in the South Alligator Valley uranium field is the best example of hydrothermal Au-PGE mineralisation associated with an unconformity-related U deposit. Although the U ore lenses contain anomalous levels of PGEs and Au, high-grade Au-PGE zones are spatially separated from the U-rich zones.

The Coronation Hill deposit and other nearby prospects are associated with the Rockhole–Palette Fault System near the unconformity between the overlying Coronation Sandstone of the El Sherana Group and pre-1860 Ma (Nimbuwah Event) basement. Coronation Hill is hosted in basement rocks, which include quartz-feldspar porphyry (Gerowie Tuff or intrusive), chloritic volcanic rocks (Shovel Billabong Andesite or Coronation Sandstone), quartz diorite (Zamu Dolerite), carbonaceous shale (Koolpin Formation), and sedimentary breccia (possibly Coronation Sandstone).

The deposit is associated with steeply south-dipping reverse faults and cross-cutting west-northwest-trending vertical faults and shears. It has a strike length of 250 m, is 50 m- to 100 m-wide, and it comprises several tabular bodies that are sub-parallel to north-northwest-trending faults. The mineralisation is present in fractures, microveinlets, quartz-carbonate-hematite veins and disseminated in the wall rock. The ores are sulphide-poor (pyrite >marcasite-pyrrhotite-sphalerite-chalcopyrite-galena), with Au associated with selenide minerals and/or pyrite. Fluid inclusion and stable isotope data suggest that metals were transported down from the unconformity by oxidised, acidic, Ca-rich brines that deposited metals by reaction with reduced rocks in the basement.

Primary mineralisation at Coronation Hill formed at  $1607 \pm 26$  Ma, and so it is likely that the South Alligator Valley region was part of a single west McArthur Basin dilational event. Most ore is hosted in sub-vertical faults and breccias in the competent volcanic cover sequence. This favoured fluid mixing,

acid buffering (forming illite), and oxidation of  $\text{Fe}^{2+}$  and reduced C-rich assemblages as important U-depositional mechanisms. However, reduction of U in fractured older pyrite (Pb model age of  $1833 \pm 67$  Ma) is an important trap in diorite. Some primary ore was remobilised at  $675 \pm 21$  Ma to form coarse uraninite+Ni-Co pyrite networks containing radiogenic Pb. Coronation Hill is polymetallic, and in this respect resembles the 'egress'-style U deposits in the Athabaskan Basin (Canada). However, these Canadian deposits are all cover-hosted. A hypothesis for further testing is that Coronation Hill is also 'egress'-style, with ores formed by fluids rising through basement-hosted fault networks (U reduction by diorite pyrite and carbonaceous shale), and into veins and breccias in the overlying Jawoyn Sub-basin volcanosedimentary succession (Orth et al., 2014).

### ***PGE mineralisation***

Coronation Hill has a pre-JORC indicated resource of 6.69 Mt grading 6.42 g/t Au, 0.30 g/t Pt, and 1.01 g/t Pd.

### ***Age of mineralisation***

U-Au mineralisation at Coronation Hill is dated as  $1607 \pm 26$  Ma (Orth et al., 2014).

### ***Current status***

Development prohibited; located in Kakadu National Park.

### ***Economic significance***

Medium-sized U-Au-Pt-Pd deposit.

### ***Major references(s)***

Ahmad, M., Wygralak, A.S., Ferenczi, P.A. and Scrimgeour, I.R., 2009. Gold deposits of the Northern Territory, second edition. Northern Territory Geological Survey Report 11, 131 pp.

Carville, D.P., Leckie, J.F., Moorhead, C.F., Rayner, J.G. and Durbin, A.A., 1990. Coronation Hill gold-platinum-palladium deposit. Australasian Institute of Mining and Metallurgy Monograph 14, 759–762.

Mernagh, T.P., Heinrich, C.A., Leckie, J.F., Carville, D.P., Gilbert, D.J., Valenta, R.K. and Wyborn, L.A.I., 1994. Chemistry of low temperature hydrothermal gold, platinum and palladium (uranium) mineralization at Coronation Hill, Northern Territory, Australia. *Economic Geology*, 89, 1053–1073.

Orth, K., Meffre, S. and Davidson, G., 2014. Age and paragenesis of mineralisation at Coronation Hill uranium deposit, Northern Territory, Australia. *Mineralium Deposita*. DOI 10.1007/s00126-013-0501-4

### ***Relevant figure(s)***

Figure 6.51, Figure 6.52, and Figure 6.53.

## **K.2.11 Devils Elbow**

### ***Geological province***

Pine Creek Orogen.

### ***Location***

Devils Elbow: 133.54603°E, -12.61238°S; Milingimbi (SD 53–02), Liverpool (5672).

### **Classification**

- 8. Hydrothermal-metamorphic; 8.F. Unconformity-type U-Au-PGEs.

### **Geological setting**

The Devils Elbow occurrence is one of several hydrothermal prospects containing anomalous U that have been located in western Arnhem Land. The Devils Elbow occurrence is related to fractures within altered amygdaloidal basalt of the ~1645 Ma Nungbalgarri Volcanics. These volcanics conformably overlie the Mamadawerre Sandstone and underlie the Gumarrimbang Sandstone. The latter unit hosts other U-Au-PGE occurrences in western Arnhem Land, whereas the former unconformably overlies basement, which includes the Tin Camp Granite and the Nimbuwah Complex. Surface samples locally returned very high U, PGE, and Au grades (see below); the best drill-hole intersection was 5 m @ 950 ppm  $U_3O_8$ .

### **PGE mineralisation**

The best assays were from surface samples, with values up to 5.8%  $U_3O_8$ , 38.1 g/t Pd, and 28.02 g/t Pd.

### **Age of mineralisation**

Mineralisation age is younger than the host basalts of the ~1645 Ma Nungbalgarri Volcanics.

### **Current status**

Exploration site.

### **Economic significance**

Occurrence.

### **Major references(s)**

Lally, J.H. and Bajwah, Z.U., 2006. Uranium deposits of the Northern Territory. Northern Territory Geological Survey Report 20, 87 pp.

### **Relevant figure(s)**

## **K.2.12 Edmund**

### **Geological province**

Arunta Orogen.

### **Location**

Edmund: 135.51775°E, -23.44680°S; Illogwa Creek (SF 53–15), Brahma (6051).

### **Classification**

- 8. Hydrothermal-Metamorphic.

### ***Geological setting***

Subsequent to the discovery of the Blackadder deposit in 2008, regional prospecting identified a number of other Ni-Cu-PGE prospects in the Irindina Province, including the Edmund prospect, which is located ~20 km to the south-southeast of Blackadder. This prospect is hosted within a felsic gneiss adjacent to a gabbro. Rock-chip samples from Edmund returned assays of up to 3.8% Cu, 488 ppm Ni, 0.16 g/t Pt+Pd+Au, and 6.6 g/t Ag. Reverse circulation drill-holes collared in 2009 returned up to 9 m @ 0.48% Ni and 0.37% Cu. The gabbro at Edmunds has not been dated, although it is possibly a correlative of the Lloyd Gabbro.

### ***PGE mineralisation***

The highest reported grade is 0.16 g/t Au+Pt+Pd in a rock chip.

### ***Age of mineralisation***

Uncertain, possibly ~409 Ma. U-Pb SHRIMP geochronology on magmatic zircons from gabbro-norite (Lloyd Gabbro) that hosts the nearby Baldrick and Blackadder Ni-Cu-PGE prospects yield a concordia age of  $409 \pm 9$  Ma.

### ***Current status***

Exploration site.

### ***Economic significance***

Occurrence.

### ***Major references(s)***

Mithril Resources Limited, 2010. Mithril Resources Limited 2010 Annual Report, 64 pp.

### ***Relevant figure(s)***

## **K.2.13 Flying Ghost**

### ***Geological province***

Pine Creek Orogen.

### ***Location***

Flying Ghost: 133.32333°E, -13.29048°S; Mount Evelyn (SD 53–05), Gilruth (5571).

### ***Classification***

- 8. Hydrothermal-Metamorphic; 8.F. Unconformity-type U-Au-PGEs.

### ***Geological setting***

The Flying Ghost U-Au-PGE prospect is one of several occurrences containing anomalous U that have been located in western Arnhem Land. These deposits are hosted by the Gumarrirbang Sandstone of the Kambolgie Subgroup, close to the contact with the unconformably underlying Gilruth Volcanics. Uranium-Au±PGE-enrichment is associated with clay in zones of intense fracturing. Mineralogically, native gold is associated with goethite and lepidocrocite. Diamond drilling at Flying

Ghost indicates that U-Au±PGE-enrichment is associated with the upper and lower contacts of the Gilruth Volcanics with the overlying Gumarrinbang Sandstone.

***PGE mineralisation***

Elevated PGEs in association with elevated U and Au.

***Age of mineralisation***

Unknown.

***Current status***

Exploration site.

***Economic significance***

Occurrence.

***Major references(s)***

Ahmad, M., Wygralak, A.S., Ferenczi, P.A. and Scrimgeour, I.R., 2009. Gold deposits of the Northern Territory, second edition. Northern Territory Geological Survey Report 11, 131 pp.

Drever, G., Thevissen, J. and Beckitt, G., 1998. Exploration Licences EL 5061 and EL 5062, Deaf Adder Project–Northern Territory, 1997 Annual Report. Cameco Australia Pty Limited. Northern Territory Geological Survey, Open File Company Report CR1998-0426.

***Relevant figure(s)***

**K.2.14 Goldeneye**

***Geological province***

Pine Creek Orogen.

***Location***

Golden Eye: 131.49869°E, -13.57210°S; Pine Creek (SD 52–08), Tipperary (5170).

***Classification***

- 6. Hydrothermal-Metamorphic; 8.F. Unconformity-type U-Au-PGEs.

***Geological setting***

The Goldeneye U-Au-PGE prospect is one of several U prospects in the developing Hayes Creek uranium field. Other prospects include Thunderball and Moonraker, but Goldeneye is the first prospect at which significant PGEs and Au have been discovered. The prospect is located within a 500 m-long, northwest-trending radiometric anomaly within structurally deformed sediments of the Mount Bonnie Formation.

***PGE mineralisation***

Platinum and Pd occur within U-rich intersections (although not always directly associated with U). The best intersection was 1 m @ 1.106 g/t Pt+Pd+Au, and 0.748% U<sub>3</sub>O<sub>8</sub>. Other intersections include 4 m @ 1.604 g/t Pt+Pd+Au (with 73 ppm U<sub>3</sub>O<sub>8</sub>) and 4 m @ 1.059 g/t Pt+Pd+Au (33 ppm U<sub>3</sub>O<sub>8</sub>).

### **Age of mineralisation**

Unknown.

### **Current status**

Exploration site.

### **Economic significance**

Occurrence.

### **Major references(s)**

MODAT (available upon request from the Northern Territory Geological Survey: <http://www.nt.gov.au>)  
Thundelarra Exploration Limited, 2010. New uranium and platinum-palladium-gold discoveries at Hayes Creek. Thundelarra Exploration Limited announcement to the Australian Securities Exchange, 10 November 2010, 5 pp.

### **Relevant figure(s)**

## **K.2.15 Gold Ridge**

### **Geological province**

Pine Creek Orogen.

### **Location**

Gold Ridge: 131.27927°E, -13.68581°S; Pine Creek (SD 52–08), Tipperary (5170).

### **Classification**

- 8. Hydrothermal-Metamorphic; ?8.F. Unconformity-type U-Au-PGEs or ?8.G. U-Au-Pd-Pt mineralisation associated with graphitic schist and carbonaceous shale.

### **Geological setting**

The Gold Ridge Au-PGE prospect in the Pine Creek Orogen is located within a roof pendant of the ~2019 Ma Wildman Siltstone (also referred to as ~1890 Ma Koolpin Formation by Sener et al., 2002) enclosed by the ~1835 Ma Fenton Granite. Laminated ferruginous siltstone, weakly schistose sedimentary rocks, and minor chert nodular siltstone are exposed in the Gold Ridge area. The sedimentary rocks were metamorphosed to greenschist facies in this area during the Nimbuwah event (~1870 Ma). The prospect was discovered in 1991 by MIM Exploration Proprietary Limited, through a stream-sediment, rock-chip, and soil geochemical program. The mineralisation was subsequently trenched and reverse-circulation drill-tested in 1992, and the small resource was proved. During 2000, ~80 ounces of Au and PGEs were mined from two small pits on the deposit by illegal miners (Sener et al., 2002). The Gold Ridge Au-PGE prospect occurs as a northwest-trending quartz breccia-filled fault zone with a dip of 50°–55° to the northeast that can be traced for 500 m. Precious metals are largely localised in a ~5-m thick graphite±pyrite-bearing mylonite (also called schist) unit structurally above a hematitic quartz breccia (Sener et al., 2002). Hanging-wall rocks are chloritised, veined, and cataclastically deformed, and the granite *sensu stricto* enveloping the deposit shows development of cataclastic zones. The mineralised structure at Gold Ridge is a shear zone within a sliver of metasedimentary rocks, bounded by the granite. The shear zone strikes NNW–north, dips at 50°–58°

east and is marked in outcrop by a hematitic quartz breccia, which forms the footwall to the mineralisation. The north-northwest to north-trending shear zones had a sinistral sense of movement.

### ***PGE mineralisation***

Significant Au-PGE grades at Gold Ridge can be traced over a strike length of 150 m and to a depth of 55 m. A pre-JORC inferred resource of 32 000 t grading 4.5 g/t Au, 0.3 g/t Pt, and 0.5 g/t Pd has been defined. Sener et al. (2002) described three major styles of mineralisation: (1) graphitic-schist hosted: graphite-kaolin-sericite-monzite. The bulk of the Au-PGE mineralisation occurs within this unit (grades up to 950 g/t Au and 7 g/t Pd and Pt). The hematitic quartz breccia that forms the footwall to the graphitic schist is barren; (2) hematitic schist hosted: hematite-goethite-kaolin-sericite-monzite, which occurs as small slivers within the graphitic schist. Assay samples of this material return lower grades than those within the more graphitic zones; and (3) hanging-wall schist: quartz-chlorite-sericite-rutile zircon. The mineralisation in this unit is confined to the narrow alteration selvages surrounding abundant quartz veinlets. The Au-PGE ore is associated with enrichment of Co, Ni, Th, and Zn, and minor Ag, As, and LREE enrichment. No anomalous U has been recorded. The Au and PGMs occur as composite grains and alloys that are intimately associated with the graphite contained in the major host unit. The Au grains are normally ~10 µm to 100 µm in diameter, and some Au grains appear to replace graphite flakes. This graphite may be a primary component of the host rock, but it is also possible that it is an alteration product introduced by hydrocarbon-rich fluids either prior to or during mineralisation. There are indications that the PGEs show zonal distribution within the Au grains. The ore is characterised by a very low sulphide content. The samples analysed show free Au and trace Pd, but no Pt-bearing phases were identified (Sener et al., 2002).

### ***Age of mineralisation***

Unknown.

### ***Current status***

Historical mine, exploration site.

### ***Economic significance***

Occurrence.

### ***Major references(s)***

- Ahmad, M., Wygralak, A.S., Ferenczi, P.A. and Scrimgeour, I.R., 2009. Gold deposits of the Northern Territory, second edition. Northern Territory Geological Survey Report 11, 131 pp.
- McGeough, M., 1992. Exploration Licence No. 7013 'PENDANT', Northern Territory, Second Annual Report: November 1992. Northern Territory Geological Survey, Open File Company Report CR1992-0645.
- Sener, A.K., Grainger, C.J. and Groves, D.I., 2002. Epigenetic gold-platinum-group element deposits: examples from Brazil and Australia. '21st Century Pt-Pd deposits: current and future potential', Mineral Deposits Studies Group, Annual Meeting, University of Southampton, England, 3 January 2002. Transactions Institution of Mining and Metallurgy, 307, January-April 2002, B65-B73.

***Relevant figure(s)***

**K.2.16 Hardtop**

***Geological province***

Pine Creek Orogen.

***Location***

Hardtop: 130.99898°E, -13.20924°S; Pine Creek (SD 52–08), Reynolds River (5071).

***Classification***

- 8. Hydrothermal-Metamorphic; 8.F. Unconformity-type U-Au-PGEs.

***Geological setting***

The Hardtop prospect is one of several small Au-Pt-Pd occurrences hosted in the Coomalie Dolostone in the area surrounding the Waterhouse Granite Complex in the Rum Jungle area.

***PGE mineralisation***

The best reported intersection was 4 m @ 0.6 g/t Pt, 0.3 g/t Pd, and 2.2 g/t Au.

***Age of mineralisation***

Unknown.

***Current status***

Exploration site.

***Economic significance***

Occurrence.

***Major references(s)***

Ahmad, M., Wygralak, A.S., Ferenczi, P.A. and Scrimgeour, I.R., 2009. Gold deposits of the Northern Territory, second edition. Northern Territory Geological Survey Report 11, 131 pp.

Williams, K.A., 1999. Final report for Exploration License 6431 Acacia area, Northern Territory 04.09.89 to 31.05.99. Northern Territory Geological Survey, Open File Company Report CR1999-0323.

***Relevant figure(s)***

**K.2.17 Jabiluka 2\***

***Geological province***

Pine Creek Orogen.

## **Location**

Jabiluka 2\*: 132.9029°E, -12.4994°S; Alligator River (SD 53–01), Cahill (5472); ~225 km east of Darwin.

## **Classification**

- 8. Hydrothermal-Metamorphic; 8.G. U-Au-Pd-Pt mineralisation associated with graphitic schist and carbonaceous sedimentary rocks.

## **Geological setting**

The Jabiluka 1 and 2 deposits occur in the lower member of the Early Proterozoic Cahill Formation, at the northeastern margin of the Nanambu Complex. Jabiluka 1 lies just west of a large outlier of the Kombolgie Subgroup, but Jabiluka 2 (300 m east of Jabiluka 1) is concealed by up to 200 m of Kombolgie sandstone. Both the Jabiluka 1 and 2 deposits occur within an open-asymmetric flexure, striking east-southeast and dipping to the south. The Jabiluka 1 deposit measures about 400 m in a northwesterly direction and 200 m in a northeasterly direction (Hegge, 1977). It dips south at 15°–30°, and in the Main Mine Series the ore zone is up to 35 m-thick. Jabiluka 2 deposit extends for at least 1000 m in a west-northwest direction and at least 400 m north–south. It dips south in a series of flexures at between 30° and 60°. The deposit is open to the south and east at depth. In the Main Mine Series the ore zones are up to 135 m-thick. Hancock et al. (1990) considered the mineralised sequence of the Cahill Formation to be overturned and the orebodies are situated along the lower limb of a recumbent fold. The metasedimentary sequence at Jabiluka consists of alternating quartz-muscovite-chlorite schist, quartz-chlorite schist, quartz-graphite schist and magnesite-dolomite. Some units are feldspathic, locally containing garnet, sillimanite, and zircon. In the vicinity of the deposits, retrograde metamorphism has resulted in chloritisation of biotite and garnet, together with sericitisation of feldspar, sillimanite, and cordierite.

The South Alligator Valley uranium field in the Pine Creek Orogen contains a number of other major U±Au±PGE deposits (Ranger 1, Koongarra, and Nabarlek (mined out)).

## **PGE mineralisation**

Palladium is the dominant PGE associated with U and Au. Palladium-bearing Au-U mineralisation occurs in graphite horizons in the western part of the Jabiluka No. 2 Orebody. The Au zone contains 2.392 Mt ore averaging 3.7 g/t Au and 0.47% U<sub>3</sub>O<sub>8</sub>, but there are no resource figures on the PGEs (ERA Limited, 1992).

## **Age of mineralisation**

Ludwig et al. (1987) reported an age of 1437 ± 40 Ma for U mineralisation at Jabiluka, however, more recent geochronological data indicates this determination is significantly too young. The age of mineralisation at Jabiluka is considered to be ~1685 Ma. LA-ICPMS data reveal initial uraninite precipitation occurred in the basement rocks at ~1680 ± 17 Ma. The oldest <sup>207</sup>Pb/<sup>206</sup>Pb ages are coincident with a <sup>40</sup>Ar/<sup>39</sup>Ar age of 1683 ± 11 Ma from one S11 illite sample from above the deposit (Polito et al., 2005).

## **Current status**

Undeveloped U-Au-PGE deposit.

### ***Economic significance***

The U resources for Jabiluka No. 1 Orebody at a cut-off grade of 0.05% U<sub>3</sub>O<sub>8</sub> are 1.3 Mt @ 0.25% U<sub>3</sub>O<sub>8</sub>, containing 3400 t of U<sub>3</sub>O<sub>8</sub> (Pancontinental Mining Limited, 1979). The U resources for the Jabiluka No. 2 Orebody at a cut-off grade of 0.2% U<sub>3</sub>O<sub>8</sub> are 31.1 Mt @ 0.53% U<sub>3</sub>O<sub>8</sub>, containing 163 000 t of U<sub>3</sub>O<sub>8</sub> (ERA Limited, 2000).

### ***Major references(s)***

- ERA Limited, 1992. Energy Resource of Australia Limited 1992 Annual Report.
- ERA Limited, 2000. Energy Resources of Australia Limited 2000 Annual Report, 60 pp.
- Hancock, M.C., Maas, R. and Wilde A.R., 1990. Jabiluka uranium gold deposits. In: Hughes, F.E. (editor), *Geology of the Mineral Deposits of Australia and Papua New Guinea*. Australasian Institute of Mining and Metallurgy, Melbourne, Monograph 14, 785–793.
- Hegge, M.R., 1977. Geologic setting and relevant exploration features of the Jabiluka Uranium Deposits. *Proceedings of the Australasian Institute of Mining and Metallurgy*, 264, 19–32.
- Lally, J.H. and Bajwah, Z.U., 2006. Uranium deposits of the Northern Territory. Northern Territory Geological Survey Report 20, 87 pp.
- Ludwig, K.R., Grauch, R.I., Nutt, C.J., Nash, J.T., Frishman, D. and Simmons, K.R., 1987. Age of uranium mineralization at the Jabiluka and Ranger deposits, Northern Territory, Australia: New U-Pb Isotope Evidence. *Economic Geology*, 82, 857–874.
- Pancontinental Mining Limited 1979. Jabiluka Project. Environmental Impact Statement, July 1979.
- Polito, P.A., Kyser, T.K., Thomas, D., Marlatt, J. and Drever, D., 2005. Re-evaluation of the petrogenesis of the Proterozoic Jabiluka unconformity-related uranium deposit, Northern Territory, Australia. *Mineralium Deposita*, 40, 257–288.

### ***Relevant figure(s)***

Figure 6.54, Figure 6.55, and Figure 6.56.

## **K.2.18 Kongo**

### ***Geological province***

Arunta Orogen.

### ***Location***

Kongo: 134.64773°E, -23.12045°S; Alice Springs (SF 53–14), Riddoch (5851).

### ***Classification***

- 8. Hydrothermal-Metamorphic; 8.D. Structurally-controlled remobilised Ni-Cu-PGE sulphides in mafic-ultramafic±felsic dykes/veins in shear zones.

### ***Geological setting***

The Kongo Cu-Au-PGE prospect is the most significant of several hydrothermal Cu-PGE-Au occurrences hosted by the Bungintina Metamorphics near the structural contact with the Irindina Province. The Bungintina Metamorphics consist of 1770 Ma–1750 Ma pelitic to psammopelitic gneiss with lesser calc-silicate rock, marble, and quartzite. The Kongo prospect consists of quartz-carbonate-tourmaline veins associated with chlorite-hematite-altered amphibolite. Although high-grade samples

have been collected at surface (see below), follow-up RAB drilling failed to intersect significant mineralisation.

***PGE mineralisation***

Rock-chip samples to 0.6 g/t Pt, 1.4 g/t Pd, 5.8 g/t Au, 6.8% Cu, and 12 g/t Ag.

***Age of mineralisation***

Unknown.

***Current status***

Exploration site.

***Economic significance***

Occurrence.

***Major references(s)***

Scrimgeour, I.R., 2013. Aileron Province. In: Ahmad, M. and Munson, T.H. (compilers), Geology and mineral resources of the Northern Territory. Northern Territory Geological Survey Special Publication 5, 12:1-12:65.

Whelan, J.A., Close, D.F., Scrimgeour, I.R., Beyer, E.E., Kositcin, N. and Armstrong, R.A., 2013. The Cu ± Au potential of the Arunta Region: Links between magmatism, tectonism, regional-scale alteration and mineralisation. Northern Territory Geological Survey Record 2013/001, 34–42.

***Relevant figure(s)***

Figure 8.18h.

**K.2.19 Lindeman's Bore\***

***Geological province***

Birrindudu Basin.

***Location***

Lindeman's Bore: 130.12832°E, -17.46228°S; Limbunya (SE 52–07), Gregorys Depot (4963).

***Classification***

- ?8. Hydrothermal-Metamorphic; ?8.G. U-Au-Pd-Pt mineralisation associated with graphitic schist and carbonaceous shale.

***Geological setting***

The Lindeman's Bore prospect is hosted by metamorphosed shales of the Birrindudu Group, which forms the base of the Paleoproterozoic Birrindudu Basin. These shales are intruded by a series of feldspar-phyric bodies. A 1 m-thick interval anomalous in Pd was part of a 7 m-thick interval grading 1.1 g/t Au. The drill-hole intersected an additional 14 m of 0.11% Cu, about 40 m down-hole from the Au-Pd intersection. Anomalous Ni was also encountered in the drill-hole. The Au-Pd intersection is approximately 80 below an unconformable contact with the Limbunya Group. Other holes in the prospect area have intersected significant Cu-Co-Au anomalism, including 1 m @ 0.07% Cu, 0.06%

Co, and 0.22 g/t Au, and hematite-chlorite alteration assemblages associated with a carbonate-sulphide assemblage.

***PGE mineralisation***

The upper Au-rich intersection included 1 m @ 0.45 g/t Pd.

***Age of mineralisation***

Unknown.

***Current status***

Exploration site.

***Economic significance***

Occurrence.

***Major references(s)***

[www.protoexploration.com.au](http://www.protoexploration.com.au) (particularly press release dated 31 March 2010)

***Relevant figure(s)***

**K.2.20 Orodruin (Mithril)**

(Braveheart also occurs within the Mordor Complex)

***Geological province***

Arunta Orogen.

***Location***

Orodruin (Mithril): 134.48134°E, -23.43826°S; Alice Springs (SF 53–14), Laughlen (5751).

***Classification***

- 4. Alkaline mafic-ultramafic intrusions; 4.A. Stratabound and disseminated Cu-Au-PGE sulphides.

***Geological setting***

The Orodruin prospect, previously known as Mithril, is hosted by ultramafic cumulate units within the ~1130 Ma Mordor Alkaline Igneous Complex. This complex intrudes Paleoproterozoic tonalitic gneiss (Artunga Gneiss) and has an oval-shape at surface. The ultramafic rocks, which comprise about 40% of the intrusive complex (eastern part), are dunitic to peridotitic in composition, and include olivine-augite, augite-olivine and augite-phlogopite-apatite-magnetite cumulates. Felsic rocks, which comprise 60% of the complex (western part), are composed mostly of phlogopite-rich syenite and shonkinite.

At Orodruin, the PGEs are hosted by ultramafic phases of the igneous complex. The highest concentrations of PGEs are located at the bases of magmatic cycles, whereas low-grade, patchy accumulations are also present in parts of the magnetite-rich upper parts of the magmatic cycles. The

PGEs are associated with a disseminated magmatic sulphide assemblage including chalcopyrite, pyrrhotite, and pentlandite along with magnetite.

### ***PGE mineralisation***

Grades of up to 1.5 g/t Pt+Pd+Au have been recorded over 1 m-thick intervals in association with anomalous Ni and Cu.

### ***Age of mineralisation***

Claoué-Long and Hoatson (2005) obtained a U-Pb zircon age for a pyroxenite from the northeast corner of the complex of  $1133 \pm 5$  Ma, which is considered the best crystallisation age for the Mordor Igneous Complex. Previous attempts to date the complex include a Rb-Sr whole-rock isochron age of  $1128 \pm 20$  Ma and Rb-Sr mineral isochron age of  $1118 \pm 17$  Ma (Langworthy and Black, 1978, recalculated by Nelson et al., 1989), and a Sm-Nd whole-rock isochron age of  $1100 \pm 280$  Ma (Nelson et al., 1989).

### ***Current status***

Exploration site.

### ***Economic significance***

Occurrence.

### ***Major references(s)***

Barnes, S.J., Anderson, J.A.C., Smith, T.R. and Bagas, L., 2008. The Mordor Alkaline Igneous Complex, central Australia: PGE-enriched disseminated sulfide layers in cumulates from a lamprophyric magma. *Mineralium Deposita*, 43, 641–662.

Claoué-Long, J.C. and Hoatson, D.M., 2005. Proterozoic mafic–ultramafic intrusions in the Arunta Region, central Australia. Part 2: Event chronology and regional correlations. *Precambrian Research*, 142, 134–158.

Langworthy, A.P. and Black, L.P., 1978. The Mordor Complex: a highly differentiated potassic intrusion with kimberlitic affinities in central Australia. *Contributions to Mineralogy and Petrology*, 67, 51–62.

Miezitis, Y., Jaireth, S. and Hoatson, D.M., 2006. Mineral potential modelling of Proterozoic mafic–ultramafic intrusions in the Arunta Region, central Australia. *Geoscience Australia Record 2006/14*, 56 pp.

Nelson, D.R., Black, L.P., McCulloch, M.T., 1989. Nd-Pb isotopic characteristics of the Mordor Complex, Northern Territory: Mid-Proterozoic potassic magmatism from an enriched mantle source. *Australian Journal of Earth Sciences*, 36, 541–551.

### ***Relevant figure(s)***

Figure 6.28, Figure 8.13, and Figure 8.17e.

## **K.2.21 Ranger 3 (Ranger 1, Number 3 Orebody)**

### ***Geological province***

Pine Creek Orogen.

### ***Location***

Ranger 3 (Ranger 1, Number 3 Orebody): 132.91500°E, -12.67510°S; Alligator River (SD 53–01), Cahill (5472).

### ***Classification***

- 8. Hydrothermal-Metamorphic; 8.F. Unconformity-type U-Au-PGEs.

### ***Geological setting***

The Ranger 3 deposit (Ranger 1, Number 3 orebody) is located 1.5 km to the north of the Ranger 1 deposit within a homogeneous succession of quartz-chlorite schist with minor chert. The Ranger deposits are hosted in the lower part of the pelitic Cahill Formation, close to the contact with the underlying Nanambu Complex. Ore zones are intensely brecciated and associated with low-angle reverse faults.

### ***PGE mineralisation***

One sample of U ore, grading 0.3% U<sub>3</sub>O<sub>8</sub>, assayed 1.1 g/t Pt and 0.98 g/t Pd.

### ***Age of mineralisation***

1737 ± 20 Ma age for mineralisation at Ranger (McKay and Mieizitis, 2001).

### ***Current status***

Operating U mine.

### ***Economic significance***

Operating U mine with minor PGEs.

### ***Major references(s)***

Lally, J.H. and Bajwah, Z.U., 2006. Uranium deposits of the Northern Territory. Northern Territory Geological Survey Report 20, 87 pp.

McKay, A.D. and Mieizitis, Y., 2001. Australia's uranium resources, geology and development of deposits. AGSO–Geoscience Australia, Mineral Resource Report 1, 184 pp.

### ***Relevant figure(s)***

## **K.2.22 RD**

### ***Geological province***

Arunta Orogen.

### ***Location***

RD: 136.34023°E, -22.60659°S; Huckitta (SF 53–11), Jervois Range (6152).

### ***Classification***

- 2. Massive to poorly layered tholeiitic mafic-dominated intrusions; 2.B. Stratabound PGE-bearing magnetite layers.

### **Geological setting**

The RD Ti-V-PGE prospect is hosted by magnetite-bearing horizons within the ~1786 Attutra Metagabbro, which intrudes ~1807 Ma rocks of the Bonya Schist. This north-trending body consists mostly of weakly recrystallised gabbro, magnetite-bearing gabbro, and massive stratabound magnetite. Obvious cyclicity and/or compositional layering are lacking. At RD, anomalous Au and PGE assays are hosted by V-Ti-rich magnetite layers within the metagabbro.

### **PGE mineralisation**

The best reported result was 16 m (47 m–63 m) @ 0.18 g/t Pt, 0.18 g/t Pd, and 0.10 g/t Au. This intersection included 10 m @ 23.5% Fe, 0.4% V<sub>2</sub>O<sub>5</sub>, and 4.6% TiO<sub>2</sub>.

### **Age of mineralisation**

The geochronology sample was a chilled gabbro from the western margin of the intrusion on the basis of its high Zr content (153 ppm Zr) and it was found to contain abundant zircons (Claoué-Long and Hoatson, 2005). The zircons are of uniform appearance, with well defined euhedral crystal shapes and indistinct growth zoning consistent with igneous zircon crystallisation. The concordia diagram in Claoué-Long and Hoatson (2005) shows a homogeneous and concordant population of zircon compositions with only four discordant grains. The 34 concordant grains agree at a weighted mean <sup>207</sup>Pb/<sup>206</sup>Pb age of 1786.4 ± 4.2 Ma for the Attutra Metagabbro Intrusion (Claoué-Long and Hoatson, 2005).

### **Current status**

Exploration site.

### **Economic significance**

Occurrence.

### **Major references(s)**

Arafura Resources Limited, 2012. Gold and PGEs add a new dimension to Arafura's Jervois vanadium project. Arafura Resources Limited announcement to the Australian Securities Exchange, 26 April 2012, 11 pp, [www.arafuraresources.com.au](http://www.arafuraresources.com.au) (press release dated 26 April 2012).

Claoué-Long, J.C. and Hoatson, D.M., 2005. Proterozoic mafic-ultramafic intrusions in the Arunta Region, central Australia. Part 2: Event chronology and regional correlations. *Precambrian Research*, 142, 134–158.

Hoatson, D.M. and Stewart, A., 2001. Field investigations of Proterozoic mafic-ultramafic in the Arunta Province, central Australia. *Geoscience Australia Record* 2001/39, 87 pp.

Miezitis, Y., Jaireth, S. and Hoatson, D.M., 2006. Mineral potential modelling of Proterozoic mafic-ultramafic intrusions in the Arunta Region, central Australia. *Geoscience Australia Record* 2006/14, 56 pp.

### **Relevant figure(s)**

Figure 8.13 and Appendix Figure K.34.

### **K.2.23 Sargent**

#### ***Geological province***

Pine Creek Orogen.

#### ***Location***

Sargent: 131.02463°E, -13.17309°S; Pine Creek (SD 52–08), Batchelor (5171).

#### ***Classification***

- 8. Hydrothermal-Metamorphic; 8.F. Unconformity-type U-Au-PGEs.

#### ***Geological setting***

The Sargent Au-PGE prospect is one of a number of small Au-Pt-Pd occurrences hosted in the Coomalie Dolostone in the area surrounding the Waterhouse Granite Complex in the Rum Jungle area. The occurrence is hosted by breccia within dolostone and shale of the Coomalie Dolostone.

#### ***PGE mineralisation***

The best intersection reported is 26 m @ 1.85 g/t Au. Minor Pt and Pd are also present.

#### ***Age of mineralisation***

Unknown.

#### ***Current status***

Exploration site.

#### ***Economic significance***

Occurrence.

#### ***Major references(s)***

MODAT (available upon request from the Northern Territory Geological Survey: <http://www.nt.gov.au>)

#### ***Relevant figure(s)***

### **K.2.24 Sargent North**

#### ***Geological province***

Pine Creek Orogen.

#### ***Location***

Sargent North: 131.02634°E, -13.15778°S; Pine Creek (SD 52–08), Batchelor (5171).

#### ***Classification***

- 8. Hydrothermal-Metamorphic; 8.F. Unconformity-type U-Au-PGEs.

### ***Geological setting***

The Sargent North Au-PGE prospect is one of several small Au-Pt-Pd occurrences hosted in the Coomalie Dolostone in the area surrounding the Waterhouse Granite Complex in the Rum Jungle area. Sargent North is hosted by hematite-quartz breccia in a succession of tremolite-chlorite schist assigned to the Coomalie Dolostone.

### ***PGE mineralisation***

A pre-JORC potential resource of 20 000–30 000 t @ 3–4 g/t Au with associated PGEs was estimated.

### ***Age of mineralisation***

Unknown.

### ***Current status***

Exploration site.

### ***Economic significance***

Occurrence.

### ***Major references(s)***

Ahmad, M., Wygralak, A.S., Ferenczi, P.A. and Scrimgeour, I.R., 2009. Gold deposits of the Northern Territory, second edition. Northern Territory Geological Survey Report 11, 131 pp.

Williams K.A., 1999. Final report for Exploration Licence 7706, Sargents area, Batchelor, Northern Territory, 23.03.92 to 22.03.99. Normandy Woodcutters Limited. Northern Territory Geological Survey, Open File Company Report CR1999-0321.

### ***Relevant figure(s)***

## **K.2.25 Stevens**

### ***Geological province***

Pine Creek Orogen.

### ***Location***

Stevens: 133.52509°E, -12.33949°S; Milingimbi (SD 53–02), Goomadeer (5673).

### ***Classification***

- 8. Hydrothermal-Metamorphic; ?8.F. Unconformity-type U-Au-PGEs.

### ***Geological setting***

The Stevens Au-PGE-Au prospect consists of quartz-chlorite-calcite-hematite veins localised in dolerite and basement rocks along the east-southeast-trending Stevens Fault. This fault separates basement of the Pine Creek Orogen from the Kombolgie Sandstone. Significant drill intersections occur over a strike length of more than 2.5 km.

***PGE mineralisation***

The best PGE intersections were 6.8 m @ 2.62 g/t Au, 0.54 g/t Pt, and 0.71 g/t Pd; and 5 m @ 6.06 g/t Au, 1.58 g/t Pt, and 2.20 g/t Pd. The best U intersection was 1 m @ 0.19% U<sub>3</sub>O<sub>8</sub>.

***Age of mineralisation***

Unknown.

***Current status***

Exploration site.

***Economic significance***

Abandoned mine.

***Major references(s)***

MODAT (available upon request from the Northern Territory Geological Survey: <http://www.nt.gov.au>)  
Uranium Equities Limited, 2007. 2006 exploration results–West Arnhem Land Joint Venture, 11 April 2007. Uranium Equities Limited announcement to the Australian Securities Exchange, 11 April 2007, 5 pp. [www.uel.com.au](http://www.uel.com.au)

***Relevant figure(s)***

## K.3 SOUTH AUSTRALIA

### K.3.1 Cooper Hill

#### ***Geological province***

Gawler Craton.

#### ***Location***

Cooper Hill: 132.68136°E, -31.78279°S; Fowler (SH 53–13), Bookabie (5434); ~90 km west-northwest of Ceduna.

#### ***Classification***

Exploration target for:

- ?2. Massive to poorly layered tholeiitic mafic-dominated intrusions; ?2.A. Segregations of Ni-Cu-Co-PGE sulphides in feeder conduits and basal contacts.

#### ***Geological setting***

An exploration target considered prospective for Voisey's Bay-style Ni-Cu-Co deposits in Proterozoic basement mafic-ultramafic intrusive rocks. The area was targeted using geophysical methods to try to identify near surface preserved magma feeder pipes thought to have been emplaced as part of the ~1590 Ma Gawler Magmatic Event. Limited historical drilling in the area (Pasminco Exploration holes BK87 and BK88) encountered peridotite and mafic rocks with elevated Ni, Cu, and PGE contents (McKinnon-Matthews et al., 2009).

#### ***PGE mineralisation***

Work conducted by Pasminco during 1994 to 1999 included ground magnetics and aircore and diamond drilling of magnetic anomalies. Ultramafic and mafic intrusives were intersected in a number of areas with assay results indicating ultramafic lithologies in a number of drill-holes (BK42: 1500 ppm Ni, 660 ppm Cu, and 1550 ppm Cr; BK1, BK2, and BK3: >1000 ppm Ni). The fresh peridotite identified in diamond holes BK087 and BK88 commonly contained more than 0.2% Ni and petrological examinations confirmed the presence of fine-grained disseminated sulphides.

An aircore-drilling component of a 'Plan for Accelerated Exploration' (PACE)-subsidised program was completed in March 2006, when 22 holes for 1017 m tested geochemical anomalies previously found in the basement weathering profile. This work defined several geochemically anomalous zones, with assayed maxima of 0.4% Ni and 287 ppb Pt+Pd occurring at the bottom of drill-hole CHAC028.

#### ***Age of mineralisation***

Unknown.

#### ***Current status***

Historical exploration site.

### ***Economic significance***

Occurrence.

### ***Major references(s)***

McKinnon-Matthews, W.J., Fowler, A. and Jenkins, A., 2009. Cooper Hill. Annual Reports and final report to licence expiry/surrender, for the period 4/7/2003 to 24/8/2009. Mithril Resources Limited, SARIG Envelope 105, 260 pp.

### ***Relevant figure(s)***

## **K.3.2 Kangaroo Dam Prospect**

### ***Geological province***

Gawler Craton.

### ***Location***

Kangaroo Dam Prospect: 134.90932°E, -29.37647°S; Coober Pedy (SG 53–06), Coober Pedy (5839); ~50 km south of Coober Pedy.

### ***Classification***

- ?8. Hydrothermal-Metamorphic.
- 12.E Others (unknown geological setting).

### ***Geological setting***

Drill-hole intersection on the western part of the Mount Wood Inlier in the Gawler Craton has identified an unusual setting of PGE mineralisation possibly related to a skarn-type mineral system associated with mafic-ultramafic igneous and sedimentary rocks. Drilling penetrated anomalous Pt and Pd in mafic rocks beneath 50 m–60 m of younger sediment near gravity anomalies tested in a series of drill-holes. Drill core included gabbro, amphibolite, garnet-rich gneiss, and pyroxenite. Follow-up drilling by Goldstream Mining NL in 2004–2005 confirmed the presence of anomalous Pt and Pd mineralisation.

### ***PGE mineralisation***

Petrographic studies of the mineralised Pt-Pd zone in drill-hole KDRC001 (1 m @ 4.1 g/t Pt+Pd) shows that the mineralisation is hosted in a hornblende-pyroxene-rich rock that may represent skarn-type alteration of metasediments or metapyroxenite. Sulphide mineralisation consists of pyrrhotite and pyrite with a maximum concentration of about 2.5% (Goldstream Mining NL, 2005a). A follow-up drill-hole at this prospect intersected 20 m @ 0.60 g/t PGEs, including 5 m @ 1.31 g/t PGEs and 1.0 m @ 4.10 g/t PGEs (Goldstream Mining NL, 2005b).

A program of five diamond drill-holes totalling 1740 m was completed in collaboration with the South Australian government's PACE drilling initiative, which partly funded the program. A total of 1401 samples comprising 27 aircore pre-collar samples and 1374 quarter core samples were collected and analysed. Assays from drill-hole KDD003 showed a mineralised intersection of 22 m @ 0.95 g/t Pt+Pd+Au from 149 m. This mineralisation is hosted within brecciated mafic gneiss with disseminated to massive pyrrhotite aggregates up to 10 cm in size. The mineralisation in KDD003 is Pd dominant with a Pd:Pt ratio of 26:1 (Goldstream Mining NL, 2005c).

### ***Age of mineralisation***

Proterozoic?

### ***Current status***

Exploration site.

### ***Economic significance***

Occurrence.

### ***Major references(s)***

Goldstream Mining NL, 2005a. Report for the quarter ended March 2005. Company announcement to the Australian Securities Exchange, 11 pp.

Goldstream Mining NL, 2005b. Annual Report 2005. Australian Securities Exchange, 78 pp.

Goldstream Mining NL, 2005c. Report for the quarter ended December 2005. Company announcement to the Australian Securities Exchange, 15 pp.

### ***Relevant figure(s)***

## **K.3.3 Lake Acraman**

### ***Geological province***

Gawler Craton.

### ***Location***

Lake Acraman: 135.00°E, -32.417°S; Gairdner (SH 53–15), Everard (5934); ~220 km west of Port Augusta.

### ***Classification***

- 12. Other occurrences; 12.B. Anomalous PGEs in sedimentary rocks related to possible impact structure.

### ***Geological setting***

The Lake Acraman region in the Gawler Ranges of central southern South Australia is believed to be the site of a pre-Cambrian meteorite impact that was responsible for a blanket of incandescent debris which was ejected some 300 km to the east over a shallow sea covering the area now known as the Flinders Ranges. Lake Acraman is a circular ephemeral playa lake about 20 km in diameter. It is deeply eroded and its original size must be inferred by indirect means, with some investigators suggesting its original diameter was up to 90 km. Outcrops of Proterozoic dacite in Lake Acraman are intensely shattered and contain shatter cones and multiple sets of shock lamellae in quartz grains.

### ***PGE mineralisation***

Researchers from the Universities of Melbourne and Adelaide have delineated anomalous Ir and Pt concentrations in sediments from Lake Acraman. Green shales containing thin bands of sand are enriched in Ir, Pt, Au, and Cu. The sediments are 1 000 times more concentrated in Ir than surrounding rocks, and Cu sulphides in the anomalous sediments are also enriched in Pt (Hoatson

and Glaser, 1989; Gostin et al., 1989; Glikson, 2013). Anomalous PGE values have been identified in sand to boulder-sized ejecta in the Acraman ejecta layer of the Bunyeroo Formation in the Flinders Ranges (Williams and Gostin, 2005).

### ***Age of mineralisation***

The age of the impact event has been estimated at ~580 Ma equating to the Ediacaran Period (Williams, 1986; Glikson, 2013).

### ***Current status***

Occurrence.

### ***Economic significance***

Occurrence.

### ***Major references(s)***

- Glikson, A.Y., 2013. The Asteroid Impact Connection of Planetary Evolution. Springer, Dordrecht. <http://dx.doi.org/10.1007/978-94-007-6328-9>, 149 pp.
- Gostin, V.A., Keays, R.R. and Wallace, M.W., 1989. Iridium anomaly from the Acraman impact ejecta horizon—impacts can produce sedimentary iridium peaks. *Nature*, 340, 542–544.
- Hoatson, D.M. and Glaser, L.M., 1989. Geology and economics of platinum-group metals in Australia. Bureau of Mineral Resources, Australia, Resource Report 5, 81 pp.
- MU Research, September Vol 4, No. 3. Insert in, The University of Melbourne Gazette, Spring 1988, 14, No. 3.
- Williams, G.E., 1986. The Acraman impact structure; source of ejecta in late Precambrian shales, South Australia. *Science*, 233, 200–203.
- Williams, G.E. and Gostin, V.A., 2005. The Acraman–Bunyeroo impact event (Ediacaran), South Australia, and environmental consequences: 25 years on. *Australian Journal of Earth Sciences*, 52, 607–620.

### ***Relevant figure(s)***

## **K.3.4 Michael Hills Copper Prospect\***

### ***Geological province***

Musgrave Province.

### ***Location***

Michael Hills Copper Prospect: 129.0250°E, -26.2583°S; Mann (SG 52–11), Davies (4745).

### ***Classification***

- ?2. Massive to poorly layered tholeiitic mafic-dominated intrusions.

### ***Geological setting***

The Michael Hills Intrusion is one of the more extensive ~1070 Ma Giles Complex cumulate sequences in the Musgrave Province. It consists of predominantly north- to northwest-dipping sequences (15°–30°) of pyroxenite, melagabbronorite, gabbronorite, leucogabbronorite, and anorthosite. Gabbronorite predominates, with gradational contacts into mela- and leucogabbronorite.

Pyroxenite horizons range between 1 m to 20 m in thickness and commonly have sharp lower contacts. Assuming no structural repetition, the intrusion has a stratigraphic thickness in excess of ~9 km. It is interpreted that the repetition of pyroxenite, gabbro, and anorthosite sequences is due to multiple intrusive pulses. The Michael Hills Copper prospect is situated approximately in the stratigraphic centre of the Michael Hills Intrusion and the surrounding geology is characterised by highly variable lithologies, lithological repetition, and layer thickness. On the basis of lithological layering surrounding the prospect, it is interpreted that Cu mineralisation accumulated during replenishment of the magma chamber with a new pulse of magma (Rutherford et al., 2008).

### ***PGE mineralisation***

The Michael Hills Copper prospect is within a predominantly pyroxenite sequence overlain by melagabbro and underlain by anorthosite and gabbro. Two samples collected at the prospect returned analytical values as shown in Appendix Table K.42.

*Appendix Table K.42 Geochemistry of samples from the Michael Hills Copper Prospect.*

<b>Lithology</b>	<b>Au (ppb)</b>	<b>Pt (ppb)</b>	<b>Pd (ppb)</b>	<b>Cu (ppm)</b>	<b>Ni (ppm)</b>	<b>Co (ppm)</b>	<b>Cr (ppm)</b>
Gabbro	310	55	83	14 000	2650	76	650
Melagabbro	390	10	29	10 000	650	47.5	950

### ***Age of mineralisation***

Mesoproterozoic.

### ***Current status***

Exploration site.

### ***Economic significance***

Occurrence.

### ***Major references(s)***

Rutherford, L., Szpunar, M., Fricke, C.E., Chalmers, N.C. and Mason, D.R., 2008. Michael Hills copper prospect, Giles Complex, central Musgrave Province. MESA Journal 49, June 2008, 16–19.

### ***Relevant figure(s)***

Figure 6.15, Figure 6.16, and Figure 8.20.

## **K.3.5 Mount Alvey**

(includes Pallatu Prospect\* and Mount Alvey East\*)

### ***Geological province***

Musgrave Province.

## Location

Mount Alvey Prospect: 130.10757°E, -26.26225°S; Mann (SG 52–11), Hanging Knoll (4945); ~475 km southwest of Alice Springs. Mount Alvey Prospect is part of Deering Hills Cu-Ni project which includes the Pallatu Ni-Cu-PGE prospect located ~18 km west-northwest of Mount Alvey.

## Classification

- ?2. Massive to poorly layered tholeiitic mafic-dominated intrusions.

## Geological setting

The Mount Alvey Pt-Pd prospect was discovered and drill tested by Rio Tinto Exploration Pty Limited in 2000 with three reverse circulation drill-holes spanning a strike length of approximately 500 m. The mineralisation is situated at the contact between a melagabbro and a gabbro within a layered mafic intrusion and strikes northeast (Mithril Resources Limited, 2007). The Ni-Cu-PGE mineralisation at Pallatu was intersected from drilling of surface EM conductors interpreted to be sourced from sulphide mineralisation and graphite-hosted within gabbros and pyroxenites interpreted to be part of the Giles Complex (Musgrave Minerals Limited, 2013).

## PGE mineralisation

All three drill-holes at the Mount Alvey Pt-Pd prospect intersected wide zones (14 m to 18 m) of elevated Pt-Pd values with highs of 0.90 g/t Pt-Pd over 4 m in RC00ALP001, 0.72 g/t Pt-Pd over 2 m in RC00ALP002 and 0.82 g/t Pt-Pd over 2 m in RC00ALP003 (see table below).

Appendix Table K.43 Key Pt, Pd, and Pt+Pd intersections at the Mount Alvey PGE prospect.

Drill-hole	From (m)	To (m)	Interval (m)	Pt (g/t)	Pd (g/t)	Pt+Pd (g/t)
RC00ALP001,	74	88	14	0.21	0.21	0.42
including	78	82	4	0.46	0.44	0.90
RC00ALP002,	92	106	14	0.19	0.18	0.37
including	94	96	2	0.39	0.33	0.72
RC00ALP003,	22	40	18	0.19	0.17	0.36
including	30	32	2	0.46	0.37	0.82

Drilling at the Pallatu Prospect intersected up to 0.5% Ni, 0.8% Cu, and up to 581 ppb Pt+Pd.

Assay results from drill-hole MAD001 on the Mount Alvey East Pt-Pd prospect in June 2008 showed significant results and included a 4 m interval grading 0.92 g/t Pt+Pd from 277 m down-hole, which sits within a broader zone of lower-grade mineralisation grading 0.62 g/t Pt+Pd over 10 m from 275 m. The Pt/Pd ratio averages 1.2:1 and the mineralisation occurs at the contact between a norite and pyroxenite. The drill-hole was targeted to test the potential eastern extension of the Mount Alvey prospect located 800 m to the west where previous explorers completed a reverse circulation drill-hole program that recorded the best PGE intersection of 0.9 g/t Pt+Pd over 4 m. The assay results suggested a strike length of mineralisation of at least 1.3 km (Mithril Resources Limited, 2008).

## Age of mineralisation

Mesoproterozoic.

### ***Current status***

Exploration sites.

### ***Economic significance***

Occurrence.

### ***Major references(s)***

Mithril Resources Limited, 2007. South Australia Musgrave tenements granted. Mithril Resources Limited announcement to the Australian Securities Exchange, 9 October 2007, 4 pp.

Mithril Resources Limited, 2008. Exploration update. Mithril Resources Limited announcement to the Australian Securities Exchange, 8 September 2008, 4 pp.

Musgrave Minerals Limited, 2013. Musgrave intersects massive nickel sulphide at Pallatu. Mithril Resources Limited announcement to the Australian Securities Exchange, 9 December 2013, 10 pp.

### ***Relevant figure(s)***

Figure 6.15, Figure 6.16, and Figure 8.20.

## **K.3.6 Nairne\***

### ***Geological province***

Delamerian Orogen.

### ***Location***

Nairne\*: 139.005043°E, -35.044923°S; Barker (SI 54–13), Mobilong (6727); ~45 km east of Adelaide.

### ***Classification***

- 8. Hydrothermal-Metamorphic.

### ***Geological setting***

The Cambrian Nairne pyritic beds occur at the base of the Kanmantoo Group, a >8 km-thick metamorphosed sequence of fine-grained quartzite, greywacke, and siltstone. The sulphides comprise pyrite, pyrrhotite, chalcopyrite, galena, sphalerite, with minor arsenopyrite and tetrahedrite. There is a strong correlation between S and graphite. The graphite varies from 1% to 2.4% in the ore beds, and with the S, is believed to be of biogenic origin. The extensive strike length of the pyritic beds (traced for 100 km) and mineral relationships suggests a sedimentary origin for the sulphides, although considerable remobilisation occurred during amphibolite-facies metamorphism.

### ***PGE mineralisation***

A Pd-bearing diantimonide (PdSb<sub>2</sub>) mineral grain measuring 6 µm by 13 µm has been reported by Graham (1978) to be in contact with chalcopyrite in a tension-gash vein sample from Ore Body 1. The PGE mineralisation appears to be hydrothermal; no mafic-ultramafic host rock is evident.

### ***Age of mineralisation***

Cambrian host rock.

### ***Current status***

Historical exploration site.

### ***Economic significance***

Occurrence.

### ***Major references(s)***

- Graham, J., 1978. Manganochromite, palladium antimonide, and some unusual mineral associations at the Nairne pyrite deposit, South Australia. *American Mineralogist*, 63, 1166–1174.
- Hoatson, D.M. and Glaser, L.M., 1989. Geology and economics of platinum-group metals in Australia. Bureau of Mineral Resources, Australia, Resource Report 5, 81 pp.

### ***Relevant figure(s)***

## **K.3.7 Taurus**

### ***Geological province***

Gawler Craton.

### ***Location***

Taurus: 135.62367°E, -29.65401°S; Billa Kalina (SH 53–07), Millers Creek (6038).

### ***Classification***

- 8. Hydrothermal-Metamorphic.

### ***Geological setting***

All of the available information on this prospect was summarised from the South Australia Geodata Database. The Taurus prospect was identified by OZ Minerals (in 2011?) as a coincident prominent NW-trending gravity, and high-amplitude magnetic anomaly. It is located northwest of a distinctive birds-eye magnetic complex of the White Hill igneous complex. Modelling of the magnetic profile indicated a steeply dipping tabular body as the source. Drilling identified a sequence of variably sheared mafic and metasedimentary rocks. Lithologies included granite, felsic gneiss, pelite, graphitic schist, dolostone, metabasalt, mafic and felsic pegmatite.

### ***PGE mineralisation***

Mineralisation included broad intervals of low-grade values of Cu, Fe, and Pt-Pd in zones of massive replacement magnetite, vein breccia, and coarse-grained mafic intrusive. Reported drill-hole intersections included: 107 m @ 0.13% Cu, 0.15 g/t PGEs; 121 m @ 0.5 g/t PGEs; and 15 m @ 1 g/t Pt, 0.66 g/t Pd. Mineralisation paragenesis was Fe metasomatism with magnetite-pyrite-chalcopyrite-pyrrhotite, apatite and titanite, and later alteration characterised by pyrite, apatite, quartz, calcite, hematite, and epidote. The main Fe metasomatism event took the form of relatively flat-lying seams to sub-horizontal vein arrays suggesting a component of vertical extension, possible east-west shortening. The Na-metasomatism event was defined by scapolite and albite, and the Ca-metasomatism event by diopside and actinolite.

The main commodities are Cu and PGEs, and the main ore minerals are chalcopyrite, Pd, and Pt. The main gangue minerals are apatite, calcite, epidote, hematite, magnetite, pyrite, pyrrhotite, and titanite.

***Age of mineralisation***

Mesoproterozoic?

***Current status***

Exploration site.

***Economic significance***

Occurrence.

***Major references(s)***

SA Geodata Database 2011. Mineral Deposit Details, Deposit Number: 9457.

***Relevant figure(s)***

**K.3.8 Wishbone**

***Geological province***

Gawler Craton.

***Location***

Wishbone: 134.5627°E, -32.91618°S; Streaky Bay (SI 53–02), Cungi (5832).

***Classification***

- 12. Others (minor or unknown economic importance); 12.E. Others (unknown geological setting).

***Geological setting***

The following summary of the available information on this prospect was sourced from the South Australia Geodata Database. The Wishbone prospect was located by aircore drilling on a magnetic anomaly targeting Ni-Cr mineralisation.

***PGE mineralisation***

Geochemistry identified low values, but anomalous Cu-Pt-Pd concentrations were associated with gabbro. The maximum Cu concentration was 1350 ppm from 26 m–28 m, with the maximum Pt+Pd concentration of 242 ppb obtained in drill-hole SBAC-019. The area is characterised with both magnetic and gravity anomalies. Follow-up diamond drilling identified gabbro and diorite cut by multiple granite dykes up to 16 m in thickness. No significant assays were returned.

***Age of mineralisation***

Unknown.

***Current status***

Exploration site.

***Economic significance***

Occurrence.

***Major references(s)***

Mithril Resources Limited, 2005. EL2861 and EL2891. Calca and Poochera (Streaky Bay Project).

Data release at partial relinquishment: Joint annual reports for the period 22/10/2001 to 13/2/2005.

Primary Industries and Resources SA Open File Envelope No. 9914, 152 pp.

SA Geodata Database 2011. Mineral Deposit Details, Deposit Number: 9457.

***Relevant figure(s)***

## K.4 QUEENSLAND

### K.4.1 Alma and Great New Zealand

#### ***Geological province***

New England Orogen.

#### ***Location***

Alma and Great New Zealand: 152.66864°E, -26.18632°S; Gympie (SG 56–10), Gympie (9445).

#### ***Classification***

- 8. Metamorphic/Hydrothermal.

#### ***Geological setting***

Although production data are not available, the historical Alma and Great New Zealand mine, which is located 0.7 km to the northeast of the Gympie post office, produced Au in 1893. Small quantities of Pt were also present. The deposit consists of a vein hosted by intermediate to mafic volcanic rocks and associated siliciclastic rocks of the Permian Rammutt Formation. It is located along the Alma and Lady Mary lines of reef. The Gympie goldfield has produced over 130 t of Au since production began in 1867. The Au is hosted by epithermal-style quartz-carbonate veins that have both parallel (e.g., Gympie-style veins) and discordant (Inglewood-style veins) relationships with host rocks, the former style of which produced the vast majority of Au.

#### ***PGE mineralisation***

Low concentrations of Pt are associated with epithermal Au veins.

Age of mineralisation: 245 ± 14 Ma.

#### ***Current status***

Mineral occurrence.

#### ***Economic significance***

Abandoned mine.

#### ***Major references(s)***

Champion D.C., Kositcin, N., Huston, D.L., Matthews, E. and Brown, C., 2009. Geodynamic synthesis of the Phanerozoic of eastern Australia and implications for metallogeny. *Geoscience Australia Record* 2009/18, 254 pp.

Cunneen, R., 1996. Recent developments in the geology of the Gympie Goldfield. *Abstracts - Geological Society of Australia* 43, 162–166.

MINOCC 2011 (available for purchase from the Geological Survey of Queensland: <http://mines.industry.qld.gov.au/geoscience/default.htm>).

**Relevant figure(s)**

**K.4.2 Broadbeach**

**Geological province**

New England Orogen.

**Location**

Broadbeach: 153.43442°E, -28.02289°S; Tweed Heads (SH 56–03), Murwillumbah (9541).

**Classification**

- 10. Placer; 10.D. Beach placers.

**Geological setting**

Broadbeach is one of several heavy-mineral-sand deposits in southeastern Queensland that contain(ed) trace quantities of Pt and Os. The deposit, which extended from Southport Spit to Broadbeach, was mined from 1944 to 1954, and produced 87 kt of heavy-mineral concentrates containing rutile, zircon, and ilmenite. Minor to trace constituents of the heavy-mineral sands include leucoxene, garnet, chromite, and cassiterite; Au and Pt are reported as trace constituents at Broadbeach. The heavy minerals are concentrated in layers of black sand that range from a centimetre to nearly half a metre in thickness. The Broadbeach deposit had a total length of ~15 km, and was up to ~250 m-wide. The heavy-mineral-sand layers have been mined to a depth of ~20 m.

**PGE mineralisation**

Platinum and Os are associated with heavy-mineral sands. Platinum is a relatively common constituent of heavy-mineral-sand deposits from eastern Australia, but Os has been rarely reported. The association of Pt and Os in the heavy-mineral sands is also rather unusual and indicates the source rocks of the PGEs may have had a hydrothermal origin, and/or the PGEs were derived from multiple sources. Alternatively, the historical status of the workings may also raise issues about the scientific identification of the Os.

**Age of mineralisation**

Quaternary.

**Current status**

Historical mine.

**Economic significance**

Occurrence.

**Major references(s)**

Ball, L.C., 1905. Gold, platinum, tinstone, and monazite in the beach sands of the south coast, Queensland. Geological Survey of Queensland Publication 198, 19 pp.

Connah, T.H., 1961. Beach sand heavy mineral deposits of Queensland. Geological Survey of Queensland Publication 302, 31 pp.

MINOCC 2011 (available for purchase from the Geological Survey of Queensland:  
<http://mines.industry.qld.gov.au/geoscience/default.htm>).

**Relevant figure(s)**

**K.4.3 Coopa**

**Geological province**

Mossman Orogen.

**Location**

Coopa: 145.73941°E , -17.42239°S; Innisfail (SE 55–06), Bartle Frere (8063).

**Classification**

- 10. Placer; 10.B. Alluvial placers derived from 'alpine- and ophiolitic-type' mafic-ultramafic intrusions.

**Geological setting**

The Coopa deposit was the first claim pegged in the Russell River goldfield and it was mined between 1886 and 1888. It is a deep-lead alluvial deposit underlying 6 m to 16 m of basalt cover and interpreted to be on a north-trending tributary of a paleo-river system. The wash is up to 0.76 m-thick. Minor quantities of fine flake Pt accompany the alluvial Au.

**PGE mineralisation**

Alluvial Pt accompanies Au.

**Age of mineralisation**

Cenozoic.

**Current status**

Historical mine.

**Economic significance**

Occurrence.

**Major references(s)**

MINOCC 2011 (available for purchase from the Geological Survey of Queensland:  
<http://mines.industry.qld.gov.au/geoscience/default.htm>).

**Relevant figure(s)**

**K.4.4 Coopooroo**

**Geological province**

Mossman Orogen.

### **Location**

Cooperoo: 145.73779°E, -17.38443°S ; Innisfail (SE 55–06), Bartle Frere (8063).

### **Classification**

- 10. Placer; 10.B. Alluvial placers derived from 'alpine- and ophiolitic-type' mafic-ultramafic intrusions.

### **Geological setting**

The Cooperoo deposit is located in the Russell River goldfield in the Boonjie Deep Lead area. It is a deep-lead alluvial deposit underlying basalt cover. The alluvium is 0.5 m-thick. Minor quantities of fine flake Pt accompany alluvial Au and cassiterite.

### **PGE mineralisation**

Alluvial Pt accompanies Au and cassiterite.

### **Age of mineralisation**

Cenozoic.

### **Current status**

Historical mine.

### **Economic significance**

Occurrence.

### **Major references(s)**

MINOCC 2011 (available for purchase from the Geological Survey of Queensland:  
<http://mines.industry.qld.gov.au/geoscience/default.htm>).

### **Relevant figure(s)**

## **K.4.5 Copper Canyon\***

### **Geological province**

Mount Isa Orogen.

### **Location**

Copper Canyon\*: 140.527406°E, -20.928331°S; Cloncurry (SF 54–02), Cloncurry (7056).

### **Classification**

- ?8. Hydrothermal-Metamorphic; ?8.G. U-Au-Pd-Pt mineralisation associated with graphitic schist and carbonaceous shale.
- ?10. Placer; 10.C. Alluvial placers.

### ***Geological setting***

Historical exploration investigated the Marimo Slate of the Mount Isa Orogen, a Proterozoic formation with carbonaceous shale units for a large-tonnage polymetallic base- and precious metal deposit, similar to that observed in the Kupferschiefer shales of central Europe.

### ***PGE mineralisation***

Historical exploration records show low, but geochemically significant Pd values from the Copper Canyon prospect, and Pt from the Mount McCabe region, ~25 km south of Cloncurry. Sporadic Au values between 1 ppm–3 ppm have been found from heavy-mineral and rock-chip sampling programs.

### ***Age of mineralisation***

Proterozoic and Cenozoic host rocks.

### ***Current status***

Historical exploration site.

### ***Economic significance***

Occurrence.

### ***Major references(s)***

Hoatson, D.M. and Glaser, L.M., 1989. Geology and economics of platinum-group metals in Australia. Bureau of Mineral Resources, Australia, Resource Report 5, 81 pp.

### ***Relevant figure(s)***

## **K.4.6 Currumbin**

### ***Geological province***

New England Orogen.

### ***Location***

Currumbin: 153.50011°E, -28.14904°S; Tweed Heads (SH 56–03), Tweed Heads (9641).

### ***Classification***

- 10. Placer; 10.D. Beach placer.

### ***Geological setting***

Currumbin is one of several heavy-mineral-sand deposits in southeastern Queensland that contain trace quantities of Pt and Os. The deposit, which is located between Currumbin Beach and Coolangatta, extends for 2.5 km and has a width of up to 250 m. The deposit has not been mined. The heavy minerals are concentrated in layers of black sand that range from a centimetre to nearly half a metre in thickness. The heavy-mineral sand layers contain rutile, which is the main commodity of interest, along with zircon, monazite, topaz, tourmaline, magnetite, and ilmenite. Minor to trace constituents of the heavy-mineral sands include leucoxene, garnet, chromite and cassiterite. Platinum, Os, and Au are reported as trace constituents at Currumbin, but their source(s) is unknown.

***PGE mineralisation***

Small flattened Pt and Os grains are associated with Au and heavy-mineral sands.

***Age of mineralisation***

Modern.

***Current status***

Occurrence, inactive (unlikely to be developed).

***Economic significance***

Occurrence.

***Major references(s)***

Ball, L.C., 1905. Gold, platinum, tinstone, and monazite in the beach sands of the south coast, Queensland. Geological Survey of Queensland Publication 198, 19 pp.

Connah, T.H., 1961. Beach sand heavy mineral deposits of Queensland. Geological Survey of Queensland Publication 302, 31 pp.

MINOCC 2011 (available for purchase from the Geological Survey of Queensland: <http://mines.industry.qld.gov.au/geoscience/default.htm>).

***Relevant figure(s)***

**K.4.7 Di**

***Geological province***

Mossman Orogen, Laura–Lakefield Basin.

***Location***

Di: 144.41376°E, -15.56071°S; Cooktown (SD 55–13), Laura (7766).

***Classification***

- 10. Placer; 10. C. Alluvial placers.

***Geological setting***

This Di prospect is located along the Mossman River. Although no prospective gravels were delineated during prospecting in the 1980s, panned concentrates commonly contained colours of Au. Platinum colours were also identified. Mining leases were granted in 1987.

***PGE mineralisation***

Placer Pt associated with Au.

***Age of mineralisation***

Cenozoic.

### ***Current status***

Exploration site–inactive.

### ***Economic significance***

Occurrence.

### ***Major references(s)***

MINOCC 2011 (available for purchase from the Geological Survey of Queensland:  
<http://mines.industry.qld.gov.au/geoscience/default.htm>).

### ***Relevant figure(s)***

## **K.4.8 Goldfind Creek**

### ***Geological province***

Etheridge Province.

### ***Location***

Goldfind Creek: 143.32358°E, -18.78670°S; Georgetown (SE 54–12), North Head (7560).

### ***Classification***

- 10. Placer; 10.C. Alluvial placers.

### ***Geological setting***

Goldfield Creek was one of a number of watercourses between the Gilbert and Robertson rivers that was mined for alluvial Au between 1870 and 1880. Mining leases were granted in 1984 from the headwaters of Goldfield Creek to its junction with the Robertson River. Platinum has also been reported in the alluvial deposits.

### ***PGE mineralisation***

Placer Pt associated with Au.

### ***Age of mineralisation***

Cenozoic.

### ***Current status***

Historical mine.

### ***Economic significance***

Occurrence.

### ***Major references(s)***

MINOCC 2011 (available for purchase from the Geological Survey of Queensland:  
<http://mines.industry.qld.gov.au/geoscience/default.htm>).

### ***Relevant figure(s)***

## **K.4.9 Goondicum Crater**

### ***Geological province***

New England Orogen.

### ***Location***

Goondicum Crater: 151.40912°E, -24.84398°S; Monto (SG 56–01), Monto (9148).

### ***Classification***

- 10. Placer, eluvial.
- 6. 'Alaskan- and Urals-type' mafic-ultramafic intrusions.

### ***Geological setting***

The Goondicum Crater ilmenite deposit is an eluvial placer deposit developed on the layered Goondicum Gabbro, which consists of layered troctolite, olivine-augite gabbro, biotite-hornblende-augite leucogabbro, ferrogabbro, anorthosite, clinopyroxenite, and syenite dykes. The body is a funnel-shaped intrusion that is circular at surface, where it has a diameter of 6 km. Layering dips 20°–30° toward the centre. It is also zoned, with a marginal poikilitic layer, followed upwards by a laminated gabbro, then by alternating leucogabbro and gabbro layers, and finally by an upper biotite-rich leucogabbro layer. Potassium-Ar analysis of hornblende indicates an intrusion age of ~96 Ma (although some doubt exists about this age).

Five resource types were recognised within the area: oxide gabbros; eluvial deposits; Cenozoic alluvials; alluvial channel deposits; and flood plain deposits. Ilmenite is the main mineral of interest in all resource types. In addition to ilmenite, these deposits also contain significant feldspar, apatite, and titanomagnetite, as well as trace Pt and Pd. The mineral resource is largely hosted by the eluvial deposits. Prior to commencement of mining, proven reserves totalled 300 kt ilmenite, 570 kt feldspar, and 110 kt apatite.

In 2004, a trial sorting plant commenced operation, with the first shipments of apatite and feldspar in mid-year. In March 2007 mining of ilmenite commenced. The mine and plant was closed and placed on care-and-maintenance in September 2008 due to flaws in plant design. Work restarted in 2013, but was stopped prior to recommissioning due to a drop in commodity prices.

### ***PGE mineralisation***

Trace quantities of Pt and Pd.

### ***Age of mineralisation***

Quaternary (eluvial deposits); ~96 Ma (age of source gabbro).

### ***Current status***

Historical mine (operated until September 2013).

### ***Economic significance***

Mine (care and maintenance).

### ***Major references(s)***

Bryan, S.E. and Purdy, D.J., 2013. Whitsunday silicic large igneous province. In: Jell, P.A. (editor), *Geology of Queensland*. Geological Survey of Queensland, 552–565.

Groen., S.G., 1993. Petrogenesis, petrochemistry, petrology and field relationships of the Goondicum Gabbro. BSc Honours thesis, Queensland University of Technology, Queensland, Australia.

MINOCC 2011 (available for purchase from the Geological Survey of Queensland: <http://mines.industry.qld.gov.au/geoscience/default.htm>).

Moore, G., 2003. The Goodicum Crater ilmenite, feldspar, apatite project. *AIG Bulletin* 38, 33–37.

### ***Relevant figure(s)***

## **K.4.10 Gympie goldfield alluvial group**

### ***Geological province***

New England Orogen.

### ***Location***

Gympie goldfield alluvial group: 152.65936°E, -26.19140°S; Gympie (SG 56–10), Gympie (9445).

### ***Classification***

- 10. Placer; 10.C. Alluvial placers.

### ***Geological setting***

Alluvial deposits at the Gympie goldfield produced Au from 1867, with most production in the early years coming from placer deposits. Between 1867 and 1872, over 9 t of Au were recorded to have been produced (the true production was probably significantly greater), virtually all from placer deposits. The deposits are Cenozoic alluvial deposits probably derived from epithermal veins hosted by intermediate to mafic volcanic rocks and associated siliciclastic rocks of the Permian Rammutt Formation. Small quantities of Pt were recorded at Brickfield Gully, near the boundary between the Lady Mary and Great Northern fault blocks.

### ***PGE mineralisation***

Minor native platinum associated with placer Au.

### ***Age of mineralisation***

Cenozoic alluvials derived from ~245 Ma epithermal vein deposits.

### ***Current status***

Historical mine.

### ***Economic significance***

Occurrence.

### **Major references(s)**

- Champion D.C., Kositcin, N., Huston, D.L., Matthews, E. and Brown, C., 2009. Geodynamic synthesis of the Phanerozoic of eastern Australia and implications for metallogeny. *Geoscience Australia Record* 2009/18, 254 pp.
- Cunneen, R., 1996. Recent developments in the geology of the Gympie Goldfield. *Abstracts - Geological Society of Australia* 43, 162–166.
- MINOCC 2011 (available for purchase from the Geological Survey of Queensland: <http://mines.industry.qld.gov.au/geoscience/default.htm>).

### **Relevant figure(s)**

## **K.4.11 Hawkwood**

### **Geological province**

New England Orogen.

### **Location**

Hawkwood: 150.87326°E, -25.78855°S; Mundubbera (SG 56–05), Auburn (9046).

### **Classification**

- ?2. Massive to poorly layered tholeiitic mafic-dominated intrusions; 2.B. Stratabound PGE-bearing magnetite layers.

### **Geological setting**

In 2012, Eastern Iron Limited announced a maiden inferred magnetite resource of 103.7 Mt grading 13.8% Fe, 1.83% TiO<sub>2</sub>, and 0.05% V at the Hawkwood deposit. The deposit is hosted by ferrogabbro that forms part of the Hawkwood Gabbro, which is presently included within the Delubra Gabbro. The Delubra Gabbro has an age of ~261 Ma.

The Hawkwood Gabbro at the prospect consists of layered magnetite-rich gabbro and pyroxenite, which form part of a differentiated mafic-ultramafic sill that intrudes felsic volcanic and volcanoclastic sedimentary rocks of the Lower Permian Narayen beds. Lam (2005) indicated that the layering in the gabbro was sub-horizontal, with the body dipping shallowly to the south. In contrast, Eastern Minerals indicate that the ferrogabbro dips steeply (80°) to the west.

Mineralogically the ferrogabbro consists of olivine, clinopyroxene, plagioclase, and orthopyroxene in a matrix of titaniferous magnetite with accessory ilmenite, and with lesser pyrrhotite and millerite, and trace pentlandite. Soil samples collected in a grid over the prospect area yielded Pt and Pd assays up to 0.115 g/t and 0.063 g/t, respectively. Analyses of trench samples yielded assays approaching 1 g/t for both metals (see below).

### **PGE mineralisation**

Trench samples have yielded grades of up to 0.71 g/t Pt, 0.90 g/t Pd, 0.55% Cu, and 0.09 g/t Au.

### **Age of mineralisation**

261.0 ± 5.7 Ma (hornblende Ar-Ar).

### **Current status**

Exploration site—active.

### **Economic significance**

Occurrence.

### **Major references(s)**

Blake, P.R. and Withnall, I.W., 2013. Yarrol Province. In: Jell, P.A. (editor), *Geology of Queensland*. Geological Survey of Queensland, 336–351.

Lam, J.S., 2005. A review of mines and metalliferous mineralisation in the Mundubbera 1:250 000 Sheet area, Queensland. *Queensland Geological Record* 2005/1.

Purdy, D.J., 2013. Granitoids of the northern New England Orogen. In: Jell, P.A. (editor), *Geology of Queensland*. Geological Survey of Queensland, 399–444.

MINOCC 2011 (available for purchase from the Geological Survey of Queensland: <http://mines.industry.qld.gov.au/geoscience/default.htm>).

[www.easterniron.com.au](http://www.easterniron.com.au) (particularly ASX announcement dated 18 May 2012)

### **Relevant figure(s)**

## **K.4.12 Hawkwood North**

### **Geological province**

New England Orogen.

### **Location**

Hawkwood North: 150.85664°E, -25.77886°S; Mundubbera (SG 56–05), Auburn (9046).

### **Classification**

- ?2. Massive to poorly layered tholeiitic mafic-dominated intrusions; 2.B. Stratabound PGE-bearing magnetite layers.

### **Geological setting**

In 2012, Eastern Iron Limited announced a maiden inferred magnetite resource of 103.7 Mt grading 13.8% Fe, 1.83% TiO<sub>2</sub>, and 0.05% V at the nearby Hawkwood deposit. This deposit and the North Hawkwood prospect are hosted by ferrogabbro that forms part of the Hawkwood Gabbro, which is presently included within the Delubra Gabbro. The Delubra Gabbro has an age of ~261 Ma.

The Hawkwood Gabbro consists of layered magnetite-rich gabbro and pyroxenite, which form part of a differentiated mafic-ultramafic sill that intrudes felsic volcanic and volcanoclastic sedimentary rocks of the Lower Permian Narayen beds.

### **PGE mineralisation**

MINOCC reports the presence of Pt and Pd.

### **Age of mineralisation**

261.0 ± 5.7 Ma (hornblende Ar-Ar).

### ***Current status***

Exploration site–active.

### ***Economic significance***

Occurrence.

### ***Major references(s)***

Blake, P.R. and Withnall I.W., 2013. Yarrol Province. In: Jell, P.A. (editor), *Geology of Queensland*. Brisbane, Geological Survey of Queensland, 336–351.

Lam, J.S., 2005. A review of mines and metalliferous mineralisation in the Mundubbera 1:250 000 Sheet area, Queensland. *Queensland Geological Record* 2005/1.

Purdy, D.J., 2013. Granitoids of the northern New England Orogen. In: Jell, P.A. (editor), *Geology of Queensland*. Brisbane, Geological Survey of Queensland, 399–444.

MINOCC 2011 (available for purchase from the Geological Survey of Queensland: <http://mines.industry.qld.gov.au/geoscience/default.htm>).

### ***Relevant figure(s)***

## **K.4.13 Jack Goodie**

### ***Geological province***

New England Orogen.

### ***Location***

Jack Goodie: 151.41960°E, -24.91998°S; Monto (SG 56–01), Monto (9148).

### ***Classification***

- 10. Placer; 10.C. Alluvial placers.

### ***Geological setting***

The Jack Goodie alluvial placer ilmenite prospect is located downstream from the Goondicum Crater ilmenite deposit, which is an eluvial placer deposit developed on the layered Goondicum Gabbro. Potassium-Ar analysis of hornblende indicates an intrusion age of ~96 Ma (some doubt exists about this age), although the age of placer formation is Quaternary.

### ***PGE mineralisation***

Trace quantities of Pt and Pd.

### ***Age of mineralisation***

Quaternary.

### ***Current status***

Exploration site–inactive.

### ***Economic significance***

Occurrence.

### ***Major references(s)***

Bryan, S.E. and Purdy, D.J., 2013. Whitsunday silicic large igneous province. In: Jell, P.A. (editor), *Geology of Queensland*. Geological Survey of Queensland, 552–565.

Groen, S.G., 1993. Petrogenesis, petrochemistry, petrology and field relationships of the Goondicum Gabbro. BSc Honours thesis, Queensland University of Technology, Queensland, Australia.

MINOCC 2011 (available for purchase from the Geological Survey of Queensland: <http://mines.industry.qld.gov.au/geoscience/default.htm>).

Moore, G., 2003. The Goodicum Crater ilmenite, feldspar, apatite project. *AIG Bulletin* 38, 33–37.

### ***Relevant figure(s)***

## **K.4.14 Kennedy Creek**

### ***Geological province***

Mossman Orogen, Hodgkinson Province.

### ***Location***

Kennedy Creek: 144.52791°E, -15.67765°S; Cooktown (SD 55–13), Butchers Hill (7866).

### ***Classification***

- 10. Placer; 10.C. Alluvial placers.

### ***Geological setting***

Exploration in 1985 and 1986 identified sub-economic Au placer deposits along a 8 km to 10 km stretch of the east branch of Kennedy Creek. The placer deposits were identified in alluvial deposits of various ages that covered the full width of the valley. In addition to Au, minor cassiterite and Pt were also recovered from the placer concentrates. Recovered Au grades were 0.093 g/m<sup>3</sup> to 0.102 g/m<sup>3</sup>.

### ***PGE mineralisation***

Native platinum in Au placer.

### ***Age of mineralisation***

Cenozoic.

### ***Current status***

Exploration site–inactive.

### ***Economic significance***

Occurrence.

### **Major references(s)**

MINOCC 2011 (available for purchase from the Geological Survey of Queensland: <http://mines.industry.qld.gov.au/geoscience/default.htm>).

### **Relevant figure(s)**

## **K.4.15 Kokomo**

### **Geological province**

Thomson Orogen.

### **Location**

Kokomo: 145.17121°E, -18.55251°S; Einasleigh (SE 55–09), Valley of Lagoons (7960).

### **Classification**

- 9. Regolith-laterite; 9.A. PGE-bearing regolith developed on ultramafic-mafic igneous rocks.

### **Geological setting**

The Kokomo deposit is one of three residual lateritic Ni-Co-Sc deposits developed on ultramafic rocks in the Greenvale area, north Queensland. The other deposits include Lucknow and Greenvale, the latter a producing mine until the early 1990s. These deposits are hosted in laterite profiles developed on ultramafic rocks of the Sandalwood Serpentinite, which, along with the Stenhouse Creek Amphibolite, constitute the Boiler Gully Complex. Lateritisation is thought to have occurred post-Cretaceous.

The Kokomo deposit is the largest of the Greenvale area deposits, having a total resource of 29.5 Mt grading 0.49% Ni, 0.08% Co, and 55 ppm Sc. It is located on a north-northeast-trending ultramafic body that is up to ~700 m-wide and ~16 km-long. The protoliths include peridotite, dunite, and pyroxenite that are thought to be sill-like bodies. The margins of the composite ultramafic body are in faulted contact with metasedimentary rocks of the Cambrian Halls Reward Metamorphics. Nickel and Co enrichment is commonly towards the base of the lateritic profile, which can be up to 50 m-thick.

### **PGE mineralisation**

The deposit is anomalous in PGEs.

### **Age of mineralisation**

Ultramafic bodies possibly emplaced in the Cambrian, with lateritic enrichment post-Cretaceous.

### **Current status**

Exploration site—active.

### **Economic significance**

Small Ni-Co-Sc deposit.

### **Major references(s)**

Fergusson, C.L., Henderson, R.A. and Withnall, I.W., 2013. Greenvale Province. In: Jell, P.A. (editor), *Geology of Queensland*. Geological Survey of Queensland, 152–159.

[www.metallicminerals.com.au](http://www.metallicminerals.com.au) (particularly ASX release dated 21 October 2013).

### **Relevant figure(s)**

## **K.4.16 Koppany**

### **Geological province**

Mount Isa Orogen.

### **Location**

Koppany: 140.02129°E, -20.76164°S; Cloncurry (SF 54–02), Marraba (6956).

### **Classification**

- 8. Hydrothermal-Metamorphic.

### **Geological setting**

The Koppany prospect is a north-striking shear-zone-hosted hydrothermal Cu-Au deposit possibly associated with diorite/gabbro sills. It is hosted by the Corella Formation and is associated with silicic, chloritic, and kaolinitic alteration zones. A 2–3 m-wide gossan is present at the surface; it averaged 1.6% Cu over 7.5 m with zones containing up to 1.1 g/t Au. The deposit is associated with a radiometric anomaly. Drilling underneath the gossan yielded a 134 m-wide (down-hole depth: 9.5 m–143.6 m) pyrrhotitic (2%–25% pyrrhotite) zone containing a 7.1 m intersection (from 47.8 m) assaying 0.3% Cu, 0.15% Ni, 0.13% Co, 0.035 g/t Au, 0.066 g/t Pd, and 0.110 g/t Pt. In addition to pyrrhotite, the prospect contains primary chalcopyrite, gypsum, chlorite, pyrite, and quartz. Secondary minerals include malachite and limonite. Hematite and marcasite are also present.

### **PGE mineralisation**

7.1 m interval @ 0.66 g/t Pd and 0.110 g/t Pt.

### **Age of mineralisation**

Paleoproterozoic (?)

### **Current status**

Exploration site–inactive.

### **Economic significance**

Occurrence.

### **Major references(s)**

MINOCC 2011 (available for purchase from the Geological Survey of Queensland: <http://mines.industry.qld.gov.au/geoscience/default.htm>).

**Relevant figure(s)**

**K.4.17 Lady Mary North**

**Geological province**

New England Orogen.

**Location**

Lady Mary North: 152.66839°E, -26.18347°S; Gympie (SG 56–10), Gympie (9445).

**Classification**

- 8. Hydrothermal-Metamorphic.

**Geological setting**

The Lady Mary North mine, which is located 0.9 km northeast of the Gympie post office, was worked intermittently between 1870 and 1892, producing 235 kg Au bullion from 2530 t of ore. Small quantities of Pt were also reported. The deposit consists of veins that are hosted by intermediate to mafic volcanic rocks and associated siliciclastic rocks of the Permian Rammutt Formation and dip steeply (70°) to the west. The Gympie goldfield has produced over 130 t of Au since production began in 1867. The Au is hosted by epithermal-style quartz-carbonate veins that have both parallel (e.g., Gympie-style veins) and discordant (Inglewood-style veins) relationships with host rocks, the former style of which produced the vast majority of Au.

**PGE mineralisation**

Low-level concentrations associated with epithermal Au veins.

**Age of mineralisation**

245 ± 14 Ma.

**Current status**

Mineral occurrence.

**Economic significance**

Abandoned mine.

**Major references(s)**

Champion D.C., Kositcin, N., Huston, D.L., Matthews, E. and Brown, C., 2009. Geodynamic synthesis of the Phanerozoic of eastern Australia and implications for metallogeny. *Geoscience Australia Record* 2009/18, 254 pp.

Cunneen, R., 1996. Recent developments in the geology of the Gympie Goldfield. *Abstracts - Geological Society of Australia* 43, 162–166.

MINOCC 2011 (available for purchase from the Geological Survey of Queensland: <http://mines.industry.qld.gov.au/geoscience/default.htm>).

## **Relevant figure(s)**

### **K.4.18 Laura River**

#### **Geological province**

Mossman Orogen, Laura–Lakefield Basin.

#### **Location**

Laura River: 144.45916°E, -15.58202°S; Cooktown (SD 55–13), Laura (7766).

#### **Classification**

- 10. Placer; 10.C. Alluvial placers.

#### **Geological setting**

The Laura River region ~200 km northwest of Cairns contains several Quaternary alluvium and lacustrine deposits. In the 1980s, Gold Copper Exploration Limited delineated significant amounts of alluvial Au and Pt in the Laura River. The mineralisation extends over a distance of 15 km in the Laura River, between Laura and the mouth of Kennedy Creek, and also in Mosman River and Kennedy Creek, which are tributaries of the Laura River. Residue concentrates from bulk alluvium samples recorded up to 840.5 ppm Pt and 6.1 ppm Pd, indicating an exceptionally high Pt/Pd ratio (Hoatson and Glaser, 1989). Gold levels averaged 0.30 g/m<sup>3</sup> for the 140 m<sup>3</sup> of bulk samples. In 1987, Gold Copper Exploration Limited announced that Laura River contained a potential mineable resource of 2.5 million cubic metres of *in situ* coarse alluvial auriferous and platiniferous gravels. Potentially mineralised Cenozoic sediments occur in the prospective areas, but the original source rocks of the PGEs and Au have not been identified.

#### **PGE mineralisation**

Native platinum and palladium are associated with an alluvial Au placer.

#### **Age of mineralisation**

Quaternary.

#### **Current status**

Exploration site–inactive.

#### **Economic significance**

Occurrence.

#### **Major references(s)**

Hoatson, D.M. and Glaser, L.M., 1989. Geology and economics of platinum-group metals in Australia. Bureau of Mineral Resources, Australia, Resource Report 5, 81 pp.

MINOCC 2011 (available for purchase from the Geological Survey of Queensland: <http://mines.industry.qld.gov.au/geoscience/default.htm>).

**Relevant figure(s)**

**K.4.19 Lucknow**

**Geological province**

New England Orogen.

**Location**

Lucknow: 152.66219°E, -26.18391°S; Gympie (SG 56–10), Gympie (9445).

**Classification**

- 8. Hydrothermal-Metamorphic.

**Geological setting**

Platinum has been reported in the Lucknow, Alma, Lady Mary Au-bearing reefs, and Warren Hasting's Shaft in the Gympie district, ~150 km north-northwest of Brisbane. The Pt occurs with native gold, galena, and pyrite in quartz veins that intrude slate, tuff, and conglomerate. In the vicinity of the reefs and in Brickfield Gully, the Pt also occurs in Au-bearing alluvium; one nugget is reported to have weighed 12.4 g.

The Lucknow mine, which is located 0.7 km north of the Gympie post office, was the site of extensive underground exploration between 1921 and 1925, although no ore was mined. A bulk sample from the upper (eastern) reef assayed 4.2 g/t Au, 2900 g/t Ag, and 2% Cu. Small quantities of Pt were also reported. The deposit consists of sub-vertical veins hosted by intermediate to mafic volcanic rocks and associated siliciclastic rocks of the Permian Rammutt Formation. The Gympie goldfield has produced over 130 t of Au since production began in 1867. The Au is hosted by epithermal-style quartz-carbonate veins that have both parallel (e.g., Gympie-style veins) and discordant (Inglewood-style veins) relationships with host rocks, the former style of which produced the vast majority of Au.

The nearby Widgee Mountain area comprising undifferentiated Paleozoic serpentinite and metamorphic rocks and Triassic granite has been of interest to exploration. Base-metal sulphide occurrences related to faults occur in granite, serpentinite, and metasediments-metavolcanics. Early exploration has shown that several prospects carry anomalous Au and PGE values (Hoatson and Glaser, 1989).

**PGE mineralisation**

Low-level concentrations of PGEs are associated with epithermal Au veins in the Lucknow deposit, and other similar hydrothermal prospects nearby.

**Age of mineralisation**

245 ± 14 Ma.

**Current status**

Mineral occurrence.

### ***Economic significance***

Abandoned mine.

### ***Major references(s)***

Champion D.C., Kositcin, N., Huston, D.L., Matthews, E. and Brown, C., 2009. Geodynamic synthesis of the Phanerozoic of eastern Australia and implications for metallogeny. *Geoscience Australia Record* 2009/18, 254 pp.

Cunneen, R., 1996. Recent developments in the geology of the Gympie Goldfield. Abstracts - Geological Society of Australia 43, 162–166.

Hoatson, D.M. and Glaser, L.M., 1989. Geology and economics of platinum-group metals in Australia. Bureau of Mineral Resources, Australia, Resource Report 5, 81 pp.

MINOCC 2011 (available for purchase from the Geological Survey of Queensland: <http://mines.industry.qld.gov.au/geoscience/default.htm>).

### ***Relevant figure(s)***

## **K.4.20 Magdalene**

### ***Geological province***

New England Orogen.

### ***Location***

Magdalene: 150.14913°E, -23.61962°S; Rockhampton (SF 56–13), Mount Morgan (8950).

### ***Classification***

- 8. Hydrothermal-Metamorphic.

### ***Geological setting***

The Magdalene deposit is hosted by the Triassic to Jurassic Bucknalla Gabbro, which is a tilted lopolith up to 2000 m-thick that is made up of a layered gabbroic suite including olivine gabbro, gabbro, troctolite, ferrogabbro, and anorthosite. This body intrudes Lower Permian mafic volcanics of the Rookwood Volcanics in the Grange Subprovince of the Yarrol Province. The body crops out over an area of approximately 10 km<sup>2</sup>. It is the only mafic-ultramafic complex out of seven in the region to contain Cu-Pd-Au mineralisation.

Although the body is layered, this layering is disrupted, a feature that Purdy (2013) suggests implies poor potential for economic mineralisation. The best drill intercepts are 10 m @ 0.42% Cu, 0.32 g/t Pd, and 0.16 g/t Au; and 6 m @ 0.32% Cu and 0.13 g/t Au. Mineralogically, primary sulphide mineralisation in the Bucknall Gabbro is characterised, in descending order of abundance, chalcopyrite, bornite and millerite. The chalcopyrite and bornite are commonly supergene altered to digenite and covellite.

### ***PGE mineralisation***

The highest PGE interval reported was 0.32 g/t Pd over 10 m.

### ***Age of mineralisation***

Triassic-Jurassic.

### ***Current status***

Exploration site–active.

### ***Economic significance***

Occurrence.

### ***Major references(s)***

MINOCC 2011 (available for purchase from the Geological Survey of Queensland: <http://mines.industry.qld.gov.au/geoscience/default.htm>).

Purdy, D.J., 2013. Granitoids of the northern New England Orogen. In: Jell, P.A. (editor), *Geology of Queensland*. Geological Survey of Queensland, 399–444.

Reeves, S.J. and Keays, R., 1995. The platinum-group element geochemistry of the Bucknalla layered complex, central Queensland. *Australian Journal of Earth Sciences* 42, 187–201.

### ***Relevant figure(s)***

## **K.4.21 Palm Beach**

### ***Geological province***

New England Orogen.

### ***Location***

Palm Beach: 153.46838°E, -28.11304°S; Tweed Heads (SH 56–03), Murwillumbah (9541).

### ***Classification***

- 10. Placer; 10.C. Beach placers.

### ***Geological setting***

Palm Beach is one of several heavy-mineral-sand deposits in southeastern Queensland that contain trace quantities of Pt and Os. The deposit, which is located at Palm Beach on the Gold Coast, extends for ~3.3 km and has a width of up to 250 m. The deposit has not been mined. The heavy minerals are concentrated in layers of black sand that range from a centimetre to nearly half a metre in thickness. The heavy-mineral-sand layers contain rutile, which is the main commodity of interest, along with zircon and ilmenite. Minor to trace constituents of the heavy-mineral sands include leucoxene, garnet, chromite, and cassiterite; Pt and Os are reported as trace constituents at Palm Beach.

### ***PGE mineralisation***

Platinum and Os are associated with heavy-mineral sands. Platinum is a relatively common constituent of heavy-mineral-sand deposits from eastern Australia, but Os has been rarely reported. The association of Pt and Os in the heavy-mineral sands is also rather unusual and indicates the source rocks of the PGEs may have had a hydrothermal origin, and/or the PGEs were derived from multiple sources. Alternatively, the historical status of the reports relating to the workings may also raise issues about the scientific identification of the Os.

### ***Age of mineralisation***

Modern.

### ***Current status***

Occurrence, inactive (unlikely to be developed).

### ***Economic significance***

Occurrence.

### ***Major references(s)***

Ball, L.C., 1905. Gold, platinum, tinstone, and monazite in the beach sands of the south coast, Queensland. Geological Survey of Queensland Publication 198, 19 pp.

Connah, T.H., 1961. Beach sand heavy mineral deposits of Queensland. Geological Survey of Queensland Publication 302, 31 pp.

MINOCC 2011 (available for purchase from the Geological Survey of Queensland: <http://mines.industry.qld.gov.au/geoscience/default.htm>).

### ***Relevant figure(s)***

## **K.4.22 Prospect Bore**

### ***Geological province***

Croydon Province.

### ***Location***

Prospect Bore: 142.25158°E, -18.89275°S; Croydon (SE 54–11), Prospect (7360).

### ***Classification***

- ?2. Massive to poorly layered tholeiitic mafic-dominated intrusions; 2.B. Stratabound PGE-bearing magnetite layers.
- ?8. Hydrothermal-Metamorphic.

### ***Geological setting***

The Prospect Bore Intrusion, located ~80 km south of Croydon in the Croydon Province of northern Queensland, was discovered in 1982 following up an aeromagnetic anomaly. The ?Proterozoic gabbroic intrusion is located on the northwest-trending Borer River fracture zone and is masked by up to 100 m of cover. In the region, variably altered gabbro, felsic volcanics, intrusive felsic porphyries, quartzite, and graphite-bearing breccias have been defined by drilling. Two percussion holes within the intrusion identified a fine-grained layered gabbro that contains 2%–3% magnetite, 3%–4% ilmenite, and minor pyrite and chalcopyrite. Strategic Minerals Corporation Limited (50%) and Golden Plateau NL (50%) during the ~1980s delineated anomalous Pt (up to 0.12 ppm), Pd (up to 0.38 ppm), and Au (up to 0.08 ppm) concentrations in a hydrothermally-altered Ti-rich gabbroic phase of the intrusion. Assays from other holes indicated average grades of 0.64% V<sub>2</sub>O<sub>5</sub> and 15.15% TiO<sub>2</sub> over a 98-m-vertical interval (34 m–132 m). This prospect is also recorded in the MINOCC database as containing Pt and Pd, although details are not given. Anomalous Au is also present, with epithermal quartz-carbonate veins

assaying up to 0.68 g/t Au over a 1 m interval. Other gabbroic intrusions to the south of the Prospect Bore Intrusion have also been reported to have anomalous concentrations of Pt and Pd.

***PGE mineralisation***

Contains anomalous concentrations of Pt and Pd.

***Age of mineralisation***

Proterozoic (inferred).

***Current status***

Exploration site–inactive.

***Economic significance***

Occurrence.

***Major references(s)***

MINOCC 2011 (available for purchase from the Geological Survey of Queensland: <http://mines.industry.qld.gov.au/geoscience/default.htm>).

***Relevant figure(s)***

#### **K.4.23 Saint George River**

***Geological province***

Mossman Orogen, Laura–Lakefield Basin.

***Location***

Saint George River: 144.02608°E, -15.63258°S; Cooktown (SD 55–13), Laura (7766).

***Classification***

- 10. Placer; 10.C. Alluvial placers.

***Geological setting***

Placer deposits extend 35 km upstream from the mouth of the Saint George River. These deposits are up to 25 m-wide and 1–1.5 m-deep.

***PGE mineralisation***

Trace quantities of Pt are associated with alluvial Au.

***Age of mineralisation***

Quaternary.

***Current status***

Mineral occurrence.

### ***Economic significance***

Occurrence.

### ***Major references(s)***

MINOCC 2011 (available for purchase from the Geological Survey of Queensland:  
<http://mines.industry.qld.gov.au/geoscience/default.htm>).

### ***Relevant figure(s)***

## **K.4.24 Saxby**

### ***Geological province***

Mount Isa Orogen.

### ***Location***

Saxby: 140.88015°E, -19.18853°S; Dobbyn (SE 54–14), Canobie (7059).

### ***Classification***

- 1. Layered tholeiitic mafic-ultramafic intrusions; 1.A. Stratabound PGE-bearing sulphide layers.

### ***Geological setting***

Follow-up drilling in 1995, which targeted an under-cover magnetic anomaly, identified olivine gabbro and gabbro-norite containing anomalous, although subeconomic Ni and Cu mineralisation. The prospect underlies 440 m or more of cover, including Neogene-Quaternary alluvial and related deposits, and the Mesozoic Carpentaria Basin. Drilling (four holes) has intersected mineralisation along a strike length of ~2 km. The best intersection was 10 m @ 0.25% Ni and 0.18% Cu (drill-hole TT001D). Anomalous Pt was also identified. Ore minerals identified in the core include pyrrhotite, pyrite, and pentlandite.

### ***PGE mineralisation***

Anomalous Pt associated with Fe and Ni sulphide minerals.

### ***Age of mineralisation***

Uncertain.

### ***Current status***

Exploration site–active.

### ***Economic significance***

Occurrence.

### ***Major references(s)***

MINOCC 2011 (available for purchase from the Geological Survey of Queensland:  
<http://mines.industry.qld.gov.au/geoscience/default.htm>).

**Relevant figure(s)**

**K.4.25 Unnamed 309578**

**Geological province**

Etheridge Province.

**Location**

Unnamed 309578: 143.18753°E, -18.45594°S; Georgetown (SE 54–12), Forest Home (7561).

**Classification**

- 9. Regolith-laterite.

**Geological setting**

The unnamed 309578 occurrence is a residual, supergene-enriched Mn-oxide deposit developed on the Paleoproterozoic Heliman Formation. Analysis of 'wad' yielded anomalous Zn (4000 ppm) and Pd (0.09 g/t).

**PGE mineralisation**

Anomalous Pd (0.09 g/t) associated with 'wad'.

**Age of mineralisation**

Cenozoic.

**Current status**

Mineral occurrence.

**Economic significance**

Occurrence.

**Major references(s)**

MINOCC 2011 (available for purchase from the Geological Survey of Queensland:

<http://mines.industry.qld.gov.au/geoscience/default.htm>).

**Relevant figure(s)**

**K.4.26 Wairambar**

**Geological province**

Mossman Orogen.

**Location**

Wairambar: 145.72535°E, -17.41372°S; Innisfail (SE 55–06), Bartle Frere (8063).

### **Classification**

- 10. Placer; 10.C. Alluvial placer (deep lead).

### **Geological setting**

The Wairambar is a deep-lead alluvial deposit. Minor quantities of fine flake Pt accompany the alluvial Au.

### **PGE mineralisation**

Alluvial Pt accompanies Au.

### **Age of mineralisation**

Cenozoic.

### **Current status**

Historical mine.

### **Economic significance**

Occurrence.

### **Major references(s)**

MINOCC 2011 (available for purchase from the Geological Survey of Queensland:  
<http://mines.industry.qld.gov.au/geoscience/default.htm>).

### **Relevant figure(s)**

## **K.4.27 Walkers Road**

### **Geological province**

New England Orogen.

### **Location**

Walkers Road: 150.89191°E, -25.81058°S; Munduberra (SG 56–05), Auburn (9046).

### **Classification**

- ?1. Layered tholeiitic mafic-ultramafic intrusions; ?1.A. Stratabound PGE-bearing sulphide layers.

### **Geological setting**

The Walkers Road Cu-Pt-Pd occurrence is hosted by the Late Permian (~261 Ma) Delubra Gabbro. The Delubra Gabbro is a medium-K calc-alkaline gabbro, with subordinate quartz diorite and granodiorite. This range in composition is interpreted as the consequence of two-stage crystal fractionation. The parent gabbro is interpreted as a modified partial mantle melt. The gabbro intrudes felsic volcanic and volcanoclastic sedimentary rocks of the Lower Permian Narayan beds and is intruded by the Cheltenham Granite. It is typically layered and includes leucogabbro, pyroxenite, and

ferrogabbro. Rock-chip samples have returned up to 1820 ppm Cu, 0.256 g/t Au, 0.135 g/t Pt, 0.174 g/t Pd, and 55.8% Fe.

***PGE mineralisation***

Up to 0.135 g/t Pt and 0.174 g/t Pd associated with Au, Cu, and Fe.

***Age of mineralisation***

261.0 ± 5.7 Ma (hornblende Ar-Ar).

***Current status***

Exploration site—active.

***Economic significance***

Occurrence.

***Major references(s)***

Blake, P.R. and Withnall, I.W., 2013. Yarrol Province. In: Jell, P.A. (editor), *Geology of Queensland*. Geological Survey of Queensland, 336–351.

Lam, J.S., 2005. A review of mines and metalliferous mineralisation in the Mundubbera 1:250 000 Sheet area, Queensland. *Queensland Geological Record* 2005/1.

MINOCC 2011 (available for purchase from the Geological Survey of Queensland: <http://mines.industry.qld.gov.au/geoscience/default.htm>).

Purdy, D.J., 2013. Granitoids of the northern New England Orogen. In: Jell, P.A. (editor), *Geology of Queensland*. Geological Survey of Queensland, 399–444.

***Relevant figure(s)***

**K.4.28 Wateranga**

***Geological province***

New England Orogen.

***Location***

Wateranga: 151.83616°E, -25.31706°S; Maryborough (SG 56–06), Mount Perry (9247).

***Classification***

The eluvial/alluvial part of the resource is:

- 10. Placer; ?10.A. Alluvial placers derived from 'Alaskan- and Urals-type' mafic-ultramafic intrusions.

The resource in the underlying mafic-ultramafic intrusion is:

- ?6. 'Alaskan- and Urals-type' mafic-ultramafic intrusions.

### ***Geological setting***

Alaskan and placer-type PGE mineralisation has been investigated in the Wateranga, Goondicum, Hawkwood, and Boyne intrusions of the Wateranga district of southern coastal Queensland. With the Fifield district of central New South Wales, the Wateranga region represents one of the major regions in Australia for exploration related to Alaskan and associated placer-type PGE mineralisation. The small composite and ovoid-shaped Paleozoic-Mesozoic complexes at Wateranga occur along major lineaments and consist of norite, olivine gabbro, pyroxenite, and anorthosite. The Wateranga Gabbro Intrusion shows evidence of differentiation and layering with the development of titaniferous magnetite horizons. The Wateranga deposits consist of both hard-rock and combined eluvial-alluvial-colluvial prospects formed by the weathering of the Wateranga Gabbro. These latter unconsolidated deposits extend over an area of approximately 6 km × 6 km and surround a core of outcropping gabbro that is up to 3.3 km-long and 2.7 km-long. A global resource (reserves plus resources) has been calculated for the unconsolidated material of 225 Mt with a grade of 4.8% ilmenite, 20% feldspar, 12% mica (muscovite and phlogopite), 0.8% apatite, and 30 ppm Sc. In addition, a global resource has also been calculated for exposed 'hard-rock' gabbro at 345 Mt averaging 34.3% feldspar.

Gabbronorite, including olivine-bearing varieties, is the most common rock type of the Wateranga Gabbro Intrusion. Other rock types include gabbro, ferrogabbro, troctolite, anorthosite, norite, hornblendite, pyroxenite, pyroxene-hornblende gabbronorite, magnetite-ilmenite-apatite-olivine-rich pyroxenite and gabbronorite, and granophyre. The hornblende-rich and oxide-rich rocks are concentrated near the northeast margin of the intrusion. Sulphide minerals (chalcopyrite, pyrrhotite, pentlandite, sphalerite and pyrite) typically constitute 0.1%–1% of the rocks and occur as intercumulus phases.

### ***PGE mineralisation***

The Queensland Department of Mines reported PGE values in a surface sample of 9 ppm and 14 ppm in a magnetite-apatite-bearing pyroxenite from the Wateranga Gabbro (Hoatson and Glaser, 1989). Check analyses of old Queensland Mines drill core failed to delineate any PGE mineralisation, but a 51-m-wide zone of titaniferous and locally apatite-rich magnetite pyroxenite may correlate with the surface material. In other petrological studies, a Rh-Ru phase has been observed as inclusions in orthopyroxene.

### ***Age of mineralisation***

246 ± 7 Ma (hornblende K-Ar)–age of primary gabbro; Quaternary–age for eluvial deposits.

### ***Current status***

Exploration site–active.

### ***Economic significance***

Occurrence.

### ***Major references(s)***

Evans, W.J., Arculus, R.J. and Ashley, P.M., 1993. Petrological variation within the Wateranga layered intrusion, southeast Queensland. In: Flood P.G. and Atchison, J.C. (editors), New England Orogen Conference Proceedings. Department of Geology and Geophysics, University of New England, Armidale, Australia, 629–635.

Hoatson, D.M. and Glaser, L.M., 1989. Geology and economics of platinum-group metals in Australia. Bureau of Mineral Resources, Australia, Resource Report 5, 81 pp.

MINOCC 2011 (available for purchase from the Geological Survey of Queensland: <http://mines.industry.qld.gov.au/geoscience/default.htm>).

Purdy, D.J., 2013. Granitoids of the northern New England Orogen. In: Jell, P.A. (editor), Geology of Queensland. Geological Survey of Queensland, 399–444.

Talusani, R.V.R., Sivell, W.J. and Ashley, P.M., 2005. Mineral chemistry, petrogenesis, and tectonic setting of the Wateranga layered intrusion, southeast Queensland, Australia. Canadian Journal of Earth Sciences, 42, 1965–1987.

### ***Relevant figure(s)***

## **K.4.29 West Coast Creek alluvials**

### ***Geological province***

New England Orogen.

### ***Location***

West Coast Creek alluvials: 152.28650°E, -26.10236°S; Gympie (SG 56–10), Goomeri (9345).

### ***Classification***

- 10. Placer; 10.C. Alluvial placer.

### ***Geological setting***

Alluvial deposits on West Coast Creek, located 23.5 km east-northeast of Goomeri, were discovered in 1868 and worked extensively until 1874, and intermittently between 1899 and 1915, and during the early 1930s. More recent mining has occurred since the 1980s. The alluvial workings extend ~4 km, with a width of 40 m to 80 m, and depths to 8 m. Minor Pt occurs with the placer Au.

### ***PGE mineralisation***

Platinum associated with placer Au.

### ***Age of mineralisation***

Quaternary.

### ***Current status***

Abandoned mine.

### ***Economic significance***

Occurrence.

### ***Major references(s)***

MINOCC 2011 (available for purchase from the Geological Survey of Queensland: <http://mines.industry.qld.gov.au/geoscience/default.htm>).

### **Relevant figure(s)**

#### **K.4.30 Westwood**

##### **Geological province**

New England Orogen.

##### **Location**

Westwood palladium: 150.14420°E, -23.62558°S; Rockhampton (SF 56–13), Mount Morgan (8950).

##### **Classification**

- 8. Hydrothermal-Metamorphic.

##### **Geological setting**

The Westwood Pd deposit is hosted by the Triassic to Jurassic Bucknalla Gabbro, which is a tilted lopolith up to 2000 m-thick that is made up of a layered gabbroic suite including olivine gabbro, gabbro, troctolite, ferrogabbro, and anorthosite. This body intrudes Lower Permian mafic volcanics of the Rookwood Volcanics in the Grantleigh Subprovince of the Yarrol Province. The body crops out over an area of approximately 10 km<sup>2</sup>.

Although the body is layered, this layering is disrupted, a feature that Purdy (2013) suggests implies poor potential for economic mineralisation. A 12 m-deep shaft was sunk at the prospect site in 1885. Minor quantities of malachite and azurite are present in the dumps. Mineralogically, primary mineralisation in the Bucknall Gabbro is characterised, in descending order of abundance, chalcopyrite, bornite, and millerite. The chalcopyrite and bornite are commonly supergene altered to digenite and covellite.

##### **PGE mineralisation**

Palladium and Au mineralisation occurs in small irregular quartz veins in a fractured dioritic rock at the Westwood Au mines. Associated minerals include malachite, azurite, chalcocite, bornite, covellite, chalcopyrite, hematite, ilmenite, magnetite, arsenopyrite, and millerite. The Pd occurs largely as porpezite (Pd-bearing Au), which forms irregular to subrounded grains up to 0.3 mm and is associated with chalcopyrite and bornite as disseminations and in veins. Highest Pd values reported from the shaft area are 10.94 ppm Pd, 6.12 ppm Au, 15.03 ppm Ag, and 2.2% Cu, and a sample from a small trench 180 m east of the shaft assayed 5.13 ppm Pd, 2.07 ppm Au, 7.83 ppm Ag, and 1.0% Cu (Hoatson and Glaser, 1989). Other published PGE assays include 3.73 g/t Pt and 6.00 g/t Pd from a surface sample that also assayed 2.11% Cu and 3.24 g/t Au (Reeves and Keays, 1995).

A number of other small (<30 km<sup>2</sup> in area) gabbroic intrusions in the Westwood district have created interest for their PGE potential. These include the Fred Creek, Midgee, Westwood, Windah, Halton, Boogargan, Eulogie Park, and Mount Gerard intrusions. These bodies appear to form a part of a 400 km-long-trending linear zone of ?Permian mafic intrusions that extends from Westwood southeast to near Gympie. Other intrusions in this zone include Goondicum, Wateranga, Wigton, and Goomboorian near Gympie.

### ***Age of mineralisation***

?Permian to Jurassic.

### ***Current status***

Historical mine.

### ***Economic significance***

Occurrence.

### ***Major references(s)***

- Hoatson, D.M. and Glaser, L.M., 1989. Geology and economics of platinum-group metals in Australia. Bureau of Mineral Resources, Australia, Resource Report 5, 81 pp.
- Purdy, D.J., 2013. Granitoids of the northern New England Orogen. In: Jell, P.A. (editor), Geology of Queensland. Geological Survey of Queensland, 399–444.
- Reeves, S.J. and Keays, R., 1995. The platinum-group element geochemistry of the Bucknalla layered complex, central Queensland. Australian Journal of Earth Sciences, 42, 187–201.
- MINOCC 2011 (available for purchase from the Geological Survey of Queensland: <http://mines.industry.qld.gov.au/geoscience/default.htm>).

### ***Relevant figure(s)***

Figure 8.18h.

## **K.4.31 Yanky Franks**

### ***Geological province***

Etheridge Province.

### ***Location***

Yanky Franks: 143.28654°E, -18.78264°S; Georgetown (SE 54–12), North Head (7560).

### ***Classification***

- 10. Placer; 10.C. Alluvial placers.

### ***Geological setting***

Yanky Franks Creek was one of a number of watercourses between the Gilbert and Robertson rivers that was mined for alluvial Au between 1870 and 1880. Mining leases were granted in 1984 for Yanky Franks Creek and an inferred resource of 2 800 000m<sup>3</sup> of auriferous gravel was estimated for Goldfind and Yanky Frank Creeks. Platinum has also been reported in the alluvial deposits.

### ***PGE mineralisation***

Placer Pt associated with Au.

### ***Age of mineralisation***

Cenozoic.

***Current status***

Historical mine.

***Economic significance***

Occurrence.

***Major references(s)***

MINOCC 2011 (available for purchase from the Geological Survey of Queensland:  
<http://mines.industry.qld.gov.au/geoscience/default.htm>).

***Relevant figure(s)***

## K.5 NEW SOUTH WALES

### K.5.1 Avondale Ni-Co-Pt Prospect

(see Fifield–Syerston area)

### K.5.2 Ballina–Tree Point

(includes PGE beach placers on north NSW coast: Ballina, Gallaghers Claim, New Zealanders Claim, McAuleys Lead, Buchanans Head, Minnie Water and Tree Point)

#### ***Geological province***

New England Orogen, Clarence Moreton Basin.

#### ***Location***

Ballina Beach workings: 153.59982°E, -28.8545°S; Tweed Heads (SH 56–03), Ballina (9640); ~3 km east of Ballina.

Gallaghers Claim: 153.44721°E, -29.12767°S; Maclean (SH 56–07), Woodburn (9539); ~2 km east-southeast of Evans Head.

New Zealander Claim: 153.45034°E, -29.13849°S; Maclean (SH 56–07), Woodburn (9539); ~3 km east-southeast of Evans Head.

McAuleys Lead: 153.35104°E, -29.25973°S; Maclean (SH 56–07), Woodburn (9539); ~3 km east-southeast of Evans Head.

Buchanans Head: 153.34481°E, -29.54964°S; Maclean (SH 56–07), Bare Point (9538); ~12 km south of Yamba.

Minnie Water: 153.295904°E, -29.76979°S; Maclean (SH 56–07), Bare Point (9538); ~11 km north of Wooli.

Tree Point: 153.29079°E, -29.79055°S; Maclean (SH 56–07), Bare Point (9538); ~8 km north of Wooli.

#### ***Classification***

- 10. Placer; 10.D. Beach placers.

#### ***Geological setting***

Heavy-mineral concentrations along the northeast coast of New South Wales.

#### ***PGE mineralisation***

Platinum grains have been reported in heavy-mineral beach sands along the New South Wales coast. Approximately 2.8 kg were produced at Ballina and Evan's Head on the northern coast. Of the seven occurrences recorded in the NSW Minview database, Buchanans Head was recorded as a Pt occurrence; New Zealanders Claim and Tree Point as Au and Pt; Ballina Workings and Minnie Waters as Au, Sn, and Pt; Gallaghers Claim and McAuleys Lead as Au and Pt.

### ***Age of mineralisation***

Quaternary?

### ***Current status***

Historical heavy-mineral-sand workings.

### ***Economic significance***

Occurrences.

### ***Major references(s)***

MinView website <http://minview.minerals.nsw.gov.au/mv2web/mv2>

### ***Relevant figure(s)***

## **K.5.3 Boonoo Boonoo River–Wylie Creek**

### ***Geological province***

New England Orogen.

### ***Location***

Boonoo Boonoo River: 152.11922°E, -28.87326°S; Warwick (SH 56–02), Drake (9340); ~30 km southeast of Stanthorpe.

Wylie Creek: 152.12123°E, -28.62281°S; Warwick (SH56–02), Drake (9340); ~19 km east-northeast of Stanthorpe.

### ***Classification***

- 10. Placer; 10.C. Alluvial placers.

### ***Geological setting***

Provenance for alluvial tin-dominated placers with minor associated PGEs near Stanthorpe in the New England Orogen include Late Silurian to Middle Triassic shelf and trough sediments, felsic to mafic volcanics, and continental sediments. Igneous activity comprises Cenozoic volcanics, Silurian to Triassic felsic to mafic volcanics and intrusives, minor ultramafic intrusives and Cenozoic mafic to felsic volcanics. Regional metamorphism ranges from very low to very high with moderate to strong folding and faulting.

### ***PGE mineralisation***

Tin-dominated modern fluvial placer with minor PGEs?

### ***Age of mineralisation***

Quaternary.

### ***Current status***

Historical alluvial workings.

### ***Economic significance***

Historical alluvial placer operation at Wylie Creek with Sn, W, Bi, Au, diamonds, and various other gemstones recovered from the area, but only alluvial Sn has been produced in significant quantities. Historical exploration reports noted '*a number of coarse angular specks of gold and a few tiny specks of platinoid (?) metal. Insignificant quantities of Au have been recovered from the creek.*' Boonoo Boonoo River is a modern fluvial placer occurrence dominated by Au and Sn, with minor Pt with historical production of 0.0039 t recorded (Minview database). The Boonoo Boonoo Gold Dredging Company began erecting a concentration plant in 1910, commencing operations in the following year. The resulting concentrate contained Au, Sn, and black sand, two tons of which were sent to Europe for evaluation. The company ceased operations in 1913 after the concentrate had been identified as a mixture of Au, Ag, Pt, and Sn, the last two in unpayable quantities (Wynn et al., 1992a,b).

### ***Major references(s)***

- Wynn, D.W., Tucker, R.M., Syvret, J.N. and Foster, J.T., 1992a. E.L. 3788. Twelve monthly report for period ended 21 March 1992a. Saracen Minerals NL GS1992/103, 244 pp.
- Wynn, D.W., Foster, J.T., Syvret, J.N. and Tucker, R.M., 1992b. E.L. 3424—Wilsons Downfall. Final Report. Saracen Minerals NL GS1991/134, 132 pp.

### ***Relevant figure(s)***

## **K.5.4 Buchanans Head**

(see Ballina–Tree Point: PGE beach placers)

## **K.5.5 Bulbodney—Hylea area**

### ***Geological province***

Lachlan Orogen.

### ***Location***

Bulbodney Platinum Prospect: 147.332505°E, -32.28781°S; Narromine (SI 55–03), Tottenham (8333); ~82 km south of Nyngan.

Keens Prospect, RAB hole BCR122: 147.300410°E, -32.297364°S; Narromine (SI 55–03), Tottenham (8333).

RAB hole BCR58: 147.316884°E, -32.297364°S; Narromine (SI 55–03), Tottenham (8333).

Drill-hole SMR2 Sampsons Tank Magnetic Anomaly: 147.267220°E, -32.097884°S; Narromine (SI 55–03), Tottenham (8333).

Hylea Tiger Creek: 147.226548°E, -32.364998°S; Narromine (SI 55–03), Tottenham (8333); 89 km south of Nyngan.

### **Classification**

- 6. 'Alaskan- and Urals-type' mafic-ultramafic intrusions; 6.A. PGE mineralisation in concentrically zoned ultramafic-mafic intrusions (Bulbodney Platinum Prospect, Hylea Tiger Creek).
- 12. Others (minor or unknown economic importance); 12.E. Others (unknown geological setting), (RAB hole BCR58, RAB hole BCR122, and drill-hole SMR2 Sampsons Tank Magnetic Anomaly, Keens Prospect were recorded in MinView database as unknown).

### **Geological setting**

The Bulbodney Platinum Prospect and drill-holes BCR58, BCR122 are in vicinity of ultramafic intrusions at Bulbodney Creek.

### **PGE mineralisation**

Drill intersections in the Bulbodney Creek Intrusive returned 16 m @ 3.4 ppm, and included 8 m @ 5.2 ppm (Helix Resources NL, 1986, 1987). A large area of anomalous Pt associated with anomalous Ni, Co, and Cr was defined in ultramafic intrusions at Hylea Tiger Creek.

### **Age of mineralisation**

Ordovician?

### **Current status**

Historical exploration sites.

### **Economic significance**

Occurrences.

### **Major references(s)**

Lea W.L., 1998. Joint final report for Exploration Licences 252 'Hylea' and 4454 'Tigers Creek' to February 1998. Volume 1 of 1 Narromine SI 55–03. PlatSearch NL. GS1998 453, 12 pp.  
Helix Resources NL, 1986. Helix Resources NL 1986 Prospectus.  
Helix Resources NL, 1987. Helix Resources NL 1987 Annual Report.

### **Relevant figure(s)**

Figure 6.35, Figure 6.36, and Figure 6.37.

## **K.5.6 Burra Alluvial**

(see Fifield–Syerston area)

## **K.5.7 Cincinnati Lead**

(see Fifield–Syerston area)

### **K.5.8 Cincinnati (Pt) Prospect**

(see Fifield–Syerston area)

### **K.5.9 Coolac**

(see Mount Mary Mines)

### **K.5.10 Copper Hill Mine**

#### ***Geological province***

Lachlan Orogen.

#### ***Location***

Copper Hill Mine: 148.86793°E, -33.05219°S; Bathurst (SI 55–08), Molong (8631); ~5 km north of Molong.

#### ***Classification***

- 8. Hydrothermal-Metamorphic; 8.E. Disseminated sulphides in alkaline to sub-alkaline porphyry Cu deposit.

#### ***Geological setting***

The Copper Hill Mine is located near the northern end of the Molong Rise, which forms part of the Molong–South Coast Anticlinorium. Geological mapping identified several centres of intense sericite-chlorite-carbonate-magnetite alteration within a major structural corridor containing several Cu and Au prospects and deposits. The Cu-Au±Pd mineralisation is hosted in zones of quartz stockwork within porphyritic dacite intrusives of the Copper Hill Intrusive complex. Stockworks occur in structural corridors in two structural orientations and trend east-southeast and north-northwest. These form a conjugate fault set and are approximately bisected by the elongate axis of the dacitic intrusion.

Copper Hill is the type example in Australia of PGEs associated with alkaline to sub-alkaline felsic porphyry igneous rocks in a magmatic-hydrothermal mineral system. Another example of PGEs in a similar geological setting to Copper Hill is from the central coast of New South Wales. Anomalous Pt, Pd, and Au concentrations have been reported at Mount Little Dromedary, 25 km south of Ulladulla near Bawley Point and Goalen Head. Hydrothermally-altered shonkinitic rock types, containing pyrite, chalcopyrite, and magnetite have also been reported from this region (Hoatson and Glaser, 1989).

#### ***PGE mineralisation***

Drilling by Cyprus in 1989 intersected significant Cu-Au-Pd mineralisation associated with a quartz-magnetite-chlorite stockwork zone at the Open-cut prospect. Maximum values in unoxidised core samples over a 1 m interval is 8.17 g/t Au and 0.91 g/t Pd. These high Au and Pd zones also have anomalous Cu up to 1.8%. A good correlation between Au, Cu, and Pd occurs in stockwork zones (Torrey, 1990: p. 50, 58; Erceg, 1992: p. 5, 6, 18).

### ***Age of mineralisation***

The porphyry Cu-Au mineralising system associated with altered dacite porphyry and quartz dacite intrusions at Copper Hill Mine is probably similar in age to the host intrusive rocks (Carr et al., 1995). Girvan (1992) indicates the CHIC was emplaced during the Late Ordovician at  $447 \pm 5$  Ma, which is consistent with the regional classification scheme (~450 Ma–445 Ma for Group 3) for these intrusions as proposed by Glen et al. (2003).

### ***Current status***

Area of historical mining with the Copper Hill mine being the oldest mined Cu deposit in NSW with mining operations commencing in 1845 (see Section 6.4). Currently an undeveloped porphyry Cu-Au deposit with advanced assessment status and JORC-compliant resources.

### ***Economic significance***

Large low-grade deposit. On 27 June 2011, Golden Cross Resources Limited reported a total Measured, Indicated, and Inferred Resource for the Copper Hill deposit of 197 Mt @ 0.31% Cu and 0.26 g/t Au. There was no mention of Pd in the resource figures.

### ***Major references(s)***

- Carr, G.R., Dean, J.A., Suppel, D.W. and Heithersay, P.S., 1995. Precise lead isotope fingerprinting of hydrothermal activity associated with Ordovician and Carboniferous metallogenic events in the Lachlan Fold Belt of New South Wales. *Economic Geology*, 90, 1467–1505.
- Erceg M., 1992. Copper Hill Exploration Licence 2290, Annual Report to 13 November, 1991. Cyprus Gold Australia Corporation. NSW GS1992/083, 529 pp.
- Girvan, S.W., 1992. Geology and mineralisation of the Copper Hill Porphyry Copper-Gold Deposit, near Molong, NSW. BSc (Hons.) thesis, Australian National University, Canberra, Australia, 75 pp.
- Glen, R.A., Crawford, A.J. and Cooke, D.R., 2003. Tectonic setting of porphyry copper-gold mineralisation in the Macquarie Arc. In: Blevin, P. Jones, M. and Chappell, B. (editors), *Magma to Mineralisation: The Ishihara Symposium*. Geoscience Australia Record 2003/14, 65–68.
- Golden Cross Resources Limited, 2011. New Copper Hill resource estimate: 197 million tonnes at 0.31% copper and 0.26 g/t gold, 3 pp.
- Hoatson, D.M. and Glaser, L.M., 1989. Geology and economics of platinum-group metals in Australia. Bureau of Mineral Resources, Australia, Resource Report 5, 81 pp.
- Scott, K.M. and Torrey, C.E., 2003. Copper Hill porphyry Cu-Au prospect, central NSW. CRC LEME 2003, 3 pp. <http://crcleme.org.au/RegExpOre/CopperHill.pdf> (last accessed 10 October 2014).
- Torrey, C.E., 1990. Copper Hill project, Exploration Licence 2290, review and exploration proposal. Cyprus Gold Australia Corporation. NSW GS1990/225, 192 pp.

### ***Relevant figure(s)***

Figure 6.50.

## **K.5.11 Drill-hole SMR2 Sampsons Tank Magnetic Anomaly**

(see Bulbodney group)

## **K.5.12 Gallaghers Claim**

(see Ballina–Tree Point: PGE beach placers)

### **K.5.13 Hylea Tiger Creek**

(see Bulbodney group)

### **K.5.14 Fifield Lead**

(see Fifield–Syerston area)

### **K.5.15 Fifield Project**

(see Fifield–Syerston area)

### **K.5.16 Fifield—Syerston area**

#### ***Geological province***

Lachlan Orogen.

#### ***Location***

The Fifield–Syerston area contains 25 PGE-bearing occurrences and deposits which fall into three main types of mineralisation: igneous related; laterite-hosted; and deep-lead placers. One of the unnamed occurrences has been labelled as 'vein-type Au-Cu-Pd'. These occurrences and deposits are listed as follows:

#### **Igneous-related (8 occurrences):**

Owendale North Pt-Cu prospect: 147.46985°E, -32.69219°S; Narromine (SI 55–03), Boona Mount (8332); 13 km north-northeast of the Fifield township, and ~370 km west-northwest of Sydney, NSW.

Murga: 147.43252°E, -32.79304°S; Narromine (SI 55–03), Boona Mount (8332).

Kelvin Grove: 147.4469°E, -32.72213°S; Narromine (SI 55–03), Boona Mount (8332).

Flemington: 147.41756°E, -32.75602°S; Narromine (SI 55–03), Boona Mount (8332).

Mount Derriwong: 147.35333°E, -32.98218°S; Narromine (SI 55–03), Boona Mount (8332).

Kars Prospect: 147.50093°E, -33.02136°S; Forbes (SI 55–07), Bogan Gate (8431).

Unnamed occurrence (NSW MinView ID No 102524): 147.41243°E, -32.80294°S; Narromine (SI 55–03), Boona Mount (8332).

Unnamed occurrence (NSW MinView ID No 102552): 147.52382°E, -32.85484°S; Narromine (SI 55–03), Tullamore (8432).

#### **Lateritic deposits (5 occurrences and deposits):**

Syerston: 147.41959°E; -32.75669°S; Narromine (SI 55–03), Boona Mount (8332); ~6.5 km northwest of the Fifield township.

## New South Wales

Owendale North residual Pt-Cu-Ni-Co Prospect: 147.47006°E, -32.69215°S; Narromine (SI 55–03), Boona Mount (8332); ~12.5 km north of the Fifield township.

Cincinnati (Pt) Prospect: 147.46866°E, -32.70992°S; Narromine (SI 55–03), Boona Mount (8332).

Milverton Residual Pt deposit: 147.47216°E, -32.71292°S; Narromine (SI 55–03), Boona Mount (8332).

Avondale Ni-Co-Pt Prospect: 147.49214°E, -32.92353°S; Narromine (SI 55–03), Boona Mount (8332); ~6.5 km northwest of the Fifield township.

Unnamed occurrence (NSW MINVIEW ID No 102555): 147.42397°E, -32.7578°S; Narromine (SI 55–03), Boona Mount (8332).

### **Deep leads and placers (11 occurrences and deposits):**

Fifield Lead: 147.451648°E, -32.795454°S; Narromine (SI 55–03), Boona Mount (8332); ~1.8 km northwest of Fifield township and ~78 km northwest of Parkes, central New South Wales.

Burra Alluvial: 147.3682°E, -32.67821°S; Narromine (SI 55–03), Boona Mount (8332).

Owendale Lead: 147.46101°E, -32.69453°S; Narromine (SI 55–03), Boona Mount (8332).

Cincinnati Lead: 147.46644°E, -32.71345°S; Narromine (SI 55–03), Boona Mount (8332).

Milverton Lead: 147.47641°E, -32.72198°S; Narromine (SI 55–03), Boona Mount (8332).

Studwick's Lead: 147.48127°E, -32.77284°S; Narromine (SI 55–03), Boona Mount (8332).

Reynolds Tank: 147.4585°E, -32.77613°S; Narromine (SI 55–03), Boona Mount (8332).

Jack's Lookout: 147.47558°E, -32.8056°S; Narromine (SI 55–03), Boona Mount (8332).

Gillenbine Lead: 147.4798°E, -32.81623°S; Narromine (SI 55–03), Boona Mount (8332).

Platina Lead: 147.4682°E, -32.84514°S; Narromine (SI 55–03), Boona Mount (8332).

Unnamed occurrence (NSW MINVIEW ID No 102277): 147.46878°E, -32.80733°S; Narromine (SI 55–03), Boona Mount (8332).

### **An unnamed vein Au-Cu deposit:**

Unnamed occurrence (NSW MINVIEW ID No 102556): 147.38124°E, -32.75162°S; Narromine (SI 55–03), Boona Mount (8332).

### **Unknown deposit type:**

Fifield Project: 147.46933°E, -32.83216°S; Narromine (SI 55–03), Boona Mount (8332); ~3 km south-southeast of Fifield township, location of Rimfire Pacific Mining NL project, no information as to type of deposit, possibly a geographical reference point for the project.

### **Classification**

- 6. 'Alaskan- and Urals-type' mafic-ultramafic intrusions; 6.A. PGE mineralisation in concentrically zoned ultramafic-mafic intrusions (Owendale North Pt-Cu Prospect, Murga, Kelvin Grove, Flemington, Mount Derriwong, Kars Prospect, and two unnamed occurrences).
- 8. Hydrothermal-Metamorphic. (Unnamed occurrence (NSW MINVIEW ID No 102556)).
- 9. Regolith-Laterite; 9.A. PGE-bearing regolith developed on ultramafic-mafic igneous rocks (Syerston, Owendale North residual Pt-Cu-Ni-Co Prospect, Cincinnati (Pt) Prospect, Milverton Residual, Avondale Ni-Co-Pt Prospect and an unnamed lateritic PGE occurrence).
- 10. Placer; 10.A. Alluvial placers derived from 'Alaskan- and Urals-type' mafic-ultramafic intrusions (Burra Alluvial, Owendale Lead, Cincinnati Lead, Milverton Lead, Studwick's Lead, Reynolds Tank, Fifield Lead, Jacks Lookout, Gillenbine Lead, Platina Lead and one unnamed occurrence).

### **Geological setting**

Composite Early Devonian intrusive complexes of the concentric 'Alaskan-type' occur in the Fifield region. These include the Owendale intrusive complex (also called Kelvin Grove Intrusion), which is a circular body consisting largely of biotite diorite, diorite, hornblendite, pyroxenite, and serpentinite. The largest body, the Tout intrusive complex (also called Flemington Intrusion), measures 5 km by 12 km, and contains hornblende melasyenite, hornblende meladiorite, hornblende pyroxenite, quartz-hornblende monzonite, and augite monzonite. The Murga intrusive complex (also called Wanda Bye Intrusion) is composed of similar rock types to the other intrusions, with hornblende pyroxenite, augite hornblendite, meladiorite, and quartz diorite predominant.

### **PGE mineralisation**

In the Fifield–Nyngan region, the PGEs occur in 'Alaskan-type' intrusions which are characterised by irregular distribution and narrow widths of mineralisation. The overlying soils, which are rarely more than 2 m-thick, and the weathered bedrock up to 40 m-thick, have anomalous Pt levels, and in some cases over extensive widths.

### **Igneous-related deposits:**

Eight occurrences (Owendale North Pt-Cu Prospect, Murga, Kelvin Grove, Flemington, Mount Derriwong, Kars Prospect (Appendix Figure K.35) and two unnamed occurrences) are hosted by the underlying ultramafic rocks.

Drilling along the southern and southeastern margins of the Owendale Intrusion delineated high-PGE levels in a medium- to coarse-grained clinopyroxenite. Significant intersections include: DDH FKD 1: 1.57 m @ 13.19 ppm Pt, 0.90 ppm Pd, and 0.5 ppm Rh; and DDH FKD 6: 0.41 m @ 10.35 ppm Pt, 0.5 ppm Pd. The mineralised clinopyroxenite is low in S (S <0.04%), Se, Te, Sb, Bi, As, and Sn and is characterised by high Pt/Pd ratios. The PGMs generally occur as euhedral, 15 µm to 30 µm crystals of Fe-platinum coexisting with erlichmanite and Al-F-sphene, fluorite, and are trapped in cracks in magnetite, usually near ilmenite. Several PGMs have been tentatively identified and include platinum-isoferroplatinum, cooperite, geversite, platarsite, sperrylite, stibiopalladinite, and erlichmanite. The concentric form of the intrusions, alkaline character of the rock types, paucity of orthopyroxene, and low Ni and Cr contents suggest the Fifield intrusions do not conform to the layered intrusive-PGE model, but may have affinities with Alaskan–Ural-type intrusions. Hydrothermal solutions possibly derived from, or driven by, late dunite intrusive plugs may have remobilised the PGEs into

monomineralic clinopyroxenite zones. Exploratory drilling in 2013 delineated new zones of fresh rock Pt mineralisation at Cincinnati and Milverton with the highest single Pt assay to date of 1 m @ 24 g/t Pt from 26 m (Platina Resources Limited, 2013a).

A different style of hard-rock PGE mineralisation has been recognised at the Tout Intrusion, 10 km southwest of the Owendale Intrusion. Anomalous Pd and Pt levels are associated with elevated Cu, Ag, and Au concentrations in pyroxenitic rocks that are traversed by a pervasive fracture zone. The metal association and structural control may indicate that hydrothermal fluids were important in remobilising the disseminated sulphides of magmatic origin into areas with a favourable structural framework. It is probable that similar base-metal sulphide-PGE associations of magmatic-hydrothermal origin will be defined in other intrusions of the Fifield–Nyngan province.

#### **Lateritic deposits:**

Five deposits (Syerston, Owendale North Pt-Cu-Ni-Co Prospect, Cincinnati (Pt) Prospect, Milverton Residual, Avondale Ni-Co-Pt Prospect and an unnamed lateritic PGE occurrence) are Pt-enriched laterites that overlie ultramafic-dominant basement rocks. All of the current published Pt and Sc Indicated and Inferred Resources are hosted in the laterite. The laterite deposits are up to 55 m-thick, and contain significant amounts of isoferroplatinum (a platinum and iron alloy), and Sc mineralisation associated with the goethite mineral component has lesser amounts of Cu, Co, and Ni.

#### **Placers:**

Eleven occurrences and deposits (Burra Alluvial, Owendale Lead, Cincinnati Lead, Milverton Lead, Studwick's Lead, Reynolds Tank, Fifield Lead, Jacks Lookout, Gillenbine Lead, Platina Lead and one unnamed occurrence) have been classed as alluvial placers and deep leads.

The Fifield district has been the largest producer of Pt in eastern Australia with total Pt and Au production of 633 kg and 197 kg, respectively (see Appendix F). The Pt has been won from placer deposits that cover an area of 5 km by 10 km in the vicinity of the Tout and Murga intrusive complexes. The Pt is usually associated with Au in Cenozoic gravels, in buried leads which have redeposited Pt eroded from Cenozoic gravels, and in recent alluvium derived from gravels and leads. The two major leads are the Platina and Fifield Leads, but drilling has shown that the alluvial Pt also occurs well away from the old mined areas. The Pt and Au occur as coarse grains generally in depressions in the bedrock and in wash dirt 10 cm above bedrock. Nuggets range up to 42 g. The Platina Lead has produced 478 kg of Pt at grades of 5 ppm to 13 ppm, and 124 kg of Au at 1.5 ppm to 4.6 ppm. The original source of the Pt is believed to be the nearby intrusive mafic-ultramafic complexes.

#### ***Age of mineralisation***

The most recent and robust geochronological methods involving the dating of zircon indicate a late Ordovician to late Silurian age (e.g., 450 Ma to 420 Ma) for the Fifield intrusions. The mineralised laterite profiles overlying these intrusions generally formed during the ?Early and/or Late Cenozoic (see Section 6.4.9.1).

#### ***Current status***

Active exploration sites.

### ***Economic significance***

The Fifield region has been a significant producer of PGEs in the past, with the vast majority of the production being sourced from deep leads and alluvial placers. Most of the current resources published in the region are hosted in lateritic deposits and include Ni, Co, Au, and Sc as potential co-products.

On 3 October 2013, Platina Resources Limited released an update on their Pt and Sc resources for the Owendale North, Cincinnati and Milverton lateritic Pt and Sc deposits. The company used a 0.3 g/t cut-off grade for Pt and a 300 ppm cut-off grade for Sc to obtain a combined Mineral Resource as follows:

- Indicated Mineral Resource: 11 Mt @ 0.55 g/t Pt, 240 ppm Sc, 0.19% Ni, 0.05% Co;
- Inferred Mineral Resource: 33 Mt @ 0.39 g/t Pt, 300 ppm Sc, 0.12% Ni, 0.05% Co; and
- Total Mineral Resource: 44 Mt @ 0.43 g/t Pt, 290 ppm Sc, 0.14% Ni, 0.05% Co.

Containing a total *in situ* content of 0.60 million ounces of Pt and 12 500 t of Sc metal.

### ***Major references(s)***

Elliott, S.J. and Martin, A.R. (editors), 1991. Geology and mineralisation of the Fifield platinum province, New South Wales. Sixth International Platinum Symposium, Perth, Western Australia. Guidebook for the Pre-Symposium Field Excursion. Geological Society of Australia, 43 pp.

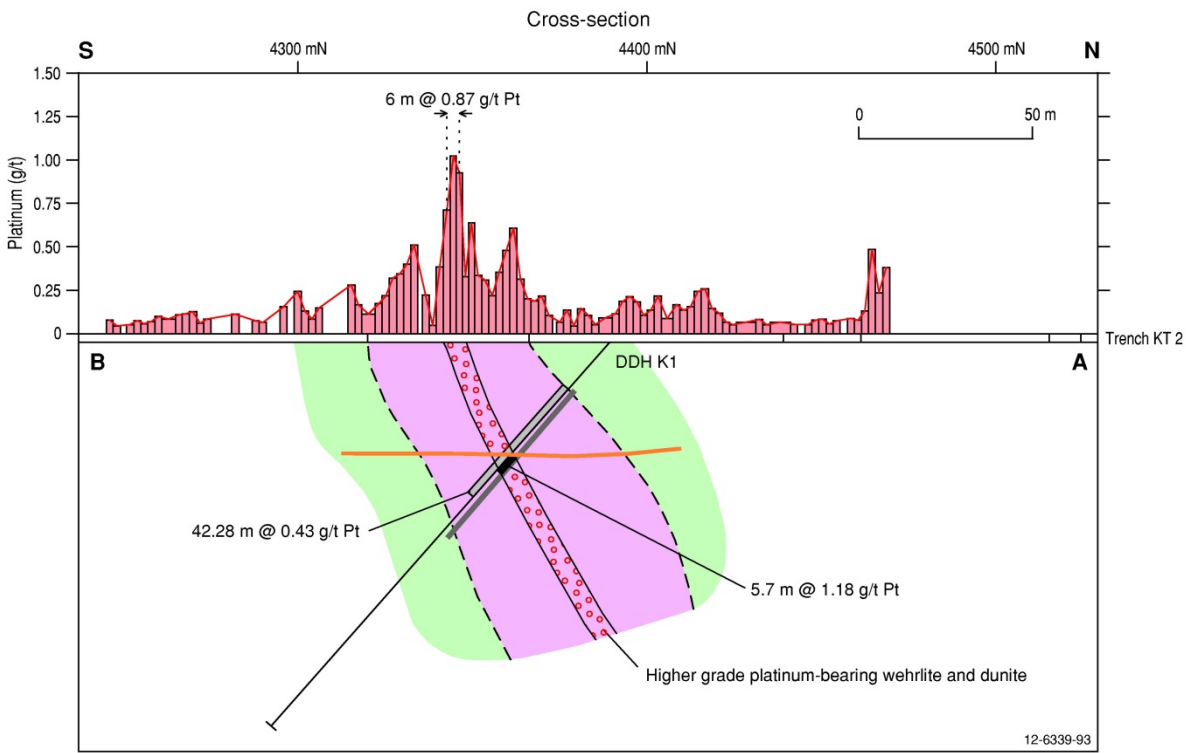
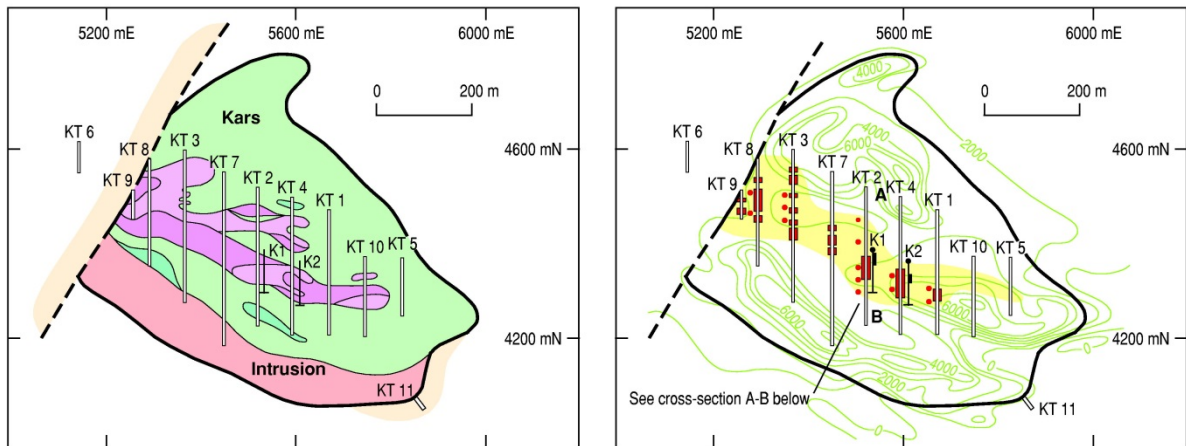
Platina Resources Limited, 2013a. Significant platinum and scandium assay results at Owendale project NSW: Highest single platinum assay to date. Platina Resources Limited announcement to the Australian Securities Exchange, 16 July 2013, 10 pp.

Platina Resources Limited, 2013b. Project update. Owendale platinum and scandium resource, NSW, Australia. Platina Resources Limited announcement to the Australian Securities Exchange, 3 October 2013, 20 pp.

Teluk, A.J., 2001. Fifield platinum project, New South Wales, Australia. Platinum metallogenesis, Ural-Alaskan type complexes. Rimfire Pacific Mining NL Technical Report 71 pp.

### ***Relevant figure(s)***

Figure 6.35, Figure 6.36, Figure 6.37, Figure 6.38, Figure 6.39, Figure 6.40, Figure 6.57, Figure 6.58, Figure 6.59, Figure 6.60, Figure 8.18g, and Appendix Figure K.35.



- Zone of anomalous platinum in soils and weathered bedrock. Values that range from 0.1-2.0 g/t Pt reflect underlying coarse-grained wehrlite and dunite
- Kars Intrusion**
- Pyroxenite
- Olivine pyroxenite
- Wehrlite, dunite
- Monzonite
- Olivine pyroxenite with dunite dykes and pods
- Sedimentary rocks
- Possible fault
- Approximate outline of Kars Intrusion
- Carbonate veining and alteration
- Base of oxidation
- Ground magnetic contours reflect magnetic phases of ultramafic intrusion
- Trench
- Trench interval with average platinum grade 0.20-0.65 g/t
- Diamond drill hole
- Diamond drill hole with platinum intersection
- RAB hole

Appendix Figure K.35 Geological interpretation of the Kars Intrusion, ~24 km south of Fifield, central New South Wales. Ground magnetic contours in top right diagram reflect magnetic ultramafic lithologies of intrusion. Anomalous platinum concentrations occur in lateritic soils and weathered bedrock overlying coarse-grained wehrlite and dunite. Schematic north-south cross-section (5525E) highlights anomalous platinum intersection associated with wehrlite and dunite in DDH K1 near the central part of the intrusion. Modified from Jones (1991).

**K.5.17 Flemington**

(see Fifield–Syerston area)

**K.5.18 Forners Prospect**

(see Mulga Springs)

**K.5.19 Gallaghers Claim**

(see Ballina–Tree Point: PGE beach placers)

**K.5.20 Gilgai Prospect**

(see Nyngan area)

**K.5.21 Gillenbine Lead**

(see Fifield–Syerston area)

**K.5.22 Honeybugle North Prospect**

(see Nyngan area)

**K.5.23 Honeybugle Yarran**

(see Nyngan area)

**K.5.24 Hylea Tiger Creek**

(see Bulbodney group)

**K.5.25 Jacks Lookout**

(see Fifield–Syerston area)

**K.5.26 Kars prospect**

(see Fifield–Syerston area)

**K.5.27 Keens Prospect, RAB hole BCR-122**

(see Bulbodney group)

### **K.5.28 Kelvin Grove**

(see Fifield–Syerston area)

### **K.5.29 Little Darling Creek Ultrabasic**

(see Mulga Springs)

### **K.5.30 Mallee Valley**

(see Nyngan area)

### **K.5.31 McAuleys Lead**

(see Ballina–Tree Point: PGE beach placers)

### **K.5.32 Milverton Lead**

(see Fifield–Syerston area)

### **K.5.33 Milverton Residual Pt deposit**

(see Fifield–Syerston area)

### **K.5.34 Mineral Claim MC127**

#### ***Geological province***

Thomson Orogen.

#### ***Location***

Mineral Claim MC127: 141.986633°E, -29.430069°S; Milparinka (SH 54–07), Olive Downs (7239); ~275 km north-northeast of Broken Hill.

#### ***Classification***

- 12. Others (minor or unknown economic importance); 12.E. Others (unknown geological setting).

#### ***Geological setting***

#### ***PGE mineralisation***

Major commodities as recorded in NSW MinView database for Mineral Claim MC127 (with very limited information) are Cu, Au, Pb, Pt, Ag; minor commodities are S, Sn, and Zn.

***Age of mineralisation***

***Current status***

Exploration site?

***Economic significance***

Occurrence.

***Major references(s)***

***Relevant figure(s)***

**K.5.35 Minnie Water**

(see Ballina–Tree Point: PGE beach placers)

**K.5.36 Monkey Hill Deep Lead**

***Geological province***

Lachlan Orogen.

***Location***

Monkey Hill Deep Lead: 149.58578°E, -33.04156°S; Bathurst (SI 55–08), Bathurst (8831); ~40 km north of Bathurst.

***Classification***

- Recorded in MinView database as a fluvial fossil placer.
- 10. Placer; 10.C. Alluvial placers.

***Geological setting***

***PGE mineralisation***

MinView database lists Au as major commodity, and Pt and diamond as minor commodities. Exploration report recorded Pt as one of the target commodities for exploration without any additional information (Kennewell, 1987).

***Age of mineralisation***

Recorded in Minview database as a 'fossil placer'.

***Current status***

Historical exploration site.

***Economic significance***

***Major references(s)***

Kennewell, P.J., 1987. Second six monthly report: EL 2746 Windeyer/Monkey Hill area. 23 June, 1987–22 December, 1987. Cluff Resources Pacific Limited, 8 pp.

**Relevant figure(s)**

**K.5.37 Mount Derriwong**

(see Fifield–Syerston area)

**K.5.38 Mount Mary Mines, Coolac\***

**Geological province**

Lachlan Orogen.

**Location**

Mount Mary Mines: 148.25934°E, -35.00505°S; Wagga Wagga (SI 55–15), Tumut (8527); ~34 km north of Tumut.

Coolac\*: 148.222536°E, -34.962046°S; Cootamundra (SI 55–11), Cootamundra (8528); ~40 km north of Tumut.

**Classification**

- 5. 'Alpine- and ophiolitic-type' mafic-ultramafic intrusions; 5.A. Podiform and stratabound chromitite.
- 8. Hydrothermal-Metamorphic.

**Geological setting**

The deposits lie within the Tumut Synclinal Zone bounded by the Gilmore Suture and the Mooney Mooney Fault. The area is generally underlain by Paleozoic sedimentary rocks with granite intrusions, and mafic to ultramafic rocks emplaced over a 100 km-strike of the Coolac serpentinite belt along the Mooney Mooney Fault. The geological formations consist of late Silurian–early Devonian age serpentinite, harzburgite, wehrlite and lherzolite and the Honeysuckle Beds comprising metabasalt, spillite, albite dolerite, metadacite, slate, siliceous metasandstone, and calc-silicates (McLennan, 1996). Rocks in the serpentinite belt show evidence of deep-seated deformation and syntectonic recrystallisation. Much speculation has been presented in regard to their genesis.

The 'alpine-type' Coolac serpentinite belt contains small deposits of podiform chromitite with minor Cu, Au, and PGEs. The linear intrusion was actively explored in 1894–1904 when approximately 32 000 t of chromite were mined from 40 podiform chromite deposits (Ashley, 1975; Franklin et al., 1992). Copper mineralisation is also related to lenses or hydrothermal pipe-like bodies of massive sulphide with intense alteration. Gold and As mineralisation is associated with the abutting Silurian Honeysuckle Beds of volcanics and metasediments, and the Young Granodiorite. In recent years companies have focussed their interest on PGE mineralisation related to the serpentinite, and have reported Pt in stream-sediment samples (0.31 ppm Pt) and tentatively identified PGM inclusions in magnetite grains and in sulphide ore from the Bogong mine at the southern end of the Coolac serpentinite belt (Helix Resources NL, 1986).

### ***PGE mineralisation***

Podiform chromite deposits in serpentinised harzburgite and pseudobreccia. Main ore mineral is chromite with minor amounts of Pt. The deposits are concentrated along a northwest-trending zone about 200 m-wide with average grades of ~49% Cr<sub>2</sub>O<sub>3</sub> (McLennan, 1996). Franklin et al. (1992) showed that both the dunitic host rocks and the chromite-bearing rocks for the Coolac serpentinite belt contain both PGEs and Au, but the chromites are more enriched in both these precious metals. The PGMs have not been identified although analyses of Ni sulphides and awaruite (Ni<sub>2</sub>Fe to Ni<sub>3</sub>Fe) occurring as fracture-fill minerals in chromite yield PGE values. Platinum-group element trends for the deposits appear to be different from those in other ophiolitic environments, which suggest the PGEs and possibly Au within them have undergone subordinate non-magmatic hydrothermal remobilisation accompanying serpentinisation alteration.

### ***Age of mineralisation***

Paleozoic?

### ***Current status***

Historical mines. 400 t averaging 48–49% chromite(?) produced from the Mount Mary mine prior to 1895. Main deposit worked by open cut 15 m-long by 9 m-deep. Several other small N-S elongate excavations (Basden, 1987).

### ***Economic significance***

Small historical mines.

### ***Major references(s)***

- Ashley, P.M., 1975. The southern serpentinite belt. In: Markham, N.L. and Basden, H. (editors), *The Mineral Deposits of New South Wales*. Geological Survey of New South Wales, 184–194.
- Basden, H., 1987. *Mineral Deposits in the Tumut 1:100 000 sheet area*. New South Wales Geological Survey report GS 1986/106, 29 pp.
- Franklin, B.J., Marshall, B., Graham, L.T. and McAndrew, J., 1992. Remobilization of PGE in podiform chromitite in the Coolac Serpentinite Belt, southeastern Australia. *Australian Journal of Earth Sciences*, 39, 365–371.
- Helix Resources NL, 1986. *Helix Resources NL 1986 Prospectus*, 47 pp.
- McLennan, R.M., 1996. Annual Report (for period 20 September 1994 to 19 September 1995) Exploration Licence 4694, Tumut–Gundagai. Imperial Mining NL., NSW GS1996/123, 88 pp.

### ***Relevant figure(s)***

## **K.5.39 Mulga Springs**

(includes other PGE occurrences in the Broken Hill region: Little Darling Creek Ultrabasic, Red Hill Silver Mining Company, Forners Prospect, Unnamed occurrence NSW MinView ID No 181767, Moorkaie)

### ***Geological province***

Curnamona Province.

### **Location**

Mulga Springs: 141.665109°E, -31.885816°S; Broken Hill (SH 54–15), Taltingan (7234); ~20 km northeast of Broken Hill.

Little Darling Creek Ultrabasic: 141.604612°E, -31.964156°S; Broken Hill (SH 54–15), Taltingan (7234); ~13 km east of Broken Hill.

Red Hill Silver Mining Company: 141.587350°E, -32.045341°S; Menindee (SI 54–03), Redan (7233); ~16 km southeast of Broken Hill.

Forners Prospect: 141.634441°E, -31.839060°S; Broken Hill (SH 54–15), Taltingan (7234); ~20 km northeast of Broken Hill.

Unnamed PGE occurrence NSW MinView ID No 181767 (Cu, Pt, Ni) also present about 200 m northwest of Forners Prospect at 141.63369°E, -31.837169°S; Broken Hill (SH 54–15), Taltingan (7234).

Moorkaie\*: 141.605602°E, -31.820155°S; exact location unknown, possibly an unnamed mineral occurrence (MinView occurrence 181865); ~9 km northwest of Mulga Springs and 3.2 km northwest of Forners Prospect.

Magnetic Hill\*: 141.275689°E, -32.135617°S; ~48 km southwest of Mulga Springs.

### **Classification**

- 8. Hydrothermal-metamorphic; 8.D. Structurally-controlled remobilised Ni-Cu-PGE sulphides in mafic-ultramafic±felsic dykes/veins in shear zones.

### **Geological setting**

PGE mineralisation occurs along the lower contacts of ultramafic intrusions in the Willyama Supergroup of the Broken Hill Domain within the Curnamona Craton. Shear zones within the Willyama Supergroup host swarms of strongly magnetic ultramafic dykes associated with variably sheared ultramafic intrusions locally intruded by the ~827 Ma Little Broken Hill Gabbro. The Little Broken Hill Gabbro shows no chilled margins with the ultramafic intrusions which are therefore considered to be of comparable age (Gibson, 1998). These ultramafic intrusions may be related to the ~825 Ma Gairdner Magmatic Event (Figure 8.8) that impacted on much of southern and central Australia (Hoatson et al., 2008).

### **PGE mineralisation**

The PGEs form small deposits with grades of several tens of ppm Pt and Pd, and a few per cent of Ni and Cu. The main deposits are Mulga Springs, Little Darling Creek and Red Hill, in the southeast of the Broken Hill Domain (Stevens and Burton, 1998). Occurrences of Pt, Ni, and Cu have also been detected in association with some ultramafic intrusions in the southwest of the Block (Barnes, 1988). Mineralisation occurs as discontinuous layers at the lower contacts of intrusions, ranging from a few centimetres to about 1.5 m in thickness, comprising pyrite, pyrrhotite, chalcopyrite, pentlandite, and magnetite. Native copper (Martin, 1987) and chromite have also been found. The intrusive bodies are altered-serpentinised harzburgite dykes and sills up to several hundred metres in outcrop length and several tens of metres in width.

An exploration report submitted by Martin (1987) noted that PGE mineralisation at the Mulga Springs prospect is hosted by remobilised Ni and Cu sulphides. Mineralisation intersected by drilling consisted predominantly of pyrite with lesser chalcopyrite, pyrrhotite, pentlandite, native copper, malachite, magnetite, bronzite, and violarite?

The Mulga Springs Prospect has been the subject of intensive exploration and research over a four-year term since September 1983. The best results are summarised in Appendix Table K.44.

*Appendix Table K.44 Selected Pt, Pd, and Au intersections for the Mulga Springs Prospect.*

Drill-hole	Depth (m)	Pt (g/t)	Pd (g/t)	Au (g/t)
MS4	14.06–15.06	18.0	24.6	1.27
MS24	25.06–27.0	1.57	3.48	0.11

A mineralised gossanous sample from the Forners Prospect described by Hodges and Dolanski (1976) assayed 0.3 ppm Au, 37.5 ppm Ag, 1.2 ppm Pt, 9.4 ppm Pd, 1.52% Cu, 0.66% Ni, 0.15% Zn, and 0.4% Pb. The sample was described as being of 'lode material' and included major components of schist, gossan, and quartz.

Impact Minerals Limited (2013) reported that a review of previous exploration results at the Red Hill Silver Mining prospect showed that around 500 t of ore were mined from the historical Red Hill Mine between 1906 and 1937, with face samples returning a grade range of 2% to 4% Cu, 2% to 3% Ni, 5 g/t to 41 g/t PGEs, and 22 g/t to 70 g/t Ag. Impact Minerals Limited also carried out rock-chip assays over a 130 m by 30 m area trending northeast from the Red Hill Mine, close to the contact between the host ultramafic intrusion and the surrounding rocks. The geochemical survey highlighted strongly anomalous grades that ranged from 1 g/t to 36 g/t PGEs and 0.2% to 6.1% Cu. Impact Minerals Limited (2014) reported further analyses of rock-chip samples grading up to 18 g/t Pt, 12 g/t Pd, 4.2% Ni, 22% Cu, 1.8 g/t Au, and 221 g/t Ag.

### ***Age of mineralisation***

Neoproterozoic or younger? The ultramafic intrusions have previously been regarded as Cambrian in age, however, the ?coeval Little Broken Hill Gabbro Intrusion has a U-Pb zircon-baddeleyite crystallisation age of  $827 \pm 9$  Ma (Wingate et al., 1998).

### ***Current status***

Exploration sites.

### ***Economic significance***

Occurrences.

### ***Major references(s)***

- Barnes, R.G., 1988. Metallogenic studies of the Broken Hill and Eurioiwie Blocks, New South Wales. 1. Styles of mineralization in the Broken Hill Block. 2. Mineral deposits of the southwestern Broken Hill Block. Geological Survey of New South Wales, Bulletin 32 (1, 2), 250 pp.
- Gibson, G.M., 1998. Regional structure in the Willyama Supergroup and its relevance to mineral exploration in the Broke Hill Inlier. In: Gibson, G.M. (compiler), Broken Hill Exploration Initiative. Abstracts of papers presented at fourth annual meeting in Broken Hill, October 19-21, 1998. Australian Geological Survey Record 1998/25, 38–40.

- Hoatson, D.M., Claoué-Long, J.C. and Jaireth, S., 2008a. Guide to using the 1:5 000 000 map of Australian Proterozoic Mafic-Ultramafic Magmatic Events. *Geoscience Australia Record* 2008/15, 140 pp.
- Hodges, I. and Dolanski, J., 1976. Metallurgical investigation of a platinum metals-bearing copper-nickel prospect. Unpublished mineralogical report No. 76/27, 6 pp.
- Impact Minerals Limited, 2013. Rock-chip samples with up to 41 g/t platinum group metals, 6% copper and 3% nickel confirmed at the Red Hill prospect, Broken Hill, NSW. Impact Minerals Limited announcement to the Sydney Securities Exchange, 16 July 2013, 7 pp.
- Impact Minerals Limited, 2014. Significant undrilled high grade platinum-palladium-nickel-copper-gold-silver anomalies at Red Hill prospect, Broken Hill, NSW. Impact Minerals Limited announcement to the Sydney Securities Exchange, 21 May 2014, 9 pp.
- Martin, A.M., 1987. Mulga Springs Prospect Broken Hill, NSW. Final Report Exploration Licence 2074, Delta Gold NL GS1987 324, 22 pp.
- Stevens, B.P.J. and Burton, G.R., 1998. The Early to Late Proterozoic Broken Hill Province, New South Wales. In: *Geology and mineral potential of major Australian mineral provinces*. AGSO Journal of Australian Geology and Geophysics, Volume 17, 81–86.
- Wingate, M.T.D., Campbell, I.H., Compston, W. and Gibson, G.M., 1998. Ion microprobe U-Pb ages for Neoproterozoic basaltic magmatism in south-central Australia and implications for the breakup of Rodinia. *Precambrian Research*, 87, 135–159.

### ***Relevant figure(s)***

Figure 6.47, Figure 6.48, Figure 6.49, and Figure 8.18h.

## **K.5.40 Murga**

(see Fifield–Syerston area)

## **K.5.41 New Zealand Claim**

(see Ballina–Tree Point: PGE beach placers)

## **K.5.42 Nyngan area**

### ***Geological province***

Lachlan Orogen.

### ***Location***

Nyngan Nickel Deposit: 147.03911°E, -32.49819°S; Nyngan (SH 55–15), Canonba (8335); ~17 km northwest of Nyngan. This deposit has only Ni and Co, with no Pt or Sc reported. There seems to be an agglomeration of Jervois Mining Limited's Nyngan Sc deposit and the Nyngan Ni-Co deposits on the Minview database.

Gilgai Prospect: 146.99593°E, -31.61098°S; Cobar (SH 55–14), Hermidale (8234); ~20 km west-southwest of Nyngan.

Nyngan Scandium Deposit\*: 146.994°E, -31.612°S; Cobar (SH 55–14), Hermidale (8234); about 20 km west-southwest of Nyngan. The Nyngan Scandium Deposit may coincide with the Gilgai Prospect.

Honeybugle North Prospect: 146.90716°E, -31.82026°S; Cobar (SH 55–14), Hermidale (8234); ~40 km southwest of Nyngan.

Honeybugle Yarran: 146.91348°E, -31.84462°S; Cobar (SH 55–14), Hermidale (8234); ~42 km southwest of Nyngan.

Yarran Park Prospect: 146.91771°E, -31.84282°S; Cobar (SH 55–14), Hermidale (8234); ~42 km southwest of Nyngan.

Mallee Valley: 146.94626°E, -31.81126°S; Cobar (SH 55–14), Hermidale (8234); about 36 km southwest of Nyngan.

### **Classification**

- ?6. 'Alaskan- and Urals-type' mafic-ultramafic intrusions; 6.A. PGE mineralisation in concentrically zoned ultramafic-mafic.
- 9. Regolith-Laterite; 9.A. PGE-bearing regolith developed on ultramafic mafic igneous rocks (the Nyngan Ni-Co deposit and the Nyngan Scandium deposit are hosted in laterite).
- ?10. Placer; ?10.A. Alluvial placers derived from Alaskan- and Urals-type mafic-ultramafic intrusions. (?Honeybugle North recorded as residual over Honeybugle Complex)

The Honeybugle prospects, Gilgai Prospect (Appendix Figure K.36), Yarran Park and Mallee Valley are recorded on Minview website as of unknown classification and are all recorded as being related to the Honeybugle Complex). The Honeybugle North prospect is recorded as a residual deposit.

### **Geological setting**

The Honeybugle Complex, 40 km southwest of Nyngan, is one of several mafic-ultramafic intrusives in a north-northwest-trending belt between Fifield and Bourke that show similarities to concentric and zoned 'Alaskan-type' mafic-ultramafic intrusions. The Honeybugle Complex comprises a southern composite zone (7 km by 18 km) of hornblende pyroxenite, lherzolite, peridotite, and anorthositic norite, while a homogeneous suite of hornblendite, monzonite, and meladiorite forms the northern subzone (7 km by 8 km). The country rocks are schists and metasediments of the Ordovician Girilambone Group (Hoatson and Glaser, 1989).

### **PGE mineralisation**

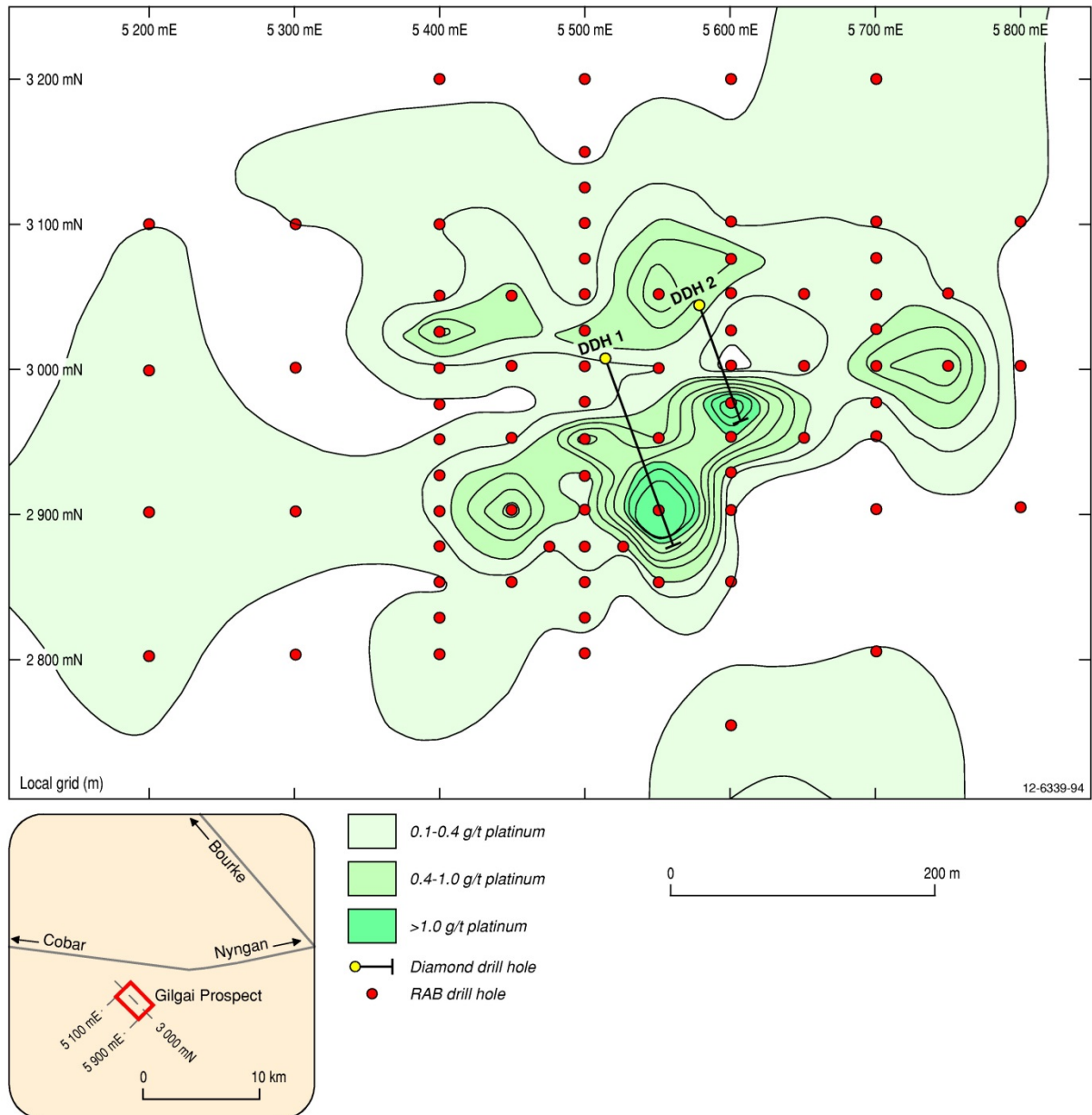
Sampling of sulphide-bearing peridotite from old dumps has returned up to 0.17 ppm Pt and 0.04 ppm Pd. Historical drill-hole intersections have returned 2 m @ 17.5 ppm for alkaline igneous rocks at the Honeybugle Complex (Helix Resources NL, 1986; 1987)

### **Age of mineralisation**

The most recent and robust geochronological methods involving the dating of zircon indicate a late Ordovician to late Silurian age (e.g., 450 to 420 million years) for the Fifield intrusions. The mineralised laterite profiles overlying these intrusions generally formed during the ?Early and/or Late Cenozoic (see Section 6.4.9.1).

### **Current status**

Exploration sites.



Appendix Figure K.36 Platinum geochemical contours (C horizon) for the Gilgai Intrusion, ~25 km west of Nyngan, central New South Wales. The covered intrusion is zoned about an olivine-rich dunite core similar to the Owendale Intrusion. The Pt geochemical anomaly in laterite has grades up to 2 g/t Pt and covers an area of 250 m by 350 m. Modified from Jones (1991).

**Economic significance**

Jervois Mining Limited reported in its 2004 Annual Report announced a resource of 16 Mt at 0.87% Ni and 0.06% Co for its Nyngan Scandium deposit of which there is 3 Mt at 290 ppm Sc and 0.22 g/t Pt. The Sc-rich portion of this deposit was updated in June 2009 as Measured Resources of 2.718 Mt at 274 ppm Sc and Indicated Resources of 9.294 Mt at 258 ppm Sc. The other occurrences in the Nyngan area are prospects with no reported PGE resources.

**Major references(s)**

Helix Resources NL, 1986. Helix Resources NL 1986 Prospectus.

Helix Resources NL, 1987. Helix Resources NL 1987 Annual Report.

Hoatson, D.M. and Glaser, L.M., 1989. Geology and economics of platinum-group metals in Australia. Bureau of Mineral Resources, Australia, Resource Report 5, 81 pp.

Jervois Mining Limited, 2005. Jervois Mining Limited 2004 Annual Report, 42 pp.

***Relevant figure(s)***

Appendix Figure K.36.

**K.5.43 Nyngan Scandium Deposit\***

(see Nyngan area)

**K.5.44 Owendale Lead**

(see Fifield–Syerston area)

**K.5.45 Owendale North Pt-Cu prospect**

(see Fifield–Syerston area)

**K.5.46 Owendale North residual Pt-Cu-Ni-Co Prospect**

(see Fifield–Syerston area)

**K.5.47 Platina Lead**

(see Fifield–Syerston area)

**K.5.48 RAB hole BCR-58**

(see Bulbodney group)

**K.5.49 Red Hill Silver Mining Company**

(see Mulga Springs)

**K.5.50 Reynolds Tank**

(see Fifield–Syerston area)

**K.5.51 Shellharbour Alluvials**

***Geological province***

Sydney Basin.

### ***Location***

Shellharbour Alluvials: 150.86999°E, -34.58341°S; Wollongong (SH 56–09), Kiama (9028); ~16 km south of Wollongong.

### ***Classification***

- 10. Placer; 10.D. Beach placers.

### ***Geological setting***

Modern beach placer.

### ***PGE mineralisation***

Tin-dominated modern beach placer with minor Au and Pt.

### ***Age of mineralisation***

Holocene.

### ***Current status***

Occurrence.

### ***Economic significance***

Occurrence.

### ***Major references(s)***

No information apart from a location on Minview and Minloc databases.

### ***Relevant figure(s)***

## **K.5.52 Studwick's Lead**

(see Fifield–Syerston area)

## **K.5.53 Syerston**

(see Fifield–Syerston area)

## **K.5.54 Talbragar River Alluvials**

### ***Geological province***

Lachlan Orogen.

### ***Location***

Talbragar River Alluvials: 148.75733°E, -32.17435°S; Dubbo (SI 55–04), Dubbo (8633); ~15 km east-northeast of Dubbo.

### **Classification**

- 10. Placer; 10.C. Alluvial placers.

### **Geological setting**

Modern fluvial placer.

### **PGE mineralisation**

Sn dominated modern fluvial placer with minor Pt.

### **Age of mineralisation**

Cenozoic?

### **Current status**

Historical exploration site.

### **Economic significance**

Occurrence.

### **Major references(s)**

No information apart from a location on NSW MinView and MINLOC databases.

### **Relevant figure(s)**

## **K.5.55 The Diggings**

### **Geological province**

Lachlan Orogen.

### **Location**

The Diggings: 149.12971°E, -32.35038°S; Dubbo (SI 55–04), Cobbora (8733); ~50 km east-southeast of Dubbo.

### **Classification**

- Classified as a modern fluvial placer in MinView database.
- 10. Placer; 10.C. Alluvial placers.

### **Geological setting**

Modern fluvial placer.

### **PGE mineralisation**

NSW MinView database recorded Au-dominant modern fluvial placer with minor Pt, Ir, and Os. Minor alluvial Au, possibly from Permian sandstone, was reported in an exploration report, but no mention of PGEs (Binns, 1984).

### ***Age of mineralisation***

Cenozoic?

### ***Current status***

Historical exploration site.

### ***Economic significance***

Occurrence.

### ***Major references(s)***

Binns, M.J., 1984. Exploration Licence 2081, Gunnegaldrie, NSW. First six-monthly report, 19 September 1983–18 March 1984. Robertson Research (Australia) Pty Limited. MinView report no GS1984/125, 187 pp.

### ***Relevant figure(s)***

## **K.5.56 Tree Point**

(see Ballina–Tree Point: PGE beach placers)

## **K.5.57 Wellington Alluvials**

### ***Geological province***

Lachlan Orogen.

### ***Location***

Wellington Alluvials: 149.10655°E, -32.6335°S; Dubbo (SI 55–04), Euchareena (8732); ~64 km southeast of Dubbo.

### ***Classification***

- 10. Placer; 10.C. Alluvial placers.

### ***Geological setting***

### ***PGE mineralisation***

MINLOC database lists Au, industrial diamond, gem diamond, and cheap gem, but no mention of Pt in reports. Only Au and industrial diamonds recorded in MinView database. Small quantities of Pt, Os, and Pd have been obtained as a by-product of Au dredging on the Macquarie River. Total recorded production during 1950–58 was less than 6.0 kg of Pt concentrate. The source of the Pt is unknown (Barrie, 1965; Hoatson and Glaser, 1989).

### ***Age of mineralisation***

Recorded in Minview database as a 'fossil placer'.

### ***Current status***

According to Intierra database, the prospect appears to be inactive since 1997.

### ***Economic significance***

A large low-grade alluvial Au deposit. Cluff Resources Limited reported an inferred resource of 38 Mt @ 0.2 g/t Au.

### ***Major references(s)***

Barrie, J., 1965. Platinum group metals. In: McLeod, I.R. (editor), Australian Mineral Industry: The Mineral Deposits. Bureau of Mineral Resources, Australia, Bulletin 72, 487–494.

Cluff Resources Limited, 1989. Cluff Resources Limited 1989 Annual Report.

Hoatson, D.M. and Glaser, L.M., 1989. Geology and economics of platinum-group metals in Australia. Bureau of Mineral Resources, Australia, Resource Report 5, 81 pp.

Vahebzadeh, B. and Boswell, M., 1988. Wellington alluvials data package for Exploration Licences 2890, 2130 and 2631. Cluff Resources Pacific Limited. NSW GS1988/238, 319 pp.

### ***Relevant figure(s)***

#### **K.5.58 Wylie Creek**

(see Boonoo Boonoo River–Wylie Creek area)

#### **K.5.59 Unnamed occurrence NSW MinView ID No 102524, 102552, 102555, 102556, 102277**

(see Fifield-Syerston area)

#### **K.5.60 Unnamed occurrence NSW MinView ID No 181767**

(see Mulga Springs)

#### **K.5.61 Yarran Park Prospect**

(see Nyngan area)

## K.6 VICTORIA

### K.6.1 East Walhalla Copper and Platinum Mine (Woods Point–Walhalla region)

(Includes Thomson River Copper Mine, Walhalla Copper Mining Co, Loch Fyne, Shamrock, Morning Star, Hunts and Maynard's Gully dyke)

#### **Geological province**

Lachlan Orogen.

#### **Location**

East Walhalla Copper and Platinum Mine: 146.462080°E, -37.938660°S; Warburton (SJ 55–06), Matlock (8122); ~105 km northeast of Wonthaggi and ~1 km east-northeast of Walhalla.

Thomson River Copper Mine (Coopers Creek): 146.427650°E, -37.985940°S; Warburton (SJ 55–06), Matlock (8122); ~5 km southwest of Walhalla.

Walhalla Copper Mining Co: 146.426760°E, -37.986760°S; Warburton (SJ 55–06), Matlock (8122); ~5 km southwest of Walhalla.

Shamrock: 146.269830°E, -37.587420°S; Warburton (SJ 55–06), Matlock (8122); ~43 km northwest of Walhalla and ~5 km east-northeast of Matlock.

Loch Fyne (New Loch Fyne): 146.230800°E, -37.612280°S; Warburton (SJ 55–06), Matlock (8122); ~42 km northwest of Walhalla and ~2 km southeast of Matlock.

Morning Star\*: 146.2456°E, -37.5686°S; Warburton (SJ 55–06), Matlock (8122); ~45 km northwest of Walhalla and ~4.5 km east-northeast of Matlock.

Hunts\*: 146.19006°E, -37.48214°S; Warburton (SJ 55–06), Mansfield (8122); ~13 km north-northwest of Matlock.

Maynard's Gully dyke\*: 146.4164°E, -37.7363°S; Warburton (SJ 55–06), Matlock (8122); ~23 km northwest of Walhalla.

#### **Classification**

- 8. Hydrothermal-metamorphic; 8.D. Structurally-controlled remobilised Ni-Cu-PGE sulphides in mafic-ultramafic±felsic dykes/veins in shear zones.

#### **Geological setting**

Widespread Cu-Ni mineralisation is hosted in mafic and ultramafic dykes of the Woods Point Dyke Swarm, but the only deposit that supported sustained mining is the Thomson River Copper Mine at Coopers Creek. The Late Devonian Woods Point Dyke Swarm, comprising ultramafic to felsic dykes, was intruded during a late Middle Devonian extension which followed the deformation of the Tabberabberan Orogeny. Gold mineralisation was introduced just after the intrusion in structurally controlled quartz veins, mostly in Walhalla Group sedimentary rocks or diorites, but Cu-Ni-PGE mineralisation was confined to the mafic and ultramafic dykes. Keays and Green (1974) noted that at

least ten of the dykes in the Woods Point Dyke Swarm contain PGEs as well as Cu-Ni mineralisation, where enrichment in Cu is usually associated with a corresponding enrichment in Pt.

### ***PGE mineralisation***

Most of the following information on the PGE mineralisation in the Woods Point–Walhalla region is sourced from VandenBerg et al. (2006).

The East Walhalla mine is located in a bulge in a member of the Woods Point Dyke Swarm. Quartz veinlets are developed along faults in a hornblendite and disseminated chalcopyrite occurs in the dyke. Small amounts of ore were produced from three small open pits and a shallow shaft. No production data are available, but samples taken in ~1917 assayed up to 0.6% Cu, 2.93 g/t Pt, 1.02 g/t Au, and 5.23 g/t Ag. Surface sampling suggested that Pd may be the dominant PGE.

Intermittent mining of the nearby Thomson River deposit commenced in 1864, and by 1879, 214 t of Cu had been mined. In the period between 1906 and 1913 a further 2540 t of ore were mined with estimated average grades of 3.75% Cu, 0.34% Ni, 12.8 ppm Ag, 1.5 ppm Au, 2.3 ppm Pt, and 3.8 ppm Pd (Cozens and Rangott, 1972; Cochrane, 1982). A historical drill-hole intersection (in 1980s) reported by Ausplat Minerals NL assayed 36 m (from a depth of 303 m) at 0.78 ppm Pt, 1.08 ppm Pd, 0.39 ppm Au, 1.25% Cu, 0.2% Ni, and 8.6 ppm Ag. CRA Exploration Pty Limited in 1981 estimated resources at 40 000 t averaging 3.2 ppm Pt, 3.6 ppm Pd, 2.7% Cu, 9.5 ppm Ag, and 2.5 ppm Au (Hoatson and Glaser, 1989; Orion Gold NL, 2013).

Mineralisation at the Thomson River Cu deposit is hosted by an intermediate to ultramafic dyke comprising gabbro, monzonite, quartz monzonite, diorite, quartz diorite, and hornblendite, with the least mafic phases generally at the centre of the intrusion. A later porphyritic intrusion occurs to the south of the main dyke. Two main ore bodies have been mined with the No 1 ore shoot entirely within sheared Norton Gully Sandstone and the No 2 ore shoot entirely within the dyke. Platinum is hosted by chalcopyrite, pyrite, pentlandite, and as sperrylite (PtAs<sub>2</sub>). Palladium has tentatively been identified by Keays and Kirkland (1972) as occurring in merenskyite (Pd,Pt)<sub>2</sub>(Te,Bi). Keays and Kirkland (1972) also noted Au was remobilised from the magmatic Cu-Ni sulphides, and redeposited in quartz-carbonate-chalcopyrite-pyrite stringers. The PGMs were less mobile than Au, with 1 µm to 10 µm-sized sperrylite grains along fissures in pyrite grains, and merenskyite situated in chalcopyrite. They believe the Au may have been transported as [AuCl<sub>4</sub>]<sup>-</sup> in oxidising and chloride-bearing solutions, or as [AuS] in slightly alkaline, sulphide-bearing (reducing) solutions.

At the Loch Fyne dyke prospect, PGE mineralisation is associated with Au, Ag, and Cu in the more mafic hornblende-rich sections of the dyke. Six samples from the most Cu-rich phase of the dyke returned up to 7.38 ppm Au, 24.88 ppm Ag, 5.63 ppm Pt, and 4.94% Cu (Cochrane, 1982).

At the Shamrock and Maynard's Gully dyke prospects, Cu-Ni-PGE mineralisation is located in the most mafic parts of the dyke. At both locations the mineralisation is present in peridotite and hornblendite, but not in diorite. The Maynard's Gully dyke has not been mined, but analyses have indicated the presence of Pt, Au, and Ag (Junner, 1920). The dyke hosts disseminated chalcopyrite with minor amounts of pyrite and pentlandite.

Drilling at the Morning Star dyke by Morning Star Gold NL between 1995 and 2005 intersected several zones of Cu-Ni massive sulphides containing up to 4 ppm PGEs, 0.6 ppm Au, and 2% Cu and Ni.

Mineralisation in the Hunt's Au mine occurs in a network of quartz veinlets developed in the Hunt's Diorite Dyke and adjacent fractured silicified sedimentary rocks. Chalcopyrite-bearing samples from the dump near the northern shaft yielded up to 1.0 ppm Pt, 2.9% Cu, 8.3 ppm Ag, and 2.9 ppm Au.

### ***Age of mineralisation***

Age of Au mineralisation is between ~370 Ma and ~376 Ma at Walhalla ( $372 \pm 2$  Ma: Foster et al., 1998) and Woods Point ( $374 \pm 2$  Ma: Bierlein et al., 2001) using  $^{40}\text{Ar}$ - $^{39}\text{Ar}$  method on sericite in hydrothermal quartz veins. The age of the Woods Point Dyke Swarm, based on Ar-Ar dates on magmatic hornblende, is considered to be around 375 Ma–380 Ma (VandenBerg, 2006: p. 124).

### ***Current status***

Exploration site. Explored by Orion Gold NL.

### ***Economic significance***

Historical mines under re-assessment.

### ***Major references(s)***

- Bierlein, F.P., Arne, D.C., Foster, D.A. and Reynolds, P., 2001. A geochronological framework for orogenic gold mineralisation in central Victoria, Australia. *Mineralium Deposita*, 36, 741–767.
- Cochrane, G.W., 1982. Copper, lead, zinc and barium deposits of Victoria. *Geological Survey of Victoria Bulletin* 61, 109–122.
- Foster, D.A., Gray, D.R., Kwak, T.A.P. and Bucher, M., 1998. Chronology and tectonic framework of turbitite-hosted gold deposits in the western Lachlan Fold Belt, Victoria,  $^{40}\text{Ar}$ - $^{39}\text{Ar}$  results. In: Ramsey, W.R.H., Bierlein, F.P. and Arne, D.C. (editors), *Mesothermal gold mineralisation in space and time*. *Ore Geology Reviews*, 13, 229–250.
- Hoatson, D.M. and Glaser, L.M., 1989. *Geology and economics of platinum-group metals in Australia*. Bureau of Mineral Resources, Australia, Resource Report 5, 81 pp.
- Junner, N.R., 1920. The geology and ore deposits of the Walhalla–Wood's Point auriferous belt. *Proceedings of the Australian Institute of Mining and Metallurgy*, 39, 127–258.
- Keays, R.R. and Green, A.H., 1974. *Geology and gold mineralisation in the Wood's Point dyke swarm*. Geological Survey of Victoria Unpublished Report, 1974/12.
- Keays, R.R. and Kirkland, M.C., 1972. Hydrothermal mobilisation of gold from copper-nickel sulfides and ore genesis at the Thomson River Copper Mine. Victoria, Australia. *Economic Geology*, 67, 1263–1275.
- Orion Gold NL, 2013. Exploration update: Walhalla polymetals project. Orion Gold NL announcement to the Australian Securities Exchange, 8 July 2013, 22 pp.
- VandenBerg, A.H.M., Cayley, R.A., Willman, C.E., Morand, V.J., Seymon, A.R., Osborne, C.R., Taylor, D.H., Haydon, S.J., McLean, M., Quinn, C., Jackson, P. and Sanford, A.C., 2006. *Walhalla–Woods Point–Tallangalook special map area geological report*. Geological Survey of Victoria Report 127. GeoScience Victoria. Department of Primary Industries, 455 pp.

### ***Relevant figure(s)***

Figure 8.18h.

## **K.6.2 Errinundra\***

### ***Geological province***

Lachlan Orogen.

### ***Location***

Errinundra (Boulder Mine)\*: 148.888050°E, -37.445930°S; Mallacoota (SJ 55–08), Bendoc (8623); Errinundra near Club Terrace in eastern Victoria.

### ***Classification***

- 8. Hydrothermal-Metamorphic.

### ***Geological setting***

Gold and Pt-Os mineralisation is associated with quartz veining in slates. The Boulder Mine was a small high-grade Au producer in the early 1900s with Au grades ranging from 85 ppm to 142 ppm. In the late 1980s, Austplat Minerals NL estimated a potential resource of 150 kg of Au at the mine.

### ***PGE mineralisation***

A sample of quartz submitted to the Victorian Mines Department in the early 1920s assayed 80.4 ppm Pt, 25.6 ppm Os, trace Au, and 17.1 ppm Ag (Kenny, 1937; Hoatson and Glaser, 1989).

### ***Age of mineralisation***

Unknown.

### ***Current status***

Historical Au mine.

### ***Economic significance***

Occurrence.

### ***Major References***

Hoatson, D.M. and Glaser, L.M., 1989. Geology and economics of platinum-group metals in Australia. Bureau of Mineral Resources, Australia, Resource Report 5, 81 pp.

Kenny, J.P.L., 1937. Boulder Mine, Errinundra. Mining and Geological Journal of Victoria, 1, 32.

### ***Relevant figure(s)***

## **K.6.3 Hunts**

(see East Walhalla Copper and Platinum Mine, Woods Point–Walhalla region)

## **K.6.4 Loch Fyne**

(see East Walhalla Copper and Platinum Mine, Woods Point–Walhalla region)

### **K.6.5 Maynards Gully Dyke**

(see East Walhalla Copper and Platinum Mine, Woods Point–Walhalla region)

### **K.6.6 Mount Leura\***

#### ***Geological province***

Lachlan Orogen.

#### ***Location***

Mount Leura: 143.15°E, -38.25°S; Colac (SJ 54–12), Corangamite (7521); Mount Leura, near Camperdown, western Victoria.

#### ***Classification***

- 12. Others (minor or unknown economic importance); 12.D. PGE-bearing ultramafic nodules and xenoliths.

#### ***Geological setting***

Occurrence located in basanites from the Newer Volcanics at Mount Leura, western Victoria (Keays et al., 1981; Hoatson and Glaser, 1989).

#### ***PGE mineralisation***

Spinel lherzolite xenoliths in basanites from the Newer Volcanics at Mount Leura, western Victoria contain pentlandite-pyrrhotite-chalcopyrite inclusions along grain boundaries and within fractures in the silicates. Discrete grains of a Pt-sulphide and Pd-stannide minerals exsolved from the pentlandite have been identified using SEM techniques (Keays et al., 1981; Hoatson and Glaser, 1989).

#### ***Age of mineralisation***

Unknown.

#### ***Current status***

Occurrence.

#### ***Economic significance***

Occurrence.

#### ***Major references(s)***

- Hoatson, D.M. and Glaser, L.M., 1989. Geology and economics of platinum-group metals in Australia. Bureau of Mineral Resources, Australia, Resource Report 5, 81 pp.
- Keays, R.R., Sewell, D.K.B. and Mitchell, R.H., 1981. Platinum and palladium minerals in upper mantle-derived lherzolites. *Nature*, 294, 646–648.

**Relevant figure(s)**

**K.6.7 Morning Star**

(see East Walhalla Copper and Platinum Mine, Woods Point–Walhalla region)

**K.6.8 Shamrock**

(see East Walhalla Copper and Platinum Mine, Woods Point–Walhalla region)

**K.6.9 Thomson River Copper Mine**

(see East Walhalla Copper and Platinum Mine, Woods Point–Walhalla region)

**K.6.10 Unnamed, GeoVic No 962436 (Turtons Creek\*)**

***Geological province***

Lachlan Orogen.

***Location***

Turtons Creek: 146.24144°E, -38.55228°S; Warragul (SJ 55–10), Foster (8120); ~10 km north of Foster, southern Victoria.

***Classification***

- 10. Placer; 10.C. Alluvial placer.

***Geological setting***

Recent alluvial placers in stream sediments. The source of the PGEs may be Cambrian greenstones, or Early Devonian sedimentary rocks in the Waratah Bay–Foster district (Douglas, 1984; Hoatson and Glaser, 1989).

***PGE mineralisation***

Alluvial Pt and/or Os is associated with Au in the Turtons Creek, Stockyard Creek, and Livingstone Creek region of Foster. The proportion of PGEs to Au is small, the former occurring as crystalline grains or in platy pieces up to 5 mm square (Ferguson, 1936; Bain et al., 1956; Douglas, 1984; Hoatson and Glaser, 1989).

***Age of mineralisation***

Quaternary.

***Current status***

Currently inactive.

### ***Economic significance***

Historical alluvial Au field.

### ***Major references(s)***

Bain, A.D.N. and Medwell, G., 1956. Victorian base metal occurrences. Geological Survey of Victoria Unpublished Report 1956/64.

Douglas, J.G., 1984. Explanatory notes on the Warragul 1:250 000 geological map. Geological Survey Report No.57. Department of Mines and Energy Victoria, 31 pp.

Ferguson, W.H., 1936. Turtons Creek Goldfield. Geological Survey of Victoria, Records 5, 249–252.

Hoatson, D.M. and Glaser, L.M., 1989. Geology and economics of platinum-group metals in Australia. Bureau of Mineral Resources, Australia, Resource Report 5, 81 pp.

### ***Relevant figure(s)***

## **K.6.11 Unnamed GeoVic No 962463 (Stockyard Creek\*)**

### ***Geological province***

Lachlan Orogen.

### ***Location***

Unnamed PGE occurrence (GeoVic No 962463): 146.20024°E, -37.65323°S; Warragul (SJ 55–10), Foster (8120); location of occurrence is in Foster, southern Victoria. This location is also known as Stockyard Creek.

### ***Classification***

- 10. Placer; 10.C. Alluvial placer.

### ***Geological setting***

Recent alluvial placers in stream sediments. The source of the PGEs may be Cambrian greenstones, or Early Devonian sedimentary rocks in the Waratah Bay–Foster district (Douglas, 1984; Hoatson and Glaser, 1989).

### ***PGE mineralisation***

The Au recorded in the Victorian database is the principal commodity. Pt (secondary commodity) and Os (minor commodity) are found in the alluvial workings as white scales or flakes and flattened grains among auriferous gravels (Bain and Medwell, 1956).

### ***Age of mineralisation***

Quaternary.

### ***Current status***

Historical alluvial Au field.

### ***Economic significance***

Occurrence.

### **Major references(s)**

- Bain, A.D.N. and Medwell, G., 1956. Victorian base metal occurrences. Geological Survey of Victoria Unpublished Report 1956/64.
- Douglas, J.G., 1984. Explanatory notes on the Warragul 1:250 000 geological map. Geological Survey Report No.57. Department of Mines and Energy Victoria, 31 pp.
- Hoatson, D.M. and Glaser, L.M., 1989. Geology and economics of platinum-group metals in Australia. Bureau of Mineral Resources, Australia, Resource Report 5, 81 pp.

### **Relevant figure(s)**

## **K.6.12 Unnamed\* (GeoVic Nos 962400, 962401)**

### **Geological province**

Lachlan Orogen.

### **Location**

Unnamed Au, PGE (962400) occurrence: 145.99697°E, -38.85524°S; Warragul (SJ 55–10), Wonthaggi (8120); ~0.5 km north-northeast of Walkerville.

Unnamed Au, PGE (962401) occurrence: 146.00576°E, -38.87722°S; Warragul (SJ 55–10), Foster (8120); ~2 km south-southeast of Walkerville.

### **Classification**

- 10. Placer; 10.D. Beach placer.

### **Geological setting**

Cambrian greenstone, mafic lava, tuff, chert, shale, and dolerite crop out along the coast from Point Grinder to Walkerville, at Waratah Bay. These rocks form the base of the structural high called the Waratah Bay Axis, and are overlain by steeply dipping Early Devonian sandstone, mudstone, shale, and conglomerate of the Liptrap Formation. Structural evidence indicates that the Cambrian greenstones underlie the area extending from the outcropping Waratah Bay greenstones and the Howqua greenstones of central Victoria.

These two unnamed Au-PGE occurrences are located on the beach in Waratah Bay. Occurrence 962401 at Bell Point and is underlain by the Cambrian mafic rocks of the Maitland Beach Volcanics (VandenBerg, 2000). Au-PGE occurrence 962400 is located on the beach about 2.6 km north of Au-PGE occurrence 962401 and is underlain by the Devonian sandstones of the Liptrap Formation. The source of the PGEs may be Cambrian greenstones, the Corduroy Creek Gabbro, or Early Devonian sedimentary rocks in the Waratah Bay–Foster district (Fergusson, 1928; Douglas, 1984; Hoatson and Glaser, 1989).

### **PGE mineralisation**

In the 2013 edition of the MINLOC database, these occurrences were only recorded for Au. Earlier versions of the database recorded both Au and PGEs for these occurrences. The presence of PGEs in beach sands in Waratah Bay is also mentioned in some reports (Fergusson, 1928; Bain and Medwell, 1956).

## Victoria

VandenBerg (2000, Tables 2.1, 2.4) noted that sub-economic concentrations of Os-Ir alloys are associated with Maitland Beach Volcanics and the Corduroy Creek Gabbro. Gold has been recorded as the principal commodity and Os as a minor commodity for this occurrence (Ferguson, 1928; Bain and Medwell, 1956).

### ***Age of mineralisation***

Quaternary.

### ***Current status***

Occurrence.

### ***Economic significance***

Subeconomic occurrence.

### ***Major references(s)***

- Bain, A.D.N. and Medwell, G., 1956. Victorian base metal occurrences. Geological Survey of Victoria Unpublished Report 1956/64.
- Douglas, J.G., 1984. Explanatory notes on the Warragul 1:250 000 geological map. Geological Survey Report No.57. Department of Mines and Energy Victoria, 31 pp.
- Ferguson, W.H., 1928. Parish of Waratah. 1:31,680 geological map. Department of Mines, Victoria.
- Hoatson, D.M. and Glaser, L.M., 1989. Geology and economics of platinum-group metals in Australia. Bureau of Mineral Resources, Australia, Resource Report 5, 81 pp.
- VandenBerg, A.H.M., Willman, C.E., Maher, S., Simons, B.A., Cayley, R.A., Taylor, D.H., Morand, V.J., Moore, D.H. and Radojkovic, A., 2000. The Tasman Fold Belt System in Victoria. Geological Survey of Victoria Special Publication, 211 pp.

### ***Relevant figure(s)***

## **K.6.13 Walhalla Copper Mining Co**

(see East Walhalla Copper and Platinum Mine, Woods Point–Walhalla region)

## K.7 TASMANIA

### K.7.1 Adamsfield Osmiridium Field

(49 alluvial PGE occurrences have been recorded in the Mineral Resources Tasmania database, including R.J. Stacey No. 9468, Stacey Bros No. 20, Stacey Bros No. 21, Williams Creek, Hall's O/C, Harrison and Brandstater, Pollards Shaft and another 42 unnamed occurrences; 10 of the occurrences including Pollard's Shaft have been named as a 'mine or prospect' whereas the remainder have been described as 'areas of alluvial workings')

#### **Geological province**

Delamerian Orogen.

#### **Location**

Adamsfield: 146.32955°E, -42.72789°S; Queenstown (SK 55–05) and Port Davey (SK 55–07), Wedge (8112); ~80 km west-northwest of Hobart, near Lake Gordon.

#### **Classification**

Historical alluvial workings are:

- 10. Placer; 10.B. Alluvial placers derived from 'alpine- and ophiolitic-type' mafic-ultramafic intrusions.

Source rocks for the PGEs are:

- 5. 'Alpine- and ophiolitic-type' mafic-ultramafic intrusions; 5.A. Podiform and stratabound chromitite.

#### **Geological setting**

The Adamsfield Complex is one of at least 20 areas in Tasmania that contain fault juxtaposed early to middle Cambrian ultramafic-mafic blocks composed of three major mineralogically and chemically different ultramafic rock successions: a high-MgO layered dunite-harzburgite succession; a layered pyroxenite-dunite succession; and a multiply intrusive layered pyroxenite-peridotite with associated gabbro succession (Varne and Brown, 1978; Brown, 1986, p. 107; Brown et al., 1989, p. 100). According to Brown (1986), Tasmanian ultramafic complexes were formed from high-temperature magmas (1200°C–1300°C) at low pressures (2 kb–5 kb), in crustal magma chambers associated with Cambrian volcanism, and not in association with ocean floor, back-arc basin or subduction-type terrains where clinopyroxene-rich ultramafic rocks are found. Brown et al. (1989: p. 63) stated that the Tasmanian ultramafic rocks are also chemically and mineralogically dissimilar to large layered bodies like the Stillwater and Bushveld complexes.

The Adamsfield Complex is a north-south-trending linear body, 15 km-long and less than 1 km-wide. An anticlinal structure exposes three major rock types that are well layered in the northern part of the complex—dunite, olivine orthopyroxenite, and orthopyroxenite (the layered dunite-harzburgite and the pyroxenite-dunite successions as described by Brown, 1986). Massive dunite and orthopyroxenite comprise the southern part. The transition between the layered rocks in the north to massive rocks in

the south is marked by a zone of intense, high-temperature deformation, where layers are folded and boudinaged (Varne and Brown, 1978).

### ***PGE mineralisation***

Most of the Os is directly derived from the ultramafic rocks as well as the late Cambrian sedimentary rocks that unconformably overlying the complex. It generally forms irregular grains, 0.5 mm to 1.5 mm across, but nuggets up to 50 g have been found. Rare Os has been reported in serpentinite, however, no occurrences have been noted in unaltered ultramafic rocks. The reclassification scheme of Harris and Cabri (1991) indicates that the 'osmiridium' from Tasmania falls within the fields of osmium, iridium, and rutheniridosmine (Figure 6.32). Past attempts at hard-rock mining have not been highly productive (Brown et al., 1989). Analyses of percussion drill samples with better assay techniques are reported to have returned 1 m @ 14 g/t Ir, 18 g/t Os, and 0.25 g/t Pt from a hole depth of 21 m (Shree Minerals Limited, 2009).

### ***Age of mineralisation***

Early- to mid-Cambrian for emplacement of the mafic-ultramafic intrusion to Cenozoic for alluvial deposits.

The Heazlewood River Complex near the northwestern corner of Tasmania has a similar geological setting and style of PGE-chromite mineralisation to the Adamsfield ultramafic-mafic intrusion. Fractionated tonalitic rocks from the upper part of the complex have a U-Pb zircon crystallisation age of  $513.6 \pm 5$  Ma (Turner et al., 1998; Turner and Bottrill, 2001). This middle Cambrian age may be indicative of the age of emplacement for the Adamsfield Intrusion and its primary PGE-chromite mineralisation. Most alluvial 'osmiridium' deposits derived from the Tasmanian ultramafic-mafic intrusions are of Cenozoic age, but may extend to the Cambrian.

### ***Current status***

Exploration sites.

### ***Economic significance***

Historical alluvial workings. Adamsfield has been a major producer of Os (production ~480 kg) from its discovery in 1925 until 1960 (Bottrill et al., 2014). Adamsfield, Savage River, Mount Stewart, and Wilson River have collectively produced ~970 kg (Hoatson and Glaser, 1989; Appendix F). Alluvial Os and chromite have been mined from the Main Creek, Adam River, and Football Hill areas in the Adamsfield district. A recent resource statement for the Halls Open Cut reported 14 500 t @ 6.5 g/t Ir, 7.3 g/t Os, and 0.13 g/t Pt. The PGE potential of the Adamsfield region, lies in the discovery of small- to moderate-sized alluvial deposits, and possibly the location of the major hard-rock source(s) of PGEs at Adamsfield.

### ***Major references(s)***

- Bottrill, R.S., Bacon, C.A. and Duncan, D. McP., 2014. Cenozoic mineral deposits. In: Corbett, K.D., Quilty, P.G. and Calver, C.R. (editors), *Geological Evolution of Tasmania*. Geological Society of Australia Special Publication 24, Geological Society of Australia (Tasmania Division), 539–548.
- Brown, A.V., 1986. *Geology of the Dundas–Mount Lindsay–Mount Youngbuck Region*. Geological Survey Tasmania. Bulletin 62, 221 pp.
- Brown, A.V., McClenaghan, M.P., Turner, N.J., Baillie, P.W., McClenaghan, J. and Calver, C.R., 1989. *Geological Atlas 1:50 000 Series, Sheet 73 (8112N)*. Huntley. Department of Mines, Tasmania, 110 pp.

- Crawford, A.J. and Berry, R.F., 1992. Tectonic implications of Late Proterozoic–Early Palaeozoic igneous rock associations in western Tasmania. *Tectonophysics*, 214, 37–56.
- Harris, D.C. and Cabri, L.J., 1991. Nomenclature of platinum-group-element alloys: review and revision. *Canadian Mineralogist*, 29, 231–237.
- Hoatson, D.M. and Glaser, L.M., 1989. Geology and economics of platinum-group metals in Australia. Bureau of Mineral Resources, Australia, Resource Report 5, 81 pp.
- Metals Exploration Limited, 1987. Adamsfield prospects southwest Tasmania. E.L. 4/85 Annual Report for the period ending 25 July 1987, 270 pp.
- Shree Minerals Limited, 2009. Shree Minerals Limited 2009 Prospectus, 1 December 2009, 160 pp.
- Turner, N.J., Black, L.P. and Kamperman, M., 1998. Dating of Neoproterozoic and Cambrian orogenies in Tasmania. *Australian Journal of Earth Sciences*, 45, 789–806.
- Turner, N.J. and Bottrill, R.S., 2001. Blue amphibole, Arthur Metamorphic Complex, Tasmania: composition and regional tectonic setting. *Australian Journal of Earth Sciences*, 48, 167–181.
- Varne, R. and Brown, A.V., 1978. The geology and petrology of the Adamsfield Ultramafic Complex, Tasmania. *Contributions to Mineralogy and Petrology*, 67, 195–207.

### ***Relevant figure(s)***

Figure 6.29, Figure 6.30, Figure 6.31, Figure 6.32, Figure 6.33, Figure 6.34, and Figure 8.17f.

## **K.7.2 Ahearne Creek**

(see Keenan Creek, Willson River–Huskisson complexes)

## **K.7.3 Alfred River**

(see Keenan Creek, Wilson River–Huskisson complexes)

## **K.7.4 Andersons Creek**

(Location 1 in Brown, 1992)

### ***Geological province***

Delamerian Orogen.

### ***Location***

Andersons Creek: 146.76879°E, -41.19667°S; Oatlands (SK 55–06), Tamar (8215); ~42 km northwest of Launceston and ~2.3 km northwest of the Barnes Hill Ni deposit.

### ***Classification***

- No actual PGE analyses recorded apart from a brief comment by Reid (1921), but minor occurrences of PGEs probably present in 'alpine- and ophiolitic-type' mafic-ultramafic intrusions and in stream sediments.
- ?5. 'Alpine- and ophiolitic-type' mafic-ultramafic intrusions; ?5.A. Podiform and stratabound chromitite.
- 10. Placer; 10.B. Alluvial placers derived from 'alpine- and ophiolitic-type' mafic-ultramafic intrusions.

### ***Geological setting***

The Andersons Creek 'osmiridium' occurrence is located within the Anderson Creek ultramafic complex (Brown, 1992). A description of the complex by the owners of the Barnes Hill lateritic Ni deposit, Proto Resources and Investments Limited in their 2008 Annual Report stated that aeromagnetics showed the complex to be a north-northwest-trending body approximately 20 km-long and up to 3 km-wide. It crops out over a length of 6.5 km, a width of 1.5 km, and plunges to the north and south beneath Permian sedimentary rocks. Dominant lithologies include serpentinite, serpentinised dunite, pyroxenite, and gabbro. Alluvial concentrations of 'osmiridium' occur in Anderson's Creek and PGE-bearing chromitites occur with specific lithologies in the complex. The Anderson Creek ultramafic complex is interpreted to be a layered Cambrian ultramafic 'wedge' that has been thrust into a sequence of Cambrian sediments lying on the eastern margin of the Precambrian Badger Head Block. The intrusion is probably early Cambrian in age and is one of ~20 discrete ultramafic-mafic complexes found mainly in the northwest and west of Tasmania. Upper Paleozoic tectonism has resulted in Ordovician Cabbage Tree Formation sediments being thrust over the eastern margin of the ultramafics. Taylor (1955) has described the petrology of the ultramafic rocks, but 'osmiridium' is not mentioned in the reports by either by Taylor or Proto Resources.

### ***PGE mineralisation***

Reid (1921) refers to this area as Salisbury District and makes only a brief comment that 'osmiridium' was known to be present in this serpentine belt for many years, but no serious attempt had been made to exploit the occurrences.

### ***Age of mineralisation***

Cambrian to Recent.

### ***Current status***

Exploration.

### ***Economic significance***

Occurrence.

### ***Major references(s)***

Brown, A.V., 1992. Platinum group elements and their host rocks in Tasmania: A summary review. In: Tasmania's development environment. Bulletin Geological Survey Tasmania 70, 48–55.

Proto Resources and Investments Limited, 2008. Proto Resources and Investments Limited 2008 Annual Report, 47 pp.

Reid, A.M., 1921. Osmiridium in Tasmania. Department of Mines Tasmania, Geological Survey Bulletin 32, 123 pp.

Taylor, B.L., 1955. Asbestos in Tasmania. Geological Survey Mineral Resources No. 9. Tasmania Department of Mines, 47 pp.

### ***Relevant figure(s)***

Figure 6.29, Figure 6.30, Figure 6.32, and Figure 8.17f.

### **K.7.5 Bald Hill**

(see Nineteen Mile Creek)

### **K.7.6 Bealy Creek**

(see Keenan Creek, Wilson River–Huskisson complexes)

### **K.7.7 Berkery Creek**

(see Keenan Creek, Wilson River–Huskisson complexes)

### **K.7.8 Boyes River Mineral Field**

#### ***Geological province***

Delamerian Orogen.

#### ***Location***

Boyes River mineral field: 146.257452°E, -42.62839°S; no name for 1:250 000 map sheet (SK 55–10), Wedge (8112); ~90 km west-northwest of Hobart and ~12 km northwest of the Adamsfield Osmiridium Field.

Six unnamed historical areas of alluvial PGE workings are located in the vicinity of the Boyes River mineral field (MRT occurrence Nos 3753.0, 3750.0, 3752.0, 3755.0, 3754.0, 3756.0).

#### ***Classification***

The PGEs in historical alluvial workings classified as:

- 10. Placer; 10.B. Alluvial placers derived from 'alpine- and ophiolitic-type' mafic-ultramafic intrusions.

The PGEs hosted in the nearby Boyes River Ultramafic Complex providing the source for the alluvial deposits classified as:

- 5. 'Alpine- and ophiolitic-type' mafic-ultramafic intrusions; 5.A. Podiform and stratabound chromitite.

#### ***Geological setting***

The Boyes River Ultramafic Complex is reported to be similar to the Adamsfield Complex (Varne and Brown, 1978). It consists of serpentinised coarsely layered ultramafic rocks. Bastite pseudomorphs, after orthopyroxene indicate a greater degree of deformation and brecciation of the sequence than is found at Adamsfield. Relict interlayered (1 cm–120 cm) dunite, orthopyroxenite, orthopyroxene-bearing dunite units in rock outcrops belong to the layered dunite-harzburgite succession (Brown et al., 1989; Brown, 1986).

### ***PGE mineralisation***

Reid (1925) noted reports of 'osmiridium' from Boyes River, however, no production has been recorded from this area.

### ***Age of mineralisation***

Cambrian to Recent.

### ***Current status***

Historical exploration sites.

### ***Economic significance***

Historical alluvial workings.

### ***Major references(s)***

Brown, A.V., McClenaghan, M.P., Turner, N.J., Baillie, P.W., McClenaghan, J. and Calver, C.R., 1989. Geological Atlas 1:50 000 Series, Sheet 73 (8112N). Huntley. Department of Mines, Tasmania, 110 pp.

Reid, A.M., 1925. Adams River osmiridium field. Unpublished Report Department of Mines Tasmania, 48–50.

Varne, R. and Brown, A.V., 1978. The geology and petrology of the Adamsfield Ultramafic Complex, Tasmania. Contributions to Mineralogy and Petrology, 67, 195–207.

### ***Relevant figure(s)***

Figure 6.29, Figure 6.30, Figure 6.32, and Figure 8.17f.

## **K.7.9 Brassy North**

(see Nineteen Mile Creek)

## **K.7.10 Burgess, Burgess Creek**

(see Nineteen Mile Creek)

## **K.7.11 Carpenter Creek**

(see Keenan Creek, Willson River–Huskisson complexes)

## **K.7.12 Castra River**

(see Stanton and Laughnan, Mt Stewart–Castray River area)

## **K.7.13 Caudrys Creek, Caudrys Prospect**

(see Nineteen Mile Creek)

### **K.7.14 Chromite Creek**

(see Keenan Creek, Willson River–Huskisson complexes)

### **K.7.15 Cuni (Five Mile)**

(see Melba Flats)

### **K.7.16 Dundas Osmiridium Field, Westerway Creek**

#### ***Geological province***

Delamerian Orogen.

#### ***Location***

Dundas Osmiridium Field: 145.43434°E, -41.89061°S; Queenstown (SK 55–05), Pieman (7914); ~15 km southwest of Rosebery.

#### ***Classification***

The PGEs in historical alluvial workings classified as:

- 10. Placer; 10.B. Alluvial placers derived from 'alpine- and ophiolitic-type' mafic-ultramafic intrusions.

#### ***Geological setting***

Historical alluvial workings about 7 km to 10 km south of the Melba Flats PGE occurrences.

#### ***PGE mineralisation***

Only a brief mention by Reid (1921) that 'osmiridium' and Au was recovered from stream beds and that peridotite outcrops in the area.

#### ***Age of mineralisation***

Cambrian to Recent?

#### ***Current status***

Historical alluvial workings.

#### ***Economic significance***

Occurrences.

#### ***Major references(s)***

Reid, A.M., 1921. Osmiridium in Tasmania. Department of Mines Tasmania, Geological Survey Bulletin 32, 123 pp.

Reid, A.M., 1925. The Dundas mineral field. Department of Mines Tasmania, Geological Survey Bulletin 36, 98 pp.

### **Relevant figure(s)**

Figure 6.29, Figure 6.30, Figure 6.32, and Figure 8.17f.

## **K.7.17 Fenton's Prospect, Fenton Creek A–B**

(see Nineteen Mile Creek)

## **K.7.18 Florentine Valley**

### **Geological province**

Delamerian Orogen, Thylacine Province.

### **Location**

Florentine Valley: 146.427518°E, -42.70141°S; no name for 1:250 000 map sheet (SK 55–10), Wedge (8112); ~72 km west-northwest of Hobart.

### **Classification**

The PGEs hosted in historical alluvial workings classified as:

- 10. Placer; 10.B. Alluvial placers derived from 'alpine- and ophiolitic-type' mafic-ultramafic intrusions.

### **Geological setting**

The historical alluvial workings at Florentine are located about 5 km east of the Adamsfield osmiridium field (Varne et al., 1978; Brown et al., 1989).

### **PGE mineralisation**

Reid (1925) noted the presence of 'osmiridium' in the Florentine Valley originating from either the Adamsfield Complex or associated Paleozoic placers.

### **Age of mineralisation**

Paleozoic to Recent?

### **Current status**

Historical alluvial workings.

### **Economic significance**

Occurrence.

### **Major references(s)**

Brown, A.V., McClenaghan, M.P., Turner, N.J., Baillie, P.W., McClenaghan, J. and Calver, C.R., 1989. Geological Atlas 1:50 000 Series, Sheet 73 (8112N). Huntley. Department of Mines, Tasmania, 110 pp.

Reid, A.M., 1925. Adams River osmiridium field. Unpublished Report Department of Mines Tasmania, 48–50.

Varne, R. and Brown, A.V., 1978. The geology and petrology of the Adamsfield Ultramafic Complex, Tasmania. *Contributions to Mineralogy and Petrology*, 67, 195–207.

**Relevant figure(s)**

Figure 6.29, Figure 6.30, Figure 6.32, and Figure 8.17f.

**K.7.19 Fourteen Mile Creek, Unnamed occurrence (MRT occurrence ID No 3845)**

**Geological province**

Delamerian Orogen.

**Location**

Fourteen Mile Creek: 146.524504°E, -42.79191°S; no name for 1:250 000 map sheet (SK 55–10), Tyenna (8212); ~64 km west-northwest of Hobart and ~16 km east-southeast of the Adamsfield Osmiridium Field.

Unnamed MRT occurrence: 3845.0: 146.56713°E, -42.81639°S; no name for 1:250 000 map sheet (SK 55–10), Tyenna (8212); ~4.5 km southeast of Fourteen Mile Creek.

**Classification**

The PGEs in historical alluvial workings classified as:

- 10. Placer; 10.B. Alluvial placers derived from 'alpine- and ophiolitic-type' mafic-ultramafic intrusions.

**Geological setting**

Fourteen Mile Creek, on the South Gordon track from Maydena, 25 km east of Adamsfield, where the PGEs are believed to be derived from the Styx River ultramafic complex (Hoatson and Glaser, 1989).

**PGE mineralisation**

Bottrill (2014) noted iridium and osmium as 'common' PGEs in alluvial deposits at Fourteen Mile Creek, platinum as moderately common, and rutheniridosmine was recorded as occurring as alluvial grains with iridium and osmium.

**Age of mineralisation**

Paleozoic to Cenozoic?

**Current status**

Historical alluvial workings.

**Economic significance**

Occurrence.

**Major references(s)**

Bottrill, R.S., 2014. Mineral deposits associated with the mafic-ultramafic complexes. In: Corbett, K.D., Quilty, P.G. and Calver, C.R. (editors), Section 4.4.7. *Geological Evolution of Tasmania*. Geological

Society of Australia Special Publication 24, Geological Society of Australia (Tasmania Division), 141–145.

Hoatson, D.M. and Glaser, L.M., 1989. Geology and economics of platinum-group metals in Australia. Bureau of Mineral Resources, Australia, Resource Report 5, 81 pp.

MRT Mineral Deposits database.

***Relevant figure(s)***

Figure 6.29, Figure 6.30, Figure 6.31, Figure 6.32, Figure 6.33, Figure 6.34, and Figure 8.17f.

**K.7.20 Fowler Creek**

(see Keenan Creek, Willson River–Huskisson complexes)

**K.7.21 Genets\***

(see Melba Flats)

**K.7.22 Gold Creek**

(see Keenan Creek, Willson River–Huskisson complexes)

**K.7.23 Gould Creek**

(see Keenan Creek, Willson River–Huskisson complexes)

**K.7.24 Gravelly Beach**

(see Spero River)

**K.7.25 Greens Creek**

(see Strongs Creek)

**K.7.26 Hall's O/C**

(see Adamsfield Osmiridium Field)

**K.7.27 Harman River**

(see Keenan Creek, Willson River–Huskisson complexes)

**K.7.28 Harrison and Brandstater**

(see Adamsfield Osmiridium Field)

### **K.7.29 Hatchet Creek**

(see Nineteen Mile Creek)

### **K.7.30 Humphries Creek**

(see Stanton and Laughnan, Mt Stewart–Castray River area)

### **K.7.31 Joint Creek**

(see Nineteen Mile Creek)

### **K.7.32 Jones Creek A–C**

(see Nineteen Mile Creek)

### **K.7.33 Keegan Creek**

(see Stanton and Laughnan, Mt Stewart–Castray River area)

### **K.7.34 Keenan Creek**

(Wilson River–Huskisson River complexes (location Nos 5 and 6 in Brown, 1992): Includes a total of about 29 alluvial occurrences including Keenan Creek, Wilson River A, B and C, Harman River, Alfred River, Limestone Creek, Gould Creek, Ahearne Creek, Merton Creek, Chromite Creek, Tributary Creek, Berkery Creek, Roberts Creek, Osmiridium Creek, Sweeney Creek, Tin Creek, Gold Creek, Kershaw Creek, Three Mile Creek, Riley Creek, Carpenter Creek, Bealy Creek, King Creek, Trinders Creek A and B, Fowler Creek, Renison Osmiridium Field\*, and Star Creek)

#### ***Geological province***

Delamerian Orogen.

#### ***Location***

Keenan Creek: 145.367971°E, -41.65642°S; Queenstown (SK 55–05), Pieman (7914); ~20 km northwest of Rosebery. Keenan Creek and Wilson River B occurrences are at the northwest end of this group of historical alluvial PGE workings.

Wilson River A: 145.37928°E, -41.6845°S; Queenstown (SK 55–05), Pieman (7914); ~17 km northwest of Rosebery.

Fowler Creek: 145.411158°E, -41.756094°S; Queenstown (SK 55–05), Pieman (7914); ~12 km west-northwest of Rosebery.

Star Creek: 145.454457°E, -41.80622°S; Queenstown (SK 55–05), Pieman (7914); ~7.7 km west-southwest of Rosebery. Star Creek is located at the southeast end of this group of alluvial PGE workings.

### **Classification**

Historical alluvial workings are:

- 10. Placer; 10.B. Alluvial placers derived from 'alpine- and ophiolitic-type' mafic-ultramafic intrusions.

Source rocks for the PGEs are:

- 5. 'Alpine- and ophiolitic-type' mafic-ultramafic intrusions; 5.A. Podiform and stratabound chromitite.

### **Geological setting**

The Wilson River and Huskisson complexes in western Tasmania are part of the Rocky Harbour Ultramafic Complex (Brown, 1989). According to Peck and Keays (1990) the ultramafic complexes were initially emplaced during the middle Cambrian and represent high-level boninitic intrusions that were deformed during the Devonian (refer to the geological setting for Heazlewood). Ford (1981) suggests the Wilson River and Huskisson River ultramafic complexes represent an extension of the Heazlewood River Complex with the intrusive Devonian Meredith Granite separating the two bodies.

### **PGE mineralisation**

According to an exploration report by Callina NL (1986), the Huskisson River Complex forms a north-south-trending ridge (Serpentinite Ridge) of dunite-harzburgite ultramafics where 'osmiridium' and Au were mined from shallow adits in fault-related shear zones. At Wilson River, 'osmiridium'-bearing limonitic, talcose joints occur in serpentinite. Possibly some of the 'osmiridium' in these joints may be detrital, with the heavy 'osmiridium' grains working their way down into joints during erosion (Bottrill, 2014). Most historical mining was directed at extensive surficial detrital deposits exposed in creeks draining the western slopes of the Huskisson River Complex with alluvial workings extending west over the Wilson River Complex. The detrital deposits appear to have originated as deep soil cover developed over the ultramafic bedrock. The soil layer was then lateritised and eroded from the Serpentinite Ridge and redeposited over the lower flanks of the ridge (Callina NL, 1986). Callina collected bulk samples in the Riley Creek area and reported a heavy-mineral content in samples of 10% to 20%. The 'osmiridium' content in the detrital unit, as estimated by hand panning, ranged from trace to 0.42 gm per cubic metre at the Riley Creek workings and up to 0.22 gm per cubic metre upslope from creek workings.

### **Age of mineralisation**

Cambrian to Cenozoic.

### **Current status**

Exploration sites.

### **Economic significance**

Historical alluvial workings. Adamsfield, Savage River, Mount Stewart, and Wilson River have collectively produced about 970 kg.

### **Major references(s)**

- Bottrill, R.S., 2014. Mineral deposits associated with the mafic-ultramafic complexes. In: Corbett, K.D., Quilty, P.G. and Calver, C.R. (editors), Section 4.4.7. Geological Evolution of Tasmania. Geological Society of Australia Special Publication 24, Geological Society of Australia (Tasmania Division), 141–145.
- Brown, A.V., 1989. Eo-Cambrian-Cambrian. In: Burrett, C.F. and Martin, E.L. (editors), Geology and Mineral Resources of Tasmania. Geological Society of Australia Inc. Special Publication 15.
- Brown, A.V., 1992. Platinum group elements and their host rocks in Tasmania: A summary review. In: Tasmania's development environment. Bulletin Geological Survey Tasmania 70, 48–55.
- Callina NL, 1986. Technical report. Wilson River, N.W. Tasmania 1986. Mineral Resources Tasmania open file report 87–2633, 49 pp.
- Ford, R.J., 1981. Platinum-group minerals in Tasmania. Economic Geology, 76, 498–504.
- Hoatson, D.M. and Glaser, L.M., 1989. Geology and economics of platinum-group metals in Australia. Bureau of Mineral Resources, Australia, Resource Report 5, 81 pp.
- Peck, D.C. and Keays, R.R., 1990. Geology, geochemistry, and origin of platinum-group element-chromitite occurrences in the Heazlewood River Complex, Tasmania. Economic Geology, 85, 765–793.

### **Relevant figure(s)**

Figure 6.29, Figure 6.30, Figure 6.31, Figure 6.32, Figure 6.33, Figure 6.34, and Figure 8.17f.

### **K.7.35 Kershaw Creek**

(see Keenan Creek, Willson River–Huskisson complexes)

### **K.7.36 King Creek**

(see Keenan Creek, Willson River–Huskisson complexes)

### **K.7.37 Limestone Creek**

(see Keenan Creek, Willson River–Huskisson complexes)

### **K.7.38 Melba Flats, Cuni (Five Mile), North Cuni (Genets\* adjoins North Cuni to the north), Nickel Reward, one Unnamed occurrence (MRT location ID 3120)**

#### **Geological province**

Delamerian Orogen.

#### **Location**

Melba Flats: 145.39954°E, -41.83609°S; Queenstown (SK 55–05), Pieman (7914); ~14 km west-southwest of Rosebery. Includes one 'unnamed' occurrence ~1.3 km northeast of Melba Flats.

#### **Classification**

- 8. Hydrothermal-Metamorphic.

The Cu-Ni-Pt-Pd deposits in the Cuni mineral field could be either modified magmatic segregations related to wall-rock assimilation, or are possibly related to Devonian granite-related hydrothermal alteration of Precambrian gabbros (Bottrill, 2014). McKeown (2005) proposed the Melba Flats Ni-Cu deposits are of hydrothermal origin where structures in a gabbro dyke host rock were important mineralising traps.

### **Geological setting**

Several small deposits with locally rich Cu-Ni-Pt-Pd sulphide ores occur within a series of highly altered gabbroic dykes in the Melba Flats–Cuni mineral field area, about 44 km northeast of Zeehan. These deposits occur over a strike length of 3 km, and appear to be largely confined to only one major gabbro dyke. Mineralisation is typically disseminated throughout the dyke, but appears to be more concentrated (massive in places) on the footwall of the dyke, which dips east at approximately 50° (McKeown, 2005).

### **PGE mineralisation**

The Ni sulphides, along with Cu sulphides (chalcopyrite), pyrite, minor Au, and PGEs are concentrated along the basal section of a gabbro dyke. The mineralisation is normally disseminated, but in places contain lenses or shoots of massive sulphide with Ni values typically in the 8%–10% Ni range. A number of mineralised pods are scattered along a three-km strike length of the gabbro dyke, several of which were historically mined for Ni and Cu, with an estimated production of 10 000 t @ 9.5% Ni and 3.5% Cu (Allegiance Mining NL, 2004d). Sperrylite and native platinum are the only PGMs recorded in the Cu-Ni-Pt-Pd pentlandite-rich ores from the Cuni mineral field northeast of Zeehan (Elliston, 1953). Palladium-bearing minerals were not observed, and Pd may occur as solid solution in pentlandite; only traces of Os, Ir, and Au occur in the ores. Other associated ore-gangue minerals include chalcopyrite, pyrite ('bravoite'), millerite, violarite, and magnetite (McKeown, 2004; Bottrill, 2014). Drilling at the North Cuni and Genets prospects intersected narrow zones of Ni-Cu-Co-Au-Pt-Pd mineralisation as shown in Appendix Table K.45 (Allegiance, 2004a,b,c,d).

*Appendix Table K.45 Ni-Cu-Co-Au-Pt-Pd mineralisation intersections in drill-holes at the North Cuni and Genets prospects. Data from Allegiance (2004a,b,c,d).*

Drill-hole	Interval (m)	Width (m)	Ni (%)	Cu (%)	Co (%)	Au (g/t)	Pt (g/t)	Pd (g/t)
MF 01	NA	0.7	9.3	4.5		0.8	0.8	1.4
MF 29	25.3–25.6	0.3	5.85	9.15		0.7	1.26	1.7
MF 32	41.55–42.3	0.75	9.2	4.55		0.92	0.9	1.55
MF 34		1.4	9.55	3.9	0.18	0.25	0.76 PGEs	
MF 38	18.9–19.7	0.8	11.5	4.3	0.18	1.23	0.95	3.2
MF 39	14.0–16.9	2.9	1.5	1.6	0.03	0.23	0.23	0.26
MF 58	37.6–39.8	2.2	4.76	3.66	0.09	0.6	0.92	1.14

Reid (1925, p. 37) reported that assaying of two samples from the Devereaux prospect in this area recorded Pt values of 0.1 ounces and 0.16 ounces.

### ***Age of mineralisation***

The dykes are of uncertain age; they lie in the Crimson Creek Formation and may actually be Neoproterozoic and thus unrelated to the Cambrian ultramafic-mafic complexes (McKeown, 2005; Bottrill, 2014).

### ***Current status***

Historical exploration sites.

### ***Economic significance***

Occurrences and a small deposit. The North Cuni–Genets deposits are reported to contain an Indicated Resource of 83 000 t @ 0.7% Ni and 0.6% Cu and 12 000 t of Inferred Resources at 1.2% Ni and 3.3% Cu (McKeown, 2005).

### ***Major references(s)***

- Allegiance Mining NL, 2004a. Securities Exchange Announcement Melba Flats Project–Tasmania, 28 April 2004, 4 pp.
- Allegiance Mining NL, 2004b. Securities Exchange Announcement Melba Flats Project–Tasmania, Genets Prospect 15 June 2004, 4 pp.
- Allegiance Mining NL, 2004c. Quarterly Report for period ending 30 September 2004, 13 pp.
- Allegiance Mining NL, 2004d. Annual Report 2004, 54 pp.
- Bottrill, R.S., 2014. Mineral deposits associated with the mafic-ultramafic complexes. In: Corbett, K.D., Quilty, P.G. and Calver, C.R. (editors), Section 4.4.7. Geological Evolution of Tasmania. Geological Society of Australia Special Publication 24, Geological Society of Australia (Tasmania Division), 141–145.
- Elliston, J., 1953. Platinoids in Tasmania. In: Edwards, A.B. (editor), Geology of Australian Mineral Deposits. 1250–1254. 5<sup>th</sup> Empire Mining and Metallurgical Congress, Australasian Institute of Mining and Metallurgy, Melbourne,
- McKeown, M.V., 2004. Melba Flats Nickel project mineral resource report. Unpublished Report Allegiance Mining NL. TCR 03\_4848.
- McKeown, M.V., 2005. Melba Project. EL43/1992. Annual Report March 2005. Allegiance Mining NL, 71 pp.
- Reid, A.M., 1925. Adams River osmiridium field. Unpublished Report Department of Mines Tasmania, 48–50.

### ***Relevant figure(s)***

Figure 6.29 and Figure 6.30.

## **K.7.39 Merton Creek**

(see Keenan Creek, Wilson River–Huskisson complexes)

## **K.7.40 Newall Creek**

### ***Geological province***

Delamerian Orogen.

### ***Location***

Newall Creek: 145.54119°E, -42.16302°S; no name for 1:250 000 map sheet (SK 55–10), Franklin (8013); ~8 km south of Queenstown.

### ***Classification***

- 10. Placer; 10.B. Alluvial placers derived from 'alpine- and ophiolitic-type' mafic-ultramafic intrusions.

### ***Geological setting***

An isolated area of historical alluvial workings about 31 km south-southeast of Dundas osmiridium field.

### ***PGE mineralisation***

An isolated area of alluvial workings located on the Newall Creek, ~900 m south of its confluence with the King River. No specific information on the PGEs.

### ***Age of mineralisation***

Paleozoic to Recent?

### ***Current status***

Historical alluvial workings.

### ***Economic significance***

Occurrence.

### ***Major references(s)***

### ***Relevant figure(s)***

Figure 6.29 and Figure 6.30.

## **K.7.41 Nickel Reward**

(see Melba Flats)

## **K.7.42 Nineteen Mile Creek**

(Heazlewood area: Includes a total of about 29 alluvial occurrences including Nineteen Mile Creek A–C, Warners Creek A–E, Fenton's Prospect and Fenton Creek A–B, Bald Hill, Joint Creek, Hatchet Creek; with Jones Creek A–C to the northeast of the main cluster of occurrences, Burgess, Burgess Creek, Brassy North to the southeast, Caudrys Creek, Caudrys Prospect, Purcells Prospect and Purcells South Workings to the southwest. Another five PGE prospects are unnamed (MRT mineral occurrence ID Nos 1356.0, 1367.0, 1354.0, 1363.0, 1364.0, 1365.0))

### ***Geological province***

Delamerian Orogen.

### **Location**

Nineteen Mile Creek A: 145.30338°E, -41.43553°S; Queenstown (SK 55–05), Arthur River (7915); ~8 km northwest of Luina.

### **Classification**

The PGE resources mined from the alluvial workings can be classified as:

- 10. Placer; 10.B. Alluvial placers derived from 'alpine- and ophiolitic-type' mafic-ultramafic intrusions.

Source of alluvial PGEs are the mafic-ultramafic complexes in the area:

- 5. 'Alpine- and ophiolitic-type' mafic-ultramafic intrusions; 5.A. Podiform and stratabound chromitite (e.g., Caudrys Prospect).

### **Geological setting**

The Heazlewood River Complex in western Tasmania is the largest and least dismembered of the Tasmanian ultramafic-mafic complexes that crops out over an area of 50 km<sup>2</sup>. It was initially emplaced during the middle Cambrian and was subsequently re-emplaced during an episode of compressional deformation during the Devonian. The complex consists of a maximum of 5 km of layered ultramafic cumulates and crosscutting gabbroic rocks and up to 3 km of overlying low-Ti tholeiitic basalt and boninite. The Heazlewood River Complex also hosts a tonalite complex and probable tectonic melanges. Cumulate layering is well developed in many parts of the complex, trending northeasterly and displaying near-vertical dips. The complex is cut by numerous faults and shear zones, commonly trending northwesterly to northerly. The cumulate rocks record variable degrees of serpentinisation. A major north-trending fault divides the complex into western and eastern sections, with very little correlation between rock types across the fault (Peck and Keays, 1990). According to Peck and Keays (1990), the complex represents a high-level boninitic intrusion. The Complex is partly overlain by eluvial deposits and alluvial stream placers, and is buried by Cenozoic lavas. Small alluvial PGE deposits are derived from the Heazlewood River Complex.

### **PGE mineralisation**

Peck and Keays (1990) identified three types of PGE-chromite occurrences in Heazlewood River Complex. Type I comprises schlieren of Cr-rich spinel hosted in primitive, olivine-rich cumulates. Type II occurs as schlieren of more aluminous spinel hosted in interlayered sequence of cumulate dunite and peridotite. Type III is more massive, occurring as irregular stringers, pods, and layers containing chromite having intermediate Cr/Al ratios. It is spatially associated with gabbroic dykes that intrude dunite-harzburgite-orthopyroxenite cyclic units and is interlayered with or enclosed by an unusual xenolith-bearing gabbro. Both type I and II chromitites are interpreted to have precipitated directly from a primitive magma and may reflect periods of magma replenishment. Type III was formed in response to mixing between ultramafic magma and volatile-rich intercumulus liquids, producing hybrid magmas having chromite as the only liquidus phase. Detailed analyses by Peck and Keays (1990) of samples of 'Type II' chromitite occurrences returned the highest PGE values in chromitite schlieren. Maximum values obtained were up to 1700 ppb Os, 1800 ppb Ir, and 2000 ppb Ru; while the maximum values of 240 ppb Rh, 1000 ppb Pt, and 72 ppb Pd were returned from samples of 'Type III' massive chromite.

Identified PGMs occur in tectonised dunite and intensely serpentinised ultramafics of the Heazlewood River Complex. Native Pt, laurite, and a possible Os-bearing sulphide (?erlichmanite) have been documented with base-metal sulphides and Ni-Fe alloys in chromitite, and native Pt or a Pt-bearing sulphide in a dunite pipe. The chromitites occur as lenticular bodies associated with pegmatitic norite in a hybrid zone interpreted to have resulted from magma mixing. Hard-rock sources are of low grade, with mining largely restricted to eluvial deposits and stream placers buried by Cenozoic lavas. Platinum-group minerals shedding from the Heazlewood River Complex have been reported in the nearby Nineteen Mile Creek; they are dominantly rutheniridosmine, which contains high Ru levels relative to PGMs from the Adamsfield Intrusion. Associated heavy minerals with the rutheniridosmine, include gold, gold alloyed with platinum, chromite, picotite, magnetite, pyrrhotite, and pyrite.

Historical alluvial mining produced 31 000 ounces of 'osmiridium' (Os-Ir-Ru alloy). The Heazlewood River Complex was the world's major supplier of Os and Ir between 1910 and 1920 (Reid, 1925; Ford, 1981; Hoatson and Glaser 1989; Peck and Keays, 1990). Osmiridium was first located in foliated serpentinite at Caudry's prospect on Bald Hill, near Heazlewood, in 1913 and produced about 250 ounces of PGEs from a zone containing magnesite, opal, and talc. The 'osmiridium' was intergrown with chromite and magnetite, which occurred in pods (Reid, 1921; Bottrill, 2014).

### ***Age of mineralisation***

Fractionated tonalitic rocks from the upper part of the Heazlewood River Complex have a U-Pb zircon crystallisation age of  $513.6 \pm 5$  Ma (Turner et al., 1998; Turner and Bottrill, 2001). This middle Cambrian age may also be relevant to other mineralised ultramafic-mafic complexes in western Tasmania, e.g., Adamsfield Intrusion and its primary PGE-chromite mineralisation. Most alluvial 'osmiridium' deposits derived from the Tasmanian ultramafic-mafic intrusions are of Cenozoic age, but may extend to the Cambrian.

### ***Current status***

Exploration.

### ***Economic significance***

Occurrences.

### ***Major references(s)***

- Bottrill, R.S., 2014. Mineral deposits associated with the mafic-ultramafic complexes. In: Corbett, K.D., Quilty, P.G. and Calver, C.R. (editors), Section 4.4.7. Geological Evolution of Tasmania. Geological Society of Australia Special Publication 24, Geological Society of Australia (Tasmania Division), 141–145.
- Ford, R. J., 1981. Platinum-group minerals in Tasmania. *Economic Geology*, 76, 498–504.
- Hoatson, D.M. and Glaser, L.M., 1989. Geology and economics of platinum-group metals in Australia. Bureau of Mineral Resources, Australia, Resource Report 5, 81 pp.
- Peck, D.C. and Keays, R.R., 1990. Geology, geochemistry and origin of platinum-group element-chromitite occurrences in the Heazlewood River Complex, Tasmania. *Economic Geology*, 85, 765–793.
- Reid, A.M., 1925. The Dundas mineral field. Department of Mines Tasmania, Geological Survey Bulletin 36, 98 pp.
- Turner, N.J., Black, L.P. and Kamperman, M., 1998. Dating of Neoproterozoic and Cambrian orogenies in Tasmania. *Australian Journal of Earth Sciences*, 45, 789–806.
- Turner, N.J. and Bottrill, R.S., 2001. Blue amphibole, Arthur Metamorphic Complex, Tasmania: composition and regional tectonic setting. *Australian Journal of Earth Sciences*, 48, 167–181.

***Relevant figure(s)***

Figure 6.29, Figure 6.30, Figure 6.31, Figure 6.32, Figure 6.33, Figure 6.34, and Figure 8.17f.

**K.7.43 North Cuni\***

(see Melba Flats)

**K.7.44 Osmiridium Beach**

(see Strongs Creek)

**K.7.45 Osmiridium Creek**

(see Keenan Creek, Willson River–Huskisson complexes)

**K.7.46 Pine Creek**

(see Stanton and Laughnan, Mt Stewart–Castray River area)

**K.7.47 Pollards Shaft**

(see Adamsfield Osmiridium Field)

**K.7.48 Purcells Prospect and Purcells South Workings**

(see Nineteen Mile Creek)

**K.7.49 Ramsay's**

(see Stanton and Laughnan, Mt Stewart–Castray River area)

**K.7.50 Renison Osmiridium Field**

(see Keenan Creek, Willson River–Huskisson complexes)

**K.7.51 Riley Creek**

(see Keenan Creek, Willson River–Huskisson complexes)

**K.7.52 R.J. Stacey No. 9468**

(see Adamsfield Osmiridium Field)

### **K.7.53 Roberts Creek**

(see Keenan Creek, Willson River–Huskisson complexes)

### **K.7.54 Rocky Boat Harbour (two locations with the same name)**

(see Strongs Creek)

### **K.7.55 Savage River Dredge, Savage River Section 1163, Unnamed PGE locations with MRT location ID 2188 (Badgers Plain), 2191, 10613**

#### ***Geological province***

Delamerian Oregon.

#### ***Location***

Savage River Dredge: 145.09891°E, -41.61715°S; Queenstown (SK 55–05), Pieman (7914); ~15 km southwest of Savage River.

Savage River Section 11663: 145.08182°E, -41.62678°S; Queenstown (SK 55–05), Pieman (7914); ~17 km southwest of Savage River.

MRT occurrence ID numbers from south to north along the Savage River:

2188.0: (Badgers Plain in Reid 1921): 145.1364°E, -41.56553°S; Queenstown (SK 55–05), Pieman (7914); ~7 km northeast of Savage River Dredge occurrence.

2191.0: 145.17784°E, -41.49909°S; Queenstown (SK 55–05), Arthur River (7915).

10613.0: 145.22864°E, -41.47286°S; Queenstown (SK 55–05), Arthur River (7915).

Whyte River: 145.18396°E, -41.62303°S; Queenstown (SK 55–05), Pieman (7914); ~7 km east of the Savage River Dredge occurrence.

#### ***Classification***

- 10. Placer; 10.B. Alluvial placers derived from 'alpine- and ophiolitic-type' mafic-ultramafic intrusions.

#### ***Geological setting***

Alluvial PGEs located along the Savage River derived from the Heazlewood River Complex located about 10 km to the northeast.

#### ***PGE mineralisation***

The Savage River area was one of the main producers of 'osmiridium' in northwest Tasmania. Reid (1921) described the alluvial mining activity along the Savage River and Whyte River, but has not recorded any production data. Reid noted that the bulk of alluvial 'osmiridium', probably further upstream at Nineteen Mile Creek, was found near and on the bedrock in the river bed. 'Osmiridium' occurs together with Au and the 'osmiridium' content in an elevated terrace was stated to be 8 to 10 grains per ton.

### ***Age of mineralisation***

Paleozoic to Cenozoic.

### ***Current status***

Historical alluvial workings.

### ***Economic significance***

Occurrences.

### ***Major references(s)***

Reid, A.M., 1921. Osmiridium in Tasmania. Department of Mines Tasmania, Geological Survey Bulletin 32, 123 pp.

### ***Relevant figure(s)***

Figure 6.29, Figure 6.30, Figure 6.31, Figure 6.32, Figure 6.33, Figure 6.34, and Figure 8.17f.

## **K.7.56 Spero River, Gravelly Beach**

### ***Geological province***

Delamerian Orogen.

### ***Location***

Spero River: 145.34878°E, -42.6333°S; no name for the 1:250 000 map sheet (SK 55–09), Spero (7912); approximately 54 km south of Strahan.

Gravelly Beach: 145.39856°E, -42.38455°S no name for the 1:250 000 map sheet (SK 55–09), Cape Sorell (7913).

### ***Classification***

The historical alluvial workings are located very close to the coast and are either stream alluvials or beach placers, possibly:

- 10. Placer; ?10.C. Alluvial placers; and
- 10. Placer; ?10.D. Beach placers.

The ages of the serpentinised peridotite and pyroxenite source rocks are unknown (Reid, 1921).

### ***Geological setting***

Either beach or stream alluvial placers.

### ***PGE mineralisation***

Only a brief mention of 'osmiridium' at Spero River and Birch's Inlet by Reid (1921). The Birch's Inlet location probably corresponds to Gravelly Beach, which is on the southern side of Macquarie Harbour and ~8 km northwest of Birch's Inlet. Reid has noted serpentinised peridotite rocks at Spero River whereas pyroxenites feature at the Birch's Inlet area. According to Reid, only small quantities of 'osmiridium' were found in the Spero River–Birch's Inlet area.

### ***Age of mineralisation***

Cenozoic.

### ***Current status***

Historical alluvial workings.

### ***Economic significance***

Occurrences.

### ***Major references(s)***

Reid, A.M., 1921. Osmiridium in Tasmania. Department of Mines Tasmania, Geological Survey Bulletin 32, 123 pp.

### ***Relevant figure(s)***

Figure 6.29, Figure 6.30, Figure 6.31, Figure 6.32, Figure 6.33, and Figure 6.34.

## **K.7.57 Stacey Bros No. 20, Stacey Bros No. 21**

(see Adamsfield Osmiridium Field)

## **K.7.58 Stanton and Loughnan**

(Mt Stewart–Castray River area: Includes Tunbridge and Kellys south of Stanton and Loughnan in the Loughnan Creek, Ramsay's and Humphries Creek; Castra River occurrence is located on the Castray River about 2 km north of Stanton and Loughnan just before the confluence of the Castray and Whyte rivers. The Pine Creek and Keegan Creek prospects are on the Pine and Keegan creeks, about 7 km southeast of the Stanton and Loughnan prospects. These two occurrences have not been described in the available literature)

### ***Geological province***

Delamerian Orogen.

### ***Location***

Stanton and Loughnan: 145.305408°E, -41.523109°S; Queenstown (SK 55–05), Pieman (7914); ~8 km east-southeast of Savage River.

### ***Classification***

The historical alluvial workings are stream placers classified as:

- 10. Placer; 10.B.Alluvial placers derived from 'alpine- and ophiolitic-type' mafic-ultramafic intrusions.

The source of the PGEs in the alluvial deposits is derived from the nearby PGE-bearing mafic-ultramafic complexes classified as:

- 5. 'Alpine- and ophiolitic-type' mafic-ultramafic intrusions; 5.A. Podiform and stratabound chromitite.

### ***Geological setting***

At Mt Stewart, 'osmiridium' was found in schlieren transecting chromite and magnetite-rich serpentinite. This area is a significant historical producer of 'osmiridium' from alluvial deposits (Bottrill, 2014).

### ***PGE mineralisation***

The following descriptions are from Reid (1921):

- Stanton and Loughnan's Reward Claim: Prevailing country rock is serpentinite intruded by granite, petrological examination of serpentinite shows presence of chromite, olivine and outlines of pyroxenes. Richest 'osmiridium' deposits were confined to Loughnan Creek where joints in serpentinite contained pockets ('schlieren') of 'osmiridium', but no 'osmiridium' was detected in samples from the wall rock. 'Osmiridium' often forms coarse grains and larger nuggets up to an ounce in weight. Production of 100 ounces of 'osmiridium' from detrital material was reported by Reid (1921) at the time of his visit. Gold, Sn, native bismuth, and chromite are also present. Granite pebbles in the Loughnan Creek suggest the source(s) for the alluvial deposits was from Meredith Range in the west.
- Humphries Creek: 'Osmiridium' in eluvial/alluvial material derived from joints in peridotite. Small nuggets of iridium, ruthenium, and iron sulphides in joints in serpentinite.
- Tunbridge and Kelly's Prospect: Serpentinised peridotite bedrock, Os, Ir, and Ru in eluvial material in weathered joints in serpentinite and also as alluvial deposits. In places 'osmiridium' nuggets in joints up to an ounce in weight. Reid (1921) reported production of 60 ounces of 'osmiridium'.
- Castra River: Located on Castray River just before its confluence with the Whyte River. Alluvial 'osmiridium' occurs together with Sn, Au, and monazite.

### ***Age of mineralisation***

Cambrian to Cenozoic.

### ***Current status***

Exploration site.

### ***Economic significance***

Historical alluvial workings.

### ***Major references(s)***

Bottrill, R.S., 2014. Mineral deposits associated with the mafic-ultramafic complexes. In: Corbett, K.D., Quilty, P.G. and Calver, C.R. (editors), Section 4.4.7. Geological Evolution of Tasmania. Geological Society of Australia Special Publication 24, Geological Society of Australia (Tasmania Division), 141–145.

Reid, A.M., 1921. Osmiridium in Tasmania. Department of Mines Tasmania, Geological Survey Bulletin 32, 123 pp.

### ***Relevant figure(s)***

Figure 6.29, Figure 6.30, Figure 6.31, Figure 6.32, Figure 6.33, Figure 6.34, and Figure 8.17f.

### **K.7.59 Star Creek**

(see Keenan Creek, Willson River–Huskisson complexes)

### **K.7.60 Strongs Creek, Tylers Creek, Osmiridium Beach, Greens Creek, Rocky Boat Harbour (two locations with the same name)**

#### ***Geological province***

Delamerian Orogen.

#### ***Location***

Strongs Creek: 146.623738°E, -43.56219°S; no name for 1:250 000 map sheet (SK 55–14), South East Cape (8210), (includes Tylers Creek);

Osmiridium Beach: 146.62744°E, -43.5649°S; no name for 1:250 000 map sheet (SK 55–14), South East Cape (8210); ~0.4 km east-southeast of Strongs Creek;

Greens Creek: 146.64236°E, -43.55324°S; no name for 1:250 000 map sheet (SK 55–14), South East Cape (8210); ~1.8 km northeast of Strongs Creek;

Rocky Boat Harbour: 146.61137°E, -43.560035°S; no name for 1:250 000 map sheet (SK 55–14), South East Cape (8210), no record of PGEs, only a geographic point of the east end of Rocky Boat Harbour.

Surprise Rivulet, another prospect called Rocky Boat Harbour (referred in this report as Surprise Rivulet) located inland: 146.64863°E, -43.53976°S; no name for 1:250 000 map sheet (SK 55–14), South East Cape (8210); 3.2 km northeast of Strongs Creek, and ~5 km inland from mouth of Surprise Rivulet, the area with serpentinite outcrop and rock chip and stream sediment sampling along the Surprise Rivulet in 1970;

Rocky Boat Plain: 146.628707°E, -43.5595°S; no name for 1:250 000 map sheet (SK 55–14), South East Cape (8210).

#### ***Classification***

- 5. 'Alpine- and ophiolitic-type' mafic-ultramafic intrusions; 5.A. Podiform and stratabound chromitite (source for alluvial and beach placer PGEs?).
- 10. Placer; 10.B. Alluvial placers derived from 'alpine- and ophiolitic-type' mafic-ultramafic intrusions (Rocky Boat Harbour (Surprise Rivulet), Rocky Plain? Greens Creek, Milford Creek\*).
- 10. Placer; 10.D. Beach placers (Strongs Creek, Tylers Creek, Osmiridium Beach, the beach location of the Rocky Boat Harbour).

#### ***Geological setting***

Serpentinite known to crop out on the western side of the Surprise Rivulet. All of the historical 'osmiridium' production appears to have been recovered from beach placers and alluvial workings.

#### ***PGE mineralisation***

Strongs Creek, Tylers Creek prospects: up to 50 ounces of 'osmiridium' reportedly recovered by prospectors in 1924 from the beach on the east side of Strongs Creek, (U.C. Services, 1970);

Rocky Boat Plain: some 'osmiridium' reportedly found (U.C. Services 1970).

Osmiridium Beach: one sample of Cambrian-Ordovician (?) conglomerate from western end of the Rocky Bay Plains beach yielded 0.07 ppm Pt, 0.01 ppm Pd, and <0.01 ppm Au (U.C. Services, 1970).

Greens Creek: a tributary of the Surprise Rivulet; fine-grained 'osmiridium' and small nuggets recovered by prospectors in 1924; four stream-sediment samples from the Greens Creek yielded <0.04 ppm to 0.11 ppm Pt, <0.01 ppm Pd, 36 ppm to 86 ppm Ni, and 4 ppm to 8 ppm Cu (U.C. Services, 1970).

Rocky Boat Harbour: located in a separate inlet; no record of PGEs.

Surprise Rivulet: another prospect called Rocky Boat Harbour (inland prospect at Surprise Rivulet); site of exploration in May 1970; analyses of 13 chip and grab samples of serpentinite rock outcrop adjoining the western side of the rivulet gave <0.02 ppm to 0.04 ppm Pt, <0.02 ppm to 0.04 ppm Pd, up to 74 ppm Cu, and 240 ppm to 3900 ppm Ni. Seven stream-sediment samples from the Surprise Rivulet did not locate any 'osmiridium', but yielded <0.03 ppm to 0.23 ppm Pt, <0.01 ppm to 0.02 ppm Pd, 30 ppm to 102 ppm Ni, and 24 ppm to 46 ppm Cu (U.C. Services, 1970).

Prospecting for 'osmiridium' is also reported to have taken place in the headwaters of the Milford Creek about 5 km northeast of Rocky Boat Harbour and one stream-sediment sample from a 1970 exploration program gave 0.17 ppm Pt (U.C. Services, 1970).

### ***Age of mineralisation***

Paleozoic to Cenozoic?

### ***Current status***

Historical alluvial and beach placer workings and historical exploration sites.

### ***Economic significance***

Occurrences.

### ***Major references(s)***

U.C. Services (Australia) Proprietary Limited, 1970. Surprise Creek. Bulletin 25, 13 pp.

U.C. Services (Australia) Proprietary Limited, 1971. Addendum to Bulletin 25, 7 pp.

MRT Mineral Deposits database

### ***Relevant figure(s)***

Figure 6.29, Figure 6.30, Figure 6.31, Figure 6.32, Figure 6.33, Figure 6.34, and Figure 8.17f.

## **K.7.61 Sweeney Creek**

(see Keenan Creek, Willson River–Huskisson complexes)

## **K.7.62 Three Mile Creek**

(see Keenan Creek, Willson River–Huskisson complexes)

### **K.7.63 Tin Creek**

(see Keenan Creek, Willson River–Huskisson complexes)

### **K.7.64 Tributary Creek**

(see Keenan Creek, Willson River–Huskisson complexes)

### **K.7.65 Trinders A and B**

(see Keenan Creek, Willson River–Huskisson complexes)

### **K.7.66 Tunbridge and Kellys**

(see Stanton and Laughnan, Mt Stewart–Castray River area)

### **K.7.67 Tylers Creek\***

(see Strongs Creek)

### **K.7.68 Unnamed PGE occurrences with MRT mineral occurrence ID Nos 1354, 1356, 1363, 1364, 1365, 1367**

(see Nineteen Mile Creek)

### **K.7.69 Unnamed PGE occurrences with MRT mineral occurrence ID Nos 2188 (Badgers Plain), 2191, 10613**

### **K.7.70 Unnamed PGE occurrence with MRT location ID No 3120**

(see Melba Flats)

### **K.7.71 Unnamed PGE occurrences with MRT occurrence ID Nos 3714, 3715, 3716, 3717, 3718, 3719, 3720, 3721, 3722, 3723, 3725, 3726, 3727, 3728, 3729, 3730, 3731, 3732, 3733, 3734, 3735, 3736, 3737, 3738, 3739, 3740, 3741, 3742, 3745, 11312, 11893, 11894, 11895, 11896, 11897, 11899, 11900, 11901, 11902, 11903, 11904, 11905**

(in historical areas of alluvial PGE workings located in the vicinity of the Adamsfield Osmiridium Field)

### **K.7.72 Unnamed PGE occurrences with MRT occurrence ID Nos 3750, 3752, 3753, 3754, 3755, 3756**

(in historical areas of alluvial PGE workings located in the vicinity of the Boyes River mineral field)

### **K.7.73 Unnamed PGE MRT occurrence ID No 3845**

(see Fourteen Mile Creek)

### **K.7.74 Unnamed prospects (MRT occurrence ID Nos 3918, 3919 and 3920)**

#### ***Geological province***

Delamerian Orogen.

#### ***Location***

Unnamed prospect: 3920.0: 146.73274°E, -43.04599°S; no name for 1:250 000 map sheet (SK 55–14), Huon (8211); ~48 km southeast of the Adamsfield Osmiridium Field.

#### ***Classification***

- 10. Placer; ?10.B. Alluvial placers derived from 'alpine- and ophiolitic-type' mafic-ultramafic intrusions.

#### ***Geological setting***

#### ***PGE mineralisation***

#### ***Age of mineralisation***

Paleozoic to Cenozoic?

#### ***Current status***

Historical alluvial workings?

#### ***Economic significance***

Occurrences.

#### ***Major references(s)***

MRT Mineral Deposits database.

#### ***Relevant figure(s)***

Figure 6.29, Figure 6.30, Figure 6.31, Figure 6.32, Figure 6.33, Figure 6.34, and Figure 8.17f.

### **K.7.75 Warners Creek A–E**

(see Nineteen Mile Creek)

### **K.7.76 Westerway Creek**

(see Dundas Osmiridium Field)

**K.7.77 Whyte River**

(see Savage River Dredge)

**K.7.78 Williams Creek**

(see Adamsfield Osmiridium Field)

**K.7.79 Wilson River A, B and C**

(see Keenan Creek, Wilson River–Huskisson complexes)

# Appendix L Pictorial library of mafic-ultramafic rocks: a guide for exploration

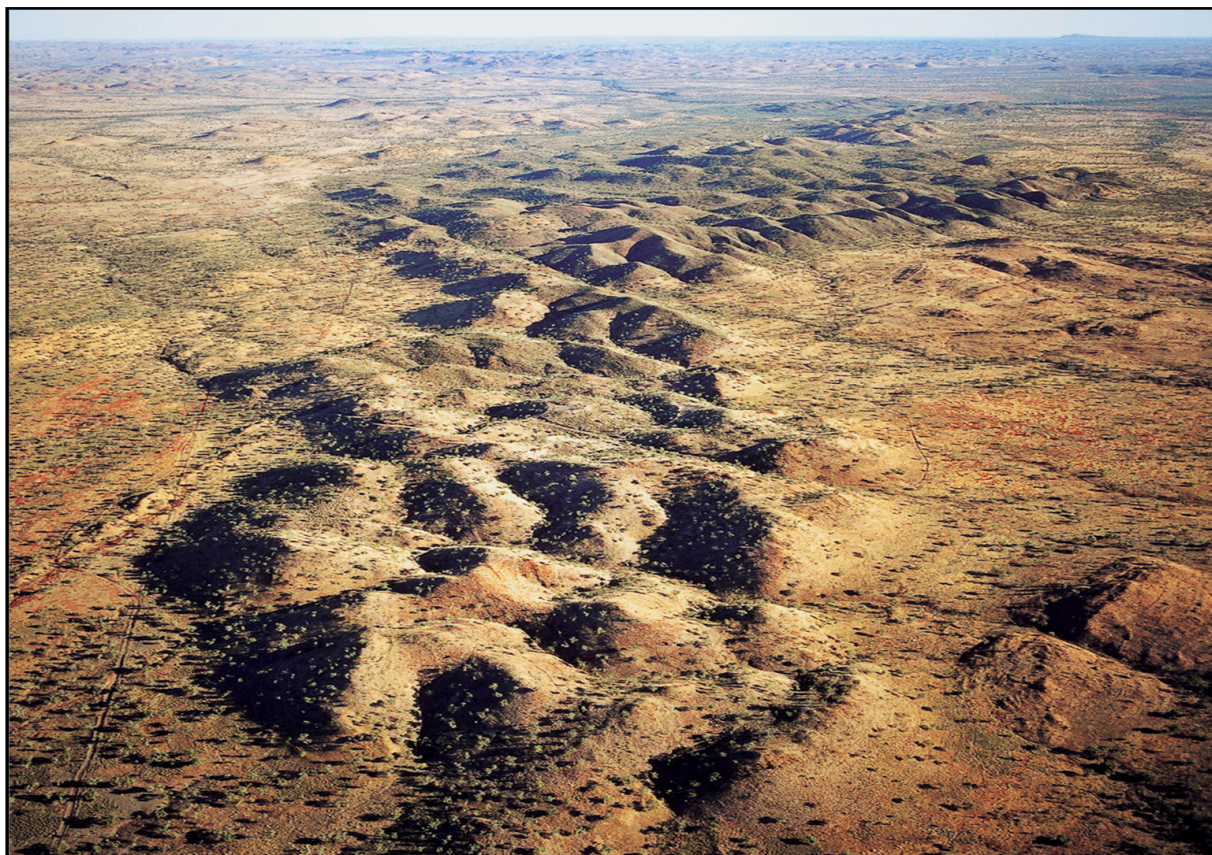
Geoscientists and companies from Australia and overseas have donated rock samples and photographs for Appendix L; these people are acknowledged on page v.

Platinum-group elements are associated with a variety of igneous rocks that are derived from tholeiitic, komatiitic, and alkaline parent magmas. A remarkable array of diagnostic rock textures involving sulphide, Cr-bearing spinel, Fe-Ti oxide, and silicate minerals provide useful clues for determining the geological environments and potential for PGE mineral-systems (see Chapter 7). Many of these rock textures are preserved in the weathering profile and therefore are useful indicators while undertaking geological mapping and drilling programs. This pictorial library contains examples of mineralisation and rock textures associated with mafic and ultramafic rocks from different orthomagmatic and hydrothermal geological settings. Examples from overseas and Australia include, such iconic (and type) localities as: the Bushveld Complex (South Africa); Stillwater Complex (Canada); Great Dyke (Zimbabwe); Noril'sk–Talnakh (Russia); Voisey's Bay (Canada); Komati Valley (South Africa); and important Australian examples, such as the Panton and Munni Muni Intrusions; Windimurra Igneous Complex; Kambalda; Mount Windarra; Flying Fox; Collurabbie; Fifield; and Avebury, among others.

Rock-types formed from intrusive tholeiitic magmatic systems are generally characterised by cumulus textures. Rock textures are invariably coarser grained than those derived from komatiitic magmas (see next paragraph) by virtue of the emplacement of the magmas at greater depths in the crust and the longer retention of heat which facilitates crystal-nucleation processes. Cumulate rocks are rocks formed by the accumulation of crystals (commonly olivine, orthopyroxene, clinopyroxene, chromite, plagioclase, Fe-Ti oxides, and sulphides) growing at or near the liquidus temperature of the parent magma. They are classified into the three textural types—orthocumulates, adcumulates, and mesocumulates based on the abundance of intercumulus (i.e., late-crystallising component) minerals. For example, adcumulates have up to 7 volume % intercumulus minerals, mesocumulates 7%–25%, and orthocumulates have 25%–50% (Irvine, 1982). In recent years, it has been recognised that cumulates can form in different parts of a magma chamber by a variety of mechanisms ranging from gravitational deposition (i.e., vertical movement), to density current and flowage differentiation (lateral movement), to *in situ* growth on the floors and walls of the magma chamber (Hoatson et al., 1992).

Komatiite sequences are often composed of multiple compound cooling units varying widely in thickness, lateral extent, and relative proportion of different rock types, representing a spectrum from rapidly cooled liquid to cumulates. Such komatiitic rocks evolve from very high-MgO magmas (>18% MgO) that formed by high degrees of partial melting in the mantle and have eruption temperatures in excess of 1600°C and local regimes of rapid cooling. Much of the diversity of textures in these rocks arises from varying proportion and morphology of original igneous olivine crystals. For example, crystal morphology in olivine±pyroxene spinifex and cumulate rocks is highly sensitive to cooling and nucleation rates, and consequently is a sensitive indicator of the crystallisation environment (Barnes, 2006). The large degrees of partial melting and the elevated eruption temperatures of komatiitic magmas are consistent with the high-geothermal gradients in the mantle during the Archean Eon and may explain why komatiitic rocks are poorly represented in Phanerozoic terranes.

## L.1 Australian examples



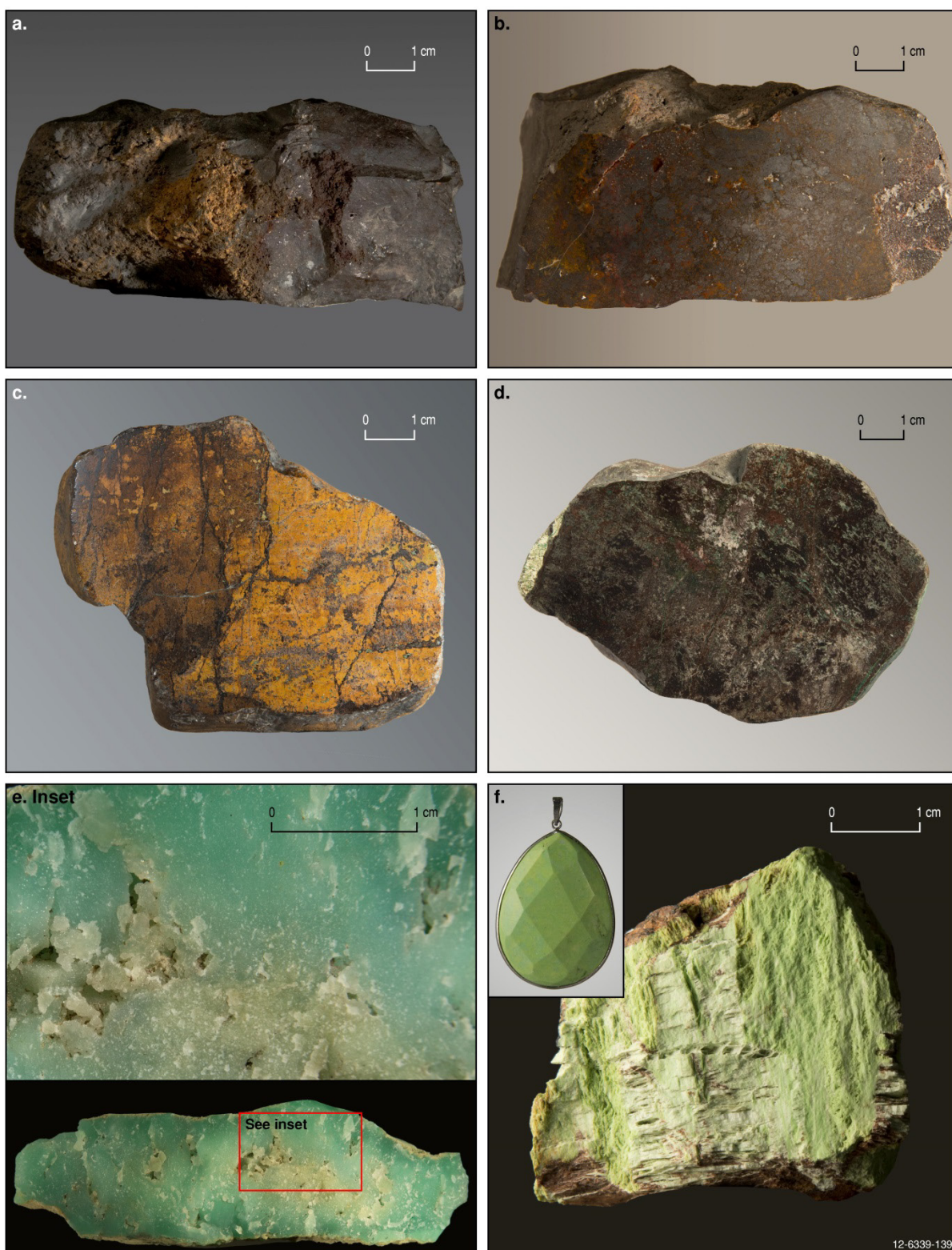
*Appendix Figure L.1 Panton Intrusion, Halls Creek Orogen, Western Australia. Oblique aerial photograph looking southwest along the synclinal axis of the Panton layered mafic-ultramafic intrusion. Platinum-group element-bearing chromitites near the contact between the ultramafic and gabbroic zones (upper central part of photograph) have been the focus of exploration since their discovery in 1962. See geology map of Figure 6.9.*



*Appendix Figure L.2 McIntosh Intrusion, Halls Creek Orogen, Western Australia. Oblique aerial photograph looking south over the McIntosh layered mafic intrusion which forms a prominent geomorphic feature (similar to the cross-section of an onion) in the East Kimberleys that is visible on satellite imagery. See Figure 6.12.*



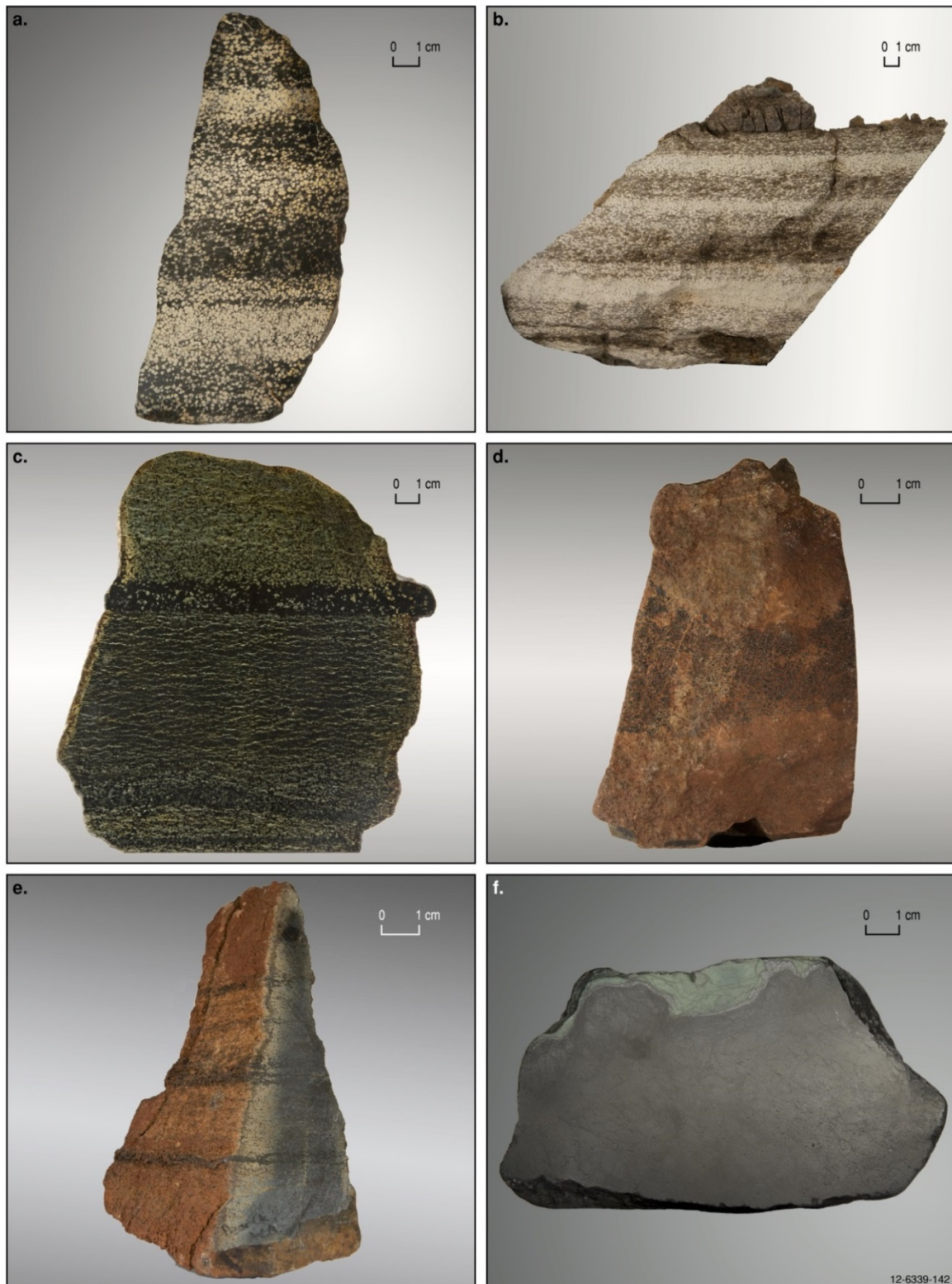
*Appendix Figure L.3 Munnii Munnii Intrusion, west Pilbara Craton, Western Australia. Vertical aerial photograph of the outcropping part of the Munnii Munnii layered mafic-ultramafic intrusion. The southwestern two-thirds of the intrusion (not shown here) is hidden by platform sedimentary and volcanic rock sequences of the Fortescue Group. See geology map of Figure 6.3.*



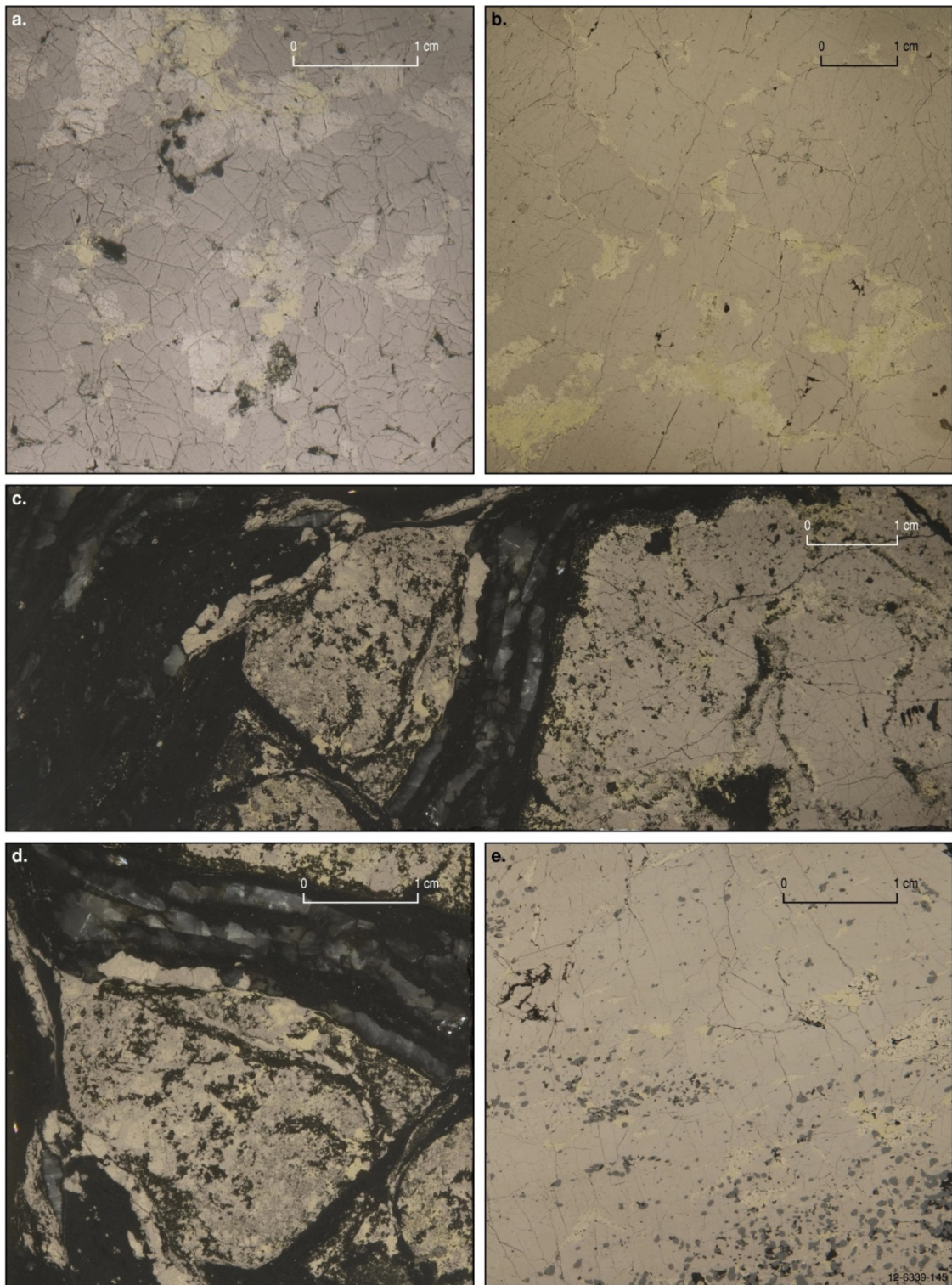
Appendix Figure L.4 Surface indicators of mineralisation at depth. (a). Ferruginous gossan ('Discovery Gossan' of Kambalda), Lunnon Ni-Cu-PGE shoot, Kambalda Dome, Yilgarn Craton, Western Australia. (b). Reverse cut face of sample shown in photo (a). (c). Ferruginous gossan, Widgee Ni-Cu deposit, Yilgarn Craton, Western Australia. (d). Ferruginous gossan with copper stains and pale-green Ni-bearing magnesite, Carr Boyd Rocks Ni-Cu-PGE deposit, Yilgarn Craton, Western Australia. (e). Chrysoprase ( $\text{NiSi}_3\text{O}_7 \cdot 10\text{H}_2\text{O}$ ), Wingellina lateritic Ni deposit, Musgrave Province, Western Australia. Inset—detail of 'bleaching' alteration near internal cavities. (f). Gaspéite ( $(\text{Ni,Mg,Fe})\text{CO}_3$ ), Kambalda Dome, Yilgarn Craton, Western Australia. Inset—gaspéite pendant.



Appendix Figure L.5 Chromitites in layered tholeiitic mafic-ultramafic intrusions. (a). Massive A chromitite (within red-flagging tape) layer (~4 g/t PGEs, 0.3% Ni, 0.1% Cu, 0.3 g/t Au), Middle Group Chromitites, Panton Intrusion, Halls Creek Orogen, Western Australia. (b). Stacked cyclic sequence of alternating thin chromite (black) and olivine (replaced by white magnesite)-chromitite layers (~1 g/t PGEs), Middle Group Chromitites, Panton Intrusion. (c). Isoclinally folded chromitites (black) in dunite, with olivine replaced by magnesite (white), Middle Group Chromitites, Panton Intrusion. (d). Parallel chromitite (black) layers (~660 ppb Pt, 490 ppb Pd, 0.12% Ni) in dunite, West McIntosh Intrusion, Halls Creek Orogen, Western Australia. (e). Chromitite (black: ~60 ppb Pt, 150 ppb Pd, 0.1% Ni) in troctolite, Wilagee Intrusion, Halls Creek Orogen, Western Australia. (f). Chromitite (black) in anorthosite, Wondinong, Windimurra Igneous Complex, Yilgarn Craton, Western Australia.



Appendix Figure L.6 Chromitites. (a). Sequence of alternating chromite (black) and olivine (replaced by white magnesite)-chromitite layers (~1 g/t PGEs), Middle Group Chromitites, Panton Intrusion, Halls Creek Orogen, Western Australia. (b). Similar olivine-chromite cumulate rock to (a). (c). Chromitite layer (~1 g/t PGEs) in partly sheared serpentinitised dunite, Lamboo Intrusion, Halls Creek Orogen, Western Australia. (d). Rare chromitite (<10 ppb Pt, 3 ppb Pd, 1.5 ppb Ir, 0.3 ppb Au) in dunite, Munni Munni Intrusion, west Pilbara Craton, Western Australia. (e). Chromitite layers in dunite, Pear Creek, East Pilbara Craton, Western Australia. (f). Podiform-nodular chromitite in serpentinitised ultramafic rock, Coolac Serpentinite, Lachlan Orogen, New South Wales.



**Appendix Figure L.7 Ni-Cu-PGE sulphide ores in tholeiitic mafic-dominated intrusions. (a).** Massive pyrrhotite (pink), interstitial pentlandite (cream) and chalcopyrite (yellow), and minor magnetite (black), basal contact, Radio Hill Intrusion, west Pilbara Craton, Western Australia. **(b).** Massive sulphides (~3.7% Ni, 1.1% Cu, 0.3% Co, 240 ppb Pt, 6312 ppb Pd, 30 ppb Ru, 1.4 ppb Ir, 5.6 ppb Au) comprising pyrrhotite, interstitial pentlandite and chalcopyrite, basal contact, Radio Hill Intrusion. **(c).** Basal contact relationships of massive and partly remobilised pyrrhotite, pentlandite, and chalcopyrite with country rocks (black) and quartz-carbonate veinlets (white), Radio Hill Intrusion. **(d).** Enlargement of left part of photo (c) sample; sample rotated 90° anticlockwise. **(e).** Massive sulphides (~3.5% Ni, 1.5% Cu, 0.3% Co, 100 ppb PGEs) comprising pyrrhotite, interstitial pentlandite and chalcopyrite, and disseminated granular magnetite, Savannah Intrusion, Halls Creek Orogen, Western Australia.



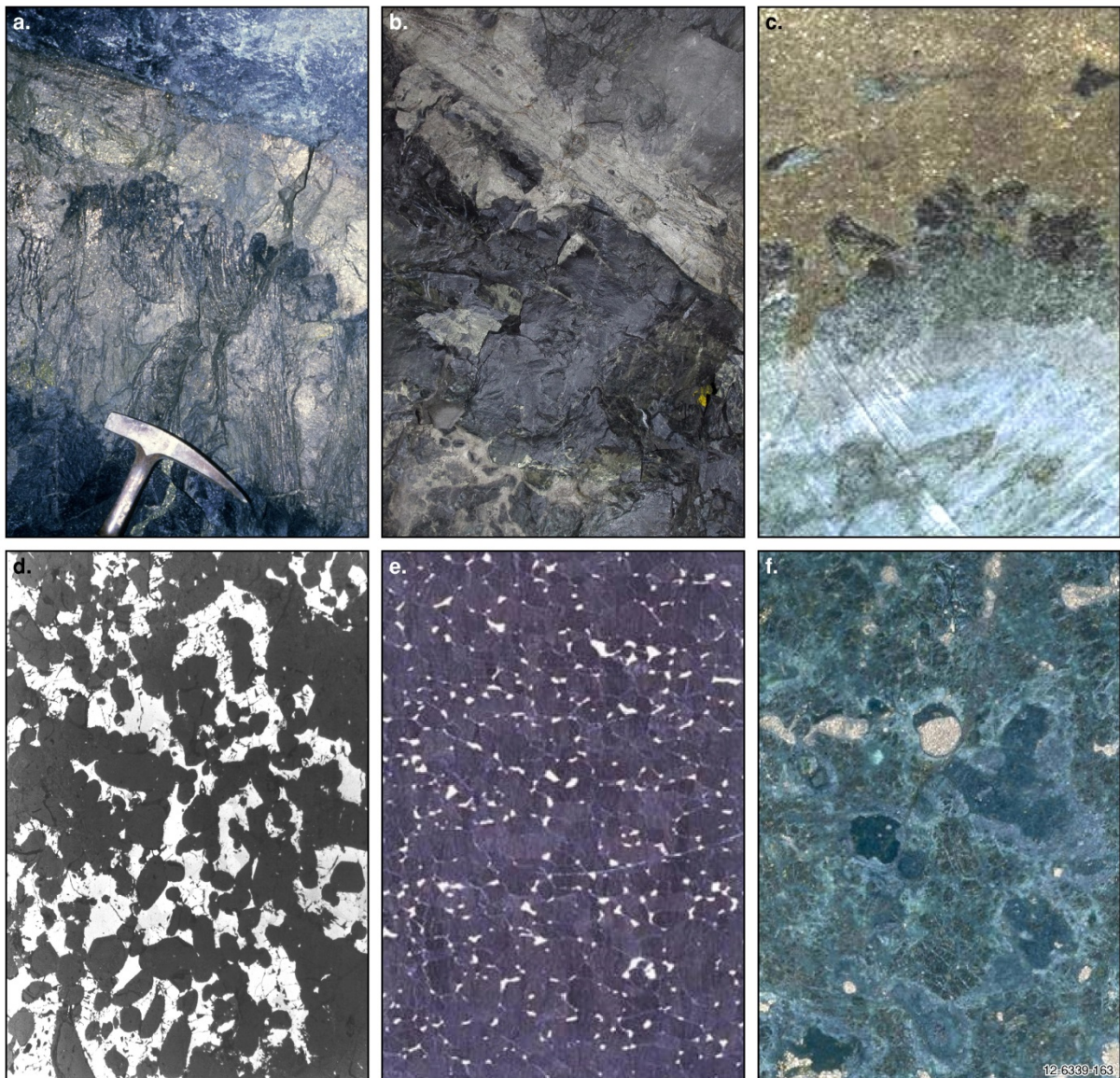
Appendix Figure L.8 Disseminated, matrix, massive, and breccia Ni-Cu-PGE sulphides. (a) Porphyritic plagioclase websterite comprising porphyritic orthopyroxene, granular clinopyroxene, interstitial plagioclase, minor biotite, and disseminated PGE-enriched chalcopyrite-pyrrhotite-pentlandite sulphides (~520 ppb Pt, 1850 ppb Pd, 200 ppb Au, 0.2% Ni, 0.3% Cu), Munni Munni Intrusion, west Pilbara Craton, Western Australia. (b) Matrix pyrrhotite-pentlandite-chalcopyrite-magnetite ore (2.55% Ni, 1.62% Cu, anomalous PGEs), Carr Boyd Rocks Intrusion, Yilgarn Craton, Western Australia. (c) Breccia pyrrhotite-pentlandite-chalcopyrite-magnetite ore (3.19% Ni, 0.33% Cu, anomalous PGEs) with quartz-rich rock fragments, Carr Boyd Rocks Intrusion. (d) Reverse view of sample (uncut face) in photo (c). (e) Massive pyrrhotite-pentlandite-chalcopyrite sulphides (7.9% Ni, 0.4% Cu, 0.2% Co), Honeymoon Well, Yilgarn Craton, Western Australia. (f) Disseminated PGE-bearing chalcopyrite-pyrrhotite-pentlandite sulphides (~0.07% Ni, 0.15% Cu, 440 ppb Pt, 710 ppb Pd, 30 ppb Rh, 20 ppb Ru, 30 ppb Ir) in peridotite, alkaline Mordor Igneous Complex, Arunta Orogen, Northern Territory.



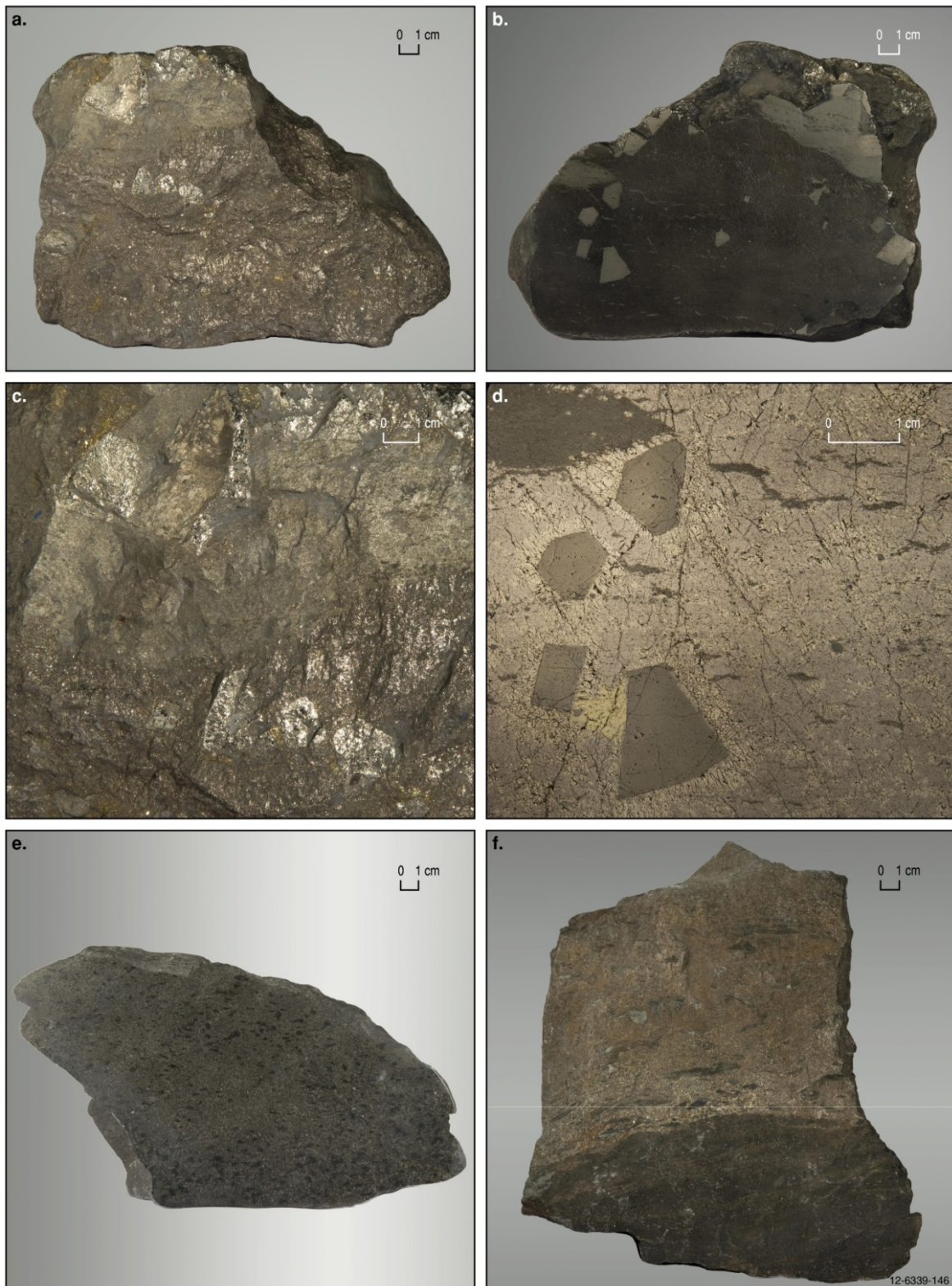
Appendix Figure L.9 Spinifex textures associated with komatiitic rocks. (a). Coarse-bladed spinifex in komatiite, Marshall Pool, Yilgarn Craton, Western Australia. The well-defined spinifex plates are probably after olivine. (b). Coarse-bladed spinifex in komatiite, Kurnalpi region, southeast of Kalgoorlie, Yilgarn Craton, Western Australia. The random plates are probably after olivine. (c). Zoned (~12 cm-thick) komatiite cooling unit equating to the  $A_2$  zone in Appendix Figure L.23. The younging directions in both photos (c) and (d) are probably down the core, Marshall Pool, Yilgarn Craton, Western Australia. (d). Matching cut pair of the sample shown in photo (c). (e). Coarse-bladed spinifex in komatiite, Ruth Well, west Pilbara Craton, Western Australia. (f). Stringy-beef spinifex in high-MgO basalt, Ultramafic Hill, west of Kambalda, Yilgarn Craton, Western Australia. Green amphibole has replaced ?clinopyroxene.



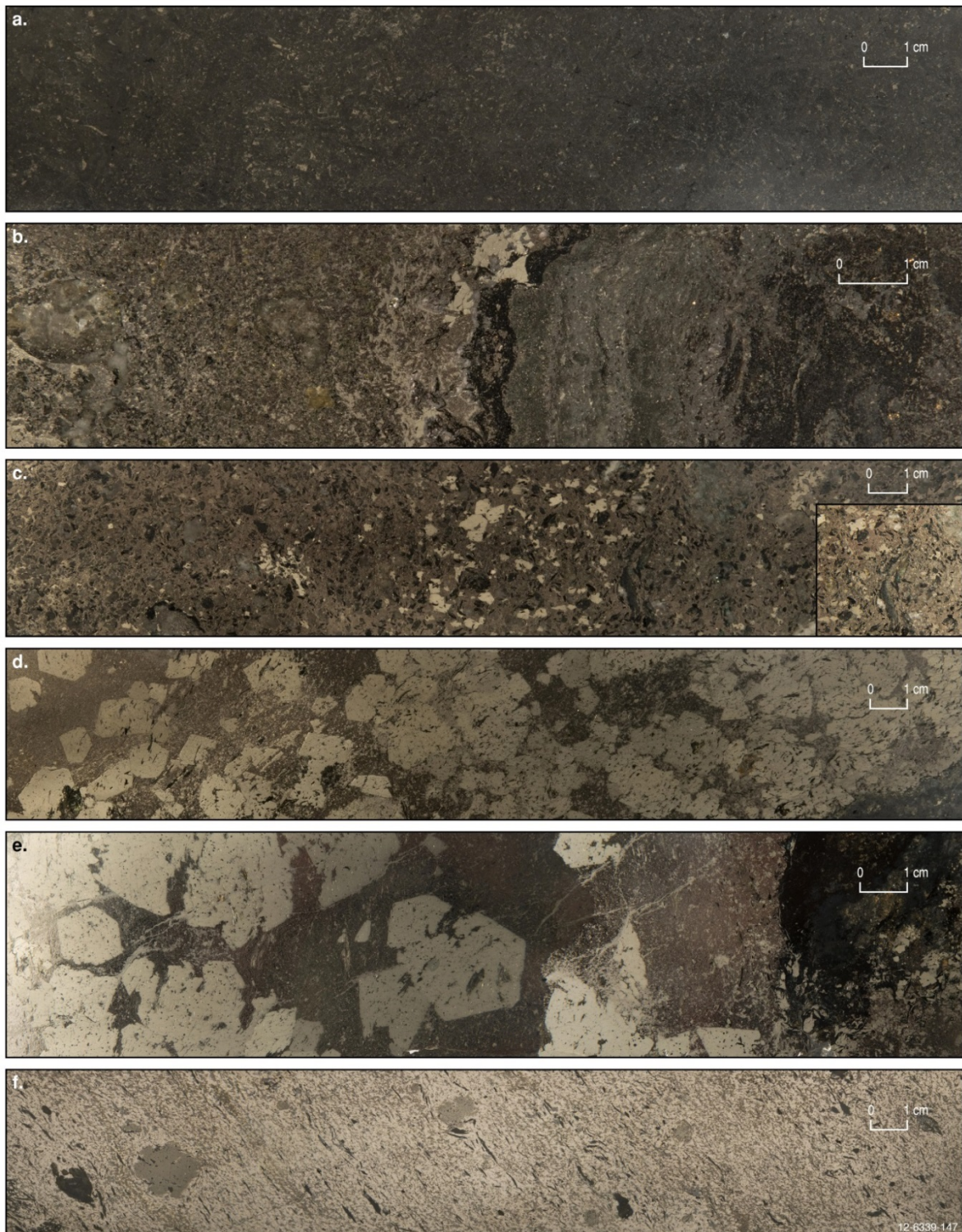
*Appendix Figure L.10 Emily Ann komatiitic-hosted Ni-Cu-PGE deposit, Yilgarn Craton, Western Australia. Massive sulphide layers and lenses separated by partly deformed and veined host rocks. The sulphide bodies have variable thicknesses, and the thickest sulphide body layer (top of photo) may represent a cross-section of a lava conduit comprising a curved basal 'embayment' contact and a flat upper contact that indicates a possible younging direction towards the bottom right of the image. Reproduced with permission from Norilsk Nickel Australia Pty Ltd.*



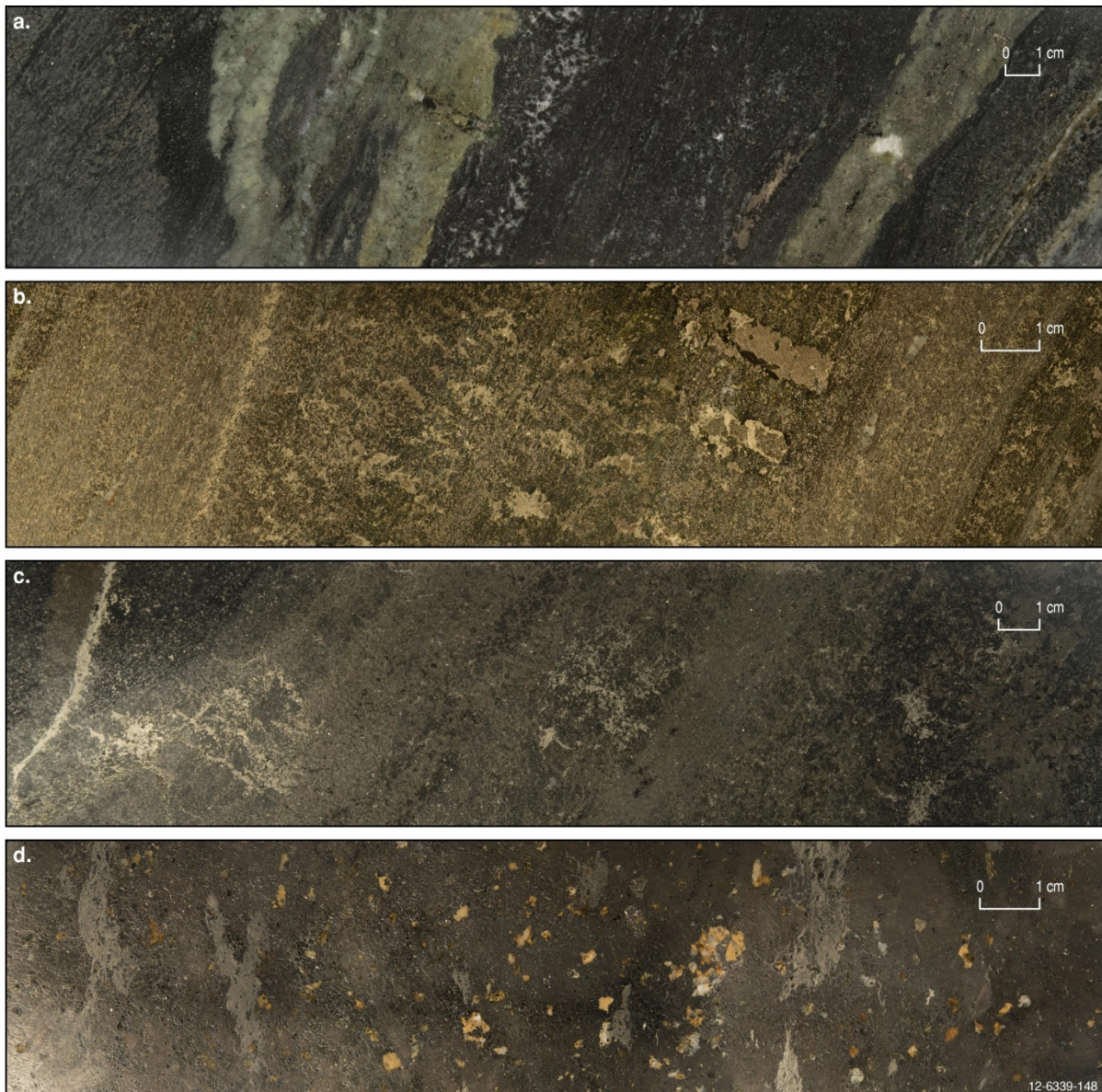
*Appendix Figure L.11 Sulphide ores associated with Ni-Cu-PGE komatiitic deposits. (a). Massive sulphide liquid melting and penetrating spinifex zone of underlying flow, Lunnon shoot, Kambalda Dome, Yilgarn Craton, Western Australia. (b). Massive pyrrhotite-pentlandite-chalcopyrite ore overlain by net-textured ore, and overlying brecciated footwall basalt, Moran shoot, Kambalda Dome. (c). Massive pyrrhotite-pentlandite ore has irregular contact with altered footwall ?basalt, Kambalda Dome. (d). Matrix pyrrhotite-pentlandite (white) making continuous interstitial matrix to serpentinised olivine (black), Katinniq deposit, Canada. (e). Disseminated pyrrhotite-pentlandite-chalcopyrite (white) in olivine adcumulate (black), ?Mount Keith, Yilgarn Craton, Western Australia. (f). Globular sulphides, Black Swan deposit, Yilgarn Craton, Western Australia.*



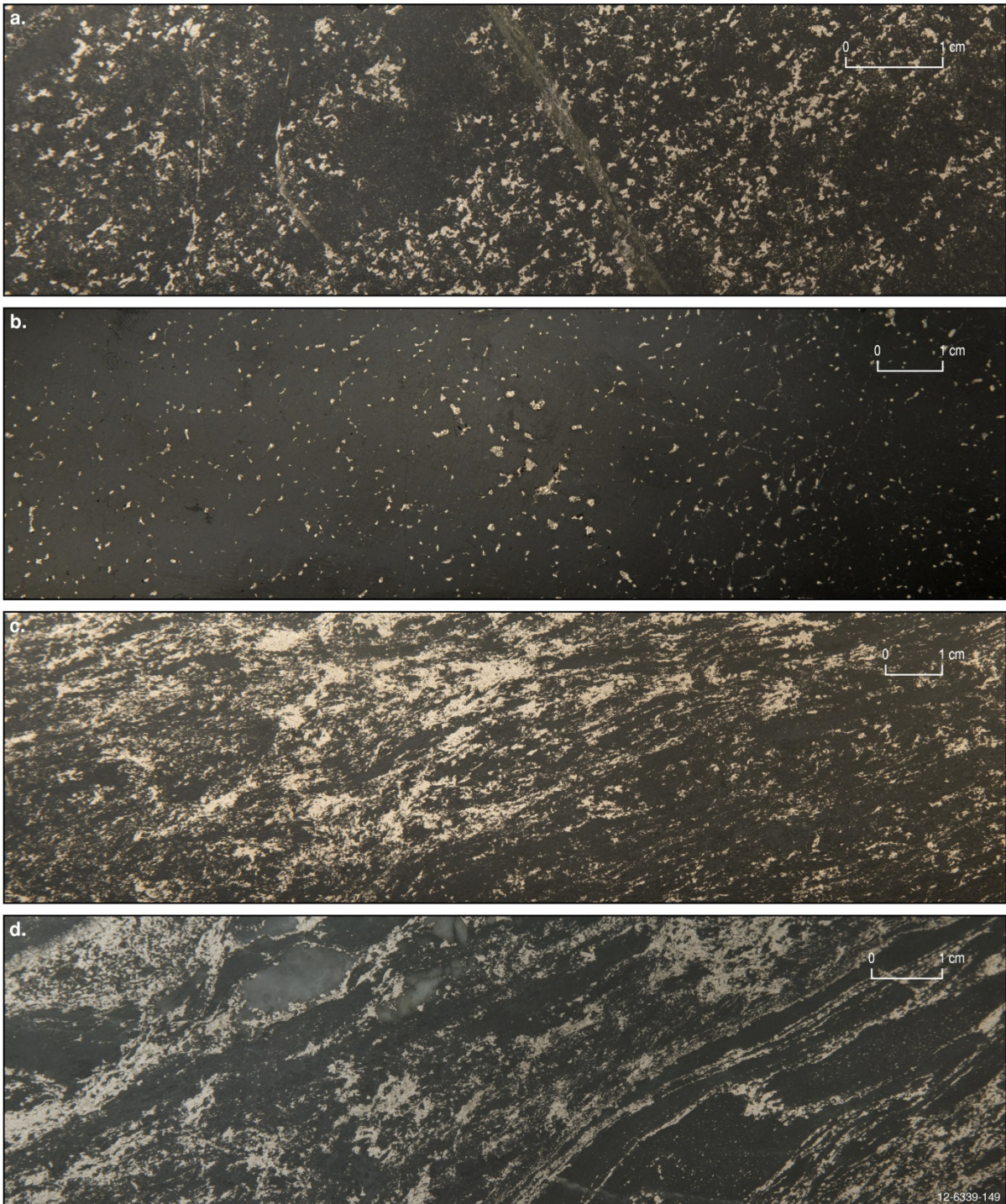
Appendix Figure L.12 Sulphide ores associated with Ni-Cu-PGE komatiitic deposits, Kambalda Dome, Yilgarn Craton, Western Australia. (a). Massive pyrrhotite-pentlandite-chalcopyrite-pyrite ore (13%–16% Ni), Long shoot (b). Reverse polished face of sample in (a) showing coarse metamorphic pyrite cubes mantled by chalcopyrite and pentlandite in pyrrhotite-rich host. (c). Enlarged upper part of photo (a) sample. (d). Enlarged left part of sample shown in photo (b) that highlights chalcopyrite and pentlandite mantling metamorphic pyrite. (e). Disseminated pyrrhotite-pentlandite-chalcopyrite (1% Ni) and wall-rock inclusions (dark), McLeay shoot. (f). Contact of massive pyrrhotite-pentlandite-chalcopyrite ore with ?metabasalt, Foster shoot.



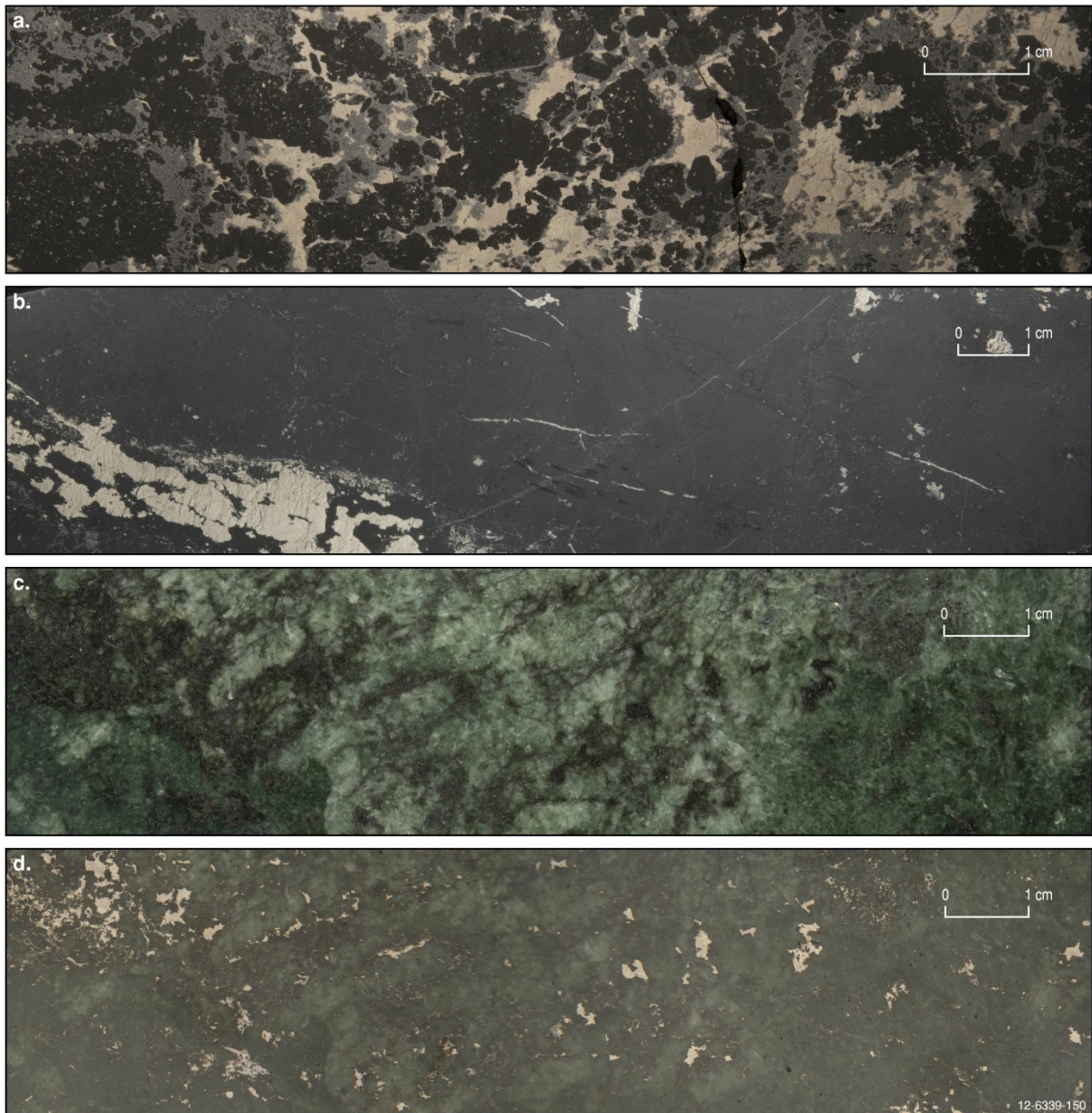
Appendix Figure L.13 Sulphide ores associated with the Flying Fox T1 Ni-Cu-PGE komatiitic deposit, Forrestania greenstone belt, Yilgarn Craton, Western Australia. (a). Disseminated sulphides (1.23% Ni, 700 ppm Cu, 0.21 ppm Pt, 0.10 ppm Pd) in ultramafic orthocumulate. (b). Chlorite-biotite-pyrite-rich reaction zone (near centre) abutting matrix sulphides (7.75% Ni, 910 ppm Cu, 0.91 ppm Pt, 0.31 ppm Pd). (c). Matrix sulphides (7.34% Ni, 1690 ppm Cu, 0.48 ppm Pt, 0.32 ppm Pd) with quartz and granite clasts in pyrrhotite, pyrite, and biotite matrix. Inset photo highlights emerald green fuchsite blades. (d). Massive pyrrhotite and pentlandite with metamorphic pyrite cubes (7.72% Ni, 4710 ppm Cu, 0.72 ppm Pt, 0.14 ppm Pd), and biotite. (e). Similar sample as in photo (d). (f). Foliated, massive pyrrhotite and pentlandite with minor chalcopyrite and secondary pyrite (8.2% Ni, 4210 ppm Cu, 0.20 ppm Pt, 0.44 ppm Pd), and biotite.



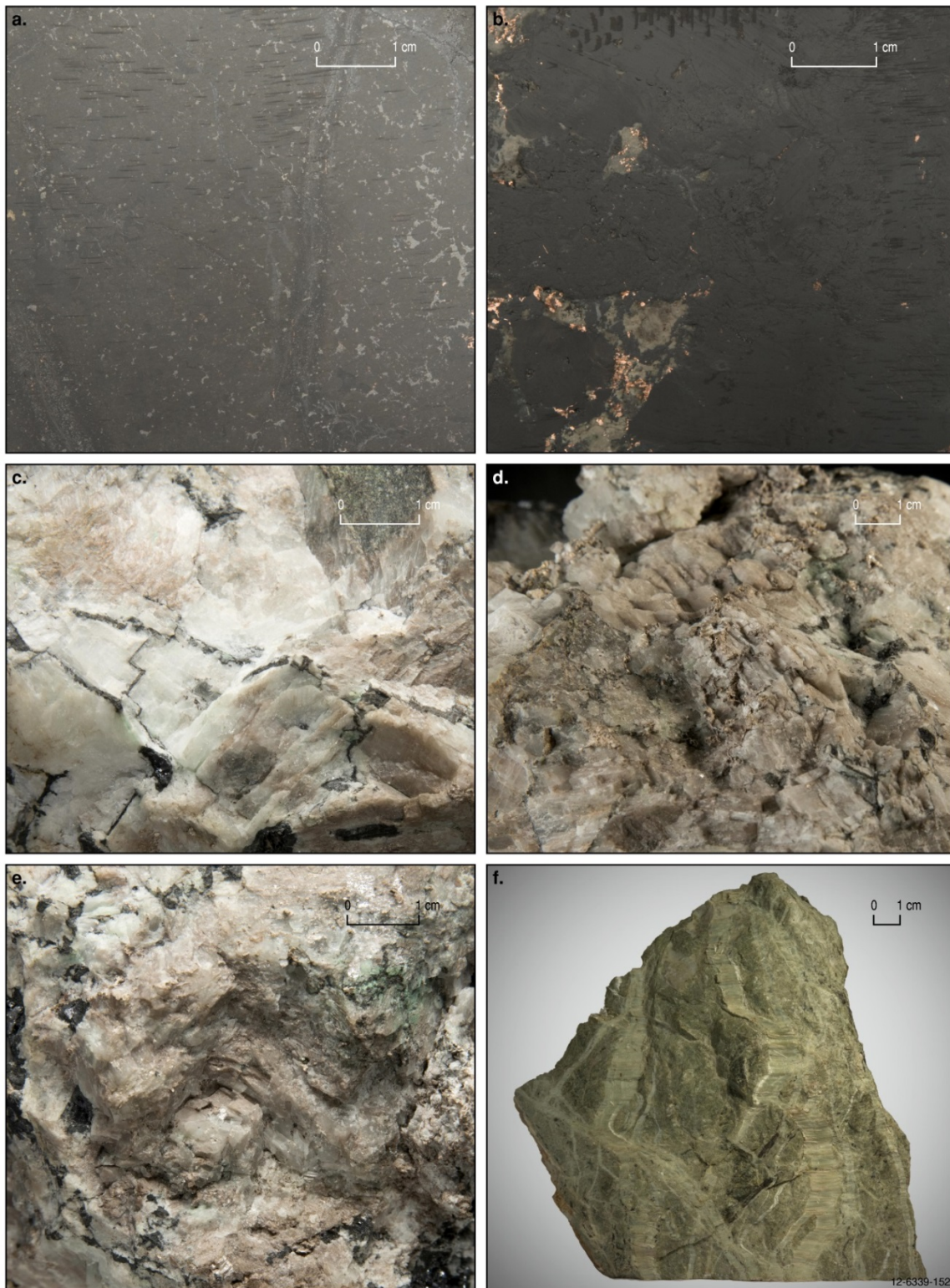
*Appendix Figure L.14 Sulphide ores associated with the Spotted Quoll Ni-Cu-PGE komatiitic deposit, Forrestania greenstone belt, Yilgarn Craton, Western Australia. (a). Disseminated low-grade pyrrhotite-pyrite-pentlandite (0.33% Ni, 0.02% Cu, 0.006 ppm Pd) in a matrix of carbonate-magnesite-magnetite-serpentine with pale-green diopside zones. (b). Stringer and disseminated pyrrhotite-pyrite-pentlandite (2.97% Ni, 0.23% Cu, 0.014 ppm Pd) in a matrix of amphibole-magnesite-serpentine. (c). Stringer pyrrhotite-pentlandite-chalcopyrite-pyrite (6.1% Ni, 0.49% Cu, 0.008 ppm Pd) in a matrix of carbonate-magnesite-magnetite. (d). Massive pyrrhotite-pentlandite-pyrite-chalcopyrite (11.12% Ni, 0.46% Cu, 0.012 ppm Pd) with minor felsic and carbonate-magnesite clasts, and magnetite.*



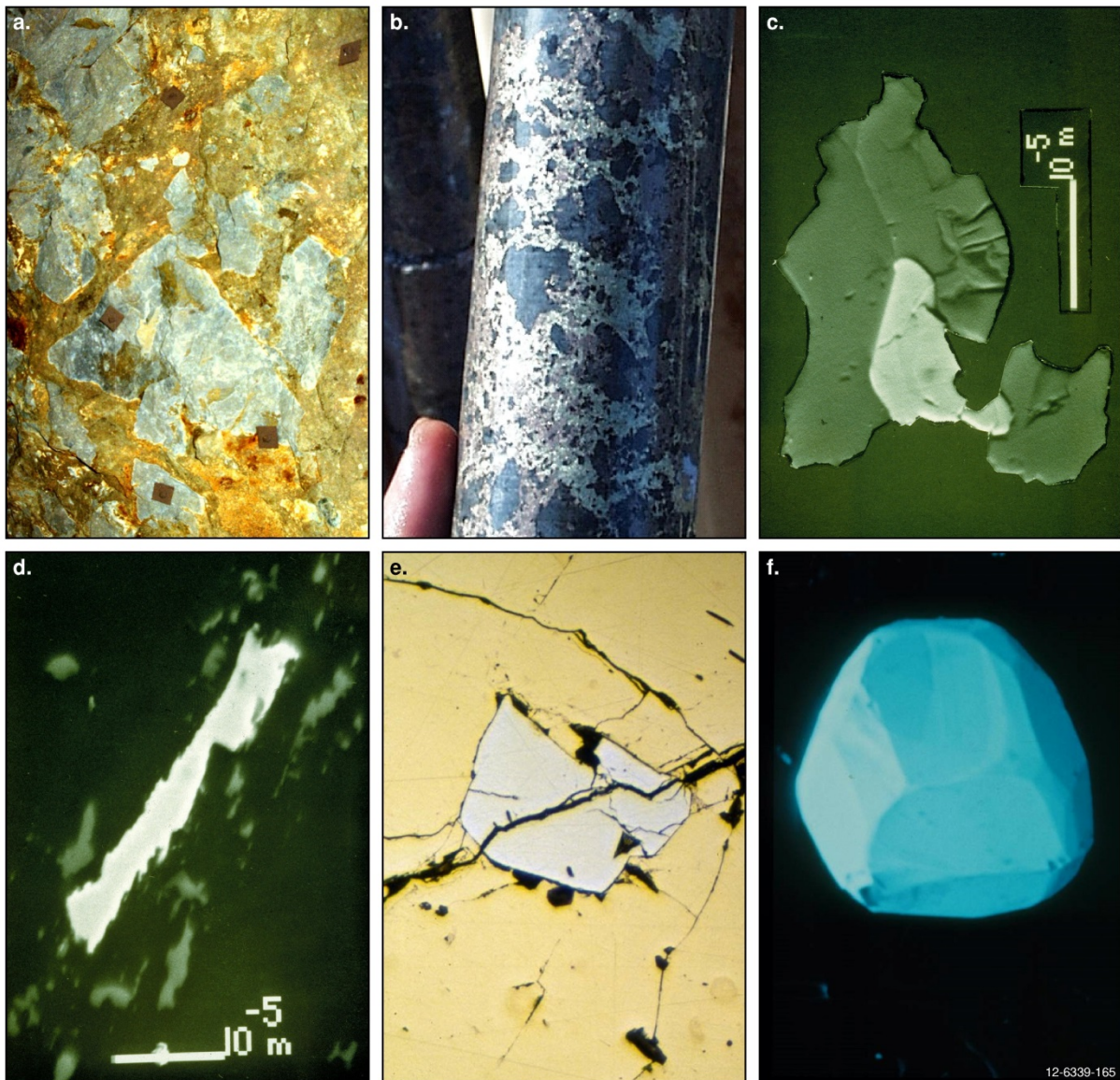
*Appendix Figure L.15 Sulphide ores associated with the Collurabbie, Mount Keith, and Mount Windarra komatiitic deposits, Yilgarn Craton, Western Australia. (a). Disseminated pyrrhotite-pentlandite (0.65% Ni, 3860 ppm Cu, 320 ppb Pt, 550 ppb Pd) in wehrlite, Collurabbie deposit. (b). Disseminated pyrrhotite-pentlandite (0.74% Ni, 180 ppm Cu) in olivine adcumulate, Mount Keith deposit. (c). Foliated, disseminated to matrix pyrrhotite-pentlandite-chalcopyrite (~4% Ni) in carbonate-serpentine-talc-magnetite komatiitic orthocumulate, Mount Windarra deposit. (d). Foliated, disseminated pyrrhotite-pentlandite-chalcopyrite-pyrite (~1% Ni) in chilled basal chlorite-tremolite-actinolite komatiite, with local ovoid-shaped milky quartz and BIF country-rock clasts, Mount Windarra deposit.*



Appendix Figure L.16 Sulphide ores associated with the hydrothermal Avebury Ni-Cu deposit, Delamerian Orogen, Tasmania. (a). Mesh-like magnetite-pentlandite-pyrrhotite ore (~2%–3% Ni) in serpentine (black). (b). Pentlandite-pyrrhotite-magnetite veins and veinlets (~1% Ni) in massive serpentine (black). (c). Disseminated pentlandite-pyrrhotite (1% Ni) in tremolite-diopside ultramafic 'skarn' (dark green and pale green). (d). Same sample as in photo (c) with 'reflected' light highlighting distribution of pentlandite-pyrrhotite.



Appendix Figure L.17 Mineralisation associated with 'Alaskan-type' intrusions and hydrothermal PGE deposits. (a). Disseminated PGE-bearing magnetite and native copper (right margin) in altered ultramafic rock ('P unit'), Owendale Intrusion, Lachlan Orogen, New South Wales. (b). Native copper in hydrothermal pegmatoidal phase of hornblende, Honeybugle Intrusion, Lachlan Orogen, New South Wales. (c). Minor PGE-bearing native silver in calcite-quartz-calcian siderite breccia host, Elizabeth Hill hydrothermal polymetallic deposit, west Pilbara Craton, Western Australia. (d). Crystalline silver wire in calcite-rich host, Elizabeth Hill. (e). Similar to (d) except additional copper (green) and lead-zinc (black) sulphides. (f). Chrysotile veins and veinlets in serpentinised dunite, Lionel Complex, Nullagine, east Pilbara Craton, Western Australia.



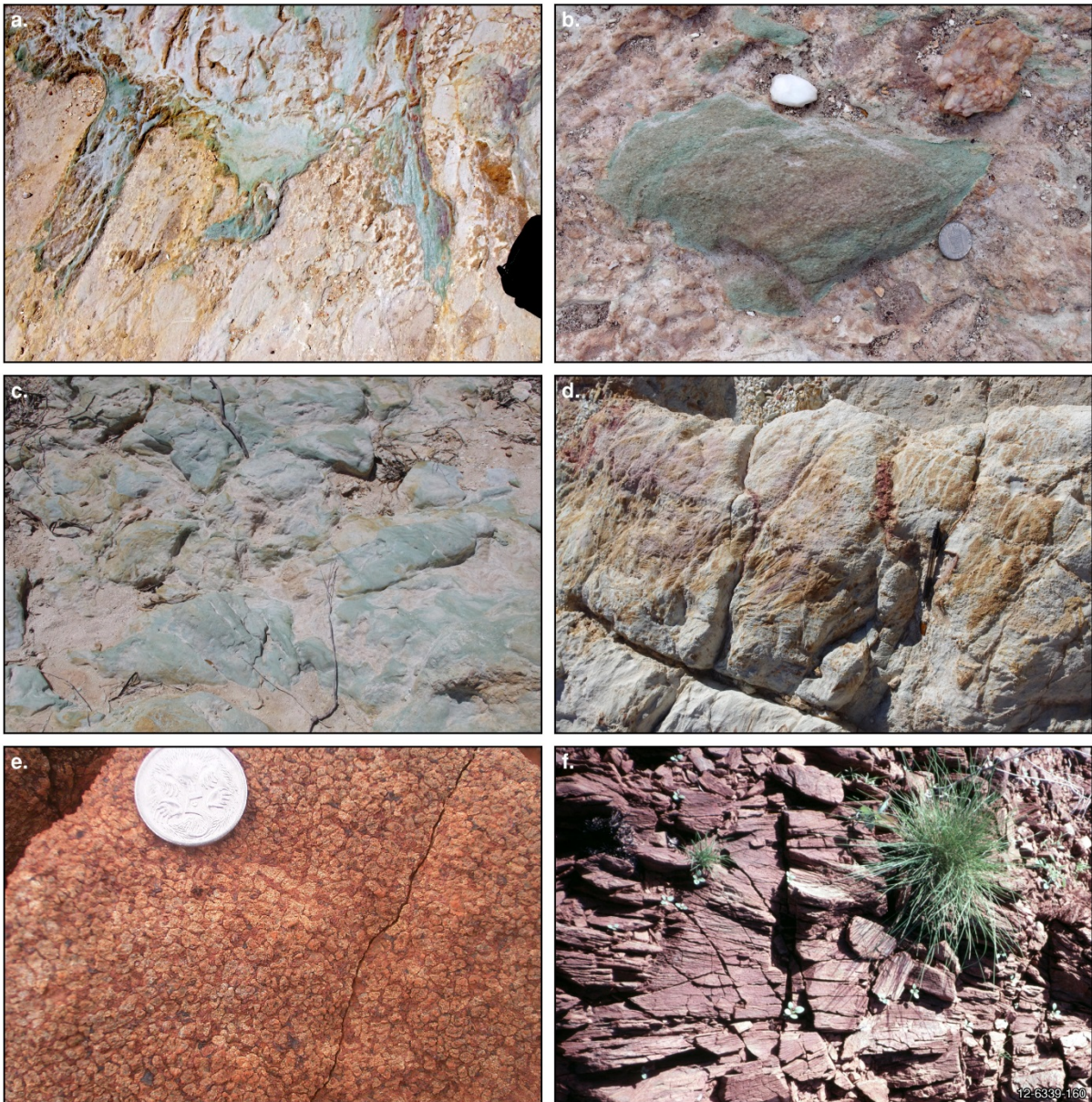
Appendix Figure L.18 Various breccia-type sulphides and platinum-group minerals. (a). Breccia ore comprising barren country-rock fragments (grey) in massive sulphides, bolted roof, Carr Boyd Rocks Ni-Cu-PGE deposit, Yilgarn Craton, Western Australia. (b). Massive Ni-Cu-PGE sulphides and country-rock breccia fragments (black), Nebo–Babel Ni-Cu-PGE deposit, Musgrave Province, Western Australia. (c). Scanning-electron microscope image of cooperite ( $PtS$ ) prism in contact with a chalcopyrite-pentlandite aggregate, porphyritic plagioclase websterite (see Appendix Figure L.8a), Munni Munni Intrusion, west Pilbara Craton, Western Australia. (d). Scanning-electron microscope image of moncheite ( $PtTe_2$ ) grain subaligned with smaller stringers of chalcopyrite, porphyritic plagioclase websterite (see Appendix Figure L.8a), Munni Munni Intrusion. (e). Sperrylite ( $PtAs_2$ ) grain enclosed in chalcopyrite, Kambalda, Yilgarn Craton, Western Australia. (f). Scanning-electron microscope image of well-crystalline sperrylite, Kambalda.



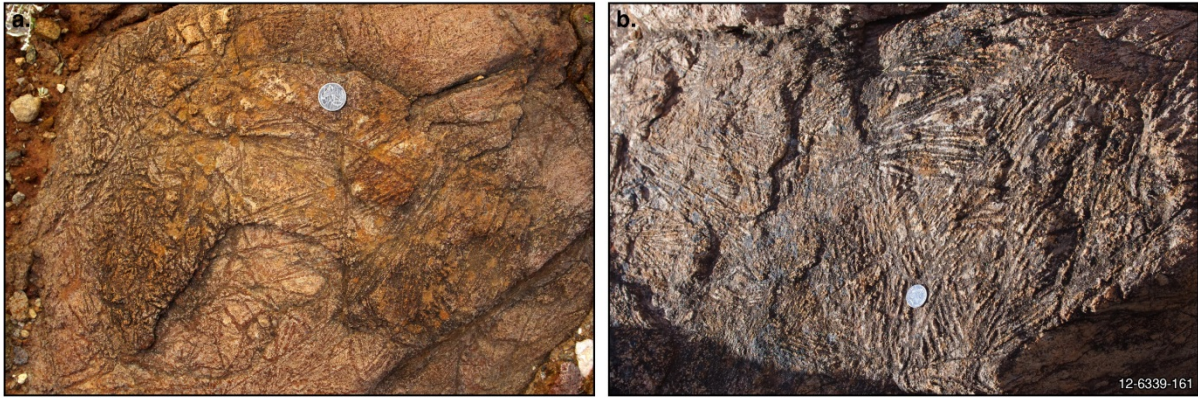
Appendix Figure L.19 Types of layering in tholeiitic mafic-ultramafic intrusions. (a). Aerial view looking southeast across the contact between the ultramafic zone (foreground) and overlying gabbroic zone (large black outcrops near Munnii Munnii Creek) of the Munnii Munnii Intrusion, west Pilbara Craton, Western Australia. Macrorhythmic layering in the ultramafic zone is defined by alternating pyroxenite cycles forming ridges and more recessive serpentinised peridotite cycles. (b). Macrorhythmic layering or 'inch-scale' layering of alternating olivine-clinopyroxene and clinopyroxene-olivine cumulates, ultramafic zone, Munnii Munnii Intrusion. (c). Interlayered mafic and felsic granulite, Mount Chapple Metamorphics, Arunta Orogen, Northern Territory. (d). Wispy compositional pyroxene layering /banding in anorthosite, Anburla Anorthosite, Arunta Orogen, Northern Territory. (e). Cyclic chromite (black) and olivine-chromite (white) layers, ultramafic series, Panton Intrusion, Halls Creek Orogen, Western Australia. (f). Looking south in Windimurra Vanadium Ltd's open-pit, multiple magnetite layers (black) in leucogabbro (white and pink), Windimurra Igneous Complex, Yilgarn Craton, Western Australia.



*Appendix Figure L.20 Commingling of mafic and felsic magmas. (a). Ellipsoidal mafic pillows with dark biotite-rich margins in partly hybridised granite, Juries mafic intrusion, Halls Creek Orogen, Western Australia. (b). Intricate cuspate and interfingering contacts, indicative of liquid-liquid relationships between mafic pillows and enclosing granite, Juries Intrusion. (c). Concentration of irregular pillow-like mafic inclusions in granite from the Toby mafic intrusion, Halls Creek Orogen. (d). Mafic pillow with cuspate and contaminated margins enclosed in fine-grained granite, Andrew Young Hills Intrusion, Arunta Orogen, Northern Territory. (e). Resorbed alkali feldspar xenocrysts in hybrid tonalite located between granite and gabbro, Andrew Young Hills Intrusion. (f). Porphyritic websterite layer (dark rock) with cuspate lower surface and planar upper surface, hosted by gabbro-norite (light rock), Munni Munni Intrusion, west Pilbara Craton, Western Australia.*

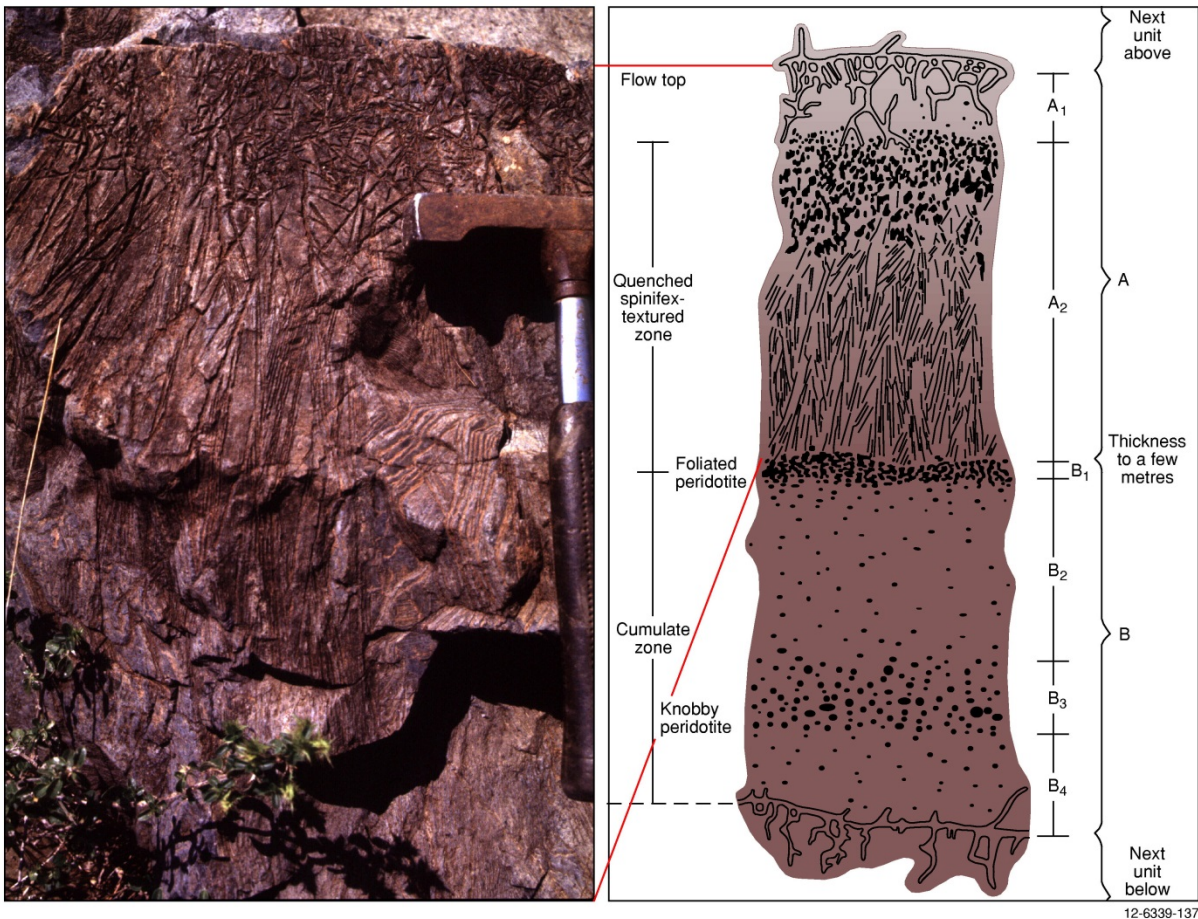


Appendix Figure L.21 Preserved komatiitic rock textures in the regolith, Yilgarn Craton, Western Australia. (a). Weathered komatiite (green) with peperite apophyses invading dacitic tuff (white), Breakaway, Kanowna, ~50 km northeast of Kalgoorlie. (b). Komatiite clast (green) in polymict agglomerate debris flow, Breakaway, Kanowna. (c). Weathered pillow-like bodies of komatiite (green) within dacite tuff (white) Breakaway, Kanowna; width of view is ~3 m. (d). Spinifex-textured A zone (centre layer) underlain by B zone, and overlain by B zone of overlying komatiitic flow, weathered saprock clay, Kanowna Town Dam. (e). Partially weathered coarse-grained olivine orthocumulate, Murrin Murrin layered lava lake komatiitic complex, Kilkenny syncline, Laverton. (f). Complete pyroxene spinifex A zone, 2 m-thick, in komatiite flow, Murrin Murrin Complex, Kilkenny Syncline.

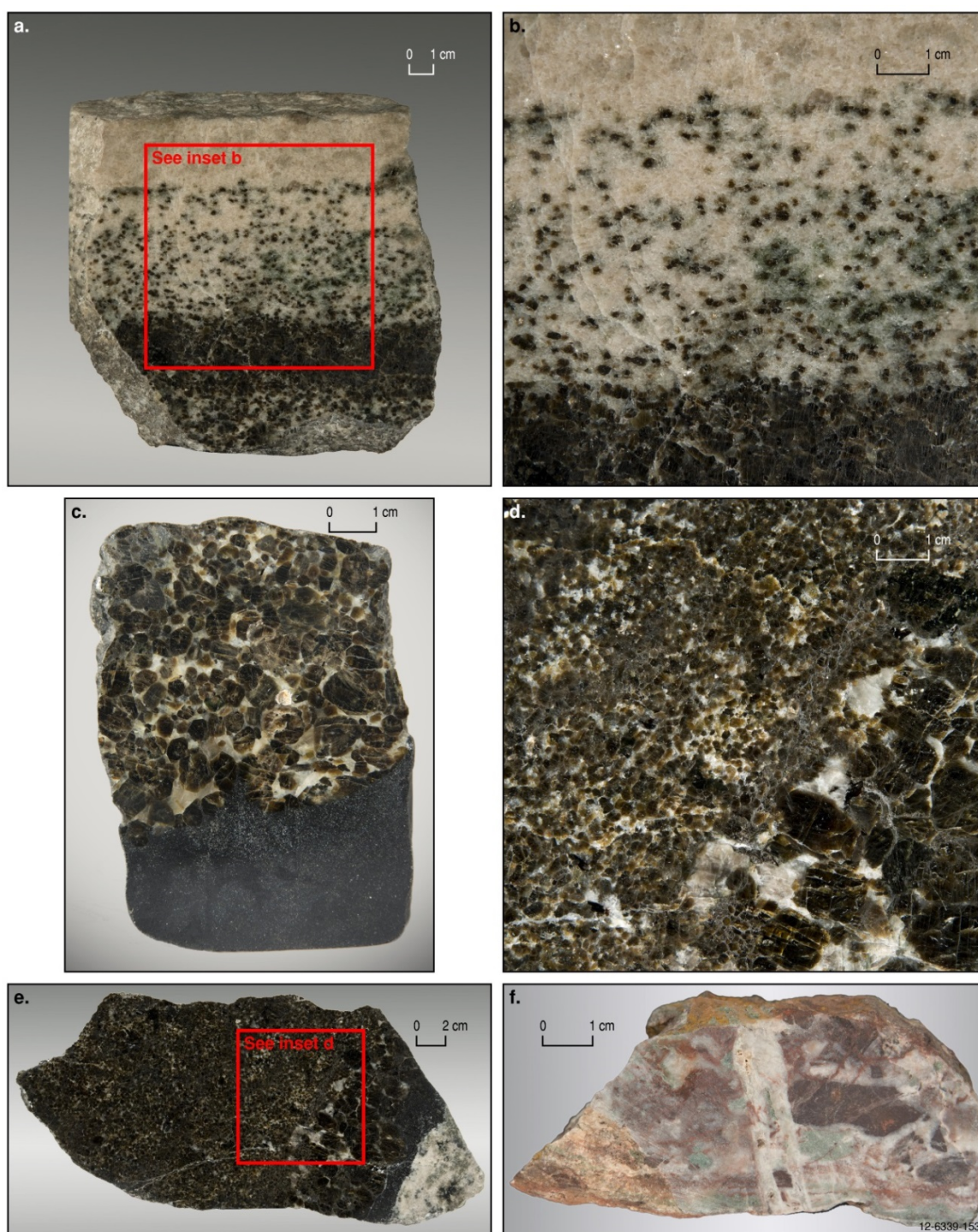


Appendix Figure L.22 Preserved spinifex textures in outcrop, Yilgarn Craton, Western Australia. (a). Olivine spinifex in outcrop, Serpentine Bay, ~15 km south of Kalgoorlie. (b). Coarse-bladed olivine spinifex in outcrop, Serpentine Bay near Mt Hunt, ~10 km south of Kalgoorlie.

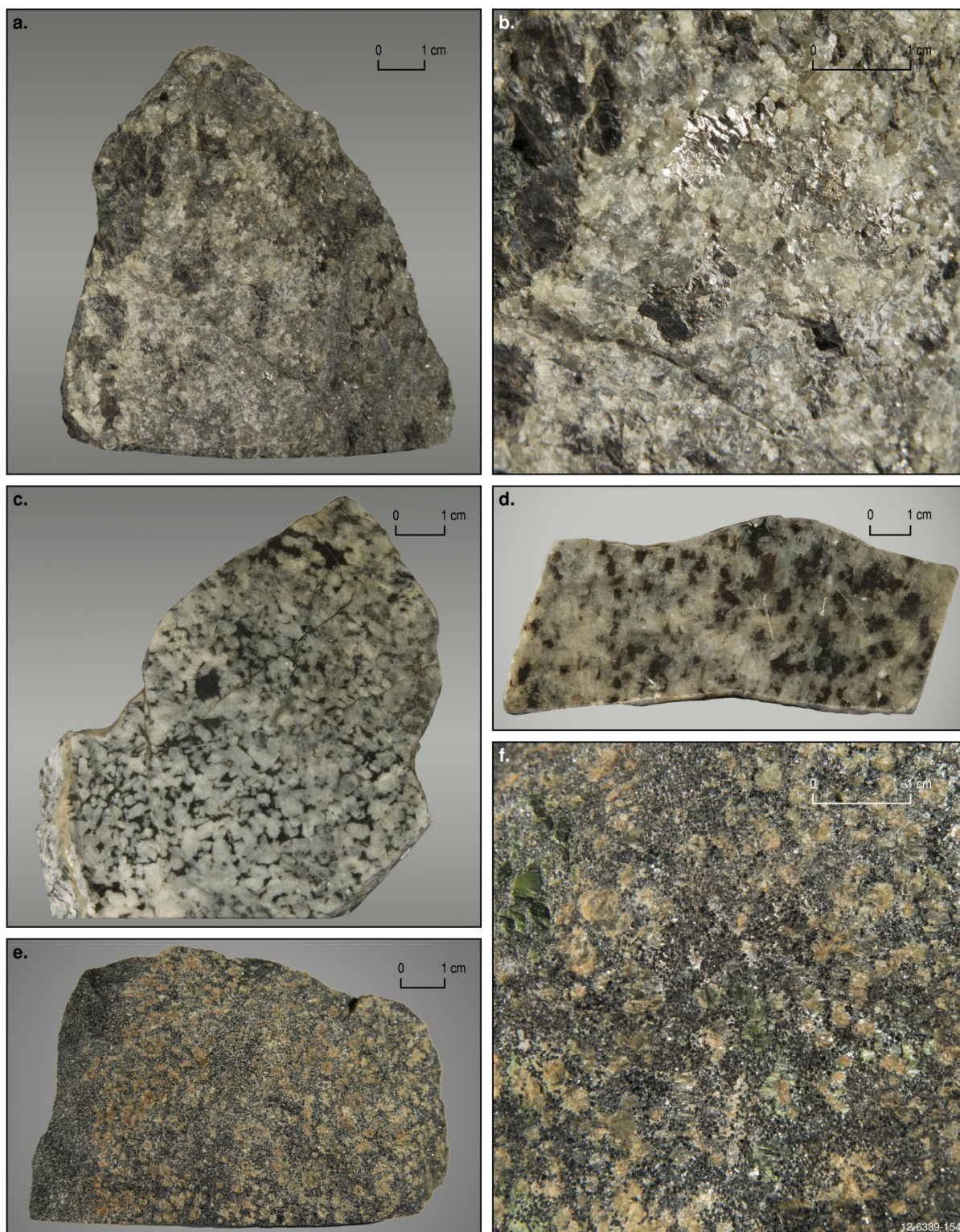
## L.2 Overseas Examples



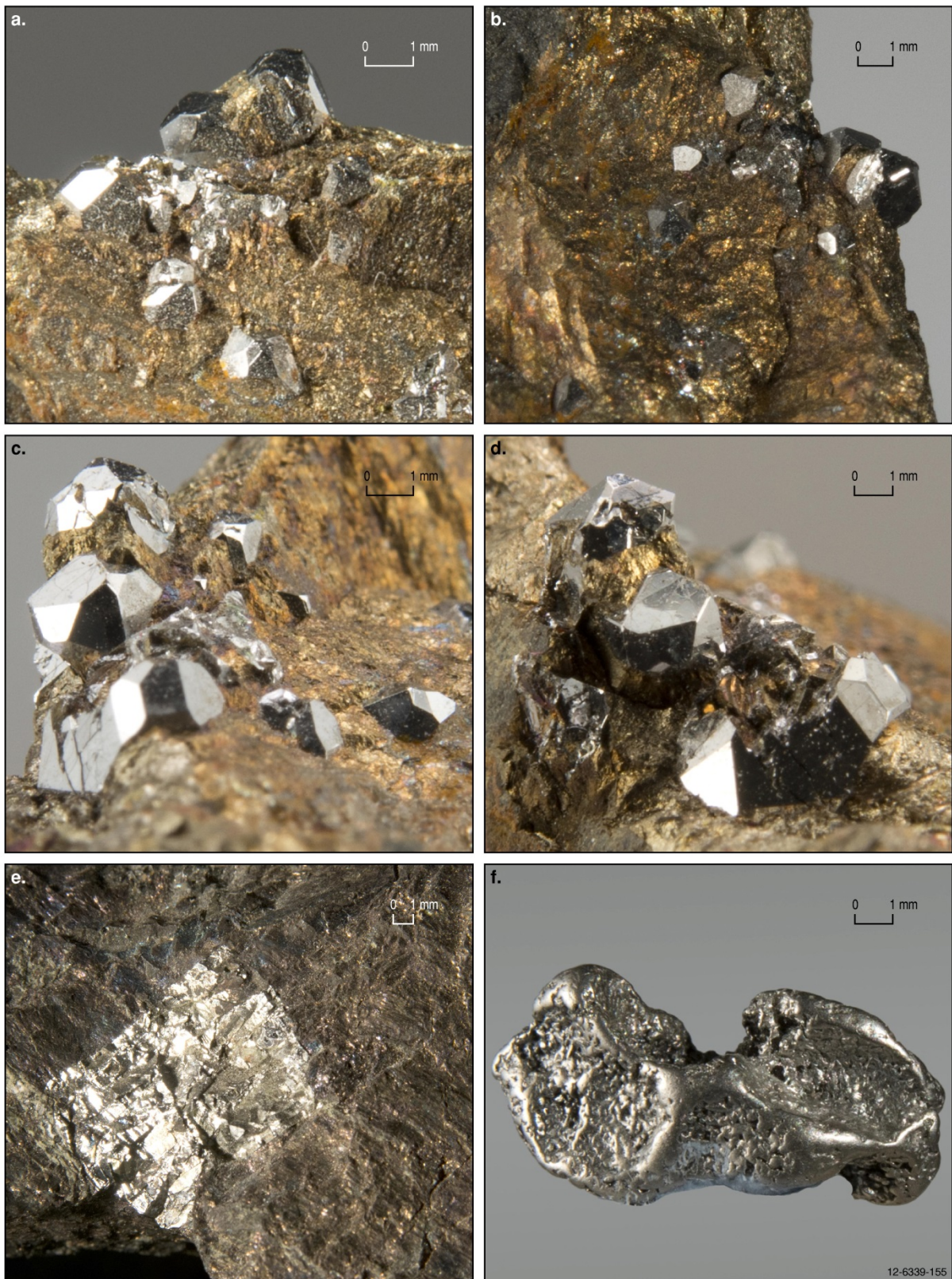
Appendix Figure L.23 Upper part of komatiite flow from the Komati Valley, Barberton greenstone belt, Republic of South Africa. This locality is considered the type example of spinifex-textured komatiites in the world. A schematic profile (right) of a complete single flow with distinct textural zones is modified from Arndt et al. (1977) and Barnes (2006).



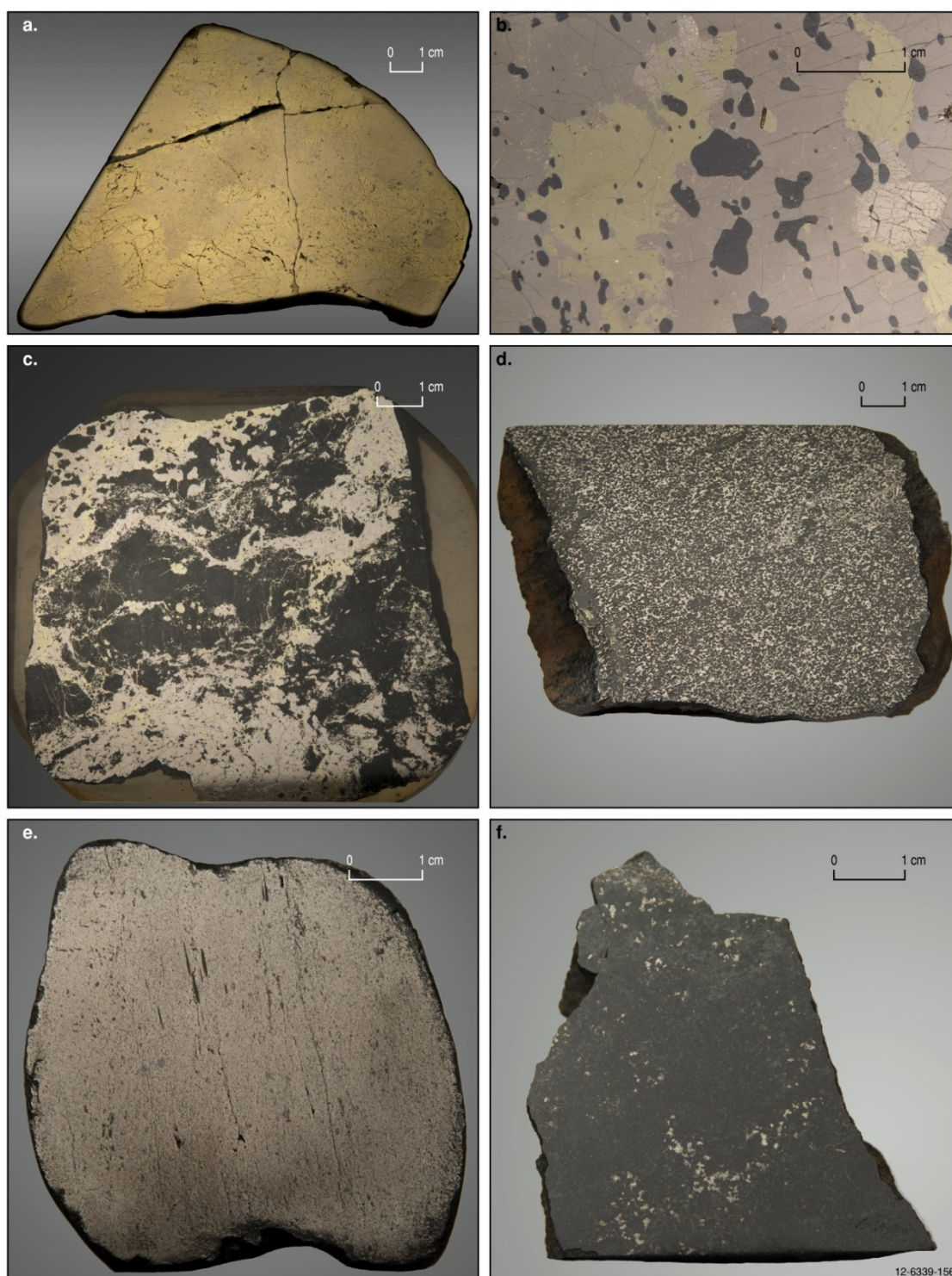
Appendix Figure L.24 Representative rock types from the Bushveld Complex, Republic of South Africa. (a). Layered gabbro-norite, overlain by plagioclase-rich norite, overlain by anorthosite (white). Hanging wall sequence to Merensky Reef. (b). Inset photo of (a) showing thin discontinuous 'isomodal' layering in the plagioclase-rich norite unit. (c). Pegmatoidal plagioclase orthopyroxene/norite comprising equigranular cumulus orthopyroxene and intercumulus plagioclase abutting fine-grained massive chromite (black) of the PGE-enriched UG-2 Chromitite layer. (d). Inset photo of (c). Pegmatoidal pyroxenite abuts fine-grained, equigranular pyroxenite containing disseminated pentlandite-chalcocopyrite-pyrrhotite-PGMs. (e). The Merensky Reef. Lithologies from right to left: anorthosite (white); thin PGE-enriched chromitite layer (black); coarse-grained pegmatoidal pyroxenite (brownish green) with disseminated PGE-bearing pentlandite-chalcocopyrite; and fine-grained, equigranular pyroxenite (brownish green) containing disseminated PGE-bearing pentlandite-chalcocopyrite-dominant sulphides. (f). Hydrothermal fault-breccia veins containing PGEs, Waterberg district, central Transvaal. The PGE component consists of 0.5% Pt as native platinum and Pt-Pd alloys.



Appendix Figure L.25 Mineralised rock types from the Stillwater Intrusion, Montana, USA. (a). Mottled 'anorthosite' of the J-M Reef comprising large oikocrystic ?clinopyroxene in cumulus plagioclase and minor PGE-enriched disseminated chalcopyrite-pentlandite-pyrrhotite. (b). Enlargement of upper central part of sample shown in (a). (c). Mineralised anorthosite with late-crystallising pyroxene minerals replaced by ?amphibole interstitial to cumulus euhedral plagioclase. (d). Footwall norite to J-M Reef comprising cumulus plagioclase and cumulus bronzite. (e). Olivine-chromite cumulate enriched in PGEs hosted by peridotite, basal parts of intrusion. (f). Enlargement of sample shown in (e).



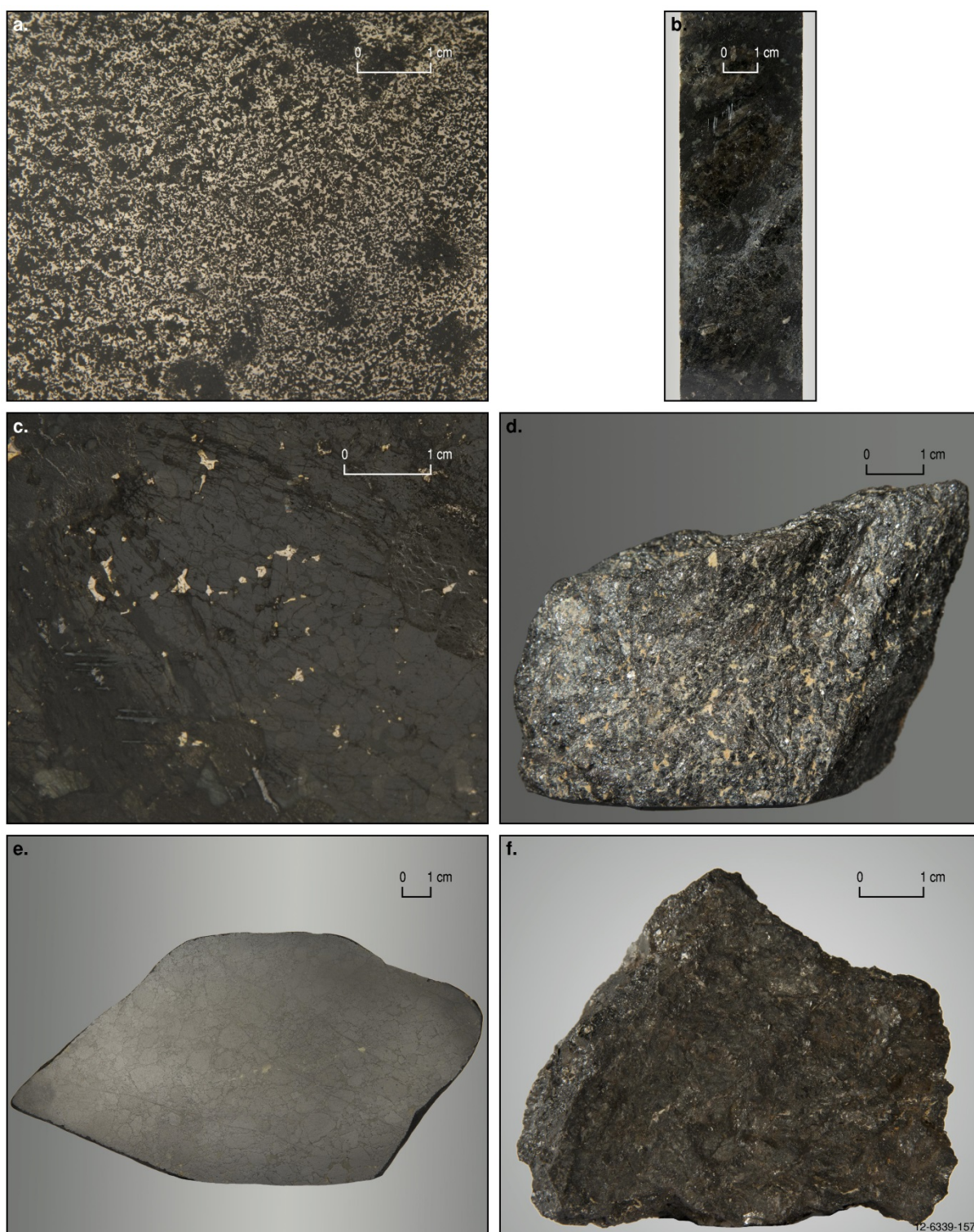
Appendix Figure L.26 Platinum-group minerals from the Noril'sk–Talnakh Ni-Cu-PGE deposits, Russia, and alluvial deposits in Goodnews Bay, Alaska. (a-d). Clusters of crystalline sperrylite ( $\text{PtAs}_2$ ) in massive chalcopyrite-bornite ore, Noril'sk–Talnakh Ni-Cu-PGE deposits, Russia. (e). Large euhedral sperrylite ( $\text{PtAs}_2$ ) in massive chalcopyrite-bornite ore, Noril'sk–Talnakh. (f). Alluvial platinum nugget, Goodnews Bay, Alaska.



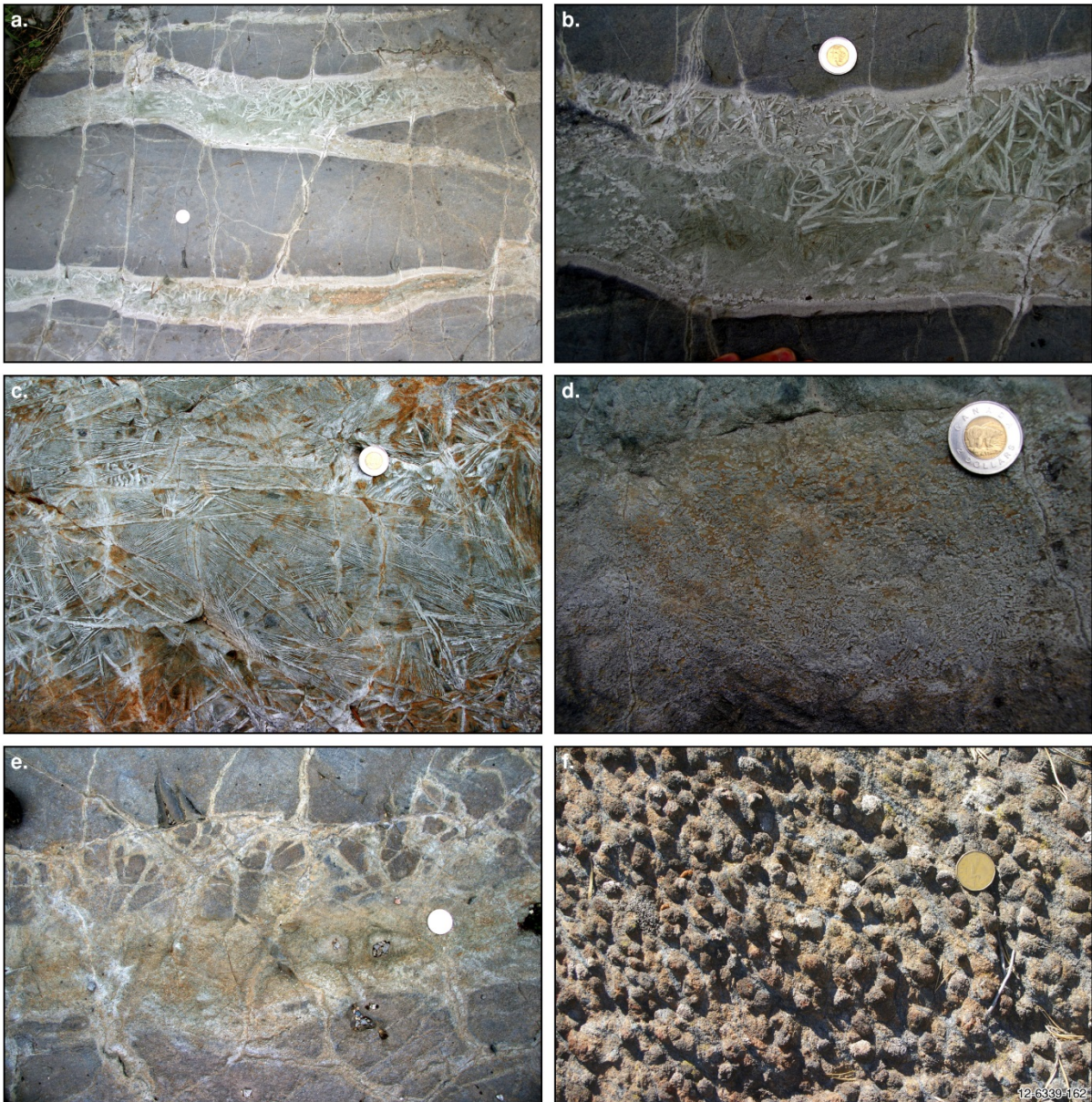
*Appendix Figure L.27 Mineralised rocks from various overseas deposits. (a). Massive chalcopyrite (yellow), pyrrhotite (pink), and minor magnetite (black) ores host a variety and abundance of PGMs (not visible), Noril'sk-Talnakh, Russia. (b). Massive pyrrhotite (pink), chalcopyrite (yellow), pentlandite (cream, fractured), and magnetite (black) ores generally host very-low concentrations of PGMs (not visible), Voisey's Bay, Canada. (c). Remobilised pyrrhotite (pink), chalcopyrite (yellow), pentlandite (cream), and magnetite ores host Pd-dominant PGMs (not visible), brecciated country-rock fragments, Sudbury Intrusion, Ontario, Canada. (d). Matrix pyrrhotite and minor chalcopyrite-pentlandite ore, Alexo Ni-Cu-PGE komatiitic deposit, Abitibi greenstone belt, Canada. (e). Massive pyrrhotite-rich ore (~1.5% Ni, 0.5% Cu, 0.5 g/t Pt, 0.5 g/t Pd), Peura-aho komatiitic deposit, Karelian Craton, eastern Finland. (f). Disseminated pyrrhotite-chalcopyrite ore (1.36% Ni, 0.19% Cu, 0.03% Co, 2.28 g/t Pt+Pd) in serpentinised peridotite, Vaara komatiitic deposit, Karelian Craton, eastern Finland.*



*Appendix Figure L.28 Massive sulphides in outcrop, Voisey's Bay nickel-copper deposit, Labrador, Canada. Glacially striated, polished, massive sulphide outcrop above ovoid massive sulphide deposit showing 'loop textures' of chalcopyrite (greenish) and ?pyrite (scattered blockier white crystals), surrounding pyrrhotite (brown), and pentlandite (not visible). Photograph taken August 2004.*



Appendix Figure L.29 Mineralised rocks from various overseas deposits. (a). Matrix pyrrhotite-pentlandite-chalcopyrite-PGE ore (4.22% Ni, 0.56% Cu, ?PGEs), Katinniq komatiitic deposit, Raglan, Canada. (b). Disseminated pentlandite-chalcopyrite-pyrrhotite in pyroxenite, Massive Sulphide Zone, Great Dyke of Zimbabwe. (c). Enlargement of upper central part of sample shown in (b), and sample rotated 90° anticlockwise. (d). Massive chromitite, Oman. (e). Massive nodular-podiform chromitite, Semail Ophiolite, Wadi Rajma, Oman. (f). Massive podiform chromitite, hosted by ophiolite, New Caledonia.



Appendix Figure L.30 Textures of komatiitic rocks from the Abitibi greenstone belt, Ontario, Canada. (a). Spinifex-textured veins within B zone of komatiite flow, Serpentine Hill. (b). Enlargement of central part of upper spinifex-vein shown in photo (a). (c). Spinifex-textured vein within B zone of komatiite flow, Serpentine Hill. (d). B<sub>1</sub> zone of komatiite flow, Serpentine Hill. (e). Polygonally jointed flow-top of komatiite flow, Serpentine Hill. (f). Poikilitic orthopyroxene (elevated mottles) in olivine cumulate, Centre Hill Intrusion, Munro Township.



Appendix Figure L.31 Textures of komatiitic rocks from Pyke Hill, Munro Township, Abitibi greenstone belt, Ontario, Canada. (a). Composite sequence of thin komatiite flows, comprising more massive B zone on far left overlying two complete zoned flows to the right (top of sequence is towards the right). (b-c). Komatiite flow with olivine-spinifex A<sub>3</sub> zone overlying and truncating layering within cumulate B zone. (d). Complete komatiite flow with olivine spinifex A zone overlying more massive cumulate B zone (top of sequence is towards the left). (e). Classical layered olivine-spinifex flows, A<sub>2</sub> zone, polygonally jointed A<sub>1</sub> flow-top. (f). Komatiitic hyaloclastite breccia.



Appendix Figure L.32 Textures of komatiitic rocks from Dundonald Beach, Abitibi greenstone belt, Ontario, Canada. (a-b). Olivine spinifex from margin of high-level komatiite sill injected into wet sediments. (c). Pyroxene spinifex in komatiitic basalt flow. (d). Olivine orthocumulate unit in komatiite flow. (e). Peperite margin of high-level komatiite sill injected into wet sediments. (f). Termination of high-level komatiite sill injected into wet sediments.